

# Description of the larva of *Platycnemis phasmovolans* Hämäläinen, 2003 (Odonata, Platycnemididae), with a key to the larvae of the subfamily Platycnemidinae from the Sino-Japanese and Oriental regions

Tosaphol Saetung Keetapithchayakul<sup>1</sup> , Quoc Toan Phan<sup>1</sup> 

<sup>1</sup> The Center for Entomology & Parasitology Research, College of Medicine and Pharmacy, Duy Tan University, 120 Hoang Minh Thao, Lien Chieu, Da Nang, Vietnam  
Corresponding author: Tosaphol Saetung Keetapithchayakul ([Keetapithchayakul.TS@gmail.com](mailto:Keetapithchayakul.TS@gmail.com))

## Abstract

The final instar larva of the rare species *Platycnemis phasmovolans* Hämäläinen, 2003 is described and illustrated here for the first time, including a new distribution record from Vietnam. The larva of *P. phasmovolans* differs from that of congeneric species by distinct morphological features, including the presence of four setae on the palpal lobe of the labium, the presence of lateral spines on abdominal S5–9, and a long terminal filament on the caudal lamella. We also provide a key to species for the known larvae of the subfamily Platycnemidinae in the Sino-Japanese and Oriental regions.

**Key words:** Biological notes, Coenagrionoidea, damselfly, identification key, new record, Platycnemidini, Vietnam, Zygoptera



Academic editor: Jan van Tol  
Received: 28 September 2024  
Accepted: 5 November 2024  
Published: 10 December 2024

ZooBank: <https://zoobank.org/4348B45F-4C9C-4E68-806F-EDB65C3C88D0>

Citation: Keetapithchayakul TS, Phan QT (2024) Description of the larva of *Platycnemis phasmovolans* Hämäläinen, 2003 (Odonata, Platycnemididae), with a key to the larvae of the subfamily Platycnemidinae from the Sino-Japanese and Oriental regions. ZooKeys 1221: 1–18. <https://doi.org/10.3897/zookeys.1221.138079>

Copyright: ©  
Tosaphol S. Keetapithchayakul & Quoc T. Phan.  
This is an open access article distributed under  
terms of the Creative Commons Attribution  
License (Attribution 4.0 International – CC BY 4.0).

## Introduction

The genus *Platycnemis* Burmeister, 1839, comprising 11 recognized species (Paulson et al. 2024), belongs to the subfamily Platycnemidinae (tribe Platycnemidini), family Platycnemididae (Dijkstra et al. 2014). This genus is widely distributed across Europe, extending eastward into Asia. The Asian species of *Platycnemis* are represented by four species from East Asia (*P. echigoana* Asahina, 1955; *P. foliacea* Selys, 1886; *P. phyllopoda* Djakonov, 1926; and *P. sasakii* Asahina, 1949) and one species from mainland Southeast Asia (*P. phasmovolans* Hämäläinen, 2003). *Platycnemis phasmovolans*, known for their elusive nature, have been documented in specific locations within central Laos and southern China, suggesting a broader but still undefined range that undoubtedly extends into northern Vietnam (Hämäläinen 2020). The species was first found in the Kaew Neua Pass area, Lak Sao district, Bolikhamsai Province in 2001 and 2002 (Hämäläinen 2003); and later, a small population was rediscovered (by Naoto Yokoi) in 2016 near the type locality (Hämäläinen 2020). While the coordinates provided in Hämäläinen (2011) are generally accurate, the actual location of the type locality is at 18°22'17.35"N, 105°09'05.84"E, which is approximately two kilometers from the Laos-Vietnam border (Hämäläinen pers. comm.). In China, a male specimen was photographed

in 2009 in the Maolan Nature Reserve in Guizhou (Pu et al. 2019), and another was recorded in 2018 near Nanning, Guangxi (Hämäläinen 2020).

The larvae of Platycnemidinae display a variety of morphological traits that are essential for species identification and add to our understanding of evolutionary relationships within the subfamily (Dijkstra et al. 2014; Orr and Dow 2015; Saetung et al. 2020). The Asian genera *Platycnemis*, *Pseudocopera* Fraser, 1922 and *Copera* Kirby, 1890, all exhibit distinctive larval morphology. The larva of *Matticnemis* Dijkstra, 2013, a monotypic genus from northern Vietnam, remains unknown. Studying platycnemidid larvae is challenging due to the high degree of morphological similarity among species, with many larvae either undescribed or with inadequate published descriptions (Keetapithchayakul et al. 2022). In this study, we describe the final instar larva of *P. phasmovolans* for the first time. We compare its characteristics with those of other described congeneric species. Additionally, we present new distribution records and provide a key to the known larvae of species of the Platycnemidinae in the Sino-Japanese and Oriental regions.

## Material and methods

Final instar larvae were collected from headwater streams of the North Central Region of Vietnam using D-frame nets and sorted manually with sieves. The larvae were transported to the laboratory and reared in plastic containers until they reached adulthood. They were fed *Aedes* larvae and provided with toothpicks as substrates to support emergence. Identification of the emerged adults was based on Hämäläinen (2003) (Figs 1, 8). Measurements and photographs were taken using a ZEISS Stemi 508 stereomicroscope equipped with an OPTIKA C-P6 Digital Camera. Illustrations were created using the Procreate application on an iPad Pro 2020, based on representative digital photographs. Final plates were assembled using AFFINITY Photo 2 version 2.5.3.

The descriptions of the larval mandibular formula, generic characteristics, and distinctive surface features of the larvae follow Watson (1956), Saetung et al. (2020) and Keetapithchayakul et al. (2022), respectively. Specimens are deposited in the Zoological Collection of Duy Tan University (ZCDTU), Da Nang City, Vietnam.

## Abbreviations used

**S1–10** abdominal segments 1–10

**A1–7** antennomeres 1–7

## Results

### *Platycnemis phasmovolans* Hämäläinen, 2003

**Material examined (larva).** VIETNAM • 1 exuviae: 1 ♂ (collected as last stadium larva, reared in laboratory); 27 Jul. 2024; 18°59'24.4"N, 104°50'17.8"E; elevation 266 m a.s.l.; Yen Khe Commune, Con Cuong District, Nghe An Province; T.S. Keetapithchayakul leg.; ZCDTU. • 7 late stadium larvae: 1 ♂ (F-0), 1 ♀ (F-0), 1 ♂ (F-1), 2 ♀♀ (F-1), 1 ♂ (F-2), 1 ♀ (F-2); 27 Jul. 2024; same site and collector as above; ZCDTU. • 2 early stadium larvae: 1 ♂, 1 ♀; 27 Jul. 2024; same site and collector as above; ZCDTU.

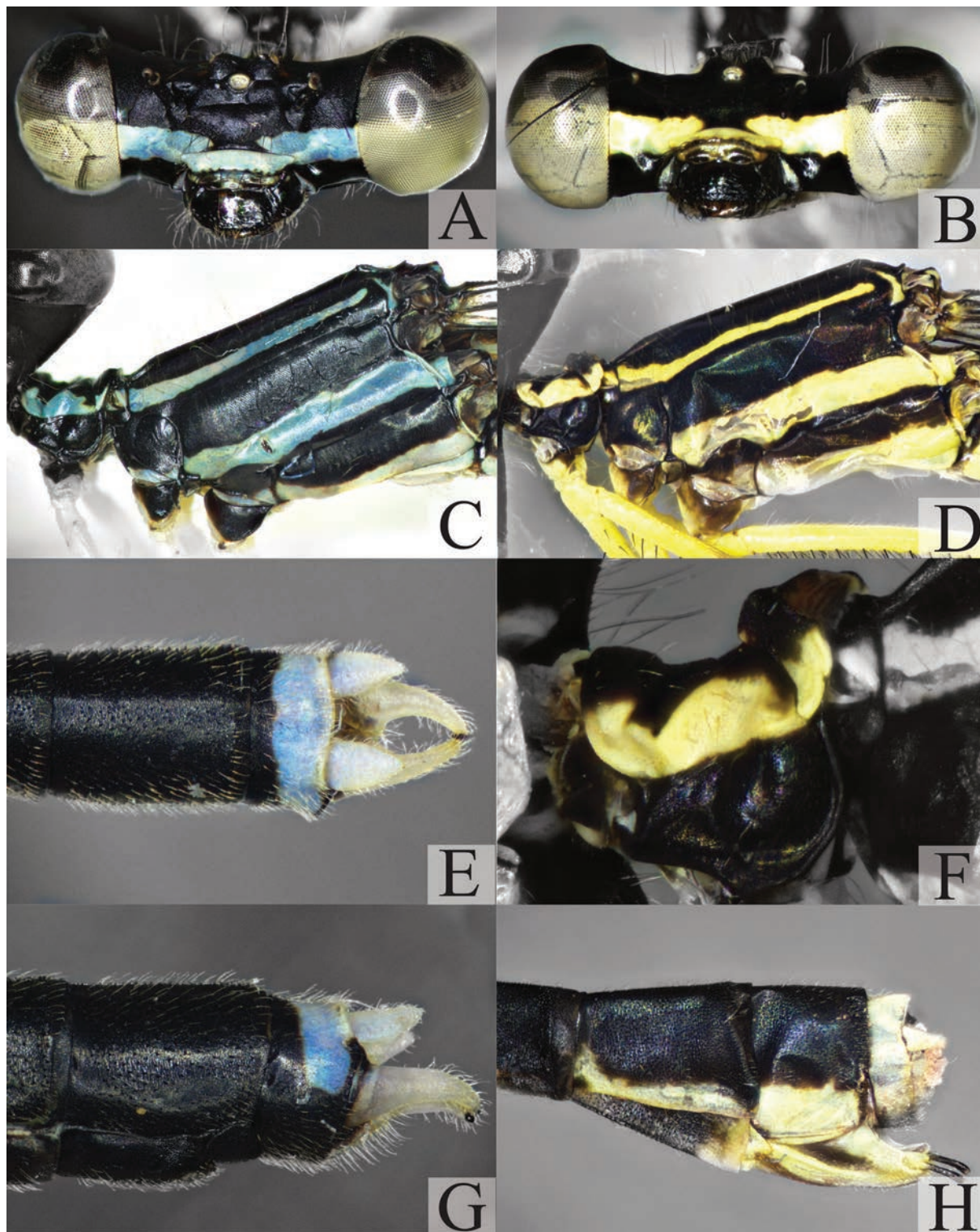
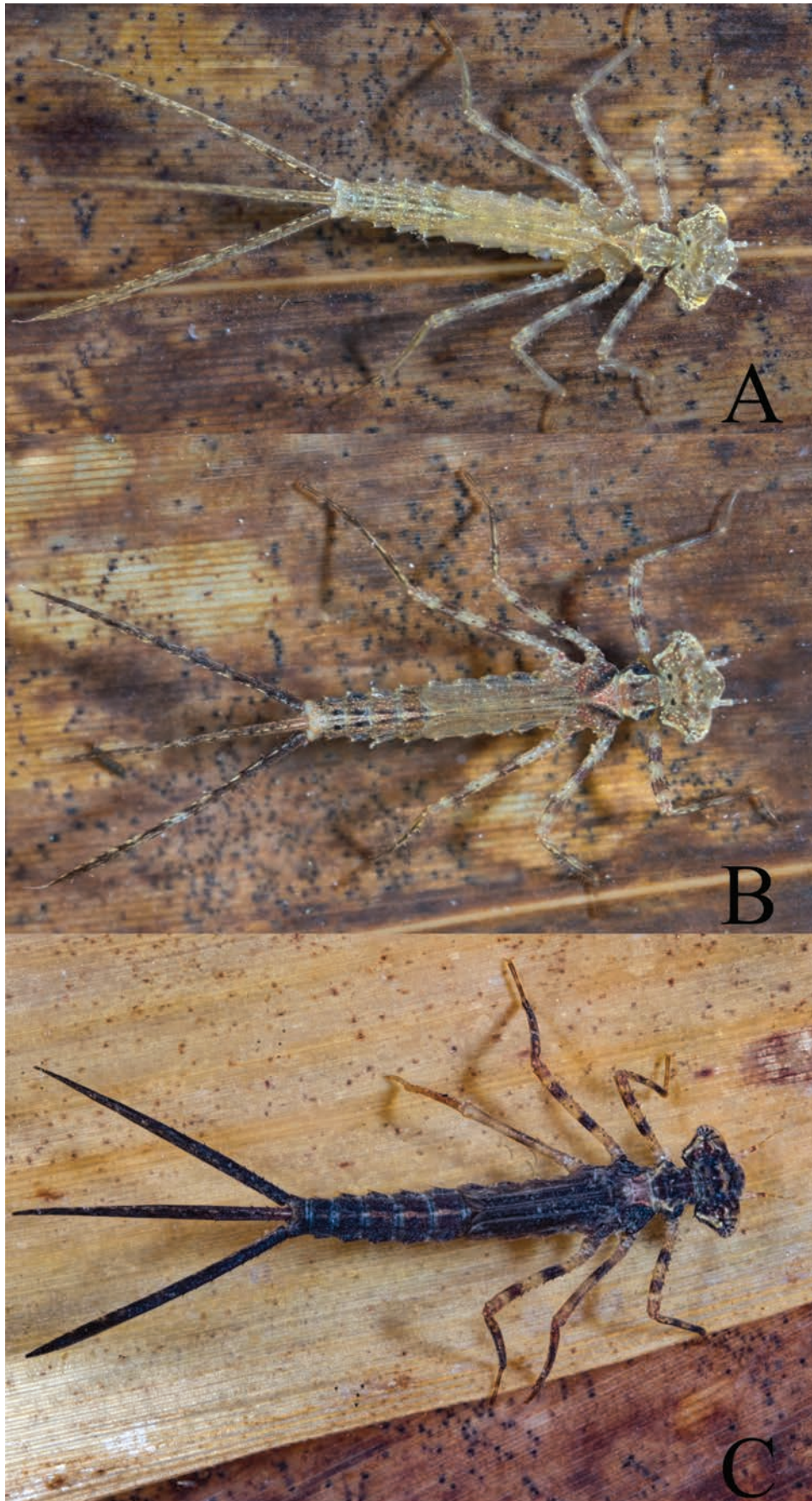


Figure 1. Adult characters of *Platycnemis phasmovolans* A, C, E, G male B, D, F, H female A, B head, frontal view C, D thorax, lateral view E abdominal tip including appendages, dorsal view F posterior pronotal lobe of prothorax in lateral view G–H abdominal tip including appendages, lateral view.

**Description of larva. (based on 1 male (exuviae) and 1 female (F-1))** Habitus (Fig. 2) slender and elongate, long thin legs, abdomen cylindrical, slightly tapered caudad, lamellae of caudal gills with terminal filament at apex; coloration varies from yellowish-brown to bright green brownish to brownish-black.



**Figure 2.** Colour variation of *Platycnemis phasmovolans* larva **A** pale yellowish-brown **B** dark yellowish-brown **C** blackish-brown.

**Head:** broad in dorsal view, roughly a strongly squashed pentagon in outline, with hind margin strongly excavated; bearing scattered simple setae; labrum flattened ventrally, outline with convex corners flanking central anterior concavity, with minute tubercles on distal half and basal glabrous; frons and vertex strongly raised with prominent ocelli; compound eyes narrow and rounded protruding postero-laterally; occiput with dense minute tubercles and scattered simple setae, convex in outline, anterior occiput with low raised prominences just behind margin of eyes (Fig. 3, indicated by red arrows); postocular lobes, rounded, scattered simple setae on anterior margin, with scattered papilliform setae and robust spiniform setae on posterior margin; genae (Figs 3B, 5A) with row of 2–3 blunt stout spines and simple setae on anterolateral margin. Antennae (Fig. 4A) filiform, 7-segmented with A2 the longest, relative length of antennomeres 0.93: 1 (0.4 mm): 0.95: 0.85: 0.58: 0.4: 0.33. Prementum (Fig. 4B) elongate subpentagonal shape, its basal hinge reaching anterior of mid coxae when mask folded; with two pairs of strong premental setae; lateral margin at base of palp with 3–4 distinct spiniform setae; with a row of 16–18 spiniform setae along distal half of lateral margin, with 1 pair long thin simple setae on middle of ventral side (Fig. 4C); ligula (Fig. 4F) strongly produced to form an obtuse angle, the two sides slightly convex; with one pair of short subapical protuberances and minute spiniform setae along margin; lobe of labial palp (Fig. 4D) 0.41 length of prementum with 4 setae on palpal lobe, outer margin with row of short spiniform setae, inner margin with weakly crenate; apex with 2 processes, the outer one truncate, but with a distinctly slanted or curved margin and bearing 5 distinct teeth, the innermost being largest and most isolated; inner process tapered then abruptly narrowed to thin acutely tipped end hook (Fig. 4E); movable hook slender and about 0.60 times as long as palpal lobe, acuminate, bent slightly inwards. Maxilla (Fig. 5B, C) galeolacinia with 7 teeth, 4 dorsal teeth approximately of the same size, apical teeth largest, 3 ventral teeth of small size. Mandible (Fig. 5D–G) with mandibular formula: L 1+1'234 a b/ R 1+1'234 y a, asymmetrical, robust with well-developed long teeth on each incisor lobe; left mandible with five incisor teeth, two molar teeth ( $a = b$ ); right mandible with five incisor teeth, one molar tooth, an additional tooth.

**Thorax:** narrower than head, with scattered simple setae, papilliform setae, and white spots. Prothorax dorsally flattened; lateral angles acute, projecting sharply at postero-lateral corners; posterior margin gently keeled midline, forming subtle ridge across posterior border, rounding at lateral edges. Synthorax robust, slightly elongated; mesepisternum with pronounced lateral keels defining boundary with mesepimeron; keels slightly raised, forming well-defined ridge; dorsal surface of mesepisternum with faint longitudinal ridges, aligned parallel to midline; mesinfraepisternum slightly convex; wing pads pale with glabrous, parallel, anterior and posterior wing pads reaching to distal margin of S6; legs almost flat and long; femora thin with dark band on posterior side, row of spiniform setae and scattered simple setae; tibial comb with scattered setae and a few tridentate setae; two claws simple with pulvilliform empodium.

**Abdomen:** cylindrical, slender, narrowing caudally, scattered simple setae, minute tubercles and white spots; abdominal terga with pale longitudinal line, posterior margin with pair of pale black spots; abdominal sterna smooth; abdominal pleura flattened on S2–S9, with scattered simple setae, and row of spiniform setae and simple setae on lateral margin, lateral spines on abdominal

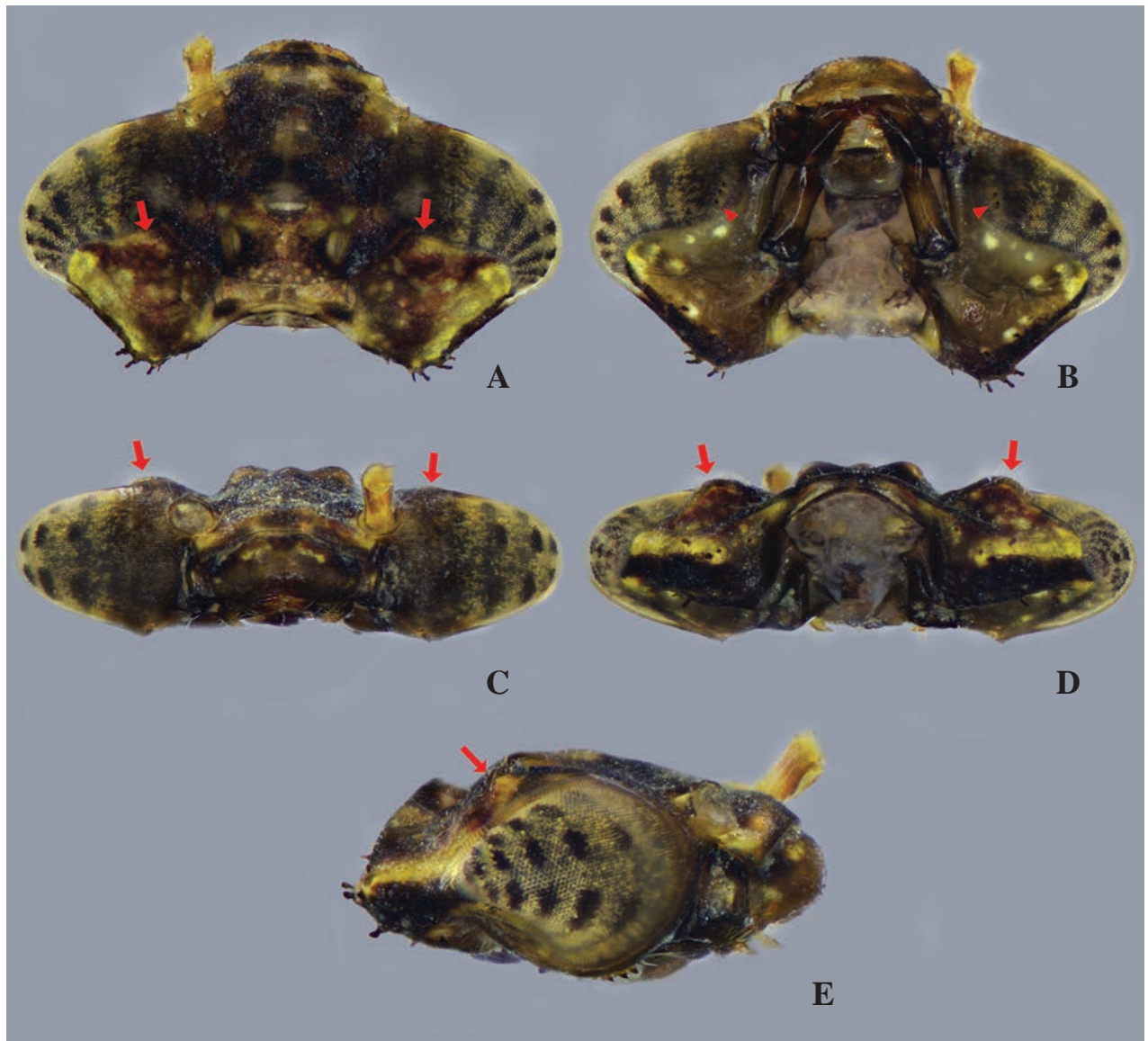


**Figure 3.** Head of *Platycnemis phasmovolans* larva **A** dorsal view **B** ventral view **C** frontal view **D** back view **E** lateral view. Arrow: prominence on occipital margin; triangle: row of spine and setae on genae.

S5–S9 ( $S9 \geq S8 \geq S7 > S6 >> S5$ ) (Fig. 6A). S10 with cluster of spiniform setae externally at the basal of cerci; male gonapophyses (Fig. 6B, C) broad-based, conical, sharply pointed, slightly divergent in ventral view, almost reaching anterior margin of S10, with a row of simple setae on ventral margin; gonopore small, O-shape embossed with median fissure; female gonapophyses (Fig. 6D, E) with two pairs of long valvae; lateral valvae terminating in sharply pointed processes, slightly divergent, with a distinct postmedian ventral spine preceded by row long simple setae on each side, extending over sternite 10; central valvae longer than lateral valvae, smooth, slender, apically rounded. Caudal lamellae (Fig. 7) long and narrow, lanceolate, with irregular light and dark-brown markings, rather sparse spiniform setae and simple setae of variable lengths along margin, median trachea; terminal filament pale and slim; a distinct median trachea with spiniform setae array on both sides, reaching terminal filament; median lamella only slightly shorter and broader than lateral lamella.

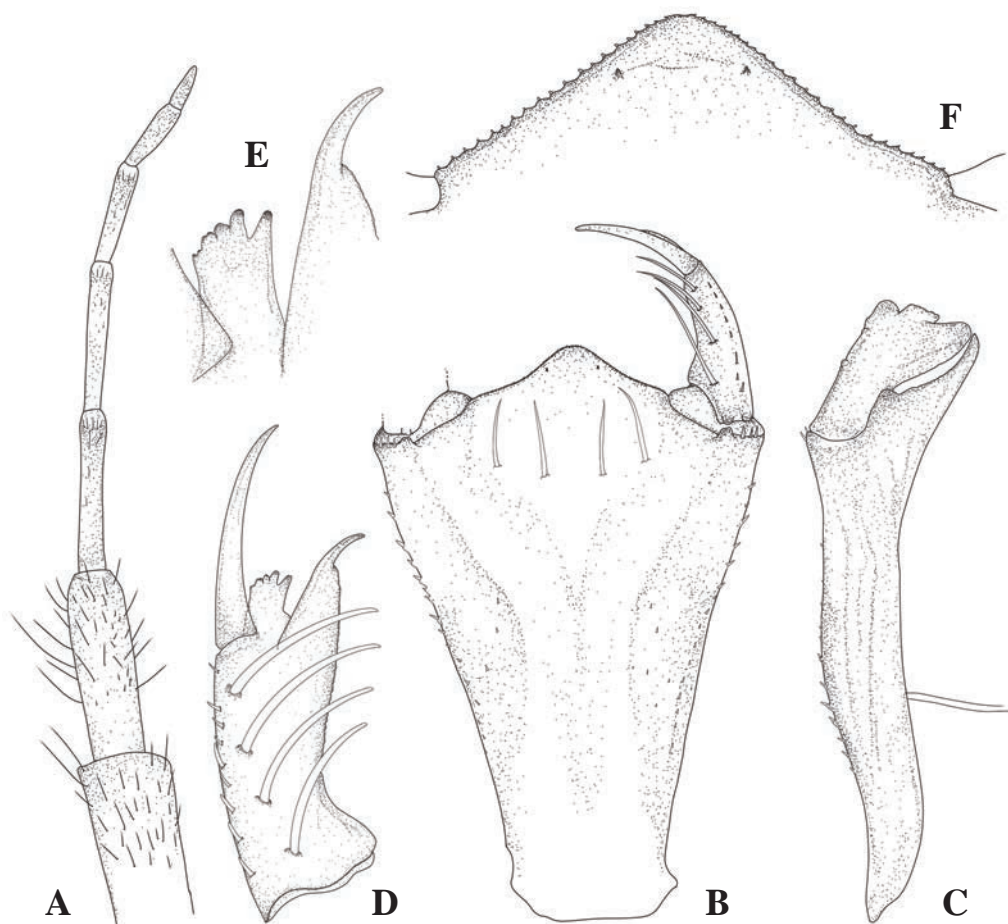


**Figure 4.** Antenna and mouth parts of *Platycnemis phasmovolans* larva **A** left antenna **B** prementum, dorsal view **C** prementum, lateral view **D** left labial palp **E** detail of distal left palpal lobe **F** ligula (median lobe).

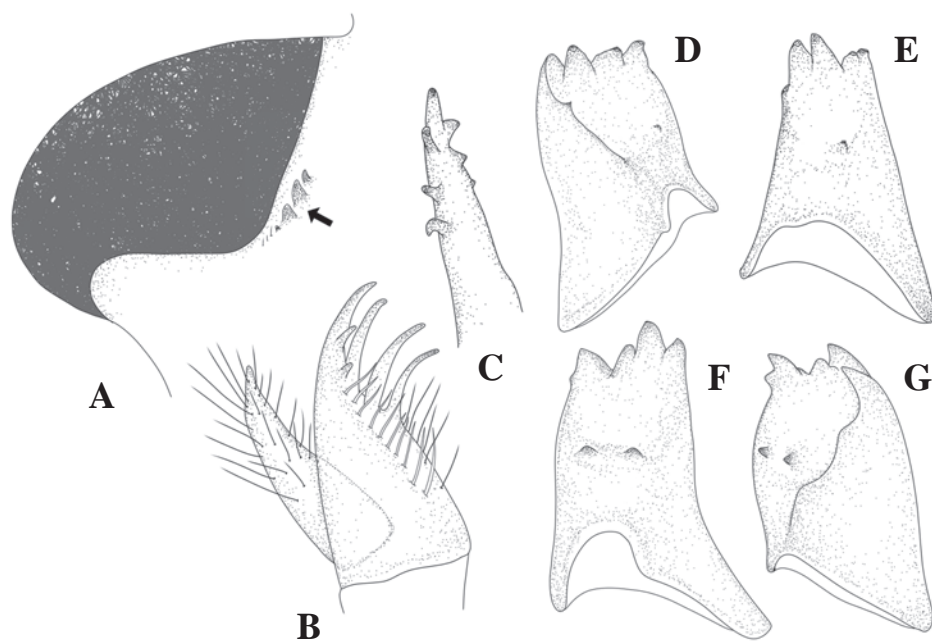


**Figure 5.** Compound eyes and mouth parts of *Platycnemis phasmovolans* larva **A** genae **B** left maxilla, dorsal view **C** left maxilla, lateral view **D** right mandible, ventro-internal view **E** right mandible, internal view **F** left mandible, internal view **G** left mandible, ventro-internal view. Arrow indicates row of spines and setae.

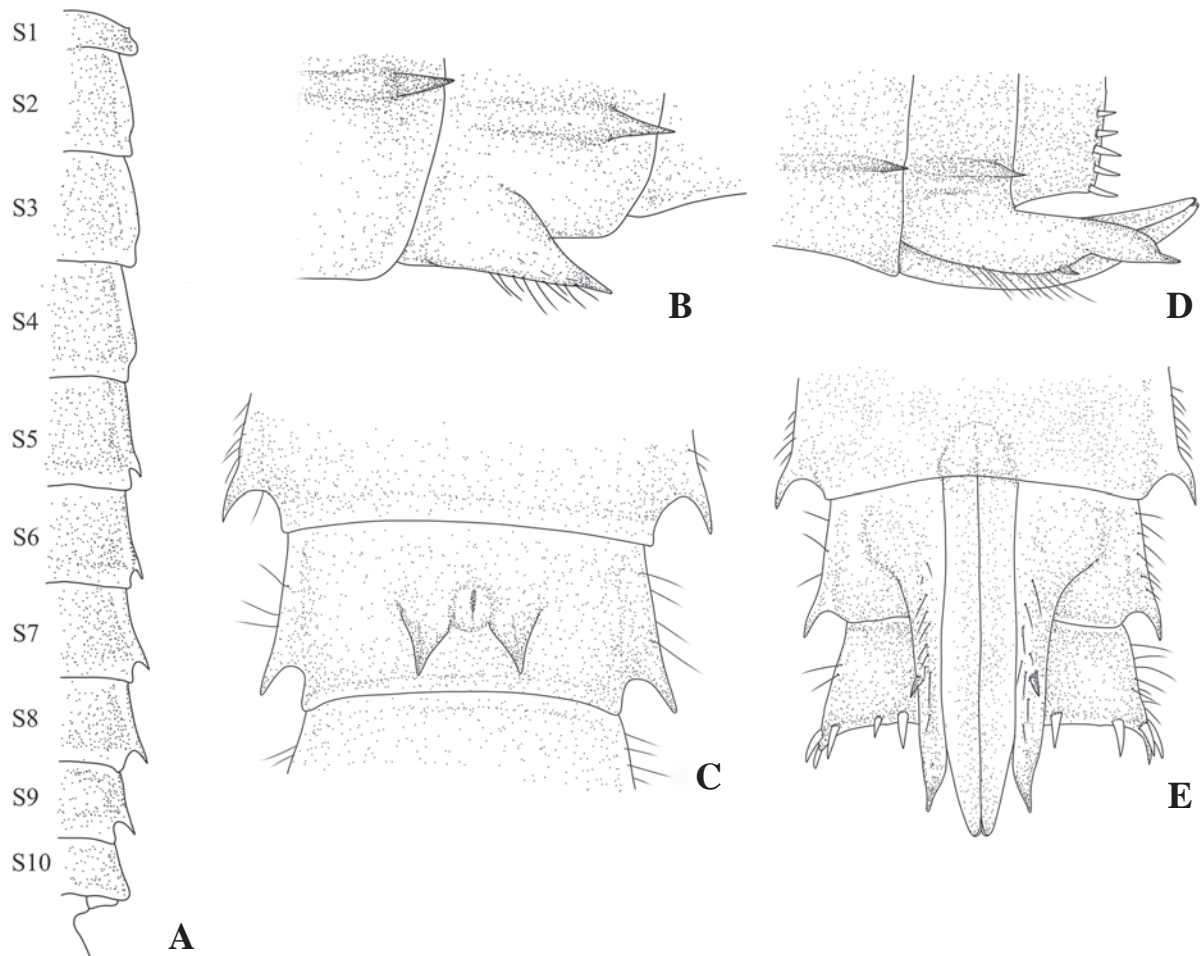


**Figure 6.** Abdomen and gonapophysis of *Platycnemis phasmovolans* larva **A** S1–10, dorsal view **B** male gonapophysis, lateral view **C** male gonapophysis, dorsal view **D** female gonapophysis, lateral view **E** female gonapophysis, dorsal view.



**Figure 7.** Caudal lamellae of *Platycnemis phasmovolans* larva **A** median lamella **B** lateral lamella.

**Material examined (adult).** VIETNAM • 4 ♂♂; 21 May 2024; 18°59'24.4"N, 104°50'17.8"E; elevation 266 m a.s.l.; Yen Khe Commune, Con Cuong District, Nghe An Province; Q.T. Phan leg.; ZCDTU. • 3 ♂♂, 2 ♀♀; 27 Jul. 2024; same site and collector as above.

**Additional observations (adult).** CHINA • 1 ♂ 26–31 May 2020; 25°18'36.0"N, 107°54'00.0"E; Maolan National Nature Reserve, Guizhou, Libo County, Province, Ruibin Song observer.

**Brief description of adult. Male** (Fig. 8A) – **Head:** black with broad bluish transverse stripe across frons and genae, broken in middle above pale blue postclypeus (Fig. 1A). **Thorax:** prothorax black with paired blue lateral markings on pronotum with irregular inner margins; propleuron entirely black (Fig. 1C); synthorax black with narrow blue antehumeral stripes, two distinct lateral stripes: one pale blue on metepisternum, the other tending to very pale blueish-yellow on lower margin of metepimeron (Fig. 1C); fore legs with femora white, except anterior side which is black in the apical third; tibiae and tarsi black; mid and hind legs with femora and tibiae wholly white, tibiae enormously dilated, feather-like, length 2.87 times and 3.22 times maximum width, respectively. **Abdomen:** black with blueish-white pattern: S1 with heart-shaped spot laterally; S2 with narrow stripes along lower margin and 1–2 markings above stripes; S3–6 with basal rings, concave dorsally, smallest on S3 and largest on S6, that on S3 incomplete dorsally; S6 marking one-third length of segment; S7 with ventro-lateral basal marking; S8–9 entirely black; posterior half of S10 dorsum blue to pale yellowish (Fig. 1G); appendages pale, as illustrated (Fig. 1E, G).

**Female** (Fig. 8B, C): As male unless otherwise stated (Fig. 1B, D, F, H): colour pattern blue replaced by yellow tending to white (Fig. 8B, C). Posterior pronotal lobe weakly developed, smooth, without spine. Tibiae not dilated. Abdomen, full stripe on S1, S2–6 the basal bands extend dorsally but do not form complete rings. S7 with on ventro-distal marking, but pale in middle; S8 with complete pale yellow broad ventral border to tergite; S9 broadly pale yellow ventrally, S10 and anal appendages entirely pale (Fig. 1H).

This description agrees almost exactly with Hämäläinen (2003) and hence we may be confident of the identity of the larvae from which specimens were bred.

**Distribution.** Lao PDR: Bolikhamsai Province, Kaew Neua Pass area (Hämäläinen 2003, 2020); Vietnam: Nghe An Province, Yen Khe Commune, Con Cuong District (this study, new record); China: Guizhou Province, Libo County, Maolan National Nature Reserve (Pu et al. 2019; this study); Guangxi Province, Hechi, Jinchengjiang District (Yu 2010; Hämäläinen 2020).

**Habitat and biology.** The larvae of *P. phasmovolans* inhabit forest pools, which are small, shallow bodies of water formed by rainwater or slow-moving streams (Fig. 9). These pools may be temporary or permanent. The larvae secrete themselves among riparian vegetation and leaf litter. The composition of the pool or stream bed where collections were made included silt (30%), small stones/pebbles/gravel/sand (5%), leaf litter (45%), and riparian/root tree debris (20%). The larval coloration acts as camouflage, allowing them to blend perfectly with their surroundings. Black larvae were typically found in dark-brown leaf litter mixed with silt or mud, whereas yellowish/brown larvae were found on riparian roots or brown/yellow leaf litter, such as bamboo leaves. The larvae were found coexisting with the larvae of *Coelliccia* spp., *Copera vittata* (Selys, 1863), and *Copera marginipes* (Rambur, 1842). Adults of *P. phasmovolans* were also observed mating and laying eggs near the larval habitats. The larvae displayed agonistic behaviour (Fig. 10), characterized by the tendency to hold the distal end of the abdomen slightly upturned, while the caudal lamellae were splayed and pointed upwards.



**Figure 8.** Adult habitus **A** male **B** female **C** immature female.

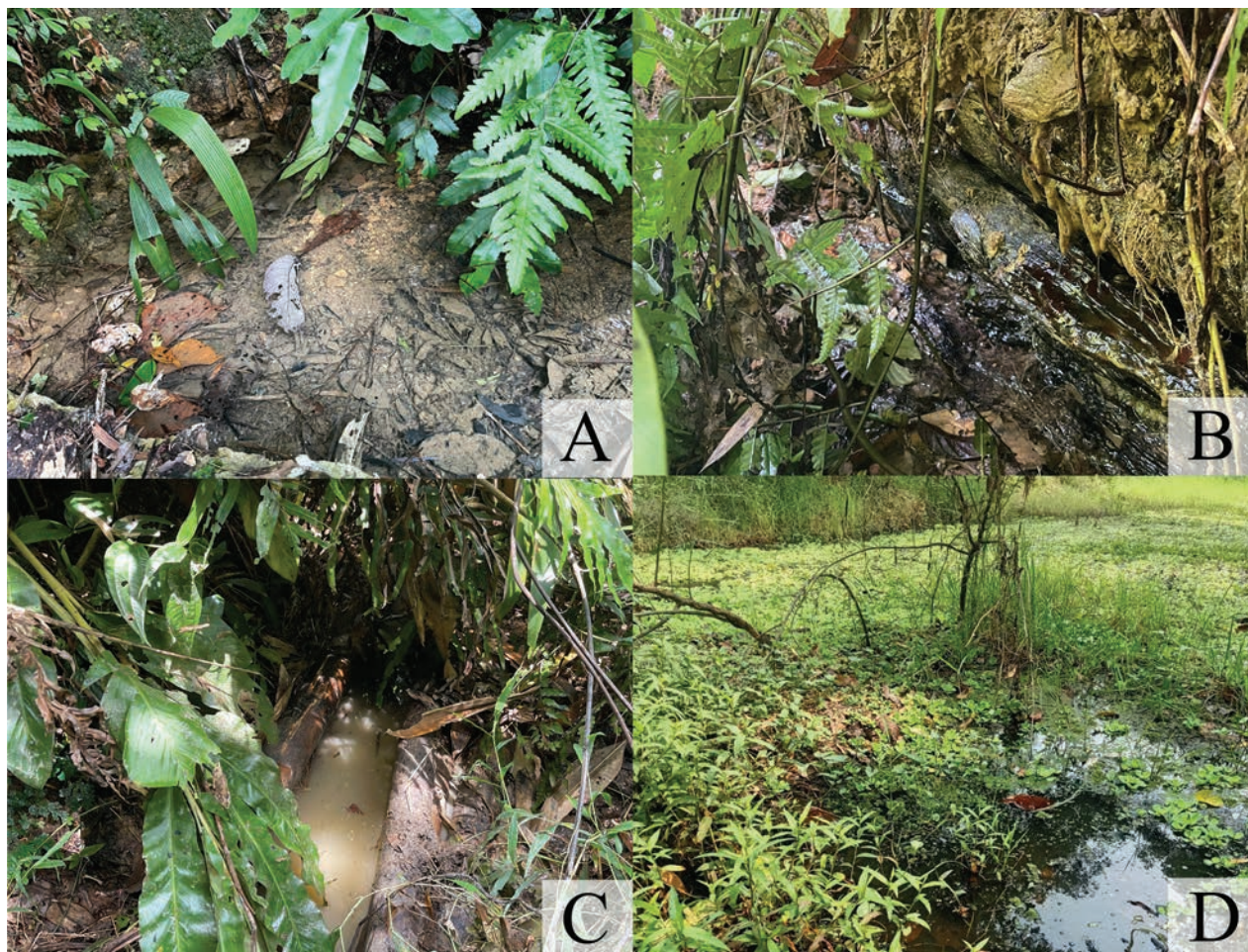


**Figure 9.** Habitat of *Platycnemis phasmovolans* larva **A** small spring-fed pool in forest **B** rainwater drainage path **C** pool in bamboo trunk (man-made) **D** seasonal forest pool

## Discussion

This study presents the first description of the larva of *P. phasmovolans*, bringing the total number of documented larval descriptions for *Platycnemis* species from Asia to four: *P. echigoana* by Eda (1965) and Ishida (1996), *P. phyllopoda* by Bae (2011) and Cho (2021), and *P. sasakii* by Ishida (1996). Given the current taxonomic status of *P. phasmovolans*, it is of interest to determine whether the larval stage shares morphological characteristics that reinforce its classification. Examination of larvae of *P. phasmovolans* and *P. phyllopoda* confirmed both share a weakly developed prominence on the anterior occiput – a feature well-developed in congeneric genera such as *Copera*, *Pseudocopera*, and *Spesbona* Dijkstra, 2013 (Deacon and Samways 2016; Saetung et al. 2020). However, this characteristic has been doubted in European species of *Platycnemis*, as it may often be overlooked.

Asian *Platycnemis* species can be distinguished from their European congeners by the presence of four palpal setae on the labial lobe, as opposed to three setae in European species (Ishida 1996; Brochard et al. 2018; this study). Although the number of palpal setae may vary among members of the family Platycnemididae, there is a notable consistency at the species level within the subfamily Platycnemidinae, typically ranging between three and four setae. The



**Figure 10.** *Platycnemis phasmovolans* larva display agonistic display behaviour.

larvae of *P. phasmovolans* differ markedly from other Asian congeneric species by having lateral spines on abdominal segments S5–9 (S7–9 in *P. echigoana*, *P. phyllopoda*, and *P. sasakii*) and narrow, lanceolate caudal gills (a broader lanceolate shape in *P. echigoana*, *P. phyllopoda*, and *P. sasakii*).

The distribution of *Platycnemis* may be restricted by its preference for specific habitats, such as pristine forests and limestone caves (as observed in China). The species appears to be restricted to regions where such conditions occur (Fig. 11C). *Platycnemis phyllopoda* has the broadest distribution, ranging from the southern subtropical regions of Guilin and Zhejiang in China to the northern temperate zones of Jilin, China, and Primorye, Russia (Zhang 2019; Kosterin 2020; iNaturalist 2024d). Regarding *P. hummeli* and *P. ulmifolia*, a thorough examination of the type specimens is necessary to assess whether they are valid synonyms of *P. phyllopoda*. Asahina (1949) originally proposed their synonymy based on observed morphological characters; however, this conclusion was reached without direct examination of the type specimens. Revisiting these types could yield important insights, allowing for verification of Asahina's taxonomic placement. In contrast, three other species have more restricted ranges: *P. foliacea* occurs in the temperate zone of Beijing and subtropical areas of Xi'an and Shanghai in China (Zhang 2019; Hämäläinen 2021; iNaturalist 2024b), while *P. echigoana* and *P. sasakii* are endemic to Japan (Ishida 1996; Hämäläinen 2021; iNaturalist 2024a, 2024e).

Recent records have expanded the known distribution of *P. phasmovolans* to Vietnam, approximately 80 km from the type locality in Laos (Fig.

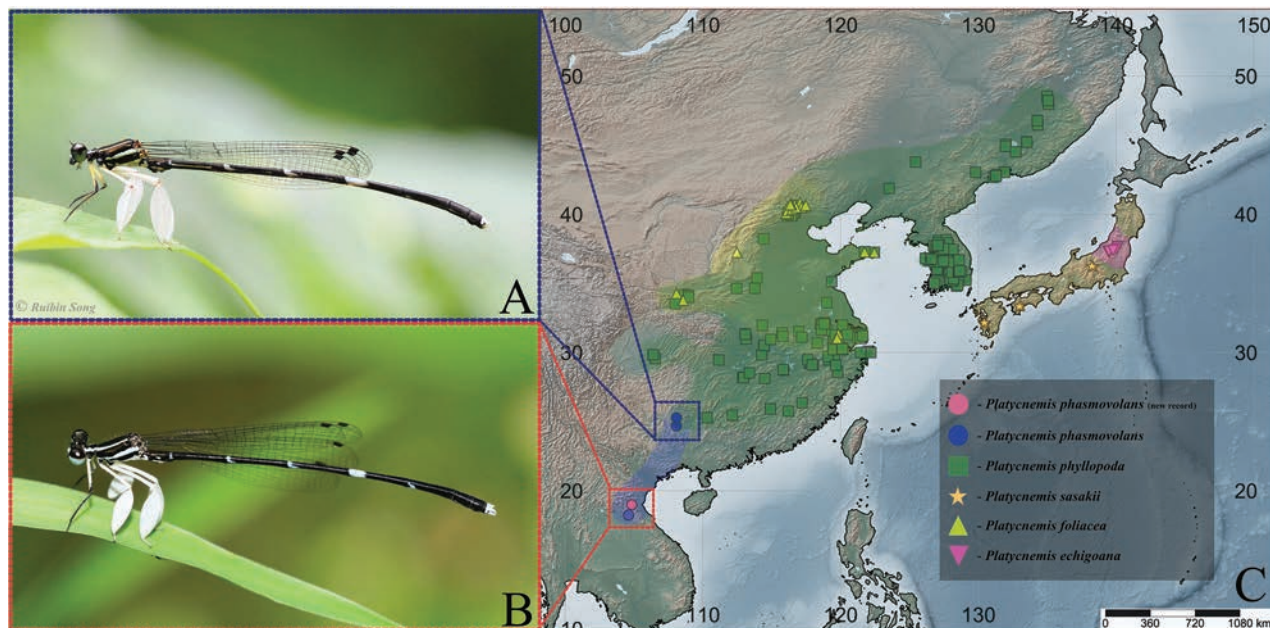


**Figure 11.** **A** adult *Platycnemis phasmovolans* male from Guizhou Province of China, photo by Rubin Song **B** adult *P. phasmovolans* male from Nghe An Province of Veitnam, photo by Phan Quoc Toan **C** distribution map of genus *Platycnemis*.

11). This finding suggests a broader range within the region, which aligns with previous predictions about the potential distribution of *P. phasmovolans* (Hämäläinen 2003, 2020). On the other hand, there are two earlier records from China (Pu et al. 2019; Hämäläinen 2020). The type locality is located c. 600 km from Nanning and c. 800 km from Maolan (Fig. 11C), raising questions about whether the specimens really are identical to *P. phasmovolans* and necessitating the collection of voucher specimens to confirm their taxonomic status. The Vietnamese and Chinese populations vary in four ways (Chinese population in parentheses): broad stripe on mesepisternum (narrow); presence of white femur on fore legs (pale yellow); marking on S6 0.35 times as long as S6 length (0.40); and presence of distinct baso-ventral stripe on S7 (ambiguous) (Fig. 11A, B). This study does not attempt to resolve the taxonomic uncertainties surrounding *Platycnemis* but aims to provide data and hypotheses that may support future analyses. The comparisons made here may offer insights into the evolutionary position of *Platycnemis* within its genus based on larval characteristics.

Currently, data on *P. phasmovolans* is significantly lacking, leading to its classification as “Data Deficient” by the IUCN (Hämäläinen 2011). GBIF (2024) provides information on the type material only. There are no records of *P. phasmovolans* available in iNaturalist (2024c), which moreover includes a misidentified photograph without any information about the source. Given these discrepancies and the possibility of undiscovered populations, intensive surveys in unexplored areas, particularly in northern Vietnam, the upper parts of Laos, and southern to southwestern China, are highly recommended. Such efforts are crucial to developing a comprehensive understanding of the distribution and ecological requirements of *P. phasmovolans* and its congeneric species across the Sino-Japanese and Indo-China regions.

## Key to the known larvae of Platycnemidinae in the Sino-Japanese and Oriental regions

The subfamily Platycnemidinae in the Sino-Japanese and Oriental regions includes 16 species in two tribes: Coperini (*Copera*, 5 species) and Platycnemidini (*Matticnemis*, 1 species; *Platycnemis*, 6 species; and *Pseudocopera*, 4 species) (Ishida 1996; Zhang 2019; Saetung et al. 2020; Kalkman et al. 2020; Cho 2021; Dow et al. 2024). The larvae of 10 species have been described based on studies by Eda (1965), Ishida (1996), Yum and Bae (2007), Bae (2011), Saetung et al. (2020), Cho (2021), and this study. This subfamily is recognized by the presence of raised prominences on the occipital margins behind the eyes and the presence of two pairs of premental setae.

- 1 Caudal lamellae with frilled borders.....**2 (Coperini: *Copera*)**
  - Caudal lamellae with elongate and smooth borders .....**4 (Platycnemidini)**
- 2 Number of fringe filaments less than 20; short, fringe filaments stout basally; sometimes poorly fimbriated.....***C. chantaburii*** [Indochina region]
  - Number of fringe filaments more than 20; long, fringe filaments stout or narrow basally .....**3**
- 3 Slender, fringe filaments stout basally; spiky, jagged appearance (Fig. 12A)..... ***C. marginipes*** [Oriental region]
  - Hair-like, slightly curved fringes, very narrow basally; wavy appearance (Fig. 12B)..... ***C. vittata*** [Oriental region]
- 4 Palpal lobe with three palpal setae; moderately produced ligula; well-developed protuberance on occipital margin; body shorter than 1.3 × length of caudal gills ..... **5 (*Pseudocopera*)**
  - Palpal lobe with four palpal setae; strongly produced ligula; poorly-developed protuberance on occipital margin; body at least as long as 1.5 × length of caudal lamellae..... **7 (*Platycnemis*)**
- 5 S8–9 without lateral spines ..... ***Ps. rubripes*** [Sino-Japan region]
  - S8–9 or S9 with lateral spines ..... **6**
- 6 Caudal lamellae length longer than 0.8× body length; with one pair seta on the terminal filament of the caudal lamellae; with lateral spine on S9 ..... ***Ps. ciliata*** [Oriental region]
  - Caudal lamellae length shorter than 0.8× body length; without one pair seta on the terminal filament of the caudal lamellae; with lateral spine on S8–9 ..... ***Ps. annulata*** [Sino-Japan region]
- 7 S5–9 with lateral spines ..... ***Pl. phasmovolans*** [Indochina region]
  - S7–9 with lateral spines ..... **8**
- 8 Postocular lobe rounded; shallow posterior lobes..... ***Pl. sasakii*** [Sino-Japan region]
  - Postocular lobe angulated; deep posterior lobes..... **9**
- 9 Ligula with small median cleft; terminal filaments on apex of caudal gills long..... ***Pl. echigoana*** [Sino-Japan region]
  - Ligula without median cleft; terminal filaments of caudal gills short or absent..... ***Pl. phyllopoda*** [Sino-Japan region]



Figure 12. Caudal gills of *Copera* spp. **A** *C. marginipes* **B** *C. vittata*.

### Acknowledgements

The authors express their gratitude to the editor (Jan van Tol) and referees, including Albert G. Orr, and Matti Hämäläinen for their valuable feedback and insightful suggestions. We also thank Ruibin Song for providing crucial information on the distribution and reference photos of *Platycnemis phasmovolans* from China. Special thanks are extended to Nguyen Tu Minh Hoang for his assistance with photography during the field trip. Our appreciation also goes to

Ho Viet Hieu and Nguyen Huy Hung (Duy Tan University) for supplying mosquito to larvae. Lastly, we are deeply grateful to Akihiko Sasamoto, Xin Yu, Sungbin Cho, and Guo-Hui Yang for their invaluable suggestions on genus *Platycnemis*.

## Additional information

### Conflict of interest

The authors have declared that no competing interests exist.

### Ethical statement

No ethical statement was reported.

### Funding

This study received partial support from the International Dragonfly Fund through the second author.

### Author contributions

Conceptualization: TSK, QTP. Investigation: QTP, TSK. Methodology: QTP, TSK. Project administration: QTP. Resources: TSK. Visualization: QTP. Writing – original draft: TSK, QTP. Writing – review and editing: TSK, QTP.

### Author ORCIDs

Tosaphol Saetung Keetapithchayakul  <https://orcid.org/0000-0001-7565-4701>

Quoc Toan Phan  <https://orcid.org/0000-0002-3154-6546>

### Data availability

All of the data that support the findings of this study are available in the main text.

## References

- Asahina S (1949) Odonata from Shansi province (North China). *Mushi* 20 (2): 27–36. [2 pls. excl]
- Bae YJ (2011) *Insect Fauna of Korea: Damselflies*, vol. 6 no. 1. National Institute of Biological Resources, Incheon.
- Brochard C, Chelmick D, Dufour C, Litman J, Martens A, Monnerat C, Reichen-Robert A-E, Robert A, Robert D, Vanappelghem C, Walter B, Wildermuth H (2018) Les larves de libellules de Paul-André Robert / Die Libellenlarven von Paul-André Robert: L'Oeuvre d'une vie / sein Lebenswerk. KNNV Publishing, Neues Museum Biel, 320 pp.
- Cho S (2021) *Korean Odonata adult and larva*. Gwangil Publishing Co, Gyeonggi, 404 pp.
- Deacon C, Samways MJ (2016) Larva of one of the world's rarest and most threatened damselflies: *Spesbona angusta* (Odonata: Platycnemididae). *Odonatologica* 45(3/4): 225–234. <https://doi.org/10.5281/zenodo.163450>
- Dijkstra K-DB, Kalkman VJ, Dow RA, Stokvis FR, Van Tol J (2014) Redefining the damselfly families: a comprehensive molecular phylogeny of Zygoptera (Odonata). *Systematic Entomology* 39(1): 68–96. <https://doi.org/10.1111/syen.12035>
- Dow RA, Choong CY, Grinang J, Lupiyaningdyah P, Ngiam RWJ, Kalkman VJ (2024) Checklist of the Odonata (Insecta) of Sundaland and Wallacea (Malaysia, Singapore, Brunei, Indonesia and Timor Leste). *Zootaxa* 5460(1): 1–122. <https://doi.org/10.11646/zootaxa.5460.1.1>

- Eda S (1965) Description of the larval stage and oviposition behavior of *Platycnemis echigoana* Asahina (Odonata). *New Entomologist* 14(5): 1–5.
- GBIF (2024) *Platycnemis phasmovolans* Hämäläinen, 2003. <https://www.gbif.org/species/1423896> [accessed 20 August 2024]
- Hämäläinen M (2003) *Platycnemis phasmovolans* sp. nov. – an extraordinary damselfly from Laos with notes on its East Asian congeners (Odonata: Platycnemididae). *Tombo, Matsumoto* 46 (1/4): 1–7.
- Hämäläinen M (2011) *Platycnemis phasmovolans*. The IUCN Red List of Threatened Species 2011: e.T190911A8840307. <https://doi.org/10.2305/IUCN.UK.2011-2.RLTS.T190911A8840307.en> [accessed 04 September 2024]
- Hämäläinen M (2020) A memorable encounter with *Platycnemis phasmovolans*, the ‘Flying Phantom Featherleg’ in Laos. *Agrion* 24(2): 84–88.
- Hämäläinen M (2021) *Platycnemis sasakii* Asahina, 1949 – a distinct species, endemic to Japan (Odonata: Platycnemididae). *Odonatologica* 50(3/4): 251–260. <https://doi.org/10.60024/zenodo.5703209>
- iNaturalist (2024a) *Platycnemis echigoana*. <https://www.inaturalist.org/taxa/358449-Platycnemis-echigoana> [accessed 20 August 2024]
- iNaturalist (2024b) *Platycnemis foliacea*. <https://www.inaturalist.org/taxa/358445-Platycnemis-foliacea> [accessed 20 August 2024]
- iNaturalist (2024c) *Platycnemis phasmovolans*. <https://www.inaturalist.org/taxa/149651-Platycnemis-phasmovolans> [accessed 20 August 2024]
- iNaturalist (2024d) *Platycnemis phyllopoda*. <https://www.inaturalist.org/taxa/325402-Platycnemis-phyllopoda> [accessed 20 August 2024]
- iNaturalist (2024e) *Platycnemis sasakii*. <https://www.inaturalist.org/taxa/1350922-Platycnemis-sasakii> [accessed 20 August 2024]
- Ishida K (1996) Monograph of Odonata larvae in Japan. Hokkaido University Press, Sapporo, 446 pp.
- Kalkman VJ, Babu R, Bedjanić M, Conniff K, Gyeltshen T, Khan MK, Subramanian KA, Zia A, Orr AG (2020) Checklist of the dragonflies and damselflies (Insecta: Odonata) of Bangladesh, Bhutan, India, Nepal, Pakistan and Sri Lanka. *Zootaxa* 4849(1): 1–84. <https://doi.org/10.11646/zootaxa.4849.1.1>
- Keetapithchayakul TS, Makbun N, Phan QT, Danaisawatdi P, Wongkamhaeng K (2022) Description of the larva of *Indocnemis orang* (Förster in Laidlaw, 1907) (Odonata: Platycnemididae: Calicnemiinae) from Thailand, with larval key to the known genera of the family Platycnemididae in Asia. *Zootaxa* 5134(4): 504–520. <https://doi.org/10.11646/zootaxa.5134.4.2>
- Kosterin OE (2020) *Platycnemis phyllopoda*. The IUCN Red List of Threatened Species 2020: e.T138183537A142390901. <https://doi.org/10.2305/IUCN.UK.2020-1.RLTS.T138183537A142390901.en> [accessed 04 September 2024]
- Orr AG, Dow RA (2015) Description of the final stadium larvae of *Onychargia atrociana* Selys, 1865 from Sarawak, identified using DNA barcoding (Odonata: Zygoptera: Platycnemididae), with an overview of larval characters in the Platycnemididae. *Zootaxa* 4040(3): 384–392. <https://doi.org/10.11646/zootaxa.4040.3.9>
- Paulson D, Schorr M, Abbott J, Bota-Sierra C, Deliry C, Dijkstra K-D, Lozano F (2024) World Odonata List. OdonataCentral, University of Alabama. <https://www.odonata-central.org/app/#/wol/> [accessed: 26 October 2024]
- Pu X, Lan H, Yu X (2019) A new record species of the genus *Platycnemis* Burmeister from China. *Journal of Chongqing Normal University (Natural Science)* 36(4): 36–39.

- Saetung T, Makbun N, Sartori M, Boonsoong B (2020) The subfamily Platycnemidinae (Zygoptera: Platycnemididae) in Thailand, with description of the final stadium larva of *Copera chantaburii* Asahina, 1984. *International Journal of Odonatology* 23(12): 1–19. <https://doi.org/10.1080/13887890.2020.1755377>
- Watson MC (1956) The utilization of mandibular armature in taxonomic studies of anisopterous nymphs. *Transactions of the American Entomological Society* 81: 155–202.
- Yu X (2010) Odonata Research. <https://www.chinaodonata.top/list/leaf/725.html?lang=en> [accessed: 26 October 2024]
- Yum JW, Bae YJ (2007) Description of the larva of *Copera tokyoensis* Asahina (Insecta: Odonata: Platycnemididae) from Korea. *Korean Journal of Systematic Zoology* 23(1): 87–89. <https://doi.org/10.5635/KJSZ.2007.23.1.087>
- Zhang H-m (2019) *Dragonflies and damselflies of China*. Vols. 1 and 2. Chongqing University Press, Chongqing, China, 14 + 1460 pp. [Bilingual, in Chinese and English]

# Moth flies (Diptera, Psychodidae) of Estonia

Jozef Oboňa<sup>1</sup>, Olavi Kurina<sup>2</sup>, Ilmar Süda<sup>3</sup>, Jan Ježek<sup>4</sup>

<sup>1</sup> Department of Ecology, Faculty of Humanities and Natural Sciences, University of Prešov, 17. novembra 1, SK – 081 16 Prešov, Slovakia

<sup>2</sup> Institute of Agricultural and Environmental Sciences, Estonian University of Life Sciences, Kreutzwaldi st 5-D, 51006 Tartu, Estonia

<sup>3</sup> Ilmar Süda FIE, Rõõmu tee 12-5, 50705 Tartu, Estonia

<sup>4</sup> Department of Entomology, National Museum, Cirkusová 1740, CZ – 193 00, Praha 9 – Horní Počernice, Czech Republic

Corresponding author: Olavi Kurina ([olavi.kurina@emu.ee](mailto:olavi.kurina@emu.ee))

## Abstract

A fundamental prerequisite for understanding and protecting biodiversity is the construction of a high-quality faunal database. The primary objective of this study was to address knowledge gaps in the biodiversity of the family Psychodidae in Estonia. Faunistic data on 45 species of moth flies (Diptera: Psychodidae) from Estonia are presented, including 30 new country-records. Sixteen species are considered important for nature conservation. An updated checklist of the family, comprising 71 species, is provided for the Baltic countries. Habitus photographs of selected Estonian species are also included.

**Key words:** Baltic countries, biodiversity, checklist, new records, Palaearctic Region, Psychodinae, Sycoracinae, Trichomyiinae

## Introduction

The moth flies (Diptera: Psychodidae) are relatively well-represented in the Palaearctic Region, with nearly 800 known species (e.g., Wagner 1990, 2018; Evenhuis et al. 2007; Salmela et al. 2014). Although, the Baltic countries belong to an area where the biodiversity of the family Psychodidae has only been superficially studied. According to Pakalniškis et al. (2006), 41 species are known in Lithuania, while Latvia, on the other hand, remains almost entirely unexplored, with only one species recorded (Salmela and Vartija 2007). Likely due to their small size and the absence of a local specialist, the moth flies were largely excluded from earlier faunistic studies in Estonia. Only Remm (1956) named *Psychoda phalaenoides* (Linnaeus, 1758) as occurring in Estonia. The first and, so far, the only list of species was published by Salmela and Piirainen (2005) for Viidumäe Nature Reserve in the Island of Saaremaa. They described a new species – *Lepimormia hemiboreale* Salmela & Piirainen, 2005 – and listed 14 additional species.

A large amount of moth fly material from various research projects has accumulated in the authors' possession over recent years. The aim of this study is to provide data on newly determined material, along with earlier published data on Estonian Psychodidae. Moreover, the list of moth flies of Baltic countries is presented.



Academic editor: Vladimir Blagoderov

Received: 27 January 2024

Accepted: 8 November 2024

Published: 10 December 2024

ZooBank: <https://zoobank.org/8CD66EA6-A8F1-46EA-9E85-D383F92BACDB>

Citation: Oboňa J, Kurina O, Süda I, Ježek J (2024) Moth flies (Diptera, Psychodidae) of Estonia. ZooKeys 1221: 19–50. <https://doi.org/10.3897/zookeys.1221.119716>

Copyright: © Jozef Oboňa et al.  
This is an open access article distributed under terms of the Creative Commons Attribution License (Attribution 4.0 International – CC BY 4.0).

## Materials and methods

A large proportion of the material was collected from forest habitats using trunk window traps (Fig. 1A, B; abbreviated as TWT; for details see Süda (2009) and Sammet et al. (2016)). Additional material was collected using Malaise traps (Fig. 1C, D; abbreviated as MT; for details see Takkis et al. (2018) and Šikora et al. (2020)). A few specimens were collected by sweep netting or handpicking. The material was collected into ethylene or propylene glycol (in the case of TWT) or ethyl alcohol (in the case of MT, sweep netting, and handpicking). In total, material was collected from 45 localities throughout the country (Fig. 2). However, individual localities may assemble several nearby collecting spots, thus, exact geographical coordinates are provided for each sample in the studied material paragraphs.

Samples from all collection methods were sorted to order and family level prior to this study. The sorted Psychodidae specimens were stored in 70% ethyl alcohol, and the majority were identified directly under a stereomicroscope without slide-mounting. Specimens of particular interest that required detailed study were mounted on microscope slides with the following procedure: the specimens were cleared (diaphanized) using chloralphenol and subsequently treated in xylol. Cleared specimens were mounted on microscope slides using Canada balsam as the mounting media. Most of the samples were identified by the first author and were then deposited in the Insect Collection of the Institute of Agricultural and Environmental Sciences, Estonian University of Life Sciences, Tartu, Estonia (**IZBE**). Otherwise, several specimens marked with INS (= Inventory Slide Number of the family Psychodidae; see Tkoč et al. 2014) were identified by the last author. This material is deposited in the National Museum, Prague, Czech Republic (**NMPC**). Habitus photographs of selected Estonian species were compiled using LAS X software from multiple gradually focused images taken in alcohol medium by a Leica K5C camera attached to a Leica 205C stereomicroscope (see also Kjærandsen et al. 2022).

The following identification keys were used: Vaillant (1971–1983); Szabó (1983); Withers (1989a, b) and numerous unnamed original papers with descriptions of new species (e.g., Ježek 1977, 1983, 1984, 1985, 1990). The nomenclature is modified from Vaillant (1971–1983) and Wagner (1990, 2018) using the classifications of Ježek and van Harten (2005, 2009), Ježek (2007), Omelková and Ježek (2012a), Oboňa and Ježek (2014), Kvitte (2014), and Kroča and Ježek (2015, 2019, 2022). The following list of species was formatted based on similar lists from other European countries such as Ježek (2005), Oboňa and Ježek (2014), and Ježek et al. (2008, 2019, 2021b).

## List of species

In the following list of species, the examined material is organized by counties from west to east and from north to south. The paragraph of the examined material is arranged as follows: county (highlighted in bold and not repeated for each sample), sample (male or/and female, without duplicates), collecting locality, geographical coordinates, collecting time range, collecting method (in case of TWT, followed by substrate tree species), collector, and INS (if material is deposited in the National Museum, Prague).

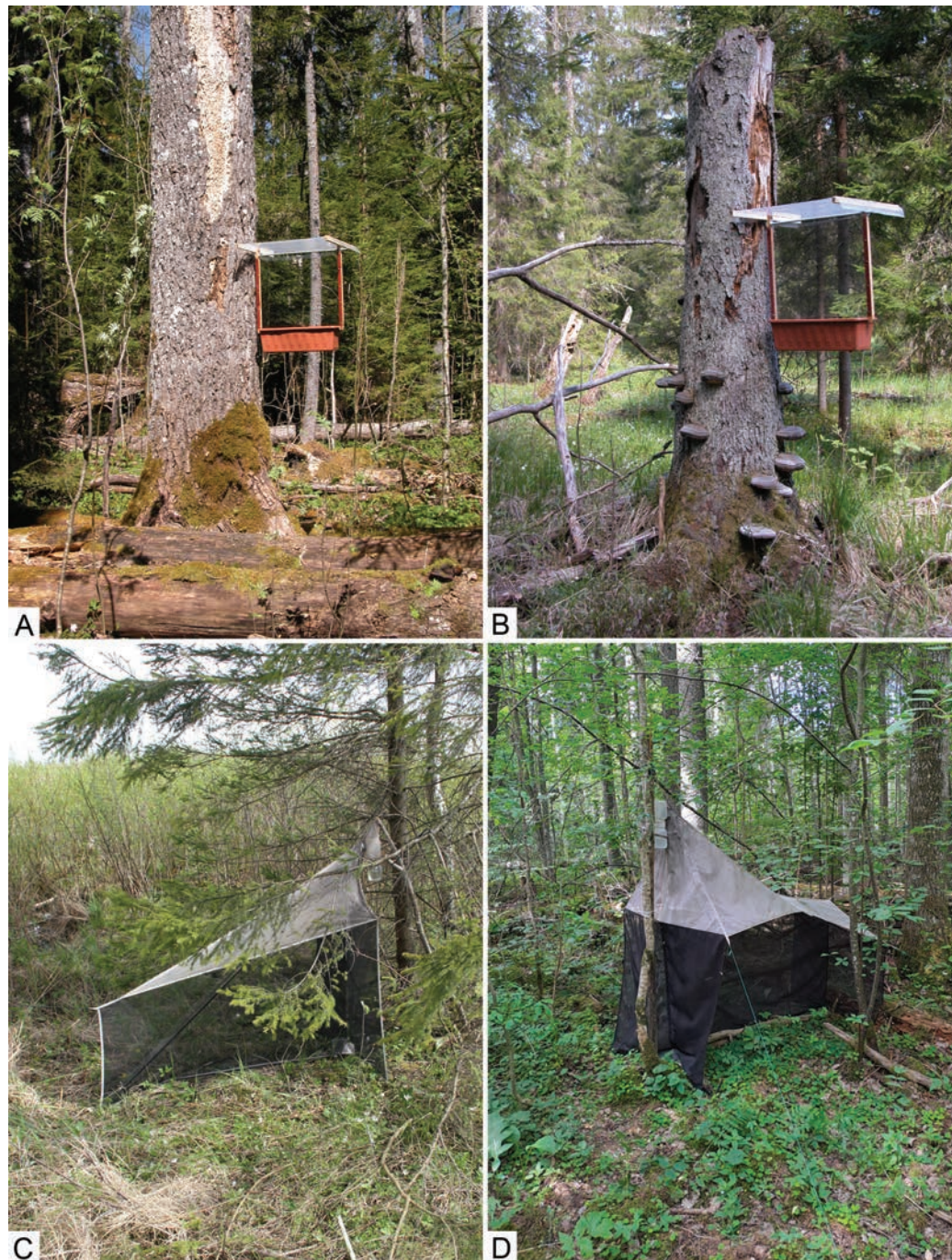


**Figure 1.** Collecting localities and the types of traps used **A** trunk window trap in Kalita NR (58°04'15"N, 24°51'37"E) **B** trunk window trap in Lahemaa NP (59°28'48"N, 25°54'24"E) **C** malaise trap near Lasila (forest patch No 75; 59°16'49.3"N, 26°13'05.2"E) **D** malaise trap in Vorbuse, Lokaatorite tee (58°25'27"N, 26°35'47"E). Photographs by IS (**A, B**), and OK (**C, D**).

The following abbreviations are used in the text: **LCA** – Limited conservation area, **MT** – Malaise trap, **NP** – Nature Park, **NR** – Nature Reserve, **PL** – Protected landscape, **TWT** – trunk window trap, ♂ – male, ♀ – female, **IS leg.** – Ilmar Sūda leg., **OK leg.** – Olavi Kurina and Co. leg. An asterisk (\*) before the species name indicates a new geographical record for Estonia.

The rarity level of each species (common, sporadically common, rare, etc.) is based on data from earlier literature, known distribution, and the abundance/frequency of the species across multiple studies. Literature sources for these

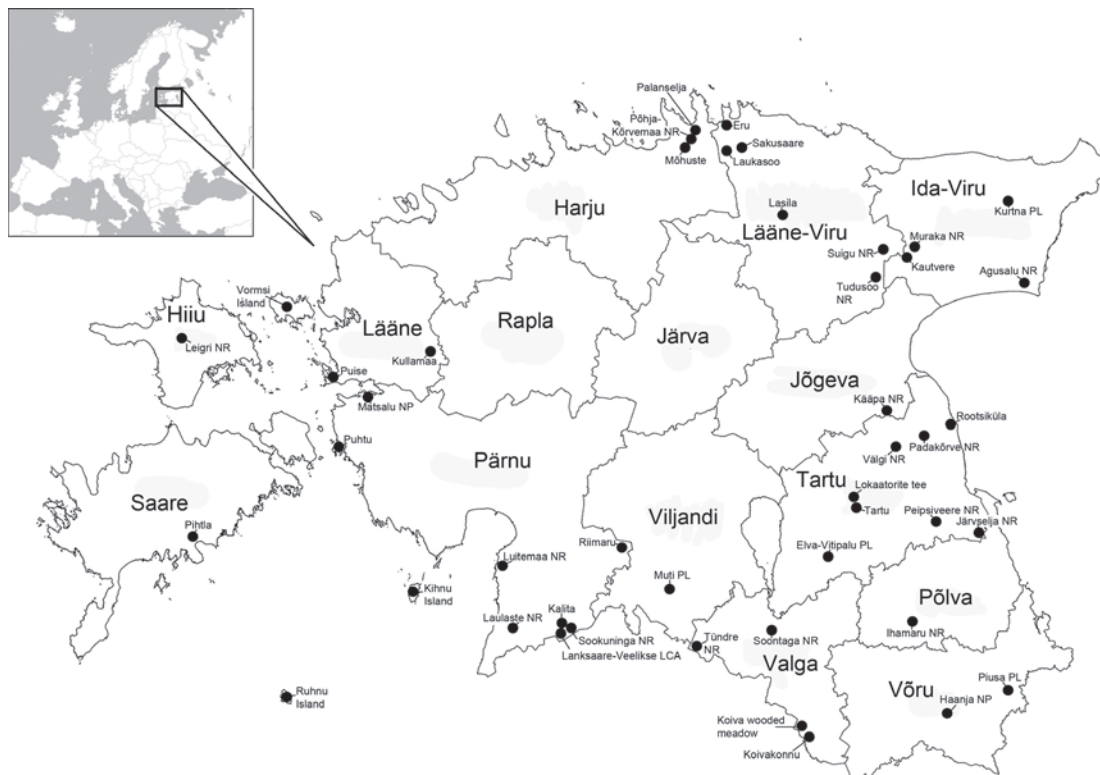


**Figure 2.** Map of Estonia showing counties (large font) and collection localities (small font). Retrieved and modified from <https://geoportaal.maaamet.ee/eng/Spatial-Data/Administrative-and-Settlement-Division-p312.html> (accessed 12 January 2024).

assessments are provided separately for each species. Species deemed important for nature conservation are those that are considered for conservation potential/status in other European countries (e.g., Ježek and Omelková 2012; Oboňa and Ježek 2014; Kroča and Ježek 2015, 2019, 2022; Ježek et al. 2019, 2021b). In accordance with IUCN categorization (IUCN 2024), these species are assessed in Czech Republic as critically endangered (CR), endangered (EN) or nationally scarce (NS). For more information, see Omelková and Ježek (2012b).

Classification and nomenclature for individual species are provided by Ježek and van Harten (2005, 2009), Ježek (2007), Ježek et al. (2018, 2020, 2021a, b, 2023a), Omelková and Ježek (2012a), Ježek and Omelková (2012), Oboňa and Ježek (2014), Kvifte (2014), and Kroča and Ježek (2015, 2019, 2022).

## Family Psychodidae

### Subfamily Sycoracinae

#### 1. *Sycorax silacea* Curtis, 1839

**Published record.** Salmela and Piirainen (2005): 304.

**Comments.** European species, sporadically common (Ježek et al. 2020; Morelli and Biscaccianti 2021).

### Subfamily Trichomyiinae

#### \*2. *Trichomyia urbica* Haliday in Curtis, 1839

**Material examined.** Läänemaa • ♂; Vormsi Island, Suuremõisa Park; 58°59'30"N, 23°11'34"E; 19.07.–19.08.2011; TWT (on old *Quercus robur* L.); IS leg. Pärnumaa • ♂; Kihnu Island; 58°08'44"N, 23°58'14"E; 29.05.–01.07.2011; TWT (on old *Aesculus hippocastanum* L.); IS leg.; • ♂; Matsalu NP; 58°42'41"N, 23°41'19"E; 11.07.–14.08.2009; TWT (on *Populus tremula* L.); IS leg.; • ♂; Lanksaare-Veelikse LCA; 58°00'11"N, 24°49'42"E; 24.07.–25.08.2017; TWT (on dead *Betula pendula* Roth); IS leg. Valgamaa • ♂; Soontaga; 58°00'03"N, 26°05'31"E; 05.06.–06.07.2015; TWT (on *Acer platanooides* L.); IS leg.

**Comments.** European and Transcaucasian species (Ježek et al. 2021a, b). Important species for nature conservation, assessed as critically endangered in the Czech Republic.

### Subfamily Psychodinae

#### Mormiini

#### Mormiina

#### \*3. *Oomormia andrenipes* (Strobl, 1910)

**Material examined.** Lääne-Virumaa • ♂; Tudusoo NR; 59°04'47"N, 26°45'38"E; 28.05.–25.06.2017; TWT (on *Populus tremula*); IS leg.; INS 33786.

**Comments.** Rather rare European species (Ježek 1984, 1994; Ježek and Omelková 2007; Kroča and Ježek 2022). Important species for nature conservation, assessed as critically endangered in the Czech Republic.

#### 4. *Lepimormia hemiboreale* Salmela & Piirainen, 2005

**Published record.** Salmela and Piirainen (2005): 302.

**Comments.** Known only from its type locality in the Viidumäe Nature Reserve, Estonia.

#### \*5. *Promormia eatoni* (Tonnoir, 1940)

**Material examined.** Pärnumaa • ♂; Kalita NR; 58°04'15"N, 24°51'37"E; 25.07.–24.08.2017; TWT (on *Populus tremula*); IS leg.; INS 33796. Lääne-Virumaa • ♂; near Lasila, forest patch No 79; 59°16'37"N, 26°13'22"E; 31.05.–28.06.2016; MT; OK leg.; INS 33782.

**Comments.** Rather rare European species (Ježek 1984, 1994; Ježek and Omelková 2007; Kroča and Ježek 2022). Important species for nature conservation, assessed as endangered in the Czech Republic.

**Paramormiini**  
**Paramormiina**

**\*6. *Lepiseodina rothschildi* (Eaton, 1912)**

**Material examined.** Saaremaa • ♂; Ruhnu Island; 57°48'22"N, 23°15'08"E; 09.06.–10.07.2012; TWT (on dead *Picea abies* (L.) H. Karst.); IS leg. Pärnumaa • ♂; Kihnu Island; 58°06'59"N, 23°59'38"E; 22.05.–11.06.2012; TWT (on old *Quercus robur*); IS leg.; • ♂; Kihnu Island; 58°09'09"N, 24°00'32"E; 22.05.–11.06.2012; TWT (on *Quercus robur*); IS leg.

**Comments.** Rather rare European species (Oboňa et al. 2021; Jaume-Schinkel et al. 2022). Important species for nature conservation, assessed as nationally scarce in the Czech Republic.

**7. *Panimerus albifacies* (Tonnoir, 1919)**

**Published record.** Salmela and Piirainen (2005): 304.

**Material examined.** Saaremaa • ♂; Ruhnu Island; 57°48'20"N, 23°14'33"E; 07.06.–10.07.2012; TWT (on dead *Alnus glutinosa* (L.) Gaertn.); IS leg.

**Comments.** European species (Ježek et al. 2021b; Jaume-Schinkel et al. 2023).

**\*8. *Panimerus notabilis* (Eaton, 1893)**

**Material examined.** Saaremaa • ♂; Ruhnu Island; 57°48'20"N, 23°14'33"E; 07.08.–05.09.2012; TWT (on dead *Alnus glutinosa*); IS leg. Pärnumaa • ♂; Kihnu Island; 58°06'59"N, 23°59'38"E; 12.07.–09.08.2012; TWT (on old *Quercus robur*); IS leg. Tartumaa • ♂; Vorbuse, Lokaatorite tee; 58°25'27"N, 26°35'47"E; 25.06.–14.07.2023; MT; OK leg.

**Comments.** Common European species (Ježek et al. 2019; Jaume-Schinkel et al. 2023).

**9. *Parajungiella consors* (Eaton, 1893)**

**Published record.** Salmela and Piirainen (2005): 304.

**Comments.** Not common European species (Kroča and Ježek 2022).

**\*10. *Parajungiella longicornis* (Tonnoir, 1919)**

**Material examined.** Pärnumaa • ♂; Riimaru; 58°16'18"N, 25°11'02"E; 17.08.–31.08.2005; TWT (on *Populus tremula*); IS leg. Lääne-Virumaa • ♂; Tudusoo NR; 59°04'47"N, 26°45'38"E; 28.05.–25.06.2017; TWT (on *Populus tremula*); IS leg.; INS 33794.

**Comments.** European and West-Siberian species (Ježek et al. 2020).

### 11. *Parajungiella pseudolongicornis* (Wagner, 1975)

**Published record.** Salmela and Piirainen (2005): 304.

**Material examined.** Lääne-Virumaa • ♂; Suigu NR; 59°09'11"N, 26°49'10"E; 26.07.–29.08.2017; TWT (on dead *Populus tremula*); IS leg.; INS 33779.

**Comments.** Rare European species (Ježek and Omelková 2012; Kroča and Ježek 2022). Important species for nature conservation, assessed as critically endangered in the Czech Republic.

### \*12. *Parajungiella serbica* (Krek, 1985)

**Material examined.** Pärnumaa • ♂; Riimaru; 58°16'19"N, 25°10'47"E; 02.06.–01.07.2006; TWT (on *Populus tremula* with *Phellinus tremulae* (Bondartsev) Bondartsev & N.P. Borisov); IS leg.

**Comments.** Rather rare European and Transcaucasian species (Ježek et al. 2020). Important species for nature conservation, assessed as critically endangered in the Czech Republic.

### 13. *Paramormia (Paramormia) polyascoidea* (Krek, 1971)

**Published record.** Salmela and Piirainen (2005): 304.

**Comments.** European, West-Siberian and Transcaucasian species (Ježek et al. 2020, 2023b).

### 14. *Peripsychoda auriculata* (Curtis, 1839)

**Published record.** Salmela and Piirainen (2005): 304.

**Material examined.** Saaremaa • ♂♂; Ruhnu Island; 57°48'15"N, 23°14'32"E; 07.06.–10.07.2012, 10.07.–07.08.2012; TWT (on *Acer platanoides*); IS leg.

**Comments.** European and Transcaucasian species (Ježek et al. 2020, 2023b; Morelli and Biscaccianti 2021).

### 15. *Seoda carthusiana* (Vaillant, 1972)

**Published record.** Salmela and Piirainen (2005): 304.

**Comments.** European species (Kročá and Ježek 2022).

### \*16. *Seoda gressica* (Vaillant, 1972)

**Material examined.** Saaremaa • ♂; Ruhnu Island; 57°47'59"N, 23°14'34"E; 26.05.–28.06.2011; TWT (on dead *Fraxinus excelsior* L.); IS leg.; INS 33783.

Pärnumaa • ♂♂; Kihnu Island; 58°07'49"N, 24°00'15"E; 22.05.–11.06.2012, 11.06.–12.07.2012; TWT (on old *Quercus robur*); IS leg.

**Comments.** Sporadically common European species (Ježek and Omelková 2012; Kroča and Ježek 2022).

**\*17. *Seoda labeculosa* (Eaton, 1893)**

**Material examined.** Lääne-Virumaa • ♂♂; near Lasila, forest patch No 24; 59°16'27"N, 26°11'44"E; 30.05.–02.07.2015, 02.08.–24.08.2015; MT; OK leg.; • ♂; near Lasila, forest patch No 31; 59°15'48"N, 26°14'17"E; 30.05.–02.07.2015; MT; OK leg.; • ♂; near Lasila, forest patch No 50; 59°16'25"N, 26°14'02"E; 02.08.–24.08.2015; OK leg.; • ♂; near Lasila, forest patch No 79; 59°16'37"N, 26°13'22"E; 28.06.–28.07.2016; MT; OK leg.; INS 33831.

**Comments.** Species known only from Europe (Ježek et al. 2019). Important for nature conservation, assessed as endangered in the Czech Republic.

**Trichopsychodina**

**18. *Feuerborniella obscura* (Tonnoir, 1919)**

**Published record.** Salmela and Piirainen (2005): 304.

**Material examined.** Pärnumaa • ♂♂; Riimaru; 58°16'19"N, 25°10'47"E; 11.06.–29.06.2005, 02.06.–01.07.2006; TWT (on *Populus tremula* with *Phellinus tremulae*); IS leg.; INS 33802, 33833.

**Comments.** European and Transcaucasian species (Oboňa et al. 2019; Ježek et al. 2020, 2021a, b, 2023b).

**\*19. *Philosepedon (Philosepedon) austriacum* Vaillant, 1974**

**Material examined.** Lääne-Virumaa • ♂; near Lasila, forest patch No 50; 59°16'25"N, 26°14'02"E; 28.07.–29.08.2016; MT; OK leg.; INS 33824.

**Comments.** European species (Ježek et al. 2020; Kroča and Ježek 2022).

**\*20. *Philosepedon (Philosepedon) dumosum* Omelková & Ježek, 2012**

**Material examined.** Pärnumaa • ♂; Luitemaa NR near Võiste; 58°12'21"N, 24°29'36"E; 23.06.–25.07.2017; TWT (on burned *Pinus sylvestris* L.); IS leg.; INS 33818.

**Comments.** Species known only from the Czech Republic (Omelková and Ježek 2012a). Important for nature conservation, assessed as nationally scarce in the Czech Republic.

**21. *Philosepedon (Philosepedon) humerale* (Meigen, 1818)**

**Published records.** Salmela and Piirainen (2005): 304.

**Material examined.** Hiiumaa • ♂; Leigri NR; 58°53'51"N, 22°35'46"E; 19.07.–03.08.2013; TWT (on *Pinus sylvestris*); IS leg. Saaremaa • ♂; Ruhnu Island, near church; 57°48'23"N, 23°14'41"E; 03.08.–11.09.2011; TWT (on old

*Quercus robur*); IS leg.; • ♂; Ruhnu Island; 57°47'55"N, 23°15'53"E; 24.05.–27.06.2011; TWT (on dead *Pinus sylvestris*); IS leg.; • ♂♂; Ruhnu Island; 57°47'59"N, 23°14'34"E; 26.05.–28.06.2011, 28.06.–03.08.2011, 07.08.–05.09.2012; TWT (on dead *Fraxinus excelsior*); IS leg.; • ♂♂; Ruhnu Island; 57°48'28"N, 23°14'32"E; 26.05.–28.06.2011, 28.06.–03.08.2011, 03.08.–11.09.2011; TWT (on dead *Fraxinus excelsior*); IS leg.; • ♂; Ruhnu Island; 57°48'01"N, 23°14'38"E; 07.08.–05.09.2012; TWT (on *Acer platanoides*); IS leg.; • ♂; Ruhnu Island; 57°48'08"N, 23°15'49"E; 06.08.–04.09.2012; TWT (on *Picea abies* with *Fomitopsis pinicola* (Sw.) P. Karst.); IS leg.; • ♂♂; Ruhnu Island; 57°48'09"N, 23°14'25"E; 07.06.–10.07.2012, 07.08.–05.09.2012; TWT (on *Fraxinus excelsior*); IS leg.; • ♂; Ruhnu Island; 57°48'09"N, 23°14'29"E; 07.08.–05.09.2012; TWT (on *Corylus avellana* L.); IS leg.; • ♂♂; Ruhnu Island; 57°48'10"N, 23°14'24"E; 07.06.–10.07.2012, 10.07.–07.08.2012, 07.08.–05.09.2012; TWT (on *Fraxinus excelsior*); IS leg.; • ♂♂; Ruhnu Island; 57°48'15"N, 23°14'32"E; 10.07.–07.08.2012, 07.08.–05.09.2012; TWT (on *Acer platanoides*); IS leg.; • ♂; Ruhnu Island; 57°48'18"N, 23°14'27"E; 07.08.–05.09.2012; TWT (on *Quercus robur*); IS leg.; • ♂; Ruhnu Island; 57°48'20"N, 23°14'33"E; 07.08.–05.09.2012; TWT (on *Alnus glutinosa*); IS leg.; • ♂; Ruhnu Island; 57°48'20"N, 23°15'30"E; 06.08.–04.09.2012; TWT (on dead *Picea abies* with *Fomitopsis pinicola*); IS leg.; • ♂; Ruhnu Island; 57°48'22"N, 23°15'08"E; 09.06.–10.07.2012; TWT (on dead *Picea abies*); IS leg.; • ♂♂; Ruhnu Island; 57°48'02"N, 23°13'42"E; 07.06.–10.07.2012, 07.08.–05.09.2012; TWT (on old *Ulmus laevis* Pallas); IS leg.; • ♂♂; Ruhnu Island; 57°48'27"N, 23°14'32"E; 09.06.–10.07.2012, 10.07.–07.08.2012, 07.08.–05.09.2012; TWT (on *Corylus avellana*); IS leg.; • ♂; Ruhnu Island; 57°47'54"N, 23°16'18"E; 06.08.–04.09.2012; TWT (on dead *Pinus sylvestris*); IS leg. **Läänemaa** • ♂♂; Vormsi Island; 59°01'18"N, 23°08'00"E; 08.05.–04.06.2012, 03.08.–11.09.2012; TWT (on *Corylus avellana*); IS leg.; • ♂♂; Vormsi Island; 58°59'30"N, 23°11'34"E; 04.06.–06.07.2011, 06.07.–19.07.2011, 06.07.–03.08.2012; TWT (on *Quercus robur*); IS leg.; • ♂♂; Vormsi Island; 58°59'26"N, 23°11'51"E; 08.05.–04.06.2012, 06.07.–03.08.2012; TWT (on *Salix fragilis* L.); IS leg.; • ♂; Vormsi Island; 58°58'11"N, 23°12'21"E; 08.05.–04.06.2012; TWT (on dead *Pinus sylvestris*); IS leg.; • ♂; Vormsi Island; 59°01'20"N, 23°08'13"E; 09.05.–04.06.2012; TWT (on dead *Alnus glutinosa*); IS leg.; • ♂; Vormsi Island; 59°00'16"N, 23°13'49"E; 10.05.–04.06.2012; TWT (on *Pinus sylvestris*); IS leg.; **Pärnumaa** • ♂; Kihnu Island; 58°06'59"N, 23°59'38"E; 02.07.–06.08.2011; TWT (on old *Quercus robur*); IS leg.; • ♂; Kihnu Island; 58°08'28"N, 23°58'47"E; 01.07.–06.08.2011; TWT (on old *Pinus sylvestris*); IS leg.; • ♂; Kihnu Island; 58°08'44"N, 23°58'14"E; 29.05.–01.07.2011; TWT (on old *Aesculus hippocastanum*); IS leg.; • ♂; Kihnu Island; 58°08'44"N, 23°58'16"E; 06.08.–13.09.2011; TWT (on old *Tilia cordata* Mill.); IS leg.; • ♂; Kihnu Island; 58°08'48"N, 23°58'17"E; 01.07.–06.08.2011; TWT (on dead *Fraxinus excelsior*); IS leg.; • ♂; Kihnu Island, Lemsi; 58°07'49"N, 24°00'15"E; 06.08.–13.09.2011; TWT (on old *Quercus robur*); IS leg.; • ♂♂; Kihnu Island; 58°06'59"N, 23°59'38"E; 22.05.–11.06.2012, 12.07.–09.08.2012; TWT (on old *Quercus robur*); IS leg.; • ♂♂; Kihnu Island; 58°07'18"N, 23°58'25"E; 23.05.–11.06.2012, 11.06.–12.07.2012; TWT (on *Pinus sylvestris*); IS leg.; • ♂♂; Kihnu Island; 58°07'49"N, 24°00'15"E; 22.05.–11.06.2012, 12.07.–09.08.2012; TWT (on old *Quercus robur*); IS leg.; • ♂♂; Kihnu Island; 58°08'07"N, 23°58'20"E; 12.07.–09.08.2012, 09.08.–08.09.2012; TWT (on *Pinus sylvestris*); IS leg.; • ♂♂; Kihnu Island;

58°08'28"N, 23°58'47"E; 23.05.–11.06.2012, 11.06.–12.07.2012, 12.07.–09.08.2012; TWT (on *Pinus sylvestris*); IS leg.; • ♂♂; Kihnu Island; 58°08'44"N, 23°58'14"E; 23.05.–11.06.2012, 11.06.–12.07.2012; TWT (on old *Aesculus hippocastanum*); IS leg.; • ♂; Kihnu Island; 58°09'09"N, 24°00'32"E; 11.06.–12.07.2012; TWT (on *Quercus robur*); IS leg.; • ♂; Puhtu; 58°33'39.4"N, 23°33'07.9"E; 10.07.–13.08.2009; TWT (on dead *Picea abies* with *Fomitopsis pinicola*); IS leg.; • ♂; Puhtu; 58°33'25"N, 23°33'04"E; 27.05.–18.06.2009; TWT (on old *Pinus sylvestris*); IS leg.; • ♂; Kalita NR; 58°04'16"N, 24°51'39"E; 25.07.–24.08.2017; TWT (on *Populus tremula*); IS leg. **Lääne-Virumaa** • ♂; Lahemaa NP, Eru; 59°34'03"N, 25°51'53"E; 26.07.–26.08.2017; TWT (on burned *Picea abies*); IS leg.; • ♂♂; Lahemaa NP, near Laukasoo; 59°28'49"N, 25°54'24"E; 23.05.–23.06.2017, 25.07.–26.08.2017; TWT (on dead *Populus tremula*); IS leg.; • ♂♂; near Lasila, forest patch No 104; 59°16'43"N, 26°17'07"E; 12.–30.05.2015, 02.07.–02.08.2015, 20.09.–21.10.2015, 31.05.–28.06.2016; MT; OK leg.; • ♂♂; near Lasila, forest patch No 24; 59°16'27"N, 26°11'44"E; 12.–30.05.2015, 30.05.–02.07.2015, 02.07.–02.08.2015, 02.–24.08.2015, 24.08.–20.09.2015, 20.09.–21.10.2015, 31.05.–28.06.2016, 05.–31.05.2016; MT; OK leg.; • ♂♂; near Lasila, forest patch No 31; 59°15'48"N, 26°14'17"E; 12.–30.05.2015, 30.05.–02.07.2015, 02.07.–02.08.2015, 02.–24.08.2015, 24.08.–20.09.2015, 20.09.–21.10.2015, 28.06.–28.07.2016; MT; OK leg.; • ♂♂; near Lasila, forest patch No 50; 59°16'25"N, 26°14'02"E; 12.–30.05.2015, 02.–24.08.2015, 31.05.–28.06.2016, 28.06.–28.07.2016, 29.08.–26.09.2016; MT; OK leg.; • ♂♂; near Lasila, forest patch No 52; 59°16'20"N, 26°13'52"E; 31.05.–28.06.2016, 28.06.–28.07.2016, 28.07.–29.08.2016, 29.08.–26.09.2016; MT; OK leg.; • ♂♂; near Lasila, forest patch No 6; 59°15'41"N, 26°12'32"E; 12.–30.05.2015, 30.05.–02.07.2015, 02.07.–02.08.2015, 02.–24.08.2015, 24.08.–20.09.2015, 20.09.–21.10.2015, 31.05.–28.06.2016, 28.07.–29.08.2016, 29.08.–26.09.2016, 26.09.–27.10.2016; MT; OK leg.; • ♂♂; near Lasila, forest patch No 7; 59°15'33"N, 26°12'41"E; 12.–30.05.2015, 02.07.–02.08.2015, 02.–24.08.2015; MT; OK leg.; • ♂♂; near Lasila, forest patch No 75; 59°16'49"N, 26°13'05"E; 30.05.–02.07.2015, 02.07.–02.08.2015, 20.09.–21.10.2015, 05.–31.05.2016, 28.07.–29.08.2016; MT; OK leg.; • ♂♂; near Lasila, forest patch No 79; 59°16'37"N, 26°13'22"E; 12.–30.05.2015, 30.05.–02.07.2015, 02.07.–02.08.2015, 02.–24.08.2015, 20.09.–21.10.2015, 05.–31.05.2016, 31.05.–28.06.2016, 28.06.–28.07.2016, 28.07.–29.08.2016, 29.08.–26.09.2016; MT; OK leg. **Ida-Virumaa** • ♂; Muraka NR; 59°05'22"N, 27°09'18"E; 15.06.–30.06.2015; TWT (on dead *Picea abies*); IS leg. **Tartumaa** • ♂; Vorbuse, Lokatorite tee; 58°25'27"N, 26°35'47"E; 10.–25.06.2023; MT; OK leg.; • ♂; Elva-Vitipalu PL; 58°10'49"N, 26°25'14"E; 13.06.–29.06.2015; TWT (on dead *Picea abies*); IS leg. **Valgamaa** • ♂♂; Soontaga; 58°00'04"N, 26°05'11"E; 07.05.–05.06.2015, 05.06.–06.07.2015, 03.–31.08.2015; TWT (on dead *Betula pendula* with *Fomes fomentarius* (L.) Fr.); IS leg.; • ♂♂; Soontaga; 58°00'04"N, 26°05'15"E; 07.05.–05.06.2015, 05.06.–06.07.2015, 06.07.–03.08.2015; TWT (on dead *Betula pendula*); IS leg.; • ♂♂; Soontaga; 58°00'01"N, 26°05'10"E; 19.05.–05.06.2015, 05.06.–06.07.2015, 06.07.–03.08.2015, 03.–31.08.2015; TWT (on dead *Populus tremula*); IS leg.; • ♂♂; Soontaga; 58°00'03"N, 26°05'31"E; 11.05.–05.06.2015, 05.06.–06.07.2015, 06.07.–03.08.2015; TWT (on *Acer platanoides*); IS leg.; • ♂; Koiva wooded meadow; 57°41'21"N, 26°11'08"E; 14.05.–

03.06.2013; TWT (on dead *Quercus robur*); IS leg.; • ♂; Koiva wooded meadow; 57°41'19"N, 26°10'59"E; 01.08.–17.08.2013; TWT (on dead *Quercus robur*); IS leg.; • ♂; Koivakonnu; 57°35'28"N, 26°19'21"E; 01.08.–17.08.2013; TWT (on dead *Quercus robur*); IS leg. **Võrumaa** • ♂; Haanja NP; 57°44'07"N, 27°03'50"E; 18.05.–20.06.2017; TWT (on dead *Populus tremula*); IS leg.; • ♂; Haanja NP; 57°44'08"N, 27°03'46"E; 20.06.–23.07.2017; TWT (on dead *Betula pendula* with *Fomes fomentarius*); IS leg.; • ♂; Piusa PL; 57°47'28"N, 27°21'57"E; 18.05.–19.06.2017, 19.06.–23.07.2017; TWT (on burned *Pinus sylvestris*); IS leg.

**Comments.** Very common European species (Ježek et al. 2020).

#### \*22. *Philosepedon (Philothreticus) soljani* Krek, 1971

**Material examined.** **Lääne-Virumaa** • ♂; near Lasila, forest patch No 50; 59°16'25"N, 26°14'02"E; 28.07.–29.08.2016; MT; OK leg.

**Comments.** European species (Ježek et al. 2017; Kroča and Ježek 2022). Important for nature conservation, assessed as nationally scarce in the Czech Republic.

#### \*23. *Philosepedon (Trichosepedon) balkanicum* Krek, 1970

**Material examined.** **Hiiumaa** • ♂; Leigri NR; 58°53'00"N, 22°35'25"E; 05.06.–18.06.2013; TWT (on dead *Picea abies*); IS leg. **Saaremaa** • ♂; Ruhnu Island; 57°48'23"N, 23°14'41"E; 03.08.–11.09.2011; TWT (on *Quercus robur*); IS leg.; • ♂; Ruhnu Island; 57°47'54"N, 23°15'26"E; 06.08.–04.09.2012; TWT (on *Pinus sylvestris*); IS leg. **Läänemaa** • ♂; Vormsi Island; 59°01'01"N, 23°12'18"E; 03.08.–01.09.2012; TWT (on *Pinus sylvestris*); IS leg.; • ♂♂; Vormsi Island; 59°01'22"N, 23°12'12"E; 19.08.–04.09.2011, 03.08.–01.09.2012; TWT (dead *Picea abies* with *Fomitopsis pinicola*); IS leg. **Pärnumaa** • ♂; Riimaru; 58°16'18"N, 25°11'02"E; 02.06.–01.07.2006; TWT (on *Populus tremula*); IS leg.; • ♂♂; Riimaru; 58°16'18"N, 25°11'02"E; 11.–29.06.2005, 17.–31.08.2005; TWT (on *Populus tremula*); IS leg.; INS 33806; • ♂; Kalita NR; 58°04'15"N, 24°51'37"E; 25.07.–24.08.2017; TWT (on *Populus tremula*); IS leg.; • ♂; Luitemaa NR near Võiste; 58°12'21"N, 24°29'34"E; 20.05.–23.06.2017; TWT (on burned *Pinus sylvestris*); IS leg.; • ♂; Kihnu Island; 58°07'49"N, 24°00'15"E; 12.07.–09.08.2012; TWT (on *Quercus robur*); IS leg. **Viljandimaa** • ♂; Muti PL; 58°08'25"N, 25°40'50"E; 21.06.–24.07.2017; TWT (on dead *Betula pendula*); IS leg. **Ida-Virumaa** • ♂; Muraka NR S of Virunurme; 59°09'52"N, 27°00'48"E; 26.05.–25.06.2017; TWT (on dead *Populus tremula*); IS leg.; • ♂; Muraka NR; 59°05'22"N, 27°09'18"E; 30.05.–15.06.2015; TWT (on dead *Picea abies*); IS leg.; • ♂; Agusalu NR; 59°02'16"N, 27°39'35"E; 30.05.–15.06.2015; TWT (on dead *Pinus sylvestris*); IS leg. **Tartumaa** • ♂; Padakõrve NR; 58°35'07"N, 27°01'09"E; 30.05.–15.06.2015; TWT (on dead *Pinus sylvestris*); IS leg.; • ♂; Järvselja NR; 58°16'52"N, 27°19'27"E; 17.05.–19.06.2017; TWT (on dead *Populus tremula*); IS leg. **Põlvamaa** • ♂; Ihamaru NR; 58°05'52"N, 26°55'33"E; 29.05.–13.06.2015; TWT (on dead *Picea abies*); IS leg.

**Comments.** European and Transcaucasian species (Kvifte 2019; Ježek et al. 2023b).

**\*24. *Trichopsychoda hirtella* (Tonnoir, 1919)**

**Material examined.** **Saaremaa** • ♂♂; Ruhnu Island, near Korsi farm; 57°48'28"N, 23°14'32"E; 26.05.–28.06.2011, 28.06.–03.08.2011; TWT (on dead *Fraxinus excelsior*); IS leg.; INS 33832; • ♂; Ruhnu Island; 57°48'08"N, 23°15'49"E; 06.08.–04.09.2012; TWT (on dead *Picea abies* with *Fomitopsis pinicola*); IS leg.; • ♂; Ruhnu Island; 57°48'09"N, 23°14'25"E; 07.08.–05.09.2012; TWT (on *Fraxinus excelsior*); IS leg.; • ♂; Ruhnu Island; 57°48'10"N, 23°14'24"E; 07.08.–05.09.2012; TWT (on *Fraxinus excelsior*); IS leg.; • ♂; Ruhnu Island; 57°48'15"N, 23°14'32"E; 10.07.–07.08.2012; TWT (on *Acer platanoides*); IS leg.; • ♂; Ruhnu Island; 57°48'18"N, 23°14'27"E; 07.08.–05.09.2012; TWT (on *Quercus robur*); IS leg.; • ♂; Ruhnu Island, near Korsi farm; 57°48'27"N, 23°14'32"E; 09.06.–10.07.2012; TWT (on *Corylus avellana*); IS leg.; • ♂; Pihtla; 21.07.2016; hand picked; M. Oras leg. **Läänemaa** • ♂; Kullamaa; 23.07.2016; sweep net; K. Sammet leg. **Pärnumaa** • ♂♂; Riimaru; 58°16'19"N, 25°10'47"E; 29.06.–13.07.2005, 02.06.–01.07.2006; TWT (on *Populus tremula* with *Phellinus tremulae*); IS leg.; INS 33788. **Lääne-Virumaa** • ♂; near Lasila, forest patch No 31; 59°15'48"N, 26°14'17"E; 02.07.–02.08.2015; MT; OK leg.; • ♂; near Lasila, forest patch No 6; 59°15'41"N, 26°12'32"E; 28.07.–29.08.2016; MT; OK leg. **Tartumaa** • ♂; Vapramäe; 15.07.2016; sweep net; OK leg. **Valgamaa** • ♂; Soontaga; 58°00'03"N, 26°05'31"E; 05.06.–06.07.2015; TWT (on *Acer platanoides*); IS leg.; • ♂; Soontaga; 58°00'04"N, 26°05'11"E; 05.06.–06.07.2015; TWT (on dead *Betula pendula* with *Fomes fomentarius*); IS leg.; • ♂; Koivakonnu; 57°35'28"N, 26°19'21"E; 16.06.–02.07.2013; TWT (on dead *Quercus robur*); IS leg.

**Comments.** European and Transcaucasian species (Ježek et al. 2020, 2023b; Morelli and Biscaccianti 2021).

**Psychodini**

**\*25. *Chodopsycha buxtoni* (Withers, 1988)**

**Material examined.** **Lääne-Virumaa** • ♂; near Lasila, forest patch No 50; 59°16'25"N, 26°14'02"E; 28.07.–29.08.2016; MT; OK leg.; INS 33825. **Valgamaa** • ♂; Koivakonnu; 57°35'28"N, 26°19'21"E; 17.08.–01.09.2013; TWT (on dead *Quercus robur*); IS leg.; INS 33834.

**Comments.** Not common European and Transcaucasian species (Ježek et al. 2023b). Important for nature conservation, assessed as nationally scarce in the Czech Republic.

**\*26. *Chodopsycha lobata* (Tonnoir, 1940)**

**Material examined.** **Lääne-Virumaa** • ♀; near Lasila, forest patch No 50; 59°16'25"N, 26°14'02"E; 28.07.–29.08.2016; MT; OK leg.; INS 33823; • ♂; Tudusoo NR; 59°05'01"N, 26°45'54"E; 27.07.–29.08.2017; TWT (on dead *Populus tremula*); IS leg.; INS 33828.

**Comments.** Common European and Transcaucasian species (Ježek et al. 2020, 2021a, b).

## 27. *Logima albipennis* (Zetterstedt, 1850)

**Published record.** Salmela and Piirainen (2005): 304.

**Material examined.** Pärnumaa • ♂♂; Riimaru; 58°16'18"N, 25°11'02"E; 03.08.–17.08.2005, 31.07.–02.09.2006; TWT (on dead *Betula pendula* with *Fomes fomentarius*); IS leg.; • ♂; Kalita NR; 58°04'15"N, 24°51'37"E; 25.07.–24.08.2017; TWT (on *Populus tremula*); IS leg.; INS 33795.

**Comments.** Cosmopolitan species (Ježek et al. 2021a, 2023a).

## \*28. *Logima satchelli* (Quate, 1955)

**Material examined.** Saaremaa • ♂; Ruhnu Island; 57°47'55"N, 23°15'53"E; 24.05.–27.06.2011; TWT (on dead *Pinus sylvestris*); IS leg.; • ♂; Ruhnu Island, near Korsi farm; 57°48'28"N, 23°14'32"E; 26.05.–28.06.2011; TWT (on dead *Fraxinus excelsior*); IS leg.; • ♂; Ruhnu Island; 57°48'09"N, 23°14'25"E; 10.07.–07.08.2012; TWT (on *Fraxinus excelsior*); IS leg.; • ♂; Ruhnu Island; 57°48'09"N, 23°14'29"E; 07.06.–10.07.2012; TWT (on *Corylus avellana*); IS leg.; • ♂; Ruhnu Island; 57°48'18"N, 23°14'27"E; 07.08.–05.09.2012; TWT (on *Quercus robur*); IS leg.; • ♂♂; Ruhnu Island, Holma; 57°48'02"N, 23°13'42"E; 29.06.–02.08.2011, 07.06.–10.07.2012; TWT (on old *Ulmus laevis*); IS leg.; • ♂♂; Ruhnu Island, Korsi farm; 57°48'27"N, 23°14'32"E; 09.06.–10.07.2012, 10.07.–07.08.2012; TWT (on *Corylus avellana*); IS leg. Läänemaa • ♂; Puise; 58°47'45"N, 23°31'22"E; 17.06.–11.07.2009; TWT (on old *Betula pendula*); IS leg.; • ♂; Vormsi Island; 58°58'33"N, 23°12'10"E; 03.08.–01.09.2012; TWT (on dead *Betula pendula* with *Fomes fomentarius*); IS leg.; • ♂; Vormsi Island; 59°01'22"N, 23°12'12"E; 03.08.–01.09.2012; TWT (on dead *Picea abies* with *Fomitopsis pinicola*); IS leg.; • ♂; Vormsi Island; 58°59'26"N, 23°11'51"E; 08.05.–04.06.2012; TWT (on *Salix fragilis*); IS leg. Pärnumaa • ♂; Kihnu Island; 58°08'07"N, 23°58'20"E; 24.05.–11.06.2012; TWT (on *Pinus sylvestris* with *Phellinus pini*); IS leg.; • ♂; Matsalu NP; 58°43'52"N, 23°42'54"E; 17.06.–11.07.2009; TWT (on dead *Betula pendula* with *Fomes fomentarius*); IS leg.; • ♂; Riimaru; 58°16'18"N, 25°11'02"E; 19.06.–03.08.2007; TWT (on *Populus tremula*); IS leg.; • ♂; Riimaru; 58°16'19"N, 25°10'47"E; 17.–31.08.2005; TWT (on *Populus tremula* with *Phellinus tremulae*); IS leg.; • ♂; Riimaru; 58°16'18"N, 25°11'02"E; 31.07.–02.09.2006; TWT (on dead *Betula pendula* with *Fomes fomentarius*); IS leg.; • ♂; Luitemaa NR near Võiste; 58°12'21"N, 24°29'36"E; 23.06.–25.07.2017; TWT (on burned *Pinus sylvestris*); IS leg. Viljandimaa • ♂; Muti PL; 58°08'25"N, 25°40'50"E; 19.05.–21.06.2017; TWT (on dead *Betula pendula* with *Fomes fomentarius*); IS leg. Harjumaa • ♂♂; Mähuste near Koitjärve; 59°24'55"N, 25°36'45"E; 01.07.–16.07.2015, 16.–30.07.2015, 15.08.–03.09.2015; TWT (on dead *Betula pendula*); IS leg.; • ♂♂; Põhja-Kõrvemaa NR; 59°25'30"N, 25°39'11"E; 15.05.–01.06.2015, 01.–16.06.2015, 16.06.–01.07.2015; TWT (on dead *Pinus sylvestris*); IS leg. Lääne-Virumaa • ♂; near Lasila, forest patch No 6; 59°15'41"N, 26°12'32"E; 31.05.–28.06.2016; MT; OK leg.; • ♂; near Lasila, forest patch No 7; 59°15'33"N, 26°12'41"E; 26.09.–27.10.2016; MT; OK leg.; • ♂; Suigu NR; 59°08'59"N, 26°49'11"E; 25.06.–26.07.2017; TWT (on *Populus tremula*); IS leg.; • ♀; Suigu NR; 59°09'11"N, 26°49'10"E; 25.06.–26.07.2017; TWT (on dead *Populus tremula*); IS leg. Ida-Virumaa • ♂; Kautvere near

Oonurme; 59°08'23"N, 26°57'10"E; 26.07.–28.08.2017; TWT (on dead *Populus tremula*); IS leg.; • ♂♂; Kurtna PL; 59°18'09"N, 27°34'08"E; 30.05.–15.06.2015, 15.–29.07.2015; TWT (on dead *Pinus sylvestris*); IS leg.; • ♂; Kurtna PL; 59°18'22"N, 27°33'53"E; 29.07.–14.08.2015; TWT (on dead *Pinus sylvestris*); IS leg.; • ♂; Agusalu NR; 59°04'16"N, 27°37'40"E; 14.–30.05.2015; TWT (on dead *Betula pendula* with *Fomes fomentarius*); IS leg.; • ♂; Agusalu NR; 59°02'17"N, 27°39'40"E; 29.07.–14.08.2015; TWT (on dead *Pinus sylvestris*); IS leg.; • ♂♂; Agusalu NR; 59°02'16"N, 27°39'35"E; 01.–14.05.2015, 30.05.–15.06.2015, 14.08.–01.09.2015; TWT (on dead *Pinus sylvestris*); IS leg.; • ♂; Agusalu NR; 59°03'56"N, 27°37'37"E; 30.04.–14.05.2015; TWT (on dead *Betula pendula*); IS leg.; • ♂; Agusalu NR; 59°04'16"N, 27°37'40"E; 30.04.–14.05.2015; TWT (on dead *Betula pendula* with *Fomes fomentarius*); IS leg.; • ♂♂; Agusalu NR; 59°07'10"N, 27°34'39"E; 30.04.–14.05.2015, 14.08.–01.09.2015; TWT (on dead *Betula pendula* with *Fomes fomentarius*); IS leg.; • ♂♂; Agusalu NR; 59°02'15"N, 27°39'42"E; 15.–30.06.2015, 14.08.–01.09.2015; TWT (on dead *Betula pendula*); IS leg. **Tartumaa** • ♂♂; Padakõrve NR; 58°35'07"N, 27°01'09"E; 30.04.–14.05.2015, 14.05.–30.05.2015, 30.05.–15.06.2015, 15.–30.06.2015, 14.08.–01.09.2015; TWT (on dead *Pinus sylvestris*); IS leg.; • ♂♂; Rootsiküla; 58°37'14"N, 27°10'47"E; 10.05.–06.06.2009, 02.–18.08.2009; TWT (on *Salix caprea* L.); IS leg.; • ♂; Vorbuse, Lokaatorite tee; 58°25'27"N, 26°35'47"E; 01.–15.10.2023; MT; OK leg.; • ♂; Välgi; 58°33'48"N, 26°52'38"E; 15.–29.07.2015; TWT (on *Populus tremula*); IS leg.; • ♂; Peipsiveere NR; 58°17'22"N, 27°08'59"E; 19.06.–22.07.2017; TWT (on dead *Populus tremula*); IS leg.; • ♂; Elva-Vitipalu PL; 58°10'49"N, 26°25'14"E; 27.04.–13.05.2015; TWT (on dead *Picea abies*); IS leg. **Põlvamaa** • ♂; Ihamaru NR; 58°06'09"N, 26°55'59"E; 27.04.–13.05.2015; TWT (on dead *Betula pendula* with *Fomes fomentarius*); IS leg. **Valgamaa** • ♂♂; Soontaga; 58°00'03"N, 26°05'31"E; 05.06.–06.07.2015, 06.07.–03.08.2015; TWT (on *Acer platanoides*); IS leg.; • ♂; Soontaga; 58°00'04"N, 26°05'11"E; 05.06.–06.07.2015; TWT (on dead *Betula pendula* with *Fomes fomentarius*); IS leg.; • ♂; Soontaga; 58°00'01"N, 26°05'10"E; 05.06.–06.07.2015; TWT (on *Populus tremula*); IS leg.; • ♂♂; Soontaga; 58°00'04"N, 26°05'15"E; 05.06.–06.07.2015, 06.07.–03.08.2015; TWT (on dead *Betula pendula*); IS leg.; • ♂; Tüdre NR; 57°56'59"N, 25°37'51"E; 21.06.–24.07.2017; TWT (on burned *Picea abies*); IS leg.; • ♂; Koiva wooded meadow; 57°41'21"N, 26°10'54"E; 17.08.–01.09.2013; TWT (on dead *Salix caprea*); IS leg.; • ♂; Koiva wooded meadow; 57°41'19"N, 26°10'59"E; 17.07.–01.08.2013; TWT (on dead *Quercus robur*); IS leg.; • ♂; Koivakonnu; 57°35'27"N, 26°19'40"E; 16.06.–02.07.2013; TWT (on dead *Betula pendula* with *Fomes fomentarius*); IS leg.; • ♂♂; Koivakonnu; 57°35'28"N, 26°19'21"E; 16.06.–02.07.2013, 01.–17.08.2013; TWT (on dead *Quercus robur*); IS leg.

**Comments.** Holarctic species (Ježek et al. 2020, 2023a, b).

#### \*29. *Logima sigma* (Kincaid, 1899)

**Material examined.** Tartumaa • ♀; Rootsiküla; 58°37'14"N, 27°10'47"E; 24.06.–15.07.2009; TWT (on dead *Salix caprea*); IS leg.; INS 33804.

**Comments.** Probably cosmopolitan species (Oboňa and Kozánek 2018; Ježek et al. 2021a).

### 30. *Psychoda phalaenoides* (Linnaeus, 1758)

**Published records.** Remm (1956): 234; Salmela and Piirainen (2005): 304.

**Material examined.** **Saaremaa** • ♂; Ruhnu Island, Holma; 57°48'02"N, 23°13'42"E; 07.08.–05.09.2012; TWT (on old *Ulmus laevis*); IS leg.; • ♂; Ruhnu Island, Korsi farm; 57°48'27"N, 23°14'32"E; 07.08.–05.09.2012; TWT (on *Corylus avellana*); IS leg.; • ♂; Ruhnu Island, Limo seashore; 57°47'37"N, 23°16'17"E; 06.08.–04.09.2012; TWT (on *Pinus sylvestris*); IS leg. **Läänemaa** • ♂; Vormsi Island; 59°01'18"N, 23°08'00"E; 08.05.–04.06.2012; TWT (on *Corylus avellana*); IS leg. **Pärnumaa** • ♂; Matsalu NP; 58°42'41"N, 23°41'19"E; 11.07.–14.08.2009; TWT (on *Populus tremula*); IS leg.; • ♂; Matsalu NP; 58°42'52"N, 23°41'23"E; 17.06.–11.07.2009; TWT (on dead *Populus tremula*); IS leg.; • ♂♂; Riimaru; 58°16'18"N, 25°11'02"E; 02.06.–01.07.2006, 19.06.–03.08.2007; TWT (on dead *Populus tremula*); IS leg.; • ♂; Riimaru; 58°16'19"N, 25°10'47"E; 02.06.–01.07.2006; TWT (on *Populus tremula* with *Phellinus tremulae*); IS leg.; • ♂; Kalita NR; 58°04'16"N, 24°51'39"E; 22.06.–25.07.2017; TWT (on *Populus tremula*); IS leg. **Viljandimaa** • ♂♂; Muti PL; 58°08'25"N, 25°40'50"E; 21.06.–24.07.2017, 24.07.–24.08.2017; TWT (on dead *Betula pendula* with *Fomes fomentarius*); IS leg. **Harjumaa** • ♂; Mähuste near Koitjärve; 59°24'55"N, 25°36'45"E; 16.07.–30.07.2015; TWT (on dead *Betula pendula*); IS leg. **Lääne-Virumaa** • ♂; Sakusaare; 59°28'58"N, 26°01'54"E; 25.07.–26.08.2017; TWT (dead *Pinus sylvestris*); IS leg.; • ♂; near Lasila, forest patch No 104; 59°16'43"N, 26°17'07"E; 02.07.–02.08.2015; MT; OK leg.; • ♂; near Lasila, forest patch No 31; 59°15'48"N, 26°14'17"E; 28.07.–29.08.2016; MT; OK leg.; • ♂♂; near Lasila, forest patch No 50; 59°16'25"N, 26°14'02"E; 28.06.–28.07.2016, 29.08.–26.09.2016, 26.09.–27.10.2016; MT; OK leg.; • ♂♂; near Lasila, forest patch No 6; 59°15'41"N, 26°12'32"E; 28.07.–29.08.2016, 26.09.–27.10.2016; MT; OK leg.; • ♂; near Lasila, forest patch No 7; 59°15'33"N, 26°12'41"E; 02.–24.08.2015; MT; OK leg.; • ♂♂; near Lasila, forest patch No 75; 59°16'49"N, 26°13'05"E; 02.07.–02.08.2015, 02.–24.08.2015, 20.09.–21.10.2015, 28.07.–29.08.2016; MT; OK leg.; • ♂♂; near Lasila, forest patch No 79; 59°16'37"N, 26°13'22"E; 02.–24.08.2015, 24.08.–20.09.2015, 05.–31.05.2016; MT; OK leg.; • ♀; Tudusoo NR; 59°04'52"N, 26°46'16"E; 26.07.–29.08.2017; TWT (on dead *Populus tremula*); IS leg. **Ida-Virumaa** • ♂; Kautvere near Oonurme; 59°08'23"N, 26°57'10"E; 26.05.–25.06.2017; TWT (on dead *Populus tremula*); IS leg.; • ♂; Muraka NR, S of Virunurm; 59°09'52"N, 27°00'48"E; 26.07.–28.08.2017; TWT (on dead *Populus tremula*); IS leg.; • ♂; Muraka NR; 59°05'22"N, 27°09'18"E; 30.04.–14.05.2015; TWT (on dead *Picea abies*); IS leg.; • ♂; Kurtna PL; 59°18'09"N, 27°34'08"E; 15.–29.07.2015; TWT (on dead *Pinus sylvestris*); IS leg.; • ♂; Kurtna PL; 59°18'22"N, 27°33'53"E; 15.–30.06.2015, 29.07.–14.08.2015; TWT (on dead *Pinus sylvestris*); IS leg.; • ♂♂; Agusalu NR; 59°02'16"N, 27°39'35"E; 01.–14.05.2015, 14.08.–01.09.2015; TWT (on dead *Pinus sylvestris*); IS leg.; • ♂; Agusalu NR; 59°02'17"N, 27°39'40"E; 15.–29.07.2015; TWT (on dead *Pinus sylvestris*); IS leg.; • ♂; Agusalu NR; 59°04'16"N, 27°37'40"E; 15.–30.06.2015; TWT (on dead *Betula pendula* with *Fomes fomentarius*); IS leg.; • ♂; Agusalu NR; 59°07'10"N, 27°34'39"E; 29.07.–14.08.2015; TWT (on dead *Betula pendula* with *Fomes fomentarius*); IS leg. **Tartumaa** • ♂; Välgi NR; 58°33'48"N, 26°52'38"E; 30.04.–14.05.2015; TWT (on *Populus tremula*); IS leg.; • ♂; Padakõrve NR; 58°35'07"N, 27°01'09"E; 30.04.–14.05.2015; TWT (on dead *Pinus sylvestris*); IS leg.; • ♂; Rootsiküla; 58°37'14"N, 27°10'47"E;

06.–24.06.2009; TWT (on dead *Salix caprea*); IS leg.; • ♂♂; Vorbuse, Lokaatorite tee; 58°25'27"N, 26°35'47"E; 30.04.–14.05.2023, 14.07.–02.08.2023, 02.08.–16.08.2023, 16.08.–30.08.2023, 30.08.–16.09.2023, 18.09.–01.10.2023, 01.10.–15.10.2023; MT; OK leg. **Valgamaa** • ♂; Soontaga; 58°00'03"N, 26°05'31"E; 05.06.–06.07.2015; TWT (on *Acer platanoides*); IS leg.; • ♂♂; Soontaga NR; 58°00'23"N, 26°03'19"E; 27.04.–13.05.2015, 29.05.–13.06.2015, 14.–28.07.2015; TWT (on dead *Picea abies*); IS leg.; • ♂; Koiva wooded meadow; 57°41'21"N, 26°11'08"E; 01.–17.08.2013; TWT (on dead *Quercus robur*); IS leg.; • ♂♂; Koivakonnu; 57°35'27"N, 26°19'40"E; 14.05.–03.06.2013, 03.–16.06.2013, 16.06.–02.07.2013, 02.–17.07.2013; TWT (on dead *Betula pendula* with *Fomes fomentarius*); IS leg.; • ♂♂; Koivakonnu; 57°35'28"N, 26°19'21"E; 14.05.–03.06.2013, 16.06.–02.07.2013, 17.08.–01.09.2013; TWT (on dead *Quercus robur*); IS leg. **Võrumaa** • ♂; Piusa PL; 57°47'28"N, 27°21'57"E; 18.05.–19.06.2017; TWT (on burned *Pinus sylvestris*); IS leg.; • ♂; Piusa PL; 57°47'33"N, 27°21'57"E; 19.06.–23.07.2017; TWT (on burned *Pinus sylvestris*); IS leg.

**Comments.** Holarctic species (Wagner 2018; Ježek et al. 2020, 2021a, b).

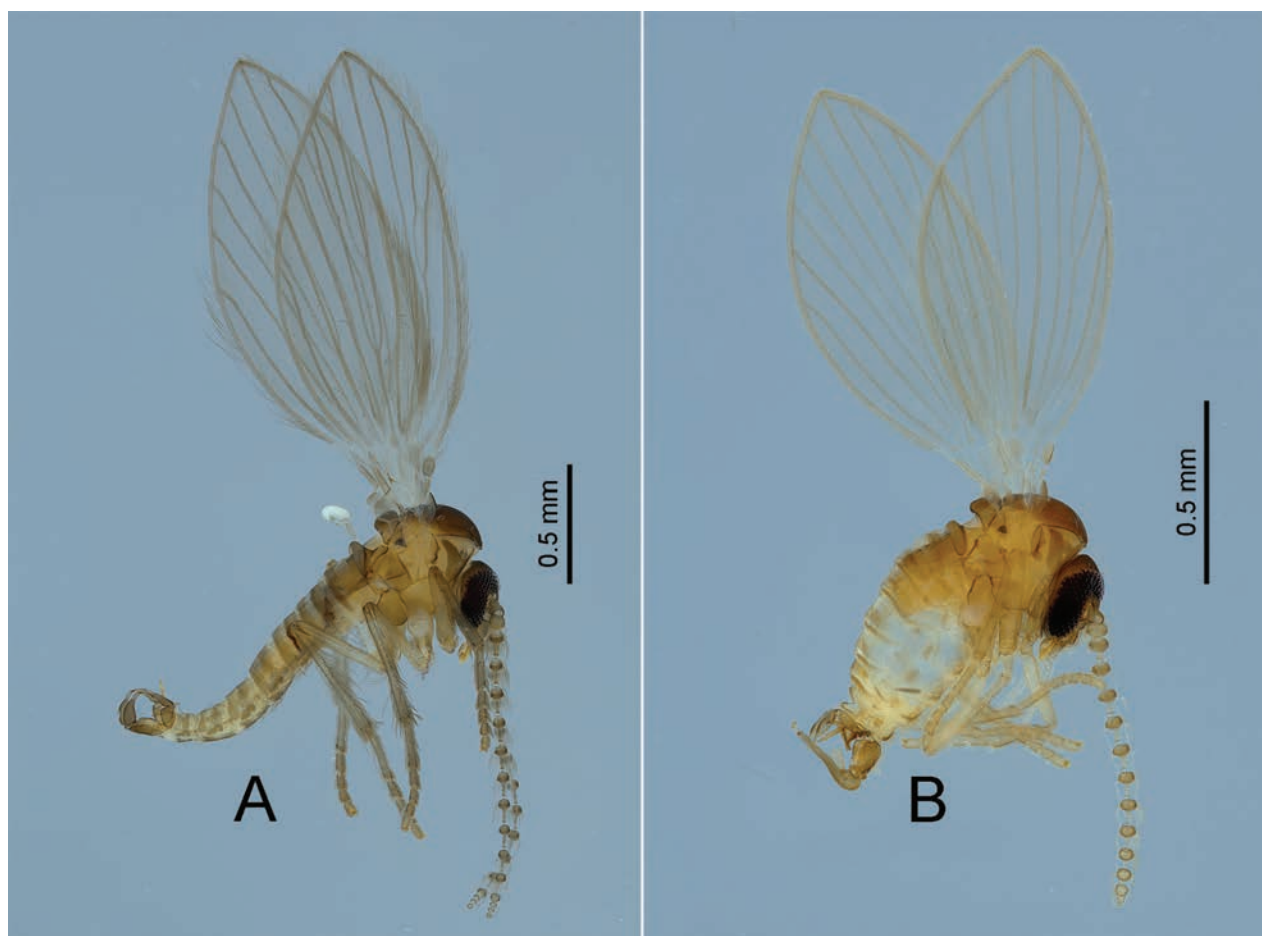
### \*31. *Psychodocha cinerea* (Banks, 1894)

Fig. 3A

**Material examined.** **Saaremaa** • ♂; Ruhnu Island; 57°47'46"N, 23°16'17"E; 06.08.–04.09.2012; TWT (on *Pinus sylvestris*); IS leg.; • ♂; Ruhnu Island; 57°47'54"N, 23°15'26"E; 06.08.–04.09.2012; TWT (on *Pinus sylvestris*); IS leg.; • ♂; Ruhnu Island; 57°48'01"N, 23°14'38"E; 07.08.–05.09.2012; TWT (on *Acer platanoides*); IS leg.; • ♂; Ruhnu Island; 57°48'06"N, 23°13'58"E; 07.08.–05.09.2012; TWT (on *Sorbus intermedia* with *Laetiporus sulphureus* (Bull.) Murrill); IS leg.; • ♂; Ruhnu Island; 57°48'09"N, 23°14'29"E; 07.08.–05.09.2012; TWT (on *Corylus avellana*); IS leg.; • ♂; Ruhnu Island; 57°48'10"N, 23°14'24"E; 10.07.–07.08.2012; TWT (on *Fraxinus excelsior*); IS leg.; • ♂; Ruhnu Island; 57°48'15"N, 23°14'32"E; 07.08.–05.09.2012; TWT (on *Acer platanoides*); IS leg.; • ♂; Ruhnu Island; 57°48'16"N, 23°16'06"E; 06.08.–04.09.2012; TWT (on dead *Pinus sylvestris*); IS leg.; • ♂; Ruhnu Island; 57°48'20"N, 23°14'33"E; 07.08.–05.09.2012; TWT (on dead *Alnus glutinosa*); IS leg.; • ♂; Ruhnu Island; 57°48'24"N, 23°15'16"E; 07.08.–05.09.2012; TWT (on dead *Salix caprea*); IS leg.; • ♂♂; Ruhnu Island, Korsi farm; 57°48'27"N, 23°14'32"E; 10.07.–07.08.2012; 07.08.–05.09.2012; TWT (on *Corylus avellana*); IS leg.; • ♂; Ruhnu Island, Limo seashore; 57°47'54"N, 23°16'18"E; 06.08.–04.09.2012; TWT (on dead *Pinus sylvestris*); IS leg.; • ♂; Ruhnu Island; 57°48'08"N, 23°15'49"E; 06.08.–04.09.2012; TWT (on dead *Picea abies* with *Fomitopsis pinicola*); IS leg. **Läänemaa** • ♂; Vormsi Island; 59°00'17"N, 23°10'58"E; 03.08.–01.09.2012; TWT (on dead *Picea abies*); IS leg.; • ♂♂; Vormsi Island; 59°01'20"N, 23°08'13"E; 09.05.–04.06.2012, 03.08.–01.09.2012; TWT (on dead *Alnus glutinosa*); IS leg.; • ♂; Vormsi Island; 58°59'26"N, 23°11'51"E; 08.05.–04.06.2012; TWT (on dead *Salix fragilis*); IS leg.; • ♂♂; Vormsi Island; 59°01'01"N, 23°12'18"E; 06.07.–03.08.2012, 03.08.–01.09.2012; TWT (on *Pinus sylvestris*); IS leg. **Pärnumaa** • ♂; Matsalu NP; 58°42'41"N, 23°41'19"E; 29.05.–17.06.2009; TWT (on *Populus tremula*); IS leg.; • ♂♂; Kihnu Island; 58°08'07"N, 23°58'20"E; 06.08.–13.09.2011, 09.08.–08.09.2012; TWT (on *Pinus sylvestris* with *Phellinus pini*); IS leg.; • ♂; Kihnu Island; 58°08'16"N, 23°58'24"E; 06.08.–13.09.2011; TWT (on dead *Pinus sylvestris*); IS leg.; • ♂; Kihnu Island; 58°08'28"N,

23°58'47"E; 11.06.–12.07.2012; TWT (on *Pinus sylvestris*); IS leg.; • ♂; Luitemaa NR near Vöiste; 58°12'21"N, 24°29'36"E; 23.06.–25.07.2017; TWT (on burned *Pinus sylvestris*); IS leg.; • ♂; Laulaste NR; 57°59'41"N, 24°32'16"E; 17.06.–03.07.2013; TWT (on dead *Picea abies* with *Fomitopsis pinicola*); IS leg.; • ♂♂; Laulaste NR; 57°59'23"N, 24°33'15"E; 17.06.–03.07.2013, 03.–18.07.2013, 02.–18.08.2013; TWT (on dead *Pinus sylvestris*); IS leg.; • ♂♂; Laulaste NR; 57°59'35"N, 24°33'35"E; 04.–17.06.2013, 03.–18.07.2013, 02.–18.08.2013; TWT (on *Betula pendula*); IS leg.; • ♂; Kalita NR, 58°04'15"N, 24°51'37"E; 25.07.–24.08.2017; TWT (on *Populus tremula*); IS leg. **Harjumaa** • ♂; Põhja-Kõrvemaa NR; 59°25'30"N, 25°39'11"E; 16.06.–01.07.2015; TWT (on dead *Pinus sylvestris*); IS leg. **Lääne-Virumaa** • ♂♂; near Lasila, forest patch No 104; 59°16'43"N, 26°17'07"E; 30.05.–02.07.2015, 12.–30.05.2015, 02.07.–02.08.2015; MT; OK leg.; • ♂♂; near Lasila, forest patch No 24; 59°16'27"N, 26°11'44"E; 30.05.–02.07.2015, 02.–24.08.2015; MT; OK leg.; • ♂♂; near Lasila, forest patch No 31; 59°15'48"N, 26°14'17"E; 12.–30.05.2015, 02.07.–02.08.2015, 02.–24.08.2015, 24.08.–20.09.2015; MT; OK leg.; • ♂♂; near Lasila, forest patch No 50; 59°16'25"N, 26°14'02"E; 02.08.–24.08.2015, 24.08.–20.09.2015; MT; OK leg.; • ♂; near Lasila, forest patch No 52; 59°16'20"N, 26°13'52"E; 26.09.–27.10.2016; MT; OK leg.; • ♂♂; near Lasila, forest patch No 6; 59°15'41"N, 26°12'32"E; 12.–30.05.2015, 29.08.–26.09.2016; MT; OK leg.; • ♂; near Lasila, forest patch No 7; 59°15'33"N, 26°12'41"E; 02.07.–02.08.2015; MT; OK leg.; • ♂; near Lasila, forest patch No 75; 59°16'49"N, 26°13'05"E; 12.–30.05.2015; MT; OK leg.; • ♂; near Lasila, forest patch No 79; 59°16'37"N, 26°13'22"E; 02.07.–02.08.2015; MT; OK leg. **Ida-Virumaa** • ♂; Muraka NR; 59°10'50"N, 27°09'44"E; 27.07.–29.08.2017; TWT (on dead *Populus tremula*); IS leg.; • ♂; Kurtna PL; 59°18'22"N, 27°33'53"E; 29.07.–14.08.2015; TWT (on dead *Pinus sylvestris*); IS leg.; • ♂; Agusalu NR; 59°02'16"N, 27°39'35"E; 14.08.–01.09.2015; TWT (on dead *Pinus sylvestris*); IS leg.; • ♂♂; Agusalu NR; 59°02'17"N, 27°39'40"E; 15.–29.07.2015, 29.07.–14.08.2015; TWT (on dead *Pinus sylvestris*); IS leg.; • ♂; Agusalu NR; 59°02'15"N, 27°39'42"E; 15.–30.06.2015; TWT (on dead *Betula pendula*); IS leg. **Jõgevamaa** • ♂♂; Kääpa NR; 58°38'58"N, 26°51'12"E; 15.–30.06.2013, 31.07.–15.08.2013; TWT (on dead *Pinus sylvestris*); IS leg. **Tartumaa** • ♂♂; Välgi NR; 58°33'48"N, 26°52'38"E; 14.05.–30.05.2015, 29.07.–14.08.2015; TWT (on *Populus tremula*); IS leg.; • ♂; Padakõrve NR; 58°36'08"N, 26°58'09"E; 31.07.–15.08.2013; TWT (on *Picea abies*); IS leg.; • ♂; Padakõrve NR; 58°35'38"N, 26°57'52"E; 15.08.–04.09.2013; TWT (on dead *Pinus sylvestris*); IS leg.; • ♂♂; Padakõrve NR; 58°35'07"N, 27°01'09"E; 14.05.–30.05.2015, 14.08.–01.09.2015; TWT (on dead *Pinus sylvestris*); IS leg.; • ♂♂; Vorbuse, Lo-kaatorite tee; 58°25'27"N, 26°35'47"E; 14.05.–29.05.2023, 25.06.–14.07.2023, 02.08.–16.08.2023, 16.08.–30.08.2023, 08.–16.09.2023, 18.09.–01.10.2023, 01.10.–15.10.2023, 15.10.–29.10.2023; MT; OK leg. **Põlvamaa** • ♂; Ihamaru NR; 58°06'09"N, 26°55'59"E; 27.04.–13.05.2015; TWT (on dead *Betula pendula* with *Fomes fomentarius*); IS leg. **Valgamaa** • ♂; Soontaga; 58°00'04"N, 26°05'11"E; 05.06.–06.07.2015; TWT (on dead *Betula pendula* with *Fomes fomentarius*); IS leg.; • ♂; Koiva wooded meadow; 57°41'26"N, 26°11'06"E; 17.08.–01.09.2013; TWT (on *Quercus robur*); IS leg.; • ♂; Koivakonnu; 57°35'27"N, 26°19'40"E; 14.05.–03.06.2013; TWT (on dead *Betula pendula* with *Fomes fomentarius*); IS leg.; • ♂♂; Koivakonnu; 57°35'28"N, 26°19'21"E; 16.06.–02.07.2013, 01.–17.08.2013; TWT (on dead *Quercus robur*); IS leg.

**Comments.** Cosmopolitan species (Ježek and Yağci 2005; Afzan and Belqat 2016; Ježek et al. 2020, 2021a, 2023b).



**Figure 3.** Lateral habitus of Estonian moth flies: the tribe Psychodini **A** *Psychodocha cinerea* (Banks, 1894) **B** *Psychodula minuta* (Banks, 1894).

**\*32. *Psychodocha gemina* (Eaton, 1904)**

**Material examined.** **Saaremaa** • ♂; Ruhnu Island, near Korsi farm; 57°48'28"N, 23°14'32"E; 03.08.–11.09.2011; TWT (on dead *Fraxinus excelsior*); IS leg. **Lääne-maa** • ♂; Vormsi Island, Suuremõisa Park; 58°59'30"N, 23°11'34"E; 06.07.–19.07.2011; TWT (on *Quercus robur*); IS leg.; • ♂; Puise; 58°47'45"N, 23°31'22"E; 11.07.–14.08.2009; TWT (on old *Betula pendula*); IS leg.; • ♂; Puise; 58°47'41"N, 23°31'28"E; 17.06.–11.07.2009; TWT (on dead *Alnus incana* with *Fomitopsis pini-cola*); IS leg. **Pärnumaa** • ♂; Riimaru; 58°16'18"N, 25°11'02"E; 13.07.–03.08.2005; TWT (on dead *Betula pendula* with *Fomes fomentarius*); IS leg. **Lääne-Virumaa** • ♂; Lahemaa NP, near Laukasoo; 59°28'49"N, 25°54'24"E; 23.05.–23.06.2017; TWT (on dead *Populus tremula*); IS leg.; • ♂♂; near Lasila, forest patch No 104; 59°16'43"N, 26°17'07"E; 20.09.–21.10.2015, 28.07.–29.08.2016; MT, OK leg.; • ♂♂; near Lasila, forest patch No 24; 59°16'27"N, 26°11'44"E; 05.–31.05.2016, 31.05.–28.06.2016, 28.07.–29.08.2016; MT; OK leg.; • ♂; near Lasila, forest patch No 31; 59°15'48"N, 26°14'17"E; 31.05.–28.06.2016; MT; OK leg.; • ♂♂; near Lasila, forest patch No 50; 59°16'25"N, 26°14'02"E; 05.–31.05.2016, 31.05.–28.06.2016, 28.06.–28.07.2016, 29.08.–26.09.2016; MT; OK leg.; • ♂; near Lasila, forest patch No 52; 59°16'20"N, 26°13'52"E; 29.08.–26.09.2016; MT; OK leg.; • ♂; near Lasila, forest patch No 6; 59°15'41"N, 26°12'32"E;

28.07.–29.08.2016; MT; OK leg.; • ♂; near Lasila, forest patch No 7; 59°15'33"N, 26°12'42"E; 29.08.–26.09.2016; MT; OK leg.; • ♂; near Lasila, forest patch No 75; 59°16'49"N, 26°13'05"E; 05.–31.05.2016, 28.07.–29.08.2016; MT; OK leg.; • ♂♂; near Lasila, forest patch No 79; 59°16'37"N, 26°13'22"E; 05.–31.05.2016, 28.06.–28.07.2016, 28.07.–29.08.2016, 29.08.–26.09.2016; MT; OK leg.; • ♂; Tudusoo NR; 59°04'47"N, 26°45'38"E; 27.07.–29.08.2017; TWT; IS leg. **Ida-Virumaa** • ♂; Muraka NR; 59°05'22"N, 27°09'18"E; 30.04.–14.05.2015; TWT (on dead *Picea abies*); IS leg. **Jõgevamaa** • ♂; Kääpa NR; 58°38'58"N, 26°51'12"E; 15.07.–31.07.2013; TWT (on dead *Pinus sylvestris*); IS leg. **Tartumaa** • ♂; Padakõrve NR; 58°35'07"N, 27°01'09"E; 15.06.–30.06.2015; TWT (on dead *Pinus sylvestris*); IS leg.; • ♂; Rootsiküla; 58°37'14"N, 27°10'47"E; 10.05.–06.06.2009; TWT (on dead *Salix caprea*); IS leg.; • ♂♂; Vorbuse, Lokaatorite tee; 58°25'27"N, 26°35'47"E; 30.04.–14.05.2023, 14.05.–29.05.2023, 10.06.–25.06.2023; MT; OK leg. **Põlvamaa** • ♂; Ihamaru NR; 58°06'11"N, 26°55'55"E; 13.–31.08.2015; TWT (on dead *Betula pendula*); IS leg. **Valgamaa** • ♂♂; Soontaga; 58°00'03"N, 26°05'31"E; 11.05.–05.06.2015, 05.06.–06.07.2015, 06.07.–03.08.2015; TWT (on *Acer platanoides*); IS leg.; • ♂; Soontaga NR; 58°01'19"N, 26°04'01"E; 28.07.–31.08.2015; TWT (on old *Quercus robur*); IS leg.; • ♂; Koiva wooded meadow; 57°41'26"N, 26°11'06"E; 14.05.–03.06.2013; TWT (on *Quercus robur*); IS leg.; • ♂; Koiva wooded meadow; 57°41'21"N, 26°11'08"E; 16.06.–02.07.2013; TWT (on dead *Quercus robur*); IS leg.; • ♂; Koivakonnu; 57°35'28"N, 26°19'21"E; 17.08.–01.09.2013; TWT (on dead *Quercus robur*); IS leg.

**Comments.** European and Transcaucasian species (Ježek et al. 2019, 2020, 2021a).

### \*33. *Psychodula minuta* (Banks, 1894)

Fig. 3B

**Material examined.** **Pärnumaa** • ♂; Kihnu Island; 58°07'49"N, 24°00'15"E; 22.05.–11.06.2012; TWT (on *Quercus robur*); IS leg.; • ♂; Laulaste NR; 57°59'23"N, 24°33'15"E; 18.–31.08.2013; TWT (on dead *Pinus sylvestris*); IS leg.; • ♂; Laulaste NR; 57°59'49"N, 24°33'30"E; 17.06.–03.07.2013; TWT (on *Pinus sylvestris*); IS leg.; • ♂; Laulaste NR; 57°59'35"N, 24°33'35"E; 18.07.–02.08.2013; TWT (on *Betula pendula*); IS leg. **Lääne-Virumaa** • ♂; near Lasila, forest patch No 104; 59°16'43"N, 26°17'07"E; 29.08.–26.09.2016; MT; OK leg.; • ♂; near Lasila, forest patch No 31; 59°15'48"N, 26°14'17"E; 20.09.–21.10.2015; MT; OK leg.; • ♂; near Lasila, forest patch No 50; 59°16'25"N, 26°14'02"E; 28.07.–29.08.2016; MT; OK leg.; • ♂♂; near Lasila, forest patch No 79; 59°16'37"N, 26°13'22"E; 12.–30.05.2015, 20.09.–21.10.2015; MT; OK leg. **Ida-Virumaa** • ♂; Agusalu NR; 59°02'16"N, 27°39'35"E; 30.05.–15.06.2015; TWT (on dead *Pinus sylvestris*); IS leg.; • ♂; Agusalu NR; 59°02'17"N, 27°39'40"E; 29.07.–14.08.2015; TWT (on dead *Pinus sylvestris*); IS leg. **Jõgevamaa** • ♂; Kääpa NR; 58°38'58"N, 26°51'12"E; 15.–31.07.2013; TWT (on dead *Pinus sylvestris*); IS leg.; • ♂; Kääpa NR; 58°39'01"N, 26°51'09"E; 15.08.–04.09.2013; TWT (on *Pinus sylvestris*); IS leg. **Valgamaa** • ♂; Soontaga; 58°00'03"N, 26°05'31"E; 05.06.–06.07.2015; TWT (on *Acer platanoides*); IS leg.

**Comments.** Holarctic species (Ježek et al. 2019, 2020, 2023b).

**\*34. *Tinearia alternata* (Say, 1824)**

**Material examined.** Saaremaa • ♀; Ruhnu Island; 57°48'20"N, 23°14'33"E; 07.08.–05.09.2012; TWT (on dead *Alnus glutinosa*); IS leg. Läänemaa • ♀; Vormsi Island; 58°58'33"N, 23°12'10"E; 03.08.–01.09.2012; TWT (on dead *Betula pendula*); IS leg. Pärnumaa • ♀; Kihnu Island, Lemsi; 58°07'49"N, 24°00'15"E; 06.08.–13.09.2011; TWT (on old *Quercus robur*); IS leg.; • ♀; Kihnu Island; 58°08'28"N, 23°58'47"E; 12.07.–09.08.2012; TWT (on *Pinus sylvestris*); IS leg.; • ♂♀; Riimaru; 58°16'18"N, 25°11'02"E; 03.–17.08.2005, 31.07.–02.09.2006; TWT (on *Populus tremula*); IS leg. Tartumaa • ♂; Tartu, Aardla 124; 58°21'10"N, 26°41'08"E; 13.05.2016; hand picked; T. Kesküla leg.

**Comments.** Cosmopolitan species (Ježek et al. 2019, 2020, 2023b).

**\*35. *Ypsydocha setigera* (Tonnoir, 1922)**

**Material examined.** Lääne-Virumaa • ♀; near Lasila, forest patch No 50; 59°16'25"N, 26°14'02"E; 28.07.–29.08.2016; MT; OK leg.; INS 33821.

**Comments.** A very common Holarctic species (Ježek and Omelková 2012).

**Pericomaini**

**\*36. *Clytocerus (Boreoclytocerus) longicorniculatus* Krek, 1987**

**Material examined.** Lääne-Virumaa • ♂; near Lasila, forest patch No 79; 59°16'37"N, 26°13'22"E; 12.–30.05.2015; MT; OK leg.

**Comments.** A species known only from Europe (Ježek et al. 2020). Important species for nature conservation, assessed as nationally scarce in the Czech Republic.

**37. *Clytocerus (Boreoclytocerus) ocellaris* (Meigen, 1804)**

Fig. 4B

**Published record.** Salmela and Piirainen (2005): 304.

**Material examined.** Saaremaa • ♂♂; Ruhnu Island, Holma; 57°48'02"N, 23°13'42"E; 29.06.–02.08.2011, 07.08.–05.09.2012; TWT (on old *Ulmus laevis* with *Polyporus squamosus*); IS leg.; • ♂; Ruhnu Island, near Korsi farm; 57°48'28"N, 23°14'32"E; 03.08.–11.09.2011; TWT (on dead *Fraxinus excelsior*); IS leg.; • ♂; Ruhnu Island; 57°48'15"N, 23°14'32"E; 07.08.–05.09.2012; TWT (on *Acer platanoides*); IS leg.; • ♂; Ruhnu Island; 57°48'24"N, 23°15'16"E; 07.08.–05.09.2012; TWT (on dead *Salix caprea*); IS leg. Läänemaa • ♂; Vormsi Island, Suuremõisa park; 58°59'30"N, 23°11'34"E; 06.07.–03.08.2012; TWT (on *Quercus robur*); IS leg.; • ♂; Vormsi Island; 59°01'01"N, 23°12'18"E; 03.08.–01.09.2012; TWT (on *Pinus sylvestris*); IS leg. Pärnumaa • ♂; Kihnu Island; 58°06'59"N, 23°59'38"E; 12.07.–09.08.2012; TWT (on old *Quercus robur*); IS leg.; • ♂; Kihnu Island; 58°07'49"N, 24°00'15"E; 22.05.–11.06.2012; TWT (on old *Quercus robur*); IS leg.; • ♂♂; Matsalu NP; 58°42'41"N, 23°41'19"E; 29.05.–17.06.2009, 11.07.–14.08.2009; TWT (on *Populus tremula*); IS leg.;

• ♂; Matsalu NP; 58°42'52"N, 23°41'23"E; 11.07.–14.08.2009; TWT (on dead *Populus tremula*); IS leg.; • ♂; Puhtu; 58°33'31"N, 23°33'08"E; 18.06.–10.07.2009; TWT (on dead *Picea abies*); IS leg.; • ♂; Sookuninga NR; 58°00'08"N, 24°52'38"E; 21.05.–22.06.2017; TWT (on dead *Populus tremula*); IS leg. **Harjumaa** • ♂; Mähuste near Koitjärve; 59°24'55"N, 25°36'45"E; 30.07.–15.08.2015; TWT (on dead *Betula pendula*); IS leg. **Lääne-Virumaa** • ♂♂; near Lasila, forest patch No 24; 59°16'27"N, 26°11'44"E; 24.08.–20.09.2015, 05.–31.05.2016, 28.07.–29.08.2016, 29.08.–26.09.2016, 26.09.–27.10.2016; MT; OK leg.; • ♂♂; near Lasila, forest patch No 31; 59°15'48"N, 26°14'17"E; 12.–30.05.2015, 02.07.–02.08.2015, 24.08.–20.09.2015, 28.07.–29.08.2016, 26.09.–27.10.2016; MT; OK leg.; • ♂♂; near Lasila, forest patch No 50; 59°16'25"N, 26°14'02"E; 12.05.–30.05.2015, 29.08.–26.09.2016; MT; OK leg.; • ♂♂; near Lasila, forest patch No 52; 59°16'20"N, 26°13'52"E; 28.07.–29.08.2016, 29.08.–26.09.2016; MT; OK leg.; • ♂♂; near Lasila, forest patch No 6; 59°15'41"N, 26°12'32"E; 28.07.–29.08.2016, 29.08.–26.09.2016; MT; OK leg.; • ♂♂; near Lasila, forest patch No 75; 59°16'49"N, 26°13'05"E; 12.–30.05.2015, 20.09.–21.10.2015, 05.–31.05.2016, 28.07.–29.08.2016; MT; OK leg.; • ♂♂; near Lasila, forest patch No 79; 59°16'37"N, 26°13'22"E; 02.–24.08.2015, 24.08.–20.09.2015, 05.–31.05.2016, 31.05.–28.06.2016, 28.06.–28.07.2016; MT; OK leg.; • ♂; Suigu NR; 59°09'01"N, 26°49'08"E; 26.07.–29.08.2017; TWT (on *Populus tremula*); IS leg.; • ♂; Suigu NR; 59°09'11"N, 26°49'10"E; 26.07.–29.08.2017; TWT (on dead *Populus tremula*); IS leg.; INS 33808; • ♂; Tudusoo NR; 59°04'47"N, 26°45'38"E; 27.07.–29.08.2017; TWT (on *Populus tremula*); IS leg.; • ♂; Tudusoo NR; 59°04'53"N, 26°46'15"E; 26.07.–29.08.2017; TWT (on *Populus tremula*); IS leg. **Ida-Virumaa** • ♂; Muraka NR; 59°10'50"N, 27°09'44"E; 25.05.–26.06.2017; TWT (on *Populus tremula*); IS leg. **Tartumaa** • ♂; Rootsiküla; 58°37'14"N, 27°10'47"E; 15.07.–02.08.2009; TWT (on dead *Salix caprea*); IS leg. **Valgamaa** • ♂♂; Soontaga; 58°00'04"N, 26°05'15"E; 05.06.–06.07.2015, 03.–31.08.2015; TWT (on dead *Betula pendula*); IS leg.; • ♂♂; Soontaga; 58°00'04"N, 26°05'11"E; 07.05.–05.06.2015, 05.06.–06.07.2015, 03.–31.08.2015; TWT (on dead *Betula pendula* with *Fomes fomentarius*); IS leg.; • ♂♂; Soontaga; 58°00'01"N, 26°05'10"E; 19.05.–05.06.2015, 06.07.–03.08.2015; TWT (on dead *Populus tremula*); IS leg.; • ♂♂; Koiva wooded meadow; 57°41'21"N, 26°11'12"E; 02.–17.07.2013, 17.08.–01.09.2013; TWT (on dead *Populus tremula*); IS leg.; • ♂; Koiva wooded meadow; 57°41'19"N, 26°10'59"E; 14.05.–03.06.2013; TWT (on dead *Quercus robur*); IS leg.; • ♂; Koivakonu; 57°35'27"N, 26°19'40"E; 14.05.–03.06.2013; TWT (on dead *Betula pendula* with *Fomes fomentarius*); IS leg.

**Comments.** European species (Ježek et al. 2019, 2020; Morelli and Biscaccianti 2021).

### \*38. *Clytocerus (Boreoclytocerus) splendidus* Ježek & Hájek, 2007

**Material examined.** **Saaremaa** • ♂; Ruhnu Island; 57°48'01"N, 23°14'38"E; 07.08.–05.09.2012; TWT (on *Acer platanoides*); IS leg.; • ♂; Ruhnu Island; 57°48'06"N, 23°13'58"E; 07.08.–05.09.2012; TWT (on *Sorbus intermedia* with *Laetiporus sulphureus*); IS leg.; • ♂; Ruhnu Island; 57°48'09"N, 23°14'25"E; 07.08.–05.09.2012; TWT (on *Fraxinus excelsior*); IS leg.; • ♂; Ruhnu Island;

57°48'10"N, 23°14'24"E; 07.08.–05.09.2012; TWT (on *Fraxinus excelsior*); IS leg.; • ♂; Ruhnu Island, Holma; 57°48'02"N, 23°13'42"E; 07.06.–10.07.2012; TWT (on old *Ulmus laevis*); IS leg. **Läänemaa** • ♂♂; Vormsi Island, 58°59'26"N, 23°11'51"E; 08.05.–04.06.2012, 06.07.–03.08.2012; TWT (on *Salix fragilis*); IS leg.; • ♂; Vormsi Island; 59°01'20"N, 23°08'13"E; 09.05.–04.06.2012; TWT (on dead *Alnus glutinosa*); IS leg. **Pärnumaa** • ♂; Kihnu Island; 58°08'07"N, 23°58'20"E; 09.08.–08.09.2012; TWT (on *Pinus sylvestris* with *Phellinus pini*); IS leg. **Lääne-Virumaa** • ♂; near Lasila, forest patch No 24; 59°16'27"N, 26°11'44"E; 12.–30.05.2015; MT; OK leg.; • ♂♂; near Lasila, forest patch No 31; 59°15'48"N, 26°14'17"E; 12.–30.05.2015, 02.07.–02.08.2015, 02.–24.08.2015, 20.09.–21.10.2015; MT; OK leg.; • ♂; near Lasila, forest patch No 50; 59°16'25"N, 26°14'02"E; 24.08.–20.09.2015; MT; OK leg.; • ♂; near Lasila, forest patch No 75; 59°16'49"N, 26°13'05"E; 02.–24.08.2015; MT; OK leg. **Tartumaa** • ♂; Rootsiküla; 58°37'14"N, 27°10'47"E; 15.07.–02.08.2009; TWT (on dead *Salix caprea*); IS leg.; INS 33809. **Valgamaa** • ♂; Koiva wooded meadow; 57°41'21"N, 26°11'12"E; 17.07.–01.08.2013; TWT (on dead *Populus tremula*); IS leg.

**Comments.** Not common European species (Ježek et al. 2018, 2019; Kroča and Ježek 2019). Important species for nature conservation, assessed as nationally scarce in the Czech Republic.

### 39. *Clytocyclus (Boreoclytocyclus) tetracorniculatus* Wagner, 1977

**Published record.** Salmela and Piirainen (2005): 304.

**Comments.** Not common European species (Kroča and Ježek 2019). Important species for nature conservation, assessed as critically endangered in the Czech Republic.

### \*40. *Pericoma albomaculata* Wahlgren, 1904

**Note.** Junior synonymous name: *Pneumia rivularis* (Berdén, 1954), see Kvitte et al. (2020).

**Material examined.** **Saaremaa** • ♂; Ruhnu Island, near Korsi farm; 57°48'28"N, 23°14'32"E; 26.05.–28.06.2011; TWT (on dead *Fraxinus excelsior*); IS leg.; • ♂; Ruhnu Island; 57°47'59"N, 23°14'34"E; 07.06.–10.07.2012; TWT (on dead *Fraxinus excelsior*); IS leg.; • ♂; Ruhnu Island; 57°48'01"N, 23°14'38"E; 07.06.–10.07.2012; TWT (on *Acer platanooides*); IS leg.; • ♂; Ruhnu Island; 57°48'15"N, 23°14'32"E; 07.06.–10.07.2012; TWT (on *Acer platanooides*); IS leg. **Läänemaa** • ♂; Vormsi Island, Suuremõisa Park; 58°59'30"N, 23°11'34"E; 06.06.–06.07.2011; TWT (on old *Quercus robur*); IS leg. **Pärnumaa** • ♂; Matsalu NP, 58°42'41"N, 23°41'19"E; 11.07.–14.08.2009; TWT (on *Populus tremula*); IS leg.; • ♂; Kalita NR; 58°04'15"N, 24°51'37"E; 25.07.–24.08.2017; TWT (on *Populus tremula*); IS leg. **Lääne-Virumaa** • ♂♂; near Lasila, forest patch No 31; 59°15'48"N, 26°14'17"E; 12.–30.05.2015, 02.07.–02.08.2015; MT; OK leg.; • ♂; near Lasila, forest patch No 50; 59°16'25"N, 26°14'02"E; 12.–30.05.2015; MT; OK leg.; • ♂; near Lasila, forest patch No 79; 59°16'37"N, 26°13'22"E; 30.05.–02.07.2015; MT; OK leg.; • ♂; Tudusoo NR; 59°04'47"N, 26°45'38"E; 28.05.–25.06.2017; TWT;

IS leg.; ♂; Tudusoo NR; 59°04'53"N, 26°46'15"E; 27.05.–25.06.2017; TWT (on *Populus tremula*); IS leg.; INS 33781. **Ida-Virumaa** ♂; Muraka NR, Mädamänniku; 59°07'07"N, 27°13'08"E; 25.05.–26.06.2017; TWT (on dead *Populus tremula*); IS leg.; INS 33799.

**Comments.** We follow the latest formal interpretation of this species by Kvifte et al. (2020). However, we consider the synonymy provided above questionable. As addressing it is beyond the scope of this paper, we postpone a detailed discussion to a future work. A Palaearctic species (Ježek et al. 2019) assessed as endangered in Czech Republic, but found to be common in Finland (Salmela et al. 2007; Salmela 2008).

#### \*41. *Pneumia compta* (Eaton, 1893)

**Material examined.** **Lääne-Virumaa** ♂; near Lasila, forest patch No 79; 59°16'37"N, 26°13'22"E; 30.05.–02.07.2015; MT; OK leg. **Ida-Virumaa** ♂; Agusalu NR; 59°04'16"N, 27°37'40"E; 14.05.–30.05.2015; TWT (on dead *Betula pendula* with *Fomes fomentarius*); IS leg.; INS 33805.

**Comments.** A Palaearctic species (Oboňa and Ježek 2014; Ježek et al. 2019; Morelli and Biscaccianti 2022). Important species for nature conservation, assessed as nationally scarce in the Czech Republic.

#### 42. *Pneumia mutua* (Eaton, 1893)

**Published record.** Salmela and Piirainen (2005): 304.

**Comments.** European species (Ježek et al. 2019).

#### \*43. *Pneumia nubila* (Meigen, 1818)

Fig. 4A

**Material examined.** **Saaremaa** ♂; Ruhnu Island; 57°47'59"N, 23°14'34"E; 26.05.–28.06.2011; TWT (on dead *Fraxinus excelsior*); IS leg.; ♂; Ruhnu Island; 57°48'15"N, 23°14'32"E; 07.08.–05.09.2012; TWT (on *Acer platanoides*); IS leg.; ♂; Ruhnu Island; 57°48'18"N, 23°14'27"E; 07.08.–05.09.2012; TWT (on *Quercus robur*); IS leg. **Läänemaa** ♂; Puise; 58°47'45"N, 23°31'22"E; 17.06.–11.07.2009; TWT (on old *Betula pendula*); IS leg. **Pärnumaa** ♂; Matsalu NP, 58°42'52"N, 23°41'23"E; 29.05.–17.06.2009; TWT (on dead *Populus tremula*); IS leg. **Harjumaa** ♂; Lahemaa NP, Palanselja; 59°32'44"N, 25°39'31"E; 26.07.–26.08.2017; TWT (on burned *Pinus sylvestris*); IS leg.; ♂; Põhja-Kõrve-maa NR; 59°25'30"N, 25°39'11"E; 15.05.–01.06.2015; TWT (on dead *Pinus sylvestris*); IS leg. **Lääne-Virumaa** ♂; Lahemaa NP, near Laukasoo; 59°28'49"N, 25°54'24"E; 25.07.–26.08.2017; TWT (on dead *Populus tremula*); IS leg. **Tartumaa** ♂; Elva-Vitipalu PL; 58°10'49"N, 26°25'14"E; 27.04.–13.05.2015; TWT (on dead *Picea abies*); IS leg.

**Comments.** Common European species (Ježek et al. 2019, 2020, 2021b), known also from Transcaucasia (Ježek et al. 2023a).

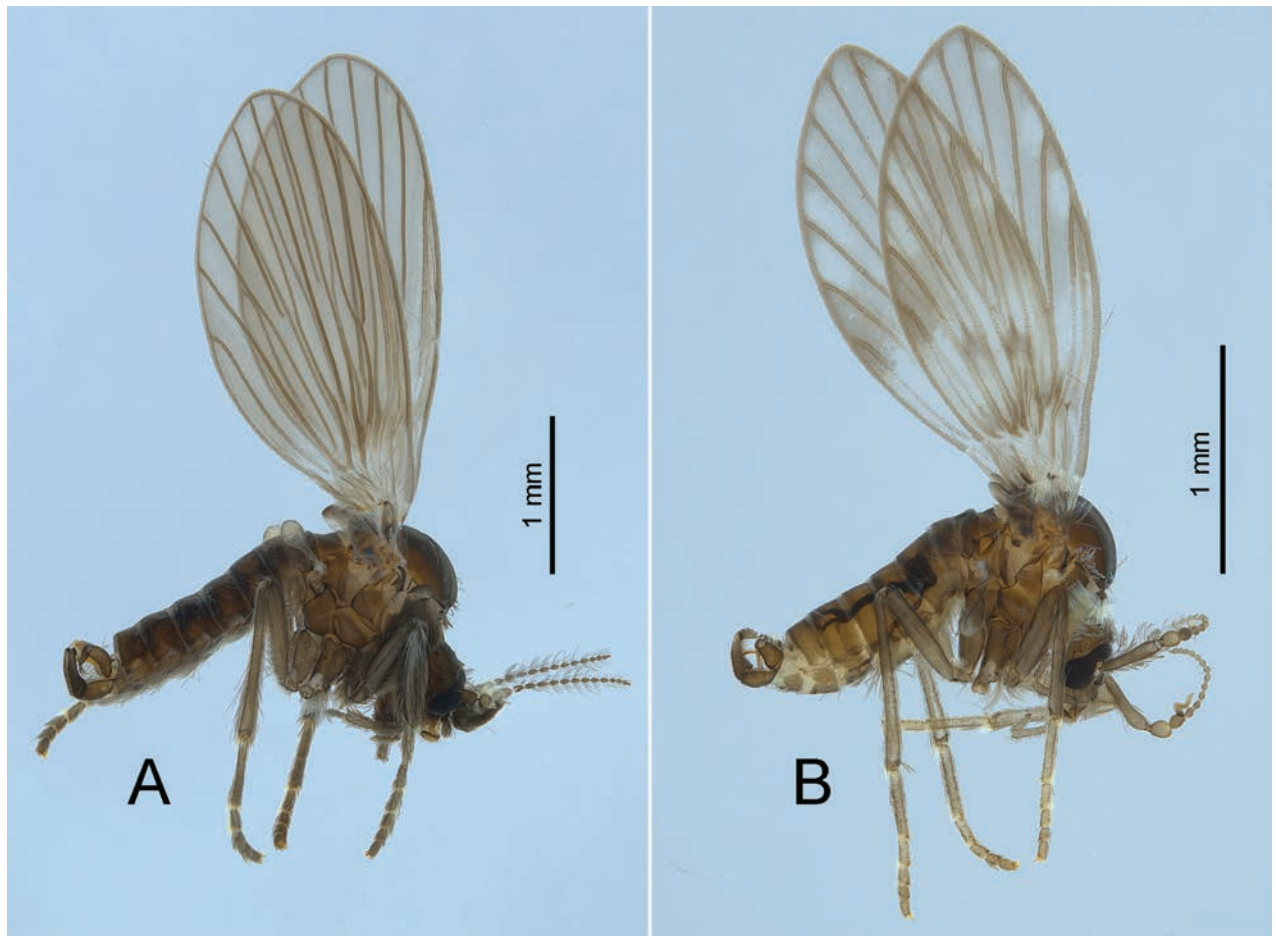


Figure 4. Lateral habitus of Estonian moth flies: the tribe Pericomaini **A** *Pneumia nubila* (Meigen, 1818) **B** *Clytocerus* (*Boreoclytocerus*) *ocellaris* (Meigen, 1804).

**\*44. *Pneumia trivialis* (Eaton, 1893)**

**Material examined.** **Saaremaa** • ♂♂; Ruhnu Island; 57°47'59"N, 23°14'34"E; 03.08.–11.09.2011, 07.08.–05.09.2012; TWT (on dead *Fraxinus excelsior*); IS leg. **Pärnumaa** • ♂; Matsalu NP; 58°42'41"N, 23°41'19"E; 29.05.–17.06.2009; TWT (on *Populus tremula*); IS leg. **Valgamaa** • ♂; Soontaga NR; 58°00'23"N, 26°03'19"E; 13.05.–29.05.2015; TWT (on dead *Picea abies*); IS leg.; • ♂; Soontaga NR; 58°01'19"N, 26°04'01"E; 29.05.–29.06.2015; TWT (on old *Quercus robur*); IS leg.

**Comments.** European and Transcaucasian species (Ježek et al. 2019, 2020, 2021a, 2023a).

**\*45. *Tonnoiriella nigricauda* (Tonnoir, 1919)**

**Material examined.** **Pärnumaa** • ♂; Matsalu NP; 58°42'41"N, 23°41'19"E; 29.05.–17.06.2009; TWT (on *Populus tremula*); IS leg. **Lääne-Virumaa** • ♂; near Lasila, forest patch No 79; 59°16'37"N, 26°13'22"E; 28.06.–28.07.2016; MT; OK leg.; INS 33791. **Valgamaa** • ♂; Soontaga; 58°00'04"N, 26°05'11"E; 05.06.–06.07.2015; TWT (on dead *Betula pendula* with *Fomes fomentarius*); IS leg.;

- ♂; Soontaga; 58°00'04"N, 26°05'15"E; 03.08.–31.08.2015; TWT (on dead *Betula pendula*); IS leg.;
- ♂; Soontaga; 58°00'03"N, 26°05'31"E; 06.07.–03.08.2015; TWT (on *Acer platanoides*); IS leg.

**Comments.** European species (Kvifte et al. 2011; Wagner 2018; Ježek et al. 2019). Important species for nature conservation, assessed as critically endangered in the Czech Republic.

## Discussion

Given the limited knowledge regarding moth fly diversity in the Baltic region, the discovery of 30 new country records in Estonia comes as no surprise. The majority of the recorded species (31 of 45; original data combined with Salmela and Piirainen (2005)) have been collected only from 1–3 localities (including 16 from a single locality), emphasizing the urgent need for further study. Conversely, seven recorded species are more widespread, having been collected from more than ten localities. Currently, a total of 71 species are documented in the Baltic countries (Table 1), while 63 species are known from Finland (including two of them marked as questionable; Salmela et al. 2014). The only species known from Latvia, *Clytocerus (B.) ocellaris*, is widely distributed in Europe as well as in the Nordic-Baltic region (Ježek and Goutner 1995).

When comparing the species lists of Lithuania, Estonia, and Finland, it is noteworthy that all countries have a remarkable proportion of unique species (Fig. 5). Considering this, it is highly likely that the number of species documented in Estonia will continue to increase. Eleven species, which are known to inhabit both Lithuania and Finland (as depicted in Fig. 3), could potentially also be found in Estonia, as there appear to be no apparent limits to their distribution. Interestingly, the genus *Ulomyia* Walker, 1856, which is known from three species in Lithuania, is absent from records in Estonia. It is possible that conducting more intensive research on the surrounding water ecosystems, including both flowing and standing water, could help fill this gap.

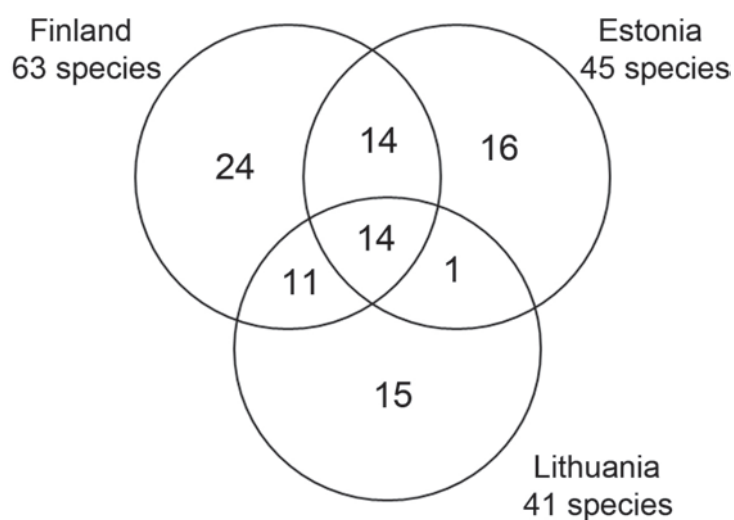


**Figure 5.** Comparison of the species diversity of moth flies in Estonia, Lithuania, and Finland. The numbers represent recorded species.

**Table 1.** An updated systematic list of the psychodids of the Baltic Countries. Lithuanian data are derived from Pakalniškis et al. (2006) and Latvian data from Salmela and Vartiija (2007).

Species	Estonia	Latvia	Lithuania
<i>Sycorax silacea</i> Haliday in Curtis, 1839	x		
<i>Trichomyia urbica</i> Haliday in Curtis, 1839	x*		
<i>Oomormia andrenipes</i> (Strobl, 1910)	x*		
<i>Lepimormia hemiboreale</i> Salmela & Piirainen, 2005	x		
<i>Promormia eatoni</i> (Tonnoir, 1940)	x*		
<i>Lepiseodina rothschildi</i> (Eaton, 1912)	x*		x
<i>Lepiseodina tristis</i> (Meigen, 1830)			x
<i>Panimerus albifacies</i> (Tonnoir, 1919)	x		
<i>Panimerus goetghebueri</i> (Tonnoir, 1919)			x
<i>Panimerus notabilis</i> (Eaton, 1893)	x*		
<i>Parajungiella consors</i> (Eaton, 1893)	x		x
<i>Parajungiella longicornis</i> (Tonnoir, 1919)	x*		
<i>Parajungiella pseudolongicornis</i> (Wagner, 1975)	x		
<i>Parajungiella serbica</i> (Krek, 1985)	x*		
<i>Paramormia (Paramormia) polyascoidea</i> (Krek, 1971)	x		
<i>Paramormia (Phyllotelmatoscopus) decipiens</i> (Eaton, 1893)			x
<i>Peripsychoda auriculata</i> (Haliday in Curtis, 1839)	x		
<i>Peripsychoda fusca</i> (Macquart, 1826)			x
<i>Psycmera integella</i> (Jung, 1956)			x
<i>Seoda britteni</i> (Tonnoir, 1940)			x
<i>Seoda carthusiana</i> (Vaillant, 1972)	x		
<i>Seoda gressica</i> (Vaillant, 1972)	x*		
<i>Seoda labeculosa</i> (Eaton, 1893)	x*		x
<i>Seoda morula</i> (Eaton, 1893)			x
<i>Feuerborniella obscura</i> (Tonnoir, 1919)	x		
<i>Philosepedon (Philosepedon) austriacum</i> Vaillant, 1974	x*		
<i>Philosepedon (Philosepedon) dumosum</i> Omelková & Ježek, 2012	x*		
<i>Philosepedon (Philosepedon) humerale</i> (Meigen, 1818)	x		x
<i>Philosepedon (Philothreticus) soljani</i> Krek, 1971	x*		
<i>Philosepedon (Trichosepedon) balkanicum</i> Krek, 1970	x*		
<i>Threticus lucifugus</i> (Walker, 1856)			x
<i>Trichopsychoda hirtella</i> (Tonnoir, 1919)	x*		
<i>Apsycha pusilla</i> (Tonnoir, 1922)			x
<i>Chodopsycha buxtoni</i> (Withers, 1988)	x*		
<i>Chodopsycha lobata</i> (Tonnoir, 1940)	x*		x
<i>Copropsychoda brevicornis</i> (Tonnoir, 1940)			x
<i>Logima albipennis</i> (Zetterstedt, 1850)	x		x
<i>Logima satchelli</i> (Quate, 1955)	x*		
<i>Logima sigma</i> (Kincaid, 1899)	x*		
<i>Psycha grisescens</i> (Tonnoir, 1922)			x
<i>Psychoda phalaenoides</i> (Linnaeus, 1758)	x		x

Species	Estonia	Latvia	Lithuania
<i>Psychodocha cinerea</i> (Banks, 1894)	x		x
<i>Psychodocha gemina</i> (Eaton, 1904)	x*		x
<i>Psychodula minuta</i> (Banks, 1894)	x*		x
<i>Tinearia alternata</i> (Say, 1824)	x*		x
<i>Ypsydocha setigera</i> (Tonnoir, 1922)	x*		x
<i>Berdeniella manicata</i> (Tonnoir, 1920)			x
<i>Clytocerus (Boreoclytocerus) longicorniculatus</i> Krek, 1987	x*		
<i>Clytocerus (Boreoclytocerus) ocellaris</i> (Meigen, 1804)	x	x	x
<i>Clytocerus (Boreoclytocerus) rivosus</i> (Tonnoir, 1919)			x
<i>Clytocerus (Boreoclytocerus) splendidus</i> Ježek & Hájek, 2007	x*		
<i>Clytocerus (Boreoclytocerus) tetracorniculatus</i> Wagner, 1977	x		
<i>Parabazarella subneglecta</i> (Tonnoir, 1922)			x
<i>Pericoma (Pachypericoma) blandula</i> Eaton, 1893			x
<i>Pericoma (Pericoma) albomaculata</i> Wahlgren, 1904	x*		
<i>Pericoma (Pericoma) diversa</i> Tonnoir, 1919			x
<i>Pericoma (Pericoma) trifasciata</i> (Meigen, 1804)			x
<i>Pneumia canescens</i> (Meigen, 1804)			x
<i>Pneumia cubitospinosa</i> (Jung, 1954)			x
<i>Pneumia compta</i> (Eaton, 1893)	x*		
<i>Pneumia extricata</i> (Eaton, 1893)			x
<i>Pneumia mutua</i> (Eaton, 1893)	x		x
<i>Pneumia nubila</i> (Meigen, 1818)	x*		x
<i>Pneumia palustris</i> (Meigen, 1804)			x
<i>Pneumia pilularia</i> (Tonnoir, 1940)			x
<i>Pneumia trivialis</i> (Eaton, 1893)	x*		
<i>Tonnoiriella nigricauda</i> (Tonnoir, 1919)	x*		
<i>Tonnoiriella pulchra</i> (Eaton, 1893)			x
<i>Ulomyia annulata annulata</i> (Tonnoir, 1919)			x
<i>Ulomyia cognata</i> (Eaton, 1893)			x
<i>Ulomyia fuliginosa</i> (Meigen, 1804)			x

\* indicates a new country-record.

Sixteen Estonian species have a conservation status in Central Europe, particularly in the Czech Republic, including six species (viz. *T. urbica*, *O. andrenipes*, *P. pseudolongicornis*, *P. serbica*, *C. (B.) tetracorniculatus*, *T. nigricauda*) classified as critically endangered, three (viz. *P. eatoni*, *P. albomaculata*, *S. labeculosa*) as endangered, and seven (viz. *L. rothschildi*, *P. (P.) soljani*, *Ch. buxtoni*, *C. (B.) longicorniculatus*, *C. (B.) splendidus*, *P. (P.) dumosum*, *P. compta*) as nationally scarce. However, one species, *P. albomaculata*, considered endangered in the Czech Republic has been found to be very common in aquatic environments in Finland (Salmela et al. 2007; Salmela 2008), highlighting the importance of sampling across a wide range of habitats. Nevertheless, given that a significant proportion of the studied material was collected from protected areas in Estonia, the knowledge regarding the potential conservation status of these species can be applied in the country's nature protection management.

## Acknowledgements

We would especially like to thank the editor and reviewers for providing constructive comments and for improving the manuscript.

## Additional information

### Conflict of interest

The authors have declared that no competing interests exist.

### Ethical statement

No ethical statement was reported.

## Funding

Jozef Oboňa was supported by the Slovak Research and Development Agency under the contract No. APVV-20-0140. Jan Ježek was supported by the Ministry of Culture of the Czech Republic (DKRVO 2024–2028/5.I.a, National Museum, 00023272). Olavi Kurina was supported by institutional research funding from the Ministry of Education and Research of Estonia and funding from the Estonian Research Council (TT14).

## Author contributions

Conceptualization: JO, OK. Data curation: JO, OK, IS. Investigation: JJ, JO, OK. Methodology: IS, OK, JO. Validation: JJ. Visualization: OK. Writing - original draft: OK, JO. Writing - review and editing: JJ, IS.

## Author ORCIDs

Jozef Oboňa  <https://orcid.org/0000-0002-1185-658X>

Olavi Kurina  <https://orcid.org/0000-0002-4858-4629>

Jan Ježek  <https://orcid.org/0000-0001-5993-4287>

## Data availability

All of the data that support the findings of this study are available in the main text.

## References

- Afzan H, Belqat B (2016) Faunistic and bibliographical inventory of the Psychodinae moth-flies of North Africa (Diptera, Psychodidae). *ZooKeys* 558: 119–145. <https://doi.org/10.3897/zookeys.558.6593>
- Evenhuis NL, Pape T, Pont AC, Thompson FC (2007) Biosystematic Database of World Diptera, Version 10. <http://www.diptera.org/biosys.htm> [accessed on 10 May 2024]
- IUCN (2024) The IUCN Red List of Threatened Species. Version 2024-1. <https://www.iucnredlist.org> [accessed on 14 October 2024]
- Jaume-Schinkel S, Morelli A, Kvifte GM, Mengual X (2022) What's inside the hole? A review of European dendrolimnetic moth flies (Diptera: Psychodidae: Psychodinae). *Diversity* 14(7): 532. <https://doi.org/10.3390/d14070532>
- Jaume-Schinkel S, Kvifte GM, Njunjić I, Schilthuizen M (2023) New records of moth flies (Diptera, Psychodidae) for the Dutch Fauna. *Biodiversity Data Journal* 11: e108636. <https://doi.org/10.3897/BDJ.11.e108636>

- Ježek J (1977) Reinstatement of the genus *Tinearia* Schellenberg (Diptera, Psychodidae). *Acta Entomologica Bohemoslovaca* 74: 232–241.
- Ježek J (1983) Contribution to the taxonomy of the genus *Logima* Eat. (Diptera, Psychodidae). *Acta Musei Nationalis Pragae* 41: 213–234.
- Ježek J (1984) Taxonomic notes on Mormiini (Diptera, Psychodidae) from the High Tatra National Park. *Acta Entomologica Bohemoslovaca* 81: 223–231.
- Ježek J (1985) Contribution to the knowledge of a new subtribe Trichopsychodina (Diptera, Psychodidae) from Czechoslovakia. *Acta Musei Nationalis Pragae* 40(2) (1984): 65–92.
- Ježek J (1990) Redescriptions of nine common palaeartic and holarctic species of Psychodini End. (Diptera: Psychodidae). *Acta Entomologica Musei Nationalis Pragae* 43: 33–83.
- Ježek J (1994) Catalogue of Holarctic and Afrotropical Mormiina End. (Diptera, Psychodidae, Psychodinae, Mormiini). *Časopis Národního Muzea, Řada přírodovědná* 162: 63–66.
- Ježek J (2005) Čeled' Psychodidae (koutulovití). In: Farkač J, Král D, Škorpík M (Eds) Červený seznam ohrožených druhů České republiky. Bezobratlí. Red list of threatened species in the Czech Republic. Invertebrates. Agentura ochrany přírody a krajiny ČR, Praha, 259–261.
- Ježek J (2007) New records of moth flies (Diptera, Psychodidae) from Poland with description of *Apsycha* gen. nov. *Acta Zoologica Universitatis Comenianae (Bratislava)* 47(2): 145–160.
- Ježek J, Omelková M (2007) Faunistic records from Czech Republic and Slovakia: Diptera, Psychodidae. *Acta Zoologica Universitatis Comenianae (Bratislava)* 47: 250–253.
- Ježek J, Omelková M (2012) Moth flies (Diptera: Psychodidae) of the Bílé Karpaty Protected Landscape Area and Biosphere Reserve (Czech Republic). In: Malenovský I, Kment P, Konvička O (Eds) Species inventories of selected insect groups in the Bílé Karpaty Protected Landscape Area and Biosphere Reserve (Czech Republic). *Acta Musei Moraviae Scientiae Biologicae, Brno*, 763–802.
- Ježek J, van Harten A (2005) Further new taxa and little-known species of non-biting moth flies (Diptera, Psychodidae) from Yemen. *Acta Entomologica Musei Nationalis Pragae* 45: 199–220.
- Ježek J, van Harten A (2009) Order Diptera, Family Psychodidae. Subfamily Psychodinae (non-biting moth flies). In: van Harten A. (Ed) *Arthropod Fauna of the United Arab Emirates, Vol. 2*. Dar Al Ummah Printing, Publishing, Distribution and Advertising, Abu Dhabi, 686–711.
- Ježek J, Yağci Ş (2005) Common non-biting moth flies (Insecta, Diptera, Psychodidae) new to the fauna of Turkey. *Acta Parasitologica Turcica* 29(3): 188–192.
- Ježek J, Vonička P, Preisler J (2008) Koutulovití (Diptera: Psychodidae) Jizerských hor a Frýdlantska. Psychodidae (Diptera) of the Jizerské hory Mts and Frýdlant region (northern Bohemia, Czech Republic). *Sborník Severočeského Muzea, Přírodní Vědy* 26: 129–151.
- Ježek J, Chvojka P, Manko P, Oboňa J (2017) Faunistic and bibliographical inventory of moth flies from Ukraine (Diptera, Psychodidae). *ZooKeys* 693: 109–128. <https://doi.org/10.3897/zookeys.693.13652>
- Ježek J, Grootaert P, Lock K, Manko P, Oboňa J (2018) Moth flies (Diptera: Psychodidae) from the Belgian transition of the Atlantic to the Central European faunal zones. *Biodiversity & Environment* 10(2): 5–17.

- Ježek J, Oboňa J, Příkryl I, Mikátová B (2019) Moth flies (Diptera: Psychodidae) of the western Hercynian mountains, Sokolov open-cast coal mines and dumps (Czech Republic). *Acta Musei Silesiae. Scientiae Naturales* 67(2018): 193–292. <https://doi.org/10.2478/cszma-2018-0015>
- Ježek J, Manko P, Oboňa J (2020) Synopsis of the Psychodidae (Diptera) fauna of Bulgaria. *Zootaxa* 4877(2): 201–240. <https://doi.org/10.11646/zootaxa.4877.2.1>
- Ježek J, Manko P, Oboňa J (2021a) Psychodidae (Diptera) of Azerbaijan and Georgia – faunistics with biodiversity notes. *ZooKeys* 1049: 15–42. <https://doi.org/10.3897/zookeys.1049.66063>
- Ježek J, Oboňa J, Manko P, Trýzna M (2021b) Moth flies (Diptera: Psychodidae) of the northern Hercynian Mountains and adjacent localities (Czech Republic). *Acta Musei Silesiae, Scientiae Naturales* 70(2): 135–182. <https://doi.org/10.2478/cszma-2021-0011>
- Ježek J, Oboňa J, Manko P (2023a) Moth flies (Diptera: Psychodidae) of Abkhazia (western Caucasus, Georgia) with some additional faunistic data from Armenia, Georgia, and Russia. *Historia Naturalis Bulgarica* 45(4): 57–82. <https://doi.org/10.48027/hnb.45.041>
- Ježek J, Manko P, Fedorčák J, Koco Š, Varga J, Shumka S, Oboňa J (2023b) Psychodidae of Albania. *Redia: Giornale di Zoologia* 106: 21–26. <https://doi.org/10.19263/REDIA-106.23.03>
- Ježek J, Goutner V (1995) Psychodidae (Diptera) of Greece. *Sborník Národního muzea v Praze. Řada B - Přírodní vědy* 50(1–4): 107–124.
- Kjærandsen J, Jakovlev J, Polevoi A, Salmela J, Kurina O (2022) A rarely seen taxonomic revision with immense value for 41 years and counting: reflections on the 1981 monograph of *Trichonta* Winnertz, 1864 (Diptera, Mycetophilidae) by Raymond Gagné, with an integrative revision of the *Trichonta vulcani* (Dziedzicki, 1889) species complex. *Proceedings of the Entomological Society of Washington* 124(3): 1–43. <https://doi.org/10.4289/0013-8797.124.3.416>
- Kročá J, Ježek J (2015) Moth flies (Psychodidae: Diptera) of the Moravskoslezské Beskydy Mts. and Podbeskydská pahorkatina Upland, Czech Republic. *Acta Musei Silesiae. Scientiae Naturales* 64: 27–50. <https://doi.org/10.1515/cszma-2015-0006>
- Kročá J, Ježek J (2019) Moth Flies (Diptera: Psychodidae) of the Moravskoslezské Beskydy Mts. and Podbeskydská pahorkatina Upland, Czech Republic, II. *Acta Musei Silesiae, Scientiae Naturales* 68(3): 201–232. <https://doi.org/10.2478/cszma-2019-0021>
- Kročá J, Ježek J (2022) Moth flies (Diptera: Psychodidae) of the Moravskoslezské Beskydy Mts. and Podbeskydská pahorkatina Uplands, Czech Republic, III. *Acta Musei Silesiae, Scientiae Naturales* 71(1) 1–29. <https://doi.org/10.2478/cszma-2022-0001>
- Kvifte GM (2014) Nomenclature and taxonomy of *Telmatoscopus* Eaton and *Seoda* Enderlein; with a discussion of parameral evolution in Paramormiini and Pericomaini (Diptera: Psychodidae, Psychodinae). *Zootaxa* 3878(4): 390–400. <https://doi.org/10.11646/zootaxa.3878.4.5>
- Kvifte GM (2019) New records of Norwegian Psychodidae, with the first description of the female of *Trichosepedon balkanicum* (Krek, 1970) comb. nov. *Norwegian Journal of Entomology* 66(1): 1–10.
- Kvifte GM, Håland Ø, Andersen T (2011) A revised checklist of Norwegian moth flies (Diptera, Psychodidae). *Norwegian Journal of Entomology* 58: 180–188.
- Kvifte GM, Salmela J, Suuronen A (2020) Taxonomic history of *Pericoma albomaculata* Wahlgren, 1904 (Diptera, Psychodidae) with new synonymies and description of *Panimerus halophilus* sp. n. *Norwegian Journal of Entomology* 67: 61–69.

- Morelli A, Biscaccianti AB (2021) New records of moth flies (Diptera Psychodidae) mainly from protected areas of Peninsular Italy. *Redia: Giornale di Zoologia* 104: 111–123. <https://doi.org/10.19263/REDIA-104.21.12>
- Morelli A, Biscaccianti AB (2022) Contribution to the knowledge of “non-Phlebotomine” Psychodidae (Diptera Nematocera) from central Italy. *Redia: Giornale di Zoologia* 105: 123–129. <https://doi.org/10.19263/REDIA-105.22.16>
- Oboňa J, Ježek J (2014) Prodrromus of moth flies (Diptera: Psychodidae) from Slovakia. *Acta Musei Silesiae. Scientiae Naturales* 63: 193–251. <https://doi.org/10.2478/cszma-2014-0020>
- Oboňa J, Kozánek M (2018) First record of *Logima sigma* (Kincaid, 1899) (Diptera: Psychodidae) from Slovakia. *Biodiversity & Environment* 10(2): 22–24.
- Oboňa J, Dvořák L, Dvořáková K, Ježek J, Kovács T, Murányi D, Slowinska I, Starý J, van der Weele R, Manko P (2019) Faunistic records of some Diptera families from the Babia Góra massif in Poland. *Dipteron. Bulletin of the Dipterological Section of the Polish Entomological Society* 35: 118–131. <https://doi.org/10.5281/zenodo.3559211>
- Oboňa J, Ježek J, Kanašová K, Manko P (2021) Hiding in plain sight: new records and endangered flies (Diptera) from a tree-hole in an urban park (Prešov, Slovakia). *Acta Musei Silesiae. Scientiae Naturales* 70: 75–81 <https://doi.org/10.2478/cszma-2021-0005>
- Omelková M, Ježek J (2012a) Two new species of *Philosepodon* Eaton (Diptera, Psychodidae, Psychodinae) from Europe, with comments on subgeneric classification. *Zootaxa* 3275: 29–42. <https://doi.org/10.11646/zootaxa.3275.1.3>
- Omelková M, Ježek J (2012b) A new species of the genus *Trichomyia* (Diptera: Psychodidae) and new faunistic data on non-phlebotomine moth flies from the Podyjí NP and its surroundings (Czech Republic). *Acta Entomologica Musei Nationalis Pragae* 52(2): 505–533.
- Pakalniškis S, Bernotienė R, Lutovinovas E, Petrašiūnas A, Podėnas S, Rimšaitė J, Sæter OA, Spungis V (2006) Checklist of Lithuanian Diptera. New and rare for Lithuania insect species 18: 16–154.
- Remm H (1956) Diptera. In: Maavara V (Ed.) Textbook for a young entomologist. Eesti Riiklik Kirjastus, Tallinn, 229–255.
- Salmela J (2008) Semiaquatic fly (Diptera, Nematocera) fauna of fens, springs, headwater streams and alpine wetlands in the northern boreal ecoregion, Finland. *W-album* 6: 1–63.
- Salmela J, Piirainen T (2005) Description of a new Psychodidae (Diptera) species from Estonia. *Entomologica Fennica* 16(4): 301–304. <https://doi.org/10.33338/ef.84274>
- Salmela J, Vartiija N (2007) New records of nematoceran flies (Diptera) from Latvia. *Latvijas entomologs* 44: 11–14.
- Salmela J, Autio O, Ilmonen J (2007) A survey on the nematoceran (Diptera) communities of southern Finnish wetlands. *Memoranda Soc. Fauna Flora Fennica* 83: 33–47.
- Salmela J, Paasivirta L, Kvifte GM (2014) Checklist of the families Chaoboridae, Dixidae, Thaumaleidae, Psychodidae and Ptychopteridae (Diptera) of Finland. *ZooKeys* 441: 37–46. <https://doi.org/10.3897/zookeys.441.7532>
- Sammet K, Talvi T, Süda I, Kurina O (2016) Pseudoscorpions (Arachnida: Pseudoscorpiones) in Estonia: new records and an annotated checklist. *Entomologica Fennica* 27(4): 149–163. <https://doi.org/10.33338/ef.60259>
- Šikora T, Jaschhof M, Kurina O (2020) Additions to the Estonian fauna of mycophagous Cecidomyiidae (Diptera), with a description of *Unicornella estonensis* gen. et sp. nov. *Zootaxa* 4851(2): 349–363. <https://doi.org/10.11646/zootaxa.4851.2.8>

- Süda I (2009) New woodland beetle species (Coleoptera) in Estonian fauna. *Forestry Studies* 50: 98–114. <https://doi.org/10.2478/v10132-011-0071-0>
- Szabó J (1983) 10. család: Psychodidae – Lepkeszúnyogok. *Fauna Hungariae* 156: 1–78.
- Takkis K, Kull T, Hallikma T, Jaksi P, Kaljund K, Kauer K, Kull Th, Kurina O, Külvik M, Lanno K, Leht M, Liira J, Melts I, Pehlak H, Raet J, Sammet K, Sepp K, Väli Ü, Laanisto L (2018) Drivers of species richness and community integrity of small forest patches in an agricultural landscape. *Journal of Vegetation Science* 29(6): 978–988. <https://doi.org/10.1111/jvs.12689>
- Tkoč M, Pecharová M, Ježek J (2014) Catalogue of the type specimens of Diptera deposited in the Department of Entomology, National Museum, Prague, Czech Republic, part 10. Moth Flies (Psychodidae). *Acta Entomologica Musei Nationalis Pragae* 54(2): 789–837.
- Vaillant F (1971–1983) 9d. Psychodidae – Psychodinae (not finished). In: Lindner E (Ed) *Die Fliegen der palaearktischen Region*. Stuttgart. Vols. 287(1971): 1–48; 291 (1972): 49–78; 292 (1972): 79–108; 305 (1974): 109–142; 310 (1975): 143–182; 313 (1977): 183–206; 317 (1978): 207–238; 320 (1979): 239–270; 326 (1981): 271–310; 328 (1983): 311–357.
- Wagner R (1990) Family Psychodidae. In: Soós A (Ed.) *Catalogue of Palaeartic Diptera*. Vol. 2. Psychodidae – Chironomidae. Akadémiai Kiadó, Budapest, 11–65.
- Wagner R (2018) Fauna Europaea: Psychodidae. In: de Jong H (Ed.) *Fauna Europaea: Diptera Nematocera*. Fauna Europaea version 2018. <https://fauna-eu.org> [accessed on 21 October 2021]
- Withers P (1989a) Moth Flies. Diptera: Psychodidae. *Dipterists Digest* 4: 1–83.
- Withers P (1989b) Some further records of Irish rot-hole moth flies (Diptera: Psychodidae), with a first record for *Telmatoscopus rothschildii*, with a figure of the male terminalia of that species. *Irish Naturalists' Journal* 23(1): 16–17.

# Complete mitochondrial genome of *Lepidocephalichthys berdmorei* and its phylogenetic status within the family Cobitidae (Cypriniformes)

Min Zhou<sup>1</sup>, Cheng Wang<sup>2</sup>, Ziyue Xu<sup>1</sup>, Zhicun Peng<sup>1</sup>, Yang He<sup>1</sup>, Ying Wang<sup>1,3</sup>

<sup>1</sup> Hubei Engineering Research Center for Protection and Utilization of Special Biological Resources in the Hanjiang River Basin, Jiangnan University, Wuhan, China

<sup>2</sup> State Key Laboratory of Freshwater Ecology and Biotechnology, Institute of Hydrobiology, Chinese Academy of Sciences, Wuhan, China

<sup>3</sup> Academy of Plateau Science and Sustainability, Qinghai Normal University, Xining, China

Corresponding author: Ying Wang ([xinyuanwangying@163.com](mailto:xinyuanwangying@163.com))

## Abstract

In this study, the complete mitochondrial genome of *Lepidocephalichthys berdmorei* was first determined by the primer walking sequence method. The complete mitochondrial genome was 16,574 bp in length, including 13 protein-coding genes (PCGs), 22 transfer RNA (tRNA) genes, two ribosomal RNA (rRNA) genes, and a control region (D-loop). The gene arrangement pattern was identical to that of other teleosts. The overall base composition was 29.9% A, 28.5% T, 25.5% C, and 16.1% G, with an A+T bias of 58.4%. Furthermore, phylogenetic analyses were conducted based on 13 PCGs from the mitochondrial genomes of 18 cobitid species using with three different methods (Neighbor-joining, Maximum likelihood, and Bayesian inference). All methods consistently showed that the four species of the genus *Lepidocephalichthys* form a monophyletic group. This study would provide effective molecular information for the *Lepidocephalichthys* species as well as novel genetic marker for the study of species identification.

**Key words:** Gene arrangement pattern, *Lepidocephalichthys berdmorei*, mitochondrial genome, phylogenetic analysis



Academic editor:

Maria Elina Bichuette

Received: 6 June 2024

Accepted: 28 October 2024

Published: 10 December 2024

ZooBank: <https://zoobank.org/DEE211BF-EF4D-42E2-AB1D-C82F8F8F4DC5>

Citation: Zhou M, Wang C, Xu Z, Peng Z, He Y, Wang Y (2024) Complete mitochondrial genome of *Lepidocephalichthys berdmorei* and its phylogenetic status within the family Cobitidae (Cypriniformes). ZooKeys 1221: 51–69. <https://doi.org/10.3897/zookeys.1221.129136>

Copyright: This is an open access article distributed under the terms of the CC0 Public Domain Dedication.

## Introduction

*Lepidocephalichthys berdmorei* (Blyth 1860) belongs to the genus *Lepidocephalichthys* within the family Cobitidae, which is widely distributed in the Irrawaddy, Sittang, Salween, Chao Phraya, Mekong basins of Burma, Thailand, and China (Kottelat and Lim 1993). According to FishBase, there are approximately 25 valid species in the genus *Lepidocephalichthys* (Froese and Pauly 2024). The lack of reliable morphological characteristics, coupled with the widespread misapplication of names, has made it challenging to differentiate this species from its close relatives. For instance, the close resemblance in physical features between *L. thermalis* and *L. berdmorei* poses a significant challenge in morphological differentiation (Kottelat 2012). Therefore, molecular information is necessary for an additional method to delimit and identify species. *Lepidocephalichthys berdmorei* is a small-sized freshwater

fish species, that inhabits hill swift streams, and lakes with sandy and gravel bottoms (Kamei et al. 2023). In recent years, due to over-exploitation, damage to spawning beds, and construction of the hydroelectric dam in the Lancang River, the wild population size of *L. berdmorei* has declined dramatically (Buj et al. 2015; Zhang et al. 2019).

The mitochondrial genome (mtDNA) is a circular double-stranded molecule consisting of 13 PCGs, 22 tRNAs, two rRNAs, and a control region (D-loop) (Anderson et al. 1981; Boore 1999; Shen et al. 2020; Chu et al. 2022; Jia et al. 2023). Traditional morphological and biological approaches have focused on the ecological characteristics of populations and reproduction, with relatively little molecular research in the genus *Lepidocephalichthys* (Gohain and Deka 2017; Trif et al. 2022). Because of its limited recombination, highly conserved gene content, maternal inheritance and moderate evolutionary speed, mtDNA is now widely used to study population genetics, phylogeny, and species identification (Avice et al. 1987; Harrison 1989; Boore and Brown 1998; Ballard and Whitlock 2004; Galtier et al. 2009; Sureandiran et al. 2023). As proof, Wang et al. (2021) successfully identified fish species from the Xiangjiaba reservoir in Jinsha River using mitochondrial DNA barcoding. Goswami et al. (2022) characterized the genetic diversity of ten loaches from northeastern India based on sequence fragments of *cox1*, *cytb*, and *16S rRNA* genes; Zhang et al. (2023) demonstrated that the evolutionary position of *Rectoris luxiensis* (Wu et al. 1977) was consistent with traditional taxonomy through phylogenetic analysis of mitochondrial genomes. Currently, four mitochondrial genomes have been reported in NCBI databases, including *L. micropogon* (Blyth 1860), *L. guntea* (Hamilton 1822), *L. hasselti* (Valenciennes and Cuvier 1846), and *L. annandalei* (Chaudhuri 1912). Nevertheless, the complete mitochondrial genome of *L. berdmorei* has not been reported until now.

In this study, the complete mitochondrial genome of *L. berdmorei* was sequenced for the first time. The variation in tRNA length, position, and size of the control region, and the codon usage bias were analyzed. Subsequently, the 13 PCGs were concatenated and utilized, with those of other cobitids, to confirm the phylogenetic position of *L. berdmorei*. Therefore, these findings will provide valuable information and contribute to future species comparison and evolutionary research.

## Materials and methods

### Sample collection and DNA extraction

An adult individual of *L. berdmorei* was obtained in 2020 from the Mengla town, Xishuangbanna Dai Autonomous Prefecture, Yunnan Province, China (21°57'70"N, 101°60'54"E) (Suppl. material 1: fig. S1). Species were identified using the original morphological descriptions in the Fauna Sinica field guides (Chen 1998). After initial morphological identification, the specimen was deposited in the Animal Genetics Center of Jiangnan University under the voucher number JHU202012029. A 40–50-mg fin clip was collected and preserved in 95% ethanol at 4 °C. Total genomic DNA was extracted from caudal fin tissue using the traditional phenol-chloroform method (Sambrook and Russell 2001).

## Mitogenome sequencing, assembly, and annotation

Eight pairs of primers (Suppl. material 1: table S1) were designed based on the mtDNA sequences of closely allied species. The PCR conditions were as follows: initial denaturation at 94 °C for 2 min, then 35 cycles of denaturation at 94 °C for 30 s, annealing at 55 °C for 30 s, and extension at 72 °C for 1 min, followed by the final extension at 72 °C for 10 min. All obtained fragments were quality-proofed and searched via BLAST in the NCBI database to confirm that the amplicon is the actual target sequence.

Sequences were assembled manually by the Seqman program using DNAs-tar v. 7.1 software (Burland 2000). The mitochondrial genome was annotated roughly following the procedure described before (Wang et al. 2011, 2018). The PCGs, rRNA genes, tRNA genes, and one control region of the mitochondrial genome were annotated by MitoAnnotator (<http://mitofish.aori.u-tokyo.ac.jp/annotation/input.html>) (Iwasaki et al. 2013). Their secondary structures of tRNAs were predicted by tRNAscan-SE (<http://lowelab.ucsc.edu/tRNAscan-SE/>; Lowe and Eddy 1997) and Forna (force-directed RNA) (Kerpedjiev et al. 2015).

The base composition and relative synonymous codon usage (RSCU) of the mitogenome were calculated and produced using PhyloSuite v. 1.2.3 (Zhang et al. 2020) and MAGA X (Kumar et al. 2018). The formulas to calculate the nucleotide composition of skew are as follows: AT-skew =  $(A - T) / (A + T)$  and GC-skew =  $(G - C) / (G + C)$  (Perna and Kocher 1995).

## Phylogenetic analyses

To verify the phylogenetic position of *L. berdmorei*, 17 mitogenome sequences from GenBank were retrieved (Suppl. material 1: table S2; Saitoh et al. 2006, 2010). The 13 PCGs for each species were concatenated and then aligned by program MAFFT using default settings (Katoh et al. 2002), and phylogenetic analyses were performed using Neighbor-joining (NJ), Maximum likelihood (ML), and Bayesian inference (BI) methods. To root the phylogenetic tree, *Syncrossus beauforti* (Smith 1931) and *S. hymenophysa* (Bleeker 1852) from Botiidae were chosen as outgroups.

A NJ phylogenetic tree was constructed using MEGA 7 (Kumar et al. 2016) with 1,000 bootstrap replicates. The ML method was assembled in RAXML 7.0.3 (Stamatakis 2006), with 1,000 bootstrap replicates. GTR + F + I + G4 was selected as best-fit model according to Bayesian Information Criteria (BIC) estimated by ModelFinder (Kalyaanamoorthy et al. 2017). The BI phylogeny was carried out using MrBayes v. 3.2.7a (Ronquist et al. 2012) under the best-fit models with 5,000,000 generations in two runs of eight chains each.

## Abbreviations

Mitogenome, mitochondrial genome; **mtDNA**, mitochondrial DNA; **PCGs**, protein-coding genes; **tRNA**, transfer RNA; **rRNA**, ribosomal RNA; **atp6** and **atp8**, ATPase 6 and ATPase 8; **cox1–3**, cytochrome oxidase subunits I–III; **cytb**, cytochrome b; **LA-PCR**, long and accurate polymerase chain reaction; **nd1–6**, NADH dehydrogenase subunits 1–6; **nd4l**, NADH dehydrogenase subunits 4L; **A+T**, A+T rich region; **RSCU**, relative synonymous codon usage; **trnA**, *tRNA*<sup>Ala</sup>;

**trnC**, *tRNA<sup>Cys</sup>*; **trnD**, *tRNA<sup>Asp</sup>*; **trnE**, *tRNA<sup>Glu</sup>*; **trnF**, *tRNA<sup>Phe</sup>*; **rrnS**, 12S rRNA; **rrnL**, 16S rRNA; **trnG**, *tRNA<sup>Gly</sup>*; **trnH**, *tRNA<sup>His</sup>*; **trnI**, *tRNA<sup>Ile</sup>*; **trnK**, *tRNA<sup>Lys</sup>*; **trnL1**, *tRNA<sup>Leu(TAA)</sup>*; **trnL2**, *tRNA<sup>Leu(TAG)</sup>*; **trnM**, *tRNA<sup>Met</sup>*; **trnN**, *tRNA<sup>Asn</sup>*; **trnP**, *tRNA<sup>Pro</sup>*; **trnQ**, *tRNA<sup>Gln</sup>*; **trnR**, *tRNA<sup>Arg</sup>*; **trnS1**, *tRNA<sup>Ser(TGA)</sup>*; **trnS2**, *tRNA<sup>Ser(GCT)</sup>*; **trnT**, *tRNA<sup>Thr</sup>*; **trnV**, *tRNA<sup>Val</sup>*; **trnW**, *tRNA<sup>Trp</sup>*; **trnY**, *tRNA<sup>Tyr</sup>*; **DHU**, Dihydrouracil; **NJ**, Neighbor-joining; **ML**, Maximum likelihood; **BI**, Bayesian inference.

## Results and discussion

### Mitogenome organization and nucleotide composition

The length of the complete mitochondrial genome of *L. berdmorei* is 16,574 bp (GenBank accession number: OP651767). The complete mitochondrial genome of *L. berdmorei* shares high similarity in gene arrangement, base composition, and codon usage pattern with those of other teleosts, indicating that the mitochondrial genome is highly conserved in evolution (Boore 1999; Taanman 1999; Broughton et al. 2001; Zou et al. 2019; Shen et al. 2020; Wang et al. 2020; Yu et al. 2021). The mitogenome is a circular double-stranded molecule with a highly conserved structure, consisting of 13 PCGs, 22 tRNA genes, two rRNA genes, and a control region (D-loop) (Fig. 1, Table 1).

The overall base composition is 29.9% for A, 16.1% for G, 25.5% for C, and 28.5% for T, which is consistent with the lowest frequency for G among the four bases in fish mitochondrial genomes, and revealing the A+T-rich content (58.4%) (Mayfield and McKenna 1978; Meyer 1993). Based on the analysis of nucleotide composition, this complete sequence exhibits a clear bias towards A and T (AT-skew = 0.02, GC-skew = -0.23) (Suppl. material 1: table S3). Both *L. berdmorei* and 58 species of Cobitidae exhibit an AT bias in their mitogenomes, but the A+T-rich content size varied among species, and it may be related to factors such as natural mutations and selection pressures during replication and transcription (Zhong et al. 2002; Yu et al. 2021). Hence, during the processes of replication and transcription, the asymmetry in nucleotide composition was used to infer the direction of gene orientation and replication (Francino and Ochman 1997; Frank and Lobry 1999; Satoh et al. 2016; Moeckel et al. 2023).

### Overlaps and non-coding intergenic spacers

Cobitidae mitogenomes range from 16,574 bp (*L. berdmorei*) to 16,646 bp (*Cobitis striata* (Ikeda, 1936)) in length (Suppl. material 1: table S2). With a few exceptions, the gene arrangements of fish mitogenomes are usually conserved (Anderson et al. 1981; Chang et al. 1994; Satoh et al. 2016; Chu et al. 2022). A typical feature in the mitochondrial genome of teleosts is the overlap of nucleotides between adjacent genes, suggesting that the size of mitochondrial DNA is very compact and economical, with potential kinetic advantages during the process of replication (Boore 1999; Curole and Kocher 1999; Taanman 1999; Wang et al. 2011; Satoh et al. 2016; Zou et al. 2017; Zou et al. 2018; Zhang et al. 2023). Similarly, in the *L. berdmorei* mitochondrial genome, there are overlaps and intervals of different lengths in all genes except for trnF/rrnS, rrnS / trnV, trnV/rrnL, rrnL/trnL2, trnM/nd2, trnC/trnY, cox2/trnK, trnG/nd3, trnR/nd4l, trnH/trnS2, trnL2/nd5, nd6/trnE, and cytb/trnT. They have the longest spacer in



**Table 1.** Organization of the mitochondrial genome of *Lepidocephalichthys berdmorei*.

Locus	Position		Size (bp)	Intergenic nucleotides <sup>a</sup>	Codon		Anti-codon	Strand <sup>b</sup>
	From	To			Start	Stop		
<i>tRNA<sup>Phe</sup>(S)</i>	1	69	69	0	–	–	GAA	H
<i>12S rRNA</i>	70	1019	950	0	–	–	–	H
<i>tRNA<sup>Val</sup>(V)</i>	1020	1091	72	0	–	–	TAC	H
<i>16S rRNA</i>	1092	2767	1676	0	–	–	–	H
<i>tRNA<sup>Leu(TAA)</sup>(L1)</i>	2768	2842	75	1	–	–	TAA	H
<i>nd1</i>	2844	3818	975	5	ATG	TAA	–	H
<i>tRNA<sup>Ala</sup>(I)</i>	3824	3895	72	-2	–	–	GAT	H
<i>tRNA<sup>Gln</sup>(Q)</i>	3894	3964	71	1	–	–	TTG	L
<i>tRNA<sup>Met</sup>(M)</i>	3966	4034	69	0	–	–	CAT	H
<i>nd2</i>	4035	5081	1047	-2	ATG	TAG	–	H
<i>tRNA<sup>Trp</sup>(W)</i>	5080	5148	69	2	–	–	TCA	H
<i>tRNA<sup>Ala</sup>(A)</i>	5151	5219	69	1	–	–	TGC	L
<i>tRNA<sup>Asn</sup>(N)</i>	5221	5293	73	30	–	–	GTT	L
<i>tRNA<sup>Cys</sup>(C)</i>	5324	5390	67	0	–	–	GCA	L
<i>tRNA<sup>Tyr</sup>(Y)</i>	5391	5459	69	1	–	–	GTA	L
<i>cox1</i>	5461	7011	1551	2	GTG	TAA	–	H
<i>tRNA<sup>Ser(TGA)</sup>(S1)</i>	7014	7084	71	1	–	–	TGA	L
<i>tRNA<sup>Asp</sup>(D)</i>	7086	7158	73	13	–	–	GTC	H
<i>cox2</i>	7172	7862	691	0	ATG	T	–	H
<i>tRNA<sup>Lys</sup>(K)</i>	7863	7938	76	1	–	–	TTT	H
<i>atp8</i>	7940	8107	168	-10	ATG	TAA	–	H
<i>atp6</i>	8098	8781	684	-1	ATG	TAA	–	H
<i>cox3</i>	8781	9566	786	-1	ATG	TAA	–	H
<i>tRNA<sup>Gly</sup>(G)</i>	9566	9638	73	0	–	–	TCC	H
<i>nd3</i>	9639	9989	351	-2	ATG	TAG	–	H
<i>tRNA<sup>Arg</sup>(R)</i>	9988	10056	69	0	–	–	TCG	H
<i>nd4l</i>	10057	10353	297	-7	ATG	TAA	–	H
<i>nd4</i>	10347	11729	1383	-1	ATG	TAG	–	H
<i>tRNA<sup>His</sup>(H)</i>	11729	11797	69	0	–	–	GTG	H
<i>tRNA<sup>Ser(GCT)</sup>(S2)</i>	11798	11866	69	1	–	–	GCT	H
<i>tRNA<sup>Leu(TAG)</sup>(L2)</i>	11868	11940	73	0	–	–	TAG	H
<i>nd5</i>	11941	13779	1839	-4	ATG	TAA	–	H
<i>nd6</i>	13776	14297	522	0	ATG	TAA	–	L
<i>tRNA<sup>Glu</sup>(E)</i>	14298	14366	69	5	–	–	TTC	L
<i>cytb</i>	14372	15512	1141	0	ATG	T	–	H
<i>tRNA<sup>Thr</sup>(T)</i>	15513	15584	72	-2	–	–	TGT	H
<i>tRNA<sup>Pro</sup>(P)</i>	15583	15652	70	0	–	–	TGG	L
D-loop	15653	16574	922	0	–	–	–	H

<sup>a</sup> Negative value indicates the overlapping sequences between adjacent genes.

<sup>b</sup> H: heavy strand; L: light strand.

## PCGs and codon usage

The length of PCGs was 11,413 bp (68.86%) and it blanketed 7 NADH dehydrogenases (*nd1–6* and *nd4l*), three cytochrome oxidases (*cox1–3*), two ATPases (*atp6* and *atp8*) and one cytochrome b (*cytb*). The size of PCGs ranged from *nd4l* (297 bp) to *nd5* (1839 bp). As in other vertebrates, the *nd6* and eight tRNA genes (*tRNA<sup>Gln</sup>*, *tRNA<sup>Ala</sup>*, *tRNA<sup>Asn</sup>*, *tRNA<sup>Cys</sup>*, *tRNA<sup>Tyr</sup>*, *tRNA<sup>Ser</sup>*, *tRNA<sup>Pro</sup>*, and *tRNA<sup>Glu</sup>*) are encoded on the light strand, and the others are encoded on the heavy strand (Fig. 1, Table 1) (Wen et al. 2017; Zou et al. 2017; Yu et al. 2021). In addition, the

bias of nucleotide composition was estimated (Suppl. material 1: table S3). All 13 PCGs showed a significant negative GC-skew. It may be that mutations in the replication process or adaptive evolution cause GC-skew. However, how to explain this unusual GC-skew needs further study.

Further analysis revealed that among 13 PCGs, most mitochondrial genes of *L. berdmorei* started with codon ATG, while only the *cox1* gene began with codon GTG. Unconventional start codons are a common phenomenon within the mitogenomes of fish (Zhang and Shen 2019; Yu et al. 2021). Eight of the PCGs are ended by TAA termination codons. The *nd2*, *nd3*, and *nd4* genes ended with TAG stop codons. The *cox2* and *cytb* use incomplete stop codons (T-) (Table 1). The relative synonymous codon usage (RSCU) denotes the differential usage of synonymous codons encoding the same amino acid. Essentially, the RSCU value was calculated by dividing the amino acids encoded by the same codons and their probability of appearing in the same codons (Sharp and Li 1986). The RSCUs of *L. berdmorei* mitogenome (Fig. 2, Table 2) show a clear preference for the usage of A and T. The total number of codons in the *L. berdmorei* mitochondrial genome is 5,524. After excluding the four stop codons (UAA(\*), UAG(\*), AGA(\*), AGG(\*)), among the 64 codons, 31 codons have an RSCU value greater than 1, indicating that these codons are prioritized more highly. For instance, six codons (UUA(L), UUG(L), CUU(L), CUC(L), CUA(L), CUG(L)) coded for leucine with preference for UUA. RSCU values for these six codons were 1.68, 0.64, 1.47, 0.65, 0.99 and 0.56, respectively. The most commonly used codon is UUU-Phe (F), followed by UUA-Leu2 (L), AAA-Lys (K), and AUU-Ile (I). The least used amino acids are Ala (GCG) and Arg (CGU). Our results show that the codon distribution is largely consistent with the mitogenomes of Cobitinae studied previously (Yu et al. 2021).

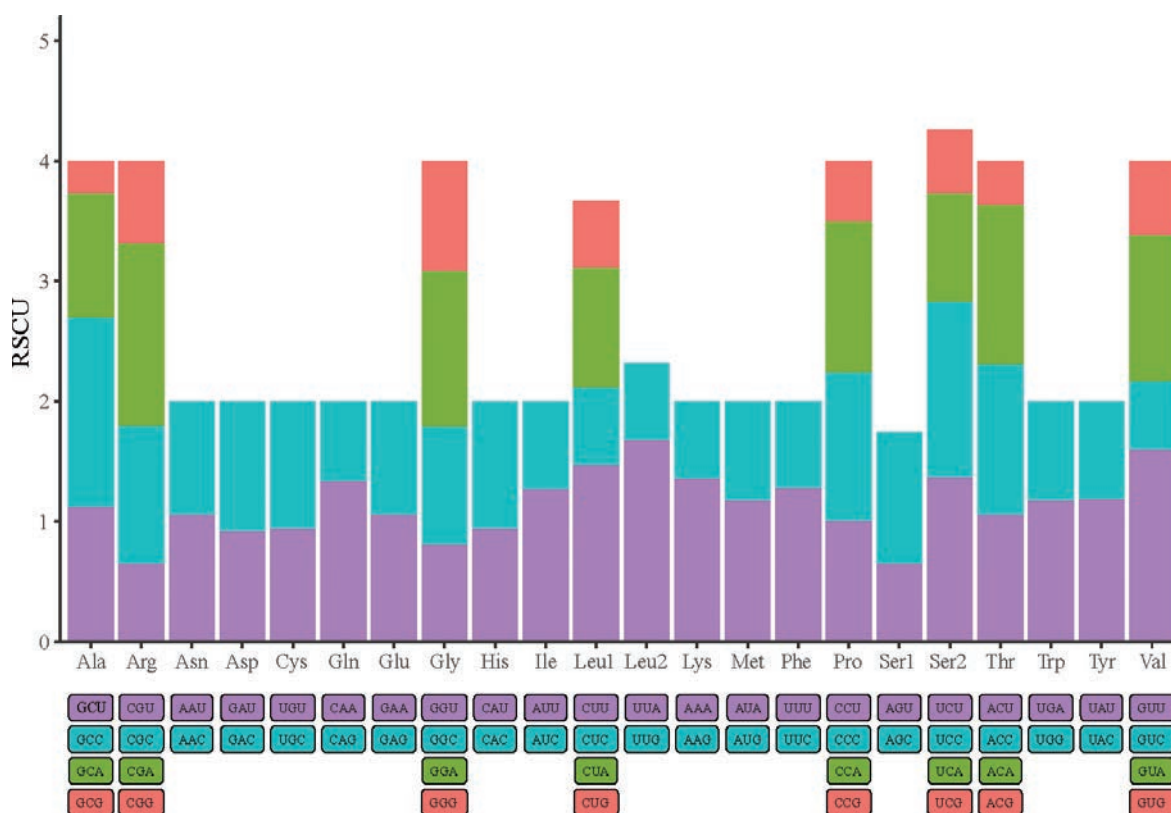


Figure 2. The relative synonymous codon usage (RSCU) of *L. berdmorei* mitogenome.

**Table 2.** Codon usage in the mitochondrial genome of *Lepidocephalichthys berdmorei*.

Codon	Count	RSCU									
UUU(F)	201	1.28	UCU(S)	103	1.37	UAU(Y)	118	1.19	UGU(C)	40	0.95
UUC(F)	113	0.72	UCC(S)	110	1.46	UAC(Y)	80	0.81	UGC(C)	44	1.05
UUA(L)	188	1.68	UCA(S)	68	0.9	UAA(*)	156	1.66	UGA(W)	75	1.18
UUG(L)	71	0.64	UCG(S)	40	0.53	UAG(*)	99	1.06	UGG(W)	52	0.82
CUU(L)	164	1.47	CCU(P)	110	1.01	CAU(H)	95	0.95	CGU(R)	21	0.65
CUC(L)	73	0.65	CCC(P)	134	1.23	CAC(H)	104	1.05	CGC(R)	37	1.15
CUA(L)	111	0.99	CCA(P)	137	1.26	CAA(Q)	156	1.34	CGA(R)	49	1.52
CUG(L)	63	0.56	CCG(P)	55	0.5	CAG(Q)	76	0.66	CGG(R)	22	0.68
AUU(I)	170	1.27	ACU(T)	102	1.06	AAU(N)	134	1.06	AGU(S)	49	0.65
AUC(I)	98	0.73	ACC(T)	120	1.25	AAC(N)	118	0.94	AGC(S)	82	1.09
AUA(M)	98	1.18	ACA(T)	128	1.33	AAA(K)	172	1.36	AGA(*)	75	0.8
AUG(M)	68	0.82	ACG(T)	35	0.36	AAG(K)	81	0.64	AGG(*)	45	0.48
GUU(V)	73	1.6	GCU(A)	82	1.13	GAU(D)	63	0.92	GGU(G)	44	0.81
GUC(V)	26	0.57	GCC(A)	114	1.57	GAC(D)	74	1.08	GGC(G)	53	0.98
GUA(V)	56	1.22	GCA(A)	75	1.03	GAA(E)	83	1.06	GGA(G)	70	1.3
GUG(V)	28	0.61	GCG(A)	20	0.27	GAG(E)	74	0.94	GGG(G)	49	0.91

### Transfer and ribosomal RNA genes

The complete mitogenome of *L. berdmorei* contains 22 tRNA genes with a size of 1,559 bp, 14 of which are located on the H-strand while the others are on the L-strand (Table 1). The 22 tRNA genes range from 67 bp to 76 bp in length, of which the shortest was *tRNA<sup>Cys</sup>* (67 bp) and the longest was *tRNA<sup>Lys</sup>* (76 bp). The color in Fig. 3 represents the type of tRNA structure in which the nucleotide is located. All tRNA genes have a typical cloverleaf secondary structure except *tRNA<sup>Ser(GCT)</sup>* lacking the Dihydrouracil (DHU) stem (Fig. 3). It is a common feature in many mitogenomes of metazoans, and can be integrated into ribosomes by adjusting its structure and function to fulfil its function of carrying and translocating amino acids (Watanabe et al. 2014; Liu et al. 2021; Xing et al. 2022).

The most prevalent non-Watson-Crick base pairs in the secondary structure of tRNAs are A-C (e.g., trnI, trnH, trnM, trnV, trnS1, trnT, trnW, and trnF), followed by T-T (trnQ and trnN), which are mostly located in the DHU, anticodon stems and acceptor (Fig. 3). And these mismatches may be modified by post-transcriptional editing processes without causing amino acid transport disorders (Tomita et al. 1996).

The lengths of *12S rRNA* and *16S rRNA* genes were 950 bp and 1,676 bp, which are located on the H strand (Table 1). They are bordered by *tRNA<sup>Phe</sup>* and *tRNA<sup>Leu(TAA)</sup>* and separated by *tRNA<sup>Val</sup>*. Both the lengths and base compositions of *12S rRNA* and *16S rRNA* are almost identical among the reported Cobitidae fishes (Kottelat and Lim 1993; Nalbant 1993; Yu et al. 2016; Shen et al. 2020; Chu et al. 2022; Ke et al. 2023). It shows a positive AT-skew (0.23) and a negative GC-skew (-0.07) (Suppl. material 1: table S3). Compared to entire mitochondrial genome, the *16S rRNA* is a non-coding gene that evolves slowly, and it contains sufficient number of polymorphisms to distinguish species (Lakra et al. 2009; Sarri et al. 2014; Hossain et al. 2019). The *12S rRNA* is also frequently considered as a DNA meta barcoding in fish identification and phylogenetic studies (Miyai et al. 2015).

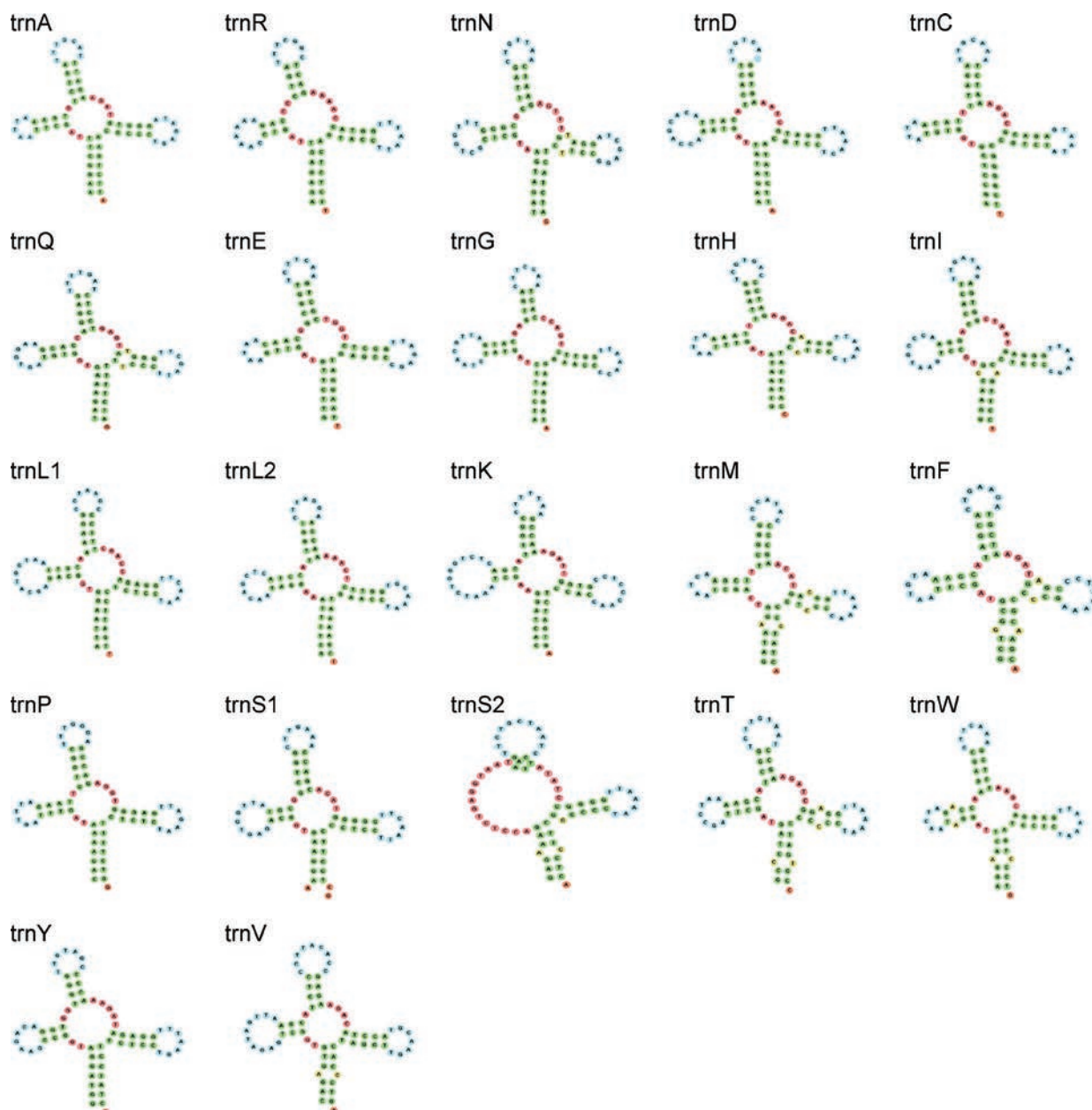


**Figure 3.** Putative secondary structure of tRNAs. Stems (typically helical) are shown in green, multiple loops (junctions) are shown in red, interior loops are shown in yellow, hairpin loops are shown in blue, and 5' and 3' unpaired regions are shown in orange.

### Control region

The only large control region of *L. berdmorei* mitogenome is the D-loop, located between the *tRNA<sup>Pro</sup>* and *tRNA<sup>Phe</sup>*, with a length of 922 bp (Fig. 1, Table 1). It plays a role in the regulation of replication and transcription and is the most rapidly evolving and changing region of the mitochondrial genome (Clayton 1982, 1991; Shadel and Clayton 1997; Zhou et al. 2014; Gao et al. 2023). The A+T-rich content of the *L. berdmorei* D-loop region is 66.27%, which is higher than the average value of the whole mitogenome (58.43%) and 13 PCGs (56.11–61.07%) (Suppl. material 1: table S3), as found in other vertebrates (Brown et al. 1986; Saccone et al. 1987; Zou et al. 2017; Ke et al. 2023).

In addition to gene duplication and insertion/deletion events, the main cause of mitochondrial genome size variation is differences in control region length (Mignotte et al. 1990; Lee et al. 1995; Pereira 2000; Minhas et al. 2023). Previous studies have demonstrated that tandem repeat sequences are prevalent in the D-loop of teleost lineage (Lee et al. 1995; Nicholls and Minczuk 2014; Jemt et al. 2015; Xu et al. 2016; Ke et al. 2023). It is worth noting that the copy number not only varies between species, but also among individuals within the same species (Norman et al. 1994; Lunt et al. 1998; Boore 1999; Xu et al. 2021). Thus, compared with the complex and large eukaryotic genome, the mitochondrial genome is simple in structure with shorter sequences, contains both conserved and highly variable regions, and can be used for taxonomic identification of species at different levels of evolution (Pereira et al. 2008; Jamandre et al. 2014; Nicholls and Minczuk 2014; Jemt et al. 2015; D'Souza and Minczuk 2018). Nevertheless, multiple duplicate regions have been found in some species that may adversely affect PCR amplification, sequencing, or both (Singh et al. 2008; Cadahía et al. 2009). As a result, researchers have avoided using this region for phylogenetic purposes, focusing instead on *rRNA* or PCGs (Slechtová et al. 2008; Wang et al. 2021; Sureandiran et al. 2023; Zhang et al. 2023).

### Phylogenetic analysis

Cobitidae belongs to Osteichthyes, Cyprinidformes, and has three subfamilies: Nemacheilinae, Botiinae and Cobitinae (Hora 1932; Nalbant 1993; Tang et al. 2005; Slechtová et al. 2008; Chu et al. 2022). Sawada (1982) proposed a phylogeny of the Cobitoidea (limited to loaches) as (Botiinae + Cobitinae) + (Nemacheilinae + Homalopterinae) based on 52 osteological characters. Nevertheless, due to their morphological similarity and frequent overlap, differentiating species within Cobitidae based solely on morphology is a challenging endeavor (Kottelat and Lim 1993; Nalbant 1993; Shen et al. 2020; Ke et al. 2023). In order to determine the phylogenetic status of *L. berdmorei* in the family Cobitidae, 17 complete mitochondrial genomes from the GenBank database were selected to reconstruct phylogenetic trees. Based on the 13 PSGs concatenated dataset, the NJ, ML and BI phylogenies generated identical topology with high bootstrap support and posterior probability values, respectively (Fig. 4). All trees presented two major clades corresponding to the outgroup. *Canthophrys* is located at the base of the phylogenetic tree. Our results are generally consistent with the traditional morphological classification and recent molecular studies (Hora 1932; Slechtová et al. 2008; Sudasinghe et al. 2024).

Firstly, the phylogenetic tree revealed that *L. guntea*, *L. hasselti*, and *L. berdmorei* clustered as a monophyletic clade, followed by a clade with *L. micropogon* with high bootstrap support. Secondly, the genus *Lepidocephalichthys* and *Pangio* which formed a sister branch with high bootstrap support and posterior probability values, which was consistent with the previous study (Slechtová et al. 2008; Yu et al. 2021). Notably, Slechtová et al. (2008) found that the genera *Lepidocephalichthys* and *Pangio* were considered as a sister group in the RAG-1 phylogeny; but this relationship was not supported by the *cytb* dataset. Meanwhile, based on *cyt b* and RAG-1 datasets, these four genera of Cobitidae (*Cobitis*, *Niwaella*, *Misgurnus*, and *Koreocobitis*) form a distinct monophyletic group (Slechtová et al. 2008). Generally, from the phylogenetic tree of genetic evolution, the evolutionary status of *L. berdmorei* was defined.

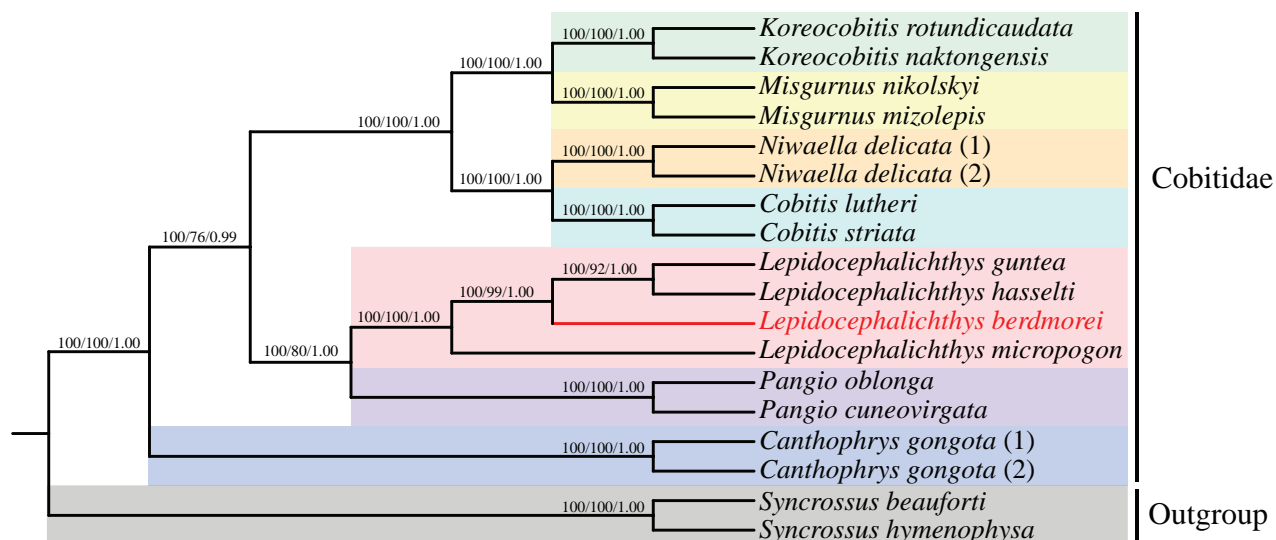


**Figure 4.** Phylogenetic tree of Cobitidae and two outgroups based on the NJ, ML and BI analysis of 13 concatenated protein-coding genes. Tree topologies produced by NJ, ML methods, and BI analysis were equivalent. The numbers at the nodes represent bootstrap support values for NJ and ML analyses and Bayesian posterior probability, sequentially, and the red branch represents the specie in this study.

## Conclusions

In conclusion, the complete mitochondrial DNA sequence of *L. berdmorei* is determined for the first time by the primer walking sequence method. The mitogenome is 16,574 bp in length, and encodes all of the 37 genes that are typical for Cobitidae fish. We compared mtDNA from *L. berdmorei* with that of other teleost and analyzed mitogenome composition, PCGs, and codon usage, transfer and ribosomal RNA genes, and noncoding regions (control region, intergenic spacers). The generated phylogenetic trees yielded convincing evidence that the genus *Lepidocephalichthys* formed a monophyletic group. These findings will provide new insights into better understanding the phylogenetic status of this intriguing and ecologically important group.

## Acknowledgements

This work was supported by grants from the National Natural Science Foundation of China (31702016), and Jiangnan University Research Project Funding Plan (2023KJZX42). We greatly appreciate the valuable suggestions of two anonymous referees.

## Additional information

### Conflict of interest

The authors have declared that no competing interests exist.

### Ethical statement

All animal protocols have been reviewed and approved by the experimental animal welfare and ethics review committee of Jiangnan University, Qinghai Normal University, and Chinese Academy of Sciences.

## Funding

This work was supported by the National Natural Science Foundation of China (Grant number 31702016) and Jiangnan University Research Project Funding Plan (Grant number 2023KJZX42).

## Author contributions

Ying Wang contributed to the concept and design of the study. Sample collection and preparation of materials were done by Cheng Wang and Zhicun Peng. Ziyue Xu, Yang He and Min Zhou performed the data analysis and interpretation, and Min Zhou wrote the first draft of the manuscript. Ying Wang revised this manuscript. All authors read and revised the manuscript and approved the final version. All authors agree to be accountable for all aspects of the manuscript.

## Author ORCIDs

Ying Wang  <https://orcid.org/0000-0002-8222-7510>

## Data availability

Genome sequence data that support the findings of this study are openly available from the GenBank at <https://www.ncbi.nlm.nih.gov/>, under accession No. OP651767.

## References

- Anderson S, Bankier AT, Barrell BG, de Bruijn MH, Coulson AR, Drouin J, Eperon IC, Nierlich DP, Roe BA, Sanger F, Schreier PH, Smith AJ, Staden R, Young IG (1981) Sequence and organization of the human mitochondrial genome. *Nature* 290(5806): 457–465. <https://doi.org/10.1038/290457a0>
- Avise JC, Arnold, J, Ball RM, Bermingham E, Lamb T, Neigel JE, Reeb CA, Saunders NC (1987) Intraspecific phylogeography: the mitochondrial DNA bridge between population genetics and systematics. *Annual Review of Ecology and Systematics* 18: 489–522. <https://doi.org/10.1146/annurev.es.18.110187.002421>
- Ballard JWO, Whitlock MC (2004) The incomplete natural history of mitochondria. *Molecular Ecology* 13(4): 729–744. <https://doi.org/10.1046/j.1365-294X.2003.02063.x>
- Bleeker P (1852) Diagnostische beschrijvingen van nieuwe of weinig bekende vischsoorten van Sumatra. Tiental I–IV. *Natuurkundig Tijdschrift Voor Nederlandsch Indië* 3: 569–608. <https://www.biodiversitylibrary.org/part/218337>
- Blyth E (1860) Report on some fishes received chiefly from the Sitang River and its tributary streams. *The Journal of the Asiatic Society of Bengal* 29: 138–174. <https://biostor.org/reference/235393>
- Boore JL (1999) Animal mitochondrial genomes. *Nucleic Acids Research* 27(8): 1767–1780. <https://doi.org/10.1093/nar/27.8.1767>
- Boore JL, Brown WM (1998) Big trees from little genomes: mitochondrial gene order as a phylogenetic tool. *Current Opinion in Genetics & Development* 8(6): 668–674. [https://doi.org/10.1016/S0959-437X\(98\)80035-X](https://doi.org/10.1016/S0959-437X(98)80035-X)
- Broughton RE, Milam JE, Roe BA (2001) The complete sequence of the zebrafish (*Danio rerio*) mitochondrial genome and evolutionary patterns in vertebrate mitochondrial DNA. *Genome Research* 11(11): 1958–1967. <https://doi.org/10.1101/gr.156801>
- Brown GG, Gadaleta G, Pepe G, Saccone C, Sbisà E (1986) Structural conservation and variation in the D-loop-containing region of vertebrate mitochondrial DNA. *Journal of Molecular Biology* 192(3): 503–511. [https://doi.org/10.1016/0022-2836\(86\)90272-X](https://doi.org/10.1016/0022-2836(86)90272-X)

- Buj I, Čaleta M, Marčić Z, Šanda R, Vukić J, Mrakovčić M (2015) Different histories, different destinies-impact of evolutionary history and population genetic structure on extinction risk of the adriatic spined loaches (genus *Cobitis*; Cypriniformes, Actinopterygii). *PLoS ONE* 10(7): e0131580. <https://doi.org/10.1371/journal.pone.0131580>
- Burland TG (2000) DNASTAR's Lasergene sequence analysis software. *Methods in Molecular Biology* 132: 71–91. <https://doi.org/10.1385/1-59259-192-2:71>
- Cadahía L, Pinsker W, Negro JJ, Pavlicev M, Urios V, Haring E (2009) Repeated sequence homogenization between the control and pseudo-control regions in the mitochondrial genomes of the subfamily Aquilinae. *Journal of Experimental Zoology Part B: Molecular and Developmental Evolution* 312B(3): 171–185. <https://doi.org/10.1002/jez.b.21282>
- Chang YS, Huang FL, Lo TB (1994) The complete nucleotide sequence and gene organization of carp (*Cyprinus carpio*) mitochondrial genome. *Journal of Molecular Evolution* 38(2): 138–155. <https://doi.org/10.1007/BF00166161>
- Chaudhuri, BL (1912) Descriptions of some new species of freshwater fishes from north India. *Records of the Zoological Survey of India* 7(5): 437–443. <https://doi.org/10.26515/rzsi/v7/i5/1912/163113>
- Chen YY (1998) *Fauna Sinica, Osteichthyes, Cypriniformes (II)*. Science Press, Beijing, 531 pp.
- Chu TJ, Yang N, Liu K (2022) Complete mitochondrial genome identification of *Niwaella nigrolinea* (Cypriniformes: Cobitidae). *Mitochondrial DNA. Part B, Resources* 7(11): 2018–2020. <https://doi.org/10.1080/23802359.2022.2149247>
- Clayton DA (1982) Replication of animal mitochondrial DNA. *Cell* 28(4): 693–705. [https://doi.org/10.1016/0092-8674\(82\)90049-6](https://doi.org/10.1016/0092-8674(82)90049-6)
- Clayton DA (1991) Nuclear gadgets in mitochondrial DNA replication and transcription. *Trends in Biochemical Sciences* 16(3): 107–111. [https://doi.org/10.1016/0968-0004\(91\)90043-U](https://doi.org/10.1016/0968-0004(91)90043-U)
- Curole JP, Kocher TD (1999) Mitogenomics: digging deeper with complete mitochondrial genomes. *Trends in Ecology & Evolution* 14(10): 394–398. [https://doi.org/10.1016/S0169-5347\(99\)01660-2](https://doi.org/10.1016/S0169-5347(99)01660-2)
- D'Souza AR, Minczuk M (2018) Mitochondrial transcription and translation: overview. *Essays in Biochemistry* 62(3): 309–320. <https://doi.org/10.1042/EBC20170102>
- Francino MP, Ochman H (1997) Strand asymmetries in DNA evolution. *Trends in Genetic* 13(6): 240–245. [https://doi.org/10.1016/S0168-9525\(97\)01118-9](https://doi.org/10.1016/S0168-9525(97)01118-9)
- Frank AC, Lobry JR (1999) Asymmetric substitution patterns: a review of possible underlying mutational or selective mechanisms. *Gene* 238(1): 65–77. [https://doi.org/10.1016/S0378-1119\(99\)00297-8](https://doi.org/10.1016/S0378-1119(99)00297-8)
- Froese R, Pauly D (2024) FishBase. World Wide Web electronic publication. <http://www.fishbase.org> [accessed May 2024]
- Galtier N, Nabholz B, Glémin S, Hurst GDD (2009) Mitochondrial DNA as a marker of molecular diversity: a reappraisal. *Molecular Ecology* 18(22): 4541–4550. <https://doi.org/10.1111/j.1365-294X.2009.04380.x>
- Gao Y, Zhang J, Wang Q, Liu Q, Tang B (2023) The complete mitochondrial genome of box tree moth *Cydalima perspectalis* and insights into phylogenetics in Pyraloidea. *Animals: An Open Access Journal from MDPI* 13(6): 1045. <https://doi.org/10.3390/ani13061045>
- Gohain AB, Deka P (2017) Length-weight relationship and relative condition factor of *Lepidocephalichthys Guntea* (Hamilton, 1822) of Ghati *Beel* of Dhemaji district of Assam, India. *International Journal of Fisheries and Aquatic Studies* 5(2): 514–517.
- Goswami M, Pavan-Kumar A, Patil G, George T, Nath R, Bhuyan RN, Siva C, Laskar MA, Sumer S (2022) Molecular identification of ornamental loaches (Cypriniformes, Co-

- bitoidei) of North East India using mitochondrial genes. *Animal Gene* 26: 200136. <https://doi.org/10.1016/j.angen.2022.200136>
- Hamilton F (1822) An account of the fishes found in the river Ganges and its branches. Printed for A. Constable and company, Edinburgh, 405 pp. <https://doi.org/10.5962/bhl.title.6897>
- Harrison RG (1989) Animal mitochondrial DNA as a genetic marker in population and evolutionary biology. *Trends in Ecology & Evolution* 4(1): 6–11. [https://doi.org/10.1016/0169-5347\(89\)90006-2](https://doi.org/10.1016/0169-5347(89)90006-2)
- Hora SL (1932) Classification, bionomics and evolution of homalopteridae fishes. *Zoological Survey of India, Calcutta*, 263–330 pp.
- Hossain MAM, Uddin SMK, Chowdhury ZZ, Sultana S, Johan MR, Rohman A, Erwanto Y, Ali ME (2019) Universal mitochondrial 16s rRNA biomarker for mini-barcode to identify fish species in Malaysian fish products. *Food Additives & Contaminants: Part A: Chemistry, Analysis, Control, Exposure & Risk Assessment* 36(4): 493–506. <https://doi.org/10.1080/19440049.2019.1580389>
- Huang Z, Liu N (2010) Advances in mitochondrial genome size variation in animals. *Life Science Research* 14(02):166–171. <https://doi.org/10.3724/SP.J.1238.2010.00512>
- Ikeda H (1936) On the sexual dimorphism and the taxonomical status of some Japanese loaches (I). *Zoological Magazine*, 48: 983–994. <https://doi.org/10.34435/zm002513>
- Iwasaki W, Fukunaga T, Isagozawa R, Yamada K, Maeda Y, Satoh TP, Sado T, Mabuchi K, Takeshima H, Miya M, Nishida M (2013) MitoFish and MitoAnnotator: a mitochondrial genome database of fish with an accurate and automatic annotation pipeline. *Molecular Biology and Evolution* 30(11): 2531–2540. <https://doi.org/10.1093/molbev/mst141>
- Jamandre BW, Durand JD, Tzeng WN (2014) High sequence variations in mitochondrial DNA control region among worldwide populations of flathead mullet *Mugil cephalus*. *International Journal of Zoology* 2014(2014): 1–9. <https://doi.org/10.1155/2014/564105>
- Jemt E, Persson Ö, Shi Y, Mehmedovic M, Uhler JP, Dávila López M, Freyer C, Gustafsson CM, Samuelsson T, Falkenberg M (2015) Regulation of DNA replication at the end of the mitochondrial D-loop involves the helicase TWINKLE and a conserved sequence element. *Nucleic Acids Research* 43(19): 9262–9275. <https://doi.org/10.1093/nar/gkv804>
- Jia W, Wei J, Niu M, Zhang H, Zhao Q (2023) The complete mitochondrial genome of *Aeschrocoristuberculatus* and *A.ceylonicus* (Hemiptera, Pentatomidae) and its phylogenetic implications. *ZooKeys* 1160: 145–167. <https://doi.org/10.3897/zookeys.1160.100818>
- Kalyaanamoorthy S, Minh BQ, Wong TKF, von Haeseler A, Jermini LS (2017) ModelFinder: fast model selection for accurate phylogenetic estimates. *Nature Methods* 14(6): 587–589. <https://doi.org/10.1038/nmeth.4285>
- Kamei M, Munilkumar S, Basudha C, Kamei M, Munilkumar S, Basudha C, Dasgupta S, Sawant PB, Romen Mangang W (2023) Breeding and larval rearing of juvenile of Burmese loach, *Lepidocephalichthys berdmorei* (Blyth, 1860): A new candidate species for aquaculture. *Journal of Experimental Zoology India* 26(1): 11–17. <https://connectjournals.com03895.2023.26.11>
- Kanu UC, Zhao G, Xie P, Li Y, Lei D, Niu J, Ma X (2016) The complete mtDNA genome of *Triplophysa strauchii* (Cypriniformes, Balitoridae, Cobitoidea): genome characterization and phylogenetic analysis. *Mitochondrial DNA. Part A, DNA Mapping, Sequencing, and Analysis* 27(4): 2637–2638. <https://doi.org/10.3109/19401736.2015.1041131>
- Katoh K, Misawa K, Kuma K, Miyata T (2002) MAFFT: a novel method for rapid multiple sequence alignment based on fast Fourier transform. *Nucleic Acids Research* 30(14): 3059–3066. <https://doi.org/10.1093/nar/gkf436>

- Ke Z, Zhou K, Hou M, Luo H, Li Z, Pan X, Zhou J, Jing T, Ye H (2023) Characterization of the complete mitochondrial genome of the elongate loach and its phylogenetic implications in Cobitidae. *Animals: An Open Access Journal from MDPI* 13(24): 3841. <https://doi.org/10.3390/ani13243841>
- Kerpedjiev P, Hammer S, Hofacker IL (2015) Forna (force-directed RNA): Simple and effective online RNA secondary structure diagrams. *Bioinformatics (Oxford, England)* 31(20): 3377–3379. <https://doi.org/10.1093/bioinformatics/btv372>
- Kottelat M (2012) *Conspectus cobitidum: an inventory of the loaches of the world (Teleostei: Cypriniformes: Cobitoidei)*. The Raffles Bulletin of Zoology Suppl 26: 1–199.
- Kottelat M, Lim KKP (1993) A synopsis of the Malayan species of *Lepidocephalichthys*, with descriptions of two new species (Teleostei: Cobitidae). *The Raffles Bulletin of Zoology* 40(2): 201–220.
- Kumar S, Stecher G, Tamura K (2016) MEGA7: molecular evolutionary genetics analysis version 7.0 for bigger datasets. *Molecular Biology and Evolution* 33(7): 1870–1874. <https://doi.org/10.1093/molbev/msw054>
- Kumar S, Stecher G, Li M, Knyaz C, Tamura K (2018) MEGA X: Molecular evolutionary genetics analysis across computing platforms. *Molecular Biology and Evolution* 35(6): 1547–1549. <https://doi.org/10.1093/molbev/msy096>
- Lakra WS, Goswami M, Gopalakrishnan A (2009) Molecular identification and phylogenetic relationships of seven Indian sciaenids (Pisces: Perciformes, Sciaenidae) based on 16S rRNA and cytochrome c oxidase subunit I mitochondrial genes. *Molecular Biology Reports* 36(5): 831–839. <https://doi.org/10.1007/s11033-008-9252-1>
- Lee WJ, Conroy J, Howell WH, Kocher TD (1995) Structure and evolution of teleost mitochondrial control regions. *Journal of Molecular Evolution* 41(1): 54–66. <https://doi.org/10.1007/BF00174041>
- Liu L, Wang Z, Yanagimoto T, Gao T, Li P (2021) The taxonomic validity and phylogenetic relationships of genus *Platycephalus* Bloch, 1785 (Teleostei: Platycephalidae) in the Northwest Pacific inferred from the mitochondrial genome. *Thalassas: An International Journal of Marine Sciences* 37: 705–715. <https://doi.org/10.1007/s41208-021-00345-w>
- Lowe TM, Eddy SR (1997) tRNAscan-SE: A program for improved detection of transfer RNA genes in genomic sequence. *Nucleic Acids Research* 25(5): 955–964. <https://doi.org/10.1093/nar/25.5.955>
- Lunt DH, Whipple LE, Hyman BC (1998) Mitochondrial DNA variable number tandem repeats (VNTRs): utility and problems in molecular ecology. *Molecular Ecology* 7(11): 1441–1455. <https://doi.org/10.1046/j.1365-294x.1998.00495.x>
- Mayfield JE, McKenna JF (1978) A-T rich sequences in vertebrate DNA. A possible explanation of q-banding in metaphase chromosomes. *Chromosoma* 67(2): 157–163. <https://doi.org/10.1007/BF00293173>
- Meyer A (1993) Evolution of mitochondrial DNA in fishes. In: Hochachka PW, Mommsen TP (ed), *Biochemistry and molecular biology of fishes*. Elsevier Science Publishers, Amsterdam, 38 pp.
- Mignotte F, Gueride M, Champagne AM, Mounolou JC (1990) Direct repeats in the non-coding region of rabbit mitochondrial DNA. Involvement in the generation of intra- and inter-individual heterogeneity. *European Journal of Biochemistry* 194(2): 561–571. <https://doi.org/10.1111/j.1432-1033.1990.tb15653.x>
- Minhas BF, Beck EA, Cheng CC, Catchen J (2023) Novel mitochondrial genome rearrangements including duplications and extensive heteroplasmy could underlie temperature adaptations in Antarctic notothenioid fishes. *Scientific Reports* 13(1): 6939. <https://doi.org/10.1038/s41598-023-34237-1>

- Miya M, Sato Y, Fukunaga T, Sado T, Poulsen JY, Sato K, Minamoto T, Yamamoto S, Yamanaka H, Araki H, Kondoh M, Iwasaki W (2015) MiFish, a set of universal PCR primers for metabarcoding environmental DNA from fishes: detection of more than 230 subtropical marine species. *Royal Society Open Science* 2(7): 150088 <https://doi.org/10.1098/rsos.150088>
- Moeckel C, Zaravinos A, Georgakopoulos-Soares I (2023) Strand asymmetries across genomic processes. *Computational and Structural Biotechnology Journal* 21: 2036–2047. <https://doi.org/10.1016/j.csbj.2023.03.007>
- Nalbant TT (1993) Some problems in the systematics of the genus *Cobitis* and its relatives (Pisces, Ostariophysi, Cobitidae). *Revue Roumaine de Biologie: Serie Biologie Animale* 38(2): 101–110.
- Nicholls TJ, Minczuk M (2014) In D-loop: 40 years of mitochondrial 7S DNA. *Experimental Gerontology* 56: 175–181. <https://doi.org/10.1016/j.exger.2014.03.027>
- Norman JA, Moritz C, Limpus CJ (1994) Mitochondrial DNA control region polymorphisms: genetic markers for ecological studies of marine turtles. *Molecular Ecology* 3(4): 363–373. <https://doi.org/10.1111/j.1365-294X.1994.tb00076.x>
- Pereira SL (2000) Mitochondrial genome organization and vertebrate phylogenetics. *Genetics and Molecular Biology* 23(4): 745–752. <https://doi.org/10.1590/S1415-47572000000400008>
- Pereira F, Soares P, Carneiro J, Pereira L, Richards MB, Samuels DC, Amorim A (2008) Evidence for variable selective pressures at a large secondary structure of the human mitochondrial DNA control region. *Molecular Biology and Evolution* 25(12): 2759–2770. <https://doi.org/10.1093/molbev/msn225>
- Perna NT, Kocher TD (1995) Patterns of nucleotide composition at fourfold degenerate sites of animal mitochondrial genomes. *Journal of Molecular Evolution* 41(3): 353–358. <https://doi.org/10.1007/BF01215182>
- Ronquist F, Teslenko M, van der Mark P, Ayres DL, Darling A, Höhna S, Larget B, Liu L, Suchard MA, Huelsenbeck JP (2012) MrBayes 3.2: efficient Bayesian phylogenetic inference and model choice across a large model space. *Systematic Biology* 61(3): 539–542. <https://doi.org/10.1093/sysbio/sys029>
- Saccone C, Attimonelli M, Sbisà E (1987) Structural elements highly preserved during the evolution of the D-loop-containing region in vertebrate mitochondrial DNA. *Journal of Molecular Evolution* 26(3): 205–211. <https://doi.org/10.1007/BF02099853>
- Saitoh K, Sado T, Mayden RL, Hanzawa N, Nakamura K, Nishida M, Miya M (2006) Mitogenomic evolution and interrelationships of the Cypriniformes (Actinopterygii: Ostariophysi): the first evidence toward resolution of higherlevel relationships of the world's largest freshwater fish clade based on 59 whole mitogenome sequences. *Journal of Molecular Evolution* 63(6): 826–841. <https://doi.org/10.1007/s00239-005-0293-y>
- Saitoh K, Chen WJ, Mayden RL (2010) Extensive hybridization and tetraploidy in spined loach fish. *Molecular Phylogenetics and Evolution* 56(3): 1001–1010. <https://doi.org/10.1016/j.ympev.2010.04.021>
- Sambrook J, Russell DW (2001) *Molecular cloning: a laboratory manual*. Cold Spring Harbor Press, New York, 58 pp.
- Sarri C, Stamatis C, Sarafidou T, Galara I, Godosopoulos V, Kolovos M, Liakou C, Tastsoglou S, Mamuris Z (2014) A new set of 16S rRNA universal primers for identification of animal species. *Food Control* 43: 35–41. <https://doi.org/10.1016/j.foodcont.2014.02.036>
- Satoh TP, Miya M, Mabuchi K, Nishida M (2016) Structure and variation of the mitochondrial genome of fishes. *BMC Genomics* 17(1): 719. <https://doi.org/10.1186/s12864-016-3054-y>

- Sawada Y (1982) Phylogeny and zoogeography of the superfamily Cobitoidea (Cyprinoidae, Cypriniformes). *Memoirs of the Faculty of Fisheries, Hokkaido University* 28: 65–223. <http://eprints.lib.hokudai.ac.jp/dspace/bitstream/2115/21871/1/2>
- Shadel GS, Clayton DA (1997) Mitochondrial DNA maintenance in vertebrates. *Annual Review of Biochemistry* 66: 409–435. <https://doi.org/10.1146/annurev.biochem.66.1.409>
- Sharp PM, Li WH (1986) An evolutionary perspective on synonymous codon usage in unicellular organisms. *Journal of Molecular Evolution* 24(1–2): 28–38. <https://doi.org/10.1007/BF02099948>
- Shen Y, Wang J, Zhang F (2020) Complete mitochondrial genome of *Parabotia bimaculata* (Cypriniformes: Cobitidae: Botiinae), an endemic riverine loach in China and phylogenetic analysis for Botiinae. *Thalassas: An International Journal of Marine Sciences* 36: 387–393. <https://doi.org/10.1007/s41208-020-00200-4>
- Singh TR, Shneor O, Huchon D (2008) Bird mitochondrial gene order: insight from 3 warbler mitochondrial genomes. *Molecular Biology and Evolution* 25(3): 475–477. <https://doi.org/10.1093/molbev/msn003>
- Slechtová V, Bohlen J, Perdices A (2008) Molecular phylogeny of the freshwater fish family Cobitidae (Cypriniformes: Teleostei): delimitation of genera, mitochondrial introgression and evolution of sexual dimorphism. *Molecular Phylogenetics and Evolution* 47(2): 812–831. <https://doi.org/10.1016/j.ympev.2007.12.018>
- Smith HM (1931) Descriptions of new genera and species of Siamese fishes. *Proceedings of the United States National Museum*: 79(2873): 1–48. <https://doi.org/10.5479/si.00963801.79-2873.1>
- Stamatakis A (2006) RAxML-VI-HPC: maximum likelihood-based phylogenetic analyses with thousands of taxa and mixed models. *Bioinformatics (Oxford, England)* 22(21): 2688–2690. <https://doi.org/10.1093/bioinformatics/btl446>
- Sudasinghe H, Dahanukar N, Raghavan R, Ranasinghe T, Wijesooriya K, Pethiyagoda R, Rüber L, Meegaskumbura M (2024) The loach genus *Lepidocephalichthys* (Teleostei: Cobitidae) in Sri Lanka and peninsular India: multiple colonizations and unexpected species diversity. *Hydrobiologia* 851: 1113–1133. <https://doi.org/10.1007/s10750-023-05321-4>
- Sureandiran B, Karuppasamy K, Sundaramanickam A, Badhul Haq MA, Arumugam U, Ajith Kumar TT (2023) First record and DNA barcode of bigeye numbfish, *Narcine Oculifera* Carvalho, Compagno & Mee, 2002 (Elasmobranchii: Torpediniformes: Narcinidae) from Indian coastal waters. *Thalassas: An International Journal of Marine Sciences* 39: 1215–1221. <https://doi.org/10.1007/s41208-023-00569-y>
- Taanman JW (1999) The mitochondrial genome: structure, transcription, translation and replication. *Biochimica et Biophysica Acta* 1410(2): 103–123. [https://doi.org/10.1016/S0005-2728\(98\)00161-3](https://doi.org/10.1016/S0005-2728(98)00161-3)
- Tang Q, Liu H, Mayden R, Xiong B (2005) Comparison of evolutionary rates in the mitochondrial DNA cytochrome *b* gene and control region and their implications for phylogeny of the Cobitoidea (Teleostei: Cypriniformes). *Molecular Phylogenetics and Evolution* 39(2): 347–357. <https://doi.org/10.1016/j.ympev.2005.08.007>
- Tomita K, Ueda T, Watanabe K (1996) RNA editing in the acceptor stem of squid mitochondrial tRNA<sup>Tyr</sup>. *Nucleic Acids Research* 24(24): 4987–4991. <https://doi.org/10.1093/nar/24.24.4987>
- Trif N, Bordeianu M, Codrea VA (2022) A Maeotian (Late Miocene) freshwater fish-fauna from Romania. *Palaeoworld* 31(1): 140–152. <https://doi.org/10.1016/j.palwor.2021.01.004>

- Valenciennes A, Cuvier G (1846) Histoire naturelle des poissons. Bertrand, Paris, 520–553 pp.
- Wang Y, Guo R, Li H, Zhang X, Du J, Song Z (2011) The complete mitochondrial genome of the Sichuan taimen (*Hucho bleekeri*): Repetitive sequences in the control region and phylogenetic implications for Salmonidae. *Marine Genomics* 4(3): 221–228. <https://doi.org/10.1016/j.margen.2011.06.003>
- Wang Y, Wen H, Yao J, Sun K, Wang W, Liu H, Yang D, Zhang F, Xiong F (2018) Complete mitochondrial genome of the Salangid icefish *Neosalanx taihuensis* (Actinopterygii: Osmeriformes: Salangidae). *Mitochondrial DNA. Part B, Resources* 3(2): 1040–1041. <https://doi.org/10.1080/23802359.2018.1511840>
- Wang IC, Lin HD, Liang CM, Huang CC, Wang RD, Yang JQ, Wang WK (2020) Complete mitochondrial genome of the freshwater fish *Onychostoma lepturum* (Teleostei, Cyprinidae): genome characterization and phylogenetic analysis. *ZooKeys* 1005: 57–72. <https://doi.org/10.3897/zookeys.1005.57592>
- Wang Y, Wen H, Zhai D, Liu H, Xiong F (2021) DNA barcoding for identification of fishes in Xiangjiaba reservoir area in the downstream section of the Jinsha River. *Conservation Genetics Resources* 13: 201–208. <https://doi.org/10.1007/s12686-021-01196-6>
- Watanabe Y, Suematsu T, Ohtsuki T (2014) Losing the stem-loop structure from metazoan mitochondrial tRNAs and co-evolution of interacting factors. *Frontiers in Genetics* 5: 109. <https://doi.org/10.3389/fgene.2014.00109>
- Wen ZY, Xie BW, Qin CJ, Wang J, Deng YY, Li R, Zou YC (2017) The complete mitochondrial genome of a threatened loach (*Beaufortia kweichowensis*) and its phylogeny. *Conservation Genetics Resources* 9: 565–568. <https://doi.org/10.1007/s12686-017-0723-3>
- Wu HW, Lin RD, Chen QX, Chen XL, He MQ (1977) Zhongguo like yulei zhi. People's Press, Shanghai, 229–394 pp.
- Wu J, He Y, Ren H, Zhang Y, Du Z, Xie M, Zhu G, Wang Q, Jiang Y, He T, Wen A (2016) The complete mitochondrial genome sequence of *Beaufortia szechuanensis* (Cypriniformes, Balitoridae). *Mitochondrial DNA. Part A, DNA Mapping, Sequencing, and Analysis* 27(4): 2535–2536. <https://doi.org/10.3109/19401736.2015.1038792>
- Xing ZP, Ling X, Wang X, Hu HY, Huang YX (2022) Novel gene rearrangement pattern in mitochondrial genome of *Ooencyrtus plautus* Huang & Noyes, 1994: new gene order in Encyrtidae (Hymenoptera, Chalcidoidea). *ZooKeys* 1124: 1–21. <https://doi.org/10.3897/zookeys.1124.83811>
- Xu DM, Yang Z, Xu N, Xiong MH, Lei P, Que YF (2016) The complete mitochondrial genome of *Lepturichthys fimbriata* (Teleostei, Balitoridae, Balitorinae). *Mitochondrial DNA. Part A, DNA Mapping, Sequencing, and Analysis* 27: 1064–1065. <https://doi.org/10.3109/19401736.2014.928869>
- Xu ZG, Wu L, Hua S, Hua C, Huang T, Zhao Y (2021) Structural variation and phylogenetic relationship of *Geospiza magnirostris* based on mitochondrial control region. *Biologia* 76: 1367–1373. <https://doi.org/10.2478/s11756-020-00669-7>
- Yu P, Ding S, Yang Q, Li X, Wan Q (2016) The complete mitochondrial genome of *Sinibotia robusta* (Cypriniformes: Cobitidae). *Mitochondrial DNA. Part A, DNA Mapping, Sequencing, and Analysis* 27(5): 3471–3472. <https://doi.org/10.3109/19401736.2015.1066353>
- Yu P, Zhou L, Yang WT, Miao LJ, Li Z, Zhang XJ, Wang Y, Gui JF (2021) Comparative mitogenome analyses uncover mitogenome features and phylogenetic implications of the subfamily Cobitinae. *BMC Genomics* 22(1): 50. <https://doi.org/10.1186/s12864-020-07360-w>

- Zhang F, Shen Y (2019) Characterization of the complete mitochondrial genome of *Rhinogobius leavelli* (Perciformes: Gobiidae: Gobionellinae) and its phylogenetic analysis for Gobionellinae. *Biologia* 74: 493–499. <https://doi.org/10.2478/s11756-018-00189-5>
- Zhang C, Ding C, Ding L, Chen L, Hu J, Tao J, Jiang X (2019) Large-scale cascaded dam constructions drive taxonomic and phylogenetic differentiation of fish fauna in the Lancang River, China. *Reviews in Fish Biology and Fisheries* 29: 895–916. <https://doi.org/10.1007/s11160-019-09580-0>
- Zhang D, Gao F, Jakovlić I, Zou H, Zhang J, Li WX, Wang GT (2020) PhyloSuite: An integrated and scalable desktop platform for streamlined molecular sequence data management and evolutionary phylogenetics studies. *Molecular Ecology Resources* 20(1): 348–355. <https://doi.org/10.1111/1755-0998.13096>
- Zhang M, Zhou Q, Xiang H, Wang J, Lan X, Luo Q, Jiang W (2023) Complete mitochondrial genome of *Rectoris luxiensis* (Teleostei, Cyprinidae): characterisation and phylogenetic implications. *Biodiversity Data Journal* 11: e96066. <https://doi.org/10.3897/BDJ.11.e96066>
- Zhong D, Zhao GJ, Zhang ZS, Xun AL (2002) Advance in the entire balance and local unbalance of base distribution in genome. *Hereditas (Beijing)* 24(3): 351–355. [in Chinese]
- Zhou X, Yu Y, Li Y, Wu J, Zhang X, Guo X, Wang W (2014) Comparative analysis of mitochondrial genomes in distinct nuclear ploidy loach *Misgurnus anguillicaudatus* and its implications for polyploidy evolution. *PLoS ONE* 9(3): e92033. <https://doi.org/10.1371/journal.pone.0092033>
- Zou YC, Xie BW, Qin CJ, Wang YM, Yuan DY, Li R, Wen ZY (2017) The complete mitochondrial genome of a threatened loach (*Sinibotia reevesae*) and its phylogeny. *Genes & Genomics* 39: 767–778. <https://doi.org/10.1007/s13258-017-0541-8>
- Zou YC, Chen M, Qin CJ, Wang YM, Li R, Qi ZM, Wen ZY (2018) Identification of the complete mitochondrial genome of *Garra pingi pingi* (Cypriniformes, Cyprinidae). *Conservation Genetics Resources* 10: 693–696. <https://doi.org/10.1007/s12686-017-0903-1>
- Zou Y, Liu T, Li Q, Wen Z, Qin C, Li R, Wang D (2019) Complete mitochondrial genome of *Hemiculter tchangii* (Cypriniformes, Cyprinidae). *Conservation Genetics Resources* 11: 1–4. <https://doi.org/10.1007/s12686-017-0949-0>

## Supplementary material 1

### Supplementary files

Authors: Min Zhou, Cheng Wang, Ziyue Xu, Zhicun Peng, Yang He, Ying Wang

Data type: docx

Explanation note: **figure S1**. Images of biological sample for this study. **table S1**. Primers used for amplification of the mitochondrial genome of *Lepidocephalichthys berdmorei*. **table S2**. Species and GenBank accession numbers of mitogenomes used in this study. **table S3**. Nucleotide contents of genes and the mitochondrial genome skew of *Lepidocephalichthys berdmorei*.

Copyright notice: This dataset is made available under the Open Database License (<http://opendatacommons.org/licenses/odbl/1.0/>). The Open Database License (ODbL) is a license agreement intended to allow users to freely share, modify, and use this Dataset while maintaining this same freedom for others, provided that the original source and author(s) are credited.

Link: <https://doi.org/10.3897/zookeys.1221.129136.suppl1>



# State of knowledge of the ladybird beetle (Coleoptera, Coccinellidae) fauna of Armenia and other Transcaucasian countries, including two new country records

Shoghik Ghazaryan<sup>1</sup>, Marine Arakelyan<sup>1,2</sup>, Astghik Ghazaryan<sup>1,2</sup>, Jerzy Romanowski<sup>3</sup>,  
Krzysztof Turlejski<sup>3</sup>, Piotr Ceryngier<sup>3</sup>

1 Department of Zoology, Yerevan State University, Yerevan, Armenia

2 Research Institute of Biology, Yerevan State University, Yerevan, Armenia

3 Institute of Biological Sciences, Cardinal Stefan Wyszyński University, Warsaw, Poland

Corresponding author: Piotr Ceryngier ([p.ceryngier@uksw.edu.pl](mailto:p.ceryngier@uksw.edu.pl))

## Abstract

Beetles (Coleoptera) have been surveyed in Armenia and other Transcaucasian countries since the first half of the 19<sup>th</sup> century. Based on the literature reports and our new data, available information was gathered on the occurrence in Armenia of one of the beetle families, the ladybirds (Coccinellidae). 84 species of Coccinellidae have been reported from this country in the literature and/or collected during our recent field survey. Two of them, *Anatis ocellata* (Linnaeus, 1758) and *Tytthaspis sedecimpunctata* (Linnaeus, 1761), have not been reported in the literature but were present in our field samples, so they can be considered species new to Armenia, and signify new country records. In addition to the 84 species unambiguously reported from Armenia, 14 were broadly reported from larger regions that include that country (Transcaucasia, the Caucasus) or its parts (the Araks valley). The recognized Coccinellidae fauna of Armenia is slightly poorer than the faunas of other Transcaucasian countries (Azerbaijan and Georgia): there are 92 species currently known to occur in Azerbaijan and 90 species in Georgia. Interestingly, the Armenian fauna contains more Caucasian endemics (10 species) and fewer non-natives (1 species) than the faunas of Azerbaijan (4 endemics and 2 non-natives) and Georgia (6 endemics and 6 non-natives).

**Key words:** Biodiversity, checklist, endemic species, non-native species, South Caucasus



Academic editor: Fedor Konstantinov

Received: 10 May 2024

Accepted: 14 October 2024

Published: 13 December 2024

ZooBank: <https://zoobank.org/4347F47D-D5CE-4562-917C-FD215FE50729>

**Citation:** Ghazaryan S, Arakelyan M, Ghazaryan A, Romanowski J, Turlejski K, Ceryngier P (2024) State of knowledge of the ladybird beetle (Coleoptera, Coccinellidae) fauna of Armenia and other Transcaucasian countries, including two new country records. ZooKeys 1221: 71–102. <https://doi.org/10.3897/zookeys.1221.127225>

Copyright: © Shoghik Ghazaryan et al.  
This is an open access article distributed under terms of the Creative Commons Attribution License (Attribution 4.0 International – CC BY 4.0).

## Introduction

The Caucasus ecoregion, a mountainous area on the border between south-eastern Europe and western Asia, covers the North Caucasus (part of Russia), the South Caucasus or Transcaucasia (Georgia, Armenia, and Azerbaijan, plus smaller separatist areas of South Ossetia and Abkhazia), north-eastern Turkey, and north-western Iran (Zazanashvili et al. 2020). Some parts of the region, such as Colchis (western Georgia) or the southern Caspian basin (south-eastern Azerbaijan and northern Iran), were Pleistocene glacial refugia (Hewitt 1999; Tarkhnishvili et al. 2012). Due to its immense biological diversity, which is at risk of rapid decline, the Caucasus was ranked by Myers et al. (2000) among the 25 globally recognized biodiversity hotspots. Shortly afterwards, part of its area (a small portion of southern

Georgia, approximately half of Armenia and the Azerbaijani enclave of Nakhchivan) was moved to the newly distinguished Irano-Anatolian hotspot (Mittermeier et al. 2004). As a result, the Caucasus ecoregion is divided between two of the 36 currently identified biodiversity hotspots (Zazanashvili et al. 2020). As Mumladze et al. (2020) point out, the region has probably been less intensively studied than many other hotspots, partly due to its tenuous political situation over the past decades.

As a country divided by the border between the Caucasus and Irano-Anatolian hotspots, Armenia is arguably an area of particularly high but as yet insufficiently recognized biodiversity. The Armenian invertebrate fauna, due to the influence of different surrounding faunas (European, Mediterranean, Irano-Turanian), as well as the diversity of landscapes and mountainous nature of the area, is rich and characterized by a high level of endemism (Kalashian et al. 2023). In this paper, we review the available data on a small part of this biodiversity, the ladybird beetles (Coccinellidae). So far, there is no paper summarizing knowledge of the ladybird fauna of Armenia, while checklists of Coccinellidae of the other Transcaucasian states, Georgia and Azerbaijan, have recently been published (Migeon and Arabuli 2022; Snegovaya and Zare Khormizi 2022). Furthermore, the ladybirds of the westernmost portion of the Russian Caucasus along the Black Sea coast were the subject of the recent, detailed study by Bieńkowski and Orlova-Bienkowskaja (2020). Hereafter, we first outline a history of coleopterological (with special reference to Coccinellidae) exploration of Armenia followed by an annotated checklist of the Armenian ladybirds based on the literature data and our unpublished records. Finally, we compare ladybird faunas of the three Transcaucasian countries, Armenia, Azerbaijan, and Georgia. We realize that most animals do not respect political boundaries, and that it would be much more biologically sound to compare the faunas of biogeographical units instead of countries. However, this would not be easy to do, given that in many cases the provided record location data is very general. Moreover, the recently published checklists for Georgian and Azerbaijani ladybirds indicate that it would be worthwhile to compile an analogous checklist for Armenia.

### **A brief history of faunistic studies of Coccinellidae in Armenia and adjacent regions**

While there is a lack of publications presenting detailed studies on the Coccinellidae fauna of Armenia, there is much data on this family scattered in books and papers of a broader scope (e.g., on insects or beetles of the region). Furthermore, some systematic works on Coccinellidae, such as species descriptions or taxonomic revisions, contain data from Armenia. Surveys and publications that have particularly contributed to the knowledge of the ladybird fauna of the Caucasus and Armenia are reviewed below in chronological order.

Entomological exploration of the Caucasus began in the first half of the 19<sup>th</sup> century. In 1827, during the Russo-Persian War, a researcher named Szovitz travelled with the Russian army to Transcaucasia to study the flora of the region. In addition to the numerous plants he collected there until 1830, he also caught some insect specimens. On his way back from the expedition, Szovitz fell ill and subsequently died in the Georgian province of Mingrelia in August 1830 (Faldermann 1835). The insects he collected were later examined by Faldermann (1835, 1837, 1838).

Another scientific expedition to the Caucasus organized by order of the Russian Tsar took place in 1829 and 1830, with the French naturalist Édouard Ménétries

(1802–1861) in charge of the zoological part. After the expedition, Ménétries (1832) published a catalogue of recorded animal species, but independently Faldermann (1835, 1837, 1838) united the data on beetles collected by Ménétries with those collected by Szovitz to compile his 'Fauna Entomologica Trans-Caucasica'.

In 1834 and 1835, the Caucasian entomofauna (mainly Coleoptera) was surveyed by the well-known Russian entomologist Victor Ivanovich Motschulsky, who often signed his works as T. Victor (Victor 1835, 1837). Then, probably in the 1840s and early 1850s, Wagner (1852) spent several years in the Caucasus, Transcaucasia, Armenia, Kurdistan, and western Persia, studying, among other things, the fauna of the region, including beetles. Other major 19<sup>th</sup> century expeditions to the Caucasus involving beetle collecting were those of Schneider and Leder in 1875–1876 (Schneider and Leder 1879) and Leder in 1878 (Leder 1879).

Apart from externally organized Caucasian expeditions, from the 1860s onwards the region was explored as part of the activities of the Caucasus Museum in Tiflis (now Tbilisi). During numerous field trips, the museum's director Gustav Radde and his colleagues collected abundant insect material, subsequently elaborated by eminent entomologists of the time. The animals, including beetles, held in the collection of the Caucasus Museum, were catalogued by Radde (1899).

In most of the publications reporting on the results of the surveys mentioned above, the locations are given imprecisely and many records cannot be attributed to the area of any currently existing country within its present borders. Based on Ménétries' (1832) description of his expedition, we can conclude that it took place outside of present-day Armenia (the present-day Russian Caucasus (including Dagestan and Chechnya) and Azerbaijan), but Szovitz's records are likely to have originated there. However, Faldermann's (1837) compilation does not indicate which of the reported species were collected by Ménétries and which by Szovitz. The area explored by Wagner's (1852) expedition was extensive, but his report lacks any information on the location of the animals collected. On the other hand, Wagner's list of the collected insects is very short and the family Coccinellidae is represented there by only three or four species (two of the four listed names are probably synonyms). Relatively detailed information on the location of the collected species of Coccinellidae can be found in the papers by Motschulsky (Victor 1837), Schneider and Leder (1879), Leder (1879), and Radde (1899). While Leder (1879) reported exclusively from the territories of present-day Georgia and Azerbaijan, some ladybird species reported by Motschulsky (Victor 1837) and, especially, Schneider and Leder (1879) and Radde (1899), were certainly collected within the present Armenian territory.

The first half of the 20<sup>th</sup> century was a time of marked stagnation in the study of the coleopterofauna of the Caucasus. In the second half of the century, the renowned Armenian coleopterist Stepan Iablokoff-Khuzorian conducted his systematic and faunistic research, much of which was devoted to Coccinellidae (e.g., Iablokoff-Khuzorian 1971, 1972, 1974, 1982, 1983). Iablokoff-Khuzorian was primarily a taxonomist, paying little attention to providing geographical details for each of the species he recorded. Therefore, as in some of the 19<sup>th</sup> century publications, the distribution data he provided often do not allow for a clear attribution to a specific country. After the period of Iablokoff-Khuzorian's research activities, from the 1990s to the present, virtually nothing has been published on ladybirds of Armenia, with the exception of reports by Kalashian et al. (2017, 2019) on the arrival and spread of the invasive harlequin ladybird, *Harmonia axyridis* (Pallas, 1773), in that country.

## Checklist of Coccinellidae reported from Armenia

The checklist includes available literature reports supplemented by previously unpublished data collected between 2018 and 2023 in all 11 provinces of Armenia by MA, AG, and M. Kalashian (National Academy of Sciences, Yerevan). The new data were recorded using standard collection methods, such as a beating tray, sweep net, or direct observation. Specimens collected by MA and AG are deposited in Research Institute of Biology of Yerevan State University, and those collected by M. Kalashian, in the Scientific Center of Zoology and Hydroecology, National Academy of Science, Yerevan.

The systematic arrangement of Coccinellidae, including the sequence of tribes, used in the checklist below follows Che et al. (2021) and the nomenclature of genera and species follows Kovář (2007). To our knowledge, for all species included in this checklist, the names provided by Kovář (2007) are valid. They are given here in bold, while the primary synonyms (provided if different from the valid names) and other synonyms (only those mentioned in the checklist) are in non-bold. The genera and species within the tribes are arranged alphabetically. Names of species that are possible but not certain to occur in Armenia (only generally reported from regions encompassing this country or its parts) are in square brackets to distinguish them from those unquestionably reported from the area of present-day Armenia. For individual species, we first provide new data (if available), including the name of the province, locality, geographical coordinates, altitude, date of collection, number of specimens collected, and the collector's name. We then list the literature reports, starting with those pointing unambiguously to Armenia and then moving on to more general location descriptions that do not exclude Armenia, such as the "Araks valley", "Transcaucasia", or the "Caucasus". At present, Araks' river source and initial course lie in Turkey, which then flows along the Turkish-Armenian border, next the border between Turkey and Nakhchivan, Iran and Nakhchivan, Iran and Armenia, and Iran and Azerbaijan. Finally, it flows to the Kura River on the Azerbaijani territory.

### Subfamily Coccinellinae Latreille, 1807

#### Tribe Stethorini Dobzhansky, 1924

##### ***Stethorus gilvifrons* (Mulsant, 1850)**

*Scymnus gilvifrons* Mulsant, 1850

**Literature data.** Armenia: Schneider and Leder (1879) (Echmiadzin, Yerevan); Jacobson (1915); Kovář (2007). Araks valley: Iablokoff-Khnzorian (1983).

##### ***Stethorus pusillus* (Herbst, 1797)**

*Scymnus pusillus* Herbst, 1797

**Literature data.** Armenia: Kovář (2007). Caucasus: Iablokoff-Khnzorian (1983).

### Tribe Coccinellini Latraille, 1807

#### *Adalia bipunctata* (Linnaeus, 1758)

*Coccinella bipunctata* Linnaeus, 1758

*Coccinella fasciatopunctata* Faldermann, 1835

**New data.** Kotayk: • Tsaghkadzor, 40.5314°N, 44.7249°E, 1841 m a.s.l., Jul. 2021, 5 exx. (leg. M. Arakelyan); Gegharkunik: • Akunk, 40.1572°N, 45.7263°E, 1965 m a.s.l., 19 Oct. 2020, 4 exx. (leg. M. Arakelyan); Vayots Dzor: • Hors, 39.8625°N, 45.2303°E, 1694 m a.s.l., 23 Jul. 2021, 1 ex. (leg. M. Arakelyan); Armavir: • river Kasagh, 40.1047°N, 44.2360°E, 870 m a.s.l., 1 Jun. 2021, 1 ex. (leg. M. Arakelyan); Syunik: • Lichk, 39.6074°N, 46.1113°E, 1929 m a.s.l., 17 May 2022, 8 exx. (leg. M. Arakelyan); Aragatsotn: • Karbi, 40.3233°N, 44.3800°E, 1303 m a.s.l., 22 Jun. 2019, 2 exx. (leg. A. Ghazaryan).

**Literature data.** Armenia: Kovář (2007). Caucasus: Heyden et al. (1891, 1906) (as *Adalia fasciatopunctata stictica* Muls.); Jacobson (1915) (as *A. fasciatopunctata* Fald.); Iablokoff-Khuzorian (1983).

#### *Adalia decempunctata* (Linnaeus, 1758)

*Coccinella decempunctata* Linnaeus, 1758

**New data.** Kotayk: • Hankavan, 40.6019°N, 44.6185°E, 1990 m a.s.l., 25.06.2021, 2 exx. (leg. M. Arakelyan); • Tsaghkadzor, 40.5313°N, 44.7249°E, 1841 m a.s.l., July, 2021, 1 ex. (leg. M. Arakelyan); Syunik: • Shenatagh, 39.38°N, 46.1322°E, 2500 m a.s.l., 18.06.2021, 1 ex. (leg. A. Ghazaryan); • Lichk, 39.6073°N, 46.1113°E, 1929 m a.s.l., 17.05.2022, 12 exx.; • Harsnadzor rest., 39.3927°N, 46.2784°E, 1929 m a.s.l., 18.05.2022, 2 exx. (leg. M. Arakelyan).

**Literature data.** Armenia: Schneider and Leder (1879); Jacobson (1915); Kovář (2007). Caucasus: Iablokoff-Khuzorian (1982, 1983).

#### *Anatis ocellata* (Linnaeus, 1758), new country record

*Coccinella ocellata* Linnaeus, 1758

**New data.** Kotayk: • Tsaghkadzor, 40.5313°N, 44.7249°E, 1841 m a.s.l., July, 2021, 1 ex. (leg. M. Arakelyan).

**Literature data.** Caucasus: Iablokoff-Khuzorian (1982, 1983).

**Remarks.** Prior to the record provided above, *A. ocellata* has not been explicitly reported as occurring in Armenia.

#### *Anisosticta caucasica* (Fleischer, 1900)

*Adonia arctica* v. *caucasica* Fleischer, 1900

**Literature data.** Armenia: Jacobson (1915) (as *Hippodamia arctica* subsp. *caucasica* Fleisch.); Kovář (2007). Araks valley: Fleischer (1900) (as *Adonia arctica* v. *caucasica*). Caucasus: Heyden et al. (1906) (as *Hippodamia arctica* v. *caucasica* Fleischer), Winkler (1927) (as *H. arctica* ?s. *caucasica* Fleisch.).

**Remarks.** There is no consensus on what Fleischer's (1900) *A. arctica* v. *caucasica* really is. While Fürsch (1977) and Kovář (2007) considered it as a distinct species belonging to the genus *Anisosticta*, according to Iablokoff-Khnzorian (1982, 1983), it is a synonym of *Hippodamia* (*Semiadalia*) *schneideri* (Weise, 1878). In his opinion, Fleischer's type is a small, untypically colored specimen of *H.* (*Semiadalia*) (= *Ceratomegilla*) *schneideri*.

***Anisosticta novemdecimpunctata* (Linnaeus, 1758)**

*Coccinella novemdecimpunctata* Linnaeus, 1758

*Anisosticta egena* Weise, 1887

**Literature data.** Armenia: Iablokoff-Khnzorian (1983) (whole Caucasus); Kovář (2007). Caucasus: Heyden et al. (1891) (as *A. 19-punctata* v. *egena* Ws.); Heyden et al. (1906) (as *A. egena* Ws.).

***Aphidecta obliterated* (Linnaeus, 1758)**

*Coccinella obliterated* Linnaeus, 1758

**Literature data.** Armenia: Kovář (2007). Caucasus: Winkler (1927).

***Bulaea lichatschovii* (Hummel, 1827)**

*Coccinella Lichatschovii* Hummel, 1827

**Literature data.** Armenia: Schneider and Leder (1879) (Echmiadzin); Jacobson (1915); Iablokoff-Khnzorian (1983) (whole Caucasus); Kovář (2007). Araks valley: Radde (1899) (as *B. Lichatschovi* var. *coronata* Weise.). Transcaucasia: Faldermann (1837). Caucasus: Weise (1879, 1885) (as *B. Lichatschovii* v. *coronata* Ws.); Heyden et al. (1891, 1906) (as *B. Lichatschovi* v. *coronata* Ws.).

**[*Bulaea lividula bocandei* Mulsant, 1850]**

*Bulaea Bocandei* Mulsant, 1850

**Literature data.** Caucasus: Weise (1885) (as *B. Lichatschovii* v. *pallida* Motsch.).

**Remark.** Biranvand et al. (2024) consider *B. lividula bocandei* a separate species, *B. bocandei* Mulsant, 1850.

***Calvia decemguttata* (Linnaeus, 1767)**

*Coccinella decemguttata* Linnaeus, 1767

*Calvia hololeuca* Mulsant, 1850 (synonymized by Iablokoff-Khnzorian (1972))

**Literature data.** Armenia: Kovář (2007). Caucasus: Mulsant (1850, 1866) (as *Calvia hololeuca*); Weise (1879, 1885) (as *Halyzia decemguttata* v. *hololeuca* Muls.); Heyden et al. (1891) (as *Halyzia decemguttata* v. *hololeuca* Muls.); Heyden et al. (1906) (as *Calvia 10-guttata* v. *hololeuca* Muls.); Iablokoff-Khnzorian (1972).

***Calvia quatuordecimguttata* (Linnaeus, 1758)**

*Coccinella quatuordecimguttata* Linnaeus, 1758

*Propylaea Rosti* Weise, 1891

**New data.** Kotayk: • Tsaghkadzor, 40.5313°N, 44.7249°E, 1841 m a.s.l., July, 2021, 2 exx. (leg. M. Arakelyan); Syunik: • Lichk, 39.6073°N, 46.1113°E, 1929 m a.s.l., 17.05.2022, 1 ex. (leg. M. Arakelyan).

**Literature data.** Armenia: Kovář (2007). Caucasus: Heyden et al. (1906) (as *Propylaea Rosti* Ws.); Jacobson (1915) (as *Propylaea Rosti* Ws.); Winkler (1927) (as *Propylaea Rosti* Ws.).

**[*Calvia quindecimguttata* (Fabricius, 1777)]**

*Coccinella quindecimguttata* Fabricius, 1777

**Literature data.** Caucasus: Iablokoff-Khnzorian (1982, 1983).

***Ceratomegilla apicalis* (Weise, 1879)**

*Adalia apicalis* Weise, 1879

**Literature data.** Armenia: Iablokoff-Khnzorian (1982, 1983); Kovář (2007). Caucasus: Weise (1885); Heyden et al. (1891, 1906); Winkler (1927).

***Ceratomegilla notata* (Laicharting, 1781)**

*Coccinella notata* Laicharting, 1781

**Literature data.** Armenia: Kovář (2007). Caucasus: Heyden et al. (1906); Winkler (1927).

***Ceratomegilla schelkovnikovi* (Dobzhansky, 1927)**

*Semiadalia schelkovnikovi* Dobzhansky, 1927

**Literature data.** Armenia: Dobzhansky (1927) (lake Sevan, Yerevan); Iablokoff-Khnzorian (1983); Kovář (2007).

**Remarks.** Dobzhansky's original spelling of the specific epithet is 'shelkovnikovi'. Type locality: lake Sevan (Goktsha-See) in Armenia.

***Ceratomegilla schneideri* (Weise, 1878)**

*Coccinella schneideri* Weise, 1878

**Literature data.** Armenia: Schneider and Leder (1879) (Alexandrapol (=Gyumri)); Jacobson (1915); Iablokoff-Khnzorian (1983); Kovář (2007). Caucasus: Weise (1879) (as *Adalia schneideri* Ws.); Weise (1885); Heyden et al. (1891, 1906); Winkler (1927).

### ***Ceratomegilla undecimnotata* (Schneider, 1792)**

*Coccinella undecimnotata* Schneider, 1792

*Coccinella Saliana* Faldermann, 1837

*Coccinella maritima* Ménétries, 1832

**Literature data.** Armenia: Iablokoff-Khuzorian (1982); Kovář (2007); Ceryngier et al. (2023) (Tigranashen, as a host of a hymenopterous parasitoid *Dinocampus coccinellae* (Schrank)). Transcaucasia: Faldermann (1837) (as *Coccinella Saliana* Fald. and *C. maritima* Ménétries). Caucasus: Weise (1879) (as *Adalia undecimnotata* Schneid.); Weise (1885); Radde (1899).

### ***Coccinella alpigrada* (Iablokoff-Khuzorian, 1957)**

*Adalia alpigrada* Iablokoff-Khuzorian, 1957

**Literature data.** Armenia: Iablokoff-Khuzorian (1957, 1982, 1983); Kovář (2007).

**Remarks.** Described from Armenia. Type locality: Yanykh, Martuni region (province Gegharkunik).

### ***Coccinella magnifica* Redtenbacher, 1843**

*Coccinella distincta* Faldermann, 1837

**New data.** Kotayk: • Arzakan, 40.4494°N, 44.6063°E, 1489 m a.s.l., 07.06.2021, 5 exx. (leg. M. Arakelyan).

**Literature data.** Armenia: Kovář (2007). Transcaucasia: Faldermann (1837) (as *C. distincta*); Iablokoff-Khuzorian (1983). Caucasus: Weise (1885) (as *C. distincta* Faldermann); Heyden et al. (1891, 1906) (as *C. distincta* Fald.); Winkler (1927) (as *C. divaricata* Ol.).

### ***Coccinella quinquepunctata* Linnaeus, 1758**

*Coccinella tripunctata* Rossi, 1790

**Literature data.** Armenia: Victor (1837) (as *Coccinella 3 punctata* Rossi); Mulsant (1866) (as *Coccinella tripunctata* Rossi), Kovář (2007).

**Remarks.** Kovář (2007) considers *Coccinella tripunctata* Rossi, 1790 a synonym of *C. quinquepunctata*. However, according to Crotch (1874), *C. tripunctata* Rossi is a variety of *Coccinella undecimpunctata* L. Iablokoff-Khuzorian (1983) states that *C. quinquepunctata* is present in the Caucasus, but not in Armenia.

### ***Coccinella septempunctata* Linnaeus, 1758**

**New data.** Syunik: • Shenatagh, 39.38°N, 46.1322°E, 2500 m a.s.l., 18.06.2021, 5 exx. (leg. A. Ghazaryan); • Kajaran, 39.1511°N, 46.16°E, 1950 m a.s.l., 13.06.2021, 14 exx. (leg. A. Ghazaryan); • Zvaravank Monastery, 39.0472°N, 46.1694°E, 1815 m a.s.l., 16.05.2022, 1 ex. (leg. M. Arakelyan); • Meghri, 38.9029°N, 46.2445°E, 610 m a.s.l., 15.05.2022, 4 exx. (leg. M. Arakelyan); • Lichk, 39.6073°N, 46.1113°E, 1929 m

a.s.l., 17.05.2022, 1 ex. (leg. M. Arakelyan); Ararat: • Azat reservoir, 40.07138°N, 44.6161°E, 1025 m a.s.l., 20.09.2021, 1 ex. (leg. M. Arakelyan); • Khosrov, 40.0458°N, 44.8982°E, 1465 m a.s.l., 28.05.2021, 2 ex. (leg. M. Arakelyan); Lori: • Mets Parni, 40.8372°N, 44.1091°E, 1680 m a.s.l., 05.06.2020, 22.06.2020, 2 ex. (leg. M. Arakelyan); Vayots Dzor: • Hors, 39.8625°N, 45.2302°E, 1694 m a.s.l., 12.06.2021, 1 ex. (leg. M. Arakelyan); • Horbategh, 39.8902°N, 45.3541°E, 1850 m a.s.l., 04.06.2023, 3 ex. (leg. M. Arakelyan); Tavush: • Voskepar, 41.0647°N, 45.0575°E, 850 m a.s.l., 26.09.2020, 1 ex. (leg. M. Arakelyan); Gegharkunik: • Dzoragyugh, 40.1694°N, 45.1986°E, 2003 m a.s.l., 06.06.2021, 1 ex. (leg. M. Arakelyan); Kotayk: • Tsaghkadzor, 40.5313°N, 44.7249°E, 1841 m a.s.l., June 2023, 3 ex. (leg. M. Arakelyan).

**Literature data.** Armenia: Jacobson (1915) (the whole Caucasus); Kovář (2007). Caucasus: Victor (1837).

### ***Coccinella undecimpunctata* Linnaeus, 1758**

**Literature data.** Armenia: Radde (1899) (Meghri); Jacobson (1915).

### ***Coccinula quatuordecimpustulata* (Linnaeus, 1758)**

*Coccinella quatuordecimpustulata* Linnaeus, 1758

**New data.** Lori: • Mets Parni, 40.8372°N, 44.1091°E, 1680 m a.s.l., 22.08.2018, 9 ex. (leg. M. Arakelyan); Syunik: • Lichk, 39.6073°N, 46.1113°E, 1929 m a.s.l., 17.05.2022, 1 ex. (leg. M. Arakelyan); Kotayk: • Gegard, 40.1553°N, 44.7913°E, 1759 m a.s.l., 22.05.2022, 1 ex. (leg. M. Arakelyan); • Tsaghkadzor, 40.5313°N, 44.7249°E, 1841 m a.s.l., June 2023, 2 ex. (leg. M. Arakelyan); Ararat: • Khosrov, 40.0458°N, 44.8982°E, 1465 m a.s.l., 28.05.2021, 2 ex. (leg. M. Arakelyan); Vayots Dzor: • Hors, 39.8625°N, 45.2302°E, 1694 m a.s.l., 12.06.2021, 1 ex. (leg. M. Arakelyan).

**Literature data.** Armenia: Radde (1899) (Helenowka (= Sevan)); Jacobson (1915); Iablokoff-Khznorian (1982, 1983); Kovář (2007).

### ***Coccinula sinuatomarginata* (Faldermann, 1837)**

*Coccinella sinuato-marginata* Faldermann, 1837

**New data.** Syunik: • Lichk, 39.6073°N, 46.1113°E, 1929 m a.s.l., 17.05.2022, 1 ex. (leg. M. Arakelyan).

**Literature data.** Armenia: Jacobson (1915); Iablokoff-Khznorian (1982, 1983); Kovář (2007). Transcaucasia: Faldermann (1837) (as *Coccinella sinuato-marginata*). Caucasus: Mulsant (1850, 1866) (as *Coccinella sinuato-marginata* Faldermann); Weise (1879, 1885); Heyden et al. (1906) (as *Synharmonia sinuatomarginata* Fald.).

### ***Halyzia sedecimguttata* (Linnaeus, 1758)**

*Coccinella sedecimguttata* Linnaeus, 1758

**New data.** Kotayk: • Tsaghkadzor, 40.5313°N, 44.7249°E, 1841 m a.s.l., July 2021, 1 ex. (leg. M. Arakelyan).

**Literature data.** Armenia: lablokoff-Khnzorian (1982); Kovář (2007). Caucasus: Winkler (1927); lablokoff-Khnzorian (1983).

### ***Harmonia axyridis* (Pallas, 1773)**

*Coccinella axyridis* Pallas, 1773

**New data.** Kotayk: • Tsaghkadzor, 40.5313°N, 44.7249°E, 1841 m a.s.l., July 2021, 2 exx. (leg. M. Arakelyan); • Hankavan, 40.6019°N, 44.6185°E, 1990 m a.s.l., 25.06.2021, 1 ex. (leg. M. Arakelyan); Shirak: • Gyumri, 40.7942°N, 43.8452°E, 1509 m a.s.l., 15.10.2020, 1 ex. (leg. M. Arakelyan); Yerevan: • Yerevan State University, 40.1817°N, 44.5261°E, 990 m a.s.l., 27.07.2020, 1 ex. (leg. M. Arakelyan); Aragatsotn: • Karbi, 40.3233°N, 44.3800°E, 1303 m a.s.l., 22.06.2019, 1 ex. (A.Ghazaryan); Lori: • Amrakits, 40.0002°N, 44.4303°E, 1380 m a.s.l., 31.05.2023, 2 exx. (leg. M. Arakelyan); • Pushkino, 40.9688°N, 44.4144°E, 1450 m a.s.l., 26.06.2023, 1 ex. (leg. M. Arakelyan); • Sanahin, 41.0873°N, 44.6661°E, 1016 m a.s.l., 28.05.2023, 1 ex. (leg. M. Arakelyan); • Privolnoye, 41.1709°N, 44.4415°E, 1629 m a.s.l., 14.06.2020, 1 ex. (leg. M. Kalashian); • Gyulagarak, 40.9620°N, 44.4696°E, 1358 m a.s.l., 09.07.2020, 15.07.2020, 20.07.2020, 3 exx. (leg. M. Kalashian); • Kachachkut, 41.1600°N, 44.5852°E, 2510 m a.s.l., 18.07.2021, 1 ex. (leg. M. Kalashian); • Margahovit, 40.70933°N, 44.66645°E, 1918 m a.s.l., 04.07.2021, 1 ex. (leg. M. Kalashian); • Odzun, 41.038577°N, 44.627781°E, 1034 m a.s.l., 30.05.2021, 1 ex. (leg. M. Kalashian); Gegharkunik: • Aygut, 40.6878°N, 45.1473°E, 1268 m a.s.l., 18.07.2020, 1 ex. (leg. M. Kalashian); • Shorzha, 40.49845°N, 45.29701°E, 1938 m a.s.l., 12.07.2021, 1 ex. (leg. M. Kalashian); Ararat: • Sipanik, 40.0796°N, 44.3637°E, 843 m a.s.l., 08.09.2020, 1 ex. (leg. M. Kalashian); • Armash, 39.796°N, 44.8415°E, 1203 m a.s.l., 07.08.2021, 1 ex. (leg. M. Kalashian); Tavush: • Gosh, 40.7409°N, 45.0334°E, 1080 m a.s.l., 18.06.2021, 1 ex. (leg. M. Kalashian).

**Literature data.** Armenia: Kalashian et al. (2017, 2019).

### ***Hippodamia tredecimpunctata* (Linnaeus, 1758)**

*Coccinella tredecimpunctata* Linnaeus, 1758

*Hippodamia signata* Faldermann, 1837

**New data.** Vayots Dzor: • Spitakavor church, 39.8297°N, 45.3644°E, 540 m a.s.l., 12.08.2020, 1 ex. (leg. M. Arakelyan).

**Literature data.** Armenia: Jacobson (1915) (as *H. tredecimpunctata* subsp. *signata* Fald.) (Yerevan); Kovář (2007). Transcaucasia: Faldermann (1837) (as *H. signata* Fald.). Caucasus: Weise (1885); Heyden et al. (1891, 1906); Winkler (1927); lablokoff-Khnzorian (1982, 1983).

### ***Hippodamia variegata* (Goeze, 1777)**

*Coccinella variegata* Goeze, 1777

**New data.** Gegharkunik: • Tsovak, 40.1819°N, 45.635°E, 1920 m a.s.l., 04.06.2021, 2 exx. (leg. M. Arakelyan); Ararat: • Ranchpar, 40.0253°N, 44.3703°E,

834 m a.s.l., 05.06.2021, 1 ex. (leg. M. Arakelyan); • Khosrov, 40.0458°N, 44.8982°E, 1465 m a.s.l., 28.05.2021, 1 ex. (leg. M. Arakelyan); Vayots Dzor: • Hors, 39.8625°N, 45.2302°E, 1694 m a.s.l., 12.06.2021, 2 exx. (leg. M. Arakelyan); Kotayk: • Hankavan, 40.6019°N, 44.6185°E, 1990 m a.s.l., 25.06.2021, 1 ex. (leg. M. Arakelyan); Tavush: • Voskepar, 41.0647°N, 45.0575°E, 850 m a.s.l., 26.09.2020, 2 exx. (leg. M. Arakelyan).

**Literature data.** Armenia: Radde (1899) (Echmiadzin); Jacobson (1915) (Yerevan); Kovář (2007); Ceryngier et al. (2023) (Nzhdeh, as a host of *D. coccinellae*).

### ***Myrrha octodecimguttata* (Linnaeus, 1758)**

*Coccinella octodecimguttata* Linnaeus, 1758

**Literature data.** Armenia: Iablokoff-Khuzorian (1983); Kovář (2007).

### ***Myzia oblongoguttata* (Linnaeus, 1758)**

*Coccinella oblongoguttata* Linnaeus, 1758

**Literature data.** Armenia: Iablokoff-Khuzorian (1982, 1983). Caucasus: Winkler (1927) (as *Paramysia oblongoguttata* L.).

### ***Oenopia conglobata* (Linnaeus, 1758)**

*Coccinella conglobata* Linnaeus, 1758

**New data.** Gegharkunik: • Akunk, 40.1572°N, 45.7263°E, 1965 m a.s.l., 19.10.2020, 3 exx. (leg. M. Arakelyan); Ararat: • Ranchpar, 40.0252°N, 44.3702°E, 834 m a.s.l., 05.06.2021, 1 ex. (leg. M. Arakelyan); Kotayk: • Tsaghkadzor, 40.5313°N, 44.7249°E, 1841 m a.s.l., July 2021, 1 ex. (leg. M. Arakelyan); Ar-mavir: • river Kasagh, 40.1046°N, 44.2359°E, 870 m a.s.l., 01.06.2021, 1 ex. (leg. M. Arakelyan); Syunik: • Lichk, 39.6073°N, 46.1113°E, 1929 m a.s.l., 17.05.2022, 2 exx. (leg. M. Arakelyan).

**Literature data.** Armenia: Iablokoff-Khuzorian (1972); Kovář (2007). Trans-caucasia: Iablokoff-Khuzorian (1983).

### ***Oenopia impustulata* (Linnaeus, 1767)**

*Coccinella impustulata* Linnaeus, 1767

*Coccinella caucasica* Motschulsky, 1837 (synonymized by Kovář (2007))

**Literature data.** Armenia: Kovář (2007). Transcaucasia: Iablokoff-Khuzorian (1983). Caucasus: Victor (1837) (as *Coccinella caucasica*); Mulsant (1850) (as *Harmonia caucasica* Motschoulsky); Heyden et al. (1891) (as *Harmonia conglobata* v. *caucasica* Motsch.); Heyden et al. (1906) (as *Synharmonia conglobata* v. *caucasica* Motsch.); Iablokoff-Khuzorian (1972).

***Oenopia lyncea agnatha* (Rosenhauer, 1847)**

*Coccinella lyncea agnatha* Rosenhauer, 1847

**Literature data.** Armenia: Iablokoff-Khnzorian (1982); Kovář (2007). Transcaucasia: Iablokoff-Khnzorian (1983).

***Oenopia oncina* (Olivier, 1808)**

*Coccinella oncina* Olivier, 1808

*Coccinella asiatica* Weise, 1885

*Coccinella persica* Faldermann, 1837

**Literature data.** Armenia: Schneider and Leder (1879) (as *Coccinella persica* Faldermann) (Echmiadzin, Tarstschai); Weise (1885) (as *Harmonia lyncea* v. *asiatica* Ws. and *H. lyncea* v. *persica* Faldermann); Jacobson (1915) (Yerevan); Kovář (2007). Transcaucasia: Faldermann (1837) (as *Coccinella persica* Faldermann); Heyden et al. (1891) (as *Harmonia lyncea* v. *asiatica* Ws.); Heyden et al. (1906) (as *Synharmonia oncina* a. *asiatica* Ws.); Iablokoff-Khnzorian (1983).

***Propylea quatuordecimpunctata* (Linnaeus, 1758)**

*Coccinella quatuordecimpunctata* Linnaeus, 1758

**New data.** Armavir: • river Kasagh, 40.1046°N, 44.2359°E, 870 m a.s.l., 01.06.2021, 2 exx. (leg. M. Arakelyan); Ararat: • Khosrov, 40.0458°N, 44.8982°E, 1465 m a.s.l., 28.05.2021, 3 exx. (leg. M. Arakelyan); Syunik: • Lichk, 39.6073°N, 46.1113°E, 1929 m a.s.l., 17.05.2022, 3 exx. (leg. M. Arakelyan); Aragatsotn: • Karbi, 40.3233°N, 44.3800°E, 1303 m a.s.l., 22.06.2019, 6 exx. (leg. M. Arakelyan); Lori: • Mets Parni, 40.8372°N, 44.1091°E, 1680 m a.s.l., 22.08.2018, 1 ex. (leg. M. Arakelyan); Kotayk: • Tsaghkadzor, 40.5313°N, 44.7249°E, 1841 m a.s.l., June 2023, 3 exx. (leg. M. Arakelyan).

**Literature data.** Armenia: Radde (1899) (as *Halyzia quatuordecimpunctata* L.) (Yerevan); Jacobson (1915) (Yerevan); Kovář (2007); Ceryngier et al. (2023) (Khor Virap, as a host of *D. coccinellae*). Caucasus: Winkler (1927).

***Psyllobora vigintiduopunctata* (Linnaeus, 1758)**

*Coccinella vigintiduopunctata* Linnaeus, 1758

**New data.** Kotayk: • Tsaghkadzor, 40.5313°N, 44.7249°E, 1841 m a.s.l., July 2021, 1 ex., June 2023, 5 exx. (leg. M. Arakelyan); Syunik: • Lichk, 39.6073°N, 46.1113°E, 1929 m a.s.l., 17.05.2022, 2 exx. (leg. M. Arakelyan); Lori: • Mets Parni, 40.8372°N, 44.1091°E, 1680 m a.s.l., 22.08.2018, 3 exx. (leg. M. Arakelyan); Aragatsotn: • Karbi, 40.3233°N, 44.3800°E, 1303 m a.s.l., 22.06.2019, 7 exx. (leg. M. Arakelyan).

**Literature data.** Armenia: Schneider and Leder (1879) (Echmiadzin, Yerevan); Radde (1899) (as *Halyzia vigintiduopunctata* L.) (Yerevan); Jacobson (1915) (Yerevan); Kovář (2007).

**[*Tytthaspis gebleri* (Mulsant, 1850)]**

*Micraspis gebleri* Mulsant, 1850

*Coccinella lineola* Gebler, 1843

**Literature data.** Caucasus: Winkler (1927) (as *Tytthaspis lineola* Gebl.).

***Tytthaspis sedecimpunctata* (Linnaeus, 1761), new country record**

*Coccinella sedecimpunctata* Linnaeus, 1761

**New data.** Lori: • Mets Parni, 40.8372°N, 44.1091°E, 1680 m a.s.l., 22.08.2018, 2 exx. (leg. M. Arakelyan); Syunik: • Lichk, 39.6073°N, 46.1113°E, 1929 m a.s.l., 17.05.2022, 1 ex. (leg. M. Arakelyan).

**Remark.** To the best of our knowledge, *T. sedecimpunctata* has not previously been reported from Armenia.

***Vibidia duodecimguttata* (Poda von Neuhaus, 1761)**

*Coccinella duodecimguttata* Poda von Neuhaus, 1761

**New data.** Vayots Dzor: • Hors, 39.8625°N, 45.2302°E, 1694 m a.s.l., 23.07.2021, 1 ex. (leg. M. Arakelyan).

**Literature data.** Armenia: Kovář (2007). Transcaucasia: Iablokoff-Khnzorian (1983).

**Tribe Epilachnini Mulsant, 1846**

***Henosepilachna argus* (Geoffroy, 1785)**

*Coccinella argus* Geoffroy, 1785

**Literature data.** Armenia: Iablokoff-Khnzorian (1980, 1981, 1983) (Araks valley in Armenia); Kovář (2007). Caucasus: Radde (1899); Jacobson (1915).

***Subcoccinella vigintiquatuorpunctata* (Linnaeus, 1758)**

*Coccinella vigintiquatuorpunctata* Linnaeus, 1758

*Coccinella colchica* Motschulsky, 1839

**New data.** Kotayk: • Arzakan, 40.4494°N, 44.6063°E, 1489 m a.s.l., 07.06.2021, 1 ex. (leg. M. Arakelyan).

**Literature data.** Armenia: Schneider and Leder (1879) (Alexandrapol (=Gyumri)); Jacobson (1915) (Yerevan); Iablokoff-Khnzorian (1980, 1983); Kovář (2007). Caucasus: Mulsant (1850) (as *Epilachna colchica* Motschoulsky); Heyden et al. (1906); Winkler (1927).

### **Tribe Scymnini Mulsant, 1846**

#### ***Clitostethus arcuatus* (Rossi, 1794)**

*Coccinella arcuata* Rossi, 1794

**Literature data.** Armenia: Iablokoff-Khnzorian (1983) (in the Caucasus reaches the Araks valley); Kovář (2007). Caucasus: Winkler (1927).

#### **[*Nephus (Bipunctatus) bipunctatus* (Kugelann, 1794)]**

*Scymnus bipunctatus* Kugelann, 1794

**Literature data.** Transcaucasia: Iablokoff-Khnzorian (1983).

#### ***Nephus (Nephus) ludyi* (Weise, 1879)**

*Scymnus ludyi* Weise, 1879

*Nephus ponticus* Iablokoff-Khnzorian, 1970

**Literature data.** Armenia: Iablokoff-Khnzorian (1970a, 1983) (as *N. ponticus* Iablokoff-Khnzorian, 1970) (Yerevan); Kovář (2007).

#### ***Nephus (Nephus) quadrimaculatus* (Herbst, 1783)**

*Sphaeridium quadrimaculatum* Herbst, 1783

**Literature data.** Armenia: Iablokoff-Khnzorian (1983) (N Armenia, Yerevan).

#### ***Nephus (Sidis) caucasicus* (Weise, 1929)**

*Scymnus caucasicus* Weise, 1929

*Scymnus plagiatus* Weise, 1878

**Literature data.** Armenia: Schneider and Leder (1879) (as *Scymnus plagiatus* Weise nov. sp.) (Yerevan); Weise (1879, 1885) (as *Scymnus (Nephus) plagiatus* Ws.) (Yerevan); Jacobson (1915) (as *N. plagiatus* Ws.) (Yerevan); Iablokoff-Khnzorian (1983) Yerevan and its vicinity); Kovář (2007). Caucasus: Heyden et al. (1891, 1906) (as *N. plagiatus*).

#### ***Scymniscus biflammulatus* (Motschulsky, 1837)**

*Scymnus biflammulatus* Motschulsky, 1837

**Literature data.** Armenia: Iablokoff-Khnzorian (1983) (almost whole Caucasus); Kovář (2007). Caucasus: Weise (1879, 1885) (as *Scymnus biflammulatus* Motsch.); Heyden et al. (1891, 1906) (as *Sidis biflammulatus* Motsch.); Jacobson (1915) (as *Sidis biflammulatus* Motsch.); Winkler (1927) (as *Sidis biflammulatus* Mtsch.).

***Scymniscus biguttatus* (Mulsant, 1850)**

*Scymnus biguttatus* Mulsant, 1850  
*Scymnus bipustulatus* Motschulsky, 1837

**Literature data.** Armenia: Jacobson (1915) (as *Sidis biguttatus* Muls.) (Yerevan). Araks valley: Heyden et al. (1906) (as *Sidis biguttatus* a. *4-guttatus* Fleisch). Caucasus: Weise (1879) (as *Scymnus (Sidis) bipustulatus* Motsch.); Weise (1885) (as *Scymnus (Sidis) biguttatus* Muls.); Winkler (1927) (as *Sidis biguttatus* Muls.).

***Scymnus (Mimopullus) pharaonis* Motschulsky, 1851**

*Scymnus pharaonis* Motschulsky, 1851  
*Scymnus (Pullus) araraticus* lablokoff-Khnzorian, 1969

**Literature data.** Armenia: lablokoff-Khnzorian (1969, 1972, 1983) (as *Scymnus (Pullus) araraticus* lablokoff-Khnzorian, 1969) (Kapan region, Yerevan vicinity); Kovář (2007).

***Scymnus (Neopullus) haemorrhoidalis* Herbst, 1797**

*Scymnus haemorrhoidalis* Herbst, 1797

**Literature data.** Armenia: Schneider and Leder (1879) (Yerevan); Jacobson (1915) (Yerevan); lablokoff-Khnzorian (1983) (whole Caucasus); Kovář (2007).

***Scymnus (Neopullus) limbatus* Stephens, 1832**

*Scymnus limbatus* Stephens, 1832

**Literature data.** Armenia: lablokoff-Khnzorian (1972, 1983) (Yerevan); Kovář (2007).

***Scymnus (Neopullus) testaceus* Motschulsky, 1837**

*Scymnus testaceus* Motschulsky, 1837

**Literature data.** Armenia: lablokoff-Khnzorian (1972, 1983) (whole Caucasus). Caucasus: Weise (1879); Heyden et al. (1891, 1906); Radde (1899).

***Scymnus (Pullus) argutus* Mulsant, 1850**

*Scymnus argutus* Mulsant, 1850

**Literature data.** Armenia: Mulsant (1850); Weise (1885); Heyden et al. (1891); lablokoff-Khnzorian (1972); Kovář (2007). Araks valley: lablokoff-Khnzorian (1983). Caucasus: Winkler (1927).

**Remark.** Described from Armenia without specifying exact locality (l'Arménie (collect. Motschoulsky)) (Mulsant 1850).

**[*Scymnus (Pullus) auritus* Thunberg, 1795]**

*Scymnus auritus* Thunberg, 1795

**Literature data.** Caucasus: Winkler (1927).

***Scymnus (Pullus) fraxini* Mulsant, 1850**

*Scymnus fraxini* Mulsant, 1850

**Literature data.** Armenia: Kovář (2007). Caucasus: Mulsant (1850); Heyden et al. (1891, 1906); Winkler (1927).

***Scymnus (Pullus) subvillosus* (Goeze, 1777)**

*Coccinella subvillosa* Goeze, 1777

**Literature data.** Armenia: Schneider and Leder (1879) (Yerevan); Jacobson (1915) (Yerevan); Kovář (2007). Caucasus: Heyden et al. (1891); Iablokoff-Khnzorian (1983).

***Scymnus (Pullus) suturalis* Thunberg, 1795**

*Scymnus suturalis* Thunberg, 1795

**Literature data.** Armenia: Kovář (2007). Caucasus: Iablokoff-Khnzorian (1983).

***Scymnus (Scymnus) apetzi* Mulsant, 1846**

*Scymnus Apetzii* Mulsant, 1846

*Scymnus stigmatopterus* Faldermann, 1837 (synonymized by Fürsch et al. (1967))

*Scymnus corpulentus* Mulsant, 1850 (synonymized by Fürsch et al. (1967))

**Literature data.** Armenia: Schneider and Leder (1879) (Echmiadzin, Yerevan); Radde (1899) (Yerevan); Jacobson (1915) (Yerevan); Fürsch et al. (1967) (lectotype of *S. stigmatopterus* Fald.) (Sadarak); Iablokoff-Khnzorian (1983) (in Transcaucasia the most common *Scymnus* species); Kovář (2007). Transcaucasia: Faldermann (1837) (as *S. stigmatopterus* Fald.); Mulsant (1850) (as *S. corpulentus*). Caucasus: Heyden et al. (1891) (as *S. corpulentus* Muls.).

**Remark.** Kovář (2007) places *S. stigmatopterus* among the taxa incertae sedis.

***Scymnus (Scymnus) flavicollis* Redtenbacher, 1843**

*Scymnus frontalis* v. *araxicola* Fleischer, 1900

**Literature data.** Armenia: Kovář (2007). Araks valley: Fleischer (1900) (as *S. frontalis* v. *araxicola*); Heyden et al. (1906) (as *S. frontalis* a. *araxicola* Fleisch.); Winkler (1927) (as *S. frontalis* a. *araxicola* Fleisch.); Fürsch et al. (1967) (as *S. araxicola* Fleischer).

***Scymnus (Scymnus) frontalis (Fabricius, 1787)***

*Coccinella frontalis* Fabricius, 1787

*Scymnus quadrivulneratus* Mulsant, 1850 (synonymized by Fürsch et al. (1967))

**Literature data.** Armenia: Schneider and Leder (1879) (Helenowka (=Sevan)); Jacobson (1915) (Yerevan); Kovář (2007). Caucasus: Heyden et al. (1891) (as *S. frontalis bimaculatus* Mot.); lablokoff-Khnzorian (1983); Winkler (1927) (as *S. 4-vulneratus* Muls.).

***Scymnus (Scymnus) inderihensis Mulsant, 1850***

**Literature data.** Armenia: lablokoff-Khnzorian (1983).

***Scymnus (Scymnus) interruptus (Goeze, 1777)***

*Coccinella interrupta* Goeze, 1777

**Literature data.** Armenia: lablokoff-Khnzorian (1983); Kovář (2007).

***Scymnus (Scymnus) magnomaculatus Fürsch, 1958***

*Scymnus quadriguttatus* Capra, 1924

**Literature data.** Armenia: lablokoff-Khnzorian (1983) (as *S. quadriguttatus* Capra, 1924); Kovář (2007).

**[*Scymnus (Scymnus) manipulus Fürsch & Kreissl, 1967*]**

**Literature data.** Araks valley: Fürsch et al. (1967).

***Scymnus (Scymnus) pallipes Mulsant, 1850***

**Literature data.** Armenia: Fürsch et al. (1967) (Saderaki, Suhulta). Caucasus: Mulsant (1850); Heyden et al. (1891); Heyden et al. (1906) (as *S. frontalis pallipes* Muls.); Winkler (1927) (as *S. frontalis a. pallipes* Muls.).

**Remark.** Fürsch et al. (1967) report that two paralectotypes of this species are from Saderaki and Suhulta in Armenia. The former name certainly refers to Sadarak in Azerbaijani exclave of Nakhchivan, while the location of the latter is unclear to us (Fürsch et al. (1967) also pointed out that the name of the locality on the label is difficult to decipher).

***Scymnus (Scymnus) rubromaculatus (Goeze, 1777)***

*Coccinella rubromaculata* Goeze, 1777

**Literature data.** Armenia: Schneider and Leder (1879) (Echmiadzin, Yerevan); Radde (1899) (Echmiadzin); Jacobson (1915) (Yerevan).

**[*Scymnus (Scymnus) suffrianioides apetzoides* Capra & Fürsch, 1967]**

*Scymnus apetzoides* Capra & Fürsch, 1967

**Literature data.** Caucasus: lablokoff-Khnzorian (1983).

**Tribe Platynaspini Mulsant, 1846**

***Platynaspis luteorubra* (Goeze, 1777)**

*Coccinella luteorubra* Goeze, 1777

*Scymnus spectabilis* Faldermann, 1837

**Literature data.** Armenia: Schneider and Leder (1879) (Yerevan); Weise (1885); Jacobson (1915) (Yerevan); Kovář (2007). Transcaucasia: Faldermann (1837) (as *Scymnus spectabilis* Fald.). Caucasus: Winkler (1927); lablokoff-Khnzorian (1983).

**Tribe Hyperaspidini Mulsant, 1846**

**[*Hyperaspis campestris* (Herbst, 1783)]**

*Coccinella campestris* Herbst, 1783

**Literature data.** Caucasus: Winkler (1927).

**[*Hyperaspis caucasica* Crotch, 1874]**

**Literature data.** Caucasus: Heyden et al. (1891) (as *Oxynychus erythrocephalus caucasicus* Crotch).

**[*Hyperaspis erythrocephala* (Fabricius, 1787)]**

*Coccinella erythrocephala* Fabricius, 1787

**Literature data.** Caucasus: Heyden et al. (1906) (as *Oxynychus erythrocephalus* a. *Guillardi* Muls.); Winkler (1927) (as *Oxynychus erythrocephalus* F.).

***Hyperaspis femorata* (Motschulsky, 1837)**

*Coccinella femorata* Motschulsky, 1837

*Hyperaspis desertorum* v. *collaris* Fleischer, 1900 (synonymized by lablokoff-Khnzorian (1971))

*Hyperaspis inaudax* Mulsant, 1853 (synonymized by lablokoff-Khnzorian (1971))

**Literature data.** Armenia: Weise (1885) (as *H. reppensis* v. *femorata* Motsch.); lablokoff-Khnzorian (1971, 1983); Kovář (2007). Araks valley: Radde (1899)

(as *H. reppensis* var. *femorata* Mot.); Fleischer (1900) (as *H. desertorum* v. *collaris*); Heyden et al. (1906) (as *Hyperaspis desertorum* a. *collaris* Fleisch.). Caucasus: Victor (1837); Mulsant (1850); Mulsant (1853) (as *H. inaudax*); Heyden et al. (1891, 1906) (as *H. reppensis* v. *femorata* Motsch. and *H. reppensis inaudax* Muls.).

#### ***Hyperaspis histeroides* (Faldermann, 1837)**

*Scymnus histeroides* Faldermann, 1837

**Literature data.** Armenia: Iablokoff-Khnzorian (1971, 1983); Kovář (2007). Transcaucasia: Faldermann (1837) (as *Scymnus histeroides*).

#### **[*Hyperaspis polita* Weise, 1885]**

**Literature data.** Caucasus: Heyden et al. (1906) (as *H. transversoguttata* v. *10-guttata* Fleischer); Winkler (1927) (as *H. transversoguttata* a. *10 guttata* Fleisch.); Iablokoff-Khnzorian (1971).

#### ***Hyperaspis transversoguttata* Weise, 1878**

**Literature data:** Armenia: Iablokoff-Khnzorian (1971) (Meghri region); Kovář (2007). Lower Araks: Iablokoff-Khnzorian (1983). Caucasus: Weise (1879); Heyden et al. (1891, 1906).

#### **Tribe Diomini Gordon, 1999**

##### ***Diomus rubidus* (Motschulsky, 1837)**

*Scymnus rubidus* Motschulsky, 1837

**Literature data.** Armenia: Kovář (2007). Eastern Caucasus: Iablokoff-Khnzorian (1983). Caucasus: Heyden et al. (1891, 1906); Winkler (1927).

#### **Tribe Chilacorini Mulsant, 1846**

##### ***Chilocorus bipustulatus* (Linnaeus, 1758)**

*Coccinella bipustulata* Linnaeus, 1758

**Literature data.** Armenia: Schneider and Leder (1879) (Echmiadzin); Radde (1899) (Echmiadzin); Jacobson (1915) (Yerevan); Kovář (2007). Caucasus: Iablokoff-Khnzorian (1983).

##### **[*Chilocorus renipustulatus* (Scriba, 1791)]**

*Coccinella renipustulata* Scriba, 1791

**Literature data.** Transcaucasia: Iablokoff-Khnzorian (1983).

***Exochomus octosignatus* (Gebler, 1830)**

*Coccinella octosignata* Gebler, 1830

**Literature data.** Armenia: Weise (1885); Jacobson (1915) (Yerevan); Tobias (1975) (Yerevan, as a host of *D. coccinellae*); Iablokoff-Khnzorian (1983); Kovář (1995, 2007). Araks valley: Radde (1899). Caucasus: Heyden et al. (1906) (as *Brumus 8-signatus* a. *conjunctus* Fleisch.).

***Exochomus quadriguttatus* Fleischer, 1900**

**Literature data.** Armenia: Iablokoff-Khnzorian (1983) (as *E. quadripustulatus* ssp. *quadriguttatus*); Kovář (1995, 2007). Araks valley: Fleischer (1900) (as *E. 4-pustulatus* v. *4-guttatus*).

***Exochomus quadripustulatus* (Linnaeus, 1758)**

*Coccinella quadripustulata* Linnaeus, 1758

**Literature data.** Armenia: Jacobson (1915) (Yerevan); Kovář (1995, 2007). Transcaucasia: Iablokoff-Khnzorian (1983). Caucasus: Weise (1885) (as *Exochomus quadripustulatus* v. *ibericus* Motsch.); Heyden et al. (1891, 1906) (as *Exochomus quadripustulatus* v. *ibericus* Motsch.).

***Exochomus undulatus* Weise, 1878**

**Literature data.** Armenia: Iablokoff-Khnzorian (1983). Caucasus: Weise (1879, 1885); Heyden et al. (1891, 1906); Winkler (1927) (as *Anexochochomus undulatus* Ws.).

***Parexochomus melanocephalus* (Zubkov, 1833)**

*Coccinella melanocephala* Zubkov, 1833

**Literature data.** Armenia: Iablokoff-Khnzorian (1983); Kovář (2007). Caucasus: Heyden et al. (1891).

***Parexochomus nigripennis* (Erichson, 1843)**

*Chilocorus nigripennis* Erichson, 1843

**Literature data.** Armenia: Jacobson (1915) (as *Exochomus flavipes* subsp. *nigripennis* Er.) (Yerevan); Iablokoff-Khnzorian (1983). Araks valley: Radde (1899) (as *Exochomus flavipes* var. *nigripennis* Er.).

***Parexochomus nigromaculatus* (Goeze, 1777)**

*Coccinella nigromaculata* Goeze, 1777  
*Exochomus collaris* Küster, 1849

**Literature data.** Armenia: Schneider and Leder (1879) (Echmiadzin, Yerevan, Tarstschai); Radde (1899) (as *Exochomus flavipes* Thnb.) (Yerevan, Echmiadzin); Jacobson (1915) (as *Exochomus flavipes* Thunb.) (Yerevan); Kovář (2007). Caucasus: Heyden et al. (1891, 1906) (as *Exochomus flavipes* v. *collaris* Küst.); lablokoff-Khznorian (1983).

***Parexochomus pubescens* (Küster, 1848)**

*Exochomus pubescens* Küster, 1848

**Literature data.** Armenia: Jacobson (1915) (Yerevan). Araks valley: Radde (1899); lablokoff-Khznorian (1983).

**Tribe Sticholotidini Weise, 1901**

***Coelopterus armeniacus* Weise, 1894**

**Literature data.** Armenia: Jacobson (1915) (Yerevan); Winkler (1927) (Yerevan); lablokoff-Khznorian (1983) (as a synonym of *C. salinus* Mulsant, 1853); Kovář (2007). Araks valley: Weise (1894); Heyden et al. (1906).

***Pharoscygnus armenus* lablokoff-Khznorian, 1970**

**Literature data.** Armenia: lablokoff-Khznorian (1970b, 1983); Kovář (2007).

**Remarks.** Described based on specimens from the Kapan region (Syunik province) (holotype) and Yeghegnadzor region (Vayots Dzor province) (paratype) in Armenia.

**Tribe Coccidulini Mulsant, 1846**

***Coccidula lithophiloides* Reitter, 1890**

**Literature data.** Armenia: Jacobson (1915) (Yerevan); lablokoff-Khznorian (1983) (Araks valley from Yerevan to Meghri); Kovář (2007); Szawaryn et al. (2021) (Echmiadzin, Yerevan). Araks: Heyden et al. (1891, 1906); Winkler (1927).

***Coccidula rufa* (Herbst, 1783)**

*Dermestes rufus* Herbst, 1783

*Coccidula unicolor* Reitter, 1890

**Literature data.** Armenia: Jacobson (1915) (as *C. unicolor* Rt.) (Yerevan). Araks: Heyden et al. (1891) (as *C. rufa* v. *unicolor* Reitt.). Caucasus: Reitter (1890); Winkler (1927) (as *C. unicolor* Rtt.).

***Coccidula scutellata* (Herbst, 1783)**

*Chrysomela scutellata* Herbst, 1783

**Literature data.** Armenia: Szawaryn et al. (2021) (Yerevan).

**Tribe Tetrabrachini Kapur, 1948**

***Tetrabrachys araxis* (Reitter, 1897)**

*Lithophilus araxis* Reitter, 1897

**Literature data.** Armenia: Jacobson (1915) (Yerevan); Iablokoff-Khnzorian (1983) (Hrazdan valley, Mt. Aragats slopes, lake Sevan shores); Kovář (2007). Araks valley: Radde (1899); Heyden et al. (1906); Winkler (1927).

***Tetrabrachys bipustulatus* (Barovskij, 1909)**

*Lithophilus bipustulatus* Barovskij, 1909

**Literature data.** Armenia: Iablokoff-Khnzorian (1974, 1983) (surroundings of Yerevan); Kovář (2007).

**Remarks.** According to Iablokoff-Khnzorian (1974), a distinct subspecies *Lithophilus* (= *Tetrabrachys*) *bipustulatus armeniacus* occurs in Armenia.

**[*Tetrabrachys caucasicus* (Weise, 1878)]**

*Lithophilus caucasicus* Weise, 1878

**Literature data.** Caucasus: Heyden et al. (1906); Winkler (1927).

***Tetrabrachys connatus* (Creutzer, 1796)**

*Tritoma connata* Creutzer, 1796

**Literature data.** Armenia: Radde (1899) (Darachichag (=Tsaghkadzor)); Jacobson (1915) (Yerevan).

**Remark.** In Jacobson's (1915) list of the distribution records of *T. connatus*, Yerevan is preceded by a question mark.

***Tetrabrachys major* (Crotch, 1874)**

*Lithophilus major* Crotch, 1874

**Literature data.** Armenia: Jacobson (1915) (Yerevan). Araks valley: Heyden et al. (1906).

**[*Tetrabrachys weisei* (Reitter, 1880)]**

*Lithophilus weisei* Reitter, 1880

**Caucasus literature data.** Heyden et al. (1906); Winkler (1927).

## Comparison of Coccinellidae faunas of Armenia, Azerbaijan, and Georgia

The checklist presented above contains 84 species that have been reported from Armenia and 14 additional species with imprecise locations (Transcaucasia, Araks valley, the Caucasus) indicating that they may or may not include Armenia. Four species reported from Armenia or adjacent areas by Jacobson (1915) and two reported by Kovář (2007) are not included, listed in Table 1 with the reasons for their exclusion.

A comparison of the reported ladybird fauna of Armenia with that of other Transcaucasian states (Azerbaijan and Georgia) is shown in Table 2. The total number of species for all the Transcaucasian countries is 116, with 84, 92, and 90 species reported from Armenia, Azerbaijan, and Georgia, respectively. Thus, the recognized ladybird fauna of Armenia is somewhat poorer than that of Azerbaijan and Georgia. However, it should be borne in mind that Armenia occupies a noticeably smaller area than the other two states: Georgia is more than twice and Azerbaijan almost three times the size of Armenia.

Approximately 12% of ladybird species reported from Transcaucasia (14 of 116 species) can be considered endemic or near-endemic to the Caucasus ecoregion (Table 3). Ten of them have been reported from Armenia (11.9% of the 84 species reported), four from Azerbaijan (4.3% of the 92 species reported), and six from Georgia (6.7% of the 90 species reported).

Another group of special interest are ladybird species non-native to the region. To our knowledge, eight such species have been reported from Transcaucasia, but the occurrence of two of them there seems unlikely, so they are not included in the list of the Transcaucasian Coccinellidae in Table 2. One of these, *Chilocorus similis* (Rossi, 1790), was reported by Schneider and Leder (1879) from Lailashi, Georgia, most probably as a result of a misidentification of *C. renipustulatus* (Scriba, 1791). The second species, *Henosepilachna vigintioctopunctata* (Fabricius, 1775), a herbivorous ladybird widely distributed in the eastern part of the Palaearctic and in the Oriental and Australian regions (Kovář 2007), was reported from Azerbaijan in an unpublished thesis cited by Snegovaya and Zare Khormizi (2022). This report likely pertains to a different species of Epilachnini. The presence in the region of the remaining six species is likely, given that each of them has been introduced in the Caucasus in the past (Table 4). All six species have been reported from Georgia, two (*Harmonia axyridis* and *Rhyzobius lophanthae*) from Azerbaijan, and only one (*H. axyridis*) from Armenia.

To conclude, the recognized ladybird fauna of Armenia, although slightly less abundant in species than those of Azerbaijan and Georgia, appears to be diverse, with a high proportion of endemic species. On the other hand, only one alien ladybird species, the harlequin ladybird (*H. axyridis*), has so far been reported from this country. The field survey revealed that this highly invasive species has become common and widespread in many parts of Armenia. The survey also shows the presence in Armenia of two ladybird species, *Anatis ocellata* and *Tytthaspis sedecimpunctata*, which had not previously been reported from the region. Further field research and examination of existing insect collections would certainly increase the number of Armenian ladybird species.

**Table 1.** Species reported from Armenia or adjacent regions, but not included in the present checklist.

Species	Justification for exclusion
<i>Oenopia doublieri</i> (Mulsant, 1846)	Jacobson (1915) reported a doubtful (with a question mark) record of <i>O. doublieri</i> from Yerevan, citing Schneider and Leder (1879) as a source of this information. Indeed, these authors reported <i>O. doublieri</i> , however, not from the Yerevan area, but from the North Caucasus (Karasu village in Kabardino-Balkaria (Russia)).
<i>Scymniscus armeniacus</i> (Canepari, 1979)	Kovář (2007) reported this species as occurring in Armenia, probably due to its specific epithet. However, Canepari (1979) described <i>S. armeniacus</i> (as <i>Nephus (Sidis) armeniacus</i> ) based on a single male specimen collected in Elisabetspol (today's Ganja in Azerbaijan). Canepari derived the name <i>armeniacus</i> from the ancient region of Armenia that covered much more extensive area than present-day Armenia.
<i>Scymnus (Scymnus) rufipes</i> (Fabricius, 1798)	Jacobson (1915) reported this species from Transcaucasia. Its identity is uncertain given some of its synonyms listed by Jacobson ( <i>S. corpulentus</i> Muls., <i>S. suffrianioides</i> J. Sahlb.). According to Kovář (2007), <i>S. corpulentus</i> is considered a synonym of <i>S. apetzi</i> Mulsant and <i>S. suffrianioides</i> is a valid species different from <i>S. rufipes</i> .
<i>Hyperaspis desertorum</i> Weise, 1885	Jacobson (1915) reported <i>H. desertorum</i> from Yerevan, which may refer either to this species or, more likely, to <i>H. femorata</i> Motschulsky, as indicated by one of the synonyms mentioned ( <i>H. desertorum</i> ab. <i>collaris</i> Fleisch.).
<i>Hyperaspis reppensis</i> (Herbst, 1783)	Jacobson's (1915) report of <i>H. reppensis</i> from Yerevan cannot be assigned to this or other related species due to the long list of synonyms given, which are currently recognized as several species (e.g., <i>H. stigma</i> A. Ol., <i>H. pseudopustulata</i> Muls., <i>H. hoffmannseggii</i> Grav., <i>H. histeroides</i> Fald., <i>H. illecebrosa</i> Chev., <i>H. femorata</i> Motsch., <i>H. quadrimaculata</i> Redt.).
<i>Pharoscymnus koenigi</i> Iablokoff-Khnzorian, 1970	According to Kovář's (2007) catalogue, <i>P. koenigi</i> occurs in both the Asiatic part of Turkey and Armenia. However, the holotype and three paratypes of <i>P. koenigi</i> , all collected in Oltu (eastern Turkey) (Iablokoff-Khnzorian 1970c), are probably the only known specimens of this species.

**Table 2.** Coccinellidae reported from the Transcaucasian countries. The Armenian data are taken from the present checklist, while those for Azerbaijan and Georgia are primarily based on recent checklists by Snegovaya and Zare Khormizi (2022) and Migeon and Arabuli (2022), respectively. A few reports from other sources are marked and footnoted. [A] after the species name indicates a species alien to the region, [E] indicates presumed endemic or nearly endemic species. Asterisks (\*) denote new country records. The footnotes are explained at the end of the table.

Species	Armenia	Azerbaijan	Georgia
<b>Microweiseinae</b>			
<b>Serangiini</b>			
<i>Serangium montazerii</i> Fürsch, 1995 [A]			+
<b>Coccinellinae</b>			
<b>Stethorini</b>			
<i>Stethorus gilvifrons</i> (Mulsant, 1850)	+	+	+
<i>Stethorus pusillus</i> (Herbst, 1797)	+	+	+
<b>Coccinellini</b>			
<i>Adalia bipunctata</i> (Linnaeus, 1758)	+	+	+
<i>Adalia decempunctata</i> (Linnaeus, 1758)	+	+	+
<i>Anatis ocellata</i> (Linnaeus, 1758)*	+	+	+
<i>Anisosticta caucasica</i> (Fleischer, 1900) [E]	+		
<i>Anisosticta novemdecimpunctata</i> (Linnaeus, 1758)	+	+	+
<i>Aphidecta obliterated</i> (Linnaeus, 1758)	+	+	+
<i>Bulaea lichatschovii</i> (Hummel, 1827)	+	+	+
<i>Calvia decemguttata</i> (Linnaeus, 1767)	+	+	+
<i>Calvia quatuordecimguttata</i> (Linnaeus, 1758)	+	+	+
<i>Calvia quindecimguttata</i> (Fabricius, 1777)		+	+
<i>Ceratomegilla apicalis</i> (Weise, 1879)	+	+	+
<i>Ceratomegilla notata</i> (Laicharting, 1781)	+	+	+
<i>Ceratomegilla schelkovnikovi</i> (Dobzhansky, 1927) [E]	+		+ <sup>1</sup>
<i>Ceratomegilla schneideri</i> (Weise, 1878) [E]	+	+	+
<i>Ceratomegilla undecimnotata</i> (Schneider, 1792)	+	+	+
<i>Coccinella alpigrada</i> (Iablokoff-Khnzorian, 1957) [E]	+		
<i>Coccinella hieroglyphica</i> Linnaeus, 1758		+	+
<i>Coccinella magnifica</i> Redtenbacher, 1843	+	+ <sup>2</sup>	+
<i>Coccinella quinquepunctata</i> Linnaeus, 1758	+	+	+

Species	Armenia	Azerbaijan	Georgia
<i>Coccinella saucerottii</i> Mulsant, 1850		+	
<i>Coccinella septempunctata</i> Linnaeus, 1758	+	+	+
<i>Coccinella undecimpunctata</i> Linnaeus, 1758	+	+	
<i>Coccinula quatuordecimpustulata</i> (Linnaeus, 1758)	+	+	+
<i>Coccinula sinuatomarginata</i> (Faldermann, 1837)	+	+	+
<i>Halyzia sedecimguttata</i> (Linnaeus, 1758)	+	+	+
<i>Harmonia axyridis</i> (Pallas, 1773) [A]	+	+	+
<i>Harmonia conformis</i> (Boisduval, 1835) [A]			+
<i>Harmonia quadripunctata</i> (Pontoppidan, 1763)		+	+
<i>Hippodamia septemmaculata</i> (DeGeer, 1775)		+	
<i>Hippodamia tredecimpunctata</i> (Linnaeus, 1758)	+	+	+
<i>Hippodamia variegata</i> (Goeze, 1777)	+	+	+
<i>Myrrha octodecimguttata</i> (Linnaeus, 1758)	+	+	+
<i>Myzia oblongoguttata</i> (Linnaeus, 1758)	+	+	+
<i>Oenopia bissexnotata</i> (Mulsant, 1850)		+	
<i>Oenopia conglobata</i> (Linnaeus, 1758)	+	+	+
<i>Oenopia impustulata</i> (Linnaeus, 1758)	+	+	+
<i>Oenopia lyncea agnatha</i> (Rosenhauer, 1808)	+	+	+
<i>Oenopia oncina</i> (Olivier, 1808)	+	+	+
<i>Propylea quatuordecimpunctata</i> (Linnaeus, 1758)	+	+	+
<i>Psyllobora vigintiduopunctata</i> (Linnaeus, 1758)	+	+	+
<i>Sospita vigintiguttata</i> (Linnaeus, 1758)			+
<i>Tythaspis sedecimpunctata</i> (Linnaeus, 1761)*	+	+	+
<i>Vibidia duodecimguttata</i> (Poda von Neuhaus, 1761)	+	+	+
<b>Epilachnini</b>			
<i>Chnootriba elaterii</i> (Rossi, 1794)		+	+
<i>Cynegetis impunctata</i> (Linnaeus, 1767)		+	
<i>Henosepilachna argus</i> (Geoffroy, 1785)	+	+	+
<i>Subcoccinella vigintiquatuorpunctata</i> (Linnaeus, 1758)	+	+	+
<b>Noviini</b>			
<i>Novius cardinalis</i> (Mulsant, 1850) [A]			+
<b>Scymnini</b>			
<i>Clitostethus arcuatus</i> (Rossi, 1794)	+	+	+
<i>Nephus (Bipunctatus) bipunctatus</i> (Kugelann, 1794)		+	+
<i>Nephus (Geminosopho) reunioni</i> (Fürsch, 1974) [A]		+	+ <sup>3</sup>
<i>Nephus (Nephus) ludyi</i> (Weise, 1879)	+		
<i>Nephus (Nephus) quadrimaculatus</i> (Herbst, 1783)	+	+	+
<i>Nephus (Nephus) redtenbacheri</i> (Mulsant, 1846)		+	+
<i>Nephus (Sidis) caucasicus</i> (Weise, 1929) [E]	+		
<i>Scymniscus armeniacus</i> (Canepari, 1979) [E]		+ <sup>4</sup>	
<i>Scymniscus biflammulatus</i> (Motschulsky, 1837)	+	+	+
<i>Scymniscus biguttatus</i> (Mulsant, 1850)	+	+	+
<i>Scymnus (Mimopullus) pharaonis</i> Motschulsky, 1851	+		
<i>Scymnus (Neopullus) haemorrhoidalis</i> Herbst, 1797	+	+	+
<i>Scymnus (Neopullus) limbatus</i> Stephens, 1832	+	+	+
<i>Scymnus (Neopullus) testaceus</i> Motschulsky, 1837	+	+	+ <sup>5</sup>
<i>Scymnus (Pullus) argutus</i> Mulsant, 1850	+	+	+
<i>Scymnus (Pullus) auritus</i> Thunberg, 1795		+	+
<i>Scymnus (Pullus) ferrugatus</i> (Moll, 1785)			+
<i>Scymnus (Pullus) fraxini</i> Mulsant, 1850	+	+	+
<i>Scymnus (Pullus) subvillosus</i> (Goeze, 1777)	+	+	+
<i>Scymnus (Pullus) suturalis</i> Thunberg, 1795	+	+	+ <sup>5</sup>
<i>Scymnus (Scymnus) apetzi</i> Mulsant, 1846	+	+	+
<i>Scymnus (Scymnus) femoralis</i> (Gyllenhal, 1827)		+	
<i>Scymnus (Scymnus) flavicollis</i> Redtenbacher, 1843	+		
<i>Scymnus (Scymnus) frontalis</i> (Fabricius, 1787)	+	+	+
<i>Scymnus (Scymnus) inderihensis</i> Mulsant, 1850	+		

Species	Armenia	Azerbaijan	Georgia
<i>Scymnus (Scymnus) interruptus</i> (Goeze, 1777)	+	+	+
<i>Scymnus (Scymnus) magnomaculatus</i> Fürsch, 1958	+	+	+
<i>Scymnus (Scymnus) marginalis</i> (Rossi, 1794)			+
<i>Scymnus (Scymnus) nigrinus</i> Kugelann, 1794		+	+
<i>Scymnus (Scymnus) pallipes</i> Mulsant, 1850	+		
<i>Scymnus (Scymnus) rubromaculatus</i> (Goeze, 1777)	+	+	+
<i>Scymnus (Scymnus) rufipes</i> (Fabricius, 1798)		+	
<b>Platynaspini</b>			
<i>Platynaspis luteorubra</i> (Goeze, 1777)	+	+	+
<b>Hyperaspidini</b>			
<i>Hyperaspis campestris</i> (Herbst, 1783)			+
<i>Hyperaspis caucasica</i> Crotch, 1874 [E]		+ <sup>6</sup>	
<i>Hyperaspis erythrocephala</i> (Fabricius, 1787)		+	+
<i>Hyperaspis femorata</i> (Motschulsky, 1837)	+	+	+
<i>Hyperaspis histeroides</i> (Faldermann, 1837)	+	+	
<i>Hyperaspis reppensis</i> (Herbst, 1783)		+	+
<i>Hyperaspis transversoguttata</i> Weise, 1878	+	+	+
<b>Diomini</b>			
<i>Diomus rubidus</i> (Motschulsky, 1837)	+	+	+
<b>Chilocorini</b>			
<i>Chilocorus bipustulatus</i> (Linnaeus, 1758)	+	+	+
<i>Chilocorus renipustulatus</i> (Scriba, 1791)		+	+
<i>Exochomus octosignatus</i> (Gebler, 1830)	+	+	+
<i>Exochomus quadriguttatus</i> Fleischer, 1900 [E]	+		+ <sup>7</sup>
<i>Exochomus quadripustulatus</i> (Linnaeus, 1758)	+	+	+
<i>Exochomus undulatus</i> Weise, 1878	+	+	+
<i>Parexochomus melanocephalus</i> (Zubkov, 1833)	+	+	+ <sup>8</sup>
<i>Parexochomus nigripennis</i> (Erichson, 1843)	+		
<i>Parexochomus nigromaculatus</i> (Goeze, 1777)	+	+	+
<i>Parexochomus pubescens</i> (Küster, 1848)	+	+	
<b>Sticholotidini</b>			
<i>Coelopterus armeniacus</i> Weise, 1894 [E]	+		
<i>Pharoscymnus armenus</i> lablokoff-Khnzorian, 1970 [E]	+		+
<i>Pharoscymnus smirnovi</i> Dobzhansky, 1927		+	+
<b>Coccidulini</b>			
<i>Coccidula lithophiloides</i> Reitter, 1890 [E]	+	+	
<i>Coccidula rufa</i> (Herbst, 1783)	+	+	+
<i>Coccidula scutellata</i> (Herbst, 1783)	+	+	+
<i>Rhyzobius lophanthae</i> (Blaisdell, 1892) [A]		+	+
<b>Tetrabrachini</b>			
<i>Tetrabrachys araxis</i> (Reitter, 1897) [E]	+	+	
<i>Tetrabrachys bipustulatus</i> (Barovskij, 1909)	+		
<i>Tetrabrachys causicus</i> (Weise, 1878) [E]			+
<i>Tetrabrachys coloratus</i> Fürsch, 1960		+	
<i>Tetrabrachys connatus</i> (Creutzer, 1796)	+	+	+
<i>Tetrabrachys major</i> (Crotch, 1874)	+		
<i>Tetrabrachys weisei</i> (Reitter, 1880) [E]			+
No. species: 116	84	92	90

<sup>1</sup> Reported by Dobzhansky (1927) from Borjomi and Bakuriani in Georgia and Mamison Pass on the Georgian-Russian border and by Kovář (2007) generally from Georgia.

<sup>2</sup> Reported by Schneider and Leder (1879) from Baku district, Azerbaijan.

<sup>3</sup> Reported from Georgia by Kovář (2007).

<sup>4</sup> Reported by Canepari (1979) from Elisabetspol (now Ganja), Azerbaijan.

<sup>5</sup> From Georgia reported by Schneider and Leder (1879) and Merkiladze and Kvavadze (2002).

<sup>6</sup> Reported from Nukha (now Shaki), Azerbaijan by Motschulsky (Victor 1837) (as *Coccinella 6 pustulata* Victor). Kovář's (2007) report from Georgia was not included, as it probably follows Motschulsky's (Victor 1837) description of the site as 'Noucha en Géorgie'.

<sup>7</sup> Reported by Kovář (1995) from Gagra in Abkhazia (formally part of Georgia) and by lablokoff-Khnzorian (1983) and Merkiladze and Kvavadze (2002) (as *E. quadripustulatus* ssp. *quadriguttatus* Fleisch, 1900) from several regions of Georgia.

<sup>8</sup> Reported by Merkiladze and Kvavadze (2002) from several regions in Georgia.

**Table 3.** Coccinellidae species with a known range restricted to or only slightly exceeding the Caucasus ecoregion.

Species	Remarks on distribution and nomenclature
<i>Anisosticta caucasica</i> (Fleischer, 1900)	For a long time, this ladybird was known only from a single type specimen that, according to Iablokoff-Khnzorian (1982), was collected by Fleischer in the Armenian part of the Araks valley. Further specimens were reported by Fürsch (1977) from Dizin in northern Iran.
<i>Ceratomegilla schelkovnikovi</i> (Dobzhansky, 1927)	It seems that the specimens collected by Dobzhansky (1927) in several locations in Armenia, Georgia, and the Russian part of the Caucasus (upper course of the Belaya River) are the only known specimens of this species.
<i>Ceratomegilla schneideri</i> (Weise, 1878)	This species is probably a Caucasian endemic. Apart from Armenia, Schneider and Leder (1879) reported it from Georgia and Azerbaijan and Iablokoff-Khnzorian (1983) added the Russian territories of Kabardino-Balkaria, Kuban region and Ossetia in the North Caucasus. Bieńkowski (2018: fig. 11C) presented a photograph of a specimen from the Republic of Adygea (NW of the North Caucasus, Russia).
<i>Coccinella alpigrada</i> (Iablokoff-Khnzorian, 1957)	Khnzorian (1957) reported several Armenian sites for <i>C. alpigrada</i> . For a long time, these were the only known sites of this species until Kovář (2005) reported it from the Erzurum Province of Turkey (Armenian Upland).
<i>Nephus caucasicus</i> (Weise, 1929)	This species was described (as <i>Scymnus plagiatus</i> Weise in Schneider & Leder, 1879) based on specimens collected near Karasu village (Kabardino-Balkaria, the North Caucasus, Russia) and Yerevan (Armenia). More recently, it was also reported from Tehran Province in northern Iran (Jafari et al. 2013).
<i>Scymniscus armeniacus</i> (Canepari, 1979)	It seems that the type specimen from Ganja in Azerbaijan (Canepari 1979) is the only known specimen of this species.
<i>Hyperaspis caucasica</i> Crotch, 1874	Motschulsky (Victor 1837) found this species in the environs of present-day Shaka in Azerbaijan and described it as <i>Coccinella 6 pustulata</i> . Subsequently, due to homonymy, Crotch (1874) replaced this name with <i>H. caucasica</i> . Kovář (2007) considered <i>Hyperaspis assimilis</i> Zaslavskij, 1966 from Tajikistan as a synonym of <i>H. caucasica</i> , while Iablokoff-Khnzorian (1983) treated both <i>H. caucasica</i> and <i>H. assimilis</i> as synonyms of <i>H. guttulata</i> Fairmaire, 1870, a species reported from the western Mediterranean region, Tajikistan, and Mongolia (Kovář 2007). A comparative examination of <i>H. caucasica</i> , <i>H. assimilis</i> , and <i>H. guttulata</i> would need to be carried out to establish their identities.
<i>Exochomus quadriguttatus</i> Fleischer, 1900	<i>Exochomus quadriguttatus</i> appears to be endemic to the Caucasus ecoregion or its range extends slightly beyond this area. It was reported from the western North Caucasus, western Georgia, Armenia, and north-eastern Anatolia (Iablokoff-Khnzorian 1983; Kovář 1995; Merkviladze and Kvavadze 2002).
<i>Coelopterus armeniacus</i> Weise, 1894	<i>Coelopterus armeniacus</i> was described based on two specimens collected in the Araks valley. Later authors consistently reported it from Armenia but, surprisingly, Kovář (2007) also mentioned Israel.
<i>Pharoscymnus armenus</i> Iablokoff-Khnzorian, 1970	It is known from Armenia and eastern Georgia (Iablokoff-Khnzorian 1970b, 1983).
<i>Coccidula lithophiloides</i> Reitter, 1890	<i>Coccidula lithophiloides</i> was described from Ordubad (Azerbaijan exclave of Nakhchivan). According to Iablokoff-Khnzorian (1983), it is common in Armenia along the Araks valley. It was also reported from several provinces of Iran (Kermanshah, Lorestan, Isfahan, and Fars; Biranvand et al. 2024), where it was described by Duverger (1983) as <i>Lithophilus naviauxi</i> .
<i>Tetrabrachys araxis</i> (Reitter, 1897)	Iablokoff-Khnzorian (1983) stated that <i>T. araxis</i> was described from Armenia, but Reitter's (1897) description was based on specimens collected in the Araks valley near Ordubad, i.e., in the Azerbaijan exclave of Nakhchivan. Nonetheless, the former author mentioned several other locations of this species within the current borders of Armenia. <i>Tetrabrachys anatolicus</i> (Pic, 1901), considered a synonym of <i>T. araxis</i> both by Iablokoff-Khnzorian (1983) and Kovář (2007), was described from Konya in southern Turkey, more than 1,000 km W-WS of the Transcaucasian locations. The identity of <i>T. anatolicus</i> needs to be examined.
<i>Tetrabrachys caucasicus</i> (Weise, 1878)	Description of this species was based on a single specimen collected in Borjomi in Georgia (Schneider and Leder 1879). Merkviladze and Kvavadze (2002) reported it also from the region of Tbilisi, and Kovář (2007) mentioned it generally from the Asiatic part of Turkey.
<i>Tetrabrachys weisei</i> (Reitter, 1880)	Reitter (1880) mentioned in general that the specimen he used to describe <i>T. weisei</i> was collected by Leder in the Caucasus. Merkviladze and Kvavadze (2002) reported it from the Tbilisi district of Georgia, and Iablokoff-Khnzorian (1974, 1983) also from Crimea.

**Table 4.** Non-native Coccinellidae reported from Transcaucasia.

Species	Information on introductions in the region
<i>Serangium montazerii</i> Fürsch, 1995	Widely released in the Black Sea coast of the Caucasus after 1973 (as <i>S. parcesetosum</i> (Sicard, 1929)) (Booth and Polaszek 1996; Bieńkowski and Orlova-Bienkowskaja 2020). Its presence in western Georgia was confirmed by Migeon and Arabuli (2022).
<i>Harmonia axyridis</i> (Pallas, 1773)	Released after 1927 in Georgia and then at the Black Sea coast of Russia (Bieńkowski and Orlova-Bienkowskaja 2020). Its presence in eastern Georgia was confirmed by Merkviladze and Kvavadze (2002). The European invasive population has been spreading in the Caucasus since ~ 2012 (Belyakova and Reznik 2013; Ukrainsky 2013).
<i>Harmonia conformis</i> (Boisduval, 1835)	Released in Georgia after 1958 (Bieńkowski and Orlova-Bienkowskaja 2020). Its presence in western Georgia was confirmed by Merkviladze and Kvavadze (2002).
<i>Novius cardinalis</i> (Mulsant, 1850)	Released in the Caucasus after 1931 (Bieńkowski and Orlova-Bienkowskaja 2020). Its presence in western Georgia was confirmed by Merkviladze and Kvavadze (2002).
<i>Nephus reunioni</i> (Fürsch, 1974)	Released in Georgia before 1987 (Bieńkowski and Orlova-Bienkowskaja 2020).
<i>Rhyzobius lophanthae</i> (Blaisdell, 1892)	Released in the Caucasus after 1947 (Bieńkowski and Orlova-Bienkowskaja 2020). Its presence in western Georgia was confirmed by Merkviladze and Kvavadze (2002).

## Acknowledgements

We are grateful to Mark Kalashian (Scientific Center of Zoology and Hydroecology, National Academy of Sciences, Yerevan) for sharing his unpublished records of *Harmonia axyridis* in Armenia.

## Additional information

### Conflict of interest

The authors have declared that no competing interests exist.

### Ethical statement

No ethical statement was reported.

### Funding

The work was supported by the Science Committee of RA, in the frames of the research project 21AG-1F033.

### Author contributions

Conceptualization: PC, SG. Data curation: SG, PC. Investigation: KT, PC, AG, MA, SG, JR. Supervision: PC. Writing - original draft: SG, PC. Writing - review and editing: PC, KT, AG, JR, MA, SG.

### Author ORCIDs

Shoghik Ghazaryan  <https://orcid.org/0009-0007-9071-6545>

Marine Arakelyan  <https://orcid.org/0000-0002-6334-5714>

Astghik Ghazaryan  <https://orcid.org/0009-0005-2840-0019>

Jerzy Romanowski  <https://orcid.org/0000-0003-1050-6403>

Krzysztof Turlejski  <https://orcid.org/0000-0001-6708-7815>

Piotr Ceryngier  <https://orcid.org/0000-0003-1085-9751>

### Data availability

All of the data that support the findings of this study are available in the main text.

## References

- Belyakova NA, Reznik SYa (2013) First record of the harlequin ladybird, *Harmonia axyridis* (Coleoptera: Coccinellidae) in the Caucasus. *European Journal of Entomology* 110: 699–702. <https://doi.org/10.14411/eje.2013.093>
- Bieńkowski AO (2018) Key for identification of the ladybirds (Coleoptera: Coccinellidae) of European Russia and the Russian Caucasus (native and alien species). *Zootaxa* 4472(2): 233–260. <https://doi.org/10.11646/zootaxa.4472.2.2>
- Bieńkowski AO, Orlova-Bienkowskaja MJ (2020) History of the biodiversity of ladybirds (Coccinellidae) at the Black Sea coast of the Russian Caucasus in the last 120 years – does the landscape transformation and establishment of *Harmonia axyridis* have an impact? *Insects* 11: 824. <https://doi.org/10.3390/insects11110824>
- Biranvand A, Fekrat L, Větřovec J, Ghobari H, Hamidi E, Zare Khormizi M, Azadbakht N, Nedvěd O, Romasi F, Ceryngier P (2024) Checklist and distribution of ladybirds (Coleoptera, Coccinellidae) in Iranian provinces. *Zootaxa* 5493 (2): 101–128. <https://doi.org/10.11646/zootaxa.5493.2.1>
- Booth RG, Polaszek A (1996) The identities of ladybird beetle predators used for whitefly control, with note on some whitefly parasitoides, in Europe. In: Brighton Crop Protection Conference – Pests & Diseases – 1996, Volume I, Brighton (England), 18–21 November 1996, 69–74.
- Canepari C (1979) Due nuove species di Scymnini paelearctici: *Nephus (Sidis) armeniacus* e *Scymnus (Pullus) folchinii* (Coleoptera: Coccinellidae). *Doriana* 5 (232): 1–5.
- Ceryngier P, Franz KW, Romanowski J (2023) Distribution, host range and host preferences of *Dinocampus coccinellae* (Hymenoptera: Braconidae): A worldwide database. *European Journal of Entomology* 120: 26–34. <https://doi.org/10.14411/eje.2023.004>
- Che L, Zhang P, Deng S, Escalona HE, Wang X, Li Y, Pang H, Vandenberg N, Ślipiński A, Tomaszewska W, Liang D (2021) New insights into the phylogeny and evolution of lady beetles (Coleoptera: Coccinellidae) by extensive sampling of genes and species. *Molecular Phylogenetics and Evolution* 156: 107045. <https://doi.org/10.1016/j.ympev.2020.107045>
- Crotch GR (1874) A Revision of the Coleopterous Family Coccinellidae. E. W. Janson, London, xv + 311 pp. <https://doi.org/10.5962/bhl.title.8975>
- Dobzhansky Th (1927) Neue und wenig bekannte Coccinelliden. *Revue Russe d'Entomologie* 21: 212–217.
- Duverger C (1983) Contribution a la connaissance des Coccinellidae d'Iran. *Nouvelle Revue d'Entomologie* 13: 73–93.
- Faldermann F (1835) Additamenta entomologica ad faunam rossicam in itineribus jussu imperatoris augustissimi annis 1827–1831 a Cl. Ménériés et Szovitz susceptis collecta, in lucem edita. *Nouveaux Mémoires de la Société Impériale des Naturalistes de Moscou* 4: 1–310.
- Faldermann F (1837) Fauna Entomologica Trans-Caucasica. Pars II. Coleoptera Trans-Caucasica. II. Heteromera. *Nouveaux Mémoires de la Société Impériale des Naturalistes de Moscou* 5: 1–412.
- Faldermann F (1838) Fauna Entomologica Trans-Caucasica. Coleoptera. Pars III. Auguste Semen, Moscou, 306 pp.
- Fleischer A (1900) Neue Coccinelliden aus der Sammlung des kais. Rathes Herrn Edmund Reiter. *Wiener entomologische Zeitung* 19: 116–120. <https://doi.org/10.5962/bhl.part.3442>
- Fürsch H (1977) Coccinellidenausbeuten aus Libanon und dem Iran im Museum Genf mit Beschreibung neuer Scymnini-Arten (Col. Cocc.). *Revue Suisse de Zoologie* 84: 645–657. <https://doi.org/10.5962/bhl.part.91413>

- Fürsch H, Kreissl E, Capra F (1967) Revision einiger europäischer *Scymnus* (s.str.)-Arten. Mitteilungen der Abteilung für Zoologie und Botanik am Landesmuseum "Joanneum" in Graz 28: 207–259.
- Hewitt GM (1999) Post-glacial re-colonization of European biota. *Biological Journal of the Linnean Society* 68: 87–112. <https://doi.org/10.1111/j.1095-8312.1999.tb01160.x>
- Heyden L v, Reitter E, Weise J (1891) *Catalogus Coleopterorum Europae, Caucasi et Armeniae rossicae*. Edmund Reitter, Berlin-Mödling-Caen, viii + 812 pp.
- Heyden Lv, Reitter E, Weise J (1906) *Catalogus Coleopterorum Europae, Caucasi et Armeniae rossicae, edition secunda*. Edmund Reitter, Berlin-Paskau-Caen, 775 pp.
- lablokoff-Khnzorian SM (1957) New species of beetles from the Armenian SSR and Nakh. ASSR. Academy of Sciences of Armenian SSR, Zoological Institute, Materials on the Study of Fauna of the Armenian SSR 3 (Zoological Collection 10): 153–183. [in Russian, with Armenian summary]
- lablokoff-Khnzorian SM (1969) Two new species of ladybird beetles from the Caucasus. *Doklady Akademii Nauk Armyanskoi SSR* 48: 247–250. [in Russian, with Armenian summary]
- lablokoff-Khnzorian SM (1970a) Two new species of the genus *Nephus* Muls. from USSR. *Doklady Akademii Nauk Armyanskoi SSR* 50: 118–121. [in Russian, with Armenian summary]
- lablokoff-Khnzorian SM (1970b) New species of beetles from Armenia and other lands of USSR. Academy of Sciences of Armenian SSR, Zoological Institute, Zoological Papers 15: 50–80. [in Russian, with Armenian and English summary]
- lablokoff-Khnzorian SM (1970c) Two new ladybird species from the Palaearctic. *Doklady Akademii Nauk Armyanskoi SSR* 50: 252–256. [in Russian, with Armenian summary]
- lablokoff-Khnzorian SM (1971) Synopsis des *Hyperaspis* Paléarctiques (Col. Coccinellidae). *Annales de la Société entomologique de France (N.S.)* 7: 163–200. <https://doi.org/10.1080/21686351.1971.12278033>
- lablokoff-Khnzorian SM (1972) Les types de Coccinellidae de la collection Motschulsky (Coléoptères Coccinellidae). *Nouvelle Revue d'Entomologie* 2: 163–184. <https://doi.org/10.1080/21686351.1971.12278033>
- lablokoff-Khnzorian SM (1974) Monographie der Gattung *Lithophilus* Froelich (Col. Coccinellidae). *Entomologische Arbeiten aus dem Museum G. Frey Tutzing bei München* 25: 148–243.
- lablokoff-Khnzorian SM (1980) Tribe Epilachnini (Coleoptera, Coccinellidae) in the fauna of the USSR. I. *Entomologicheskoye Obozreniye* 59: 297–310. [in Russian]
- lablokoff-Khnzorian SM (1981) Tribe Epilachnini (Coleoptera, Coccinellidae) in the fauna of the USSR. II. *Entomologicheskoye Obozreniye* 60: 849–859. [in Russian]
- lablokoff-Khnzorian SM (1982) Les Coccinelles Coléoptères – Coccinellidae Tribu Coccinellini des régions Palearctique et Orientale. Paris, Boubée, 568 pp.
- lablokoff-Khnzorian SM (1983) Review of the coccinellid fauna of the USSR. Academy of Sciences of Armenian SSR, Institute of Zoology, Zoological Papers 19: 94–161. [in Russian, with Armenian and English summary]
- Jacobson GG (1915) Beetles of Russia and western Europe – a guide to beetle identification. Izd. A.F. Devrien, St. Petersburg, issue XI, 865–1024. [in Russian]
- Jafari R, Fursch H, Zarei Khormizi M (2013) A checklist of the Scymninae (Coleoptera: Coccinellidae) of Iran. *International Research Journal of Applied and Basic Sciences* 5: 154–160.
- Kalashian MYu, Ghrejyan TL, Karagyan GH (2017) Harlequin ladybird *Harmonia axyridis* Pall. (Coleoptera, Coccinellidae) in Armenia. *Russian Journal of Biological Invasions* 8: 313–315. <https://doi.org/10.1134/S207511171704004X>

- Kalashian MYu, Ghrejyan TL, Karagyan GH (2019) Expansion of harlequin ladybird *Harmonia axyridis* Pall. (Coleoptera, Coccinellidae) in Armenia. Russian Journal of Biological Invasions 10: 153–156. <https://doi.org/10.1134/S2075111719020073>
- Kalashian M, Aghababyan K, Zarikyan N, Gabrielyan B, Arakelyan M, Ghazaryan A (2023) Fauna of Armenia. In: Fayvush G (Ed.) Biodiversity of Armenia. Springer Nature Switzerland AG, 165–282. [https://doi.org/10.1007/978-3-031-34332-2\\_5](https://doi.org/10.1007/978-3-031-34332-2_5)
- Khnzorian SM (1957) New species of beetles from the Armenian SSR and Nakh. ASSR. Academy of Sciences of the Armenian SSR – Institute of Zoology, Materials for the Study of the Fauna of the Armenian SSR, III, Zoological Collection 10: 153–183. [in Russian, with Armenian summary]
- Kovář I (1995) Revision of the genera *Brumus* Muls. and *Exochomus* Redtb. (Coleoptera, Coccinellidae) of the Palaearctic region. Part I. Acta Entomologica Musei Nationalis Pragae 44: 5–124.
- Kovář I (2005) Revision of the Palaearctic species of the *Coccinella transversoguttata* species group with notes on some other species of the genus (Coleoptera: Coccinellidae). Acta Entomologica Musei Nationalis Pragae 45: 129–164.
- Kovář I (2007) Family Coccinellidae Latreille, 1807. In: Löbl I, Smetana A (Eds) Catalogue of Palaearctic Coleoptera. Vol. 4. Elateroidea, Derodontoidea, Bostrichoidea, Lymexyloidea, Cleroidea, Cucujoidea. Apollo Books, Stenstrup, Denmark, 71–74, 568–631.
- Leder H (1879) Beitrag zur kaukasischen Käfer-Fauna. Verhandlungen der kaiserlich-königlichen zoologisch-botanischen Gesellschaft in Wien 29: 451–488.
- Ménétries E (1832) Catalogue raisonné des objets de zoologie recueillis dans un voyage au Caucase et jusqu'aux frontières actuelles de la Perse entrepris par ordre de S. M. l'Empereur. Académie Impériale des Sciences, St.-Petersbourg, 271 + xxxiii + iv pp. <https://doi.org/10.5962/bhl.title.51784>
- Merkviladze MS, Kvavadze ES (2002) List of ladybirds (Coleoptera, Coccinellidae) of Georgia. Proceedings of the Institute of Zoology, Tbilisi 21: 149–155.
- Migeon A, Arabuli T (2022) Rediscovery of *Serangium montazerii* Fürsch in Georgia and updated list of the Coccinellidae of Georgia. Caucasia 1: 1–6. <https://doi.org/10.3897/caucasiana.1.e60966>
- Mittermeier RA, Robles-Gil P, Hoffmann M, Pilgrim J, Brooks T, Mittermeier CG, Lamoreux J, Da Fonseca GAB (2004) Hotspots Revisited: Earth's Biologically Richest and Most Endangered Terrestrial Ecoregions. CEMEX, Mexico City, 391 pp.
- Mulsant E (1850) Species des Coléoptères trimères sécuripapes. Annales des Sciences Physiques et Naturelles d'Agriculture et d'Industrie (Deuxième Série) 2: xv + 1104 pp. <https://doi.org/10.5962/bhl.title.8953>
- Mulsant E (1853) Supplément a la monographie des Coléoptères trimères sécuripapes. Annales de la Société Linnéenne de Lyon (nouvelle série) 1: 129–298. <https://doi.org/10.5962/bhl.title.60609>
- Mulsant E (1866) Monographie des Coccinellides, 1<sup>re</sup> Partie – Coccinelliens. F. Savy / Deyrolle, Paris, 294 pp.
- Mumladze L, Japoshvili B, Anderson EP (2020) Faunal biodiversity research in the Republic of Georgia: a short review of trends, gaps, and needs in the Caucasus biodiversity hotspot. Biologia 75: 1385–1397. <https://doi.org/10.2478/s11756-019-00398-6>
- Myers N, Mittermeier RA, Mittermeier CG, da Fonseca GAB, Kent J (2000) Biodiversity hotspots for conservation priorities. Nature 403: 853–858. <https://doi.org/10.1038/35002501>
- Radde G (1899) Die Sammlungen des kaukasischen Museums. Band I. Zoologie. Typographie der Kanzelei des Landescheffs, Tiflis, 520 pp.

- Reitter E (1880) Bestimmungs-Tabellen der europäischen Coleopteren. I. Enthaltend die Familien: Cucujidae, Telnatophilidae, Tritomidae, Mycetidae, Endomychidae, Lyctidae und Sphindidae. Verhandlungen der kaiserlich-königlichen zoologisch-botanischen Gesellschaft in Wien 29: 71–100.
- Reitter E (1890) Neue Coleopteren aus Europa, den angrenzenden Ländern und Sibirien, mit Bemerkungen über bekannte Arten. Zehnter Theil. Deutsche Entomologische Zeitschrift 1890, Heft 1: 165–176. <https://doi.org/10.1002/mmnd.48018900324>
- Reitter E (1897) Dreissig neue Coleopteren aus russisch Asien und der Mongolei. Deutsche Entomologische Zeitschrift 1897, Heft 2: 209–228. <https://doi.org/10.1002/mmnd.48018970115>
- Schneider O, Leder H (1879) Beiträge zur Kenntniss der kaukasischen Käferfauna. Verhandlungen des naturforschenden Vereines in Brünn 17: 3–99.
- Snegovaya N, Zare Khormizi M (2022) Checklist of lady beetles (Coleoptera: Coccinellidae) in Azerbaijan Republic. Munis Entomology & Zoology 17: 1142–1154.
- Szawaryn K, Nedvĕd O, Biranvand A, Czerwiński T, Nattier R (2021) Revision of the genus *Coccidula* Kugelann (Coleoptera, Coccinellidae). ZooKeys 1043: 61–85. <https://doi.org/10.3897/zookeys.1043.65829>
- Tarkhnishvili D, Gavashelishvili A, Mumladze L (2012) Palaeoclimatic models help to understand current distribution of Caucasian forest species. Biological Journal of the Linnean Society 105: 231–248. <https://doi.org/10.1111/j.1095-8312.2011.01788.x>
- Tobias VI (1975) A Review of the Braconidae (Hymenoptera) of the USSR. Amerind Publishing Co. Pvt. Ltd., New Delhi, viii + 164 pp.
- Ukrainsky AS (2013) The multicoloured Asian lady beetle *Harmonia axyridis* Pall. (Coleoptera, Coccinellidae) in North Caucasus, Russia. Eurasian Entomological Journal 12: 35–38. [in Russian, with English abstract]
- Victor T [Motschulsky VI] (1835) Description de quelques Coléoptères recueillis dans un voyage au Caucase et dans les provinces transcaucasiennes russes en 1834 et 1835. Nouveaux Mémoires de la Société Impériale des Naturalistes de Moscou 4: 313–323.
- Victor T [Motschulsky VI] (1837) Description de quelques Coléoptères recueillis dans un voyage au Caucase et dans les provinces transcaucasiennes russes en 1834 et 1835. Nouveaux Mémoires de la Société Impériale des Naturalistes de Moscou 5: 413–425.
- Wagner M (1852) Reise nach Persien und dem Lande der Kurden. Zweiter Band. Arnoldische Buchhandlung, Leipzig, iv + 315 pp.
- Weise J (1879) Bestimmungs-Tabellen der europäischen Coleopteren. II. Coccinellidae. Zeitschrift für Entomologie (Neue Folge) 7: 88–156.
- Weise J (1885) Bestimmungs-Tabellen der europäischen Coleopteren. II. Heft. Coccinellidae. II. Auflage. Mödling, 83 pp.
- Weise J (1894) *Coelopterus armeniacus*. Deutsche Entomologische Zeitschrift 1894: 144. <https://doi.org/10.1002/mmnd.48018940549>
- Winkler A (1927) Catalogus Coleopterorum regionis palaearticae. Pars 7. Albert Winkler, Wien, 753–880.
- Zazanashvili N, Manvelyan K, Askerov E, Mousavi M, Krever V, Kalem S, Garforth M (2020) The boundaries and bio-physical features of the Caucasus ecoregion. In: Zazanashvili N, Garforth M, Bitsadze M (Eds) Ecoregional Conservation Plan for the Caucasus, 2020 Edition: Supplementary Reports. WWF, KfW, Tbilisi, 9–20.

# Polyclads (Platyhelminthes) in the southern Gulf of Mexico: unveiling biodiversity and descriptions of two new species

Daniel Cuadrado<sup>1</sup>, Alejandro Hernández-González<sup>2</sup>, Carolina Noreña<sup>1</sup>, Nuno Simões<sup>2,3,4</sup>

1 Department of Biodiversity and Evolutionary Biology, National Museum of Natural Science, MNCN (CSIC), Madrid 28006, Spain

2 Universidad Nacional Autónoma de México, Merida, Mexico

3 Laboratorio Nacional de Resiliencia Costera, México, Mexico

4 International Chair for Coastal and Marine Studies, Harte Research Institute for Gulf of Mexico Studies, Corpus Christi, USA

Corresponding authors: Daniel Cuadrado ([cuadradopm@hotmail.com](mailto:cuadradopm@hotmail.com)); Nuno Simões ([ns@ciencias.unam.mx](mailto:ns@ciencias.unam.mx))

## Abstract

The order Polycladida (Platyhelminthes) in Mexico has historically received limited attention from researchers, primarily due to challenges associated with its low detectability and the scarcity of specialists. This study addresses part of the gap by conducting a comprehensive assessment of polyclad diversity in the southern Gulf of Mexico. Our investigation revealed a total of 27 distinct species, belonging to 17 genera and 12 families, within the suborders Cotylea and Acotylea. Our findings include the identification of 17 species previously undocumented in the Gulf of Mexico. This represents a significant expansion of the region's known polyclad biodiversity. By revising the polyclad records in the Gulf of Mexico, the known species count has increased from 31 to 50. Furthermore, our research unveiled the presence of two new species, *Stylochoplana sisalensis* sp. nov. and *Emprostopharynx hartei* sp. nov., also marking the first time a species of the genus *Emprostopharynx* has been reported for the Atlantic coast of the Americas.

**Key words:** Campeche, flatworms, histological analysis, marine invertebrates, new record, Quintana Roo, species discovery, taxonomy, Yucatan



Academic editor: Christopher Glasby

Received: 24 May 2024

Accepted: 25 October 2024

Published: 13 December 2024

ZooBank: <https://zoobank.org/EE34B942-57D8-456C-A6D5-F8046BB3A71E>

**Citation:** Cuadrado D, Hernández-González A, Noreña C, Simões N (2024) Polyclads (Platyhelminthes) in the southern Gulf of Mexico: unveiling biodiversity and descriptions of two new species. ZooKeys 1221: 103–144. <https://doi.org/10.3897/zookeys.1221.128260>

Copyright: © Daniel Cuadrado et al.  
This is an open access article distributed under terms of the Creative Commons Attribution License (Attribution 4.0 International – CC BY 4.0).

## Introduction

The Gulf of Mexico (GoM) is renowned for being one of the largest marine ecosystems worldwide, due to its unique combination of hydrographic factors, biological productivity, and population diversity. Covering more than 1.5 million km<sup>2</sup>, the GoM boasts a broad range of marine habitats, from coral reefs to fishing banks and coastal areas, making it a globally significant ecosystem (Chávez-Hidalgo 2009). Additionally, the interaction of ocean currents, winds, and unique geomorphological features contributes to the distinctive dynamics of this marine ecosystem. This optimal environment supports marine life and makes the GoM an essential area for the reproduction, feeding, and migration of numerous marine species (Gil-Agudelo et al. 2020).

Polyclads, marine flatworms, have not received much attention from researchers in Mexico. There are several reasons for the difficulty of observing these small organisms, including their ability to mimic their surround-

ings. More than 1000 species of polyclads are known worldwide according to Tyler et al. (2006–2024). Despite this, research on these organisms in GoM is limited. The largest number of records and species known in the Gulf of Mexico region was discovered in the initial studies conducted by Pearse and Wharton (1938) and by Hyman (1940, 1944, 1954) along the US coasts of Louisiana, Texas, and Florida. *Prostheceraeus crozieri*, a species also studied in this work, was documented in Florida by Newman et al. (2000). Quiroga et al. (2004a, 2004b) identified 124 species in the Gulf of Mexico and the Caribbean, while 40 species were found in Florida and 26 species were distributed throughout the Gulf of Mexico (Hooge and Newman 2009). Lastly, Quiroga (2008) described two new polyclad species in Louisiana, which is the latest discovery to date. The study conducted by Rawlinson (2008) focused on the polyclad species of the Caribbean Sea, which included Florida.

The present work is a significant contribution to the region as it addresses the shortage of species records and the urgent need to update the biodiversity inventory of the order Polycladida in the Gulf of Mexico (GoM). By examining 142 specimens, we identified 27 taxa that belong to 12 families and 17 genera, increasing the known species count from 31 to 50 (Suppl. material 1: table S1, Fig. 1). The Gulf documentation now includes 17 species that were not previously recorded and the discovery of two new species, which are described below.

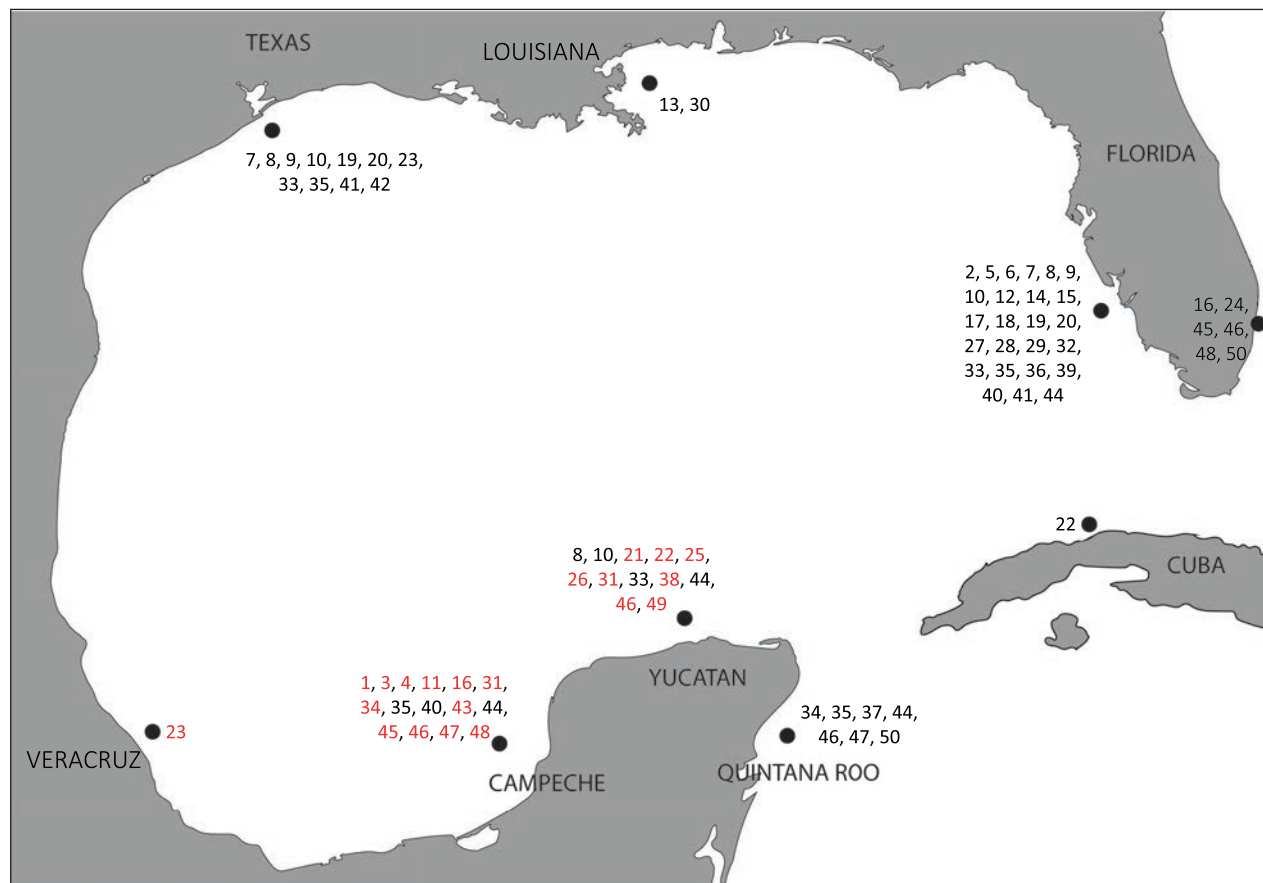
## Materials and methods

### Sampling sites and processing of material

The study material from the southern Gulf of Mexico was obtained through direct field collection using scuba diving and snorkelling in the subtidal (Fig. 2). Comprehensive information about external features was meticulously recorded using notes, photographs, and drawings. Details regarding pigmentation, colour patterns, movement, size, and the presence or absence of tentacles or eyes were documented and have been used for the species descriptions. Additionally, dorsal structures such as papillae, stripes, warts, or any type of epithelial or dermal formations were compiled. Photographs in the field in their habitat were taken whenever it was possible with a Canon G16. Photographs of the living specimens were taken to document their colouration. Whenever possible, the photographs were taken on a black background using transmitted light with a Nikon D90 camera equipped with a Micro Nikkor 60 mm lens.

### Histological processing

To ensure proper fixation, individuals were first anaesthetised with a seawater/magnesium chloride solution (7%). A small tissue sample was extracted and preserved in absolute ethanol for future molecular studies, and the entire specimen was then fixed in Bouin's solution (saturated picric acid solution, formaldehyde, and acetic acid in a 15:5:1 proportion) for histological studies (Romeis



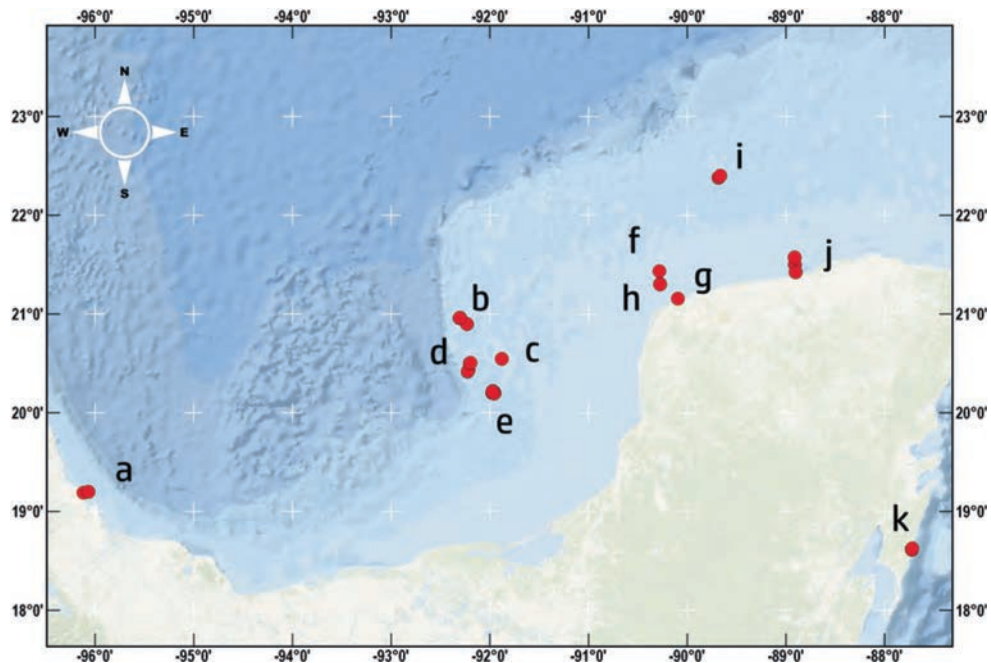


**Figure 2.** Sampling sites in the southern Gulf of Mexico and the Mexican Caribbean **a** Veracruz **b** West Triangles reef and East **c** reefs Banco Nuevo and Banco Pera **d** Banco Obispos north and south **e** Cayo Arcas **f** reef Madagascar **g** Punta Piedra **h** Bajo de Sisal **i** Alacranes Reef **j** Dzilam de Bravo **k** Mahahual.

### Abbreviations used in the figures

**cg:** cement glands, **co:** copulatory organ, **ct:** connective tissue, **de:** ejaculatory duct, **dlv:** Lang's vesicle duct, **e:** stylet, **ed:** ejaculatory duct, **e-gpt:** epithelial-glandular prostate tissue, **ev:** external vagina, **fa:** female atrium, **fg:** female gonopore, **i:** intestine, **iv:** internal vagina, **lv:** Lang's vesicle, **m:** muscle layer, **ma:** male atrium, **mb:** marginal band, **mg:** male gonopore, **ml:** marginal line, **oc:** cerebral ocelli/eyes, **om:** marginal ocelli/eyes, **ot:** tentacular ocelli/eyes, **ov:** oviduct, **p:** pharynx, **pa:** papillae, **pp:** penis papilla, **pt:** pseudotentacles, **pte:** pseudotentacle eyes, **pv:** prostatic vesicle, **s:** sucker, **sg:** shell glands, **sv:** seminal vesicle, **t:** tentacle, **va:** vagina, **vd:** vas deferens.

### DNA extraction and amplification

Total genomic DNA was extracted from each sample following the phenol-chloroform protocol (Chen et al. 2010). DNA concentration and purity of the extraction were measured using a NanoDrop Fluorospectrometer (Thermo Fisher Scientific). Sequences of the ribosomal gene 28S of the investigated Polycladida species were studied. All PCRs were performed using Taq DNA polymerase of Mastermix (Invitrogen, Carlsbad, CA) following the manufacturer's protocol in a total volume of 25 µl. Sequences of approximately 1100 bp of the 28S gene were amplified with degenerated primers designed by Cuadrado et al. (2021): forward primer (5'-AGCCCAGCACCGAATCCT3') and reverse (5'-GCAAACCAAGTAGGGTGTGCGC-3'). The PCR consisted of an initial denaturation step at 95 °C (3 min), followed by a pre-cycle of 5 cycles of denaturation at 96 °C (30 sec), annealing at 55 °C (30 sec) and extension at 72 °C (1 min), followed by 40 cycles of denaturation at 95 °C (30 sec), annealing at 59 °C (30 sec) and extension at 72 °C (1 min), with a final extension of 10 min at 72 °C.

The PCR products were observed using TBE gel electrophoresis in 1.5% agarose gel stained with SYBER Safe and visualised under UV light. PCR products were sent to Macrogen for clean-up and sequencing. Lastly, obtained forward and reverse sequences were combined using the program Geneious Prime v. 2020.2.4 (<http://www.geneious.com>, Kearse et al. 2012) using the alignment-transition/transversion with the consensus sequence tool and manually created.

All sequences obtained in the present study have been deposited in the GenBank database under the accession numbers included in Suppl. material 1: table S2.

## Results

### Polycladida

#### Suborder Cotylea

#### Periceloidea Bahia, Padula & Schrödl, 2017

#### Pericelidae Laidlaw, 1902

#### *Pericelis* Laidlaw, 1902

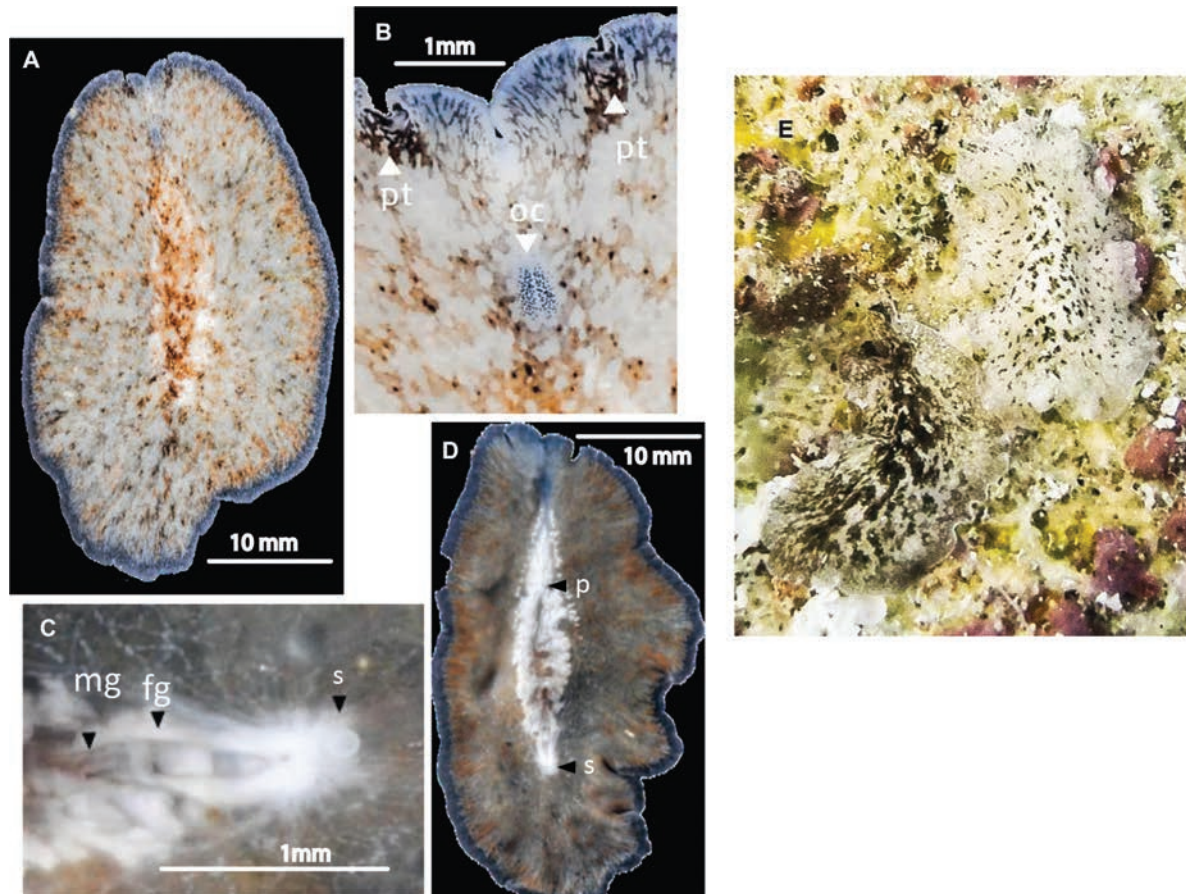
#### *Pericelis cata* Marcus & Marcus, 1968

Fig. 3

**Material examined. Campeche coast, MEXICO** • 1; Cayos sumergidos del Oeste; 20.9°N, 92.2°W; 0 m; 10 Sep. 2017; A. Gutiérrez leg.; CRPPY-0011 • 1; Cayos sumergidos del Oeste; 20.9°N, 92.2°W; 13 m; 14 Sep. 2017; A. Gutiérrez leg.; CRPPY-0020 • 1; Cayos sumergidos del Oeste; 21.0°N, 92.3°W; 10 m; 9 Sep. 2017; F. Márquez leg.; CRPPY-0022 • 2; Cayos sumergidos del Oeste; 20.4°N, 92.2°W; 10.8 m; 14 Sep. 2017; A. Gutiérrez leg.; CRPPY-0024 • 1; Cayos sumergidos del Oeste; 20.5°N, 92.2°W; 26 m; 13 Sep. 2017; X. Vital leg.; CRPPY-0025; **Quintana Roo coast, MEXICO** • 1; Mahahual; 18.6°N, 87.7°W; 13.4 m; 18 Mar. 2018; A. Hernández leg.; CRPPY-0040; **Campeche coast, MEXICO** • 1; Cayo Arcas; 20.2°N, 92.0°W; 5 m; 19 Apr. 2018; A. Hernández leg.; CRPPY-0046 • 1; Cayo Arcas; 20.2°N, 92.0°W; 4.7 m; 19 Apr. 2018; A. Hernández leg.; CRPPY-0051 • 1; Cayo Arcas; 20.2°N, 92.0°W; 6.3 m; 22 Apr. 2018; A. Hernández leg.; CRPPY-0065 • 1; Cayo Arcas; 20.2°N, 92.0°W; 3.2 m; 24 Apr. 2018; A. Hernández leg.; CRPPY-0078 • 1; Cayo Arcas; 20.2°N, 92.0°W; 7.7 m; 25 Apr. 2018; A. Hernández leg.; CRPPY-0083.

**Distribution.** This species was previously recorded in Curaçao (Marcus and Marcus 1968); the Caribbean coast of Colombia (Quiroga et al. 2004a, 2004b); Cabo Frío, Salvador, and Alagoas, Brazil (Queiroz et al. 2013; Bahia et al. 2014, 2015; Bahia and Schrödl 2018); Canary Islands, Spain (Cuadrado et al. 2017). This is a new record for the coasts of Campeche (Gulf of Mexico), and Quintana Roo (Mexican Caribbean). New record for the Gulf of Mexico.

**Description.** Body oval with multiple marginal folds, 4 cm in length and 2.5 cm in width. Dorsally, pattern of dark pigmentation is interrupted by spots where the white parenchyma is observed. Towards the margin, the white patches become smaller, and the space between them decreases, with scattered black dots. The tentacles are subtle marginal folds, with a clear separation between them, characteristic of the genus *Pericelis* (Fig. 3A, B). Marginal eyes are arranged irregularly around the entire body margin (Fig. 3A, B). Dorsally, the tentacular and cerebral eyes are arranged in two elongated clusters (Fig. 3B).



**Figure 3.** *Pericelis cata* **A** dorsal view **B** frontal region, cerebral eyes and pseudotentacles **C** location of the sucker, male and female gonopores **D** ventral view **E** *P. cata* in situ.

**Remarks.** *Pericelis cata* morphology found in the Gulf of Mexico corresponds to the original description by Marcus and Marcus (1968), characterised by the position of the pseudotentacles, the elongated cerebral eye clusters, and the colour pattern: white and black spots on a brown background (Fig. 3A–D). The pigmentation of the specimens sampled in the Gulf of Mexico is different from that described in the original description of *P. cata*. The Mexican species displays a basal colour of white, with brown spots and freckles (as seen in Fig. 3E).

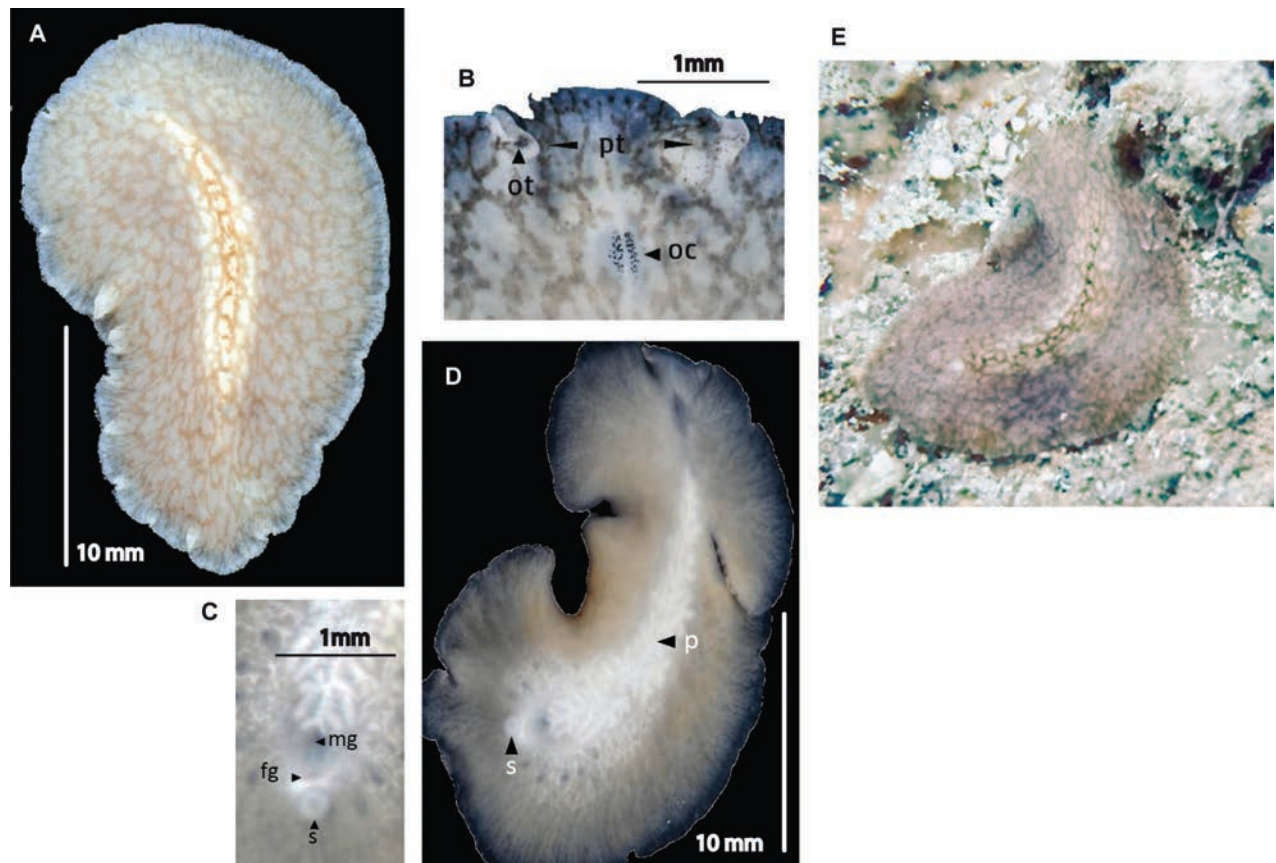
#### ***Pericelis orbicularia* (Schmarda, 1859)**

Fig. 4

**Material examined.** Yucatan coast, MEXICO • 1; Punta Piedra, Sisal; 21.2°N, 90.1°W; 1 m; 30 Apr. 2018; A. Hernández leg.; CRPPY-0087 • 1; Dzilam; 21.5°N, 88.9°W; 9.3 m; 8 May 2018; A. Hernández leg.; CRPPY-0091 • 1; 12 slides; Dzilam; 21.5°N, 88.9°W; 13 m; 10 May 2018; A. Hernández leg.; CRPPY-0097.

**Distribution.** *Pericelis orbicularia* is known from the south coast of Jamaica (Schmarda 1859); Port Aransas, Texas, USA (Hyman 1955); and Key Biscayne (Florida, USA; Marcus and Marcus 1968). This is the first record for the coast of Yucatan (Mexico).

**Description.** Body oval-shaped, 2 cm in length and 1 cm in width, with small pseudotentacles, less than 1 mm. Dorsal surface exhibits an orange to light



**Figure 4.** *Pericelis orbicularia* **A** dorsal view **B** shape of pseudotentacles, pseudotentacular eyes, cerebral eyes **C** male and female gonopores, sucker **D** ventral view **E** *P. orbicularia* in situ.

brown reticulated pattern on a regular creamy beige background (Fig. 4A, D, E). The pigmentation corresponds to the colouration described by Hyman (1955) for specimens of Port Aransas, Texas. According to Hyman, *Pericelis orbicularia* presents “a reddish-brown network on a paler ground”. Cerebral eyes are arranged in two elongated clusters. Tentacular and marginal eyes scattered along the margin. A swelling in the body’s midline is caused by the highly folded pharynx and the copulatory organ (Fig. 4A, B, E). *Pericelis orbicularia* was observed to secrete an abundant and viscous mucus. **Reproductive system.** The male and female copulatory apparatus are located just posterior to the pharynx and before the prominent sucker, 0.5 mm distance between them. Live specimens exhibit distinct female and male gonopores, but in our fixed specimens, the gonopores appear as a concavity, giving the impression of a single gonopore (Fig. 4C, D). The male copulatory apparatus shows an anteroposterior orientation, including a highly muscular seminal vesicle and an ejaculatory duct lined with glandular epithelium.

#### **Prosthiostomidae Lang, 1884**

##### ***Prosthiostomum* Quatrefage, 1845**

##### ***Prosthiostomum utarum* Marcus, 1952**

Fig. 5A

**Material examined.** Quintana Roo coast, MEXICO • 1; Mahahual; 18.6°N, 87.7°W; 13.4 m; 18 Mar. 2018; A. Hernández leg.; CRPPY-0041.

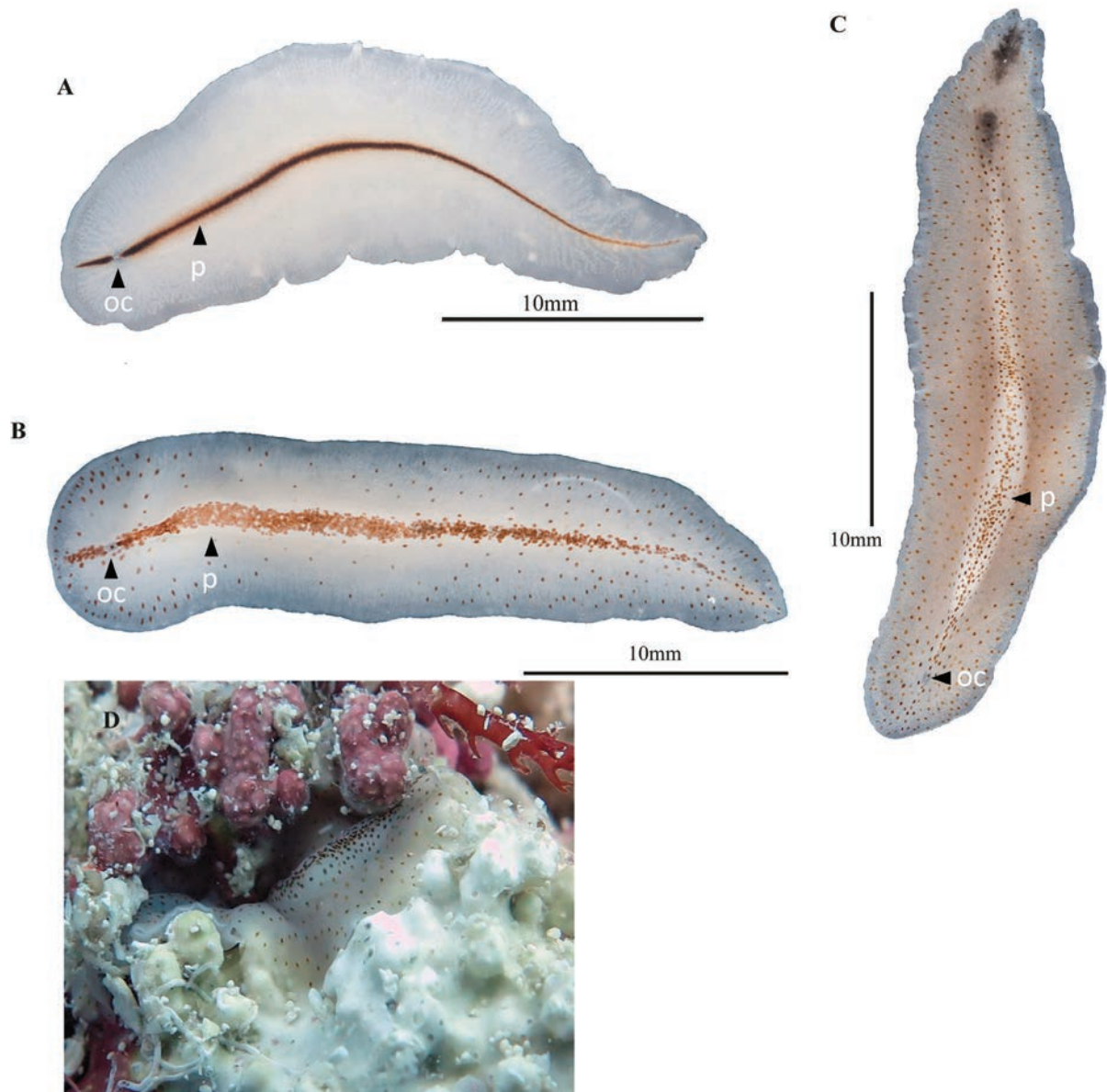


**Figure 5.** A *Prosthiostomum utarum* dorsal view B *Enchiridium periommatum* in situ C *Enchiridium evelinae* dorsal view D *Enchiridium evelinae* in situ.

**Distribution.** This species was described from Sao Sebastiao Island, Brazil (type locality; Marcus 1952) and the Praia das Conchas, Cabo Frío, Brazil (Bahia et al. 2014; Bahia and Schrödl 2018), as well as on the Atlantic coast of Florida. It has also been recorded in the Caribbean Sea, Colombia (Quiroga et al. 2004a, 2004b). The discovery of *Prosthiostomum utarum* on the coast of Quintana Roo presents a new record for this species in the Mexican Caribbean Sea.

**Description.** Body shape elongated, 3 cm in length and 0.7 cm in width with a rounded anterior end and a pointed posterior end (Fig. 5A). Predominantly white tonalities and distinctive brown pigmentation along the midline and the anterior region. Cerebral eyes organised in two elongated clusters. Marginal eyes along the anterior region.

**Remarks.** *Prosthiostomum utarum*, originally described as *Lurymare utarum* (Marcus, 1952), was recently reassigned to the genus *Prosthiostomum* based on the work of Litvaitis et al. (2019) based on the 28S gene. The morphology of

Gulf of Mexico specimens corresponds to the original description by Marcus (1952). A comprehensive investigation, including both morphological and molecular aspects, is necessary for accurate delimitation of the genera *Lurymare* and *Prosthiostomum*.

### ***Enchiridium* Bock, 1913**

#### ***Enchiridium evelinae* Marcus, 1949**

Fig. 5C, D

**Material examined.** Yucatan coast, MEXICO • 1; Bajos de Sisal; 21.2°N, 90.0°W; 1 m; 10 Sep. 2017; A. Hernández leg.; CRPPY-0033.

**Distribution.** Recorded in São Paulo (Marcus 1950), Rio Grande do Norte, and Alagoas (Bahia et al. 2012, 2014, 2015; Bahia and Schrödl 2018) in Brazil and Panama (Rawlinson 2008). It is also known in Curaçao (Marcus and Marcus 1968). This work represents a new record for the Yucatan coast. New record for the Gulf of Mexico.

**Description.** Body shape elongated, 3 cm in length and 1 cm in width. Body cream-coloured with brown, orange, and yellow spots arranged densely along the midline and paler towards the margins (Fig. 5C, D). Tubular pharynx extends to ~ 1/3 of the body's length. Reproductive male apparatus with an enclosed seminal vesicle and two prostatic vesicles included in a common muscular bulb, and a long penis papilla armed with a stylet opening in a long male atrium.

**Remarks.** The spots disappear after fixation and, according to Marcus (1950), the pigmentation of these spots is lipoid (Fig. 5C, D). The specimens recorded here have a lower density of dots compared to the specimens described in Bahia et al. (2014: fig. 14).

### ***Enchiridium periommatum* Bock, 1913**

Fig. 5B

**Material examined.** Yucatan coast, MEXICO • 1; Arrecife Alacranes; 22.4°N, 89.7°W; 1 m; 3 Nov. 2017; A. Hernández leg.; CRPPY-0001 • 1; Arrecife Alacranes; 22.4°N, 89.7°W; 1 m; 3 Nov. 2017; A. Hernández leg.; CRPPY-0003 • 2; Arrecife Alacranes; 22.4°N, 89.7°W; 1 m; 4 Nov. 2017; A. Hernández leg.; CRPPY-0005 • 1; Arrecife Alacranes; 22.4°N, 89.7°W; 2 m; 4 Nov. 2017; A. Hernández leg.; CRPPY-0007; Quintana Roo coast, MEXICO • 1; Mahahual; 18.6°N, 87.7°W; 15 m; 18 Mar. 2018; A. Hernández leg.; CRPPY-0042; Yucatan coast, MEXICO • 1; Dzilam; 21.5°N, 88.9°W; 13 m; 10 May 2018; A. Hernández leg.; CRPPY-0098.

**Distribution.** The species was originally described in Thatch Island, US Virgin Islands (Bock 1913), later collected in Jamaica (Hyman 1955), and also known from Texas to Florida, Gulf of Mexico (Hyman 1955). This is a new record for the coasts of Campeche and Quintana Roo (Mexico).

**Description.** Body elongated, 1.5 cm in length and 0.5 cm in width, with a rounded anterior end and a tapered posterior end. Marginal eyes densely distributed along the anterior margin; cerebral eyes in a heart-shaped cluster. Translucent white background speckled with dense brown to orange spots that

gradually decrease in number towards the edges (Fig. 5B). Pharynx, male and female reproductive organs, as well as the sucker are located in the anterior 1/2 of the body, a distinctive feature of this species.

**Pseudocerotoidea Faubel, 1984**

**Euryleptidae Stimpson, 1857**

***Eurylepta* Ehrenberg, 1831**

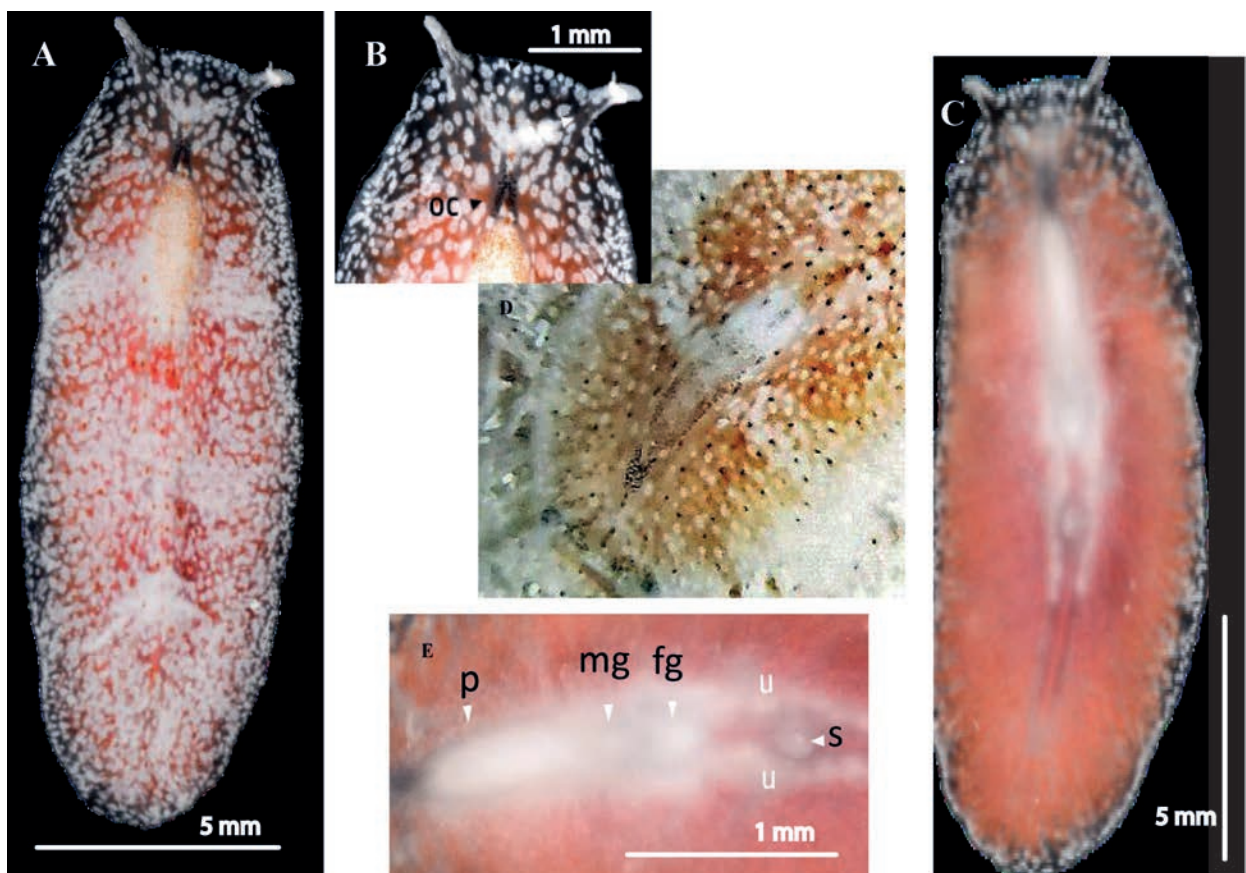
***Eurylepta aurantiaca* Heath & McGregor, 1912**

Fig. 6

**Material examined.** Yucatan coast, MEXICO • 1; Dzilam; 21.5°N, 88.9°W; 9.3 m; 8 May 2018; A. Hernández leg.; CRPPY-0088.

**Distribution.** The species was recorded in Monterey Bay, California (Heath and McGregor 1912); Washington State, USA (Hyman 1955), the Caribbean Sea of Colombia (Quiroga et al. 2004a, 2004b); Brazil (Bahia et al. 2014); India (Pitale and Apte 2019). This work represents a new record for the Yucatan coast. New record for the Gulf of Mexico.

**Description.** Body shape elliptical, 1.7 cm in length and 0.5 cm in width, with a translucent to orange-pink colouration, white spots on the dorsal side, and a reddish median line with reddish dots (Fig. 6A, B, D). Intestinal branches apparent (Fig. 6C, E). Whitish tentacles. Cerebral eyes are in two elongated clusters,



**Figure 6.** *Eurylepta aurantiaca* **A** dorsal view **B** anterior region, cerebral eyes **C** ventral view **D** *Eurylepta aurantiaca* in situ **E** detail of pharynx, male and female gonopores, uteri, and sucker.

and tentacular eyes in the basal region of the tentacles. Two frontal eye clusters located between the tentacles.

**Remarks.** The specimen collected from the Mexican coast exhibits a pigmentation characterised by a pinkish orange hue, as illustrated in Fig. 6A, congruent with the characterisation reported by Bahia et al. (2014).

***Prostheceraeus* Schmarda, 1859**

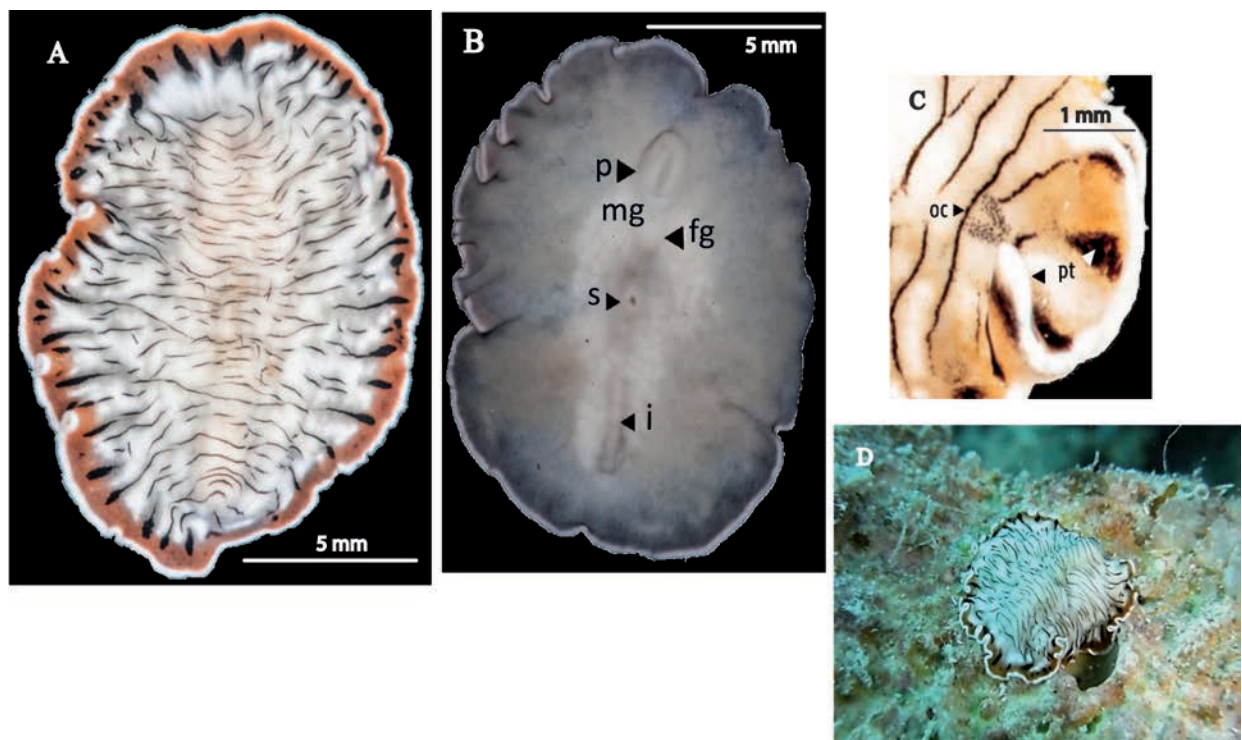
***Prostheceraeus crozieri* (Hyman, 1939)**

Fig. 7

**Material examined.** Campeche coast, MEXICO • 1; Cayos sumergidos del Oeste; 20.4°N, 92.2°W; 18 m; 14 Sep. 2017; A. Gutiérrez leg.; CRPPY-0018 • 1; Cayo Arcas; 20.2°N, 92.0°W; 16.3 m; 20 Aug. 2018; A. Hernández leg.; CRPPY-0108.

**Distribution.** Recorded in the east coast of Florida and the Florida Keys, Bermuda (Crozier 1917; Hyman 1939); Curaçao (Marcus and Marcus 1968); Jamaica, the Gulf of Mexico, and the Caribbean (Hyman 1952). New record for the coast of Campeche, Mexico.

**Description.** Oval or circular-shaped body, 2.3 cm in length and 0.8 cm in width, with a semi-transparent white-beige background with transverse wavy black lines. The lines alternately end in a black spot or an orange blotch. Dorsal surface with white spots and a submarginal semi-transparent and marginal narrow white band (Fig. 7A, C, D). Ventral surface creamy white (Fig. 7B). Marginal orange tentacles long with black and white tips. Cerebral eye is distributed in two elongated clusters, each containing ~ 35 eyes (Fig. 7A, C). The anatomy of the reproductive system agrees with that described by Hyman (1939).



**Figure 7.** *Prostheceraeus crozieri* **A** dorsal view **B** ventral view. Detail of mouth and pharynx, female gonopore, sucker, intestine **C** cerebral eyes and pseudotentacles **E** *P. crozieri* in situ.

**Remarks.** The specimen from the Gulf of Mexico aligns with the description of *Prostheceraeus crozieri* provided by Hyman (1939). Newman et al. (2000) transferred both *Pseudoceros crozieri* Hyman, 1939 and *Prostheceraeus zebra* Hyman, 1955 to *Maritigrella crozieri* due to the presence of a tubular pharynx and the lack of uterine vesicles. Litvaitis et al. (2019) reclassified *Maritigrella crozieri* as *Prostheceraeus* based on the description and illustration of *Prostheceraeus zebra* by Hyman (1955).

**Biology.** *Prostheceraeus crozieri* is documented as a primary consumer of the sea squirt *Ecteinascidia turbinata*. Although this ascidian species was prolific within the research areas, the occurrence of *Prostheceraeus crozieri* was limited.

### **Pseudocerotidae Lang, 1884**

#### ***Pseudoceros* Lang, 1884**

#### ***Pseudoceros bicolor* Verrill, 1901**

Fig. 8

**Material examined.** **Yucatan coast, MEXICO** • 1; Arrecife Alacranes; 22.4°N, 89.7°W; 3 m; 4 Nov. 2017; A. Hernández leg.; CRPPY-0008; **Campeche coast, MEXICO** • 1; Cayos sumergidos del Oeste; 20.4°N, 92.2°W; 10 m; 14 Sep. 2017; A. Hernández leg.; CRPPY-0015 • 1; Cayos sumergidos del Oeste; 20.4°N, 92.2°W; 11.1 m; 13 Sep. 2017; D. Ortigosa leg.; CRPPY-0027 • 1; Cayos sumergidos del Oeste; 20.4°N, 92.2°W; 11.7 m; 14 Sep. 2017; D. Ortigosa leg.; CRPPY-0028; **Yucatan coast, MEXICO** • 1; Bajos de Sisal; 21.2°N, 90.0°W; 1 m; 22 Feb. 2018; A. Hernández leg.; CRPPY-0032; **Quintana Roo coast, MEXICO** • 1; Mahahual; 18.6°N, 87.7°W; 7.7 m; 17 Mar. 2018; A. Hernández leg.; CRPPY-0039; **Campeche coast, MEXICO** • 1; Cayo Arcas; 20.2°N, 92.0°W; 6.4 m; 19 Apr. 2018; A. Hernández leg.; CRPPY-0048 • 1; Cayo Arcas; 20.2°N, 92.0°W; 2.2 m; 20 Apr. 2018; A. Hernández leg.; CRPPY-0052 • 2; Cayo Arcas; 20.2°N, 92.0°W; 2.2 m; 20 Apr. 2018; A. Hernández leg.; CRPPY-0054 • 1; Cayo Arcas; 20.2°N, 92.0°W; 2.2 m; 20 Apr. 2018; A. Hernández leg.; CRPPY-0055 • 1; Cayo Arcas; 20.2°N, 92.0°W; 2.2 m; 21 Apr. 2018; A. Hernández leg.; CRPPY-0061 • 1; Cayo Arcas; 20.2°N, 92.0°W; 2.2 m; 22 Apr. 2018; A. Hernández leg.; CRPPY-0063 • 2; Cayo Arcas; 20.2°N, 92.0°W; 6.3 m; 22 Apr. 2018; A. Hernández leg.; CRPPY-0067 • 1; Cayo Arcas; 20.2°N, 92.0°W; 7.5 m; 23 Apr. 2018; A. Hernández leg.; CRPPY-0069 • 1; Cayo Arcas; 20.2°N, 92.0°W; 5.9 m; 23 Apr. 2018; A. Hernández leg.; CRPPY-0070 • 1; Cayo Arcas; 20.2°N, 92.0°W; 5.3 m; 23 Apr. 2018; A. Hernández leg.; CRPPY-0072 • 1; Cayo Arcas; 20.2°N, 92.0°W; 5.3 m; 24 Apr. 2018; A. Hernández leg.; CRPPY-0074 • 1; Cayo Arcas; 20.2°N, 92.0°W; 9.9 m; 25 Apr. 2018; A. Hernández leg.; CRPPY-0081 • 1; Cayo Arcas; 20.2°N, 92.0°W; 7.7 m; 25 Apr. 2018; A. Hernández leg.; CRPPY-0084 • 1; Cayo Arcas; 20.2°N, 92.0°W; 3.4 m; 18 Aug. 2018; A. Hernández leg.; CRPPY-0106 • 1; Cayo Arcas; 20.2°N, 92.0°W; 3.4 m; 18 Aug. 2018; A. Hernández leg.; CRPPY-0107.

**Distribution.** Recorded in the Birds Islands, Bermuda (Verrill 1901); Curaçao (Marcus and Marcus 1968); the Caribbean coast of Colombia (Quiroga et al. 2004a); Florida, Virgin Islands, Jamaica, Belize, Honduras, Caribbean coast of Panama (Rawlinson 2008; Litvaitis et al. 2019); Brazil (Bahia and Padula 2009; Bahia et al. 2014, 2015; Bahia and Schrödl 2018). New record for the coasts of Campeche, Yucatán, and Quintana Roo (Mexican Caribbean), Mexico.

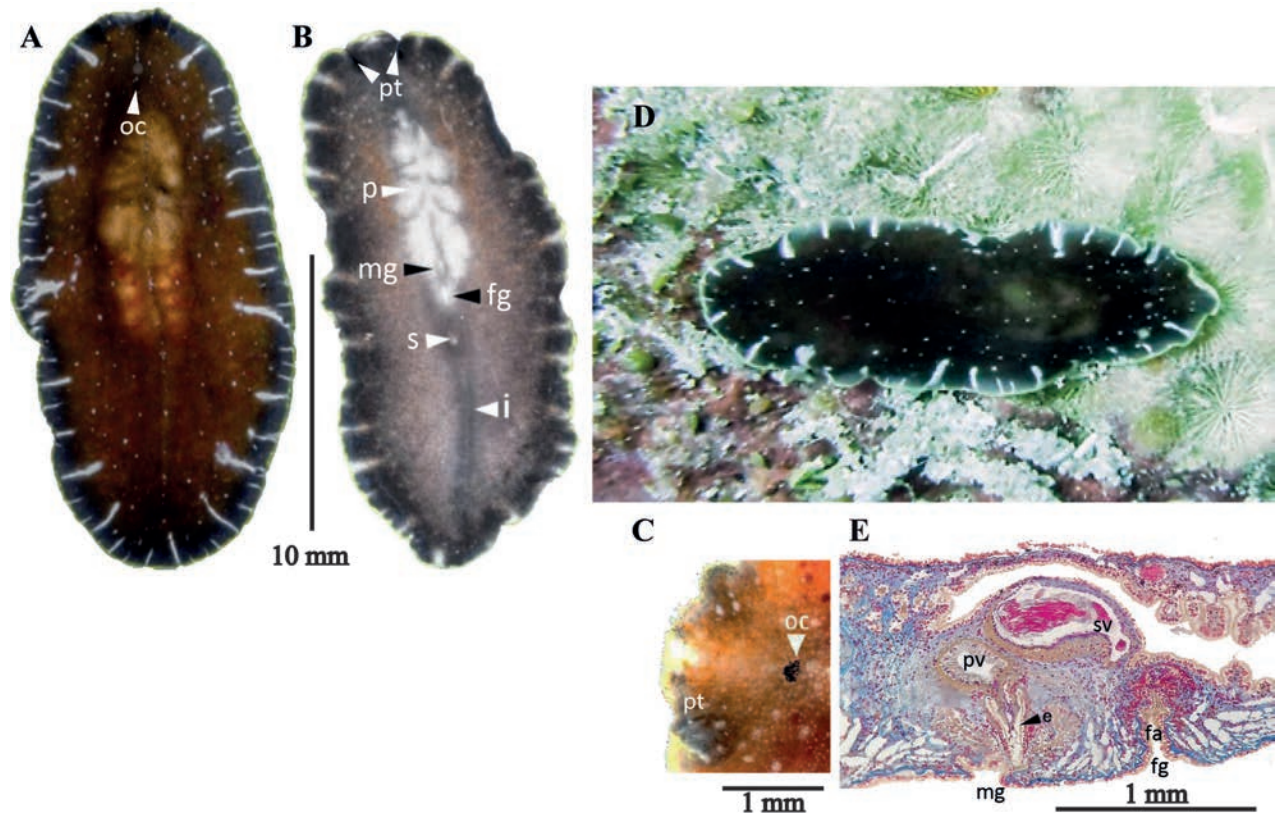


**Figure 8.** *Pseudoceros bicolor* **A** dorsal view **B** ventral view, sucker, oral pore, pharynx, male gonopore, female gonopore and intestine **C** detail of tentacular eyes, pseudotentacles **D** *P. bicolor* in situ **E** sagittal section, prostatic vesicle, seminal vesicle, male gonopore, stylet, vagina, female gonopore, female atrium Azan stained.

**Description.** Body shape elongated with rounded anterior and posterior end, 2.5 cm in length and 1 cm in width. Dorsal pigmentation ranges from yellow to dark brown, with scattered white dots on its dorsal surface and with a yellowish or pale green marginal rim. Conspicuous dark marginal band interrupted by transverse white stripes (Fig. 8A, B, D). Pseudotentacles are simple folds with two clusters of eyes between them. Cerebral eyes arranged in the shape of an arrowhead, marginal eyes very numerous (Fig. 8C). Male and female gonopores located in the mid-region of the body, sucker posteriorly (Fig. 8B, E).

**Remarks.** The pigmentation observed in *P. bicolor* in Yucatan aligns with the morphotype seen in Brazil (Litvaitis et al. 2010: fig. 4N). Preliminary analysis of the sequences obtained for the species (Suppl. material 1: table S2) suggests that Mexican specimens appear to have a closer genetic relationship to those in Brazil than those in the Caribbean Sea and nearby regions. A comparative molecular analysis will help to understand their genetic relationship with other morphotypes described in the literature.

***Pseudoceros rawlinsonae* Bolaños, Quiroga & Litvaitis, 2007**

Fig. 9

**Material examined.** Yucatan coast, MEXICO • 1; Bajos de Sisal; 21.2°N, 90.0°W; 1 m; 22 Feb. 2018; A. Hernández leg.; CRPPY-0029; Quintana Roo coast, MEXICO • 1; Mahahual; 18.6°N, 87.7°W; 5.3 m; 17 Mar. 2018; A. Hernández leg.;

CRPPY-0036; **Campeche coast, Mexico** • 1; Cayo Arcas; 20.2°N, 92.0°W; 9.3 m; 21 Apr. 2018; A. Hernández leg.; CRPPY-0056 • 1; Cayo Arcas; 20.2°N, 92.0°W; 5 m; 25 Apr. 2018; A. Hernández leg.; CRPPY-0085.

**Distribution.** *Pseudoceros rawlinsonae* has been recorded in the Caribbean Sea: Virgin Islands, Honduras, Jamaica, Bahamas, Curaçao; the Gulf of Mexico, Florida (Bolaños et al. 2007; Litvaitis et al. 2010, 2019); Brazil (Bahia et al. 2014, 2015; Bahia and Schrödl 2018). This is the first record for the coasts of Quintana Roo (Mexican Caribbean), Campeche and Yucatán, Mexico.

**Description.** Body shape elongated with rounded anterior and posterior end, 1.2 cm in length and 0.5 cm in width. Pigmentation brownish yellow to black with scattered white dots (Fig. 9A, D). A white marginal band with grey to black stripes encircles body margin. A characteristic golden yellow or orange marginal line marks external rim. Pseudotentacles simple folds (Fig. 9A, B). Cerebral eyes arranged in arrowhead shape, tentacular eyes more densely arranged along margins of pseudotentacles. Two frontal eye clusters positioned between two pseudotentacles. Ruffled pharynx in anterior region, oral pore situated centrally. Female and male gonopores separate and located in mid-region of the body, with sucker posterior to them (Fig. 9C).

**Remarks.** *Pseudoceros bicolor* and *P. rawlinsonae* are closely related. Externally, the primary distinguishing features between the two are the prominent white submarginal band and the orange rim that characterise *P. rawlinsonae*. A study by Litvaitis et al. (2010) provided a detailed comparison between both species, examining both morphological and molecular data, specifically through analysis of the 28S gene.

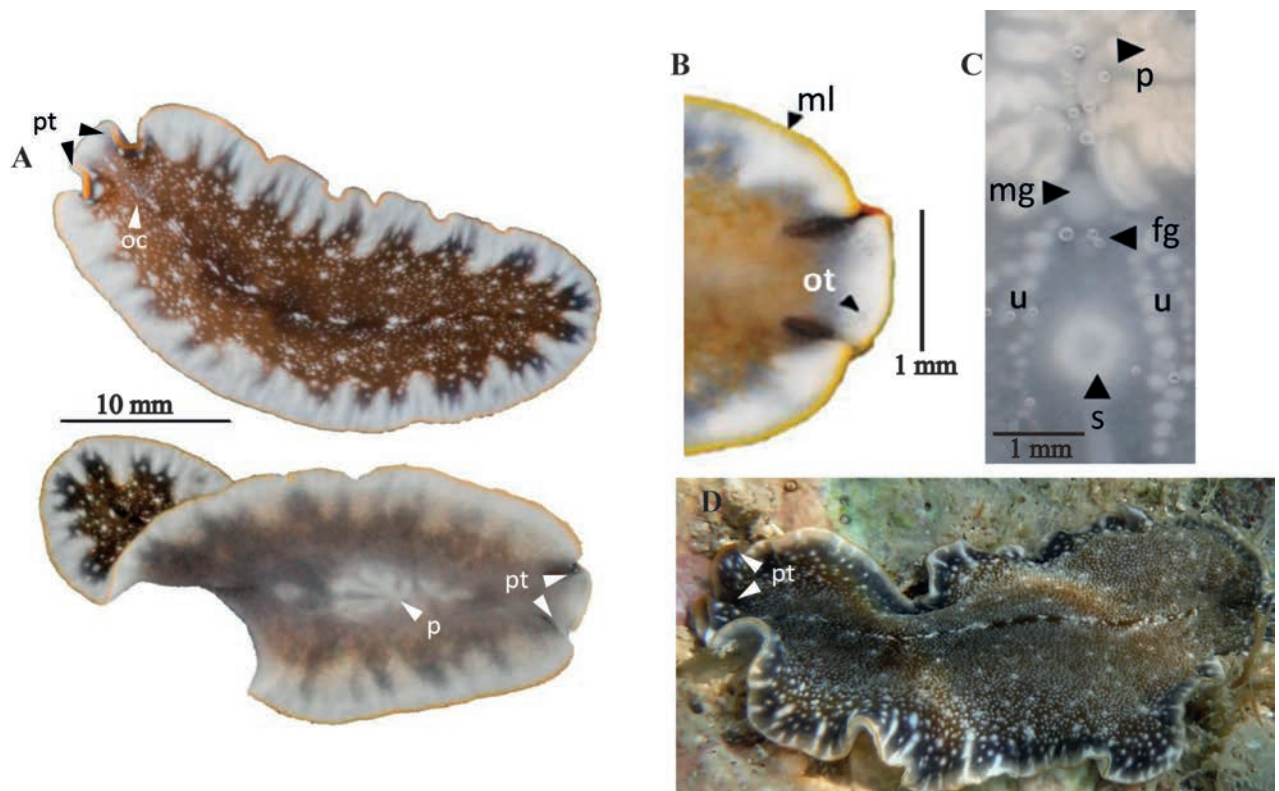


**Figure 9.** *Pseudoceros rawlinsonae* **A** anterior end with pseudotentacles **B** dorsal y ventral view **C** ventral detail of pharynx, male and female gonopore, uteri and sucker **D** *P. rawlinsonae* in situ.

***Pseudoceros bolool* Newman & Cannon, 1994**

Fig. 10

**Material examined.** Campeche coast, MEXICO • 1; Cayo Arcas; 20.2°N, 92.0°W; 3.2 m; 24 Apr. 2018; A. Hernández leg.; CRPPY-0079.

**Distribution.** Recorded in Heron Island and One Tree Island, Australia; Madang, Papua New Guinea (Newman and Cannon 1994); Shivrajpur, Gujarat (Thakkar et al. 2017); Andaman and Nicobar Island, India (Sreeraj and Raghunathan 2015); Caribbean Sea and Florida (Rawlinson 2008). This is the first record for the Campeche coast. New record for the Gulf of Mexico.

**Description.** Body shape elongated with rounded anterior margin, tapering posteriorly, 3.5 cm in length and 1 cm in width. Margins slightly wavy. Ground colour velvety black, without any specific additional pattern, but with a small stain, devoid of pigment, present in area of cerebral eyes (Fig. 10A, B). Greyish ventrally. A characteristic bulge marks main intestinal trunk in body midline (Fig. 10C). Pseudotentacles simple folds of anterior margin. Cluster of cerebral eyes horseshoe-shaped at anterior end (Fig. 10A).

**Remarks.** Within *Pseudoceros*, *P. bolool* and *P. velutinus* (Blanchard, 1847) share several external and internal morphological characters, characterised by a uniform velvety black coloration, without spots, bands, or marginal lines.

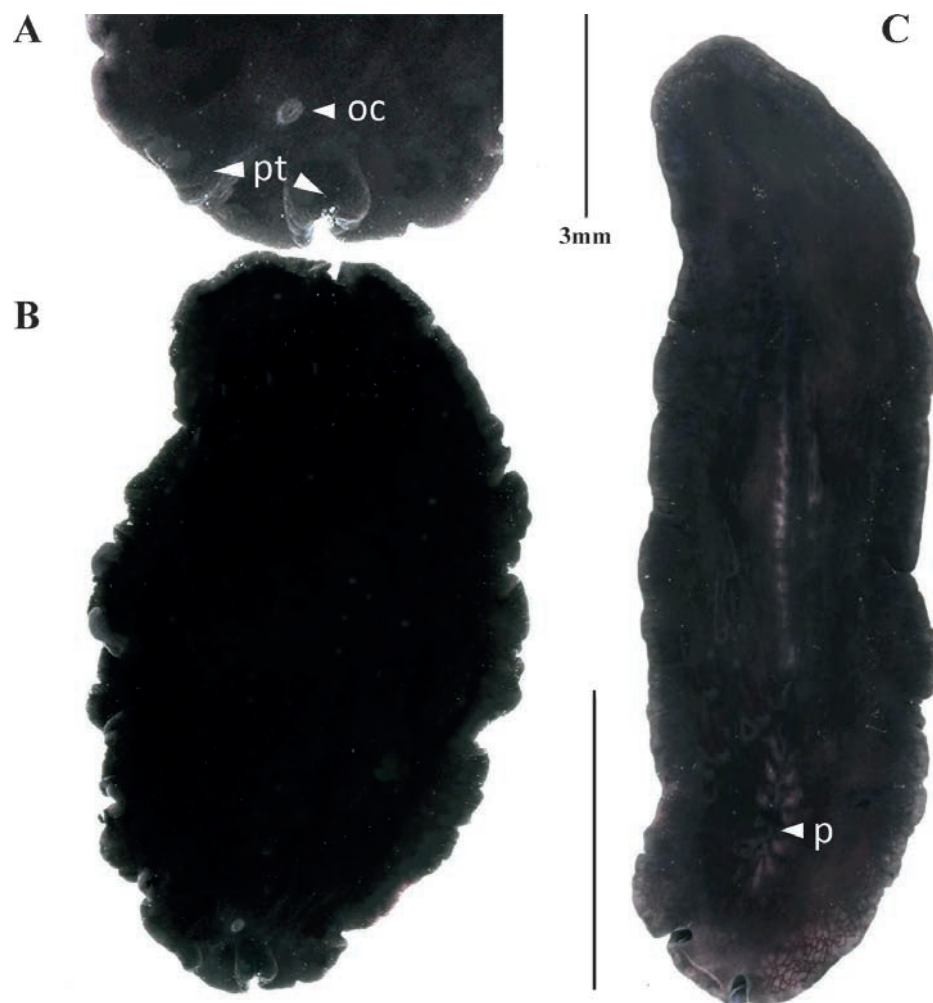


**Figure 10.** *Pseudoceros bolool* **A** detail of the shape of the pseudotentacles and cerebral eyes **B** dorsal view **C** ventral view.

While both species share several external and internal morphological traits, they can be distinguished by the ventral coloration: *P. velutinus* has a bluish violet background whereas *P. bolool* is grey, and by their marginal folds, which are broader in *P. velutinus* and more subtly defined in *P. bolool*. The specimen found in the Gulf of Mexico matches the original description of *P. bolool*. This species has been previously reported from the Australasian region (Newman and Cannon 1994, 1998) and the Indomalayan region (Dixit et al. 2021). Prior to this study, *P. bolool* was cited in Florida by Rawlinson (2008).

***Pseudoceros juani* Bahia, Padula, Lavrado & Quiroga, 2014**

Fig. 11

**Material examined.** Campeche coast, MEXICO • 1; Cayo Arcas; 20.2°N, 92.0°W; 5 m; 26 Apr. 2018; A. Hernández leg.; CRPPY-0086.

**Distribution.** Cabo Frío, Brazil (Bahia et al. 2014). First record for the Gulf of Mexico (Campeche, Mexico).

**Description.** Elongated and elliptical body, 1.5 cm in length and 0.5 cm in width (Fig. 11A). Margin slightly wavy. Dorsal surface brick-orange with white dots and small black spots (Fig. 11A, B). Translucent whitish marginal band with a yellowish line visible (Fig. 11B). Pseudotentacles brick-orange, short, and as simple folds. Cluster of cerebral eyes horseshoe-shaped. Pseudotentacular eyes present. Two clusters of marginal eyes situated between pseudotentacles. Pharynx ruffled and butterfly-shaped (Fig. 11C).

**Remarks.** Specimens of *Pseudoceros juani* from Brazil show a darker colouration, characterised by more abundant and smaller dots distributed along the middle dorsal line. Additionally, the white marginal band with a yellow line is more conspicuous in the Brazilian exemplar. Disparities in the distribution of

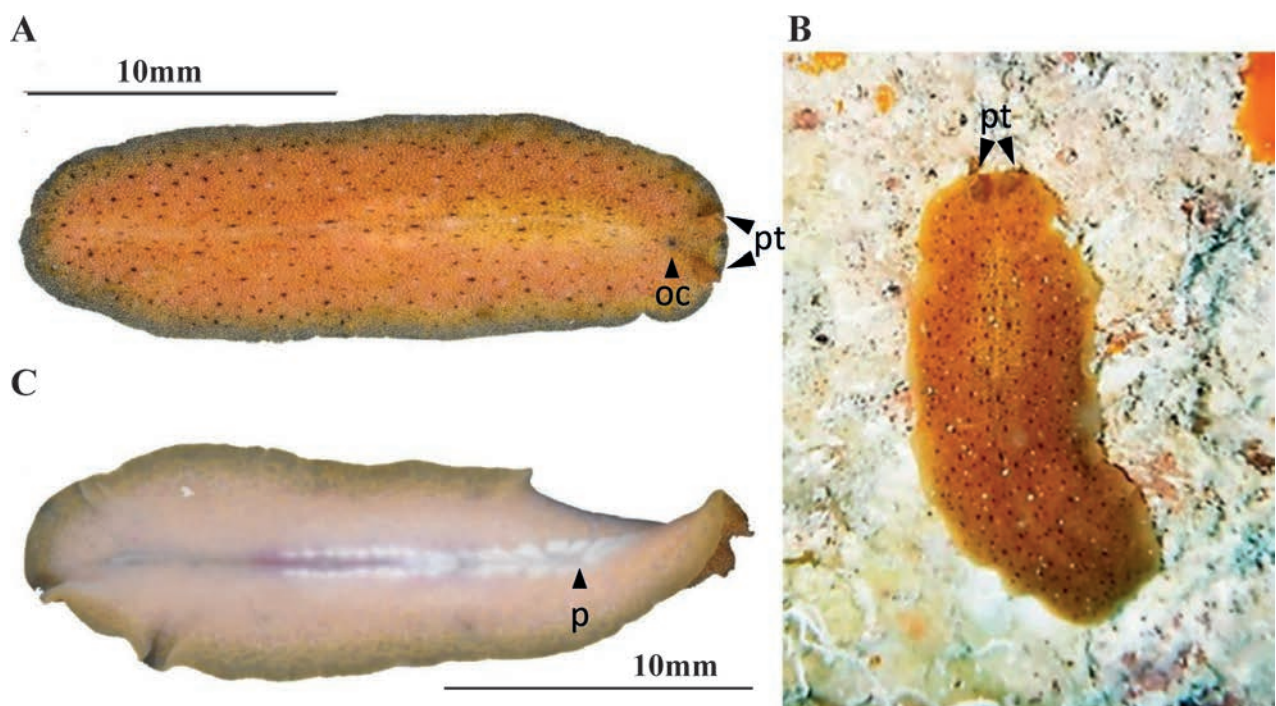


Figure 11. *Pseudoceros juani* A dorsal view B In situ C ventral view.

the dorsal dots and the lighter tones of the final brown band may be attributed to the maturity state of the individuals. Brazilian individuals are longer than those from the Gulf of Mexico.

***Pseudobiceros* Faubel, 1983**

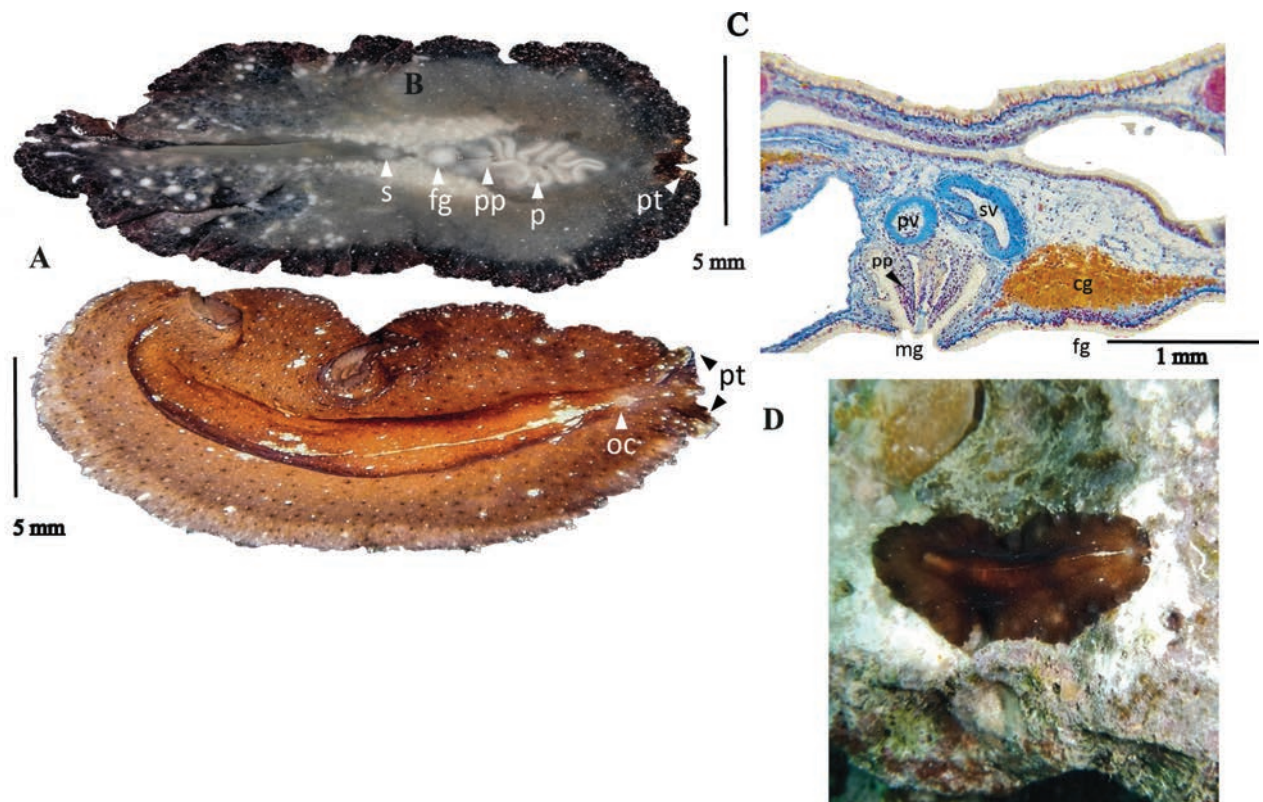
***Pseudobiceros caribbensis* Bolaños, Quiroga & Litvaitis, 2007**

Fig. 12

**Material examined.** Campeche coast, MEXICO • 1; Cayos sumergidos del Oeste; 20.4°N, 92.2°W; 13 m; 14 Sep. 2017; A. Hernández leg.; CRPPY-0014 • 1; Cayos sumergidos del Oeste; 20.4°N, 92.2°W; 10.8 m; 14 Sep. 2017; A. Gutiérrez leg.; CRPPY-0019 • 3; Cayo Arcas; 20.2°N, 92.0°W; 4.1 m; 21 Apr. 2018; A. Hernández leg.; CRPPY-0057 • 1; Cayo Arcas; 20.2°N, 92.0°W; 2.2 m; 21 Apr. 2018; A. Hernández leg.; CRPPY-0058 • 1; Cayo Arcas; 20.2°N, 92.0°W; 9.3 m; 24 Apr. 2018; A. Hernández leg.; CRPPY-0075 • 1; Cayo Arcas; 20.2°N, 92.0°W; 4.4 m; 17 Aug. 2018; A. Hernández leg.; CRPPY-0105.

**Distribution.** Recorded in Curaçao, Jamaica, Florida, and Honduras (Bolaños et al. 2007); Belize (Rawlinson 2008). This is the first record for the Gulf of Mexico (Campeche coast, Mexico).

**Description.** Elongated and elliptical body, 2 cm in length and 1 cm in width, Dorsal background pigmentation caramel-brown with dispersed, darker tonalities. Small white and black spots scattered across entire surface. Median longitudinal thickening traversed with two large white patches, white median



**Figure 12.** *Pseudobiceros caribbensis* **A** dorsal view **B** ventral view **C** sagittal section of the reproduction organs (stained with AZAN) **D** in situ.

line more visible in anterior ½ of body, especially between patches. One patch situated near pharynx in first 1/3 of body, and second in posterior region of body (Fig. 12A, B, D). Ventral surface appears greyish with darker edges and dispersed white spots (Fig. 12B). Multiple marginal folds. Pseudotentacles complex with multiple folds. Cluster of cerebral eyes horseshoe shaped, situated in a pale rounded area. Ruffled pharynx located in first 1/3 of body, with a centred mouth. Two male copulatory openings in middle body region, behind the pharynx, located near female gonopore and sucker (Fig. 12C). Configuration of reproductive system matches that provided in the original description (Bolaños et al. 2007).

***Pseudobiceros splendidus* (Lang, 1884)**

Fig. 13

**Material examined.** Yucatan coast, MEXICO • 1; Bajos de Sisal; 21.2°N, 90.0°W; 1 m; 22 Feb. 2018; A. Hernández leg.; CRPPY-0030.

**Distribution.** Originally described from Naples, Italy (Lang 1884). Recorded in Bermuda, Puerto Rico, Mid Turtle Shoal, Hawk Channel, Florida Keys, and the Atlantic coast of Florida, USA (Lang 1884; Hyman 1939, 1955; Litvaitis et al. 2019); Forte de Itaipú, Santos, São Paulo, Extremoz, Rio Grande de Norte, and Cabo Frío, Rio de Janeiro, Brazil (Marcus 1950; Bahia et al. 2012, 2014); Heron Island and One Tree Island, Great Barrier Reef, Australia; Hawaii, USA; Madang, Papua New Guinea; Rottneest Island, Western Australia; Andaman and Nicobar

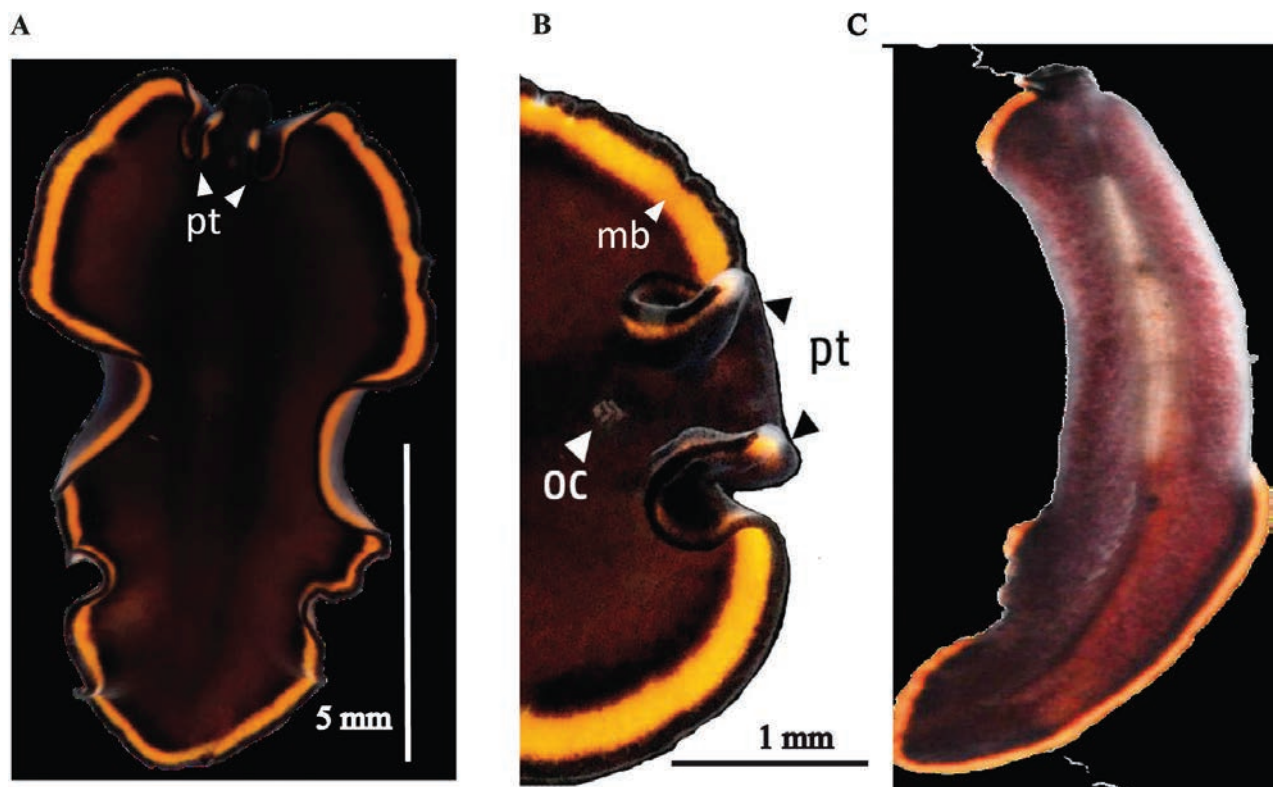


**Figure 13.** *Pseudobiceros splendidus* **A** dorsal view **B** detail of colouration and marginal bands, pseudotentacles, and cluster of cerebral eyes **C** ventral view.

Islands, India; Indonesia; Maldives; South Africa; Singapore (Newman and Cannon 1994, 1997; Marquina et al. 2015; Litvaitis et al. 2019). New records for the Yucatan coast and Gulf of Mexico.

**Description.** Body shape elongated with rounded anterior end and tapered posterior end, 1 cm in length and 0.5 cm in width. Velvety, wine-coloured background with a submarginal orange and marginal black band, interrupted at level of the pseudotentacles (Fig. 13A, C). Cerebral eyes located in a pigmentation-less area (Fig. 13B). Ruffled pharynx in the first 1/3 of the body, with the mouth. Two male copulatory organs are located close to the female gonopore and near the pharynx. Ventral sucker centred in the second corporal 1/3.

**Remarks.** Specimens of *Pseudobiceros splendidus* studied show a colouration pattern similar to the specimens from Florida, illustrated in Litvaitis et al. (2019: fig. 9A). Litvaitis et al. (2019) grouped the closely related and similar species *Pseudobiceros evelinae*, *P. periculosus*, and *P. hymanae* into a single species, *P. splendidus*. This grouping is based on the results obtained through the molecular analyses of 28S and the few morphological differences found between these species (Litvaitis et al. 2019).

**Biology.** The samples were collected under rocks associated with ascidians, possibly the primary food source of this species.

#### ***Pseudobiceros pardalis* (Verrill, 1900)**

Fig. 14

**Material examined.** Quintana Roo coast, MEXICO • 1; Mahahual; 18.6°N, 87.7°W; 5.3 m; 17 Mar. 2018; A. Hernández leg.; CRPPY-0113.

**Distribution.** Original description from Bermuda (Verrill 1900); Bocas del Toro, Panamá, Caribbean Sea (Bolaños et al. 2007; Marcus 1950); Rio de Janeiro and Alagoas, Brazil (Bahia et al. 2012, 2014, 2015). New record for the coast of Quintana Roo (Mexican Caribbean).

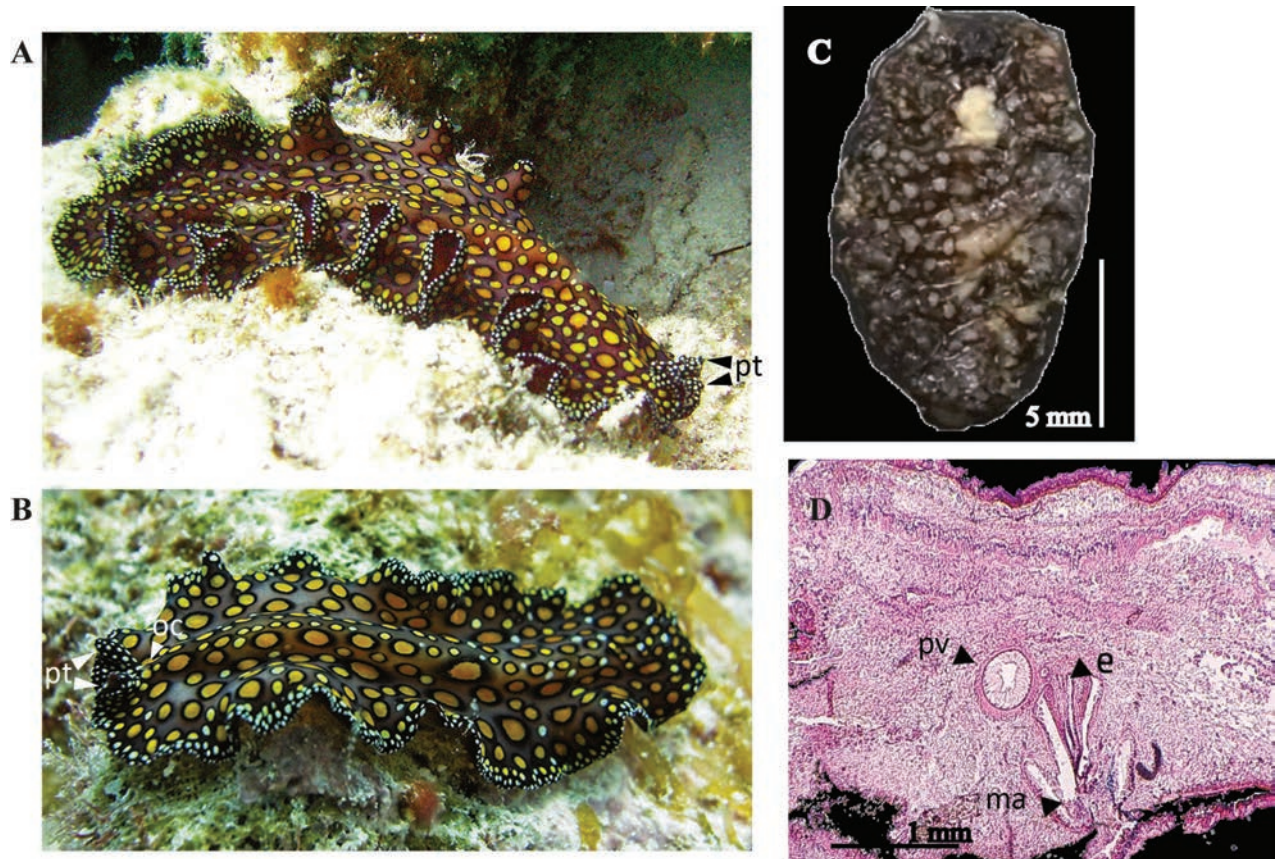
**Description.** Body shape elongated with rounded anterior and tapering posteriorly, 1.3 cm in length and 0.7 cm in width. Body margins slightly wavy. Purple-brown background, darker at the margins, with yellow and orange spots outlined by a black circle, and tiny white spots along the entire body margin (Fig. 14A, B, C). Ventral surface characterised by a light purple shade, more translucent towards the margin. Two external and prominent male gonopores, together with the female gonopore located in the ventral midline (Fig. 14D). Additionally, a ventral sucker is present, situated in the centre of the body.

#### ***Phrikoceros* Newman & Cannon, 1996**

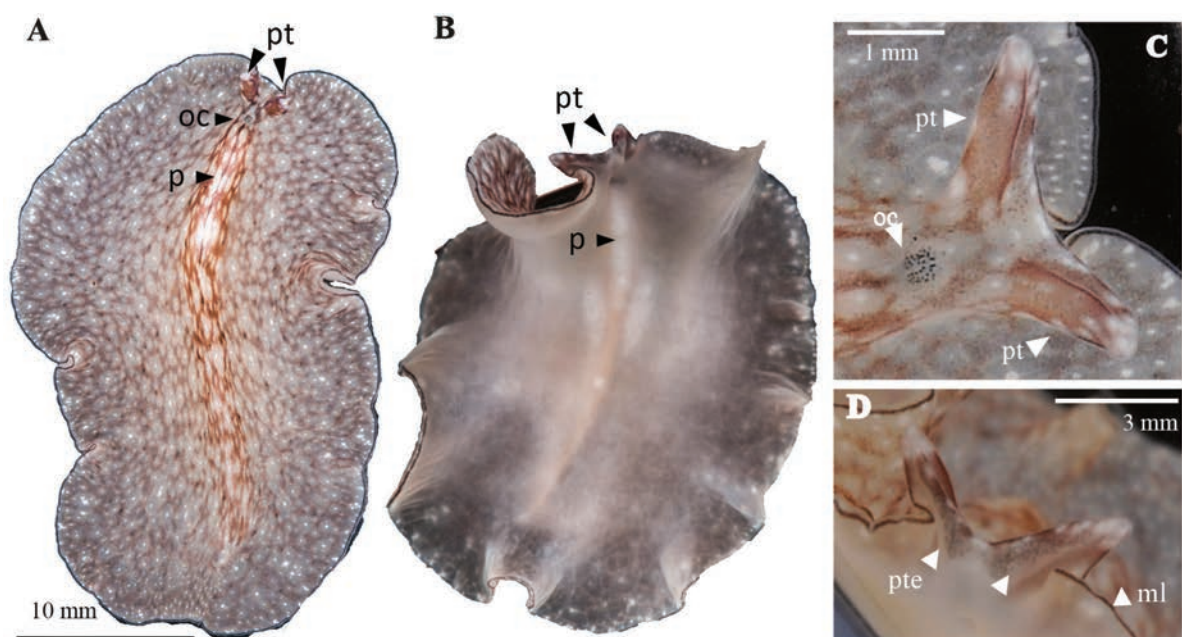
##### ***Phrikoceros mopsus* (Marcus, 1952)**

Fig. 15

**Material examined.** Campeche coast, MEXICO • 1; Cayos sumergidos del Oeste; 20.4°N, 92.2°W; 13 m; 14 Sep. 2017; A. Gutiérrez leg.; CRPPY-0021; **Quintana Roo coast, MEXICO** • 1; Mahahual; 18.6°N, 87.7°W; 13.6 m; 18 Mar. 2018; A. Hernández leg.; CRPPY-0043.



**Figure 14.** *Pseudobiceros pardalis* **A, B** photographs by Christine Loew and Matteo Cassela in Playa del Carmen (Mexico) **C** Specimen preserved for museum collections **D** sagittal section of the male reproductive system, prostatic vesicle stylet, male atrium (hematoxylin-eosin stain).



**Figure 15.** *Phrikoceros mopsus* **A** dorsal view **B** ventral view **C** detail of the pseudotentacles and cerebral **D** marginal line and pseudotentacular eyes.

**Distribution.** *Phrikoceros mopsus* was originally described in São Paulo, south-eastern Brazil (Marcus 1952). Later it was recorded in Antigua and Barbuda, Curaçao (Marcus and Marcus 1968); Argentina (Brusa et al. 2009; Bulnes et al. 2011); Brazil (Bahia et al. 2012, 2014, 2017; Bahia and Schrödl 2018); Colombia (Quiroga et al. 2004a); India (Sreeraj and Raghunathan 2015). This is the first record for the Campeche coast and Quintana Roo (Mexican Caribbean). New record for the Gulf of Mexico.

**Description.** Body shape oval and elongated, with an extremely delicate consistency and a wavy margin, 3 cm in length and 1.5 cm in width. Marginal pseudotentacles deeply folded. Dorsally, with the characteristic small white spots on a caramel brown background, body midline darker. Marginal black rim, interrupted in the distal region of the pseudotentacles. (Fig. 15A, B). Two cerebral eyes clusters horseshoe-shaped and slightly separated. Pseudotentacular eyes grouped in two clusters placed ventrally and dorsally (Fig. 15C, D). Ventral surface beige (Fig. 15B). Ruffled pharynx and oral opening in the first 1/3 of the body, close to male and female gonopores. Ventral sucker in the middle of the body (Fig. 15B).

### ***Thysanozoon* Grube, 1840**

#### ***Thysanozoon brocchii* (Risso, 1818)**

Fig. 16

**Material examined.** Campeche coast, MEXICO • 1; Cayo Arcas; 20.2°N, 92.0°W; 6.3 m; 22 Apr. 2018; A. Hernández leg.; CRPPY-0068 • 1; Cayo Arcas; 20.2°N, 92.0°W; 13.2 m; 24 Apr. 2018; A. Hernández leg.; CRPPY-0076.

**Distribution.** The species was described from Naples, Italy (Risso 1818). It is considered a cosmopolitan species, reported in the Mediterranean Sea, the United Kingdom, and southern and western Africa. In the western Atlantic, *Thysanozoon brocchii* has been recorded in the Gulf of Mexico (Hyman 1952; Marcus and Marcus 1968); Caribbean coast of Colombia (Quiroga et al. 2004a, 2004b); Brazil (Bahia et al. 2014, 2015, 2017; Bahia and Schrödl 2018); Canary Islands (De Vera et al. 2009); Argentina (Brusa et al. 2009). In the Pacific it has been recorded in Japan and New Zealand (Prudhoe 1985). The record for Cayo Arcas, Campeche, represents the first record for Mexico.

**Description.** Body oval-shaped and firm consistency, 1.5 cm in length and 0.5 cm in width. Background colour ranges from brown to yellowish-ochre. Two stripes of paler cream spots, one longitudinally and the other perpendicular, form an inverted cross (Fig. 16A, B). The dorsal surface is covered with characteristic papillae, decreasing in size towards the margin. Pseudotentacles complex with multiple folds (Fig. 16D). Ruffled pharynx located in the first 1/3 of the body, with the oral opening in the middle. Two male copulatory apparatus and positioned close to the female organ in the ventral central region of the body. Sucker at the beginning of the second 1/2 of the body (Fig. 16C).

**Remarks.** *Thysanozoon brocchii* is noted for the abundance of papillae covering its dorsal surface and its cosmopolitan distribution. Various morphological descriptions with distinct colour patterns occur for different localities (Bahia et al. 2014). Molecular analysis of the different populations of this species is needed to identify potential divergences among the cited locations.

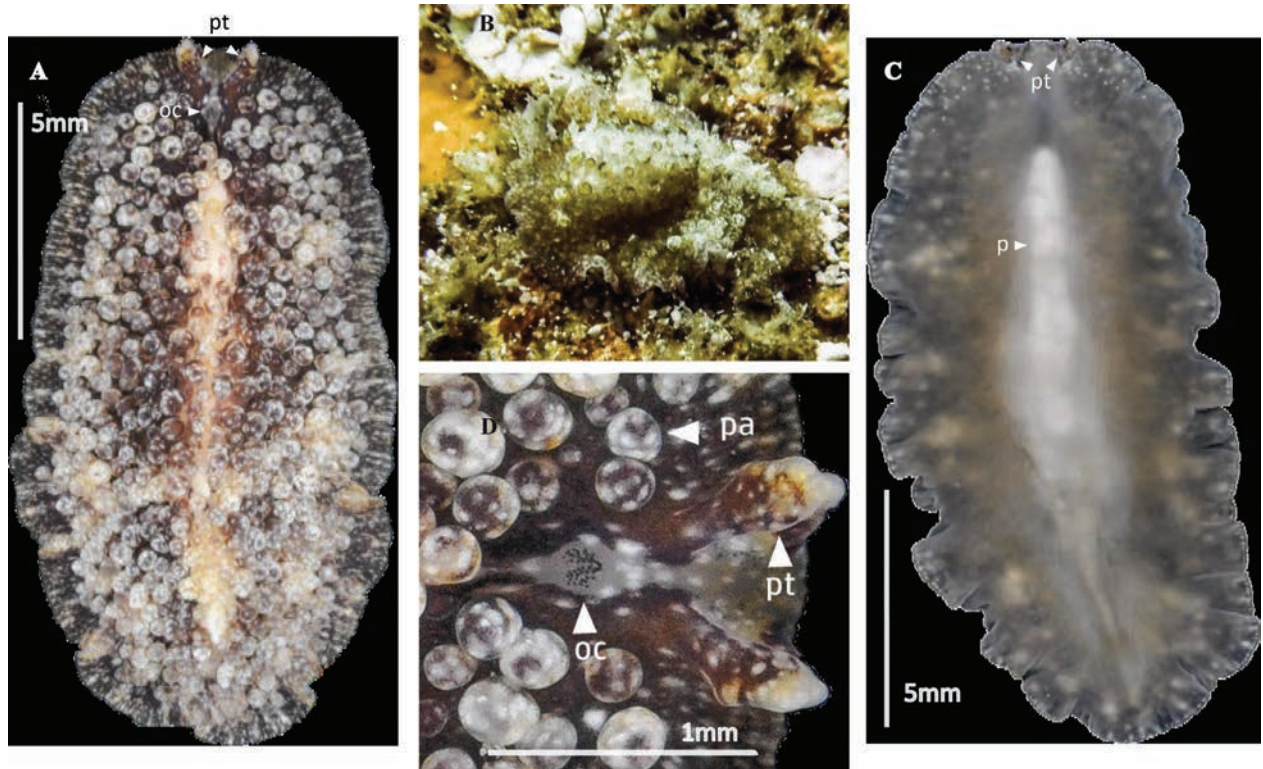


**Figure 16.** *Thysanozoon brocchii* **A** dorsal view **B** In situ **C** ventral view **D** detail of the dorsal surface; papillae, cerebral eyes, and pseudotentacles.

#### Suborder Acotylea

**Discoceloidea** Dittmann, Cuadrado, Aguado, Noreña, & Egger, 2019

**Cryptocelididae** Laidlaw, 1903

***Phaenocelis*** Stummer-Traunfels, 1933

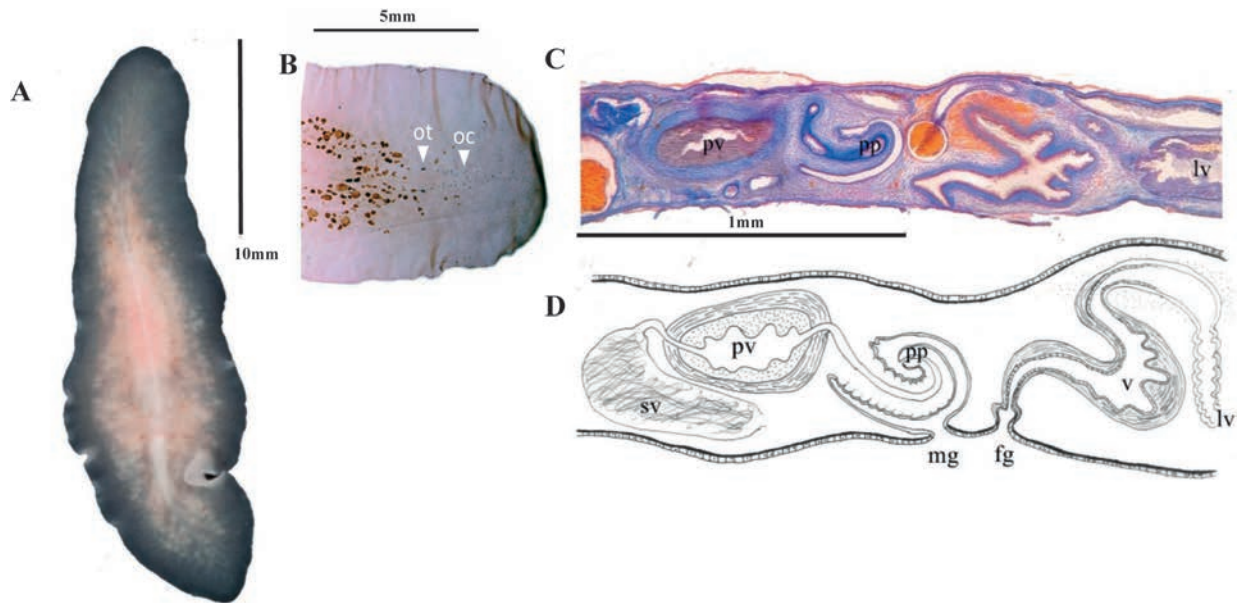
***Phaenocelis medvedica*** Marcus, 1952

Fig. 17

**Material examined.** Campeche coast, MEXICO • 1; Cayo Arcas; 20.2°N, 92.0°W; 6.2 m; 20 Aug. 2018; A. Hernández leg.; CRPPY-0109 • 1; Cayo Arcas; 20.2°N, 92.0°W; 3.3 m; 20 Aug. 2018; A. Hernández leg.; CRPPY-0112.

**Distribution.** *Phaenocelis medvedica* was recorded in Brazil (Marcus 1952; Bahia et al. 2015; Bahia and Schrödl 2018); Caribbean coast of Colombia (Quiroga et al. 2004a, 2004b). New record for the Campeche coast and Gulf of Mexico.

**Description.** Body shape elongated with rounded anterior end and pointed posterior end, 0.45 cm in length and 0.2 cm in width. Translucent pinkish colouration, including two longitudinal dark brown rows parallel to the main body's axis (Fig. 17A). Two elongated clusters of cerebral eyes and two small groups of tentacular eyes sparsely distributed. Small marginal eyes along the entire body margin. (Fig. 17B). Pharynx central, occupies 1/3 of the body size. Male and female reproductive organs located in the second 1/2 of the body with the morphological features of *P. medvedica*. **Reproductive system.** The male reproductive system consists of a large and muscular interpolated prostatic vesicle, a slightly muscular seminal vesicle, and a large, coiled cirrus. Female copulatory organ with a bulbous vagina and large Lang's vesicle (Fig. 17C, D).



**Figure 17.** *Phaenocelis medvedica* **A** dorsal view **B** detail of the marginal, cerebral and tentacular ocelli **C** sagittal section of the reproductive system **D** sagittal reconstruction of male and female apparatus.

***Phaenocelis peleca* Marcus & Marcus, 1968**

Fig. 18

**Material examined.** Campeche coast, MEXICO • 2; Cayo Arcas; 20.2°N, 92.0°W; 2.2 m; 20 Apr. 2018; A. Hernández leg.; CRPPY-0053 • 1; Cayo Arcas; 20.2°N, 92.0°W; 9.3 m; 24 Apr. 2018; A. Hernández leg.; CRPPY-0077.

**Distribution.** Piscadera Bay, Curaçao, Caribbean Sea (Marcus and Marcus 1968). New record from the Campeche coast and Gulf of Mexico.

**Description.** Body shape oval and tapers in the posterior region, 4 cm in length, 2 cm in width. Compact consistency. Milky-translucent colouration, with translucent margin (Fig. 18A, C). Intestinal branches visible through transparency. Well-differentiated tentacular eyes; cerebral eyes in scattered, elongated clusters; abundant marginal eyes along the entire body margin (Fig. 18B). Pharynx ruffled, elongated and narrow. Male and female gonopores close to the oral pore. **Reproductive system.** Male reproductive system (Fig. 18D, E) consists of a short, curved penis papilla, an elongated prostatic vesicle, and a short seminal vesicle with distally broad seminal ducts. Female reproductive system, poorly developed in the studied specimens (Fig. 18D, E), consists of an elongated vagina externa, surrounded by cement cells, a vagina interna and Lang’s vesicle.

**Remarks.** The specimen of the Gulf of Mexico aligns with the description of *Phaenocelis peleca* provided by Marcus and Marcus (1968). Nonetheless, Mexican *P. peleca* specimens are larger than Caribbean ones (4 cm vs 2 cm), but present a short penis papilla compared to that given in the original description. Female apparatus differences are also observed, with the Cayo Arcas *P. peleca* having an elongated Lang’s vesicle compared to the round one in Caribbean individuals. These differences may be due to specimen size and maturity.

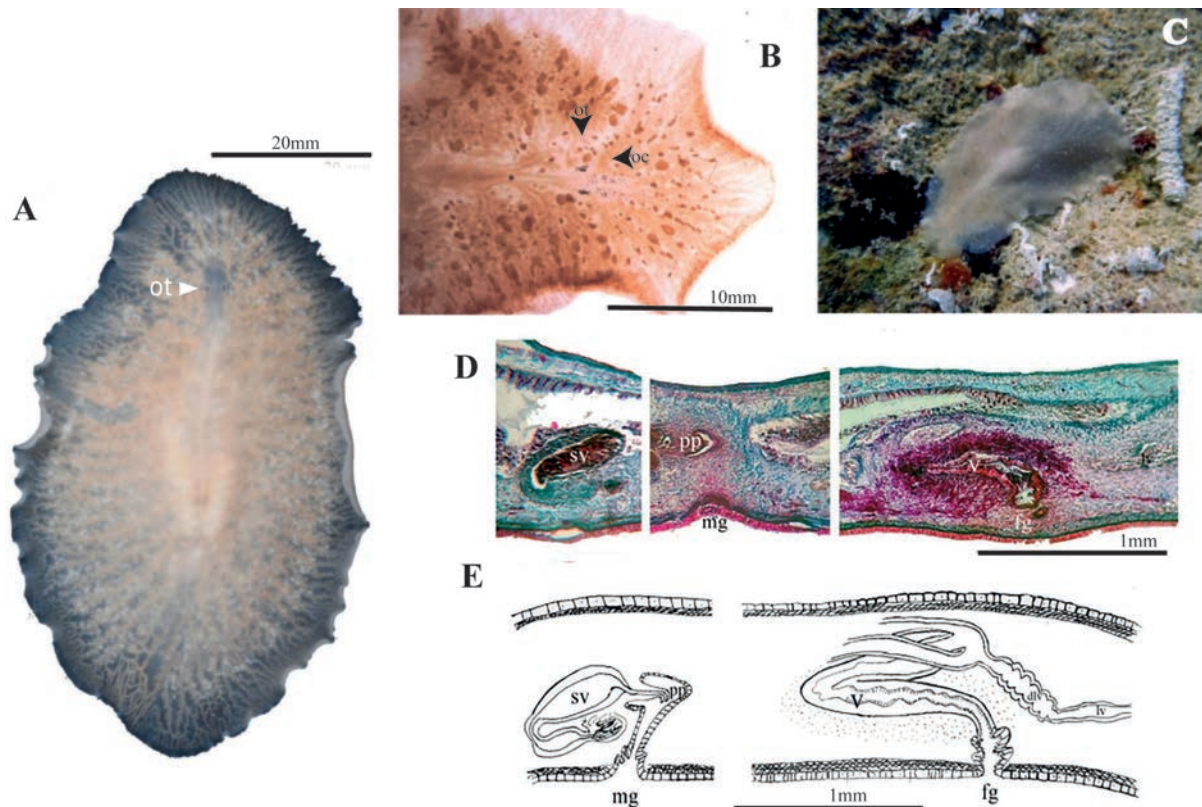


**Figure 18.** *Phaenocelis peleca* **A** live animal photographed on black background **B** anterior end with tentacular eyes and cerebral eyes **C** in situ **D** sagittal section of the reproductive system **E** sagittal reconstruction of male and female copulatory organs.

**Leptoplanoidea** Faubel, 1984  
**Stylochoplanidae** Faubel, 1983  
***Stylochoplana*** Stimpson, 1857

***Stylochoplana sisalensis* sp. nov.**

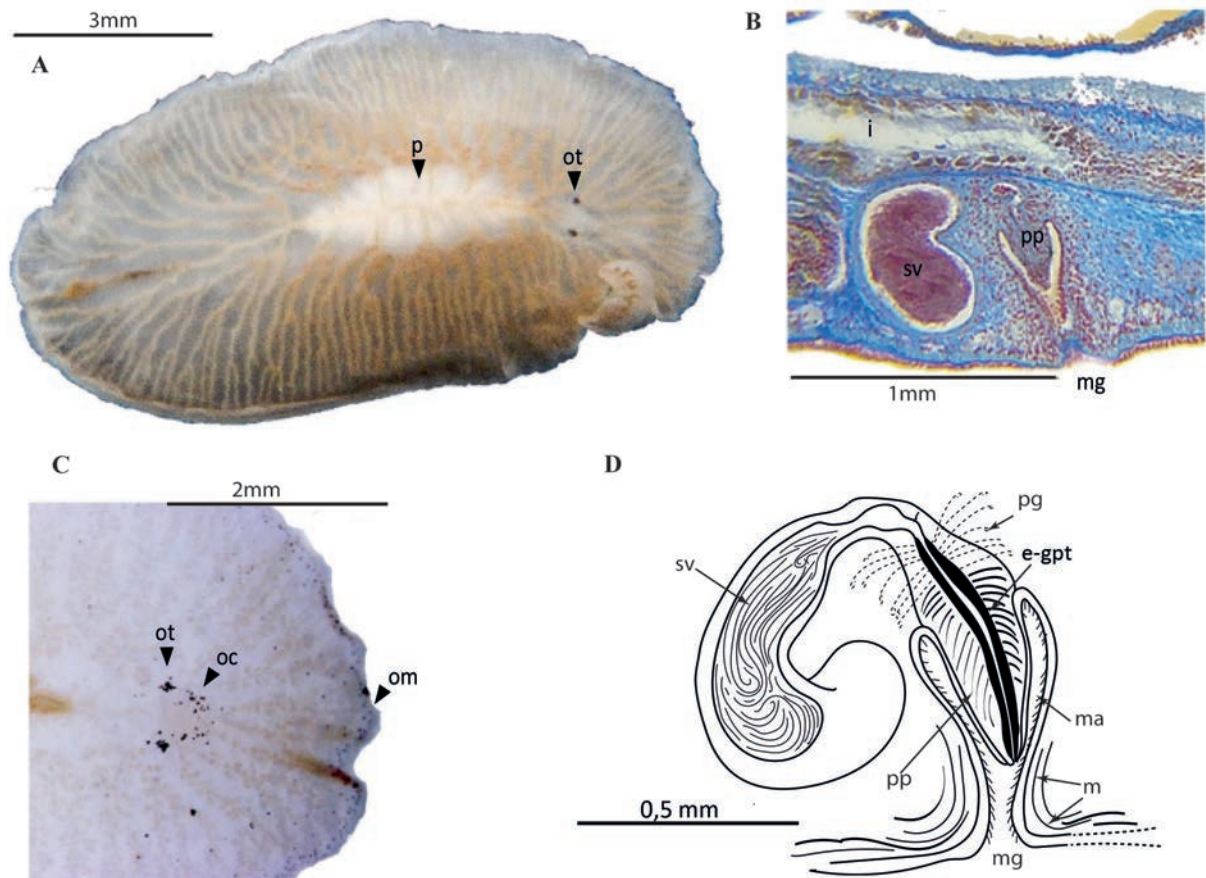
<https://zoobank.org/962C25B2-2F1B-4A9F-8897-B458D326398A>

Fig. 19

**Material examined. Holotype:** Campeche coast, MEXICO • 1; 9 slides; Cayos sumergidos del Oeste; 20.4°N, 92.2°W; 0 m; 11 Sep. 2017; A. Hernández leg.; CRPPY-0013. **Paratypes:** Campeche coast, MEXICO • 1; Cayo Arcas; 20.2°N, 92.0°W; 6.2 m; 20 Aug. 2018; A. Hernández leg.; CRPPY-0110 • 1; Cayo Arcas; 20.2°N, 92.0°W; 3.3 m; 20 Aug. 2018; A. Hernández leg.; CRPPY-0111.

**Distribution.** Found in submerged West Keys of Reef Triángulos and Cayo Arcas, Campeche coast, Mexico.

**Description.** Body shape oval with rounded anterior and posterior end, 10 mm long and 5 mm wide. Whitish translucent colour with a pale brown tonality due to the gut contents. A network of independent intestinal branches, not anastomosing, extends to the body's margin (Fig. 19A). Presence of two compact clusters tentacular eyes (12–17 eyes per cluster), two scattered clusters of cerebral eyes (15–20 eyes per cluster, distributed within 0.03 mm in front of the tentacular eyes) and some marginal eyes in the frontal region (Fig. 19B). Ruffled pharynx located in the second 1/3 of the body.



**Figure 19.** *Stylochoplana sisalensis* sp. nov. **A** dorsal view **B** sagittal section of a male copulatory organ without a prostatic vesicle, only showing a penis papilla **C** anterior end with cerebral and marginal eyes **D** sagittal reconstruction of the reproductive system.

**Reproductive system.** Testes dorsal and ovaries ventral. Seminal vesicle well developed, elongated and wide surrounded by thin muscular walls. The ejaculatory duct runs upward, backward, and then curves downward before widening as it enters the penis papilla. Lining of walls of this internal dilation forms epithelial glandular prostate tissue which functions as a prostatic vesicle. The glandular prostate epithelium stores the secretion from the extra-vesicular glands (Fig. 19B, D). Conical, naked penis papilla (without a stylet) covered by a non-ciliated, flat epithelium. It projects into a deep male atrium, with a tall ciliated epithelium (Fig. 19C). The female copulatory organ was barely developed in the only specimen observed, so it could not be described in detail.

**Etymology.** The name *sisalensis* is dedicated to the town where the research centre is located, the UNAM campus in Sisal, Yucatán province, Mexico.

**Remarks.** Currently, the genus *Stylochoplana* comprises 25 valid species worldwide. This genus is one of the most species-rich within the order Polycladida and has been divided into different informal groups by several authors (Bock 1913; Marcus and Marcus 1968) since it was described by Stimpson (1857). *Stylochoplana sisalensis* is included in group B of Bock (1913) or B1 of Marcus and Marcus (1968), characterised by tentacles absent, unarmed papilla peneal, absence of penial pocket, and Lang's vesicle present. This group includes the following species:

- *S. chilensis* (Schmarda, 1859): with epithelial-glandular prostate tissue (Stummer-Traunfels 1933).
- *S. chloranota* (Boone, 1929): with interpolated prostatic vesicle (Hyman 1953).
- *S. graffi* (Laidlaw, 1906): with interpolated prostatic vesicle (Bock 1913).
- *S. longipenis* Hyman, 1953: with interpolated prostatic vesicle.
- *S. minuta* Hyman, 1959: with epithelial-glandular prostate tissue, but forms a receptacle or container in the proximal region of the papilla peneal.
- *S. nadiae* (Melouk, 1941): without data.
- *S. suosensis* Kato, 1943: with epithelial-glandular prostate tissue. The female apparatus is not known, and so it is unknown whether the species belongs to B1 (with Lang's vesicle) or B2 (without Lang's vesicle).
- *S. utunomii* Kato, 1943: with epithelial-glandular prostate tissue.
- *S. walsergia* Marcus & Marcus, 1968 (no. 12): with epithelial-glandular prostate tissue.

*Stylochoplana sisalensis* sp. nov. presents the greatest similarity with *S. walsergia* from Brazil, *S. chilensis* from Chile, *S. utunomii* from Japan, and *S. minuta* from the Palau Islands (Micronesia). These species are all characterised by the presence of a well-developed and elongated seminal vesicle, as well as an ejaculatory duct that widens and is covered by a prostatic glandular epithelium. All other species in this group present an isolated, more or less elongated and interpolated prostatic vesicle.

On the other hand, the species of Marcus' Group B1 present a very similar female copulatory apparatus directed towards the anterior region and, at the level of the internal vagina, then curving towards the posterior region. In the middle of the female duct, the oviduct opens and the internal epithelium thickens to form Lang's duct that ends in the rounded Lang's vesicle.

*Stylochoplana sisalensis* differs from *S. walsergia* by the location of the prostate tissue and the shape of the penis papilla. In *S. walsergia*, the prostatic dilation is included entirely in the penis papilla and surrounded by the male atrium, while in *S. sisalensis* the penis papilla encloses only 1/2 of the prostatic tissue and the common male duct. This characteristic is shared by *S. chilensis*, but not with *S. utunomii* in which the prostate tissue is practically outside the penis papilla, a short protrusion within the male atrium. As in *S. suosensis*, we lack data on the female apparatus, but we assume that its arrangement is like that of the entire Marcus group B of *Stylochoplana*.

### ***Emprostopharynx* Bock, 1913**

#### ***Emprostopharynx hartei* sp. nov.**

<https://zoobank.org/0E7C472E-3BC9-4326-916A-CF91C641F5D1>

Fig. 20

**Material examined. Holotype:** Yucatan coast, MEXICO • 1; 18 Slides; Dzilam; 21.5°N, 88.9°W; 13 m; 10 May 2018; A. Hernández leg.; CRPPY-0095. **Paratypes:** Yucatan coast, MEXICO • 4; Dzilam; 21.5°N, 88.9°W; 14 m; 9 May 2018; A. Hernández leg.; CRPPY-0092 • 3; Dzilam; 21.5°N, 88.9°W; 14 m; 9 May 2018; A. Hernández leg.; CRPPY-0093.

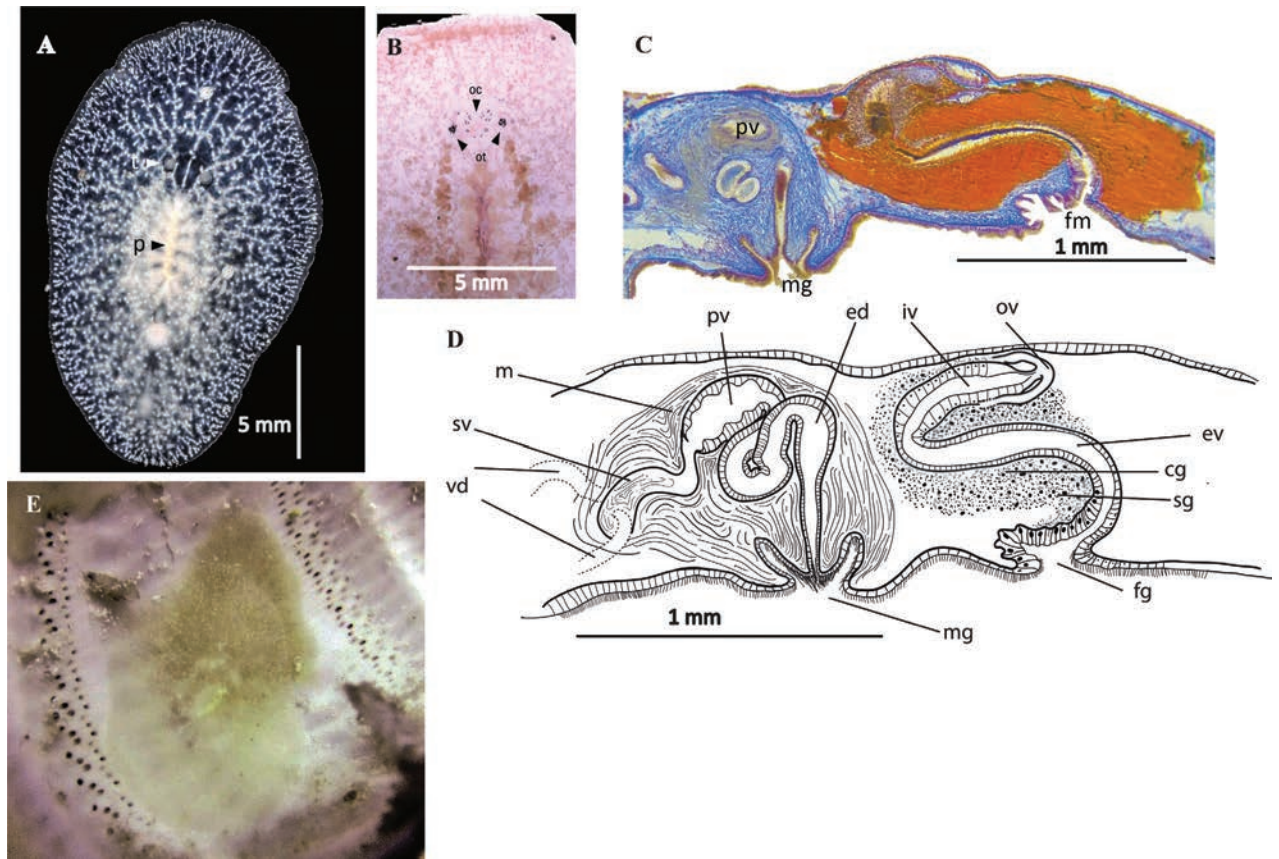


**Figure 20.** *Emprostopharynx hartei* sp. nov. **A** photographed on a black background, where the intestinal branches and pharynx are patent **B** anterior end with tentacular eyes and cerebral eyes **C** histological sagittal section (Azan stained) at the level of the reproductive system **D** sagittal reconstruction of the reproductive system **E** specimen in situ, showing natural colouration. Abbreviations: ot tentacular eyes, oc cerebral eyes

**Distribution.** Dzilam de Bravo, Yucatan, Mexico.

**Description.** Body shape elliptical, 10 mm length and 7 mm width. Body constitution solid with a translucent background (Fig. 20A). Conspicuous whitish intestinal branches extend towards margins. Body periphery with a white dotted line. Nuchal tentacles rounded and prominent, with 20–30 eyes per tentacle. Two small clusters of cerebral eyes close to the tentacles are, 12–20 eyes per cluster (Fig. 20B). Ruffled pharynx centrally positioned. Oral pore located at pharynx centre. Dorsal pore dorsally in the last body 1/3, visible when examined in vivo (Fig. 20A, E). **Reproductive system.** Male and female copulatory apparatus situated posterior to the pharynx, in the second 1/2 of the body. Male copulatory organ immersed in a muscular bulb: the seminal vesicle, prostatic vesicle, ejaculatory duct, and an elongated penis papilla covered with long cilia with a sclerotised appearance. Elongated seminal vesicle receives the vasa differentia separately at its proximal end. Distally the seminal vesicle connects to the prostatic vesicle through a narrow duct. Prostatic vesicle lined with a thick wavy epithelium and extending into a long duct that surrounds the ejaculatory duct. The ejaculatory duct is ciliated and discharges in the penis papilla. A narrow and shallow male atrium houses the penis papilla (Fig. 20C, D). Female reproductive system characterised by a short, wide, muscular atrium covered by a well-developed ciliated epithelium. A narrow tubular vagina externa leads from the atrium towards the wider vagina interna, lined with glandular epithe-

lium. At its distal end, the vagina interna divides into two oviducts that turn towards the anterior region. Both sections of the vagina, but especially the vagina interna, are surrounded by dense masses of cement and shell glands. Lang's vesicle is absent (Fig. 20C, D).

**Etymology.** The species name *hartei* is dedicated to the conservationist Edward H. Harte, in recognition of his lifelong commitment to environmental conservation and his significant contributions to marine science and the protection of marine ecosystems.

**Remarks.** Currently, the genus *Emprostopharynx* is composed of nine species: *E. gracilis* (Heath & McGregor, 1912); *E. hancocki* (Hyman, 1953); *E. heroniensis* Beveridge, 2018; *E. lysiosquillae* Oya, Nakajima & Kajihara, 2022; *E. opisthoporus* Bock, 1913; *E. pallida* (Quatrefage, 1845); *E. vanhoeffeni* Bock, 1931; *E. onubensis* Pérez-García, Gouveia, Calado, Noreña & Cervera, 2024; and *E. rasae* Prudhoe, 1968. The genus is distributed mainly within the Pacific Ocean, except for *E. pallida* and *E. onubensis*, which are native to the Mediterranean, and *E. vanhoeffeni* found in the Cape Verde Islands (Bock 1931) and Morocco (Prudhoe 1985). *Emprostopharynx hartei* sp. nov. lacks marginal eyes as do *E. pallida*, *E. onubensis*, *E. hancocki*, *E. gracilis*, and *E. heroniensis*. Still, it can be distinguished from the other *Emprostopharynx* species by the presence of tentacles, which *E. hartei* shares only with *E. hancocki* and *E. gracilis* (Pérez-García et al. 2024).

Regarding the internal characteristics between *Emprostopharynx hartei* and *E. hancocki*, in both species, the distal region of the papilla peneal is covered by a series of bristles, thickened, or with pseudosclerotised cilia (the styliform development of the basal membrane mentioned by Faubel 1983, 1984). This pseudosclerotised formation differentiates these two species from the other species of *Emprostopharynx*, which either present a true stylet (*E. vanhoeffeni* and *E. lysiosquillae*) or show a naked papilla peneal, without hard structures (*E. heronensis*, *E. gracilis*, *E. onubensis*, *E. opisthoporus*, *E. pallidus*, and *E. rasae*).

The main difference between *Emprostopharynx hancocki* and *E. hartei* is found at the level of the arrangement and shape of the reproductive system. The seminal vesicle and the prostatic vesicle in *E. hancocki* barely present a small constriction between one organ and another, while in *E. hartei* the transition between the seminal vesicle and the prostatic vesicle is marked by a tube-like narrowing. In addition, the prostatic vesicle in *E. hartei* empties through an elongated sinuous extension until the papilla peneal.

The distinction between *Emprostopharynx gracilis* and *E. hartei* lies in the structural and morphological characteristics of the distal region of the male copulatory apparatus. *Emprostopharynx hartei* has an elongated prostatic vesicle that leads to a long ejaculatory duct. The duct ends in a papilla peneal surrounded by a flattened atrium. In contrast, *E. gracilis* is characterised by a rounded prostatic vesicle and a short and robust papilla peneal that opens into a long and deep atrium. Within the female reproductive system, we can observe differences between *E. hartei* and *E. gracilis*. For instance, the female atrium in *E. hartei* is elongated and narrow, whereas in *E. gracilis* it is short and widened. Additionally, the thickening of the vagina is distinct in the two species: in *E. hartei*, the thickening is located in the proximal region, while in *E. gracilis* it is found in the distal region.

**Notoplanidae Marcus & Marcus, 1966**  
***Notoplana* Laidlaw, 1903**

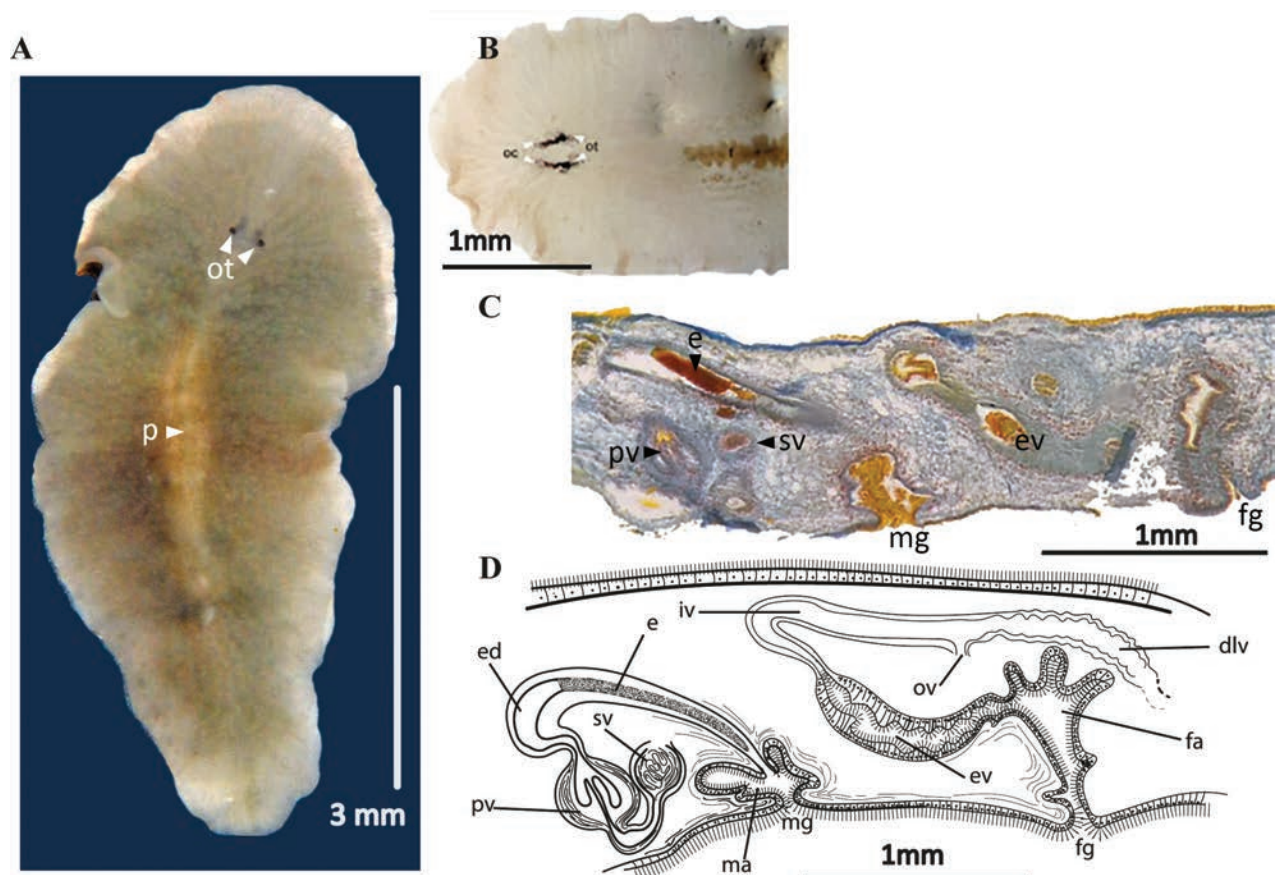
***Notoplana annula* Marcus & Marcus, 1968**

Fig. 21

**Material examined.** Campeche coast, MEXICO • 5; Cayos sumergidos del Oeste; 20.4°N, 92.2°W; 5 m; 10 Sep. 2017; A. Hernández leg.; CRPPY-0009 • 8; Cayos sumergidos del Oeste; 20.4°N, 92.2°W; 0 m; 10 Sep. 2017; A. Gutiérrez leg.; CRPPY-0010 • 1; Cayos sumergidos del Oeste; 20.4°N, 92.2°W; 0 m; 11 Sep. 2017; A. Hernández leg.; CRPPY-0012 • 5; Cayos sumergidos del Oeste; 20.4°N, 92.2°W; 11 m; 11 Sep. 2017; A. Gutiérrez leg.; CRPPY-0016 • 2; Cayos sumergidos del Oeste; 20.4°N, 92.2°W; 13 m; 14 Sep. 2017; A. Gutiérrez leg.; CRPPY-0017 • 1; Cayos sumergidos del Oeste; 20.4°N, 92.2°W; 13 m; 14 Sep. 2017; A. Gutiérrez leg.; CRPPY-0023.

**Distribution.** Recorded in Piscadera Bay and Fuik Bay, Curaçao and Virginia Key, Florida (Marcus and Marcus 1968). New record in the Gulf of Mexico: Campeche, Mexico.

**Description.** Body shape elongated and smooth, 0.7 cm in length and 0.3 cm in width. Pigmentation varies from whitish beige to greenish hues. Intestinal extensions well-branched, not anastomosing, extending to body margin, with contents visible due to transparency (Fig. 21A). Tentacular eyes form rounded cluster located in the brain, crossed by two, parallel, elongated clusters of cere-



**Figure 21.** *Notoplana annula* **A** dorsal view **B** detail of cerebral and tentacular eyes **C** histological section of male and female copulatory organs **D** sagittal reconstruction of the reproductive system.

bral eyes. Marginal eyes absent (Fig. 21B). Pharynx elongated, tapering along midsection of body. Male and female gonopores positioned posterior to the pharynx in the second 1/2 of the body.

Heading as above. Male copulatory system comprises an elongated seminal vesicle with two broad sperm ducts proximally (Fig. 21C, D). Prostatic vesicle interpolated, connected via a narrowing to the ejaculatory duct and the penis papilla. Ejaculatory duct with thin, long, curved stylet covered with a penial sheath. Atrium wide proximally and tubular distally. Female apparatus comprises a wide, densely ciliated female antrum, a ciliated external vagina with a sinuous course, the internal vagina, and Lang's vesicle. Cement glands open into the vagina externa and oviducts into the vagina interna (Fig. 21C, D).

**Notocomplanidae Litvaitis, Bolaños & Quiroga, 2019**

***Notocomplana* Faubel, 1983**

***Notocomplana ferruginea* (Schmarda, 1859)**

Fig. 22

**Material examined.** Yucatan coast, MEXICO • 1; Arrecife Alacranes; 22.4°N, 89.7°W; 1 m; 4 Nov. 2017; A. Hernández leg.; CRPPY-0004; Veracruz coast, MEXICO • 6; Veracruz; 19.2°N, 96.1°W; 1 m; 31 Sep. 2018; A. Hernández leg.; CRPPY-0101 • 7; Veracruz; 19.2°N, 96.1°W; 2 m; 1 Sep. 2018; A. Hernández leg.; CRPPY-0103.

**Distribution.** The species was described from Jamaica (Schmarda 1859); Colombia, Antilles, and Bahamas (Hyman 1955; Marcus and Marcus 1968;

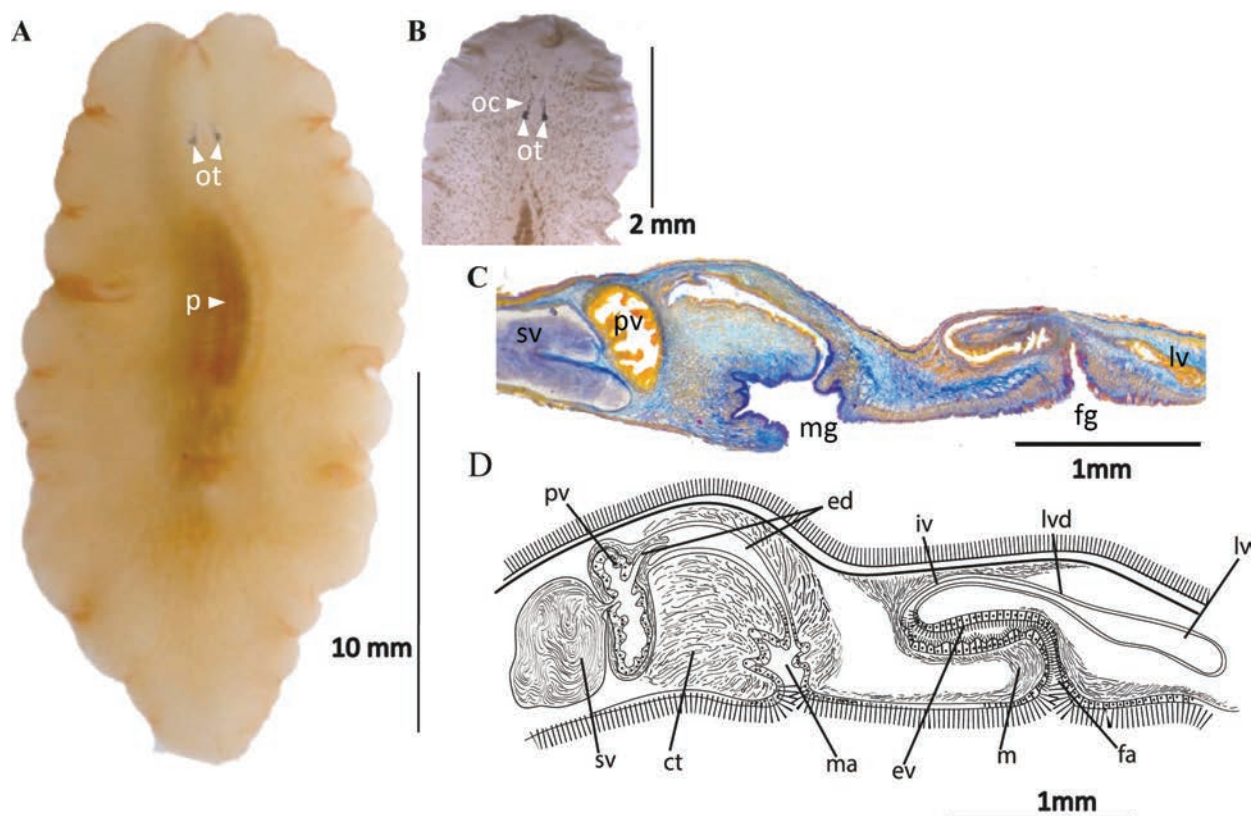


**Figure 22.** *Notocomplana ferruginea* **A** dorsal view **B** approach to the tentacular, cerebral and ruffled pharynx **C** sagittal section of the reproductive system **D** sagittal reconstruction of male and female apparatus.

Quiroga et al. 2004a, 2004b). New record for the coasts of Veracruz and Yucatán. New record for the Gulf of Mexico.

**Description.** Body shape oval with rounded anterior and tapered posterior end, margins pale, wavy, 2.5 cm in length and 1 cm in width. Translucent beige colouration, darker in the middle region of the pharynx (Fig. 22A). Two groups of well-defined cerebral and tentacular eyes (Fig. 23B). No marginal eyes. A short stylet is present. Prostatic vesicle interpolated. Male atrium very muscular. An elongated atrium, a muscular vagina externa and interna as well as Lang's vesicle form the female copulatory apparatus (Fig. 22C, D).

**Remarks.** Research conducted by Oya and Kajihara (2017) and Litvaitis et al. (2019) has led to the transfer of species within *Melloplana*, a genus belonging to the family Pleioplanidae, to the genus *Notocomplana* (family Notoplanidae). This transfer is based on analysis of the mitochondrial gene Cox1 (Oya and Kajihara 2017) and the nuclear gene 28S (Litvaitis et al. 2019). Only a few morphological differences between *Melloplana* and *Notocomplana* have been identified. The main distinction lies in the orientation of the prostatic vesicle chambers: *Melloplana* prostatic chambers are perpendicular to the intra-vesicular ejaculatory duct, whereas *Notocomplana* chambers are longitudinally arranged (Faubel 1983). However, both *Melloplana* and *Notocomplana* lack a stylet.

Considering the limited morphological variation between the genera and recent molecular analyses, there is a tendency to propose eliminating the genus *Melloplana*, as well as the family Pleioplanidae. However, Pleioplanidae also includes other genera like *Izmira*, *Pleioplana*, and *Laqueusplana*, which are poorly known. Therefore, additional molecular analyses and morphological evidence are necessary to confirm the elimination of the family Pleioplanidae (Dittmann et al. 2019).

## **Gnesiocerotidae Marcus & Marcus, 1966**

### ***Gnesioceros* Diesing, 1862**

#### ***Gnesioceros sargassicola* Mertens, 1832**

Fig. 23A

**Material examined.** Quintana Roo coast, MEXICO • 2; Mahahual; 18.6°N, 87.7°W; 7.7 m; 17 Mar. 2018; A. Hernández leg.; CRPPY-0037.

**Distribution.** Currently, *Gnesioceros sargassicola* is known from Bermuda (Hyman 1939) and Florida to Texas, Gulf of Mexico US coast (Hyman 1954); on *Sargassum* algae, near the west coast of Africa (Moseley 1877); Boa Vista Island, Cape Verde (Laidlaw 1903); Gaira Bay, Colombia (Quiroga 2008); Curaçao, Bonaire, Little Bonaire, (Netherlands Antilles, Caribbean), Saint Barthelemy, France Antilles; Bahia Fosforescente, Puerto Rico; Marine Biological Station, Virginia Key, Florida, USA; Central Atlantic Ocean, Sargasso Sea (Marcus and Marcus 1968). New record for the coasts of Mahahual, Quintana Roo (Mexican Caribbean).

**Description.** Dorsoventrally flattened body, anteriorly widened with a shallow constriction after the tentacles, undulated body margins, and a blunt-tailed posterior end, 0.8 cm in length and 0.3 cm in width. Yellowish grey background colouration with numerous, rounded, orange or brown spots. Narrow elongated pharyngeal pouch with a central oral opening (Fig. 23A).

**Biology.** Associated with *Sargassum* algae.

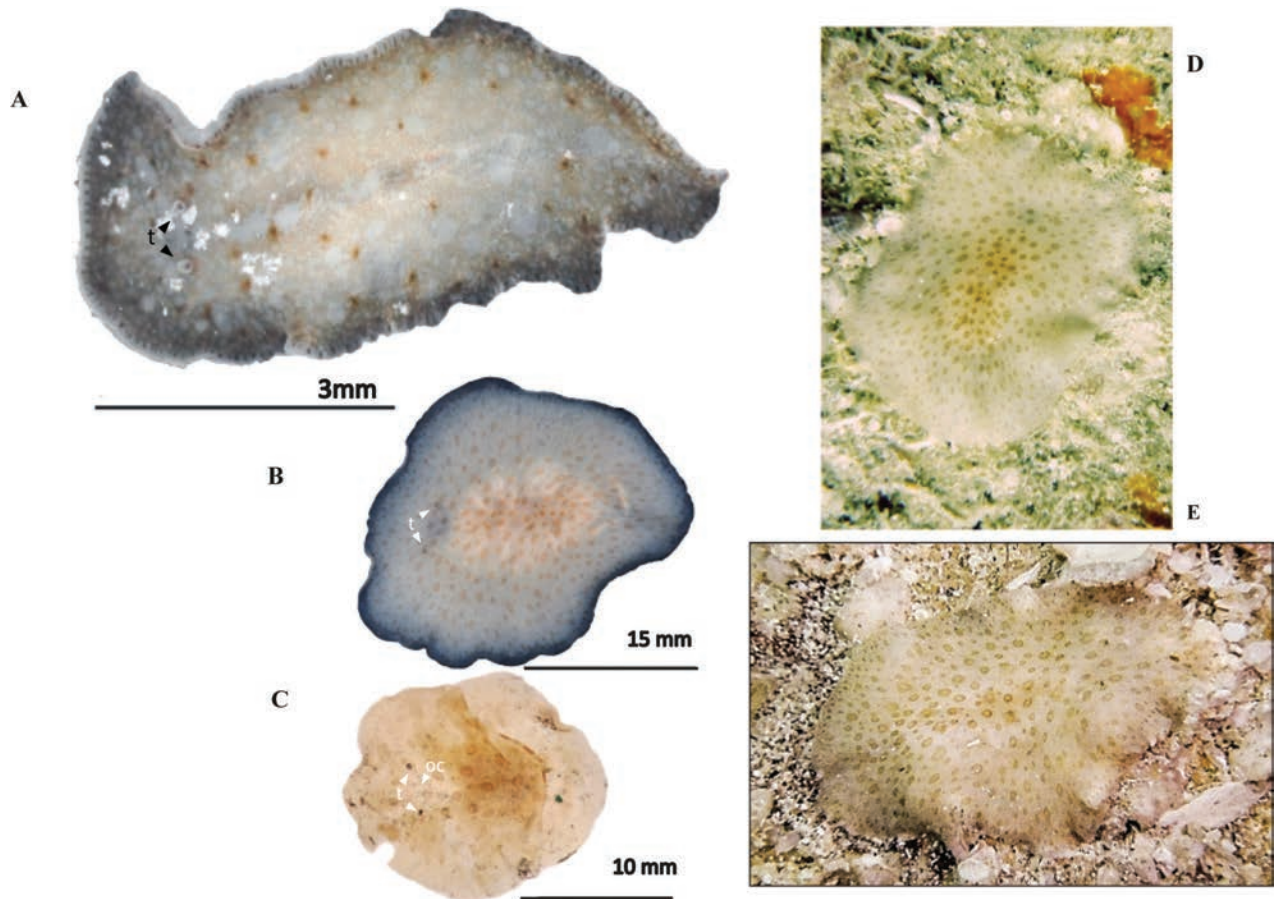


**Figure 23.** **A** *Gnesioceros sargassicola* Photograph in situ of the specimen captured **B–E** *Idioplana atlantica* **B** dorsal view of a live individual photographed on a black background **C** specimen photographed after fixation **D, E** specimens photographed in situ with the characteristic pigmentation rings.

**Stylochoidea Poche, 1926**

**Idioplanidae Dittmann, Cuadrado, Aguado, Noreña & Egger, 2019**

***Idioplana* Woodworth, 1898**

***Idioplana atlantica* (Bock, 1913)**

Fig. 23B–E

**Material examined.** Yucatan coast, MEXICO • 3; Dzilam; 21.5°N, 88.9°W; 13 m; 10 May 2018; A. Hernández leg.; CRPPY-0096.

**Distribution.** *Idioplana atlantica* was originally recorded off St Thomas Island (USA Virgin Island, Caribbean Sea; Bock 1913). Similar morphotypes of this species have been reported in Bocas del Toro (Panama, Caribbean Sea; Litvaitis 2014–2024; Quiroga et al. 2004b); Aguadores Beach near Santiago de Cuba (Caribbean Sea; Catalá et al. 2016). New record for the coasts of Yucatán, Mexico.

**Description.** Body shape oval, with a rounded posterior end and a more pointed anterior end, 2 cm in length and 1 cm in width. Firm and dense consistency. Background colour ranges from yellowish-white to amber. Dorsally, is covered by dark rings with cream-pigmented inner. The shape of these rings is variable, appearing more rounded anteriorly and elongated posteriorly. Also, the central rings are larger compared to those along the body's margin (Fig. 23B, C, D, E). Near the anterior end, two cylindrical nuchal tentacles are present. Tentacular

eyes immersed along the tentacles (Fig. 23E). Two elongated scattered clusters of cerebral eyes and the marginal eyes limited to the anterior of the body.

**Remarks.** Yucatan specimens show a resemblance to those documented by Litvaitis (2014–2024), as well as by Kate Rawlinson in Bocas del Toro, Panama (<https://www.invertebase.org/portal/taxa/index.php?taxauthid1&taxon=146957&clid=57>). In these instances, organisms identified as *Idioplana atlantica* (Bock, 1913) exhibit rounded dark rings. However, the type description of *Idioplana atlantica*, based on fixed material, does not mention rounded spots or rings. The specimen documented by Bock (1913) exhibits a homogeneous yellowish colouration with a slightly orange tone in the central region, while the ventral side is white-grey. Also, the marginal eyes encircle the entire body edge, and the cerebral eyes are dispersed but abundantly present in the brain region. The living specimen and preserved Yucatan specimen displays dark rings covering its dorsal surface. Furthermore, marginal eyes are either absent or barely noticeable on the anterior end. The absence of pigmentation noted by Bock could be attributed to the fixation process. This differs from the Mexican material, where pigmentation remains intact throughout fixation processing. Also, the Bocas del Toro specimens (Litvaitis 2014–2024) show specimens with and without pigmentation.

Although some doubts have arisen about the identity of this species, the presence or absence of pigmentation spots in the preserved specimens of *Idioplana* described from the Gulf of Mexico does not provide sufficient evidence to confirm the existence of a new species. Therefore, we have decided to classify the *Idioplana* specimens found in Yucatan as *I. atlantica*. Further morphological and molecular studies will be necessary to determine whether it represents a distinct species.

## **Stylochidae Stimpson, 1857**

### ***Stylochus* Ehrenberg, 1831**

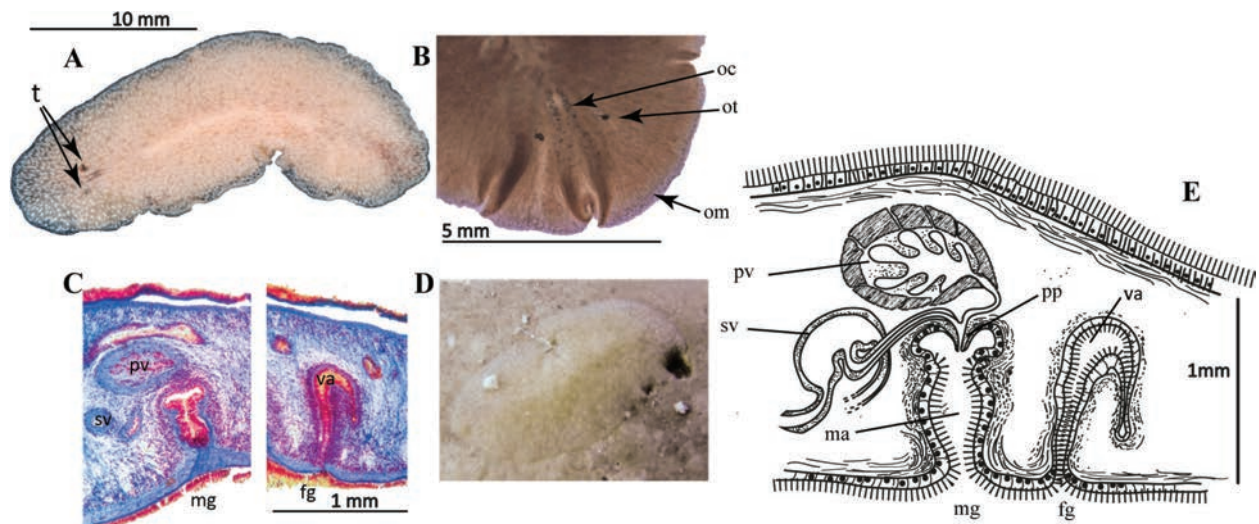
#### ***Stylochus sixteni* Marcus, 1947**

Fig. 24

**Material examined.** Yucatan coast, MEXICO • 1; Dzilam; 21.5°N, 88.9°W; 9.3 m; 8 May 2018; A. Hernández leg.; CRPPY-0090 • 1; 12 slides; Dzilam; 21.5°N, 88.9°W; 13 m; 10 May 2018; A. Hernández leg.; CRPPY-0099.

**Distribution.** The species was originally described in Cape Verde (Bock 1931). New record for the Gulf of Mexico (Yucatan).

**Description.** Elongated oval body shape, firm and fleshy consistency. In live specimens, body measures 20 mm in length, and 7 mm in width, whereas in fixed specimens, measures are reduced to 10 mm length, and 8 mm in width. Rounded nuchal tentacles visible. Pale beige colouration, translucent near the margins. Small white spots, denser along the midline and a white dotted line along the entire body margin (Fig. 24A, D). Two elongated clusters of cerebral eyes between nuchal tentacles. Densely packed tentacular eyes. Marginal eyes in the first 1/3 of the body, up to the level of the tentacles (Fig. 24B). Ruffled pharynx centrally located, oral opening at its centre. **Reproductive system.** Male and female copulatory apparatus posterior to pharynx, near second 1/2 of body. Male apparatus comprises a free prostatic vesicle and a small kidney-shaped seminal vesicle. Ejaculatory duct penetrates through an anteroposterior-orient-



**Figure 24.** *Stylochus sixteni* **A** live animal, photographed on a black background, tentacles **B** anterior end, marginal, cerebral and tentacular eyes, after fixation **C** sagittal section through the reproductive system (stained with AZAN) **D** specimen in situ **E** sagittal reconstruction of male and female copulatory organs.

ed penis papilla into the deep atrium. Penis papilla, small, conical. Male atrium heart-shaped, deep (Fig. 24C, E). Female apparatus simple, anteroposteriorly oriented, slightly muscular vagina, and small ciliated female atrium (Fig. 24C, E).

**Remarks.** To avoid confusion between *Stylochus crassus* Verrill, 1893 (from the coast of Maryland, USA) and *S. crassus* Bock, 1931 (from the coast of Cape Verde Island), Marcus (1947) renamed the specimens described by Bock (1931) as *Stylochus sixteni*. The specimen captured on the coast of Yucatan is most similar to the specimen described by Bock (1931). The major difference between the specimens described by Bock (1931) and *Stylochus sixteni* from the Gulf of Mexico is the distance of the reproductive system from the posterior end of the animal. The reproductive organs, in Bock's description, are close to the body end, while in the Yucatan specimens, they are near to the posterior end, but not so close as in Bock's. However, this may be due to the difference in size, since the specimens from Cape Verde measured 10 mm, while those from the Yucatan coast measured 20 mm (Fig. 24E).

### Hoploplanidae Stummer-Traunfels, 1933

#### *Hoploplana* Laidlaw 1902

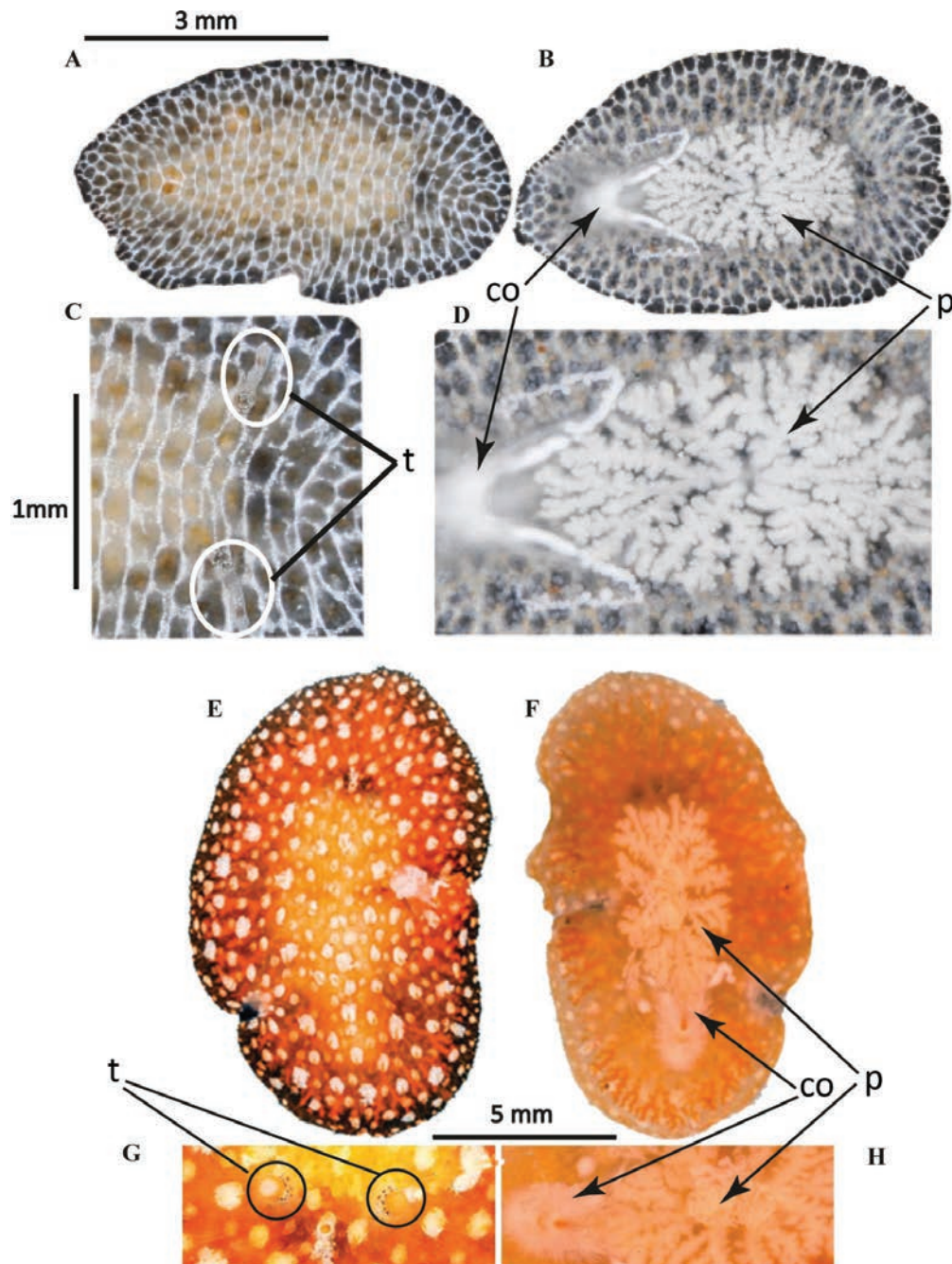
#### *Hoploplana inquilina* (Wheeler, 1894)

Fig. 25A–D

**Material examined.** Yucatan coast, MEXICO • 1; Dzilam; 21.5°N, 88.9°W; 9.3 m; 8 May 2018; A. Hernández leg.; CRPPY-0089.

**Distribution.** *Hoploplana inquilina* has been observed off St. Thomas Island, Caribbean (Hyman 1939). It has been reported in the Gulf of Mexico, Bermuda, and the Central North Atlantic (Prudhoe 1985); Cayman Islands, Caribbean (Hyman 1954). Additionally, it has been found in shells in Massachusetts (Hyman 1939, 1940). Specimens have also been documented in the mantle-cavity of *Urosalpinx cinerea* and *Eupleura caudata* in New Jersey (Schlechter 1943), and in the mantle-cavity of *Thais floridana* in Florida and Louisiana (Hyman 1944, 1954).

**Description.** Body shape oval, 5 mm in length and 3 mm in width. Translucent bluish-to-grey background colour with a distinctive white reticulum on the dorsal surface that does not correspond to the intestine (Fig. 25A, B). This network extends to the periphery, appearing white in reflected light and black in transmitted light, as described by Wheeler (1894). Delicate tubular nuchal tentacles present. Two clusters of small, rounded cerebral eyes situated between the nuchal tentacles, with tentacular eyes at the base (Fig. 25C). Ruffled pharynx, branched intestine, and reproductive system milky white and visible dorsally and ventrally (Fig. 25B, D).



**Figure 25.** A–D *Hoploplana inquilina* A dorsal view B ventral view C anterior end, tentacles and tentacular eyes D ventral view, ruffled pharynx and reproduction organs E–H *Hoploplana divae* E dorsal view F ventral view G anterior end, tentacles H ventral view, ruffled pharynx and reproduction organ.

### ***Hoploplana divae* Marcus, 1950**

Fig. 25E–H

**Material examined.** Campeche coast, MEXICO • 1; Cayo Arcas; 20.2°N, 92.0°W; 5.3 m; 23 Apr. 2018; A. Hernández leg.; CRPPY-0073 • 1; Cayo Arcas; 20.2°N, 92.0°W; 13.2 m; 24 Apr. 2018; A. Hernández leg.; CRPPY-0080.

**Distribution.** Originally described in São Paulo, Southeast of Brazil (Marcus 1950) and later by Bahia and Schrödl (2018). *Hoploplana divae* has been documented in Rio Grande do Norte, Brazil (Bahia et al. 2012) and Curaçao (Marcus and Marcus 1968). This study marks a novel record for the Campeche coast and new record for the Gulf of Mexico.

**Description.** Body shape oval with rounded anterior and posterior end, 1.2 cm in length and 0.6 cm in width. Two small cylindrical nuchal tentacles (Fig. 25E, G). Tentacular eyes at base of tentacles. Cerebral eyes two sparse clusters, extending towards anterior and posterior regions of body. Colouration semi-translucent, orange to pinkish. Dorsal epidermis covered with numerous semi-cylindrical whitish papillae. Largest papillae in posterior region. Highly folded ruffled pharynx, characteristic of the species of the genus *Hoploplana*. Oral opening situated in the anterior 1/2 of the body (Fig. 25F, H). Male and female gonopores close to each other, distinctly separated and open near the posterior end (Fig. 25F, H).

## **Conclusions**

This study provides a valuable contribution to our knowledge of Polycladida diversity in the southern regions of the Gulf of Mexico. Our research reveals the presence of 27 polyclad species, belonging to 17 genera and 12 families. By revising the polyclad records in the Gulf of Mexico, we have increased the known species count from 31 to 50. It is noteworthy that this is the first known report of marine flatworms along the coasts of Campeche, Yucatan, and Quintana Roo.

This study has identified 17 species that were previously unknown in the Gulf of Mexico, thus expanding their known distribution ranges. Some of the notable findings include the extension of distribution ranges for *Enchiridium evelinae*, *Pseudoceros juani*, *Phaenocelis peleca*, *Stylochus sixteni*, and *Hoploplana divae*. Additionally, this study has introduced two new species, *Stylochoplana sisalensis* sp. nov. and *Emprostopharynx hartei* sp. nov. The latter marks the first report of its genus on the Atlantic coast of the Americas.

This work highlights the rich diversity of Polycladida along the Atlantic coastline of Mexico. It also emphasises the importance of exploring and documenting under-researched species, particularly in regions home to abundant fauna. Ultimately, our study contributes to the development of a comprehensive atlas of unrecorded species, which will help to enhance conservation efforts and advance our knowledge of marine biodiversity in the Gulf of Mexico.

## **Acknowledgements**

We thank Patricia Guadarrama from the Ecology and microscopy laboratory, UMDI-Sisal, UNAM, México; Diana Ugalde and Tonali Mendoza for support on field trip logistics and project administration; to Efrain Chavez and

Quetzalli Hernandez for help during SCUBA diving collections; to Pedro Homa, Raul Castillo, and Diana Ugalde for their work on the UNAM-Sisal scientific collection. We thank Gregory Arjona and Danilú Couoh from Aquatic Pathology Laboratory of CINVESTA-IPN Mérida for their help with histology preparations. We also thank the anonymous reviewers for their valuable comments and suggestions, which greatly improved the quality of this manuscript.

## **Additional information**

### **Conflict of interest**

The authors have declared that no competing interests exist.

### **Ethical statement**

No ethical statement was reported.

### **Funding**

Field and lab work was financed by grants to NS by the Harte Research Institute with Harte Charitable Foundation funds and CONABIO-NE018. AHG received CONACyT scholarship number #629884.

### **Author contributions**

DC and AHG took the lead in writing the manuscript, developed the conception of the research, contributed to data interpretation. NS wrote respective parts of the manuscript and acquired funds. CN analysed the samples, wrote parts of the manuscript, and mostly contributed to histological interpretation. All authors edited and reviewed the manuscript.

### **Author ORCIDs**

Daniel Cuadrado  <https://orcid.org/0000-0001-5565-3023>

Alejandro Hernández-González  <https://orcid.org/0000-0002-1557-5582>

Carolina Noreña  <https://orcid.org/0000-0002-4580-7460>

Nuno Simões  <https://orcid.org/0000-0001-7490-3147>

### **Sampling and field studies**

The samples were collected under the collection permit N. PPF / DGOPA-295/17 and PPF / DGOPA-079/19, issued by Mexico's State Secretariat of Agriculture, Livestock, Rural Development, Fisheries, and Food (SAGARPA). Access to Alacranes Reef National Park was authorised by the Park authorities and we appreciate the possibility of using their facilities in Perez Island.

### **Data availability**

Whole body specimens and the histological preparations of those specimens under study were deposited at the 'Colección regional de Policlados de la Península del Yucatán, Mexico' (CRPPY), located at the Multidisciplinary Teaching and Research Unit of Sisal, Faculty of Sciences, National Autonomous University of Mexico (UMDI-Sisal, FC-UNAM). All sequences obtained in the present study have been deposited in the GenBank (Suppl. material 1: table S2).

## References

- Bahia J, Padula V (2009) First record of *Pseudoceros bicolor* and *Pericelis cata* (Platyhelminthes: Polycladida) from Brazil. *Marine Biodiversity Records* 2: 1–5. <https://doi.org/10.1017/S1755267209000918>
- Bahia J, Schrödl M (2018) Brazilian Polycladida (Rhabditophora: Platyhelminthes): Rediscovery of Marcus' type material and general revision. *Zootaxa*, 4490(1): 1–121. <https://doi.org/10.11646/zootaxa.4490.1.1>
- Bahia J, Padula V, Delgado M (2012) Five new records and morphological data of polyclad species (Platyhelminthes: Turbellaria) from Rio Grande do Norte, northeastern Brazil. *Zootaxa* 3170: 31–44. <https://doi.org/10.11646/zootaxa.3170.1.3>
- Bahia J, Padula V, Passeri Lavrado H, Quiroga S (2014) Taxonomy of *Cotylea* (Platyhelminthes: Polycladida) from Cabo Frio, southeastern Brazil, with the description of a new species. *Zootaxa* 3873: 495–525. <https://doi.org/10.11646/zootaxa.3873.5.3>
- Bahia J, Padula V, Dorigo Correia M, Sovierzoski H (2015) First records of the order Polycladida (Platyhelminthes, Rhabditophora) from reef ecosystems of Alagoas State, north-eastern Brazil, with the description of *Thysanozoon alagoensis* sp. nov. *Journal of the Marine Biological Association of the United Kingdom* 95: 1653–1666. <https://doi.org/10.1017/S0025315415000922>
- Bahia J, Padula V, Schrödl M (2017) Polycladida phylogeny and evolution: Integrating evidence from 28S rDNA and morphology. *Organisms, Diversity & Evolution* 17(3): 653–678. <https://doi.org/10.1007/s13127-017-0327-5>
- Bock S (1913) Studien ber Polycladen. *Zoologiska bidrag fran Uppsala* 2: 31–344.
- Bock S (1931) Die Polycladen der Deutschen Südpolar-Expedition 1901–1903. *Deutsche Südpolar-Expedition* 20: 259–304.
- Bolaños DM, Quiroga SY, Litvaitis MK (2007) Five new species of cotylean flatworms (Platyhelminthes, Polycladida) from the wider Caribbean. *Zootaxa* 1650: 1–23. <https://doi.org/10.11646/zootaxa.1650.1.1>
- Brusa F, Damborenea C, Quiroga S (2009) First records of Pseudocerotidae (Platyhelminthes: Polycladida: Cotylea) from Patagonia, Argentina. *Zootaxa* 2283: 51–59. <https://doi.org/10.11646/zootaxa.2283.1.5>
- Bulnes VN, Albano MJ, Obenat SM, Cazzaniga NJ (2011) Three Pseudocerotidae species (Platyhelminthes, Polycladida, Cotylea) from the Argentinean coast. *Zootaxa* 2990: 30–44. <https://doi.org/10.11646/zootaxa.2990.1.2>
- Catalá A, Diez Y, Yuanis D (2016) Nuevos registros de Polycladida (Platyhelminthes) para Cuba. *Revista Investigaciones Marinas* 36: 94–104. <https://revistas.uh.cu/rim/article/view/5574>
- Chávez-Hidalgo A (2009) *Conectividad de los arrecifes coralinos del Golfo de Mexico y Caribe mexicano Maestra en Manejo de Recursos Marinos*. PhD Thesis, Instituto Politecnico Nacional. Centro Interdisciplinario de Ciencias Marinas. <http://www.repositoriodigital.ipn.mx/handle/123456789/13669>
- Chen H, Rangasamy M, Tan SY, Wang H, Siegfried BD (2010) Evaluation of five methods for total DNA extraction from western corn rootworm beetles. *Public Library of Science ONE* 5: e11963. <https://doi.org/10.1371/journal.pone.0011963>
- Crozier WJ (1917) On the Pigmentation of a Polyclad. *Proceedings of the American Academy of Arts and Sciences* 52(11): 725–730. <https://doi.org/10.2307/20025707>
- Cuadrado D, Moro L, Noreña C (2017) The Polycladida (Platyhelminthes) in the Canary Islands. New genus, species and records. *Zootaxa* 4312(1): 38–68. <https://doi.org/10.11646/zootaxa.4312.1.2>

- Cuadrado D, Rodríguez J, Moro L, Grande C, Noreña C (2021) Polycladida (Platyhelminthes, Rhabditophora) from Cape Verde and related regions of Macaronesia. *European Journal of Taxonomy* 736: 1–43. <https://doi.org/10.5852/ejt.2021.736.1249>
- De Vera A, Moro L, Bacallado JJ, Hernández F (2009) Contribución al conocimiento de la biodiversidad de policlados (Platyhelminthes, Turbellaria) en las Islas Canarias. *Revista de la Academia Canaria de Ciencias* 20(4): 45–59. <https://biostor.org/reference/140805>
- Dittmann IL, Cuadrado D, Aguado MT, Noreña C, Egger B (2019) Polyclad phylogeny persists to be problematic. *Organisms Diversity and Evolution* 19: 585–608. <https://doi.org/10.1007/s13127-019-00415-1>
- Dixit S, Manjebayakath H, Saravanane N (2021) Pseudocerotid Polyclads of Lakshadweep Islands. Centre for Marine Living Resources and Ecology, Ministry of Earth Sciences, Government of India, Kochi, 24 pp.
- Faubel A (1983) The Polycladida, Turbellaria; Proposal and establishment of a new system. Part I. The Acotylea. *Mitteilungen aus dem Hamburgischen Zoologischen Museum und Institut* 80: 17–12.
- Faubel A (1984) The Polycladida, Turbellaria; Proposal and establishment of a new system. Part II. The Cotylea. *Mitteilungen aus dem Hamburgischen Zoologischen Museum und Institut* 81: 189–259.
- Gil-Agudelo DL, Cintra-Buenrostro CE, Brenner J, González-Díaz P, Kiene W, Lustic C, Pérez-España H (2020) Coral Reefs in the Gulf of Mexico Large Marine Ecosystem: Conservation Status, Challenges, and Opportunities. *Frontiers in Marine Science* 6: 2296–7745. <https://doi.org/10.3389/fmars.2019.00807>
- Heath H, McGregor EA (1912) New Polyclads from Monterey Bay, California. *Proceedings of the Academy of Natural Sciences of Philadelphia* 31: 455–480. <https://www.jstor.org/stable/4063474>
- Hooge MD, Newman LJ (2009) Turbellarians (Acoelomorpha and Free-Living Platyhelminthes) of the Gulf of Mexico Gulf of Mexico. In: Felder DL, Camp DK (Eds) *Gulf of Mexico—Origins, Waters, and Biota*. Texas A&M University Press.
- Hyman LH (1939) Some polyclads of the New England coast, especially of the Woods Hole region. *Biological Bulletin of the Marine Biological* 127–152. <https://doi.org/10.2307/1537854>
- Hyman LH (1940) The polyclad flatworms of the Atlantic Coast of the United States and Canada. *Proceedings of the United States National Museum* 89: 449–492. <https://doi.org/10.5479/si.00963801.89-3101.449>
- Hyman LH (1944) Marine Turbellaria from the Atlantic Coast of North America. *Proceedings of the United States National Museum* 1266: 1–15.
- Hyman LH (1952) Further notes on the turbellarian fauna of the Atlantic coast of the United States. *Biological Bulletin of the Marine Biological Laboratory of Woods Hole* 103: 195–200. <https://doi.org/10.2307/1538446>
- Hyman LH (1953) The polyclad flatworms of the Pacific coast of North America. *Bulletin American Museum Natural History* 100: 269–391.
- Hyman LH (1954) Free-living flatworms (Turbellaria) of the Gulf of Mexico. *Fishery Bulletin of the Fish and Wildlife Service, United States* 55: 301–302. <http://hdl.handle.net/1969.3/19215>
- Hyman LH (1955) Some polyclad flatworms from the West Indies and Florida. *Proceedings of the United States National Museum* 104: 115–150. <https://doi.org/10.5479/si.00963801.104-3341.115>
- Kearse M, Moir R, Wilson A, Stones-Havas S, Cheung M, Sturrock S, Buxton S, Cooper A, Markowitz S, Duran C, Thierer T, Ashton B, Meintjes P, Drummond A (2012) Gene-

- ious basic: An integrated and extendable desktop software platform for the organization and analysis of sequence data. *Bioinformatics* 28(12): 1647–1649. <https://doi.org/10.1093/bioinformatics/bts199>
- Laidlaw FF (1903) On the marine fauna of Zanzibar and British East Africa, from collections made by Cyril Crossland in the years of 1901 and 1902. – Turbellaria Polycladida. Part I. The Acotylea. *Proceedings of the Zoological Society of London* 1903(2): 99–13.
- Lang A (1884) Die Polycladen (Seeplanarien) des Golfes von Neapel und der angrenzenden Meeresabschnitte. Eine Monographie. *Fauna und Flora des Golfes von Neapel* 11. Engelmann, Leipzig. <https://doi.org/10.5962/bhl.title.10545>
- Litvaitis MK (2014–2024) InvertEBase. <http://invertebase.org>
- Litvaitis MK, Bolaños DM, Quiroga SY (2010) When names are wrong and colours deceive: unravelling the *Pseudoceros bicolor* species complex (Turbellaria: Polycladida). *Journal of Natural History* 44(13): 829–845. <https://doi.org/10.1080/00222930903537074>
- Litvaitis MK, Bolaños DM, Quiroga SY (2019) Systematic congruence in Polycladida (Platyhelminthes, Rhabditophora): are DNA and morphology telling the same story? *Zoological Journal of the Linnean Society* 20: 1–27. <https://doi.org/10.1093/zoolinnean/zlz007>
- Marcus E (1947) Turbellarios Marinhos do Brasil (5). *Boletins da Faculdade de Filosofia, Ciências e Letras da Universidade de So Paulo Zoologia* 12: 99–215. <https://doi.org/10.11606/issn.2526-4877.bsffclzoologia.1947.125220>
- Marcus E (1949) Turbellaria Brasileiros (7). *Boletins da Faculdade de Filosofia, Ciências e Letras da Universidade de So Paulo Zoologia* 14: 7–156. <https://doi.org/10.11606/issn.2526-4877.bsffclzoologia.1949.129106>
- Marcus E (1950) Turbellaria Brasileiros (9). *Boletins da Faculdade de Filosofia, Ciências e Letras da Universidade de So Paulo Zoologia* 15: 5–190. <https://doi.org/10.11606/issn.2526-4877.bsffclzoologia.1950.125192>
- Marcus E (1952) Turbellaria Brasileiros (10). *Boletins da Faculdade de Filosofia, Ciências e Letras da Universidade de So Paulo Zoologia* 17: 5–186. <https://doi.org/10.11606/issn.2526-4877.bsffclzoologia.1952.125189>
- Marcus E, Marcus E (1966) Systematische Übersicht der Polykladen. *Abhandlungen der Senckenbergischen Naturforschenden Gesellschaft* 511: 1–95.
- Marcus E, Marcus E (1968) Polycladida from Curaao and faunistically related regions. *Studies on the Fauna of Curaao and other Caribbean Islands* 26: 1–134.
- Marquina D, Teresa Aguado M, Noreña C (2015) New records of Cotylea (Polycladida, Platyhelminthes) from Lizard Island, Great Barrier Reef, Australia, with remarks on the 32 distribution of the *Pseudoceros* Lang, 1884 and *Pseudobiceros* Faubel, 1984 species of the Indo-Pacific Marine Region. *Zootaxa* 4019(1): 354–377. <https://doi.org/10.11646/zootaxa.4019.1.14>
- Moseley HN (1877) On *Stylochus Pelagicus*, a new species of pelagic planarian, with notes on other pelagic species, on the larval forms of *Thysanozoon*, and of a gymnosomatous pteropod. *Microscopical Journal* 17: 23–32. <https://doi.org/10.1242/jcs.s2-17.65.23>
- Newman LJ, Cannon LR (1994) *Pseudoceros* and *Pseudobiceros* (Platyhelminthes, Polycladida, Pseudocerotidae) from eastern Australia and Papua New Guinea. *Memoirs of the Queensland Museum* 37: 205–266.
- Newman LJ, Cannon LR (1997) Nine new species of *Pseudobiceros* (Platyhelminthes: Polycladida) from the Indo-Pacific. *The Raffles Bulletin of Zoology* 45: 341–368.
- Newman LJ, Cannon LR (1998) New *Pseudoceros* (Platyhelminthes, Polycladida) from the Indo-Pacific with twelve new species from Australia and Papua New Guinea. *The Raffles Bulletin of Zoology* 46: 293–323.

- Newman LJ, Norenburg JL, Reed S (2000) Taxonomic and biological observations on the tiger flatworm, *Maritigrella crozieri* (Hyman, 1939), new combination (Platyhelminthes, Polycladida, Euryleptidae) from Florida waters. *Journal of Natural History* 34: 799–808. <https://doi.org/10.1080/002229300299264>
- Oya Y, Kajihara H (2017) Description of a new *Notocomplana* species (Platyhelminthes: Acotylea), new combination and new records of Polycladida from the northeastern Sea of Japan, with a comparison of two different barcoding markers. *Zootaxa* 4282: 526–542. <https://doi.org/10.11646/zootaxa.4282.3.6>
- Palombi A (1928) Report on the Turbellaria. Zoological results of the Cambridge Expedition to the Suez Canal. 1924. *Transactions of the Zoological Society of London* 22(5): 579–630. <https://doi.org/10.1111/j.1096-3642.1928.tb00208.x>
- Pearse AS, Wharton GW (1938) The oyster leech, *Stylochus inimicus* Palombi, associated with oysters on the coast of Florida. *Ecological Monographs* 8: 605–655. <https://doi.org/10.2307/1943085>
- Pérez-García P, Gouveia F, Calado G, Noreña C, Cervera JL (2024) Acotylea (Platyhelminthes, Polycladida) from the southern and western Iberian Peninsula, with the description of five new species. *Zoosystematics and Evolution* 100(4): 1487–1513. <https://doi.org/10.3897/zse.100.128211>
- Pitale R, Apte D (2019) Intertidal Euryleptid polyclads and description of a new *Stylostomum* Lang, 1884 from Maharashtra, India. *Zootaxa* 4652(2): 317–339. <https://doi.org/10.11646/zootaxa.4652.2.5>
- Plehn M (1896) Polycladen von Ambon. *Zoologische forschungsreisen in Australien und dem Malayischen Archipel. Denkschrift der Medizinisch-Naturwissenschaftlichen Gesellschaft in Jena* 8: 327–334.
- Prudhoe S (1982) Polyclad turbellarians from the southern coasts of Australia. *Records of the South Australian Museum (Adelaide)* 18(16): 361–384.
- Prudhoe S (1985) A monograph on polyclad Turbellaria. Oxford University Press, Oxford, New York, Toronto, 259 pp.
- Queiroz V, Sales L, Neves EG, Johnsson R (2013) *Pericelis cata* Marcus and Marcus, 1968 (Platyhelminthes: Polycladida): First record from northeast of Brazil. *Check List* 9(3): 628–630. <https://doi.org/10.15560/9.3.628>
- Quiroga SY (2008) Systematics and Taxonomy of Polyclad Flatworms with a special emphasis on the morphology of the nervous system. University of New Hampshire 110.
- Quiroga SY, Bolaos DM, Litvaitis MK (2004a) A checklist of polyclad flatworms (Platyhelminthes: Polycladida) from the Caribbean coast of Colombia, South America. *Zootaxa* 633: 1–12. <https://doi.org/10.11646/zootaxa.633.1.1>
- Quiroga SY, Bolaños M, Litvaitis MK (2004b) Policládidos (Platyhelminthes: “Turbellaria”) del Atlántico Tropical Occidental. *Biota Colombiana* 5(2): 159–172.
- Rawlinson K (2008) Biodiversity of coastal polyclad flatworm assemblages in the wider Caribbean. *Marine Biology* 153: 769–778. <https://doi.org/10.1007/s00227-007-0845-3>.
- Risso A (1818) Sur quelques gastéropodes nouveaux, nudibranches et tectibranches observés dans la mer de Nice. *Journal de Physique chimie et Histoire Naturelle* 87: 368–376.
- Romeis B (1989) *Mikroskopische Technik* (17<sup>th</sup> ed., revised and expanded by Böck P). Urban und Schwarzenberg, München Wien Baltimore, 697 pp. <https://doi.org/10.1002/jobm.3620300221>
- Schlechter V (1943) Two flatworms from the oyster-drilling snail *Thais floridanahaysae* Clench. *Journal Parasitol* 29: 362. <https://doi.org/10.2307/3272618>

- Schmarda LK (1859) Neue Turbellarien, Rotatorien und Anneliden beobachtet und gesammelt auf einer Reise um die Erde 1853 bis 1857. Neue wirbellose Thiere 1: 1–66. <https://doi.org/10.5962/bhl.title.85313>
- Sreeraj CR, Raghunathan C (2015) A report on the coral reef dwelling polyclads of Nicobar Islands, India. *Proceedings of the International Academy of Ecology and Environmental Sciences* 5: 83–88.
- Stimpson W (1857) *Prodromus descriptionis animalium evertibratorum, quae in Expeditione ad Oceanum Pacificum Septentrionalem a Republica Federata missa, Johanne Rodgers Duce, observavit et descripsit. Pars I, Turbellaria Dendrocoela*. *Proceedings of the Academy of Natural Sciences of Philadelphia* 9: 19–31. <https://doi.org/10.5962/bhl.title.51447>
- Stummer-Traunfels R (1933) Polycladida. In *Bronn's Klassen und Ordnungen des Tierreichs, Band IV. Akademische Verlagsgesellschaft* 4[Abt. 1c, Lief. 179]: 3521–3523, 3485–3596.
- Thakkar NJ, Shah PD, Sarma KJ, Mankodi PC (2017) First record and description of marine flatworm *Pseudoceros bolool* (Newman & cannon, 1994) from Gujarat state. *International Journal of Zoology Studies* 2(5): 56–57.
- Tyler S, Schilling S, Hooge M, Bush LF (2006–2024) Turbellarian taxonomic database. <http://turbellaria.umaine.edu>
- Verrill AE (1893) Marine planarians of New England. *Transactions of the Connecticut Academy of Arts and Science* 8: 459–520
- Verrill AE (1900) Additions to the Turbellaria, Nemertina, and Annelida of the Bermudas. *Transactions of the Connecticut Academy of Arts and Science* 10: 595–670. <https://doi.org/10.5962/bhl.part.7035>
- Verrill AE (1901) Additions to the fauna of the Bermudas from the Yale Expedition of 1901, with notes on other species. *Transactions of the Connecticut Academy of Arts and Science* 11: 15–62. <https://biostor.org/reference/57677>
- Wheeler WM (1894) *Planocera inquilina*, a polyclad inhabiting the branchial chamber of *Sicotypus canaliculatus* Oil. *Journal of Morphology* 9 195–201. <https://doi.org/10.1002/jmor.1050090203>

## Supplementary material 1

### Supplementary information

Authors: Daniel Cuadrado, Alejandro Hernández-González, Carolina Noreña, Nuno Simões

Data type: docx

Explanation note: **table S1**. Polycladida of the Gulf of Mexico, updated and with species studied, new records for the Gulf of Mexico and new species added. **table S2**. GenBank accession numbers of the molecular sequences generated in this study of 28S from Polycladida of the Gulf of Mexico.

Copyright notice: This dataset is made available under the Open Database License (<http://opendatacommons.org/licenses/odbl/1.0/>). The Open Database License (ODbL) is a license agreement intended to allow users to freely share, modify, and use this Dataset while maintaining this same freedom for others, provided that the original source and author(s) are credited.

Link: <https://doi.org/10.3897/zookeys.1221.128260.suppl1>

# Six new species of micropterous *Paederus* (Coleoptera, Staphylinidae, Paederinae) from China

Yi Yang<sup>1</sup>, Sophie Chen<sup>2</sup>, Zhong Peng<sup>1</sup>

<sup>1</sup> College of Life Sciences, Shanghai Normal University, 100 Guilin Road, 1<sup>st</sup> Educational Building 323 Room, Shanghai, 200234, China

<sup>2</sup> Shanghai American School, 1600 Lingbai Road, Shanghai, 200120, China

Corresponding author: Zhong Peng ([lathrobium@163.com](mailto:lathrobium@163.com))

## Abstract

Six new species of the genus *Paederus* Fabricius, 1775 from China are described: *P. chentangus* **sp. nov.** (Xizang: Chentang), *P. mirus* **sp. nov.** (Xizang: Xiayadong), *P. songi* **sp. nov.** (Chongqing: Polaoxiang), *P. trispinosus* **sp. nov.** (Hubei: Houhe), *P. (Harpo-paederus) yei* **sp. nov.** (Hubei: Cuijia'ao), and *P. zhaoi* **sp. nov.** (Zhejiang: Majian). A key to the micropterous *Paederus* species of mainland China is given.

**Key words:** New species, rove beetles, taxonomic key

## Introduction

The genus *Paederus* Fabricius, 1775 was previously represented in mainland China by 55 known species and in Taiwan by 25 known species (Assing 2017, 2020, 2022). According to a key provided by Li et al. (2016), 31 micropterous species of *Paederus* were previously reported from mainland China. In recent years, three additional species have been described (Assing 2017; Cheng and Peng 2019; Assing 2020), thus raising the total number of micropterous species known from mainland China to 34. The *Paederus* fauna of over 50 mountain ranges in China has not been examined and most of these ranges have suitable habitats for the micropterous *Paederus*, suggesting that the true diversity of the genus is far greater than currently known.

A study of the micropterous *Paederus* material of mainland China yielded six new species.

## Materials and methods

The genitalia and other dissected parts were mounted on plastic slides and attached to the same pin as the respective specimens. Photographs were taken with a Canon EOS 7D camera with a MP-E 65 mm macro lens or with a Canon G9 camera mounted on an Olympus CX 31 microscope.

The following abbreviations are used in the text, with all measurements in millimeters:



Academic editor: Adam Brunke

Received: 31 August 2024

Accepted: 11 November 2024

Published: 13 December 2024

ZooBank: <https://zoobank.org/74B1036C-9E80-4F7C-9BBB-D61763088A2B>

Citation: Yang Y, Chen S, Peng Z (2024) Six new species of micropterous *Paederus* (Coleoptera, Staphylinidae, Paederinae) from China. ZooKeys 1221: 145–164. <https://doi.org/10.3897/zookeys.1221.135891>

Copyright: © Yi Yang et al.  
This is an open access article distributed under terms of the Creative Commons Attribution License (Attribution 4.0 International – CC BY 4.0).

Body length (**BL**) from the anterior margin of the labrum to the abdominal apex; forebody length (**FL**) from the anterior margin of the labrum to the posterior margin of the elytra; head length (**HL**) from the anterior clypeal margin to the occipital constriction; maximum width of head (**HW**); length of antenna (**AnL**); length of pronotum (**PL**) along midline; maximum width of pronotum (**PW**); elytral length (**EL**) at the suture from the apex of the scutellum to the posterior margin of the elytra (at the sutural angles); maximum width of the elytra (**EW**); maximum width of abdomen (**AW**); length of aedeagus (**AL**) from the apex of the dorsal plate or the parameres (whichever forms the apex of the aedeagus) to the base of the aedeagal capsule.

All material treated in this paper is deposited in the Insect Collection of Shanghai Normal University, Shanghai, China (**SNUC**). The type labels are cited in the original spelling; different labels are separated by slashes.

## Results

### *Paederus chentangus* Yang & Peng, sp. nov.

<https://zoobank.org/1436E3DD-0963-4800-BE95-CAD08EC18C76>

Figs 1A, 2, 8, 9

**Type material. Holotype.** CHINA – Xizang Prov. • ♂; glued on a card with two labels as follows: “China: Xizang Prov., Dingjie County, Chentang Town, Xiuxiongma Vill., alt. 27°54'11"N, 87°22'42"E, 2700–3000 m, 25.VI.2021, Peng, Yin & Zhang leg.” “HOLOTYPE: *Paederus chentangus* sp. n., Yang & Peng des. 2024” [red handwritten label]; SNUC. **Paratypes.** CHINA – Xizang Prov. • 8 ♂♂, 12 ♀♀; Dingjie County, Chentang Town, Xiuxiongma Vill., alt. 27°54'11"N, 87°22'42"E, 2700–3000 m, 25.VI.2021, Peng, Yin & Zhang leg; SNUC • 4 ♂♂, 12 ♀♀; Dingjie County, Chentang Town, Ganma Zangbu, 27°51'38"N, 87°24'59"E, alt. 2300 m, 30.VII.2022, Peng, Song, Yin & Zhang leg; SNUC • 3 ♀♀; Dingjie County, Chentang Town, Ganma Zangbu, 27°51'50"N, 87°24'24"E, alt. 2400 m, 28.VI.2021, Z. Peng leg; SNUC.

**Description.** Measurements (in mm) and ratios: BL: 9.39–11.22; FL: 4.43–5.00; HL: 1.25–1.37; HW: 1.47–1.57; AnL: 2.78–3.17; PL: 1.34–1.57; PW: 1.42–1.50; EL: 1.05–1.12; EW: 1.49–1.62; AW: 1.62–1.69; AL: 1.72–1.74; HL/HW: 0.84–0.87; HW/PW: 0.98–1.05; HL/PL: 0.87–0.93; PL/PW: 0.95–1.05; EL/PL: 0.71–0.78; diameter of eye: 0.37–0.42.

Habitus as in Figs 1A, 8. Coloration: head and abdomen black; antennae light brown, sometimes antennomeres 4–11 infusate; pronotum red; elytra black with bluish-green hue; legs black with blackish-brown tarsi.

Head (Fig. 1A) transverse, widest across eyes; punctation coarse and moderately dense; interstices glossy. Eyes distinctly convex. Antennae slender, antennomere 4 approximately 3.8 times as long as broad and antennomere 10 nearly twice as long as broad. Mandibles (Fig. 2A, B) each with apically bifid molar tooth, without evident sexual dimorphism.

Pronotum (Fig. 1A) weakly transverse or as long as broad, strongly convex in cross section; punctures distinctly sparser and shallower than that of head.

Elytra (Fig. 1A) nearly trapeziform; punctation coarse, well defined, and dense. Hind wings reduced. Metatarsomere I shorter than combined length of metatarsomeres II and III.

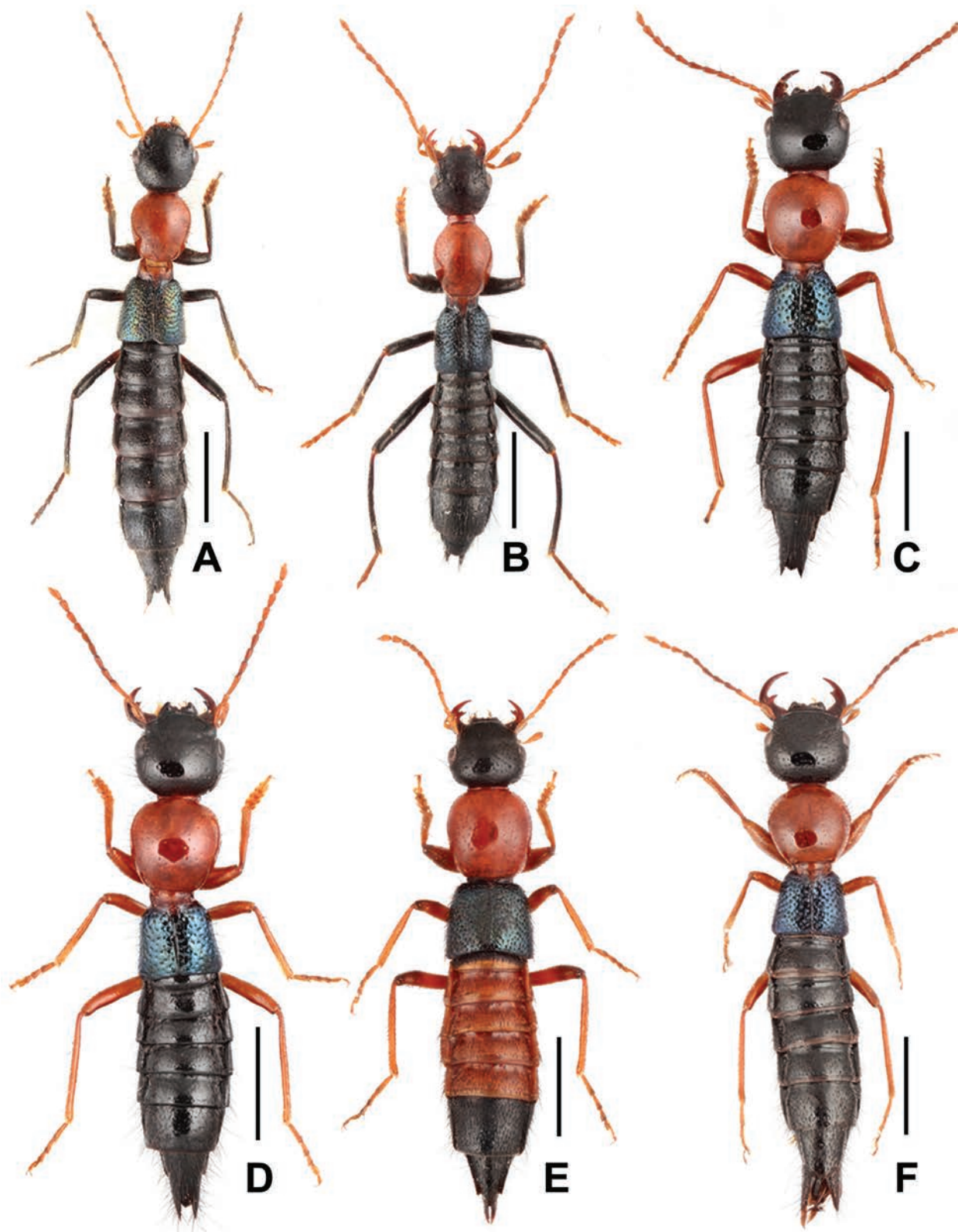


**Figure 1.** Habitus of *Paederus* species **A** *P. chentangus* **B** *P. mirus* **C** *P. songi* **D** *P. trispinosus* **E** *P. yei* **F** *P. zhaoi*. Scale bars: 2.0 mm.

Abdomen slightly broader than elytra; punctation dense; interstices with distinctly transverse microsculpture; posterior margin of tergite VII without palisade fringe.

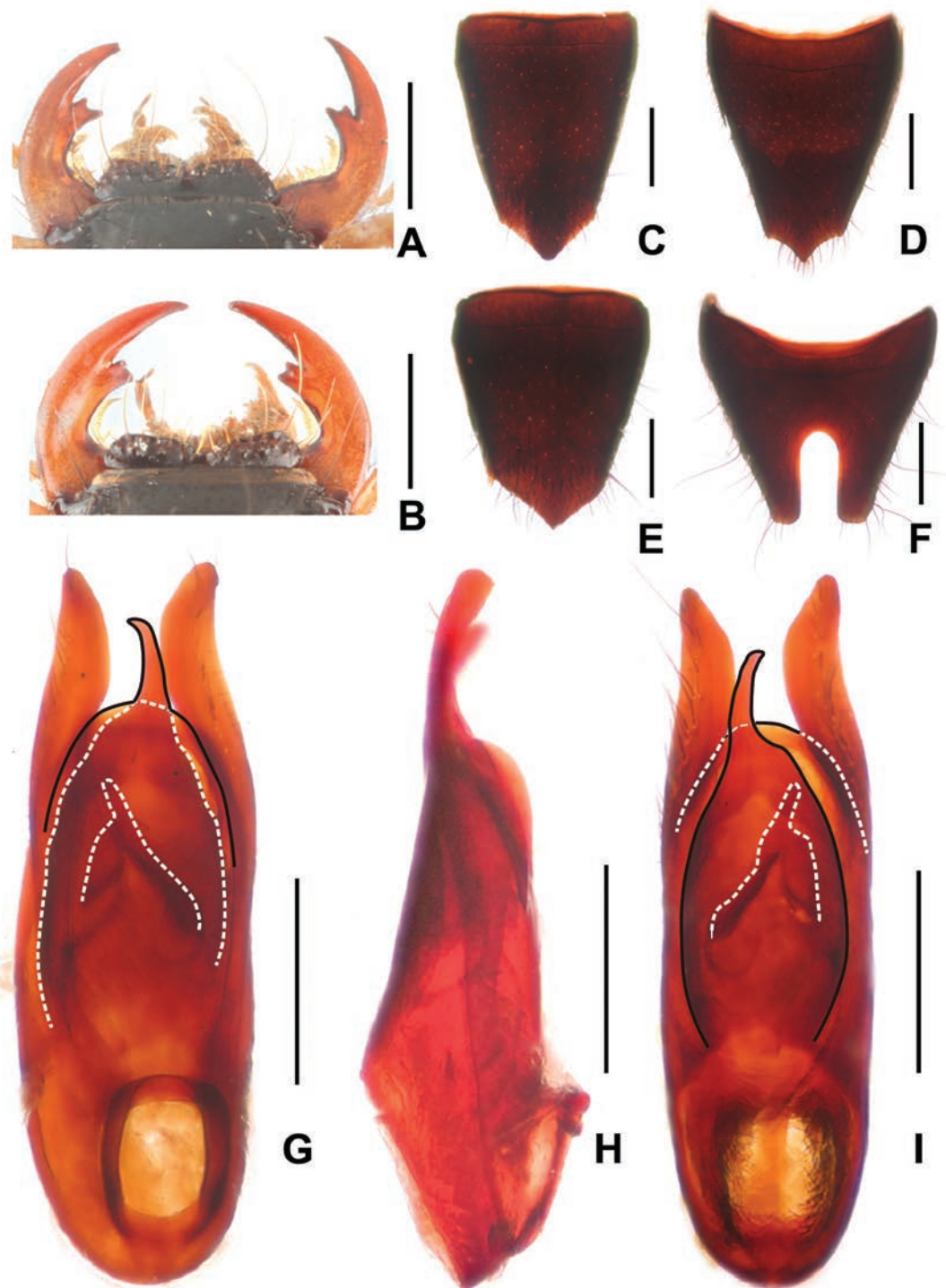


**Figure 2.** *Paederus chentangus* **A** female mouthparts **B** male mouthparts **C** female tergite VIII **D** female sternite VIII **E** male tergite VIII **F** male sternite VIII **G** aedeagus in ventral view **H** aedeagus in lateral view **I** aedeagus in dorsal view. Scale bars: 0.5 mm.

**Male.** Anterior margin of labrum (Fig. 2B) in middle with semicircular median excision; posterior margin of tergite VIII (Fig. 2E) pointed in middle; sternite VII unmodified; sternite VIII (Fig. 2F) with deep posterior excision, this excision approximately 0.4 times as long as sternite VIII; aedeagus as in Fig. 2G–I, ventral plate apically convex in ventral view; dorsal plate asymmetric, apically acute and not reaching apices of parameres in ventral view; parameres weakly

asymmetric and apically distinctly curved in lateral view; internal sac with single distinctive sclerotized spine.

**Female.** Anterior margin of labrum (Fig. 2A) in middle with shallow median excision. Posterior margin of tergite VIII (Fig. 2C) strongly convex; posterior margin of sternite VIII (Fig. 2D) obtusely pointed in middle.

**Distribution and biological notes.** The species was found in three localities in the Chentang area, to the south of Dingjie, southern Xizang. The specimens were sifted from moss, grass roots and loose gravel in shrub habitats at altitudes of 2300–3000 m (Figs 8, 9).

**Etymology.** The species is named after its type locality (Chentang).

**Comparative notes.** Based on the sexual characters and the external characters, closer affiliations with other *Paederus* species from Xizang are not evident. However, the highly similar male sexual characters, particularly the similarly derived morphology of the aedeagus, suggest that *P. chentangus* is very closely related to *P. megascutum* Willers, 1999 from Nepal. It differs from *P. megascutum* by the shape of the head (weakly transverse in *P. megascutum*), by the shorter elytra, and particularly by the stouter parameres and the curved ventral plate of the aedeagus in ventral view. For illustrations of *P. megascutum*, see Willers (1999: figs 7, 14, 114).

#### ***Paederus mirus* Yang & Peng, sp. nov.**

<https://zoobank.org/D8356E73-3E02-40F7-8609-F0D60478A008>

Figs 1B, 3, 10

**Type material. Holotype.** CHINA – Xizang Prov. • ♂; glued on a card with two labels as follows: “China: Xizang Prov., Yadong County, Xiayadong, 27°23'48"N, 88°50'02"E, alt. 3000 m, 01.VIII.2021, Peng, Yin & Zhang leg.” “HOLOTYPE: *Paederus mirus* sp. n., Yang & Peng des. 2024” [red handwritten label]; SNUC.

**Paratypes.** CHINA – Xizang Prov. • 3 ♀♀: Yadong County, Xiayadong, 27°23'48"N, 88°50'02"E, alt. 3000 m, 01.VIII.2021, Peng, Yin & Zhang leg; SNUC • 1 ♀: Yadong County, Xiayadong, 27°23'48"N, 88°50'02"E, alt. 2750 m, 10.VIII.2010, Wen-Xuan Bi leg; SNUC.

**Description.** Measurements (in mm) and ratios: BL 9.10–9.45, FL 4.42–4.77, HL 1.26–1.32, HW 1.29–1.35, AnL: 3.24–3.78; PL: 1.50–1.57; PW: 1.26–1.29; EL: 1.01–1.09; EW: 1.24–1.27; AW: 1.51–1.59; AL: 0.95; HL/HW: 0.96–0.98; HW/PW: 1.02–1.05; HL/PL: 0.84–0.85; PL/PW: 1.19–1.21; EL/PL: 0.67–0.69; diameter of eye: 0.32–0.33.

Habitus as in Fig. 1B. Coloration: head and abdomen black; antennae light brown; pronotum red; elytra black with faint bluish hue; legs black with dark brown tarsi.

Head (Fig. 1B) weakly transverse, widest across eyes; punctation distinctly coarse and sparse; interstices glossy. Eyes distinctly convex. Antennae distinctly slender, antennomere 4 nearly four times as long as broad and antennomere 10 nearly twice as long as broad. Labrum (Fig. 3A, B) without evident sexual dimorphism, anterior margin in middle with U-shaped median excision, with small projection on either side of median excision. Mandibles (Fig. 3A, B) each with apically bifid molar tooth, without sexual dimorphism.

Pronotum (Fig. 1B) nearly oviform, strongly convex in cross section; punctures sparser and shallower than on head.

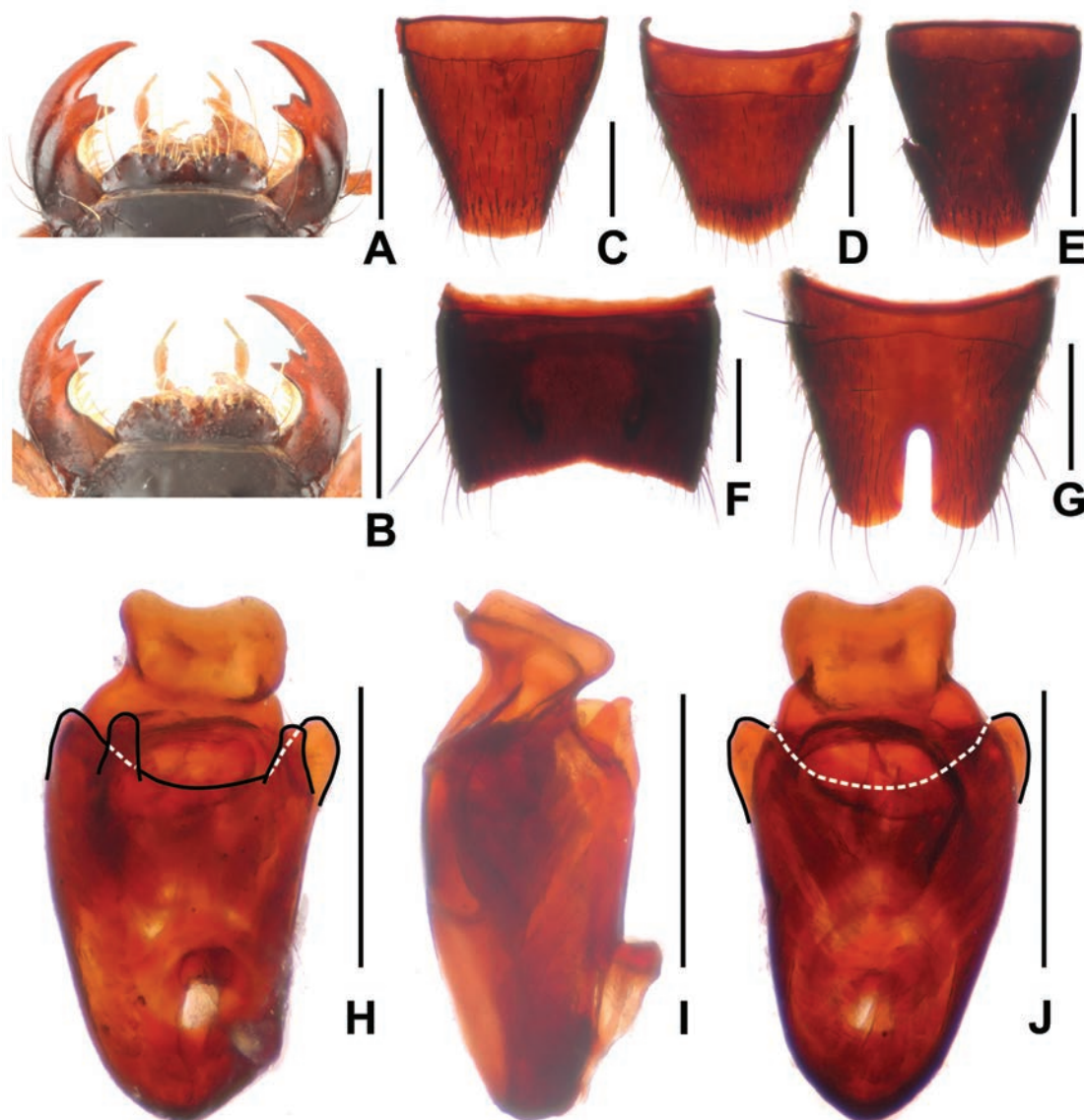


**Figure 3.** *Paederus mirus* **A** female mouthparts **B** male mouthparts **C** female tergite VIII **D** female sternite VIII **E** male tergite VIII **F** male sternite VII **G** male sternite VIII **H** aedeagus in ventral view **I** aedeagus in lateral view **J** aedeagus in dorsal view. Scale bars: 0.5 mm.

Elytra (Fig. 1B) slightly slender, humeral angles obsolete; punctation coarse, well defined, and dense. Hind wings reduced. Metatarsomere I as long as combined length of metatarsomeres II and III.

Abdomen broader than elytra; punctation dense; interstices with shallow microsculpture; posterior margin of tergite VII without palisade fringe; posterior margin of tergite VIII (Fig. 3C, E) weakly convex, shape subject to some variation, but without evident sexual dimorphism.

**Male.** Sternites III–VI unmodified; sternite VII (Fig. 3F) strongly transverse, with deep median impression without modified pubescence, posterior margin broadly concave; sternite VIII (Fig. 3G) with deep posterior excision, this excision approximately 0.4 times as long as sternite VIII; aedeagus as in Fig. 3H–J and strongly derived; ventral plate nearly truncate; dorsal plate weakly asymmetric, apically bifid and conspicuous; parameres very short; internal sac without sclerotized spine.

**Female.** Posterior margin of sternite VIII (Fig. 3D) convex.

**Distribution and biological notes.** The species was discovered in two localities situated to southern Yadong, southern Xizang. Some specimens were sifted from moss and leaf litter in montane primary mixed and coniferous forests at an altitude of 3000 m (Fig. 10).

**Etymology.** The specific epithet *mirus* means “strange, wonderful”, referring to the shape of the aedeagus.

**Comparative notes.** *Paederus mirus* is characterized particularly by the distinctive shape of the aedeagus and additionally by the shape and chaetotaxy of the male sternite VII, as well as by the slender habitus and antennae. Based on the sexual characters, closer affiliations with other *Paederus* species are not evident.

***Paederus songi* Yang & Peng, sp. nov.**

<https://zoobank.org/ED02AC7E-1878-4FD6-B4E3-D67865AB93DA>

Figs 1C, 4

**Type material. Holotype.** CHINA – **Chongqing** • ♂; glued on a card with two labels as follows: “China: Chongqing City, Shizhu County, Huangshui Town, Polaoxiang, Near Dafengbao, 30°13'04"N, 108°24'50"E, alt. 1550 m, 27.IX.2023, Xiao-Bin Song leg.” “HOLOTYPE: *Paederus songi* sp. n., Yang & Peng des. 2024” [red handwritten label]; SNUC. **Paratypes.** CHINA – **Chongqing** • 1 ♀; Shizhu County, Huangshui Town, Polaoxiang, Near Dafengbao, 30°13'04"N, 108°24'50"E, alt. 1550 m, 27.IX.2023, Xiao-Bin Song leg; SNUC.

**Description.** Measurements (in mm) and ratios: BL 8.11–9.55, FL 4.45–5.02, HL 1.49–1.52, HW 1.54–1.71, AnL: 2.94–3.31; PL: 1.54–1.72; PW: 1.59–1.68; EL: 0.95–1.02; EW: 1.55–1.60; AW: 1.73–1.79; AL: 2.25; HL/HW: 0.89–0.97; HW/PW: 0.97–1.02; HL/PL: 0.88–0.97; PL/PW: 0.97–1.02; EL/PL: 0.59–0.62; diameter of eye: 0.38–0.45.

Habitus as in Fig. 1C. Coloration: head and abdomen black; antennae brown to light brown; pronotum red; elytra black with distinctly bluish hue; legs brown with paler tarsi.

Head (Fig. 1C) transverse, widest across eyes; punctation coarse and sparse; interstices glossy. Eyes distinctly convex. Antennae slender, antennomere 4 approximately 3.4 times as long as broad and antennomere 10 nearly twice as long as broad.

Pronotum (Fig. 1C) nearly as long as broad, strongly convex in cross section; punctures slightly sparser than on head.

Elytra (Fig. 1C) trapeziform; punctation distinctly coarse, well defined, and moderately dense. Hind wings reduced. Metatarsomere I slightly shorter than combined length of metatarsomeres II and III.

Abdomen broader than elytra; punctation dense; interstices with distinctly transverse microsculpture; posterior margin of tergite VII without palisade fringe.

**Male.** Mandibles (Fig. 4B) each with weakly bifid molar tooth at apex. Labrum (Fig. 4B) with distinctly concave anterior margin, with U-shaped median excision and with broad lateral projection on either side. Posterior margin of tergite VIII (Fig. 4E) convex; sternite VII unmodified; sternite VIII (Fig. 4F) with deep posterior excision, this excision approximately 0.4 times as long as sternite VIII; aedeagus as in Fig. 4G–I, ventral plate asymmetric in ventral view; dorsal plate asymmetric, apically acute in dorsal view and not reaching apices of

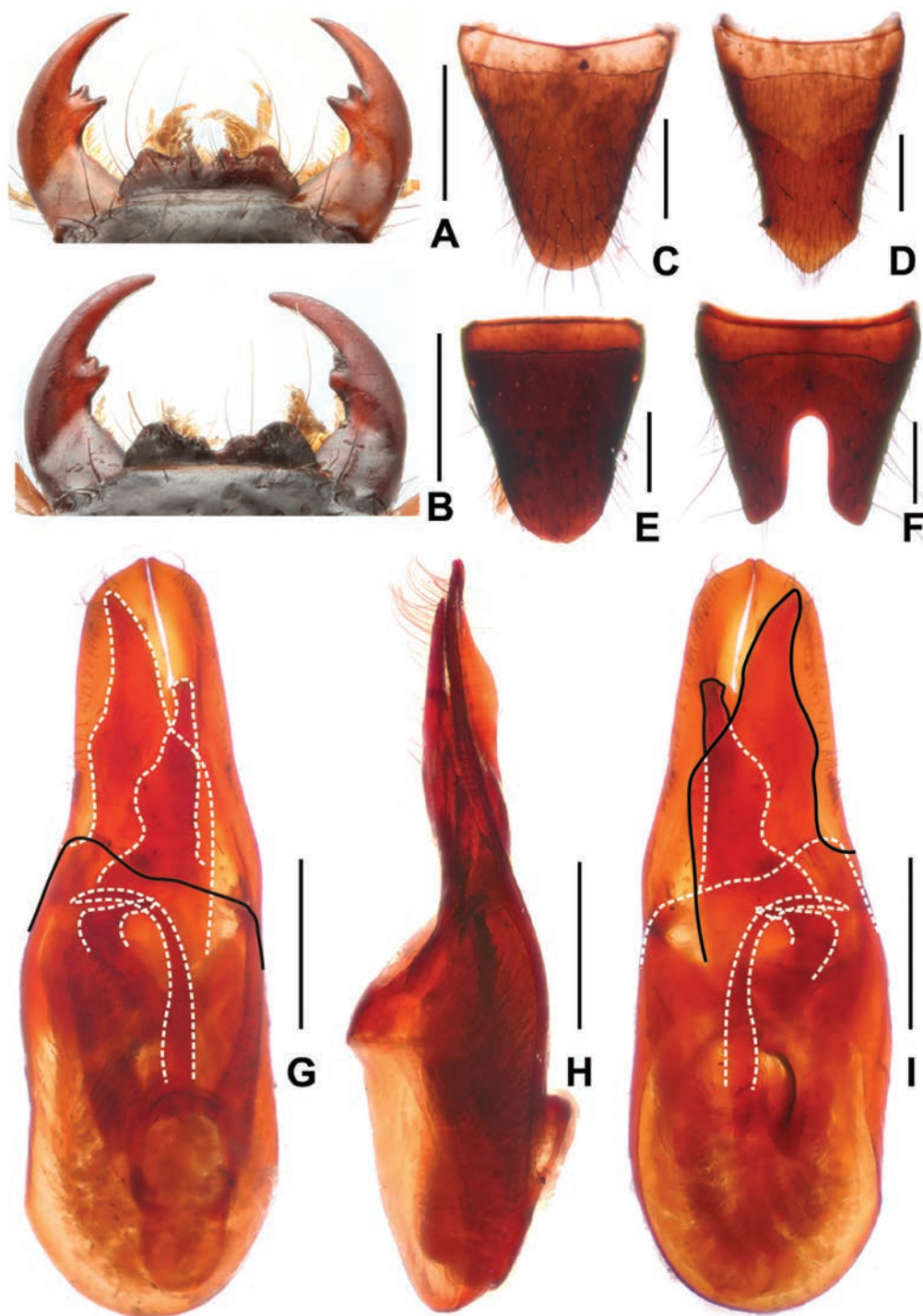


**Figure 4.** *Paederus songi* **A** female mouthparts **B** male mouthparts **C** female tergite VIII **D** female sternite VIII **E** male tergite VIII **F** male sternite VIII **G** aedeagus in ventral view **H** aedeagus in lateral view **I** aedeagus in dorsal view. Scale bars: 0.5 mm.

parameres; parameres asymmetric and weakly curved in lateral view; internal sac with pair of long sclerotized spines and single very short sclerotized spine.

**Female.** Mandibles (Fig. 4A) each with bifid molar tooth of similar shape. Labrum (Fig. 4A) with U-shaped median excision and with broad lateral projection on either side, as well as a small projection on either side of median excision. Tergite VIII (Fig. 4C) oblong, with convex posterior margin; posterior margin of sternite VIII (Fig. 4D) strongly convex.

**Distribution and biological notes.** The type locality is in northeastern Shizhu, eastern Chongqing. The specimens were sifted from moist leaf litter and roots in a secondary deciduous forest with bamboo at an altitude of 1550 m (Song pers. comm.). The paratype is teneral.

**Etymology.** The species is named after Xiao-Bin Song, who collected the type specimens. He is a renowned specialist on mainly Palaearctic Paussinae.

**Comparative notes.** The external and particularly the male sexual characters leave no doubt that this species belongs to the *P. biacutus* group. Among the species of this group, it appears to be most closely allied to *P. sinisterobliquus* Li, Zhou & Solodovnikov, 2013, with which it shares the similar morphology of the aedeagus. It is distinguished from *P. sinisterobliquus* by slightly larger body size, by the stouter pronotum, by three distinctly sclerotized spines of the internal sac and the larger parameres of the aedeagus, as well as by the shape of the female sternite VIII.

***Paederus trispinosus* Yang & Peng, sp. nov.**

<https://zoobank.org/5AB15EEF-ED8D-461D-9696-F78D262EDFCE>

Figs 1D, 5, 11

**Type material. Holotype.** CHINA – Hubei Prov. • ♂; glued on a card with two labels as follows: “China: Hubei Prov., Wufeng County, Houhe N.R., 30°11'53"N, 110°35'40"E, alt. 1480 m, 12.V.2020, Wen-Xuan Bi leg.” “HOLOTYPE: *Paederus trispinosus* sp. n., Yang & Peng des. 2024” [red handwritten label]; SNUC. **Paratypes.** CHINA – Hubei Prov. • 4 ♂♂, 2 ♀♀; Wufeng County, Houhe N.R., 30°11'53"N, 110°35'40"E, alt. 1480 m, 12.V.2020, Wen-Xuan Bi leg; SNUC • 1 ♂; Wufeng County, Houhe N.R., 30°05'10"N, 110°33'04"E, alt. 1150 m, 30.IV.2004, Li-Zhen Li leg; SNUC.

**Description.** Measurements (in mm) and ratios: BL 9.11–9.67, FL 4.56–4.91, HL: 1.35–1.54; HW: 1.49–1.69; AnL: 3.08–3.22; PL: 1.49–1.67; PW: 1.50–1.67; EL: 1.00–1.10; EW: 1.47–1.54; AW: 1.67–1.74; AL: 2.14–2.17; HL/HW: 0.90–0.93; HW/PW: 0.99–1.02; HL/PL: 0.90–0.93; PL/PW: 0.97–1.01; EL/PL: 0.65–0.68; diameter of eye: 0.38–0.43.

Habitus as in Fig. 1D. Coloration: head and abdomen black; antennae brown, sometimes antennomeres 4–8 infuscate; pronotum red; elytra black with distinctly bluish hue; legs with brown femora, and with brown to light brown tibiae and tarsi.

Head (Fig. 1D) transverse, widest across eyes; punctation coarse and sparse; interstices glossy. Eyes distinctly convex. Antennae slender, antennomere 4 approximately 3.3 times as long as broad and antennomere 10 1.8 times as long as broad. Mandibles (Fig. 5A, B) each with apically bifid molar tooth, without evident sexual dimorphism.

Pronotum (Fig. 1D) nearly as long as broad, strongly convex in cross section; punctures slightly sparser than on head.

Elytra (Fig. 1D) trapeziform; punctation distinctly coarse, defined and moderately dense. Hind wings reduced. Metatarsomere I as long as combined length of metatarsomeres II and III.

Abdomen distinctly broader than elytra; punctation dense; interstices with distinctly transverse microsculpture; posterior margin of tergite VII without palisade fringe.

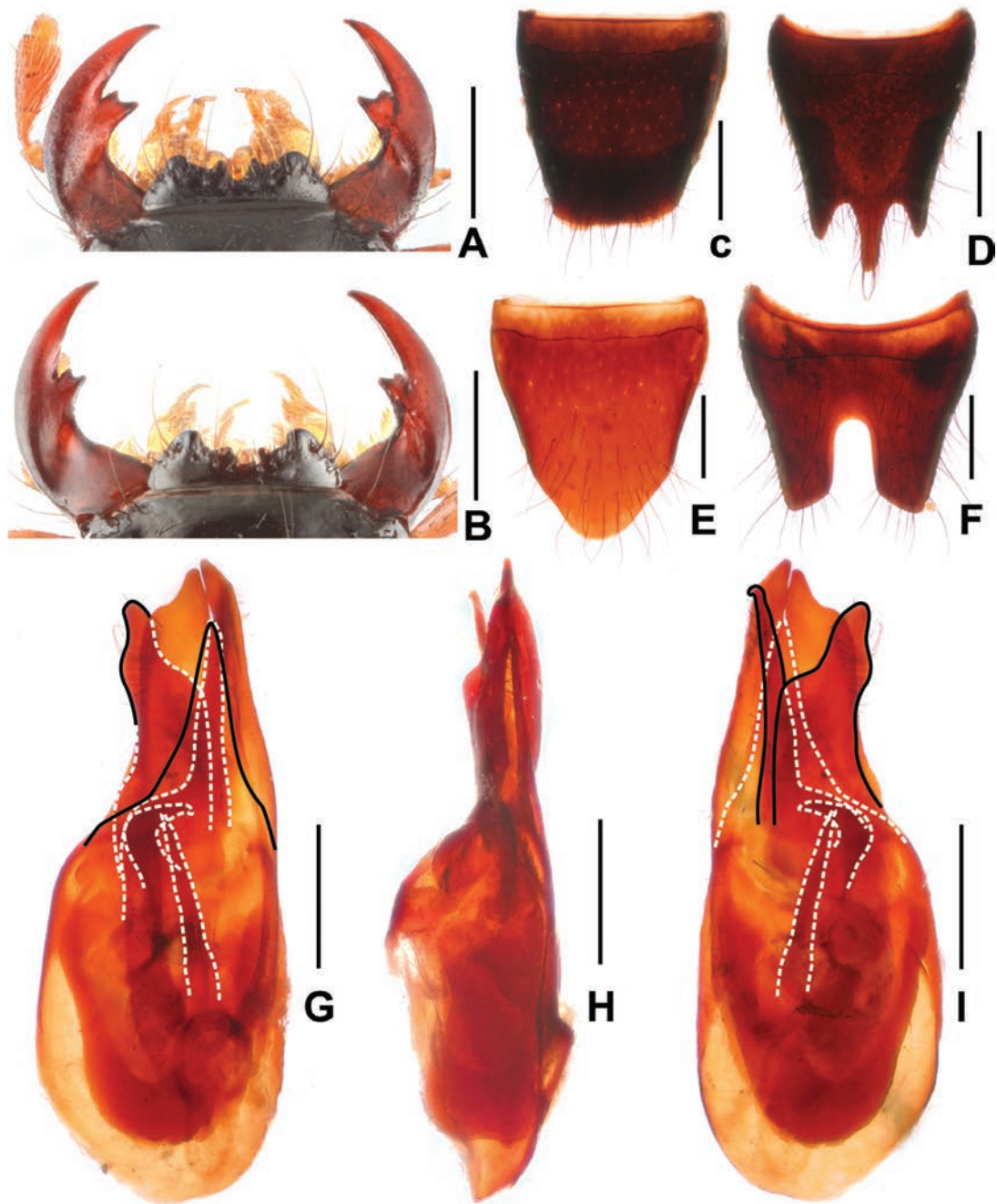


**Figure 5.** *Paederus trispinosus* **A** female mouthparts **B** male mouthparts **C** female tergite VIII **D** female sternite VIII **E** male tergite VIII **F** male sternite VIII **G** aedeagus in ventral view **H** aedeagus in lateral view **I** aedeagus in dorsal view. Scale bars: 0.5 mm.

**Male.** Labrum (Fig. 5B) with distinctly concave anterior margin, with U-shaped median excision and with large lateral projection on either side, as well as indistinct projection on either side of median excision. Posterior margin of tergite VIII (Fig. 5E) strongly convex; sternite VII unmodified; sternite VIII (Fig. 5F) with deep posterior excision, this excision approximately 0.3 times as long as sternite VIII; aedeagus as in Fig. 5G–I, ventral plate long and apically acute in ventral view; dorsal plate asymmetric and strongly sclerotized, with obtusely acute apical portion and not reaching apices of parameres; parameres distinctly asymmetric and apically straight in lateral view; internal sac with three distinctive sclerotized spines.

**Female.** Labrum (Fig. 5A) with U-shaped median excision and with broad lateral projection on either side, as well as a small projection on either side of median excision. Posterior margin of tergite VIII (Fig. 5C) weakly convex; posterior margin of sternite VIII distinctly trifurcate as in Fig. 5D.

**Distribution and biological notes.** The species was found in two localities in the Houhe Natural Reserve, to western Wufeng, Hubei. Some specimens were sifted from leaf litter, grass roots and the soil along a forest path at an altitude of 1480 m (Fig. 11).

**Etymology.** The specific epithet of this new species consists of the Latin suffix *tri-* (which means “three”) and the Latin adjective *spinus* (which means “spiny”). The name (a Latin adjective) refers to three distinctive sclerotized spines in the internal sac of the aedeagus.

**Comparative notes.** The external and particularly the male sexual characters leave no doubt that this species belongs to the *P. biacutus* group. This new species is distinguished from other species of this group by the shape of female tergite VIII and the morphology of the aedeagus (the distinctly asymmetric dorsal plate and parameres, as well as two long sclerotized spines and one hooked sclerotized spine in the internal sac).

***Paederus (Harpopaederus) yei* Yang & Peng, sp. nov.**

<https://zoobank.org/54D298FE-9877-443A-8C9A-CD6DF6CB782B>

Figs 1E, 6

**Type material. Holotype.** CHINA – Hubei Prov. • ♂; glued on a card with two labels as follows: “China: Hubei Prov., Baokang County, Cuijia’ao, 31.72°N, 111.13°E, alt. 1550 m, 31.VII.2021, Mao Ye leg.” “HOLOTYPE: *Paederus (Harpopaederus) yei* sp. n., Yang & Peng des. 2024” [red handwritten label]; SNUC.

**Paratypes.** CHINA – Hubei Prov. • 6 ♂♂, 5 ♀♀; Baokang County, Cuijia’ao, 31.72°N, 111.13°E, alt. 1550 m, 31.VII.2021, Mao Ye leg; SNUC • 3 ♂♂: Baokang County, Longping, alt. 1100 m, 15.VII.2017, Lu Qiu leg; SNUC.

**Description.** Measurements (in mm) and ratios: BL 9.43–10.02, FL 4.46–5.01, HL 1.20–1.25, HW 1.44–1.54, AnL: 2.67–2.79; PL: 1.49–1.67; PW: 1.49–1.69; EL: 1.14–1.20; EW: 1.64–1.74; AW: 1.62–1.74; AL: 1.94–1.99; HL/HW: 0.81–0.83; HW/PW: 0.91–0.97; HL/PL: 0.75–0.81; PL/PW: 0.98–1.01; EL/PL: 0.72–0.76; diameter of eye: 0.30–0.38.

Habitus as in Fig. 1E. Coloration: head and apex of abdomen black; labrum blackish brown; antennae brown, with the four basal and two apical segments yellowish brown; pronotum red; elytra black with faint bluish hue; first four abdominal segments reddish brown; legs with dark brown femora and protibiae, and with brown to light brown meso- and metatibiae and tarsi.

Head (Fig. 1E) transverse, widest across eyes; punctation coarse and sparse; interstices glossy. Eyes convex. Antennae not particularly slender, antennomere 4 approximately 3.1 times as long as broad and antennomere 10 1.7 times as long as broad. Labrum (Fig. 6A, B) with U-shaped median excision and with broad lateral projection on either side, as well as small projection on either side of median excision. Mandibles (Fig. 6A, B) each apically with bifid molar tooth, without sexual dimorphism.

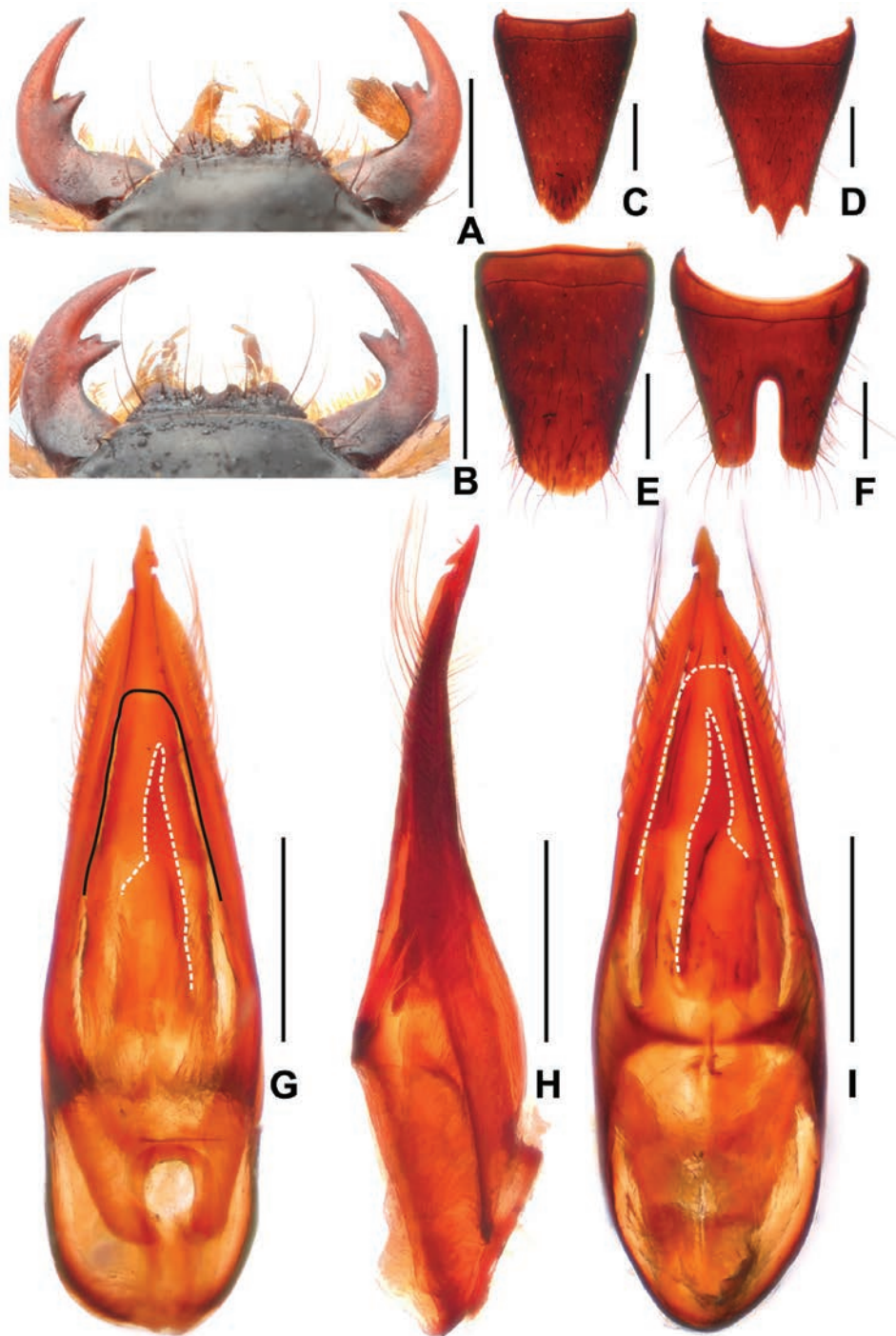


**Figure 6.** *Paederus yei* **A** female mouthparts **B** male mouthparts **C** female tergite VIII **D** female sternite VIII **E** male tergite VIII **F** male sternite VIII **G** aedeagus in ventral view **H** aedeagus in lateral view **I** aedeagus in dorsal view. Scale bars: 0.5 mm.

Pronotum (Fig. 1E) as long as broad, moderately convex in cross section; punctuation similar to that of head, but somewhat finer.

Elytra (Fig. 1E) nearly parallel-sided, wider than long; punctuation coarse, well defined, and dense. Hind wings reduced. Metatarsomere I shorter than combined length of metatarsomeres II and III.

Abdomen as broad as elytra or somewhat broader than elytra; punctuation dense; interstices with shallow microsculpture; posterior margin of tergite VII without palisade fringe.

**Male.** Posterior margin of tergite VIII (Fig. 6E) strongly convex; sternite VII unmodified; sternite VIII (Fig. 6F) with deep posterior excision, this excision approximately 0.4 times as long as sternite VIII; aedeagus as in Fig. 6G–I and nearly symmetric; ventral plate very weakly sclerotized; dorsal plate long and weakly curved in lateral view, extending beyond apices of parameres, dorsally with two rows of 4–5 denticles at some distance from hooked apex; parameres slender and weakly curved in lateral view; internal sac with single long sclerotized spine.

**Female.** Tergite VIII (Fig. 6C) oblong, posterior margin of strongly convex; posterior margin of sternite VIII trifurcate as in Fig. 6D.

**Distribution and biological notes.** The species was discovered in two localities situated to southwestern Baokang, western Hubei. Some specimens were sifted from leaf litter in a mixed deciduous forest with shrubs at an altitude of 1550 m (Ye pers. comm.).

**Etymology.** The species is named for Mao Ye, who collected some of the type specimens.

**Comparative notes.** The geographically closest *Harpopaederus* species are *P. apfelsinicus* Willers, 2001, *P. cultellatus* Assing, 2015, and *P. multidenticulatus* Li, Solodovnikov & Zhou, 2014. *Paederus yei* is distinguished from them by the stouter pronotum, particularly by the smaller aedeagus of different morphology (dorsal plate with hooked apex; shape of the internal structure), and by the oblong female tergite VIII. For illustrations of *P. apfelsinicus* see Willers (2001: figs 16–23), of *P. cultellatus* see Assing (2015: figs 55–62), and of *P. multidenticulatus* see Li et al. (2014: fig. 2A–H).

***Paederus zhaoi* Yang & Peng, sp. nov.**

<https://zoobank.org/B0F75D94-6D81-4D0E-8527-A3F131020410>

Figs 1F, 7, 12, 13

**Type material. Holotype.** CHINA – Zhejiang Prov. • ♂; glued on a card with two labels as follows: “China: Zhejiang Prov., Zhuji City, Majian Town, Near Longmen, 29.76°N, 119.89°E, 700–1000 m, 27.IX.2023, Tie-Xiong Zhao leg.” “HOLOTYPE: *Paederus zhaoi* sp. n., Yang & Peng des. 2024” [red handwritten label]; SNUC.

**Paratypes. Zhejiang Prov.** • 3 ♂♂, 2 ♀♀; Zhuji City, Majian Town, Near Longmen, 29.76°N, 119.89°E, 700–1000 m, 27.IX.2023, Tie-Xiong Zhao leg.; SNUC.

**Description.** Measurements (in mm) and ratios: BL 9.99–10.42, FL 4.65–4.78, HL 1.41–1.57, HW 1.56–1.82, AnL: 3.00–3.33; PL: 1.54–1.64; PW: 1.67–1.82; EL: 1.02–1.10; EW: 1.57–1.64; AW: 1.64–1.79; AL: 2.24–2.29; HL/HW: 0.85–0.92; HW/PW: 0.88–1.00; HL/PL: 0.88–0.91; PL/PW: 0.95–1.00; EL/PL: 0.66–0.68; diameter of eye: 0.33–0.37.

Habitus as in Figs 1F, 12. Coloration: head and abdomen black; antennae light brown, sometimes antennomeres 4–8 infusate; pronotum red; elytra black with distinctly bluish hue; legs with brown femora, and with brown to light brown tibiae and tarsi.

Head (Fig. 1F) transverse, widest across eyes; punctation coarse and sparse; interstices glossy. Eyes distinctly convex. Antennae slender, antennomere 4 approximately 3.2 times as long as broad and antennomere 10 1.7 times as long as broad.

Pronotum (Fig. 1F) weakly transverse or as long as broad, strongly convex in cross section; punctures sparser and slightly finer than on head.

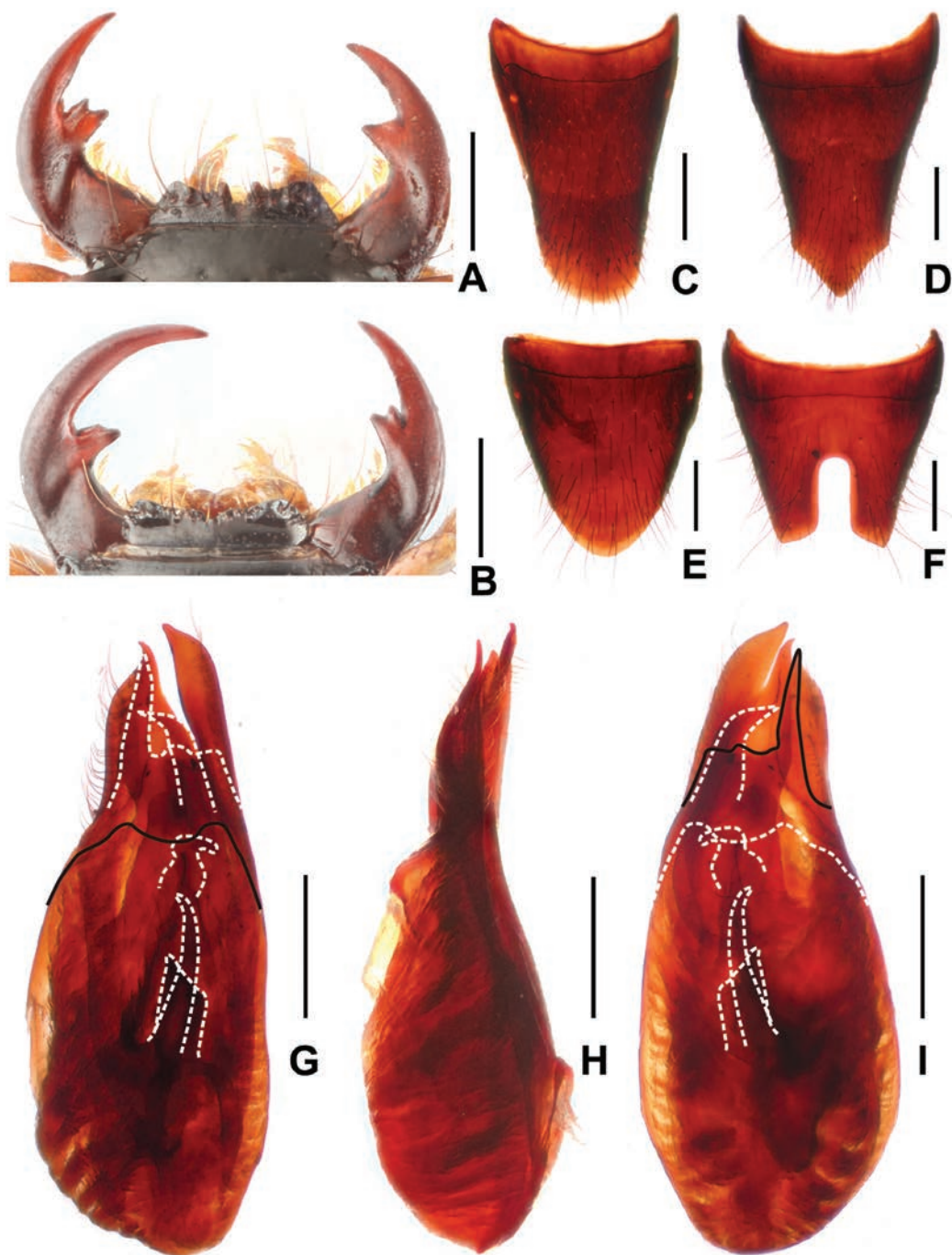
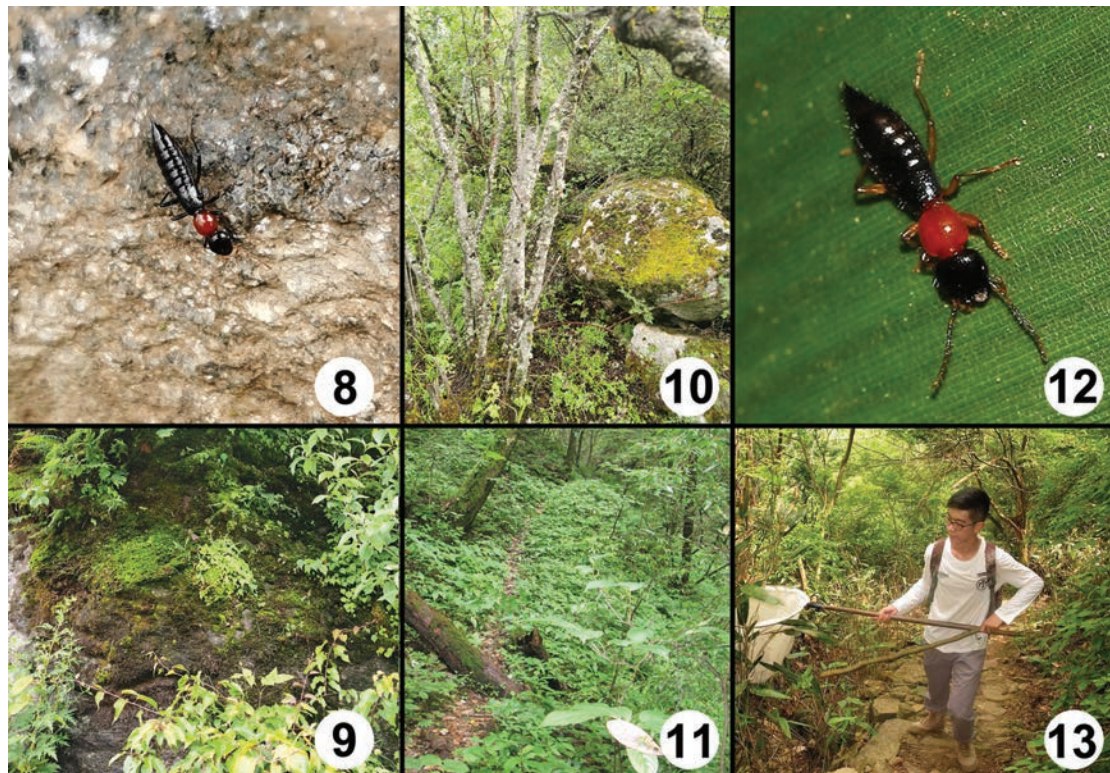


**Figure 7.** *Paederus zhaoi* **A** female mouthparts **B** male mouthparts **C** female tergite VIII **D** female sternite VIII **E** male tergite VIII **F** male sternite VIII **G** aedeagus in ventral view **H** aedeagus in lateral view **I** aedeagus in dorsal view. Scale bars: 0.5 mm.

Elytra (Fig. 1F) trapeziform; punctation distinctly coarse, well-defined, and dense. Hind wings reduced. Metatarsomere I as long as combined length of metatarsomeres II and III.

Abdomen broader than elytra; punctation dense; interstices with distinctly transverse microsculpture; posterior margin of tergite VII without palisade fringe.

**Male.** Mandibles (Fig. 7B) each apically with small bifid molar tooth. Labrum (Fig. 7B) with shallowly concave anterior margin, and with V-shaped median excision. Posterior margin of tergite VIII (Fig. 7E) convex; sternite VII unmodified; sternite VIII (Fig. 7F) with deep posterior excision, this excision approximately 0.4 times



Figures 8–13. **8** *Paederus chentangus* walking on a stone **9** habitat of *Paederus chentangus* **10** habitat of *Paederus mirus* **11** habitat of *Paederus trispinosus* **12** *Paederus zhaoi* walking on a blade of grass **13** Tie-Xiong Zhao collecting *Paederus zhaoi* at Majian, Zhejiang.

as long as sternite VIII; aedeagus as in Fig. 7G–I, ventral plate weakly asymmetric and apically concave in ventral view; apically acute dorsal plate of distinctive shape and nearly reaching apices of parameres; parameres distinctly asymmetric, apically curved in lateral view and acute in ventral view; internal sac with three distinctive sclerotized spines and with one additional dark membranous structure.

**Female.** Left mandible (Fig. 7A) with apically bifid molar tooth; right mandible (Fig. 7A) with single-pointed middle tooth. Labrum (Fig. 7A) with U-shaped median excision and with broad lateral projection on either side, as well as small projection on either side of median excision. Tergite VIII (Fig. 7C) oblong, with convex posterior margin; posterior margin of sternite VIII (Fig. 7D) strongly convex.

**Distribution and biological notes.** The type locality is situated to the west of Zhuji, central Zhejiang. The specimens were collected by hand on grasses and by sweep-netting of shrubs and shaking of branches both in shrub habitats with oak and bamboo at altitudes of 700–1000 m (Fig. 13).

**Etymology.** The species is named after Tie-Xiong Zhao, who collected the type specimens.

**Comparative notes.** The external and particularly the male sexual characters leave no doubt that this species belongs to the *P. biacutus* group. Among the species of this group, it appears to be most closely allied to *P. jianyueae* Peng & Li, 2014, with which it shares the similar morphology of the aedeagus. It is distinguished from *P. jianyueae* by the longer antennae, particularly the morphology of the aedeagus (distinctly asymmetric parameres; shape of the internal structure), and by the shape of the female tergite VIII and sternite VIII. For illustrations of *P. jianyueae* see Peng et al. (2014: figs 7, 8).

**Key to the micropterous *Paederus* species of mainland China**

According to recent contributions (Assing 2017; Cheng and Peng 2019; Assing 2020), three additional Chinese micropterous *Paederus* species have been described. This paper presents taxonomic and faunistic data for six new species. Therefore, the recently published key of the micropterous *Paederus* species from mainland China (Li et al. 2016) should be modified.

- |   |   |   |
|---|---|---|
| 1 | Male mandibles with dorsal tooth.....   | 2   |
| – | Male mandibles without dorsal tooth .....   | 9   |
| 2 | Internal sac of aedeagus with two spines.....   | 3   |
| – | Internal sac of aedeagus with one spine .....   | 4   |
| 3 | HL/PL more than 1.00. Male right mandible with small dorsal tooth; internal sac of aedeagus with one long curved spine and one short spine. Posterior margin of female tergite VIII truncate..... |   |
|   | ..... <b><i>P. (Gnathopaederus) szechuanus</i> (Chapin, 1927)</b>   |   |
| – | HL/PL no more than 0.95. Male right mandible with large dorsal tooth; internal sac of aedeagus with two short spines. Posterior margin of female tergite VIII convex.....                         | <b><i>P. (Gnathopaederus) bursavacua</i> Willers, 2001</b>        |
| 4 | Smaller species, length of body: 7.2 mm. Length of antenna no more than 3.0 mm .....  | <b><i>P. (Gnathopaederus) jilongensis</i> Li &amp; Zhou, 2009</b> |
| – | Larger species, length of body more than 8.0 mm. Length of antenna more than 3.3 mm.....  | 5   |
| 5 | Male sternite V–VI with shallow median impression posteriorly, this impression with weakly modified setae.....  |   |
|   | ..... <b><i>P. (Gnathopaederus) zhangmuensis</i> Cheng &amp; Peng, 2019</b>   |   |
| – | Male sternite V–VI without median impression and modified setae posteriorly.....  | 6   |
| 6 | Dorsal plate of aedeagus straight in lateral view and internal sac with one short spine .....   | <b><i>P. (Gnathopaederus) cheni</i> Peng &amp; Li, 2015</b>       |
| – | Dorsal plate of aedeagus weakly curved in lateral view and internal sac with one long spine .....   | 7   |
| 7 | Male left mandible with large dorsal tooth; internal spine of aedeagus apically extending nearly to apex of dorsal plate .....  |   |
|   | ..... <b><i>P. (Gnathopaederus) furcillatus</i> Assing, 2017</b>  |   |
| – | Male left mandible with small dorsal tooth; internal spine of aedeagus far from reaching apex of dorsal plate .....   | 8   |
| 8 | Smaller species, length of body: 8.3–10.5 mm. Male right mandible with small dorsal tooth; smaller aedeagus with slenderer parameres .....  |   |
|   | ..... <b><i>P. (Gnathopaederus) yunnanensis</i> Willers, 2001</b>   |   |
| – | Larger species, length of body 11.6–12.4 mm. Male right mandible with large dorsal tooth; larger aedeagus with stouter parameres .....  |   |
|   | ..... <b><i>P. (Gnathopaederus) xuei</i> Peng &amp; Li, 2015</b>  |   |
| 9 | Coloration of abdomen black .....   | 10  |
| – | Abdomen bicoloured (usually segments III–VI reddish and segments VII–X black) .....   | 21  |

- 10 Coloration of head brown. Male sternite VI with distinct median impression posteriorly ..... ***P. lateralis* Li, Solodovnikov & Zhou, 2014**
- Coloration of head black. Male sternite VI without median impression posteriorly ..... **11**
- 11 Male sternite VII with deep median impression posteriorly. Parameres of aedeagus very short..... ***P. mirus* Yang & Peng, sp. nov.**
- Male sternite VII without impression posteriorly. Parameres long and conspicuous..... **12**
- 12 Small species, length of body no more than 8.5 mm..... ***P. sinisterobliquus* Li, Zhou & Solodovnikov, 2013**
- Large species, length of body larger than 9.0 mm..... **13**
- 13 Maximum width of pronotum no more than 1.50 mm. Parameres of aedeagus apically distinctly curved in lateral view ..... ***P. chentangus* Yang & Peng, sp. nov.**
- Maximum width of pronotum more than 1.54 mm. Parameres of aedeagus apically weakly curved or straight in lateral view ..... **14**
- 14 Internal sac of aedeagus with two spines ..... **15**
- Internal sac of aedeagus with three spines ..... **17**
- 15 Maximum width of abdomen more than 2.1 mm. Parameres of aedeagus slender. Female sternite IX longer..... ***P. parvidenticulatus* Li, Zhou & Solodovnikov, 2013**
- Maximum width of abdomen no more than 2.0 mm. Parameres of aedeagus stout. Female sternite IX shorter..... **16**
- 16 HL/HW more than 0.95. Aedeagus with apically hooked dorsal plate in dorsal view and two long sclerotized spines in internal sac. Female sternite VIII with elliptic depression posteriorly..... ***P. volutobliquus* Li, Zhou & Solodovnikov, 2013**
- HL/HW no more than 0.90. Aedeagus with apically acute dorsal plate in dorsal view and two short sclerotized spines in internal sac. Female sternite VIII without depression ..... ***P. nanlingensis* Peng & Li, 2016**
- 17 Legs with infusate apical portion of femora. Aedeagus with apically hooked dorsal plate in dorsal view ..... ***P. biacutus* Li, Zhou & Solodovnikov, 2013**
- Legs with brown femora. Aedeagus with apically acute dorsal plate in dorsal view ..... **18**
- 18 Parameres of aedeagus symmetric and slender in ventral view..... ***P. jianyueae* Peng & Li, 2014**
- Parameres of aedeagus asymmetric and stouter in ventral view ..... **19**
- 19 Internal sac of aedeagus with one additional dark membranous structure. Female right mandible with single-pointed middle tooth ..... ***P. zhaoi* Yang & Peng, sp. nov.**
- Internal sac of aedeagus without dark membranous structure. Female right mandible with small bifid molar tooth apically ..... **20**
- 20 Ventral plate of aedeagus short and broad. Posterior margin of female sternite VIII strongly convex ..... ***P. songi* Yang & Peng, sp. nov.**
- Ventral plate of aedeagus long and slender. Posterior margin of female sternite VIII distinctly trifurcate ..... ***P. trispinosus* Yang & Peng, sp. nov.**

21	Aedeagus stout, with short and stout dorsal plate in dorsal view .....	22
–	Aedeagus slender, with long and slender dorsal plate in dorsal view .....	24
22	Legs reddish with infusate apical portion of femora. Aedeagus with apically acute dorsal plate in dorsal view .....	<b><i>P. tibetanus</i> Cameron, 1928</b>
–	Legs yellowish brown. Aedeagus with apically convex dorsal plate in dorsal view .....	23
23	Male labrum with sinuate anterior margin. Aedeagus with short parameres. Female sternite VIII with truncate median process posteriorly .....	<b><i>P. describendus</i> Willers, 2001</b>
–	Male labrum with deeply excavate anterior margin. Aedeagus with long parameres. Posterior margin of female sternite VIII convex.....	<b><i>P. daicongchaoi</i> Peng &amp; Li, 2016</b>
24	Dorsal plate of aedeagus not reaching apices of parameres .....	25
–	Dorsal plate of aedeagus extending beyond apices of parameres.....	29
25	Segments III–VI of abdomen reddish and with black patch in middle; elytra with pronounced impression.....	<b><i>P. (Harpopaederus) gottschei</i> Kolbe, 1886</b>
–	Segments III–VI of abdomen pale-reddish and without black patch in middle; elytra without impression.....	26
26	Dorsal plate of aedeagus without denticles .....	<b><i>P. (Harpopaederus) antennocinctus</i> Willers, 2001</b>
–	Dorsal plate of aedeagus with conspicuous denticles .....	27
27	Internal sac of aedeagus with one long and apically acute moderately sclerotized structure .....	<b><i>P. (Harpopaederus) willersi</i> Assing, 2020</b>
–	Internal sac of aedeagus with one basal clip-shaped structure and one asymmetric apical structure.....	28
28	Length of aedeagus: 2.4 mm. Female tergite VIII apically narrower .....	<b><i>P. (Harpopaederus) deplectens</i> Assing, 2015</b>
–	Length of aedeagus: 2.7 mm. Female tergite VIII apically broader .....	<b><i>P. (Harpopaederus) chinensis</i> Bernhauer, 1931</b>
29	Dorsal plate of aedeagus without denticles .....	30
–	Dorsal plate of aedeagus with denticles.....	31
30	Length of aedeagus: 1.4 mm; internal sac without sclerotized basal structures .....	<b><i>P. (Harpopaederus) xui</i> Peng &amp; Li, 2015</b>
–	Length of aedeagus: 2.0 mm; internal sac with one clip-shaped, weakly sclerotized basal structure ....	<b><i>P. (Harpopaederus) edentulus</i> Assing, 2015</b>
31	Legs with blackish metatibiae.....	32
–	Coloration of metatibiae much paler (usually yellowish) .....	33
32	Length of aedeagus: 2.4–2.7 mm, with apically stouter dorsal plate. Female sternite VIII with short median process posteriorly.....	<b><i>P. (Harpopaederus) apfelsinicus</i> Willers, 2001</b>
–	Length of aedeagus: 2.9 mm, with apically more slender dorsal plate. Female sternite VIII with long median process posteriorly .....	<b><i>P. (Harpopaederus) lineodenticulatus</i> Li &amp; Zhou, 2007</b>
33	Forebody longer than 5.8 mm. Aedeagus conspicuously long (2.7 mm)....	<b><i>P. (Harpopaederus) minicus</i> Assing, 2015</b>
–	Forebody no more than 5.5 mm. Aedeagus shorter .....	34
34	Internal sac of aedeagus with one long, apically acute and sclerotized apical structure.....	35
–	Internal sac of aedeagus without distinctly sclerotized apical structure .....	38

- 35 Aedeagus 2.4 mm long, with longer apical portion of the dorsal plate .....  
..... *P. (Harpopaederus) cultellatus* Assing, 2015
- Aedeagus 1.9–2.1 mm long, with shorter apical portion of the dorsal  
plate.....36
- 36 Dorsal plate of aedeagus with hooked apex. Posterior margin of female  
sternite VIII trifurcate ..... *P. (Harpopaederus) yei* Yang & Peng, sp. nov.
- Dorsal plate of aedeagus with acute apex. Female sternite VIII posteriorly  
with median process of triangular shape .....37
- 37 Tibiae usually yellowish; mandibles and shape of head without sexual di-  
morphisms. Aedeagus with moderately sclerotized apical internal struc-  
ture ..... *P. (Harpopaederus) agnatus* Eppelsheim, 1889
- Tibiae distinctly infuscate basally; mandibles and shape of head with pro-  
nounced sexual dimorphisms. Aedeagus with strongly sclerotized apical  
internal structure ..... *P. (Harpopaederus) konfuzius* Willers, 2001
- 38 Femora brown. Dorsal plate of aedeagus with 20 small denticles; param-  
eres apically weakly curved in lateral view .....  
..... *P. (Harpopaederus) multidenticulatus* Li, Zhou & Solodovnikov, 2014
- Femora bicoloured. Dorsal plate of aedeagus with several large denticles;  
parameres apically hooked in lateral view.....39
- 39 Head transverse (HL/HW: 0.90). Dorsal plate of aedeagus with short api-  
cal portion. Female sternite VIII with strongly convex posterior margin .....  
..... *P. (Harpopaederus) brevior* Li, Zhou & Solodovnikov, 2014
- Head weakly transverse (HL/HW: 0.99). Dorsal plate of aedeagus with  
long apical portion. Female sternite VIII with long median process posteri-  
orly.....*P. (Harpopaederus) gracilacutus* Li & Zhou, 2007

## Acknowledgements

All the collectors mentioned in the text are acknowledged for their fieldwork. Two anonymous reviewers are thanked for comments on a previous version of the manuscript.

## Additional information

### Conflict of interest

The authors have declared that no competing interests exist.

### Ethical statement

No ethical statement was reported.

### Funding

The present study was supported by the National Natural Science Foundation of China (No. 31872965), GDAS Special Project of Science and Technology Development (No. 2020GDASYL–20200102021, 2020GDASYL–20200301003) and Science and Technology Commission of Shanghai Municipality, China (19QA1406600) awarded to Zi-Wei Yin.

### Author contributions

Conceptualization: SC. Writing – original draft: ZP. Writing – review and editing: YY.

## Author ORCIDs

Yi Yang  <https://orcid.org/0000-0003-1132-9103>

Sophie Chen  <https://orcid.org/0009-0007-3396-9810>

Zhong Peng  <https://orcid.org/0000-0001-5959-1536>

## Data availability

All of the data that support the findings of this study are available in the main text.

## References

- Assing V (2015) On the *Harpopaederus* fauna of China (Coleoptera: Staphylinidae: Paederinae). *Linzer Biologische Beiträge* 47(1): 163–190. <https://doi.org/10.1002/jor.1100120417>
- Assing V (2017) Two new species and additional records of micropterous *Paederus* from China and Taiwan (Coleoptera: Staphylinidae: Staphylininae). *Linzer Biologische Beiträge* 49(1): 253–263.
- Assing V (2020) On the taxonomy and zoogeography of *Paederus*. V. Two new species from Laos and China, a new synonymy, new subgeneric assignments, and new records from the Palaearctic region (Coleoptera: Staphylinidae: Paederinae). *Acta Musei Moraviae, Scientiae Biologicae* 105(1): 91–102.
- Assing V (2022) On the taxonomy and zoogeography of *Paederus*. VI. Two new species from Nepal and new records from the Palaearctic and Oriental regions (Coleoptera: Staphylinidae: Paederinae). *Contributions to Entomology* 72(1): 75–79. <https://doi.org/10.3897/contrib.entomol.72.e87241>
- Cheng ZF, Peng Z (2019) A new species and additional records of brachypterous *Paederus* (Coleoptera, Staphylinidae) of mainland China and Taiwan. *Zootaxa* 4686(1): 127–132. <https://doi.org/10.11646/zootaxa.4686.1.7>
- Li XY, Zhou HZ, Solodovnikov A (2013) Five new species of the genus *Paederus* Fabricius from mainland China, with a review of the Chinese fauna of the subtribe Paederina (Coleoptera: Staphylinidae: Paederinae). *Annals of the Entomological Society of America* 106(5): 562–574. <https://doi.org/10.1603/AN13008>
- Li XY, Solodovnikov A, Zhou HZ (2014) Two new species and a new synonym of the genus *Paederus* Fabricius (Coleoptera: Staphylinidae: Paederinae) from China. *Zootaxa* 3847(3): 431–436. <https://doi.org/10.11646/zootaxa.3847.3.7>
- Li QL, Li LZ, Gu FK, Peng Z (2016) New data on brachypterous *Paederus* (Coleoptera, Staphylinidae) of mainland China. *Zootaxa* 4184(3): 576–588. <https://doi.org/10.11646/zootaxa.4184.3.11>
- Peng Z, Li LZ, Zhao MJ (2014) New data on the *Paederus biacutus* species group from mainland China (Coleoptera: Staphylinidae: Paederinae). *ZooKeys* 419: 117–128. <https://doi.org/10.3897/zookeys.419.7764>
- Willers J (1999) Der Artenbestand der Gattung *Paederus* Fabricius s.l. (Coleoptera, Staphylinidae) von Nepal. *Veröffentlichungen des Naturkundemuseums Erfurt* 18: 121–162.
- Willers J (2001) Neue asiatische Arten der Gattung *Paederus* Fabricius s.l. aus der Sammlung des Naturhistorischen Museums Basel (Coleoptera, Staphylinidae). *Entomologica Basiliensia* 23: 287–309.

# A new species of *Laena* Dejean (Coleoptera, Tenebrionidae) from Sichuan Province, China, with an updated key

Haizhi Wang<sup>1</sup>, Zhonghua Wei<sup>1</sup>, Guodong Ren<sup>2</sup>

<sup>1</sup> College of Life Sciences, China West Normal University, 637009, Nanchong, Sichuan Province, China

<sup>2</sup> College of Life Sciences, Hebei University, 071002, Baoding, Hebei Province, China

Corresponding author: Zhonghua Wei ([wzh1164@126.com](mailto:wzh1164@126.com))

## Abstract

In this study, we describe and illustrate a new species of the genus *Laena* Dejean, 1821, *Laena costata* **sp. nov.**, which was collected in Micangshan Nature Reserve of Sichuan Province, China. Additionally, the COI mitochondrial gene was sequenced to provide additional evidence for this new species' validity. The results of phylogenetic analyses suggest that this new species is sister to *L. maowenica* Schawaller, 2008. Furthermore, an updated key to *Laena* species from Sichuan Province is provided.

**Key words:** DNA barcoding, Lagriinae, Laenini, new species

## Introduction

The genus *Laena* Dejean, 1821 belongs to the tribe Laenini Seidlitz, 1895 of the family Tenebrionidae Latreille, 1802 (Bouchard et al. 2021), which is one of the largest genera in the subfamily Lagriinae Latreille, 1825. *Laena* species recorded in China appear endemic, except for *L. leonhardi* Schuster, 1916 and *L. brunkei* Schawaller & Bellersheim, 2023 (Schawaller 2001; Schawaller and Bellersheim 2023), and most *Laena* species appear to have narrow distribution ranges. Given China's complex terrain and diverse ecological environments, it is likely that many undescribed *Laena* species exist within the country.

The Micangshan Nature Reserve, located in northern part of Sichuan Province, borders on Shaanxi Province. An insect diversity survey was initiated in the Micangshan Nature Reserve from 2023 to 2024, during which the genus *Laena* was found. Specimens of *Laena* were collected by sifting leaf litter. After examining the collected specimens, two *Laena* species were identified: *L. qinlingica* Schawaller, 2001 and *L. costata* sp. nov. This study provided a description and illustrations of this new species, as well as the results of DNA barcoding. Molecular species identification was conducted using newly sequenced COI data (Table 1),



Academic editor: Fedor Konstantinov

Received: 23 July 2024

Accepted: 17 November 2024

Published: 13 December 2024

ZooBank: <https://zoobank.org/EA20F573-24FB-48A9-AEB5-7DB685FDDC69>

Citation: Wang H, Wei Z, Ren G (2024) A new species of *Laena* Dejean (Coleoptera, Tenebrionidae) from Sichuan Province, China, with an updated key. ZooKeys 1221: 165–173. <https://doi.org/10.3897/zookeys.1221.132774>

Copyright: © Haizhi Wang et al.

This is an open access article distributed under terms of the Creative Commons Attribution License (Attribution 4.0 International – CC BY 4.0).

along with previously published COI sequences of *Laena* species (Wei and Ren 2023, 2024). An updated key to *Laena* species from Sichuan Province, modified from Wei et al. (2020), is provided. Seven *Laena* species (*L. baogua* Schawaller, 2021, *L. chunyang* Schawaller, 2021, *L. dentithoraxa* Wei & Ren, 2023, *L. grebennikovi* Schawaller, 2021, *L. mounigouica* Wei & Ren, 2023, *L. wannian* Schawaller, 2021, and *L. costata* sp. nov.) are added to this key.

## Materials and methods

The examined specimens of the genus *Laena* were collected in the Micangshan Nature Reserve of Sichuan Province, China, and are deposited at the Museum of China West Normal University (MCWNU). All examined specimens were collected by sifting leaf litter. The specimens were examined using an Olympus SZX10 stereomicroscope. Images were taken using a Canon EOS 9D Mark III camera with a Laowa FF 25 mm F2.8 Ultra Macro 2.5–5× lens.

The sequences of the mitochondrial gene COI were used for molecular species identification. The leg muscles were used for DNA extraction using the Ezup Column Animal Genomic DNA Purification Kit (Shanghai, China). The sequences were obtained using polymerase chain reaction (PCR) amplification with the primer pair LCO1490 and HCO2198 (Folmer et al. 1994) and the settings used in Wei and Ren (2023). The PCR products were sequenced by Sangon Biotech Co. Ltd (Shanghai, China) after examined using 1.0% agarose gel electrophoretic analysis.

*Anaedus brunneus* (Ziegler, 1844), *Grabulax darlingtonia* Kanda, 2016, and three species of the genus *Hypolaenopsis* Masumoto, 2001 were chosen as outgroups in this study. The newly available DNA sequences were checked and edited using SeqMan v. 7.1.0. Then the new COI sequences (Table 1) and previously known 34 sequences (GenBank accession nos. OR682144–OR682149, OR721926, OR721927, OR721930–OR721939, OR721941–OR721953) were aligned using Clustal W (Thompson et al. 1994) and trimmed using trimmAl v. 1.2 (Capella-Gutiérrez et al. 2009). Based on Bayesian information criterion, the best substitution model, GTR+I+G4+F, was calculated using ModelFinder (Kalyaanamoorthy et al. 2017) that plugged into PhyloSuite v. 1.2.2 (Zhang et al. 2020). The maximum-likelihood (ML) tree was constructed using IQ-TREE v. 1.6.6 (Nguyen et al. 2015) which was also integrated in PhyloSuite. To estimate node reliability, we performed ML analysis using 1,000 ultrafast bootstrapping and 1,000 SH-aLRT iterations.

**Table 1.** COI GenBank accession numbers and voucher information of *Laena* species provided in this study.

Name	Collection site	GenBank accession no.
<i>Laena qinlingica</i> Schawaller, 2001	China, Sichuan Province, Wangcang County, Micangshan Nature Reserve, Jinchangba, 32.4985°N, 106.6234°E, elev. 1880 m	PQ059651
<i>Laena costata</i> sp. nov.	China, Sichuan Province, Wangcang County, Micangshan Nature Reserve, Jinchangba, 32.4985°N, 106.6234°E, elev. 1880 m	PQ059650
<i>Laena habashanica</i> Schawaller, 2001	China, Yunnan Province, Habaxueshan, Habacun, elev. 2870 m	PQ059648
<i>Laena tryznai</i> Schawaller, 2001	China, Sichuan Province, Xiangcheng County, Redazhen, elev. 3200 m	PQ059647
<i>Laena quinquagesima</i> Schawaller, 2008	China, Yunan Province, Xianggelila, elev. 3200–3500 m	PQ059649

## Results

### Tribe Laenini Seidlitz, 1895

### Genus *Laena* Dejean, 1821

#### *Laena costata* sp. nov.

<https://zoobank.org/FF55FC90-0D17-4216-8A80-68263966C07A>

Fig. 1A–F

**Type material. Holotype:** CHINA • ♂; Sichuan Province, Wangcang County, Micangshan Nature Reserve, Jinchangba; 32.4985°N, 106.6234°E, elev. 1880 m; 2024-IV-21; Zhonghua Wei leg.; MCWNU. **Paratypes:** CHINA – Sichuan Province • 1♀; Wangcang County, Micangshan Nature Reserve, Jinchangba; 32.4985°N, 106.6234°E, elev. 1880 m; 2024-IV-21; Zhonghua Wei leg.; MCWNU • 1♂; Wangcang County, Micangshan Nature reserve, Shiziba; 32.6554°N, 106.5581°E, elev. 1750 m; 2023-IX-7; Zhonghua Wei leg.; MCWNU.

**Description. Male.** Body length 6.4–7.2 mm. Body (Fig. 1B) blackish brown, antennae, maxillary palps, and tibiae reddish brown, tarsi light brown; body dorsum rough and covered with dense punctures bearing short setae. Epistome trapezoidal, each lateral part with two longer setae, surface with dense large punctures bearing short setae; anterior margin distinctly concave. Frontoclypeal suture shallow, straight at middle. Genae ridge-like, strongly raised; surface with dense small punctures. Eyes elliptical and slightly prominent laterally. Frons slightly prominent at middle of anterior portion; surface with dense and large punctures, each puncture with a short seta. Antennae reaching posterior margin of pronotum; antennomere III about 1.7× as long as antennomere II.

Pronotum (Fig. 1C) nearly circular, widest at anterior 1/3, approximately as wide as long; anterior margin nearly straight; lateral margins finely beaded; posterior margin neither bent downwards nor beaded; disc slightly convex, with a longitudinal groove and a pair of shallow depressions at middle, surface with dense and large punctures, distance between punctures equal to 0–1× puncture diameter, each puncture with a short seta; anterior angles rounded and posterior angles obtuse. Prothoracic hypomera with punctures as large as those on pronotal disc, bearing short setae. Prosternal process widest at posterior margin, bent downwards behind coxae; surface with fused large punctures which bear very short setae.

Elytra (Fig. 1D) elongate-oval, approximately 1.5 times as long as wide, widest at middle; strongly prolonged at apices; humeral angles rounded; lateral sides curved; surface rough, without striate, with rows of punctures; punctures in rows bearing short setae, distinctly larger than those on pronotum; intervals with dense fine punctures which bear short setae, intervals I, II, IV and VI flat, III slightly convex, V and VII distinctly convex and ridged, IX with two setigerous pores at posterior portion.

Legs slender. Femora without teeth on inner sides. Tibiae hooked at inner apex; mesotibiae slightly curved on inner sides.

Punctures on abdominal ventrites gradually becoming smaller from ventrite I to V.

Aedeagus (Fig. 1E, F) subfusiform, 1.94–1.96 mm in length. Parameres trapezoidal, widest at base and gradually narrowed from base to apex; apex abruptly widened and strongly arcuated.

**Female.** All the tibiae not hooked at inner sides of apex.

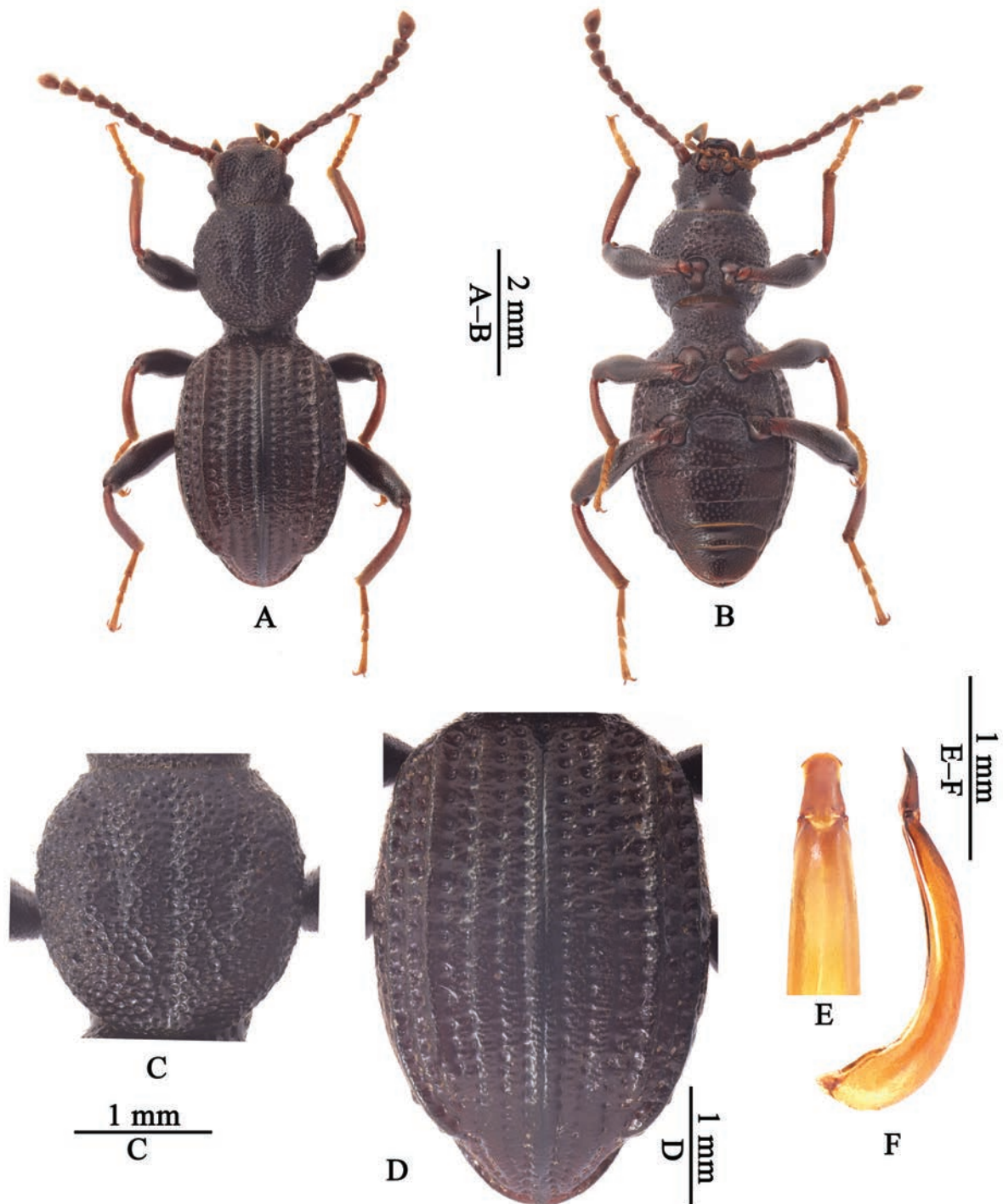


**Figure 1.** The holotype of *Laena costata* sp. nov. **A, B** habitus, in dorsal and ventral views **C** pronotum **D** elytra **E, F** aedeagus, in dorsal (apical portion) and lateral views.

**Diagnosis.** In the phylogenetic tree (Fig. 3), *Laena costata* sp. nov., *L. maowenica* Schawaller, 2008, and *L. bifoveolata* Reitter, 1889 form a clade, and the new species appear sister to *maowenica* Schawaller, 2008, but the relationships are not statistically supported. Based on morphological characteristics, *Laena costata* sp. nov. is similar to *L. bifoveolata* Reitter, 1889, *L. bowaica* Schawaller, 2001, *L. haigouica* Schawaller, 2001, *L. maowenica* Schawaller, 2008 and *L. mounigouica* Wei & Ren, 2023 shared with them body surface having the dense punctures, the pronotal disc

with a longitudinal groove and two median impressions, and non-dentate femora without teeth. This new species can be distinguished from the latter by the following characters: (1) body surface rough, with dense punctures; (2) elytral interval III slightly convex, intervals V and VII distinctly convex and ridged; (3) parameres with apex distinctly broadened and constricted at sides near apex; (4) humeral angles arcuated and not prominent; (5) male tibiae hooked at inner apex.

**Distribution.** China: Sichuan.

**Etymology.** The name is in reference to the elevated and ridged elytral intervals V and VII; *costata*, Latin, meaning ribbed.

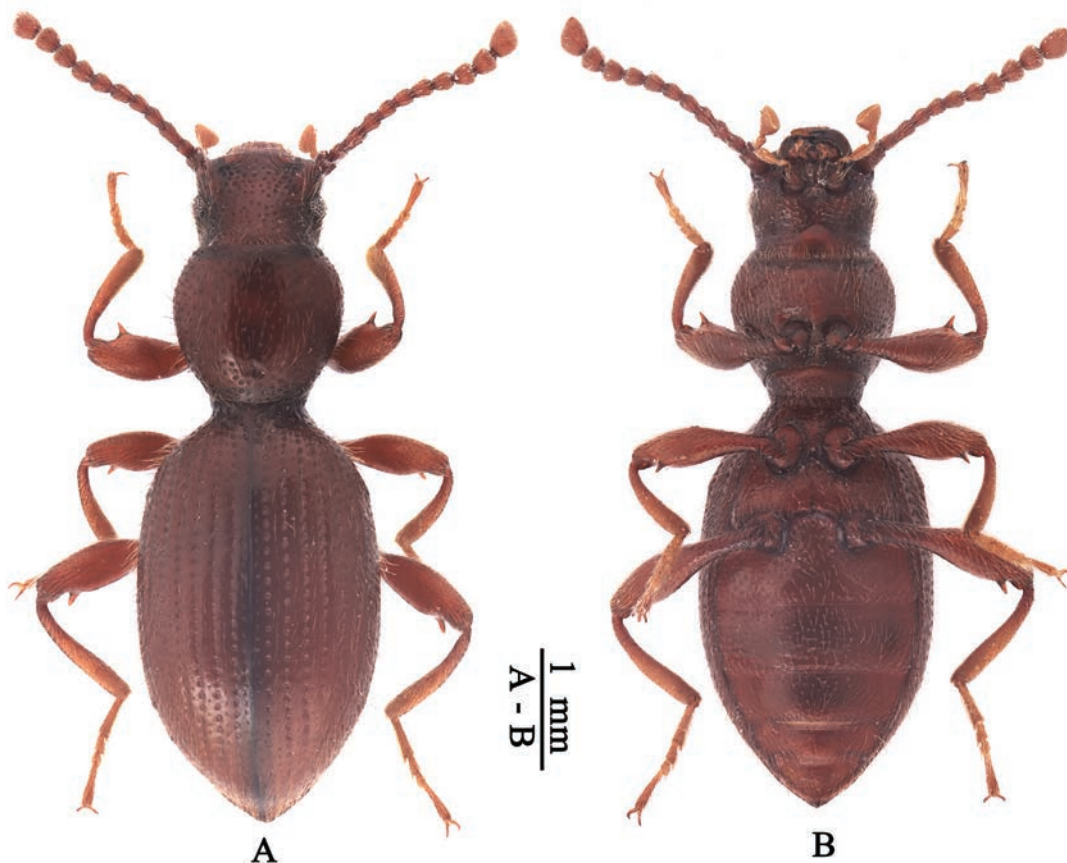
***Laena qinlingica* Schawaller, 2001**

Fig. 2A, B

*Laena qinlingica* Schawaller, 2001: 32; Schawaller 2008: 406; Yuan and Ren 2018: 700; Wei et al. 2020: 527.

**Examined material.** CHINA – Sichuan Province • 2♀ (in 95% ethanol); Wangcang County, Micangshan Nature reserve, Shuiliandong; 2023-IX-8; Zhonghua Wei leg.; MCWNU • 2♂5♀ (2♂4♀ in 95% ethanol); Wangcang County, Micangshan Nature reserve, Jinchangba; 32.4985°N, 106.6234°N, elev. 1880 m; 2024-IV-21; Zhonghua Wei leg.; MCWNU.

**Distribution.** China: Sichuan, Shaanxi.



**Figure 2.** The habitus of *Laena qinlingica* Schawaller, 2001 **A** habitus in dorsal view **B** habitus in ventral view.

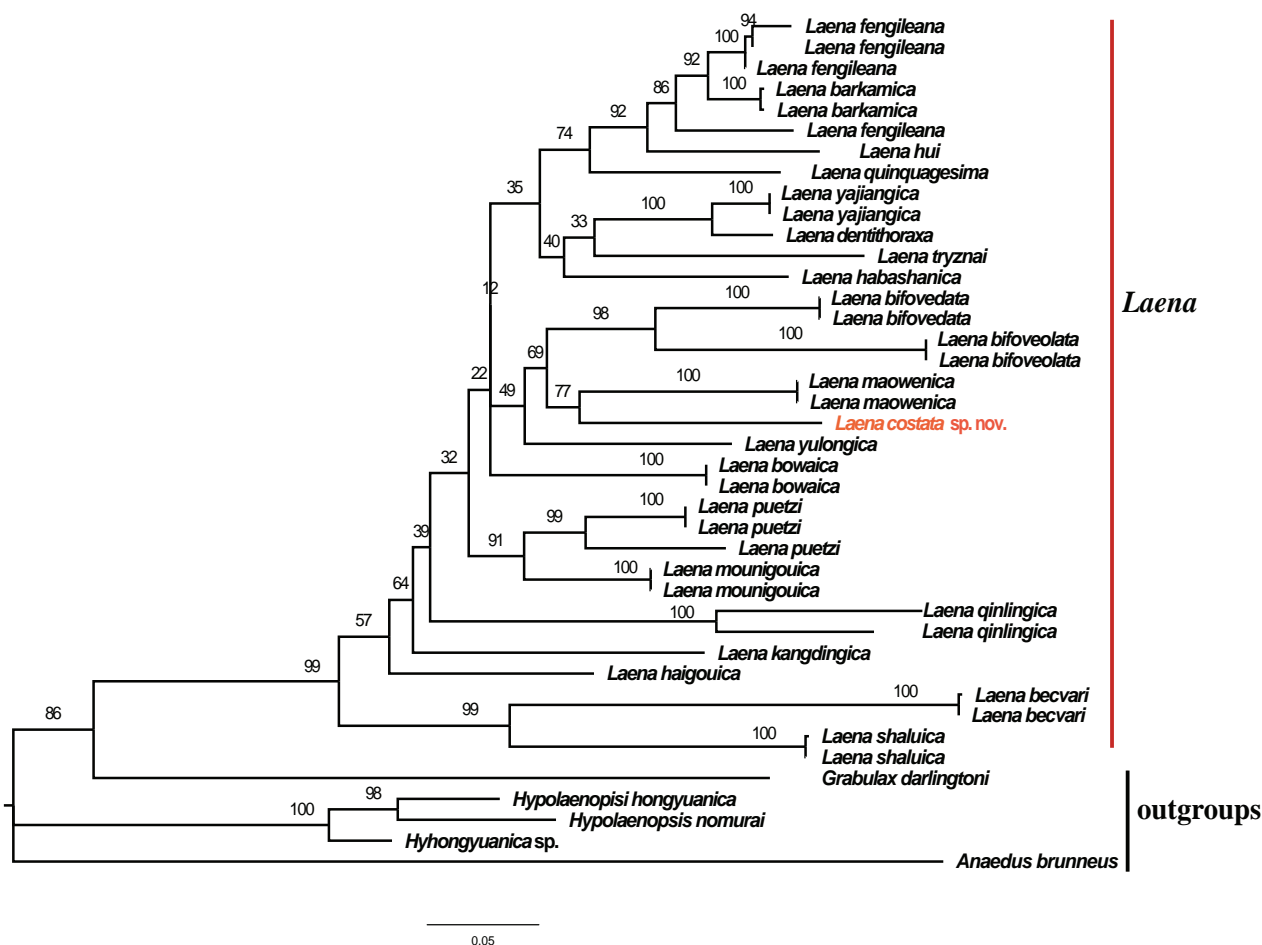


Figure 3. The maximum-likelihood tree of *Laena* species based on available COI sequences. The values on the branches show ultrafast bootstrap supports.

### An updated key to *Laena* species from Sichuan Province modified from Wei et al. (2020)

The couplets 5, 10, 11, 25 and 41 of the key to *Laena* from Sichuan Province provided by Wei et al. (2020) should be modified as follows to include *Laena baogua* Schawaller, 2021, *L. chunyang* Schawaller, 2021, *L. costata* sp. nov., *L. dentithoraxa* Wei & Ren, 2023, *L. grebennikovi* Schawaller, 2021, *L. mounigouica* Wei & Ren, 2023, and *L. wannian* Schawaller, 2021.

- 5 Femora with opposite teeth.....5a
- Femora each with a tooth or angle or spine ..... 6
- 5a Lateral margins of pronotum beaded; pro- and mesofemora each with single tooth, metafemora with opposite teeth ..... ***L. grebennikovi***
- Lateral margins of pronotum not beaded; all femora with opposite teeth... ..5b
- 5b Male protibiae strongly curved at basal third; pronotum with feeble longitudinal impression and on each side with an indistinct impression; body length 8.2–8.5 mm.....***L. baogua***
- Male protibiae weakly curved at base; pronotum with an impression at middle of base; body length 10.6–11.9 mm..... ***L. latitarsia***
- ...

- 10 Pronotum with lateral margins not beaded ..... **10a**
- Pronotum with lateral margins beaded or partially beaded ..... **16**
- 10a Lateral margins of pronotum serrated ..... *L. dentithoraxa*
- Lateral margins of pronotum arcuated ..... **11**
- 11 Elytral intervals V and VII convex or only interval VII convex; male tibiae not hooked or meso- and metatibiae hooked at inner apex ..... **11a**
- Elytral intervals V and VII not convex; male metatibiae hooked at inner apex ..... **13**
- 11a Male tibiae not hooked at inner apex ..... **11b**
- Male meso- and metatibiae hooked at inner apex ..... **12**
- 11b Pronotal disc with a pair of impressions at middle; elytral intervals with a few scattered fine punctures ..... *L. chungyang*
- Pronotal disc without impressions at middle; elytral intervals with a row of fine punctures ..... *L. wannian*
- ...
- 25 Elytral interval VII convex, swollen and knob-shaped at shoulder ..... **25a**
- Elytral interval VII not convex and not knob-shaped at shoulder ..... **27**
- 25a Lateral margins of pronotum beaded; elytral interval VII not swollen .....  
..... *L. costata sp. nov.*
- Lateral margins of pronotum not beaded; elytral interval VII swollen ..... **26**
- ...
- 41 Elytral intervals with small scattered punctures; all male tibiae hooked at inner apex ..... **41a**
- Elytral intervals with a regular row of small punctures; male meso- and metatibiae hooked at inner apex, without granules ..... **42**
- 41a Male metatibiae with granules on inner sides; elytral intervals with a row of punctures, interval IX with two setiferous pores ..... *L. hengduanica*
- Male metatibiae without granules on inner sides; elytral intervals with scattered fine punctures, interval IX with three setiferous pores .....  
..... *L. mounigouica*

## Acknowledgements

We thank the staff of the Micangshan Nature Reserve Administration for providing help in sample collection. We also appreciate the reviewers and academic editor for improving the quality of this manuscript.

## Additional information

### Conflict of interest

The authors have declared that no competing interests exist.

### Ethical statement

No ethical statement was reported.

### Funding

This study was supported by the Biodiversity Survey and Monitoring of the Micang Mountains National Nature Reserve (KH2023-016) and the Sichuan Provincial Natural Science Foundation (2024NSFSC0076).

## Author contributions

Conceptualization: ZHW, GDR. Data curation: HZW, ZHW. Formal analysis: ZHW. Visualization: HZW, ZHW. Writing – original draft: HZW, ZHW. Writing – review and editing: ZHW.

## Author ORCIDs

Zhonghua Wei  <https://orcid.org/0000-0001-7349-9939>

Guodong Ren  <https://orcid.org/0000-0001-5808-9122>

## Data availability

All of the data that support the findings of this study are available in the main text.

## References

- Bouchard P, Bousquet Y, Aalbu RL, Alonso-Zarazaga MA, Merkl O, Davies AE (2021) Review of genus-group names in the family Tenebrionidae (Insecta, Coleoptera). *ZooKeys* 1050: 1–633. <https://doi.org/10.3897/zookeys.1050.64217>
- Capella-Gutiérrez S, Silla-Martínez JM, Gabaldón T (2009) TrimAl: a tool for automated alignment trimming in large-scale phylogenetic analyses. *Bioinformatics* 25(15): 1972–1973. <https://doi.org/10.1093/bioinformatics/btp348>
- Folmer O, Black M, Hoeh W, Lutz R, Vrijenhoek R (1994) DNA primers for amplification of mitochondrial cytochrome c oxidase subunit I from diverse metazoan invertebrates. *Molecular Marine Biology and Biotechnology* 3(5): 294–299.
- Kalyaanamoorthy S, Minh BQ, Wong TKF, von Haeseler A, Jermin LS (2017) ModelFinder: fast model selection for accurate phylogenetic estimates. *Nature Methods* 14(6): 587–589. <https://doi.org/10.1038/nmeth.4285>
- Nguyen LT, Schmidt HA, von Haeseler A, Minh BQ (2015) IQ-TREE: a fast and effective stochastic algorithm for estimating maximum-likelihood phylogenies. *Molecular Biology and Evolution* 32(1): 268–274. <https://doi.org/10.1093/molbev/msu300>
- Schawaller W (2001) The genus *Laena* Latreille (Coleoptera: Tenebrionidae) in China, with descriptions of 47 new species. *Stuttgarter Beitrriigezur Naturkunde Serie A (Biologie)* 632: 1–62.
- Schawaller W (2008) The genus *Laena* Latreille (Coleoptera: Tenebrionidae) in China (part 2) with descriptions of 30 new species and a new identification key. *Stuttgarter Beitrriige zur Naturkunde A, Neue Serie* 1: 387–411.
- Schawaller W, Bellersheim A (2023) New species and records of *Laena* Dejean (Coleoptera: Tenebrionidae: Lagriinae) from Vietnam, southeastern China, and Korea. *Zootaxa* 5296(4): 540–550. <https://doi.org/10.11646/zootaxa.5296.4.3>
- Thompson JD, Higgins DG, Gibson TJ (1994) Clustal W: Improving the sensitivity of progressive multiple sequence alignment through sequence weight, position-specific gap penalties and weight matrix choice. *Nucleic Acids Research* 22(22): 4673–4680. <https://doi.org/10.1093/nar/22.22.4673>
- Wei ZH, Ren GD (2023) Two new species of the genus *Laena* (Coleoptera, Tenebrionidae, Lagriinae) from northern Sichuan in China based on morphological and molecular data. *ZooKeys* 1173: 71–83. <https://doi.org/10.3897/zookeys.1173.103125>
- Wei ZH, Ren GD (2024) Review of the genus *Laena* Dejean, 1821 (Coleoptera, Tenebrionidae) from Gansu Province, China, with the description of a new species. *ZooKeys* 1190: 121–130. <https://doi.org/10.3897/zookeys.1190.114201>

- Wei ZH, Zhao XL, Ren GD (2020) Taxonomic study of the genus *Laena* from Sichuan in China, with description of four new species (Coleoptera: Tenebrionidae). *Journal of Asia-Pacific Entomology* 23(2): 516–528. <https://doi.org/10.1016/j.aspen.2019.12.016>
- Yuan CX, Ren GD (2018) Tenebrionidae. In: Yang XK (Ed.) *Insect fauna of the Qinling Mountains. Coleoptera I*. World Book Publishing Xi'an Co. Ltd, Xi'an, 697–701.
- Zhang D, Gao F, Jakovlić I, Zou H, Zhang J, Li WX, Wang GT (2020) PhyloSuite: An integrated and scalable desktop platform for streamlined molecular sequence data management and evolutionary phylogenetics studies. *Molecular Ecology Resources* 20(1): 348–355. <https://doi.org/10.1111/1755-0998.13096>



# Annotated checklist of Sarcophagidae (Diptera) of Jamaica, with new records

Latoya Foote-Gordon<sup>1</sup>, Eric Garraway<sup>1</sup>, Thomas Pape<sup>2</sup>, Eliana Buenaventura<sup>3</sup>

1 Department of Life Sciences, University of the West Indies, Mona, Kingston, Jamaica

2 Natural History Museum of Denmark, Copenhagen, Denmark

3 Grupo de Entomología Universidad de Antioquia – GEUA, Universidad de Antioquia, Medellín, Colombia

Corresponding author: Latoya Foote-Gordon ([latoyafote@yahoo.com](mailto:latoyafote@yahoo.com))

## Abstract

An annotated checklist of the Sarcophagidae of Jamaica is presented based on material collected from 2018 to 2024, supplemented with specimens in museum collections as well as literature records. The checklist comprises 45 species from 21 genera, of which 23 species from 15 genera were collected during the present study and identified based on male terminalia. The following species are recorded from Jamaica for the first time: *Bahamiola orbitalis* Dodge, *Peckia (Sarcodexia) dominicana* (Lopes), *Tapacura mariarum* Tibana & Lopes, and *Lepidodexia (Harpagopyga) diversipes* (Coquillet).

**Key words:** Caribbean, checklist, diversity, flesh flies, Jamaica, Miltogramminae, Sarcophaginae, taxonomy



Academic editor: Filippo Di Giovanni

Received: 30 August 2024

Accepted: 24 October 2024

Published: 13 December 2024

ZooBank: <https://zoobank.org/6B22A82F-C506-4232-8020-72CD1410DB01>

Citation: Foote-Gordon L, Garraway E, Pape T, Buenaventura E (2024) Annotated checklist of Sarcophagidae (Diptera) of Jamaica, with new records. ZooKeys 1221: 175–203. <https://doi.org/10.3897/zookeys.1221.135698>

Copyright: © Latoya Foote-Gordon et al. This is an open access article distributed under terms of the Creative Commons Attribution License (Attribution 4.0 International – CC BY 4.0).

## Introduction

The family Sarcophagidae or flesh flies is a diverse family of Diptera, currently with 172 genera and 3094 described species (Pape et al. 2011; Buenaventura and Pape 2013), which are classified into three subfamilies: Miltogramminae, Paramacronychiinae, and Sarcophaginae. Members of the family are diverse in their feeding habits, including coprophagy, parasitism, predation and necrophagy (Lopes 1982; Mullen et al. 1984; Ferrar 1987; Bänziger and Pape 2004; Vairo et al. 2015; Buenaventura 2021).

Flesh flies of the large subfamily Sarcophaginae show a variable degree of synanthropy or preference for human-modified environments (Beltran et al. 2012; Yepes-Gaurisas et al. 2013; Valverde-Castro et al. 2017; Buenaventura et al. 2021a), and several species have importance for forensic sciences (Oliveira and Vasconcelos 2010; Segura et al. 2011; Cherix et al. 2012; Szpila et al. 2015; Villet et al. 2017), while others may be mechanical carriers of pathogens (Sukontason et al. 2006) or play a role as general (Howlett et al. 2016) or more specific (Wisniewska et al. 2019) pollinators. Flesh flies are hypothesized to have originated in the Neotropical region (Buenaventura et al. 2021b; Buenaventura 2021; Yan et al. 2021), with species predominantly belonging to the subfamily Sarcophaginae. However, further research is warranted to elucidate their evolutionary history, ecological roles and geographical distribution.

This paper aims to update the list of species of Sarcophagidae from Jamaica based on data obtained from recent collections (2018–2024), specimens in the insect collection in the Department of Life Sciences of the University of the West Indies (**DLSUWI**) and the Natural History Museum of Jamaica (**NHMJ**), and literature records. Research on Sarcophagidae diversity from Caribbean islands has yielded the numbers given in Table 1.

**Table 1.** Sarcophagidae diversity of Caribbean Islands.

Caribbean Island	Number of Species
Antigua (Pape 1996)	1
Barbados (Pape 2024)	1
Cayman Island (Pape 1996)	1
Curaçao (Pape 2024)	1
Guadeloupe (Pape 1996)	2
Grenadines (Pape 1996)	2
St. Lucia (Pape 1996)	3
St. Vincent (Pape 1996)	5
British Virgin Islands (Pape 1996)	4
United States Virgin Islands (Pape 1996)	4
Turks and Caicos Island (Pape 1996)	7
Haiti (Pape 1996)	8
Martinique (Pape 1996)	9
Puerto Rico (Curran 1928)	30
Dominica (Pape 2024)	36
Trinidad & Tobago (Pape 2024)	39
Jamaica (Dodge 1965b; Pape 1989)	39
Bahamas (Dodge 1965a)	43
Cuba (Pape 2024)	55

To date, there are no records of Sarcophagidae species on Caribbean islands such as St. Kitts and Nevis and Grenada. However, the number of flesh fly species documented in the Caribbean archipelago is expected to increase with further field research and more intensive sampling efforts.

Dodge (1965b) provides the most comprehensive documentation of Jamaican Sarcophagidae, recording 39 species, 16 of which were described as new. Few collections or biological observations of Sarcophagidae have been documented from Jamaica since the 1960s (Freeman and Taffe 1974; Freeman and Jayasingh 1975; Pape 1989; Foote 2014; Foote-Gordon and Garraway 2023a, 2023b, 2023c), and the knowledge of Jamaican Sarcophagidae is certainly incomplete.

This research aims to expand the understanding of flesh fly diversity and distribution in Jamaica through comprehensive field collections, a systematic review of historical literature, and the analysis of museum specimens housed at the Natural History Museum of Jamaica and the Department of Life Sciences of the University of the West Indies.

## Materials and methods

### Study area

Jamaica is situated in the tropical zone approximately 18 degrees north of the equator and is part of the archipelago of the Caribbean Islands. The island measures 232 km in length, with a width ranging from approximately 48 to 80 km and encompasses an area of 10,992 km<sup>2</sup> (Wilson 2004).

The study area encompasses twelve habitat types (Table 2), such as coastal and freshwater mangrove forests, dry and wet limestone forests, wet and dry forests, wet and dry montane forests, inland wetlands, urban and suburban communities, and rural farms. A total of 17 sampling localities were selected across these habitat types (Fig. 1, Table 2).

**Table 2.** List of sampling localities of Sarcophagidae in Jamaica between 2018 and 2024.

	Locality	Geographic coordinates	Altitude (m)	Habitat description
<b>A</b>	Merrywood, St. Elizabeth	18°13'04"N, 77°51'02"W	220	Rural farm
<b>B</b>	Windsor, Trelawny	18°21'09"N, 77°38'47"W	98	Wet limestone forest
<b>CD</b>	Rio Bueno property, St. Ann	18°28'30"N, 77°26'41"W	25	Dry limestone forest
		18°28'01"N, 77° 27'51"W	10	Solitary wasp nest
<b>E</b>	Belair, St. Ann	18°27'23"N, 77°21'08"W	15	Dry limestone forest
<b>F</b>	Green Grotto, St. Ann	18°05'15"N, 77°24'57"W	15	Freshwater mangrove forest
<b>G</b>	Roaring River, St. Ann	18°24'52"N, 77°09'32"W	94	Dry limestone forest
<b>H</b>	Hardware Gap, Portland	18°05'15"N, 76°42'13"W	1050	Wet montane forest
<b>I</b>	Comfort Castle, Portland	18°03'14"N, 76°24'46"W	147	Wet montane forest, rural/farm community
<b>J</b>	Bowden Pen, St. Thomas	18°02'27"N, 76°23'55"W	290	Wet limestone forest
<b>K</b>	Salt Hill, St. Andrew	18°02'00"N, 76°40'29"W	1210	Dry montane forest and farmlands
<b>L</b>	Red Light, St. Andrew	18°03'36"N, 76°43'23"W	988	Dry forest and suburban community
<b>M</b>	Mona, St. Andrew	18°00'22"N, 76°45'00"W	180	Urban community
<b>N</b>	Port Royal, St. Andrew	17°56'29"N, 76°50'02"W	4	Coastal mangrove forest
<b>O</b>	Newport, Manchester	17°57'17"N, 77°29'41"W	715	Suburban community
<b>PQ</b>	Mason River, Clarendon	18°11'47"N, 77°15'35"W	700	Inland wetland

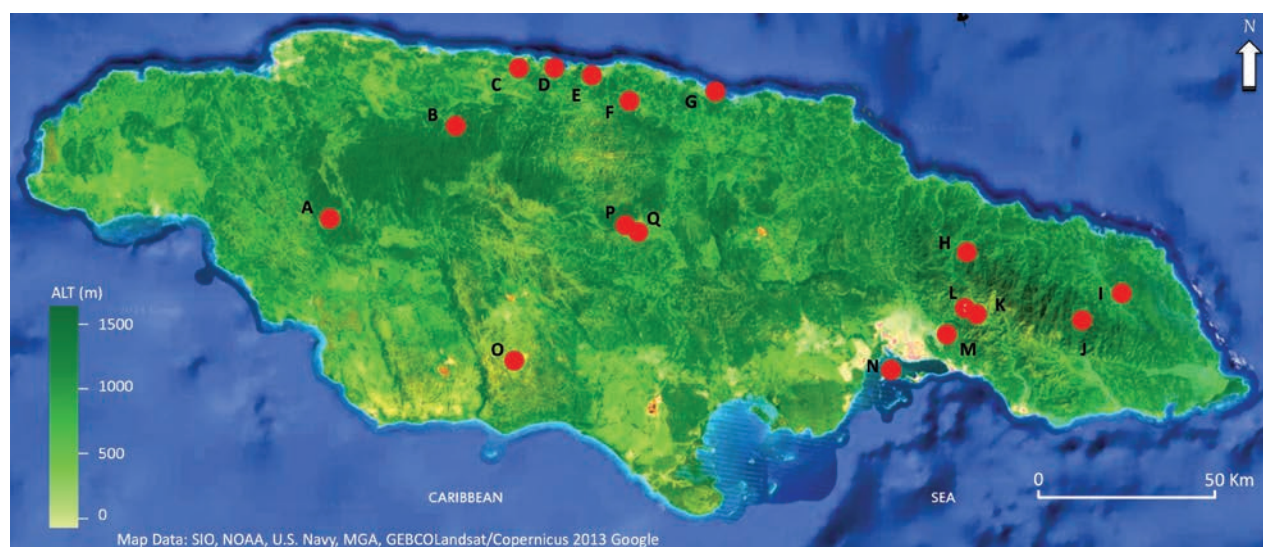


**Figure 1.** Distribution of sampling sites in Jamaica between 2018 and 2024. **A** Merrywood, St. Elizabeth; **B** Windsor, Trelawny; **C, D** Rio Bueno, St. Ann; **E** Belair, St. Ann; **F** Green Grotto, St. Ann; **G** Roaring River, St. Ann; **H** Hardware Gap, Portland; **I** Comfort Castle, Portland; **J** Bowden Pen, St. Thomas; **K** Salt Hill, St. Andrew; **L** Red Light, St. Andrew; **M** Mona, St. Andrew; **N** Port Royal, St. Andrew; **O** Newport, Manchester; **P, Q** Mason River, Clarendon.

## Specimen sampling, identification, and documentation

Field expeditions were carried out between 2018 and 2024. Sample collection was conducted throughout the year, regardless of rainy and dry seasons, depending on the availability of resources. Many of the flies were collected with Van Someren-Rydon (VSR) traps and plastic bottle traps (Hwang and Turner 2005), and a few were collected with hand nets. Traps were baited separately with various decomposing meats, such as chicken and pork, and fermented fruits. At each site, two VSR traps were placed at a minimum height of 1.5 m above ground and spaced at least 50 m apart. The traps were left in place for a minimum of 4 h and a maximum of 12 h.

Specimens were collected and preserved in 95% ethanol. Flesh flies were carefully pinned, and their terminalia extended for detailed examination and taxonomic identification. Taxonomic identifications were made of males only, as females are difficult to identify. Taxonomic keys, descriptions, and illustrations by Dodge (1965a, b), Giroux and Wheeler (2009), and Buenaventura and Pape (2013) were used to identify species.

Neotropical distribution data were taken from 'A taxonomic database to all flesh flies' (Pape 2024), and distribution in Jamaica is based on the specimens collected during the present study and specimens from the insect collections of the Department of Life Sciences, University of the West Indies (DLSUWI) and the Natural History Museum of Jamaica (NHMJ).

Photographs of male terminalia were produced with a Leica M205 C stereo microscope system camera.

## Format of checklist

The checklist is arranged in alphabetical order, first by subfamily, then by genus and species. Each species entry starts with a valid species name, the authority, and the year of publication. For all collected specimens and museum material, the following information is recorded: locality and date of collection, number and sex of specimens, collector(s), and depository. Entries are separated by semicolons. For localities with multiple hierarchical levels, a comma separates the exact sampling site from the main locality or parish. Species previously recorded from Jamaica have their published records listed in a section titled "Literature records", while species recorded from Jamaica for the first time are indicated as "New records." For each species, the general distribution within the Neotropical region is also provided. Remarks are included when applicable.

## Results

A total of 731 specimens of flesh flies from Jamaica were examined from field expeditions, which included 325 females and 406 males, with 45% of the males belonging to only four species (Table 3). The survey revealed new records of flesh flies for the island, namely *Bahamiola orbitalis* Dodge, 1965, *Peckia (Sarcodexia) dominicana* Lopes, 1982, *Tapacura mariarum* Tibana & Lopes, 1985, and *Lepidodexia (Harpagopyga) diversipes* (Coquillett, 1900). These new records increased the total number of flesh fly species known

**Table 3.** Abundance and distribution of the most common and widespread species during the study. Only males are included.

Species	Number of individuals	Localities
<i>Bahamiola orbitalis</i>	94	5
<i>Oxysarcodexia peltata</i>	46	10
<i>Peckia chrysostoma</i>	29	8
<i>Peckia nicasia</i>	14	6

from the country to 45 (Table 4). Most of the species belong to the genus *Peckia* Robineau-Desvoidy, 1830 with six species, followed by *Oxysarcodexia* Townsend, 1917 with three species. The remaining 13 genera are represented by one or two species each. The rarest species found within the genus *Peckia* are *Peckia (Euboettcheria) buethni* (Dodge, 1965) and *Peckia (Peckia) hillifera* (Aldrich, 1916), each with only one individual, found in Rio Bueno, St. Ann and in Belair, St. Ann, respectively.

## Checklist

### Subfamily Miltogramminae Lioy, 1864

#### Genus *Amobia* Robineau-Desvoidy

##### 1. *Amobia floridensis* (Townsend, 1892)

**Literature records.** Dodge (1965b); Lopes (1969); Freeman and Taffe (1974); Freeman and Jayasingh (1975); Pape (1996).

**Neotropical distribution.** Belize, Brazil, Costa Rica, Cuba, Ecuador, Galápagos Is, Guyana, Jamaica, Panama, Peru, Puerto Rico, Trinidad & Tobago, Venezuela.

#### Genus *Metopia* Meigen

##### 2. *Metopia argyrocephala* (Meigen, 1824)

**Literature records.** Johnson (1919, as *Metopia leucocephala*); Gowdey (1926); Dodge (1965b); Lopes (1969); Pape (1996).

**Neotropical distribution.** Belize, Cuba, Dominican Republic, Ecuador, El Salvador, Guatemala, Jamaica, Mexico, Peru, Puerto Rico.

**Newly collected material.** • Rio Bueno Property, St. Ann; 31 May 2018; 1 ♂; E. Buenaventura leg. (DLSUWI).

**Remarks.** Collected during the present study with a sweep net near nests of solitary wasps.

#### Genus *Opsidia* Coquillett

##### 3. *Opsidia jamaica* Pape, 1989

**Literature records.** Pape (1989); Pape (1996).

**Neotropical distribution.** Jamaica.

**Genus *Senotainia* Macquart**

**4. *Senotainia rubriventris* Macquart, 1846**

**Literature records.** Johnson (1919); Dodge (1965b); Lopes (1969); Pape (1996).

**Neotropical distribution.** Bahamas, Jamaica, Puerto Rico.

**5. *Senotainia trilineata* (Wulp, 1890)**

**Literature records.** Johnson (1919); Dodge (1965b); Lopes (1969); Pape (1996).

**Neotropical distribution.** Bahamas, Costa Rica, El Salvador, Jamaica, Mexico, Nicaragua, Peru.

**Subfamily Sarcophaginae Macquart, 1834**

**Genus *Argoravinia* Townsend, 1917**

**6. *Argoravinia candida* (Curran, 1928)**

**Literature records.** Dodge (1965b); Lopes (1969); Pape (1996); Carvalho-Filho and Esposito (2012).

**Neotropical distribution.** Cuba, Jamaica, Puerto Rico.

**7. *Argoravinia rufiventris* (Wiedemann, 1830)**

**Literature records.** Dodge (1965b, as *Argoravinia modesta*); Lopes (1969); Pape (1996); Livingstone (2006); Dufek et al. (2015); Sousa et al. (2015).

**Neotropical distribution.** Argentina, Brazil, Colombia, Jamaica, Trinidad & Tobago.

**Newly collected material.** • Mona, St. Andrew; 06 Sep. 2018; 46 ♂; L. Foote leg. (DLSUWI).

**Museum material.** • Rio Cobre, St. Catherine; 23 Sept. 1954; 1 ♂; T. H. Farr leg. (NHMJ).

**Remarks.** Found associated with corpses, hence of potential forensic importance (Dufek et al. 2015). It is known to infest turtle eggs (Smith 2001; Livingstone 2006). In the current study, it was collected in VSR traps containing decomposing chicken. It has been collected from the carcasses of bears, deer and swine in Louisiana using pitfall traps and manual sampling (Grindley-Watson 2004). *Argoravinia rufiventris* is associated with human faeces, fish and bovine spleen (Barbosa 2019). It is also collected from pig carcasses (Barros et al. 2008).

**Genus *Bahamiola* Dodge, 1965**

**8. *Bahamiola orbitalis* Dodge, 1965**

**Neotropical distribution.** Bahamas, Jamaica (New record).

**Newly collected material.** • Windsor, Trelawny; 01 Jun. 2018; 38 ♂; L. Foote and E. Buenaventura leg. (DLSUWI) • Green Grotto, St. Ann, 31 May 2018; 19 ♂;

L. Foote and E. Buenaventura leg. (DLSUWI) • Belair, St. Ann; 31 May 2018; 16 ♂; L. Foote and E. Buenaventura leg. (DLSUWI) • Rio Bueno Property, St. Ann; 31 May 2018; 2 ♂; L. Foote and E. Buenaventura leg. (DLSUWI) • Red Light, St. Andrew; 19 Mar. 2024; 19 ♂; L. Foote leg. (DLSUWI).

**Remarks.** The genus contains two species, *Bahamiola orbitalis* and *Bahamiola gregori* Rohdendorf, 1971. This study presents the first record of the genus and species in Jamaica. It was collected in VSR traps with decomposing chicken and was the most frequently collected species during the study.

### Genus *Blaesoxipha* Loew, 1861

#### 9. *Blaesoxipha (Kellymyia) jamacoorum* (Dodge, 1965)

Fig. 2

**Literature records.** Dodge (1965b); Lopes (1969); Pape (1996).

**Neotropical distribution.** Jamaica.

**Newly collected material.** • Roaring River, St. Ann; 19 Oct. 2018; 2 ♂; L. Foote leg. (DLSUWI) • Mason River, Clarendon; 26 Nov. 2019; 1 ♂; L. Foote leg. (DLSUWI) • Red Light, St. Andrew; 19 Mar. 2024; 3 ♂; L. Foote leg. (DLSUWI).



Figure 2. *Blaesoxipha (Kellymyia) jamacoorum*. Male terminalia, lateral view; endemic to Jamaica. Scale bar: 1 mm.

**Museum material.** • Mocho, Clarendon; 16 Nov. 1978; 1 ♂; J. Simpson leg. (DLSUWI) • Jacksonville; 05 Oct 1997; 1 ♂; M. Peddie leg. (DLSUWI) • Highgate, St. Mary; 05 Oct. 2008; 1 ♂; M. Grant leg. (DLSUWI) • Windsor, Trelawny; 28 Sep. 2014; 1 ♂; D. Wilkins leg. (DLSUWI) • Lewisburg, St. Mary; 18 Oct. 2015; 1 ♂; Heslop leg. (DLSUWI) • Halse Hall, Clarendon; Mona, St. Andrew; 27 Oct. 2016; 2 ♂; K. Minott leg. (DLSUWI).

**Remarks.** Collected on overripe mango fruit by Dodge (1965b). In this study, it was collected from decomposing chicken and pork.

#### 10. *Blaesoxipha (Gigantotheca) plinthopyga* (Wiedemann, 1830)

**Literature records.** Johnson (1919); Lopes (1941); Dodge (1965b); Pape (1996); Mello-Patiu (2016).

**Neotropical distribution.** American Virgin Is, Bahamas, Brazil, Costa Rica, Cuba, Dominica, Dominican Republic, El Salvador, Galápagos Is, Guatemala, Guyana, Jamaica, México, Nicaragua, Panamá, Puerto Rico, Venezuela.

**Newly collected material.** • Mona, St. Andrew; 26 Jun. 2018; 10 ♂; L. Foote leg. (DLSUWI).

**Museum material.** • Morant Bay, St. Thomas; 28 Jan. 1989; 1 ♂; (DLSUWI) • Stony Hill, St. Andrew; 17 May 1992; 1 ♂; J. Rodent leg. (DLSUWI) • Meadowbrook Estate, Kingston; 21 Oct 2003; 1 ♂; C. McIntosh leg. (DLSUWI) • Spanish Town, St. Catherine; 18 Nov. 2006; 1 ♂; T. McIntyre leg. (DLSUWI) • Havendale, Kingston; 09 Nov. 2011; 1 ♂; P. Sutherland leg. (DLSUWI) • Mona, St. Andrew; 17 Mar. 2015; 2 ♂; Gilles-Lee leg. (DLSUWI) • Downtown, Kingston; 07 Nov. 1946; 2 ♂, 5 ♀; G. B. Thomspen leg. (NHMJ) • Downtown, Kingston; 18 Dec. 2013; 6 ♂, 4 ♀; L. Wright leg. (NHMJ).

**Remarks.** This widely distributed species was reported on a human corpse in the USA (Wells and Smith 2013), and it is considered medically and forensically important (Barbosa 2019). Dodge (1965b) mentions specimens that were “bred from dead crocodile.” During the study period, it was reared from buried pork bait in Jamaica.

#### Genus *Boettcheria* Parker, 1914

##### 11. *Boettcheria parkeri* (Aldrich, 1916)

Fig. 3

**Literature records.** Johnson (1919); Dodge (1965b); Lopes (1969); Pape (1996).

**Neotropical distribution.** Jamaica.

**Newly collected material.** • Bowden Pen, St. Thomas; 05 Jun. 2018; 7 ♂; E. Buenaventura leg. (DLSUWI) • Salt Hill, St. Andrew; 26 Feb. 2024; 1 ♂; L. Foote leg. (DLSUWI).

**Museum material.** • Hermitage Reservoir, St. Andrew; 30 May 1954; 2 ♂; T. H. Farr leg. (NHMJ) • Corn Puss Gap, St. Thomas; 04 Aug. 1948; 1 ♂; R. P. Bengry leg. (NHMJ) • Unity Valley, St. Ann; 14 Nov. 1954; 1 ♂; T. H. Farr leg. (NHMJ).

**Remarks.** *Boettcheria parkeri* is still the only species of *Boettcheria* known from Jamaica (Pape 1996), and as for most other species in this genus, the biology is unknown. It was collected in a VSR trap baited with decomposing



Figure 3. *Boettcheria parkeri*. Male terminalia, lateral view; endemic to Jamaica. Scale bar: 1 mm.

chicken and pork. Members of the genus are often listed as carrion flies (Ramírez-Mora et al. 2012) and are found in a variety of habitats, from old-growth forests to urban areas (Dahlem and Downes 1996).

#### Genus *Chrysagria* Townsend

##### 12. *Chrysagria duodecimpunctata* Townsend, 1935

**Literature records.** Dodge (1965b, as *Sarcophartiomyia tenta*); Lopes (1969, as *Sarcophartiomyia tenta*); Pape (1996); Mello-Patiu (2016).

**Neotropical distribution.** Argentina, Brazil, Colombia, Dominica, Ecuador, Guatemala, Jamaica, Mexico, Peru.

#### Genus *Dexosarcophaga* Townsend, 1917

##### 13. *Dexosarcophaga ruthae* (Dodge, 1965)

**Literature records.** Dodge (1965b); Lopes (1969); Mello (1996); Pape (1996).

**Neotropical distribution.** Jamaica.

**Remarks.** The type series was collected “over broken nest of *Nasutitermes*” (Dodge 1965b).

#### Genus *Helicobia* Coquillett, 1895

##### 14. *Helicobia morionella* (Aldrich, 1930)

**Literature records.** Dodge (1965b); Lopes (1969); Pape (1996); Mello-Patiu (2016); Dufek (2019); Dufek et al. (2020).

**Neotropical distribution.** American Virgin Is, Argentina, Bahamas, Brazil, Colombia, Costa Rica, Cuba, Dominica, Ecuador, El Salvador, Guatemala, Haití, Jamaica, México, Puerto Rico, Venezuela.

**Newly collected material.** • Rio Bueno Property, St. Ann; 31 May 2018; 1 ♂; L. Foote and E. Buenaventura leg. (DLSUWI) • Belair, St. Ann; 31 May 2018; 1 ♂; L. Foote and E. Buenaventura leg. (DLSUWI).

**Museum material.** • Windsor Hotel, St. Ann; 19 Mar. 1955; 1 ♂; T. H. Farr leg. (NHMJ) • Ferry, St. Andrew, 30 Oct. 1946; 1 ♂; G. B. Thompson leg. (NHMJ) • Ferry, St. Andrew; 03 Oct. 1954; 2 ♂; T. H. Farr leg. (NHMJ) • Mona, St. Andrew; 20 Jan. 1947; 2 ♂; G. B. Thompson leg. (NHMJ).

**Remarks.** This necrophagous species is considered to be of forensic importance (Early and Goff 1986). It was collected from a decomposing crab and decomposing chicken in the present study.

#### 15. *Helicobia rapax* (Walker, 1849)

**Literature records.** Johnson (1919, as *Sarcophaga helicis*); Dodge (1965b); Lopes (1969); Pape (1996); Mello-Patiu (2016).

**Neotropical distribution.** Argentina, Belize, Brazil, Cuba, Dominica, Ecuador, El Salvador, Jamaica, Martinique, Mexico, Panama, Peru, Puerto Rico.

**Museum material.** • Road to Holly Mount, St. Andrew; 24 Sept. 1954; 1 ♂; R. P. Bengry leg. (NHMJ) • Mona, St. Andrew; 30 Jan. 1947; 1 ♂; G. B. Thompson leg. (NHMJ) • Half Way Tree, St. Andrew; 06 Aug. 1950; 1 ♂; R. B. Bengry leg. (NHMJ) • Troy, Trelawny; 25 Sept. 1954; 1 ♂; T. H. Farr leg. (NHMJ).

#### Genus *Lepidodexia* Brauer & Bergenstamm, 1891

#### 16. *Lepidodexia (Harpagopyga) albihirta* (Dodge, 1965)

**Literature records.** Dodge (1965b); Lopes (1969); Pape (1996).

**Neotropical distribution.** Jamaica.

#### 17. *Lepidodexia (Harpagopyga) atrata* (Dodge, 1965)

**Literature records.** Dodge (1965b); Lopes (1969); Pape (1996).

**Neotropical distribution.** Jamaica.

#### 18. *Lepidodexia (Harpagopyga) dissimilis* (Dodge, 1965)

**Literature records.** Dodge (1965b); Lopes (1969); Pape (1996)

**Neotropical distribution.** Jamaica.

#### 19. *Lepidodexia (Harpagopyga) diversipes* (Coquillet, 1900)

**Neotropical distribution.** Cuba, Puerto Rico, Jamaica (New record).

**Museum material.** Hardware Gap, Portland; 27 Jul. 1949; 1 ♂; C. B. Lewis leg. (NHMJ).

**20. *Lepidodexia (Harpagopyga) nigribimbo* (Dodge, 1965)**

**Literature records.** Dodge (1965b); Lopes (1969); Pape (1996).

**Neotropical distribution.** Jamaica.

**21. *Lepidodexia (Harpagopyga) villipes* (Dodge, 1965)**

**Literature records.** Dodge (1965b); Lopes (1969); Pape (1996).

**Neotropical distribution.** Jamaica.

**Genus *Oxysarcodexia* Townsend, 1917**

**22. *Oxysarcodexia bakeri* (Lopes, 1945)**

**Literature records.** Dodge (1965b); Lopes (1969); Pape (1996); Mello-Patiu (2016); Souza et al. (2020).

**Neotropical distribution.** Bahamas, Brazil, Chile, Colombia, Cuba, Dominica, Ecuador, El Salvador, Galápagos Is, Guadeloupe, Haití, Honduras, Jamaica, México, Panamá, Puerto Rico, Turks & Caicos Is, Venezuela.

**Newly collected material.** • Belair, St. Ann; 31 May 2018; 1 ♂; L. Foote and E. Buenaventura leg. (DLSUWI) • Green Grotto, St. Ann; 31 May 2018; 1 ♂; L. Foote and E. Buenaventura leg. (DLSUWI) • Merrywood, St. Elizabeth; 24 May 2021; 1 ♂; R. Daley leg. (DLSUWI) • Newport, Manchester; 18 Aug. 2023; 1 ♂; R. Daley leg. (DLSUWI) • Red Light, St. Andrew; 20 Mar. 2024; 1 ♂; L. Foote leg. (DLSUWI) • Comfort Castle, Portland; 27 Mar. 2024; 1 ♂; L. Foote leg. (DLSUWI).

**Museum material.** • Cross Roads, St. Andrew; 05 Sep. 1954; 2 ♀, 1 ♂; T. H. Farr leg. (NHMJ) • Rio Cobre, St. Catherine; 28 Feb. 1954; 1 ♀; T. H. Farr leg. (NHMJ) • Negril, Westmoreland; 19 Jul. 1954; 1 ♀; T. H. Farr leg. (NHMJ) • Molland Bay, St. Thomas; 28 Nov. 1954; 1 ♂; T. H. Farr leg. (NHMJ) • Swamp, St. Thomas; 04 Feb. 1955; 1 ♂; T. H. Farr leg. (NHMJ) • Chovey House, St. Mary; 12 Sept. 1954; 1 ♂; T. H. Farr leg. (NHMJ) • Discovery Bay, St. Ann; 11 Nov. 2012; 1 ♂; Wisdom leg. (DLSUWI) • Woodford, St. Andrew; 08 Nov. 2013; 1 ♂; T. Barrett leg. (DLSUWI) • Windsor, Trelawny; 31 Oct. 2015; 2 ♂; E. Reid leg. (DLSUWI).

**Remarks.** Ubiquitous species with a preference for human settlements (Yepes-Gaurisas et al. 2013). Reports of coprophagous (Flores and Dale 1995) and necrophagous (Yepes-Gaurisas et al. 2013) habits.

**23. *Oxysarcodexia chaetopygialis* (Williston, 1896)**

**Literature records.** Dodge (1965b); Lopes (1969); Pape (1996); Souza et al. (2020).

**Neotropical distribution.** Jamaica, St. Vincent.

#### 24. *Oxysarcodexia corolla* Dodge, 1965

**Literature records.** Dodge (1965b); Lopes (1969); Pape (1996); Souza et al. (2020).

**Neotropical distribution.** Jamaica.

**Newly collected material.** • Hardware Gap, Portland; 29 May 2018; 5 ♂; L. Foote and E. Buenaventura leg. (DLSUWI) • Bowden Pen, St Thomas; 05 Jun. 2018; 2 ♂; L. Foote and E. Buenaventura leg. (DLSUWI) • Red Light, St. Andrew; 26 Feb. 2024; 1 ♂; L. Foote leg. (DLSUWI).

**Remarks.** Little is known about the species except its morphology described by Dodge (1965b). Specimens were collected in a VSR trap baited with decomposing chicken in this study.

#### 25. *Oxysarcodexia dorisae* Dodge, 1965

**Literature records.** Dodge (1965b); Lopes (1969); Pape (1996); Souza et al. (2020).

**Neotropical distribution.** Jamaica.

#### 26. *Oxysarcodexia peltata* (Aldrich, 1916)

**Literature records.** Johnson (1919); Dodge (1965b); Lopes (1946, 1969); Pape (1996); Souza et al. (2020).

**Neotropical distribution.** Bahamas, Cuba, Dominica, Guadeloupe, Jamaica, Mexico, Panama, Puerto Rico, San Andres Islands, St. Lucia, St. Vincent.

**Newly collected material.** • Green Grotto, St. Ann; 31 May 2018; 11 ♂; L. Foote and E. Buenaventura leg. (DLSUWI) • Belair, St. Ann; 31 May 2018; 7 ♂; L. Foote and E. Buenaventura leg. (DLSUWI) • Windsor, Trelawny; 01 Jun. 2018; 5 ♂; L. Foote and E. Buenaventura leg. (DLSUWI) • Bowden Pen, St. Thomas; 05 Jun. 2018; 2 ♂; L. Foote and E. Buenaventura leg. (DLSUWI) • Hardware Gap, Portland; 29 May 2018; 3 ♂; L. Foote and E. Buenaventura leg. (DLSUWI) • Merrywood, St. Elizabeth; 24 May 2021; 2 ♂; R. Daley leg. (DLSUWI) • Newport, Manchester; 18 Aug. 2023; 2 ♂; R. Daley leg. (DLSUWI) • Red Light, St. Andrew; 20 Feb. 2024; 1 ♂; L. Foote leg. (DLSUWI) • Comfort Castle, Portland; 27 Mar. 2024; 10 ♂; L. Foote leg. (DLSUWI).

**Museum material.** • 4 miles South of Buff Bay, Portland; 14 Mar. 1947; 1 ♂; G. B. Thompson leg. (NHMJ) • Quickstep, Trelawny; 10 Mar. 1949; 1 ♀; C. B. Lewis leg. (NHMJ) • Hermitage Dam, St. Andrew; 21 Jan. 1947; 1 ♂; C. B. Lewis leg. (NHMJ) • Negril, Westmoreland; 19 Jul. 1954; 1 ♀; T. H. Farr leg. (NHMJ) • Whitfield Hall, St. Thomas; Dec. 1954; 1 ♀; G.R. Proctor leg. (NHMJ) • Ferry, St. Andrew; 03 Oct. 1954; 2 ♂; T. H. Farr leg. (NHMJ) • Beverly Hills, St. Andrew; 26 Dec. 1954; 1 ♀; (NHMJ) • Long Mountain, St. Andrew; 19 Sep. 1954; 2 ♀, 1 ♂; T. H. Farr leg. (NHMJ) • Rock Hall, St. Andrew; 17 Oct. 1984; 1 ♂; P. Coward leg. (DLSUWI) • Hope Gardens, St. Andrew; 09 Nov. 2003; 2 ♂; V. Thompson leg. (DLSUWI) • Spanish Town, St. Catherine; 02 Nov. 2011; 1 ♂; K. Reid leg. (DLSUWI) • Mona, St. Andrew; 10 Apr. 2014; 2 ♂; S. Matthew leg. (DLSUWI) • Discovery Bay, St. Ann; 14 Sep. 2014; 2 ♂; J. Dixon leg. (DLSUWI) • Roaring River, St. Ann; 03 Oct. 2014; 1 ♂; S. McKenzie leg. (DLSUWI).

**Remarks.** Known for its role as a pollinator of the White Mangrove, *Laguncularia racemosa* (Sánchez-Núñez and Mancera-Pineda 2012). It was collected from decomposing chicken during the present study. *Oxysarcodexia peltata* was the second most frequently collected species during the sampling period, with a presence confirmed across ten localities.

**Genus *Peckia* Robineau-Desvoidy, 1830**

**27. *Peckia (Euboettcheria) buethni* Dodge, 1965**

Fig. 4

**Literature records.** Dodge (1965b); Lopes (1969); Pape (1996); Buenaventura and Pape (2013).

**Neotropical distribution.** Jamaica.

**Newly collected material.** Rio Bueno Property, St. Ann; 31 May 2018; 1 ♂; L. Foote and E. Buenaventura leg. (DLSUWI).

**Remarks.** This species is only known from Jamaica. Dodge (1965b) first described it from Papine, Kingston, approximately 114 km from its collection locality in this study. Its biology is unknown. However, specimens were collected in a VSR trap baited with decomposing chicken in the present study.



**Figure 4.** *Peckia (Euboettcheria) buethni*. Male terminalia, lateral view; endemic to Jamaica. Scale bar: 1 mm.

## 28. *Peckia (Peckia) chrysostoma* (Wiedemann, 1830)

**Literature records.** Lopes (1941; Dodge (1965b); Lopes (1969); Pape (1996); Buenaventura and Pape (2013); Mello-Patiu (2016); Dufek (2019); Dufek et al. (2020); Toma et al. (2020).

**Neotropical distribution.** American Virgin Is, Argentina, Bahamas, Belize, Bolivia, Brazil, Chile, Colombia, Costa Rica, Dominica, Ecuador, French Guiana, Galápagos Is, Guatemala, French Guiana, Guyana, Jamaica, Mexico, Nicaragua, Panama, Peru, Surinam, Trinidad & Tobago, Venezuela.

**Newly collected material.** • Rio Bueno Property, St. Ann; 31 May 2018; 1 ♂; L. Foote and E. Buenaventura leg. (DLSUWI) • Belair, St. Ann; 31 May 2018; 2 ♂; L. Foote and E. Buenaventura leg. (DLSUWI) • Green Grotto, St. Ann; 31 May 2018; 3 ♂; L. Foote and E. Buenaventura leg. (DLSUWI) • Windsor, Trelawny; 01 Jun. 2018; 2 ♂; L. Foote and E. Buenaventura leg. (DLSUWI) • Bowden Pen, St. Thomas; 05 Jun. 2018; 5 ♂; L. Foote and E. Buenaventura leg. (DLSUWI) • Mona, St. Andrew; 17 Jun. 2018; 10 ♂; L. Foote leg. (DLSUWI) • Newport, Manchester; 18 Aug. 2023; 4 ♂; R. Daley leg. (DLSUWI) • Comfort Castle, Portland; 27 Mar. 2024; 2 ♂; L. Foote leg. (DLSUWI).

**Museum material.** • Copa Cabana, St. Thomas; 24 Jan. 1989; 1 ♂; N. Knight leg. (DLSUWI) • Gordon Town, St. Andrew; 15 Jan. 2009; 1 ♂; J. Wynter leg. (DLSUWI) • May Pen, Clarendon; 21 Nov. 2010; 1 ♂; T. Gooden leg. (DLSUWI) • Guys Hill, St. Catherine; 23 Nov. 2011; 2 ♂; D. Allen leg. (DLSUWI) • Green Grotto, St. Ann; 13 Nov. 2010; 1 ♂; D. Herro leg. (DLSUWI) • Discovery Bay, St. Ann; 14 Sept. 2014; 1 ♂; J. Dixon leg. (DLSUWI) • Windsor, Trelawny; 04 Oct. 2014; 1 ♂; Hanchard leg. (DLSUWI) • Mona, St. Andrew; 23 Sept. 2014; 3 ♂; R. Daley leg. (DLSUWI) • Roaring River, St. Ann; 05 Nov. 2016; 1 ♂; S. McKenzie leg. (DLSUWI).

**Remarks.** *Peckia (Peckia) chrysostoma* is one of the most widely distributed species in the genus *Peckia* (Buenaventura and Pape 2013). It has been reported as a coloniser of human corpses in Brazil (Vasconcelos et al. 2014), and Dodge (1965b) mentions specimens from Jamaica that were “bred from crocodile”. Specimens have been recorded as collected from stinkhorn fungus (*Phallus* sp.; Phallales: Basidiomycota) and flowers of *Casearia* sp. (Salicaceae) (Camargo et al. 2018).

## 29. *Peckia (Sarcodexia) dominicana* (Lopes, 1982)

Fig. 5

**Neotropical distribution.** Dominican Republic, Jamaica (new record).

**Newly collected material.** • Windsor, Trelawny; 01 Jun. 2018; 1 ♂; L. Foote and E. Buenaventura leg. (DLSUWI) • Hardware Gap, Portland; 29 May 2018; 2 ♂; L. Foote and E. Buenaventura leg. (DLSUWI) • Red Light, St. Andrew; 20 Mar. 2024; 1 ♂; L. Foote leg. (DLSUWI).

**Remarks.** Previously known only from the Dominican Republic. This study reports *Peckia (Sarcodexia) dominicana* as a new record for Jamaica and adds to its distribution within the Caribbean. Little is known about the biology of *P. dominicana*. It was collected in a VSR trap baited with decomposing chicken in the present study.



**Figure 5.** *Peckia (Sarcodexia) dominicana*. Male terminalia, postero-lateral view; Antillean species, new record from Jamaica. Scale bar: 1 mm.

### 30. *Peckia (Peckia) hillifera* (Aldrich, 1916)

**Literature records.** Buenaventura and Pape (2013); (Camargo et al. 2018).

**Neotropical distribution.** Bahamas, Brazil, Cuba, Jamaica, México, Panamá, Puerto Rico, Trinidad & Tobago, Venezuela.

**Newly collected material.** • Belair, St. Ann; 31 May 2018; 1 ♂; L. Foote and E. Buenaventura leg. (DLSUWI).

**Remarks.** Specimens have been reared from a dead crab [*Ucides cordata* (Linnaeus)] (Camargo et al. 2018).

### 31. *Peckia (Sarcodexia) lambens* (Wiedemann, 1830)

**Literature records.** Townsend (1892, 1993, both as *Sarcodexia sternodontis*); Johnson (1908, 1919, both as *Sarcophaga sternodontis*); Lopes (1969, as *Sarcodexia sternodontes*); Pape (1996); Buenaventura and Pape (2013); Vairo et al. (2011); Vairo et al. (2014); Mello-Patiu (2016); Dufek (2019); Dufek et al. (2020); Ramírez-Mora et al. (2022).

**Neotropical distribution.** Argentina, Bahamas, Bolivia, Brazil, Cayman Is, Chile, Colombia, Costa Rica, Cuba, Ecuador, El Salvador, Galápagos Is, Guadeloupe, Guyana, Haití, Honduras, Jamaica, México, Panamá, Paraguay, Perú, Puerto Rico, St. Vincent and the Grenadines, Trinidad & Tobago, Venezuela.

**Newly collected material.** • Green Grotto, St. Ann; 31 May 2018; 3 ♂; L. Foote and E. Buenaventura leg. (DLSUWI) • Belair, St. Ann; 31 May 2018; 2 ♂; L. Foote and E. Buenaventura leg. (DLSUWI) • Red Light, St. Andrew; 26 Feb. 2024; 3 ♂; L. Foote leg. (DLSUWI) • Newport, Manchester; 18 Aug. 2023; 2 ♂; R. Daley leg. (DLSUWI) • Comfort Castle, Portland; 27 Mar. 2024; 2 ♂; L. Foote leg. (DLSUWI).

**Museum material.** • Cambridge District, St. Elizabeth; 23 Nov. 2013; 1 ♂; Bailey leg. (DLSUWI) • August Town, St. Andrew; 09 Nov. 2017; 1 ♂; Dacosta leg. (DLSUWI).

**Remarks.** Known as a saprophagous and necrophagous species in the Neotropics (Lopes de Carvalho and Linhares 2001; Vairo et al. 2015). It has been reported on human corpses and is considered one of the most important saprophagous species of forensic importance (Vairo et al. 2015). It has been collected from decomposing fish, bovine spleen and faeces (Barbosa 2019). Known parasitoid of the yellowtail moth (*Hylesia metabus*) and the fall armyworm (*Spodoptera frugiperda*) (Toma et al. 2018).

### 32. *Peckia (Euboettcheria) nicasia* (Lopes, 1941)

**Literature records.** Dodge (1965b); Lopes (1941, 1969); Pape (1996); Buenaventura and Pape (2013).

**Neotropical distribution.** Jamaica.

**Newly collected material.** • Windsor, Trelawny; 01 Jun. 2018; 3 ♂; L. Foote and E. Buenaventura leg. (DLSUWI) • Green Grotto, St. Ann; 31 May 2018; 1 ♂; L. Foote and E. Buenaventura leg. (DLSUWI) • Hardware Gap, Portland; 29 May 2018; 2 ♂; L. Foote and E. Buenaventura leg. (DLSUWI) • Bowden Pen, St. Thomas; 05 Jun. 2018; 1 ♂; L. Foote and E. Buenaventura leg. (DLSUWI) • Mona, St. Andrew; 12 Jun. 2018; 2 ♂; L. Foote leg. (DLSUWI) • Red Light, St. Andrew; 20 Mar. 2024; 5 ♂; L. Foote leg. (DLSUWI).

**Museum material.** • Cinchona Morce's Gap, St. Andrew; 21 Aug. 1949; 1 ♀; R. B. Bengry & R. Hart leg. (NHMJ) • Hermitage Reservoir, St. Andrew; 30 May 1954; 1 ♂; T. H. Farr leg. (NHMJ) • Southwest of Ecclesdown, Portland; 24 Aug. 1954; 1 ♂; T. H. Farr leg. (NHMJ) • Fern Gully, St. Ann; 11 Jul. 1954; 1 ♂; T. H. Farr leg. (NHMJ) • Hermitage Dam, St. Andrew; 31 May 1954; 1 ♂; R. B. Bengry leg. (NHMJ) • Long Mountain, St. Andrew; 26 Jun. 1955; 1 ♂; T. H. Farr leg. (NHMJ) • Benson Avenue; 12 Sep. 2007; 1 ♂; A. Sherman leg. (DLSUWI) • Bowden Pen, St. Thomas; 04 Nov. 2011; 1 ♂; T. Stephenson; (DLSUWI) • Roaring River, St. Ann; 03 Oct. 2014; 2 ♂; Bennett leg. (DLSUWI) • Dolphin Head Mountain, Hanover; 01 Oct. 2014; 1 ♀; L. Wright leg. (NHMJ).

**Remarks.** The species was collected in a VSR trap baited with decomposing chicken during the present study. It has previously been collected from decomposing pig carrion (Foote 2014).

### Genus *Ravinia* Robineau-Desvoidy, 1863

#### 33. *Ravinia effrenata* (Walker, 1861)

**Literature records.** Johnson (1919; as *Sarcophaga (Ravinia) quadrisetosa*, see Dodge 1965b); Hall (1928, as *Sarcophaga adamsii*); Lopes (1969, as *Chaetoravinia adamsi*); Pape (1996); Mello-Patiu (2016); Ramírez-Mora et al. (2022).

**Neotropical distribution.** Bahamas, Brazil, Colombia, Costa Rica, Cuba, Dominica, Dominican Republic, El Salvador, Guatemala, Jamaica, México, Panamá, Perú, St. Vincent.

**Newly collected material.** • Rio Bueno Property, St. Ann; 31 May 2018; 6 ♂; L. Foote and E. Buenaventura leg. (DLSUWI) • Belair, St. Ann; 31 May 2018; 2 ♂; L. Foote and E. Buenaventura leg. (DLSUWI) • Newport, Manchester; 18 Aug. 2023; 2 ♂; R. Daley leg. (DLSUWI).

**Museum material.** • Amity Hall, St. Catherine; 23 Mar. 1947; 1 ♂; C. B. Thompson leg. (NHMJ) • West of Jacob's Hut, Clarendon; 28 Sept. 1954; 1 ♂; T. H. Farr leg. (NHMJ).

**Remarks.** Species collected from decomposing fish (sardines), human faeces (Barbosa 2019) and fruit (Valverde-Castro et al. 2017).

### Genus *Sarcodexiopsis* Townsend, 1917

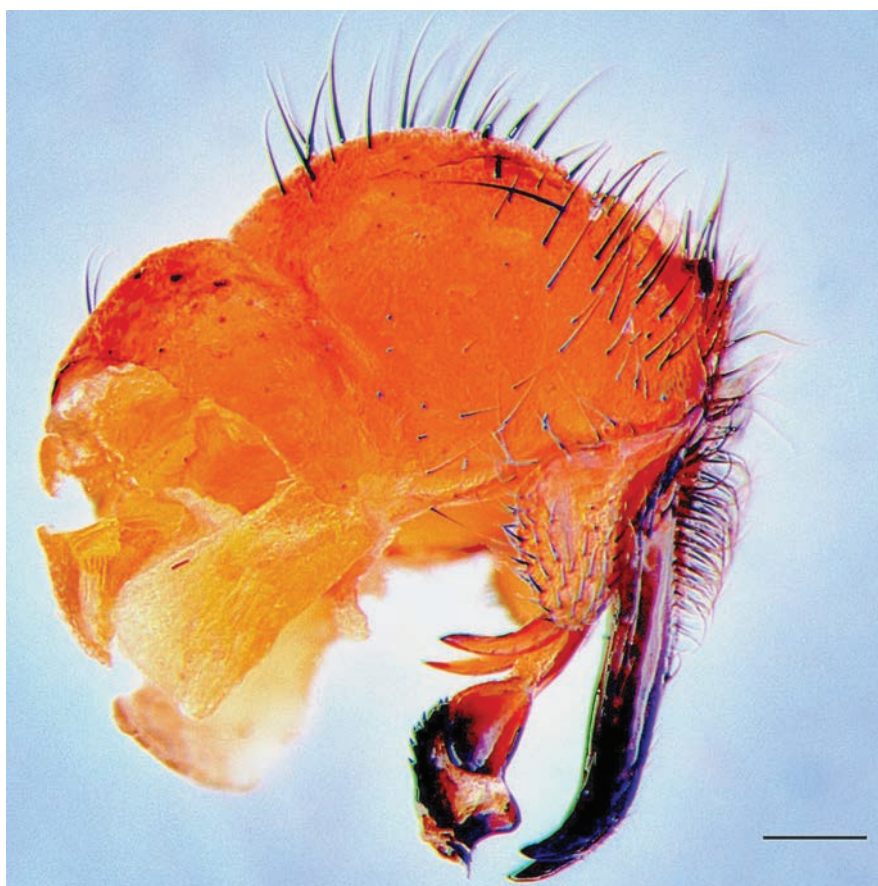
#### 34. *Sarcodexiopsis welchi* (Hall, 1930)

Fig. 6

**Literature records.** Pape (1996).

**Neotropical distribution.** Bahamas, British Virgin Is, Cuba, Jamaica, Puerto Rico.

**Newly collected material.** • Belair, St. Ann; 31 May 2018; 1 ♂; L. Foote and E. Buenaventura leg. (DLSUWI).



**Figure 6.** *Sarcodexiopsis welchi*. Male terminalia, lateral view; Antillean species. Scale bar: 1 mm.

**Genus *Sarcofahrtiopsis* Hall, 1933**

**35. *Sarcofahrtiopsis diembroma* Dodge, 1965**

**Literature records.** Dodge (1965b); Lopes (1969); Pape (1996).

**Neotropical distribution.** Jamaica.

**Remarks.** This species is still known only from the original type series consisting of two females. The holotype from Second Breakfast Spring, St. Andrew (deposited in Washington State University), and a female paratype from Hermitage, St. Andrew, stated to be in the "Science Museum, Institute of Jamaica" (now Natural History Museum of Jamaica) but were not located.

**36. *Sarcofahrtiopsis farri* Dodge, 1965**

**Literature records.** Dodge (1965b); Lopes (1969); Pape (1996); Pape and Méndez (2004).

**Neotropical distribution.** Costa Rica, Jamaica.

**Newly collected material.** • Green Grotto, St. Ann; 31 May 2018; 3 ♂; L. Foote and E. Buenaventura leg. (DLSUWI) • Belair, St. Ann; 31 May 2018; 3 ♂; L. Foote and E. Buenaventura leg. (DLSUWI) • Rio Bueno Property, St. Ann; 31 May 2018; 2 ♂; L. Foote and E. Buenaventura leg. (DLSUWI).

**Museum material.** • Ferry, St. Andrew; 03 Oct. 1954; 1 ♂; T. H. Farr leg. (NHMJ) • Rio Cobre, St. Catherine; 05 Jun. 1952; 1 ♂; R. P. Bengry leg. (NHMJ) • Colonel Ridge, Clarendon; 18 Nov. 1946; 1 ♂; G. B. Thompson leg. (NHMJ).

**37. *Sarcofahrtiopsis jamaicensis* Dodge, 1965**

**Literature records.** Dodge (1965b); Lopes (1969); Pape (1996).

**Neotropical distribution.** Jamaica.

**Museum material.** • Hermitage Dam, St. Andrew; 03 May 1954; 1 ♂; R. P. Bengry leg. (NHMJ).

**38. *Sarcofahrtiopsis paterna* Dodge, 1965**

**Literature records.** Dodge (1965b); Pape and Méndez (2004).

**Neotropical distribution.** Cuba, Jamaica, Puerto Rico.

**Remarks.** The presence of this species in Jamaica is based on one male paratype with no further data (Dodge 1965b).

**Genus *Sarcophaga* Meigen, 1826**

**39. *Sarcophaga (Liopygia) ruficornis* (Fabricius, 1794)**

**Literature records.** Pape (2024).

**Neotropical distribution.** Brazil, Colombia, Jamaica, Panamá, Venezuela.

**Newly collected material.** • Mona, St. Andrew; 07 Sep. 2018; 1 ♂; L. Foote leg. (DLSUWI).

**Remarks.** This is the first record from Jamaica documented with explicit reference to a collected specimen. Considered to be synanthropic and of forensic relevance (Barbosa 2019). Larvae were found to cause myiasis in toads (*Bufo melanostictus* Schneider) (Roy and Dasgupta 1977). It has been collected from decomposing bovine spleen and fish (Barbosa 2019) as well as from human cadavers (Kavitha et al. 2013). The optimum temperature for the development of *S. ruficornis* larvae is 20–35 °C (Nassu et al. 2014).

#### **Genus *Tapacura* Tibana & Lopes, 1985**

#### **40. *Tapacura mariarum* Tibana & Lopes, 1985**

Fig. 7

**Neotropical distribution.** Brazil, Jamaica (new record).

**Newly collected material.** Green Grotto, St. Ann; 31 May 2018; 4 ♂; L. Foote and E. Buenaventura leg. (DLSUWI).



**Figure 7.** *Tapacura mariarum*. Male terminalia, lateral view; new record from Jamaica. Scale bar: 1 mm.

**Remarks.** New record of this genus and species from Jamaica. The genus *Tapacura* presently contains two species, *Tapacura mariarum* recorded in the Neotropics (Brazil) and *Tapacura mexicana* Lopes, 1988 known only from the Nearctic (México) (Mello-Patiu and de Souza Neto 2007). There is no information on the biology of the species. It was collected from a VSR trap baited with decomposing chicken in the present study.

### Genus *Titanogrypa* Townsend, 1860

#### 41. *Titanogrypa (Airypel) cryptopyga* Lopes, 1956

**Literature records.** Dodge (1965b, as *Airypel molluscoyperda*); Lopes (1969); Pape (1996); Dufek (2019); Dufek et al. (2020).

**Neotropical distribution.** Argentina, Bolivia, Brazil, Cuba, Guyana, Jamaica, Trinidad & Tobago.

**Museum material.** • Ferry, St. Andrew; 03 Oct. 1954; 1 ♂; T. H. Farr leg. (NHMJ).

**Remarks.** Probably a scavenger. Dodge (1965b) gave label data from the holotype and a paratype: “Emerged Nov. 8, 1902, in Pittsburgh, Pa. Pupae received with shells received from near Mandeville, Jamaica”.

#### 42. *Titanogrypa (Sarconeiva) fimbriata* (Aldrich, 1916)

**Literature records.** Johnson (1919); Dodge (1965b); Lopes (1969); Pape (1996); Vairo et. al (2011); Dufek (2019); Dufek et al. (2020).

**Neotropical distribution.** Argentina, Brazil, Dominica, Dominican Republic, Jamaica, México, Panamá, Perú, Venezuela.

**Newly collected material.** • Bowden Pen, St. Thomas; 05 Jun. 2018; 4 ♂; L. Foote and E. Buenaventura leg. (DLSUWI).

**Museum material.** • Mona, St. Andrew; 07 May 1989; 1 ♂; J. Lawrence leg. (DLSUWI) • Mona, St. Andrew; 17 Nov. 2009; 1 ♂; T. Henry leg. (DLSUWI).

**Remarks.** Considered to be of forensic relevance (Barbosa 2019). It has been recorded from decomposition studies in Brazil (Mello-Patiu et al. 2014), on gastropods/molluscs (Barker 2004), and decomposing sardines (Barbosa 2019).

### Genus *Tricharaea* (Sarcophagula) Wulp, 1887

#### 43. *Tricharaea canuta* (Wulp, 1896)

**Literature records.** Dodge (1965b); Lopes (1969); Pape (1996); Mello-Patiu (2016); Ramírez-Mora et al. (2022).

**Neotropical distribution.** Brazil, Colombia, Costa Rica, Cuba, Dominica, Ecuador, El Salvador, Galápagos Is, Guatemala, Honduras, Jamaica, México, Paraguay, Perú.

**Newly collected material.** • Mona, St. Andrew; 07 Sep. 2018; 1 ♂; L. Foote leg. (DLSUWI).

**Remarks.** Synanthropic species of forensic relevance (Barbosa 2019). It has been collected from human faeces and decomposing bovine spleen (Barbosa 2019).

#### 44. *Tricharaea (Sarthromyia) femoralis* (Schiner, 1868)

**Literature records.** Johnson (1908, 1919).

**Neotropical distribution.** Bahamas, Brazil, Costa Rica, Cuba, Dominica, French Guiana, Honduras, Panama, Puerto Rico, Surinam, Trinidad & Tobago, Turks & Caicos Is., Venezuela.

**Museum material.** • Holland Bay, St. Thomas; 16 Mar. 1989; 8 ♀; T. H. Farr leg. (NHMJ) • Holland Bay, St. Thomas; 16 Nov. 1988; 5 ♀; R. A. Boothe leg. (NHMJ).

#### 45. *Tricharaea (Sarcophagula) occidua* (Fabricius, 1794)

**Literature records.** Johnson (1908, as *Sarcophagula imbecilla*; 1919); Dodge (1965b); Dufek et al. (2020).

**Neotropical distribution.** American Virgin Is., Argentina, Bolivia, Brazil, Chile, Colombia, Cuba, Dominica, Ecuador, El Salvador, Galápagos Is, Guatemala, Guyana, Haiti, Honduras, Jamaica, Mexico, Panama, Paraguay, Peru, Puerto Rico, St. Vincent Is., Venezuela.

**Museum material.** • Swamp, St. Thomas; 03 Nov. 1955; 1 ♀; T. H. Farr leg. (NHMJ) • Half Way Tree, St. Andrew; 06 Aug. 1950; 2 ♀; R. B. Bengry leg. (NHMJ) • Windsor Hotel, St. Ann; 20 Sep. 1959; 1 ♀; T. H. Farr leg. (NHMJ) • Ferry, St. Andrew; 03 Oct. 1954; 1 ♀; T. H. Farr leg. (NHMJ).

**Remarks.** Only females were studied in the present study, and their separation from *T. canuta* (Wulp, 1896) remains tentative.

## Discussion

The updated checklist for Jamaica includes 45 species, four of which are new records. The number of genera in Jamaica has increased to 21 with the addition of the genera *Bahamiola* and *Tapacura*.

With the addition of *Peckia (Sarcodexia) dominicana* to the checklist, *Peckia* becomes the most speciose flesh fly genus in Jamaica with a total of six species: *P. buethni*, *P. chrysostoma*, *P. dominicana*, *P. hillifera*, *P. lambens*, and *P. nicasia*. Some species of *Peckia* were quite rare. Only one individual of *P. buethni* was collected in this study. Previous record of *P. buethni* was one male in Papine, St. Andrew (southern Jamaica), collected by W. Büthn (BMNH). Similarly, only one individual of *P. hillifera* was collected in this study. Previous record of *P. hillifera* was one male in Milk River bath, St. Thomas (southern Jamaica), collected by Wirth and Farr (ZMUC). This pattern suggests that *P. buethni* and *P. hillifera* are rare in Jamaica, despite their relatively wide distribution.

*Lepidodexia* subgenus *Harpagopyga* Aldrich contains 15 nominal species, 14 of which occur in the Neotropical region (Pape 1996). Dodge (1965b) documented five species of *Lepidodexia* from Jamaica, all of which are endemic to the island. An additional species, *L. diversipes*, is here added to the records of *Lepidodexia* from Jamaica, increasing the total species number to six. Of note, no specimens collected during the present study, suggesting low abundance, a very narrow distribution, or sparse collecting for flesh flies in Jamaica.

*Oxysarcodexia* consists of 91 described species worldwide and is considered one of the most species-rich genera in the Neotropics (Souza et al. 2020).

Jamaica has five species of *Oxysarcodexia*, making it one of the most speciose genera on the island after *Peckia* and *Lepidodexia*. There are two endemic species of *Oxysarcodexia* recorded for Jamaica: *O. corolla* and *O. dorisae*. Only the female of *O. dorisae* is known, while both the male and the female of *O. corolla* are known. *Oxysarcodexia corolla* was found in a wet limestone forest, wet forest, and a rural area in St. Andrew, which might indicate a preference for environments with low anthropogenic impact. All other known species of *Oxysarcodexia* in Jamaica are widely distributed.

*Bahamiola orbitalis* was previously known only from the Bahamas (Grand Bahama Is.; Dodge 1965a). With 94 individuals across five locations, the species is common and widely distributed (Table 4).

*Tapacura mariarum* was previously known only from Brazil (Tibana and Lopes 1985), and the present record represents a significant range extension. Four individuals were collected at the Green Grotto, St. Ann. This species is likely to have a restricted geographical range in Jamaica, and its occurrence at a single locality may suggest a limited distribution in the island.

MacArthur and Wilson (1967) demonstrated that the number of species on an island is correlated with its size and proximity to the mainland. The Caribbean islands share several species due to their proximity and shared geological histories. According to Crews and Esposito (2020) islands are sources of diversity with dispersal from a large island source to smaller islands. Notably, Cuba, the largest island of the Greater Antilles (Fig. 8, Table 4), has the largest number of known species of Sarcophagidae. There are 15 species shared between Jamaica and Cuba, which may be attributed mainly to their close proximity, as Jamaica is approximately 145 km from the southeastern coast of Cuba. Winds may further facilitate species dispersal between these islands (Kirk-Spriggs and Muller 2017).

**Table 4.** Total number of endemics and percentage endemism of Sarcophagidae known from islands of the Greater Antilles.

Island	Number of endemics	Percentage of endemics (%)	Number of species	Size of island (km <sup>2</sup> )
Jamaica	15	33	45	10,992
Cuba	14	25	55	109,884
Hispaniola	3	14	19	76,192
Puerto Rico	4	13	30	8,870

Hispaniola is situated 190 km east of Jamaica. A total of 19 species of Sarcophagidae have been identified on the island, and of these, eight species are shared with Jamaica. It is noteworthy that Hispaniola is approximately seven times larger than Jamaica (Table 4), suggesting that Hispaniola may be under-sampled or inadequately studied. Another factor suggesting low sampling efforts on the island of Hispaniola is the low number of species shared between the two countries of the island. Eight species are recorded from the Haitian part and 13 from the Dominican Republic. Only two species are found in both countries, indicating inadequate sampling.

Puerto Rico, the smallest island in the Greater Antilles (Table 4), is the furthest from Jamaica, located at a distance of 923 km. Despite this distance, Puerto Rico and Jamaica share 12 species, which may reflect extensive sampling efforts in Puerto Rico.

Several species previously thought to be endemic to other islands have been found in Jamaica. It is unclear whether these species were recently introduced to Jamaica or if their endemism to other islands was mistakenly identified. A genetic analysis of these populations is needed to resolve these uncertainties.

Compared to other islands in the Greater Antilles, Jamaica is notable for its high endemism of Sarcophagidae. With an area of 10,992 km<sup>2</sup>, Jamaica is the third largest island in the Greater Antilles (Fig. 8). The island's diverse geography, which includes complex topography such as extensive karst limestone regions, mountains and plains, along with a range of biomes from xerophytic conditions receiving less than 60 cm of annual precipitation to wet forests receiving more than 700 cm, has fostered numerous centres of speciation (Aitken-Soux et al. 1981), contributing to its high endemism. Specific regions, such as the Cockpit Country, are known to be local centres of endemism due to their distinctive geomorphology, characterized by isolated conical hills and depressions (Sweeting 1958), which limit species dispersal and create distinct microhabitats.

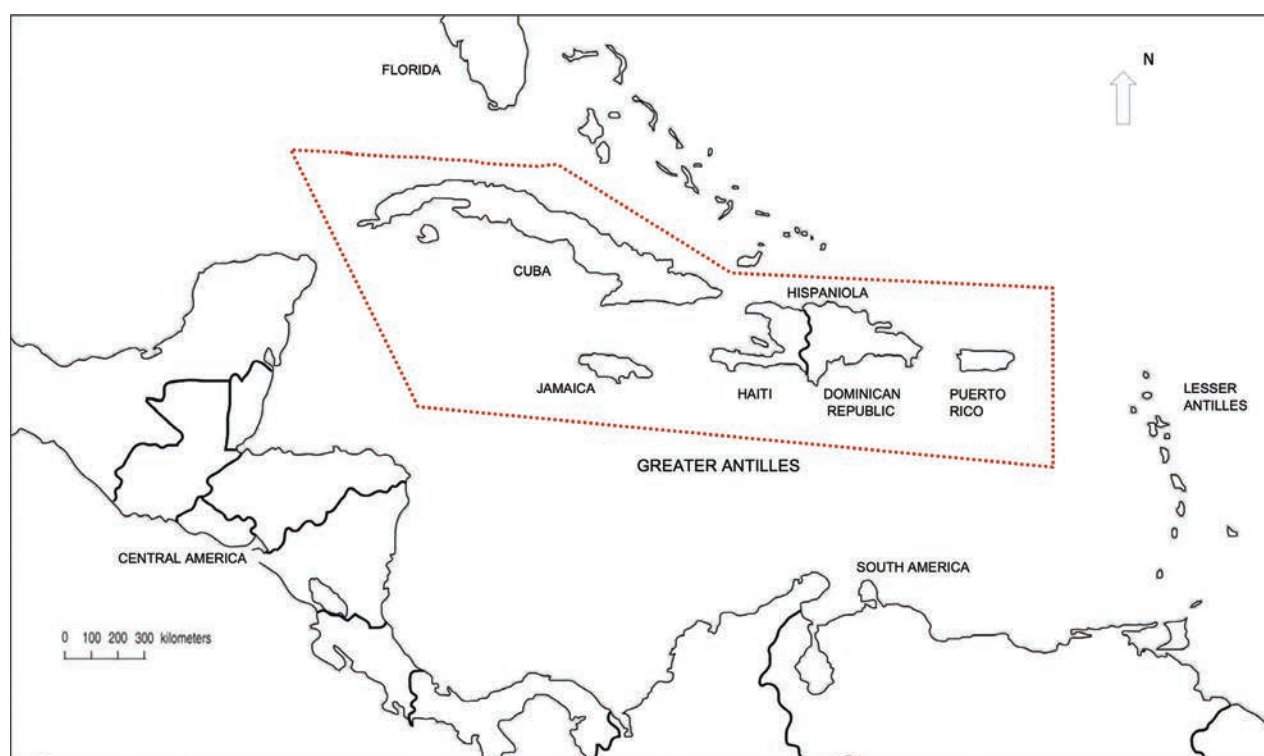


Figure 8. Map of the Caribbean region, highlighting the Greater Antilles.

## Acknowledgements

Latoya Foote-Gordon acknowledges the support of the National History Museum of Jamaica, Smithsonian National Museum of Natural History, USA, and the Natural History Museum of Denmark, University of Copenhagen, Denmark, for this project. We are grateful to Taneisha Barrett at the University of Hong Kong for the photographs. The authors would like to thank the reviewers for their insightful comments and suggestions, which greatly improved the quality of this manuscript. We also express our sincere gratitude to the editors for their guidance and support throughout the review process.

## Additional information

### Conflict of interest

The authors have declared that no competing interests exist.

### Ethical statement

No ethical statement was reported.

### Funding

National History Museum of Jamaica, Smithsonian National Museum of Natural History, USA, and the Natural History Museum of Denmark, University of Copenhagen, Denmark.

### Author contributions

Conceptualization: LFG. Data curation: LFG, EB. Formal analysis: LFG. Funding acquisition: LFG. Investigation: EB, LFG. Methodology: LFG. Resources: EG, LFG. Supervision: EG, TP. Validation: EB, TP. Writing - original draft: LFG. Writing - review and editing: LFG, EB, TP, EG.

### Author ORCIDs

Latoya Foote-Gordon  <https://orcid.org/0009-0001-6713-0550>

Eric Garraway  <https://orcid.org/0009-0004-5586-1649>

Thomas Pape  <https://orcid.org/0000-0001-6609-0609>

Eliana Buenaventura  <https://orcid.org/0000-0002-5265-815X>

### Data availability

All of the data that support the findings of this study are available in the main text.

## References

- Aitken-Soux P, Wahab AH, Johnson IE (1981) Country-level action plan- Jamaica. IICA Biblioteca, Venezuela, 18 pp.
- Bänziger H, Pape T (2004) Flowers, faeces and cadavers: natural feeding and laying habits of flesh flies in Thailand (Diptera: Sarcophagidae, *Sarcophaga* spp.). *Journal of Natural History* 38(13): 1677–1694. <https://doi.org/10.1080/0022293031000156303>
- Barbosa TM (2019) Sarcophagidae (Diptera) no bioma caatinga: revisão taxonômica do subgênero *Titanogrypa* (*Cucullomyia*) e avaliação do potencial de espécies como bioindicadoras de conservação ambiental. PhD Thesis, Universidade Federal de Pernambuco, Recife, Brazil. <https://repositorio.ufpe.br/handle/123456789/34067>
- Barker GM (2004) Natural enemies of terrestrial molluscs. CABI Publishing, Wallingford, Oxfordshire, 644 pp. <https://doi.org/10.1079/9780851993195.0085>
- Barros RM, Mello-Patiu CA, Pujol-Luz JR (2008) Sarcophagidae (Insecta, Diptera) associated to the decay process of *Sus scrofa* Linnaeus (Suidae) carcasses in a cerrado area of distrito federal, Brazil. *Revista Brasileira de Entomologia* 52(4): 606–609. <https://doi.org/10.1590/S0085-56262008000400011>
- Beltran Y, Pinilla T, Segura NA, Bello FJ (2012) Synanthropy of Calliphoridae and Sarcophagidae (Diptera) in Bogotá, Colombia. *Neotropical Entomology* 41(3): 237–242. <https://doi.org/10.1007/s13744-012-0036-x>
- Buenaventura E (2021) Museomics and phylogenomics with protein-encoding ultra-conserved elements illuminate the evolution of life history and phallic morphology

- of flesh flies (Diptera: Sarcophagidae). *BMC Ecology and Evolution* 21(70): 1–18. <https://doi.org/10.1186/s12862-021-01797-7>
- Buenaventura E, Pape T (2013) Revision of the new world genus *Peckia* Robineau-Desvoidy (Diptera: Sarcophagidae). *Zootaxa* 3622(1): 1–87. <https://doi.org/10.11646/zootaxa.3622.1.1>
- Buenaventura E, Valverde-Castro C, Wolff M (2021a) New carrion-visiting flesh flies (Diptera: Sarcophagidae) from tropical dry forests of Colombia and their phylogenetic affinities. *Acta Tropica* 213: 105720. <https://doi.org/10.1016/j.actatropica.2020.105720>
- Buenaventura E, Lloyd MW, Perilla-López JM, González VL, Thomas-Cabianca A, Dikow T (2021b) Protein-encoding ultraconserved elements provide a new phylogenomic perspective of Oestroidea flies (Diptera: Calyptratae). *Systematic Entomology* 46: 5–27. <https://doi.org/10.1111/syen.12443>
- Camargo SLX, Carvalho-Filho FS, Esposito CM (2018) The genus *Peckia* Robineau-Desvoidy (Diptera: Sarcophagidae) in the Brazilian Amazon: a new species, new records, descriptions of female terminalia and key to species. *Zootaxa* 4483(1): 1–35. <https://doi.org/10.11646/zootaxa.4483.1.1>
- Carvalho LML, Linhares AX (2001) Seasonality of insect succession and pig carcass decomposition in a natural forest area in south-eastern Brazil. *Journal of Forensic Science* 46(3): 604–608. <https://doi.org/10.1520/JFS15011J>
- Carvalho-Filho FS, Esposito CM (2012) Revision of *Argoravinia* Townsend (Diptera: Sarcophagidae) of Brazil with the description of two new species. *Zootaxa* 3256: 1–26. <https://doi.org/10.11646/zootaxa.3256.1.1>
- Cherix D, Wyss C, Pape T (2012) Occurrences of flesh flies (Diptera: Sarcophagidae) on human cadavers in Switzerland, and their importance as forensic indicators. *Forensic Science International* 220(1–3): 158–163. <https://doi.org/10.1016/j.forsci-int.2012.02.016>
- Crews SC, Esposito LA (2020) Towards a synthesis of the Caribbean biogeography of terrestrial arthropods. *BMC Ecology Biology* 20: 12. <https://doi.org/10.1186/s12862-019-1576-z>
- Curran CH (1928) Insects of Porto Rico and the Virgin Islands. Diptera or two-winged flies. *Scientific Survey of Porto Rico and the Virgin Islands* 11: 1–118.
- Dahlem G, Downes Jr W (1996) Revision of the genus *Boettcheria* in America North of Mexico (Diptera: Sarcophagidae). *Insecta Mundi: A Journal of World Insect Systematics* 10(1–4): 77–103. <https://digitalcommons.unl.edu/cgi/viewcontent.cgi?article=1361&context=insectamundi>
- Dodge RH (1965a) The Sarcophagidae (Diptera) of the West Indies. I. The Bahamas Islands. *Annals of the Entomological Society of America* 58(4): 474–497. <https://doi.org/10.1093/aesa/58.4.474>
- Dodge RH (1965b) The Sarcophagidae (Diptera) of the West Indies II. Jamaica. *Annals of the Entomological Society of America* 58(4): 497–517. <https://doi.org/10.1093/aesa/58.4.497>
- Dufek MI (2019) Comunidades de Calliphoridae y Sarcophagidae (Diptera: Calyptratae) en áreas naturales y disturbados del Chaco Oriental. PhD Thesis, Universidad Nacional del Nordeste, Argentina, 179 pp.
- Dufek MI, Osharov EB, Mulieri PR (2015) Preliminary survey and inventory of Calliphoridae and Sarcophagidae (Diptera) in the Province of Corrientes, Argentina, with new records of species with forensic importance. *Revista de La Sociedad Entomológica Argentina* 74(1–2): 37–46. <https://ri.conicet.gov.ar/handle/11336/208116>

- Dufek MI, Mello-Patiu CA, Mulieri PR (2020). Inventory of Sarcophaginae (Diptera: Sarcophagidae) for the Humid Chaco, a poorly surveyed ecoregion of South America. *Journal of Natural History* 54(5–6): 367–403. <https://doi.org/10.1080/00222933.2020.1764646>
- Early M, Goff ML (1986) Arthropod succession patterns in exposed carrion on the island of O'ahu, Hawaiian islands, USA. *Journal of Medical Entomology* 23(5): 520–531. <https://doi.org/10.1093/jmedent/23.5.520>
- Ferrar P (1987) A guide to the breeding habits and immature stages of Diptera Cyclorhapha. *Entomonograph* 8(1–2): 1–907. <https://doi.org/10.1163/9789004533936>
- Flores VI, Dale WE (1995) Un estudio sobre la ecología de las moscas Sarcophagidae en la costa central Peruana. *Revista Peruana de Entomología* 38: 13–17.
- Foote L (2014) An introduction to the study of insects of forensic importance in Jamaica. Master's Thesis, University of the West Indies, Mona, Jamaica.
- Foote-Gordon L, Garraway E (2023a) Ultrastructure Morphology of the Antennae of *Bahamiola orbitalis* (Diptera: Sarcophagidae). *Caribbean Journal of Science* 53(1): 51–58. <https://doi.org/10.18475/cjos.v53i1.a5>
- Foote-Gordon L, Garraway E (2023b) Ultrastructure morphology of the antennae of three *Peckia* species; *Peckia dominicana*, *P. nicasia*, *P. chrysostoma* (Diptera: Sarcophagidae). *Caribbean Journal of Science* 53(2): 198–209. <https://doi.org/10.18475/cjos.v53i2.a4>
- Foote-Gordon L, Garraway E (2023c) Ultrastructure Morphology of the Antennae of *Oxysarcodexia corolla* and *Oxysarcodexia peltata* (Diptera: Sarcophagidae). *Caribbean Journal of Science* 53(2): 384–390. <https://doi.org/10.18475/cjos.v53i2.a19>
- Freeman BE, Jayasingh DB (1975) Population dynamics of *Pachodynerus nasidens* (Hymenoptera) in Jamaica. *Oikos* 26(1): 86–91. <https://doi.org/10.2307/3543282>
- Freeman BE, Taffe CA (1974) Population dynamics and nesting behaviour of *Eumenes colona* (Hymenoptera) in Jamaica. *Oikos* 25: 388–394. <https://doi.org/10.2307/3543961>
- Giroux M, Wheeler T (2009) Systematics and phylogeny of the subgenus *Sarcophaga* (*Neobellieria*) (Diptera: Sarcophagidae). *Annals of the Entomological Society of America* 102(4): 567–587. <https://doi.org/10.1603/008.102.0401>
- Gowdey CC (1926) *Catalogus Insectorum Jamaicensis*. *Entomological Bulletin* 4: 1–114.
- Grindley-Watson EJ (2004) Faunal succession of necrophilous insects on wildlife carcasses in Louisiana. *Journal of Medical Entomology* 40(3): 338–347. <https://doi.org/10.1603/0022-2585-40.3.338>
- Hall DG (1928) *Sarcophaga pallinervis* and related species in the Americas. *Annals of the Entomological Society of America* 21: 331–352[ 4 pls]. <https://doi.org/10.1093/aesa/21.2.331>
- Howlett BG, Davidson MM, Pattermore DE, Walker MK, Nelson WR (2016) Seasonality of calliphorid and sarcophagid flies across Canterbury arable farms requiring pollinators. *New Zealand Plant Protection* 69: 290–295. <https://doi.org/10.30843/nzpp.2016.69.5899>
- Hwang C, Turner BD (2005) Spatial and temporal variability of necrophagous Diptera from urban to rural areas. *Medical and Veterinary Entomology* 19(4): 379–391. <https://doi.org/10.1111/j.1365-2915.2005.00583.x>
- Johnson CW (1908) The Diptera of the Bahamas, with notes and description of one new species. *Psyche* 15: 69–80. <https://doi.org/10.1155/1908/81853>
- Johnson CW (1919) A revised list of Diptera of Jamaica. *Bulletin Museum of Natural History* 41: 441–449. <http://hdl.handle.net/2246/1354>

- Kavitha R, Nazni WA, Tan TC, Lee HL, Azirun MS (2013) Review of forensically important entomological specimens collected from human cadavers in Malaysia (2005–2010). *Journal of Forensic and Legal Medicine* 20(5): 480–482. <https://doi.org/10.1016/j.jflm.2013.03.007>
- Kirk-Spriggs AH, Muller BS (2017) Biogeography of Diptera. *Manual of Afrotropical Diptera* 1: 203–238.
- Livingstone SR (2006) Sea turtle ecology and conservation on the north coast of Trinidad, West Indies. PhD Thesis, University of Glasgow, Scotland, 263 pp. <https://theses.gla.ac.uk/4323/>
- Lopes HS (1941) Sobre alguns sarcófagídeos neotrópicos da coleção do Museu Britânico (Diptera). *Arquivos de Zoologia, São Paulo* 2(16): 357–388. <https://doi.org/10.11606/issn.2176-7793.19412357-388>
- Lopes HS (1946) Contribuição ao conhecimento das espécies do gênero *Oxysarcodexia* Townsend, 1917 (Diptera Sarcophagidae). *Boletim de la Escuela Nacional de Veterinaria (Rio de Janeiro)* 1: 62–134.
- Lopes HS (1969) Family Sarcophagidae. In: Papavero N (Ed.) *A catalog of the Diptera of the Americas south of the United States* 103: 1–88. Departamento de Zoologia, Secretaria da Agricultura, São Paulo.
- Lopes HS (1982) On *Eumacronychia sternalis* Allen (Diptera, Sarcophagidae), with larvae living on eggs and hatchlings [sic] of the East Pacific Green Turtle. *Revista Brasileira de Biologia* 42: 425–429.
- MacArthur RH, Wilson EO (1967) *The theory of island biogeography*. Princeton University Press, 224 pp.
- Mello CA (1996) Revision of the genus *Farrimyia* Dodge, 1965 (Diptera, Sarcophagidae) – Parte I. *Revista brasileira de Biologia* 56: 459–471.
- Mello-Patiu CA (2016) Family Sarcophagidae. *Zootaxa* 4122(1): 884–903. <https://doi.org/10.11646/zootaxa.4122.1.75>
- Mello-Patiu CA, de Souza Neto SP (2007) Revisão das duas espécies de *Tapacura* Tibana & Lopes, 1985 (Diptera: Sarcophagidae: Sarcophaginae). *Biota Neotropica* 7(1): 1–4. <https://doi.org/10.1590/S1676-06032007000100021>
- Mello-Patiu CA, Paseto ML, Faria LS, Mendes J, Linhares AX (2014) Sarcophagid flies (Insecta, Diptera) from pig carcasses in Minas Gerais, Brazil, with nine new records from the Cerrado, a threatened neotropical biome. *Revista Brasileira de Entomologia* 58(2): 142–146. <https://doi.org/10.1590/S0085-56262014000200005>
- Mullen GR, Trauth SE, Sellers JC (1984) Association of a miltogrammine fly, *Eumacronychia nigricornis* Allen (Diptera: Sarcophagidae), with the brood burrows of *Sceloporus undulatus* (Latrielle) [sic] (Reptilia: Lacertillia [sic]). *Journal of the Georgia Entomological Society* 19: 1–6.
- Nassu MP, Thyssen PJ, Linhares AX (2014) Developmental rate of immatures of two fly species of forensic importance: *Sarcophaga (Liopygia) ruficornis* and *Microcerella halli* (Diptera: Sarcophagidae). *Parasitology Research* 113(1): 217–222. <https://doi.org/10.1007/s00436-013-3646-2>
- Oliveira TC, Vasconcelos SD (2010) Insects (Diptera) associated with cadavers at the Institute of Legal Medicine in Pernambuco, Brazil: Implications for forensic entomology. *Forensic Science International* 198(1–3): 97–102. <https://doi.org/10.1016/j.forsciint.2010.01.011>
- Pape T (1989) Revision of *Opsidia* Coquillett (Diptera: Sarcophagidae). *Entomologica Scandinavica* 20(2): 229–241. <https://doi.org/10.1163/187631289X00302>

- Pape T (1996) Catalogue of Sarcophagidae of the World (Insecta: Diptera). *Memoirs of Entomology International* 8: 1–558.
- Pape T (2024) Family: Sarcophagidae a taxonomic database to all flesh flies. <https://diptera.dk/sarco/index.php> [Accessed on 06 May 2024]
- Pape T, Méndez J (2004) Two new species of *Sarcophahrtiopsis* (Diptera: Sarcophagidae). *Zootaxa* 485: 1–7. <https://doi.org/10.11646/zootaxa.485.1.1>
- Pape T, Blagoderov V, Mostovski MB (2011) Order Diptera Linnaeus, 1758. *Zootaxa* 3148: 222–229. <https://doi.org/10.11646/zootaxa.3148.1.42>
- Ramírez-Mora MA, Buenaventura E, Gómez-P LM, Amat E (2012) Updated checklist and new records of calyptratae carrion flies (Diptera, Schizophora) from Valle de Aburrá and other localities in Colombia. *Entomotropica* 27(1): 27–35. <https://doi.org/10.22201/ib.20078706e.2012.2.983>
- Ramírez-Mora MA, Durango-Manrique Y, Gomez GF (2022) New records and distributional data of (Diptera: Sarcophaginae) from Colombia. *Revista de la Sociedad Entomológica Argentina* 81(2): 49–56. <https://doi.org/10.25085/rsea.80205>
- Roy P, Dasgupta B (1977) *Sarcophaga ruficornis* Fabr. (Sarcophagidae: Diptera) as a parasite of the common indian toad. *Proceedings of the Indian Academy of Sciences* 86(3): 207–209. <https://doi.org/10.1007/BF03050949>
- Sánchez-Núñez DA, Mancera-Pineda JE (2012) Pollination and fruit set in the main neotropical mangrove species from the southwestern Caribbean. *Aquatic Botany* 103: 60–65. <https://doi.org/10.1016/j.aquabot.2012.06.004>
- Segura NA, Bonilla MA, Usaquén W, Bello García FJ (2011) Entomofauna resource distribution associated with pig cadavers in Bogotá DC. *Medical and Veterinary Entomology* 25(1): 46–52. <https://doi.org/10.1111/j.1365-2915.2010.00933.x>
- Smith JM (2001) Glasgow University Exploration Society Trinidad Expedition 2001. <http://www.glasgowexsoc.org.uk/reports/trinidad2001.pdf> [Accessed 15 January 2024]
- Sousa JRP, Carvalho-Filho FS, Esposito MC, Meyer M (2015) Distribution and abundance of necrophagous flies (Diptera: Calliphoridae and Sarcophagidae) in Maranhão, Northeastern Brazil. *Journal of Insect Science* 15(1): 70. <https://doi.org/10.1093/jisesa/iev054>
- Souza CM, Pape T, Thyssen PJ (2020) *Oxysarcodexia* Townsend, 1917 (Diptera: Sarcophagidae)-a centennial conspectus. *Zootaxa* 4841(1): 1–126. <https://doi.org/10.11646/zootaxa.4841.1.1>
- Sukontason KL, Piangjai S, Bunchu N, Chaiwong T, Sripakdee D, Boonsriwong W, Vogtsberger RC, Sukontason K (2006) Surface ultrastructure of the puparia of the blow fly, *Lucilia cuprina* (Diptera: Calliphoridae), and flesh fly, *Liosarcophaga dux* (Diptera: Sarcophagidae). *Parasitology Research* 98(5): 482–487. <https://doi.org/10.1007/s00436-005-0102-y>
- Sweeting MM (1958) The karstlands of Jamaica. *The Geographical Journal* 124(2): 184–199. <https://doi.org/10.2307/1790245>
- Szpila K, Mađra A, Jarmusz M, Matuszewski S (2015) Flesh flies (Diptera: Sarcophagidae) colonising large carcasses in Central Europe. *Parasitology Research* 114(6): 2341–2348. <https://doi.org/10.1007/s00436-015-4431-1>
- Tibana R, Lopes HS (1985) On Brazilian Sarcophagidae (Diptera) with description of two new genera and four new species. *Revista Brasileira de Entomologia* 29(2): 189–198.
- Toma R, Roel A, Miranda R (2018) First record of *Peckia* (*Sarcodexia*) *lambens* (Wiedemann, 1830) (Diptera: Sarcophagidae) parasitizing *Spodoptera frugiperda* (Smith, 1797) (Lepidoptera: Noctuidae) in Brazil. *Arquivos do Instituto Biológico* 84: e0302016. <https://doi.org/10.1590/1808-1657000302016>

- Toma R, Koller WW, Mello-Patiu CA, Mello RL (2020) New records of Sarcophagidae (Insecta: Diptera) collected in Cerrado fragments in the municipality of Campo Grande, Mato Grosso do Sul state, Brazil. *EntomoBrasilis* 13: e0873. <https://doi.org/10.12741/ebrasilis.v13.e0873>
- Townsend CHT (1892) A dextiid parasite of a longicorn beetle. *Journal of the Institute of Jamaica* 1: 105–106.
- Vairo KP, Mello-Patiu CA, Carvalho CJB (2011) Pictorial identification key for species of Sarcophagidae (Diptera) of potential forensic importance in southern Brazil. *Revista Brasileira de Entomologia* 55(3): 333–347. <https://doi.org/10.1590/S0085-56262011005000033>
- Vairo KP, Ururahy-Rodrigues A, Moura MO, Mello-Patiu CA (2014) Sarcophagidae (Diptera) with forensic potential in Amazonas: a pictorial key. *Tropical Zoology* 27(4): 140–152. <https://doi.org/10.1080/03946975.2014.981482>
- Vairo KP, Queiroz MMC, Mendonca PM, Barbosa RR, Carvalho CJB (2015) Description of immature stages of the flesh fly *Peckia (Sarcodexia) lambens* (Wiedemann) (Diptera: Sarcophagidae) provides better resolution for taxonomy and forensics. *Tropical Zoology* 28(3): 114–125. <https://doi.org/10.1080/03946975.2015.1057435>
- Valverde-Castro C, Buenaventura E, Sánchez-Rodríguez JD, Wolff M (2017) Flesh flies (Diptera: Sarcophagidae: Sarcophaginae) from the Colombian Guajira biogeographic Province, an approach to their ecology and distribution. *Zoologia* 34: 1–11. <https://doi.org/10.3897/zoologia.34.e12277>
- Vasconcelos SD, Soares TF, Costa DL (2014) Multiple colonization of a cadaver by insects in an indoor environment: first record of *Fannia trimaculata* (Diptera: Fanniidae) and *Peckia (Peckia) chrysostoma* (Sarcophagidae) as colonizers of a human corpse. *International Journal of Legal Medicine* 128(1): 229–233. <https://doi.org/10.1007/s00414-013-0936-2>
- Villet MH, Clitheroe C, Williams KA (2017) The temporal occurrence of flesh flies (Diptera, Sarcophagidae) at carrion-baited traps in Grahamstown, South Africa. *African Invertebrates* 58(1): 1–8. <https://doi.org/10.3897/AfrInvertebr.58.9537>
- Wells JD, Smith JL (2013). First report of *Blaesoxipha plinthopyga* (Diptera: Sarcophagidae) from a human corpse in the U.S.A. and a new state geographic record based on specimen genotype. *Journal of Forensic Sciences* 58(5): 1378–1380. <https://doi.org/10.1111/1556-4029.12246>
- Wilson A (2004) *Jamaica the Land*. Crabtree Publishing Company, New York, 32 pp.
- Wisniewska N, Lipinska MM, Golebiowski M, Kowalkowska AK (2019) Labellum structure of *Bulbophyllum echinolabium* JJ Sm. (section *Lepidorhiza* Schltr., *Bulbophyllinae* Schltr., *Orchidaceae* Juss.). *Protoplasma* 256: 1185–1203. <https://doi.org/10.1007/s00709-019-01372-4>
- Yan L, Buenaventura E, Pape T, Kutty SN, Bayless KM, Zhang D (2021) A phylotranscriptomic framework for flesh fly evolution (Diptera, Calyptratae, Sarcophagidae). *Cladistics* 37: 540–558. <https://doi.org/10.1111/cla.12449>
- Yepes-Gaurisas D, Sánchez-Rodríguez JD, Mello-Patiu CA, Wolff ME (2013) Synanthropy of Sarcophagidae (Diptera) in La Pintada, Antioquia-Colombia. *Revista de Biología Tropical* 61(3): 1275–1287. <https://www.scielo.sa.cr/pdf/rbt/v61n3/a22v61n3.pdf>



# Taxonomic notes of jumping spiders (Araneae, Salticidae) from Guangxi, Hainan, Sichuan, Xizang and Yunnan, China

Cheng Wang<sup>1</sup>, Xiaoqi Mi<sup>1</sup>, Shuqiang Li<sup>2,3</sup>, Xiang Xu<sup>4</sup>

<sup>1</sup> Guizhou Provincial Key Laboratory for Biodiversity Conservation and Utilization in the Fanjing Mountain Region, Tongren University, Tongren, Guizhou 554300, China

<sup>2</sup> Institute of Zoology, Chinese Academy of Sciences, Beijing 100101, China

<sup>3</sup> University of Chinese Academy of Sciences, Beijing, China

<sup>4</sup> College of Life Science, Hunan Normal University, Changsha 410081, Hunan, China

Corresponding author: Shuqiang Li ([lisq@ioz.ac.cn](mailto:lisq@ioz.ac.cn))

## Abstract

Twenty-one new species of jumping spiders from five provinces of South China are described: *Cheliceroides jinxini* sp. nov. (♂), *Dendroicius qiong* sp. nov. (♂♀), *Icius deer-gong* sp. nov. (♂♀), *Irura qiuhang* sp. nov. (♂♀), *I. yarlungzangbo* sp. nov. (♂♀), *Mintonia shiwandashan* sp. nov. (♂), *Myrmarachne kuan* sp. nov. (♂♀), *Nandicius xiefengi* sp. nov. (♂♀), *Pancorius medog* sp. nov. (♀), *P. yingjiang* sp. nov. (♂♀), *Piranthus maddisoni* sp. nov. (♂♀), *Simaetha hainan* sp. nov. (♂♀), *Stertinus lhoba* sp. nov. (♂♀), *Synagelides kongmingi* sp. nov. (♂♀), *S. xuandei* sp. nov. (♂♀), *S. yunchang* sp. nov. (♂♀), *S. yidei* sp. nov. (♂), *S. zilongi* sp. nov. (♂♀), *Yaginumaella dawweishan* sp. nov. (♂♀), *Y. moinba* sp. nov. (♂♀), and *Y. pingbian* sp. nov. (♂♀). *Nepalicius* Prószyński, 2016, **syn. nov.** is proposed as a junior synonym of *Okinawicius* Prószyński, 2016. Three new combinations are proposed: *O. nepalicus* (Andreeva, Hęciak & Prószyński, 1984), **comb. nov.** and *O. seychellensis* (Wanless, 1984), **comb. nov.** transferred from *Nepalicius*, and *O. daoxianensis* (Peng, Gong & Kim, 2000), **comb. nov.** transferred from *Philaeus* Thorell, 1869. The unknown females of *O. nepalicus*, *Padillothorax exilis* (Cao & Li, 2016) and *Siler hanoicus* Prószyński, 1985 are described for the first time. Distribution maps of the studied specimens are also provided.

**Key words:** Morphology, new combination, new species, synonym, taxonomy



Academic editor: Yuri Marusik

Received: 27 August 2024

Accepted: 25 November 2024

Published: 17 December 2024

ZooBank: <https://zoobank.org/B61D8EFC-2753-4B88-8A36-DAB1F37D96BB>

**Citation:** Wang C, Mi X, Li S, Xu X (2024) Taxonomic notes of jumping spiders (Araneae, Salticidae) from Guangxi, Hainan, Sichuan, Xizang and Yunnan, China. ZooKeys 1221: 205–277. <https://doi.org/10.3897/zookeys.1221.135640>

Copyright: © Cheng Wang et al.  
This is an open access article distributed under terms of the Creative Commons Attribution License (Attribution 4.0 International – CC BY 4.0).

## Introduction

Salticidae, the largest family in Araneae, currently contains 6702 extant species in 685 genera distributed worldwide (WSC 2024). The taxonomic study of the family from China has a relatively long history, but it has been in rapid development until recently four decades (WSC 2024). A series of continuous taxonomic studies from some tropical areas, such as Xishuangbanna, Yunnan, and Hainan provinces, and taxonomic studies and revisions on several genera of Chrysillini Simon, 1901 and Euophryini Simon, 1901 have significantly increased our knowledge (Wang et al. 2023; WSC 2024). Peng et al. (1993) and Peng (2020) also conducted two comprehensive taxonomic works.

To date, at least 773 nominal species (including the species described in the present work) under 144 genera have been recorded in China (Metzner 2024; WSC 2024), and the species number far exceeds the figure for nearby countries such as India (349), Vietnam (180), and even the most species-rich countries worldwide, such as Australia (537) and Brazil (714) (Metzner 2024). However, the taxonomic study of the family from China remains unsatisfactory because most regions have not been adequately studied, even some hot spot provinces such as Hainan and Yunnan, where new species or records are continuously being discovered. Moreover, it is also limited by high rates of poorly studied species that cannot be precisely identified or known only from a single sex, and quite a few genera cannot be adequately defined. As stated by Li (2020), Luo and Li (2024), Zhang et al. (2023), Lu et al. (2022), the true diversity of Chinese spiders could reach very high.

In our recent examination of jumping spiders from the five provinces of south China, more than twenty species were recognized as new to science, and the unknown females of three species were found. The goals of the present work are to (re)describe those species (all are the members of the subfamily Salticinae Blackwall, 1841 except *Mintonia shiwandashan* sp. nov. belongs to the subfamily Spartaestinae Wanless, 1984) and propose a synonym and three new combinations.

## Materials and methods

Specimens were collected by beating shrubs or sieving leaf litter and preserved in 80% or absolute ethanol. They are deposited in the Institute of Zoology, Chinese Academy of Sciences in Beijing (**IZCAS**), China, and Tongren University (**TRU**) in Tongren, China. Methods followed Wang et al. (2024).

All measurements are given in millimeters. Leg measurements are given as: total length (femur, patella, tibia, metatarsus, tarsus). References to figures in the cited papers are listed in lowercase type (fig. or figs), and figures in this paper are noted with an initial capital (Fig. or Figs). Abbreviations used in the text and figures are as follows: **AERW** anterior eye row width; **AME** anterior median eye; **ALE** anterior lateral eye; **AG** accessory gland; **AL** anterior tegular lobe; **AR** atrial ridge; **AS** anterior chamber of spermatheca; **At** atrium; **BTA** baso-retrolateral tibial apophysis; **CD** copulatory duct; **CF** cymbial flange; **CO** copulatory opening; **CP** cymbial process; **CR** prolateral cymbial ridged portion; **DCA** dorsal cymbial apophysis; **DCE** dorsal cymbial extension; **DCP** dorsal cymbial process; **DD** dorsal denticle of retrolateral tibial apophysis; **DTA** dorsal tibial apophysis; **DTP** dorsal tibial process; **E** embolus; **EFL** eye field length; **F** epigynal fold; **FD** fertilization duct; **H** epigynal hood; **JS** junction duct of spermatheca; **MA** median apophysis; **MTP** membranous tegular peak; **PCA** prolateral cymbial apophysis; **PERW** posterior eye row width; **PB** patellar bump of male palp; **PL** posterior tegular lobe; **PME** posterior median eye; **PCA** prolateral cymbial apophysis; **PFA** prolateral femoral apophysis; **PLE** posterior lateral eye; **PS** posterior chamber of spermatheca; **PTA** prolateral tibial apophysis; **PTgA** prolateral tegular apophysis; **RCA** retrolateral cymbial apophysis; **RTA** retrolateral tibial apophysis; **S** spermatheca; **Se** septum; **SD** sperm duct; **TB** tegular bump; **TL** tegular lobe; **UI** U-shaped incision of embolic disc; **VTA** ventral tibial apophysis; **VTP** ventral tibial process.

## Results

### Family Salticidae Blackwall, 1841

#### Genus *Cheliceroides* Żabka, 1985

**Type species.** *Cheliceroides longipalpis* Żabka, 1985; type locality Cuc Phuoug, Vietnam.

**Comments.** This monotypic genus was considered a synonym of *Colopus* Simon, 1902 by Logunov (2021) but was recently revalidated by Lin et al. (2024a). It is placed in the tribe Hasariini Simon, 1903 by Maddison (2015), but that has been confirmed as doubtful, and its phylogenetic placement remains uncertain (Lin et al. 2024a).

#### *Cheliceroides jinxini* sp. nov.

<https://zoobank.org/AF3ECB2E-C8A4-444E-914F-96A97EDDFE42>

Figs 1, 2, 47

**Type material. Holotype** ♂ (TRU-JS 0729), CHINA: • Yunnan Province, Menghai County, Bameng Village (22°08.1'N, 100°31.56'E, ca 2030 m), 1.VII.2023, J.X. Liu et al. leg.

**Etymology.** The specific name is a patronym in honor of the collector; noun (name) in the genitive case.

**Diagnosis.** *Cheliceroides jinxini* sp. nov. resembles *C. longipalpis* in habitus and palpal structure, but can be distinguished by the following: 1) presence of a raised tegular portion (Fig. 1A, B) vs absent (Lin L. et al. 2024a: figs 9–11, 16); 2) male palpal tibia ~ 1/5 of cymbial length (Fig. 1A, B) vs approx. as long as cymbium (Lin et al. 2024a: figs 9–11, 16); 3) embolus (E) originating at ca 4 o'clock position (Fig. 1A, B) vs ca 2 o'clock position (Lin et al. 2024a: fig. 10); and 4) chelicerae unmodified, and presence of one retromarginal tooth (Fig. 2D) vs modified, and two retromarginal teeth (Logunov 2021: figs 2, 4).

**Description. Male** (Figs 1, 2). Total length 5.40. Carapace 2.60 long, 2.04 wide. Abdomen 2.68 long, 1.64 wide. Eye sizes and interdistances: AME 0.64, ALE 0.36, PLE 0.30, AERW 1.96, PERW 1.80, EFL 1.24. Legs: I 5.99 (1.75, 1.08, 1.45, 1.08, 0.63), II 5.12 (1.58, 0.95, 1.18, 0.88, 0.53), III 5.67 (1.83, 0.88, 1.20, 1.13, 0.63), IV 5.89 (1.83, 0.80, 1.28, 1.35, 0.63). Carapace dark except anterior half of thoracic part red-brown, covered with dense dark and white setae, with clusters of bilateral, dense white scales. Chelicerae red-brown, with two promarginal teeth and one retromarginal tooth. Legs overall yellow except femora I dark brown, patellae, tibiae, and metatarsi I yellow-brown, spiny. Dorsum of abdomen yellow laterally, with anterior, transverse, arc-shaped setal stripes, and central, longitudinal, dark patch; venter pale brown, with dark spots.

**Palp** (Fig. 1A, B): femur length/width ratio ca 3.32; patella slightly wider than long; tibia short, ~ 2× wider than long in ventral view; retrolateral tibial apophysis (RTA) broadened into sub-quadrangular portion at base, then tapered to blunt end slightly curved inward; cymbium flat, ~ 1.5× longer than wide in ventral view; tegulum almost round, with swollen retrolateral portion; embolus (E)

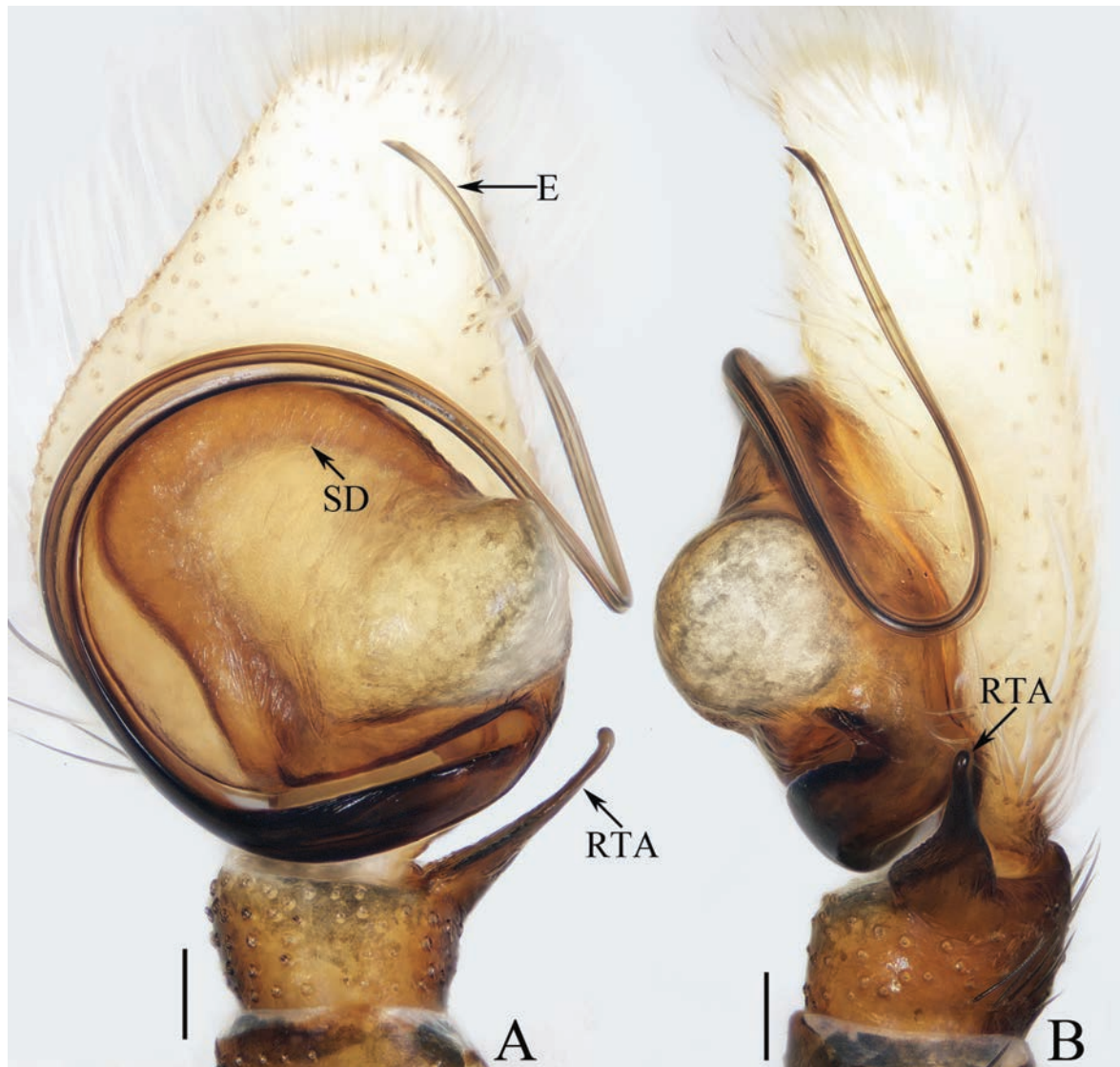


**Figure 1.** Male palp of *Cheliceroides jinxini* sp. nov., holotype **A** ventral **B** retrolateral. Abbreviations: E embolus; RTA retrolateral tibial apophysis; SD sperm duct. Scale bars: 0.1 mm.

long, arising at ca 4 o'clock position, extending circularly (ca 340°) along tegulum before strongly curving 180°, then antero-prolaterally extending into acutely pointed tip at apex of cymbium.

**Female.** Unknown.

**Distribution.** Known only from the type locality in Yunnan, China (Fig. 47).

**Comments.** The new species is considered a member of the genus because it shares a series of characters with *C. longipalpis*, such as the similar habitus, pattern, and long and whip-like embolus. However it is also obviously different from the latter by the unmodified chelicerae with one retromarginal tooth (vs modified, elongated chelicerae with two retromarginal teeth; Logunov 2021: figs 3, 9), the C-shaped sperm duct (vs S-shaped; Logunov 2021: fig. 5), and only the cymbium bears dense white setae (vs all segments except coxae and femora are densely covered with white setae; Logunov 2021: figs 2, 4). Therefore, the generic position of this species remains uncertain. Discovering its unknown female and obtaining enough molecular evidence could be helpful in confirming this issue.

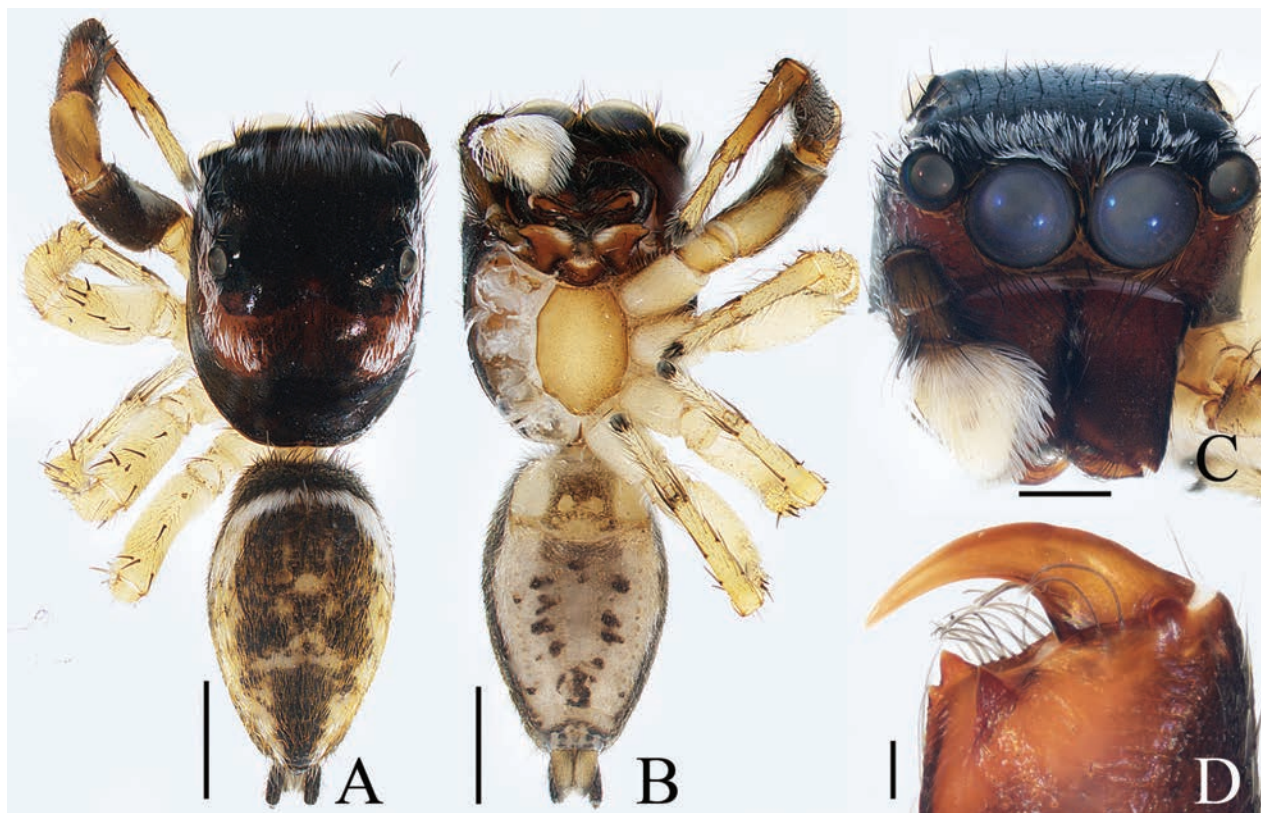


**Figure 2.** *Cheliceroides jinxini* sp. nov., holotype **A** habitus, dorsal **B** ditto, ventral **C** carapace, frontal **D** chelicera, posterior. Scale bars: 1.0 mm (**A**, **B**); 0.5 mm (**C**); 0.1 mm (**D**).

### Genus *Dendroicius* Lin & Li, 2020

**Type species.** *Dendroicius hotaruae* Lin & Li, 2020; type locality Menglun Township, Mengla County, Yunnan, China.

**Comments.** This monotypic genus was not placed in any of the subfamilies and tribes of Salticidae. Judging from the conformation of the male palp, and particularly in having a tegular bump, it belongs to Chrysillini Simon, 1901. It is only known from the original description (WSC 2024).

### *Dendroicius qiong* sp. nov.

<https://zoobank.org/A1C42A54-F6D7-4CCF-8BA0-F916BB5544D5>

Figs 3, 4, 47

**Type material.** **Holotype** ♂ (TRU-JS 0730), CHINA: • Hainan Province, Baoting Li and Miao Autonomous County, Maogan Township, 124 road (18°39.32'N, 109°32.45'E, ca 530 m), 4.VIII.2023, C. Wang et al. leg. **Paratypes** • 1 ♂ (TRU-JS 0731), same data as for holotype; • 2 ♀ (TRU-JS 0823, 0824), same locality as for holotype, 4.IX.2024, C. Wang and S. K. Li leg.

**Etymology.** The specific name refers to the short name of type locality (Hainan Province); noun in apposition.

**Diagnosis.** *Dendroicius qiong* sp. nov. resembles *D. hotaruae* in having similar habitus and copulatory organs, especially the presence of a pair of white lateral setal stripes across the whole surface of carapace, but can be easily



**Figure 3.** Male palp of *Dendroicius qiong* sp. nov., holotype **A** palp, prolateral **B** ditto, ventral **C** ditto, retrolateral. Abbreviations: CP cymbial process; DD dorsal denticle of retrolateral tibial apophysis; DTA dorsal tibial apophysis; E embolus; RTA retrolateral tibial apophysis; TB tegular bump; TL tegular lobe. Scale bars: 0.1 mm.

distinguished by the absence of latero-terminal tibial apophysis and mesal branch of dorsal tibial apophysis (Fig. 3C) vs present (Lin and Li 2020: fig. 3C) and by the distance between copulatory openings (CO), which is  $\sim 3/4$  of epigynal width, and the C-shaped copulatory ducts (CD) (Fig. 4A–C) vs distance between copulatory openings  $\sim 1/3$  of epigynal width, and nearly S-shaped copulatory ducts (Lin and Li 2020: fig. 4A, B).

**Description. Male** (Figs 3, 4D, E, G, H). Total length 2.91. Carapace 1.40 long, 0.89 wide. Abdomen 1.53 long, 0.80 wide. Eye sizes and interdistances: AME 0.28, ALE 0.14, PLE 0.13, AERW 0.80, PERW 0.84, EFL 0.47. Legs: I 2.19 (0.68, 0.45, 0.53, 0.33, 0.20), II 1.74 (0.53, 0.33, 0.38, 0.30, 0.20), III 1.63 (0.55, 0.25, 0.30, 0.33, 0.20), IV 2.19 (0.70, 0.33, 0.53, 0.40, 0.23). Carapace almost rectangular, yellow-brown except eye field dark, covered with dense dark setae; fovea indistinct. Chelicerae red-brown, with two promarginal teeth and one retro-marginal tooth. Legs pale except femora dark brown, with two pairs of spines on tibiae and metatarsi I. Dorsum of abdomen grey, with six longitudinal, dark green and green-brown stripes extending across complete surface; venter pale.

**Palp** (Fig. 3A–C): femur length/width ratio ca 2.0; patella almost as long as wide in retrolateral view; tibia almost as long as patella in retrolateral view;

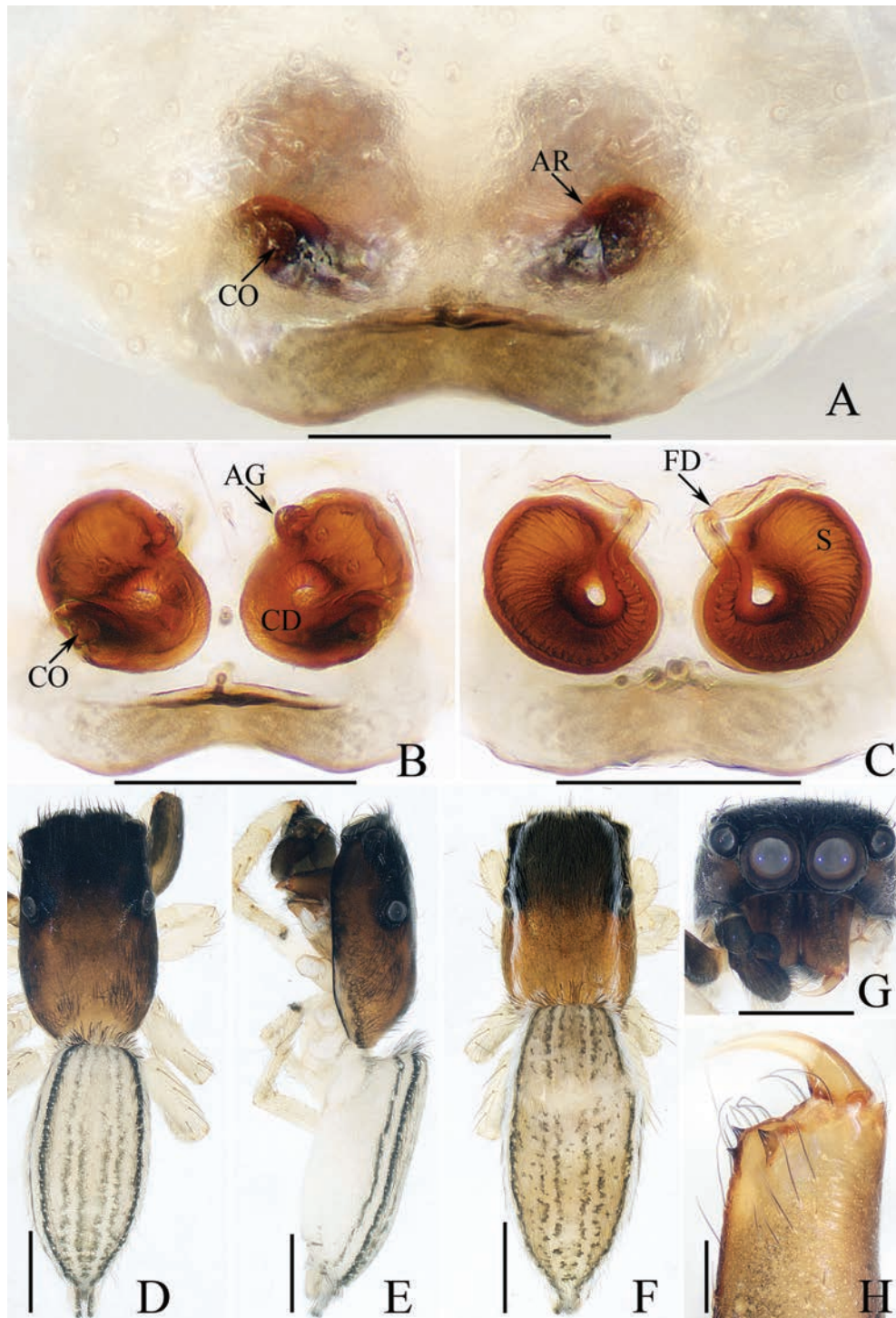


**Figure 4.** *Dendroicius qiong* sp. nov. **D, E, G, H** male holotype and **A–C, F** female paratype (TRU-JS 0823) **A, B** epigyne, ventral **C** vulva, dorsal **D, F** habitus, dorsal **E** ditto, lateral **G** carapace, frontal **H** chelicera, posterior. Abbreviations: AG accessory gland; AR atrial ridge; CD copulatory duct; CO copulatory opening; FD fertilization duct; S spermatheca. Scale bars: 0.1 mm (**A–C, H**); 0.5 mm (**D–G**).

retrolateral tibial apophysis (RTA) lamellar, with dorsal spinous denticle (DD); dorsal tibial apophysis (DTA) wider than long, with several anteromarginal denticles; cymbium  $\sim 1.8\times$  longer than wide, with almost horizontal tip and flat baso-retrolateral process (CP); tegulum elongate-oval, swollen at posterior half, with irregular anterior lobe (TL) and small disto-retrolateral bump (TB); embolus

(E) strongly sclerotized, tapered, almost as long as anterior tegular lobe, slightly curved medially and pointed apically.

**Female** (Fig. 4A–C, F). Total length 2.66. Carapace 1.12 long, 0.77 wide. Abdomen 1.64 long, 0.80 wide. Eye sizes and interdistances: AME 0.26, ALE 0.13, PLE 0.12, AERW 0.70, PERW 0.74, EFL 0.49. Legs: I 1.49 (0.48, 0.28, 0.30, 0.25, 0.18), II 1.31 (0.40, 0.28, 0.25, 0.20, 0.18), III 1.41 (0.45, 0.20, 0.30, 0.28, 0.18), IV 1.99 (0.63, 0.30, 0.48, 0.35, 0.23). Habitus (Fig. 4F) similar to that of male except paler and with pair of longitudinal, white setal stripes laterally on carapace.

**Epigyne** (Fig. 4A–C) wider than long, with posterior concave > 3× wider than long; atrium (At) oval, paired, with anterior arc-shaped ridges (AR); copulatory openings (CO) almost round, laterally opened, separated from each other ~ 3/4 epigynal width; copulatory ducts (CD) curved into C-shape, and with small terminal accessory glands (AG); spermathecae (S) elongated.

**Distribution.** Known only from the type locality in Hainan, China (Fig. 47).

### Genus *Icius* Simon, 1876

**Type species.** *Marpissa hamata* C. L. Koch, 1846; type locality Naples, Italy.

**Comments.** *Icius*, one of the most species-rich genera of Chrysillini, comprises 47 species widely distributed in five continents (Maddison 2015; WSC 2024). The genus has not been revised recently, and 20 of its species are known only from a single sex (WSC 2024). The species are rather diverse in habitus and copulatory organs, especially the south and east Asian and African members, indicating that it is likely polyphyletic.

#### *Icius deergong* sp. nov.

<https://zoobank.org/B0961AB8-F6A6-4E8B-B7AA-E18C6341DB1A>

Figs 5, 6, 47

**Type material. Holotype** ♂ (TRU-JS 0732), CHINA: • Xizang Autonomous Region, Medog County, Beibeng Township, Deergong Village, Yarlung Zangbo National Nature Reserve (29°10.84'N, 95°8.67'E, ca 1670 m), 25.V.2024, X.Q. Mi et al. leg.

**Paratypes** • 1 ♂ 3 ♀ (TRU-JS 0733–0736), same data as for holotype.

**Etymology.** The specific name refers to the type locality, Deergong Village; noun in apposition.

**Diagnosis.** *Icius deergong* sp. nov. resembles *I. yadongensis* Hu, 2001 in general shape of copulatory organs, especially the invert infundibuliform base of copulatory duct, but can be easily distinguished by the bifurcated retrolateral tibial apophysis (RTA), the presence of epigynal septum (Se) and proximally touching copulatory ducts (CD) (Figs 5B, C, 6A–D) vs non-bifurcated retrolateral tibial apophysis, lacking septum and copulatory ducts apart from each other proximally (Hu 2001: fig. 8–247-2, 3, 5–7).

**Description. Male** (Figs 5, 6E, F, H, I). Total length 2.56. Carapace 1.16 long, 0.71 wide. Abdomen 1.43 long, 0.60 wide. Eye sizes and interdistances: AME 0.23, ALE 0.11, PLE 0.11, AERW 0.63, PERW 0.69, EFL 0.51. Legs: I 1.77 (0.53, 0.33, 0.40, 0.28, 0.23), II 1.42 (0.43, 0.25, 0.28, 0.23, 0.23), III 1.47 (0.43, 0.23, 0.30, 0.28, 0.23), IV 1.99 (0.60, 0.30, 0.48, 0.38, 0.23). Carapace elongated, grey-brown

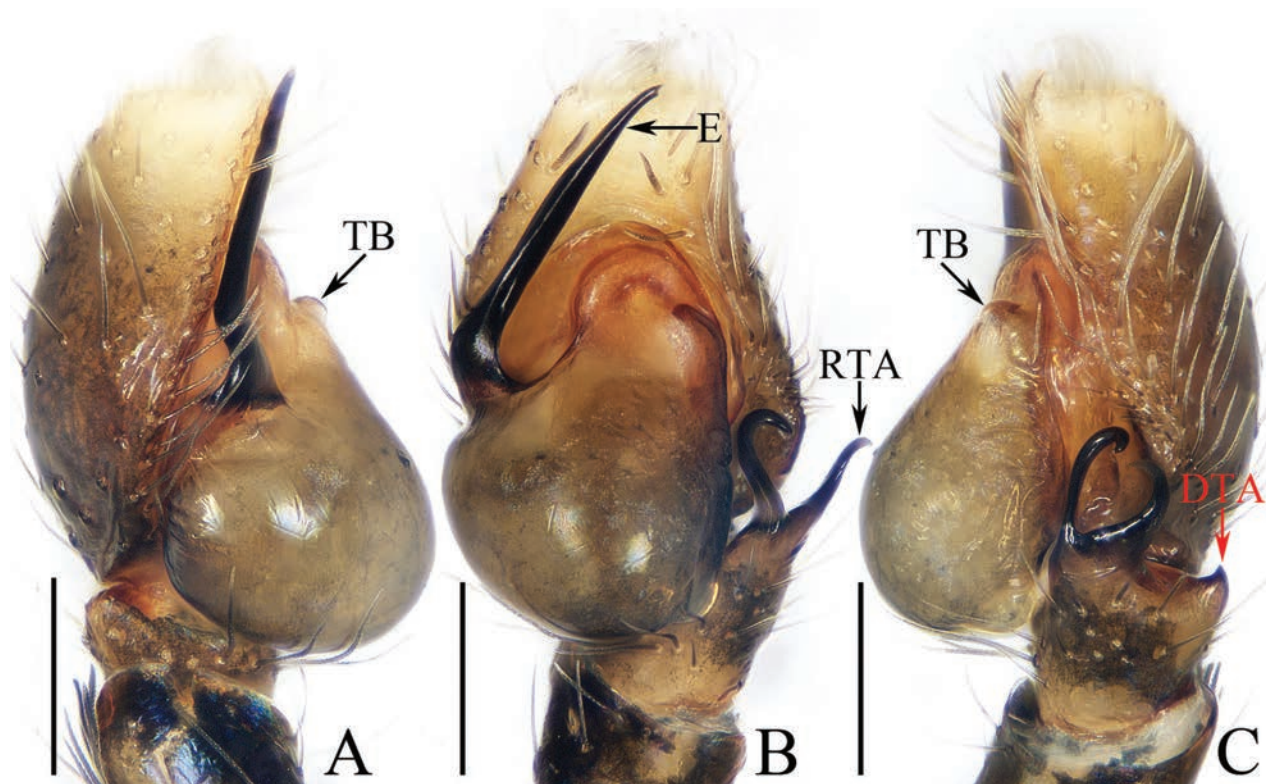


**Figure 5.** Male palp of *Icius deergong* sp. nov., paratype (TRU-JS 0733) **A** prolateral **B** ventral **C** retrolateral. Abbreviations: DTA dorsal tibial apophysis; E embolus; RTA retrolateral tibial apophysis; TB tegular bump. Scale bars: 0.1 mm.

except eye field dark, with marginal white scale-like setal stripe; fovea indistinct. Chelicerae with two promarginal teeth and one retromarginal tooth. Legs pale with dark stripes except femora, patellae, and tibiae I dark brown; legs I with thickened femora, patellae, and tibiae, covered with cluster of dark ventral setae on patellae and tibiae. Dorsum of abdomen mainly dark brown, covered with dense dark setae, with several transverse, pale yellow lateral stripes; venter pale.

**Palp** (Fig. 5A–C): femur length/width ratio ca 2.0; patella slightly wider than long in retrolateral view; tibia ~ 2/3 of patellar length in retrolateral view; retrolateral tibial apophysis (RTA) strongly sclerotized, bifurcated basally with two slender, hook-shaped rami pointed apically; dorsal tibial apophysis (DTA) tiny, with pointed tip; cymbium ~ 1.35× longer than wide; tegulum ~ 1.43× longer than wide, with small, antero-retrolateral bump (TB); embolus (E) originating at ca 9:30 o'clock position, curved ventrally at base, and with rather blunt tip.

**Female** (Fig. 6A–D, G). Total length 2.88. Carapace 1.20 long, 0.73 wide. Abdomen 1.78 long, 0.90 wide. Eye sizes and interdistances: AME 0.24, ALE 0.11, PLE 0.11, AERW 0.63, PERW 0.73, EFL 0.55. Legs: I 1.64 (0.50, 0.28, 0.38, 0.25, 0.23), II 1.38 (0.40, 0.25, 0.30, 0.23, 0.20), III 1.49 (0.45, 0.23, 0.30, 0.28, 0.23), IV 2.11 (0.65, 0.35, 0.45, 0.43, 0.23). Habitus (Fig. 6G) similar to that of male except darker, and without cluster of dark ventral setae on patellae and tibiae I.

**Epigyne** (Fig. 6A–D) longer than wide; atrium (At) large, occupying most region of posterior 2/5, separated by narrow septum (Se); copulatory openings (CO) almost round, touching each other; copulatory ducts (CD) tapered into invert infundibuliform on proximal half, then acutely narrowed and forming ca 90° curves; spermathecae (S) almost spherical, with posteriorly extending portions.

**Distribution.** Known only from the type locality in Xizang, China (Fig. 47).

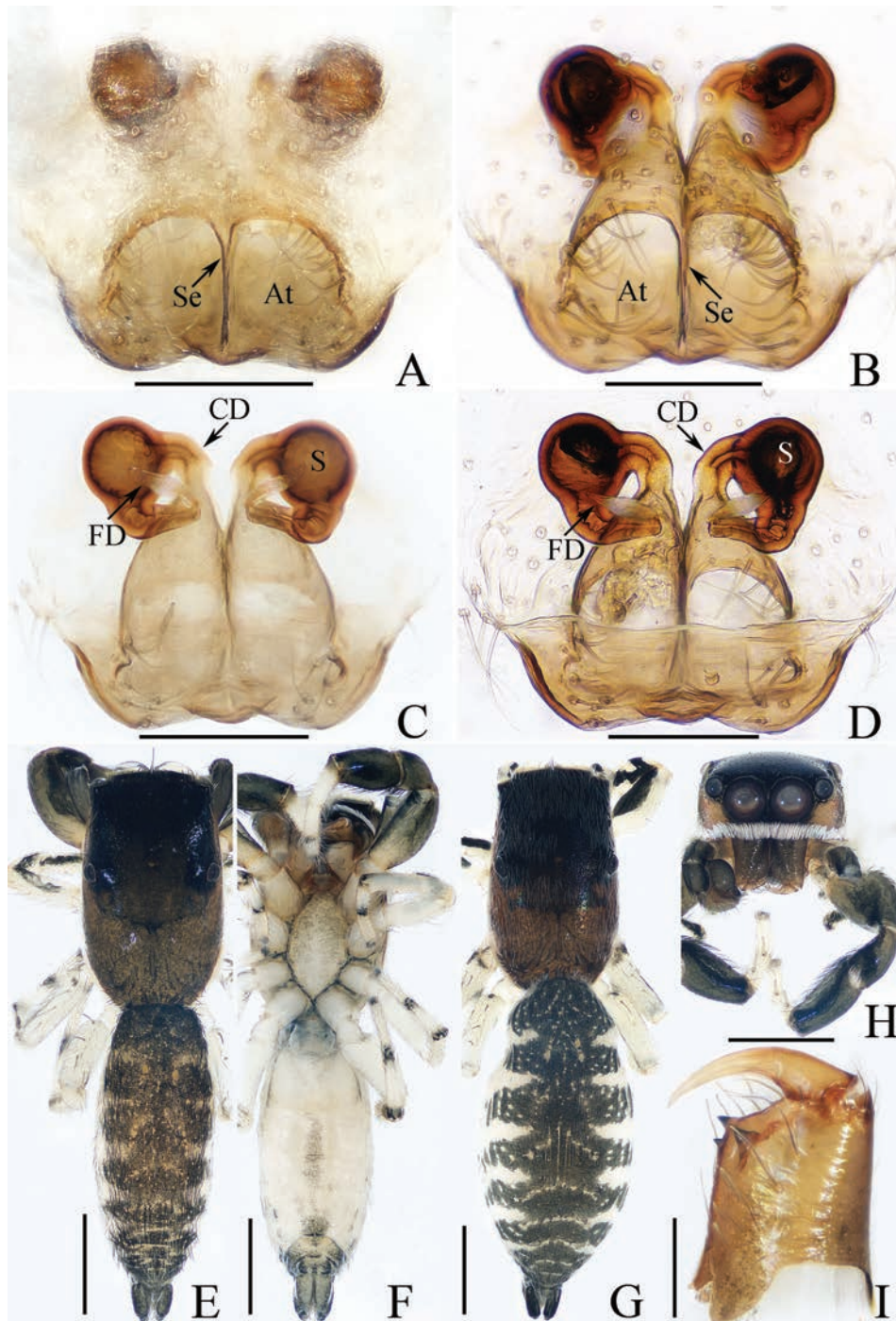


**Figure 6.** *Icius deergong* sp. nov., **E, F, H, I** male holotype and **A–D, G** female paratype (TRU-JS 0734) **A, B** epigyne, ventral **C, D** vulva, dorsal **E, G** habitus, dorsal **F** ditto, ventral **H** carapace and leg I, frontal **I** chelicera, posterior. Abbreviations: At atrium; CD copulatory duct; FD fertilization duct; S spermatheca ; Se septum. Scale bars: 0.1 mm (**A–D, I**); 0.5 mm (**E–H**).

### Genus *Irura* Peckham & Peckham, 1901

**Type species.** *Irura pulchra* Peckham & Peckham, 1901; type locality Ceylon, now Sri Lanka.

**Comments.** This genus is assigned to the subtribe Simaethina Simon, 1903, within the Vicirini Simon, 1901 (Maddison 2015), and contains 21 species

known from east, south, and southeast Asia (WSC 2024). The genus is rather poorly studied, as the generotype is lacking diagnostic drawings, and nearly 30% of its species are known only from a single sex (WSC 2024). Moreover, based on our recent study, several Chinese species are mismatched (female and male belong to different species) and need further revision. The following two species are placed in the genus due to similar habitus and copulatory organs to most *Irura* species.

***Irura qiuhangi* sp. nov.**

<https://zoobank.org/0743067C-2711-42DE-A8BB-61C2B7496F91>

Figs 7, 8, 48

**Type material.** **Holotype** ♀ (TRU-JS 0737), CHINA: • Yunnan Province, Menghai County, Menghai Township, Manliang Village (21°56.36'N, 100°28.37'E, elevation undetailed), 18.III.2024, Hang Qiu leg. **Paratype** • 1 ♂ (TRU-JS 0738), same data as for holotype.

**Etymology.** The specific name is a patronym in honor of the collector; noun (name) in the genitive case.

**Diagnosis.** The female of *Irura qiuhangi* sp. nov. resembles that of *I. uniprocessa* Mi & Wang, 2016 in having a similar atrium (At) and transversely extended anterior chamber of spermatheca (AS), but can be easily distinguished by the rounded posterior chamber of spermatheca (PS) (Fig. 8B) vs elongated (Mi and Wang 2016: figs 1G, 2e). The male of *I. qiuhangi* sp. nov. resembles that of *I. shendurney* Asima, Caleb & Prasad, 2024 in the point of origin of the embolus (E) and the form of cymbial process (CP), but can be easily distinguished by the absence of tibial apophysis (Fig. 7B, C) vs retrolateral apophysis present (Asima et al. 2024: figs 41, 44).

**Description. Female** (Fig. 8A, B, D–G). Total length 2.65. Carapace 1.34 long, 1.44 wide. Abdomen 1.38 long, 1.53 wide. Eye sizes and interdistances: AME 0.30, ALE 0.17, PLE 0.16, AERW 1.11, PERW 1.34, EFL 0.49. Legs: I 3.63 (1.05, 0.75, 0.98, 0.50, 0.35), II (0.75, 0.45, 0.45, 0.40, missing), III 2.12 (0.65, 0.38, 0.43, 0.38, 0.28), IV (0.88, 0.43, 0.53, missing, missing). Carapace orange-brown, with pair of round dots behind PMEs, followed by oval, brown patch, covered with pale brown long setae and scales. Chelicerae red-brown, incised on base of anterior surface, with two promarginal teeth and one retromarginal fissentate tooth with four cusps. Leg I robust, with two pairs of ventral spines on tibiae and metatarsi. Abdomen oval, dorsum pale yellow, with two pairs of large depressions; venter pale, with small pale brown dots medially.

**Epigyne** (Fig. 8A, B) ~ 1.8× wider than long; atrium (At) almost square, divided by narrow septum (Se); copulatory openings (CO) beneath lateral portions of atrium; copulatory ducts (CD) weakly sclerotized, curved at base, and connected to distal ends of junction ducts of spermathecae (JS); spermathecae (S) divided into transversely extending, kidney-shaped anterior chamber (AS) and round posterior chamber (PS); fertilization ducts (FD) originating from antero-inner portions of posterior chamber of spermatheca.

**Male** (Figs 7, 8C). Total length 2.62. Carapace 1.38 long, 1.58 wide. Abdomen 1.35 long, 1.68 wide. Eye sizes and interdistances: AME 0.31, ALE 0.18, PLE 0.17, AERW 1.19, PERW 1.50, EFL 0.61. Legs: I 4.75 (1.50, 1.15, 1.00, 0.65,

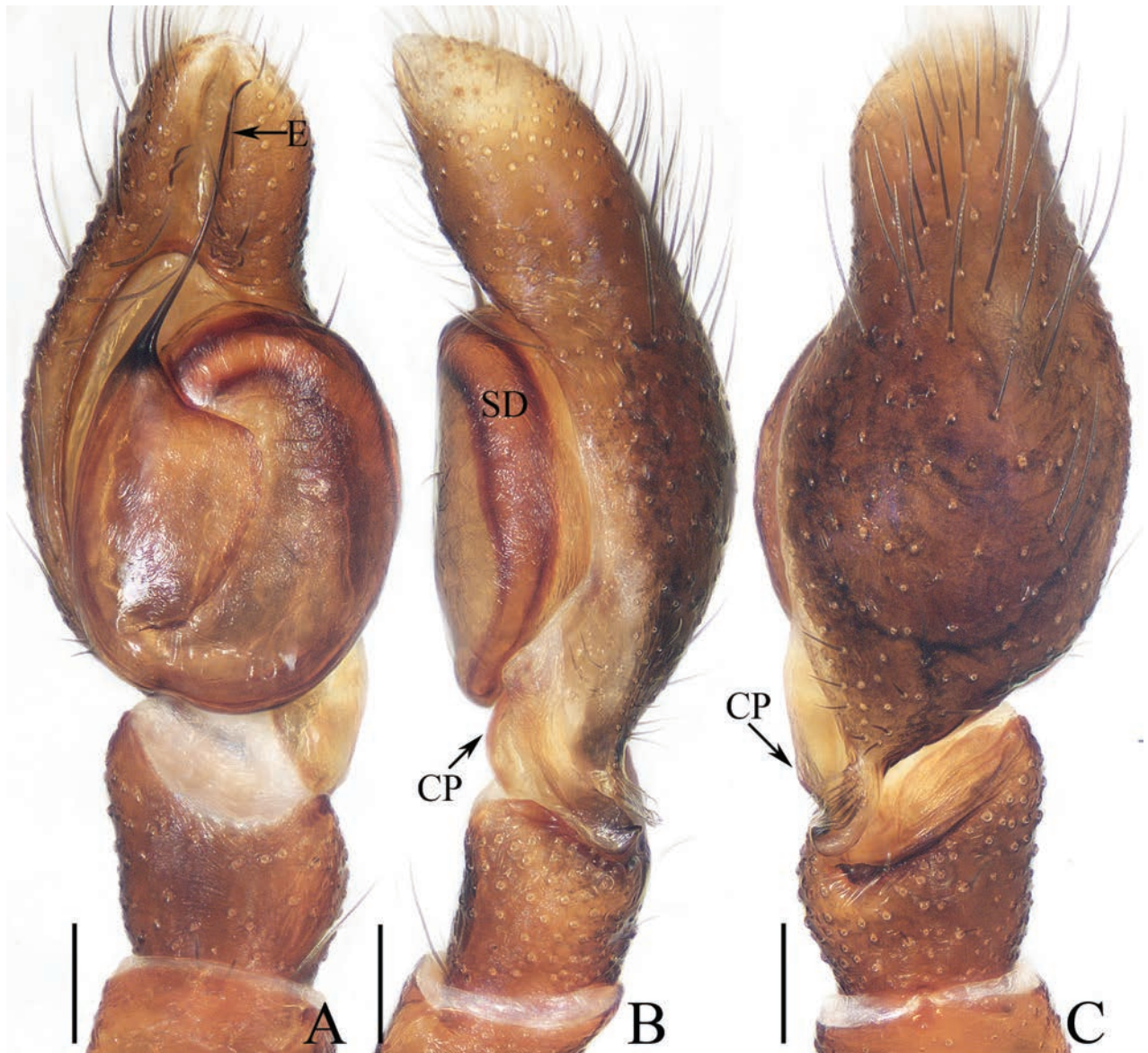


**Figure 7.** Male palp of *Irura qiuhangi* sp. nov., paratype (TRU-JS 0738) **A** ventral **B** retrolateral **C** dorsal. Abbreviations: CP cymbial process; E embolus; SD sperm duct. Scale bars: 0.1 mm.

0.45), II 2.68 (0.90, 0.50, 0.50, 0.48, 0.30), III 2.19 (0.75, 0.38, 0.38, 0.40, 0.28), IV 2.70 (0.90, 0.50, 0.50, 0.50, 0.30). Carapace (Fig. 8C) red-brown, with central irregular dark patch on cephalon, covered with dense thin setae and scales. Abdomen (Fig. 8C) oval, dorsum with irregular brown patch, and without similar shallow depressions as in female; venter brown.

**Palp** (Fig. 7A–C): femur length/width ratio ca 2.8; patella ~ 1.4× longer than wide; tibia slightly longer than wide, lacking apophyses; cymbium ~ 2× longer than wide, with sizeable baso-retrolateral process (CP) curved medially and with pointed end; tegulum flat, almost round, with sperm duct (SD) extending along submargin; embolus (E) originating at ca 10 o'clock position, ~ 5/6 tegular length, flagelliform.

**Distribution.** Known only from the type locality in Yunnan, China (Fig. 48).

**Comments.** As the female can be more easily distinguished from other congeners than the male, it was chosen as the holotype.

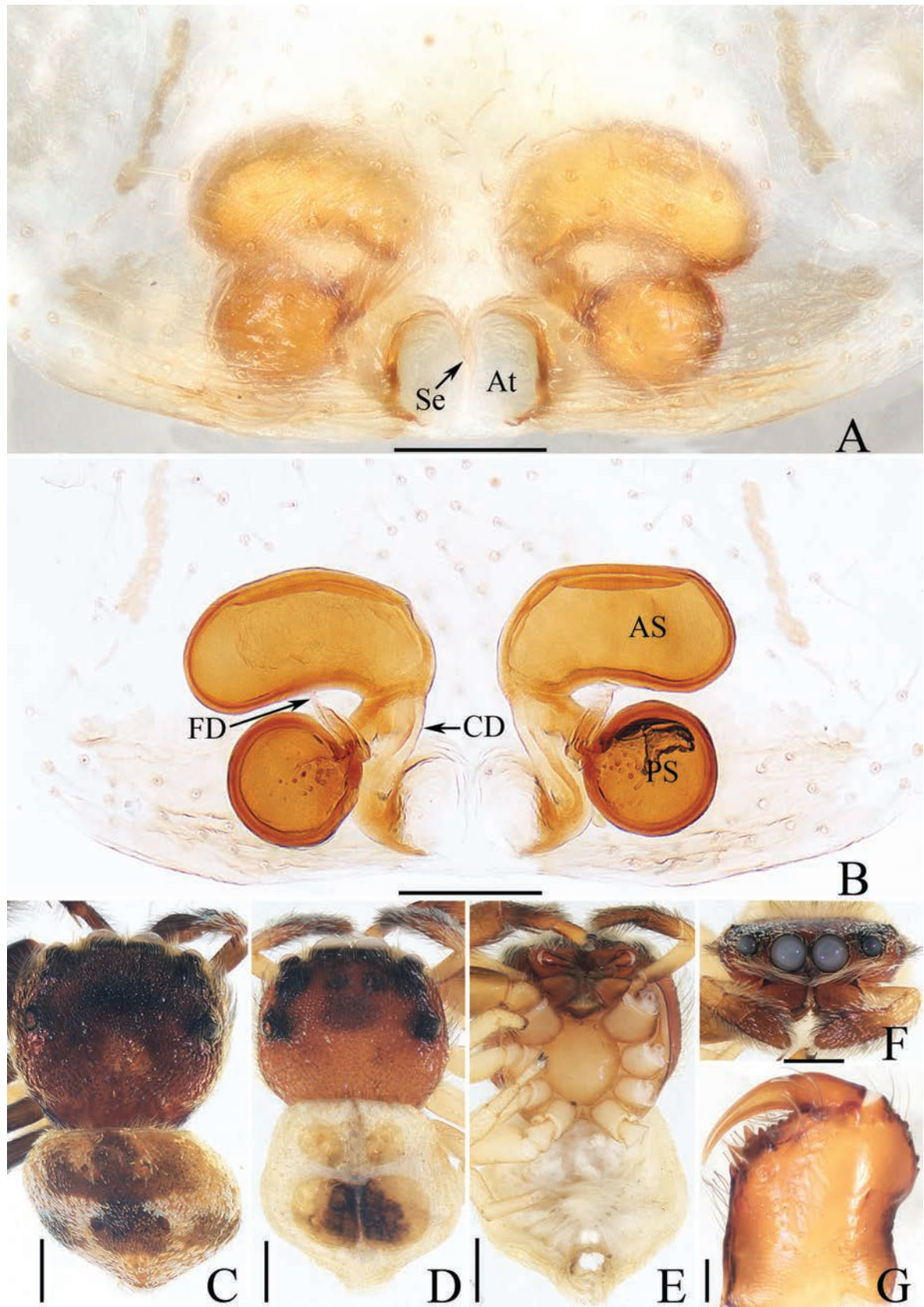


**Figure 8.** *Irura qihangi* sp. nov., **A, B, D–G** female holotype and **C** male paratype (TRU-JS 0738) **A** epigyne, ventral **B** vulva, dorsal **C, D** habitus, dorsal **E** ditto, ventral **F** carapace, frontal **G** chelicera, posterior. Abbreviations: At atrium; AS anterior chamber of spermatheca; CD copulatory duct; FD fertilization duct; PS posterior chamber of spermatheca; Se septum. Scale bars: 0.1 mm (**A, B, G**); 0.5 mm (**C–F**).

***Irura yarlungzangbo* sp. nov.**

<https://zoobank.org/34323023-3011-48DA-B5B9-0BF3A5FFA9DC>

Figs 9, 10, 47

**Type material. Holotype** ♀ (TRU-JS 0739), CHINA: • Xizang Autonomous Region, Medog County, Beibeng Township, Deergong Village, Yarlung Zangbo National Nature Reserve (29°10.84'N, 95°8.67'E, ca 1670 m), 25.V.2024, X.Q. Mi et al. leg.

**Paratypes** • 1 ♂ 2 ♀ (TRU-JS 0740–0742), same data as for holotype.

**Etymology.** The specific name refers to the Yarlung Zangbo National Nature Reserve, the type locality; noun in apposition.

**Diagnosis.** The female of *Irura yarlungzangbo* sp. nov. resembles that of *I. zhangae* Gan, Wang & Peng, 2017 in having a similar epigyne, but can be easily distinguished by the anterior chamber of spermatheca (AS), ~ 1.3× longer than wide (Fig. 10B) vs ~ 2× longer than wide (Gan et al. 2017: fig. 2F, G, 3D, E), and by the absence of an incision between copulatory openings (Fig. 10A) vs having a square incision between copulatory openings (Gan et al. 2017: figs 2F, G, 3D, E). The male can be easily distinguished by the presence of dorsal cymbial extension (DCE), which bears several retromarginal spines (Fig. 9B, C) vs absent in other congeners (see Metzner 2024).

**Description. Female** (Fig. 10A, B, D–G). Total length 3.78. Carapace 1.43 long, 1.65 wide. Abdomen 2.05 long, 1.65 wide. Eye sizes and interdistances: AME 0.38, ALE 0.22, PLE 0.19, AERW 1.31, PERW 1.55, EFL 0.74. Legs: I 3.28 (1.05, 0.75, 0.65, 0.48, 0.35), II 2.31 (0.75, 0.45, 0.45, 0.38, 0.28), III 2.02 (0.63, 0.35, 0.38, 0.38, 0.28), IV 2.49 (0.85, 0.43, 0.50, 0.43, 0.28). Carapace red-brown, covered with thin brown setae and pale scales, with pair of dark spots centrally on eye field. Chelicerae incised on base of anterior surface, with two promarginal teeth and one retromarginal fissidentate tooth with three cusps. Leg I robust, with two pairs of ventral spines on tibiae and metatarsi. Abdomen oval, dorsum mainly pale, with two pairs of anterior muscle depressions and medio-posterior shallow depressions surrounded by brown C-shaped stripes; venter with dark brown posterior half, and two pairs of pale yellow dotted lines.

**Epigyne** (Fig. 10A, B) ~ 1.65× wider than long, weakly sclerotized; copulatory openings (CO) postero-marginally located, opened posterolaterally, separated by > 1/3 epigynal width; copulatory ducts (CD) thin, slightly curved proximally and distally, and connected to distal portions of junction ducts of spermathecae (JS); spermathecae (S) divided into oval anterior chamber (AS) and spherical posterior chamber (PS); fertilization ducts (FD) originating at antero-inner margins of anterior chamber of spermatheca.

**Male** (Figs 9, 10C, H). Total length 2.63. Carapace 1.29 long, 1.37 wide. Abdomen 1.41 long, 1.22 wide. Eye sizes and interdistances: AME 0.35, ALE 0.20, PLE 0.15, AERW 1.14, PERW 1.31, EFL 0.65. Legs: I 3.53 (1.05, 0.75, 0.78, 0.50, 0.45), II 2.34 (0.75, 0.43, 0.45, 0.43, 0.28), III 2.00 (0.63, 0.33, 0.38, 0.38, 0.28), IV missing. Carapace (Fig. 10C) brown, covered with purplish gold scales. Chelicerae (Fig. 10H) similar to that of female except retromarginal fissidentate tooth only with two cusps. Legs brown, mingled with green. Abdomen (Fig. 10C) oval, dorsum mainly dark brown, covered with purplish gold scales, with pair of pale median patches and transverse, posterior, pale band; venter dark brown.

**Palp** (Fig. 9A–C): femur length/ width ratio ca 2.72; patella ~ 1.6× longer than wide in retrolateral view; tibia slightly longer than patella, with well-developed,



**Figure 9.** Male palp of *Irura yarlungzangbo* sp. nov., paratype (TRU-JS 0740) **A** ventral **B** retrolateral **C** dorsal. Abbreviations: CP cymbial process; E embolus; DCE dorsal cymbial extension; DTP dorsal tibial process; RTA retrolateral tibial apophysis; SD sperm duct. Scale bars: 0.1 mm.

lamellar retrolateral apophysis (RTA) and swollen dorsal process (DTP); cymbium ~ 2× longer than wide, with weakly sclerotized retrolateral process (CP) partly covered by retrolateral tibial apophysis and with pointed end, and well developed, posteriorly extending dorsal extension (DCE) bearing several retromarginal spines; tegulum flat, oval; embolus (E) filiform, 1.2× longer than tegulum, originating at ca 9 o'clock position.

**Distribution.** Known only from the type locality in Xizang, China (Fig. 47).

#### Genus *Mintonia* Wanless, 1984

**Type species.** *Mintonia tauricornis* Wanless, 1984; type locality Sarawak, Indonesia.

**Comments.** This genus is placed in the subtribe Spartaeina Wanless, 1984 within the Spartaeini Wanless, 1984 (Maddison 2015). To date, ten species have been described, and all are restricted to Southeast Asia (WSC 2024). A significant taxonomic study of the genus was done by Wanless (1984, 1987), who described eight new species and first illustrated the transferred species, *Mintonia ramipalpis* (Thorell, 1890). However, seven species described by him are only known from a single sex.

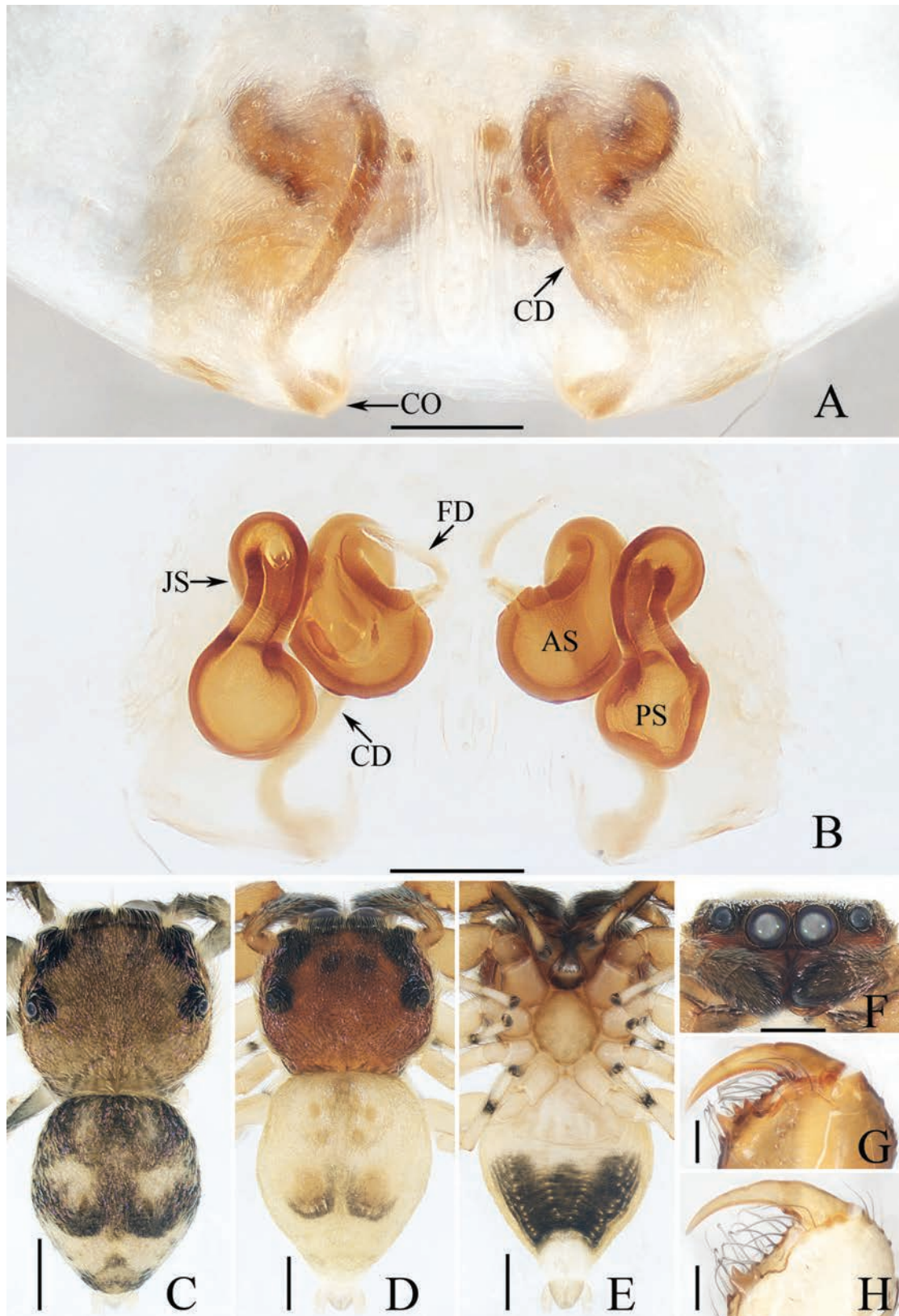


**Figure 10.** *Irura yarlungzangbo* sp. nov. **A, B, D–G** female holotype and **C, H** male paratype (TRU-JS 0740) **A** epigyne, ventral **B** vulva, dorsal **C, D** habitus, dorsal **E** ditto, ventral **F** carapace, frontal **G, H** chelicera, posterior. Abbreviations: AS anterior chamber of spermatheca; CD copulatory duct; CO copulatory opening; FD fertilization duct; JS junction duct of spermatheca; PS posterior chamber of spermatheca. Scale bars: 0.1 mm (**A, B, G, H**); 0.5 mm (**C–F**).

***Mintonia shiwandashan* sp. nov.**

<https://zoobank.org/6CB986A6-0998-4233-898A-3AA4652F30F8>

Figs 11, 47

**Type material.** *Holotype* ♂ (TRU-JS 0743), CHINA: • Guangxi Zhuang Autonomous Region, Fangchenggang City, Shiwandashan National Nature Reserve, Wanglue Station (21°54.23'N, 107°54.18'E, ca 310 m), 30.IV.2021, A.L. He et al. leg.

**Etymology.** The specific name refers to the type locality: Shiwandashan National Nature Reserve; noun in apposition.

**Diagnosis.** *Mintonia shiwandashan* sp. nov. resembles *M. breviramis* Wanless, 1984 in having very short embolus (E), but can be easily distinguished by the presence of baso-retrolateral and dorsal tibial apophyses, and by the bifurcated retrolateral tibial apophysis (RTA) (Fig. 11B, C) vs lacking baso-retrolateral and dorsal tibial apophyses and having non-bifurcated retrolateral tibial apophysis (Wanless 1984: fig. 12A, B).

**Description. Male** (Fig. 11). Total length 5.10. Carapace 2.43 long, 2.05 wide. Abdomen 2.62 long, 1.71 wide. Eye sizes and interdistances: AME 0.62, ALE 0.38, PLE 0.34, AERW 2.00, PERW 1.86, EFL 1.19. Legs: I 5.92 (1.70, 0.88, 1.53, 1.18, 0.63), II 5.43 (1.60, 0.85, 1.30, 1.10, 0.58), III 5.08 (1.50, 0.50, 1.25, 1.25, 0.58), IV 6.86 (1.95, 0.78, 1.68, 1.75, 0.70). Carapace pale yellow except eye field dark, with elevated and square cephalon, covered with brown and golden thin setae; fovea dark. Chelicerae yellow, with three promarginal and seven smaller retromarginal teeth. Legs yellow, tinged with brown, spiny. Dorsum of abdomen pale to brown, covered with golden and dark setae, with two well-visible pairs of anteromedian muscle depressions; venter pale, with two pairs of dotted lines medially.

**Palp** (Fig. 11A–C): femur length/width ratio ca 3.3; patella ~ 1.5× longer than wide in retrolateral view; tibia slightly longer than wide in ventral view, with almost half-round, lamellar base-retrolateral apophysis (BTA); ventral tibial apophysis (VTA) almost sub-triangular; retrolateral tibial apophysis (RTA) strongly sclerotized, bifurcated with two blunt rami; dorsal tibial apophysis (DTA) bar-shaped, with blunt end in dorsal view; cymbium ~ 1.47× longer than wide in ventral view; tegulum oval; embolus (E) strongly sclerotized, broad, with tapered projection.

**Female.** Unknown.

**Distribution.** Known only from the type locality in Guangxi, China (Fig. 47).

**Comments.** Although the new species is similar to *Portia jianfeng* Song & Zhu, 1998 in palpal structure, it has not been considered to be a member of *Portia* Karsch, 1878 because it lacks tufts on the abdomen and a pronounced dorso-basal flange on the cymbium, which are diagnostic for *Portia* (Wanless 1984). The new species is provisionally placed in the genus *Mintonia* due to the general similarity of palpal structure to current congeners.

**Genus *Myrmarachne* MacLeay, 1839**

**Type species.** *Myrmarachne melanocephala* MacLeay, 1839; type locality India.

**Comments.** *Myrmarachne*, the species-richest genus of the subtribe Myrmarachnina Simon, 1901 within the tribe Myrmarachnini Simon, 1901 (Maddison and Szűts 2019), contains 192 nominal species widely distributed

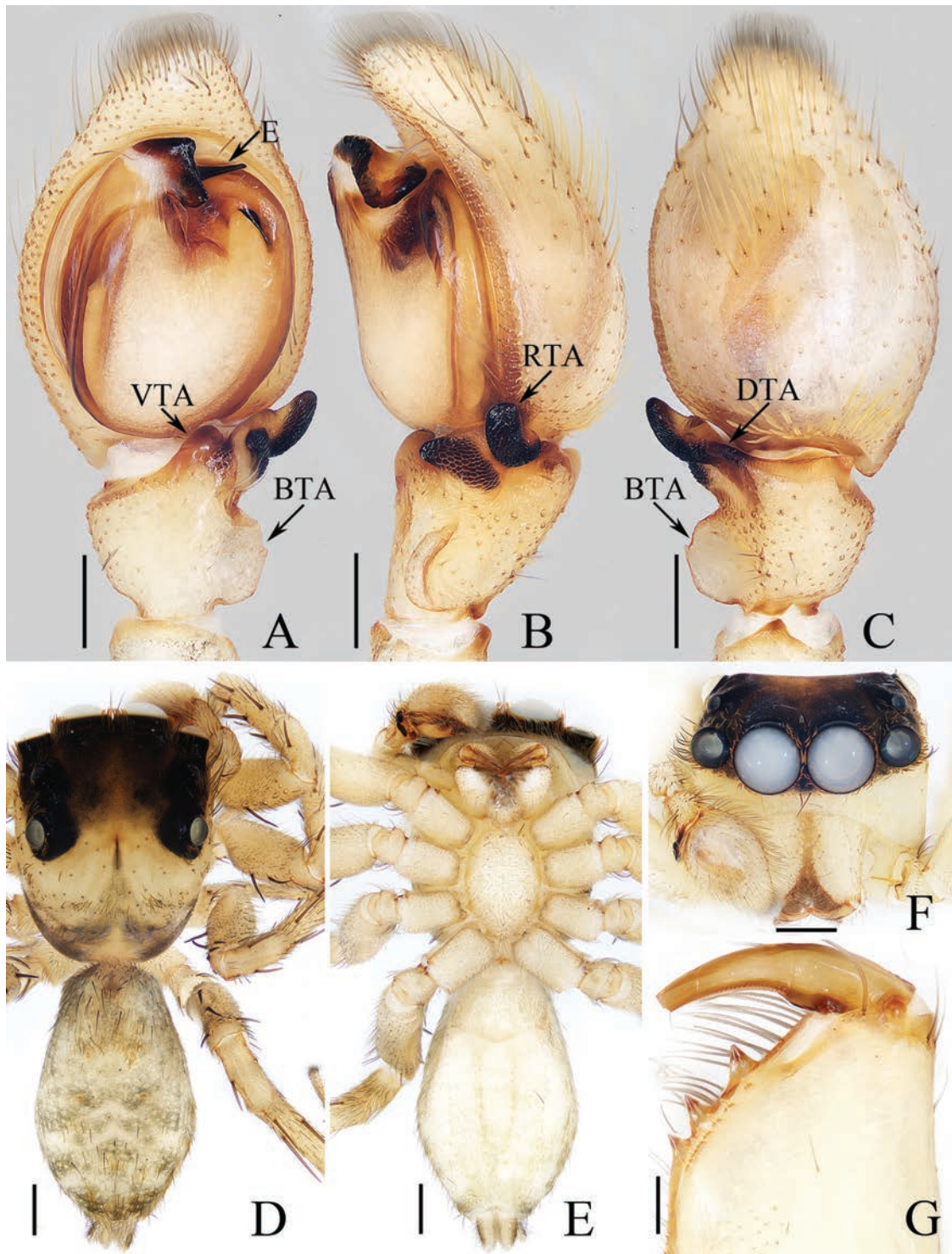


**Figure 11.** *Mintonia shiwandashan* sp. nov., holotype **A** palp, ventral **B** ditto, retrolateral **C** ditto, dorsal **D** habitus, dorsal **E** ditto, ventral **F** carapace, frontal **G** chelicera, posterior. Abbreviations: BTA baso-retrolateral tibial apophysis; DTA dorsal tibial apophysis; E embolus; RTA retrolateral tibial apophysis; VTA ventral tibial apophysis. Scale bars: 0.2 mm (**A–C, G**); 0.5 mm (**D–F**).

all over the globe (WSC 2024). *Myrmarachne* is one of the most poorly studied genera among the Salticidae since ~ 48.95% of its species are known only from a single sex or sub-adult specimen, > 50 species have not been illustrated or lack essential diagnostic drawings. Moreover, many of its species share similar copulatory organs and present several color patterns, making them difficult to

identify. There is no doubt that a few of its species could be potential synonyms or the “missing” sex of another congener. In addition, Prószyński (2016) split and resurrected eleven genera from *Myrmarachne* according to morphological characters. However, this conclusion has not been supported by the subsequent molecular evidence (Yamasaki et al. 2018; Maddison and Szűts 2019). Thus, the phylogenetic relationship between *Myrmarachne* and the mentioned eleven genera remains uncertain.

***Myrmarachne kuan* sp. nov.**

<https://zoobank.org/99B67F00-8D9E-4D75-AF2D-A5B0E7D327B4>

Figs 12, 13, 48

**Type material.** **Holotype** ♂ (TRU-JS 0744), CHINA: • Yunnan Province, Pingbian Miao Autonomous County, around Tuanpo Reservoir (22°58.33'N, 103°41.25'E, ca 1560 m), 15.V.2024, C. Wang et al. leg. **Paratypes** • 2 ♂ 5 ♀ (TRU-JS 0745–0751), same data as for holotype; • 1 ♀ (IZCAS-Ar 45282), Hainan, Lingshui County, Diaoluoshan National Nature Reserve, Power Station (18°39.84'N, 109°55.81'E, ca 100 m), 20.IV.2009, G. Tang leg.

**Etymology.** The specific name is a noun and comes from Chinese Pinyin ‘kuan’, meaning broad, which refers to the broadened thoracic part.

**Diagnosis.** The male of *Myrmarachne kuan* sp. nov. resembles that of *M. salaputium* Yamasaki, 2018 in general shape of the palp, but can be easily distinguished by the flat cephalon that is lower than thoracic part in lateral view (Fig. 13E) vs elevated cephalon that is much higher than thoracic part (Yamasaki et al. 2018: fig. 45). The female resembles those of *M. lambirensis* Yamasaki & Ahmad, 2013 in having a similar epigyne, but can be easily distinguished by the presence of an epigynal hood (H), and by the sclerotized portions of copulatory ducts curved into circles at base (Fig. 13A, B) vs epigynal hood absent, and sclerotized portions of copulatory ducts slightly curved into C-shapes (Yamasaki and Ahmad 2013: fig. 23D–F).

**Description. Male** (Figs 12, 13C–E, G). Total length 3.72. Carapace 1.80 long, 0.98 wide. Abdomen 1.61 long, 0.83 wide. Eye sizes and interdistances: AME 0.30, ALE 0.15, PLE 0.14, AERW 0.89, PERW 0.98, EFL 0.65. Legs: I 2.91 (0.83, 0.40, 0.88, 0.50, 0.30), II 2.32 (0.65, 0.38, 0.58, 0.43, 0.28), III 2.39 (0.70, 0.33, 0.53, 0.53, 0.30), IV 3.19 (0.95, 0.43, 0.80, 0.68, 0.33). Carapace flat, covered with sparse white scales, with laterally broadened thoracic part. Chelicerae elongated, with six promarginal and five tiny retromarginal teeth. Legs slender, with one, eight, and four ventral spines on patellae, tibiae, and metatarsi I, respectively. Abdomen slightly constricted at anterior 1/5, dorsum mainly dark, covered with several white scales; venter dark brown.

**Palp** (Fig. 12A–C): femur length/width ratio ca 2.5; patella ~ 1.4× longer than wide in retrolateral view; tibia broad, with prolateral projected portion, and tapered retrolateral apophysis (RTA) approximately as long as tibia, slightly curved inward distally, and with rather pointed tip; cymbium length/width ratio ca 1.37, tapered at distal 1/4; tegulum flat and round, with sperm duct extending along submargin circularly; embolus (E) originating at ca 6 o'clock position of tegulum, making ca 540° course and terminating at ca 1:30 o'clock position.



**Figure 12.** Male palp of *Myrmarachne kuan* sp. nov., paratype (TRU-JS 0745) **A** ventral **B** retrolateral **C** dorsal. Abbreviations: E embolus; RTA retrolateral tibial apophysis; SD sperm duct. Scale bars: 0.1 mm.

**Female** (Fig. 13A, B, F, H). Total length 4.33. Carapace 1.88 long, 0.86 wide. Abdomen 1.96 long, 1.12 wide. Eye sizes and interdistances: AME 0.30, ALE 0.15, PLE 0.14, AERW 0.87, PERW 0.92, EFL 0.61. Legs: I 2.44 (0.68, 0.40, 0.68, 0.40, 0.28), II 2.02 (0.58, 0.38, 0.50, 0.33, 0.23), III 2.12 (0.60, 0.33, 0.48, 0.48, 0.23), IV 3.03 (0.90, 0.45, 0.75, 0.63, 0.30). Habitus (Fig. 13F) similar to that of male except less-developed chelicerae (Fig. 13H) with six larger retromarginal teeth.

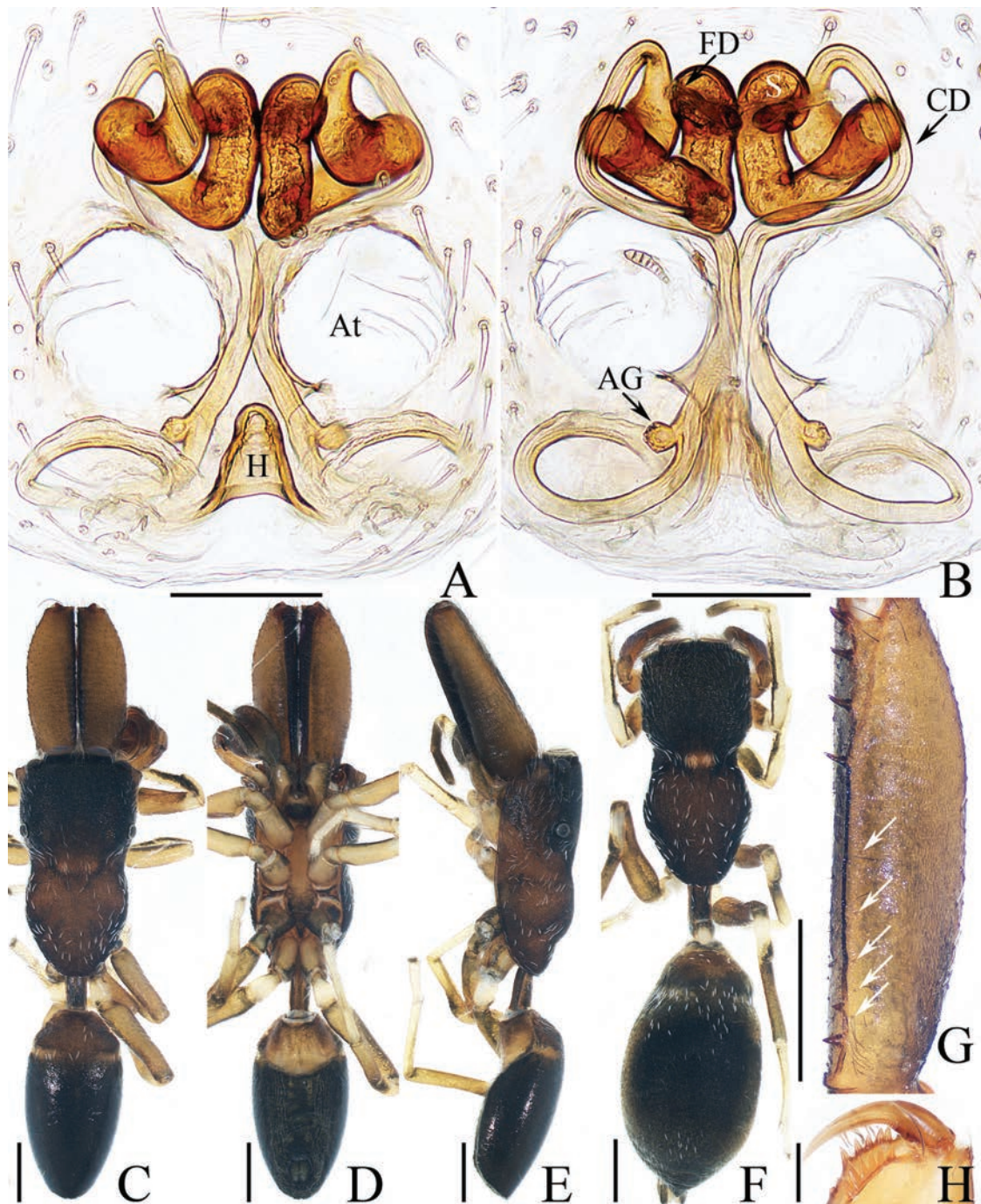


**Figure 13.** *Myrmarachne kuan* sp. nov. **C–E, G** holotype and **A, B, F, H** female paratype (TRU-JS 0747) **A** epigyne, ventral **B** vulva, dorsal **C, F** habitus, dorsal **D** ditto, ventral **E** ditto, lateral **G, H** chelicera, posterior. Abbreviations: AG accessory gland; At atrium; CD copulatory duct; FD fertilization duct; H epigynal hood; S spermatheca. Scale bars: 0.1 mm (**A, B, H**); 0.5 mm (**C–G**).

**Epigyne** (Fig. 13A, B) longer than wide, with posterior, bell-shaped hood (H); atrium (At) paired, almost round; copulatory openings (CO) invisible; sclerotized portions of copulatory ducts slender, forming complicated coils, and with short accessory glands (AG) on position of proximal 2/5; spermathecae (S) elongated, folded twice; fertilization ducts (FD) originating from antero-inner portions of spermathecae.

**Distribution.** China (Hainan, Yunnan; Fig. 48).

## Genus *Nandicius* Prószyński, 2016

**Type species.** *Phintella mussooriensis* Prószyński, 1992; type locality Mussoorie, India.

**Comments.** This genus was recently considered to be a member of Chrysellini (Yang & Zhang, 2024). To date, 13 species are known from Afghanistan to Japan (WSC 2024). Within the genus, many species (> 46%) are known only from a single sex (WSC 2024), and several members most likely are misplaced and need to be further revised, such as *N. proshynskii* Wang & Li, 2021 (Yunnan, China), *N. shihaitaoi* Wang & Li, 2023 (Hainan, China), and *N. woongilensis* Kim & Lee, 2016 (Korea). The first two could be related to *Icius indicus* (Simon, 1901), and the last one may belong to *Pseudeuophrys* Dahl, 1912.

### *Nandicius xiefengi* sp. nov.

<https://zoobank.org/277A2491-14F1-4E0A-871C-9D4BF0506035>

Figs 14, 15, 48

**Type material.** **Holotype** ♂ (TRU-JS 0752), CHINA: • Xizang Autonomous Region, Medog County, Damu Township, Zhu Village (29°29.73'N, 95°25.86'E, ca 1740 m), 27.V.2024, X.F. Wang. leg. **Paratype** 1 ♀ (TRU-JS 0753), same data as for holotype.

**Etymology.** The specific name is a patronym in honor of the collector; noun (name) in the genitive case.

**Diagnosis.** The male of *Nandicius xiefengi* sp. nov. resembles that of *N. gyrongensis* (Hu, 2001) in having similar retrolateral tibial apophysis (RTA), but can be easily distinguished by the following: 1) embolus (E) curved towards antero-retrolateral side (Fig. 14B) vs antero-prolateral side (Yang and Zhang 2024: figs 155, 161); 2) posterior tegular lobe (PL) extending posteriorly (Fig. 14B) vs extending prolatero-posteriorly (Yang and Zhang 2024: figs 155, 161). The female of *N. xiefengi* sp. nov. can be easily distinguished from congeners by the anteriorly located epigynal hood (H) (Fig. 15A) vs posteriorly located in the others (see Metzner 2024).

**Description. Male** (Figs 14, 15C, D, F, G). Total length 3.68. Carapace 1.84 long, 1.32 wide. Abdomen 1.95 long, 1.08 wide. Eye sizes and interdistances: AME 0.34, ALE 0.16, PLE 0.15, AERW 1.08, PERW 1.11, EFL 0.81. Legs: I 3.88 (1.05, 0.65, 0.90, 0.90, 0.38), II 2.64 (0.78, 0.48, 0.60, 0.45, 0.33), III 2.74 (0.93, 0.43, 0.50, 0.53, 0.35), IV 3.12 (0.93, 0.43, 0.70, 0.68, 0.38). Carapace mainly dark brown, with pair of elongated, dark patches centrally on cephalon, and longitudinal, orange band extending from middle between PMEs to posterior end, covered with dense pale and dark setae. Chelicerae orange, with two promarginal teeth and one retromarginal tooth. Legs pale except legs I mottled with dark. Dorsum of abdomen mainly green-brown, with longitudinal, irregular pale patch extended over whole surface, and two pairs of median muscle depressions; venter pale laterally, and dark brown centrally, with pair of longitudinal, central dotted lines.

**Palp** (Fig. 14A–C): femur length/width ratio ca 3.2; patella almost as long as wide in retrolateral view; tibia ~1.3× wider than long in retrolateral view;

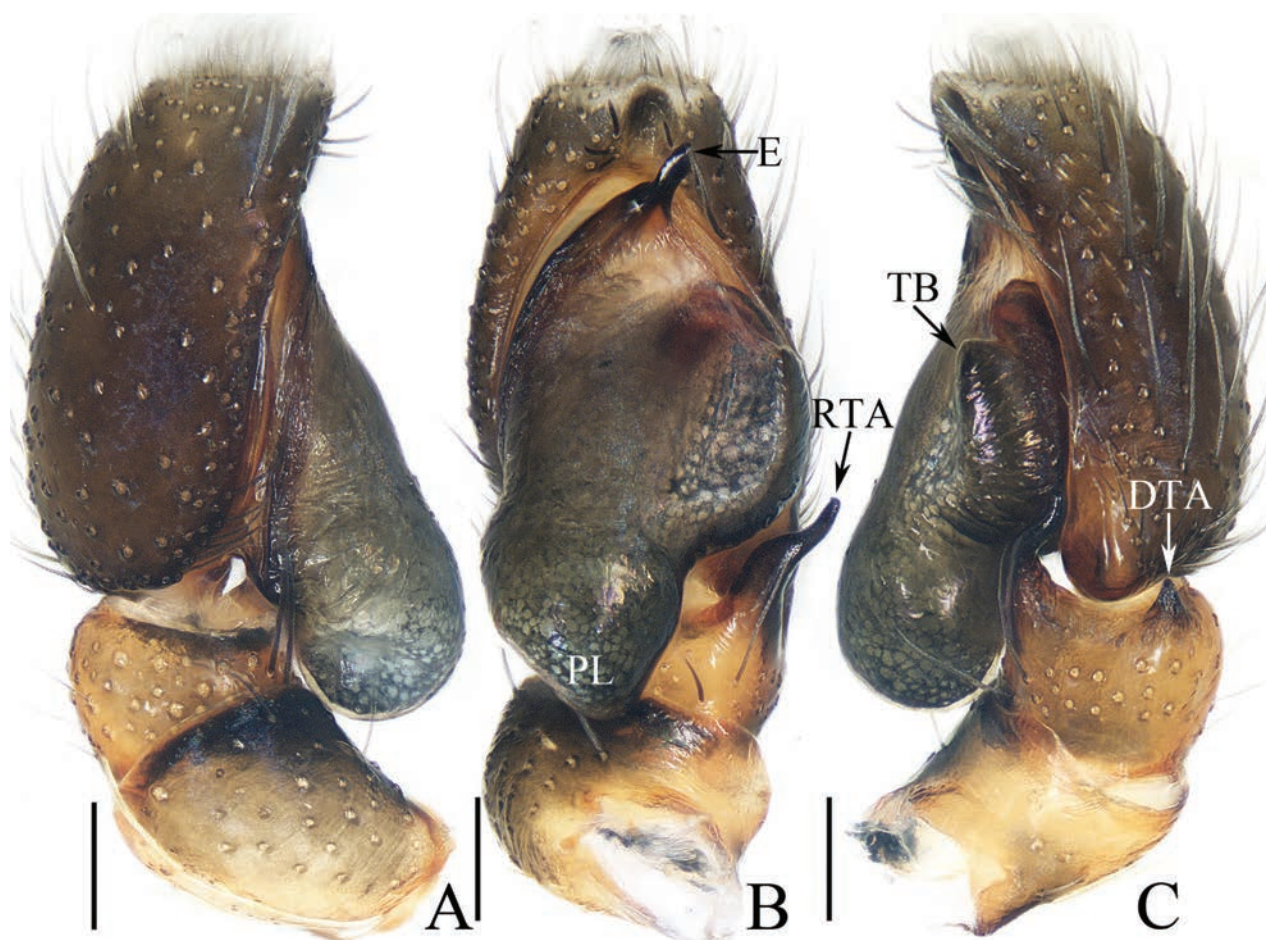


**Figure 14.** Male palp of *Nandicius xiefengi* sp. nov., holotype **A** prolateral **B** ventral **C** retrolateral. Abbreviations: DTA dorsal tibial apophysis; E embolus; PL posterior tegular lobe; RTA retrolateral tibial apophysis; TB tegular bump. Scale bars: 0.1 mm.

retrolateral tibial apophysis (RTA) strongly sclerotized, curved medially, and with rather blunt tip; dorsal tibial apophysis (DTA) sub-triangular; cymbium ~ 1.6× longer than wide, with hollow against embolus; tegulum longer than cymbium, swollen medio-posteriorly, with posteriorly extended posterior lobe (PL), and disto-retrolateral bump (TB); embolus (E) strongly sclerotized, short, slightly curved, with rather blunt end.

**Female** (Fig. 15A, B, E). Total length 4.24. Carapace 1.68 long, 1.14 wide. Abdomen 2.41 long, 1.46 wide. Eye sizes and interdistances: AME 0.32, ALE 0.16, PLE 0.16, AERW 0.98, PERW 1.06, EFL 0.71. Legs: I 2.56 (0.75, 0.50, 0.63, 0.38, 0.30), II 2.31 (0.70, 0.45, 0.53, 0.35, 0.28), III 2.56 (0.78, 0.43, 0.50, 0.55, 0.30), IV 3.29 (1.03, 0.48, 0.80, 0.68, 0.30). Habitus (Fig. 15E) similar to that of male but paler.

**Epigyne** (Fig. 15A, B) > 2× wider than long, with pair of anterior hoods (H) lateral to atrium (At); atrium almost square, with pair of lateral auricle-shaped ridges (AR); copulatory openings (CO) posteriorly located on atrium, irregular; copulatory ducts (CD) strongly curved circularly at proximal, then curved to C-shape, with bar-shaped, terminal accessory glands (AG); spermathecae (S) sub-spherical, with antero-inner extensions.

**Distribution.** Known only from the type locality in Xizang, China (Fig. 48).

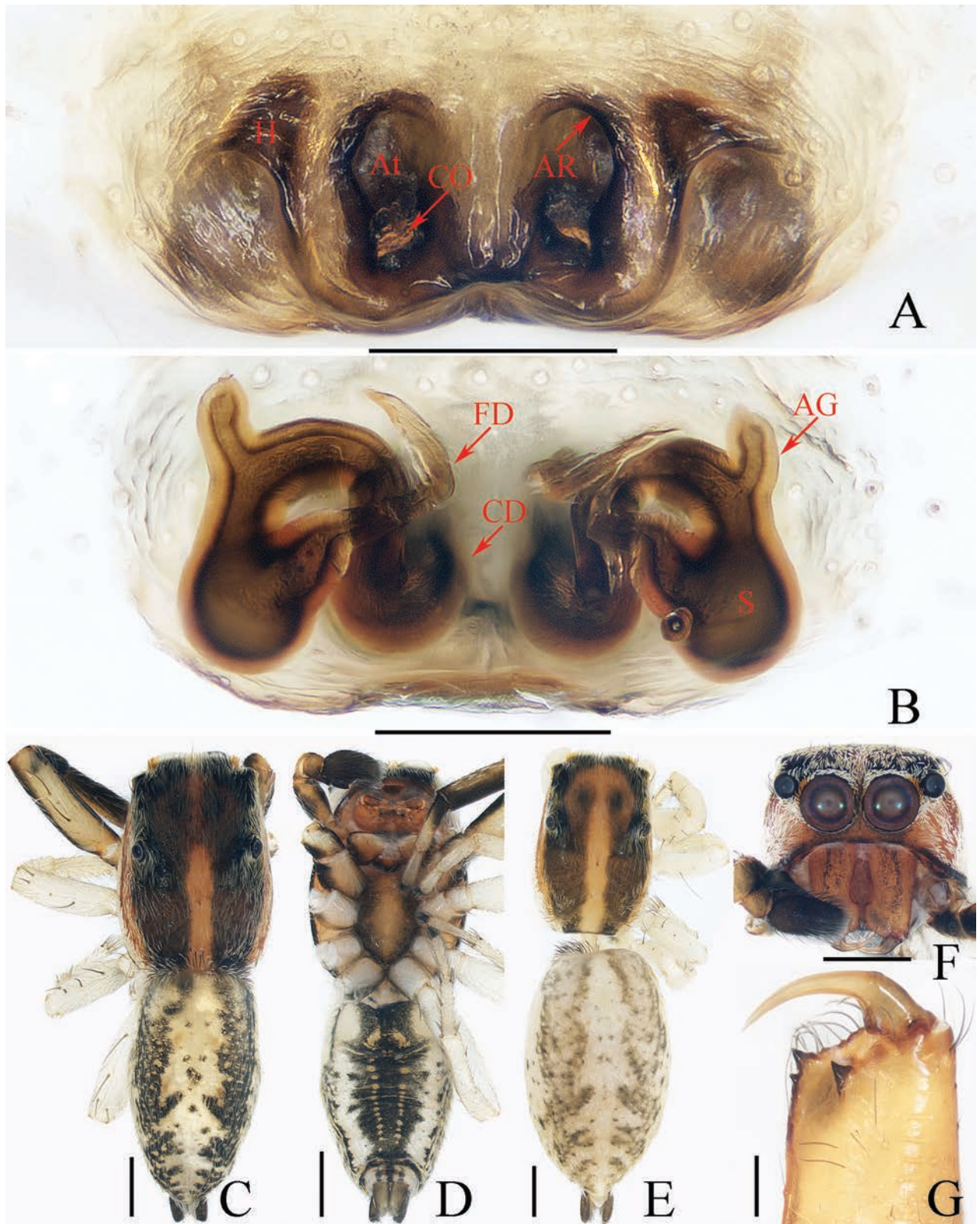


**Figure 15.** *Nandicius xiefengi* sp. nov. **C, D, F, G** male holotype and **A, B, E** female paratype (TRU-JS 0753) **A** epigyne, ventral **B** vulva, dorsal **C, E** habitus, dorsal **D** ditto, ventral **F** carapace, frontal **G** chelicera, posterior. Abbreviations: AG accessory gland; AR atrial ridge; At atrium; CD copulatory duct; CO copulatory opening; FD fertilization duct; H epigynal hood; S spermatheca. Scale bars: 0.1 mm (**A, B, G**); 0.5 mm (**C–F**).

## Genus *Okinawicius* Prószyński, 2016

*Okinawicius* Prószyński, 2016: 22.

*Nepalicius* Prószyński, 2016: 21. Syn. nov.

**Type species.** *Pseudicius okinawaensis* Prószyński, 1992; type locality Okinawa.

**Diagnosis and description.** See Prószyński (2016).

**Composition.** This genus currently includes 12 species: *Okinawicius daitaricus* (Prószyński, 1992) (♀); *O. daoxianensis* (Peng, Gong & Kim, 2000), comb. nov. (♂); *O. delesserti* (Caporiacco, 1941) (♂); *O. modestus* (Simon, 1885) (♀); *O. nepalicus* (Andreeva, Hęciak & Prószyński, 1984), comb. nov. (♂♀); *O. okinawaensis* (Prószyński, 1992) (♀); *O. seychellensis* (Wanless, 1984), comb. nov. (♂♀); *O. sheherezadae* (Prószyński, 1989) (♀); *O. shirinae* (Prószyński, 1989) (♂); *O. sindbadi* (Prószyński, 1989) (♂); *O. tekdi* Tripathi & Kulkarni, 2024 (♂♀); *O. tokaraensis* (Bohdanowicz & Prószyński, 1987) (♂♀).

**Comments.** Both *Nepalicius* and *Okinawicius* were described by Prószyński (2016). They are considered to be congeneric because the newly discovered females of *N. nepalicus* (the generotype of *Nepalicius*) share consistent habitus and epigyne with *O. okinawaensis* (the generotype of *Okinawicius*, known only from females), especially the copulatory ducts that form several coils in a plane almost perpendicular to the vertical axis. Thus, *Nepalicius* is proposed as a synonym of *Okinawicius*. We act as First Revisor per ICZN (1999). *Okinawicius daoxianensis* (Peng, Gong & Kim, 2000), comb. nov. is transferred due to it having the round tegulum encircled by embolus and with dorsal ramus of retrolateral tibial apophysis reduced to a triangular protuberance, which is consistent with *O. nepalicus*. As Yang et al. (2024) mentioned, some *Afraflacilla* species, only known by males, may also belong to *Okinawicius*. Moreover, the relationship between *Okinawicius* and *Afraflacilla* also needs further attention.

### *Okinawicius nepalicus* (Andreeva, Hęciak & Prószyński, 1984), comb. nov.

Figs 16, 17, 47

*Icius nepalicus* Andreeva, Hęciak & Prószyński, 1984: 372, figs 49–51 (holotype ♂, not examined).

*Pseudicius nepalicus*: Prószyński, 1992: 106, figs 67, 69–72 (♂).

*Nepalicius nepalicus*: Prószyński, 2016: 22, fig. 7A, B (transferred from *Pseudicius*).

**Note.** For a complete reference list of the species, see WSC (2024).

**Material examined.** 2 ♂ 3 ♀ (TRU-JS 0754–0758), CHINA: • Xizang Autonomous Region, Medog County, Beibeng Township, Deergong Village, Yarlung Zangbo National Nature Reserve (29°10.84'N, 95°8.67'E, ca 1670 m), 25.V.2024, X.Q. Mi et al. leg.

**Diagnosis.** This species resembles *O. tokaraensis* in having very similar habitus and copulatory organs, especially the epigynal structure, but differs in: 1) embolus (E) originating at ca 4 o'clock position (Fig. 16A, D) vs ca 6:30 – ca 9:00 o'clock position (Yang et al. 2024: figs 80–83); 2) membranous portions of copulatory ducts make 2 coils (Fig. 17B) vs ~ 3 coils (Yang et al. 2024: figs 89, 91, 93, 99–101).



Figure 16. Male palp of *Okinawicius nepalicus* (Andreeva, Hęciak & Prószyński, 1984) **A–C** TRU-JS 0754 **D–F** TRU-JS 0755 **A, D** ventral **B, E** retrolateral **C, F** dorsal. Abbreviations: E embolus; RTA retrolateral tibial apophysis; TB tegular bump. Scale bars: 0.1 mm.

**Re-description. Male** (Figs 16, 17C, D, F, G). Total length 3.69. Carapace 1.79 long, 1.25 wide. Abdomen 2.01 long, 1.17 wide. Eye sizes and interdistances: AME 0.32, ALE 0.19, PLE 0.18, AERW 1.01, PERW 1.02, EFL 0.77. Legs: I 3.79 (1.13, 0.75, 1.00, 0.63, 0.28), II 2.53 (0.80, 0.48, 0.55, 0.40, 0.30), III 2.65 (0.80,

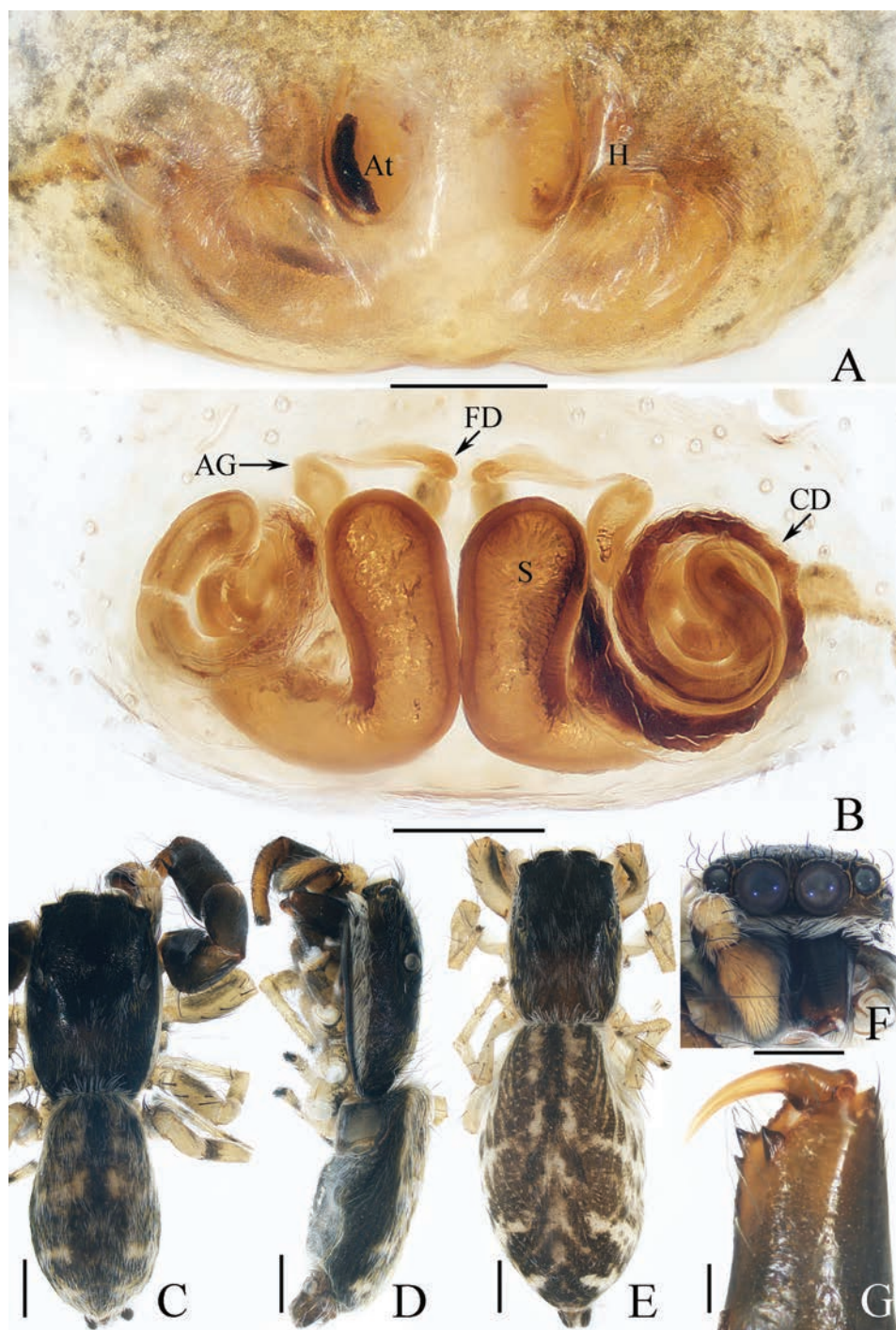


**Figure 17.** *Okinawicius nepalicus* (Andreeva, Hęciak & Prószyński, 1984) **C, D, F, G** male (TRU-JS 0754) and **A, B, E** female (TRU-JS 0756) **A** epigyne, ventral **B** vulva, dorsal **C, E** habitus, dorsal **D** ditto, lateral **F** carapace, frontal **G** chelicera, posterior. Abbreviations: AG accessory gland; At atrium; CD copulatory duct; FD fertilization duct; H epigynal hood; S spermatheca. Scale bars: 0.1 mm (**A, B, G**); 0.5 mm (**C–F**).

0.40, 0.55, 0.60, 0.30), IV 3.34 (1.00, 0.50, 0.83, 0.73, 0.28). Carapace dark, with marginal white setal band, covered with dense pale, golden and dark setae. Chelicerae mainly dark, with two promarginal teeth and one retromarginal tooth. legs I with thickness femora, patellae and tibiae, and single pro-ventral spine on tibiae. Dorsum of abdomen dark brown, with four pairs of transverse, pale stripes laterally; venter colored as dorsum.

**Palp** (Fig. 16A–F): femur length/width ratio ca 2.44; patella almost as long as wide in retrolateral view; tibia ~ 1.6× wider than long in ventral view, with strongly sclerotized retrolateral apophysis (RTA) bifurcated into sub-triangular ventral ramus and sub-semicircular dorsal ramus; cymbium ~ 1.54× longer than wide; tegulum almost round, with prolatero-posterior bump (TB) and antero-retrolateral swollen portion; embolus (E) originating at ca 4 o'clock position, coiled in less than complete circle, with rather blunt tip.

**Female** (Fig. 17A, B, E). Total length 4.40. Carapace 1.72 long, 1.14 wide. Abdomen 2.86 long, 1.64 wide. Eye sizes and interdistances: AME 0.34, ALE 0.17, PLE 0.15, AERW 0.91, PERW 1.01, EFL 0.71. Legs: I 2.79 (0.88, 0.63, 0.63, 0.40, 0.25), II 2.28 (0.65, 0.5, 0.5, 0.38, 0.25), III 2.55 (0.75, 0.45, 0.50, 0.55, 0.30), IV 3.52 (1.08, 0.58, 0.83, 0.73, 0.30). Habitus (Fig. 17E) similar to that in male except paler and with thinner femora, patellae, and tibiae I.

**Epigyne** (Fig. 17A, B) ~ 2× wider than long, with pair of anteriorly located hoods (H) ~ 1.5× longer than wide; atrium (At) almost oval; copulatory openings (CO) indistinct; copulatory ducts (CD) forming ~ 2 coils, with terminal bar-shaped accessory glands (AG) curved medially; spermathecae (S) tube-shaped, touching each other.

**Distribution.** China (Xizang; Fig. 47), India (Tamil Nadu), Nepal (Kathmandu).

**Comments.** Although the male specimens described here are almost identical to the holotype, they also have some differences, such as the origin of embolus, which arises at ca 4 o'clock position (vs ca 3 o'clock in the holotype; see Andreva et al. 1984: fig. 49), those are here considered as interspecific variations.

### Genus *Padillothorax* Simon, 1901

**Type species.** *Padillothorax semiostrinus* Simon, 1901; type locality Malaysia.

**Comments.** This genus is considered to be a member of *Baviini* Simon, 1901 (Maddison 2015; Maddison et al. 2020). It has always been poorly known, from only two nominal species until a proper redefinition was provided by Maddison et al. (2020), who first illustrated the generotype, proposed three new combinations and added two new members. Further taxonomic attention to the genus is also essential because three members, including the generotype, remain known only from a single sex and *P. taprobanicus* Simon, 1902 lacks diagnostic drawings (WSC 2024).

### *Padillothorax exilis* (Cao & Li, 2016)

Figs 18, 19, 48

*Bavia exilis* Cao & Li, in Cao, Li & Žabka, 2016: 54, figs 7A–D, 8A, B (holotype ♂, not examined).

*Bavirecta exilis*: Kanesharatnam and Benjamin 2018: 8 (transferred from *Bavia*).

*Padillothorax exilis*: Maddison et al. 2020: 65 (transferred from *Bavirecta*).

**Material examined.** 1 ♂ 1 ♀ (TRU-JS 0759–0760), CHINA: • Hainan Province, Qiongzong County, Limushan National Nature Reserve (19°9.35'N, 109°44.70'E, ca 620 m), 6.VIII.2023, C. Wang et al. leg.

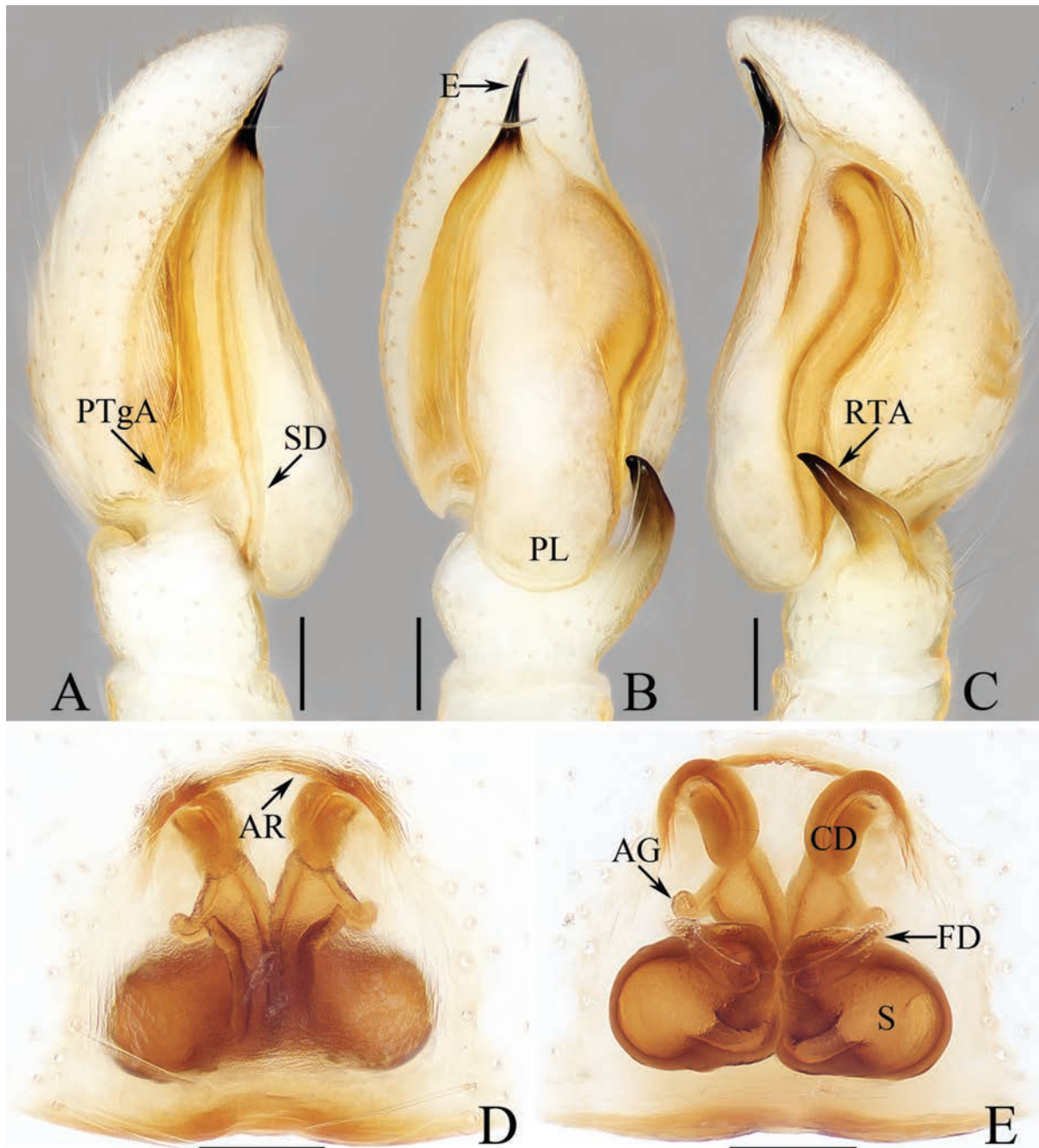


**Figure 18.** Copulatory organs of *Padillothorax exilis* (Cao & Li, 2016) **A–C** male palp (TRU-JS 0759) and **D, E** epigyne (TRU-JS 0760) **A** prolateral **B** ventral **C** retrolateral **D** epigyne, ventral **E** vulva, dorsal. Abbreviations: AG accessory gland; AR atrial ridge; CD copulatory duct; E embolus; FD fertilization duct; PL posterior tegular lobe; PTgA prolateral tegular apophysis; RTA retrolateral tibial apophysis; S spermatheca; SD sperm duct. Scale bars: 0.1 mm.

**Diagnosis.** The male was diagnosed in Cao et al. (2016). The female resembles that of *P. casteti* (Simon, 1900) in the general shape of epigyne, but differs in: 1) presence of accessory glands (AG) of copulatory ducts (Fig. 18D, E) vs absent (see the drawings in Prószyński 1987: 78); 2) copulatory ducts (CD) curved distally and connected to the dorsal surface of spermathecae (S) (Fig. 18E) vs straight distally and connected to the ventral surface of spermathecae (see the drawings in Prószyński 1987: 78).

**Description. Male.** See Cao et al. (2016).

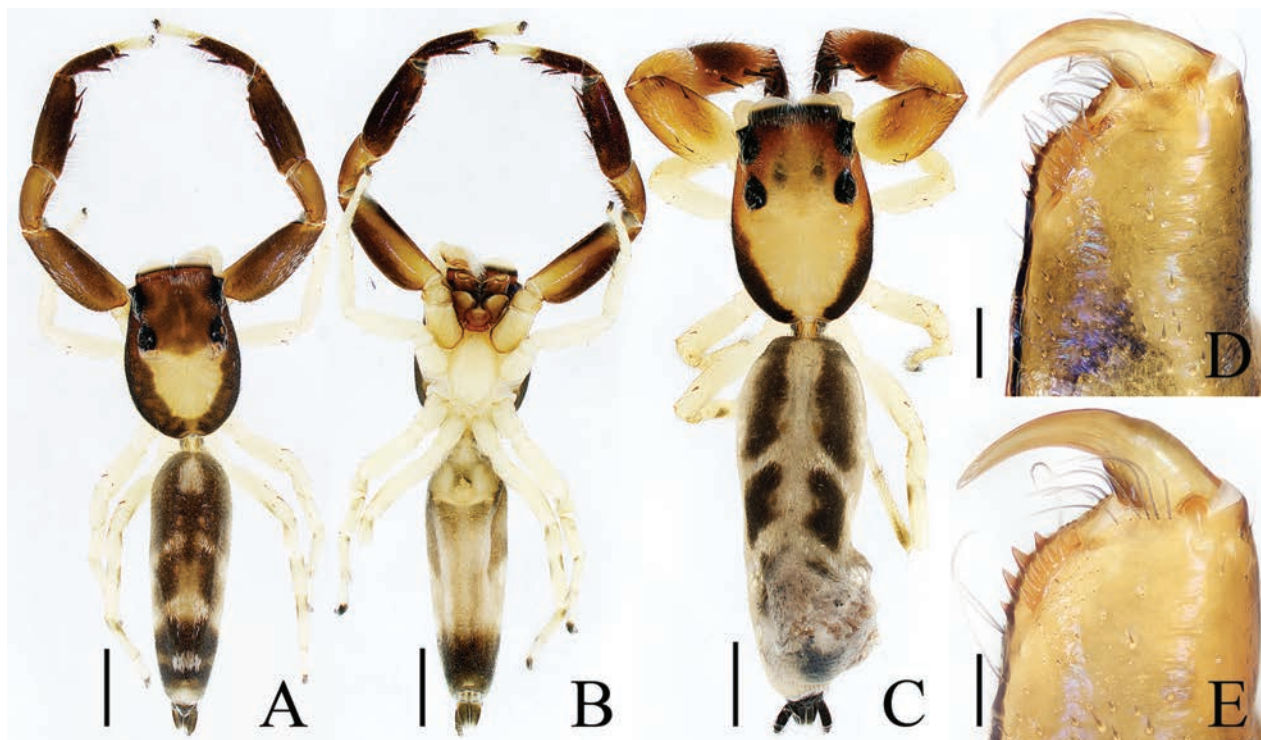


**Figure 19.** *Padillothorax exilis* (Cao & Li, 2016) **A, B, D** male (TRU-JS 0759) and **C, E** female (TRU-JS 0760) **A, C** habitus, dorsal **B** ditto ventral **D, E** chelicera, posterior. Scale bars: 1.0 mm (**A–C**); 0.1 mm (**D, E**).

**Female** (Figs 18D, E, 19C, E). Total length 5.36. Carapace 1.86 long, 1.32 wide. Abdomen 3.36 long, 1.23 wide. Eye sizes and interdistances: AME 0.45, ALE 0.18, PLE 0.18, AERW 1.14, PERW 1.05, EFL 0.77. Legs: I 5.24 (1.53, 0.93, 1.40, 0.88, 0.50), II 3.51 (1.00, 0.65, 0.85, 0.63, 0.38), III 3.18 (0.95, 0.60, 0.55, 0.70, 0.38), IV 4.36 (1.25, 0.65, 1.03, 1.05, 0.38). Carapace mainly yellow, with pair of dark stripes laterally on thoracic part, covered with sparse setae, denser on eye base. Chelicerae yellow, with four promarginal and seven retromarginal teeth. Leg I robust, with thickened femora, three and two pairs of ventral spines on tibiae and metatarsi, respectively. Dorsum of abdomen with symmetrical, alternating pale and dark patches; venter pale.

**Epigyne** (Fig. 18D, E) ~ 1.3× wider than long; atrium (At) with anterior arc-shaped ridge (AR), copulatory openings (CO) slit-shaped, partly covered by atrial ridge; copulatory ducts (CD) thickened in walls at proximal 1/3, strongly curved distally, and with medially located, laterally extended accessory glands (AG) forming round ends; spermathecae (S) oval, touching each other.

**Distribution.** China (Yunnan, Hainan; Fig. 48).

### Genus *Pancorius* Simon, 1902

**Type species.** *Ergane dentichelis* Simon, 1899; type locality Padang, Indonesia.

**Comments.** *Pancorius* is placed in the subtribe *Plexippina* Simon, 1901 within the tribe *Plexippini* Simon, 1901 (Maddison 2015), and comprises 46 species restricted to Asia (WSC 2024). The genus is poorly studied and its generotype is only known from limited diagnostic drawings, resulting in it not being precisely delimited. In addition, members are rather diverse in habitus and copulatory organs, and several species, such as *P. guiyang* Yang, Gu & Yu, 2023,

*P. inexpectatus* Logunov, 2024, *P. lui* Gan, Mi & Wang, 2022, and *P. nyingchi* Wang, Mi & Li, 2024 were tentatively placed, indicating that they could be polyphyletic. Moreover, half its species are only known from a single sex (WSC 2024).

***Pancorius medog* sp. nov.**

<https://zoobank.org/60603398-7E09-433D-ADF6-1F078E7D4B96>

Figs 20, 47

**Type material. Holotype** ♀ (TRU-JS 0761), CHINA: • Xizang Autonomous Region, Medog County, Beibeng Township, Deergong Village, Yarlung Zangbo National Nature Reserve (29°10.84'N, 95°8.67'E, ca 1670 m), 25.V.2024, X.Q. Mi et al. leg.

**Paratypes** • 3 ♀ (TRU-JS 0762–0764), same data as for holotype.

**Etymology.** The specific name is named after the type locality, Medog County; noun in apposition.

**Diagnosis.** *Pancorius medog* sp. nov. resembles that of *P. nyingchi* Wang, Mi & Li, 2024 in having a central epigynal hood (H), longitudinal band on the dorsum of abdomen, but can be easily distinguished by the following: 1) epigynal hood opened posteriorly (Fig. 20A) vs opened ventro-posteriorly (Wang et al. 2024: fig. 12A); 2) the distinct spermathecae (S) (Fig. 20B) vs indistinct (Wang et al. 2024: fig. 12B); 3) presence of central yellow area bearing pale thin setae on carapace (Fig. 20C) vs absent (Wang et al. 2024: fig. 12E).

**Description. Female** (Fig. 20). Total length 5.19. Carapace 2.31 long, 1.78 wide. Abdomen 3.01 long, 2.03 wide. Eye sizes and interdistances: AME 0.52, ALE 0.27, PLE 0.25, AERW 1.67, PERW 1.67, EFL 1.03. Legs: I 4.08 (1.25, 0.75, 1.00, 0.63, 0.45), II 3.72 (1.13, 0.70, 0.88, 0.58, 0.43), III 4.18 (1.40, 0.63, 0.90, 0.80, 0.45), IV 4.72 (1.45, 0.68, 1.08, 1.03, 0.48). Carapace orange-brown on cephalon and dark on thoracic part, with central yellow area bearing pale thin setae, covered with pale, dark brown and golden setae. Chelicerae red-brown, with two promarginal teeth and one retromarginal tooth. Legs pale, spiny. Dorsum of abdomen grey-brown, with longitudinal, sub-fusiform central stripe extended across whole surface; venter mainly pale brown, with central, longitudinal, non-consecutive, dark patches.

**Epigyne** (Fig. 20A, B) longer than wide, with central, posteriorly opened hood (H) with inverted V-shaped margin; atrium (At) sub-square, located anteriorly; copulatory openings (CO) slit-shaped; copulatory ducts (CD) short, curved into U-shape and then folded to connect to antero-inner portions of spermathecae; spermathecae (S) almost spherical, with anterior extended extensions.

**Male.** Unknown.

**Distribution.** Known only from the type locality in Xizang, China (Fig. 47).

***Pancorius yingjiang* sp. nov.**

<https://zoobank.org/C4E290D2-5E94-4C5B-8DF3-A14C58250BFD>

Figs 21, 22, 48

**Type material. Holotype** ♀ (TRU-JS 0765), CHINA: • Yunnan Province, Dehong Dai Autonomous Prefecture, Yingjiang County, Tongbiguan Township, Banggetong (24°35.96'N, 97°38.48'E, elevation undetailed) 3.V.2024, H. Qiu leg. **Paratypes** •

3 ♂ (TRU-JS 0766–0768), same data as for holotype.

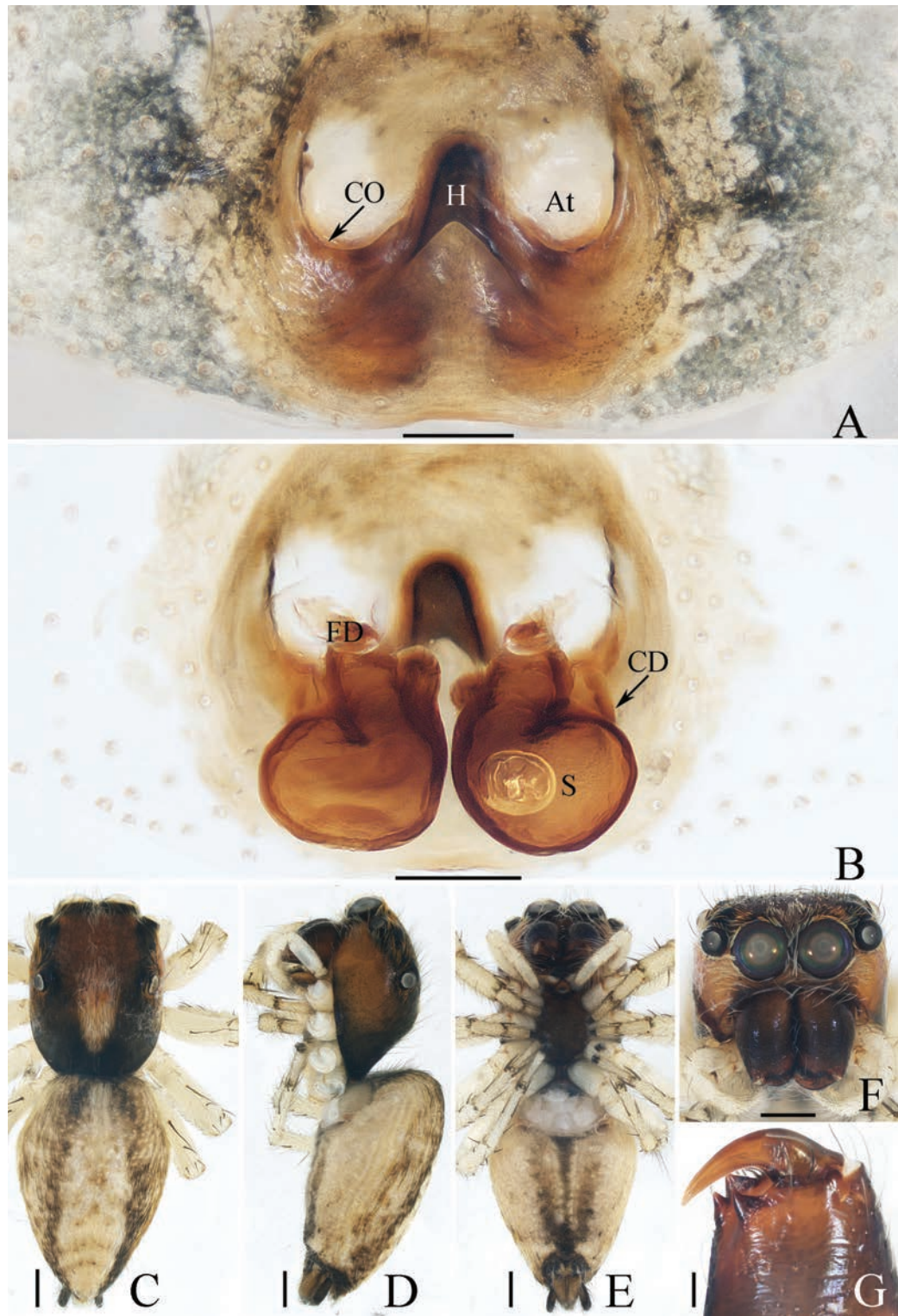


**Figure 20.** *Pancorius medog* sp. nov., holotype **A** epigyne, ventral **B** vulva, dorsal **C** habitus, dorsal **D** ditto, lateral **E** ditto, ventral **F** carapace, frontal **G** chelicera, posterior. Abbreviations: At atrium; CO copulatory opening; CD copulatory duct; FD fertilization duct; H epigynal hood; S spermatheca. Scale bars: 0.1 mm (**A**, **B**, **G**); 0.5 mm (**C**–**F**).

**Etymology.** The species name comes from the type locality, Yingjiang County; noun in apposition.

**Diagnosis.** *Pancorius yingjiang* sp. nov. resembles that of *P. manipuriensis* (Biswas & Biswas, 2004) in having a similar male palp and a small, anteriorly

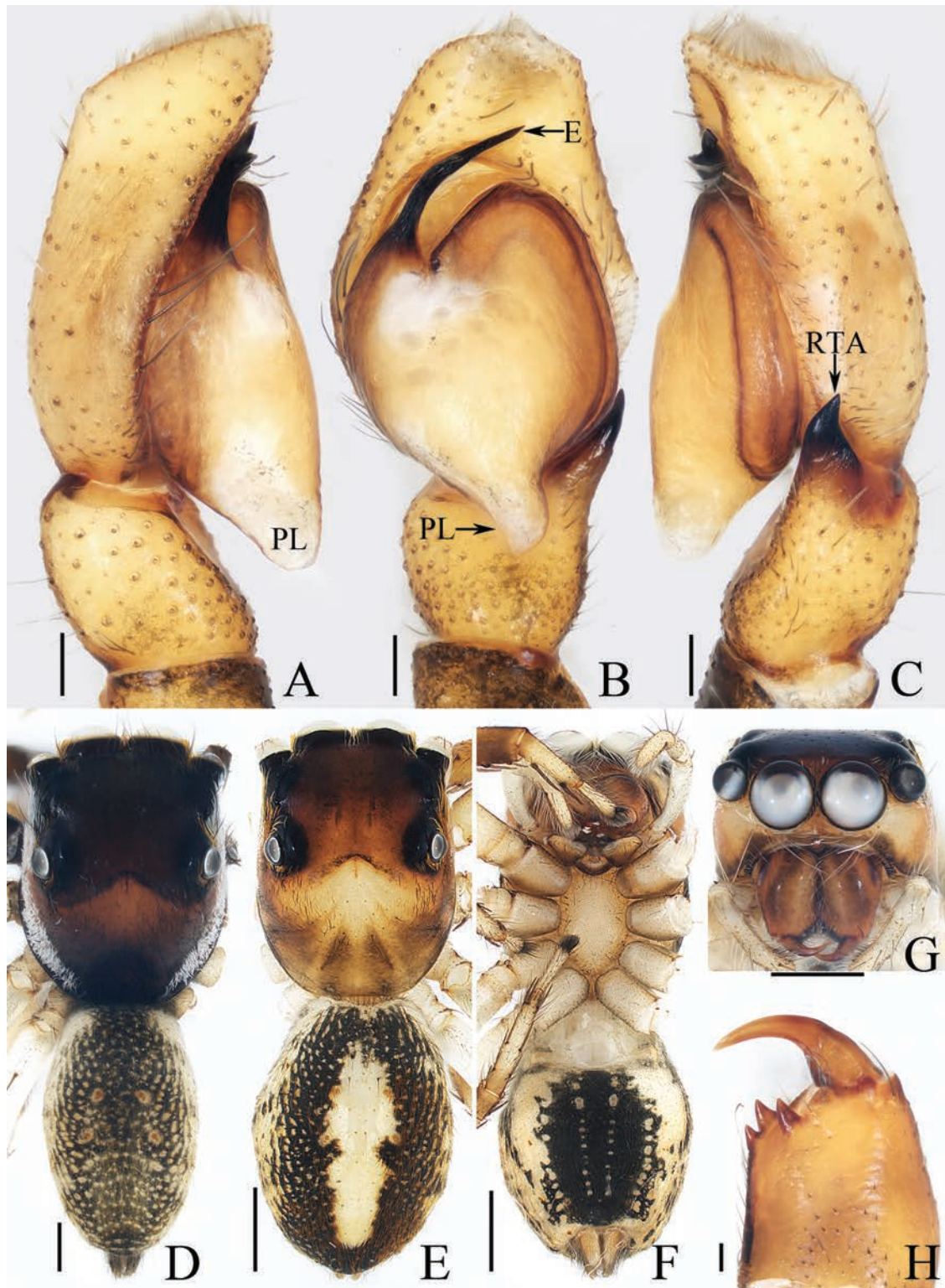


**Figure 21.** *Pancorius yingjiang* sp. nov. **E–H** female holotype and **A–D** male paratype (TRU-JS 0766) **A** palp, prolateral **B** ditto, ventral **C** ditto, retrolateral **D**, **E** habitus, dorsal **F** ditto, ventral **G** carapace, frontal **H** chelicera, posterior. Abbreviations: E embolus; PL posterior tegular lobe; RTA retrolateral tibial apophysis. Scale bars: 0.5 mm (**D**, **G**); 1.0 mm (**E**, **F**); 0.1 mm (**A–C**, **H**).

located epigynal hood (H), but can be easily distinguished by the following: 1) copulatory openings (CO) opened anteriorly (Fig. 22A, B) vs opened opposite (Caleb 2023: figs 21, 22); 2) epigynal hoods (H) posterior to copulatory openings (CO) (Fig. 22A, B) vs lateral to copulatory openings (Caleb 2023:

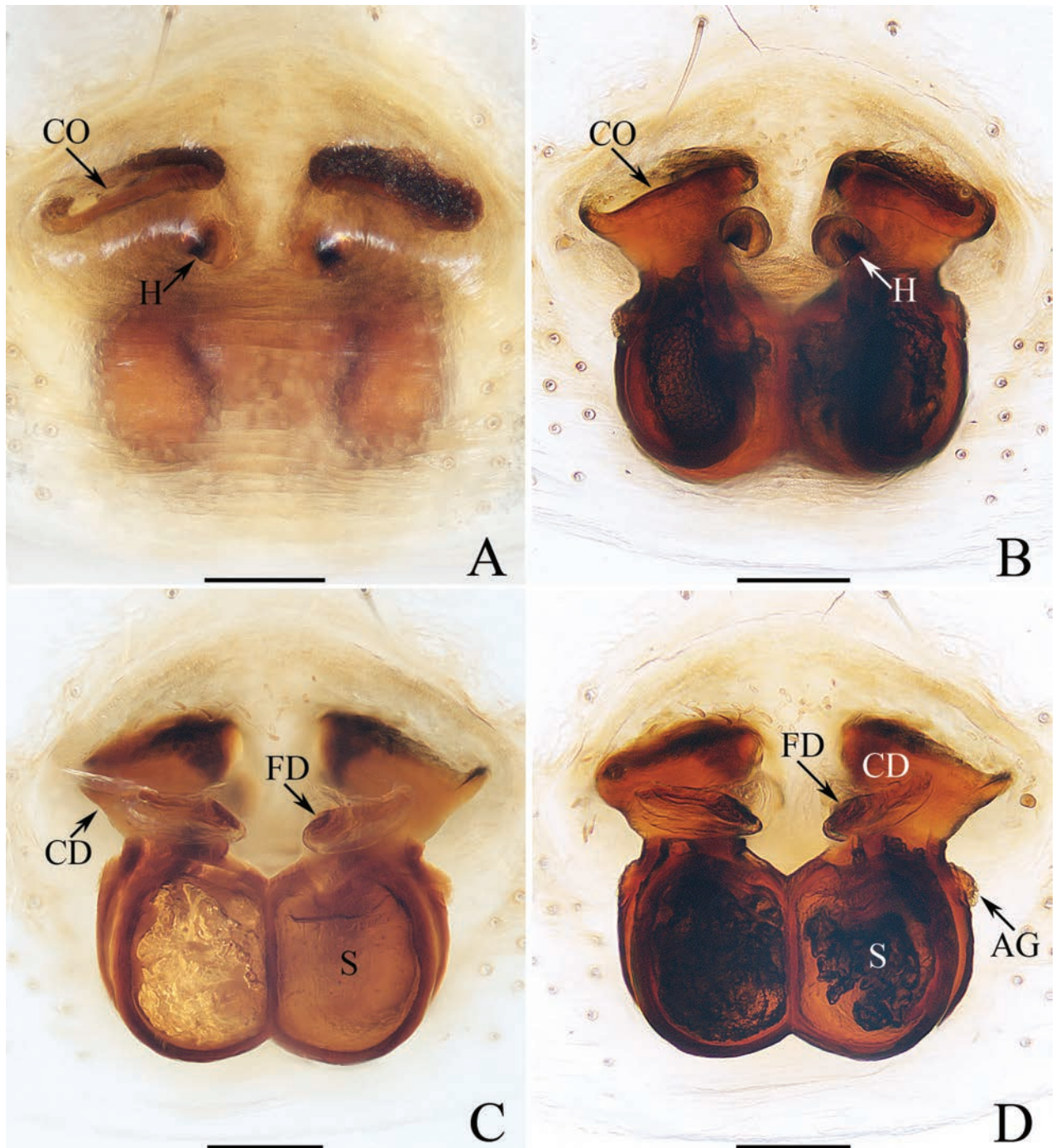


**Figure 22.** Epigyne of *Pancorius yingjiang* sp. nov., female holotype **A, B** epigyne, ventral **C, D** vulva, dorsal. Abbreviations: AG accessory gland; CO copulatory opening; CD copulatory duct; FD fertilization duct; H epigynal hood; S spermatheca. Scale bars: 0.1 mm.

figs 21, 22); 3) retrolateral tibial apophysis (RTA) directed towards ca 12 o'clock position in ventral view (Fig. 21B) vs ca 2 o'clock position (Caleb 2023: fig. 15).

**Description. Female** (Figs 21E–H, 22). Total length 6.40. Carapace 3.03 long, 2.40 wide. Abdomen 3.23 long, 2.43 wide. Eye sizes and interdistances: AME 0.72, ALE 0.43, PLE 0.38, AERW 2.30, PERW 2.20, EFL 1.40. Legs: I 6.16 (1.88, 1.18, 1.50, 1.00, 0.60), II 5.56 (1.63, 1.10, 1.25, 0.95, 0.63), III 6.61 (2.13, 1.00, 1.45, 1.35, 0.68), IV 6.97 (2.13, 0.98, 1.55, 1.63, 0.68). Carapace yellow-brown, covered with dark golden and pale setae, with irregular yellow

area anteriorly on thoracic part. Chelicerae brawny, with two promarginal teeth and one retromarginal tooth. Legs pale, mingled with red-brown, spiny. Dorsum of abdomen dark and spotted laterally, with central, longitudinal, pale stripe and two pairs of median muscle depressions; venter dark centrally, with pair of dotted lines.

**Epigyne** (Fig. 22A–D) with pair of anterior, small hoods (H) below copulatory openings (CO); copulatory openings slit-shaped, opened anteriorly, and apart from each other < 1/2 their width; copulatory ducts (CD) broad, with small, mediolateral accessory glands (AG); spermathecae (S) almost round, touching each other.

**Male** (Fig. 21A–D). Total length 5.23. Carapace 2.66 long, 2.14 wide. Abdomen 2.63 long, 1.60 wide. Eye sizes and interdistances: AME 0.66, ALE 0.40, PLE 0.37, AERW 2.06, PERW 1.97, EFL 1.26. Legs: I 6.84 (2.00, 1.08, 1.78, 1.25, 0.73), II 5.64 (1.75, 0.90, 1.33, 1.03, 0.63), III 6.54 (2.08, 0.90, 1.38, 1.45, 0.73), IV 6.82 (2.03, 0.85, 1.43, 1.58, 0.93). Habitus (Fig. 21D) similar to that of female except carapace darker, and without central, longitudinal, pale stripe on dorsum of abdomen.

**Palp** (Fig. 21A–C): femur length/width ratio ca 3.34; patella ~ 1/2 femoral length; tibia slightly longer than wide, with strongly sclerotized, tapered retrolateral apophysis (RTA) curved distally and with pointed tip; cymbium ~ 1.5× longer than wide; tegulum slightly swollen posteriorly, with well-developed posterior lobe (PL) with blunt end; embolus (E) arising from anteroprolateral portion of tegulum, with median sub-triangular extension and pointed end.

**Distribution.** Known only from the type locality in Yunnan, China (Fig. 48).

**Comments.** As the female can be more easily distinguished from other congeners than the male, it is proposed as the holotype.

## Genus *Piranthus* Thorell, 1895

**Type species.** *Piranthus decorus* Thorell, 1895; type locality Palon, Myanmar.

**Comments.** *Piranthus* is considered as a member of the tribe Baviini Simon, 1901 (Maddison 2015; Maddison et al. 2020). To date, six species are known from tropical Asia (WSC 2024), of which four were described by Maddison et al. (2020). The genus is relatively well studied because all members are known from diagnostic drawings, and only two are known from a single sex (WSC 2024). Besides the below-described new species, the generotype has also been found in Hainan, China.

### *Piranthus maddisoni* sp. nov.

<https://zoobank.org/62C62771-5D33-41E5-AB29-F0831674E7D7>

Figs 23, 24, 47

**Type material.** **Holotype** ♂ (TRU-JS 0769), CHINA: • Hainan Province, Changjiang Li Autonomous County, Bawangling National Nature Reserve (19°7.12'N, 109°9.34'E, ca 640 m), 24.IV.2021, F.E. Li leg. **Paratype** • 1 ♀ (IZCAS-Ar 45283), Lingshui County, Diaoluoshan (18°40.22'N, 109°53.67'E, ca 260 m), 14.IV.2009, G. Tang leg.

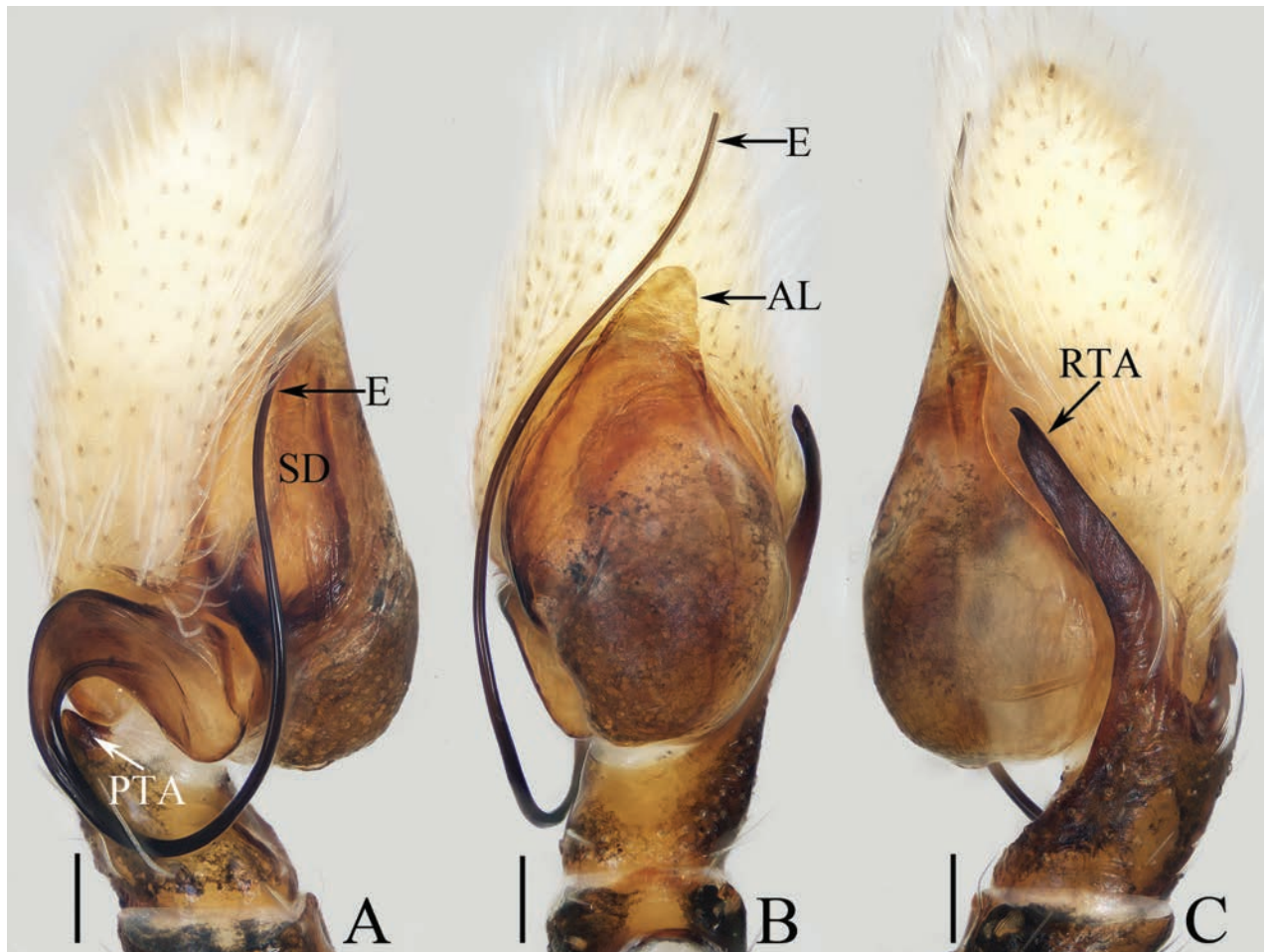


**Figure 23.** Male palp of *Piranthus maddisoni* sp. nov., holotype **A** prolateral **B** ventral **C** retrolateral. Abbreviations: AL anterior tegular lobe; E embolus; PTA prolateral tibial apophysis; RTA retrolateral tibial apophysis; SD sperm duct. Scale bars: 0.1 mm.

**Etymology.** The specific name is a patronym in honor of Prof. Wayne P. Maddison (Vancouver, Canada), the leading specialist in jumping spiders, who has made significant contributions to the taxonomy of salticids worldwide; noun (name) in the genitive case.

**Diagnosis.** *Piranthus maddisoni* sp. nov. resembles that of *P. bakau* Maddison, 2020 in having similar habitus, pattern, and palpal structure, but differs in: 1) retrolateral tibial apophysis (RTA) not broadened at base, and forming an incision at distal end in retrolateral view (Fig. 23C) vs broadened into a dorsal prominent portion and lacking similar incision (Maddison et al. 2020: fig. 239); 2) presence of a well-developed anterior tegular lobe (AL) (Fig. 23B) vs indistinct (Maddison et al. 2020: fig. 238); 3) base of septum (Se) < 1/4 of epigynal width (Fig. 24A) vs ~ 1/3 of epigynal width (Maddison et al. 2020: fig. 240).

**Description. Male** (Figs 23, 24D, E, G–I). Total length 6.10. Carapace 2.78 long, 2.15 wide. Abdomen 3.27 long, 1.61 wide. Eye sizes and interdistances: AME 0.55, ALE 0.26, PLE 0.26, AERW 1.51, PERW 1.59, EFL 1.12. Legs: I 5.25 (1.75, 1.00, 1.25, 0.75, 0.50), II 4.51 (1.38, 0.90, 1.10, 0.68, 0.45), III 3.76 (1.13, 0.70, 0.70, 0.80, 0.43), IV 5.04 (1.58, 0.75, 1.18, 1.08, 0.45). Carapace almost oval, dark, and covered with dense white setae. Chelicerae red-brown, with three promarginal and five retromarginal teeth. Legs I and II yellow except

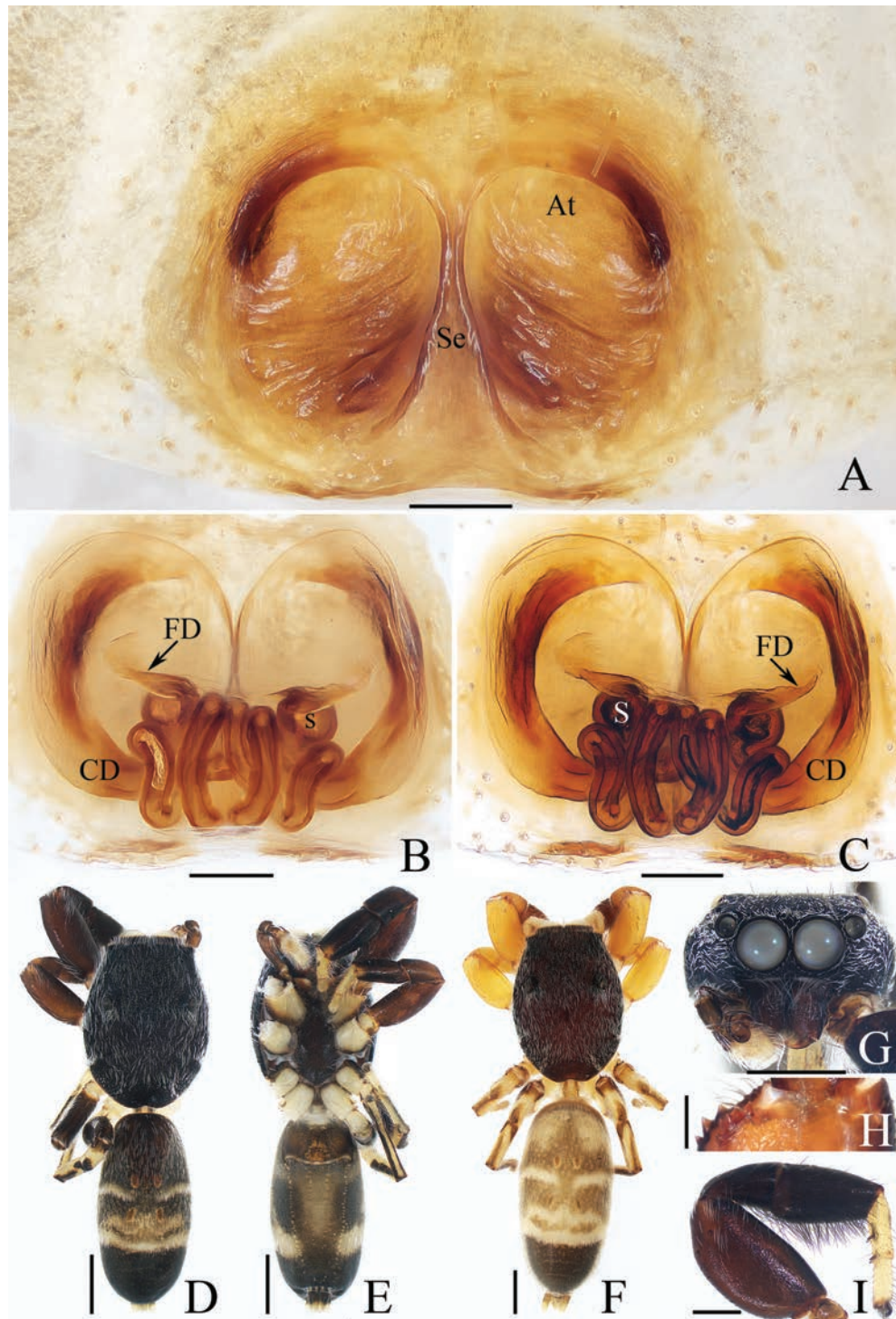


**Figure 24.** *Piranthus maddisoni* sp. nov. **D, E, G–I** male holotype and **A–C, F** female paratype (IZCAS-Ar 45283) **A** epigyne, ventral **B, C** vulva, dorsal **D, F** habitus, dorsal **E** ditto, ventral **G** carapace, frontal **H** chelicera, posterior **I** leg I, prolateral. Abbreviations: At atrium; CD copulatory duct; FD fertilization duct; S spermatheca; Se septum. Scale bars: 0.1 mm (**A–C, H**); 1.0 mm (**D–G**); 0.5 mm (**I**).

thickness femora, patellae, and tibiae dark brown, bearing pale setae on patellae and tibiae I. Dorsum of abdomen with two pairs of muscle depressions, pair of transverse, pale setal stripes followed by big transverse pale grey band medially, covered by anterior scutum ~ 1/3 abdominal length; venter colored as dorsum, with pair of oval postero-lateral pale spots and median dotted lines.

**Palp** (Fig. 23A–C): femur length/width ratio ca 2.5; patella ~ 1.4× longer than wide in retrolateral view; tibia slightly longer than wide, with sub-triangular disto-prolateral apophysis (PTA) and blade-shaped retrolateral apophysis (RTA) longer than tibia, slightly curved at proximal 1/3, and forming shallow incision at distal end; cymbium pale, > 1.5× longer than wide; tegulum elongate-oval, swollen medio-posteriorly, with lamellar, anteriorly extended antero-marginal sub-triangular lobe (AL); embolus (E) arising at baso-prolateral corner of tegulum, with broad base extended anticlockwise, and then acutely narrowed into flagelliform portion.

**Female** (Fig. 24A–C, F). Total length 8.34. Carapace 3.47 long, 2.53 wide. Abdomen 4.53 long, 2.20 wide. Eye sizes and interdistances: AME 0.43, ALE 0.26, PLE 0.26, AERW 1.48, PERW 1.60, EFL 1.05. Legs: I 4.89 (1.65, 1.03, 1.08, 0.63, 0.50), II 4.83 (1.50, 1.05, 1.15, 0.68, 0.45), III 4.24 (1.30, 0.80, 0.78, 0.93, 0.43), IV 6.00 (1.80, 1.00, 1.40, 1.30, 0.50). Habitus (Fig. 24F) similar to that of male except paler and without dorsal abdominal scutum.

**Epigyne** (Fig. 24A–C) ~ 1.2× wider than long; atrium (At) almost oval, separated by basally broadened septum (Se); copulatory openings (CO) anteriorly located, partly visible; copulatory ducts (CD) long, broadened and flat proximally, and then forming complicated coils; spermathecae (S) spherical, separated from each other ~ 2× their diameter.

**Distribution.** Known only from the type locality in Hainan, China (Fig. 47).

**Comments.** Although the male and female were collected in different places, they share consistent habitus, and pattern and thus they are considered to be conspecific, but this may need further confirmation.

## Genus *Siler* Simon, 1889

**Type species.** *Siler cupreus* Simon, 1889; type locality Yokohama, Japan.

**Comments.** *Siler*, a member of Chrysillini, comprises 12 species, mainly distributed in east and southeast Asia (Maddison 2015; WSC 2024). The genus has not been revised recently. Like most salticid genera, a high rate (58.3%) of its species are known only from a single sex. In addition, three species are only known from the original description, and *S. pulcher* Simon, 1901 has never been illustrated (WSC 2024).

### *Siler hanoicus* Prószyński, 1985

Figs 25, 26, 48

*Siler hanoicus* Prószyński, 1985: 75, figs 21, 22 (holotype ♂, not examined); Żabka, 1985: 447, figs 571, 572 (♂).

**Material examined.** 1 ♂ 1 ♀ (TRU-JS 0770–0771), CHINA: • Guangxi Zhuang Autonomous Region, Fangchenggang City, Shiwandashan National Nature Reserve, west border of Pinglong Station (21°50.73'N, 107°53.24'E, ca 430 m), 30.IV.2024, A.L. He et al. leg.

**Diagnosis.** *Siler hanoicus* resembles that of *S. cupreus* in the general shape of copulatory organs but differs in: 1) embolus (E) curved (Fig. 25B) vs straight

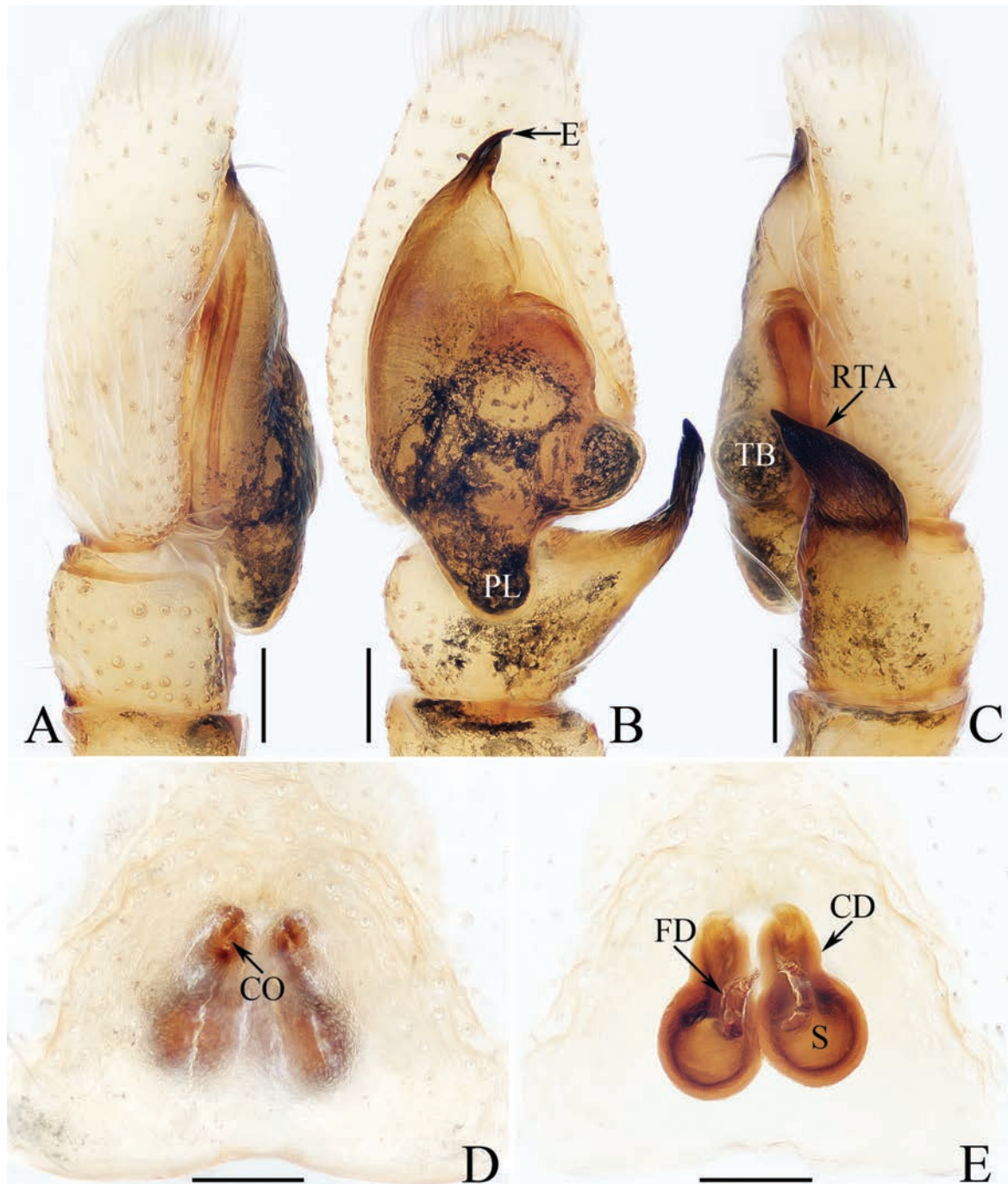


**Figure 25.** Copulatory organs of *Siler hanoicus* Prószyński, 1985 **A–C** male palp (TRU-JS 0770) and **D, E** eigyne (TRU-JS 0771) **A** prolateral **B** ventral **C** retrolateral **D** epigyne, ventral **E** vulva, dorsal. Abbreviations: CD copulatory duct; CO copulatory opening; E embolus; FD fertilization duct; PL posterior tegular lobe; RTA retrolateral tibial apophysis; S spermatheca; TB tegular bump. Scale bars: 0.1 mm.

(Peng 2020: fig. 296b); 2) retrolateral tibial apophysis (RTA) curved ventrally in retrolateral view (Fig. 25C), vs anteriorly extending before curved ventrally (Peng 2020: fig. 296b); 3) presence of a pair of atrial ridges (AR) (Fig. 25D), vs absent (Peng 2020: fig. 296f).

**Re-description. Male** (Figs 25, 26A, B, D, E). Total length 4.09. Carapace 2.03 long, 1.49 wide. Abdomen 2.11 long, 1.37 wide. Eye sizes and interdistances: AME 0.41, ALE 0.21, PLE 0.19, AERW 1.16, PERW 1.37, EFL 0.94. Legs: I 4.16



**Figure 26.** *Siler hanoicus* Prószyński, 1985 **A, B, D, E** male (TRU-JS 0770) and **C** female (TRU-JS 0771) **A, C** habitus, dorsal **B** ditto, ventral **D** carapace, frontal **E** chelicera, posterior. Scale bars: 0.5 mm (**A–D**); 0.1 mm (**E**).

(1.35, 0.70, 0.95, 0.73, 0.43), II 3.23 (1.00, 0.50, 0.75, 0.63, 0.35), III 4.07 (1.13, 0.48, 1.18, 0.85, 0.43), IV (1.50, missing, missing, missing, missing). Carapace brown except cephalon dark, covered with pale scales on face and around PMEs; fovea red. Chelicerae yellow, mingled with dark, with two promarginal teeth and one retromarginal tooth. Legs yellow except tibiae I dark, covered with dense, dark, ventral setae on patellae and tibiae I. Dorsum of abdomen dark, mingled with green, with irregular anterior scutum ~ 1/3 abdominal length; venter colored as dorsum.

**Palp** (Fig. 25A–C): femur length/width ratio ca 2.5; patella ~ 1.2× longer than wide in retrolateral view; tibia ~ as long as wide in retrolateral view; retrolateral tibial apophysis (RTA) strongly sclerotized, curved ventrally to rather pointed tip in retrolateral view; cymbium pale yellow, ~ 1.6× longer than wide; tegulum length/width ratio ca 1.53, with posteriorly extended posterior lobe (PL) with blunt end, and sub-spherical retrolateral tegular bump (TB); embolus (E) originating from most anterior portion of tegulum, slightly curved, and with blunt end.

**Female** (Figs 25D, E, 26C). Total length 5.14. Carapace 2.29 long, 1.67 wide. Abdomen 2.90 long, 1.81 wide. Eye sizes and interdistances: AME 0.43, ALE 0.26, PLE 0.26, AERW 1.48, PERW 1.60, EFL 1.05. Legs: I 4.61 (1.55, 0.68, 1.10, 0.83, 0.45), II 3.91 (1.25, 0.63, 0.88, 0.75, 0.40), III 4.64 (1.38, 0.63, 1.00, 1.13, 0.50), IV 6.18 (1.68, 0.80, 1.50, 1.70, 0.50). Carapace (Fig. 26C) similar to that of male. Dorsum of abdomen (Fig. 26C) with inconsecutive, anterior, orange, arc-shaped setal stripes followed by alternate pale and dark setal patches; venter dark.

**Epigyne** (Fig. 25D, E) sub-triangular; atrium (At) anteriorly located, with arc-shaped lateral ridges (AR); copulatory openings (CO) small, partly visible; copulatory ducts (CD) thick, posteriorly extended; spermathecae (S) touching each other, spherical.

**Distribution.** China (Guangxi; Fig. 48); Vietnam (Hanoi).

## Genus *Simaetha* Thorell, 1881

**Type species.** *Simaetha thoracica* Thorell, 1881; type locality Australia.

**Comments.** The genus was assigned by Maddison (2015) in the subtribe Simaethina Simon, 1903 within the tribe Vicirini Simon, 1901, and is represented by 23 nominal species, mainly distributed from South Asia to Australia (WSC 2024). Although a detailed revision of Oceanian species has been done by Žabka (1994), the genus remains poorly studied because nearly half (11) of the species are known only from a single sex, and four species cannot be precisely identified due to lack of diagnostic drawings (WSC 2024).

### *Simaetha hainan* sp. nov.

<https://zoobank.org/7FCE4F94-E617-42E1-AC89-FC806BB826A7>

Figs 27, 28, 48

**Type material.** **Holotype** ♂ (IZCAS-Ar 45284), CHINA: • Hainan Province, Lingshui County, Diaoluoshan National Nature Reserve (18°39.96'N, 109°35.81'E, ca 80 m), 15.IV.2009, G. Tang leg. **Paratypes** • 1 ♀ (IZCAS-Ar 45285), same data as for holotype; • 1 ♂ (IZCAS-Ar 45286), Diaoluoshan National Nature Reserve (18°40.44'N, 109°52.72'E, ca 580 m), 16.IV.2009, G. Tang leg; • 1 ♂ (IZCAS-Ar 45287), Diaoluoshan National Nature Reserve (18°40.44'N, 109°52.60'E, ca 490 m), 10.VIII.2010, G. Tang leg; • 1 ♀ (IZCAS-Ar 42288), Qiongzong County, Yinggeling National Nature Reserve, Yinggezui Station (19°03.05'N, 109°33.75'E, ca 690 m), 25.VIII.2010, G. Zhou leg; • 2 ♂ (TRU-JS 0772–0773), Ledong County, Jianfeng Township, Jianfengling National Nature Reserve, Main Peak (18°43.11'N, 108°52.32'E, ca 1400 m), 16.IV.2019, C. Wang & Y.F. Yang leg.

**Etymology.** The specific name is after the type locality, Hainan; noun in apposition.

**Diagnosis.** *Simaetha hainan* sp. nov. resembles that of *S. cheni* Wang & Li, 2021, in having the blade-shaped retrolateral tibial apophysis (RTA), the presence of antero-marginal protuberances on anterior surface of chelicerae, but differs in: 1) embolus (E) straight (Fig. 27A) vs curved prolaterally at distal portion (Wang and Li 2021: fig. 18B); 2) tibia slightly longer than wide in retrolateral view (Fig. 27B) vs wider than long (Wang and Li 2021: fig. 18C); 3) epigynal hood (H) posteriorly located, and approximately half the length of anterior chamber of spermatheca (Fig. 28A) vs anteriorly located and < 1/4 length of anterior chamber of spermatheca (Wang and Li 2021: fig. 19A, B).

**Description. Male** (Figs 27, 28C, D, F, G). Total length 2.74. Carapace 1.32 long, 1.08 wide. Abdomen 1.50 long, 1.06 wide. Eye sizes and interdistances: AME 0.32, ALE 0.16, PLE 0.16, AERW 0.90, PERW 1.04, EFL 0.64. Legs: I 2.41 (0.78, 0.50, 0.50, 0.33, 0.30), II 1.76 (0.53, 0.30, 0.38, 0.30, 0.25), III 1.63 (0.50, 0.25, 0.33, 0.30, 0.25), IV 2.06 (0.73, 0.30, 0.45, 0.33, 0.25). Carapace red-brown, covered with pale and golden scales, with central dark patch on cephalon. Chelicerae red-yellow, with base-lateral protuberances on anterior surface, two promarginal teeth and one retromarginal fissentate tooth with two cusps. Leg I robust, with enlarged femora, and three and two pairs of ventral spines on tibiae and metatarsi, respectively. Dorsum of abdomen red-brown, covered completely by large scutum; venter brown, with two pairs of dotted lines medially.

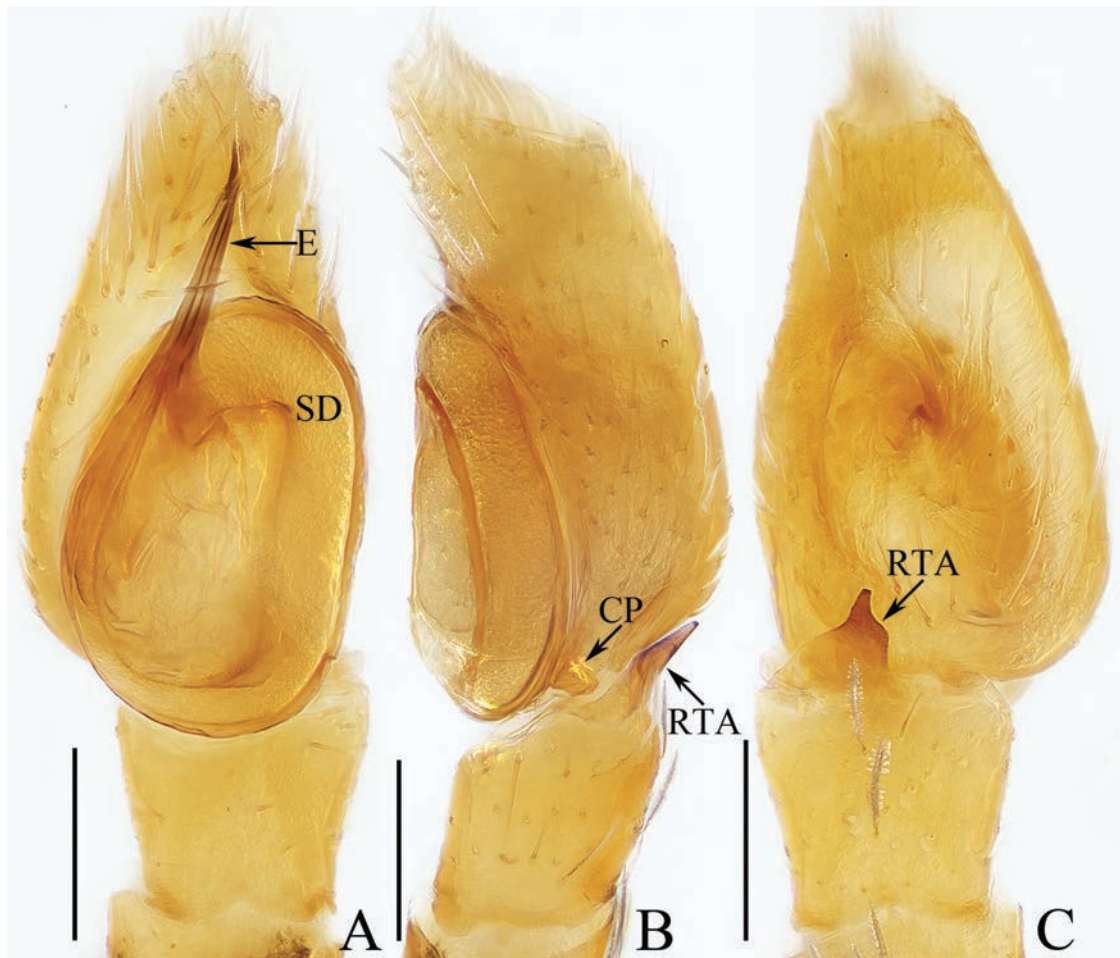


**Figure 27.** Male palp of *Simaetha hainan* sp. nov., holotype **A** ventral **B** retrolateral **C** dorsal. Abbreviations: CP cymbial process; E embolus; RTA retrolateral tibial apophysis; SD sperm duct. Scale bars: 0.1 mm.

**Palp** (Fig. 27A–C): femur length/width ratio ca 3.2; patella ~ 1.5× longer than wide in retrolateral view; tibia slightly longer than wide, with lamellar retrolateral apophysis (RTA) acutely narrowed at distal portion and blunt apically in dorsal view; cymbium ~ 1.8× longer than wide, with baso-retrolateral process (CP); tegulum oval; embolus (E) originating at ca 10:30 o'clock position, straight, tapered to rather blunt tip.

**Female** (Fig. 28A, B, E). Total length 3.16. Carapace 1.34 long, 1.07 wide. Abdomen 1.95 long, 1.08 wide. Eye sizes and interdistances: AME 0.32, ALE 0.17, PLE 0.17, AERW 0.97, PERW 1.08, EFL 0.74. Legs: I 2.11 (0.75, 0.45, 0.38, 0.28, 0.25), II 1.89 (0.58, 0.35, 0.38, 0.33, 0.25), III 1.68 (0.50, 0.25, 0.35, 0.33, 0.25), IV 2.24 (0.83, 0.28, 0.50, 0.38, 0.25). Habitus (Fig. 28E) similar to that of male except without base-lateral protuberances on anterior surface of chelicerae.

**Epigyne** (Fig. 28A, B) ~ 1.7× wider than long, with posterior, sub-triangular hood (H) ~ 1/2 length of anterior chamber of spermatheca (AS); copulatory openings (CO) lateral to hood; copulatory ducts (CD) slightly curved medially, connected to antero-inner portions of anterior chamber of spermatheca, with small terminal accessory glands (AG); spermathecae (S) divided into oval anterior chamber extended posteriorly and spherical posterior chamber (PS); fertilization ducts (FD) arising from antero-inner portions of posterior chamber of spermatheca.

**Distribution.** Known only from the type locality in Hainan, China (Fig. 48).

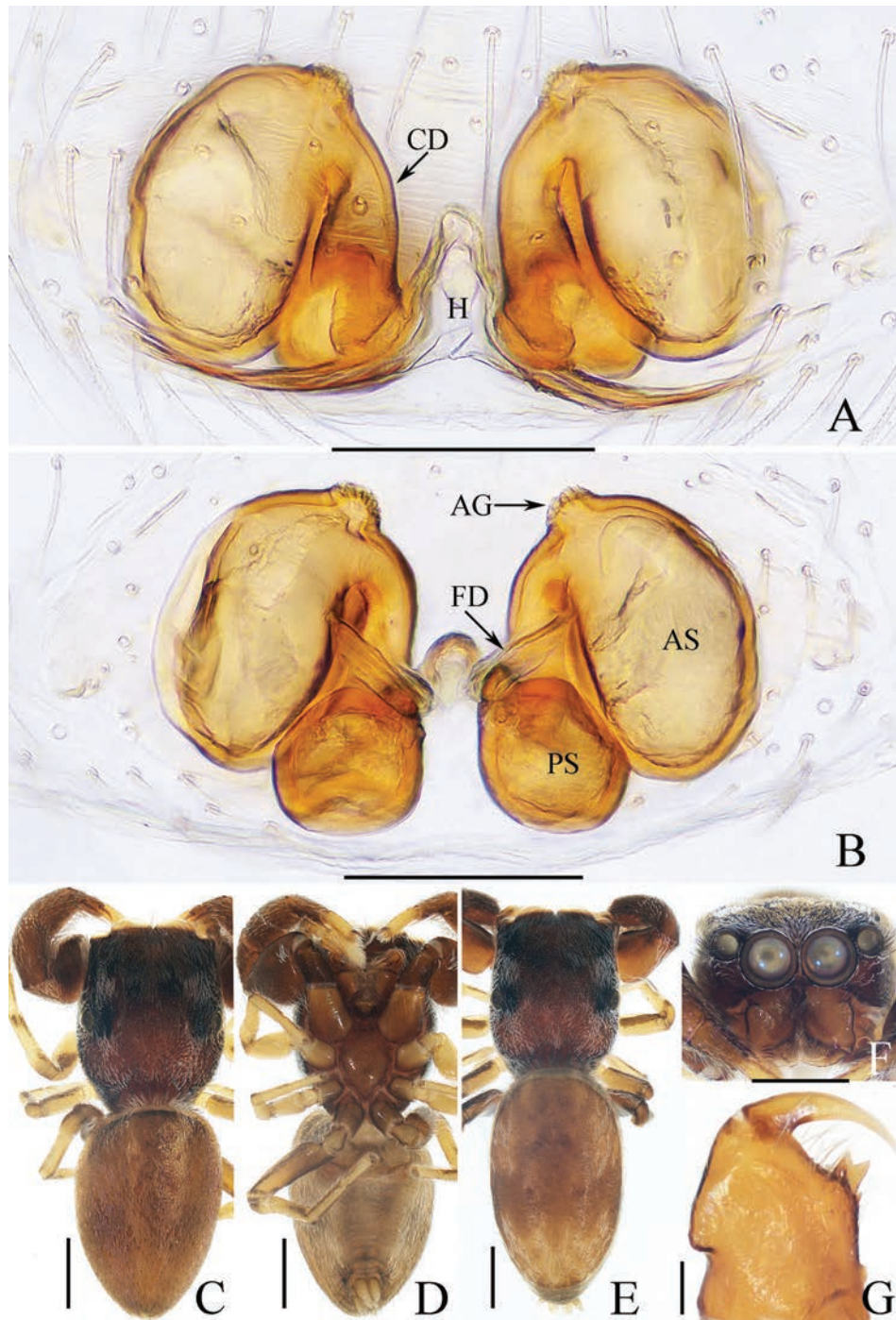


**Figure 28.** *Simaetha hainan* sp. nov. **C, D, F, G** male holotype and **A, B, E** female paratype (IZCAS-Ar 45285) **A** epigyne, ventral **B** vulva, dorsal **C, E** habitus, dorsal **D** ditto, ventral **F** carapace, frontal **G** chelicera, anterior. Abbreviations: AG accessory gland; AS anterior chamber of spermatheca; CD copulatory duct; FD fertilization duct; H epigynal hood; PS posterior chamber of spermatheca. Scale bars: 0.1 mm (**A, B, G**); 0.5 mm (**C–F**).

### Genus *Stertinus* Simon, 1890

**Type species.** *Stertinus dentichelis* Simon, 1890; type locality Mariana Is.

**Comments.** *Stertinus*, is considered a member of *Simaethina* (Maddison 2015). Currently, 16 species have been placed in this genus, primarily from east and southeast Asia (WSC 2024). The genus is poorly defined because the

generotype is lacking essential diagnostic drawings, and most of its species were assigned to the genus based only on the similarity to some of the known congeners (Wang et al. 2024).

***Stertinus lhoba* sp. nov.**

<https://zoobank.org/339A1A0E-A710-4B62-81AE-77367D097F6D>

Figs 29, 30, 47

**Type material. Holotype** ♂ (TRU-JS 0774), CHINA: • Xizang Autonomous Region, Medog County, Beibeng Township, Deergong Village, Yarlung Zangbo National Nature Reserve (29°10.84'N, 95°8.67'E, ca 1670 m), 25.V.2024, X.Q. Mi et al. leg.

**Paratypes** • 2 ♀ (TRU-JS 0775–0776), same data as for holotype.

**Etymology.** The specific name is after the Lhoba ethnic group, one of the two significant national minorities in Medog; noun in apposition.

**Diagnosis.** *Stertinus lhoba* sp. nov. resembles that of *S. liqingae* Wang, Mi & Li, 2024 in general shape of copulatory organs, especially the epigyne structure, but differs in: 1) retrolateral tibial apophysis (RTA) almost equal in width in retrolateral view (Fig. 29B) vs almost tapered (Wang et al. 2024: fig. 15C); 2) epigyne has a fold (F) (Fig. 30A, B) vs a hood (Wang et al. 2024: fig. 16A, B); 3) anterior chamber of spermatheca (AS) almost posteriorly extending (Fig. 30B, C) vs transversely extending (Wang et al. 2024: fig. 16B, C).

**Description. Male** (Figs 29, 30D, E, G, H). Total length 2.78. Carapace 1.28 long, 1.13 wide. Abdomen 1.60 long, 1.13 wide. Eye sizes and interdistances: AME 0.30, ALE 0.16, PLE 0.15, AERW 0.95, PERW 1.08, EFL 0.60. Legs: I 2.87 (0.90, 0.63, 0.68, 0.38, 0.28), II 2.04 (0.63, 0.38, 0.45, 0.30, 0.28), III 1.91 (0.60, 0.30, 0.40, 0.33, 0.28), IV 2.29 (0.75, 0.38, 0.50, 0.38, 0.28). Carapace mainly red-brown, covered with golden and pale setae, with central, irregular dark patch on cephalon. Chelicerae red-brown, with two promarginal teeth and one much larger pillar-shaped retromarginal tooth. Leg I robust, with enlarged femora and tibiae, and two pairs of ventral spines on tibiae and metatarsi. Dorsum of abdomen pale yellow, mingled with dark brown, covered wholly by scutum, with longitudinal, irregular central dark patch; venter dark with median dotted lines.

**Palp** (Fig. 29A, B): femur length/width ratio ca 4.0; patella ~ 1.4× longer than wide in retrolateral view; tibia almost as long as wide in retrolateral view, with short retrolateral apophysis (RTA) slightly curved outwards and blunt apically; cymbium ~ 2× longer than tibia in ventral view, with sub-triangular baso-retrolateral process (CP); tegulum nearly oval, with sperm duct (SD) extending along submargin; embolus (E) originating from antero-prolateral portion of tegulum, slightly curved prolaterally at median portion and with pointed tip directed towards ca 11 o'clock position.

**Female** (Fig. 30A–C, F). Total length 2.72. Carapace 1.15 long, 1.01 wide. Abdomen 1.68 long, 1.10 wide. Eye sizes and interdistances: AME 0.30, ALE 0.16, PLE 0.15, AERW 0.90, PERW 1.01, EFL 0.58. Legs: I 1.94 (0.63, 0.40, 0.40, 0.28, 0.23), II 1.62 (0.50, 0.33, 0.33, 0.23, 0.23), III 1.59 (0.50, 0.28, 0.30, 0.28, 0.23), IV 2.23 (0.70, 0.45, 0.45, 0.38, 0.25). Habitus (Fig. 30F) similar to that of male except smaller retromarginal cheliceral tooth, and without dorsal abdominal scutum.

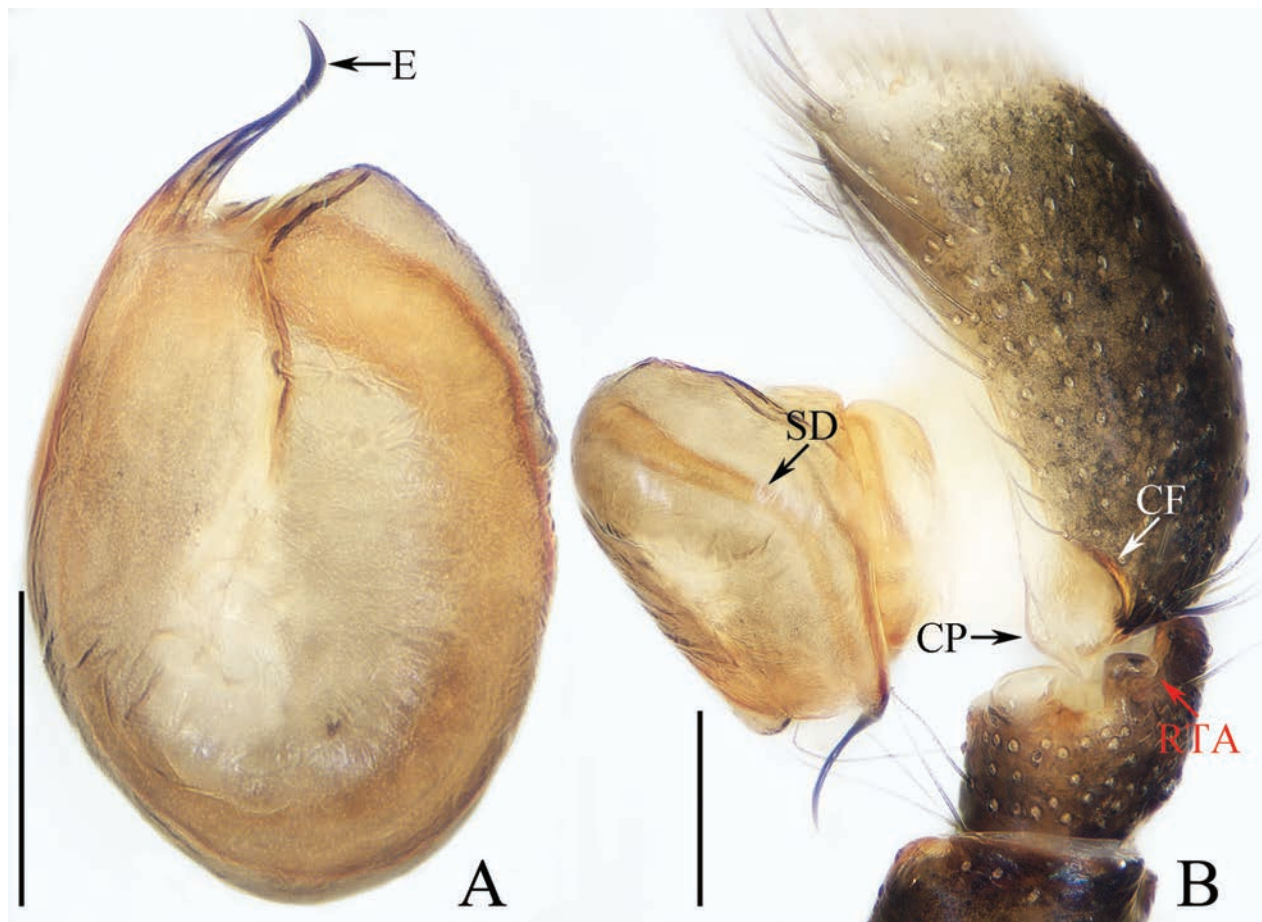


**Figure 29.** *Sertinius lhoba* sp. nov., holotype **A** bulb, ventral **B** palp, retrolateral. Abbreviations: CF cymbial flange; CP cymbial process; E embolus; RTA retrolateral tibial apophysis; SD sperm duct. Scale bars: 0.1 mm.

**Epigyne** (Fig. 30A–C) ~ 1.46× wider than long, with sub-labiate central fold (F); copulatory openings (CO) small, beneath lateral portion of fold; copulatory ducts (CD) short, without distinct border; spermathecae (S) divided into oval anterior chamber (AS) and spherical posterior chamber (PS); fertilization ducts (FD) originating from antero-inner portions of posterior chamber of spermatheca.

**Distribution.** Known only from the type locality in Xizang, China (Fig. 47).

### Genus *Synagelides* Strand, 1906

**Type species.** *Synagelides agoriformis* Strand, 1906; type locality Japan.

**Comments.** *Synagelides* is placed in the tribe Agoriini Simon, 1901 (Madison, 2015). To date, 78 nominal species have been described from east to southeast Asia, of which more than 60% are recorded from China (WSC 2024). The genus is relatively well studied because all its species are known from diagnostic drawings. However, > 41% of its species are only known from a single sex. The species described below are consistent in having hollowed fovea, two promarginal teeth and one retromarginal tooth on chelicerae, sub-triangular prolateral femoral apophysis (PFA), enlarged male palpal patella with a disto-prolateral bump (PB), and short male palpal tibia with a flat and broad ventral process (VTP).

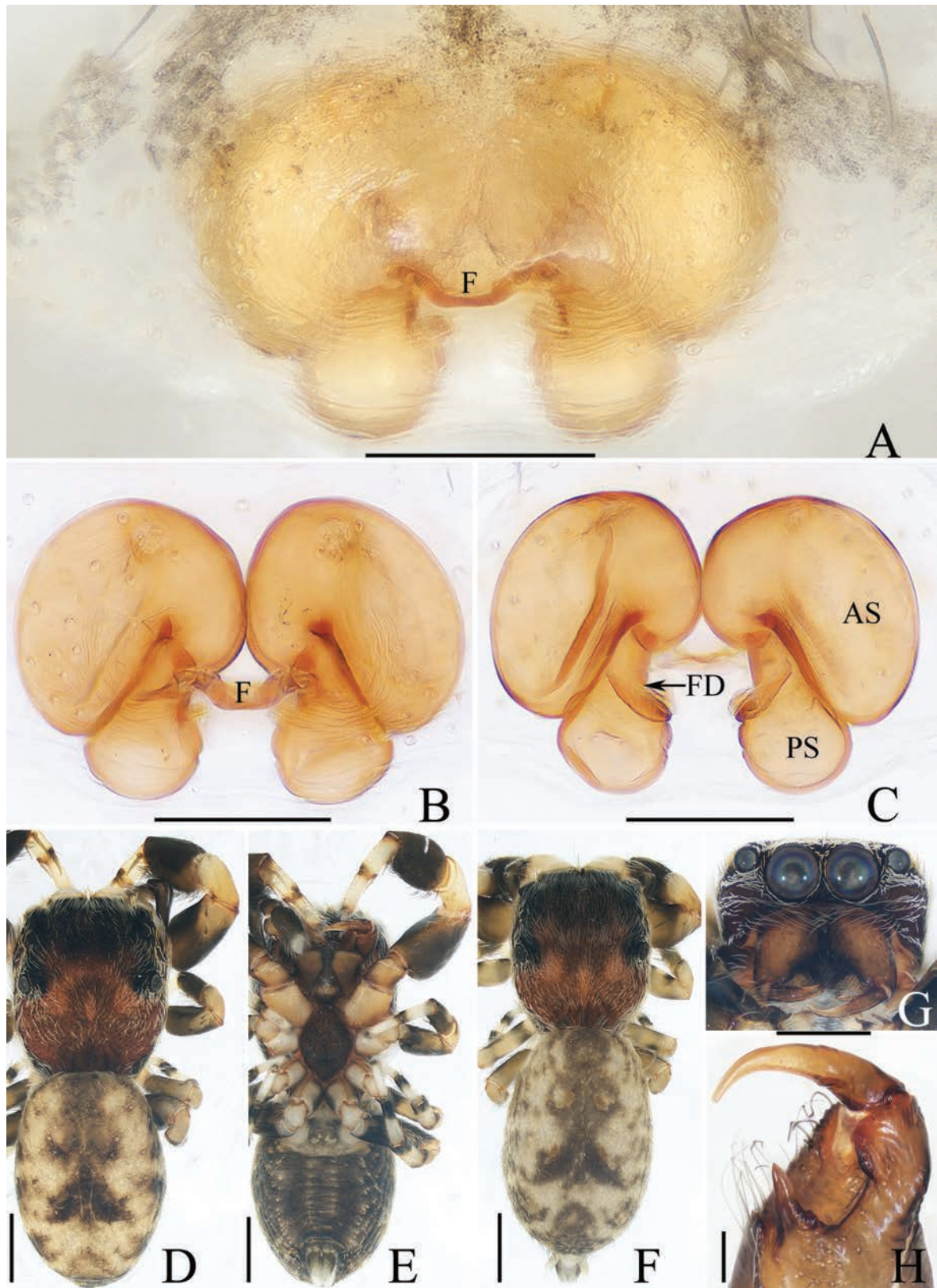


**Figure 30.** *Sertinius lhoba* sp. nov. **D, E, G, H** male holotype and **A–C, F** female paratype (TRU-JS 0775) **A, B** epigyne, ventral **C** vulva, dorsal **D, F** habitus, dorsal **E** ditto, ventral **G** carapace, frontal **H** chelicera, posterior. Abbreviations: AS anterior chamber of spermatheca; F epigynal fold; FD fertilization duct; PS posterior chamber of spermatheca. Scale bars: 0.1 mm (**A–C, H**); 0.5 mm (**D–G**).

***Synagelides kongmingi* sp. nov.**

<https://zoobank.org/2C8CCDDE-E317-4DD2-966E-626BC653C4DB>

Figs 31, 32, 47

**Type material.** *Holotype* ♂ (TRU-JS 0777), CHINA: • Sichuan Province, Bazhong City, Nanjiang County, Guangwu Township, Guangwushan-Nuoshuihe National Geopark (32°40.76'N, 106°46.11'E, ca 1010 m), 3.VI.2022, A.L. He et al. leg.

*Paratypes* • 1 ♂ 2 ♀ (TRU-JS 0778–0780), Sandaoguan Scenic Area (32°39.57'N, 106°44.36'E, ca 1470 m), 4.VIII.2022, A.L. He et al. leg.

**Etymology.** The specific name is a patronym in honor of a famous wise strategist Zhuge Kongming; noun (name) in the genitive case.

**Diagnosis.** *Synagelides kongmingi* sp. nov. resembles that of *S. tianquan* Wang, Mi & Li, 2024 in having very similar habitus and copulatory organs, but differs in: 1) retrolateral cymbial apophysis (RCA) with a smooth edge in dorsal view (Fig. 31D) vs a shallow incision on inner edge (Wang et al. 2024: fig. 18D); 2) presence of a groove between the retrolateral cymbial apophysis and dorsal cymbial process (Fig. 31D) vs absent (Wang et al. 2024: fig. 18D); 3) spermathecae (S) transversely extending (Fig. 32C, D) vs anteriorly extending at lateral portions (Wang et al. 2024: fig. 19B); 4) accessory glands (AG) visible (Fig. 32C, D) vs invisible (Wang et al. 2024: fig. 19B).

**Description.** **Male** (Figs 31, 32E, F, H, I). Total length 3.42. Carapace 1.53 long, 1.15 wide. Abdomen 1.84 long, 1.10 wide. Eye sizes and interdistances: AME 0.36, ALE 0.20, PLE 0.18, AERW 1.08, PERW 1.18, EFL 0.89. Legs: I 3.73 (1.18, 0.90, 0.90, 0.45, 0.30), II 2.54 (0.75, 0.43, 0.58, 0.50, 0.28), III 2.61 (0.75, 0.38, 0.60, 0.60, 0.28), IV 3.51 (1.00, 0.50, 0.88, 0.80, 0.33). Carapace mainly red-brown, covered with sparse, thin setae. Legs mainly yellow except enlarged femora I brown, with lateral stripes on femora, patellae, tibiae, and metatarsi II, III, IV, and four and two pairs of ventral spines on tibiae and metatarsi I, respectively. Dorsum of abdomen divided into brown, pale and dark portions, with pair of transverse, anterior, pale stripes bearing white setae, and longitudinal, central scutum extending through anterior 1/3; venter pale, without distinct markings.

**Palp** (Fig. 31A–D): femur length/width ratio ca 1.8; patella ~ 1.5× longer than wide in retrolateral view; tibia ~ 1/3 patellar length, with flat retrolateral apophysis (RTA) abruptly narrowed distally to blunt tip directed ca 11 o'clock position; cymbium length/width ratio ca 1.6, with flat prolateral and horn-shaped retrolateral apophyses, as well as sheet-shaped dorsal process (DCP); tegulum swollen; median apophysis (MA) irregular, slightly bent towards ventrally at median portion; embolus (E) flat, and curved into invert C-shape at base, and followed by slightly curved, thinner, whip-shaped portion.

**Female** (Fig. 32A–D, G). Total length 3.42. Carapace 1.53 long, 1.15 wide. Abdomen 1.84 long, 1.10 wide. Eye sizes and interdistances: AME 0.36, ALE 0.20, PLE 0.18, AERW 1.08, PERW 1.18, EFL 0.89. Legs: I 3.33 (1.00, 0.75, 0.85, 0.43, 0.30), II 2.29 (0.65, 0.38, 0.53, 0.45, 0.28), III 2.54 (0.75, 0.38, 0.58, 0.55, 0.28), IV 3.44 (1.00, 0.45, 0.88, 0.78, 0.33). Carapace (Fig. 32G) similar to that of male except paler. Dorsum of abdomen (Fig. 32G) pale brown; venter pale.

**Epigyne** (Fig. 32A–D) ~ 1.27× wider than long; atrium (At) occupies anterior 1/3, separated by broad, longitudinal septum (Se) grooved medio-posteriorly and bearing invert cup-shaped anterior hood (H), with pair of lateral arc-shaped

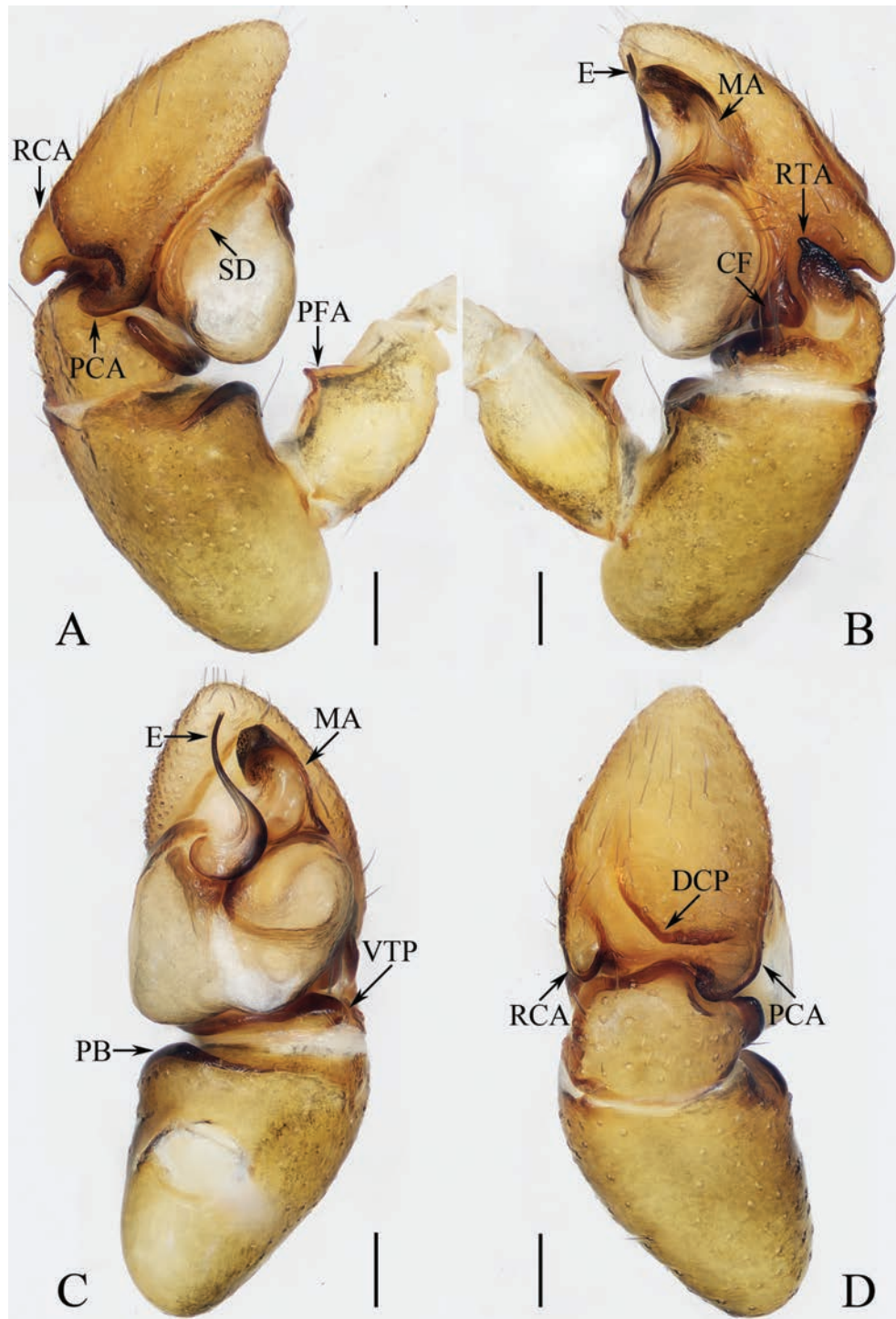


**Figure 31.** Male palp of *Synagelides kongmingi* sp. nov., paratype (TRU-JS 0778) **A** prolateral **B** retrolateral **C** ventral **D** dorsal. Abbreviations: CF cymbial flange; DCP dorsal cymbial process; E embolus; MA median apophysis; PB patellar bump of male palp; PCA prolateral cymbial apophysis; PFA prolateral femoral apophysis; RCA retrolateral cymbial apophysis; RTA retrolateral tibial apophysis; SD sperm duct; VTP ventral tibial process. Scale bars: 0.1 mm.

ridges (AR) antero-laterally; copulatory openings (CO) invisible; copulatory ducts (CD) strongly curved at proximal 1/3, and connected to antero-inner portions of spermathecae, with short, transversely extended, terminal accessory glands (AG); spermathecae (S) oval, separated by ~ 1/8 of their width.

**Distribution.** Known only from the type locality in Sichuan, China (Fig. 47).

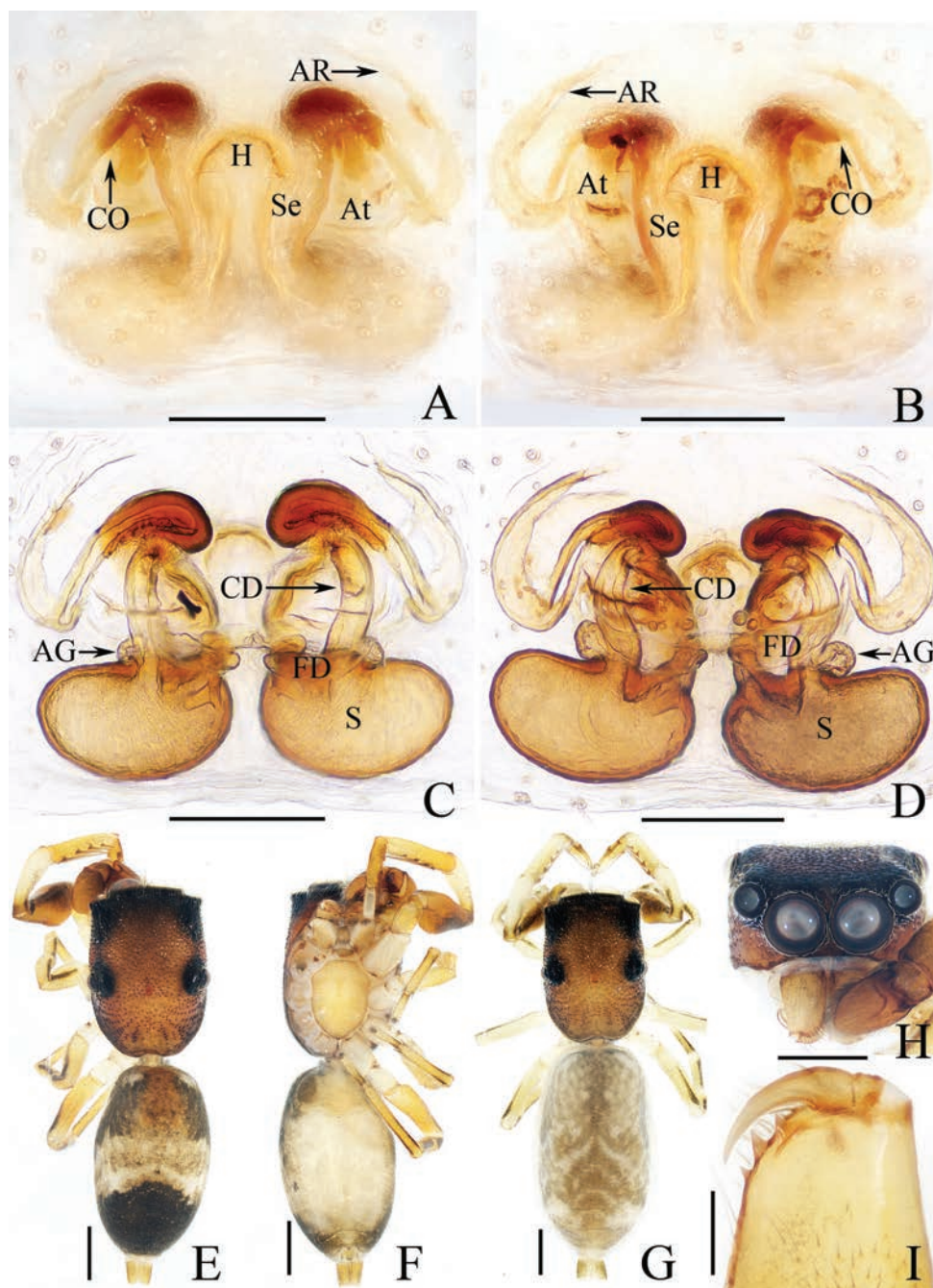


**Figure 32.** *Synagelides kongmingi* sp. nov. **E, F, H, I** holotype **A, C, G** female paratype (TRU-JS 0779) **B, D** female paratype (TRU-JS 0780) **A, B** epigyne, ventral **C, D** vulva, dorsal **E, G** habitus, dorsal **F** ditto, ventral **H** carapace, frontal **I** chelicera, posterior. Abbreviations: AG accessory gland; At atrium; AR atrial ridge; CD copulatory duct; CO copulatory opening; FD fertilization duct; H epigynal hood; S spermatheca; Se septum. Scale bars: 0.1 mm (**A–D, I**); 0.5 mm (**E–H**).

***Synagelides xuandei* sp. nov.**

<https://zoobank.org/7B3C45E2-7239-462B-BB03-A92DBF9510BF>

Figs 33, 34, 47

**Type material.** **Holotype** ♂ (TRU-JS 0781), CHINA: • Guangxi Zhuang Autonomous Region, Laibing City, Jinxiu Yao Autonomous County, Yinshan Park (24°10.07'N, 110°14.48'E, ca 1310 m), 8.XI.2021, A.L. He et al. leg. **Paratypes** • 3 ♂ 7 ♀ (TRU-JS 0782–0791), same data as for holotype.

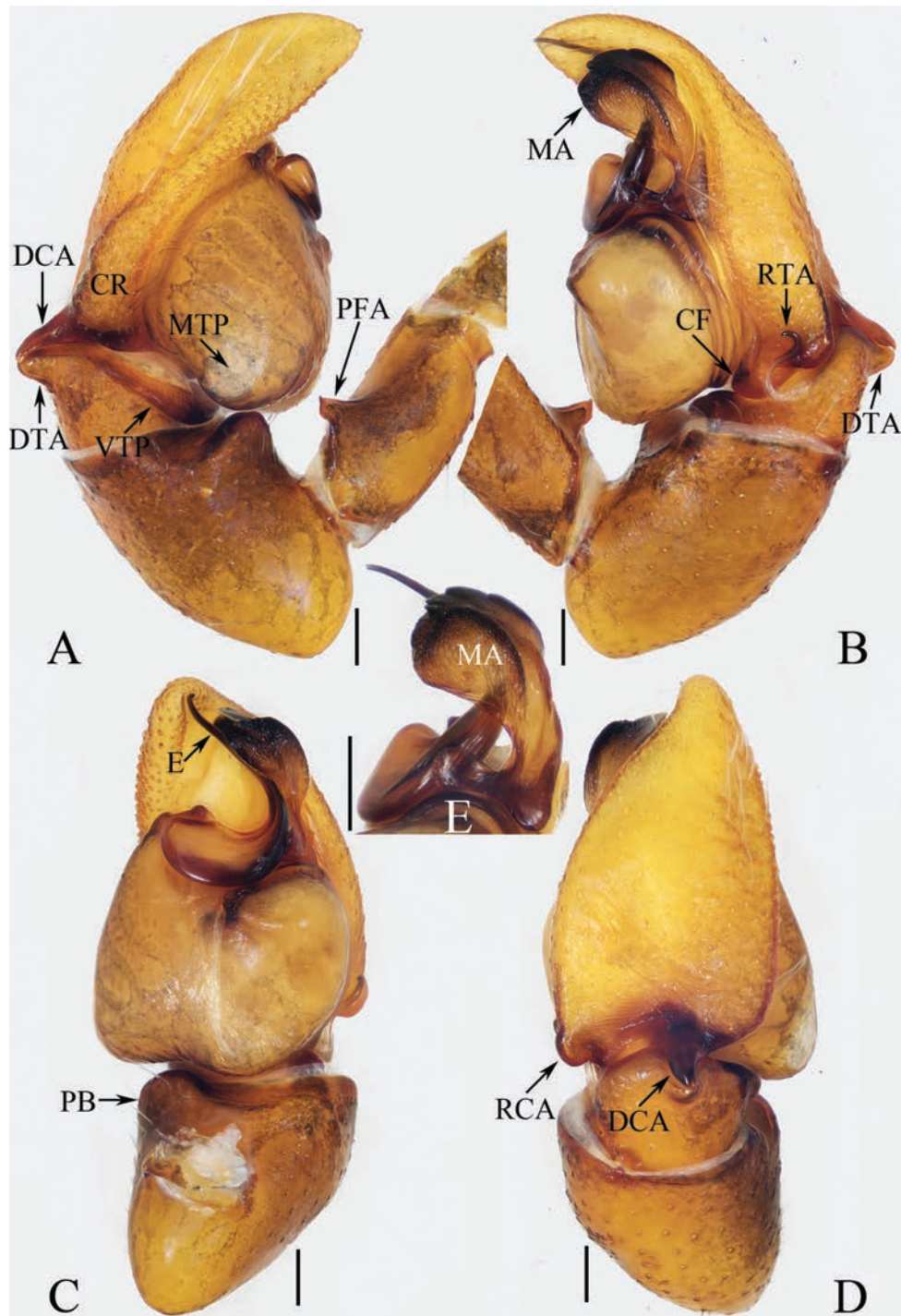


**Figure 33.** Male palp of *Synagelides xuandei* sp. nov. **A–D** holotype and **E** paratype (TRU-JS 0782) **A** prolateral **B** retrolateral **C** ventral **D** dorsal **E** embolus and median apophysis, retrolateral. Abbreviations: CF cymbial flange; CR cymbial ridge; DCA dorsal cymbial apophysis; DTA dorsal tibial apophysis; E embolus; MA median apophysis; MTP membranous tegular peak; PB patellar bump of male palp; PFA prolateral femoral apophysis; RCA retrolateral cymbial apophysis; RTA retrolateral tibial apophysis; VTP ventral tibial process. Scale bars: 0.1 mm.

**Etymology.** The specific name is after Mr. Liu Xuande, who is the first emperor of Shu during the Three Kingdoms of ancient China; noun (name) in the genitive case.

**Diagnosis.** The male of *Synagelides xuandei* sp. nov. is similar to *S. huangxin* Lin & Li, 2024 in general shape of the palp, but can be distinguished by the

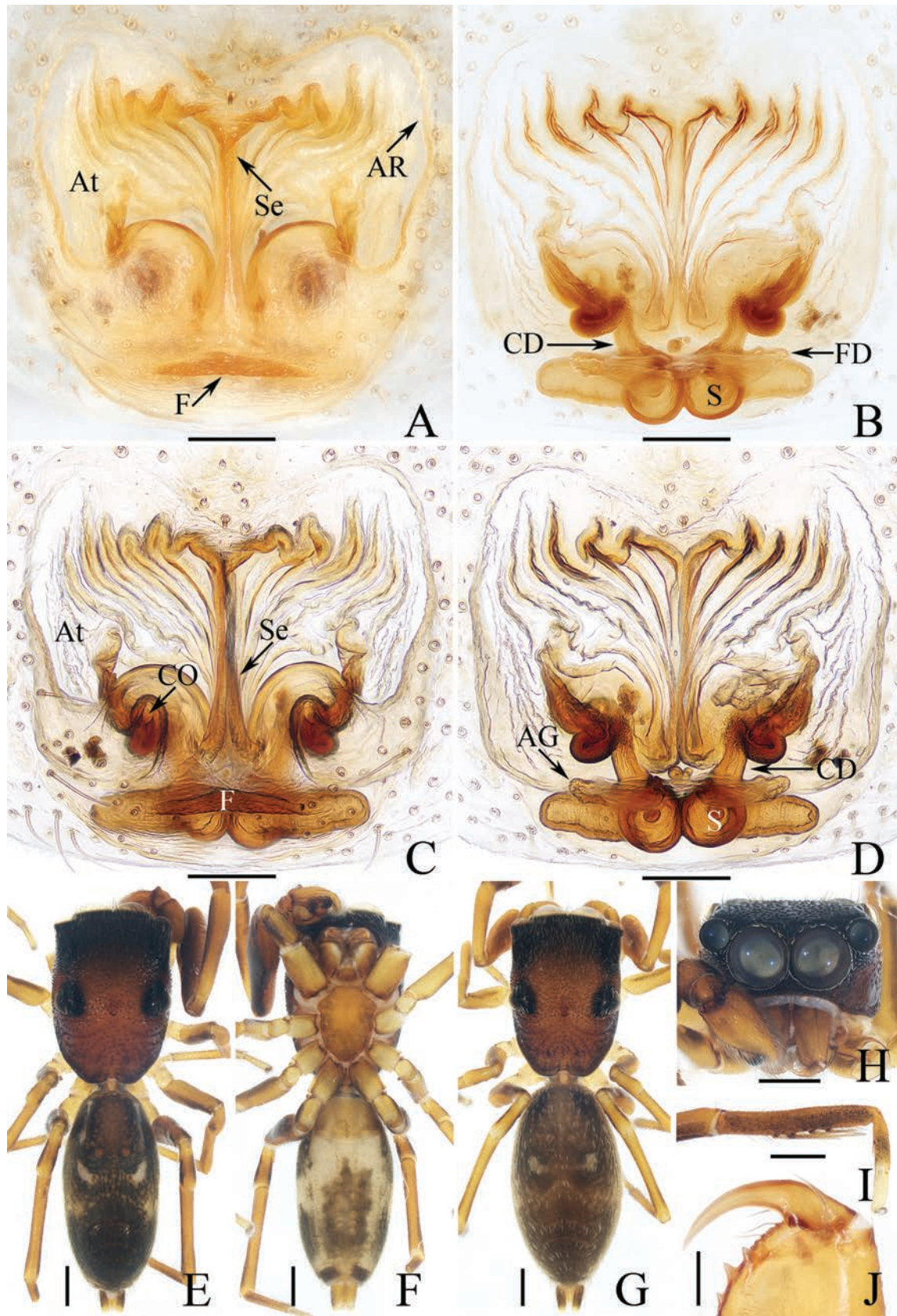


**Figure 34.** *Synagelides xuandei* sp. nov. **E, F, H–J** holotype and **A–D, G** female paratype (TRU-JS 0785) **A, C** epigyne, ventral **B, D** vulva, dorsal **E, G** habitus, dorsal **F** ditto, ventral **H** carapace, frontal **I** tibia and metatarsi I, prolateral **J** chelicera, posterior. Abbreviations: AG accessory gland; AR atrial ridge; CD copulatory duct; CO copulatory opening; F epigynal fold; FD fertilization duct; S spermatheca; Se septum. Scale bars: 0.1 mm (**A–D, J**); 0.5 mm (**E–I**).

median apophysis (MA), which is widest distally and has a base elongate-oval lamellar branch (Fig. 33B, E) vs almost tapered at distal half and lacking similar branch (Lin et al. 2024b: fig. 47B). The female of this species resembles that of *S. subgambosus* Wang, Mi, Irfan & Peng, 2020 in general shape of epigyne, especially the rugulose atrium (At), but can be easily distinguished the copulatory ducts (CD), which are strongly curved at proximal half (Fig. 34B–D) vs straight (Wang et al. 2020: fig. 12B, C).

**Description. Male** (Figs 33, 34E, F, H–J). Total length 4.63. Carapace 2.07 long, 1.48 wide. Abdomen 2.52 long, 1.22 wide. Eye sizes and interdistances: AME 0.50, ALE 0.27, PLE 0.26, AERW 1.46, PERW 1.48, EFL 1.15. Legs: I 5.86 (1.85, 1.68, 1.45, 0.58, 0.30), II 3.72 (1.13, 0.58, 0.95, 0.73, 0.33), III 3.91 (1.15, 0.53, 0.95, 0.95, 0.33), IV 5.27 (1.38, 0.68, 1.43, 1.35, 0.43). Carapace mainly red-brown, covered with thin setae. Legs mainly red-brown, with four and two pairs of ventral spines on tibiae and metatarsi I. Dorsum of abdomen dark brown, with pair of longitudinal, anterolateral, pale setal stripes and pair of oblique, median, pale setal patches; venter pale, with broad, central dark brown patch.

**Palp** (Fig. 33A–E): femur length/width ratio ca 2.1; patella ~ 1.6× longer than wide in retrolateral view; tibia short, with sub-triangular dorsal apophysis (DTA) and slender, S-shaped retrolateral apophysis (RTA); cymbium ~ 1.8× longer than wide, with prolateral ridged portion (CR), blunt retrolateral apophysis (RCA) and tapered baso-dorsal apophysis (DCA) with pointed end; tegulum swollen; median apophysis (MA) large, broadened and forming mesal ridge, with base, elongate-oval lamellar branch extended ventrally; embolus (E) forming half-round disc at base, then tapered and curved into rather blunt tip.

**Female** (Fig. 34A–D, G). Total length 4.88. Carapace 2.02 long, 1.39 wide. Abdomen 2.72 long, 1.47 wide. Eye sizes and inter-distances: AME 0.50, ALE 0.28, PLE 0.26, AERW 1.51, PERW 1.49, EFL 1.21. Legs: I 4.83 (1.50, 1.23, 1.25, 0.55, 0.30), II 3.63 (1.10, 0.55, 0.90, 0.78, 0.30), III 3.94 (1.13, 0.53, 0.95, 0.98, 0.35), IV 5.40 (1.45, 0.70, 1.40, 1.40, 0.45). Habitus (Fig. 34G) similar to that of male except paler and with much shallow similar patterns.

**Epigyne** (Fig. 34A–D) slightly longer than wide, with broad posterior fold (F) ~ 1/3 atrial width; atrium (At) crinkly, occupied anterior 3/5 and separated by narrow septum (Se), with pair of lateral ridges (AR); copulatory openings (CO) invisible; copulatory ducts (CD) strongly curved at proximal, and connected to inner portions of spermathecae, with bar-shaped, terminal accessory glands (AG); spermathecae (S) touching each other, with spherical inner portions and transversely extended, elongate-oval outside portions.

**Distribution.** Known only from the type locality in Guangxi, China (Fig. 47).

### ***Synagelides yidei* sp. nov.**

<https://zoobank.org/D9A6BA46-20F4-458E-950E-7231D9986C9F>

Figs 35, 36, 48

**Type material. Holotype** ♂ (TRU-JS 0792), CHINA: • Guangxi Zhuang Autonomous Region, Laibing City, Jinxiu Yao Autonomous County, Yinshan Park (24°10.07'N, 110°14.48'E, ca 1310 m), 8.XI.2021, A.L. He et al. leg. **Paratypes** • 1 ♂ (TRU-JS 0793), same data as for holotype; • 1 ♂ (TRU-JS 0794), Shengtangshan Scenic Area (23°58.05'N, 110°6.53'E, ca 1520 m), 11.X.2021, A.L. He et al. leg.

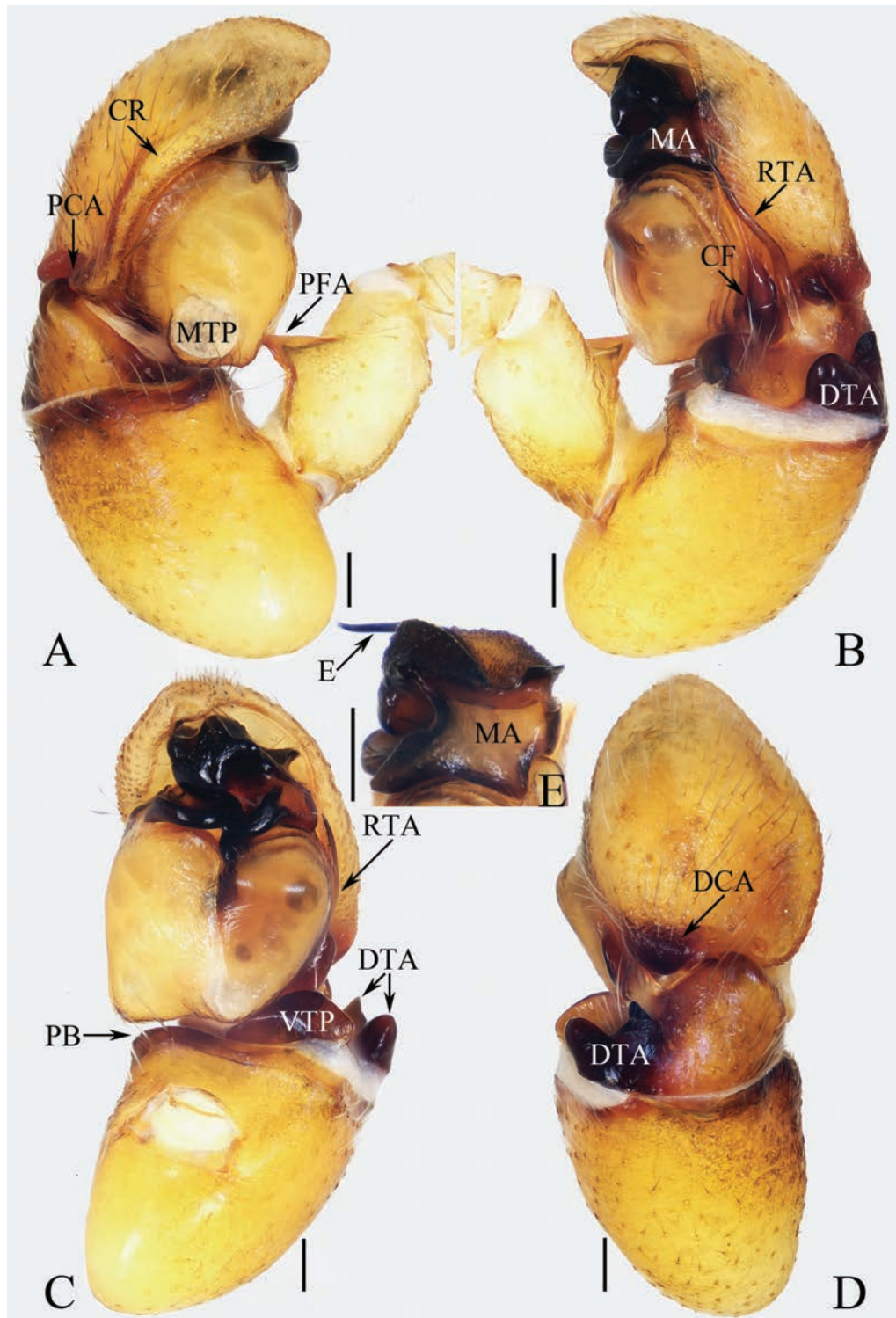


**Figure 35.** Male palp of *Synagelides yidei* sp. nov. **A–D** holotype and **E** paratype (TRU-JS 0793) **A** prolateral **B** retrolateral **C** ventral **D** dorsal **E** embolus and median apophysis, retrolateral. Abbreviations: CF cymbial flange; CR prolateral cymbial ridge; DCA dorsal cymbial apophysis; DTA dorsal tibial apophysis; E embolus; MA median apophysis; MTP membranous tegular peak; PB patellar bump of male palp; PCA prolateral cymbial apophysis; PFA prolateral femoral apophysis; RTA retrolateral tibial apophysis; VTP ventral tibial process. Scale bars: 0.1 mm.

**Etymology.** The specific name is after Mr. Zhang Yide, who is one of the famous Shu Generals in the Three Kingdoms of ancient China; noun (name) in the genitive case.

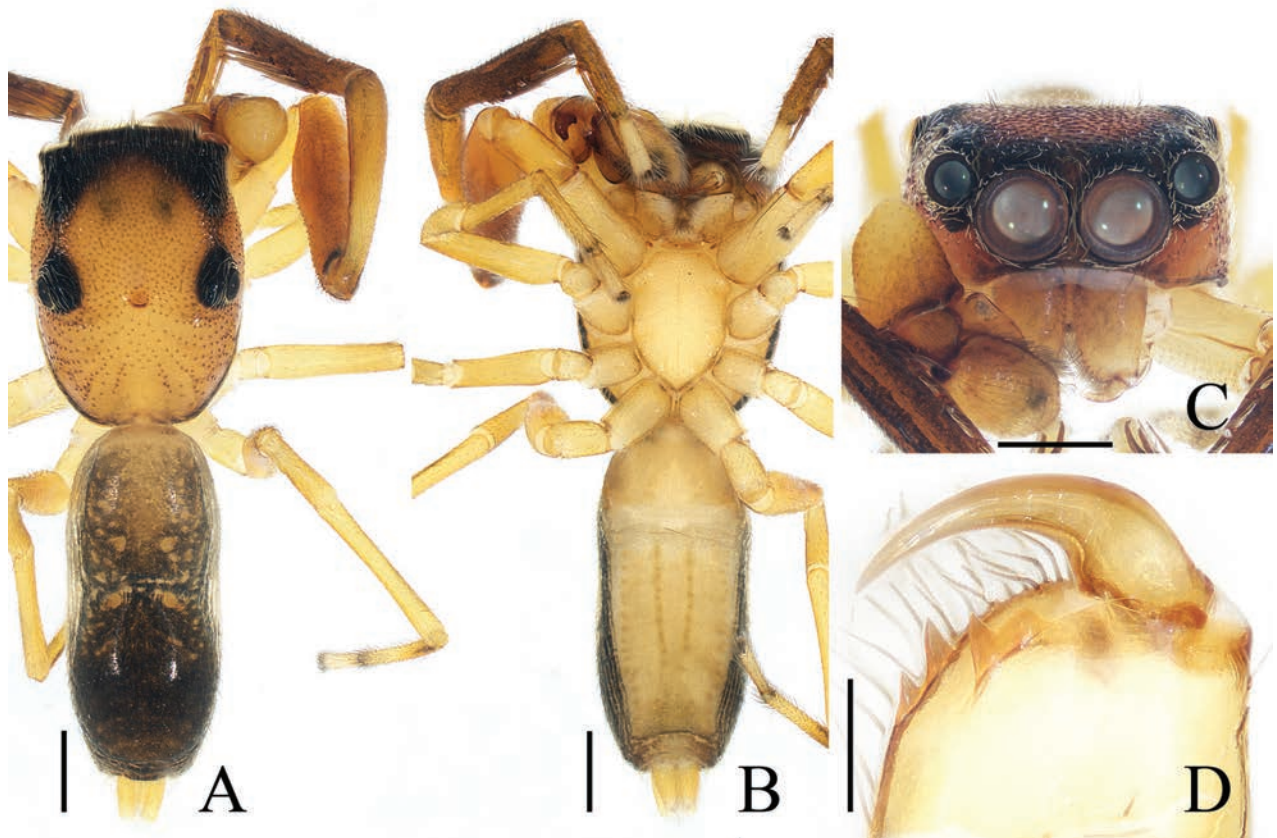


**Figure 36.** *Synagelides yidei* sp. nov., holotype **A** habitus, dorsal **B** ditto, ventral **C** carapace, frontal **D** chelicera, posterior. Scale bars: 0.5 mm (**A–C**); 0.1 mm (**D**).

**Diagnosis.** *Synagelides yidei* sp. nov. can be easily distinguished from other known male congeners by the bifurcated dorsal tibial apophysis (DTA) (Fig. 35B–D) vs absent or not bifurcated in congeners (see Metzner 2024).

**Description. Male** (Figs 35, 36). Total length 3.93. Carapace 1.76 long, 1.34 wide. Abdomen 2.23 long, 0.95 wide. Eye sizes and interdistances: AME 0.42, ALE 0.23, PLE 0.21, AERW 1.18, PERW 1.30, EFL 0.97. Legs: I 7.13 (2.25, 2.05, 1.63, 0.75, 0.45), II 3.51 (1.03, 0.55, 0.88, 0.70, 0.35), III 3.57 (0.98, 0.53, 0.88, 0.83, 0.35), IV 4.79 (1.28, 0.70, 1.30, 1.13, 0.38). Carapace mainly yellow, with pair of indistinct dark patches anteriorly on square cephalon. Legs slender, bear four and two pairs of ventral spines on tibiae and metatarsi I. Abdomen slightly constricted medially, dorsum dark brown posteriorly, with two pairs of median, yellow muscle depressions; venter pale, with pair of central, dotted lines.

**Palp** (Fig. 35A–E): femur length/width ratio ca 1.68; patella ~ 1.5× longer than wide in retrolateral view; dorsal tibial apophysis (DTA) bifurcated with two short, blunt rami; retrolateral tibial apophysis (RTA) tapered, slender, > 1/2 cymbial length, and pointed apically; cymbium with prolateral ridged portion (CR), strongly sclerotized, blunt baso-dorsal apophysis (DCA) and prolateral apophysis (PCA); tegulum swollen; median apophysis (MA) irregular, retrolateral to embolus; embolus (E) forming disc at base, then twisted into blunt end.

**Female.** Unknown.

**Distribution.** Known only from the type locality in Guangxi, China (Fig. 48).

***Synagelides yunchangi* sp. nov.**

<https://zoobank.org/0477C6C3-63F4-4281-BBF2-3C23EC7F2F4B>

Figs 37, 38, 47

**Type material.** *Holotype* ♂ (TRU-JS 0795), CHINA: • Guangxi Zhuang Autonomous Region, Laibing City, Jinxiu Yao Autonomous County, Shengtangshan Scenic Area (23°58.05'N, 110°6.53'E, ca 1520 m), 11. X.2021, A.L. He et al. leg.

*Paratypes* • 4 ♂ 2 ♀ (TRU-JS 0796–0801), same data as for holotype.

**Etymology.** The specific name is after Mr. Guan Yunchang, who is one of the famous Shu Generals in the Three Kingdoms of ancient China; noun (name) in the genitive case.

**Diagnosis.** *Synagelides yunchangi* sp. nov. resembles that of *S. gambosus* Xie & Yin, 1991, in having very similar copulatory organs, but can be distinguished by the following: 1) ratio of the constricted portion of median apophysis (MA) to the broadest portion ~ 1/2 in retrolateral view (Fig. 37B) vs ~ 1/3 (Peng 2020: fig. 326d); 2) presence of an U-shaped incision (UI) on the anterior margin of embolic disc (Fig. 37C) vs very shallow, near C-shaped incision (Peng 2020: fig. 326b); 3) septum (Se) almost Y-shaped, and ~ 3/5 of atrial width (Fig. 38A–C) vs approximately T-shaped, and > 4/5 of atrial width (Peng 2020: fig. 326f); 4) atrial ridge (AR) approximately auricle-shaped (Fig. 38A–C) vs approximately L-shaped (Peng 2020: fig. 326f); 5) presence of a pair of anterolateral, pale stripes on dorsum of abdomen (Fig. 36E, G) vs pair of round spots (Peng 2020: fig. 326a).

**Description. Male** (Figs 37, 38E, F, H, I). Total length 3.87. Carapace 1.85 long 1.34 wide. Abdomen 1.96 long, 1.05 wide. Eye sizes and interdistances: AME 0.45, ALE 0.25, PLE 0.21, AERW 1.36, PERW 1.40, EFL 1.11. Legs: I 4.41 (1.38, 1.15, 1.10, 0.50, 0.28), II 2.94 (0.88, 0.45, 0.68, 0.63, 0.30), III 3.19 (0.93, 0.45, 0.73, 0.78, 0.30), IV 4.19 (1.15, 0.50, 1.13, 1.08, 0.33). Carapace red-brown, with longitudinal, anteromedian, paired, dark patches on cephalon. Legs slender, with four and two pairs of ventral spines on tibiae and patellae I. Dorsum of abdomen brown at anterior half and dark posteriorly, with pair of anterolateral pale stripes followed by paired yellow spots and transverse, pale patches; venter pale, without patterns.

**Palp** (Fig. 37A–D): femur length/width ratio ca 1.79; patella ~ 1.8× longer than wide; tibia ~ 1/3 patellar length, with slender, S-shaped retrolateral apophysis (RTA) and sub-triangular dorsal apophysis (DTA); cymbium ~ 1.6× longer than wide, with tapered, spine-shaped baso-dorsal apophysis (DCA); tegulum swollen; median apophysis (MA) irregular, broadened and swollen distally; embolus (E) flat and forming round disc at base, and then acutely narrowed to whip-shaped portion.

**Female** (Fig. 38A–D, G). Total length 4.77. Carapace 2.03 long, 1.47 wide. Abdomen 2.67 long, 1.41 wide. Eye sizes and inter-distances: AME 0.50, ALE 0.27, PLE 0.24, AERW 1.50, PERW 1.48, EFL 1.20. Legs: I 4.38 (1.33, 1.05, 1.20, 0.50, 0.30), II 3.14 (0.98, 0.48, 0.75, 0.63, 0.30), III 3.44 (1.00, 0.48, 0.78, 0.85, 0.33), IV 4.43 (1.25, 0.50, 1.20, 1.13, 0.35). Habitus (Fig. 38G) similar to that of male except slightly darker.

**Epigyne** (Fig. 38A–D) almost as long as wide, with transverse, lamellar, posterior fold (F); atrium (At) large, occupies anterior 3/5, separated by Y-shaped septum (Se), with pair of auricle-shaped lateral ridges (AR); copulatory openings (CO) beneath baso-lateral portions of atrial ridges; copulatory ducts (CD) thin, anterior half curved into C-shape, posterior half posteriorly descending with short, transversely extending accessory glands (AG); spermathecae touched, with spherical inner portions.

**Distribution.** Known only from the type locality in Guangxi, China (Fig. 47).

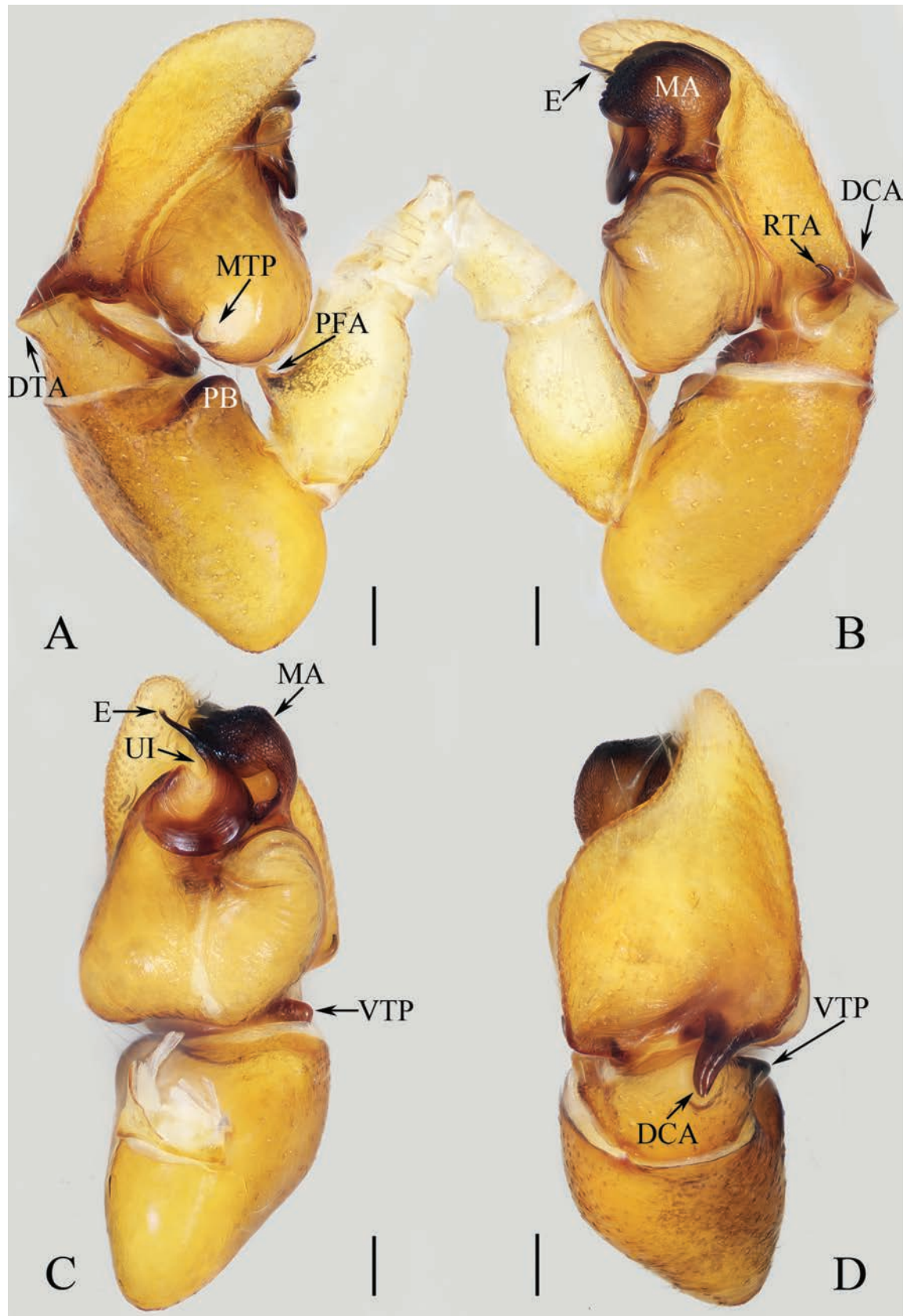


**Figure 37.** Male palp of *Synagelides yunchangi* sp. nov., holotype **A** prolateral **B** retrolateral **C** ventral **D** dorsal. Abbreviations: DCA dorsal cymbial apophysis; DTA dorsal tibial apophysis; E embolus; MA median apophysis; MTP membranous tegular peak; PB patellar bump of male palp; PFA prolateral femoral apophysis; RTA retrolateral tibial apophysis; UI U-shaped incision of embolic disc; VTP ventral tibial process. Scale bars: 0.1 mm.

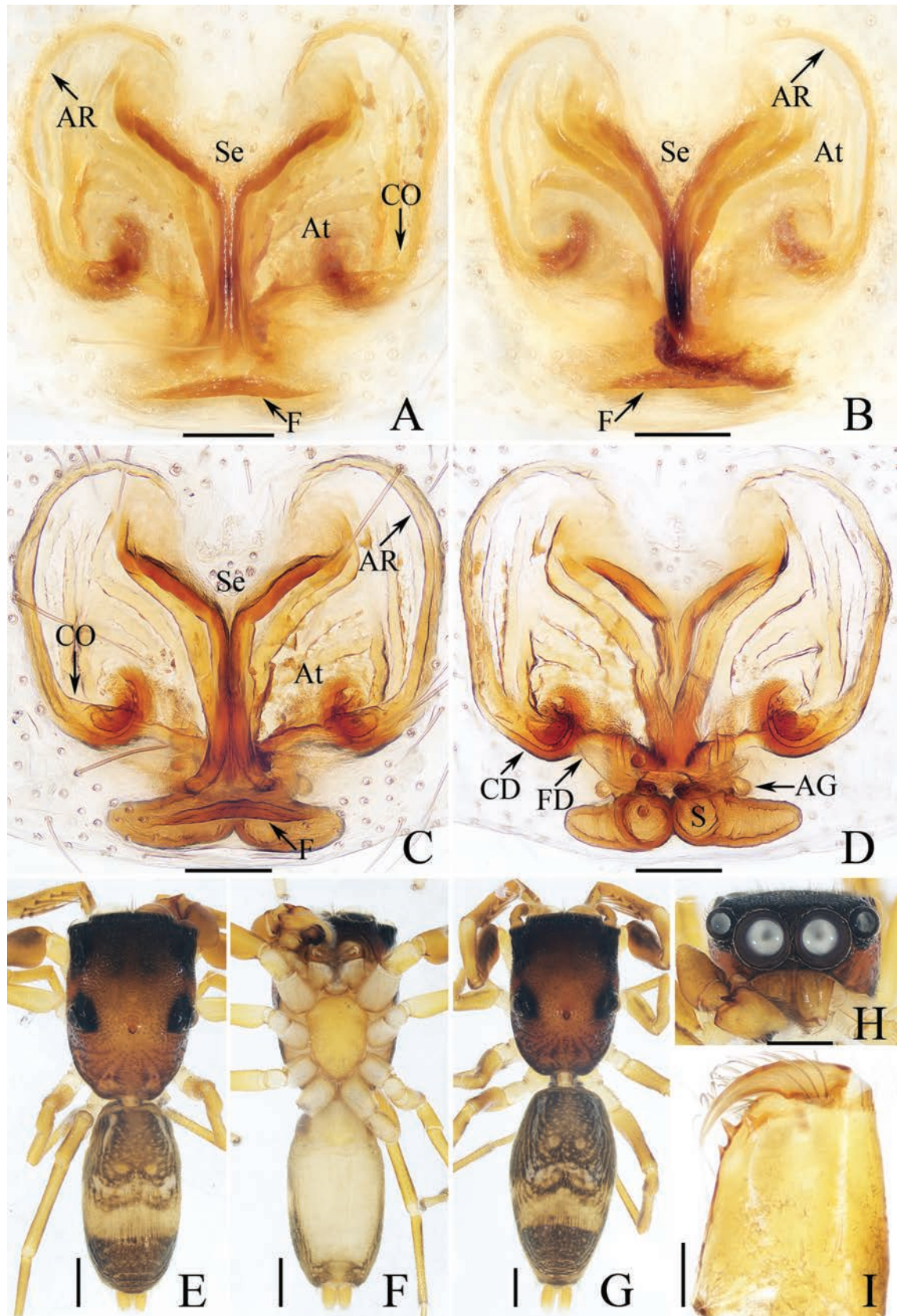


**Figure 38.** *Synagelides yunchangi* sp. nov. **E, F, H, I** male holotype **A, C, D, G** female paratype (TRU-JS 0800) **B** female paratype (TRU-JS 0801) **A–C** epigyne, ventral **D** vulva, dorsal **E, G** habitus, dorsal **F** ditto, ventral **H** carapace, frontal **I** chelicera, posterior. Abbreviations: AG accessory gland; At atrium; AR atrial ridge; CD copulatory duct; CO copulatory opening; F epigynal fold; FD fertilization duct; S spermatheca; Se septum. Scale bars: 0.1 mm (**A–D, I**); 0.5 mm (**E–H**).

***Synagelides zilongi* sp. nov.**

<https://zoobank.org/80BEA892-2AA3-4BB4-8A21-1DE32F673C9A>

Figs 39, 40, 48

**Type Material.** **Holotype** ♂ (TRU-JS 0802), CHINA: • Yunnan Province, Wenshan City, Wenshan National Nature Reserve, Bozhushan (23°22.19'N, 103°55.17'E, ca 2730 m), 14.V.2024, C. Wang et al. leg. **Paratypes** • 1 ♂ 2 ♀ (TRU-JS 0803–0805), same data as for holotype.

**Etymology.** The specific name is after Mr. Zhao Zilong, who is one of the famous Shu Generals in the Three Kingdoms of ancient China; noun (name) in the genitive case.

**Diagnosis.** *Synagelides zilongi* sp. nov. resembles that of *S. jingzhao* Yang, Zhu & Song, 2007 in the habitus and general shape of copulatory organs, but can be easily distinguished by the following: 1) retrolateral tibial apophysis (RTA) ~ 1/2 of cymbial length in retrolateral view (Fig. 39B) vs ~ 3/5 of cymbial length (Yang et al. 2007: fig. 1F); 2) epigynal hood (H) ~ 3× longer than wide (Fig. 40A–D) vs just slightly longer than wide (Yang et al. 2007: fig. 1B); 3) presence of four pairs of ventral spines on tibiae I (Fig. 40I) vs five pairs (see the description in Yang et al. 2007: 1).

**Description. Male** (Figs 39, 40E, F, H–J). Total length 3.18. Carapace 1.43 long, 1.09 wide. Abdomen 1.72 long, 0.78 wide. Eye sizes and inter-distances: AME 0.34, ALE 0.19, PLE 0.18, AERW 1.02, PERW 1.11, EFL 0.83. Legs: I 4.54 (1.38, 1.20, 1.13, 0.50, 0.33), II 2.53 (0.75, 0.40, 0.60, 0.50, 0.28), III 2.59 (0.75, 0.38, 0.60, 0.58, 0.28), IV 3.49 (0.95, 0.48, 0.93, 0.83, 0.30). Carapace yellow-brown to dark, with longitudinal, dark, thin stripe centrally on cephalon. Legs slender, with four and two pairs of ventral spines on patellae and metatarsi I. Dorsum of abdomen dark, with pair of anterolateral, pale dots followed by paired, dark yellow dots, and inconsistent, transverse, white stripes bearing sparse white setae medially; venter pale, mingled with dark, with longitudinal, dark stripe extending from epigastric groove to posterior 1/3.

**Palp** (Fig. 39A–E): femur length/width ratio ca 1.67; patella ~ 1.5× longer than wide; tibia ~ 1/3 patellar length; dorsal tibial apophysis (DTA) strongly sclerotized, directed towards ca 1:30 o'clock position apically in retrolateral view; retrolateral tibial apophysis (RTA) tapered into pointed tip reaches base of median apophysis (MA), with small, spinous ramus located on ventral margin of anterior 1/3; cymbium with prolateral ridged portion (CR), and blunt baso-dorsal apophysis (DCA); tegulum swollen; median apophysis (MA) irregular, retrolateral to embolus; embolus (E) broadened at base, twisted into blunt end.

**Female** (Fig. 40A–D, G). Total length 4.45. Carapace 1.88 long, 1.39 wide. Abdomen 2.58 long, 1.36 wide. Eye sizes and inter-distances: AME 0.42, ALE 0.24, PLE 0.21, AERW 1.29, PERW 1.42, EFL 1.01. Legs: I 4.27 (1.28, 0.98, 1.13, 0.55, 0.33), II 2.89 (0.88, 0.45, 0.68, 0.58, 0.30), III 3.07 (0.88, 0.43, 0.73, 0.73, 0.30), IV 4.27 (1.20, 0.58, 1.13, 1.03, 0.33). Habitus (Fig. 40G) similar to that of male except paler and wider abdomen.

**Epigyne** (Fig. 40A–D) ~ 1.15× longer than wide, with tube-shaped anterior hood (H) ~ 3× longer than wide; atrium (At) oval, with pair of arc-shaped lateral ridges (AR); septum (Se) wide, narrowest medially; copulatory openings (CO) baso-lateral to narrowest portion of septum; copulatory ducts (CD) slender, curved into U-shape at anterior 2/3, with short, bar-shaped accessory

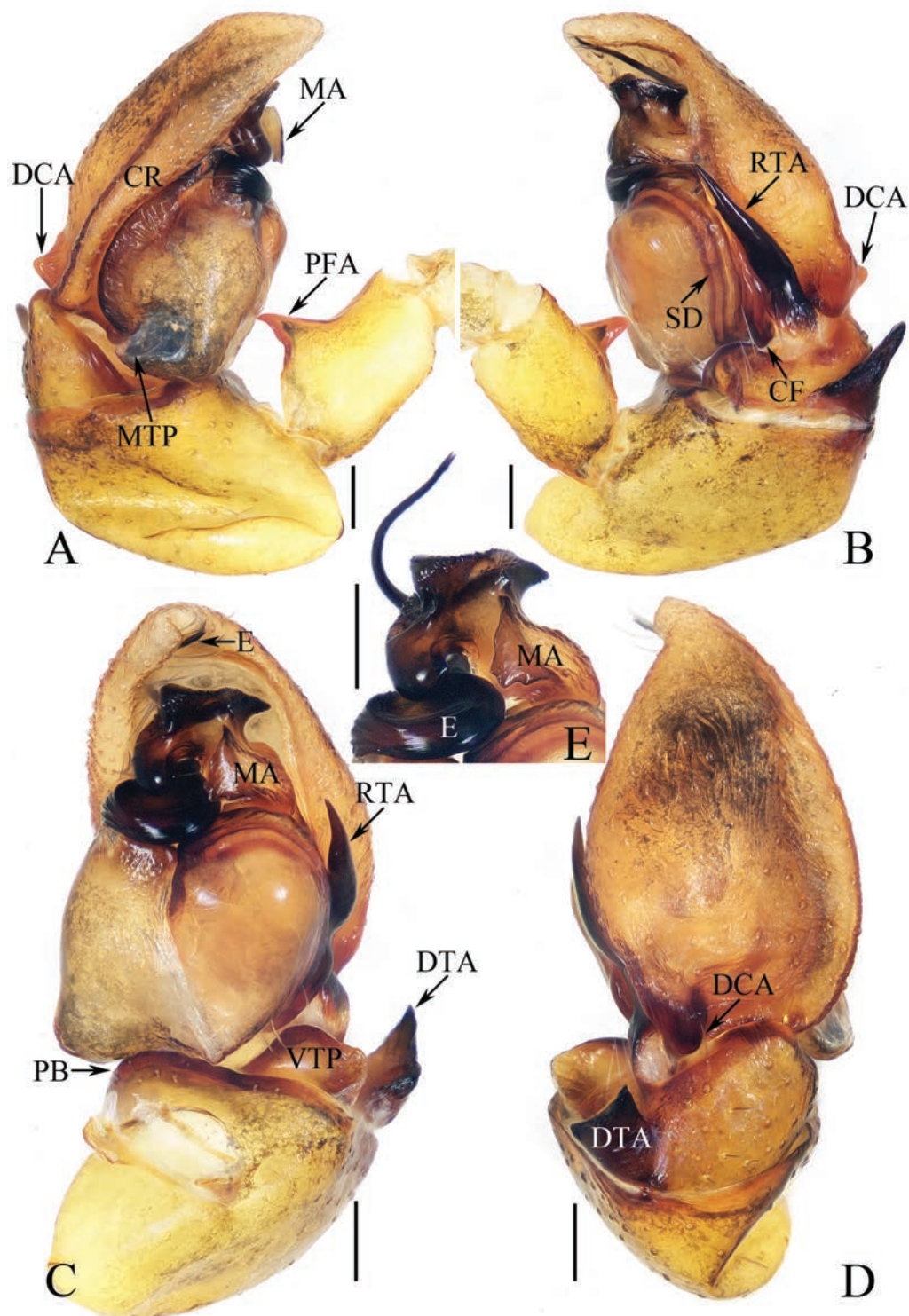


**Figure 39.** Male palp of *Synagelides zilongi* sp. nov. **A–D** holotype and **E** paratype (TRU-JS 0803) **A** prolateral **B** retrolateral **C** ventral **D** dorsal **E** embolus and median apophysis, ventral. Abbreviations: CF cymbial flange; CR prolateral cymbial ridge; DCA dorsal cymbial apophysis; DTA dorsal tibial apophysis; E embolus; MA median apophysis; MTP membranous tegular peak; PB patellar bump of male palp; PFA prolateral femoral apophysis; RTA retrolateral tibial apophysis; SD spermatheca; VTP ventral tibial process. Scale bars: 0.1 mm.

glands (AG); spermathecae (S) elongate-oval, touching each other, ~ 1.8× longer than wide.

**Distribution.** Known only from the type locality in Yunnan, China (Fig. 48).

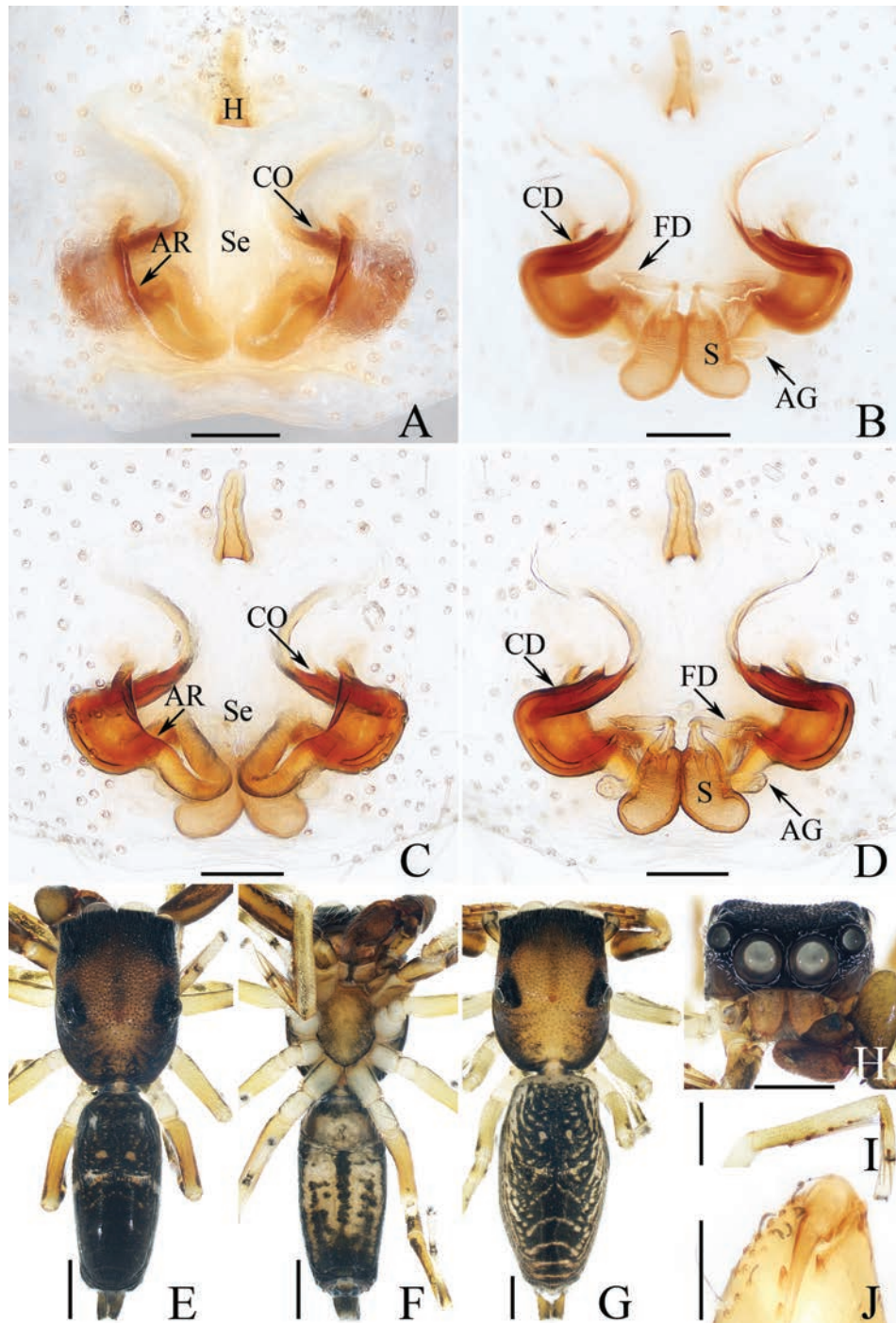


**Figure 40.** *Synagelides zilongi* sp. nov. **E, F, H–J** male holotype and **A–D, G** female paratype (TRU-JS 0804) **A, C** epigyne, ventral **B, D** vulva, dorsal **E, G** habitus, dorsal **F** ditto, ventral **H** carapace, frontal **I** tibia and metatarsi I, prolateral **J** chelicera, ventral. Abbreviations: AG accessory gland; AR atrial ridge; CD copulatory duct; CO copulatory opening; FD fertilization duct; H epigynal hood; S spermatheca; Se septum. Scale bars: 0.1 mm (**A–D, J**); 0.5 mm (**E–I**).

### Genus *Yaginumaella* Prószyński, 1979

**Type species.** *Pellenes ususudi* Yaginuma, 1972; type locality Hidaka District, Hokkaido, Japan.

**Comments.** *Yaginumaella*, a member of Plexippini (Maddison 2015), is represented by 17 species restricted in east, south, and southeast Asia (WSC 2024).

The genus is relatively poorly studied because it has never been widely revised, and more than 35% of species are known only from a single sex (WSC 2024). Moreover, the relationship between the genus and *Ptocasius* Simon, 1885 remains controversial, and thus the generic position of many related species cannot be ultimately confirmed (Logunov 2024; Wang et al. 2024).

***Yaginumaella dawuishan* sp. nov.**

<https://zoobank.org/06D6603D-1E63-4D32-91A7-05A9AEE538A8>

Figs 41, 42, 47

**Type material. Holotype** ♂ (TRU-JS 0806), CHINA: • Yunnan Province, Pingbian Miao Autonomous County, Daweishan National Nature Reserve (22°54.81'N, 103°42.02'E, ca 2040 m), 15.V.2024, C. Wang et al. leg. **Paratypes** • 2 ♂ 6 ♀ (TRU-JS 0807–0814), same data as for holotype.

**Etymology.** The specific name refers to type locality; noun (name) in apposition.

**Diagnosis.** *Yaginumaella dawuishan* sp. nov. resembles that of *Y. ususudi* (Yaginuma, 1972) in the general shape of copulatory organs, but can be distinguished by the following: 1) embolus (E) slightly curved, and with terminal broadened part (Fig. 41B) vs curved into a C-shape and without similar broadened part (Bohdanowicz and Prószyński 1987: fig. 307); 2) retrolateral tibial apophysis (RTA) tapered into a pointed tip in retrolateral view (Fig. 41C) vs almost equal in width from the base to the distal portion, and with a blunt tip (Bohdanowicz and Prószyński 1987: fig. 308); 3) epigynal hood (H) slightly longer than wide (Fig. 42A) vs > 2.5× wider than long (Bohdanowicz and Prószyński 1987: fig. 309).

**Description. Male** (Figs 41, 42C, D, F, G). Total length 4.46. Carapace 2.18 long, 1.75 wide. Abdomen 2.39 long, 1.36 wide. Eye sizes and interdistances: AME 0.51, ALE 0.30, PLE 0.28, AERW 1.59, PERW 1.54, EFL 0.98. Legs: I 4.76 (1.55, 0.83, 0.88, 0.90, 0.60), II 4.20 (1.25, 0.70, 1.00, 0.75, 0.50), III 4.82 (1.50, 0.63, 1.08, 1.08, 0.53), IV 5.02 (1.55, 0.63, 1.13, 1.18, 0.53). Carapace sub-square, with pair of bilateral pale setal bands and pair of longitudinal, dark brown stripes separated by central pale-yellow stripe on thoracic part. Legs pale except legs I darker, with three and two pairs of ventral spines on tibiae and metatarsi I. Dorsum of abdomen dark brown, with longitudinal, central pale band bearing sparse sliver spots, followed by several arc-shaped transverse pale stripes; venter pale, with central, longitudinal, irregular dark patch.

**Palp** (Fig. 41A–C): femur length/width ratio ca 3.4; patella ~ 1.4× longer than wide in retrolateral view; tibia as long as retrolateral tibial apophysis (RTA); retrolateral tibial apophysis tapering to pointed tip directed anteriorly; cymbium ~ 1.6× longer than wide; tegulum ca 1.5× longer than wide, with posteriorly extended posterior lobe (PL); embolus (E) originating at ca 9 o'clock position, slightly curved, and terminating at 12 o'clock position, with broadened terminal part.

**Female** (Fig. 42A, B, E). Total length 4.63. Carapace 1.77 long, 1.40 wide. Abdomen 2.80 long, 1.97 wide. Eye sizes and interdistances: AME 0.47, ALE 0.23, PLE 0.20, AERW 1.30, PERW 1.25, EFL 0.90. Legs: I 4.23 (1.30, 0.75, 1.00, 0.70, 0.48), II 3.94 (1.20, 0.68, 0.93, 0.65, 0.48), III 4.84 (1.50, 0.68, 1.05, 1.08, 0.53), IV 5.02 (1.55, 0.63, 1.13, 1.18, 0.53). Habitus (Fig. 42E) similar to that of male except darker.

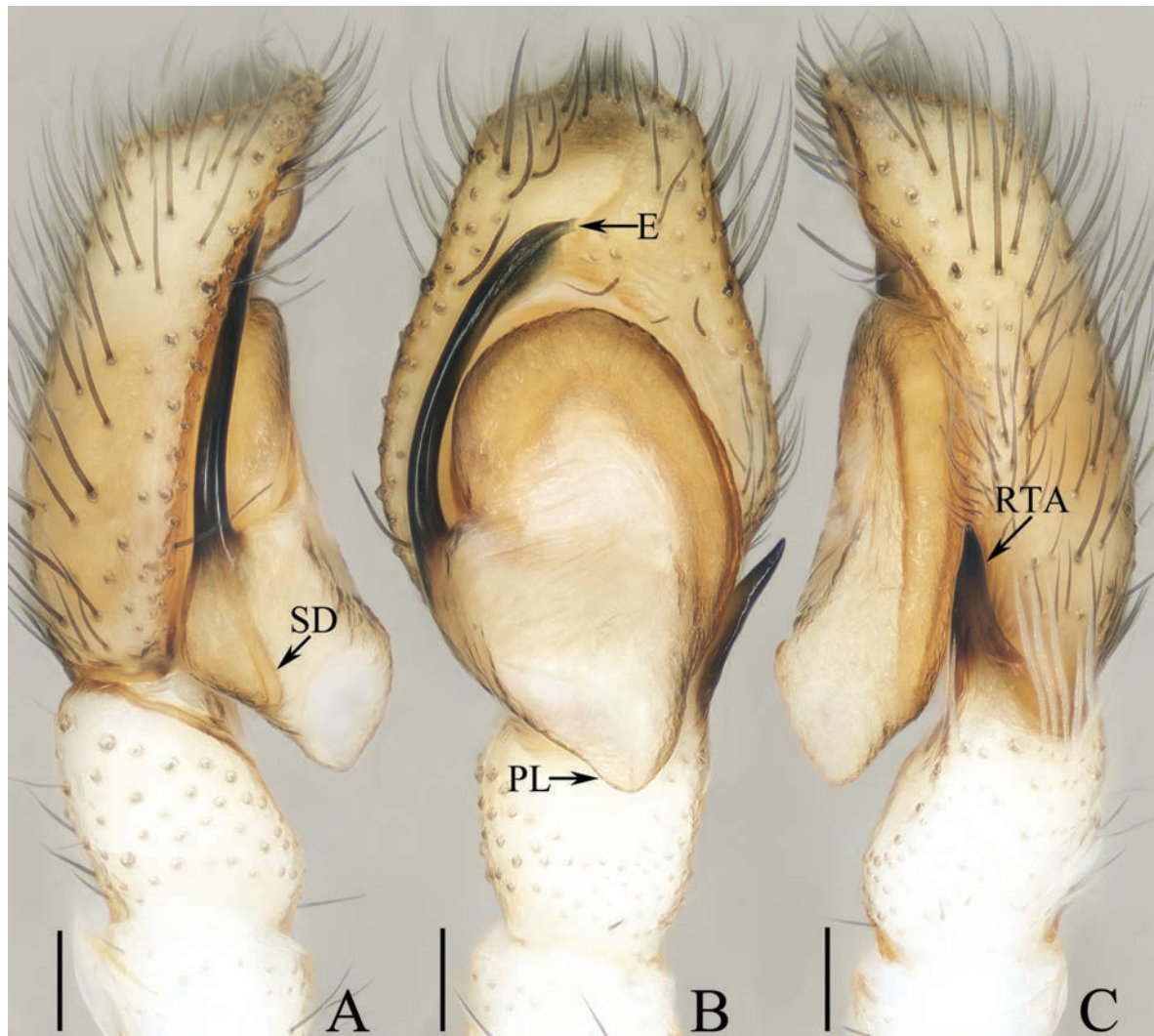


**Figure 41.** Male palp of *Yaginumaella daweishan* sp. nov., holotype **A** prolateral **B** ventral **C** retrolateral. Abbreviations: E embolus; PL posterior tegular lobe; RTA retrolateral tibial apophysis; SD sperm duct. Scale bars: 0.1 mm.

**Epigyne** (Fig. 42A, B) approximately as long as wide, with pair of hoods (H) posteriorly to copulatory openings (CO), and  $\sim 1.5\times$  longer than wide; atrium (At) oval, located anteriorly; copulatory ducts (CD) broad, forming complicated path; spermathecae (S) almost oval.

**Distribution.** Known only from the type locality in Yunnan, China (Fig. 47).

***Yaginumaella moinba* sp. nov.**

<https://zoobank.org/0706CACB-A27D-4E22-A3C9-DEA584C425BB>

Figs 43, 44, 47

**Type material. Holotype** ♂ (TRU-JS 0815), CHINA: • Xizang Autonomous Region, Medog County, Beibeng Township, Deergong Village, Yarlung Zangbo National Nature Reserve (29°10.84'N, 95°8.67'E, ca 1670 m), 25.V.2024, X.Q. Mi et al. leg.

**Paratypes** • 2 ♂ 1 ♀ (TRU-JS 0816–0818), same data as for holotype.

**Etymology.** The specific name is after the Mionba ethnic group, one of the two significant national minorities in Medog; noun in apposition.

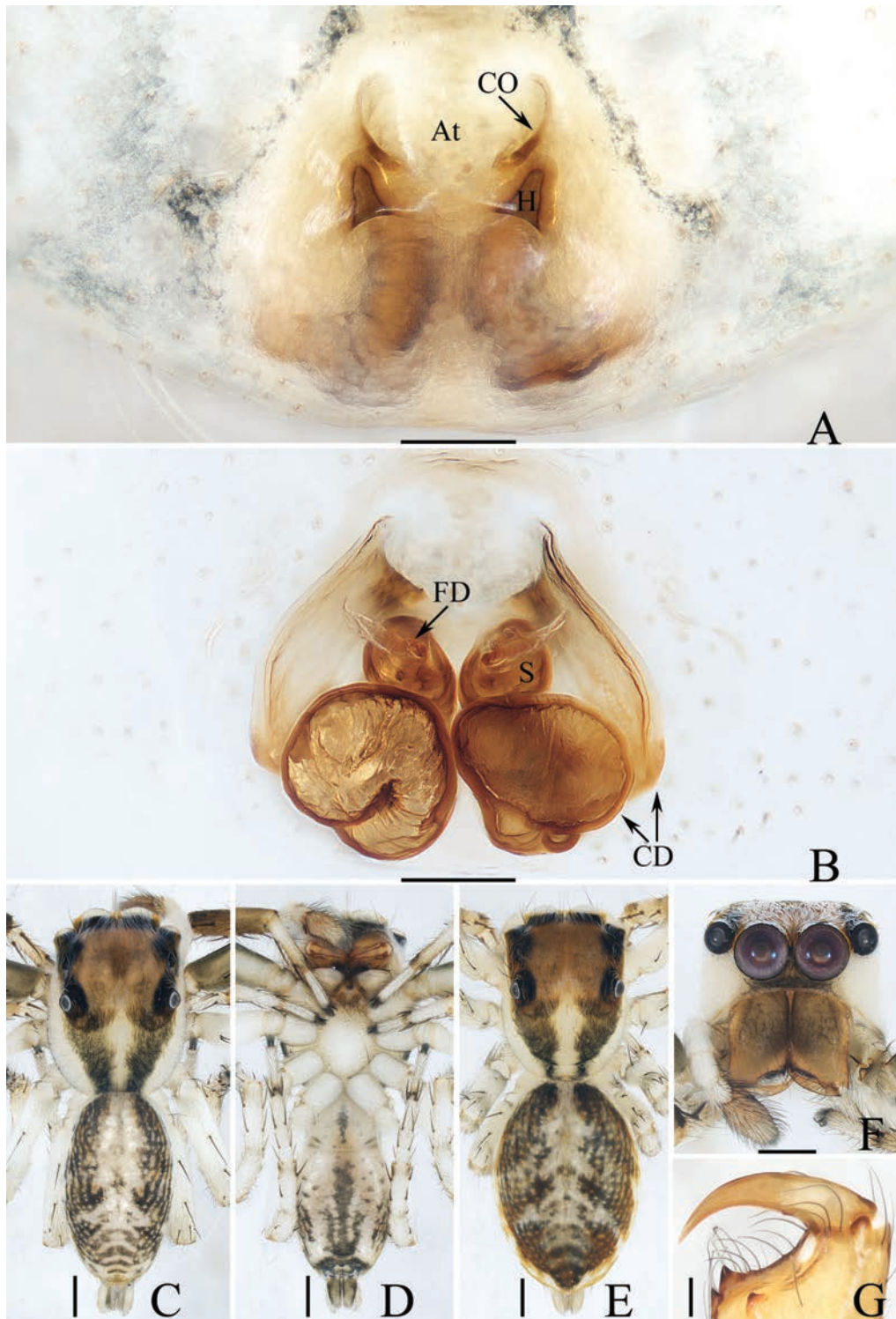


**Figure 42.** *Yaginumaella daweshan* sp. nov. **C, D, F, G** male holotype and **A, B, E** female paratype (TRU-JS 0809) **A** epigyne, ventral **B** vulva, dorsal **C, E** habitus, dorsal **D** ditto, ventral **F** carapace, frontal **G** chelicera, posterior. Abbreviations: At atrium; CD copulatory duct; CO copulatory opening; FD fertilization duct; H epigynal hood; S spermatheca. Scale bars: 0.1 mm (**A, B, G**); 0.5 mm (**C–F**).

**Diagnosis.** The male of *Yaginumaella moinba* sp. nov. resembles that of *Y. curvata* Li, Liu & Peng, 2024 in the general shape of palpal structure, but can be distinguished by the following: 1) embolus arising at ca 8:30 o'clock position (Fig. 43A, B) vs ca 6:30 o'clock position (Li et al. 2024: fig. 4A); 2) retrolateral

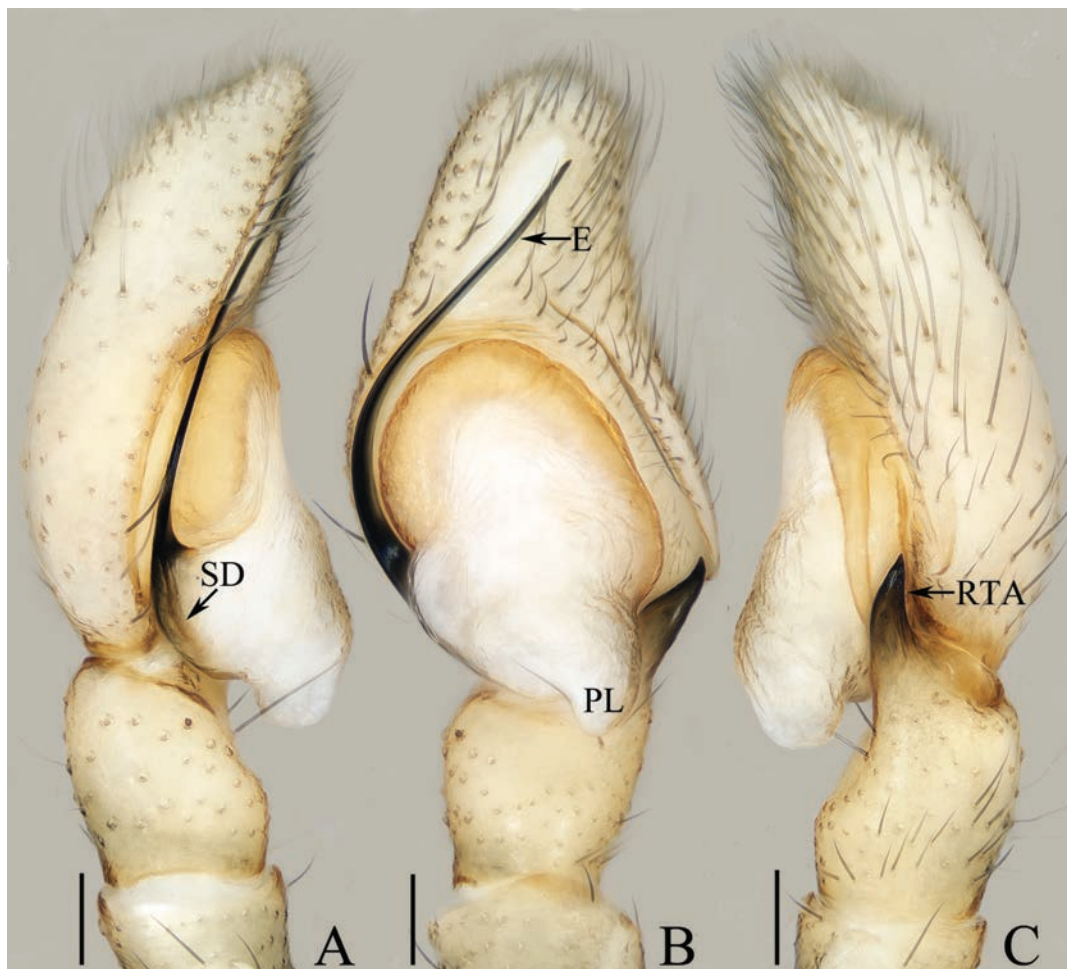


**Figure 43.** Male palp of *Yaginumaella moinba* sp. nov., holotype **A** prolateral **B** ventral **C** retrolateral. Abbreviations: E embolus; PL posterior tegular lobe; RTA retrolateral tibial apophysis; SD sperm duct. Scale bars: 0.1 mm.

tibial apophysis (RTA) apically directed towards ca 12:30 o'clock position in retrolateral view (Fig. 43C) vs ca 1:30 o'clock (Li et al. 2024: fig. 4B). The female of this species resembles that of *Y. pingbian* sp. nov. in having anterolaterally located, bell-shaped epigynal hood (H), but can be easily distinguished by the copulatory ducts, which are extending into an approximate S-shape (Fig. 44B–D) vs extending into approximate L-shape at beginning (Fig. 46B).

**Description. Male** (Figs 43, 44E, F, H, I). Total length 3.94. Carapace 1.94 long, 1.54 wide. Abdomen 2.00 long, 1.23 wide. Eye sizes and interdistances: AME 0.46, ALE 0.24, PLE 0.20, AERW 1.36, PERW 1.29, EFL 0.89. Legs: I 4.18 (1.20, 0.68, 1.10, 0.70, 0.50), II 3.86 (1.20, 0.63, 0.95, 0.63, 0.45), III 4.39 (1.28, 0.63, 1.03, 0.95, 0.50), IV 4.59 (1.28, 0.55, 1.13, 1.13, 0.50). Carapace pale yellow except baso-lateral part of face and area behind AMEs brown. Legs pale yellow, with dark brown patches on femora I, and three and two pairs of ventral spines on tibiae and metatarsi I. Dorsum of abdomen with irregular green-brown patches and sliver spots; venter grey centrally and covered with dense sliver spots laterally.

**Palp** (Fig. 43A–C): femur length/width ratio ca 3.5; patella ~ 1.45× longer than tibia; tibia ~ 1.3× longer than wide in retrolateral view, with tapered retrolateral apophysis (RTA) shorter than tibia, slightly curved medially and pointed apically; cymbium ~ 1.5× longer than wide in ventral view; tegulum almost oval, slightly swollen medio-posteriorly, with tapered, somewhat curved posterior

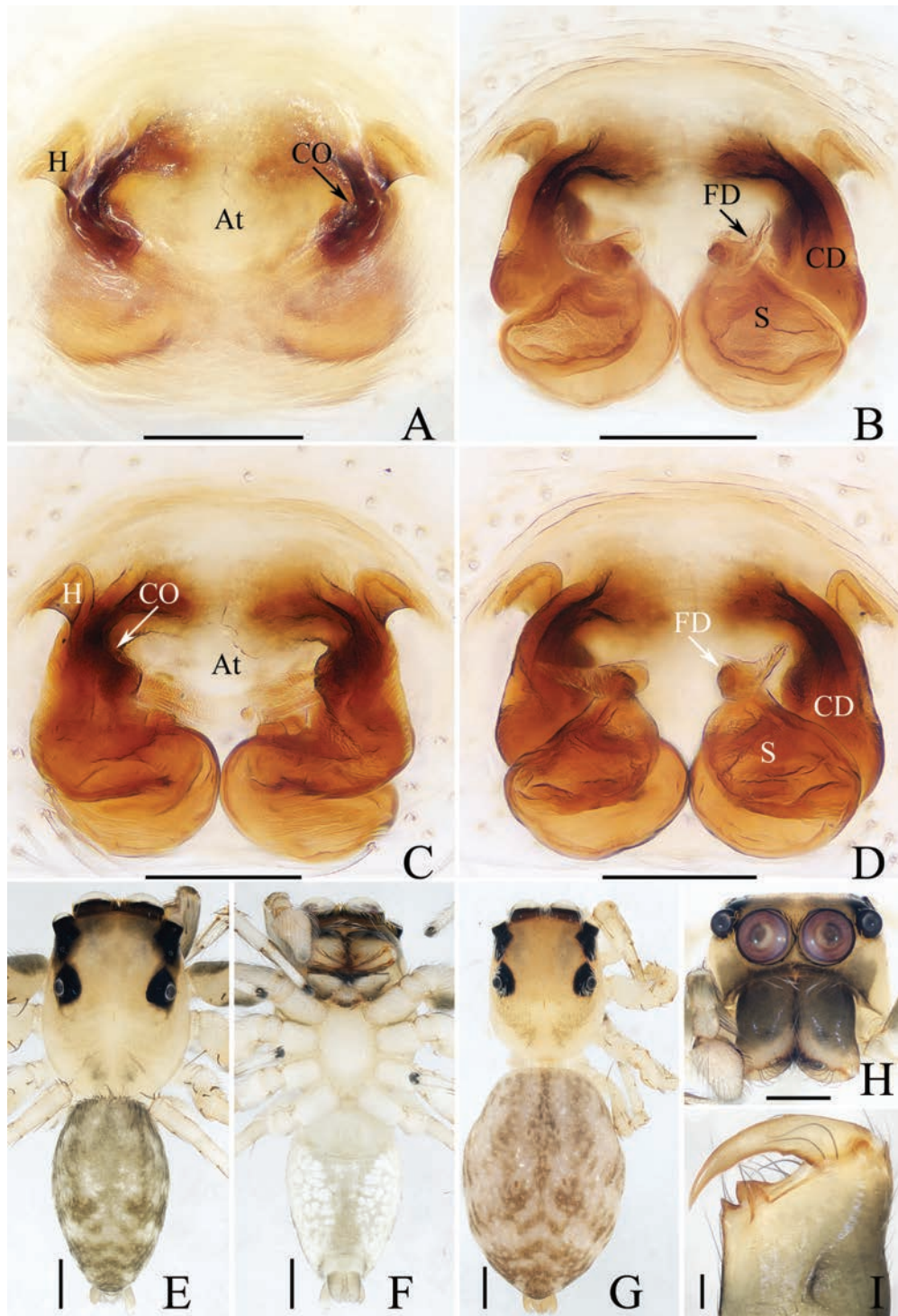


**Figure 44.** *Yaginumaella moinba* sp. nov. **E, F, H, I** male holotype and **A–D, G** female paratype (TRU-JS 0818) **A, C** epigyne, ventral **B, D** vulva, dorsal **E, G** habitus, dorsal **F** ditto, ventral **H** carapace, frontal **I** chelicera, posterior. Abbreviations: At atrium; CD copulatory duct; CO copulatory opening; FD fertilization duct; H epigynal hood; S spermatheca. Scale bars: 0.1 mm (**A–D, I**); 0.5 mm (**E–H**).

lobe (PL); embolus (E) originating at ca 8:30 o'clock position, curved clockwise along the tegulum at anterior half, and terminating at ca 1 o'clock position.

**Female** (Fig. 44A–D, G). Total length 4.63. Carapace 1.77 long, 1.40 wide. Abdomen 2.80 long, 1.97 wide. Eye sizes and interdistances: AME 0.47, ALE 0.23, PLE 0.20, AERW 1.30, PERW 1.25, EFL 0.90. Legs: I 3.23 (0.90, 0.65, 0.75,

0.50, 0.43), II 3.07 (0.88, 0.60, 0.68, 0.48, 0.43), III 3.66 (1.08, 0.60, 0.75, 0.75, 0.48), IV 3.86 (1.13, 0.55, 0.85, 0.85, 0.48). Habitus (Fig. 44G) similar to that of male except dorsum of abdomen brown.

**Epigyne** (Fig. 44A–D) ~ 1.3× wider than long, with pair of anterior hoods (H) lateral to transversely oval atrium (At) and copulatory openings (CO); copulatory ducts (CD) curved into ca S-shape; spermathecae (S) oval, separated from each other by ~ 1/4 of their width.

**Distribution.** Known only from the type locality in Xizang, China (Fig. 47).

***Yaginumaella pingbian* sp. nov.**

<https://zoobank.org/5A9A8D0B-A854-402D-AFC6-5D3045DC751B>

Figs 45, 46, 47

**Type material.** **Holotype** ♂ (TRU-JS 0819), CHINA: • Yunnan Province, Pingbian Miao Autonomous County, Daweishan National Nature Reserve (22°54.81'N, 103°42.02'E, ca 2040 m), 15.V.2024, C. Wang et al. leg. **Paratypes** • 3 ♀ (TRU-JS 0820–0822), same data as for holotype.

**Etymology.** The species name refers to the type locality: Pingbian Miao Autonomous County; noun in apposition.

**Diagnosis.** *Yaginumaella pingbian* sp. nov. resembles that of *Y. erlang* Wang, Mi & Li, 2024 in its habitus and general shape of copulatory organs, but can be easily distinguished by the following: 1) male palpal tibia approximately~ as long as wide in retrolateral view (Fig. 45C) vs wider than long (Wang et al. 2024: fig. 20C); 2) central longitudinal band on thoracic part in male ~ 1/4 of carapace width (Fig. 46C) vs < 1/5 (Wang et al. 2024: fig. 21C); 3) epigynal hood

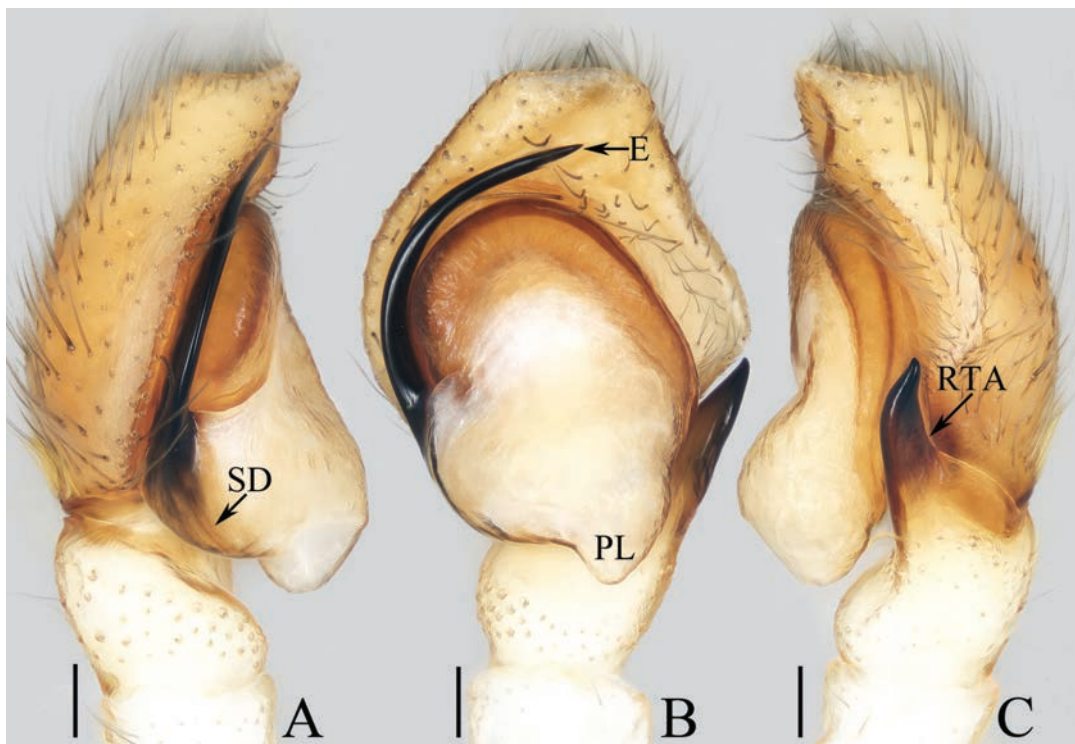


**Figure 45.** Male palp of *Yaginumaella pingbian* sp. nov., holotype **A** prolateral **B** ventral **C** retrolateral. Abbreviations: E embolus; PL posterior tegular lobe; RTA retrolateral tibial apophysis; SD sperm duct. Scale bars: 0.1 mm.

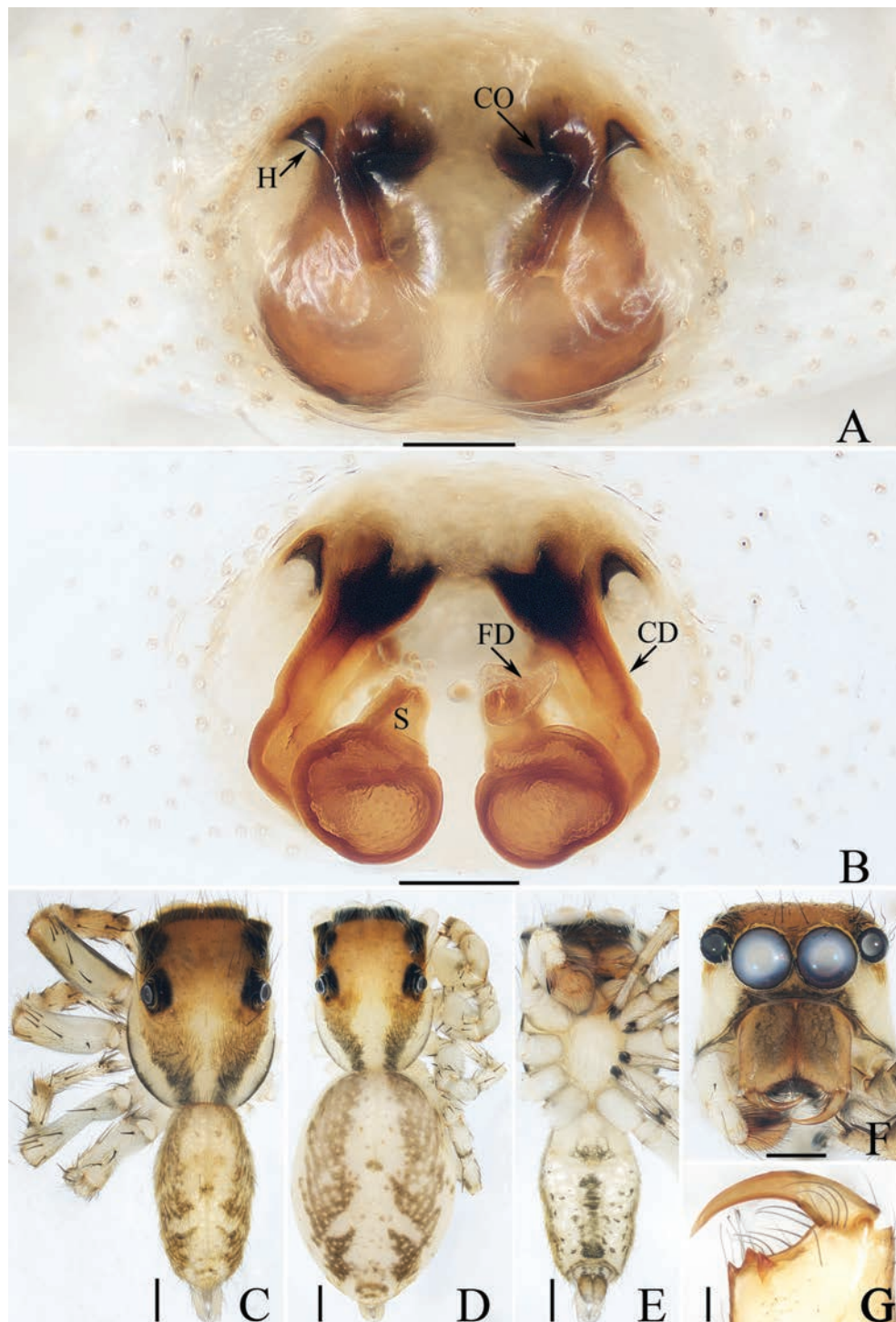


**Figure 46.** *Yaginumaella pingbian* sp. nov. **C, E–G** male holotype and **A, B, D** female paratype (TRU-JS 0820) **A** epigyne, ventral **B** vulva, dorsal **C, D** habitus, dorsal **E** ditto, ventral **F** carapace, frontal **G** chelicera, posterior. Abbreviations: CD copulatory duct; CO copulatory opening; FD fertilization duct; H epigynal hood; S spermatheca. Scale bars: 0.1 mm (**A, B, G**); 0.5 mm (**C–F**).

(H) strongly sclerotized, opened towards 6: 30 o'clock position (Fig. 46A) vs weakly sclerotized, opened towards ca 7:30 o'clock position (Wang et al. 2024: fig. 21A). The female also somewhat resembles that of *Y. moinba* sp. nov., but can be easily distinguished by the copulatory ducts (CO), which are extending into L-shape at beginning (Fig. 46B) vs approximately S-shape (Fig. 44B–D).

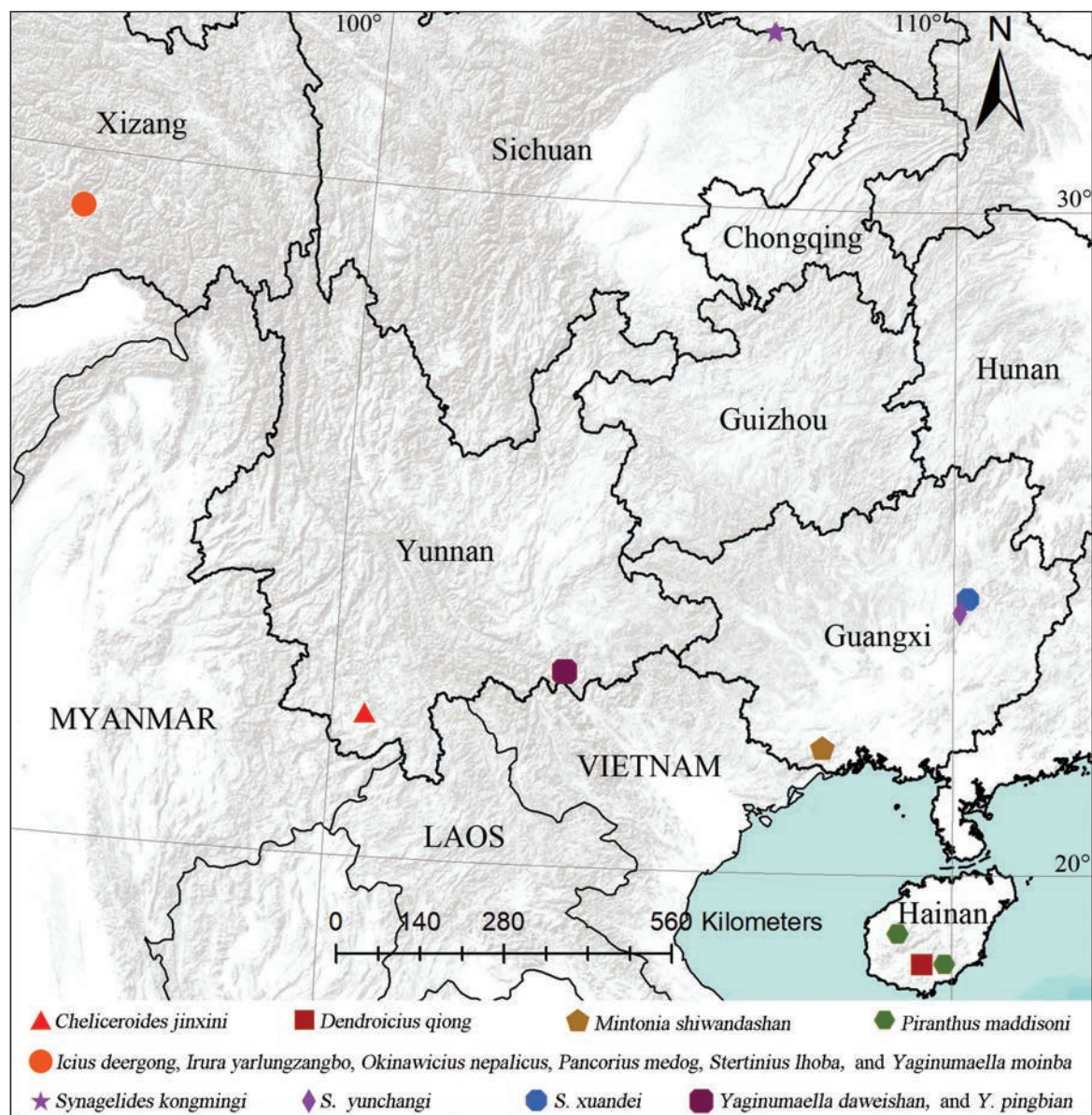


**Figure 47.** Distributional records of *Cheliceroides jinxini* sp. nov., *Dendroicius qiong* sp. nov., *Icius deergong* sp. nov., *I. yarlungzangbo* sp. nov., *Mintonia shiwandashan* sp. nov., *Okinawicius nepalicus* (Andreeva, Hęciak & Prószyński, 1984), *Pancorius medog* sp. nov., *Piranthus maddisoni* sp. nov., *Stertinius lhoba* sp. nov., *Synagelides kongmingi* sp. nov., *S. yunchangi* sp. nov., *S. xuandei* sp. nov., *Yaginumaella daweshan* sp. nov., *Y. moinba* sp. nov., and *Y. pingbian* sp. nov.

**Description. Male** (Figs 45, 46C, E–G). Total length 4.37. Carapace 2.31 long, 1.76 wide. Abdomen 2.20 long, 1.19 wide. Eye sizes and interdistances: AME 0.52, ALE 0.30, PLE 0.28, AERW 1.63, PERW 1.56, EFL 0.98. Legs: I 4.79 (1.50, 0.78, 1.13, 0.85, 0.53), II 4.26 (1.30, 0.75, 0.95, 0.73, 0.53), III 4.56 (1.43, 0.70, 1.00, 0.95, 0.48), IV 5.08 (1.50, 0.65, 1.18, 1.20, 0.55). Carapace mainly orange-yellow, covered with dark and golden setae, with pair of lateral pale bands bearing pale setae and longitudinal, central pale stripe extending across thoracic part. Legs pale, mingled with orange-brown, with lateral dark brown stripes on femora I, and three and two pairs of ventral spines on tibiae and metatarsi I. Dorsum of abdomen brown, with longitudinal, central, broad pale band extending across whole surface and bifurcated at posterior 1/3; venter pale, with longitudinal, central inconsecutive green-brown stripes.

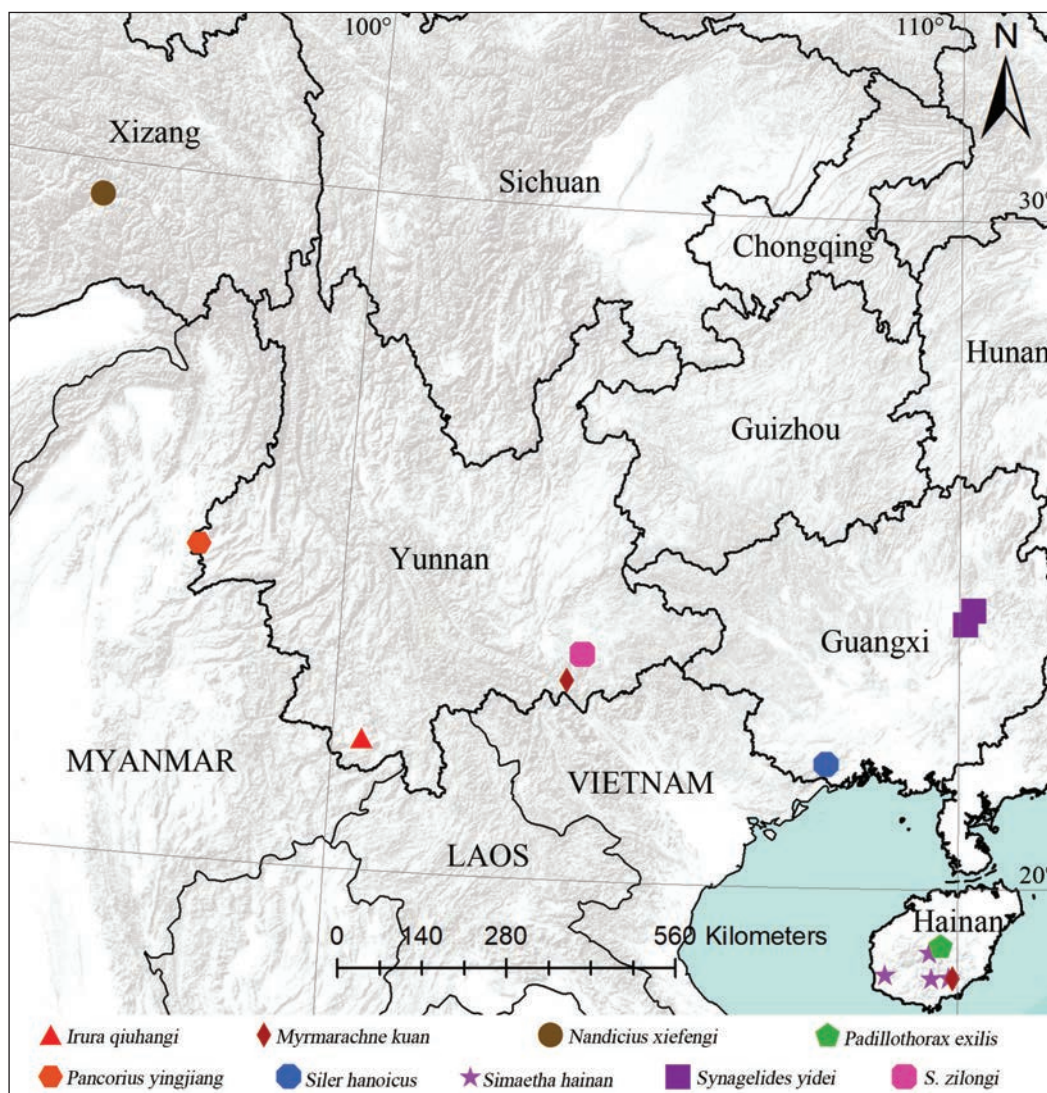


**Figure 48.** Distributional records of *Irura qiuhangi* sp. nov., *Myrmarachne kuan* sp. nov., *Nandicius xiefengi* sp. nov., *Padillothorax exilis* (Cao & Li, 2016), *Pancorius yingjiang* sp. nov., *Siler hanoicus* Prószyński, 1985, *Simaetha hainan* sp. nov., *Synagelides yidei* sp. nov., and *S. zilongi* sp. nov.

**Palp** (Fig. 45A–C): femur length/width ratio ca 3.0; patella ~ 1.15× longer than wide in retrolateral view; tibia almost as long as wide in retrolateral view; retrolateral tibial apophysis (RTA) tapered, longer than tibia, curved distally into pointed tip; cymbium ca 1.2× longer than wide, with almost horizontal tip; tegulum nearly oval, with posteriorly extending posterior lobe (PL), embolus (E) originating at ca 8:30 o’clock position of bub, curved into C-shape.

**Female** (Fig. 46A, B, D). Total length 5.32. Carapace 2.20 long, 1.64 wide. Abdomen 3.24 long, 2.28 wide. Eye sizes and interdistances: AME 0.52, ALE 0.32, PLE 0.28, AERW 1.60, PERW 1.56, EFL 1.04. Legs: I 4.18 (1.25, 0.75, 1.00, 0.68, 0.50), II 3.94 (1.25, 0.70, 0.88, 0.63, 0.48), III 4.89 (1.58, 0.75, 0.93, 1.03, 0.60), IV 5.22 (1.58, 0.70, 1.18, 1.18, 0.58). Habitus (Fig. 46D) similar to that of male.

**Epigyne** (Fig. 46A, B) ~ 1.3× wider than long, with pair of sub-triangular, anterior hoods (H) lateral to copulatory openings (CO); copulatory ducts (CD) run into L-shape at beginning, and with complex distal curves; spermathecae (S) without distinct border.

**Distribution.** Known only from the type locality in Yunnan, China (Fig. 47).

## Acknowledgments

The manuscript benefited greatly from comments by Yuri M. Marusik (Magadan, Russia), Wayne Maddison (Vancouver, Canada), Dmitri V. Logunov (St Petersburg, Russia), and Galina N. Azarkina (Novosibirsk, Russia). Danni Sherwood (London, UK) and Nathalie Yonow (Wales, UK) checked the English and made other comments in the final draft. Guo Tang (late), Guo Zheng (Shenyang), E-Feng Li (Guiyang), Ai-Lan He (Shaoguan), Jin-Xin Liu (Changsha), Zong-Guang Huang (Changsha), Rong-Rong Liao (Changsha), Yun Liang (Changsha), Yu Hui (Changsha), Qin Li (Changsha), Xue-Mei Yang (Changsha), Yin-Li Wen (Changsha), Zhao Ye (Changsha), Yang Liu (Changsha), Hang Qiu (Kunming), Shi-Kai Li (Tongren), Xu-Fei Zhu (Tongren), Zhong-Jie Pan (Tongren) and Xie-Feng Wang (Tongren) helped with fieldwork.

## Additional information

### Conflict of interest

The authors have declared that no competing interests exist.

### Ethical statement

No ethical statement was reported.

### Funding

This research was supported by the Science & Technology Fundamental Resources Investigation Program of China (2023FY100200), the National Natural Science Foundation of China (NSFC 32200369, 32070429, 31471963), the Animal Resources Survey Project of Hainan Tropic Rainforest National Park, the Scientific Monitoring of Yarlung Zangbo Grand Canyon National Nature Reserve, Project the Open Project of Ministry of Education Key Laboratory for Ecology of Tropic Islands, Hainan Normal University, China (HNSF-OP-202201, HNSF-OP-2024-1), the Doctoral Research Foundation of Tongren University (trxyDH2102), and the high-level innovative talent training project of Guizhou Province (2024-(2022)-050).

### Author contributions

SL designed the study. CW, XM, SL, XX performed morphological species identification. CW finished the species descriptions and took the photos. CW, XM, and SL drafted and revised the manuscript. All authors read and approved the final version of the manuscript.

### Author ORCIDs

Cheng Wang  <https://orcid.org/0000-0003-1831-0579>

Xiaoqi Mi  <https://orcid.org/0000-0003-1744-3855>

Shuqiang Li  <https://orcid.org/0000-0002-3290-5416>

Xiang Xu  <https://orcid.org/0000-0001-9485-5373>

### Data availability

All of the data that support the findings of this study are available in the main text.

## References

Andreeva EM, Hęciak S, Prószyński J (1984) Remarks on *Icius* and *Pseudicius* (Araneae, Salticidae) mainly from central Asia. *Annales Zoologici, Warszawa* 37: 349–375.

- Asima A, Caleb JTD, Prasad G (2024) On a collection of jumping spiders (Araneae: Salticidae) from the Shendurney Wildlife Sanctuary, India. *European Journal of Taxonomy* 932: 252–270. <https://doi.org/10.5852/ejt.2024.932.2531>
- Bohdanowicz A, Prószyński J (1987) Systematic studies on East Palaearctic Salticidae (Araneae), IV. Salticidae of Japan. *Annales Zoologici, Warszawa* 41: 43–151.
- Caleb JTD (2023) Deciphering mysteries: on the identity of five enigmatic jumping spiders from northeast India, China and Philippines (Araneae, Salticidae). *Zootaxa* 5230(3): 391–400. <https://doi.org/10.11646/zootaxa.5230.3.8>
- Cao Q, Li S, Žabka M (2016) The jumping spiders from Xishuangbanna, Yunnan, China (Araneae, Salticidae). *ZooKeys* 630: 43–104. <https://doi.org/10.3897/zookeys.630.8466>
- Gan JH, Wang C, Peng XJ (2017) Three new spider species of *Irura* Peckham & Peckham, 1901 from China (Araneae: Salticidae). *Zootaxa* 4226(2): 273–282. <https://doi.org/10.11646/zootaxa.4226.2.7>
- Hu JL (2001) Spiders in Qinghai-Tibet Plateau of China. Henan Science and Technology Publishing House, 658 pp.
- ICZN (1999) International Code of Zoological Nomenclature. 4<sup>th</sup> edn. The International Trust for Zoological Nomenclature. London, UK, 305 pp.
- Li S (2020) Spider taxonomy for an advanced China. *Zoological Systematics* 45(2): 73–77. <https://doi.org/10.11865/zs.202011>
- Li SL, Liu P, Peng XJ (2024) Three new species of jumping spiders (Araneae, Salticidae) from Hunan, China. *ZooKeys* 1204: 301–312. <https://doi.org/10.3897/zookeys.1204.122887>
- Lin YJ, Li S (2020) Two new genera and eight new species of jumping spiders (Araneae, Salticidae) from Xishuangbanna, Yunnan, China. *ZooKeys* 952: 95–128. <https://doi.org/10.3897/zookeys.952.51849>
- Lin L, Yang ZY, Zhang JX (2024a) Revalidation of the jumping spider genus *Cheliceroidea* Žabka, 1985 based on molecular and morphological data (Araneae, Salticidae). *ZooKeys* 1196: 243–253. <https://doi.org/10.3897/zookeys.1196.117921>
- Lin YJ, Li S, Mo HL, Wang XH (2024b) Thirty-eight spider species (Arachnida: Araneae) from China, Indonesia, Japan and Vietnam. *Zoological Systematics* 49(1): 4–98. <https://doi.org/10.11865/zs.2024101>
- Logunov DV (2021) Jumping spiders (Araneae: Salticidae) of the Na Hang Nature Reserve, Tuyen Quang Province, Vietnam. *Arachnology* 18(9): 1021–1055. <https://doi.org/10.13156/arac.2021.18.9.1021>
- Logunov DV (2024) Jumping spiders (Araneae: Salticidae) of the Bidoup Nui Ba National Park, Lam Dong Province, Vietnam. *Arachnology* 19(8): 1074–1099. <https://doi.org/10.13156/arac.2024.19.8.1074>
- Lu Y, Chu C, Zhang XQ, Li S, Yao ZY (2022) Europe vs. China: *Pholcus* (Araneae, Pholcidae) from Yanshan-Taihang Mountains confirms uneven distribution of spiders in Eurasia. *Zoological Research* 43(4): 532–534. <https://doi.org/10.24272/j.issn.2095-8137.2022.103>
- Luo YF, Li S (2024) Indian monsoon drove the dispersal of the thoracica group of *Scytodes* spitting spiders. *Zoological Research* 45(1): 152–159. <https://doi.org/10.24272/j.issn.2095-8137.2023.364>
- Maddison WP (2015) A phylogenetic classification of jumping spiders (Araneae: Salticidae). *The Journal of Arachnology* 43(3): 231–292. <https://doi.org/10.1636/arac-43-03-231-292>
- Maddison WP, Szűts T (2019) Myrmarachnine jumping spiders of the new subtribe *Levieina* from Papua New Guinea (Araneae, Salticidae, Myrmarachnini). *ZooKeys* 842: 85–112. <https://doi.org/10.3897/zookeys.842.32970>

- Maddison WP, Beattie I, Marathe K, Ng PYC, Kanesharatnam N, Benjamin SP, Kunte K (2020) A phylogenetic and taxonomic review of baviine jumping spiders (Araneae, Salticidae, Baviini). *ZooKeys* 1004: 27–97. <https://doi.org/10.3897/zookeys.1004.57526>
- Metzner H (2024) Jumping spiders (Arachnida: Araneae: Salticidae) of the world. [Accessed 10 Jul. 2024] <https://www.jumping-spiders.com>
- Mi XQ, Wang C (2016) A new species of *Irura* Peckham & Peckham, 1901 (Araneae: Salticidae) from Yunnan Province, China. *Sichuan Journal of Zoology* 35(3): 400–403.
- Peng XJ (2020) *Fauna Sinica, Invertebrata* 53, Arachnida: Araneae: Salticidae. Science Press, Beijing, 612 pp.
- Peng XJ, Xie LP, Xiao XQ, Yin CM (1993) Salticids in China (Arachnida: Araneae). Hunan Normal University Press, 270 pp.
- Prószyński J (1987) Atlas rysunków diagnostycznych mniej znanych Salticidae 2. *Zeszyty Naukowe Wyższej Szkoły Rolniczo-Pedagogicznej, Siedlcach*, 172 pp.
- Prószyński J (1985) On *Siler*, *Silerella*, *Cyllobelus* and *Natta* (Araneae, Salticidae). *Annales Zoologici, Warszawa* 39: 69–85.
- Prószyński J (1992) Salticidae (Araneae) of India in the collection of the Hungarian National Natural History Museum in Budapest. *Annales Zoologici, Warszawa* 44: 165–277.
- Prószyński J (2016) Delimitation and description of 19 new genera, a subgenus and a species of Salticidae (Araneae) of the world. *Ecologica Montenegrina* 7: 4–32. <https://doi.org/10.37828/em.2016.7.1>
- Wang C, Li S (2021) On ten species of jumping spiders from Xishuangbanna, China (Araneae, Salticidae). *ZooKeys* 1062: 123–155. <https://doi.org/10.3897/zookeys.1062.72531>
- Wang C, Mi XQ, Irfan M, Peng XJ (2020) On eight species of the spider genus *Synagelides* Strand, 1906 from China (Araneae: Salticidae). *European Journal of Taxonomy* 724(1): 1–33. <https://doi.org/10.5852/ejt.2020.724.1153>
- Wang C, Mi XQ, Wang WH, Gan JH, Irfan M, Zhong Y, Peng XJ (2023). Notes on twenty-nine species of jumping spiders from South China (Araneae: Salticidae). *European Journal of Taxonomy* 902: 1–91. <https://doi.org/10.5852/ejt.2023.902.2319>
- Wang C, Mi XQ, Li S (2024) Eleven species of jumping spiders from Sichuan, Xizang, and Yunnan, China (Araneae, Salticidae). *ZooKeys* 1192: 141–178. <https://doi.org/10.3897/zookeys.1192.114589>
- Wanless FR (1987) Notes on spiders of the family Salticidae. 1. The genera *Spartaeus*, *Mintonia* and *Taraxella*. *Bulletin of the British Museum of Natural History (Zool.)* 52: 107–137. <https://doi.org/10.5962/p.18302>
- Wanless (1984) A review of the spider subfamily Spartaestinae nom. n. (Araneae: Salticidae) with descriptions of six new genera. *Bulletin of the British Museum of Natural History (Zool.)* 46: 135–205. <https://doi.org/10.5962/bhl.part.15964>
- World Spider Catalog (2024) World Spider Catalog. Version 25.0. Natural History Museum Bern, <http://wsc.nmbe.ch>. [accessed on 3 Jul.2024] <https://doi.org/10.24436/2>
- Yamasaki T, Ahmad AH (2013) Taxonomic study of the genus *Myrmarachne* of Borneo (Araneae: Salticidae). *Zootaxa* 3710: 501–556. <https://doi.org/10.11646/zootaxa.3710.6.1>
- Yamasaki T, Hashimoto Y, Endo T, Hyodo F, Itioka T, Meleng P (2018) New species of the ant-mimicking genus *Myrmarachne* MacLeay, 1839 (Araneae: Salticidae) from Sarawak, Borneo. *Zootaxa* 4521(3): 335–356. <https://doi.org/10.11646/zootaxa.4521.3.2>

- Yang ZY, Zhang JX (2024) On eight species of Chrysillini from Xizang, China (Araneae: Salticidae: Salticinae). *Zootaxa* 5447(2): 151–187. <https://doi.org/10.11646/zootaxa.5447.2.1>
- Yang ZZ, Zhu MS, Song DX (2007) Report of two new species of the genus *Synagelides* Strand, 1906 from China (Araneae: Salticidae). *Journal of Dali University* 6(2): 1–4.
- Yang ZY, Wang WH, Zhang JX (2024) On a new genus and seven species of Chrysillini from China (Araneae: Salticidae: Salticinae). *Zootaxa* 5477(2): 101–135. <https://doi.org/10.11646/zootaxa.5477.2.1>
- Żabka M (1985) Systematic and zoogeographic study on the family Salticidae (Araneae) from Vietnam. *Annales Zoologici, Warszawa* 39: 197–485.
- Żabka M (1994) Salticidae (Arachnida: Araneae) of Oriental, Australian and Pacific regions, X. Genus *Simaetha* Thorell. *Records of the Western Australian Museum* 16: 499–534.
- Zhang QQ, Li Y, Lin YC, Li S, Yao ZY, Zhang XQ (2023) Regression of East Tethys resulted in a center of biodiversity: A study of Mysmenidae spiders from the Gaoligong Mountains, China. *Zoological Research* 44(4): 737–738. <https://doi.org/10.24272/j.issn.2095-8137.2023.206>



# A new genus, *Sinodromus* gen. nov., with two new species and the first description of the female of *Philodromus guiyang* Long & Yu, 2022 (Arachnida, Araneae, Philodromidae) from China

Zhong-jing Wang<sup>1\*</sup>, Yan-bin Yao<sup>2\*</sup>, Zi-ying Tang<sup>1\*</sup>, Wen-hui Li<sup>1</sup>, Ke-ke Liu<sup>1</sup>, Xiang Xu<sup>3</sup>

1 College of Life Science, Jinggangshan University, Ji'an 343009, Jiangxi, China

2 Jinshan College of Fujian Agriculture and Forestry University, Fuzhou 350007, Fujian, China

3 College of Life Science, Hunan Normal University, Changsha 410081, Hunan, China

Corresponding authors: Ke-ke Liu ([kekeliu@jgsu.edu.cn](mailto:kekeliu@jgsu.edu.cn)); Xiang Xu ([xux@hunnu.edu.cn](mailto:xux@hunnu.edu.cn))

## Abstract

Three species of the spider family Philodromidae are reported from the south of China. A new genus, *Sinodromus* gen. nov., is described from Jiangxi, Fujian, and Hunan Provinces. It can be distinguished from other genera of Philodromidae by the tegular apophysis of the palp and the cymbial process, as well as by its uniquely striped abdomen. The type species, *S. fujianensis* sp. nov., and a second species, *S. perbrevis* sp. nov., are described and illustrated; these species occur in bamboo forests in hilly areas. Additionally, the female of *Philodromus guiyang* Long & Yu, 2022 is described for the first time from Jiangxi and Hunan Provinces. All species are illustrated with SEM micrographs, and their distributions are mapped.

**Key words:** Distribution, hilly land, running crab spiders, taxonomy



Academic editor: Sarah Crews

Received: 26 September 2024

Accepted: 21 November 2024

Published: 20 December 2024

ZooBank: <https://zoobank.org/7EE4D14C-4869-4130-ABF6-DF42B903476B>

Citation: Wang Z-jing, Yao Y-bin, Tang Z-ying, Li W-hui, Liu K-ke, Xu X (2024) A new genus, *Sinodromus* gen. nov., with two new species and the first description of the female of *Philodromus guiyang* Long & Yu, 2022 (Arachnida, Araneae, Philodromidae) from China. ZooKeys 1221: 279–296. <https://doi.org/10.3897/zookeys.1221.137930>

Copyright: © Zhong-jing Wang et al.  
This is an open access article distributed under terms of the Creative Commons Attribution License (Attribution 4.0 International – CC BY 4.0).

## Introduction

Philodromidae Thorell, 1870, commonly known as small running crab spiders, is a relatively small but globally distributed spider family consisting of 528 species in 29 genera (WSC 2024). They are free-living, agile spiders commonly found on plants or on the soil surface (Jocqué and Dippenaar-Schoeman 2006). Currently, 59 species in seven genera are recorded or described from China (Li 2020; WSC 2024). The majority of Chinese philodromid spiders have been reported from the Tibetan Plateau in the western part of the country, while other regions of China remain poorly studied (Li and Lin 2016). Thus, there are still many undescribed species of small running crab spiders in the northern and southern parts of China.

While examining philodromid spider material collected in the southern part of China, namely from Hunan, Jiangxi, and Fujian Provinces over the last 10 years, we discovered two undescribed species from one new genus and the first female of *Philodromus guiyang* Long & Yu, 2022. The present paper provides detailed descriptions of these three species.

\* These authors contributed equally to this work.

## Materials and methods

Specimens were examined using a Jiangnan SZ6100 stereomicroscope with a KUY NICE CCD camera. Male and female copulatory organs in this paper were dissected and examined in 80–85% ethanol. The endogynes were cleaned with pancreatin (Álvarez-Padilla and Hormiga 2007). All specimens were photographed with an Olympus CX43 compound microscope with a KUY NICE CCD camera. For SEM photographs, the specimens were dried under natural conditions, sprayed with gold with a small ion-sputtering apparatus (ETD-2000), or were uncoated, and then photographed with a Zeiss EVO LS15 scanning electron microscope.

All measurements were made using a stereomicroscope (AxioVision SE64 rel. 4.8.3) and are given in millimeters. Leg measurements are given as total length (femur, patella, tibia, metatarsus, tarsus).

Depositories of all specimens examined are abbreviated as:

**ASM-JGSU** Animal Specimen Museum, College of Life Science, Jinggangshan University, Ji'an, China.

**HNU** Hunan Normal University, Changsha, China.

Terminology of the male and female copulatory organs follows Kubcová (2004) and Kastrygina and Kovblyuk (2016). The abbreviations used in the text and figures are:

### Eyes

<b>ALE</b>	anterior lateral eye;
<b>AME</b>	anterior median eye;
<b>MOA</b>	median ocular area;
<b>PLE</b>	posterior lateral eye;
<b>PME</b>	posterior median eye.

### Male palp

<b>Con</b>	conductor;
<b>CP</b>	cymbial process;
<b>Em</b>	embolus;
<b>RTA</b>	retrolateral tibial apophysis;
<b>SD</b>	sperm duct;
<b>TA</b>	tegular apophysis;
<b>VTA</b>	ventro-prolateral tibial apophysis.

### Epigyne

<b>At</b>	atrium;
<b>CD</b>	copulatory duct;
<b>CO</b>	copulatory opening;
<b>ET</b>	epigynal tooth;
<b>FD</b>	fertilization duct;
<b>GA</b>	glandular appendage;

<b>GM</b>	glandular mound;
<b>MS</b>	median septum;
<b>Spe</b>	spermatheca.

## Taxonomy

### Family Philodromidae Thorell, 1870

Currently, approximately 43% of philodromid species are known from a single sex and juveniles: 167 of these were described from females, 39 from males, and 21 from juveniles (WSC 2024). There are seven genera reported in China: *Apollophanes* O. Pickard-Cambridge, 1898, *Philodromus* Walckenaer, 1826, *Pulchellodromus* Wunderlich, 2012, *Psellonus* Simon, 1897, *Rhysodromus* Schick, 1965, *Thanatus* C. L. Koch, 1837, and *Tibellus* Simon, 1875 (WSC 2024). Some of these are widely distributed in Asia, America, and Europe, such as *Apollophanes punctipes* (O. Pickard-Cambridge, 1891), *Philodromus emarginatus* (Schränk, 1803), *Pulchellodromus medius* (O. Pickard-Cambridge, 1872), *Rhysodromus alascensis* (Keyserling, 1884), *Thanatus arcticus* Thorell, 1872, and *Tibellus oblongus* (Walckenaer, 1802) (WSC 2024). Currently, 59 known species in those seven genera above have been reported from China (Li and Lin 2016; WSC 2024). Only three new species have been described from China in the past 10 years (WSC 2024).

### Genus *Philodromus* Walckenaer, 1826

#### *Philodromus guiyang* Long & Yu, 2022

Figs 1A–D, 2A–E, 8A, 9A, B

Common name: 贵阳逍遥蛛

*Philodromus guiyang* Long & Yu in Long et al. 2022: 118, figs 2A–D, 3A–D (holotype male from Guiyang, Guizhou Province, illustrations examined).

**Additional material examined. CHINA:** Jiangxi Province • 2♂, 5♀, Ji'an City, Jishui County, Dadong Mountain, 27°15'14.71"N, 115°10'50.50"E, 607 m a.s.l., 2 March 2023, K. Liu, Z. Jiang, Z. Deng, X. Chen leg. (20230302, Phi-07, ASM-JGSU) • 1♂, 1♀, Ji'an City, Jinggangshan County Level City, Ciping Town, Jingzhu Mountain, 26°32'45.20"N, 114°06'32.46"E, 1158 m a.s.l., 2 May 2024, Z. Jiang, Z. Wang leg. (20240502, Phi-07, ASM-JGSU) • 1♀, Ciping Town, Huangyangjie Scenic Spot, 26°37'30.33"N, 114°7'8"E, 1384 m a.s.l., 13 August 2024, L. Luo, Y. Yao, Z. Wang leg. (20240813, Phi-07, ASM-JGSU), other data same as previous • 2♀, Shangrao City, Guangfeng District, Tongbo Mountain, Shazi Ridge, 28°09'10.78"N, 118°17'41.31"E, 751 m a.s.l., 11 July 2023, K. Liu, Z. Jiang, C. Li leg. (20230711, Phi-07, ASM-JGSU) • 1♀, Qianshan County, Wangwu Line, Wuyishan Town, near Yu Huizhen Hope Primary School, 27°57'05.51"N, 117°49'12.74"E, 463 m a.s.l., 9 July 2023 (20230709, Phi-07, ASM-JGSU), other data same as previous; Hunan Province • 6♀, Xinning County, Bajiaozhai, Langshan, Bajiaozhai, 26°16'.673N, 110°44.262'E, 839 m a.s.l., 22 July 2015, H. Yin, B. Zhou, J. Gan, Y. Gong, W. Liu, C. Zeng, Z. Chen, B. He, Y. Huang, X. Wu leg. (Phi-07, HNU).

**Diagnosis.** The female of this species resembles that of *P. subaureolus* Bösenberg & Strand, 1906 (see Yin et al. 2012: 1250, fig. 672b, c) in having

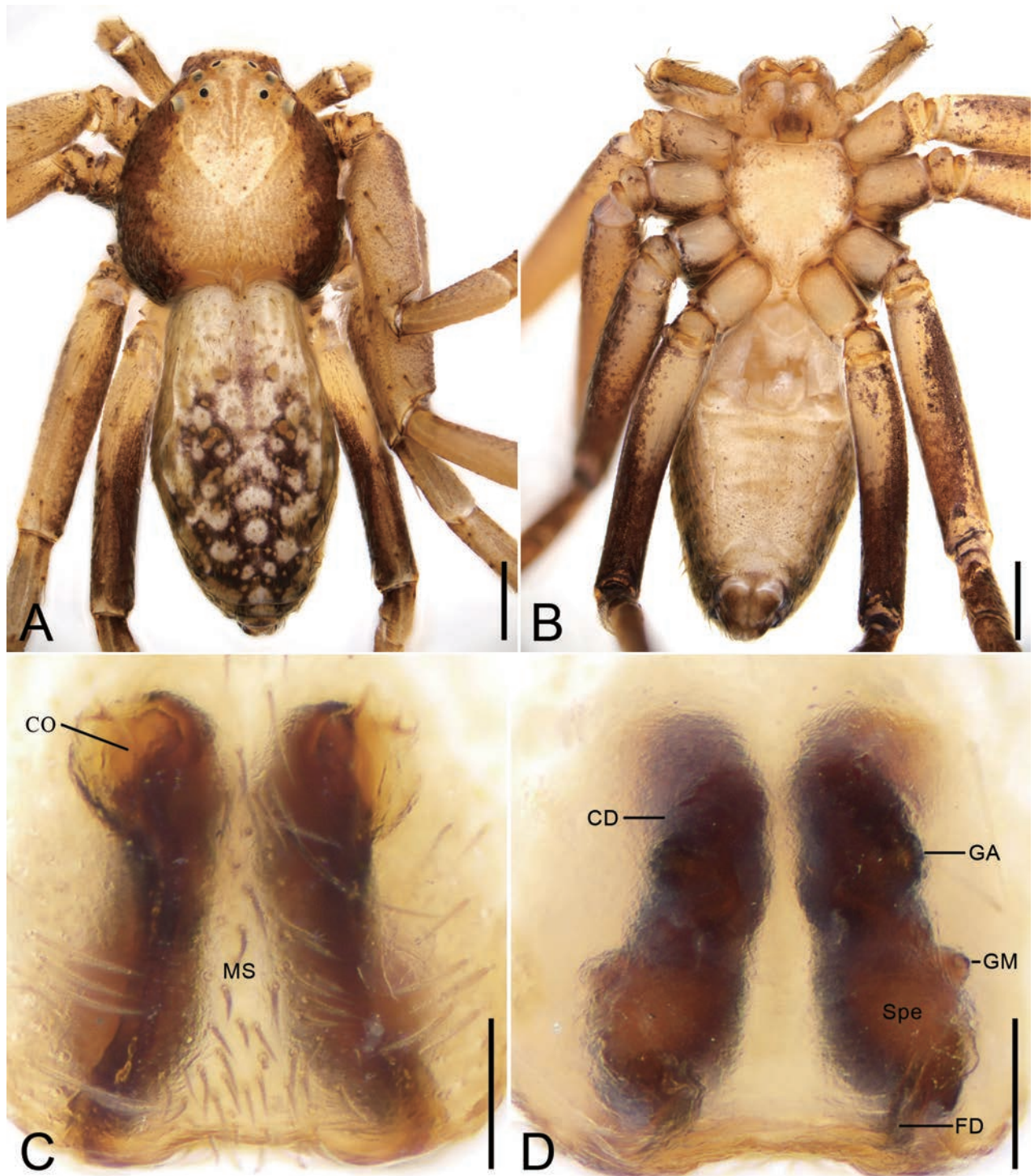


**Figure 1.** *Philodromus guiyang* Long & Yu, 2022, female **A** habitus, dorsal view **B** same, ventral view **C** epigyne, ventral view **D** vulva, dorsal view. Abbreviations: CD – copulatory duct, CO – copulatory opening, FD – fertilization duct, GA – glandular appendage, GM – glandular mound, MS – median septum, Spe – spermatheca. Scale bars: 0.5 mm (**A**, **B**); 0.1 mm (**C**, **D**).

widely separated oval spermathecae, but it can be easily separated from it by the broad median septum (vs narrow) and the broad copulatory ducts (vs narrow) (Fig. 1C, D). For the male diagnosis, see Long et al. (2022).

**Description. Female.** Habitus as in Figs 1A, B, 9A, B. Total length 2.95, carapace 1.24 long, 1.3 wide. Eye sizes and interdistances (Fig. 1A): AME 0.06, ALE 0.07, PME 0.07, PLE 0.08, AME–AME 0.17, AME–ALE 0.08, PME–PME 0.31, PME–PLE 0.17,



**Figure 2.** *Philodromus guiyang* Long & Yu, 2022, male **A** habitus, dorsal view **B** same, ventral view **C** right palp, retrolateral view **D** same, ventral view **E** same, prolateral view. Scale bars: 0.5 mm (**A**, **B**); 0.1 mm (**C**–**E**).

AME–PME 0.18, AME–PLE 0.3, ALE–ALE 0.3, PLE–PLE 0.72, ALE–PLE 0.17. MOA 0.28 long, front width 0.29, back width 0.43. Chelicerae with three promarginal teeth and no retromarginal teeth. Leg measurements: I 5.42 (1.59, 0.7, 1.22, 1.08, 0.83); II 6.26 (1.86, 0.76, 1.56, 1.13, 0.95); III 4.12 (1.45, 0.32, 0.89, 0.88, 0.58); IV 4.47 (1.45, 0.48, 1.04, 0.99, 0.51); spination: I Fe: d6; Ti: d4, p3, r2, v6; Mt: d4, p2, r2, v6; II Fe: d4; Ti: d4, p2, v6; Mt: d4, p4, r3, v6; III Fe: d2, p1; Ti: d4, p2, v4; Mt: d4, p2, r2, v6; IV Fe: d4, p1; Ti: d4, v6; Mt: d4, p2, r3, v6. Abdomen 1.71 long, 1.12 wide.

**Coloration** (Fig. 1A, B). Carapace white to red-brown, laterally with broad red-brown stripes. Medially with a white V-shaped mark. Chelicerae and endites yellow to brown. Labium brown. Sternum white to brown, laterally with brown spots. Legs white to dark brown, with many dark brown stripes or annulations. Abdomen white to dark brown, with many white spots and yellow muscle sigilla; venter white to yellowish.

**Epigyne** (Figs 1C, D, 8A). Copulatory openings located at antero-lateral part of epigyne. Median septum broad, sub-posterior part slightly constricted. Copulatory ducts broad, anteriorly curved, posteriorly slightly separated. Glandular appendages slightly protruding, very small, directed laterally. Spermathecae oval, widely separated. Glandular mounds mastoid-like, located on anterolateral part of spermathecae, directed anterolaterally. Fertilization ducts long, more than 2/3 length of spermathecae, directed anterolaterally.

**Male.** See Long et al. (2022) for description; habitus is shown in Fig. 2A, B and the palp is shown in Fig. 2C–E.

**Remarks.** This species is numerous in subtropical broad-leaved forests. The specimens were collected on shrubs and broad-leaved trees by sieving.

**Distribution.** Known from Guizhou (Long et al. 2022), Hunan (Fig. 10), and Jiangxi (Fig. 10), China. It may be broadly distributed in southern China.

### Genus *Sinodromus* Yao & Liu, gen. nov.

<https://zoobank.org/00C43736-D4E3-438C-91E9-5D460295BDF4>

**Type species.** *Sinodromus fujianensis* Yao & Liu, sp. nov.

**Diagnosis.** The new genus is similar to *Tibellus* Simon, 1875 in having a similar habitus (cf. Figs 3–7, 8B, C and Kastrygina and Kovblyuk 2016: figs 1A, 2A, 3A, 4A, 5A, B, 6A, B), but it can be easily distinguished from *Tibellus* (cf. Figs 3–7, 8B, C and Kastrygina and Kovblyuk 2016: figs 1C, G, H, J, K, 2C, G, H, 3F, G, 4C, F, G, 5D, J, K, 6D, F, G) by the very small PME, nearly as long as 1/2 of the AME diameter (vs the large PME as long as AME diameter), the palp with two tibial apophyses (vs one), the presence of a cymbial process (vs absent), the epigyne with a pair of teeth (vs absent), and the relatively thin, tube-shaped copulatory ducts (vs broad). Species of *Sinodromus* gen. nov. also resemble those of *Pulchellodromus* Wunderlich, 2012 in having a blunt cymbium and spine-like RTA (cf. Figs 4A–C, 5A, B, D, E and Lecigne et al. 2019: fig. 3F and Song and Zhu 1997: fig. 134C, D), but the genus can be easily distinguished from *Pulchellodromus* by the slender habitus (vs relatively broad), the male palp with a ventro-prolateral tibial apophysis (vs absent), the well-developed conductor with scaly serrations (vs the undeveloped conductor lacking scaly serrations), and the epigyne with a pair of teeth anterolaterally (vs absent) (cf. Figs 3–7, 8B, C and Lecigne et al. 2019: figs 4F, 5F and Song and Zhu 1997: fig. 134A, B).

**Description.** Small spiders, body length 2.5–4.5 mm. Male habitus with more black spots than in females. **Eyes:** AME, ALE, and PLE oval, with relatively large eye cups, PME rounded, smaller than other eyes, with small eye cups, anterior eye row and posterior eye row strongly recurved. Chelicerae with two promarginal teeth and no retromarginal teeth. Broad brown median band present on carapace and abdomen, and white or grey bands present on carapace and abdomen laterally. Abdomen elongate, with a notch anteromedially and pointed at posterior end.

**Male palp:** tibia with two apophyses, ventro-prolateral and retrolateral, both finger-like; cymbium with blunt postero-retrolateral process, directed towards base of retrolateral tibial apophysis; sperm duct slender, curving back on itself, located medially; conductor large, covers embolus, with scaly serrations; tegular apophysis thick and large, slightly sclerotized; embolus spine-like. Epigyne with conspicuous epigynal teeth anterolaterally; median septum triangular; copulatory openings located laterally to median septum; copulatory ducts tube-shaped; spermathecae oval, slightly separated.

**Species composition.** *S. fujianensis* sp. nov. (type species) and *S. perbrevis* sp. nov.

**Distribution.** China (Fujian, Hunan, and Jiangxi Provinces; Fig. 10).

**Etymology.** The genus name is formed from a combination of *sino-* from the Latin “Sinae” referring to China, and *-dromus*, from “Philodromidae”; the gender is masculine.

#### ***Sinodromus fujianensis* Yao & Liu, sp. nov.**

<https://zoobank.org/58446CA8-10D4-4F41-B533-4B3A957649B2>

Figs 3–6, 8B, 9C–F

Common name: 福建华逍遥蛛

**Type material. CHINA:** Fujian Province: **Holotype** • ♂: Fuzhou City, Cangshan District, Jinshan College of Fujian Agriculture and Forestry University, 26°2'21.12"N, 119°19'56.66"E, 24 February 2024, Y. Yao leg. (20240224, Phi-5, ASM-JGSU). **Paratypes** • 2♂, 2♀, the same data as the holotype • 2♂, 1♀, Fuzhou City, Yongtai County, Geling Town, Yangxi Village, Tianmen Mountain, 25°49'7.6"N, 119°1'5.07"E, 320 m a.s.l., 23 March 2024, Y. Yao, Q. Wu, and Z. Chen leg. (20240323, Phi-5, ASM-JGSU). Jiangxi Province • 1♀, Ji'an City, Jinggangshan County Level City, Huang'ao Town, Jiebei Group, 26°28'40.8"N, 114°14'16.8"E, 297 m a.s.l., 6 April 2015, Z. Chen, G. Li, K. Liu, Z. Meng, Y. Zhao leg. (20150406, Phi-5, ASM-JGSU).

**Diagnosis.** Males of the new species are easily distinguished from other philodromid spiders by the following combination of morphological characteristics: (1) the thumb-like retrolateral tibial apophysis with a membranous basal apophysis on the male palpal tibia, (2) the tegular apophysis with several ridges, and (3) the conductor with scale-like serrations (Figs 4A–E, 5A–M). The female resembles that of *Sinodromus perbrevis* sp. nov. in having spermathecae with a short stalk and crescent-shaped fertilization ducts, but it can be separated by the triangular epigynal teeth (vs oval), the copulatory openings located at the mediolateral part of the epigyne (vs anterolateral), and the very short copulatory ducts (vs relatively long) (cf. Figs 6A, B, 8B, 7C, D, 8C).

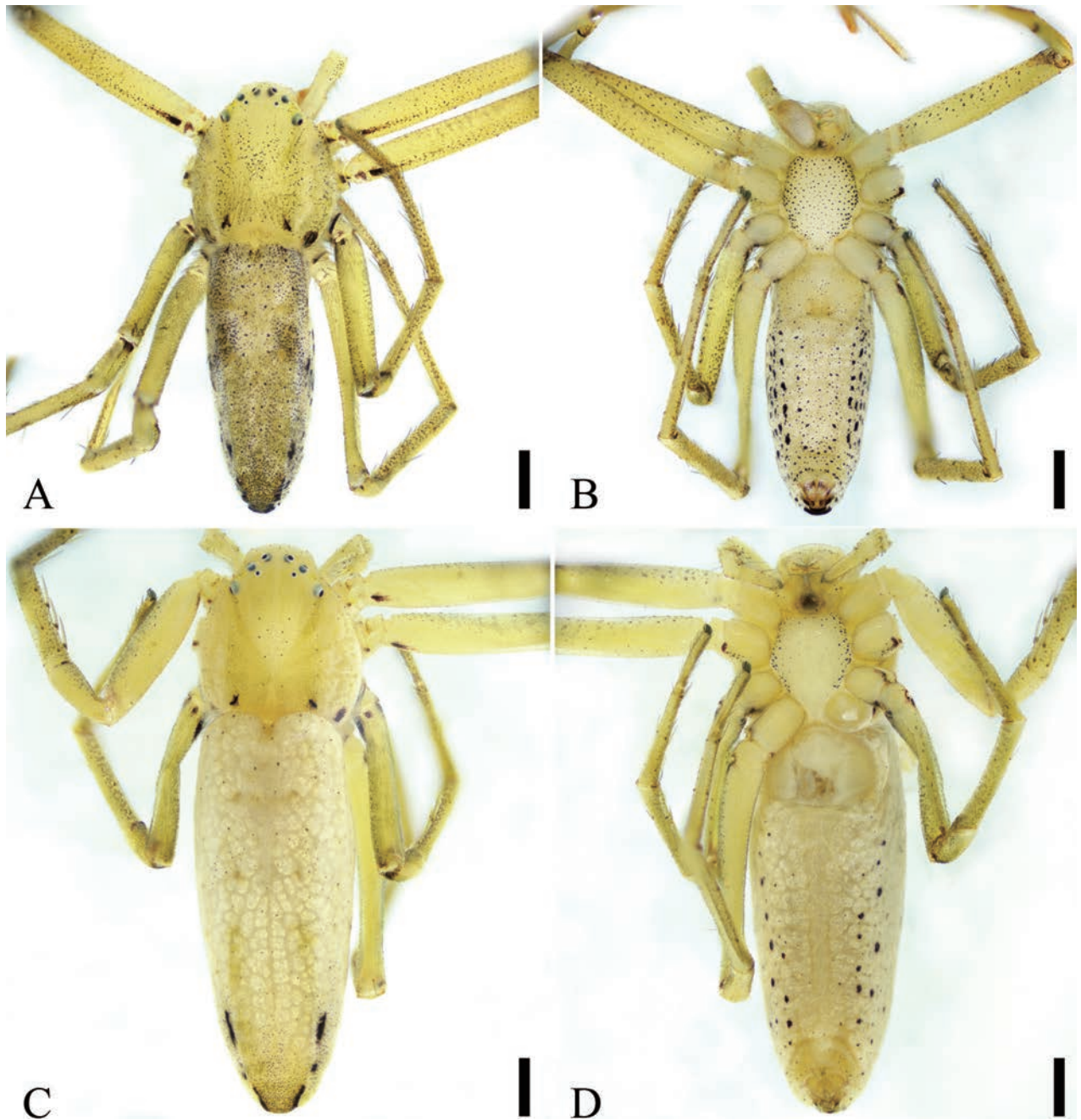


**Figure 3.** *Sinodromus fujianensis* sp. nov., habitus **A** male holotype, dorsal view **B** same, ventral view **C** female paratype, dorsal view **D** same, ventral view. Scale bars: 0.5 mm.

**Description. Male (holotype).** Habitus as in Figs 3A, B, 9C, D. Total length 3.83. Carapace medially with dense yellowish-brown setae, laterally with dense white setae, 1.46 long, 1.30 wide. Eye sizes and interdistances (Fig. 3A): AME 0.05, ALE 0.06, PME 0.03, PLE 0.07, AME–AME 0.14, AME–ALE 0.09, PME–PME 0.24, ALE–ALE 0.41, PME–PLE 0.22, PLE–PLE 0.68, ALE–PLE 0.23, AME–PME 0.11, AME–PLE 0.34. MOA 0.15 long, 0.22 front width, 0.30 back width. Chelicerae with two promarginal teeth (proximal larger) and no retromarginal teeth. Leg measurements: I 6.64 (1.91, 0.60, 1.68, 1.53, 0.92); II 8.32 (2.34, 0.82,

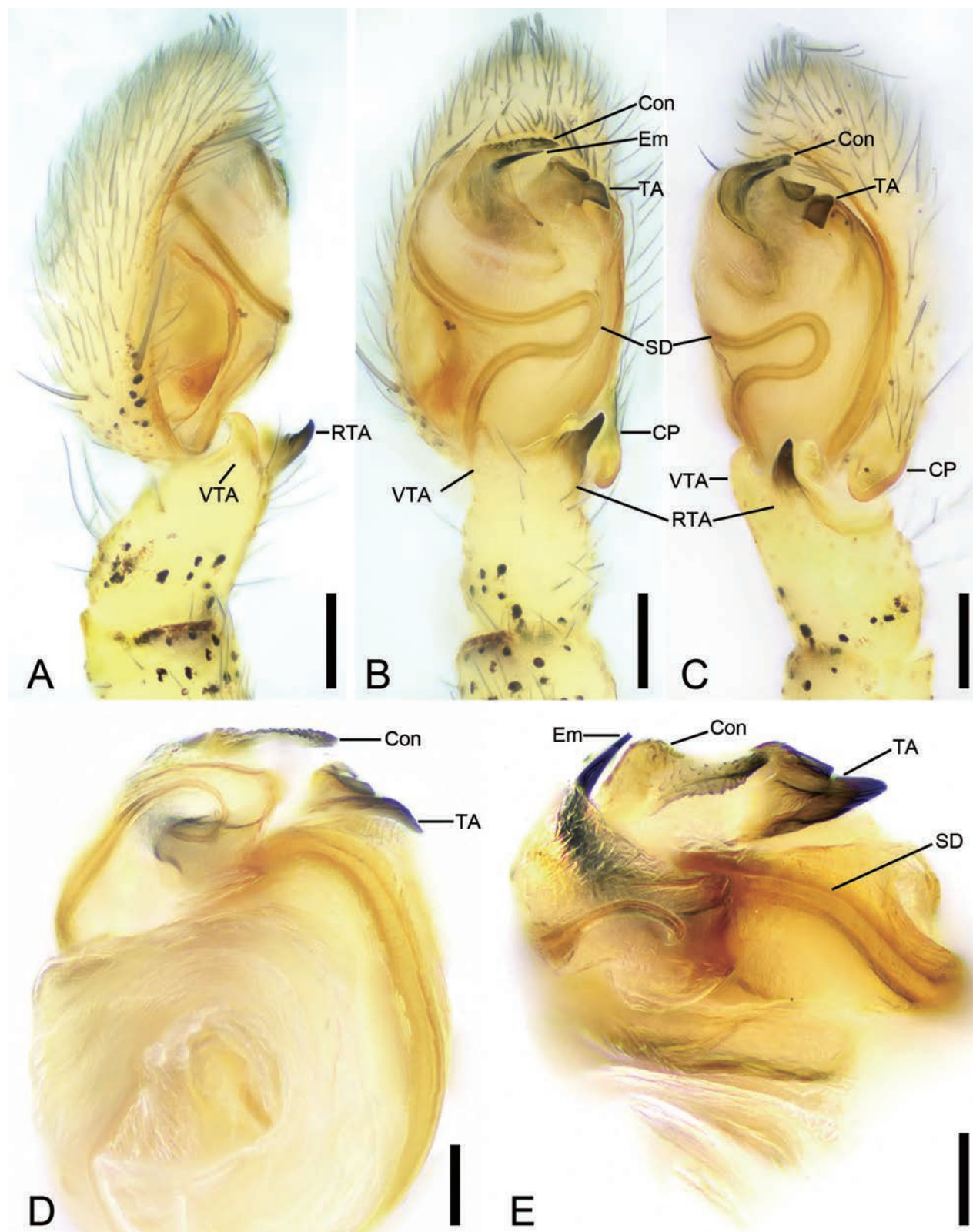


**Figure 4.** *Sinodromus fujianensis* sp. nov., male palp **A** holotype, prolatral view, slightly ventral **B** same, ventral view **C** same, ventro-retrolateral view **D** paratype, detail of palpal tegulum, posterior view **E** same, ventral view, slightly frontal. Abbreviations: Con – conductor, CP – cymbial process, Em – embolus, RTA – retrolateral tibial apophysis, SD – sperm duct, TA – tegular apophysis, VTA – ventro-prolateral tibial apophysis. Scale bars: 0.1 mm (**A–C**); 0.05 mm (**D, E**).

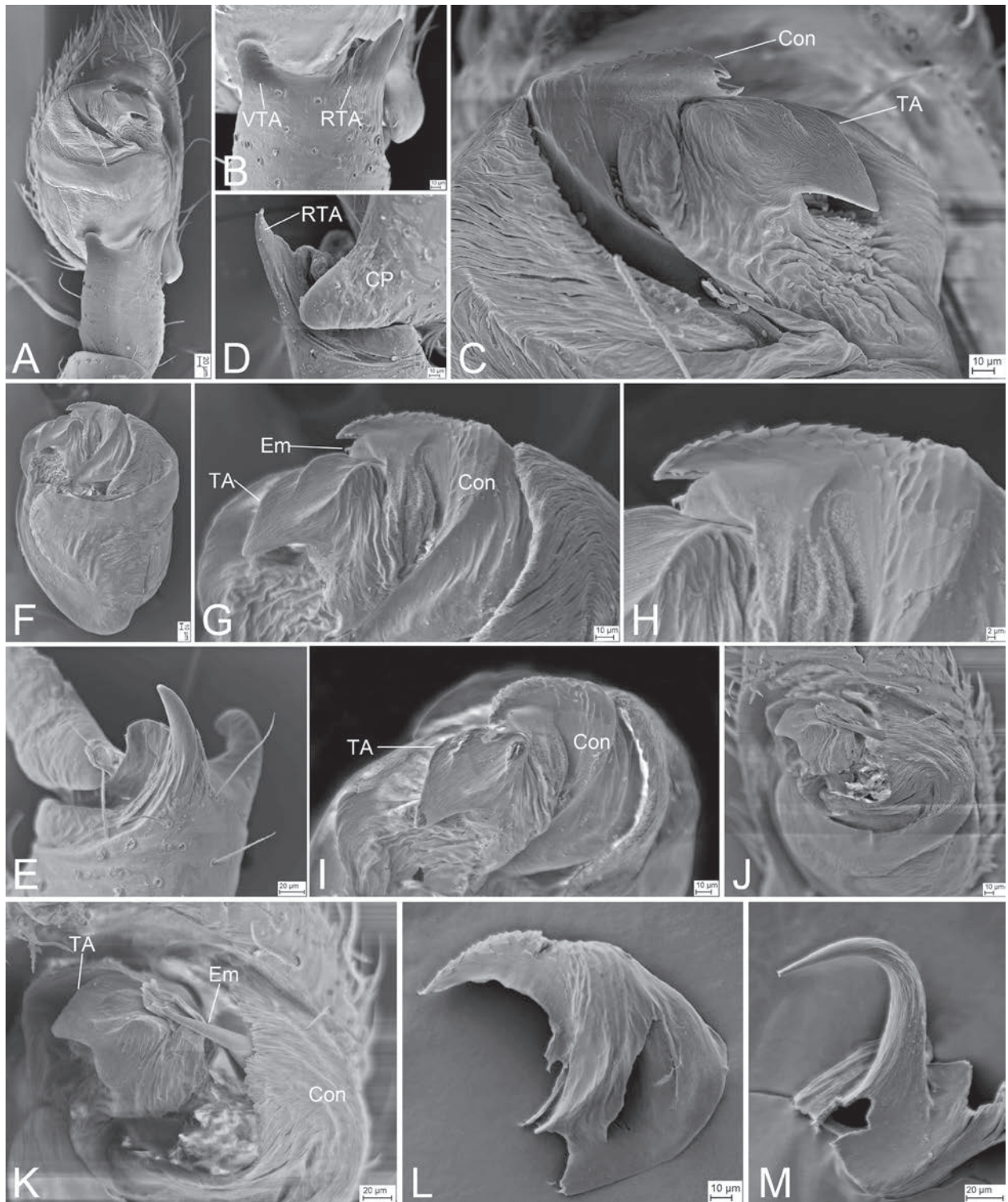


**Figure 5.** SEMs of *Sinodromus fujianensis* sp. nov., male palp of paratypes **A** left palp, ventral view **B** same, detail of ventro-prolateral and retrolateral tibial apophyses, ventral view **C** same, detail of anterior tegulum, ventral view **D** detail of retrolateral tibial apophysis and cymbial process, retrolateral view **E** right palp, detail of tibial apophyses, prolateral view **F** same, tegulum, ventral view **G** same, detail of anterior tegulum, ventral view **H** same, detail of conductor, ventral view **I** same, detail of anterior tegulum, retrolatero-ventral view **J** same, detail of anterior tegulum, ventral view, slightly frontal **K** same, detail of tegular apophysis and embolic tip after removing part of conductor, ventral view, slightly frontal **L** same, detail of conductor, ventral view **M** same, detail of embolus, ventral view. Abbreviations: Con – conductor, CP – cymbial process Em – embolus, RTA – retrolateral tibial apophysis, TA – tegular apophysis, VTA – ventro-prolateral tibial apophysis.

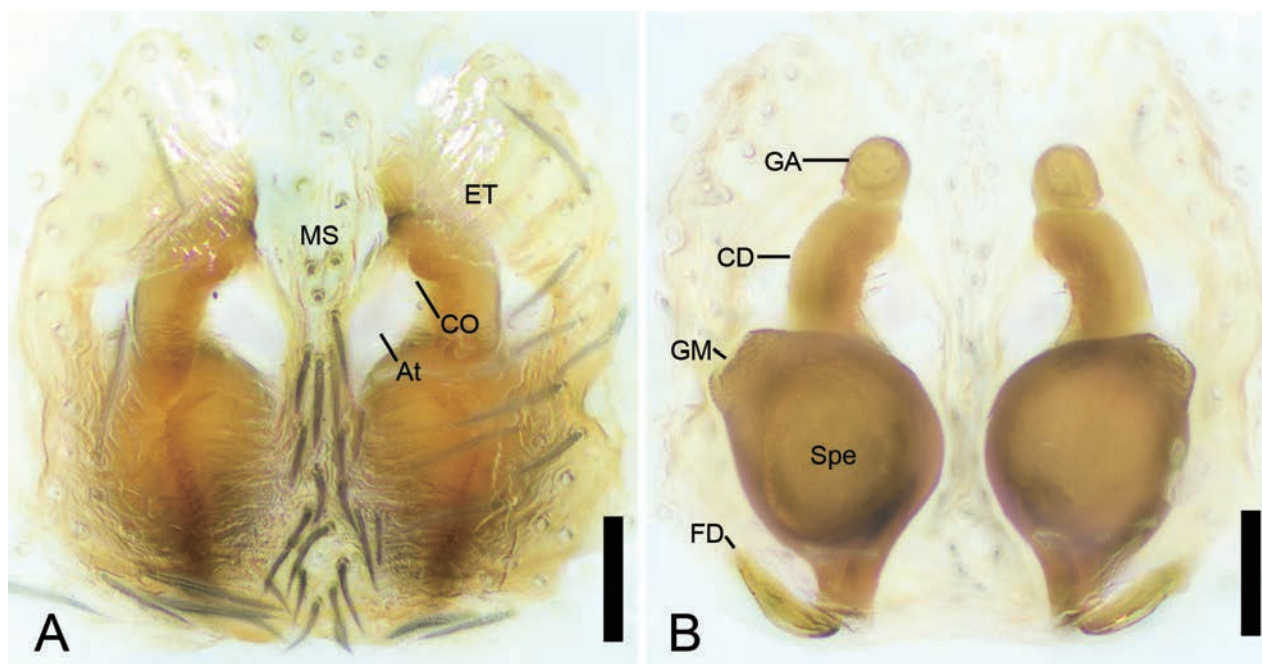


**Figure 6.** *Sinodromus fujianensis* sp. nov., female epigyne of paratype **A** epigyne, ventral view **B** vulva, dorsal view. Abbreviations: At – atrium, CD – copulatory duct, CO – copulatory opening, ET – epigynal tooth, FD – fertilization duct, GA – glandular appendage, GM – glandular mound, MS – median septum, Spe – spermatheca. Scale bars: 0.05 mm.

2.14, 1.97, 1.05); III 5.18 (1.63, 0.54, 1.22, 1.17, 0.62); IV 6.37 (2.12, 0.65, 1.29, 1.57, 0.74). Leg spination: I Pa: d1, p1, r1; Ti: d2, p2, r2, v5; Mt: d1, p2, r2, v2; II Pa: v1; Ti: d2, p2, r2, v5; Mt: d1, p1, r2, v1; III Pa: v1; Ti: d2, p1, r2, v3; Mt: d2, p2, r3, v3; IV Fe: d2; Pa: d1; Ti: d2, p2, r1; Mt: d2, p2, r3. Abdomen (Fig. 3A, B) medially with dense yellow-brown setae, laterally with dense white setae, 2.47 long, 0.91 wide.

**Coloration** (Figs 3A, B, 9C, D). Carapace yellow, with many black dots, laterally with broad yellowish stripes, posteriorly with two pairs of black spots. Chelicerae and endites yellow. Labium yellow, with brown spot posteriorly. Sternum shield-like, yellowish, with dense black dots. Legs with many black dots. Abdomen yellowish to yellow, dorsally with dense black dots, medially with broad yellow stripe, laterally with grey stripes; venter with many pairs of black spots bilaterally.

**Palp** (Figs 4A–E, 5A–M). Tibia with two apophyses, the ventro-prolateral one short, slightly curved dorsally toward posterior part of tegulum, the retrolateral one finger-like, with a membranous basal apophysis. Cymbial process strongly protruding, approaching the base of retrolateral tibial apophysis. Sperm duct thin, curving back on itself, clearly visible from posterior to prolateral part. Tegular apophysis thick, horn-like, with a blunt basal apophysis. Conductor slightly sclerotized, longer than embolus, covers embolus, with many scaly serrations. Embolus short, hook-shaped, tapering to a point.

**Female (paratype).** Habitus as in Figs 3C, D, 9E, F. As in male, except as noted. Total length 5.00. Carapace: 1.50 long, 1.45 wide. Eye sizes and interdistances (Fig. 3C): AME 0.05, ALE 0.05, PME 0.03, PLE 0.06, AME–AME 0.19, AME–ALE 0.11, PME–PME 0.29, ALE–ALE 0.48, PME–PLE 0.24, PLE–PLE 0.80, ALE–PLE 0.22, AME–PME 0.13, AME–PLE 0.36. MOA 0.16 long, 0.28 front width, 0.36 back width. Leg measurements: I 5.22 (1.46, 0.70, 1.31, 1.10, 0.65); II 6.38 (1.76, 0.83, 1.61, 1.39, 0.79); III 4.32 (1.33, 0.50, 1.02, 0.97, 0.50); IV 6.05 (1.97, 0.63,

1.47, 1.33, 0.65). Leg spination: I Fe: d1; Ti: d2, p2, r5, v4; Mt: p3, r3, v3; II Ti: d2, p3, r3, v3; Mt: p3, r3, v2; III Ti: d2, p2, r1, v2; Mt: p3, r1, v3; IV Pa: v1; Ti: d1, p2, r1, v2; Mt: p1, r3, v6. Abdomen 3.50 long, 1.41 wide.

**Coloration** (Figs 3C, D, 9E, F). Paler than male. Carapace yellowish to yellow, with sparse black dots. Sternum laterally with many black dots. Legs yellowish white, with sparse dark spots. Abdomen with abundant silver spots and sparse black dots on surface.

**Epigyne** (Figs 6A, B, 8B) slightly longer than wide. Epigynal teeth lamellar, subtriangular, located anterolaterally on epigyne. Atrium small, separated by median septum. Median septum narrow, anteriorly subtriangular. Copulatory openings directed posteriorly, located on the sides of the antero-lateral part of median septum, slightly covered by epigynal teeth. Glandular appendages located at the beginning part of copulatory ducts, directed anteriorly. Copulatory ducts slightly curved, slightly shorter than spermathecae. Spermathecae slightly separated, round, with a short stalk. Glandular mounds slightly protruding, truncate, located on anterolateral part of spermathecae, directed laterally. Fertilization ducts nearly as long as 1/2 of spermathecal width, directed antero-laterally.

**Biology.** The coloration and habitus are the same as the grassland community from which they are collected and provides them with camouflage.

**Distribution.** Known from the type locality in Fujian Province, as well as Jiangxi Province, China (Fig. 10).

**Etymology.** The specific name refers to the type locality.

***Sinodromus perbrevis* Yao & Liu, sp. nov.**

<https://zoobank.org/87AD4F3D-EBE1-4D80-A70D-E9540A33B613>

Figs 7, 8C

Common name: 短华逍遥蛛

**Type material. CHINA:** Jiangxi Province: **Holotype** • ♀, Ji'an City, Jinggangshan County Level City, Ciping Town, Huangyangjie Scenic Spot, 26°37'21.6"N, 114°6'21.6"E, 958 m a.s.l., 5 April 2014, Z. Chen, K. Liu, Z. Meng, Y. Tang, X. Huang leg. (20140405, Phi-06, ASM-JGSU). **Paratypes** • 1♀, Ji'an City, Jinggangshan County Level City, JingZhu Mountain, 26°29'45.6"N, 114°4'44.4"E, 1146 m a.s.l., 20 December 2015, K. Liu, Z. Chen, Z. Meng, Q. Chen, S. Wu, P. Gong leg. (20151220, Phi-06, ASM-JGSU). Hunan Province • 1♀, Hengshan Mountain, 27°16.504'N, 112°42.304'E, 815 m a.s.l., 1–7 May 2007, G. Tang, P. Hu, Q. Wang leg. (Phi-06, HNU) • 1♀, 1 May 2008, Q. Wang leg., other data same as previous (Phi-06, HNU).

**Diagnosis.** The female of this species can be easily distinguished from *S. fujianensis* sp. nov. by the oval epigynal teeth (vs triangular) and the short copulatory ducts (vs relatively long) (cf. Figs 7C, D, 8C, 6A, B, 8B).

**Description.** Habitus as in Fig. 7A, B. Total length 3.52. Carapace 1.34 long, 1.21 wide. Eye sizes and interdistances (Fig. 7A): AME 0.04, ALE 0.08, PME 0.03, PLE 0.06, AME–AME 0.18, AME–ALE 0.12, PME–PME 0.28, PME–PLE 0.2, AME–PME 0.12, AME–PLE 0.32, ALE–ALE 0.44, PLE–PLE 0.67, ALE–PLE 0.15. MOA 0.21 long, front width 0.25, back width 0.34. Chelicerae with three promarginal teeth and no retromarginal teeth. Leg (Fig. 7A, B) measurements:

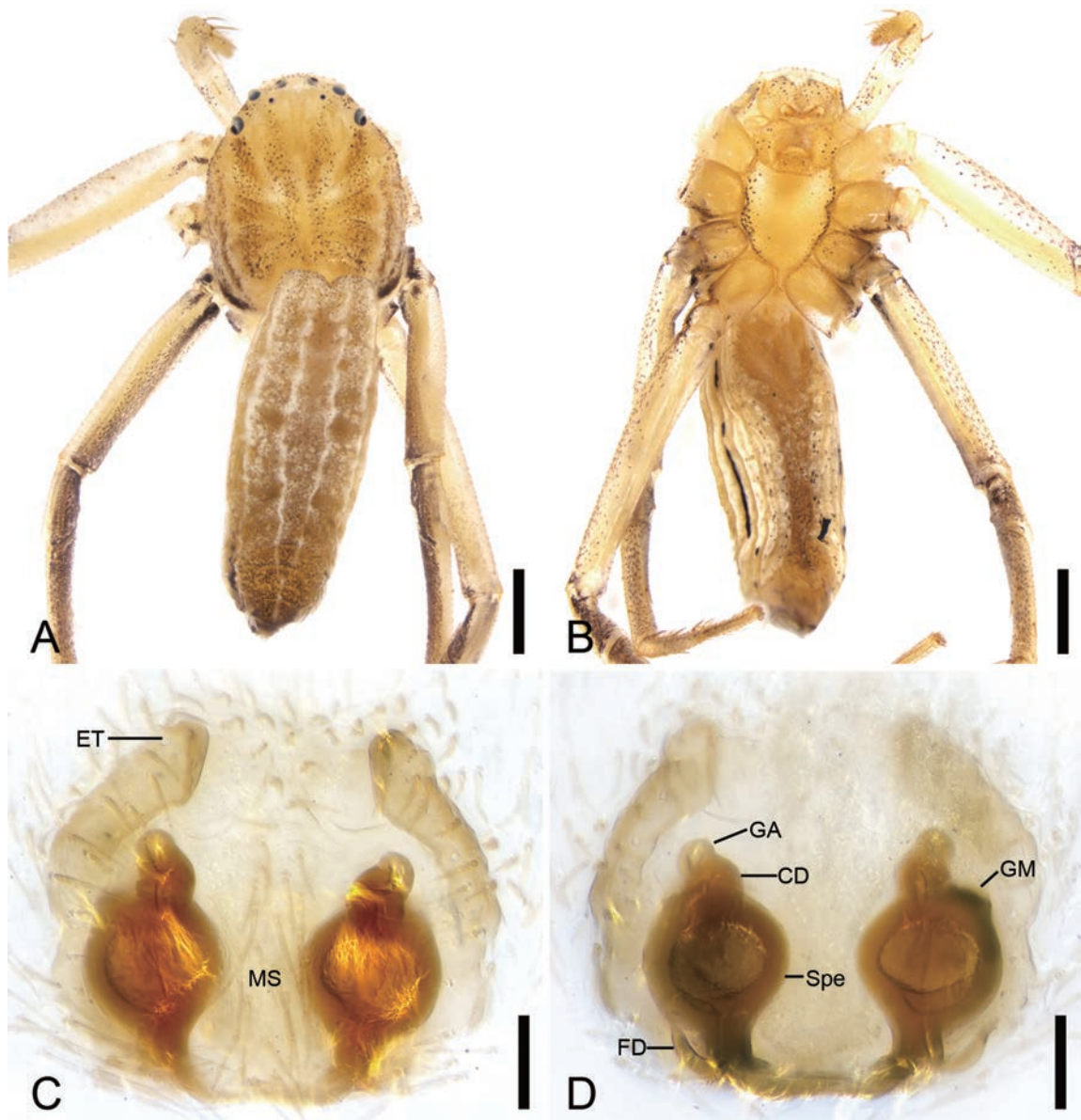


**Figure 7.** *Sinodromus perbrevis* sp. nov., female holotype **A** habitus, dorsal view **B** same, ventral view **C** epigyne, ventral view **D** vulva, dorsal view. Abbreviations: CD – copulatory duct, ET – epigynal tooth, FD – fertilization duct, GA – glandular appendage, GM – glandular mound, MS – median septum, Spe – spermatheca. Scale bars: 0.5 mm (**A, B**); 0.1 mm (**C, D**).

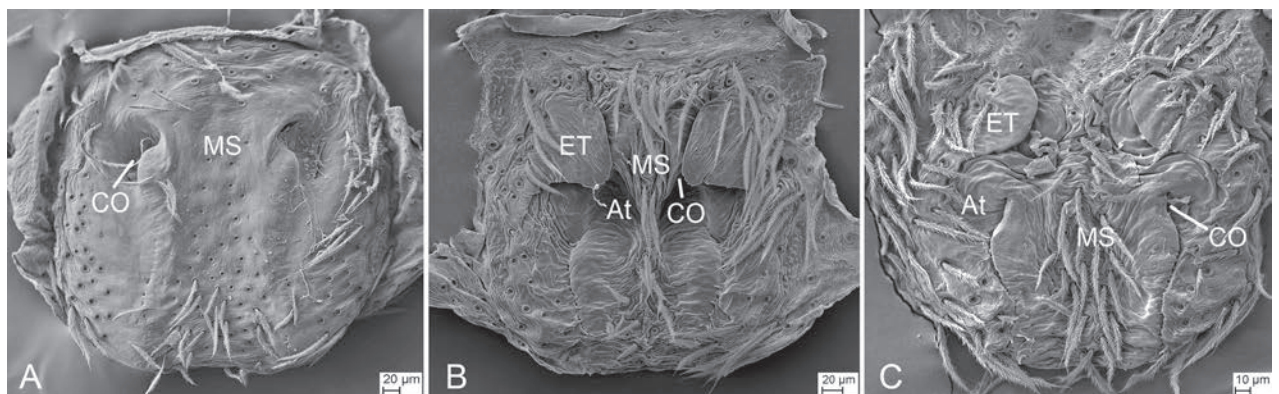


**Figure 8.** SEM pictures of epigynes, ventral view **A** *Philodromus guiyang* Long & Yu, 2022 **B** *Sinodromus fujianensis* sp. nov. **C** *S. perbrevis* sp. nov.. Abbreviations: At – atrium, CO – copulatory opening, ET – epigynal tooth, MS – median septum.

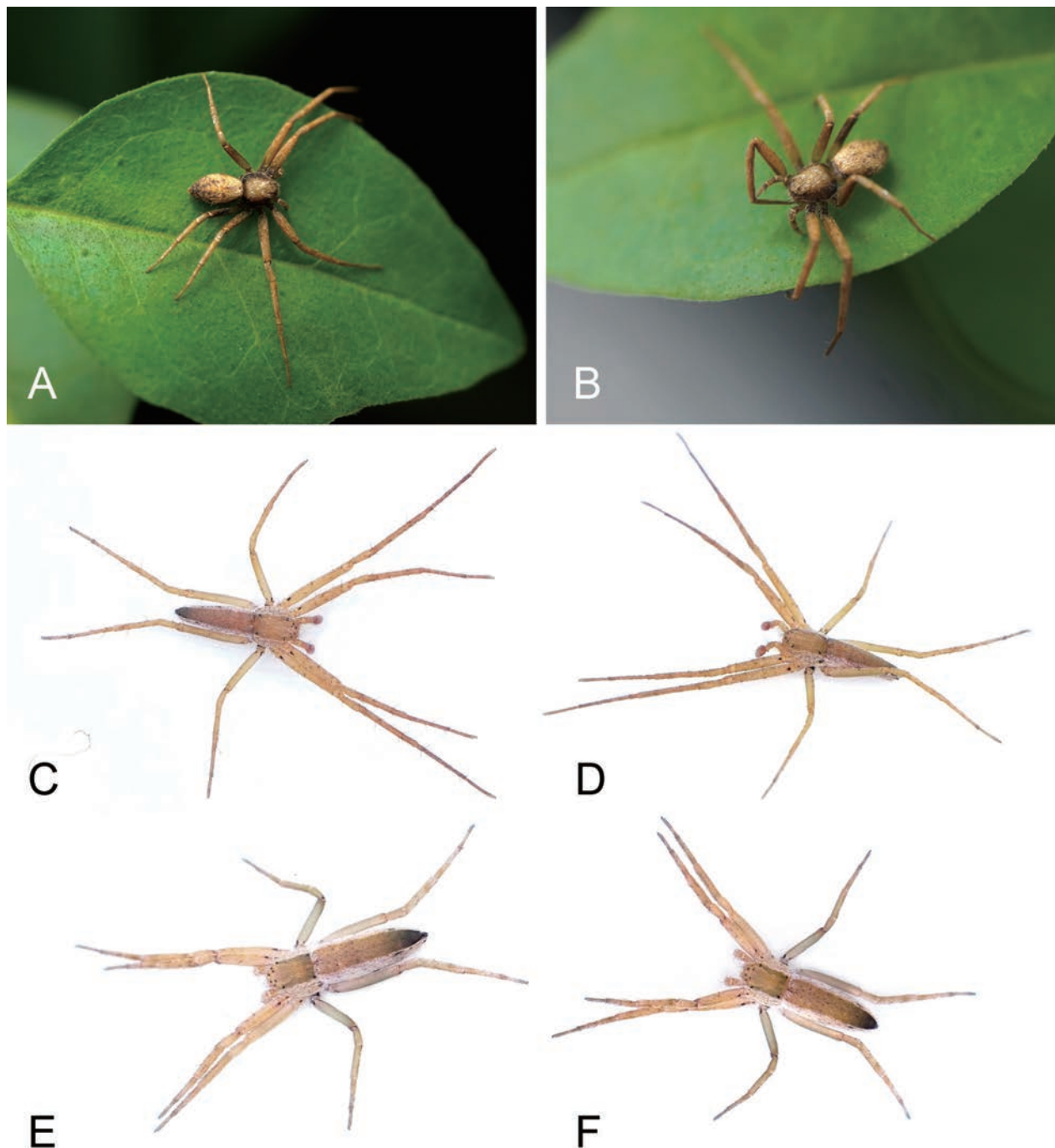


Figure 9. **A, B** living specimen of *Philodromus guiyang* Long & Yu, 2022 **C, D** *Sinodromus fujianensis* sp. nov., male **E, F** *S. fujianensis*, female.

I and II missing; III 1.26 (0.42, 0.16, 0.28, 0.25, 0.15); IV 5.3 (1.82, 0.63, 1.18, 1.06, 0.61); spination: III Ti: r2; Mt: d1, r1, v8; IV Ti: v2; Mt: r2, v6. Abdomen (Fig. 7A, B) 2.18 long, 0.79 wide.

**Coloration** (Fig. 7A, B). Carapace yellow, with three pairs of stripes, each one including many black spots, laterally with dark brown stripes. Chelicerae yellowish, with sparse black spots. Endites and labium yellow, with sparse black spots. Sternum yellowish to yellow, laterally with many black dots. Legs with many small black dots. Abdomen yellowish to brown, dorsally with small dense black dots; venter with a broad brown stripe medially.

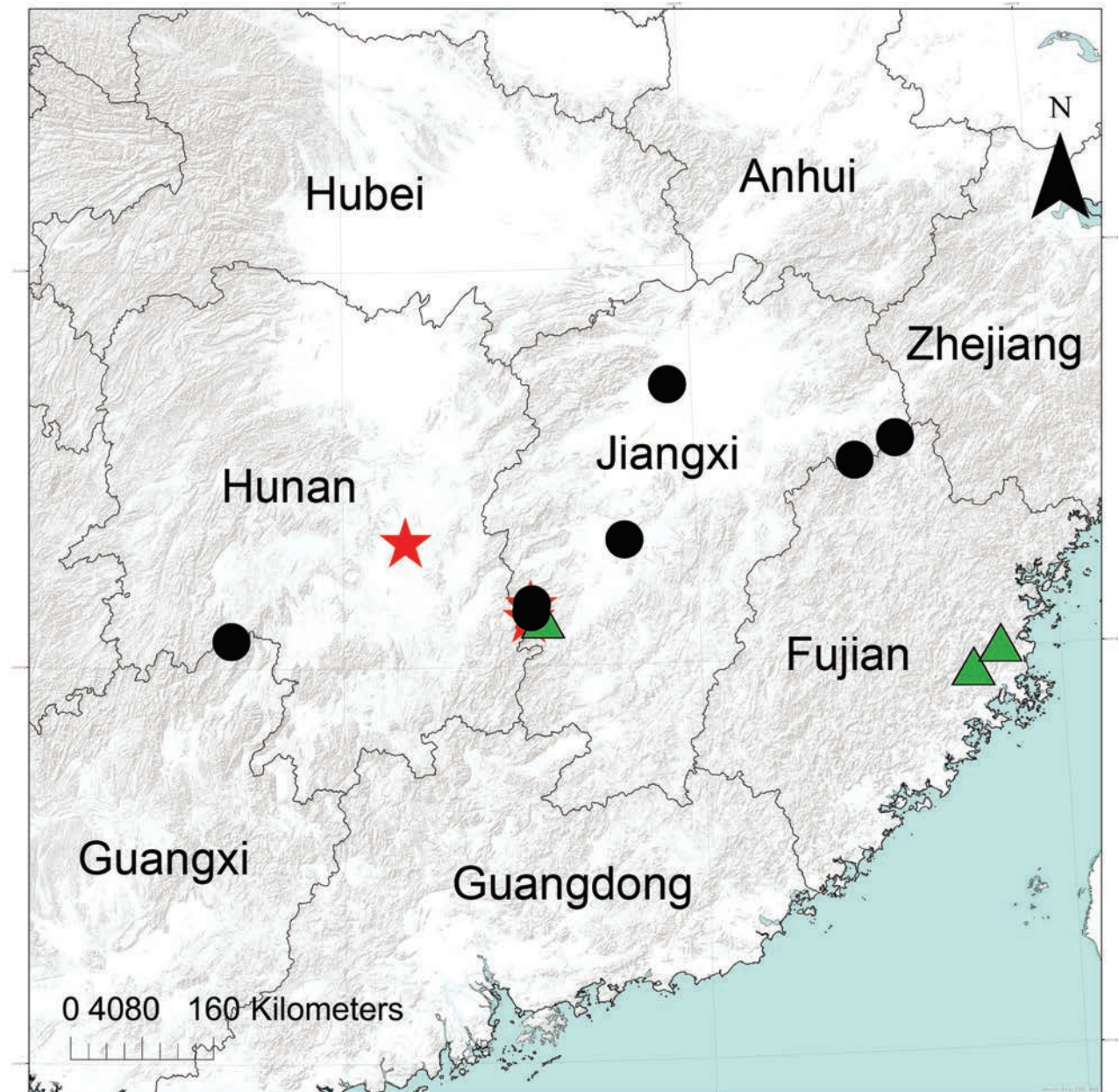


Figure 10. Distributional records of *Philodromus guiyang* Long & Yu, 2022 (black circles), *Sinodromus fujianensis* sp. nov. (green triangles) and *S. perbrevis* sp. nov. (red stars) from China.

**Epigyne** (Figs 7C, D, 8C) nearly as long as wide. Epigynal teeth lamellar, ear-shaped, located antero-laterally. Atrium moderately large, anteromedially located. Median septum narrow, anteriorly subtriangular. Copulatory openings directed laterally, located on the sides of the antero-lateral part of median septum, not covered by epigynal teeth. Glandular appendages small, mastoid like, located at the origin of the copulatory ducts, directed anterolaterally. Copulatory ducts very short, strongly bent dorsally. Spermathecae widely separated, globular, with a short stalk. Glandular mounds slightly protruding, cap-like, located on antero-lateral part of spermathecae, directed laterally. Fertilization ducts nearly as long as 1/2 of spermathecal width, directed antero-laterally.

**Male.** Unknown.

**Distribution.** Known from the type locality in Jiangxi, and from Hunan Province, China (Fig. 10).

**Etymology.** The specific name comes from the Latin word *perbrevis*, referring to the very short copulatory ducts; adjective.

## Discussion

Currently, with this addition of the two new species, 62 species of philodromids have been classified in eight genera in China. Surprisingly, there are no detailed keys for these genera. The main reasons are: 1) most species of *Thanatus* are known from only a single female (WSC 2024), and it is very difficult to classify the generic characters; 2) the genus *Thanatus* is very large, and the morphological variation within its supposed members is so broad that the assignment of several species to this genus has been questioned (e.g. many species from South China should be re-assigned to the genus *Apollophanes*); 3) the descriptions of *Rhysodromus* and *Tibellus* from China are superficial, and only a few illustrations have been provided (e.g. Song and Zhu 1997; Hu 2001). The new genus has a tegular apophysis (Fig. 5C), which is absent in *Apollophanes* (Dondale and Redner 1975), *Philodromus* (Dondale and Redner 1978), *Pulchellodromus* (Wunderlich 2012), *Psellonus* (Malamel et al. 2019, Lin et al. 2024), *Rhysodromus* (Kastrygina and Kovblyuk 2016), *Thanatus* (Dippenaar-Schoeman et al. 2022), and *Tibellus* (Dippenaar-Schoeman et al. 2022).

Beating as a collecting method has allowed us to simultaneously obtain many specimens from the subtropical forest habitat. The new genus, *Sinodromus* gen. nov., is distributed in the south of China. It is likely that additional species in this genus will be described in the future, extending the distribution.

## Acknowledgements

We are grateful to Qun-zhen Wu, Qin-ang Wu, and Zu-bin Chen (from Chonglinyequ Cultural Creativity Co., Ltd), and Zhi-wu Chen, Guang-feng Li, Cong-zheng Li, Ze-yuan Meng, Yu-bao Tang, Qian-qian Chen, Sha Wu, Pei-chong Gong, Xing-tong Chen and Yi-fan Zhao (from Jinggangshan University, China) and Guo Tang, Peng Hu, Hai-qiang Yin, Bing Zhou, Jia-hui Gan, Yu-hui Gong, Wang Liu, Chen Zeng, Zhuo-er Chen, Bing-yan He, Ya-zhou Huang, Xin-zhou Wu and Qiao-bing Wang (from Hunan Normal University) for collecting the specimens. We also thank Dr Nathalie Yonow for improving the English of the manuscript, and Mr Ye-jie Lin, the reviewer Dr Rahşen S. Kaya, and the subject editor Dr Sarah Crews for providing detailed corrections and suggestions.

## Additional information

### Conflict of interest

The authors have declared that no competing interests exist.

### Ethical statement

No ethical statement was reported.

## Funding

This study was supported by the Natural Science Foundation of China (32000301/32070429).

## Author contributions

Yan-bin Yao, Ke-ke Liu and Xiang Xu designed the MS. Zhong-jing Wang, Yan-bin Yao, Zi-ying Tang and Wen-hui Li provided the data. Ke-ke Liu drafted the early MS.

## Author ORCIDs

Zhong-jing Wang  <https://orcid.org/0009-0000-6377-6840>

Yan-bin Yao  <https://orcid.org/0000-0002-2560-9299>

Zi-ying Tang  <https://orcid.org/0009-0006-8513-456X>

Wen-hui Li  <https://orcid.org/0000-0002-8074-9526>

Ke-ke Liu  <https://orcid.org/0000-0001-7822-3667>

Xiang Xu  <https://orcid.org/0000-0001-9485-5373>

## Data availability

All of the data that support the findings of this study are available in the main text.

## References

- Álvarez-Padilla F, Hormiga G (2007) A protocol for digesting internal soft tissues and mounting spiders for scanning electron microscopy. *The Journal of Arachnology* 35(3): 538–542. <https://doi.org/10.1636/Sh06-55.1>
- Dippenaar-Schoeman AS, Haddad CR, Foord SH, Lotz LN (2022) The Philodromidae of South Africa. Version 2. South African National Survey of Arachnida Photo Identification Guide, Irene, 53 pp. <https://doi.org/10.5281/zenodo.6634009>
- Dondale CD, Redner JH (1975) Revision of the spider genus *Apollophanes* (Araneida: Thomisidae). *The Canadian Entomologist* 107(11): 1175–1192. <https://doi.org/10.4039/Ent1071175-11>
- Dondale CD, Redner JH (1978) The insects and arachnids of Canada, Part 5. The crab spiders of Canada and Alaska, Araneae: Philodromidae and Thomisidae. Research Branch Agriculture Canada Publication 1663: 1–255.
- Hu JL (2001) Spiders in Qinghai-Tibet Plateau of China. Henan Science and Technology Publishing House, 658 pp.
- Jocqué R, Dippenaar-Schoeman AS (2006) Spider families of the world. Musée Royal de l’Afrique Central Tervuren, 336 pp.
- Kastrygina ZA, Kovblyuk MM (2016) The spider genus *Rhysodromus* Schick, 1965 in the Crimea (Aranei: Philodromidae). *Arthropoda Selecta* 25(3): 283–292. <https://doi.org/10.15298/arthscl.25.3.08>
- Kubcová L (2004) A new spider species from the group *Philodromus aureolus* (Araneae, Philodromidae) in Central Europe. In: Thaler K (Ed.) *Diversität und Biologie von Web-spinnen, Skorpionen und anderen Spinnentieren*. *Denisia* 12: 291–304.
- Lecigne S, Cornic JF, Oger P, Van Keer J (2019) *Celerrimus* n. gen. (Araneae, Philodromidae) et description de *Celerrimus duffeyi* n. sp., une espèce très singulière d’Europe occidentale. *Revue Arachnologique* (2) 6: 32–51.
- Li S (2020) Spider taxonomy for an advanced China. *Zoological Systematics* 45(2): 73–77. <https://doi.org/10.11865/zs.202011>

- Li SQ, Lin YC (2016) Species Catalogue of China (Vol. 2). Animals. Invertebrates (1). Arachnida: Araneae. Science Press, Beijing, 549 pp.
- Lin YJ, Li SQ, Mo HL, Wang XH (2024) Thirty-eight spider species (Arachnida: Araneae) from China, Indonesia, Japan and Vietnam. *Zoological Systematics* 49(1): 4–98. <https://doi.org/10.11865/zs.2024101>
- Long FY, Deng LJ, Mao JL, Yu H (2022) A survey of genus *Philodromus* (Araneae: Philodromidae) from Guiyang, Guizhou, China, with description of a new species. *Acta Arachnologica Sinica* 31(2): 113–120. <https://doi.org/10.3969/j.issn.1005-9628.2022.02.009>
- Malamel JJ, Nafin KS, Sankaran PM, Sebastian PA (2019) Taxonomic revision of the monotypic genus *Psellonus* Simon, 1897 (Araneae, Philodromidae). *Zootaxa* 4543(3): 442–450. <https://doi.org/10.11646/zootaxa.4543.3.9>
- Song DX, Zhu MS (1997) Fauna Sinica: Arachnida: Araneae: Thomisidae, Philodromidae. Science Press, Beijing, 259 pp.
- World Spider Catalog (2024) World Spider Catalog. Natural History Museum Bern. Version 25.5. <https://wsc.nmbe.ch/> [accessed 1 August 2024]
- Wunderlich J (2012) Fifteen papers on extant and fossil spiders (Araneae). *Beiträge zur Araneologie* 7: 1–246.
- Yin CM, Peng XJ, Yan HM, Bao YH, Xu X, Tang G, Zhou QS, Liu P (2012) Fauna Hunan: Araneae in Hunan, China. Hunan Science and Technology Press, Changsha, 1590 pp.

# First record of the family Calliopiidae (Crustacea, Malacostraca, Amphipoda) from Korean waters, with description of new species *Calliopus ulleungensis* sp. nov.

Kyung-Won Kim<sup>1</sup>, Young-Hyo Kim<sup>1</sup>

<sup>1</sup> Department of Biological Sciences, Dankook University, Cheonan 31116, Republic of Korea  
Corresponding author: Young-Hyo Kim ([yhkim@dankook.ac.kr](mailto:yhkim@dankook.ac.kr))

## Abstract

A new species of the family Calliopiidae was collected from the East Sea of Korea. *Calliopus ulleungensis* sp. nov. is similar to *C. columbianus* Bousfield & Hendrycks, 1997 in having numerous calceoli on the posteromedial margins of antennae and a weakly carinate body. However, the new species can be distinguished from *C. columbianus* by the shorter process on peduncular article 3 of antenna 1, subrectangular eyes, and fewer articles in the antenna flagellum. This species, along with *C. ezoensis* Shimoji et al. 2020, occurs in the Western Pacific. The females of the two species are morphologically very similar, but the males of *C. ezoensis* are easily distinguishable, as the gnathopod 1 is larger than gnathopod 2. The new species is fully illustrated and extensively compared with related species. In this paper, both *Calliopus* and Calliopiidae are reported from Korea for the first time. A key to species of *Calliopus* is also provided.

**Key words:** Amphipod, calliopiid, key, morphology, new record, taxonomy



Academic editor: Rachael Peart  
Received: 11 October 2024  
Accepted: 19 November 2024  
Published: 20 December 2024

ZooBank: <https://zoobank.org/D142F735-B3A8-463C-89DD-48975E019800>

**Citation:** Kim K-W, Kim Y-H (2024) First record of the family Calliopiidae (Crustacea, Malacostraca, Amphipoda) from Korean waters, with description of new species *Calliopus ulleungensis* sp. nov. ZooKeys 1221: 297–307. <https://doi.org/10.3897/zookeys.1221.139066>

Copyright: © Kyung-Won Kim & Young-Hyo Kim. This is an open access article distributed under terms of the Creative Commons Attribution License (Attribution 4.0 International – CC BY 4.0).

## Introduction

The family Calliopiidae G.O. Sars, 1893 represents a moderately sized group within the amphipods. Members of this family display a range of morphologically diverse forms that share many symplesiomorphies but only a few synapomorphies (Bousfield and Hendrycks 1997). In previous studies, the family was grouped with Eusiridae due to the following morphological similarities: well-developed eyes, body often with dorsal carina, slender antennae, generally degenerated accessory flagellum, feeble gnathopods, and uropod 3 with rami subsimilar in length (Sars 1893; Barnard and Karaman 1991; Bousfield and Hendrycks 1997). However, with the establishment of the suborder Senticaudata, the family Calliopiidae was reclassified and is now positioned in a category that places it systematically distant from Eusiridae (Lowry and Myers 2013).

The genus *Calliopus* Lilljeborg, 1865 currently comprises nine species (Horton et al. 2024). The genus was originally described as *Calliope* Spence

Bate, 1857, with *Calliope leachii* Spence Bate, 1857 as the type species. Later, as the genus *Calliopius* was established by Lilljeborg in 1865, *Calliope leachii* was considered a junior subjective synonym of *Amphithoe laeviuscula* Krøyer, 1838. The genus *Calliopius* is characterized by reduced accessory flagellum, fused on peduncular article 3; subchelate gnathopods, and entire telson (Bate 1857). In this paper, we describe and illustrate a new species of *Calliopius* in the Korean amphipod fauna. This is also first record of the family Calliopiidae from Korean waters. Additionally, we provide a key to *Calliopius* species.

## Materials and methods

Specimens were collected from subtidal waters around Ulleungdo island, East Sea, Korea (Fig. 1). The collected specimens were fixed in 95% ethanol for preservation and later dissected in glycerol on Cobb's aluminum hole slides. The materials were examined under stereoscopic (Olympus SZX 10) and compound microscopes (Olympus BX 51), and drawings and measurements were made with the aid of a drawing tube. Line drawings were produced using Clip Studio Paint software (Celsys, Japan). Body length was measured from the tip of the rostrum to the posterior end of the urosome, along the dorsal parabolic line of the body. The examined specimens are deposited at the National Marine Biodiversity Institute of Korea (MABIK), Secheon, Korea, and the Department of Biological Science, Dankook University (DKU), Cheonan, Korea.

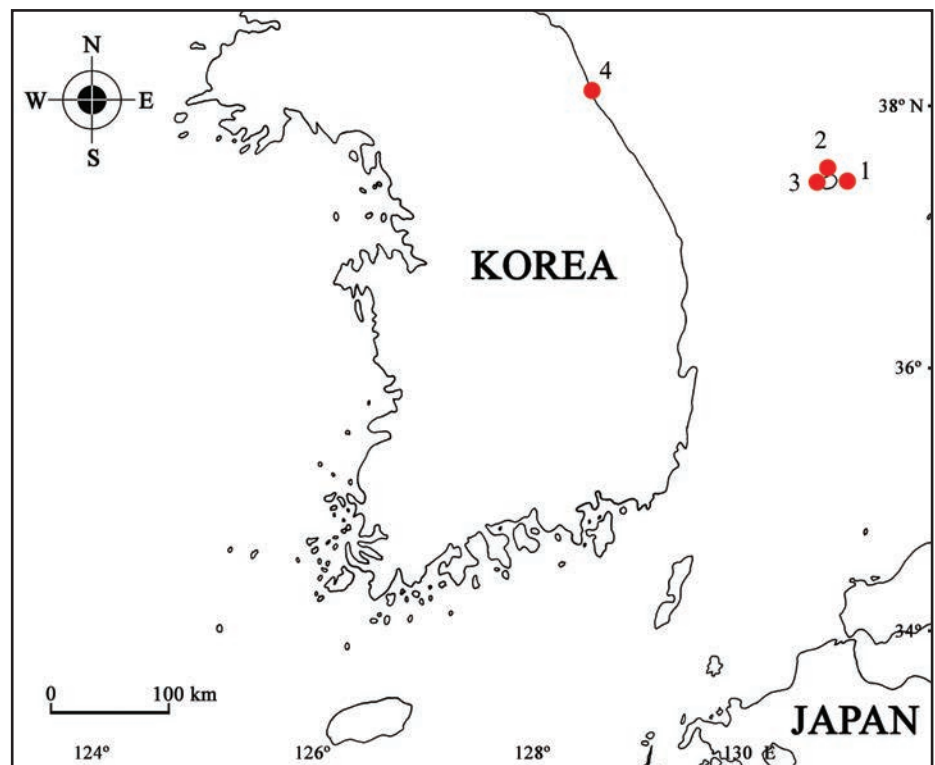


**Figure 1.** Collecting sites of the *Calliopius ulleungensis* sp. nov.: 1 = Ulleungdo Island (site 1); 2 = Ulleungdo Island (site 2); 3 = Taeha-ri; 4 = Bongpo-ri.

## Taxonomy

**Order Amphipoda Latreille, 1816**

**Family Calliopiidae G.O. Sars, 1893**

**Korean name: Kal-li-o-pe-yeop-sae-u-gwa, new**

**Genus *Calliopius* Lilljeborg, 1865**

**Korean name: Kal-li-o-pe-yeop-sae-u-sok, new**

**Type species.** *Calliopius laeviusculus* (Krøyer, 1838).

***Calliopius ulleungensis* sp. nov.**

<https://zoobank.org/85C8913F-106E-435B-9D09-456EEC991326>

Figs 2–6

**Korean name: Ul-leung- kal-li-o-pe-yeop-sae-u, new**

**Type material. Holotype:** • ♂, 13.6 mm, dissected (appendages on one slide), MABIK CR00257942, South Korea: Ulleungdo Island (site 1), Gyeongsangbuk-do, 37°30'30"N, 130°58'12"E, collected from floating algae (*Sargassum horneri*) K.W. Kim leg., 24 May 2023. **Paratypes:** • 1 ♀, 11.5 mm, dissected (appendages on one slide), DKUAMP202408; • 9 ♂♂, 28 ♀♀, DKUAMP202409, same station data as holotype.

**Additional material.** • 2 ♂♂, 8 ♀♀ Ulleungdo Island (site 2), Gyeongsangbuk-do, 37°32'33"N, 130°50'28"E, collected by conical net, K.W. Kim leg., 23 May 2023; • 1 ♂, Taeha-ri, Seo-myeon, Ulleungdo Island, Gyeongsangbuk-do, 37°30'52"N, 130°47'36"E, collected by hand net, Y.H. Kim leg., 24 May 2023; • 5 ♂♂, 10 ♀♀ Bongpo-ri, Toseong-myeon, Goseong-gun, Gangwon-do, 38°14'32"N, 128°34'28"E, collected from brown algae, Y.H. Kim leg., 20 Jul 2023.

**Diagnosis.** Eyes well developed, subrectangular. Antenna 1 calceolate, peduncular article 3 with distoventral process; flagellum callynophorate, longer than peduncle. Antenna 2 calceolate, densely setose, slightly flattened; gland cone bluntly pointed; flagellum longer than peduncle. Mandibles, incisor with six-seven dentate, lacinia mobilis on both sides, molar triturative. Gnathopods subchelate, moderate, subsimilar; propodus ovoid, palmar margin with numerous setae, six strong robust spines, palmar corner with four medial robust spines; dactylus falcate. Uropod 3 rami foliaceous. Telson linguiform, entire.

**Description. Holotype, adult male,** MABIK CR00257942.

**Body** (Figs 2A, 3A) 13.6 mm long, pleonite 7–urosome 2 weakly carinated, laterally compressed; eyes well developed, subrectangular.

**Epimera** (Fig. 3B), epimeron 1 posteroventral corner minutely pointed, with marginal simple setae, 10 clusters of setae ventrally; epimeron 2 posteroventral corner pointed, with 18 clusters of setae ventrally; epimeron 3 with posteroventral cusp, 12 ventral setae.

**Antenna 1** (Fig. 3C) peduncular articles stout, cylindrical, less setose, articles 2–3 calceolate medioventrally, article 3 with obtuse short process distoventrally, length ratio of peduncular articles 1–3 = 1.00: 0.69: 0.35; flagellum longer than peduncle, 28-articulate, callynophore, two calceoli distomedially on each article from second flagellum; accessory flagellum minute.

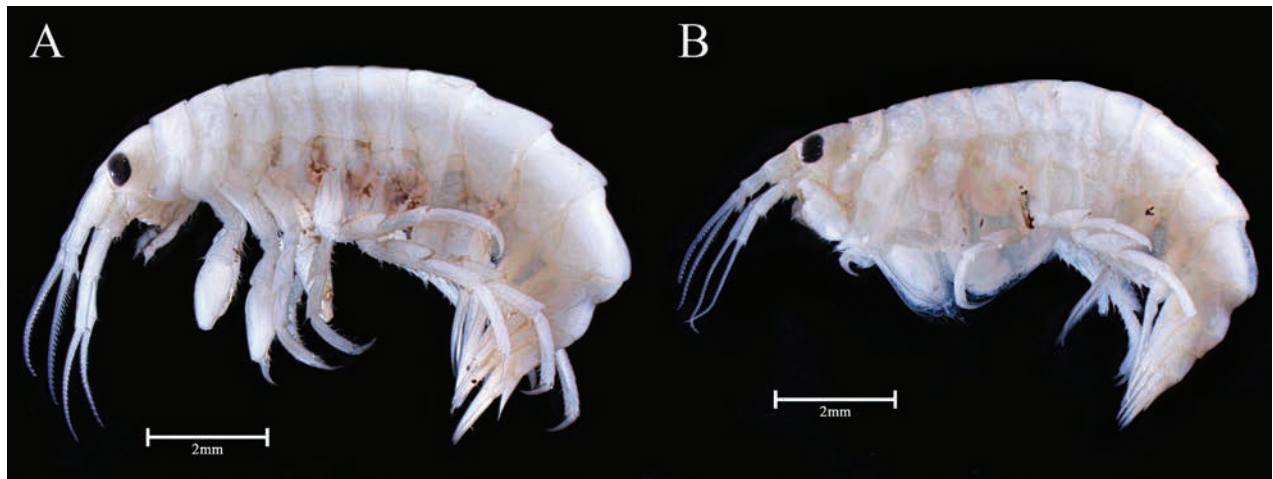


Figure 2. *Calliopius ulleungensis* sp. nov. **A** holotype male, 13.6 mm **B** paratype female, 11.6 mm. Scale bars: 2.0 mm.

**Antenna 2** (Fig. 3D) setose; peduncular articles 2–3 short, peduncular articles 3–4 with medial setal rows; peduncular article 4, half of ventrodistal portion with calceoli; peduncular article 5 slender, with two or three rows of calceoli; length ratio of peduncular articles 3–5 = 1.00: 2.11: 2.20; flagellum slightly depressed, 23-articulate, two calceoli distomedially on each article from second flagellum.

**Upper lip** (Fig. 3E) semicircular, apically round, pubescent.

**Lower lip** (Fig. 3F), inner plate indistinct, densely pubescent; outer plate distally expanded, pubescent mediodistally; mandibular process developed.

**Left mandible** (Fig. 3G), incisor with six blunt teeth, lacinia mobilis with six teeth; accessory setal row with eight setae between lacinia mobilis and molar; molar triturative surface well developed, with pappose seta; palp 3-articulate; article 1 short, distally setose; article 2 midmedially broadened, with unequal simple setae; article 3 narrowing distally, three apical setae; length ratio of articles 1–3 = 1.00: 3.51: 4.40.

**Right mandible** (Fig. 3H) similar to left mandible; incisor with seven blunt teeth, lacinia mobilis with five apical teeth; accessory setal row of seven setae between lacinia mobilis and molar.

**Maxilla 1** (Fig. 3I), inner plate subrectangular, with four pappose setae apically; outer plate, apical margin with 11 dentate setal teeth; palp biarticulate; article 1 short, unarmed; article 2 elongated ovate, swollen distally, with 11 robust setae.

**Maxilla 2** (Fig. 3J), inner plate apex and medial margins setose with a plumose seta on surface; outer plate large, broad, with row of mediodistal setae.

**Maxilliped** (Fig. 3K), inner plate subrectangular, medial margin with six plumose setae submarginally, apex with four plumose and four stout robust setae; outer plate semicircular, apex slightly beyond end of palp article 2, apex and medial margin straight with marginal blunt robust setae; palp 4-articulate, article 1 short, articles 2 with distal robust setae, article 3 distal half covered with rows of setae, article 4 falcate.

**Gnathopod 1** (Fig. 4A) subchelate, densely setose; coxa with small robust setae posteriorly; basis subrectangular, relatively long, broadened distally, anterior margin with minute setae, posterolateral margins setose, with cluster of pinnate setae posterodistally; ischium short, 0.27× basis, with distal setae; merus subtriangular, 0.41× basis; carpus with subtriangular posterior lobe, with

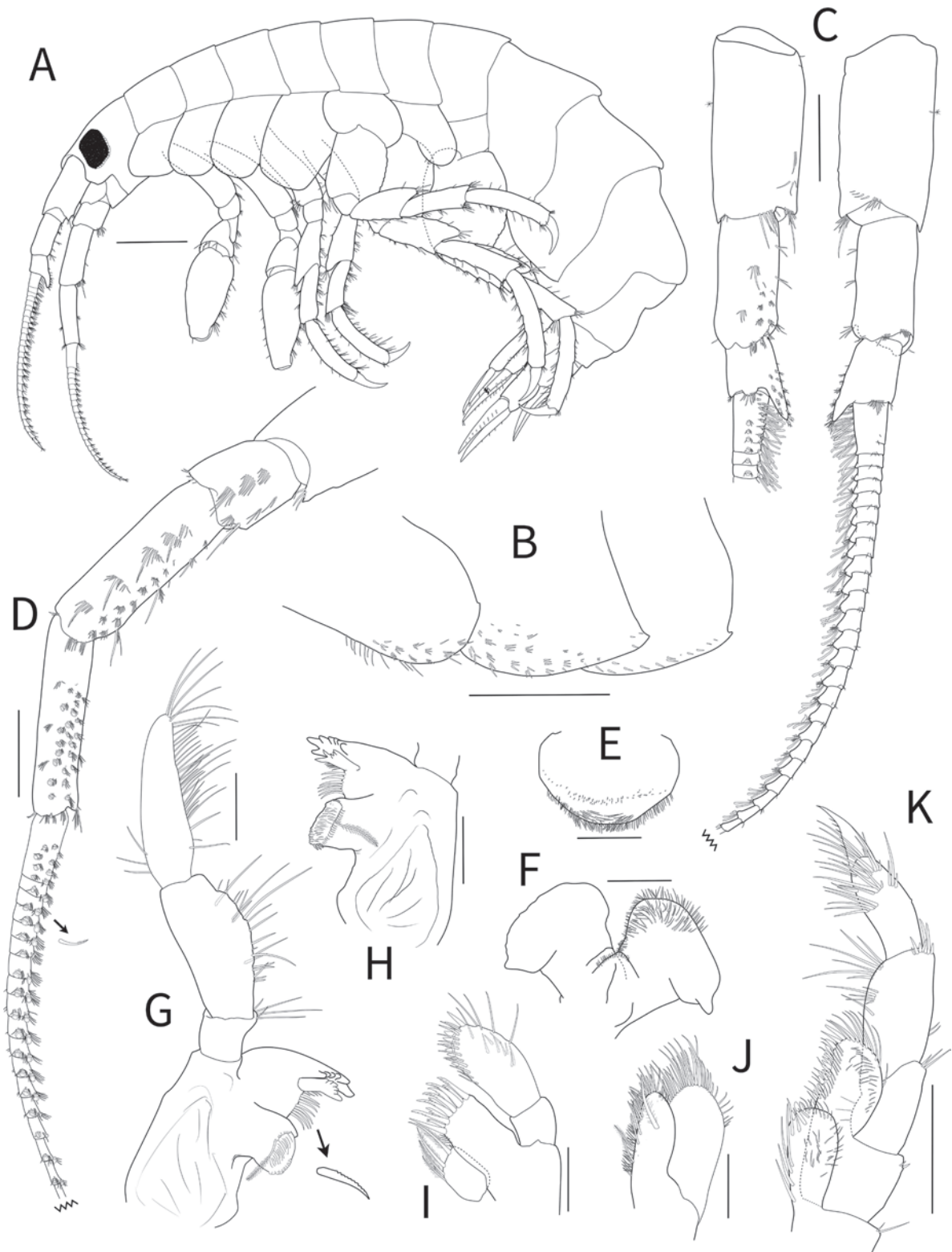


**Figure 3.** *Calliopius ulleungensis* sp. nov. holotype male, 13.6 mm **A** habitus **B** epimeron **C** antenna 1, medial margin and lateral margin **D** antenna 2, medial margin **E** upper lip **F** lower lip **G** left mandible **H** right mandible **I** maxilla 1 **J** maxilla 2. **K** maxilliped. Scale bars: 1.0 mm (**A**, **B**); 0.5 mm (**C**, **D**, **K**); 0.2 mm (**E**–**J**).

apical setae; propodus ovoid, longer than basis; palmar margin with numerous plumose setae, with six strong robust spines, palmar corner with four medial robust spines; dactylus elongated, falcate, 0.55× propodus.

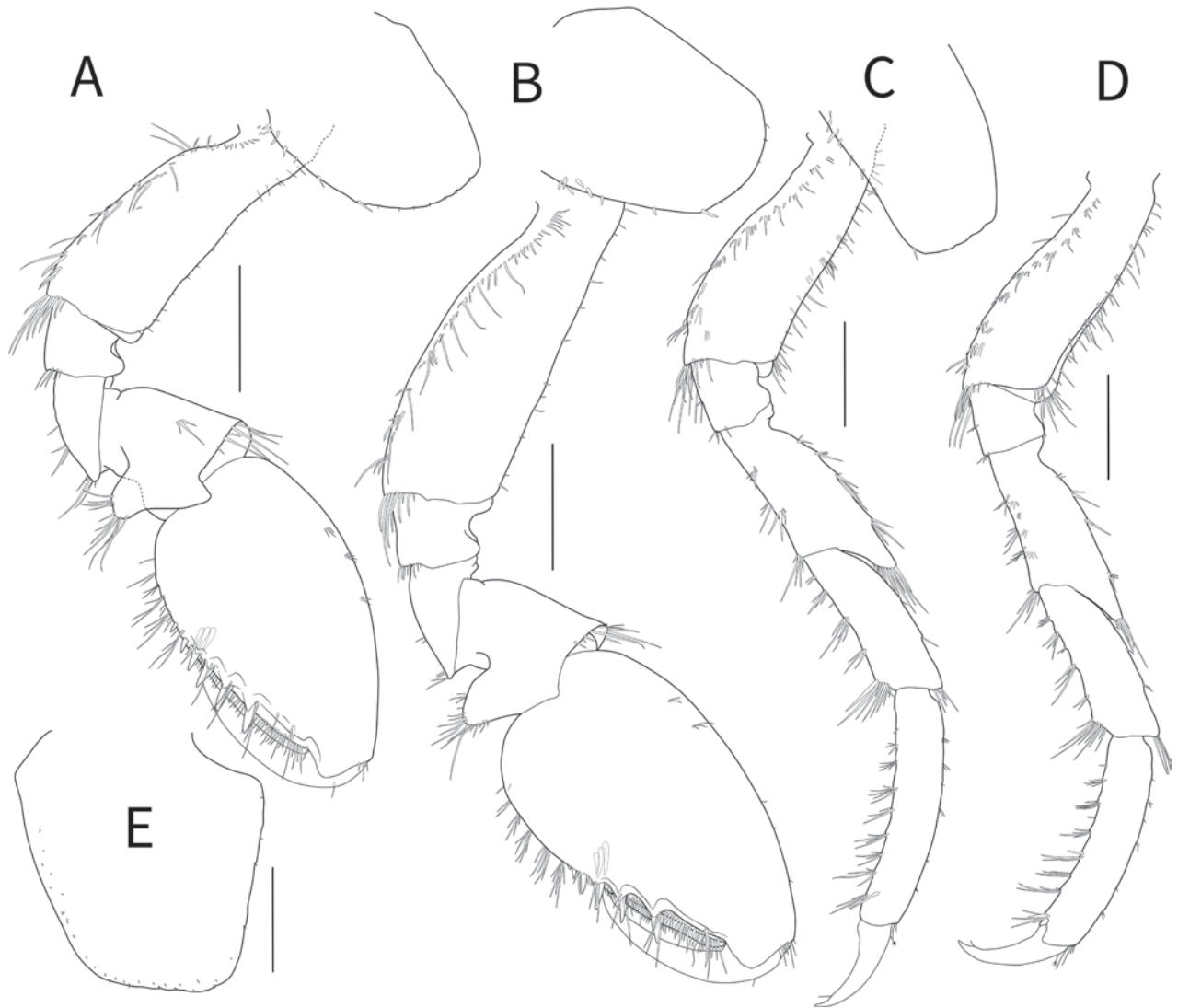


**Figure 4.** *Calliopiopus ulleungensis* sp. nov. holotype male, 13.6 mm **A** gnathopod 1 **B** gnathopod 2 **C** pereopod 3 **D** pereopod 4 **E** coxa 4, left. Scale bars: 0.5 mm.

**Gnathopod 2** (Fig. 4B) subsimilar to gnathopod 1 but elongated; basis 1.1× that of gnathopod 1; propodus slightly longer; palmar corner with five medial robust spines.

**Pereopod 3** (Fig. 4C) setose; basis subsimilar to that of gnathopod 1, anterior margin setose, merus with four cluster of robust setae, produced anterodistally with cluster of seta; carpus subrectangular, expanded distally, with postero-marginal cluster of thick setae; propodus rectangular, slightly convex; dactylus falcate, length ratio of basis–dactylus = 1.00: 0.22: 0.75: 0.65: 0.89: 0.37.

**Pereopod 4** (Fig. 4D) similar to pereopod 3, slightly shortened. coxa (Fig. 4E) broad; length ratio of basis–dactylus = 1.00: 0.31: 0.77: 0.74: 0.89: 0.38.

**Pereopod 5** (Fig. 5A), coxa bilobate, wider than long; basis subrectangular, expanded posteroventally with 10 minute setae, anterior margin with marginal short robust setae and distal long robust setae; ischium subquadrate; with antero-marginal robust setae; merus with robust setae on both margin, produced posterodistally, with cluster of seta; carpus subrectangular, expanded distally; propodus rectangular, slightly convex; dactylus falcate, length ratio of basis–dactylus = 1.00: 0.24: 0.77: 0.85: 1.06: 0.45.

**Pereopod 6** (Fig. 5B) similar to pereopod 5, posterior lobe distally elongated, basis broader than that of pereopod 5, anterolateral margin with row of setae; length ratio of basis–dactylus = 1.00: 0.22: 0.79: 0.85: 1.06: 0.45.

**Pereopod 7** (Fig. 5C) similar, but longer than either pereopods 5 or 6; basis broad, twice the area of that of pereopod 5, posterior lobe over end of ischium, anterodistal margin with short robust setae; length ratio of basis–dactylus = 1.00: 0.18: 0.70: 0.79: 1.01: 0.32.

**Uropod 1** (Fig. 5D), peduncle subrectangular, each margin with dorsal row of robust setae.; outer ramus  $\times 0.40$  peduncle, with 11 robust setae on laterally, four robust setae on medially, two robust setae on apex; inner ramus  $\times 0.5$  peduncle, with nine dorsolateral robust setae and seven dorsomedial robust setae, apex on two robust setae.

**Uropod 2** (Fig. 5E), peduncle subrectangular; outer ramus  $0.86\times$  peduncle, with seven dorsolateral robust setae and five dorsomedial robust setae, apex on two robust setae; inner ramus  $1.45\times$  peduncle, with 14 dorsolateral robust setae and nine dorsomedial robust setae, apex on two robust setae.

**Uropod 3** (Fig. 5F). peduncle short, both rami foliaceous; outer ramus  $1.62\times$  peduncle, with 11 dorsolateral and 14 dorsomedial robust setae; inner ramus subequal to outer ramus, with 21 dorsolateral and 9 dorsomedial robust setae.

**Telson** (Fig. 5G) linguiform, entire, 1.61 times as long as wide, with 2 setules on each side.

**Paratype, adult ovigerous female**, DKUAMP202408.

**Body** (Figs 2A, 6A) 11.6 mm long, laterally plump, coxae broader than male.

**Antenna 1** (Fig. 6B) similar to that of male, peduncular articles shortened; length ratio of peduncular articles 1–3 = 1.00: 0.65: 0.32; flagellum 28-articulate.

**Antenna 2** (Fig. 6C) similar to that of male, peduncular articles shortened; length ratio of peduncular articles 3–5 = 1.00: 1.58: 1.60; flagellum 25-articulate.

**Gnathopod 1** (Fig. 6D) similar to that of male but reduced, more setose; propodus ovoid, longer than basis; palmar margin with numerous plumose setae, six strong robust spines, palmar corner with four medial robust spines.

**Gnathopod 2** (Fig. 6E) subsimilar to gnathopod 1 but elongated; coxa expanded, similar in length with basis; basis  $1.1\times$  that of gnathopod 1; propodus slightly longer; palmar margin with numerous plumose setae, seven strong robust spines, palmar corner with four medial robust spines.

**Remarks.** *Calliopius ulleungensis* sp. nov. resembles several Pacific region species, *C. behringi* Gurjanova, 1951 from King Island, Bering Sea, *C. pacificus* Bousfield & Hendrycks, 1997 from Alaska, USA, and *C. carinatus* Bousfield & Hendrycks, 1997 and *C. columbianus* Bousfield & Hendrycks, 1997 both from British Columbia, Canada, in having two to numerous rows of calceoli on the peduncular articles on the antennae. Among them, *C. behringi* and *C. carinatus* can be easily distinguished by their strong body carination, elongated posterodistal process on antenna 1 peduncular article 3.

In general, *Calliopius ulleungensis* sp. nov. is similar to *C. columbianus*. However, the new species can be distinguished from *C. columbianus* by the following characteristics (*C. columbianus* characters in parentheses): 1) eyes subrectangular (vs ovate); 2) antenna 1, posterodistal process of peduncular article 3 reaching half of flagellar article 1 (vs reaching the end of flagellar article 1); 3) antennae flagellum with fewer than 30 articles (vs with more than 30 articles, up

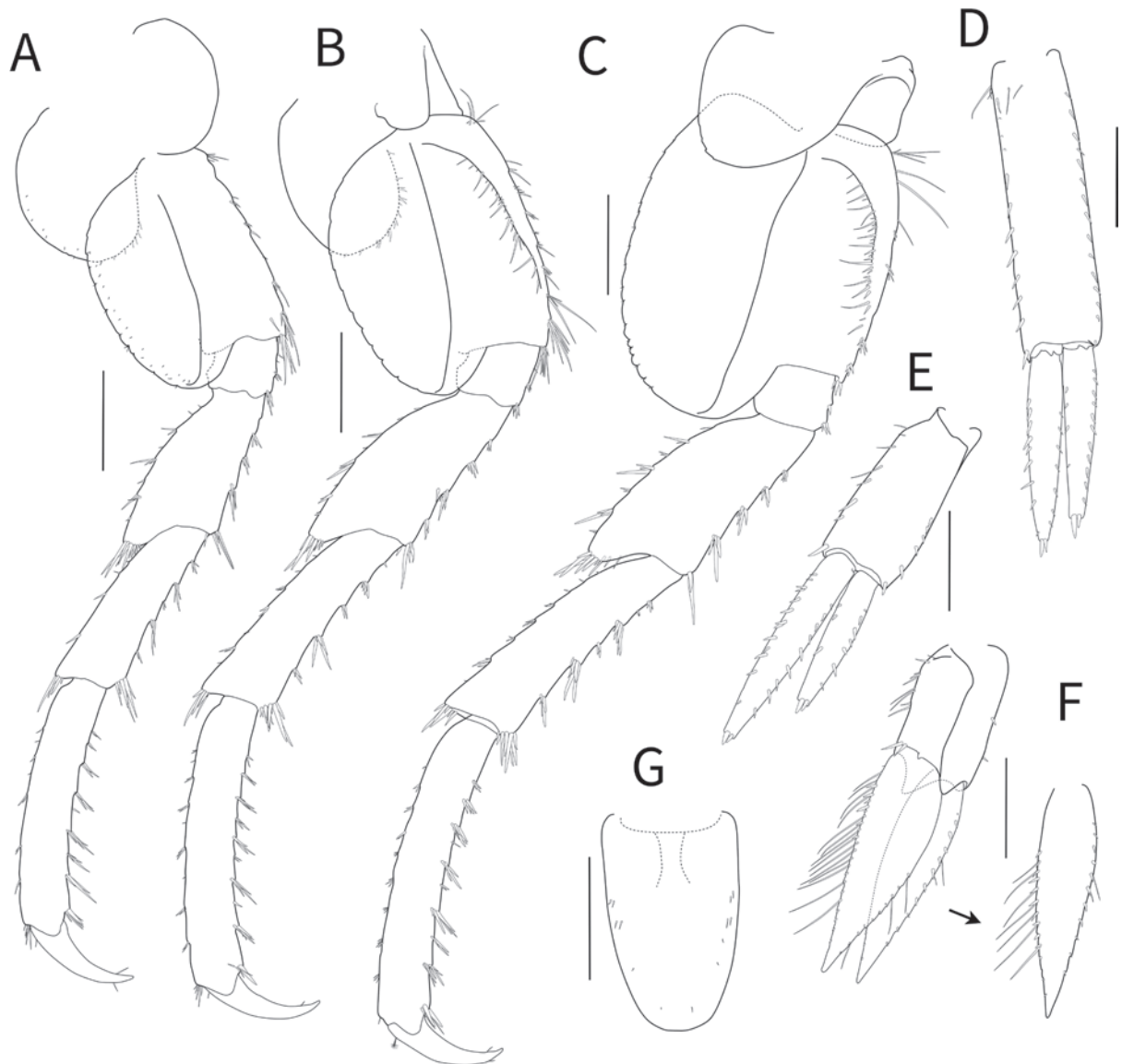


**Figure 5.** *Calliopius ulleungensis* sp. nov. holotype, male, 13.6 mm **A** pereopod 5 **B** pereopod 6 **C** pereopod 7 **D** uropod 1 **E** uropod 2 **F** uropod 3, outer ramus **G** telson. Scale bars: 0.5 mm.

to 40); and 4) maxilla 1, inner plate with 4 apical pappose setae (vs with 5 apical pappose setae). *Calliopius ulleungensis* is geographically close to *C. ezoensis*. The collection sites of *C. ezoensis* are on the southern and northeastern coasts of Hokkaido (Shimoji et al. 2020), connected to the collection site of *C. ulleungensis* across the Tugaru Strait and La Pérouse Strait. The females of both species are morphologically similar, with two or more rows of calceoli and a short process on the third article of antenna 1 peduncle. However, the new species can be distinguished from *C. ezoensis* by the following characteristics (*C. ezoensis* characters in parentheses): 1) male antennae with two or more rows of calceoli (vs one row of calceoli); 2) male gnathopod 2 larger than gnathopod 1 (vs gnathopod 1 larger than gnathopod); 3) in female antenna 2 peduncular article 4–5, rows of calceoli start from 1/4 of the basal (vs from half of the basal).

**Etymology.** The species name is derived from the type locality, Ulleungdo Island located off the East Sea of Korea.

**Distribution.** Korea (Gangwon-do, Ulleungdo Island, East Sea).

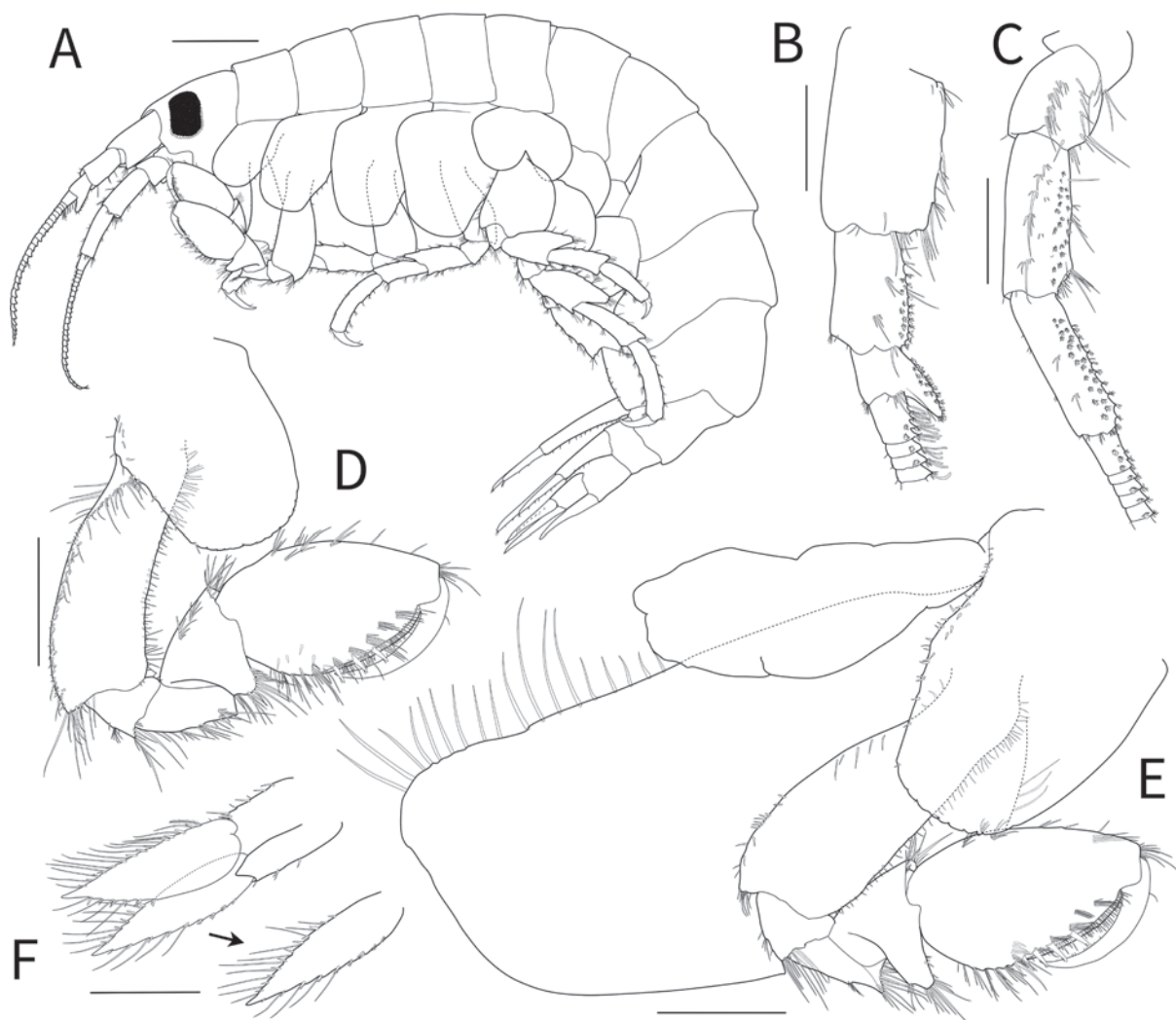


Figure 6. *Calliopius ulleungensis* sp. nov. paratype, female, 11.6 mm A habitus B antenna 1, medial margin C antenna 2, medial margin D gnathopod 1 E gnathopod 2 F uropod 3. Scale bars: 1.0 mm (A); 0.5 mm (B–F).

**Key to species of the genus *Calliopius* from Western Pacific (modified from Bousfield and Hendrycks 1997)**

- 1 Pacific (Antennae, calceoli present in one or two rows on posterior surface of peduncular articles, especially in females).....2
- Atlantic (Antennae, calceoli present in two to several rows on posterior surface of peduncular articles, especially in females) .....7
- 2 Antenna 1, posterodistal process of peduncular article 3 elongate, extending along 4–6 basal flagellum; uropod 2, outer ramus short, 0.5× inner ramus ..... ***Calliopius behringi* Gurjanova, 1951**
- Antenna 1, posterodistal process of peduncular article 3 short, not extending or reaching end of flagellar article 1; uropod 2, outer ramus moderate, 0.7× inner ramus) ..... **3**
- 3 Pereonite 5 to pleonite 2 distinctly carinate, with dorsal tubercles; epimeron 2, facial setae in 5–7 submarginal rows..... ***C. carinatus* Bousfield & Hendrycks, 1997**
- Pereonites to pleonites not or weakly carinate, without dorsal tubercles; epimeron 2, facial setae in two or three submarginal rows..... **4**

- 4 Antennal flagella short (<20 articles); pereopods 5–7, dactyli large, heavy, > 1/3 length of propodus; maxilla 1, inner plate with 2 apical setae..... **C. pacificus Bousfield & Hendrycks, 1997**
- Antennal flagella elongate (>20 articles); pereopods 5–7, dactyli small, < 1/3 length of propodus; maxilla 1, inner plate with four or five apical setae..... **5**
- 5 Antenna 1, posterodistal process of peduncular article 3 reaching distal end of flagellar article 1; antennal flagella over 30 articles..... **C. columbianus Bousfield & Hendrycks, 1997**
- Antenna 1, posterodistal process of peduncular article 3 not reaching end of flagellar article 1; antennal flagella usually 30 articles ..... **6**
- 6 Eye ovate; gnathopod 1 distinctly larger than 2 in male; uropod 3, outer ramus with seven laterally marginal robust setae..... **C. ezoensis Shimoji, Nakano & Tomikawa, 2020**
- Eye subrectangular; gnathopod 1 slightly smaller than 2 in male; uropod 3, outer ramus with 11 laterally marginal robust setae... **C. ulleungensis sp. nov.**
- 7 Uropod 3, rami conspicuously setose on inner and outer margins..... **8**
- Uropod 3, rami conspicuously setose on inner margin only..... **9**
- 8 Antenna 1, posterodistal process of peduncular article 3 elongate, exceeding flagellar article 1; epimeron 2, facial spines in submarginal row... **C. laeviusculus (Krøyer, 1838)**
- Antenna 1, posterodistal process of peduncular article 3 short, length < flagellar article 1; epimeron 2, facial spines in three submarginal rows ..... **C. sablensis Bousfield & Hendrycks, 1997**
- 9 Coxae 1–4, distal margin distinctly crenulate; pereopods 5–7, dactyli strong, length > 1/3 propodus ..... **C. crenulatus Chevreux & Fage, 1925**
- Coxae 1–4, distal margin nearly smooth; pereopods 5–7, dactyli short, slender, length < 1/3 propodus..... **C. rathkii (Zaddach, 1844)**

## Acknowledgements

We would like to express our sincere gratitude to Editor Dr Rachael Peart, National Institute of Water and Atmospheric Research (NIWA), Wellington, New Zealand, for their valuable guidance and constructive feedback during the review process. We also greatly appreciate the suggestions and comments given from reviewers: Dr Alan Myers National University of Ireland, Cork, Ireland, and Dr Azman Abdul Rahim of the Marine Ecosystem Research Centre (EKOMAR), Malaysia. Their helpful comments greatly improved the manuscript.

## Additional information

### Conflict of interest

The authors have declared that no competing interests exist.

### Ethical statement

No ethical statement was reported.

### Funding

This work was supported by the management of Marine Fishery Bio-resources Center (2024) funded by the National Marine Biodiversity Institute of Korea (MABIK).

## Author contributions

Kyung-Won Kim: Specimen collection; species identification; original draft writing; illustrations and measurements. Young-Hyo Kim: Conceptualization; species identification; funding acquisition; project administration; review and editing.

## Author ORCIDs

Kyung-Won Kim  <https://orcid.org/0000-0003-2152-9555>

Young-Hyo Kim  <https://orcid.org/0000-0002-7698-7919>

## Data availability

All of the data that support the findings of this study are available in the main text.

## References

- Barnard JL, Karaman GS (1991) The families and genera of marine gammaridean Amphipoda (except marine gammaroids). Record of the Australian Museum, Supplement 13, 866 pp. <https://doi.org/10.3853/j.0812-7387.13.1991.367>
- Bate CS (1857) A synopsis of the British edriophthalmous Crustacea—Part I. Amphipoda. The Annals and Magazine of Natural History (Series 2) 19: 135–152. <https://doi.org/10.1080/00222935708697715>
- Bousfield EL, Hendrycks EA (1997) The amphipod superfamily Eusiroidea in the North American Pacific Region. II. Family Calliopiidae. Systematics and distributional ecology. Amphipacifica 2(3): 3–66.
- Horton T, Lowry J, De Broyer C, Bellan-Santini D, Coleman CO, Corbari L, Costello MJ, Danieli M, Dauvin JC, Fišer C, Gasca R, Grabowski M, Guerra-García JM, Hendrycks E, Hughes L, Jaume D, Jazdzewski K, Kim YH, King R, Krapp-Schickel T, LeCroy S, Lörz AN, Mamos T, Senna AR, Serejo C, Sket B, Souza-Filho JF, Tandberg AH, Thomas JD, Thurston M, Vader W, Väinölä R, Vonk R, White K, Zeidler W (2024) World Amphipoda Database. *Calliopius* Lilljeborg, 1865. Accessed through: World Register of Marine Species <https://www.marinespecies.org/aphia.php?p=taxdetails&id=101511> [2024-08-01]
- Kröyer H (1838) Grönlands Amphipoder. Det Kongelige Danske Videnskabernes Selskabs Naturvidenskabelige og Mathematisk Afhandlinger, Series 4 7: 229–326. [pls 1–4] <https://doi.org/10.5962/bhl.title.13024>
- Latreille PA (1816) Nouveau Dictionnaire d'histoire naturelle, appliquée aux arts, à l'Agriculture, à l'Economie rurale et domestique, à la Médecine, etc. Par une Société de Naturalistes et d'Agriculteurs. Vol. 1. Nouvelle Édition. Deterville, Paris, 467–469.
- Lilljeborg W (1865) On the *Lysianassa magellanica* H. Milne Edwards, and on the Crustacea of the suborder Amphipoda and subfamily Lysianassina found on [sic] the coast of Sweden and Norway. Nova Acta Regiae Societatis Scientiarum Upsaliensis 6(1): 1–38. [pls 1–5] <https://doi.org/10.5962/bhl.title.6806>
- Lowry JK, Myers AA (2013) A phylogeny and classification of the Senticaudata suborder. (Crustacea: Amphipoda). Zootaxa 3610(1): 1–80. <https://doi.org/10.11646/zootaxa.3610.1.1>
- Sars GO (1893) Amphipoda. Part XIX. Pardaliscidae (concluded), Eusiridae. An account of the Crustacea of Norway, with short descriptions and figures of all the species. Vol. I. A. Cammermeyer, Christiania 413–432. [pls 145–152]
- Shimoji R, Nakano T, Tomikawa K (2020) A new species of *Calliopius* (Crustacea: Amphipoda: Calliopiidae) from Japan. Proceedings of the Biological Society of Washington 133(1): 7–17. <https://doi.org/10.2988/20-00001>



# Integrative review of *Xylomoia strix*, *X. retinax* and *X. stangelmaieri* (Lepidoptera, Noctuidae, Xyleninae, Apameini)

Risto Haverinen<sup>1,2</sup>, Aleksander Pototski<sup>2,3</sup>, Marko Mutanen<sup>4</sup>, Darius Mikalauskas<sup>5</sup>, Roman V. Yakovlev<sup>6,7,8</sup>, Günter C. Müller<sup>9,10</sup>, Alexey M. Prozorov<sup>9,11,12</sup>, Aidas Saldaitis<sup>13</sup>

1 Ripako Oy, Vantaa, Finland

2 Estonian Society of Lepidopterologists, Tallinn, Estonia

3 Lasnamäe Gymnasium, Tallinn, Estonia

4 Ecology and Genetics Research Unit, P.O. Box 3000, FI-90014 University of Oulu, Oulu, Finland

5 Lithuanian Entomological Society, Akademijos str. 2, 08412 Vilnius-21, Lithuania

6 Laboratory of Biodiversity and Ecology, Tomsk State University, Lenina pr. 36, RUS-634050 Tomsk, Russia

7 Western Caspian University, Istiglaliyyat Street, 31. Baku 1001, Azerbaijan

8 Samarkand State University, University blv. 15, 140104 Samarkand, Uzbekistan

9 University of Sciences, Techniques and Technologies of Bamako, BP 1805 Bamako, Mali

10 Kuvim Center for the Study of Infectious and Tropical Diseases, Hadassah Medical School, The Hebrew University, Kalman Ya'akov Man St., 91120 Jerusalem, Israel

11 Ludwig-Maximilians-University of Munich, Großhaderner str. 2, D-82152 Planegg-Martinsried, Germany

12 Bavarian Natural History Collections (SNSB-ZSM), Münchhausen str. 21, D-81247 Munich, Germany

13 Nature Research Centre, Akademijos str. 2, 08412 Vilnius-21, Lithuania

Corresponding author: Risto Haverinen ([r.haverinen@luukku.com](mailto:r.haverinen@luukku.com))



Academic editor: Kevin Keegan

Received: 16 July 2024

Accepted: 25 October 2024

Published: 23 December 2024

ZooBank: <https://zoobank.org/29DE1440-2C8F-4B06-A9F9-78494E587455>

Citation: Haverinen R, Pototski A, Mutanen M, Mikalauskas D, Yakovlev RV, Müller GC, Prozorov AM, Saldaitis A (2024) Integrative review of *Xylomoia strix*, *X. retinax* and *X. stangelmaieri* (Lepidoptera, Noctuidae, Xyleninae, Apameini). ZooKeys 1221: 309–342. <https://doi.org/10.3897/zookeys.1221.132205>

Copyright: © Risto Haverinen et al.  
This is an open access article distributed under terms of the Creative Commons Attribution License (Attribution 4.0 International – CC BY 4.0).

## Abstract

The relationship of *Xylomoia strix* Mikkola, 1980; *Xylomoia retinax* Mikkola, 1998; and *Xylomoia stangelmaieri* Mikkola, 1998 is reconsidered based on 59 genitalia slides (37 males and 22 females) and 40 barcodes of adults collected from the type localities and areas in-between. Due to lack of stable morphologic differences, apart from the wing coloration of *X. retinax*, and low genetic distance between the three, they are considered as three subspecies of *X. strix*: the nominotypical one *X. strix stangelmaieri* **stat. nov.** and *X. strix retinax* **stat. nov.** Included are photographs of all specimens covering 37 adults, and 28 male and 18 female genitalia, as well as a phylogenetic tree and a map showing collecting localities.

**Key words:** DNA barcoding, European fauna, morphology, new status, Palearctic

*The article is dedicated to Kari Nupponen (15.01.1962–2.12.2021), a Finnish lepidopterologist, whose main interest was in the family Scythrididae. The first two authors of the article participated in many joint expeditions, traveling together with Kari around the world for nearly twenty years.*

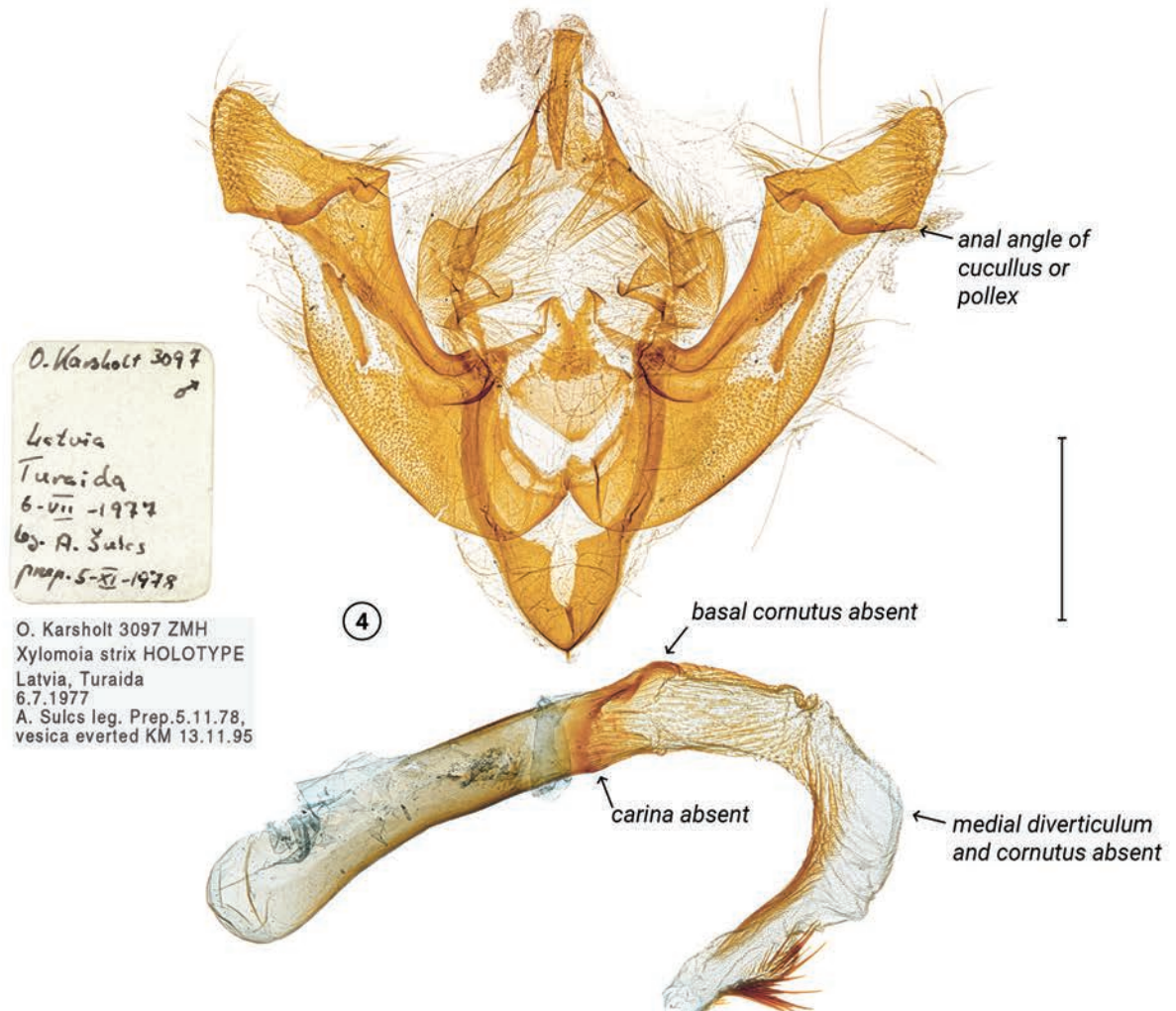
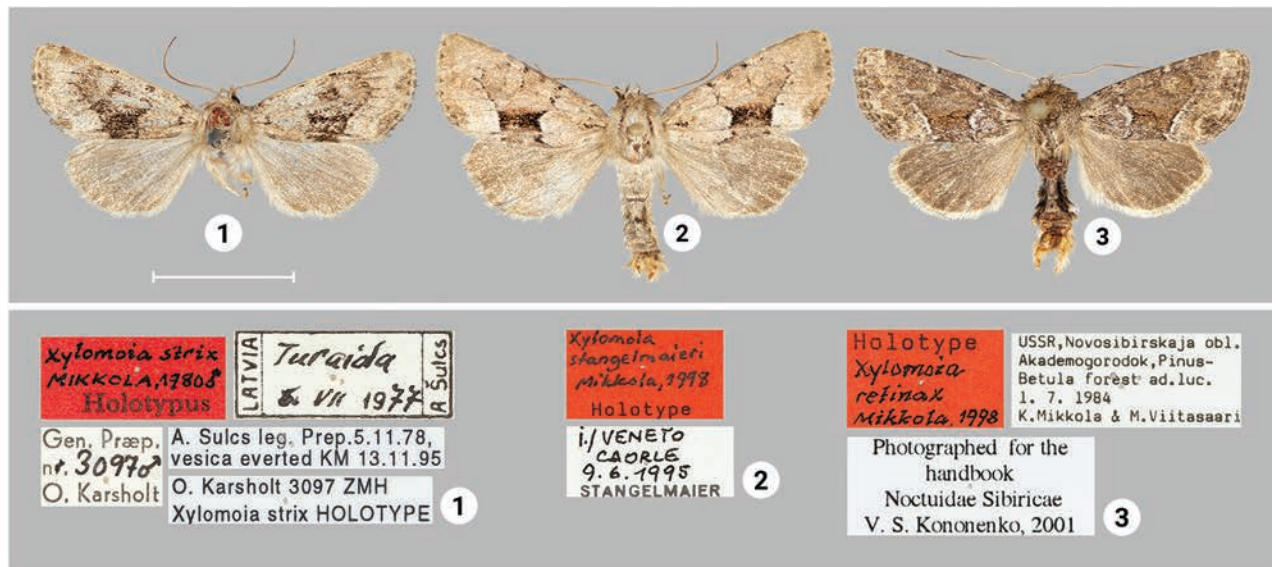
## Introduction

*Xylomoia* Staudinger, 1892 is a Holarctic genus from the tribe Apameini containing eight species (Mikkola 1998; Lafontaine and Schmidt 2010; Kononenko 2016a, 2016b): 1) *X. chagnoni* Barnes & McDunnough, 1917; type locality (TL):

Canada, “Quebec, Rouville Co. and Mt St Hilaire;” 2) *X. indirecta* (Grote, 1875); TL: Canada, “British Columbia, Vancouver Island;” 3) *X. apameoides* (Hacker, 1989); TL: Turkey, “Prov. Hakkari, Yüksekova;” 4) *X. fusei* Sugi, 1976; TL: Japan, “Gumma Pref., Itakura;” 5) *X. graminea* (Graeser, 1889); TL: “Russia, Amurland, Khabarovka;” 6) *X. strix* Mikkola, 1980; TL: “Latvia, Turaida;” 7) *X. retinax* Mikkola, 1998; TL: “Russia, Western Siberia, Akademgorodok (40 km SE Novosibirsk);” and 8) *X. stangelmaieri* Mikkola, 1998; TL: “N Italy, Venezia Giulia, Caorle.” The latter three, here termed the *strix* group, are evidently very closely related and are of particular interest.

*Xylomoia strix* is a widespread European species recorded for Finland, Estonia, Latvia, Lithuania, Poland, Belarus, Ukraine, and European Russia (Mikkola 1980; Šulcs and Šulcs 1983; Skou 1991; Nowacki and Sekuła 1994; Karvonen 1996; Klyuchko et al. 2001; Zilli et al. 2005; Savenkov and Šulcs 2010; Pekarsky and Korb 2012 as *X. retinax*; Ivinskis and Rimšaitė 2013; Sachkov 2013; Nowacki and Pałka 2014; Haverinen et al. 2016; Aarvik et al. 2017; Anikin et al. 2017; Geryak et al. 2018; Ūsaitis et al. 2019; Derzhinsky 2019; Matov et al. 2019, 2023; Bolshakov and Makarichev 2020; Haverinen et al. 2021). *Xylomoia retinax* is recorded from Irkutsk westwards to Novosibirsk, Omsk, Chelyabinsk, Yaroslavl, and is also found in Altai Republic in Russia (Mikkola 1998; Nupponen and Fibiger 2002; Sviridov 2002; Zilli et al. 2005; Knyazev et al. 2015, 2016; Volynkin and Ivanova 2016; Matov et al. 2019, 2023; Knyazev 2020). The border between two species seems to lie between the Volga River and Ural Mountains but it is not precisely defined: specimens originated from Tatarstan, Samara, and Saratov Oblasts were identified as *X. strix* (e.g., Matov et al. 2019, 2023), while specimens collected approximately 500 km eastwards from the Volga River, near Miass in Chelyabinsk Oblast, were attributed to *X. retinax* (Mikkola 1998). *Xylomoia stangelmaieri* is even rarer, it is only known from around the type locality, the Adriatic coast near Venice in northern Italy, and is unknown elsewhere (Mikkola 1998).

The primary types of *X. strix* (Fig. 1) and *X. stangelmaieri* (Fig. 2) are similar in appearance, while *X. retinax* (Fig. 3) is darker than the other two and lacks the dark contrasting pattern in the medial field of the forewing. Among the holotype males, genitalia were studied only for *X. strix*, whereas paratype males were dissected for *X. retinax* and *X. stangelmaieri*. The phallus of the holotype specimen of *X. strix* lacks “the basal cornutus/spines of the vesica, and the medial diverticulum and cornutus of it, present in all other species of the clade” (Mikkola 1998). Later publications do not contain a description of the phallus of any other *X. strix*. Phalli of the paratype males of *X. retinax* and *X. stangelmaieri*, in contrary to *X. strix*, do have the ventral spines of phallus (also called *carina*), and basal and medial cornuti – as in the original description. Instead of morphological investigation, the before-mentioned authors (except Mikkola 1998) focused on the biology and ecology of *X. strix*, leaving unclear whether its holotype exhibits a unique aberration or the species as a whole lacks the spiky features on phallus. Morphological variability of *X. retinax* and *X. stangelmaieri* also was not thoroughly studied. Sviridov (2002), for instance, mentioned that specimens of *X. retinax* from Yaroslavl Oblast have a curved medial cornutus, which he considered a potential reason to establish a new subspecies and suggested that it was in need of detailed investigation. To understand the morphological variability of each taxon, its distribution area, and taxonomic



Figures 1–4. Adults and male genitalia of *Xylomoia* spp. with labels (ZMHF). **1, 4** HT male of *X. strix*, lacking features of phallus are indicated with arrows **2** HT male of *X. stangellaieri* **3** HT male of *X. retinax*. Scale bars: 1 cm (for adults); 1 mm (for genitalia).

status, a large quantity of adults had to be accumulated. We analyze published data and add original discoveries in morphology, phylogeny, and natural history of the *X. strix* group and reconsider the systematic position of the related taxa.

Abbreviations of the depositories used:

<b>ASV</b>	collection of A. Saldaitis (Vilnius, Lithuania);
<b>CEO</b>	collection of E. Õunap (Tartu, Estonia);
<b>CJK</b>	collection of J. Karvonen (Helsinki, Finland);
<b>CKTN</b>	collection of K. & T. Nupponen (Espoo, Finland);
<b>CKP</b>	collection of K. Pałka (Lublin, Poland);
<b>CMR</b>	collection of M. Rantala (Kerava, Finland);
<b>CNC</b>	Canadian National Collection of Insects, Arachnids and Nematodes (Montreal, QC, Canada);
<b>CPI</b>	collection of P. Ivinskis (Vilnius, Lithuania);
<b>CRH</b>	collection of R. Haverinen (Vantaa, Finland);
<b>DMV</b>	collection of D. Mikalauskas (Vilnius, Lithuania);
<b>PFC</b>	Canadian Forest Service, Pacific Forestry Centre (Victoria, BC, Canada);
<b>ZMHF</b>	Zoological Museum, University of Helsinki (Finland);
<b>ZMUO</b>	collection of Zoological Museum of the University of Oulu (Finland).

Other abbreviations used:

<b>GS</b>	genitalia slide;
<b>HT</b>	holotype;
<b>PT</b>	paratype;
<b>TL</b>	type locality.

## Materials and methods

Adults were photographed with a Nikon D3300, a Nikon 40mm f/2.8G and a Nikon R1C1. Slides were photographed using a Leica MC170 HD. All images were processed with Photoshop CS6, and color plates were made with InDesign CS6.

Genitalia preparations were made following Hardwick (1950). The distal one third of the abdomen of each specimen was put into a separate 50 ml Falcon tube with 10 ml of 13% solution of potassium hydroxide (KOH). Several tubes with abdomens and KOH were placed into a small pot with hot water for 20 min. The tubes thereafter were removed from the pot and the abdomens were rinsed with water several times to remove any remaining scales and soft tissue. Cleaned abdominal parts were then transferred into separate cells of the Corning Costar 96 Well Cell Culture Cluster with a small quantity of water to keep them moist during preparation. Sequentially, abdomens were cleaned with a soft brush and dissected using Dumont Tweezers Style 5 and micro scissors in a Petri dish under the microscope. The phallus was extracted and vesica everted with an insulin syringe and a 32G or 33G needle for mesotherapy. The vesica was stained with Evans blue (Evans and Schulemann 1914; Cooksey 2013). The dissected genitalia were rinsed in 50, 70, and 96% ethanol and then mounted on a microscope slide in Euparal and covered with a cover slip. Morphological terminology partially follows Pierce (1909), Mikkola (1998), and Volynkin (2024).

**Table 1.** Data on specimens and their barcodes deposited in BOLD and used in the phylogenetic analysis.

Taxon / BIN number	#	Process ID / Sample ID	Specimen details and collecting data (depository)
<i>X. strix stangelmaieri</i> / BOLD:ABA9763	1	LEFIJ4675-16 / KN00913	male, <b>Italy</b> , Veneto, Valle Vecchia, 45.616°N, 12.916°E, 3 m, 15.04.2015, leg. R. Haverinen (CKTN)
	2	LEFIJ4676-16 / KN00914	female, <b>Italy</b> , Veneto, Valle Vecchia, 45.616°N, 12.916°E, 3 m, 15.04.2015, leg. R. Haverinen (CKTN)
	3	LEFIJ4677-16 / KN00915	male, <b>Italy</b> , Veneto, Valle Vecchia, 45.616°N, 12.916°E, 3 m, 15.04.2015, leg. R. Haverinen (CKTN)
	4	LEFIJ7558-18 / MM24198	female, <b>Italy</b> , Veneto, Valle Vecchia, 45.6167°N, 12.9333°E, 3 m, 16.04.2014, leg. R. Haverinen and M. Hirvonen (CRH)
	5	LEFIJ7559-18 / MM24199	male, <b>Italy</b> , Veneto, Valle Vecchia, 45.6167°N, 12.9333°E, 3 m, 16.04.2014, leg. R. Haverinen and M. Hirvonen (CRH)
	6	LEFIJ7560-18 / MM24200	male, <b>Italy</b> , Veneto, Valle Vecchia, 45.6167°N, 12.9333°E, 3 m, 16.04.2014, leg. R. Haverinen and M. Hirvonen (CRH)
	7	LEPAL476-17 / MM06019	female, <b>Italy</b> , Veneto, Valle Vecchia, 45.61°N, 12.93°E, 3 m, 29.06.2014, leg. R. Haverinen and M. Hirvonen (CRH)
	8	LEPAL482-17 / MM24002	male, <b>Italy</b> , Veneto, Valle Vecchia, 45.61°N, 12.93°E, 3 m, 15.06.2014, leg. R. Haverinen and M. Hirvonen (CRH)
<i>X. strix strix</i> / BOLD:ADA4423	9	LEFID225-10 / MM06083	male, <b>Latvia</b> , Turaida, leg. R. Haverinen (ZMUO)
	10	LEFIJ4666-16 / MM25269	adult, <b>Finland</b> , Nylandia, Hanko, 65.0158°N, 25.6574°E, 15.07.1994, leg. J. Karvonen (CJK)
	11	LEFIJ4668-16 / KN00906	male, <b>Latvia</b> , Turaida, 57.166°N, 24.85°E, 20 m, 30.06.2005, leg. T. Nupponen (CKTN)
	12	LEFIJ4669-16 / KN00907	female, <b>Latvia</b> , Turaida, 57.166°N, 24.85°E, 20 m, 7.07.2005, leg. K. Nupponen (CKTN)
	13	LEFIJ7512-18 / MM24023	adult, <b>Estonia</b> , Misso, 58.6481°N, 25.9169°E, 3.07.2012, leg. E. Õunap (CEO)
	14	LEFIJ7513-18 / MM24024	adult, <b>Estonia</b> , Misso, 58.6481°N, 25.9169°E, 3.07.2012, leg. E. Õunap (CEO)
	15	LEFIJ7544-18 / MM24106	larva, <b>Russia</b> , Lotoshinskiy district, Moscow region, Sevastino village, 56.3877°N, 35.7431°E, 20.08.2014, leg. A. Komrakov (ZMOU)
	16	LEFIJ7561-18 / MM24201	male, <b>Russia</b> , Saratov district, settlement Zonalny, 51.5833°N, 46.1°E, 15 m, 16.05.2014, leg. R. Haverinen and A.Belik (CRH)
	17	LEFIJ7562-18 / MM24202	male, <b>Russia</b> , Saratov district, settlement Zonalny, 51.5833°N, 46.1°E, 15 m, 16.05.2014, leg. R. Haverinen and A.Belik (CRH)
	18	LEFIJ7563-18 / MM24203	female, <b>Russia</b> , Saratov district, settlement Zonalny, 51.5833°N, 46.1°E, 15 m, 16.05.2014, leg. R. Haverinen and A.Belik (CRH)
	19	LEFIJ7564-18 / MM24204	female, <b>Russia</b> , Saratov district, settlement Zonalny, 51.5833°N, 46.1°E, 15 m, 16.05.2014, leg. R. Haverinen and A.Belik (CRH)
	20	LEFIJ7565-18 / MM24205	female, <b>Russia</b> , Saratov district, settlement Zonalny, 51.5833°N, 46.1°E, 15 m, 16.05.2014, leg. R. Haverinen and A.Belik (CRH)
	21	LEFIJ21338-21 / MM27347	male, <b>Russia</b> , Orenburgskaya Oblast, near Kuvandyk village, 225 m, 25.06.2019, leg. M. Rantala (CMR)
	22	LEFIJ21339-21 / MM27348	female, <b>Russia</b> , Orenburgskaya Oblast, near Kuvandyk village, 225 m, 25.06.2019, leg. M. Rantala (CMR)
	23	LEPAL477-17 / MM06020	male, <b>Poland</b> , Skvyhiozyn, 52.0685°N, 19.4357°E, 16.04.2014, leg. K. Pałka (CKP)
	24	LEPAL478-17 / MM06021	male, <b>Poland</b> , Skvyhiozyn, 52.0685°N, 19.4357°E, 20.05.2013, leg. K. Pałka (CKP)
	25	LEPAL479-17 / MM06022	male, <b>Poland</b> , Malice, 52.0685°N, 19.4357°E, 23.05.2014, leg. K. Pałka (CKP)
	26	LEPAL480-17 / MM06023	male, <b>Poland</b> , Malice, 52.0685°N, 19.4357°E, 16.05.2014, leg. K. Pałka (CKP)
	27	LEPAL481-17 / MM24001	male, <b>Estonia</b> , vs Valga, Koiva River, Koikküla, 57.63 N, 26.23 E, 16.05.2014, leg. R. Haverinen (CRH)

Taxon / BIN number	#	Process ID / Sample ID	Specimen details and collecting data (depository)
<i>X. strix strix</i> / BOLD:ADA4423	28	LEPAL483-17 / MM24003	female, <b>Estonia</b> , Põlvamaa, Veski, 57.83°N, 27.51°E, 15.06.2014, leg. R. Haverinen (CRH)
	29	LEPAL484-17 / MM24004	male, <b>Estonia</b> , Põlvamaa, Veski, 57.83°N, 27.51°E, 16.04.2014, leg. R. Haverinen (CRH)
	30	LEPAL485-17 / MM24005	female, <b>Russia</b> , Saratov district, settlement Zonalny, 51.58°N, 46.1°E, 20.06.2014, leg. R. Haverinen, K. Nupponen, A. Pototski and A. Belik (CRH)
	31	LEPAL486-17 / MM24006	male, <b>Russia</b> , Saratov district, settlement Zonalny, 51.58°N, 46.1°E, 20.06.2014, leg. R. Haverinen, K. Nupponen, A. Pototski and A. Belik (CRH)
	32	LEPAL487-17 / MM24007	male, <b>Estonia</b> , Saaremaa, Kogula, 58.28°N, 22.25°E, 19.06.2014, leg. R. Haverinen (CRH)
	33	LEPAL488-17 / MM24008	male, <b>Estonia</b> , Saaremaa, Kogula, 58.28°N, 22.25°E, 19.06.2014, leg. R. Haverinen (CRH)
	34	LEPAL489-17 / MM24021	larva, <b>Estonia</b> , Koiva River, Koikküla, 58.6481°N, 25.9169°E, 24.08.2014, leg. R. Haverinen (CRH)
<i>X. strix retinax</i> / BOLD:ADA4423	35	LEFIJ4670-16 / KN00908	male, <b>Russia</b> , Novosibirsk district, Novosibirsk, Akademgorodok, 59.0394°N, 98.6705°E, 110 m, 13.09.2014, leg. R. Haverinen and A. Pototski (CKTN)
	36	LEFIJ4671-16 / KN00909	male, <b>Russia</b> , Novosibirsk district, Novosibirsk, Akademgorodok, 59.0394°N, 98.6705°E, 110 m, 13.09.2014, leg. R. Haverinen and A. Pototski (CKTN)
	37	LEFIJ4672-16 / KN00910	female, <b>Russia</b> , Novosibirsk district, Novosibirsk, Akademgorodok, 59.0394°N, 98.6705°E, 110 m, 13.09.2014, leg. R. Haverinen and A. Pototski (CKTN)
	38	LEFIJ4673-16 / KN00911	male, <b>Russia</b> , Novosibirsk district, Novosibirsk, Akademgorodok, 59.0394°N, 98.6705°E, 110 m, 13.09.2014, leg. R. Haverinen and A. Pototski (CKTN)
	39	LEFIJ4674-16 / KN00912	female, <b>Russia</b> , Novosibirsk district, Novosibirsk, Akademgorodok, 59.0394°N, 98.6705°E, 110 m, 13.09.2014, leg. R. Haverinen and A. Pototski (CKTN)
	40	LEFIJ7511-18 / MM24022	larva, <b>Russia</b> , Novosibirsk, 59.0394°N, 98.6705°E, leg. R. Haverinen and A. Pototski (CRH)
<i>X. graminea</i> / BOLD:ADN5882	41	LEFIJ7545-18 / MM24107	male, <b>Lithuania</b> , Kalniskes, 55.2944°N, 23.946°E, 21.06.2013, leg. P. Ivinskis (ZMUO)
	42	LEFIJ7546-18 / MM24108	<b>Lithuania</b> , Kalniskes, 55.2944°N, 23.946°E, 21.06.2013, leg. P. Ivinskis
<i>X. chagnoni</i> / BOLD:AAE4227	43	RDNMG580-08 / CNC LEP00052404	adult, <b>Canada</b> , Ontario, Stittsville, 45.2005°N, 75.98°W, 131.066 m, 4.07.2003, leg. J. Troubridge (CNC)
	44	RDNMG581-08 / CNC LEP00052405	adult, <b>Canada</b> , Ontario, Stittsville, 45.2005°N, 75.98°W, 131.066 m, 15.07.2003, leg. J. Troubridge (CNC)
<i>X. indirecta</i> / BOLD:AAB1776	45	LHLEP387-06 / UBC- 2006-1537	male, <b>Canada</b> , British Columbia, Maple Ridge, UBC Research Forest, 49.266°N, 122.573°W, 158 m, 1.08.2006, leg. A. Li and J. Derhousoff (PFC)
	46	LHLEP388-06 / UBC- 2006-1538	male, <b>Canada</b> , British Columbia, Maple Ridge, UBC Research Forest, 49.266°N, 122.573°W, 158 m, 1.08.2006, leg. A. Li and J. Derhousoff (PFC)

COI barcodes of 46 specimens from BOLD projects were used for this study (Ratnasingham and Hebert 2007, 2013). The samples were collected in seven countries and stored in nine entomological collections (Table 1). One leg from each individual was used for analysis. Legs were stored in tubes with 96% ethanol. The sequences were obtained at the Biodiversity Institute of Ontario, Canada. DNA isolation, PCR amplification, and DNA sequencing followed standard protocols (Hebert et al. 2003; deWaard et al. 2008).

Sequence alignment and calculation of pairwise distances were conducted using MEGA X (Kumar et al. 2018). Maximum Likelihood (ML) analysis of the aligned COI sequences was conducted using IQ-TREE 2.2.0 (Minh et al. 2020) under HKY+F+I nucleotide substitution model as preferred to by ModelFinder (Kalyaanamoorthy et al. 2017), and with 1000 ultrafast bootstrap replicates.

The tree rooted to *X. chagnoni* + *X. indirecta* was constructed using FigTree 1.4.4 and polished with CorelDraw 24.5.0.731 and InDesign CC 2019.

Map of ecoregions was taken from ecoregions.appspot.com (see Dinerstein et al. 2017).

## Review of morphology

**Wing coloration** (Figs 1–3, 5–41). In general, two types of wing coloration are distinguished: 1) *X. stangelmaieri* + *X. strix* with a dark area in the medial field, and 2) *X. retinax* without a dark area in the medial field. *Xylomoia stangelmaieri* has a narrow blackish streak with reddish brown margins (Figs 5–10), whereas *X. strix* has this streak varying from narrow to wide with more or less pronounced reddish-brown edges. It may expand towards the costa covering medial field (Figs 11–15, 19, 26). Otherwise, all three species are similar. Tinge of wing coloration does vary from greyish to brownish even in adults collected from the same location. This may be due to some variety of mineral composition of the soil that is picked up by the host plant.

**Male genitalia** (Figs 42–68). Four of the five genitalia of *X. stangelmaieri* exhibit an anal angle of cucullus (*pollex* sensu Pierce 1909; also see Volynkin 2024) which is better pronounced than in *X. strix* and *X. retinax* (also see Mikola 1998). In addition, the shape of the uncus, valva, and saccus as well as the presence or absence of a carina, the basal or medial cornuti on the phallus vary within each species. Such variability is not exclusive for *Xylomoia* and is known for other Apameini like *Hydraecia* Guenée, 1841 and *Photedes* Lederer, 1857.

**Female genitalia** (Figs 69–89). *Xylomoia retinax* lacks fold of ductus bursae (Figs 87–89), whereas both *X. stangelmaieri* and *X. strix* exhibit it. Otherwise, shape of the bursa copulatrix and number of signa vary within each species.

*Xylomoia retinax* is distinguished from *X. stangelmaieri* and *X. strix* by lack of dark medial field on forewing and lack of fold of ductus bursae in female genitalia; *X. stangelmaieri* is distinguished from *X. strix* and *X. retinax* by a better pronounced pollex on the cucullus (four studied genitalia out of five).

## Review of phylogeny

The Maximum Likelihood (ML) tree revealed five well-defined clusters (Fig. 90): 1) *X. stangelmaieri*, 2) *X. strix* + *X. retinax*, 3) *X. graminea*, 4) *X. chagnoni*, and 5) *X. indirecta*. Each of them has high bootstrap value above 80. Both clusters of *X. stangelmaieri* and *X. strix* + *X. retinax* have several weakly supported sub-clusters that are also unsupported by morphological features or distribution.

Pairwise divergences calculated between *X. stangelmaieri* and *X. strix* vary from 1.48 to 2.3% and between *X. stangelmaieri* and *X. retinax* from 1.37 to 2.13%, whereas *X. strix* and *X. retinax* have a maximum divergence of 0.33% which is reflected in their intermixed positions on the ML tree. All three taxa have 2.13–2.63% *p*-distance from their sister species *X. graminea*. Much higher *p*-distances are calculated between the Eurasian and North American species being running as high as 6.99–8.36%, and *p*-distance between West Canadian *X. indirecta* and East Canadian *X. chagnoni* from 5.93 to 6.23%.

*Xylomoia strix* and *X. retinax* form a monophyletic clade with a maximum divergence of 0.33% within the clade, whereas *X. stangelmaieri* has an average *p*-dis-

tance of 1.84% from the clade *X. strix* + *X. retinax*; *X. graminea* is a sister species to the *X. strix* group with an average *p*-distance of 2.38%; two Canadian species have an average *p*-distance of 7.68% from European taxa and 6.08% between themselves, which is up to 2.5 times higher than between any European taxa.

## Review of natural history

*Xylomoia strix* with the closely related *X. retinax* and *X. stangelmaieri* were rather recently described and had remained enigmatic species with unknown biology. The species were only associated with wet habitats near various bodies of water without a particular host plant (Mikkola 1998). Comprehensive investigation of the biology of *X. strix* and its relatives was initiated after 2004, when RH and his daughter Inna found a connection between *X. strix* and *Equisetum hyemale*, apparently the host plant, which was later confirmed by Ahola and Silvonen (2007). Knowing that, RH and AP, together with the late Finnish lepidopterist K. Nupponen, systematically travelled across Europe and to places in Russia for nearly twenty years to unveil the biology and distribution of *X. strix* and its congeners.

Known environments inhabited by *X. strix* in Latvia, Poland, and Ukraine were wetlands, whereas in Estonia the environments were a dry forest meadow and a pine forest (Mikkola 1980; Karvonen 1996). Adults were collected in “deep, dark, wet forest areas close to rivers and or lakes [...] in late June to mid-July” (Zilli et al. 2005). The natural history and distribution of *X. strix* were thoroughly studied in Estonia, where more than 110 localities with growing *E. hyemale* were discovered (Haverinen et al. 2016). More than 80 of them were investigated by RH and AP together with K. Nupponen, and in half of them, *X. strix* was collected. Four field trips were taken to Russia in: 1) 2014 and 2) the first half of May 2015 to Saratov, where caterpillars were found on narrow stems of *E. hyemale* near a growth of *E. hyemale* where stems seemed to be too thin for caterpillars; 3) the first half of May 2015 to Moscow Oblast, where some stems of *E. hyemale* were found with holes bored by caterpillars of *X. strix*; and 4) September 2019 to Luzhsky District of Leningrad Oblast, where two populations of *E. hyemale* were found and a total of 24 caterpillars were collected, from which 16 adults later emerged (Haverinen et al. 2021). The complete life cycle of *X. strix* was described in detail by Haverinen et al. (2016).

Adults of *X. retinax* were collected in: “birch-pine forest at the verge of a slope down to a nearby creek valley” (Mikkola 1998); “old forest patch nearby moist meadow [...] in the end of June – beginning of July” (Zilli et al. 2005); “patch of mixed-grass meadow among ravines abundantly overgrown with sea buckthorn”, and “forest in front of a vast clearing with meadow vegetation” (Knyazev et al. 2015). In mid-September 2014, RH and AP travelled to Novosibirsk, Russia from where only seven specimens of *X. retinax* were known. More than one thousand caterpillars, each inside of an individual stem of long thick plants of *E. hyemale*, were found near Novosibirsk Reservoir and transported to Finland for breeding. Feeding of *X. strix* on *E. hyemale* had also been reported by Knyazev et al. (2016) and Geryak et al. (2018).

The natural history of *X. stangelmaieri* was only known from the original description. Mikkola (1998) wrote that the species was “Found in a wetland habitat on the Adriatic Coast in late May and early June. The moths were caught by light beyond the sandy coastline near marshy lagoons at sea level. The plants in this

area included the following (G. Stangelmaier, personal comm.): *Pinus pinea*, *Elaeagnus angustifolia*, *Tamarix* sp., *Rubus fruticosus*, *Aristolochia*, *Filipendula*, *Salsola*, *Suaeda*, *Arthrocnemum*, *Crithmum*, *Datura*, *Phragmites communis*, *Juncus*, *Typha latifolia* and *Scirpus*." The type locality, Valle Vecchia near Venice, Italy, remains the only known locality where *X. stangelmaieri* occurs. RH visited it for the first time in 2007 and subsequently in 2009, when knowledge about the host plant of *X. strix* was shared with G. Stangelmaier and some plants of *Equisetum* damaged by *X. stangelmaieri* were found. Wine-baited traps were set near the type locality in the last week of April 2010 by RH and his daughter, and 49 specimens of *X. stangelmaieri* were collected by J.-P. Kaitila two weeks later. In March–April 2014, RH together with M. Hirvonen found a large number of caterpillars in stems of *Equisetum* plants near Venice: most of them had been collected in a pine forest, while some had been found on dry sand dunes. In the first half of December 2014, RH and AP collected numerous plants with caterpillars and handed them to K. Silvonen and T. Nupponen for breeding. The area was visited again by RH in 2015 and K. Nupponen in 2016. At the end of March 2024 RH, AP, and I. Jürjendal went again to collect *Equisetum* plants to identify the species to which they belonged. They grow up to 150 cm long, may branch, and have thin stems so that caterpillar stretch up to 3–4 cm to fit into them. Plants appeared to be neither *Equisetum ramosissimum* nor *E. hyemale*, but, probably, a hybrid or even triploid. Caterpillars of *X. stangelmaieri* deliberately chose *E. hyemale* over another species when offered them in laboratory conditions. They hibernated from mid-November to mid-March in the middle part of the stem in contrary to *X. strix* that overwintered in the lower part of the stems under snow cover. In nature *X. stangelmaieri* may often be parasitized by *Necremnus* sp. (Eulophidae; V. Vikberg, pers. comm. 02 Mar 2015) or eaten by birds, spiders, or black ants (*Myrmica* sp.).

The natural history of other *Xylomoia* species remains relatively unknown, but even these crumbs of information are very important. Bury and Czudec (2019) reared *X. graminea*, a sister species to the *X. strix* group, on *Phragmites australis* under laboratory conditions. They noted that "Just like its related species *X. graminea* is associated with primeval moist habitats, predominantly lush sedge meadows, transitory bogs and rush communities (Buszko 2004, 2010; Bury and Zajda 2012)." Rockburne and Lafontaine (1976) stated that *X. chagnoni*'s host plant was *Phalaris arundinacea*. Both *Phragmites australis* and *Phalaris arundinacea* belong to the family Poaceae, while *E. hyemale*, the host plant of both *X. strix* and *X. retinax*, belongs to the family Equisetaceae. The only cohesive feature of Equisetaceae and Poaceae, in this case, is a meaty stem with an external hard covering suitable for caterpillars to bore through, feed, and develop inside, including safe overwintering. Otherwise, the two families are phylogenetically distant and may be a good differentiating feature to distinguish the groups of species within *Xylomoia*.

*Xylomoia strix* is included in annexes II and IV of the Council of Europe Directive 92/43/EEC of 21 May 1992 among animal species of Community importance, the preservation of which requires the designation of special protection areas and requires strict protection. In addition, *X. strix* is marked with an asterisk, which means that the species is of a primary importance among the species whose preservation requires the creation of special protected areas (Annex II) and belongs to the list of species in need of strict protection (Annex IV) (Council Directive 1992).

## Results

Considering similarity of wing coloration (*X. retinax* is distinguished by the lack of a dark medial field), male genitalia (*X. stangelmaieri* is distinguished by bigger pollex), female genitalia (*X. retinax* is distinguished by the lack of fold on ductus bursae), genetic divergence (*X. stangelmaieri* does cluster separately from *X. strix* + *X. retinax*), and natural history (two of the three species feed on one species of Equisetaceae instead of Poaceae like *X. graminea* and *X. chagnoni*), we suggest all three taxa of the *X. strix* group as populations that still may be undergoing speciation. Two previously established species are downgraded to subspecific status: *X. strix stangelmaieri* stat. nov. and *X. strix retinax* stat. nov. Diagnosis, intrasubspecific variability, and updated distributions are provided below for each subspecies, except for *X. strix stangelmaieri* due to lack of any new collection data.

### *Xylomoia strix strix* Mikkola, 1980

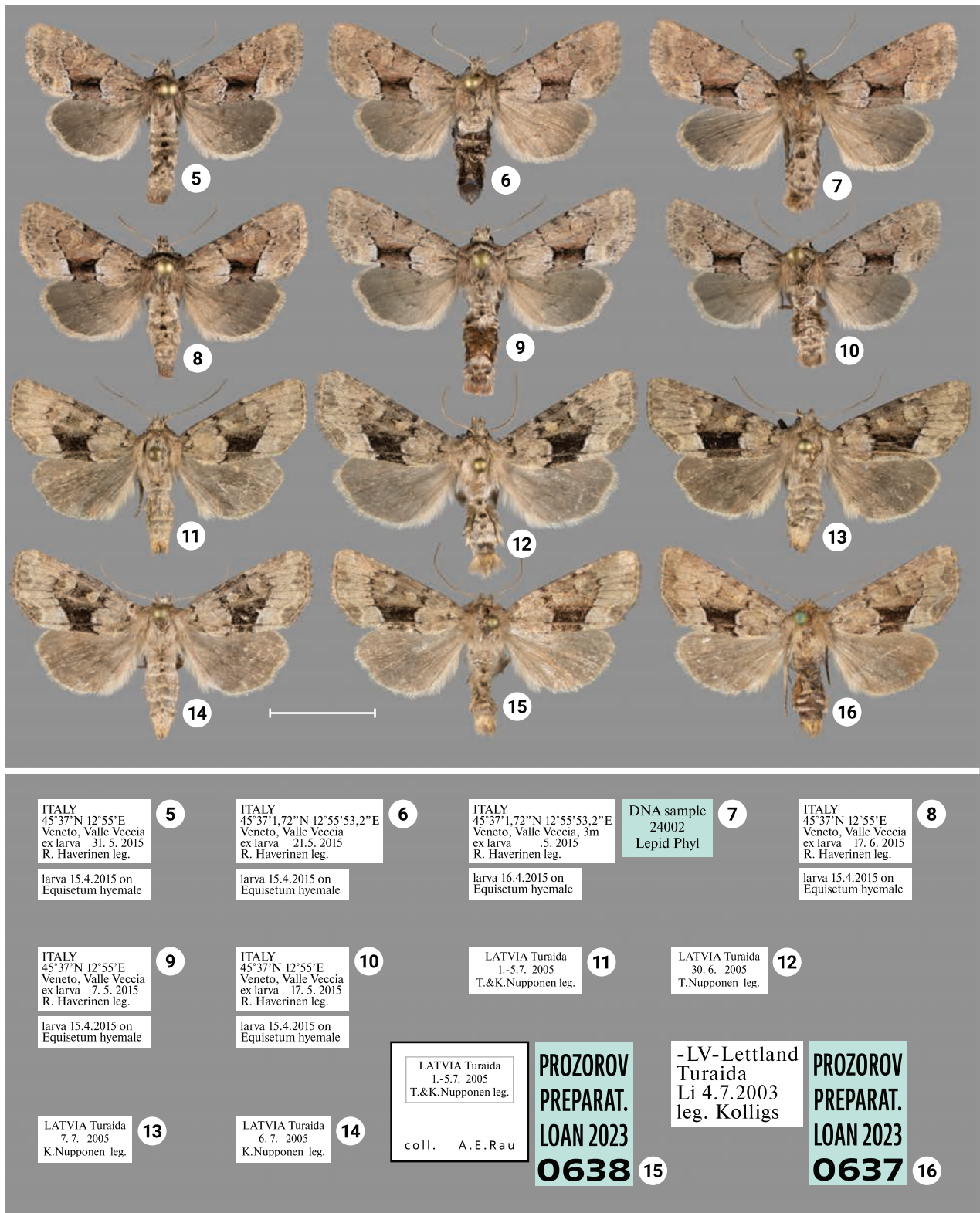
Figs 1, 4, 11–35, 46–64, 72–86

*Xylomoia strix strix* Mikkola, 1980: Notulae Entomologicae 60: 220. TL: “Latvia, Turaida.” Holotype male, ZMHF [examined].

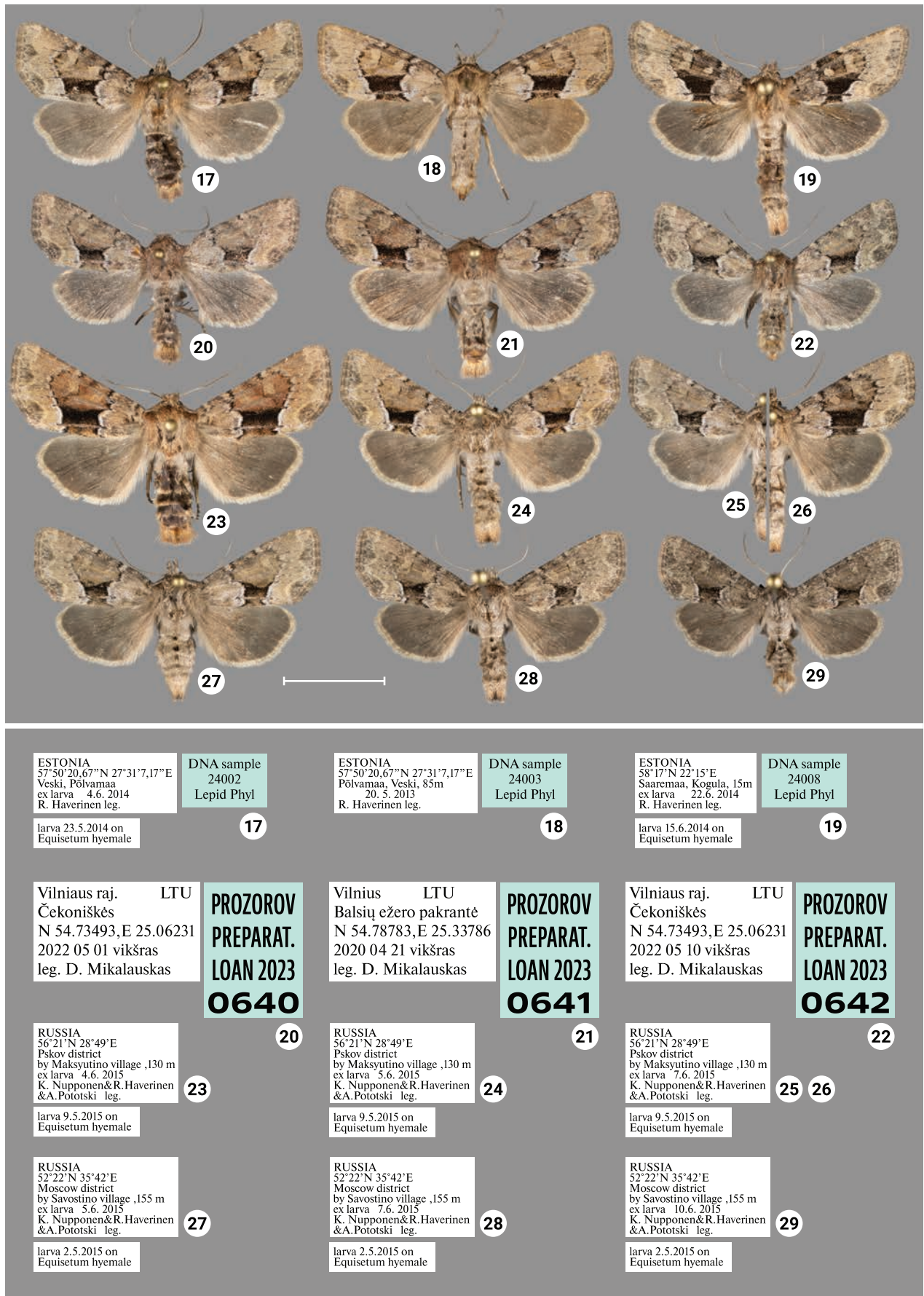
**Diagnosis.** Distinguished from *X. strix stangelmaieri* by broader dark field on forewings (Figs 11–35) and smaller pollex (Figs 46–64), from *X. strix retinax* by actual presence of dark field on forewing (Figs 11–35) and fold of ductus bursae (Figs 72–86); from both subspecies genetically, having an average *p*-distance of 1.89% from *X. strix stangelmaieri* and 0.33% from *X. strix retinax*. Average *p*-distance between *X. strix strix* and *X. graminea* is 2.55%, *X. strix strix* and *X. chagnoni*, 7.64%, and *X. strix strix* and *X. indirecta*, 8.05% (Fig. 90). Found in north, central, and east Europe with the westernmost presence in the Volga region (Figs 91, 92).

**Variability. Adults.** Blackish streak in medial field varies from narrow (e.g., Figs 20, 22, 33) to wide (e.g., 18, 23), its reddish-brown bounds vary from well-pronounced (e.g., Figs 15, 21) to non-existing (e.g., Figs 12, 19). Dark streak may expand towards costa and cover medial field (Figs 11–15, 19, 26). Forewings may have somewhat reddish (Figs 16, 23, 30, 33), yellowish (Figs 11–15, 18, 24, 26) or greyish tinge (Figs 22, 25, 27–29, 31–32, 34–35); submarginal field may be pale- (e.g., Fig. 11) or dark-colored (e.g., Fig. 17).

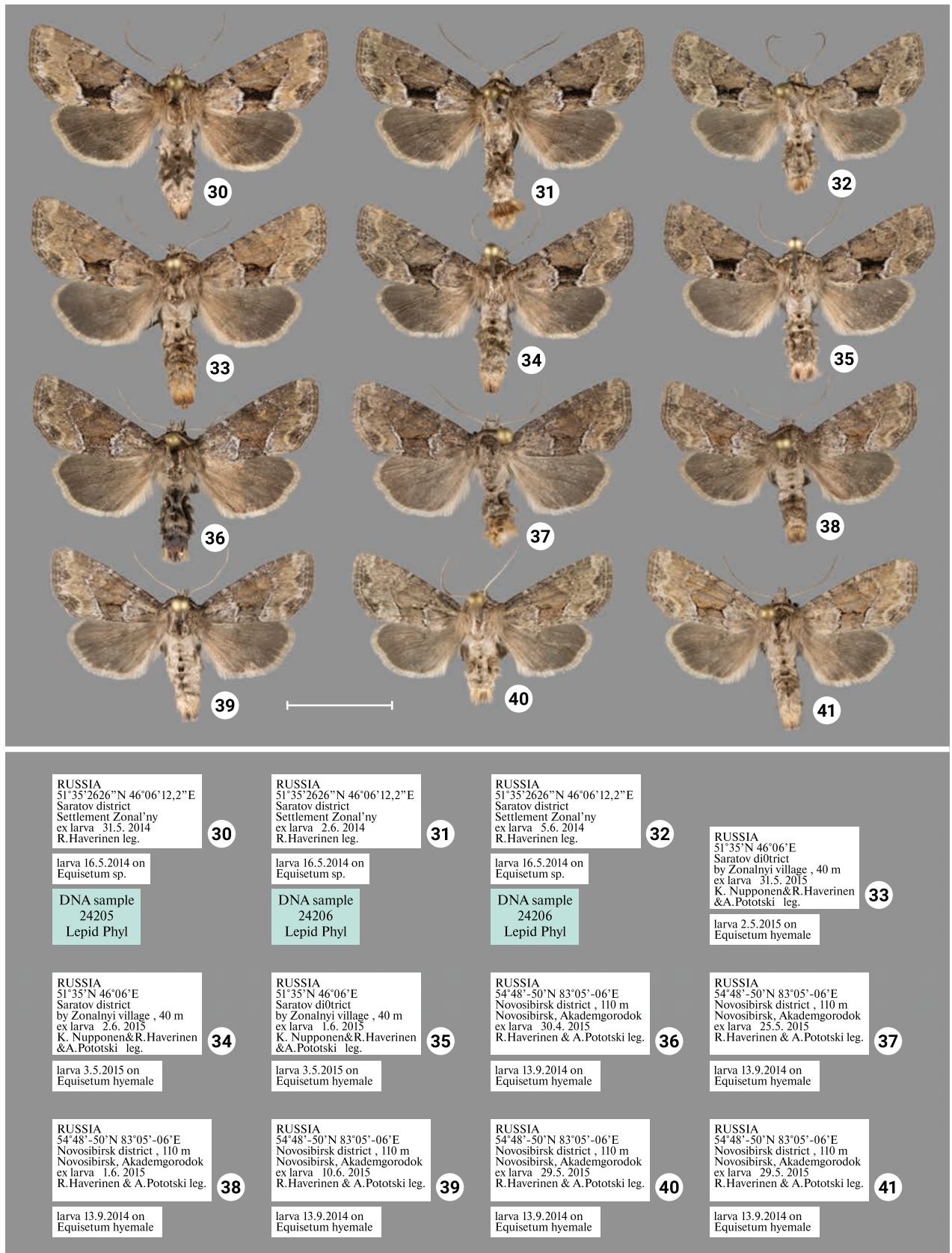
**Male genitalia.** Uncus may gradually get thin towards apex (e.g., Figs 46, 59) or only be thin near its apex (e.g., Figs 51, 58), saccus may be relatively small and narrow (e.g., Figs 48, 62) or large (e.g., Figs 54, 63), carina may be reduced (Figs 56–57, 59, 61) or well-developed (e.g., Figs 48, 60, 64), basal cornutus varies in size from small (e.g., Fig. 61) to large (e.g., Fig. 58) and may be more or less bent, medial cornutus may be almost straight (e.g., Fig. 46), c-shaped (e.g., Fig. 62) or s-shaped (e.g., Fig. 60) and varies in size.



Figures 5–16. Adults of *Xylomoia strix* ssp. with labels. 5–10 *X. strix stangellaeri* (CRH) 11–16 *X. strix strix* 11–14 CRH 15, 16. ASV. Scale bar: 1 cm.



Figures 17–29. Adults of *Xylomoia strix strix* with labels. 17–19, 23–29 CRH 20–22 ASV. Scale bar: 1 cm.



Figures 30–41. Adults of *Xylomoia strix* ssp. with labels (CRH). 30–35 *X. strix strix* 36–41 *X. strix retinax*. Scale bar: 1 cm.

**Female genitalia.** Antevaginal plate slightly varies in thickness, bursa copulatrix may narrow around connection with ductus bursae (e.g., Fig. 76) and may have one (Figs 73, 74, 77, 85) or two (Fig. 86) frontal signa, hind signum varies in size.

**Distribution area.** Finland, Estonia, Latvia, Lithuania, Poland, Belarus, Ukraine, and Russia (Leningrad, Yaroslavl, Moscow, Tula, Saratov, Samara Oblasts and Republic of Tatarstan).

***Xylomoia strix stangelmaieri* Mikkola, 1998, stat. nov.**

Figs 2, 5–10, 42–45, 69–71

*Xylomoia strix stangelmaieri* Mikkola, 1998: Systematic Entomology 23: 182.

TL: "N Italy, Venezia Giulia, Caorle." Holotype male, ZMHF [examined].

**Diagnosis.** Distinguished from *X. strix strix* by somewhat narrower dark field on forewings and from *X. strix retinax* by actual presence of this dark field (Figs 5–10) and fold of ductus bursae (Figs 69–71); from both subspecies by bigger pollex in male genitalia (Figs 42, 43, 45) and genetically, having an average *p*-distance of 1.89% from *X. strix strix* and 1.75% from *X. strix retinax*. Average *p*-distance between *X. strix stangelmaieri* and *X. graminea* is 2.28%, *X. strix stangelmaieri* and *X. chagnoni*, 6.77%, *X. strix stangelmaieri* and *X. indirecta*, 8.06% (Fig. 90). Very local, so far found only on the Adriatic coast near Venice in northern Italy (Figs 91, 92).

**Variability. Adults.** Forewings may have reddish (Figs 5–8) or greyish tinge (Fig. 10), submarginal field may be paler (Figs 6, 7, 9, 10) or darker in color (Figs 5, 8). **Male genitalia.** Uncus may gradually narrow towards apex (Fig. 44) or be narrow only near its apex (Figs 42, 43, 45), pollex may be barely noticeable (Fig. 44) or well pronounced (Figs 42, 43, 45), saccus may be narrow (Figs 42, 43) or wide (Figs 44, 45), carina vary in size from small (Fig. 42) to large (Fig. 44), basal cornutus vary in size from small (Fig. 44) to large (Fig. 43), medial cornutus may be straight (Fig. 43) or curved (Figs 42, 44, 45). **Female genitalia.** Antevaginal plate may be narrow (Fig. 71) or thick (Fig. 70), bursa copulatrix may be narrow around connection with ductus bursae (Fig. 71); bursa copulatrix may have one (Fig. 70), two (Fig. 69), or three (Fig. 71) frontal signa; hind signum slightly varies in size.

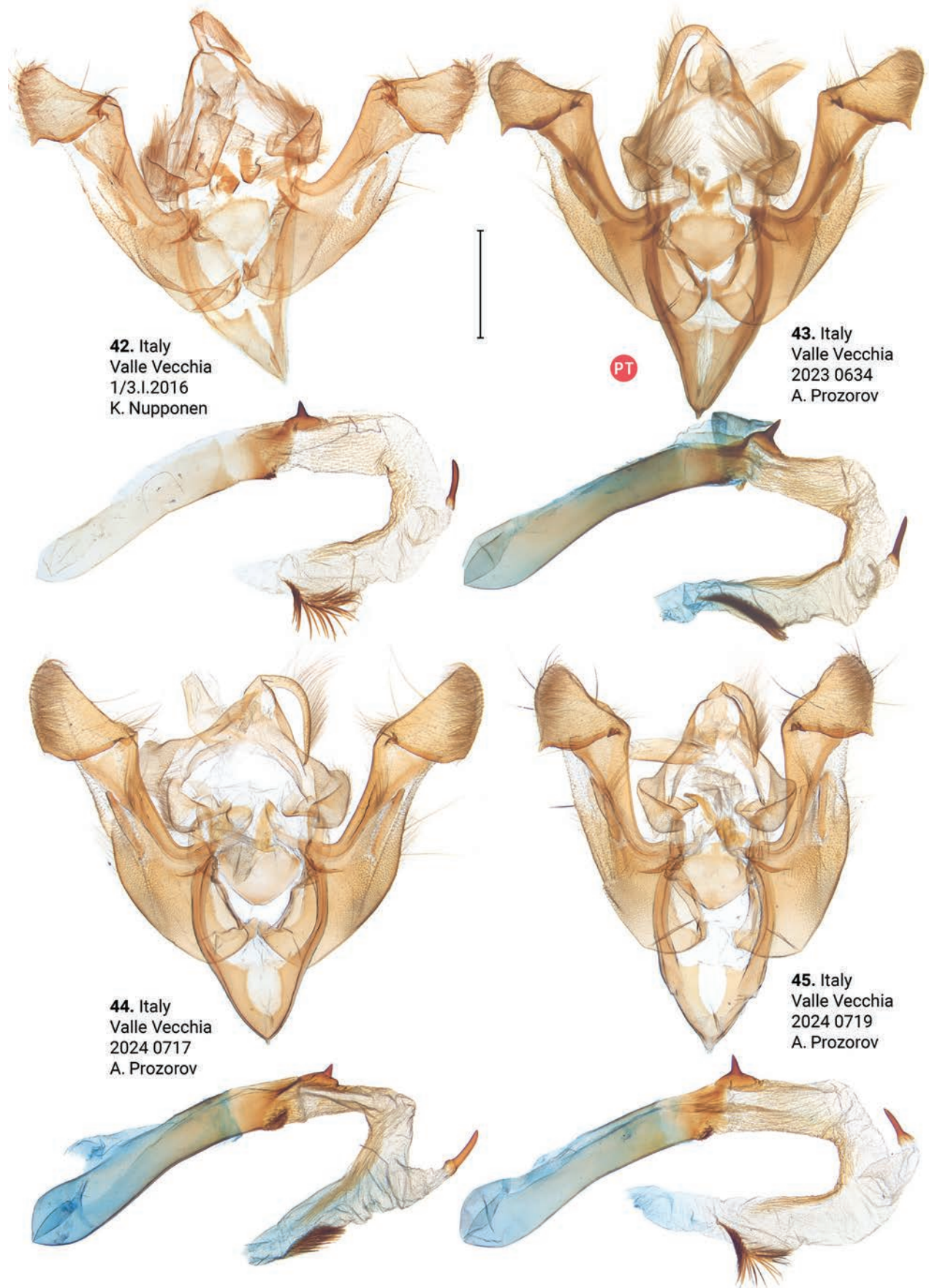
***Xylomoia strix retinax* Mikkola, 1998, stat. nov.**

Figs 3, 36–41, 65–68, 87–89

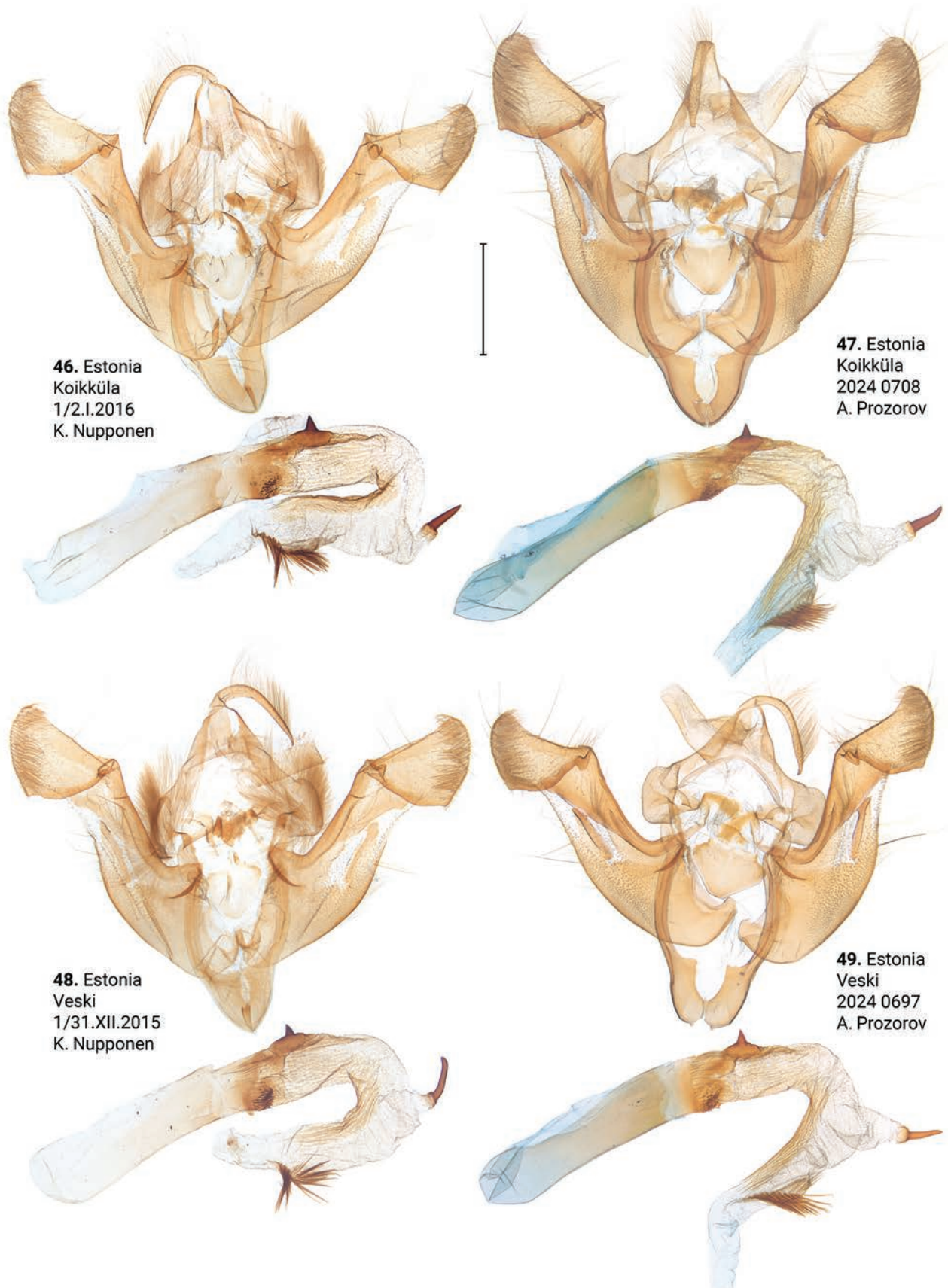
*Xylomoia strix retinax* Mikkola, 1998: Systematic Entomology 23: 181. TL: "Russia, Western Siberia, Akademgorodok (40 km SE Novosibirsk)." Holotype

male, ZMHF [examined].

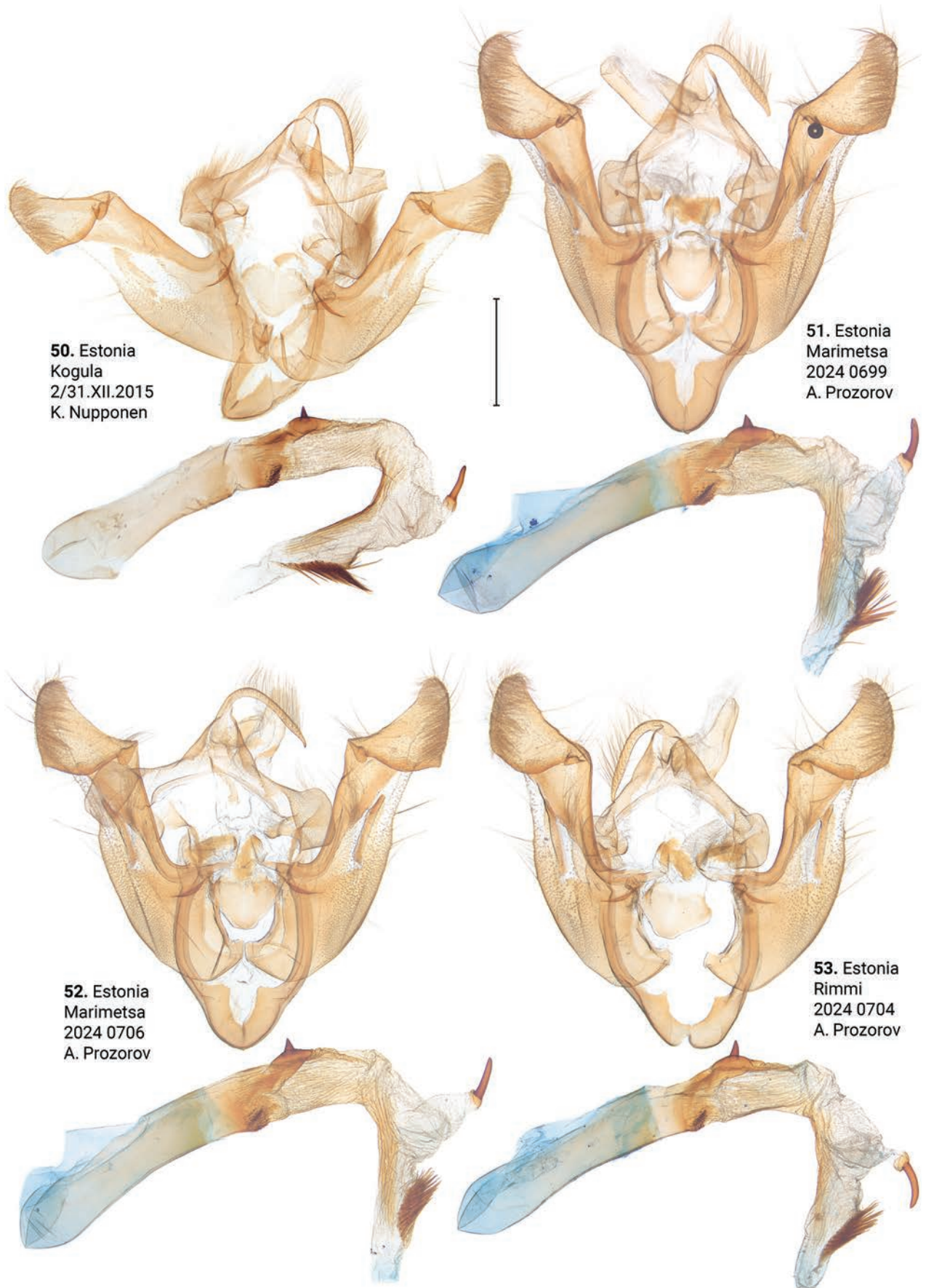
**Diagnosis.** Distinguished from *X. strix stangelmaieri* by smaller pollex (Figs 65–68), from both congeners by lack of dark medial field on forewing (Figs 36–41), fold of ductus bursae (Figs 87–89) and genetically, having an average *p*-distance of 1.75% from *X. strix stangelmaieri* and 0.33% from *X. strix strix*.



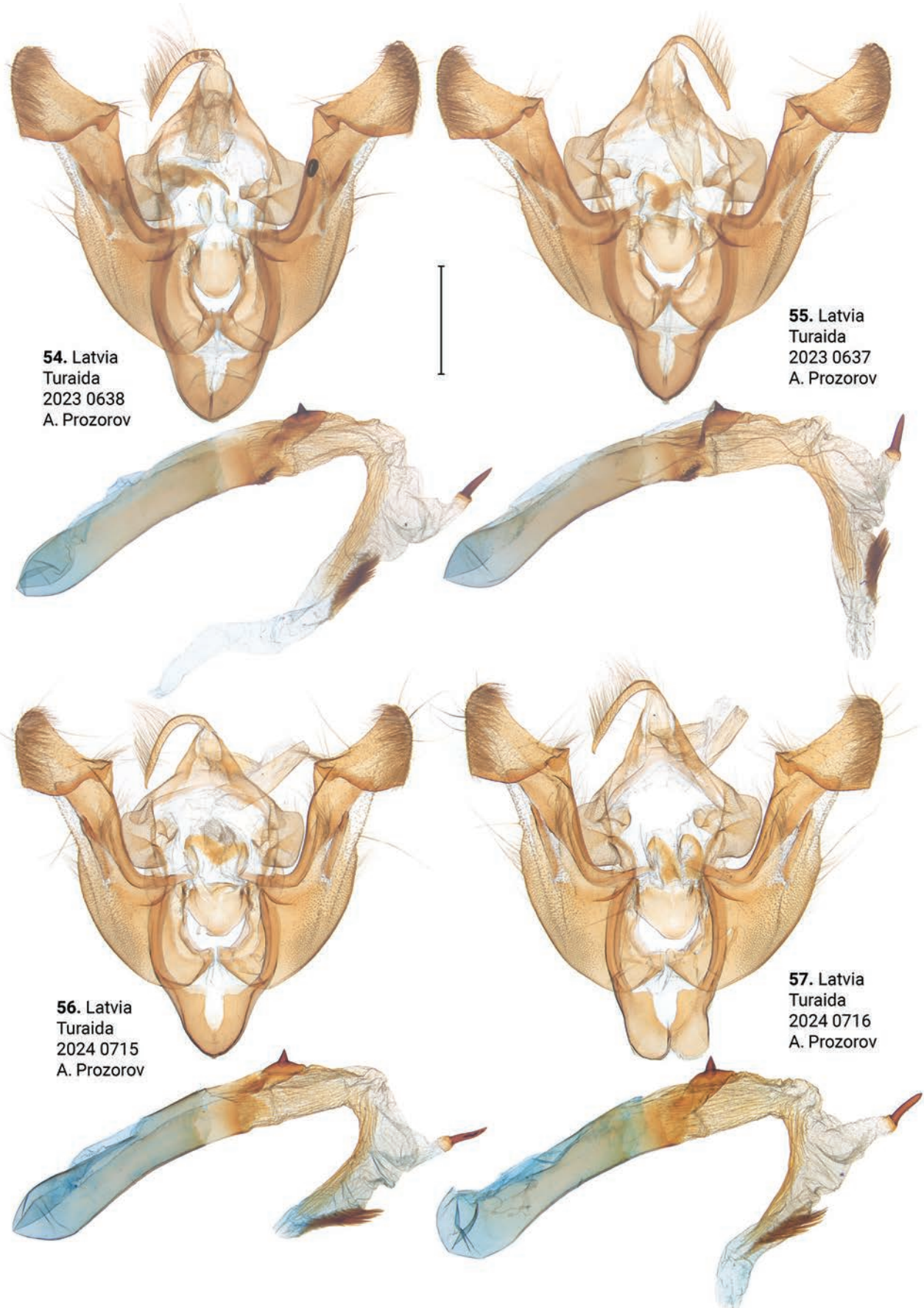
Figures 42–45. Male genitalia of *Xylomoia strix stangellaieri*. Depositories: **42, 44–45** CRH **43** ASV. Scale bar: 1 mm.



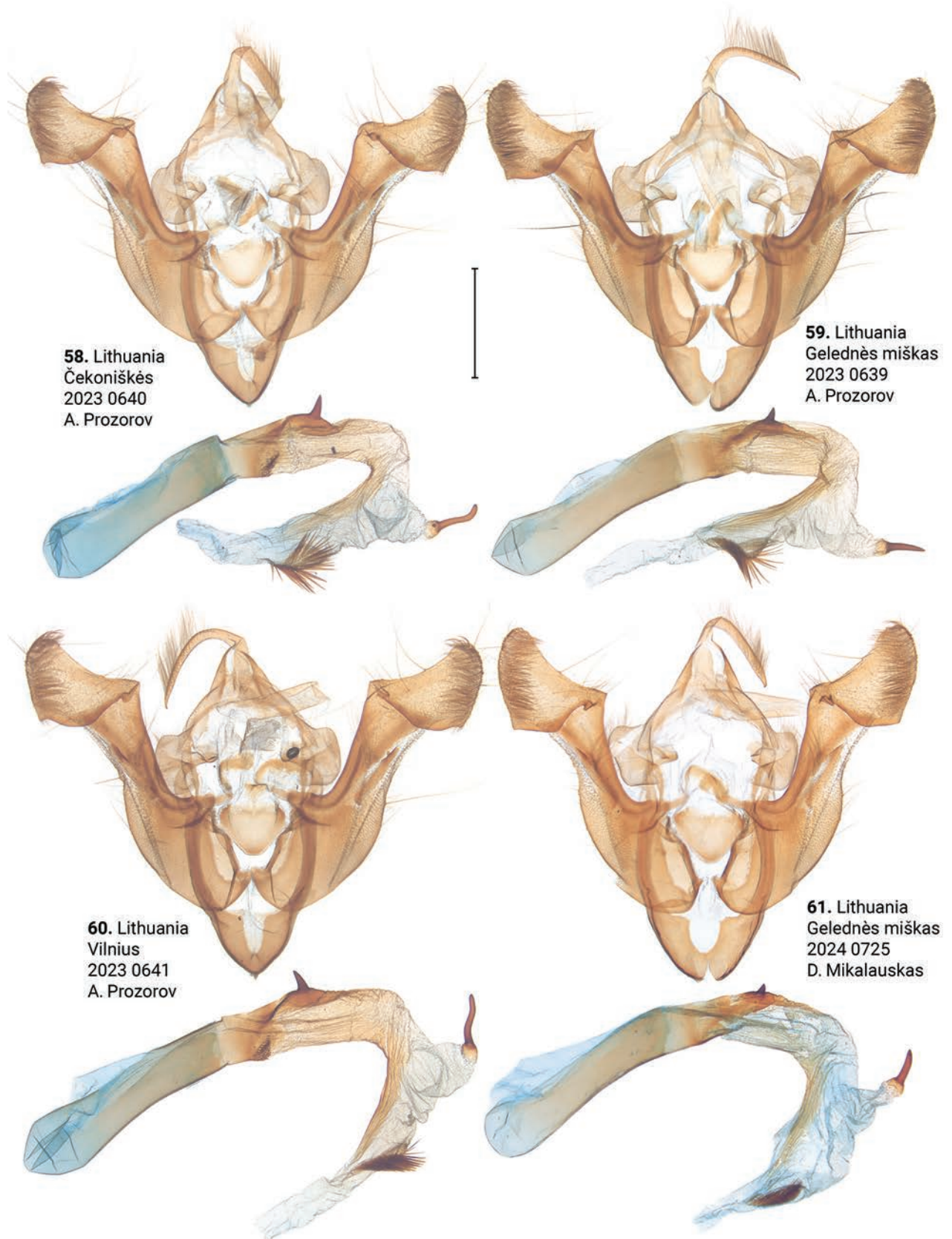
Figures 46–49. Male genitalia of *Xylomoia strix strix* (CRH). Scale bar: 1 mm.



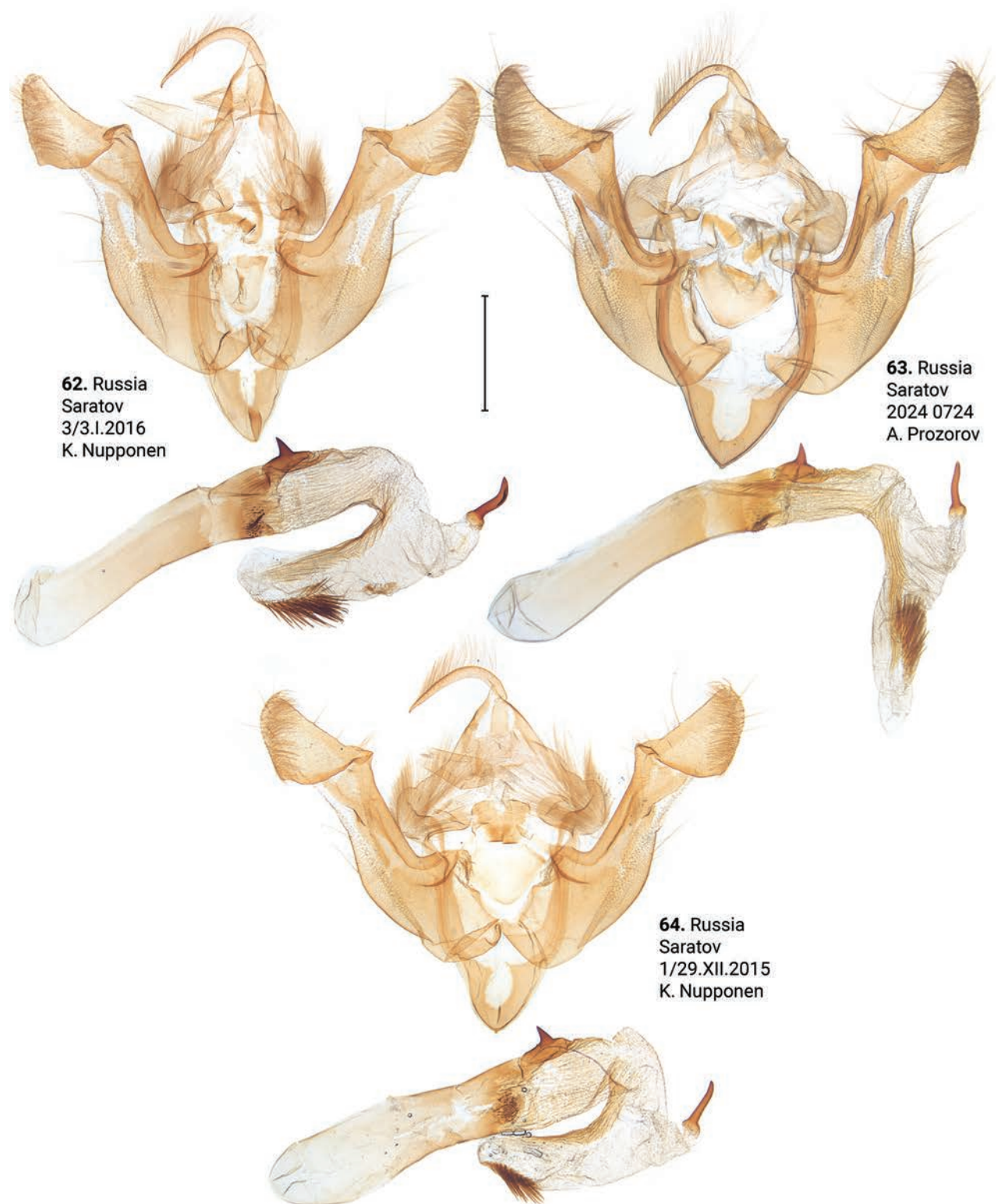
Figures 50–53. Male genitalia of *Xylomoia strix strix* (CRH). Scale bar: 1 mm.



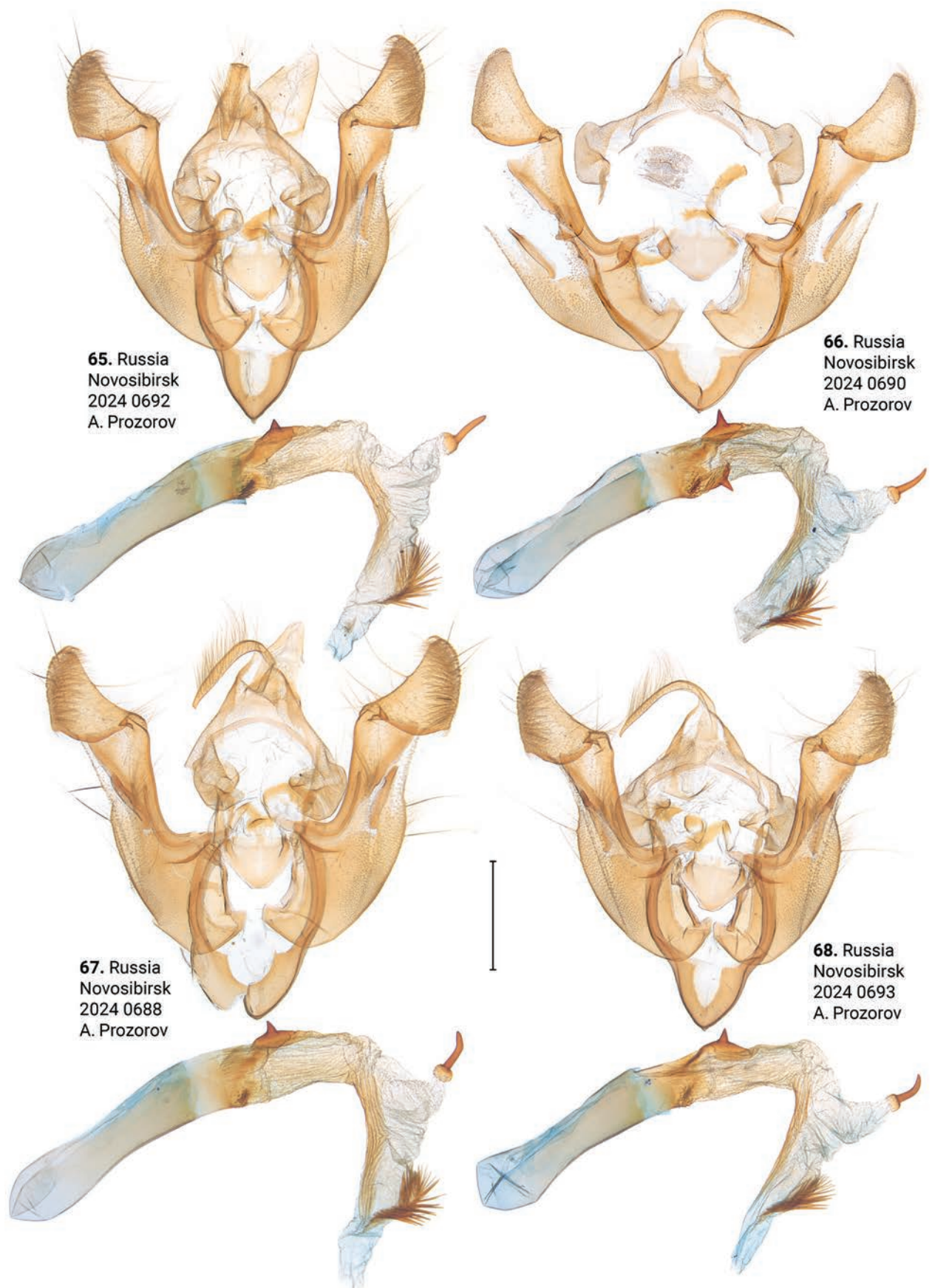
Figures 54–57. Male genitalia of *Xylomoia strix strix*. Depositories: **54, 55** ASV **56, 57** CRH. Scale bar: 1 mm.



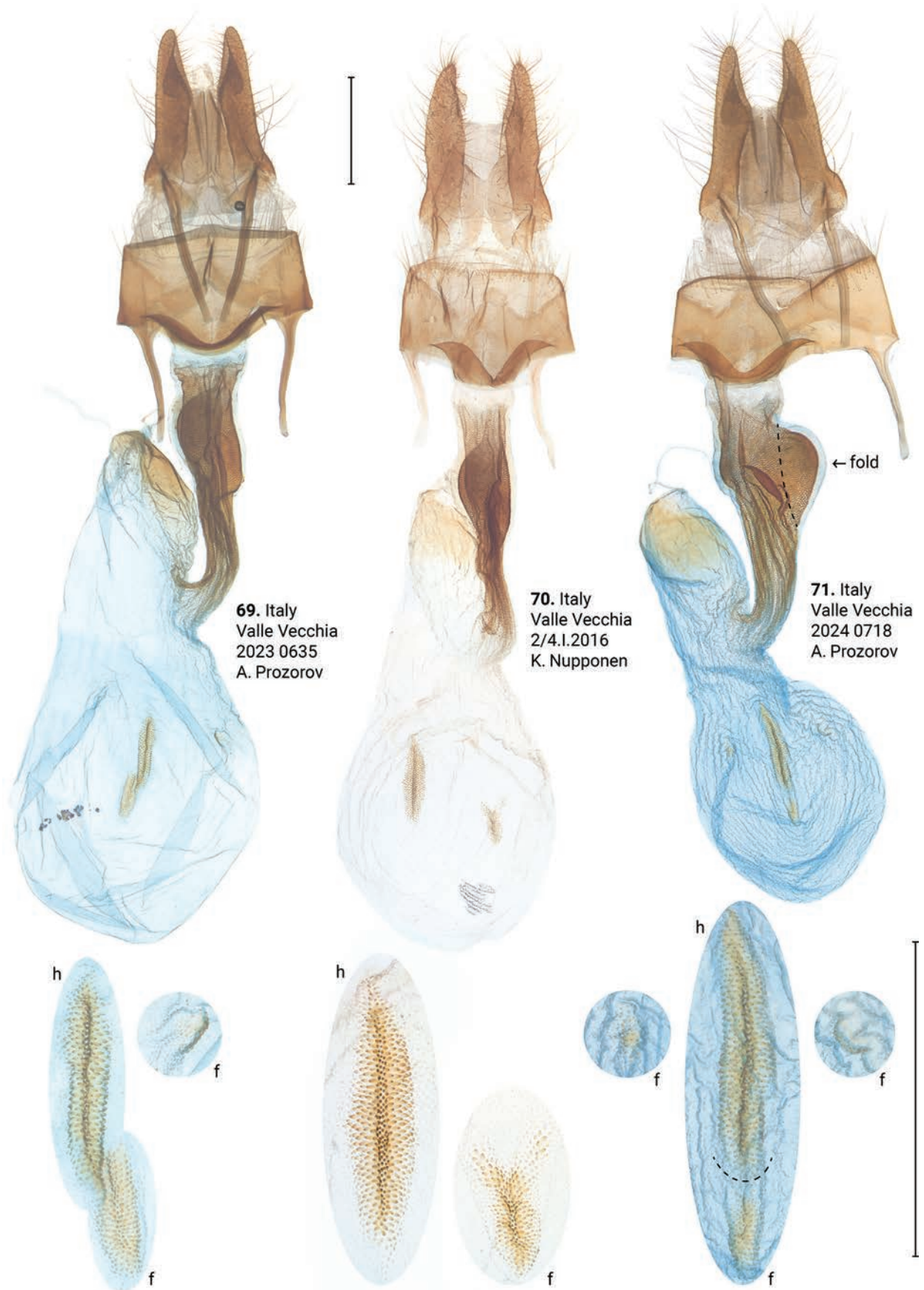
Figures 58–61. Male genitalia of *Xylomoia strix strix* (ASV). Scale bar: 1 mm.



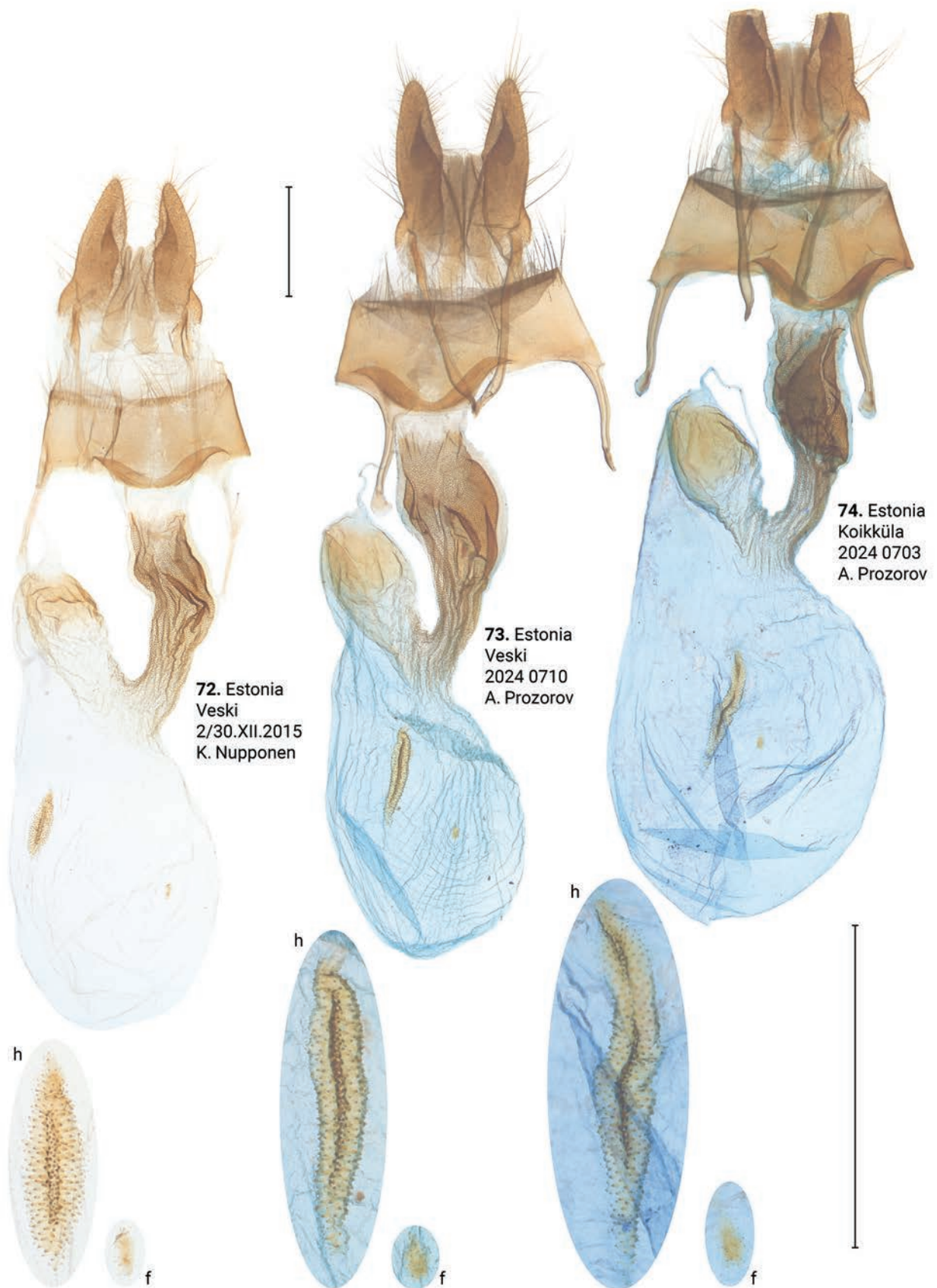
Figures 62–64. Male genitalia of *Xylomoia strix strix* (CRH). Scale bar: 1 mm.



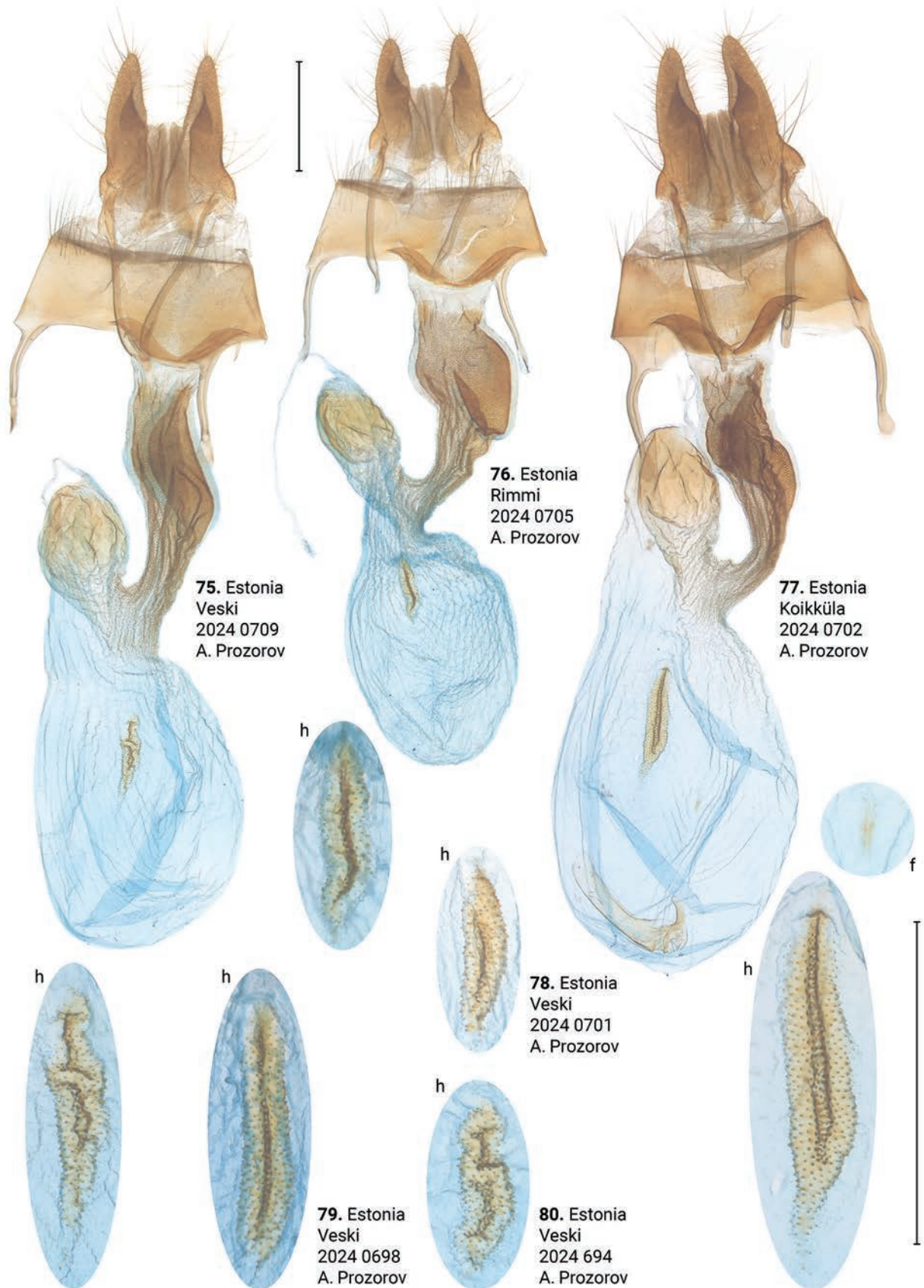
Figures 65–68. Male genitalia of *Xylomoia strix retinax* (CRH). Scale bar: 1 mm.



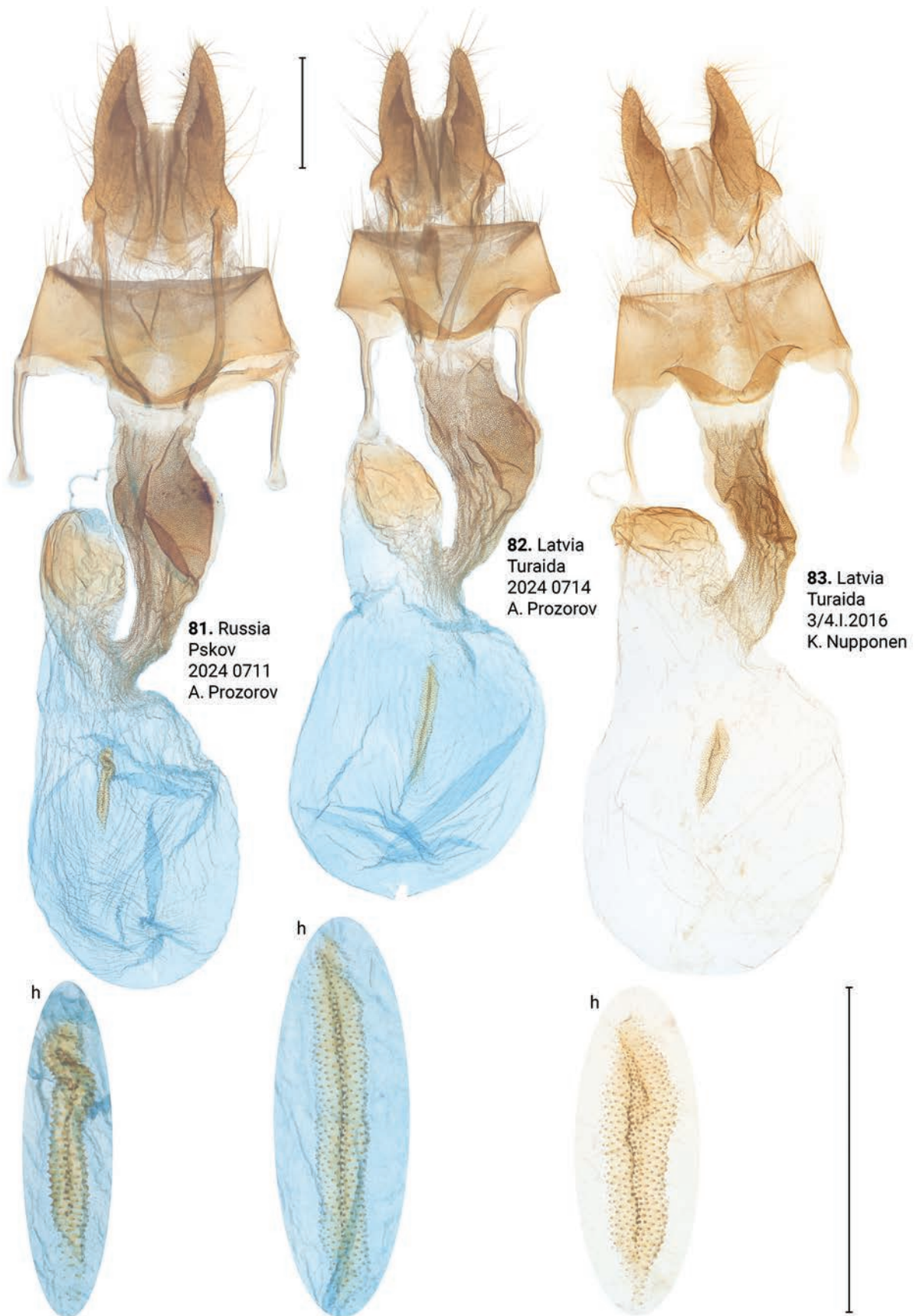
Figures 69–71. Female genitalia of *Xylomoia strix stangelmaieri*. Abbreviations: f – frontal signum, h – hind signum. Depositories: **69** ASV **70, 71** CRH. Scale bar: 1 mm.



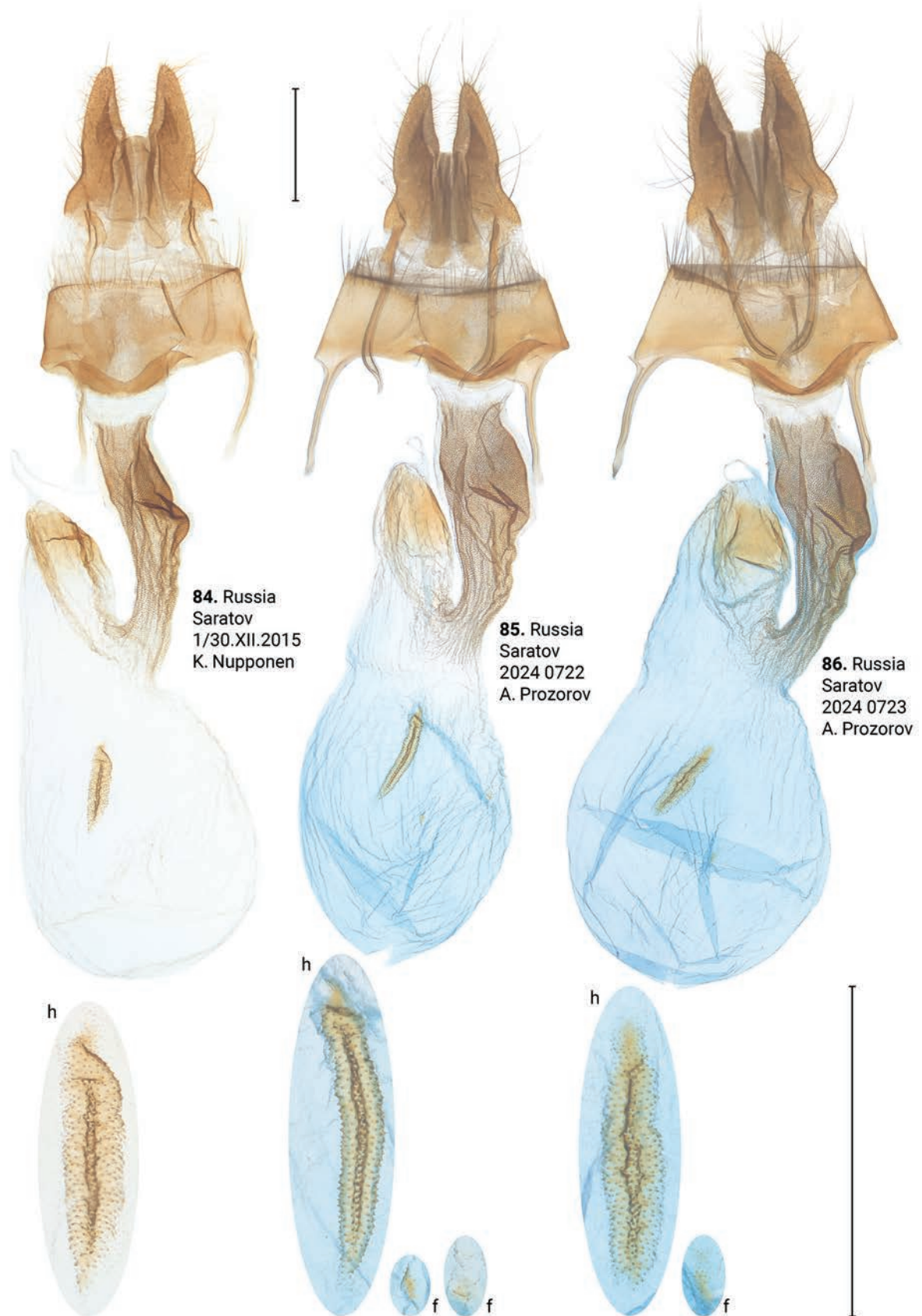
Figures 72–74. Female genitalia of *Xylomoia strix strix* (CRH). Abbreviations: f – frontal signum, h – hind signum. Scale bar: 1 mm.



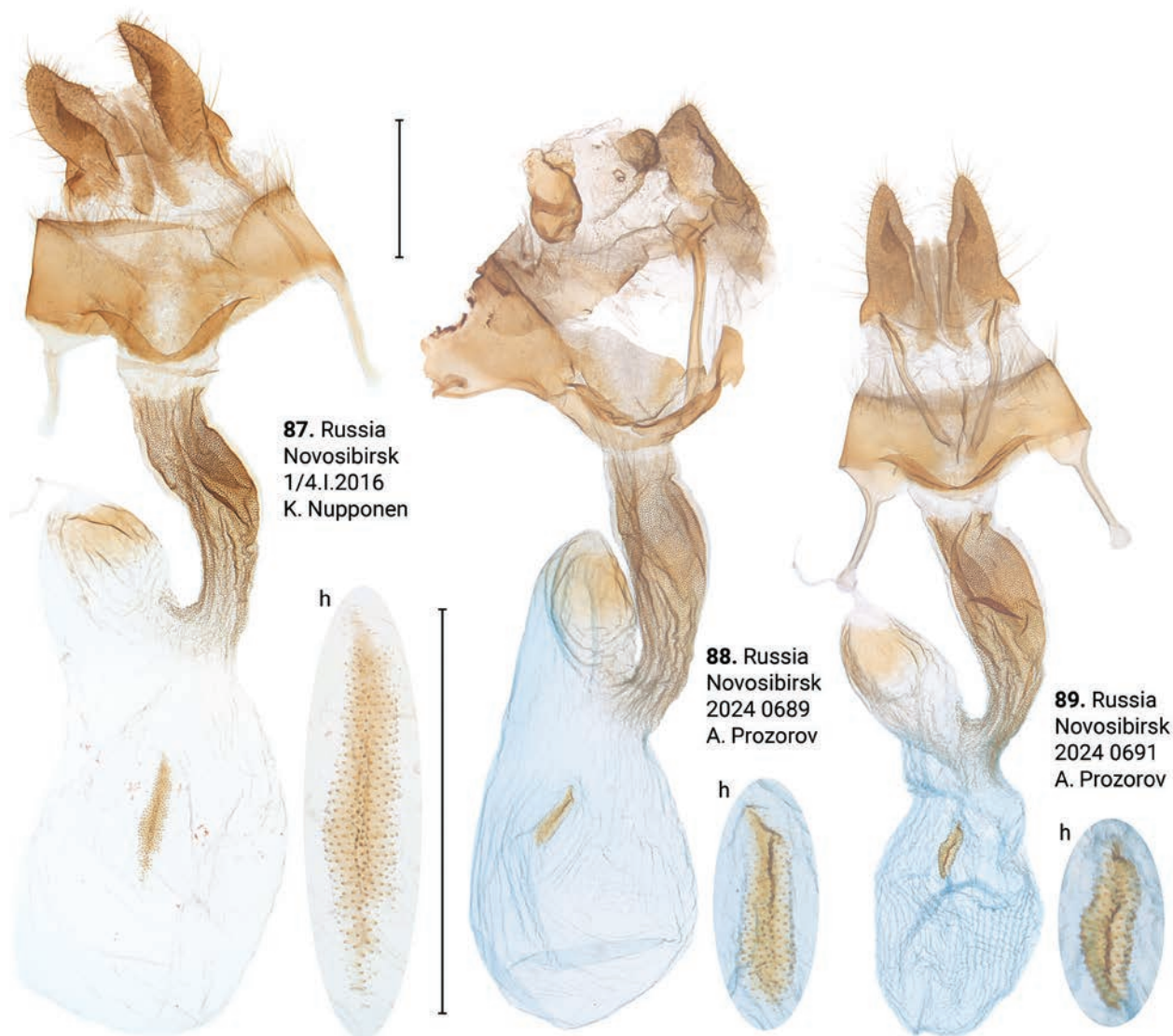
Figures 75–80. Female genitalia of *Xylomoia strix strix* (CRH). Abbreviations: f – frontal signum, h – hind signum. Scale bar: 1 mm.



**Figures 81–83.** Female genitalia of *Xylomoia strix strix* (CRH). Abbreviations: f – frontal signum, h – hind signum. Scale bar: 1 mm.



**Figures 84–86.** Female genitalia of *Xylomoia strix strix* (CRH). Abbreviations: f – frontal signum, h – hind signum. Scale bar: 1 mm.



Figures 87–89. Female genitalia of *Xylomoia strix retinax* (CRH). Abbreviations: h – hind signum. Scale bar: 1 mm.

Average *p*-distance between *X. strix retinax* and *X. graminea* is 2.36%, *X. strix retinax* and *X. chagnoni*, 7.22%, and *X. strix retinax* and *X. indirecta*, 8.13% (Fig. 90).

**Variability. Adults.** May be dark-colored with brownish tinge (Figs 36–38) or pale-colored with yellowish tinge (Figs 39–41), submarginal area may be dark (e.g., Fig. 36) or pale (e.g., Fig. 38). **Male genitalia.** Uncus may gradually get thin towards apex (Figs 66, 68) or only be thin near its apex (Figs 65, 67), saccus varies in size, carina may be more (e.g., Fig. 65) or less pronounced (e.g., Fig. 67), additional cornutus similar to the basal one may be present near carina (Fig. 66), basal cornutus varies in size from small (e.g., Fig. 65) to large (e.g., Fig. 66), medial cornutus may be almost straight (Fig. 65) or c-shaped (e.g., Fig. 67). **Female genitalia.** Antevaginal plate slightly varies in thickness, bursa copulatrix and hind signum vary in size (Figs 87–89).

**Distribution area.** Russia (Orenburg, Chelyabinsk, Omsk, Novosibirsk Oblasts and Altai Republic).

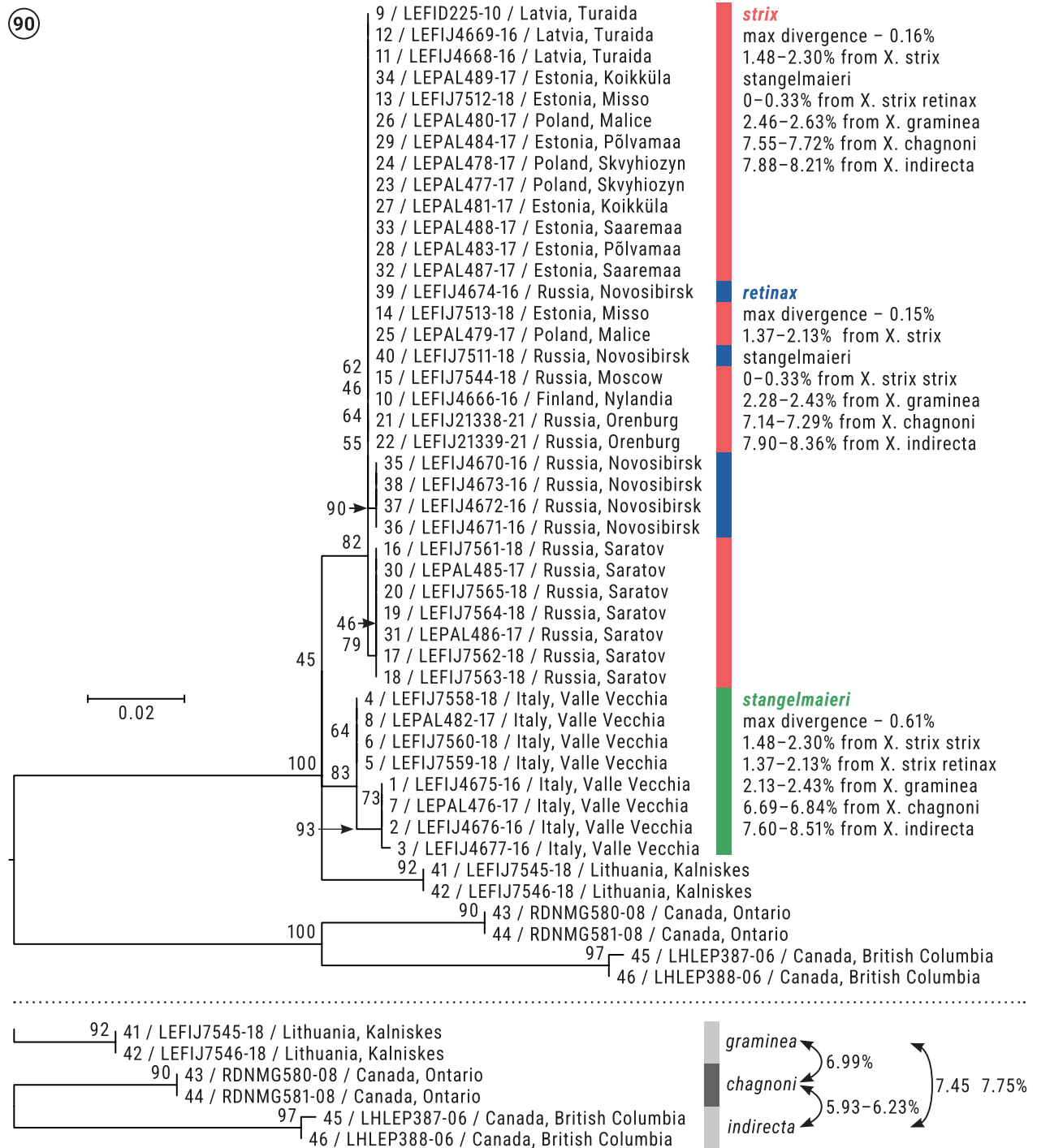
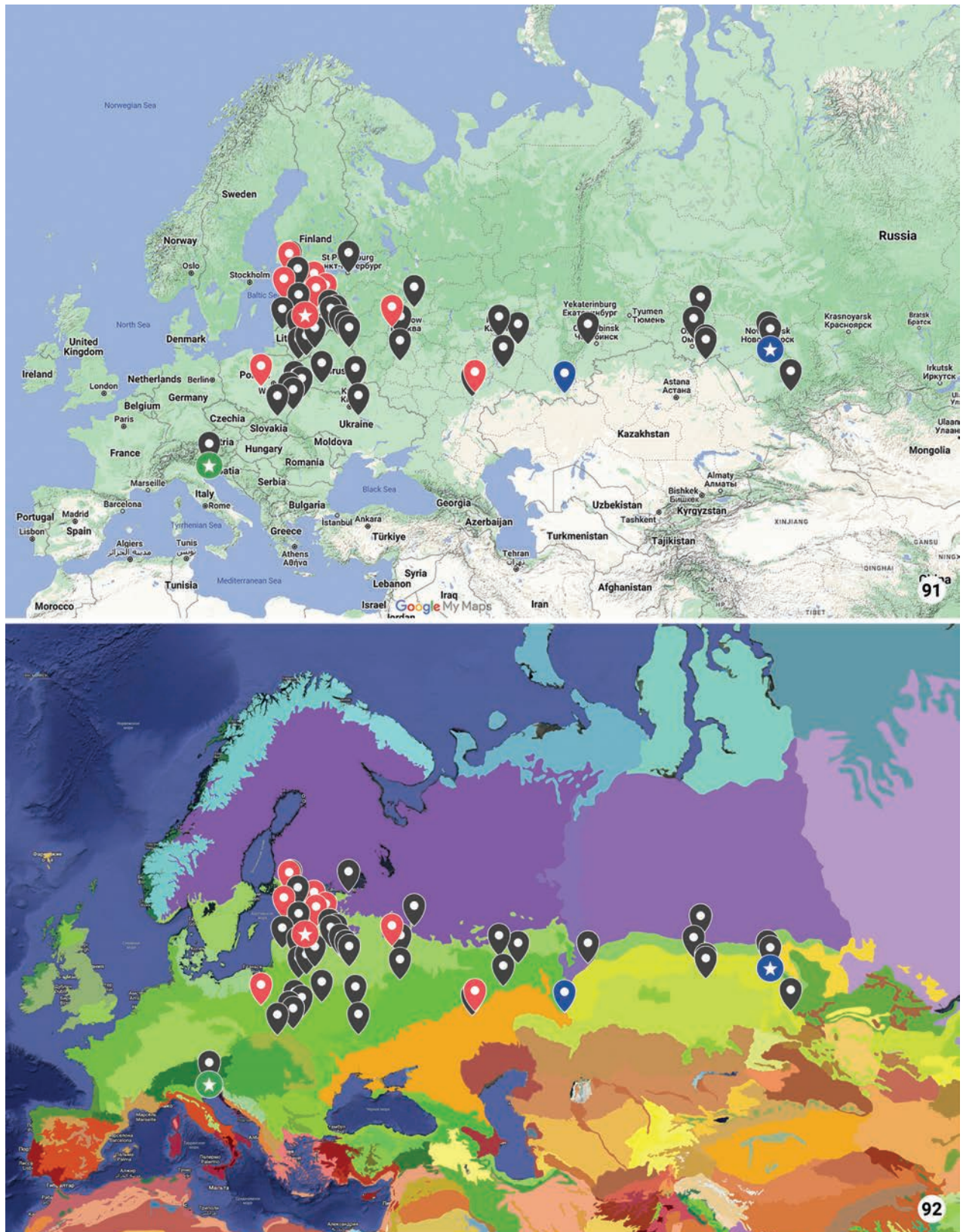


Figure 90. Phylogenetic tree (Maximum Likelihood, HKY+F+I, 1000 ultrafast bootstrap replicates) for *Xylomoia* spp. built in IQ-TREE 2.2.0 and pairwise distances (%) computed for each pair of taxa in MEGA X.



Figures 91, 92. Collecting localities of *Xylomoia strix* subspecies: *X. strix stangelmaieri* in Italy, *X. strix strix* in Europe, and *X. strix retinax* in Asia. Colored tags mark collecting locations from where adults were barcoded. Circles with stars mark type localities **91** physical map **92** map of ecoregions: green colors indicate forests and steppes, purple – taiga (see ecoregions.appspot.com).

## Acknowledgments

We thank Timo Nupponen for invaluable help with breeding, preparing, and labeling the huge number of different *Xylomoia* caterpillars. Many thanks to the senior author's daughter Inna Antikainen, who has been his source of inspiration for the last 20 years of his research, from the first step to the present day. We are grateful to Marjut Hirvonen, Jari-Pekka Kaitila, Markus Rantala, the late Kimmo Silvonen (Finland), Sami Haapala, Iiti Jürjendal (Estonia), Aleksei Belik, Stanislav Korb, Andrei Komrakov, Oleg Kosterin, Alexej Matov, and Sergei Shaposhnikov (Russia) for various types of assistance. We thank Mukta Joshi for her help with the ML analysis. We greatly appreciate the help of Herb Friend (New York, USA) with English language editing. We are deeply indebted to the reviewers, Alberto Zilli and Péter Gyulai, for their time and efforts to improve the quality and clarity of the manuscript.

## Additional information

### Conflict of interest

The authors have declared that no competing interests exist.

### Ethical statement

No ethical statement was reported.

### Funding

Ripako Oy (Ltd.), Vantaa, Finland.

### Author contributions

Conceptualization: AS. Data curation: RH, MM. Formal analysis: GCM, AS, RVY, MM. Investigation: RH, AP, DM. Project administration: RH. Supervision: AS. Validation: AS. Visualization: AMP. Writing – original draft: AMP. Writing – review and editing: GCM, AS, AP, RH, DM, RVY, MM.

### Author ORCIDs

Risto Haverinen  <https://orcid.org/0000-0001-8072-847X>

Aleksander Pototski  <https://orcid.org/0000-0002-1843-3627>

Marko Mutanen  <https://orcid.org/0000-0003-4464-6308>

Darius Mikalauskas  <https://orcid.org/0009-0004-2145-8747>

Roman V. Yakovlev  <https://orcid.org/0000-0001-9512-8709>

Günter C. Müller  <https://orcid.org/0000-0002-7024-0179>

Alexey M. Prozorov  <https://orcid.org/0000-0002-5668-0741>

Aidas Saldaitis  <https://orcid.org/0000-0003-0999-3996>

### Data availability

All of the data that support the findings of this study are available in the main text.

## References

Aarvik L, Bengtsson BA, Elven H, Ivinskis P, Jürivete U, Karsholt O, Mutanen M, Savenkov N (2017) Nordic-Baltic Checklist of Lepidoptera. Norwegian Journal of Entomology Supplement 3: 1–236.

- Ahola M, Silvonen K (2007) Pohjoisen Euroopan yökkösten toukat [Larvae of Northern European Noctuidae]. Volume 1. Kuvaseppälä Yhtiöt Oy, Vaasa, 657 pp.
- Anikin VV, Sachkov SA, Zolotuhin VV (2017) "Fauna Lepidopterologica Volgo-Uralensis": from P. Pallas to present days. Proceedings of the Museum Witt Munich 7: 1–696.
- Barnes W, McDunnough J (1917) A new Canadian noctuid. Canadian Entomologist 49: 320–321. <https://doi.org/10.4039/Ent49320-9>
- Bolshakov LV, Makarichev NI (2020) Additions and corrections to the fauna of Lepidoptera of the Tula Province. 9. Eversmannia 61: 68–73.
- Bury J, Czudec P (2019) Comments on the occurrence and biology of *Xylomoia graminea* (Graeser, 1889) (Lepidoptera: Noctuidae) from south-eastern Poland. Fragmenta Faunistica 62(1): 39–46. <https://doi.org/10.3161/00159301FF2018.61.2.039>
- Bury J, Zajda W (2012) Distribution of *Xylomoia graminea* (Graeser, 1889) (Lepidoptera: Noctuidae) in Poland – review of previous studies and new data. Fragmenta Faunistica 55: 139–145. <https://doi.org/10.3161/00159301FF2012.55.2.139>
- Buszko J (2004) Sówka puszczykówka. In: Adamski P, Bartel R, Bereszyski A, Kapel A, Witkowski Z (Eds) Gatunki Zwierząt (z wyjątkiem ptaków). Poradniki ochrony siedlisk i gatunków. Natura 2000. Podręcznik metodyczny. Ministerstwo Środowiska, Warszawa, 6: 63–64.
- Buszko J (2010) Ksylomka striks (sówka puszczykówka) *Xylomoia strix* Mikkola, 1980. In: Makomaska-Juchiewicz M (Ed.) Monitoring gatunków zwierząt. Przewodnik metodyczny. I. Biblioteka Monitoringu Środowiska. Inspekcja Ochrony Środowiska, Warszawa, 408 pp.
- Cooksey C (2013) Quirks of dye nomenclature. 1. Evans blue. Biotechnic & Histochemistry, 89(2): 111–113. <https://doi.org/10.3109/10520295.2013.822560>
- Council Directive (1992) Council Directive 92/43/EEC of 21 May 1992 on the conservation of natural habitats and of wild fauna and flora. Official Journal L 206, 22/07/1992, 0007–0050. <http://data.europa.eu/eli/dir/1992/43/2013-07-01>
- Derzhinsky EA (2019) New findings of noctuid *Xylomoia strix* (Lepidoptera, Noctuidae) in Belarus Poozerje. In: Science for education, production, economics. Materials of 71<sup>st</sup> regional scientific and practical conference of teachers, researchers and graduate students. Vitebsk 1: 42–43.
- deWaard JR, Ivanova NV, Hajibabaei M, Hebert PDN (2008) Assembling DNA Barcodes. In: Martin CC (Ed.) Environmental Genomics. Humana Press, Totowa, New Jersey, 275–294. [https://doi.org/10.1007/978-1-59745-548-0\\_15](https://doi.org/10.1007/978-1-59745-548-0_15)
- Dinerstein E, Olson D, Joshi A, Vynne C, Burgess ND, Wikramanayake E, Hahn N, Palminteri S, Hedao P, Noss R, Hansen M, Locke H, Ellis EC, Jones B, Barber CV, Hayes R, Kormos C, Martin V, Crist E, Sechrest W, Price L, Baillie JEM, Weeden D, Suckling K, Davis C, Sizer N, Moore R, Thau D, Birch T, Potapov P, Turubanova S, Tyukavina A, De Souza N, Pintea L, Brito JC, Llewellyn OA, Miller AG, Patzelt A, Ghazanfar SA, Timberlake J, Klöser H, Shennan-Farpón Y, Kindt R, Barnekow Lillesø J-P, Van Breugel P, Graudal L, Vogé M, Al-Shammari KF, Saleem M (2017) An Ecoregion-Based Approach to Protecting Half the Terrestrial Realm. BioScience 1(6): 1–12. <https://doi.org/10.1093/biosci/bix014>
- Evans HM, Schulemann W (1914) The action of vital stains belonging to the benzidine group. Science 39(1004): 443–454. <https://doi.org/10.1126/science.39.1004.443>
- Geryak YuM, Voytko PL, Kanarsky YuV, Chorny TZ (2018) Supplement to the fauna of Noctuoidea (Lepidoptera, Insecta) of the Volyn Region. Scientific basis for preserving biotic diversity 9(16): 119–134.
- Graeser L (1889) Beiträge zur Kenntniss der Lepidopteren-Fauna des Amurlandes. Berliner Entomologische Zeitung 33: 309–414. <https://doi.org/10.1002/mmnd.47918880407>

- Grote AR (1875) Supplement to the list of North American Noctuidae. Bulletin of the Buffalo Society of natural History 2: 209–223.
- Guenée A (1841) Noctuarum europaeorum index methodicus, classificationis in Ann. Soc. entom gallic. editae tabulam fingens (1). Annales de la Société entomologique de France 10: 235–250.
- Hacker H (1989) Beiträge zur systematischen Erfassung der Noctuidae des vorder- und zentralasiatischen Raumes. Neue taxonomische und faunistische Erkenntnisse zur Fauna Vorderasiens und Ägyptens (Lepidoptera, Noctuidae). Atalanta 19: 157–187.
- Hardwick DF (1950) Preparation of slide mounts of lepidopterous genitalia. Canadian Entomologist 82(11): 231–235. <https://doi.org/10.4039/Ent82231-11>
- Haverinen R, Nupponen K, Pototski A (2016) New data on the distribution and bionomics of *Xylomoia strix* Mikkola, 1980 in the Baltic countries (Lepidoptera, Noctuidae). Lepinfo 22: 1–7.
- Haverinen R, Pototski A, Matov A (2021) *Xylomoia strix* (Lepidoptera, Noctuidae) recorded in Leningrad region, Russia. Lepinfo 24: 103–105.
- Hebert PDN, Cywinska A, Ball SL, deWaard JR (2003) Biological identifications through DNA barcodes. Proceedings of the Royal Society B 270(1512): 313–321. <https://doi.org/10.1098/rspb.2002.2218>
- Ivinskis P, Rimšaitė J (2013) Data on new and rare Lepidoptera species for Lithuanian fauna. New and Rare for Lithuania Insect Species 25: 31–36.
- Kalyaanamoorthy S, Minh BQ, Wong TKF, Von Haeseler A, Jermiin LS (2017) ModelFinder: Fast model selection for accurate phylogenetic estimates. Nature Methods 14: 587–589. <https://doi.org/10.1038/nmeth.4285>
- Karvonen J (1996) *Xylomoia strix* jälleen Suomesta. Baptria 21: 51–52.
- Klyuchko ZF, Pljushch IG, Sheshurak PN (2001) Annotated catalogue of noctuids (Lepidoptera, Noctuidae) of the Ukraine fauna. Zoology Institute of Ukrainian Academy of Sciences, Kiev, 884 pp.
- Knyazev SA (2020) Catalogue of Lepidoptera of Omsk Oblast (Russia). Macrolepidoptera. Families: Hepialidae, Brachodidae, Cossidae, Sesiidae, Limacodidae, Zygaenidae, Thyrididae, Drepanidae, Uraniidae, Geometridae, Lasiocampidae, Lemoniidae, Endromididae, Saturniidae, Sphingidae, Notodontidae, Lymantriidae, Arctiidae, Syntomidae, Erebiidae, Nolidae, Noctuidae, Hesperidae, Papilionidae, Pieridae, Lycaenidae, Nymphalidae, Satyridae. Acta Biologica Sibirica 6: 139–226. <https://doi.org/10.3897/abs.6.e53005>
- Knyazev SA, Ivonin VV, Dubatolov VV, Vasilenko SV, Ponomaryov KB (2015) New records of Lepidoptera from the South of West Siberia. Amurian zoological journal VII(1): 43–50. <https://doi.org/10.33910/1999-4079-2015-7-1-43-50>
- Knyazev SA, Ivonin VV, Vasilenko SV (2016) New and interesting findings of butterflies and moths (Insecta, Lepidoptera) in Omsk and Novosibirsk provinces. Amurian zoological journal VIII (4): 254–272. <https://doi.org/10.33910/1999-4079-2016-8-4-254-272>
- Kononenko VS (2016a) Noctuidae. In: Leley AS (Ed.) Annotated catalogue of the insects of Russian Far East. Volume II. Lepidoptera. Vladivostok, Dalnauka, 812 pp.
- Kononenko VS (2016b) Noctuidae: Cuculliinae – Noctuinae, part (Lepidoptera). Noctuoidea Sibiricae. Part 3. Proceedings of the Museum Witt Munich 5: 1–497.
- Kumar S, Stecher G, Li M, Knyaz Ch, Tamura K (2018) MEGA X: Molecular Evolutionary Genetics Analysis across Computing Platforms. Molecular Biology and Evolution 35(6): 1547–1549. <https://doi.org/10.1093/molbev/msy096>
- Lafontaine JD, Schmidt BCh (2010) Annotated check list of the Noctuoidea (Insecta, Lepidoptera) of North America north of Mexico. ZooKeys 40: 1–239. <https://doi.org/10.3897/zookeys.40.414>

- Lederer J (1857) Die Noctuinen Europa's mit Zuziehung einiger bisher meist dazu gezählter Arten des asiatischen Russland's, Kleinasien's, Syrien's und Labrador's. Friedrich Manz, Wien, 251 pp. <https://doi.org/10.5962/bhl.title.60460>
- Matov AYu, Kononenko VS, Sviridov AV (2019) In: Sinev SYu (Ed.) Catalogue of the Lepidoptera of Russia. Second edition. Zoological Institute RAS, St. Petersburg, 448 pp.
- Matov AYu, Kononenko VS, Sviridov AV (2023) Catalogue of the Lepidoptera of Russia [online version] Ver. 2.3. [https://www.zin.ru/publications/books/Lepidoptera\\_Russia](https://www.zin.ru/publications/books/Lepidoptera_Russia)
- Mikkola K (1980) Two new noctuid species from Northern Europe: *Polia sabmeana* n. sp. and *Xylomoia strix* n. sp. (Lepidoptera, Noctuidae: Hadeninae and Amphipyriinae). *Notulae Entomologicae* 60: 217–222.
- Mikkola K (1998) Revision of the genus *Xylomoia* Staudinger (Lepidoptera: Noctuidae), with descriptions of two new species. *Systematic Entomology* 23: 173–186. <https://doi.org/10.1046/j.1365-3113.1998.00055.x>
- Minh BQ, Schmidt HA, Chernomor O, Schrepf D, Woodhams MD, Von Haeseler A, Lanfear R, Teeling E (2020) IQ-TREE 2: New Models and Efficient Methods for Phylogenetic Inference in the Genomic Era. *Molecular Biology and Evolution* 37: 1530–1534. <https://doi.org/10.1093/molbev/msaa015>
- Nowacki J, Pałka K (2014) Nowe stanowisko *Xylomoia strix* Mikkola, 1980 (Lepidoptera: Noctuidae) w Polsce. *Wiadomości entomologiczne* 33: 38–41.
- Nowacki J, Sekuła W (1994) *Xylomoia strix* Mikkola, 1980 – nowy dla fauny Polski przedstawiciel sówkowatych (Lepidoptera, Noctuidae). *Wiadomości Entomologiczne* 13(3): 195–196.
- Nupponen K, Fibiger M (2002) Contribution to the knowledge of the fauna of Bombyces, Sphingines and Noctuidae of the Southern Ural Mountains, with description of a new *Dichagyris* (Lepidoptera: Lasiocampidae, Endromidae, Saturniidae, Sphingidae, Notodontidae, Noctuidae, Pantheidae, Lymantriidae, Nolidae, Arctiidae). *Phegea* 30(4): 121–185.
- Pekarsky ON, Korb SK (2012) The first finding of *Xylomoia retinax* Mikkola, 1998 in Lower Volga region (Lepidoptera: Noctuidae). *Eversmannia* 31–32: 114.
- Pierce FN (1909) The genitalia of the group Noctuidae of the Lepidoptera of the British Islands: An account of the morphology of the male clasping organs. A.W. Duncan, Liverpool, 88 pp. <https://doi.org/10.5962/bhl.title.8998>
- Ratnasingham S, Hebert PD (2007) BOLD: The Barcode of Life Data System (<http://www.barcodinglife.org>). *Molecular Ecology Notes* 7(3): 355–364. <https://doi.org/10.1111/j.1471-8286.2007.01678.x>
- Ratnasingham S, Hebert PD (2013) A DNA-Based Registry for All Animal Species: The Barcode Index Number (BIN) System. *PLoS ONE* 8(8): e66213. <https://doi.org/10.1371/journal.pone.0066213>
- Rockburne EW, Lafontain JD (1976) The cutworm moths of Ontario and Quebec. Printing and Publishing Supply and Services Canada, Ottawa, 164 pp.
- Sachkov SA (2013) The new for Samara area species of Lepidoptera. 4<sup>th</sup> report. *Bulletin of Samara University* 3(104): 188–199. <https://doi.org/10.18287/2541-7525-2013-19-3-188-199>
- Savenkov N, Šulcs I (2010) Latvijas Tauriņi. Katalogs. Tallinn, 176 pp.
- Skou P (1991) Nordens ugler. Danmarks dyreliv. Bind 5. Stensrup, 566 pp.
- Sugi S (1976) A new species of the genus *Xylomoia* Staudinger (Lepidoptera, Noctuidae, Amphipyriinae). *Tinea* 10: 63–66.
- Šulcs A, Šulcs I (1983) Zur Kenntnis von *Xylomoia strix* Mikkola, 1980 (Lep., Noctuidae). *Entomologische Nachrichten und Berichte* 27(5): 227–228.

- Sviridov AV (2002) Noctuid moths (Lepidoptera) new for different areas of the Russian Federation, 1. Russian Entomological Journal 11(4): 445–450.
- Ūsaitis T, Mikalauskas D, Bačianskas V (2019) New and rare for the Lithuanian fauna Lepidoptera species recorded in 2019. Bulletin of the Lithuanian Entomological Society 3(31): 79–98.
- Volynkin AV (2024) On the terminology of the genitalia structures of lichen moths (Lepidoptera: Erebidæ: Arctiinae: Lithosiini) with some references to Noctuidæ. Ecologica Montenegrina 73: 176–207. <https://doi.org/10.37828/em.2024.73.18>
- Volynkin AV, Ivanova MS (2016) First record of *Xylomoia retinax* Mikkola, 1998 (Lepidoptera: Noctuidæ) from Altai Republic, Russia. Far Eastern Entomologist 324: 13–14.
- Zilli A, Ronkay L, Fibiger M (2005) Noctuidæ Europeæ. Volume 8. Apameini. Entomological Press, Sorø, 323 pp.

# Parazoanthidae (Cnidaria, Zoantharia) associated with glass sponges on the Nishi-Shichito Ridge, northwestern Pacific Ocean, with the description of a new species

Hiroki Kise<sup>1</sup>, James Davis Reimer<sup>2,3</sup>, Akira Iguchi<sup>1,4</sup>, Yuji Ise<sup>5</sup>, Shinji Tsuchida<sup>6</sup>, Yoshihiro Fujiwara<sup>6</sup>

1 Geological Survey of Japan, National Institute of Advanced Industrial Science and Technology, AIST Tsukuba Central 7, 1-1-1 Higashi, Tsukuba, Ibaraki 305-8567, Japan

2 Molecular Invertebrate Systematics and Ecology Laboratory, Graduate School of Engineering and Science, University of the Ryukyus, 1 Senbaru, Nishihara, Okinawa 903-0213, Japan

3 Tropical Biosphere Research Center, University of the Ryukyus, 1 Senbaru, Nishihara, Okinawa 903-0213, Japan

4 Research Laboratory on Environmentally-conscious Developments and Technologies (E-code), National Institute of Advanced Industrial Science and Technology (AIST), Tsukuba 305-8567, Japan

5 Kuroshio Biological Research Foundation, 560 Nishidomari, Otsuki, Hata, Kochi 788-0333, Japan

6 Research Institute for Global Change (RIGC), Japan Agency for Marine-Earth Science and Technology (JAMSTEC), 2-15 Natsushima-cho, Yokosuka, Kanagawa 237-0061, Japan

Corresponding author: Hiroki Kise ([h.kise@aist.go.jp](mailto:h.kise@aist.go.jp))



Academic editor: Bert W. Hoeksema

Received: 4 July 2024

Accepted: 28 September 2024

Published: 27 December 2024

ZooBank: <https://zoobank.org/8D02638F-C398-4B9A-AA2F-4CCFC633252E>

**Citation:** Kise H, Reimer JD, Iguchi A, Ise Y, Tsuchida S, Fujiwara Y (2024) Parazoanthidae (Cnidaria, Zoantharia) associated with glass sponges on the Nishi-Shichito Ridge, northwestern Pacific Ocean, with the description of a new species. ZooKeys 1221: 343–362. <https://doi.org/10.3897/zookeys.1221.131258>

Copyright: © Hiroki Kise et al.

This is an open access article distributed under terms of the Creative Commons Attribution License (Attribution 4.0 International – CC BY 4.0).

## Abstract

Seamounts are biodiversity hotspots that face increasing threats from anthropogenic activities. Seamounts host diverse sessile suspension-feeding organisms such as sponges and anthozoans, which are crucial for seamount ecosystems as they construct three-dimensional habitats utilized by numerous other animals. Therefore, accurate identification of seamount fauna, in particular of sessile suspension-feeding organisms, is of paramount importance for robust conservation efforts. This study focused on Zoantharia, a sessile anthozoan group, and specifically the family Parazoanthidae, known for associations with many different host taxa, prominently including octocorals and sponges. We collected Parazoanthidae specimens from northwestern Pacific seamounts and formally describe a new species, *Vitrumanthus flosculus* Kise & Reimer, **sp. nov.**, based on morphological and molecular analyses. We also report the complete mitochondrial genomes of this new species and the related species *Churabana kuroshioae*. Our results reconfirm the phylogenetic positions of these two species within Parazoanthidae, while demonstrating much remains to be learned about the benthic diversity of northwestern Pacific seamounts.

**Key words:** Baseline data, Hexasterophora, mitochondrial genome, mitogenome, MPA, phylogeny, seamount, taxonomy, zoantharian

## Introduction

Seamounts are diversity hotspots for deep-sea organisms (Worm et al. 2003; Samadi et al. 2006; Clark et al. 2010; Morato et al. 2010; Rowden et al. 2010), harboring diverse assemblages of sessile suspension-feeding organisms due to turbulent and hydrodynamic water flowing around their peaks, which delivers

planktonic food and nutrients to the benthos in the immediate area (Clark et al. 2010; Watling and Auster 2017). Seamount habitats and their fauna face threats from anthropogenic activities, such as bottom trawling that may damage or destroy these diverse marine animal forests (Worm et al. 2006; Clark et al. 2007; Althaus et al. 2009; Rossi et al. 2022). Sessile suspension-feeding organisms, especially sponges and anthozoans, play important roles in seamount communities, as they construct three-dimensional habitats utilized by numerous other animals such as crustaceans, ophiuroids, and polychaetes (Glasby and Watson 2001; Buhl-Mortensen and Mortensen 2004; Mosher and Watling 2009; Watling et al. 2011; Bracken-Grissom et al. 2018; Okanishi and Mah 2020; Komai et al. 2022). Sponges and anthozoans are vulnerable to damage from anthropogenic activities, as they are often large, fragile, long-lived, and extremely slow-growing (Probert et al. 1997; Clark et al. 2016; Molodtsova and Opresko 2017). It has been estimated that the recovery of these organisms from such anthropogenic damage will take decades to centuries (Clark et al. 2016). Therefore, accurate identification and documentation of seamount fauna, in particular of sessile suspension-feeding organisms, is important to generate robust baseline datasets that can be utilized to better protect the biological communities of seamounts.

The order Zoantharia is a group of sessile cnidarians consisting of > 300 species (Reimer and Sinniger 2024). In the deep sea, species of zoantharians within the family Parazoanthidae are known to associate with many different host taxa, prominently including octocorals and sponges (e.g., Carlgren 1923; Sinniger et al. 2005, 2013; Reimer et al. 2008, 2019; Carreiro-Silva et al. 2017; Kise et al. 2022; Montenegro et al. 2024). Four zoantharian genera have been reported to be associated with Hexasterophora sponges; *Churabana* Kise, Montenegro & Reimer, 2021, *Parachurabana* Kise, 2023, *Thoracactis* Gravier, 1918, and *Vitrumanthus* Kise, Montenegro & Reimer, 2022. *Churabana*, *Parachurabana*, and *Thoracactis* are monotypic genera while *Vitrumanthus* includes three species from the Pacific and Atlantic oceans. Although the Hexasterophora-zoantharian association thus has a wide distribution across the global oceans (Reiswig and Wheeler 2002; Dohrmann et al. 2011; Reiswig and Dohrmann 2014; Van Soest et al. 2014; Montenegro et al. 2020; Kise et al. 2022, 2023), the diversity of these associations is still poorly known. In this study, we collected specimens of *Churabana* and *Vitrumanthus* from the Shoho and An'ei seamounts along the Nishi-Shichito Ridge in the northwestern Pacific Ocean, and formally describe one species, *Vitrumanthus flosculus* sp. nov., utilizing a combination of morphological observations and molecular phylogenetic analyses. In addition, we report the complete mitochondrial genomes of two Hexasterophora-associated species, *Churabana kuroshioae* and *Vitrumanthus flosculus* sp. nov., which further reinforce the phylogenetic position of these species within Parazoanthidae.

## Materials and methods

### Specimen collection

Hexasterophora-associated zoantharians were collected from Shoho and An'ei seamounts on 29 November 2020 and 17 October 2021 by the remotely operated vehicle (KM-ROV) aboard the R/V Kaimei at depths of 400 and 770 m, respectively (Fig. 1). Photographs of the specimens were taken in situ for gross exter-

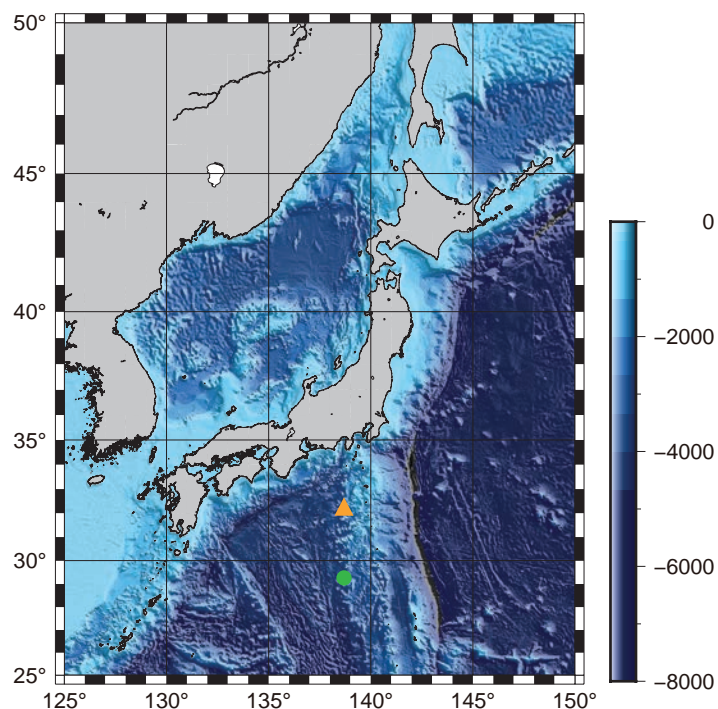


**Figure 1.** Research area and location of sampling sites. Enclosed symbols indicate sampling sites of two species examined in this study. *Vitrumanthus flosculus* sp. nov. (orange triangle) and *Churabana kuroshioae* (green circle).

nal morphological observation before collection using a camera mounted on the *KM-ROV*. Upon specimen retrieval, each specimen was anesthetized with magnesium chloride and subsequently fixed in 10% seawater formalin with subsamples preserved in 99.5% ethanol. The specimens examined in this study have been deposited in the National Museum of Nature and Science, Tsukuba, Japan (**NSMT**).

### DNA extraction, sequencing, and assembly

Tissues preserved in 99.5% ethanol were used for DNA extraction with a spin-column DNeasy Blood and Tissue Extraction kit following the manufacturer's instructions (Qiagen, Hilden, Germany). Extracted DNA was quantified using a Qubit dsDNA BR assay kit (ThermoFisher Scientific, Waltham, USA). Whole-genome shotgun sequencing was performed by Bioengineering Lab. Co., Ltd. (Sagamihara, Japan) with DNBSEQ-G400 platforms (MGI Tech, Shenzhen, China) to produce pair-end 200 bp reads. The raw reads were filtered using Trimmomatic v. 0.39 (Bolger et al. 2014) with default parameters. Filtered reads were de novo assembled with GetOrganelle v.1.7.5 (Jin et al. 2020), which used implemented SPAdes v.3.6.2 genome assembler (Bankevich et al. 2012) with K-mer = 115. The mitochondrial genome annotation was performed with MITOS webserver (Bernt et al. 2013), and manually inspected and adjusted using Geneious Prime 2022.1.1 (<https://www.geneious.com>). Transfer RNA genes were identified using the tRNAscan-SE v2.0 (Chan et al. 2021). The annotated mitochondrial genomes were deposited in GenBank with the accession numbers PQ554681 and PQ554682. Sequences of Cox1 (mitochondrial cytochrome c oxidase subunit I), 12S rDNA (mitochondrial 12S ribosomal DNA), and 16S rDNA (mitochondrial 16S ribosomal DNA) were extracted from newly obtained

mitochondria genomes. Three nuclear sequences, 18S rDNA (nuclear 18S ribosomal DNA), ITS rDNA (nuclear internal transcribed spacer region of ribosomal DNA), and 28S rDNA (nuclear 28S ribosomal DNA) were recovered from filtered and trimmed reads according to reference fragment sequences of *Churabana kuroshioae* (Accession numbers: MK377416, MZ329753, and MZ329743) and *Vitrumanthus schrieri* (Accession numbers: MZ329701, MZ329735, and MZ329712) using the Geneious Read Mapper (<https://www.geneious.com>).

### Molecular phylogenetic analyses

Partial fragments of mitochondrial genes (Cox1, 12S rDNA, and 16S rDNA) and of the nuclear genes (18S rDNA, ITSrDNA, and 28S rDNA) were added to the alignment dataset used in Kise et al. (2023). In addition, previously reported sequences of *Thoracactis topsenti* (Kise et al. 2024) were also added to the alignment dataset. GenBank accession numbers used for phylogenetic analyses in this study are listed in Suppl. material 1. Subsequently, these sequences were manually trimmed and realigned using MAFFT (Kato and Standley 2013) with the auto algorithm under default parameters for all genetic markers, and finally these alignments for each genetic marker were concatenated (hereafter six-gene dataset). Phylogenetic analyses were performed on the concatenated dataset using maximum likelihood (ML) and Bayesian inference (BI). ModelTest-NG v.0.1.6 (Darriba et al. 2020) under the Akaike information criterion was used to select the best-fitting model for each molecular marker independently for both ML and BI analyses. The best-selected models for ML and BI analyses are listed in Suppl. material 2. The final dataset consisted of 5148 bp and was used for ML and BI analyses. ML analyses were performed by RAXML-NG (Kozlov et al. 2019) with 1000 bootstrap replicates. BI analyses were performed with MrBayes; four Markov chain Monte Carlo (MCMC) heated chains were run for 5,000,000 generations with the temperature of the heated chain set to 0.2. Chains were sampled every 200 generations. Burn-in was set to 1,250,000 generations, at which point the average standard deviation of split frequency was consistently below 0.01. Tracer v.1.7.1 (Rambaut et al. 2018) was used to inspect the convergence of MCMC.

In addition, 13 protein-coding genes were extracted from newly sequenced mitochondrial genomes and other zoantharian mitochondrial genomes listed in Polisenio et al. (2020) and Fourreau et al. (2023) (Suppl. material 3). These protein-coding genes were individually aligned using MAFFT with the auto algorithm under default parameters. The concatenated dataset consisted of 35 zoantharian species and 13025 sites. For this mitochondrial genome dataset, ML reconstruction was performed using IQ-TREE2 (Minh et al. 2020) with best-fitting models for each protein-coding gene selected using ModelFinder (Kalyaanamoorthy et al. 2017) implemented in the IQ-TREE2 under Bayesian information criterion (Suppl. material 4). Support for each node was evaluated using 10,000 ultrafast bootstrap (UFBoot2) approximations (Hoang et al. 2018). BI was performed with MrBayes v.3.2.7 (Ronquist et al. 2012); four Markov chain Monte Carlo (MCMC) heated chains were run for 5,000,000 generations with the temperature of the heated chain set to 0.2. Chains were sampled every 200 generations. Best-fitting models for BI analyses were selected from models available in MrBayes using IQ-TREE2 (-mset mrbayes) (Suppl. material 4). Burn-in was set

to 1,250,000 generations, at which point the average standard deviation of split frequency was consistently below 0.01. Tracer v.1.7.1 (Rambaut et al. 2018) was used to inspect the convergence of MCMC. The mitochondrial genomes of two antipatharian species, *Stichopathes luetkeni* Brook, 1889 and *Myriopathes japonica* (Brook, 1889), were used as outgroups according to Polisenio et al. (2020).

## Morphological observations

External morphological characteristics were observed and dissected under a Stemi 305 microscope (Carl Zeiss, Oberkochen, Germany), and photographs were taken using a Zeiss Axiocam 208 color camera (Carl Zeiss, Oberkochen, Germany). In addition, in-situ photographs were used for morphological observations. Internal morphological characters were examined by histological sections; 10–15-mm thickness serial sections were made with a microtome (Leica RM2145, Leica Biosystems, Wetzlar, Germany) and stained with haematoxylin and eosin after desilication with 20% hydrofluoric acid for 18–24 h. Classification of marginal muscle shapes followed Swain et al. (2015). Cnidae analyses were conducted using undischarged nematocysts and spirocysts from tentacles, column, actinopharynx, and mesenterial filaments using a Nikon Eclipse80i stereomicroscope (Nikon, Tokyo, Japan), and photographs were taken by a Nikon DS-Qi2 (Nikon, Tokyo, Japan). Cnidae sizes were measured using ImageJ v.1.45s (Rasband 2012). The reported frequencies were the relative amounts based on numbers from all slides in the cnidae analyses. Cnidae classification generally followed England (1991) and Ryland and Lancaster (2004) except for the treatment of basitrichs and microbasic b-mastigophores as in Kise et al. (2019).

## Results

### Taxonomic account

**Order Zoantharia Rafinesque, 1815**

**Suborder Macrocnemina Haddon & Shackleton, 1891**

**Family Parazoanthidae Delage & Hérouard, 1901**

**Genus *Vitrumanthus* Kise, Montenegro & Reimer, 2022**

**Type species.** *Vitrumanthus schrieri* Kise, Montenegro & Reimer, 2022.

**Diagnosis.** Parazoanthidae characterized by obligate symbiotic relationship with massive hexasterophoran and Demospongiae sponges. Preserved polyps 0.3–3.1 mm in length, 0.8–3.4 mm in diameter. Azooxanthellate. Cyclically transitional marginal musculature.

***Vitrumanthus flosculus* Kise & Reimer, sp. nov.**

<https://zoobank.org/BD579CA0-C245-4CBD-85DA-389A18CBAD7E>

Figs 2–5

**Material examined. Holotype** • NSMT-Co 1898, Shoho Seamount, Nishi-Shichito Ridge, Japan (32°19.73'N, 138°44.28'E), 400 m depth, November 29, 2020.

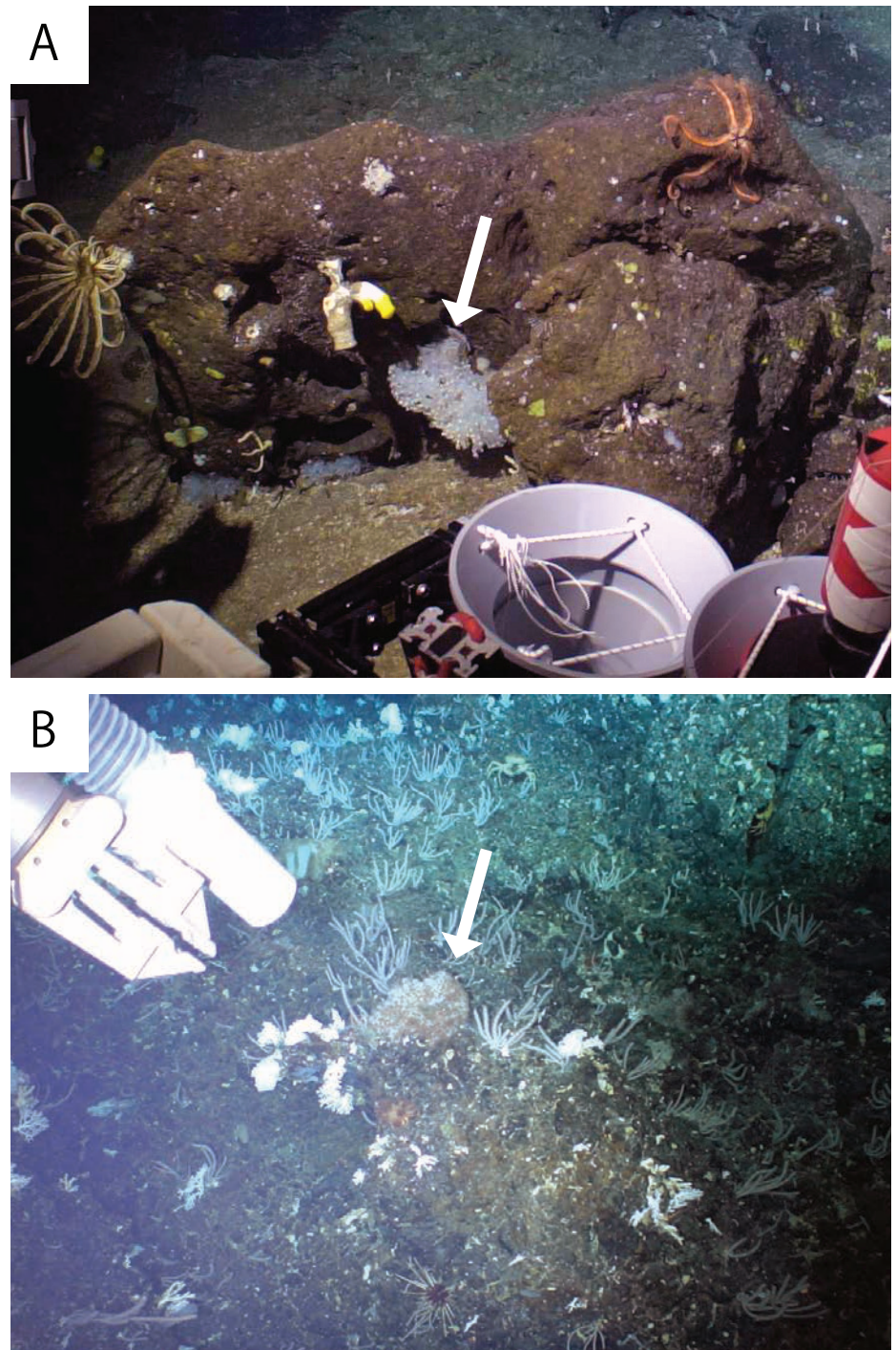


**Figure 2.** In-situ image of **A** *Vitrumanthus flosculus* sp. nov. and **B** *Churabana kuroshioae*. White arrows indicate each species associated with Hexasterophora sponges.

**Type locality.** Shoho Seamount, Nishi-Shichito Ridge, Japan.

**Etymology.** “*flosculus*” meaning “small flower” or “floweret” in Latin.

**Description. External morphology.** Colonial macrocnemic zoantharians associated with host hexasterophoran sponge *Farrea* Bowerbank, 1862 (Fig. 2A). Solitary or colonial polyps rise irregularly from all over the three-dimensional structure of host hexasterophoran sponge with base of polyps embedded in tissue of sponge (Fig. 3A). Preserved specimens consist of cylindrical polyps (Fig. 3B, C), dark brown in coloration. The living polyps and

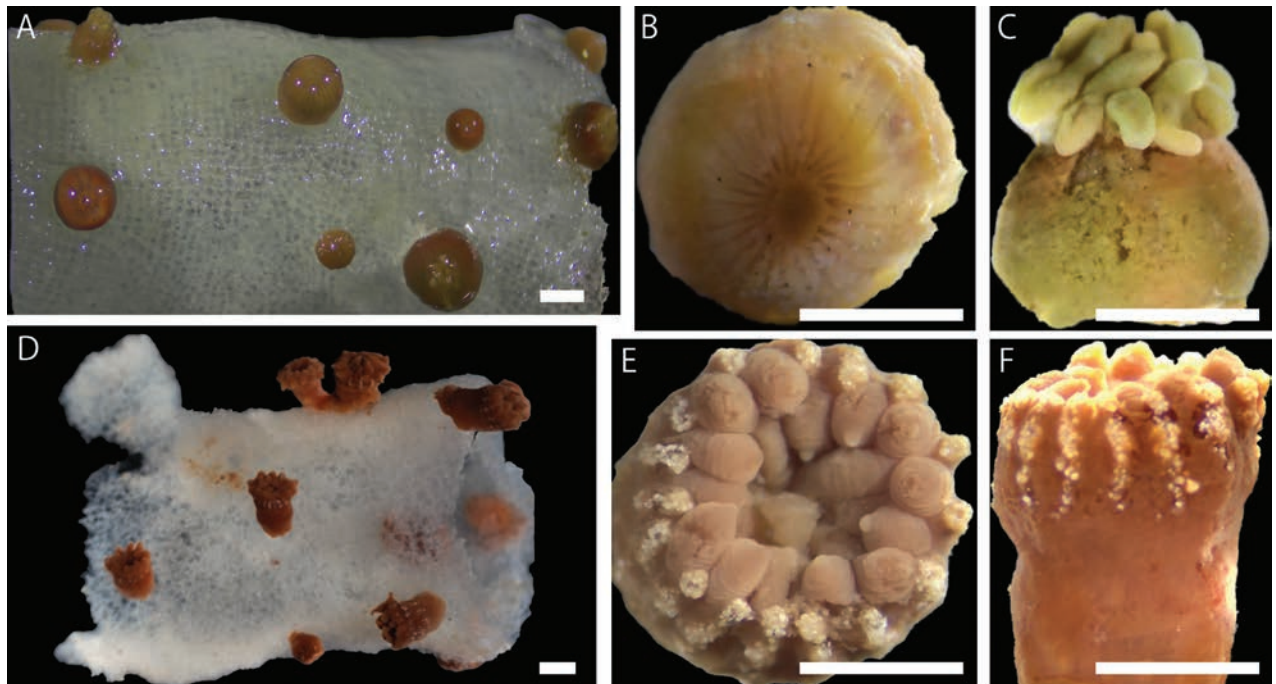


**Figure 3.** Images of external morphology of (A–C) *Vitrumanthus flosculus* sp. nov. and (D–F) *Churabana kuroshioae*. A preserved polyps attached to *Farrea* sp. B and C close-up image of a preserved polyp D preserved polyps attached to *Pararete* sp. E and F close-up image of a preserved polyp. Scale bars: 1.0 mm (A–C); 2.0 mm (D–F).

tentacles transparent yellowish in coloration. Surface of column smooth and ectoderm continuous (Fig. 3C). No encrustations of sand and silica particles in ectoderm of capitulum but ectoderm of scapus encrusted with small-sized sand and silica particles. Contracted preserved polyps 1.5–2.5 mm in height, 1.0–2.5 mm in diameter. Capitulary ridges indiscernible when contracted. Tentacles 22–26 in number.

**Internal morphology.** Zooxanthellae absent. Cyclically transitional marginal musculature (Fig. 4A–C). Encircling sinus or mesogleal canal present and basal canals of mesenteries absent (Fig. 4E). Mesenteries 22–26 in number, in brachycnemic arrangement (Fig. 4D). Mesoglea thickness 20–30  $\mu\text{m}$ . Siphonoglyph distinct and V-shaped. Mesenterial filaments present. Complete mesenteries fertile (Fig. 4E).

**Cnidae.** Basitrichs and microbasic b-mastigophores, microbasic p-mastigophores, holotrichs, special b-mastigophores, and spirocysts (see Fig. 5, Table 1 for sizes and distributions).

**Habitat and distribution.** Northwestern Pacific Ocean: known from the Shoho Seamount, Nishi-Shichito Ridge, Japan at a depth of 400 m. The new species was found on a glass sponge, *Farrea* sp., attached to rocks on the summit of the Shoho Seamount.

**Associated host.** *Farrea* sp.

**Remarks.** Regarding host sponges, *Vitrumanthus flosculus* sp. nov. is associated with *Farrea*, while other *Vitrumanthus* species are associated with other, different host sponges (*Vitrumanthus schrieri*: *Verrucocoeloidea*, *Parahigginsia* and *Cyrtaulon*, *Vitrumanthus vanderlandi*: *Aphrocallistes*, and *Vitrumanthus oligomyarius*: *Tretochone*). *Vitrumanthus flosculus* sp. nov. has holotrich nematocysts in all tissues we examined, while *V. vanderlandi* does not have holotrichs

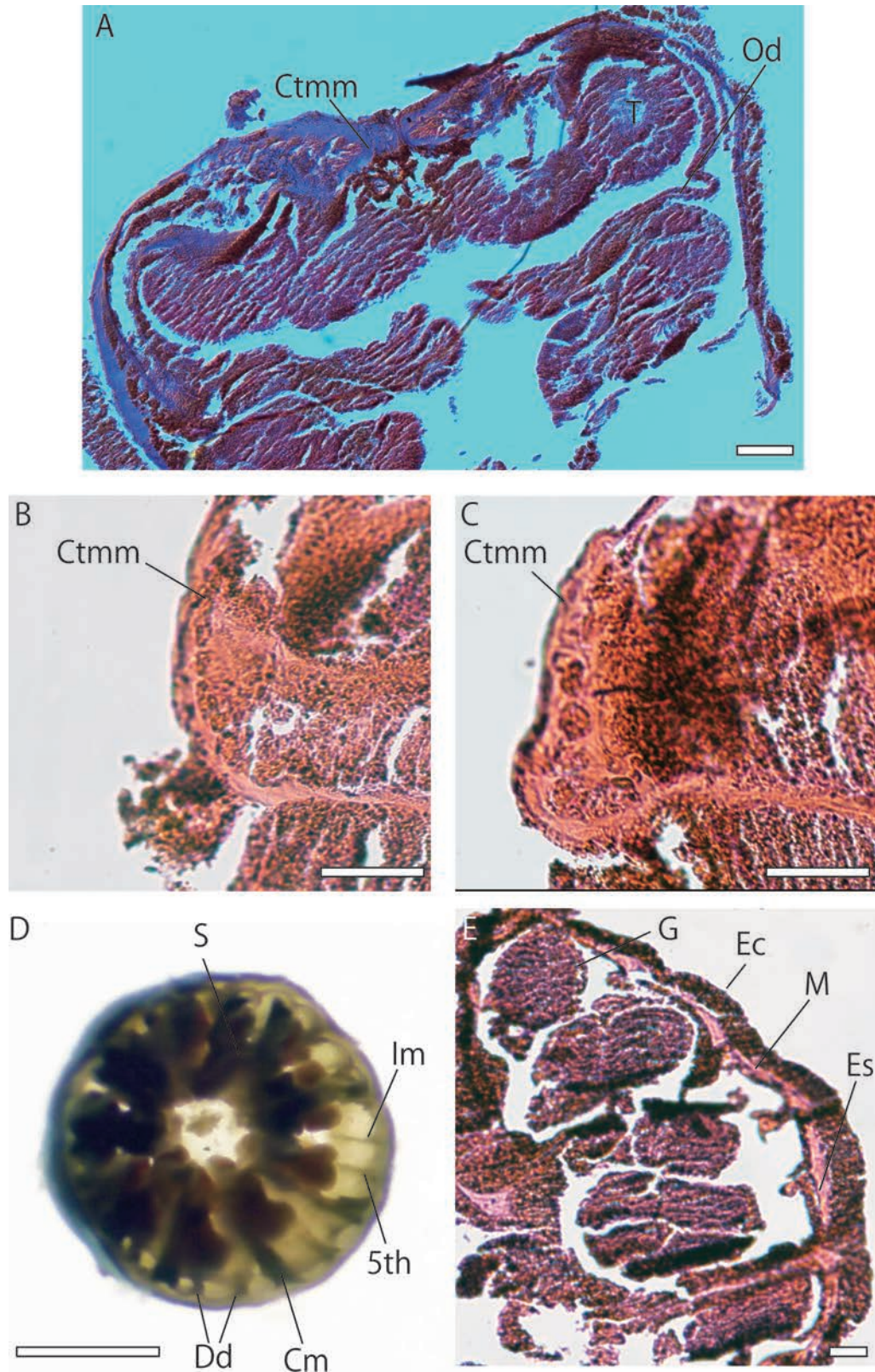


**Figure 4.** Images of internal morphology of *Vitrumanthus flosculus* sp. nov. **A** longitudinal section of a polyp **B** and **C** closed-up image of cyclically transitional marginal musculature **D** transverse-section of polyp at level of actinopharynx by hand-cutting **E** transverse-section of polyp. **Ctmm** cyclically transitional marginal musculature, **CM** complete mesentery, **Dd** dorsal directives, **Ec** ectoderm, **Es** encircling sinus, **IM** incomplete mesentery, **G** gonads, **M** mesoglea, **Od** oral disk, **T** tentacles, **S** siphonoglyph, **5<sup>th</sup>** 5<sup>th</sup> mesentery from dorsal directives. Scale bars: 100  $\mu$ m (**A**); 50  $\mu$ m (**B**, **C**, **E**); 1 mm (**D**).

## *Vitrumanthus flosculus* sp. nov.

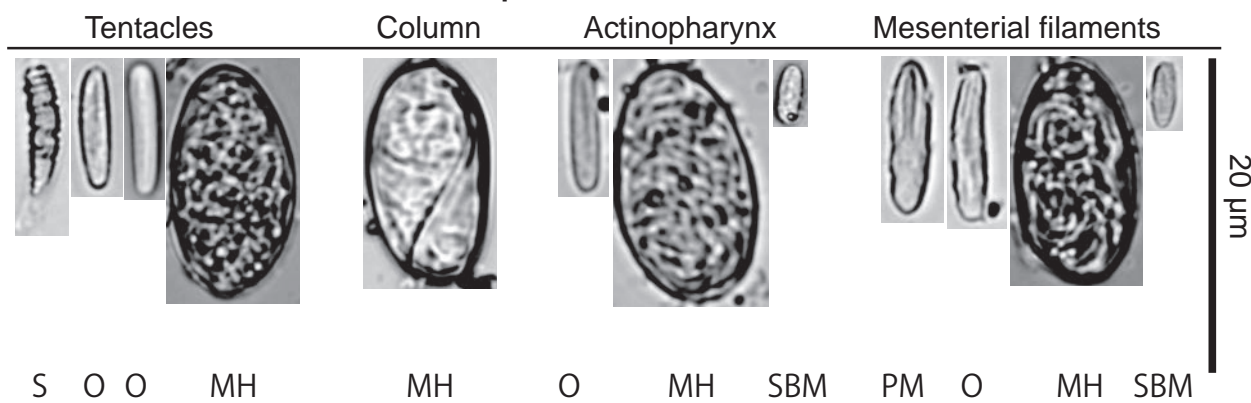


**Figure 5.** Cnidae in the tentacles, column, actinopharynx and mesenterial filaments of *Vitrumanthus flosculus* sp. nov. **HM** holotrich medium **O** basitrichs and microbasic b-mastigophores **PM** microbasic p-mastigophores **S** spirocysts **SBM** special microbasic b-mastigophores.

**Table 1.** Cnidae types and sizes observed in this study. Frequency: relative abundance of cnidae type in decreasing order; numerous, common, occasional, rare. *N* = number of cnidae measured.

Tissue	Type of cnidae	<i>Vitrumanthus flosculus</i> sp. nov.			
		Length (min-max, mean)	Width (min-max, mean)	Frequency	n
Tentacle	Spirocysts	18.5–8.5, 12.7	3.3–1.3, 2.0	Numerous	215
	Basitrichs and microbasic b-mastigophores	12.4–8.5, 10.4	3.2–1.4, 2.1	Numerous	73
	Holotrichs (M)	20.5	9.7	Rare	1
Column	Holotrich (M)	20.9–17.0, 18.7	11.9–8.7, 10.0	Common	25
Actinopharynx	Basitrichs and microbasic b-mastigophores	18.2–8.7, 12.0	3.5–1.6, 2.3	Common	38
	Special microbasic b-mastigophores	8.6–7.0, 7.8	3.3–1.6, 2.3	Common	13
	Holotrichs (L)	19.7–13.0, 17.5	11.3–8.5, 10.2	Common	18
Mesenterial filaments	Basitrichs and microbasic b-mastigophores	14.7–7.9, 11.8	3.1–1.4, 1.9	Common	21
	Microbasic p-mastigophores	16.9–10.7, 13.2	3.7–2.5, 3.3	Common	32
	Special microbasic b-mastigophores	9.3–7.2, 8.1	3.0–2.1, 2.5	Occasional	5
	Holotrichs (M)	22.2–15.4, 18.6	11.3–7.6, 9.4	Common	25

in any tissues. The surface of the column is smooth in *Vitrumanthus flosculus* sp. nov. with no encrustation of sand and silica particles in the ectoderm of capitulum, while the surface of the column is rough in *V. schrieri* with encrustation in the ectoderm of capitulum. The mesenteric arrangement of both *Vitrumanthus flosculus* sp. nov. and *V. oligomyarius* is brachycnemic, an exceptional characteristic for species within the suborder Macrocnemina. However, these two species can be distinguished by their numbers of tentacles and the sizes of the polyps; *Vitrumanthus flosculus* sp. nov. has 22–26 tentacles, while *V. oligomyarius* has 32–36 tentacles. *Vitrumanthus flosculus* sp. nov. has relatively smaller polyps than those of *V. oligomyarius* (1.5–2.5 mm in height and 1.0–2.5 mm in diameter vs. 0.5–3.1 mm in height and 1.2–3.4 mm in diameter). Furthermore, the host sponges of *Vitrumanthus flosculus* sp. nov. and *V. oligomyarius* are different (*Farrea* vs. *Tretochone*).

*Parachurabana* is a monotypic genus, and the diagnostic feature of this genus is described as having an association with Farreidae sponges. Although *Vitrumanthus flosculus* sp. nov. is associated with *Farrea* sp., *Vitrumanthus flosculus* sp. nov. can be easily distinguished from *Parachurabana* by the different shape of its sphincter muscle (cyclically transitional vs. cteniform endodermal

marginal musculature) and different mesenterial arrangement (brachycnemic vs macrocnemic arrangement). The diagnosis of *Parachurabana* may need to be updated based on examinations of additional specimens.

### Genus *Churabana* Kise, Montenegro & Reimer, 2021

**Type species.** *Churabana kuroshioae* Kise, Montenegro & Reimer, 2021.

**Diagnosis.** (modified from the diagnosis given by Kise et al. 2022). Parazoanthidae with obligate symbiotic relationship with *Pararete* sponges. Preserved polyps 3.0–10.0 mm in height, 2.8–5.0 mm in diameter. Azooxanthellate. Cteniform endodermal marginal musculature.

**Remarks.** We modified the generic diagnosis based on a newly collected specimen of *Churabana kuroshioae*. This species seems to have host specificity to *Pararete* species based on this study and Kise et al. (2022), although further investigations are required to confirm this.

### *Churabana kuroshioae* Kise, Montenegro & Reimer, 2021

**Material examined.** • NSMT-Co 1899, An'ei Seamount, Nishi-Shichito Ridge, Japan (29°17.03'N, 138°37.85'E), 770 m depth, October 17, 2021.

**Type locality.** Near Iejima Island, Motobu, Okinawa, Japan.

**Description.** External morphology. Parazoanthidae associated with host hexasterophoran sponge *Pararete ljima*, 1927. Approximately 100 truncated cone-shaped cylindrical polyps in preserved specimen. Solitary or colonial polyps rise irregularly from host *Pararete* sponges (Figs 2B, 3D). The living and preserved polyps dark brown and tentacles brown in coloration. Ectoderm and mesoglea of capitulum encrusted with numerous and comparatively large sizes of sand and silica particles (approximately < 100 µm). No encrustations of sand and silica particles in the ectoderm or mesoglea of scapus (Fig. 3F). Contracted preserved polyps 3.0–10.0 mm in height, 2.8–5.0 mm in diameter. Capitulary ridges discernible when contracted, 15–16 in number, and 30–32 tentacles (Fig. 3E).

**Habitat and distribution.** Northwestern Pacific Ocean: *Churabana kuroshioae* was originally reported from the Ryukyu Archipelago, Japan at depths of 520–650 m (Kise et al. 2022). The findings in this study reveal that this species is also distributed at the An'ei Seamount, Nishi-Shichito Ridge, Japan at a depth of 770 m. *Churabana kuroshioae* was found on the summit of An'ei Seamount on glass sponge *Pararete* sp. attached to rocky substrate.

**Associated host.** *Pararete* sp.

**Remarks.** The polyp coloration of *Churabana kuroshioae* is cream-pink or beige with cream or whitish transparent tentacles in the original description, while the specimen of *C. kuroshioae* collected from An'ei Seamount has dark brown polyps with brown tentacles. As well, the polyp sizes of the specimen examined in this study were relatively larger than that of the original description (3.0–4.0 mm in height, 2.8–4.0 mm in diameter) by Kise et al. (2022). Based on the results of molecular phylogenetic analyses, the differences in coloration and polyp sizes found in this study are considered intraspecific variation, although detailed molecular analyses in the future may warrant reconsideration of this.

### Mitochondrial genome

The complete mitochondrial genome sizes of *Churabana kuroshioae* and *Vitrumanthus flosculus* sp. nov. were 22,738 and 20,556 bp, respectively. The mitochondrial gene order and content of these two species were the same, including 13 protein-coding genes, two rRNA genes, and two transfer RNA genes. The sequences of the protein-coding region covered 54.0% (*Churabana kuroshioae*) and 58.8% (*Vitrumanthus flosculus* sp. nov.) of the mitochondrial genomes, while GC contents of *Churabana kuroshioae* and *Vitrumanthus flosculus* sp. nov. were 49.8% and 50.0%, respectively. Regarding stop codons, both *C. kuroshioae* and *V. flosculus* sp. nov. have either TAA and TAG for all protein-coding genes, with the start codon being ATG. The mitochondrial base composition was A: 22.6%, T: 27.6%, G: 26.1%, C: 23.7% in *C. kuroshioae*, and A: 22.2%, T: 27.8%, G: 26.3%, C: 23.6% in *V. flosculus* sp. nov.

### Molecular phylogeny

ML and BI phylogenetic analyses based on the six-gene dataset indicated that *Churabana* and *Vitrumanthus* were both monophyletic clades with complete support (ML = 100%, BI = 1). *Churabana* was sister to *Thoracactis* (ML = 88%, BI = 0.96). ML and BI phylogenetic topologies were congruent (Fig. 6). *Vitrumanthus flosculus* sp. nov. was sister to *Vitrumanthus oligomyarius* and *Vitrumanthus vanderlandi* (ML = 68%, BI = 0.99).

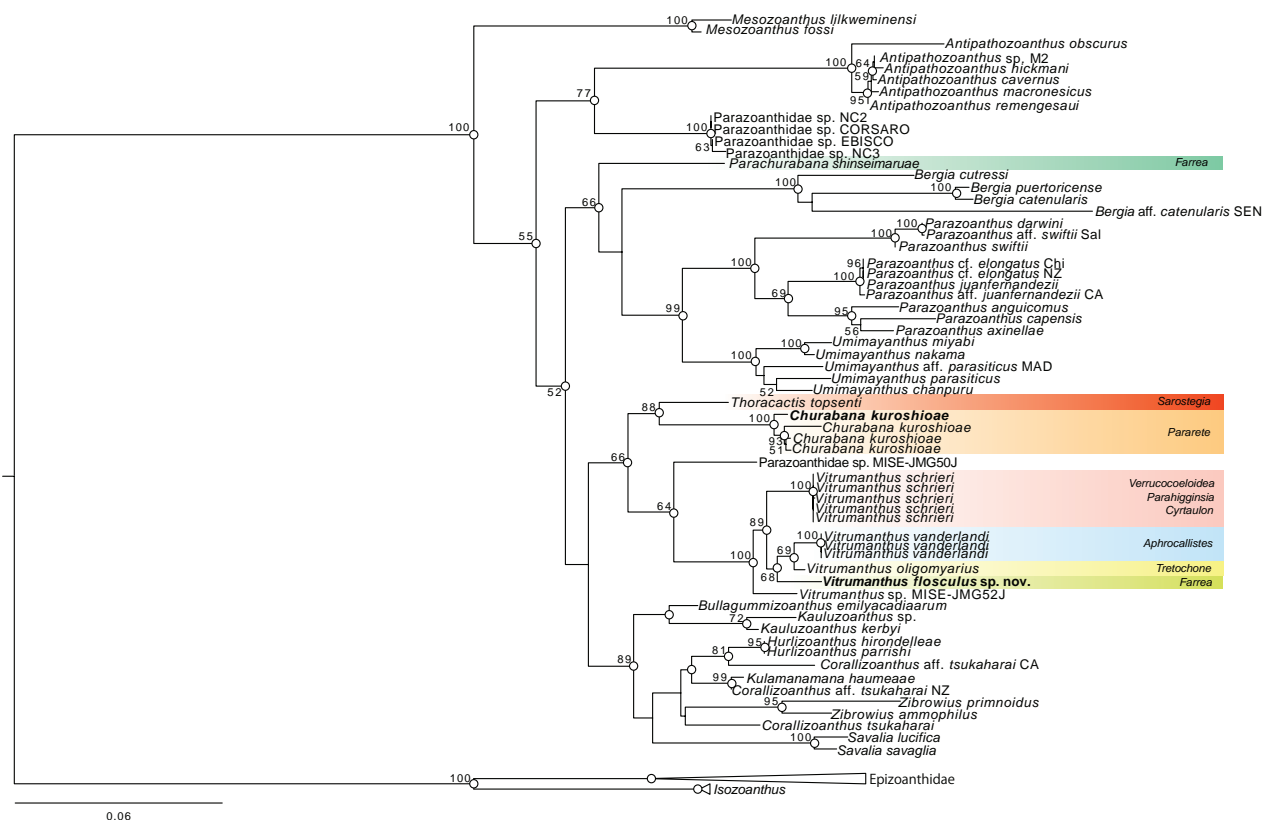
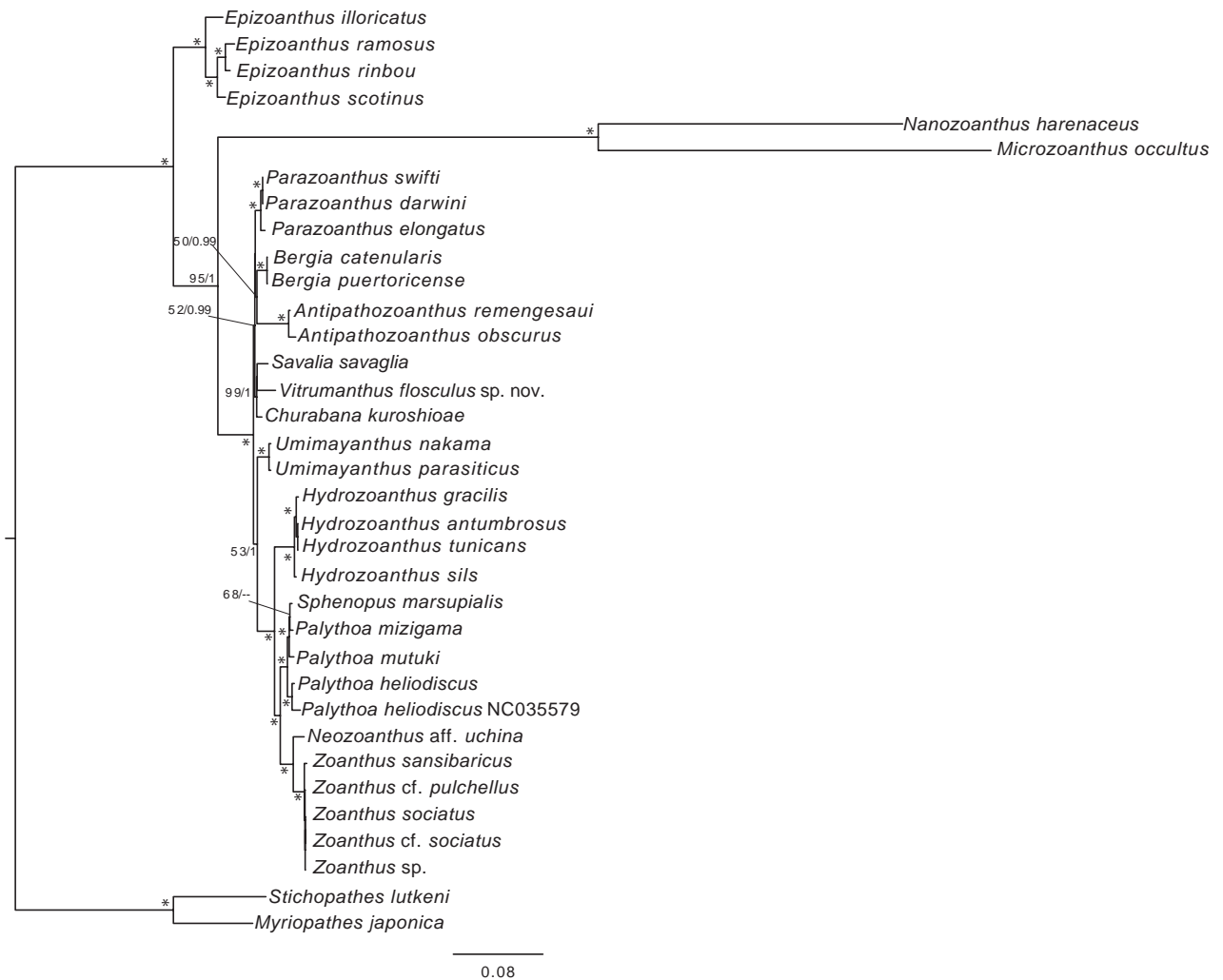


Figure 6. Maximum-likelihood tree based on combined dataset of COXI, 12S rDNA, 16S rDNA, 18S rDNA, 28S rDNA, and ITS rDNA sequences. Numbers at nodes represent ML bootstrap values (>50% are shown). White circles on nodes indicate high support of Bayesian posterior probabilities (PP) (>0.95).



**Figure 7.** Maximum-likelihood tree based on complete mitochondrial genome dataset. Numbers at each node indicates ML bootstrap value and Bayesian posterior probabilities. Asterisks indicate ML/BI = 100/1.00.

ML and BI phylogenetic topologies based on the complete mitochondrial genome dataset were also congruent (Fig. 7). *Churabana* and *Vitrumanthus* formed a monophyletic clade with *Savalia savaglia* (Bertoloni, 1819) with strong support (ML = 99%, BI = 1).

## Discussion

*Thoracactis topsenti* was the first zoantharian species to be described as Hexasterophora-associated (Gravier 1918). Subsequent studies have more recently described three Parazoanthidae genera associated with hexasterophorans from the Indo-Pacific and the Atlantic (Kise et al. 2022, 2023). Although *Thoracactis* was originally placed in the family Epizoanthidae, Kise et al. (2024) have recently transferred *T. topsenti* to Parazoanthidae based on molecular phylogenetic and morphological results, indicating that the association with Hexasterophora is unique to the family Parazoanthidae. Kise et al. (2023) found that Hexasterophora-associated species were not monophyletic, but instead that *Parachurabana* was recovered as basal to Demospongiae-associated species (*Bergia*, *Parazoanthus*, and *Umimayanthus*), indicating that Parazoanthidae species may have

switched its host from Hexasterophora to Demospongiae. However, the phylogenetic tree based on a six-gene dataset of this study and previous studies have shown weak support at some nodes in Parazoanthidae. Therefore, further studies using phylogenetically informative loci, as mentioned below, are needed to better understand the evolutionary history of host switching in Parazoanthidae.

This study sequenced the complete mitochondrial genomes of *Churabana* and *Vitrumanthus* for the first time. The mitochondrial gene arrangements of these two genera were in the same order as those of other zoantharians (Poliseno et al. 2020), further reinforcing the conservative nature of zoantharian mitochondrial gene orders.

Based on both our six-gene and complete mitochondrial genome analyses, it is apparent that much of the diversity of Parazoanthidae has comparatively recently evolved, resulting in weak support at many generic-level nodes, with short genetic distances as reported in Poliseno et al. (2020). Perhaps more robust genomic analytical methods (e.g., ultra-conserved elements; Cowman et al. 2020; Quattrini et al. 2020) may help resolve the weak phylogenetic structure of Parazoanthidae, which would then help in taxonomic reconsideration of the family. Most of the genera contained within Parazoanthidae have been erected since 2008 (12/17 genera), with each genus erected based on its uniqueness from other genera, and little consideration has yet been given to the phylogeny and taxonomy of the family. It may be time to reconsider the framework of Parazoanthidae, and it is hoped that the current study provides the impetus to begin this future work.

Shoho and An'ei seamounts are on the Nishi-Shichito Ridge, which has been designated as a marine protected area (MPA) (Ministry of the Environment of Japan 2020), and recent studies have described a number of previously unknown species including sea pens, sea stars, ribbon worms, and parasitic crustacean from the Shoho and An'ei seamounts (Hookabe et al. 2021, 2023; Kobayashi et al. 2022; Jimi et al. 2023; Kushida et al. 2024). Our results echo these recent studies, highlighting the overall lack of diversity studies in this MPA. Documentation of local faunal biodiversity is one important key for effective monitoring of MPAs, and further taxonomic studies of many taxa are needed to better understand the true marine diversity of this MPA.

## Acknowledgements

We thank the captain and crew of the R/V Kaimei, the operation team of KM-ROV, and all the research members during the KM20-10C and KM21-E04 cruises. This research was performed by the Environment Research and Technology Development Fund (JPMEERF20S20700) of the Environmental Restoration and Conservation Agency Provided by the Ministry of Environment of Japan.

## Additional information

### Conflict of interest

The authors have declared that no competing interests exist.

### Ethical statement

No ethical statement was reported.

## Funding

This study was supported by the Environment Research and Technology Development Fund (JPMEERF20S20700) of the Environmental Restoration and Conservation Agency Provided by the Ministry of Environment of Japan. This study was also partially supported by the Research Laboratory on Environmentally Conscious Developments and Technologies (E-code) at the National Institute of Advanced Industrial Science and Technology. The first author was supported in part by JSPS KAKENHI grant number 23KJ2206 from the Japan Society for the Promotion of Science. We thank an anonymous reviewer and the journal editor for their valuable comments that improved this work.

## Author contributions

Data curation: HK. Formal analysis: HK. Funding acquisition: YF, AI. Investigation: HK, YI. Project administration: YF, ST. Resources: YI, JDR, YF. Validation: HK. Visualization: HK. Writing - original draft: HK. Writing - review and editing: ST, YI, JDR, AI, YF.

## Author ORCIDs

Hiroki Kise  <https://orcid.org/0000-0002-4099-6469>

James Davis Reimer  <https://orcid.org/0000-0003-0453-8804>

Akira Iguchi  <https://orcid.org/0000-0002-8894-1977>

Yuji Ise  <https://orcid.org/0009-0009-4887-611X>

Shinji Tsuchida  <https://orcid.org/0000-0002-8600-2386>

Yoshihiro Fujiwara  <https://orcid.org/0000-0002-1833-1866>

## Data availability

All of the data that support the findings of this study are available in the main text or Supplementary Information. Obtained sequences have been deposited in NCBI GenBank (accession number PQ308072–PQ308077 and PQ554681–PQ554682).

## References

- Althaus F, Williams A, Schlacher TA, Kloser RJ, Green MA, Barker BA, Bax NJ, Brodie P, Schlacher-Hoenlinger MA (2009) Impacts of bottom trawling on deep-coral ecosystems of seamounts are long-lasting. *Marine Ecology Progress Series* 397: 279–294. <https://doi.org/10.3354/meps08248>
- Bankevich A, Nurk S, Antipov D, Gurevich AA, Dvorkin M, Kulikov AS, Lesin VM, Nikolenko SI, Pham S, Pribelski Ad, Pyshkin AV, Sirotkin AV, Vyahhi N, Tesler GI, Alekseyev MA, Pevzner PA (2012) SPAdes: a new genome assembly algorithm and its applications to single-cell sequencing. *Journal of Computational Biology* 19(5): 455–477. <https://doi.org/10.1089/cmb.2012.0021>
- Bernt M, Donath A, Jühling F, Externbrink F, Florentz C, Fritzsche G, Pütz J, Middendorf M, Stadler PF (2013) MITOS: improved de novo metazoan mitochondrial genome annotation. *Molecular Phylogenetics and Evolution* 69(2): 313–319. <https://doi.org/10.1016/j.ympev.2012.08.023>
- Bolger AM, Lohse M, Usadel B (2014) Trimmomatic: a flexible trimmer for Illumina sequence data. *Bioinformatics* 30(15): 2114–2120. <https://doi.org/10.1093/bioinformatics/btu170>
- Bowerbank JS (1862) On the anatomy and physiology of the Spongiadae. Part III On the generic characters, the specific characters, and on the method of examination. *Philosophical Transactions of the Royal Society* 152(2): 1087–1135. <https://doi.org/10.1098/rstl.1862.0044>

- Bracken-Grissom H, Widder E, Johnsen S, Messing C, Frank T (2018) Decapod diversity associated with deep-sea octocorals in the Gulf of Mexico. *Crustaceana* 91(10): 1267–1275. <https://doi.org/10.1163/15685403-00003829>
- Brook G (1889) Report on the Antipatharia collected by H.M.S. Challenger during the years 1873–76. Report on the Scientific Results of the Voyage of H.M.S. Challenger during the years 1873–76. *Zoology* 32[part 80]: [i–iii,]1–222 [pl. 1–15]. <http://www.19thcenturyscience.org/HMSC/HMSC-Reports/Zool-80/README.html>
- Buhl-Mortensen L, Mortensen, PB (2004) Symbiosis in deep-water corals. *Symbiosis*.
- Carlgren O (1923) Ceriantharia and Zoantharia. *Wissensch Ergebn Deutsch Tiefsee-Exp Dampfer 'Valdivia' 1898–99* 19(7): 242–337.
- Carreiro-Silva M, Ocaña O, Stanković D, Sampaio I, Porteiro FM, Fabri MC, Stefanni S (2017) Zoantharians (Hexacorallia: Zoantharia) associated with cold-water corals in the Azores region: new species and associations in the deep sea. *Frontiers in Marine Science* 4: 88. <https://doi.org/10.3389/fmars.2017.00088>
- Chan PP, Lin BY, Mak AJ, Lowe TM (2021) tRNAscan-SE 2.0: improved detection and functional classification of transfer RNA genes. *Nucleic Acids Research* 49(16): 9077–9096. <https://doi.org/10.1093/nar/gkab688>
- Clark MR, Vinnichenko VI, Gordon JD, Beck-Bulat GZ, Kukharev NN, Kakora AF (2007) Large-scale distant-water trawl fisheries on seamounts. *Seamounts: Ecology, Fisheries, and Conservation* 12: 361–399. <https://doi.org/10.1002/9780470691953.ch17>
- Clark MR, Rowden AA, Schlacher T, Williams A, Consalvey M, Stocks KI, Rogers AD, O'Hara TD, White M, Shank TM, Hall-Spencer JM (2010) The ecology of seamounts: structure, function, and human impacts. *Annual Review of Marine Science* 2: 253–278. <https://doi.org/10.1146/annurev-marine-120308-081109>
- Clark MR, Althaus F, Schlacher TA, Williams A, Bowden DA, Rowden AA (2016) The impacts of deep-sea fisheries on benthic communities: a review. *ICES Journal of Marine Science* 73(suppl\_1): i51–i69. <https://doi.org/10.1093/icesjms/fsv123>
- Cowman PF, Quattrini AM, Bridge TC, Watkins-Colwell GJ, Fadli N, Grinblat M, Roberts TE, McFadden CS, Miller DJ, Baird AH (2020) An enhanced target-enrichment bait set for Hexacorallia provides phylogenomic resolution of the staghorn corals (Acroporidae) and close relatives. *Molecular Phylogenetics and Evolution* 153: 106944. <https://doi.org/10.1016/j.ympev.2020.106944>
- Darriba D, Posada D, Kozlov AM, Stamatakis A, Morel B, Flouri T (2020) ModelTest-NG: a new and scalable tool for the selection of DNA and protein evolutionary models. *Molecular Biology and Evolution* 37(1): 291–294. <https://doi.org/10.1093/molbev/msz189>
- Delage Y, Hérouard E (1901) Zoanthidés. – Zoanthidae. In *Traité de Zoologie concrète, 2eme partie. Les Cœlentérés*. C. Reinwald, Paris, 654–667.
- Dohrmann M, Haen KM, Lavrov DV, Wörheide G (2011) Molecular phylogeny of glass sponges (Porifera, Hexactinellida): increased taxon sampling and inclusion of the mitochondrial protein-coding gene, cytochrome oxidase subunit I. In *Ancient Animals, New Challenges* (pp. 11–20). Springer, Dordrecht. <https://doi.org/10.1007/s10750-011-0727-z>
- England KW (1991) Nematocysts of sea anemones (Actiniaria, Ceriantharia and Corallimorpharia: Cnidaria): nomenclature. *Hydrobiologia* 216: 691–697. <https://doi.org/10.1007/BF00026532>
- Fourreau CJL, Kise H, Santander MD, Pirro S, Maronna MM, Polisenio A, Santos MEA, Reimer JD (2023) Genome sizes and repeatome evolution in zoantharians (Cnidaria: Hexacorallia: Zoantharia). *PeerJ* 11: e16188. <https://doi.org/10.7717/peerj.16188>

- Glasby CJ, Watson C (2001) A new genus and species of Syllidae (Annelida: Polychaeta) commensal with octocorals. *Beagle: Records of the Museums and Art Galleries of the Northern Territory, The Beagle* 17: 43–51. <https://doi.org/10.5962/p.286289>
- Gravier C (1918) Note sur une actinie (*\*Thoracactis\** n. g., *\*topsenti\** n. sp.) et un annélide polychète (*\*Hermadion Fauveli\** n. sp.), commensaux d'une Éponge siliceuse (*\*Sarostegia oculata\** Topsent). *Bulletin de l'Institut océanographique de Monaco* 344: 1–20. <https://doi.org/10.5962/bhl.part.8664>
- Hoang DT, Chernomor O, Von Haeseler A, Minh BQ, Vinh LS (2018) UFBoot2: improving the ultrafast bootstrap approximation. *Molecular Biology and Evolution* 35(2): 518–522. <https://doi.org/10.1093/molbev/msx281>
- Hookabe N, Jimi N, Yokooka H, Tsuchida S, Fujiwara, Y (2021) *Lacydonia shohoensis* (Annelida, Lacydoniidae) sp. nov.—a new lacydonid species from deep-sea sunken wood discovered at the Nishi-Shichito Ridge, north-western Pacific Ocean. *Journal of the Marine Biological Association of the United Kingdom* 101(6): 927–933. <https://doi.org/10.1017/S0025315421000862>
- Hookabe N, Kohtsuka H, Fujiwara Y, Tsuchida S, Ueshima R (2023) Three new species in *Tetrastemma* Ehrenberg, 1828 (Nemertea, Monostilifera) from sublittoral to upper bathyal zones of the northwestern Pacific. *ZooKeys* 1146: 135–146. <https://doi.org/10.3897/zookeys.1146.95004>
- Jimi N, Kobayashi I, Moritaki T, Woo SP, Tsuchida S, Fujiwara Y (2023) Insights into the diversification of deep-sea endoparasites: Phylogenetic relationships within *Dendrogaster* (Crustacea: Ascothoracida) and a new species description from a western Pacific seamount. *Deep Sea Research Part I: Oceanographic Research Papers* 196: 104025. <https://doi.org/10.1016/j.dsr.2023.104025>
- Jin JJ, Yu WB, Yang JB, Song Y, DePamphilis CW, Yi TS, Li DZ (2020) GetOrganelle: a fast and versatile toolkit for accurate de novo assembly of organelle genomes. *Genome Biology* 21(1): 1–31. <https://doi.org/10.1186/s13059-020-02154-5>
- Kalyaanamoorthy S, Minh BQ, Wong TK, Von Haeseler A, Jermiin LS (2017) ModelFinder: fast model selection for accurate phylogenetic estimates. *Nature Methods* 14: 587–589. <https://doi.org/10.1038/nmeth.4285>
- Katoh K, Standley DM (2013) MAFFT multiple sequence alignment software version 7: improvements in performance and usability. *Molecular Biology and Evolution* 30(4): 772–780. <https://doi.org/10.1093/molbev/mst010>
- Kise H, Montenegro J, Ekins M, Moritaki T, Reimer JD (2019) A molecular phylogeny of carcinoecium-forming *Epizoanthus* (Hexacorallia: Zoantharia) from the Western Pacific Ocean with descriptions of three new species. *Systematics and Biodiversity* 17(8): 773–786. <https://doi.org/10.1080/14772000.2019.1693439>
- Kise H, Montenegro J, Santos MEA, Hoeksema BW, Ekins M, Ise Y, Higashiji T, Fernandez-Silva I, Reimer JD (2022) Evolution and phylogeny of glass-sponge-associated zoantharians, with a description of two new genera and three new species. *Zoological Journal of the Linnean Society* 194(1): 323–347. <https://doi.org/10.1093/zoolinnean/zlab068>
- Kise H, Nishijima M, Iguchi A, Minatoya J, Yokooka H, Ise Y, Suzuki A (2023) A new hexactinellid-sponge-associated zoantharian (Porifera, Hexasterophora) from the northwestern Pacific Ocean. *ZooKeys* 1156: 71–85. <https://doi.org/10.3897/zookeys.1156.96698>
- Kise H, Montenegro J, Corrêa PV, Clemente MV, Sumida PY, Hoeksema BW, Reimer JD (2024) A taxonomic revision of the sponge-associated genus *Thoracactis* Gravier, 1918 (Anthozoa: Zoantharia) based on an integrated approach. *Contributions to Zoology* 93(3): 229–251. <https://doi.org/10.1163/18759866-bja10059>

- Kobayashi I, Yamamoto M, Fujiwara Y, Tsuchida S, Fujita T (2022) First record of the family Myxasteridae (Asteroidea: Velatida) from western north Pacific with description of a new species of *Asthenactis*. *Species Diversity* 27(2): 251–258. <https://doi.org/10.12782/specdiv.27.251>
- Komai T, Tsuchida S, Fujiwara Y (2022) New record of a rarely collected caridean shrimp *Bathypalaemonella pandaloides* (Rathbun, 1906) (Decapoda: Bathypalaemonellidae) from the West Mariana Ridge, northwestern Pacific. *Zootaxa* 5129(2): 272–284. <https://doi.org/10.11646/zootaxa.5129.2.7>
- Kozlov AM, Darriba D, Flouri T, Morel B, Stamatakis A (2019) RAxML-NG: a fast, scalable and user-friendly tool for maximum likelihood phylogenetic inference. *Bioinformatics* 35(21): 4453–4455. <https://doi.org/10.1093/bioinformatics/btz305>
- Kushida Y, Kise H, Iguchi A, Fujiwara Y, Tsuchida S (2024) Description of the fifth sea pen species that attaches to hard substrates by modifying its peduncle. *Deep Sea Research Part I: Oceanographic Research Papers* 203: 104212. <https://doi.org/10.1016/j.dsr.2023.104212>
- Minh BQ, Schmidt HA, Chernomor O, Schrempf D, Woodhams MD, Von Haeseler A, Lanfear R (2020) IQ-TREE 2: new models and efficient methods for phylogenetic inference in the genomic era. *Molecular Biology and Evolution* 37(5): 1530–1534. <https://doi.org/10.1093/molbev/msaa015>
- Ministry of the Environment of Japan (2020) Ministry of the Environment of Japan. <https://www.env.go.jp/nature/naturebiodic/kaiyo-hogoku.html> [Accessed 20<sup>th</sup> Mar 2024]
- Molodtsova TN, Opresko DM (2017) Black corals (Anthozoa: Antipatharia) of the Clarion-Clipperton fracture zone. *Marine Biodiversity* 47(2): 349–365. <https://doi.org/10.1007/s12526-017-0659-6>
- Montenegro J, Hoeksema BW, Santos MEA, Kise H, Reimer JD (2020) Zoantharia (Cnidaria: Hexacorallia) of the Dutch Caribbean and one new species of *Parazoanthus*. *Diversity* 12(5): 190. <https://doi.org/10.3390/d12050190>
- Montenegro J, Fromont J, Richards Z, Kise H, Gomez O, Hoeksema BW, Reimer JD (2024) Museum collections as untapped sources of undescribed diversity of sponge-zoantharian associations with the description of six new species of *Umimayanthus* (Zoantharia: Parazoanthidae) from Western Australia and eastern Indonesia. *Contributions to Zoology* 1: 1–57. <https://doi.org/10.1163/18759866-bja10069>
- Morato T, Hoyle SD, Allain V, Nicol SJ (2010) Seamounts are hotspots of pelagic biodiversity in the open ocean. *Proceedings of the National Academy of Sciences* 107(21): 9707–9711. <https://doi.org/10.1073/pnas.0910290107>
- Mosher CV, Watling L (2009) Partners for life: a brittle star and its octocoral host. *Marine Ecology Progress Series* 397: 81–88. <https://doi.org/10.3354/meps08113>
- Okanishi M, Mah CL (2020) Overlooked biodiversity from museum collections: four new species and one new genus of Ophiuroidea (Echinodermata) from Antarctica and adjacent regions with notes on multi-armed ophiuroids. *Marine Biodiversity* 50(5): 1–26. <https://doi.org/10.1007/s12526-020-01080-w>
- Poliseno A, Santos MEA, Kise H, Macdonald B, Quattrini AM, McFadden CS, Reimer JD (2020) Evolutionary implications of analyses of complete mitochondrial genomes across order Zoantharia (Cnidaria: Hexacorallia). *Journal of Zoological Systematics and Evolutionary Research* 58(4): 858–868. <https://doi.org/10.1111/jzs.12380>
- Probert PK, Mcknight DG, Grove SL (1997) Benthic invertebrate bycatch from a deep-water trawl fishery, Chatham Rise, New Zealand. *Aquatic Conservation: Marine and Freshwater Ecosystems* 7(1): 27–40. [https://doi.org/10.1002/\(SICI\)1099-0755\(199703\)7:1<27::AID-AQC214>3.0.CO;2-9](https://doi.org/10.1002/(SICI)1099-0755(199703)7:1<27::AID-AQC214>3.0.CO;2-9)

- Quattrini AM, Rodríguez E, Faircloth BC, Cowman PF, Brugler MR, Farfan GA, Hellberg ME, Kitahara MV, Morrison CL, Paz-García DA, Reimer JD, McFadden CS (2020) Palaeoclimate ocean conditions shaped the evolution of corals and their skeletons through deep time. *Nature Ecology & Evolution* 4(11): 1531–1538. <https://doi.org/10.1038/s41559-020-01291-1>
- Rafinesque CS (1815) *Analyse de la nature: or, Tableau de l'univers et des corps organisés*. Palermo, Italy, 224 pp. <https://doi.org/10.5962/bhl.title.106607>
- Rambaut A, Drummond AJ, Xie D, Baele G, Suchard MA (2018) Posterior summarization in Bayesian phylogenetics using Tracer 1.7. *Systematic Biology* 67(5): 901–904. <https://doi.org/10.1093/sysbio/syy032>
- Rasband WS (2012) *ImageJ: Image processing and analysis in Java*. *Astrophysics Source Code Library* 1: e06013.
- Reimer JD, Sinniger F (2024) World List of Zoantharia. Zoantharia. [World Register of Marine Species] <https://www.marinespecies.org/aphia.php?p=taxdetails&id=607338> [on 2024-04-27]
- Reimer JD, Nonaka M, Sinniger F, Iwase F (2008) Morphological and molecular characterization of a new genus and new species of parazoanthid (Anthozoa: Hexacorallia: Zoantharia) associated with Japanese Red Coral. *Coral Reefs* 27: 935–949. <https://doi.org/10.1007/s00338-008-0389-0>
- Reimer JD, Kise H, Santos MEA, Lindsay DJ, Pyle RL, Copus JM, Bowen BW, Nonaka M, Higashiji T, Benayahu Y (2019) Exploring the biodiversity of understudied benthic taxa at mesophotic and deeper depths: examples from the order Zoantharia (Anthozoa: Hexacorallia). *Frontiers in Marine Science* 6: 305. <https://doi.org/10.3389/fmars.2019.00305>
- Reiswig HM, Dohrmann M (2014) Three new species of glass sponges (Porifera: Hexactinellida) from the West Indies, and molecular phylogenetics of Euretidae and Auloplacidae (Sceptrulophora). *Zoological Journal of the Linnean Society* 171: 233–253. <https://doi.org/10.1111/zoj.12138>
- Reiswig HM, Wheeler B (2002) Family Euretidae Zittel, 1877. In: Hooper JNA, Van Soest RWM, Willenz P (Eds) *Systema Porifera*. Springer, Boston, MA, 1301–1331. [https://doi.org/10.1007/978-1-4615-0747-5\\_135](https://doi.org/10.1007/978-1-4615-0747-5_135)
- Ronquist F, Teslenko M, van der Mark P, Ayres DL, Darling A, Höhna S, Larget B, Liu L, Suchard MA, Huelsenbeck JP (2012) MrBayes 3.2: efficient Bayesian phylogenetic inference and model choice across a large model space. *Systematics Biology* 61(3): 539–542. <https://doi.org/10.1093/sysbio/sys029>
- Rossi S, Bramanti L, Horta P, Allcock L, Carreiro-Silva M, Coppari M, Denis V, Hadjioannou L, Isla E, Jimenez C, Johnson M, Mohn C, Orejas C, Ramšak A, Reimer J, Rinkevich B, Rizzo L, Salomidi M, Samaai T, Schubert N, Soares M, Thurstan R, Vassallo P, Ziveri P, Zorrilla-Pujana J (2022) Protecting global marine animal forests. *Science* 376(6596): 929–929. <https://doi.org/10.1126/science.abq7583>
- Rowden AA, Dower JF, Schlacher TA, Consalvey M, Clark MR (2010) Paradigms in seamount ecology: fact, fiction and future. *Marine Ecology* 31: 226–241. <https://doi.org/10.1111/j.1439-0485.2010.00400.x>
- Ryland JS, Lancaster JE (2004) A review of zoanthid nematocyst types and their population structure. *Hydrobiologia* 530: 179–187. <https://doi.org/10.1007/s10750-004-2685-1>
- Samadi S, Botton L, Macpherson E, De Forges BR, Boisselier MC (2006) Seamount endemism questioned by the geographic distribution and population genetic structure of marine invertebrates. *Marine Biology* 149(6): 1463–1475. <https://doi.org/10.1007/s00227-006-0306-4>

- Sinniger F, Montoya-Burgos JI, Chevaldonne P, Pawlowski J (2005) Phylogeny of the order Zoantharia (Anthozoa, Hexacorallia) based on the mitochondrial ribosomal genes. *Marine Biology* 147: 1121–1128. <https://doi.org/10.1007/s00227-005-0016-3>
- Sinniger F, Ocaña OV, Baco AR (2013) Diversity of zoanths (Anthozoa: Hexacorallia) on Hawaiian seamounts: description of the Hawaiian gold coral and additional zoanths. *PLoS ONE* 8: e52607. <https://doi.org/10.1371/journal.pone.0052607>
- Swain TD, Schellinger JL, Strimaitis AM, Reuter KE (2015) Evolution of anthozoan polyp retraction mechanisms: convergent functional morphology and evolutionary allometry of the marginal musculature in order Zoanthidea (Cnidaria: Anthozoa: Hexacorallia). *BioMed Central Evolutionary Biology* 15: 1–19. <https://doi.org/10.1186/s12862-015-0406-1>
- Van Soest RW, Meesters EH, Becking LE (2014) Deep-water sponges (Porifera) from Bonaire and Klein Curaçao, Southern Caribbean. *Zootaxa* 387: 401–443. <https://doi.org/10.11646/zootaxa.387.5.1>
- Watling L, Auster PJ (2017) Seamounts on the high seas should be managed as vulnerable marine ecosystems. *Frontiers in Marine Science* 4: 14. <https://doi.org/10.3389/fmars.2017.00014>
- Watling L, France SC, Pante E, Simpson A (2011) Biology of deep-water octocorals. *Advances in Marine Biology* 60: 41–122. <https://doi.org/10.1016/B978-0-12-385529-9.00002-0>
- Worm B, Lotze HK, Myers RA (2003) Predator diversity hotspots in the blue ocean. *Proceedings of the National Academy of Sciences* 100(17): 9884–9888. <https://doi.org/10.1073/pnas.1333941100>
- Worm B, Barbier EB, Beaumont N, Duffy JE, Folke C, Halpern BS, Jackson JBC, Lotze HK, Micheli F, Palumbi SR, Sala E, Selkoe KA, Stachowicz JJ, Watson R (2006) Impacts of biodiversity loss on ocean ecosystem services. *Science* 314(5800): 787–790. <https://doi.org/10.1126/science.1132294>

## Supplementary material 1

### GenBank accession numbers used for phylogenetic analyses in this study

Authors: Hiroki Kise, James Davis Reimer, Akira Iguchi, Yuji Ise, Shinji Tsuchida, Yoshihiro Fujiwara

Data type: xlsx

Copyright notice: This dataset is made available under the Open Database License (<http://opendatacommons.org/licenses/odbl/1.0/>). The Open Database License (ODbL) is a license agreement intended to allow users to freely share, modify, and use this Dataset while maintaining this same freedom for others, provided that the original source and author(s) are credited.

Link: <https://doi.org/10.3897/zookeys.1221.131258.suppl1>

## Supplementary material 2

### Best fitting models for ML and BI phylogenetic analyses based on six-gene dataset

Authors: Hiroki Kise, James Davis Reimer, Akira Iguchi, Yuji Ise, Shinji Tsuchida, Yoshihiro Fujiwara

Data type: xlsx

Copyright notice: This dataset is made available under the Open Database License (<http://opendatacommons.org/licenses/odbl/1.0/>). The Open Database License (ODbL) is a license agreement intended to allow users to freely share, modify, and use this Dataset while maintaining this same freedom for others, provided that the original source and author(s) are credited.

Link: <https://doi.org/10.3897/zookeys.1221.131258.suppl2>

## Supplementary material 3

### Information of Zoantharian species used for phylogenomic analyses of mitochondrial genomes

Authors: Hiroki Kise, James Davis Reimer, Akira Iguchi, Yuji Ise, Shinji Tsuchida, Yoshihiro Fujiwara

Data type: xlsx

Copyright notice: This dataset is made available under the Open Database License (<http://opendatacommons.org/licenses/odbl/1.0/>). The Open Database License (ODbL) is a license agreement intended to allow users to freely share, modify, and use this Dataset while maintaining this same freedom for others, provided that the original source and author(s) are credited.

Link: <https://doi.org/10.3897/zookeys.1221.131258.suppl3>

## Supplementary material 4

### Best fitting models for ML and BI phylogenetic analyses based on complete mitochondrial genome dataset

Authors: Hiroki Kise, James Davis Reimer, Akira Iguchi, Yuji Ise, Shinji Tsuchida, Yoshihiro Fujiwara

Data type: xlsx

Copyright notice: This dataset is made available under the Open Database License (<http://opendatacommons.org/licenses/odbl/1.0/>). The Open Database License (ODbL) is a license agreement intended to allow users to freely share, modify, and use this Dataset while maintaining this same freedom for others, provided that the original source and author(s) are credited.

Link: <https://doi.org/10.3897/zookeys.1221.131258.suppl4>

# First formal record of the feeding habits of Saileriolidae (Hemiptera, Heteroptera, Pentatomomorpha, Pentatomoidea), with redescription of *Bannacoris hyalinus* (Schaefer & Ashlock, 1970), comb. nov. endemic to Vietnam

Jun Souma<sup>1</sup>, Cuong Viet Canh Le<sup>2</sup>, Thai-Hong Pham<sup>2,3</sup>

1 Shirakami Research Center for Environmental Sciences, Faculty of Agriculture and Life Science, Hirosaki University, Aomori, Japan

2 Mienrung Institute for Scientific Research, Vietnam National Museum of Nature, Vietnam Academy of Science and Technology, Hue, Vietnam

3 Graduate School of Science and Technology, Vietnam Academy of Science and Technology, Hanoi, Vietnam

Corresponding authors: Jun Souma ([kodokusignal@gmail.com](mailto:kodokusignal@gmail.com)); Thai-Hong Pham ([phamthai@vnmn.vast.vn](mailto:phamthai@vnmn.vast.vn))

## Abstract

In the present study, the rare true bug *Bannacoris hyalinus* (Schaefer & Ashlock, 1970), **comb. nov.** (Hemiptera, Heteroptera, Pentatomomorpha, Pentatomoidea, Saileriolidae), which is endemic to Vietnam, is redescribed and transferred from the genus *Saileriola* China & Slater, 1956 to the genus *Bannacoris* Hsiao, 1964 based on morphological characteristics. Adults and nymphs of this species congregate in groups of several individuals and suck sap from the abaxial side of the leaves of *Litsea* sp. (Lauraceae). They cause visible feeding damage on the adaxial side of *Litsea* leaves, similar to that caused by members of the heteropteran family Tingidae Laporte, 1832 (Cimicomorpha, Miroidea). The new knowledge of *B. hyalinus* **comb. nov.** also represents the first formal record of the feeding habits of Saileriolidae China & Slater, 1956. An identification key to all four species of this family is provided.

**Key words:** Host plant, phytophagous insect, rare species, Tingidae, Urostylididae



Academic editor: Wenjun Bu  
Received: 19 August 2024  
Accepted: 7 November 2024  
Published: 31 December 2024

ZooBank: <https://zoobank.org/0845BEEE-7645-4D58-8FC9-C972F1B2696E>

**Citation:** Souma J, Le CVC, Pham T-H (2024) First formal record of the feeding habits of Saileriolidae (Hemiptera, Heteroptera, Pentatomomorpha, Pentatomoidea), with redescription of *Bannacoris hyalinus* (Schaefer & Ashlock, 1970), comb. nov. endemic to Vietnam. ZooKeys 1221: 363–375. <https://doi.org/10.3897/zookeys.1221.135026>

Copyright: © Jun Souma et al.  
This is an open access article distributed under terms of the Creative Commons Attribution License (Attribution 4.0 International – CC BY 4.0).

## Introduction

The true bug family Saileriolidae China & Slater, 1956 (Hemiptera, Heteroptera, Pentatomomorpha, Pentatomoidea) comprises the following four species in three genera distributed in Asia: *Bannacoris arboreus* Hsiao, 1964 from China and Thailand; *Ruckesona vitrella* Schaefer & Ashlock, 1970 from Thailand; *Saileriola hyalina* Schaefer & Ashlock, 1970 from Vietnam; and *S. sandakanensis* China & Slater, 1956 from Malaysia (Borneo Island) (China and Slater 1956; Hsiao 1964; Schaefer and Ashlock 1970; Hsiao and Ching 1977; Rider 2006; Rider et al. 2018). This family was previously assigned to the pentatomoid family Urostylididae Dallas, 1851 (China and Slater 1956), but it was elevated to the family rank owing to the non-monophyly of Urostylididae (Grazia et al. 2008), which was supported by subsequent studies using the morphological characteristics of extant and fossil species (Yao et al. 2012, 2013). Nevertheless, recent studies partially or completely

based on molecular data have recovered the sister relationship between Saileriolidae and Urostylididae, and these studies continued to treat Saileriolidae at the family rank (Wu et al. 2016; Zhou and Rédei 2020; Ye et al. 2022; Duan et al. 2023).

If it is reasonable to treat Saileriolidae as a family rank, there should be significant differences not only in morphological but also ecological characteristics between Saileriolidae and Urostylididae. Although the life history of Urostylididae has been reported in some Japanese species (Kobayashi and Tachikawa 2004; Kaiwa et al. 2014), the biological information of Saileriolidae is poorly understood (Rider et al. 2018; Schuh and Weirauch 2020). Current biological information on Saileriolidae based on the published literature is as follows: (i) several adults and nymphs of *R. vitrella* were collected from a “palm at the water margin” (Arecaceae), therefore the indeterminate palm could be a host plant for this species (cf. Schaefer and Ashlock 1970; Schuh and Weirauch 2020); (ii) the guts of adults and nymphs of *R. vitrella* contain green fragments similar to chloroplasts, suggesting that this species does not feed exclusively on sap but also ingests chloroplasts from leaves and/or stems (Schaefer and Ashlock 1970); and (iii) *B. arboreus* was collected from leaves of an indeterminate banana *Musa* sp. (Musaceae) (cf. Rider et al. 2018). Additionally, in the biological information not formally published, several adults and nymphs of this species have been observed congregating on the abaxial side of banana leaves (<https://spain.inaturalist.org/taxa/1360964-Bannacoris-arboreus>). In conclusion, more field surveys and formal publications on the relevant biological information are needed to elucidate the life history of Saileriolidae.

Meanwhile, the two known species of the genus *Saileriola* China & Slater, 1956 seem to be rare because only the old holotype is known (cf. China and Slater 1956; Schaefer and Ashlock 1970). In the original description, *R. vitrella* and *S. hyalina* were not compared with *B. arboreus*, and the general habitus of *S. hyalina* was not illustrated (cf. Schaefer and Ashlock 1970), making the identification key to the species incomplete and the identification of *S. hyalina* difficult. Therefore, a taxonomic study based on field surveys should be conducted to rediscover the two species of *Saileriola* and to provide an updated identification key to the four known species of the family, including *B. arboreus*.

Recently, the first author rediscovered *S. hyalina* in Bạch Mã National Park, Thừa Thiên Huế Province, Vietnam, with the help of the second and third authors. In addition, the first author observed the feeding habits of this species. Furthermore, *S. hyalina* is consistent with the diagnostic characters of the genus *Bannacoris* Hsiao, 1964 based on the examination of morphological characteristics by the first author. In the present study, we redescribe *S. hyalina* and propose a new combination, *Bannacoris hyalinus* (Schaefer & Ashlock, 1970), comb. nov., which is transferred from *Saileriola* to *Bannacoris*. Moreover, we report on the biology of *B. hyalinus* comb. nov., providing the first formal record of the feeding habits of Saileriolidae. We also provide an identification key to the four known species of Saileriolidae.

## Materials and methods

The morphological characteristics of the specimens were observed, drawn, and measured using a stereoscopic microscope (SZX16; Olympus, Tokyo, Japan) equipped with an ocular grid. To examine the male and female genitalia, first, the terminalia was removed from the body after softening the specimens in

hot water. The removed terminalia was then immersed in a hot 15% potassium hydroxide (KOH) solution for 5 min. For further observation, the paramere and phallus were immersed in 99% ethanol and removed from the genital capsule. Male and female genitalia were preserved in small polyethylene vials containing a 50% aqueous solution of glycerin. Male and female genitalia were observed after the angles were fixed with a gel (Museum Gel Clear; Ready America, California, USA) and placed on a microscope slide. The polyethylene vial was mounted on a pin with the respective specimens. The specimens were photographed using a digital camera (EOS 90D; Canon, Tokyo, Japan) equipped with a zoom lens (18–35 mm F1.8 DC HSM; SIGMA, Kanagawa, Japan) and a digital microscope (Dino-Lite Premier M; Opto Science, Tokyo, Japan). Photographs of living individuals and habitats were taken using a compact digital camera (Tough TG-6; Olympus, Tokyo, Japan) and a smartphone (iPhone 14; Apple, California, USA), respectively. The image stacks of the specimens were processed using a Zerene Stacker (Zerene Systems, Richland, WA, USA). All illustrations and photographs were edited using Adobe Photoshop 2024 v. 25.11. Morphological terms were generally assigned according to Tsai et al. (2011).

The specimens examined in this study have been deposited at the Vietnam National Museum of Nature, Hanoi, Vietnam (**VNMN**).

The species distribution map was created and edited using Adobe Photoshop, and geographic coordinates were obtained from Google Maps (<https://www.google.co.jp/maps>).

## Results

### Taxonomy

#### Genus *Bannacoris* Hsiao, 1964

*Bannacoris* Hsiao, 1964: 283. Type species by original designation: *Bannacoris arboreus* Hsiao, 1964.

**Diagnosis.** *Bannacoris* can be distinguished from the two other known saileriolid genera, *Ruckesona* Schaefer & Ashlock, 1970 and *Saileriola* China & Slater, 1956, by a combination of the following characters: head with a median sulcus on vertex (without a median sulcus on vertex in *Ruckesona*); compound eye separated from anterior margin of pronotum (close to anterior margin of pronotum in *Ruckesona* and *Saileriola*); a pair of ocelli closer together than a diameter of ocellus (separated by more than 3.0 times of a diameter of ocellus in *Ruckesona*); antennomere I more than 1.5 times as long as antennomere II (less than 1.5 times in *Ruckesona*); lateral margin of pronotum serrate in anterior part (nearly straight in *Saileriola*), without distinct spine (with two distinct spines in *Saileriola*); and corium of forewing mostly punctate (punctate only along claval and median furrows in *Saileriola*).

**Remarks.** The following characters in the original description are the diagnostic characters of the family Saileriolidae, partly including misinterpretation, and are unable to distinguish this genus from other saileriolid genera (Hsiao 1964; Schaefer and Ashlock 1970; Rider et al. 2018; present study): ostiole of metathoracic scent gland quite small (absent in original description); peritreme absent; and tarsi three-segmented (two-segmented in original description).

Additionally, hindwing venation, which differs between *Ruckesona* and *Saileriola*, was not considered in the present study because of the lack of a detailed description of the type species of *Bannacoris*, *B. arboreus* (cf. Hsiao 1964). Thus, based on the original descriptions of the three known saileriolid genera (China and Slater 1956; Hsiao 1964; Schaefer and Ashlock 1970) and the first author's examination, we provisionally redefine the morphological characteristics shared by *Bannacoris* species, as described in the Diagnosis section above, and propose a new combination, *Bannacoris hyalinus* (Schaefer & Ashlock, 1970), comb. nov., which is transferred from *Saileriola* to *Bannacoris*. In conclusion, the genus *Bannacoris* comprises two species, *B. arboreus* from China and Thailand and *B. hyalinus* comb. nov. from Vietnam (Hsiao 1964; Schaefer and Ashlock 1970; Rider et al. 2018; present study).

***Bannacoris hyalinus* (Schaefer & Ashlock, 1970), comb. nov.**

Figs 1A, B, 2A–G, 3A–D, 4A, B

*Saileriola hyalina* Schaefer & Ashlock, 1970: 631. Holotype: ♂, Vietnam: 7 km SE of Dilinh (Djiring), 990 m [= Lâm Đồng Province, Di Linh District, Bảo Thuận?]; Bernice P. Bishop Museum, Honolulu, Hawaii, USA.

**Material examined. Non-types** (5 ♂♂ 4 ♀♀, VNMN): VIETNAM • Thừa Thiên Huế Province, Phú Lộc District, Bạch Mã National Park, Lộc Trì, Đường mòn Đổ Quyên; 16°11'34"N, 107°50'52"E; 6.vi.2024; leg. J. Souma.

**Diagnosis.** *Bannacoris hyalinus* comb. nov. can be distinguished from the only other congener, *B. arboreus*, by the following characters: head, pronotum, and scutellum mostly yellowish brown (Figs 1A, B, 2A) (mostly reddish to dark brown in *B. arboreus*); corium of forewing mostly hyaline (Fig. 2D) (reddish to dark brown in middle part in *B. arboreus*), not punctate in an area enclosed by Sc (subcostal) vein and medial furrow (entirely punctate in *B. arboreus*); dorso-lateral process of genital capsule undeveloped (Figs 2E, 3A) (protruding posteriorly in *B. arboreus*); and ventromedian process concave in posterior margin (gently curved outward in *B. arboreus*).

**Redescription.** Most parts of head, antennomeres I–IV, pronotum except for anterior and lateral margins, ventral surface of thoracic parts, most parts of scutellum, legs except for claws, and abdomen yellowish brown; antennomere V, compound eye, ocellus, anterior margin of scutellum, Sc (subcostal) vein of forewing, claws, and punctures on body dark brown; anterior and lateral margins of pronotum, and outer part of semi-elliptical ridge in anteromedial part of scutellum whitish brown; forewing except for Sc vein and punctures hyaline; setae on body yellowish (Figs 1A, B, 2A–F, 4A, B).

Body (Fig. 1A, B) ovate, 1.5–1.6 times as long as maximum width across abdomen. Head (Fig. 2A–C) declivent, mostly punctate, longer than maximum width across compound eyes in cranial view, with a median sulcus on vertex, sparsely bearing minute setae. Antenniferous tubercle annulate, placed anterior to compound eye. Clypeus distinctly surpassing mandibular plate at both apices. Compound eye round, separated from anterior margin of pronotum. A pair of ocelli placed along midline of vertex, closer together than a diameter of ocellus. Antenna smooth on surface; antennomere I longest among antennomeres, more than

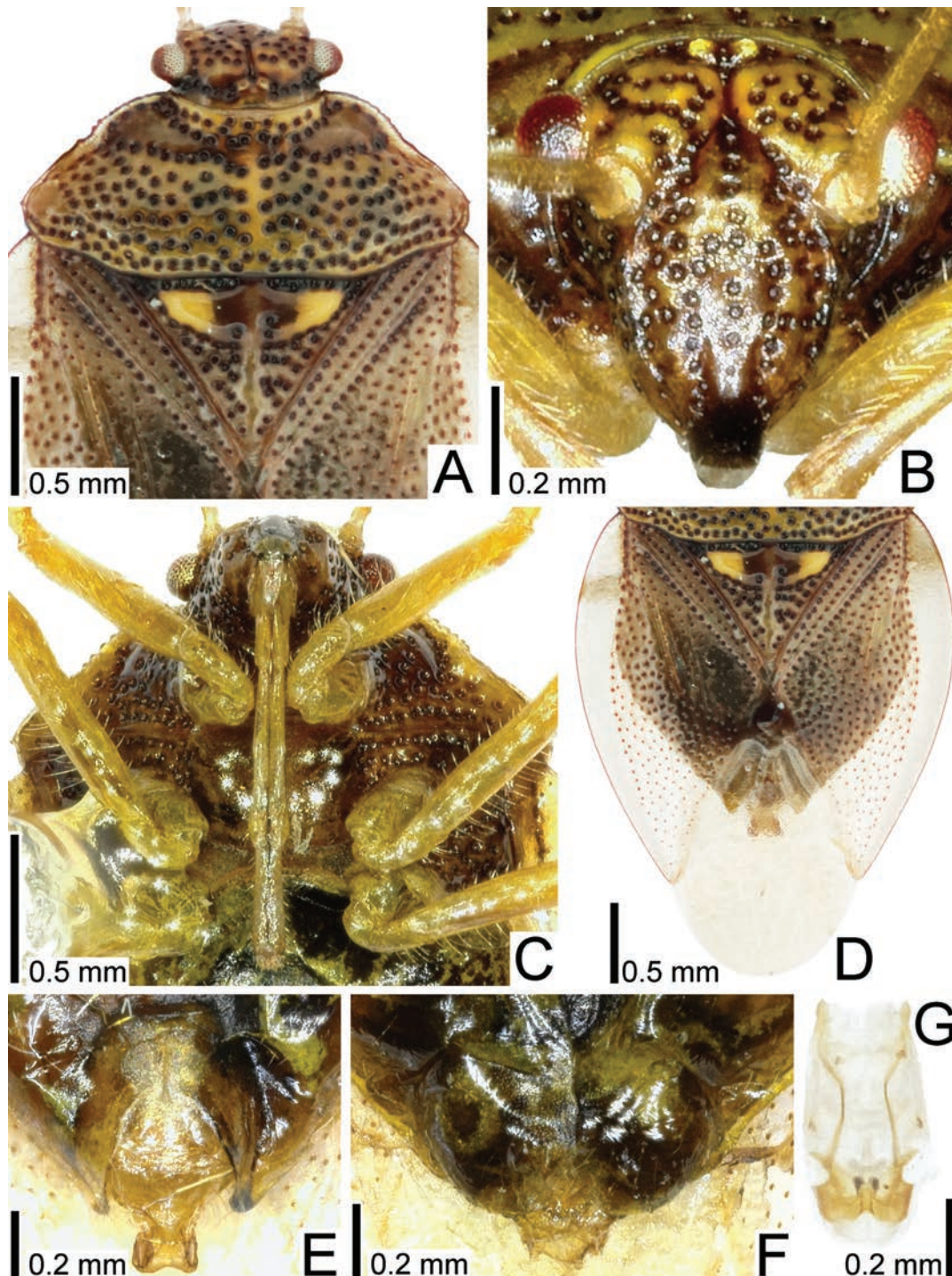


Figure 1. Dorsal habitus of *Bannacoris hyalinus* comb. nov. from Vietnam. **A** male **B** female.

1.5 times as long as antennomere II, bearing minute setae throughout its length; antennomere II longer than antennomere IV, bearing minute setae throughout its length; antennomere III shortest among antennomeres, bearing minute setae throughout its length; antennomere IV as long as antennomere V, bearing minute and long setae throughout its length; antennomere V bearing minute and long setae throughout its length. Labium reaching anterior part of abdominal sternite III. Buccula semi-elliptical in lateral view, highest in middle part.

Thorax (Figs 1A, B, 2A, C) mostly punctate. Pronotum trapezoidal in dorsal view, shorter than its maximum width, punctate except for callus; lateral margin serrate in anterior part, without distinct spine, bearing minute setae throughout its length; humeral angle rounded. Scutellum triangular, shorter than its maximum width, semi-elliptically raised in anteromedial part, punctate except for midline and semi-elliptical ridge. Forewing (Fig. 2D) oblong; anterior margin gently curved outward; clavus shorter than membrane, with 2 rows of punctures throughout its length; corium punctate except in an area enclosed by Sc vein and medial furrow, bearing minute setae in anterior part; membrane provided with several indistinct longitudinal veins; Sc vein, basal part of Cu (cubital) vein, and claval and medial furrows distinct. Epimera and episterna punctate except metepimeron. Sterna smooth on surface. Legs smooth on surface; femora and tibiae cylindrical, bearing setae throughout their length.

Abdomen (Figs 1A, B, 2D–F) longer than combined length of head and pronotum; posterior margin of sternite VI concave in male, undulate in female; sternite VII concave in posterior margin of male, with a longitudinal cleft in female. Genital



**Figure 2.** Detailed morphological images of *Bannacoris hyalinus* comb. nov. from Vietnam **A** head, pronotum, and scutellum, dorsal view **B** head, cranial view **C** head and thorax, ventral view **D** forewing, dorsal view **E** male terminalia, ventral view **F** female terminalia, ventral view **G** phallus, ventral view.

capsule (Fig. 3A) elliptical in dorsal and ventral views, smooth on surface, bearing setae in posterior part; lateral margin gently curved outward; dorsolateral process undeveloped; ventromedian process widened apically, concave in posterior margin. Paramere (Fig. 3B, C) elongate; crown widened apically, bearing three setae from cuticular sockets along outer margin of dorsum; neck constricted; stem widened apically. Phallus (Fig. 2G) oblong; basal plate and phalotheca

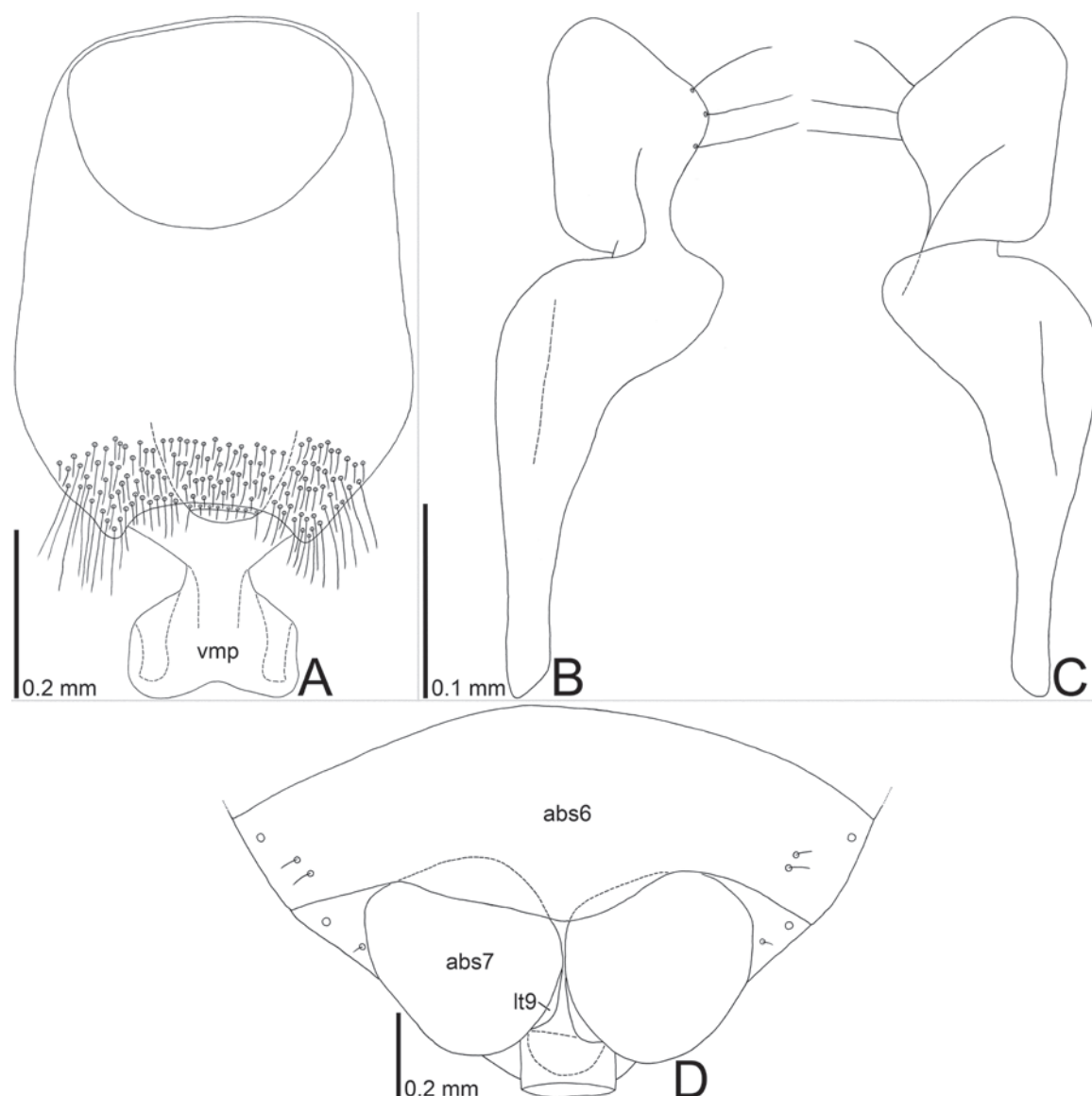


**Figure 3.** Line drawings of *Bannacoris hyalinus* comb. nov. from Vietnam **A** genital capsule, dorsal view **B** paramere, dorsal view **C** paramere ventral view **D** female terminalia, ventral view. Abbreviations: abs6, abs7, abdominal sternites VI, VII; lt9, laterotergite IX; vmp, ventromedian process.

coriaceous; conjunctiva with two pairs of sclerites. Female terminalia (Fig. 3D) semicircular in ventral view, protruding posteriad in middle part; laterotergite VIII reduced; valvifer VIII reduced; laterotergite IX rounded in outer margin.

Measurements (male:  $n = 5$ ; female:  $n = 4$ ). Body length with forewing 3.5–3.8 mm in male and 3.9–4.0 mm in female, maximum width across forewings 2.3–2.4 mm in male and 2.5 mm in female; head length in cranial view 0.9 mm in both sexes, maximum width across compound eyes 0.8 mm in both sexes; length of antennomeres I–V in both sexes 1.5 mm, 0.8 mm, 0.2 mm, 0.6 mm, and 0.6 mm, respectively; length of labial segments I–IV in both sexes 0.3 mm, 0.3 mm, 0.3 mm, and 0.4 mm, respectively; pronotum length 0.7 mm in both sexes, maximum width 1.8 mm in male and 1.9–2.0 mm in female; scutellum length 0.8 mm in male and 0.9 mm in female, maximum width 1.0 mm in male and 1.1 mm in female; forewing length 2.8–2.9 mm in male and 3.0–3.1 mm in female, maximum width 1.2 mm in male and 1.3 mm in female.

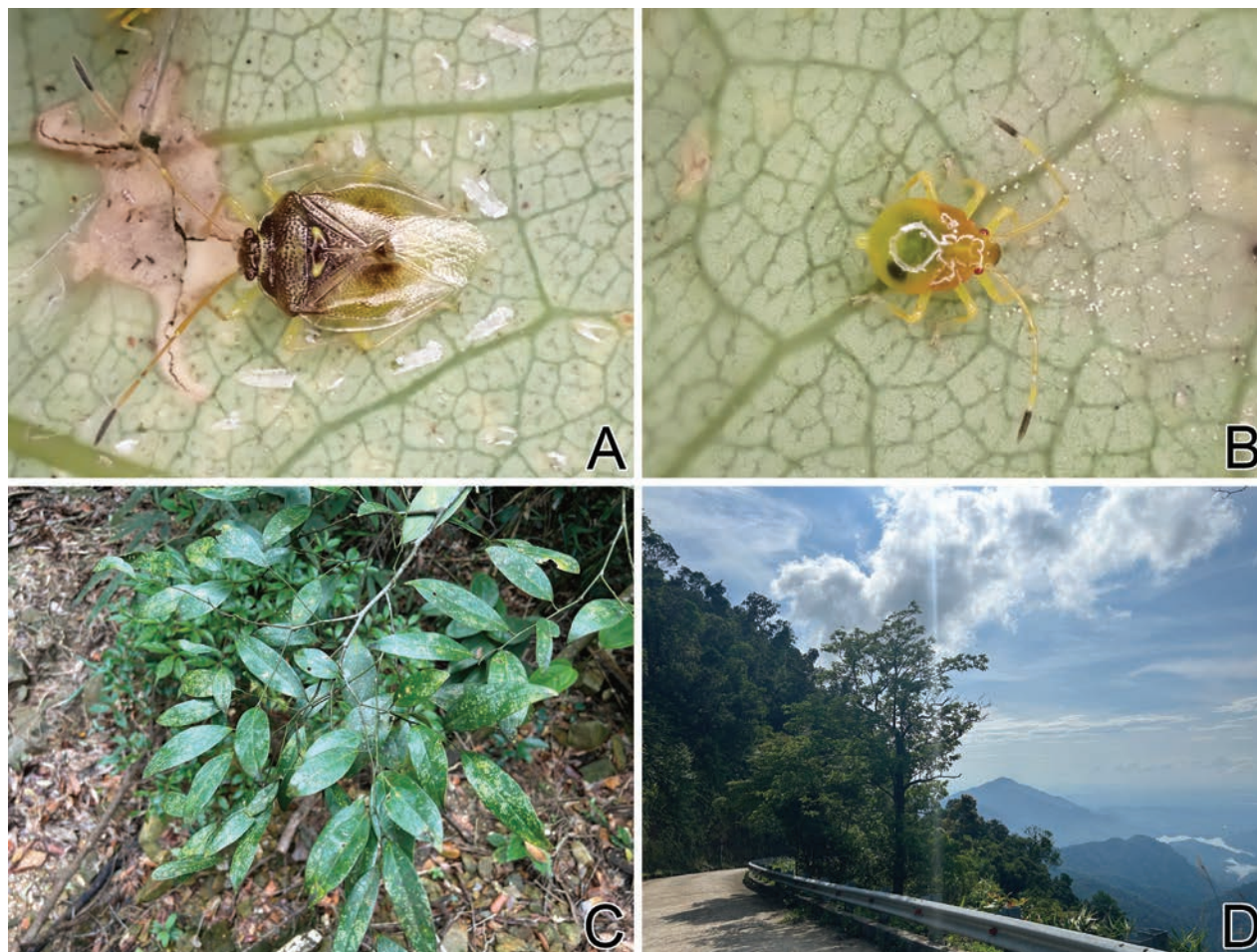


**Figure 4.** Photographs regarding *Bannacoris hyalinus* comb. nov. from Bạch Mã National Park, Thừa Thiên Huế Province, Vietnam **A** living adult **B** living nymph **C** host plant (*Litsea* sp.) **D** surrounding habitat.

**Remarks.** The nine specimens recorded above (Fig. 1A, B) matched well with the original description and illustrations of *Bannacoris hyalinus* comb. nov. (Schaefer and Ashlock 1970) in terms of morphological characteristics, especially the structure of the head (Fig. 2B) and the shape of the genital capsule (Figs 2E, 3A) and paramere (Fig. 3B, C). Therefore, we identified the specimens studied as *B. hyalinus* comb. nov. and redescribed this species in the above section.

In the original description (Schaefer and Ashlock 1970), *B. hyalinus* comb. nov. was not compared with the only other congener, *B. arboreus*, making the identification of the two species difficult. However, based on the comparison among the nine specimens of *B. hyalinus* comb. nov. and the illustrations (Hsiao 1964; Hsiao and Ching 1977), photographs (Hsiao and Ching 1977; Rider et al. 2018; <https://spain.inaturalist.org/taxa/1360964-Bannacoris-arboreus>), and original description (Hsiao 1964) of *B. arboreus*, the five characters described in the Diagnosis section above were recognized to easily differentiate *B. hyalinus* comb. nov. from *B. arboreus*.

**Distribution.** Vietnam (Thừa Thiên Huế Province, Lâm Đồng Province) (Fig. 5) (Schaefer and Ashlock 1970; present study).

**Host plant.** Adults and nymphs of *Bannacoris hyalinus* comb. nov. were observed to congregate in groups of several on the abaxial side of leaves of

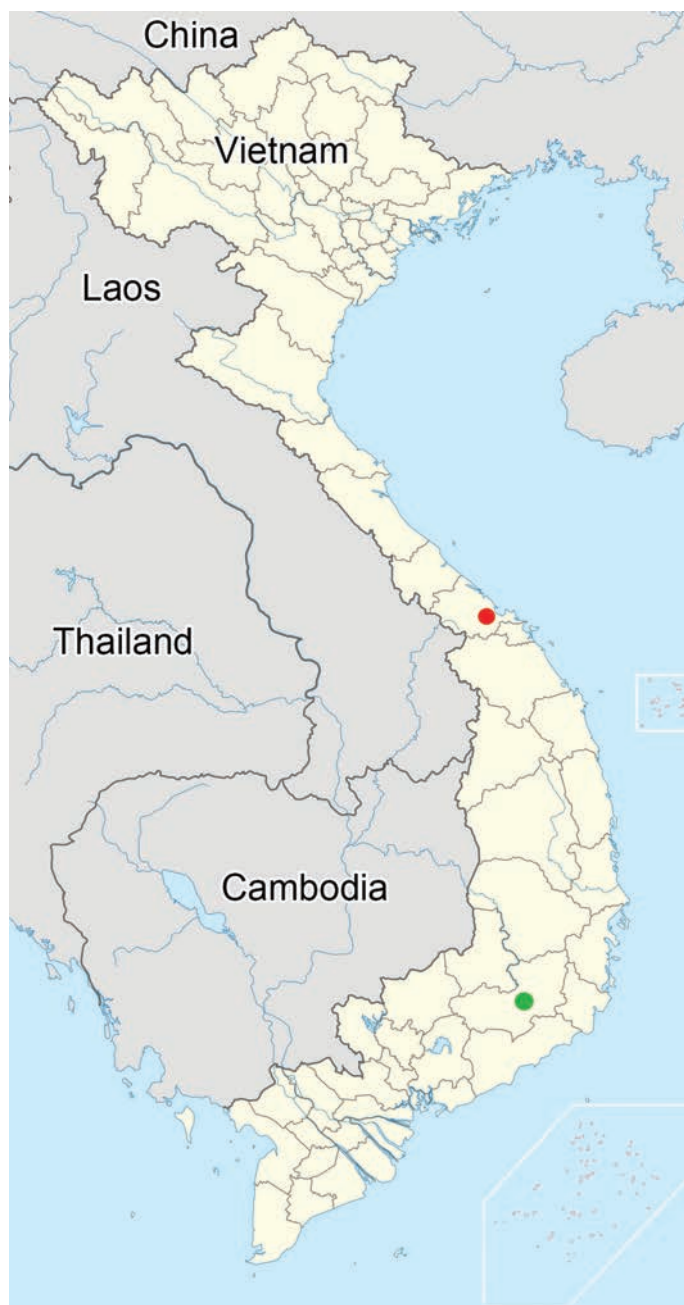


**Figure 5.** Collection sites of *Bannacoris hyalinus* comb. nov.: red circle = new record; green circle = known record.

*Litsea* sp. (Lauraceae) (Fig. 4C) in Bạch Mã National Park, Thừa Thiên Huế Province, Vietnam (Fig. 4D), by the first author. In addition, nymphs were observed sucking sap from the abaxial side of the leaves of this lauraceous tree in captivity. Thus, *Litsea* sp. is considered the host plant of *B. hyalinus* comb. nov., the biological information of which was unknown in the original description (Schaefer and Ashlock 1970).

The adaxial side of the leaves apparently damaged by this saileriolid species was irregularly yellowed in the field and in captivity, suggesting the possibility that *B. hyalinus* comb. nov. feeds on leaf chlorophyll.

**Bionomics.** *Bannacoris hyalinus* comb. nov. inhabits evergreen broad-leaved forests in the mountainous areas of Vietnam with a subtropical climate.

Adults were collected in May 1960 and June 2024 (Schaefer and Ashlock 1970; present study), and nymphs were observed in June 2024 (present study).

### Key to the species of the family Saileriolidae

Modified after the key provided by Schaefer and Ashlock (1970).

- 1 Head without a median sulcus on vertex; a pair of ocelli separated by more than 3.0 times of a diameter of ocellus; antennomere I less than 1.5 times as long as antennomere II ..... ***Ruckesona vitrella* Schaefer & Ashlock, 1970**
- Head with a median sulcus on vertex (Figs 1A, B, 2A–C); a pair of ocelli closer together than a diameter of ocellus; antennomere I more than 1.5 times as long as antennomere II ..... **2**
- 2 Compound eye close to anterior margin of pronotum; lateral margin of pronotum nearly straight in anterior part, with two distinct spines; corium of forewing punctate only along claval and median furrows ..... ***Saileriola sandakanensis* China & Slater, 1956**
- Compound eye separated from anterior margin of pronotum (Figs 1A, B, 2A); lateral margin of pronotum serrate in anterior part, without distinct spine; corium of forewing mostly punctate (Fig. 2D) ..... **3**
- 3 Head, pronotum, and scutellum mostly yellowish brown (Figs 1A, B, 2A–C); corium of forewing mostly hyaline (Fig. 2D), not punctate in an area enclosed by Sc (subcostal) vein and medial furrow ..... ***Bannacoris hyalinus* (Schaefer & Ashlock, 1970), comb. nov.**
- Head, pronotum, and scutellum mostly reddish to dark brown; corium of forewing reddish to dark brown in middle part, entirely punctate ..... ***B. arboreus* Hsiao, 1964**

### Discussion

In this study, the feeding habits of Saileriolidae was formally reported for the first time based on observations of *Bannacoris hyalinus* comb. nov. endemic to Vietnam. This saileriolid species congregates in groups of several individuals and sucks sap from the abaxial side of the leaves of *Litsea* sp. (Fig. 4C). According to previous knowledge, *B. arboreus* and *Ruckesona vitrella* were collected from the leaves of indeterminate banana *Musa* sp. (Musaceae) and indeterminate palm (Arecaceae), respectively (cf. Schaefer and Ashlock 1970; Rider et al. 2018), and several adults and nymphs of *B. arboreus* were observed congregating on the abaxial side of banana leaves (<https://spain.inaturalist.org/taxa/1360964-Bannacoris-arboreus>). Therefore, members of Saileriolidae may generally suck sap from the abaxial side of the leaves. Moreover, the adaxial side of the leaves apparently damaged by *B. hyalinus* comb. nov. was irregularly yellowed, and the guts of adults and nymphs of *R. vitrella* contained green fragments similar to chloroplasts (Schaefer and Ashlock 1970), suggesting that members of Saileriolidae feed on leaf chlorophyll, as speculated in an earlier study (Schaefer and Ashlock 1970).

The feeding habits of Saileriolidae and folivorous taxa of the heteropteran family Tingidae Laporte, 1832 (Cimicomorpha, Miroidea), which feed on leaf chlorophyll, are similar in that in groups of several individuals congregate and

suck sap on the abaxial side of the leaves, causing irregular yellowing on the adaxial side (cf. Ishihara and Kawai 1981; Yasunaga et al. 1993; Schuh and Weirauch 2020; Souma 2022). Nevertheless, since Saileriolidae and Tingidae belong to the infraorders Pentatomomorpha Leston, Pendergrast & Southwood, 1954 and Cimicomorpha Leston, Pendergrast & Southwood, 1954, respectively, and are distantly related (Schuh and Weirauch 2020; Ye et al. 2022), the similarity in feeding habits does not reflect phylogenetic relationships.

Meanwhile, the feeding habits of the pentatomoid family Urostylididae, which is a sister group of Saileriolidae (Wu et al. 2016; Zhou and Rédei 2020; Ye et al. 2022; Duan et al. 2023), differs from that of Saileriolidae as follows: (i) the first instar nymphs suck from a jelly-like substance enclosing the egg mass and develop into the second or third instar nymphs (Kobayashi and Tachikawa 2004; Kaiwa et al. 2014); (ii) the second or third instar nymphs to adults suck sap from various parts of host plants such as sprouts, shoots, leaves, and young fruits (Kobayashi and Tachikawa 2004); and (iii) adults and nymphs are not known to congregate on the abaxial side of leaves and cause visible feeding damage on the adaxial side. Furthermore, the photograph of the indeterminate egg mass, probably from *B. arboreus*, is not enclosed by a jelly-like substance (<https://spain.inaturalist.org/taxa/1360964-Bannacoris-arboreus>). Thus, young nymphs of this saileriolid species may suck sap from the host plant. In conclusion, although the life history of Saileriolidae is still not completely known, the differences in the feeding habits of Saileriolidae and Urostylididae possibly support the rationality of the treatment of previous studies that the former is not a subfamily of the latter but an independent family (Grazia et al. 2008; Yao et al. 2012, 2013; Wu et al. 2016; Zhou and Rédei 2020; Ye et al. 2022; Duan et al. 2023).

## Acknowledgements

We sincerely thank Wenjun Bu (Nankai University, China) and the anonymous reviewer of Zookeys for their critical comments on the manuscript. We express our gratitude to Toshiya Hirowatari, Kohei Matsuura, Toshiharu Mita, Sadahisa Yagi (Kyushu University, Japan), local guides, national park staff, and colleagues of the second and third authors for their help and support during the field surveys. We thank Editage ([www.editage.com](http://www.editage.com)) for the English language editing.

## Additional information

### Conflict of interest

The authors have declared that no competing interests exist.

### Ethical statement

No ethical statement was reported.

### Funding

This study was partially supported by a Bilateral Collaborations (JPJSBP120249601) grant from the Japan Society for the Promotion of Science, Tokyo, Japan, to Toshiharu Mita. The Vietnam Academy of Science and Technology (VAST) funded the present study under grant number NCSX02.01/25-27 and project code QTBY01.08/22-23.

## Author contributions

Conceptualization: JS. Data curation: JS. Funding acquisition: JS. Investigation: JS. Methodology: JS. Project administration: JS, CVCL, T-HP. Resources: JS. Software: JS. Supervision: JS, CVCL, T-HP. Validation: JS. Visualization: JS. Writing – original draft: JS. Writing – review and editing: JS, CVCL, T-HP.

## Author ORCIDs

Jun Souma  <https://orcid.org/0000-0002-2238-5015>

Cuong Viet Canh Le  <https://orcid.org/0000-0002-1430-6305>

Thai-Hong Pham  <https://orcid.org/0000-0002-4763-3679>

## Data availability

All of the data that support the findings of this study are available in the main text.

## References

- China WE, Slater JA (1956) A new subfamily of Urostylidae from Borneo (Hemiptera: Heteroptera). *Pacific Science* 10(4): 410–414.
- Duan Y, Fu S, Ye Z, Bu W (2023) Phylogeny of Urostylididae (Heteroptera: Pentatomoidea) reveals rapid radiation and challenges traditional classification. *Zoologica Scripta* 52(3): 264–278. <https://doi.org/10.1111/zsc.12582>
- Grazia J, Schuh RT, Wheeler WC (2008) Phylogenetic relationships of family groups in Pentatomoidea based on morphology and DNA sequences (Insecta: Heteroptera). *Cladistics* 24(6): 932–976. <https://doi.org/10.1111/j.1096-0031.2008.00224.x>
- Hsiao TY (1964) New species and new record of Hemiptera-Heteroptera from China. *Acta Zootaxonomica Sinica* 1(2): 283–292. [in Chinese with English summary]
- Hsiao TY, Ching HL (1977) Urostylidae. In: Hsiao TY, Jen SC, Cheng LI, Liu SL, Ching HL (Eds) *A Handbook for the Determination of the Chinese Hemiptera-Heteroptera*. Vol. I. Science Press, Beijing, 181–197 + 302–304. [pls. 30–32] [in Chinese with English summary]
- Ishihara R, Kawai S (1981) Feeding habits of the azalea lace bug, *Stephanitis pyrioides* (Scott) (Hemiptera: Tingidae). *Japanese Journal of Applied Entomology and Zoology* 25(3): 200–202. <https://doi.org/10.1303/jjaez.25.200>
- Kaiwa N, Hosokawa T, Nikoh N, Tanahashi M, Moriyama M, Meng XY, Maeda T, Yamaguchi K, Shigenobu S, Ito M, Fukatsu T (2014) Symbiont-supplemented maternal investment underpinning host's ecological adaptation. *Current Biology* 24(20): 2465–2470. <https://doi.org/10.1016/j.cub.2014.08.065>
- Kobayashi T, Tachikawa S (2004) [Illustrated Eggs and Nymphs of Pentatomoids. Morphology and Ecology]. Yokendo, Tokyo, 7 + 323 pp. [in Japanese]
- Rider DA (2006) Family Urostylididae Dallas, 1851. In: Aukema B, Rieger C (Eds) *Catalogue of the Heteroptera of the Palaearctic Region*. Vol. 5, Pentatomomorpha II. The Netherlands Entomological Society, Amsterdam, 102–116.
- Rider DA, Schwertner CF, Vilímová J, Rédei D, Kment P, Thomas DB (2018) Higher systematics of the Pentatomoidea. In: McPherson JE (Ed.) *Invasive Stink Bugs and Related Species (Pentatomoidea): Biology, Higher Systematics, Semiochemistry, and Management*. CRC Press, Boca Raton, 25–201. [pls 2.25–2.32] <https://doi.org/10.1201/9781315371221-2>
- Schaefer CW, Ashlock PD (1970) A new genus and new species of Saileriolinae (Hemiptera: Urostylidae). *Pacific Insects* 12(3): 629–639.

- Schuh RT, Weirauch C (2020) True Bugs of the World (Hemiptera: Heteroptera). Classification and natural history (Second Edition). Siri Scientific Press, Manchester, 768 pp. [32 pls]
- Souma J (2022) Integrative taxonomy of the Lauraceae-feeding species of the genus *Stephanitis* (Hemiptera, Heteroptera, Tingidae) from Japan. *Deutsche Entomologische Zeitschrift* 69(2): 219–281. <https://doi.org/10.3897/dez.69.89864>
- Tsai JF, Rédei D, Yeh GF, Yang MM (2011) Jewel Bugs of Taiwan (Heteroptera: Scutelleridae). National Chung Hsing University, Taichung, 309 pp.
- Wu YZ, Yu SS, Wang YH, Wu HY, Li XR, Men XY, Zhang YW, Rédei D, Xie Q, Bu WJ (2016) The evolutionary position of Lestoniidae revealed by molecular autapomorphies in the secondary structure of rRNA besides phylogenetic reconstruction (Insecta: Hemiptera: Heteroptera). *Zoological Journal of the Linnean Society* 177(4): 750–763. <https://doi.org/10.1111/zoj.12385>
- Yao YZ, Ren D, Rider DA, Cai WZ (2012) Phylogeny of the infraorder Pentatomomorpha based on fossil and extant morphology, with description of a new fossil family from China. *PLoS ONE* 7(5): e37289. <https://doi.org/10.1371/journal.pone.0037289>
- Yao YZ, Cai WZ, Rider DA, Ren D (2013) Primipentatomidae fam. nov. (Hemiptera: Heteroptera: Pentatomomorpha), an extinct insect family from the cretaceous of north-eastern China. *Journal of Systematic Palaeontology* 11(1): 63–82. <https://doi.org/10.1080/14772019.2011.639814>
- Yasunaga T, Takai M, Yamashita I, Kawamura M, Kawasaki T (1993) A Field Guide to Japanese Bugs. Terrestrial Heteropterans. Zenkoku Noson Kyoiku Kyokai Publishing, Tokyo, Japan, 380 pp. [in Japanese]
- Ye F, Kment P, Rédei D, Luo JY, Wang YH, Kuechler SM, Zhang WW, Chen PP, Wu HY, Wu YZ, Sun XY, Ding L, Wang YR, Xie Q (2022) Diversification of the phytophagous lineages of true bugs (Insecta: Hemiptera: Heteroptera) shortly after that of the flowering plants. *Cladistics* 38(4): 403–428. <https://doi.org/10.1111/cla.12501>
- Zhou YY, Rédei D (2020) From lanceolate to plate-like: gross morphology, terminology, and evolutionary trends of the trichophoran ovipositor. *Arthropod Structure & Development* 54: 100914. <https://doi.org/10.1016/j.asd.2020.100914>



# Diversity of ectoparasitic bat flies (Diptera, Hippoboscoidea) in inter-Andean valleys: evaluating interactions in the largest inter-Andean basin of Colombia

Camila López-Rivera<sup>1</sup>, Laura Natalia Robayo-Sánchez<sup>2</sup>, Alejandro Ramírez-Hernández<sup>2,3</sup>,  
Jerson Andrés Cuéllar-Saénz<sup>2</sup>, Juan Diego Villar<sup>4</sup>, Jesús Alfredo Cortés-Vecino<sup>2</sup>,  
Fredy A. Rivera-Páez<sup>1</sup>, Paula Andrea Ossa-López<sup>1</sup>, Erika M. Ospina-Pérez<sup>1</sup>, Jose J. Henao-Osorio<sup>1</sup>,  
Alexandra Cardona-Giraldo<sup>1</sup>, Javier Racero-Casarrubia<sup>5</sup>, Miguel E. Rodríguez-Posada<sup>6</sup>,  
Darwin M. Morales-Martínez<sup>7</sup>, Marylin Hidalgo<sup>4</sup>, Héctor E. Ramírez-Chaves<sup>1,8</sup>

1 Grupo de Investigación GEBIOME, Departamento de Ciencias Biológicas, Facultad de Ciencias Exactas y Naturales, Universidad de Caldas, Calle 65 No. 26-10, 170004, Manizales, Caldas, Colombia

2 Grupo de Investigación Parasitología Veterinaria, Laboratorio de Parasitología Veterinaria, Facultad de Medicina Veterinaria y de Zootecnia, Universidad Nacional de Colombia, Carrera 30 No. 45-03, 111321, Bogotá D.C., Colombia

3 Grupo Epidemiología y Salud Pública, Universidad de La Salle, Bogotá D. C., Colombia

4 Grupo Enfermedades Infecciosas, Departamento de Microbiología, Pontificia Universidad Javeriana, Bogotá D.C., Colombia

5 Grupo de Investigación Biodiversidad Unicórdoba, Facultad de Ciencias Básicas, Universidad de Córdoba, Montería, Córdoba, Colombia

6 Fundación Reserva Natural La Palmita, Centro de Investigación, Grupo de investigaciones territoriales para el uso y conservación de la biodiversidad, Bogotá, Colombia

7 Museum of Natural Science and Department of Biological Sciences, Louisiana State University, 119 Foster Hall 70803, Baton Rouge, Louisiana, USA

8 Centro de Museos, Museo de Historia Natural, Universidad de Caldas, Manizales, Colombia

Corresponding author: Héctor E. Ramírez-Chaves ([hector.ramirez@ucaldas.edu.co](mailto:hector.ramirez@ucaldas.edu.co))

## Abstract

Flies belonging to the families Streblidae and Nycteribiidae are highly specialized arthropods that feed on the blood of bats. Their morphology varies and has adapted throughout their coevolutionary history with hosts. Bat flies are often associated with specific bat species and can establish distinct infracommunities. Interaction networks have been used to better understand these associations, revealing interaction modules between bats and their parasites. The Magdalena River basin is the largest in Colombia, encompassing a wide variety of climatic and ecological conditions, with up to 98 bat species reported. We conducted field trips to capture bats and bat flies in different locations along the basin and reviewed literature records and biological collections to gather additional data on interactions between bats and bat flies in this region. We found a high diversity of bats and bat flies in the Magdalena River basin, revealing a medium specialization and modularity in these interactions. We identified bat fly infracommunities and negative associations between certain bat fly species, suggesting competition for resources within hosts. The specialization is similar to that reported in degraded and fragmented habitats where the availability of shelters decreases, favoring the overcrowding of bats, forming multi-species colonies. In conclusion, our study provides important information on the interactions between bats and bat flies in the Magdalena River basin, expanding knowledge about the diversity and structure of these communities in inter-Andean landscapes.

This article is part of:  
**Biology of Pangolins and Bats**



Academic editor: Pierfilippo Cerretti  
Received: 21 May 2024  
Accepted: 3 November 2024  
Published: 31 December 2024

ZooBank: <https://zoobank.org/8A419F59-A628-48AC-B296-19633549A038>

Copyright: © Camila López-Rivera et al.  
This is an open access article distributed under terms of the Creative Commons Attribution License (Attribution 4.0 International – CC BY 4.0).

**Key words:** Chiroptera, Dry Forest, Magdalena River, Nycteribiidae, specialization, Streblidae

**Citation:** López-Rivera C, Robayo-Sánchez LN, Ramírez-Hernández A, Cuéllar-Sáenz JA, Villar JD, Córtes-Vecino JA, Rivera-Páez FA, Ossa-López PA, Ospina-Pérez EM, Henao-Osorio JJ, Cardona-Giraldo A, Racero-Casarrubia J, Rodríguez-Posada ME, Morales-Martínez DM, Hidalgo M, Ramírez-Chaves HE (2024) Diversity of ectoparasitic bat flies (Diptera, Hippoboscoidea) in inter-Andean valleys: evaluating interactions in the largest inter-Andean basin of Colombia. *ZooKeys* 1221: 377–400. <https://doi.org/10.3897/zookeys.1221.127890>

## Introduction

Ectoparasitic flies of the families Streblidae and Nycteribiidae (Diptera: Hippoboscoidea) are highly specialized hematophagous arthropods associated with bats (Wenzel et al. 1966; Marshall 1982). Currently, Nycteribiidae are considered monophyletic, while Streblidae are paraphyletic with the New World Streblidae placed apart from all Old-World taxa (Dittmar et al. 2006; 2015). The morphology of bat flies' species within Streblidae and Nycteribiidae is highly variable (Dick and Patterson 2006). Species within Nycteribiidae have dorsoventrally flattened bodies, but also have reduced eyes and all species are apterous (Dick and Patterson 2006). In contrast, species of Streblidae can have laterally compressed, dorsoventrally flattened or uncompressed bodies, reduced compound eyes, and the wings may be normal, reduced, or absent (Dick and Patterson 2006; Dick and Miller 2010; Dick and Dittmar 2014).

The morphological adaptations of bat flies can be attributed in part to coevolutionary history with their hosts (Poinar and Brown 2012). Most bat flies are monoxenes (host-specific), but others may be oligoxenes (associated with more than one species of the same genus), pleioxenes (associated with more than one species of the same subfamily or family), and to a lesser extent, polyoxenes (associated with different species of different families) (Wenzel et al. 1966; Dick 2005; Dick and Gettinger 2005; Dick and Miller 2010). Similarly, bats may have associations with a limited number of coexisting but spatially segregated morphologically distinct bat flies, which can form “infracommunities” (ter Hofstede et al. 2004; Dick 2005; ter Hofstede and Fenton 2005; Dick and Patterson 2006). Based on the region of the host body where the bat flies are typically found, there are three ecomorphological groups: (1) wing crawlers, which include flies that predominantly inhabit the wing membrane; (2) fur runners, which are flies that particularly have long hind legs and are found mainly on the hairy body, moving on the surface of the fur; and (3) fur swimmers, which include species characterized by a compressed head and body, usually possessing ctenidia, adapted to navigate through the fur of the host (ter Hofstede et al. 2004; Dick 2005).

The study of host-parasite interactions is critical to uncovering ecological and coevolutionary patterns and processes, and is key in the study of emerging infectious diseases (Swann et al. 2015). Ecologically, interaction networks reveal modules or interaction groups that are formed when bats share the same species of ectoparasites (Grilli et al. 2016), providing insight into the structure and interconnectedness of host and ectoparasite assemblages (Blüthgen et al. 2006). Also, interaction networks can determine the ecological role of each species and the complexity of their interactions (Lindeman 1942; Pilosof et al. 2017). In terms of coevolution, the interaction studies can determine how closely related the parasitic species are in the phylogeny or whether these species share ecological traits (Patterson et al. 2008; Zarazúa-Carbajal et al. 2016; Durán et al. 2018; Hernández-Martínez et al. 2018).

Despite bat flies being generally distributed globally due to the wide range of their bat hosts, the tropics exhibit greater species richness and endemism (Guerrero 1994; Dittmar et al. 2015). This phenomenon is often associated with the high diversity of bat species in tropical areas (Hutson et al. 2001). Unfortunately, knowledge of bat fly-bat interactions has been restricted to fragmented records at a local scale (Zapata-Mesa et al. 2024). For example, in the Neotropics,

Colombia is home to one of the highest bat species diversity globally with 222 species (Ramírez-Chaves et al. 2021). Nevertheless, the richness of bat flies in the country is underestimated. Colombia has records of 81 species of Streblidae and 11 of Nycteribiidae (Dick et al. 2016; Graciolli et al. 2016; Pastrana-Montiel et al. 2019; Wolff et al. 2023), which is a lower diversity compared with neighboring countries such as Brazil, which has 181 bat species (Garbino et al. 2022), with 84 species of Streblidae and 26 Nycteribiidae, respectively (Graciolli 2018). A similar situation occurs in Venezuela, where 172 bat species have been reported (Delgado-Jaramillo et al. 2016), with 121 species of Streblidae and 10 of Nycteribiidae, respectively (Bezerra et al. 2016; Laurenço et al. 2016).

Extensive research on bat flies in Colombia has spanned more than four decades (Marinkelle and Grose 1981; Herrera-Sepúlveda 2013; Durán et al. 2018; Calonge-Camargo and Pérez-Torres 2018; Liévano-Romero et al. 2019), but numerous information gaps persist regarding the presence, diversity, distribution, and ecological interactions of these ectoparasitic flies (Durán et al. 2018; Liévano-Romero et al. 2019). Recent studies have provided new insights into bat-fly interactions in various natural regions of the country, such as the Orinoquia (Liévano-Romero et al. 2019; López Rivera et al. 2022; Ospina-Pérez et al. 2023), the Caribbean (Durán et al. 2018; Calonge-Camargo and Pérez-Torres 2018), and the Andes (Tamsitt and Fox 1970; Tarquino-Carbonell et al. 2015; Ascuntar-Osnas et al. 2020; Raigosa-Álvarez et al. 2020). However, there remains a gap in knowledge in the Andean region and the inter-Andean basins such as the one formed by the Magdalena River.

The inter-Andean basin of the Magdalena River covers 257,000 km<sup>2</sup> and represents 24% of Colombia's continental territory (Restrepo and Syvitski 2006). This basin is critical for host-parasite interaction studies for many reasons. First, the Magdalena River basin harbors a rich bat fauna with nearly 98 bat species (IAvH 2021), representing nearly 45% of the country's bat species; however, there is limited information regarding the ectoparasitic flies that coexist with them. Second, the Magdalena River basin has more than 30 million inhabitants, around 79% of the country's population (Restrepo and Syvitski 2006). Third, the basin has undergone significant deforestation being one of the areas with most dramatic forest reduction in Colombia between the years 1970 and 2000 (Etter et al. 2008). Considering the last two events, a dense human population and high deforestation rates, the Magdalena River basin is an ideal region for studying of the effects of habitat degradation of the prevalence of parasites, and on the emerging infectious diseases, especially in animals considered as vectors, such as bats and their parasites. In this context, this study seeks to unveil the extent of species richness within Streblidae and Nycteribiidae to elucidate the complex interactions with bats in the main inter-Andean basin of Colombia.

## Materials and methods

### Study area

The Magdalena River forms the largest inter-Andean basin of Colombia covering 257,438 km<sup>2</sup> of national territory. It originates at the head of the Colombian Massif at an elevation of 3,865 m in the Puracé National Natural Park and flows into the Caribbean Sea in Bocas de Ceniza in the Department of Atlántico. This basin exhibits a great diversity of geological, edaphic, climatic, hydraulic,

sedimentological, and morpho-dynamic conditions, forming a highly complex socio-ecological system (Gallo-Vélez et al. 2023). It crosses 1,540 km from south to north along 13 departments of Colombia, where 79% of the country's population resides, making it an area of economic importance since 80% of Colombia's GDP is generated there. The Magdalena River basin is significantly influenced by human activity, including deforestation, poor soil conservation and mining practices (Restrepo and Syvitski 2006).

Due to its geographical location, the climate of the region is tropical, primarily determined by altimetric variations, the relief topography and the influence of the Intertropical Confluence Zone, which generates two wet and two dry periods that occur interspersed throughout the year (León et al. 2000). Other factors that influence the climatic characteristics of the Magdalena River basin are precipitation, temperature, relative humidity, sunlight, and wind, which can create microclimates around the basin (IDEAM 2001; Nardini et al. 2020). According to Holdridge (1978), the Magdalena River basin encompasses five altitudinal zones: the tropical zone (0–1,000 m), the premontane zone (1,000–2,000 m), the submontane zone (2,000–3,000 m), and the Andean zone (3,000–4,000 m). The Magdalena River Basin supports ecosystems of Andean forests (26.36%), paramo (1.96%), xerophytic vegetation (3.01%), and wetlands (2.56%).

### Field trips

We conducted field trips in 12 localities in the Magdalena River basin between March, July and September 2021, April and November 2022, and January and March 2023. Specific dates for each locality are shown in Table 1. Four sampling sites were in the Department of Caldas at elevations between 170 and 650 m (Table 1). Five localities were in the Department of Cundinamarca, with elevations between 800 and 1,900 m. Three localities were within the Department of Cesar, with elevations between 50 and 200 m (Table 1; Fig. 1).

To capture bats, we installed 5 nylon mist nets (12.0 m × 2.5 m, and mesh size 36 mm) for five nights at each sampled location. Mist nets were randomly placed and operated between 18:00 and 22:00 hours. We placed bats individually in cotton bags and identified them using taxonomic keys (i.e., Gardner 2008; Díaz et al. 2021). To mitigate possible contamination between samples, the cloth bags used for bat sampling were cleaned and employed only once each night. We collected some specimens from the captured individuals to confirm identifications and deposited them in the Mammals (M) and Ectoparasites (Ec) collections of the Museo de Historia Natural, Universidad de Caldas (MHN-UCa), Colombia.

We manually collected bat flies using entomological tweezers. The collected bat flies were placed in Eppendorf tubes with 70% ethanol to prevent desiccation during transport to the laboratory. For the identification of Streblidae and Nycteribiidae specimens, we used the dichotomous keys and descriptions from Wenzel et al. (1966), Wenzel (1976), Guerrero (1994, 1995, 1998), Autino et al. (1999), and Graciolli (2004). All the collections were conducted under permits granted by the National Authority for Environmental Licenses (ANLA) to the Universidad de Caldas, as stipulated in Resolution 02497 of 2018, and to the National University of Colombia through Resolution 01435 of September 3, 2018, and to the Universidad de Caldas as stipulated in resolution 854 of 20 May 2019, modified by resolution 519 of 3 March 2022.

**Table 1.** Sampling localities (1–14) of bats and bat flies between 2021 and 2023 in the departments of Caldas, Cesar and Cundinamarca in the Magdalena River basin in Colombia. Localities obtained from the literature (15–16), and from specimens housed at the ectoparasite collection (MHN-UCa-Ec) of the Museo de Historia Natural de la Universidad de Caldas (localities 17–26).

Number	Department, Municipality	Localities	Latitude, Longitude	Elevation (m)	Dates
1	Caldas, La Dorada	Vereda La Atarraya, near La Miel River	5,72015, -74,72697	178	8/11/2022
2	Caldas, La Dorada	Vereda La Atarraya, Jardín Botánico del Magdalena	5,67694, -74,74417	224	9/11/2022
3	Caldas, Norcasia	Vereda Las Delicias, near the Manso River	5,67261, -74,84481	214	6/04/2022
4	Caldas, Norcasia	Vereda La Estrella, finca El Encanto	5,62775, -74,86806	654	7/04/2022
5	Cundinamarca, Villeta	Vereda Mave	4,94047, -74,45944	1289	15/01/2023
6	Cundinamarca, Villeta	Vereda Cune, Reserva Forestal la Playita	5,04239, -74,50117	1042	17/07/2022
7	Cundinamarca, Villeta	Vereda Cune, Finca Chamorro	5,03258, -74,49281	1044	12/02/2023
8	Cundinamarca, Villeta	Vereda Cune, Finca Choquenzá	5,05314, -74,49375	1271	17/01/2023
9	Cundinamarca, Villeta	Vereda Bagazal	4,98789, -74,48969	868	18/01/2023
10	Cundinamarca, Villeta	Vereda Salitre Blanco	5,05064, -74,49117	1324	12/07/2022
11	Cundinamarca, Villeta	Vereda La Esmeralda	5,05511, -74,54386	1999	17/03/2023
12	Cesar, Jagua de Ibirico	Mina Cerro Largo	9,54533, -73,28578	209	23/09/2021
13	Cesar, El Paso	Mina El Descanso	9,72156, -73,42611	64	17/09/2023
14	Cesar, La Loma	Mina La Loma	9,60972, -73,52089	56	05/03/2021 and 08/07/2021
15	Tolima, Ambalema	Chorrillo	4,43330, -74,80000	273	08/2012 and 11/2012
16	Tolima, Melgar		4,20358, -74,64337	322	04/1962
17	Caldas, Samaná	Vereda Lagunilla	5,60813, -74,94997	866	24/11/2021
18	Caldas, Samaná	Vereda Piedras verdes	5,60736, -74,94446	760	07/11/2021
19	Caldas, Samaná	Vereda La Reforma	5,58329, -74,95034	884	26/11/2021
20	Caldas, Samaná	Parque Nacional Natural Selva de Florencia	5,51642, -75,04292	1478	20/02/2018
21	Huila, Acevedo	Vereda La Ilusion	1,66045, -76,02625	1515	21/10/2021
22	Cundinamarca, La Palma		5,36056, -74,38972	1447	12/09/2018
23	Cundinamarca, Tenjo	Vereda Churunguaro	4,87532, -74,14609	2612	27/09/2018
24	Cundinamarca, Guachetá	Vereda Guachetá Alto	5,38556, -73,68555	2688	22/09/2018
25	Cundinamarca, Sasaima	RFPP Peñas del Aserradero	4,88008, -74,43585	2295	04/10/2018
26	Cundinamarca, La Vega	Vereda San Antonio	4,94875, -74,38367	1372	10/11/2018

## Review of records in the literature and biological collections

To compile additional records within the study area, we reviewed and identified bat and associated bat flies from different locations in the Magdalena River basin encompassing the departments of Caldas, Cundinamarca, Huila, Santander, and Tolima, deposited in the MHN-UCa-Ec collection. Additionally, we conducted searches for studies on ectoparasitic flies associated with bats in the Magdalena River Basin region. We reviewed the available information retrieved from search engines such as Science Direct, Web of Science, SciELO, Scopus, and Google Scholar, using the keywords ((fly\*) OR (flies) AND (Streblidae\*) OR (Nycteribiidae) AND (bat\*) AND (Colombia\*)). The last search was performed in October 2023. We also reviewed references and sources cited in the publications to obtain as much information as possible for creating interaction

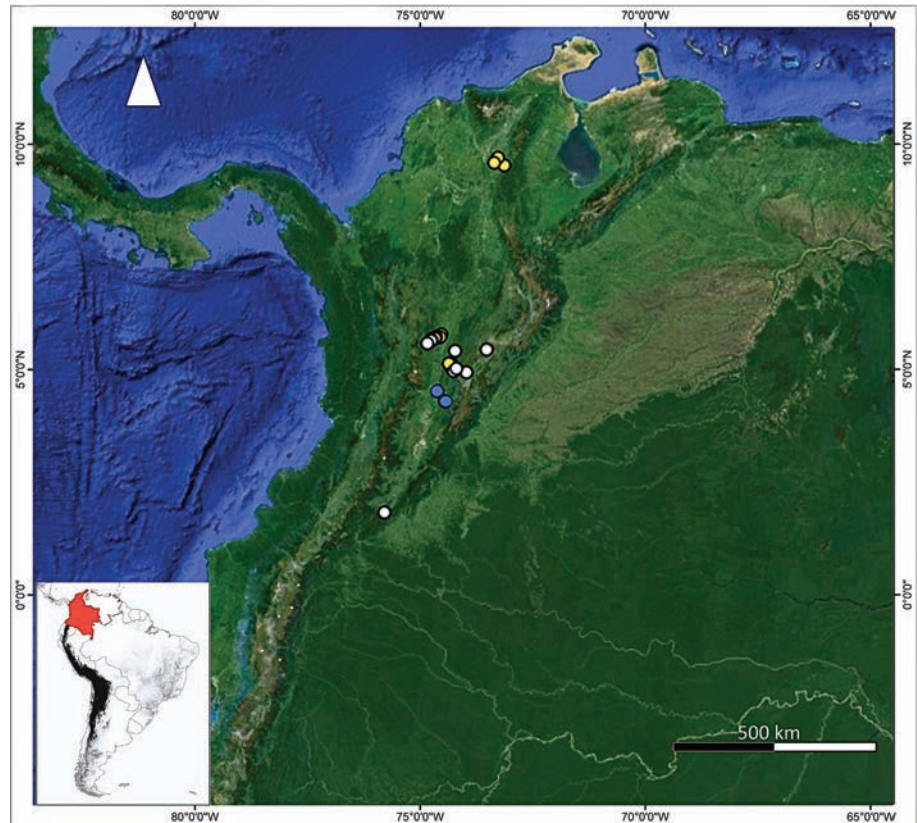


**Figure 1.** Locality records of bat flies (Nycteribiidae and Streblidae) in the inter-Andean Magdalena River basin, Colombia. Yellow circles indicate localities where field trips were conducted, blue circles are localities reported in the literature, and white circles indicate records of specimens in the ectoparasite collection of the Museo de Historia Natural de la Universidad de Caldas (MHN-UCa-Ec). The Magdalena River basin is indicated in green.

networks. We considered articles that included records of interactions between bat flies and bats in the Magdalena River Basin region, with no temporal restrictions. This approach enabled us to consolidate a more comprehensive data set for our study. We updated the taxonomic names of bat and bat fly's species reported in the literature. In the case of the fly reported as *Paratrichobius cf. longicrus* by Tamsitt and Fox (1970) we listed these records as *P. longicrus* when constructing the interaction network. Similarly, we considered the records of the bats *Sturnira liliium* and *S. parvidens* as part of *S. cf. giannae*, while *S. liliium* is restricted to the South Cone in Argentina, Brazil, Bolivia, Paraguay, and Uruguay; and *S. parvidens* is restricted to Mexico, Guatemala, Belize, Honduras, El Salvador, Nicaragua and Costa Rica (Mammal Diversity Database, 2023).

### Diversity, structure, and metrics of bat-fly ectoparasitic network

We analyzed the coexistence of bat fly species and their hosts, using the Kendall correlation, which is suitable for small samples and allows for the observation of negative relationships. We excluded infracommunities reported in only one individual as analysis was not possible in such cases. The analyses were performed using the Bipartite package v. 2.20 (Dormann et al. 2008), and the network graphics were created using the "plotweb" function and the "plotModuleWeb" function from the same package, implemented in R software v. 4.3.2 (R Core Team 2022).

To construct the interaction network between bats and bat flies, we classified the associations as primary, non-primary, or accidental, following the criteria established by Dick (2007). Primary associations are defined as those host species infested by  $\geq 5\%$  of the total number of individuals of a species of parasite. Additionally, we reviewed the literature to check if associations that were below 5% had been reported previously and if so, we included them in the network. For the data obtained from the review of the MHN-UCa-Ec, we only considered the associations that have been previously reported in the literature. To evaluate host-ectoparasite interactions in the Magdalena River Basin, we unified the data obtained from the different sources mentioned earlier, constructing a two-dimensional matrix through the quantitative summation of the three data sets (fieldwork, literature, and collection specimens).

We also performed bipartite interaction networks, in which bat and ectoparasite species are represented by nodes, and interacting species are linked by lines, with line width proportional to the frequency of each interaction (Blüthgen et al. 2006). Additionally, we evaluated network properties such as complementary specialization ( $H_2'$ ), specialization at the species level ( $d'$ ), connectance ( $C$ ), and modularity ( $M$ ) (Dormann et al. 2009; Fortuna et al. 2010; Mello et al. 2016). The complementary specialization index ( $H_2'$ ) measures both the degree of niche complementarity between species and specialization at the species level (Blüthgen et al. 2006; Blüthgen 2010). This index ranges from 0 (unspecialized network) to 1 (perfectly specialized network). The variation of species-level specialization measures (standardized Kullback-Leibler distance or divergence,  $d'$ ) provides valuable information about the structural properties of a network. The  $C$  index represents the number of interactions or links observed in the network, between bats and their ectoparasitic flies considering the total number of potential interactions. It takes values from 0 to 1 where 0 indicates that there are no connections and 1 that denotes that most of the nodes in the network interact with each other (Blüthgen et al. 2006). We calculated Modularity ( $M$ ) to identify subgroups of species that are more connected to each other than to the rest of the network (modules) (Fortuna et al. 2010). Modularity ranges from 0 to 1, with a value of 1 indicating a highly modular network and 0 a non-modular network. We use the DIRTLPawd+ algorithm to compute modularity (Dormann and Strauss 2014; Beckett 2016). In addition, we used a null model to test the significance of specialization ( $H_2'$ ) and modularity ( $M$ ) based on 1000 randomly generated matrices based on a Patefield null model (Dormann et al. 2009). Finally, we standardized modularity by calculating the ZQ score (ZQ), where values greater than 1.96 represent differences from the null model (Carstensen et al. 2016).

## Results

### Data collection

During the field work, we captured 376 bats belonging to 31 species, 22 genera, and four families. Of these, 285 bats of 25 species of Phyllostomidae and one species of Noctilionidae carried bat flies. In total we collected 588 bat flies belonging to 23 species, 10 genera and a single family (Streblidae). The most common bat species captured were *Carollia perspicillata* ( $n = 176$ ), *Carollia brevicauda* ( $n = 38$ ), *Glossophaga soricina* ( $n = 23$ ), and *Artibeus lituratus* ( $n = 18$ ).

The most abundant species of bat flies were *Trichobius joblingi* ( $n = 301$ ) and *Speiseria ambigua* ( $n = 50$ ), mainly associated with species of the genus *Carollia* (Table 2). The literature review added records of 107 bats of eight species of the family Phyllostomidae, of which 51 were being parasitized by 170 bat flies belonging to 14 species of Streblidae. The most frequently reported bat species in the literature were *Carollia perspicillata* (49), *Artibeus planirostris* (20), and *Desmodus rotundus* (16). Similarly, the most abundant bat fly's species recorded in the literature were *T. joblingi* ( $n = 114$ ) and *T. costalimai* ( $n = 82$ ), mainly associated with *Carollia perspicillata* and *Phyllostomus discolor*, respectively (Table 3). The review of specimens housed at the MHN-UCa-Ec added 145 bat flies belonging to 20 species, 11 genera, and two families (Streblidae and Nycteribiidae), linked to 67 bats of 19 species of Phyllostomidae, and two species of Vespertilionidae. *Carollia perspicillata* ( $n = 23$ ) and *T. joblingi* ( $n = 48$ ) were the most abundant bat and bat fly species (Table 3). For Nycteribiidae, all specimens recorded belong to the genus *Basilia*. The male specimens of *Basilia* deposited at the MHN-UCa-Ec could not be identified to the species level, since the majority of identification keys available correspond to females. We identified *Basilia juquiensis* males because they were collected with females (Fig. 2), and the latter are characterized by having the sternite almost twice as long as it is wide, sternite III covered by sternite II, and sternite VI divided longitudinally.



Figure 2. Micrographs of *Basilia juquiensis* (MHN-UCa-Ec 849), female (A, B) ventral view and (C) dorsal view; male (D) ventral (E) dorsal view. Scale bars: 0.5 mm.

**Table 2.** Bat-fly interactions including bat species, number of infested individuals, their respective bat flies, abundance, prevalence of these relationships in the study area. The localities where the associations were documented correspond to Table 1. M (Mammals) and Ec (Ectoparasite): museum vouchers of bat and fly's specimens deposited at the MHN-UCa.

Bat species	<i>n</i>	No. of infested bats	Bat flies	<i>n</i>	Prevalence %	Voucher	Locality
<b>Emballonuridae</b>							
<i>Saccopteryx leptura</i>	2	0	0	0	0	M-3969, M-4223	1, 3
<i>Rhynchonycteris naso</i>	3	0	0	0	0	M-3970, 3971, 4222	2, 3
<b>Molossidae</b>							
<i>Cynomops greenhalli</i>	1	0	0	0	0	M-4221	2
<i>Molossops griseiventer</i>	1	0	0	0	0	M-4220	2
<i>Molossus molossus</i>	2	0	0	0	0	M-4357, 4358	9
<b>Noctilionidae</b>							
			<b>Streblidae</b>				
<i>Noctilio albiventris</i>	4	4	<i>Paradyschira parvuloides</i>	5	100	Ec-1364, 1390, 1392	14
		1	<i>Trichobius joblingi</i>	2	25	Ec-1384	14
<b>Phyllostomidae</b>							
<i>Carollia brevicauda</i>	38	2	<i>Speiseria ambigua</i>	3	5.26	Ec-1019, 1326	4, 14
		1	<i>Strebla guajiro</i>	1	2.63	M-4341; Ec-1700	5
		19	<i>Trichobius joblingi</i>	40	50	M-4339-4341; Ec-936, 941-944, 1023, 1025, 1217, 1317, 1328, 1632, 1687, 1689, 1691, 1694, 1701, 1758, 1767	2, 3, 5, 7, 8, 10, 14
		2	<i>Trichobius uniformis</i>	7	5.26	M-4105-4106; Ec-1629-1630	10
<i>Carollia castanea</i>	9	3	<i>Speiseria ambigua</i>	3	33.33	M-3974; Ec-934, 1015, 1538	3, 4
		6	<i>Trichobius joblingi</i>	6	66.67	M-4117; Ec-935, 1022, 1190, 1220, 1227, 1684	2, 3, 4, 6
<i>Carollia perspicillata</i>	176	38	<i>Speiseria ambigua</i>	45	21.59	M-4108, 4109, 4340; Ec-937, 938, 950, 1011, 1013, 1021, 1369, 1373, 1376, 1382, 1386, 1396, 1398, 1400, 1408, 1412, 1415, 1484, 1490, 1492, 1497, 1501, 1504, 1506, 1512, 1515, 1528, 1531, 1541, 1546, 1551, 1555, 1637, 1640, 1649, 1654, 1658, 1755	3, 4, 5, 12, 13, 10
		1	<i>Strebla guajiro</i>	1	0.57	M-4343; Ec-1702	4
		1	<i>Strebla christinae</i>	1	0.57	Ec-1381	14
		5	<i>Strebla hertigi</i>	5	2.84	M-4109; Ec-1014, 1026, 1647, 1505, 1545	4, 13
		2	<i>Trichobius costalimai</i>	11	1.14	Ec-1332, 1403	14
		1	<i>Trichobioides perspicillatus</i>	1	0.57	Ec-1404	14
		97	<i>Trichobius joblingi</i>	217	55.11	M-4102-4104, 4107-4109, 4338, 4340; Ec-939, 940, 949, 951, 1024, 1027, 1083, 1212, 1215, 1218, 1222, 1224, 1314, 1322, 1323, 1329, 1331, 1333, 1336, 1341, 1343, 1370-1372, 1374, 1375, 1378, 1380, 1385, 1387, 1388, 1394, 1397, 1405, 1406, 1410, 1413, 1414, 1416, 1417, 1419, 1480, 1482, 1489, 1491, 1493, 1495, 1496, 1498-1500, 1502, 1503, 1509, 1510, 1513, 1516, 1521, 1522, 1526, 1527, 1530, 1532, 1533, 1540, 1542, 1543, 1544, 1547, 1548, 1550, 1554, 1623, 1624, 1628, 1633, 1635, 1636, 1638, 1639, 1641-1644, 1648, 1652, 1653, 1657, 1686, 1688, 1690, 1692, 1693, 1696, 1756, 1757	1, 2, 3, 4, 5, 7, 10, 12, 13, 14
		1	<i>Trichobius persimilis</i>	3	0.57	Ec-1020	4
		1	<i>Trichobius uniformis</i>	1	0.57	Ec-1340	14
	<i>Anoura cadenai</i>	1	1	<i>Trichobius joblingi</i>	2	100	M-4355; Ec-1629
<i>Anoura luismanueli</i>	3	1	<i>Anastrebla modestini</i>	2	33.33	M-4428-4430; Ec-1794	11

Bat species	n	No. of infested bats	Bat flies	n	Prevalence %	Voucher	Locality
<i>Glossophaga soricina</i>	23	2	<i>Paraeuctenoides longipes</i>	2	8.70	Ec-1487, 1553	14
		1	<i>Speiseria ambigua</i>	1	4.35	Ec-1549	14
		9	<i>Trichobius joblingi</i>	14	39.13	Ec-1321, 1338, 1339, 1342, 1399, 1483, 1486, 1523, 1529	14
		9	<i>Trichobius uniformis</i>	19	39.13	M-4096; Ec-1334, 1335, 1337, 1401, 1402, 1552, 1646, 1655, 1660	10
<i>Trinycteris nicefori</i>	1	1	<i>Strebla alvarezii</i>	3	100	M-4255; Ec-1197	1
<i>Lonchorrhina aurita</i>	1	1	<i>Speiseria ambigua</i>	1	100	M-3973; Ec-957	3
		1	<i>Trichobius</i> sp.	4	100	Ec-958	3
<i>Micronycteris megalotis</i>	1	0	0	0	0	M-4094	10
<i>Micronycteris microtis</i>	2	0	0	0	0	M-4254, 4356	3, 11
<i>Lophostoma nicaraguae</i>	3	1	<i>Strebla tonatidae</i>	3	33.33	M-4236, 4238, 1198	1
		2	<i>Trichobius mendezi</i>	4	66.67	Ec-1196, 1202	1
<i>Lophostoma silvicola</i>	8	1	<i>Mastoptera guimaraesi</i>	1	12.50	Ec-1324	14
		5	<i>Trichobius joblingi</i>	30	62.50	Ec-1391, 1409, 1507, 1508, 1511	14
<i>Phylloderma stenops</i>	1	1	<i>Strebla christinae</i>	3	100	M-3972; Ec-948	3
<i>Phyllostomus discolor</i>	18	1	<i>Strebla hertigi</i>	1	5.56	Ec-1683	10
		1	<i>Paratrachobius longicrus</i>	1	5.56	Ec-1315	14
		8	<i>Trichobioides perspicillatus</i>	26	44.44	M-4113, 4114; Ec-1669, 1671, 1674-1676, 1678, 1680, 1682	10
		7	<i>Trichobius costalimai</i>	29	38.89	Ec-1670, 1672, 1673, 1677, 1679, 1681, 1188	10
<i>Phyllostomus hastatus</i>	12	4	<i>Mastoptera guimaraesi</i>	14	33.33	Ec-1194, 1770, 1771, 1792	1, 9
		4	<i>Strebla hertigi</i>	8	33.33	Ec-1760-1762, 1791	5, 9
		4	<i>Trichobius dugesioides</i>	2	33.33	M-4334; Ec-1195, 1763, 1769, 1772	1, 5, 9
<i>Artibeus aequatorialis</i>	8	2	<i>Aspidoptera phyllostomatis</i>	2	25	M-3987, 4251; Ec-945, 1205, 1206, 1666	6
		4	<i>Megistopoda aranea</i>	6	50	M-3989, 4111; Ec-959, 1662, 1665	3, 6, 14
		1	<i>Trichobius joblingi</i>	1	12.50	Ec-1316-1319	14
<i>Artibeus lituratus</i>	18	5	<i>Paratrachobius longicrus</i>	13	27.78	M-4099-4100-4336; Ec-1488, 1634, 1645, 1661, 1698	8, 10, 14
		2	<i>Trichobius joblingi</i>	3	11.11	Ec-1383, 1656	10, 14
<i>Dermanura anderseni</i>	7	0	0	0	0	M-3979, 3980, 4243, 4248, 4252, 4253, 4258	1, 2, 3
<i>Mesophylla macconnelli</i>	1	0	0	0	0	M-3981	3
<i>Platyrrhinus helleri</i>	4	0	0	0	0	M-3984, 3985, 4244, 4249	1, 2, 3
<i>Sturnira cf. giannae</i>	21	4	<i>Aspidoptera delatorrei</i>	10	30.77	M-4097, 4098, 4353; Ec-1192, 1204, 1219, 1225, 1226, 1228, 1622, 1651, 1764	1, 2, 10
		20	<i>Megistopoda proxima</i>	26	95.23	M-4097, 4098, 4115, 4116, 4241, 4352; Ec-1193, 1395, 1517, 1518, 1524, 1534-1536, 1539, 1621, 1650, 1667, 1685, 1695, 1697, 1765, 1766, 1768, 1793	1, 6, 7, 8, 10, 11, 14
<i>Sturnira luisi</i>	3	1	<i>Aspidoptera delatorrei</i>	2	33.33	M-3978; Ec-961	3,
		1	<i>Megistopoda proxima</i>	3	33.30	M-3977, 4250; Ec-952, 1204	2, 3
<i>Uroderma convexum</i>	2	0	0	0	0	M-3986, 4240	1, 3
<i>Vampyressa thuyone</i>	2	0	0	0	0	M-3982, 3983	3

**Table 3.** Bat species with associated bat flies recorded in the literature and museum specimens at the MHN-UCa-Ec. The *n* of infested bats is shown only for records in the literature. The localities where the associations were documented correspond to Table 1.

Bat species (n- infested bats)	Bat fly species	<i>n</i>	Reference/Voucher	Locality
<b>Phyllostomidae</b>	<b>Streblidae</b>			
<i>Carollia brevicauda</i> (3)	<i>Mastoptera minuta</i>	1	Tarquino-Carbonell et al. 2015	15
	<i>Strebla guajiro</i>	1	Tarquino-Carbonell et al. 2015	15
	<i>Trichobius joblingi</i>	14	Tarquino-Carbonell et al. 2015/ Ec-847, 866, 869	15
<i>Carollia castanea</i> (4)	<i>Speiseria ambigua</i>	1	Ec-853	19
	<i>Trichobius joblingi</i>	3	Ec-531	19
	<i>Trichobius persimilis</i>	3	Ec-854, 860	17, 19
<i>Carollia perspicillata</i> (23)	<i>Megistopoda proxima</i>	4	Ec-845	18
	<i>Paratrachobius longicrus</i>	6	Ec-865, 868	17
	<i>Speiseria ambigua</i>	19	Tamsitt and Fox 1970; Tarquino-Carbonell et al. 2015/ Ec-529, 533, 856	15, 16, 17, 18
	<i>Strebla guajiro</i>	2	Tamsitt and Fox 1970; Tarquino-Carbonell et al. 2015	15, 16
	<i>Strebla hertigi</i>	2	Ec-858	17
	<i>Trichobius joblingi</i>	144	Tamsitt and Fox 1970; Tarquino-Carbonell et al. 2015/ Ec-97, 527, 528, 534, 535, 844, 846, 848, 851, 855, 857, 859, 864, 867, 871	15, 16, 17, 18, 19, 20
	<i>Trichobius tiptoni</i>	3	Ec-1821	22
<i>Desmodus rotundus</i>	<i>Trichobius parasiticus</i>	53	Tarquino-Carbonell et al. 2015	15
<i>Anoura aequatoris</i> (1)	<i>Exastinion decepticum</i>	2	Ec-1825	25
<i>Anoura caudifer</i> (1)	<i>Anastrebla caudiferae</i>	1	Ec-1822	24
	<i>Anastrebla mattadeni</i>	1	Tamsitt and Fox 1970	16
<i>Anoura geoffroyi</i> (2)	<i>Exastinion decepticum</i>	3	Ec-1816	23
<i>Anoura</i> sp. (3)	<i>Exastinion decepticum</i>	1	Ec-1831	26
	<i>Anastrebla caudiferae</i>	1	Ec-1829	26
<i>Anoura peruana</i>	<i>Exastinion clovisi</i>	1	Tamsitt and Fox 1970	16
<i>Choeroniscus</i> sp. (1)	<i>Strebla hertigi</i>	1	Ec-530	20
<i>Glossophaga soricina</i>	<i>Trichobius dugesii</i>	1	Tamsitt and Fox 1970	16
	<i>Trichobius uniformis</i>	1	Tarquino-Carbonell et al. 2015	15
<i>Lonchophylla robusta</i> (1)	<i>Trichobius lonchophyllae</i>	1	Ec-1817	22
<i>Lophostoma nicaraguae</i> (5)	<i>Mastoptera minuta</i>	2	Ec-861, 863	17
	<i>Trichobius affinis</i>	3	Ec-862, 870	17, 18
	<i>Trichobius persimilis</i>	1	Ec-852	17
<i>Phylloderma stenops</i> (1)	<i>Strebla christinae</i>	6	Ec-689	18
<i>Phyllostomus discolor</i> (1)	<i>Trichobius costalimai</i>	82	Tamsitt and Fox 1970	16
	<i>Trichobioides perspicillatus</i>	73	Tamsitt and Fox 1970/ Ec-1819	16, 22
	<i>Strebla consocius</i>	1	Tamsitt and Fox, 970	16
	<i>Strebla hertigi</i>	7	Tamsitt and Fox 1970	16
<i>Phyllostomus hastatus</i>	<i>Trichobius longipes</i>	3	Tarquino-Carbonell et al. 2015	15
	<i>Mastoptera minuta</i>	35	Tarquino-Carbonell et al. 2015	15
<i>Artibeus aequatorialis</i>	<i>Megistopoda aranea</i>	2	Tamsitt and Fox 1970	16
	<i>Paratrachobius longicrus</i>	1	Tamsitt and Fox 1970	16

Bat species (n- infested bats)	Bat fly species	n	Reference/Voucher	Locality
<i>Artibeus lituratus</i>	<i>Aspidoptera phyllostomatis</i>	2	Tarquino-Carbonell et al. 2015	15
	<i>Megistopoda aranea</i>	2	Tarquino-Carbonell et al. 2015	15
	<i>Paratrachobius</i> cf. <i>longicrus</i>	23	Tamsitt and Fox 1970	16
<i>Artibeus planirostris</i>	<i>Megistopoda aranea</i>	3	Tarquino-Carbonell et al. 2015	15
<i>Artibeus</i> sp. (2)	<i>Megistopoda aranea</i>	2	Ec-1836	26
	<i>Aspidoptera phyllostomatis</i>	1	Ec-1837	26
<i>Enchistenes hartii</i> (1)	<i>Paratrachobius sanchezi</i>	1	Ec-100	20
<i>Platyrrhinus vittatus</i> (1)	<i>Paratrachobius longicrus</i>	1	Ec-75	20
<i>Sturnira bogotensis</i> (1)	<i>Megistopoda proxima</i>	1	Ec-73	20
	<i>Trichobius petersoni</i>	3	Ec-1821	22
<i>Sturnira erythromos</i> (2)	<i>Trichobius petersoni</i>	3	Ec-1817, 1820	22
<i>Sturnira</i> cf. <i>giannae</i> (7)	<i>Aspidoptera delatorrei</i>	3	Ec-685, 688, 751	21
	<i>Megistopoda proxima</i>	20	Tamsitt and Fox 1970; Tarquino-Carbonell et al. 2015/ Ec-526, 532, 536, 687, 1820	15, 16, 18, 20, 22
<i>Sturnira ludovici</i> (2)	<i>Megistopoda proxima</i>	3	Ec-1823	25
	<i>Trichobius petersoni</i>	2	Ec-1824	25
<b>Vespertilionidae</b>	<b>Nycteribiidae</b>			
<i>Myotis keaysi</i> (1)	<i>Basilisa</i> sp.	1	Ec-752	21
<i>Myotis riparius</i> (2)	<i>Basilisa</i> sp.	2	Ec-74	20
	<i>Basilisa juquiensis</i>	4	Ec-849	17

### Structure and metrics of the bat-fly ectoparasitic network

The bat-fly bat interaction network for the Magdalena River Basin exhibited high specialization ( $H_2' = 0.74$ ) and low connectance ( $C = 0.06$ ). Likewise, the specialization index by bat fly species indicating that 23.68% of species were highly specialized ( $d' = 0.936-1$ ). The results obtained from the reciprocal specialization index at the species level ( $d'$ ) revealed that the species *Anastrebla modestini*, *Exastinion clovisi*, *Paratrachobius sanchezi*, *Strebla alvarezii*, *S. christinae*, *Trichobius lonchophyllae*, and *T. parasiticus* each had a value of 1, indicating high reciprocal specialization. These species were followed by *Exastinion. decepticum* ( $d' = 0.97$ ) and *Paradyschiria parvuloides* ( $d' = 0.93$ ). In contrast, the species with the lowest values in the specialization index were *Strebla guajiro* ( $d' = 0.11$ ) and *S. consocius* ( $d' = 0.11$ ), *S. hertigi* ( $d' = 0.19$ ), and *Speiseria ambigua* ( $d' = 0.28$ ), suggesting lower specialization compared to the aforementioned species (Suppl. material 1: table S1).

Of the 38 species of bat flies included in our interaction network, 19 were associated with a single bat species: *A. mattadeni*, *A. modestini*, *B. fuquiensis*, *E. clovisi*, *P. parvuloides*, *Paraeuctenoides longipes*, *Paratrachobius sanchezi*, *S. alvarezii*, *S. christinae*, *S. consocius*, *S. tonatidae*, *Trichobioides perspicillatus*, *Trichobius affinis*, *T. dugesii*, *T. dugesioides*, *T. lonchophyllae*, *T. longipes*, *T. mendezii*, and *T. parasiticus*. The bat fly species with the greatest number of interactions were *T. joblingi* (9) and *Megistopoda proxima* (6). The bat species with the most associations were *C. perspicillata* (8), *A. lituratus* (5), and *Lophostoma nicaraguae*, *Phyllostomus discolor* and *P. hastatus* (5). Additionally, 16 of the 37 bat species used to create the interaction network were associated with only one bat fly species (Suppl. material 1: fig S1). Moreover, we recorded high modularity for the interaction network ( $M = 0.64$ ), forming 13 modules of related species. Most modules exhibited medium (the fly interacts with the host bat species with a noticeable,

but not constant, frequency) to low (the fly interacts with the host bat species on rare occasions or under specific conditions) interaction strength (Fig. 3), except for the first module, which showed high interaction strength (the bat fly interacts with the host species frequently and regularly). This indicates a strong dependence of the fly on that particular bat for its survival and reproduction, specifically between *C. perspicillata* and *T. joblingi*. Most modules were formed by phylogenetically similar host, either from the same genus (modules 3 and 11 in Fig. 3) or from the same family (module 1 and 10 of Fig. 3). Comparisons with null models showed differences (ZQ = 83.51) indicating that the observed indices result from ecological processes rather than random chance. Furthermore, the comparison between the observed  $H_2'$  value (0.74) and the null model values revealed significant differences (p-value = 0.00) (Suppl. material 1: fig. S2).

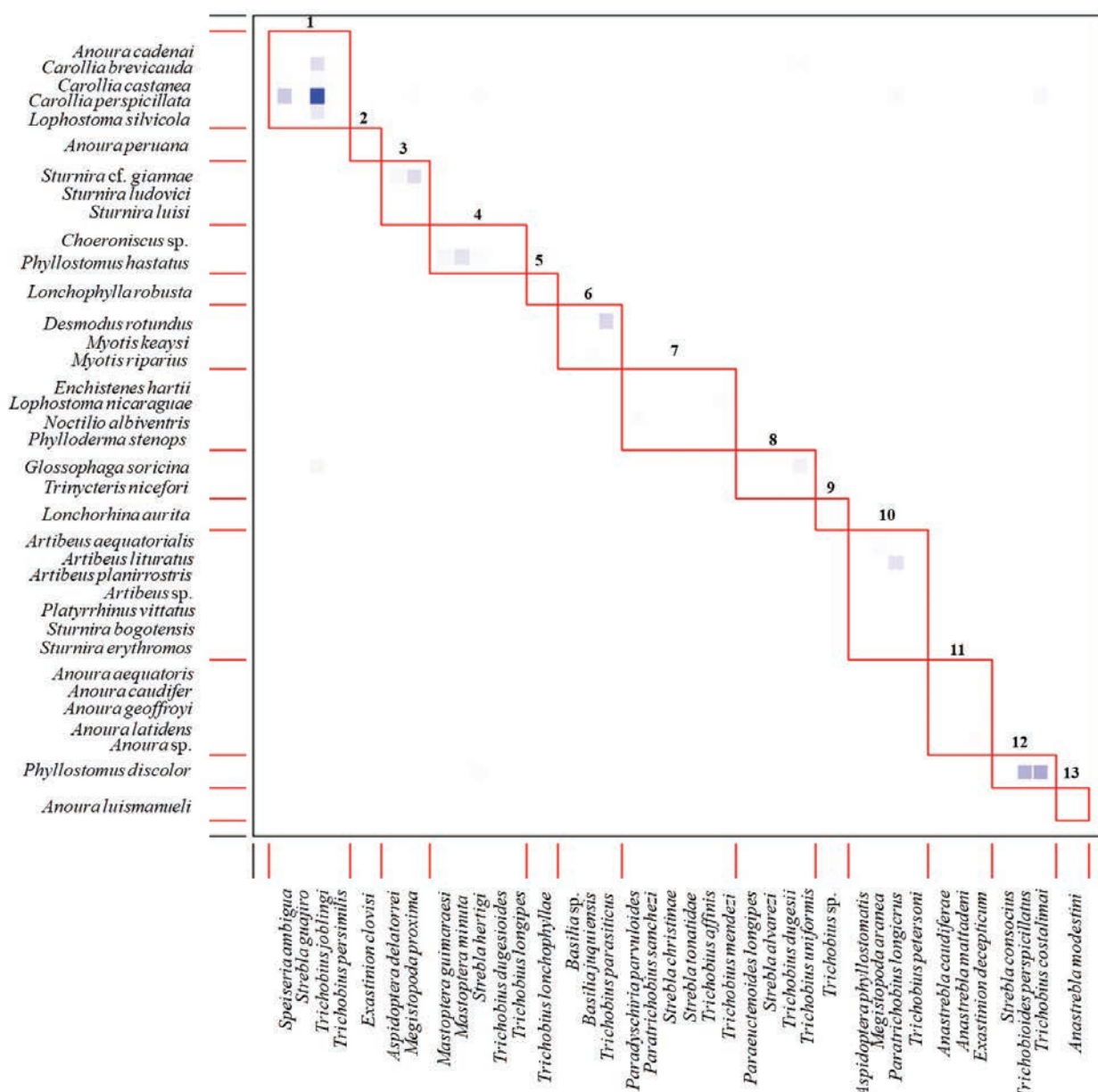
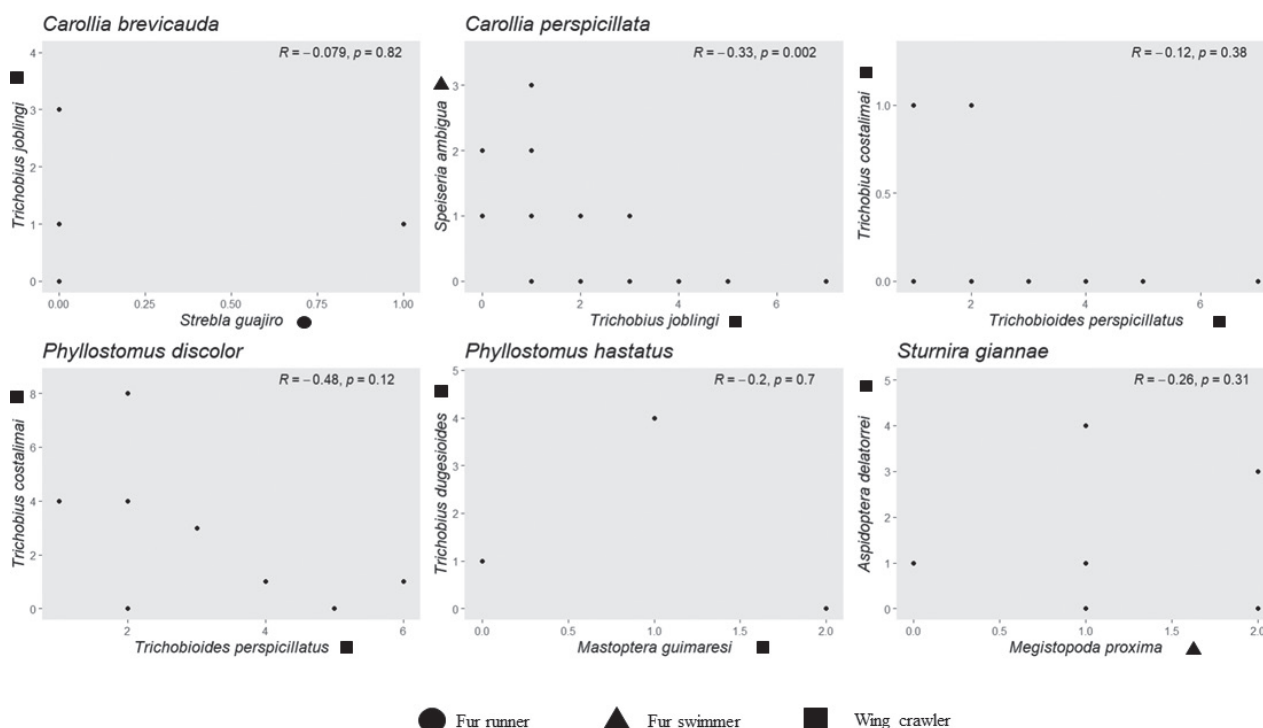


Figure 3. Modularity network generates in the bipartite bat-bat fly network in the inter-Andean Magdalena River basin of Colombia. The intensity of the blue box colors indicates the strength (intensity or frequency) of the interaction, due to the number of fly individuals involved.

We identified infracommunities associated with six bat species within Phyllostomidae: *A. aequatorialis*, *C. brevicauda*, *C. perspicillata*, *P. discolor*, *P. hastatus*, and *S. giannae* (Table 4). However, co-occurrence analyses of bat-fly species could be conducted for only five bat species (Table 4) due to the limited sample size of *A. aequatorialis*. The interaction between *T. joblingi* and *S. ambigua* on *C. perspicillata* showed negative interactions ( $z = -2.867, -0.311$ ,  $p\text{-value} < 0.05$ ), while the remaining five pairs showed positive or null density correlations (Table 4; Fig. 4). Notably, *Carollia perspicillata* was parasitized by two species of bat flies belonging to two different ecomorphological groups: wing crawlers and fur runners (Fig. 5).

**Table 4.** Co-occurrence analyses (Kendall correlation) of bat fly species on their specific host bat species. Bold p-value indicates statistical significance ( $p < 0.05$ ).

Infracommunity	n	z-value	tau	p-value
<b><i>Carollia brevicauda</i></b>	23			
<i>Strebla guajiro</i> + <i>Trichobius joblingi</i>	1	-1.574	-0.537	0.12
<b><i>Carollia perspicillata</i></b>	115			
<i>Speiseria ambigua</i> + <i>T. joblingi</i>	25	-2.867	-0.311	<b>0.002</b>
<i>S. hertigi</i> + <i>T. joblingi</i>	3	-0.872	-0.122	0.382
<b><i>Phyllostomus discolor</i></b>	9			
<i>Trichobius costalimai</i> + <i>Trichobioides perspicillatus</i>	6	-1.562	-0.48	0.118
<b><i>Phyllostomus hastatus</i></b>	9			
<i>Mastoptera guimaresi</i> + <i>Trichobius dugesioides</i>	1	-0.382	-0.2	0.702
<b><i>Sturnira giannae</i></b>	11			
<i>Aspidoptera delatorrei</i> + <i>Megistopoda proxima</i>	2	-1.022	-0.259	0.306



**Figure 4.** Scatterplots of densities for all bat fly species pairs occurring on their respective host bat species along the inter-Andean Magdalena River basin of Colombia.



**Figure 5.** *Carollia perspicillata* parasitized by two species of bat flies belonging to two different ecomorphological groups *Trichobius joblingi* (wing crawler) and *Speiseria ambigua* (fur runner). Photograph: Carlos González Salazar.

## Discussion

This study extends knowledge of bat flies interactions in the Magdalena River basin and in Colombia, as we included the largest number of species of both bats (42 spp.) and bat flies (35 spp.) in the inter-Andean valleys of the country. The families Phyllostomidae (Chiroptera) and Streblidae (Diptera) were the most diverse, which was expected due to the positive correlation with capture methods (mist nets) in Neotropical regions (Dick and Gettinger 2005; Patterson et al. 2008). In contrast, bat flies within Nycteribiidae are rarely represented due to the low number of captures of their host bat families such as Vespertilionidae. In this context, the diversity of Nycteribiidae is underestimated and represents a gap to be filled in the future. Similarly, the presence of nycteribiids in other poorly represented bat families such as Emballonuridae and Molossidae should be assessed. These families have low capture rates with mist nets due to their elusive behavior and foraging activity between and above the forest canopy (Bonaccorso 1979; Muñoz Arango 2001; Gardner 2008; Tarquino-Carbonell et al. 2015). New records or associations are therefore expected. For example, of the 35 species of bat flies recorded in the Magdalena River basin, *Basilia juquiensis* associated with the bat *Myotis riparius* from Samaná, Caldas (Fig. 2) is a new record for Colombia. This fly was previously known only from Brazil and Venezuela, associated with *Myotis nigricans* and *M. riparius* (Graciolli 2004).

Our results indicate a predominance of certain bat fly species, such as *Trichobius joblingi*, which is the most common ectoparasite of bats in the Magdalena River basin. This dominance is largely attributed to its close association

with bats of the genus *Carollia*, particularly *C. perspicillata* which is considered its main host (Wenzel et al. 1966; Fritz 1983). Given the high abundance of *C. perspicillata* in the study area, the prevalence of *T. joblingi* was anticipated. Associations with other bat species are likely, in some cases, accidental (Wenzel 1976; Komeno and Linhares 1999; Barbier and Graciolli 2016).

The Magdalena River basin is experiencing high levels of deforestation due to intense human activity, which has significantly altered the original landscape (Restrepo and Syvitski 2006). Consequently, the elevated prevalence of bat flies in this region may correlate with the intensity of landscape transformation. While this study focused on a specific region, the prevalence of bat fly observed aligns with findings from studies conducted in urban areas of the tropical region (Zarazúa-Carbajal et al. 2016; Hernández-Martínez et al. 2018; Urbietta et al. 2021). In these urban areas, the responses of bat ectoparasites to habitat loss and fragmentation tend to be host- and parasite-specific (Pilosof et al. 2012; Bolívar-Cimé et al. 2018; Hiller et al. 2020, 2021; Eriksson et al. 2023). For instance, Mello et al. (2023) found that certain bat fly species, including *Megistopoda proxima*, *Strebla guajiro*, and *Trichobius joblingi* are more prevalent in deforested areas. Generally, disturbed and fragmented sites lead to a reduction in the availability of high-quality roosts, which can result in the overcrowding of bats and the formation of multi-species colonies (Brändel et al. 2020; Kelm et al. 2021). Under such conditions, ectoparasites may switch primary hosts, resulting in a loss of specialization in their interactions and facilitating horizontal transfer (Lewis 1995; Dick and Patterson 2006; Patterson et al. 2006 Garbino and Tavares 2018; Saldaña-Vázquez et al. 2019).

Additionally, our results indicate medium modularity in the interactions between bats and bat flies, which correlates with medium specialization and low connectivity (Blüthgen et al. 2006; Durán et al. 2018). The identified subgroups reflect the niche differentiation of bat flies among their hosts (Blüthgen et al. 2006). Most modules are formed by the phylogenetic preference of different bat fly species for specific bat species. For instance, we observed that species of the genus *Anoura* (*Anoura aequatoris*, *A. caudifer*, *A. geoffroyi*, *A. latidens*, and *Anoura* sp.) were parasitized by *Anastrebla caudifera* and *Exastinion decepticum* (Fig. 3). It is likely that the parasites select phylogenetically related hosts due to their phenotypic similarities (Wiens et al. 2010; Lima et al. 2012). The close evolutionary relationship between bat flies and bats, with the phenotypic similarities among phylogenetically related bats, may serve as a filter for parasite species (Dick and Patterson 2006; Wiens et al. 2010; Urbietta et al. 2021).

The infracommunities and parasite associations identified in this study align with previous findings (Fritz 1983; Dick 2005; Bezerra et al. 2016; Dornelles et al. 2017; Bezerra and Bocchiglieri 2018) and may result from ecomorphological differentiation, where unrelated parasites coexist on the same host and spatially segregate within the host's body (Dick 2005). In all documented cases, the infracommunities comprised parasite species from different genera and primarily from different ecomorphological groups (Dick 2005; Hiller et al. 2018). In our findings, all the relationships between pairs of bat fly species were negative, with only one pair exhibiting a significantly negative correlation, interpreted as potential competition for limited resources, between *S. ambigua* and *T. joblingi* on *C. perspicillata*. This suggests that while the presence of one bat fly species does not preclude the presence of another, their abundances are negatively correlated (density compensation) (Wenzel et al. 1966; Dick and Patterson 2006; Presley

2007; Tello et al. 2008). Consequently, negative correlations between pairs of species on the same host may serve as a mechanism to maintain ectoparasite populations within the host's tolerable limit (Komeno and Linhares 1999).

In conclusion, our results indicate that interactions between bats and bat flies may vary based on habitat conservation status, potentially leading to lower specialization in degraded and fragmented landscapes. While our study did not directly assess this relationship, we recommend that future research delve deeper into how habitat conservation influences the specialization of these interactions. Additionally, our results suggest that different species of bat flies can coexist and share the same resource (bats), with their morphological traits likely playing a role in this coexistence. Overall, this study enhances our understanding of bat flies-bats interactions in the Magdalena River basin and expands the known distribution of certain bat fly species within the country.

## Acknowledgements

We thank the Museo de Historia Natural de la Universidad de Caldas, for allowing the use of the MHN-UCa collections facilities. Thanks the program "Relación, distribución, taxonomía de especies de garrapatas asociadas a mamíferos silvestres en zonas endémicas de rickettsiosis en Colombia. Un acercamiento a la comprensión de la relación vectores patógenos-reservorios", granted by the Ministerio de Ciencia, Tecnología e Innovación - Minciencias (Code: 120385270267 and CTO 80740- 200-2021). Mateo Ortiz Giraldo, Julio Chacón Pacheco helped during different parts of this project.

## Additional information

### Conflict of interest

The authors have declared that no competing interests exist.

### Ethical statement

No ethical statement was reported.

### Funding

This work was supported by the program "Relación, distribución, taxonomía de especies de garrapatas asociadas a mamíferos silvestres en zonas endémicas de rickettsiosis en Colombia. Un acercamiento a la comprensión de la relación vectores patógenos-reservorios" (Code: 120385270267), specifically to the project "Mamíferos silvestres y su relación con rickettsias asociadas a garrapatas en dos zonas del Departamento de Cundinamarca: aproximación eco-epidemiológica y genómica" (Code: 71800), granted by the Ministerio De Ciencia, Tecnología e Innovación - Minciencias (CTO 80740- 200-2021).

### Author contributions

CLR and HERC, conceptualization. CL-R, LNRS, ARH, JACV, JACS, JRC, JDV, FARP, PAOL, JJHO, ACG, EMOP, DMMM, MERP, MH, HERC revised the manuscript, contributed critically to the drafts, and approved the final version for publication. CLR, LNRS, ARH, JACS, JDV, JJHO, JRC, ACG, HERC carried out field trips. CLR, EMOP and HERC created and organized the figures of the manuscript. ARH, JACV, FARP, PAOL, MH, HERC, searched for funding of this project.

## Author ORCIDs

Camila López-Rivera  <https://orcid.org/0009-0003-5414-7956>  
Laura Natalia Robayo-Sánchez  <https://orcid.org/0000-0002-4074-1001>  
Alejandro Ramírez-Hernández  <https://orcid.org/0000-0001-8689-5930>  
Jerson Andrés Cuéllar-Saénz  <https://orcid.org/0000-0003-2257-8981>  
Juan Diego Villar  <https://orcid.org/0009-0006-8820-1908>  
Jesús Alfredo Cortés-Vecino  <https://orcid.org/0000-0003-2641-604X>  
Fredy Arvey Rivera-Páez  <https://orcid.org/0000-0001-8048-5818>  
Paula Andrea Ossa-López  <https://orcid.org/0000-0002-9079-4988>  
Erika M. Ospina-Pérez  <https://orcid.org/0000-0001-5784-6216>  
Jose J. Henao-Osorio  <https://orcid.org/0000-0002-8618-8539>  
Alexandra Cardona-Giraldo  <https://orcid.org/0000-0002-7534-994X>  
Javier Racero-Casarrubia  <https://orcid.org/0000-0001-5989-4174>  
Darwin M. Morales-Martinez  <https://orcid.org/0000-0001-5786-4107>  
Marylin Hidalgo  <https://orcid.org/0000-0001-8960-0616>  
Héctor E. Ramírez-Chaves  <https://orcid.org/0000-0002-2454-9482>

## Data availability

All of the data that support the findings of this study are available in the main text or Supplementary Information.

## References

- Ascuntar-Osnas O, Montoya-Bustamante S, González-Chávez B (2020) Records of Streblidae (Diptera: Hippoboscoidea) in a tropical dry forest fragment in Colombia. *Biota Colombiana* 21(1): 16–27. <https://doi.org/10.21068/c2020.v21n01a02>
- Autino AG, Claps GL, Barquez RM (1999) Insectos ectoparásitos de murciélagos de las Yungas de la Argentina. *Acta Zoológica Mexicana* 78(78): 119–169. <https://doi.org/10.21829/azm.1999.78781921>
- Beckett SJ (2016) Improved community detection in weighted bipartite networks. *Royal Society open science* 3(1): 140536. <https://doi.org/10.1098/rsos.140536>
- Barbier E, Gracioli G (2016) Community of bat flies (Streblidae and Nycteribiidae) on bats in the Cerrado of Central-West Brazil: hosts, aggregation, prevalence, infestation intensity, and infracommunities. *Studies on Neotropical Fauna and Environment* 51(3): 176–87. <https://doi.org/10.1080/01650521.2016.1215042>
- Bezerra RHS, Bocchiglieri A (2018) Association of ectoparasites (Diptera and Acari) on bats (Mammalia) in a Restinga habitat in northeastern Brazil. *Parasitology Research* 117(11): 3413–3420. <https://doi.org/10.1007/s00436-018-6034-0>
- Bezerra RHS, Vasconcelos PF, Bocchiglieri A (2016) Ectoparasitas de morcegos (Mamíferos: Chiroptera) em fragmentos de Mata Atlântica no nordeste do Brasil. *Parasitology Research* 10: 3759–3765. <https://doi.org/10.1007/s00436-016-5137-8>
- Blüthgen N (2010) Why network analysis is often disconnected from community ecology: a critique and an ecologist's guide. *Basic and Applied Ecology* 11(3): 185–195. <https://doi.org/10.1016/j.baae.2010.01.001>
- Blüthgen N, Menzel F, Blüthgen N (2006) Measuring specialization in species interaction networks. *BMC ecology* 6(1): 1–12. <https://doi.org/10.1186/1472-6785-6-9>
- Bolívar-Cimé B, Cuxim-Koyoc A, Reyes-Novelo E, Morales-Malacara JB, Laborde J, Flores-Peredo R (2018) Habitat fragmentation and the prevalence of parasites

- (Diptera, Streblidae) on three Phyllostomid bat species. *Biotropica* 50(1): 90–97. <https://doi.org/10.1111/btp.12489>
- Bonaccorso F (1979) Foraging and reproductive ecology in a Panamanian bat community. *Bulletin of the Florida Museum of Natural History* 24(4): 359–408. <https://doi.org/10.58782/flmnh.dobh1085>
- Brändel SD, Hiller T, Halczok TK, Kerth G, Page RA, Tschapka M (2020) Consequences of fragmentation for Neotropical bats: The importance of the matrix. *Biological Conservation* 252: 108792. <https://doi.org/10.1016/j.biocon.2020.108792>
- Calonge-Camargo B, Pérez-Torres J (2018) Ectoparasites (Polyctenidae, Streblidae, Nycteribiidae) of bats (Mammalia: Chiroptera) from the Caribbean region of Colombia. *Therya* 9(2): 171–178. <https://doi.org/10.12933/therya-18-492>
- Carstensen DW, Sabatino M, Morellato LPC (2016) Modularity, pollination systems, and interaction turnover in plant-pollinator networks across space. *Ecology* 97(5): 1298–1306. <https://doi.org/10.1890/15-0830.1>
- Delgado-Jaramillo M, García FJ, Machado M (2016) Diversidad de murciélagos (Mammalia: Chiroptera) en las áreas de protección estricta de Venezuela. *Ecotrópicos* 29(1–2): 28–42.
- Díaz MM, Solari S, Gregorin R, Aguirre L F, Barquez RM (2021) Clave de identificación de los murciélagos neotropicales / Chave de identificação dos morcegos neotropicais. *Publicación especial No. 4*, 124 pp.
- Dick CW (2005) Ecology and host specificity of Neotropical bat flies (Diptera: Streblidae) and their chiropteran hosts. Unpublished. Ph.D Dissertation. Texas Tech University, Lubbock, TX, USA.
- Dick CW (2007) High host specificity of obligate ectoparasites. *Ecological Entomology* 32(5): 446–450. <https://doi.org/10.1111/j.1365-2311.2007.00836.x>
- Dick CW, Dittmar K (2014) Parasitic Bat Flies (Diptera: Streblidae and Nycteribiidae): Host Specificity and Potential as Vectors. In: Klimpel S, Mehlhorn H (Eds) *Bats (Chiroptera) as Vectors of Diseases and Parasites. Parasitology Research Monographs*, vol 5. Springer, Berlin, Heidelberg, 131–155. [https://doi.org/10.1007/978-3-642-39333-4\\_6](https://doi.org/10.1007/978-3-642-39333-4_6)
- Dick CW, Gettinger D (2005) A faunal survey of streblid flies (Diptera: Streblidae) associated with bats in Paraguay. *Journal of Parasitology* 91(5): 1015–1024. <https://doi.org/10.1645/GE-536R.1>
- Dick CW, Miller JA (2010) Streblidae (bat flies). In: Brown BV, Borkent A, Cumming JM, Wood DM, Woodley NE and Zumbado M (Eds) *Manual of Central American Diptera*, NRC Research Press, Ottawa 2: 1249–1260.
- Dick CW, Patterson BD (2006) Bat flies: Obligate ectoparasites of bats. In: Morand S, Krasnov BR, Poulin R (Eds) *Micromammals and Macroparasites*. Springer, Tokyo, 179–194. [https://doi.org/10.1007/978-4-431-36025-4\\_11](https://doi.org/10.1007/978-4-431-36025-4_11)
- Dick CW, Graciolli G, Guerrero R (2016) Family Streblidae. *Zootaxa* 4122(1): 784–802. <https://doi.org/10.11646/zootaxa.4122.1.67>
- Dittmar K, Porter ML, Murray S, Whiting MF (2006) Molecular phylogenetic analysis of nycteribiid and streblid bat flies (Diptera: Brachycera, Calypttratae): Implications for host associations and phylogeographic origins. *Molecular phylogenetics and evolution* 38(1): 155–170. <https://doi.org/10.1016/j.ympev.2005.06.008>
- Dittmar K, Morse SF, Dick CW, Patterson BD (2015) Bat fly evolution from the Eocene to the Present (Hippoboscoidea, Streblidae and Nycteribiidae). In Morand S, Krasnov BR and Littlewood DTJ (Eds), *Parasite Diversity and Diversification: Evolutionary Ecology*

- Meets Phylogenetics Cambridge University Press, Cambridge, 246–264. <https://doi.org/10.1017/CBO9781139794749.017>
- Dormann CF, Strauss R (2014) A method for detecting modules in quantitative bipartite networks. *Methods in Ecology and Evolution* 5(1): 90–98. <https://doi.org/10.1111/2041-210X.12139>
- Dormann CF, Gruber B, Fründ J (2008) Introducing the bipartite package: analysing ecological networks. *Interaction* 1(0.2413793): 8–11.
- Dormann CF, Fründ J, Blüthgen N, Gruber B (2009) Indices, graphs and null models: analyzing bipartite ecological networks. *The Open Ecology Journal* 2(1): 7–24. <https://doi.org/10.2174/1874213000902010007>
- Dornelles GD, Graciolli G, Odon A, Bordignon MO (2017) Infracommunities of Streblidae and Nycteribiidae (Diptera) on bats in an ecotone area between Cerrado and Atlantic Forest in the state of Mato Grosso do Sul. *Iheringia. Série Zoologia* 107: e2017044. <https://doi.org/10.1590/1678-4766e2017044>
- Durán AA, Saldaña-Vázquez RA, Graciolli G, Peinado LC (2018) Specialization and modularity of a bat fly antagonistic ecological network in a dry tropical forest in northern Colombia. *Acta Chiropterologica* 20(2): 503–510. <https://doi.org/10.3161/15081109ACC2018.20.2.020>
- Eriksson A, Filion A, Labruna MB, Muñoz-Leal S, Poulin R, Fischer E, Graciolli G (2023) Effects of forest loss and fragmentation on bat-ectoparasite interactions. *Parasitology Research* 122: 1391–1402. <https://doi.org/10.1007/s00436-023-07839-x>
- Etter A, McAlpine C, Possingham H (2008) Historical patterns and drivers of landscape change in Colombia since 1500: A regionalized spatial approach. *Annals of the Association American Geographers* 98(1): 2–23. <https://doi.org/10.1080/00045600701733911>
- Fortuna MA, Stouffer DB, Olesen JM, Jordano P, Mouillot D, Krasnov BR, Poulin R, Bascompte J (2010) Nestedness versus modularity in ecological networks: two sides of the same coin? *Journal of Animal Ecology* 79(4): 811–817. <https://doi.org/10.1111/j.1365-2656.2010.01688.x>
- Fritz GN (1983) Biology and ecology of bat flies (Diptera: Streblidae) on bats in the genus *Carollia*. *Journal of Medical Entomology* 20(1): 1–10. <https://doi.org/10.1093/jmedent/20.1.1>
- Gallo-Vélez D, Restrepo JC, Newton A (2023) Assessment of the Magdalena River delta socio-ecological system through the Circles of Coastal Sustainability framework. *Frontiers in Earth Sciences* 11: 1058122. <https://doi.org/10.3389/feart.2023.1058122>
- Garbino GS, Tavares VC (2018) Roosting ecology of Stenodermatinae bats (Phyllostomidae): evolution of foliage roosting and correlated phenotypes. *Mammal Review* 48(2): 75–89. <https://doi.org/10.1111/mam.12114>
- Garbino GST, Gregorin R, Lima IP, Loureiro L, Moras L, Moratelli R, Nogueira MR, Pavan AC, Tavares VC, Nascimento MC, Novaes RLM, Peracchi AL (2022) Updated checklist of Brazilian bats: versão 2020. Comitê da Lista de Morcegos do Brasil—CLMB. Sociedade Brasileira para o Estudo de Quirópteros.
- Gardner AL (Ed.) (2008) *Mammals of South America, Volume 1: Marsupials, Xenarthrans, Shrews, and Bats (Vol. 1)*. University of Chicago Press, Chicago, 669 pp. <https://doi.org/10.7208/chicago/9780226282428.001.0001>
- Graciolli G (2004) Nycteribiidae (Diptera, Hippoboscoidea) no Sul do Brasil. *Revista Brasileira de Zoologia* 21(4): 971–985. <https://doi.org/10.1590/S0101-81752004000400035>

- Gracioli G (2018) Streblidae in Catálogo Taxonômico da Fauna do Brasil. PNUD. <http://fauna.jbrj.gov.br/fauna/faunadobrasil/2624> [accessed October 2023]
- Gracioli G, Dick CW, Guerrero R (2016) Family Nycteribiidae. *Zootaxa* 4122 (1): 780–783. <https://doi.org/10.11646/zootaxa.4122.1.66>
- Grilli J, Rogers T, Allesina S (2016) Modularity and stability in ecological communities. *Nature Communications* 7: 12031. <https://doi.org/10.1038/ncomms12031>
- Guerrero R (1994) Catálogo de los Streblidae (Diptera: Pupipara) parásitos de murciélagos (Mammalia: Chiroptera) del Nuevo Mundo. I Clave para los géneros y Nycterophiliinae. *Acta Biologica Venezuelica* 14(4): 61–75.
- Guerrero R (1995) Catálogo de los Streblidae (Diptera: Pupipara) parásitos de murciélagos (Mammalia: Chiroptera) del Nuevo Mundo. V. Trichobiinae con alas reducidas o ausentes y misceláneos. *Boletín de Entomología Venezolana* 10: 135–160.
- Guerrero R (1998) Notes on Neotropical batflies (Diptera, Streblidae). I. The genus. *Acta Parasitologica* 43(2): 86–93.
- Hernández-Martínez J, Morales-Malacara JB, Alvarez-Añorve MY, Amador-Hernández S, Oyama K, Avila Cabadilla LD (2018) Drivers potentially influencing host–bat fly interactions in anthropogenic neotropical landscapes at different spatial scales. *Parasitology* 146(1): 74–88. <https://doi.org/10.1017/S0031182018000732>
- Herrera-Sepúlveda MT (2013) Comparación de la carga de ectoparásitos entre harenes y grupos mixtos de la población de *Carollia perspicillata* en la cueva Macaregua (Santander, Colombia). Facultad de Ciencias. Pontificia Universidad Javeriana, Bogotá, 45 pp.
- Hiller T, Honner B, Page RA, Tschapka M (2018) Leg structure explains host site preference in bat flies (Diptera: Streblidae) parasitizing neotropical bats (Chiroptera: Phyllostomidae). *Parasitology* 145(11): 1475–1482. <https://doi.org/10.1017/S0031182018000318>
- Hiller T, Brändel, SD, Honner B, Page RA, Tschapka M (2020) Parasitization of bats by bat flies (Streblidae) in fragmented habitats. *Biotropica* 52(3): 488–501. <https://doi.org/10.1111/btp.12757>
- Hiller T, Vollstädt MG, Brändel SD, Page RA, Tschapka M (2021) Bat–bat fly interactions in Central Panama: host traits relate to modularity in a highly specialised network. *Insect Conservation and Diversity* 14(5): 686–699. <https://doi.org/10.1111/icad.12508>
- Holdridge LR (1978) *Ecología basada en zonas de vida* (No. 83). Agroamérica, San José.
- Hutson AM, Mickleburgh SP, Racey PA (comp.) (2001) *Microchiropteran bats: global status survey and conservation action plan*. IUCN/SSC Chiroptera Specialist Group. IUCN, Gland, Switzerland and Cambridge, UK, x + 258 pp. <https://doi.org/10.2305/IUCN.CH.2001.SSC-AP.1.en>
- IAvH (2021) Instituto de Investigación de Recursos Biológicos Alexander von Humboldt, Agencia Nacional de Hidrocarburos. Línea base general de mamíferos para el valle medio del Magdalena - VMM. v1.3. Instituto de Investigación de Recursos Biológicos Alexander von Humboldt. Dataset/Samplingevent. <https://doi.org/10.15472/mbw96>
- IDEAM (2001) *Estudio Ambiental de la Cuenca Magdalena-Cauca y elementos para su ordenamiento territorial*. Reporte técnico y base de datos de Arcinfo, Bogotá, Colombia, Instituto de Hidrología, Meteorología y Estudios Ambientales (IDEAM), 984 pp.
- Kelm DH, Toelch U, Jones MM (2021) Mixed-species groups in bats: non-random roost associations and roost selection in neotropical understory bats. *Frontiers in Zoology* 18: 1–12. <https://doi.org/10.1186/s12983-021-00437-6>

- Komeno CA, Linhares AX (1999) Batflies parasitic on some phyllostomid bats in Southeastern Brazil: parasitism rates and host-parasite relationships. *Memórias do Instituto Oswaldo Cruz* 94: 151–156. <https://doi.org/10.1590/S0074-02761999000200004>
- Laurenço EC, Almeida JC, Famadas KM (2016) Richness of ectoparasitic flies (Diptera: Streblidae) of bats (Chiroptera)—a systematic review and meta-analysis of studies in Brazil. *Parasitology Research* 115: 4379–4388. <https://doi.org/10.1007/s00436-016-5223-y>
- León GE, Zea JA, Eslava JA (2000) Circulación general del Trópico y la zona de confluencia intertropical en Colombia”. *Meteorología Colombiana* 1: 31–38.
- Lewis SE (1995) Roost fidelity of bats: a review. *Journal of Mammalogy* 76(2): 481–496. <https://doi.org/10.2307/1382357>
- Liévano-Romero KS, Rodríguez-Posada ME, Cortés-Vecino JA (2019) Nuevos registros de ectoparásitos de murciélagos en sabanas inundables de la Orinoquía colombiana. *Mastozoología neotropical* 26(2): 377–389. <https://doi.org/10.31687/saremMN.19.26.2.0.13>
- Lima Jr DP, Giacomini HC, Takemoto RM, Agostinho AA, Bini LM (2012) Patterns of interactions of a large fish-parasite network in a tropical floodplain. *Journal of Animal Ecology* 81(4): 905–13. <https://doi.org/10.1111/j.1365-2656.2012.01967.x>
- Lindeman RL (1942) The trophic-dynamic aspect of ecology. *Ecology* 23(4): 399–417. <https://doi.org/10.2307/1930126>
- López Rivera C, Flórez Padilla JM, Méndez Urbano F, Ospina-Pérez EM, Velásquez-Guarín D, Mejía-Fontecha IY, Ossa-López PA, Rivera-Páez FA, Ramírez-Chaves HE (2022) Interaction networks between bats (Mammalia: Chiroptera) and ectoparasitic flies (Diptera: Hippoboscoidea): a specificity relationship in the Colombian Orinoquia region. *Acta Chiropterologica* 24(2): 379–394. <https://doi.org/10.3161/150811094CC2022.24.2.008>
- Mammal Diversity Database (2023) Mammal Diversity Database (Version 1.12.1) [Data set]. Zenodo. <https://doi.org/10.5281/zenodo.10595931> [accessed October 2023]
- Marinkelle C, Grose ES (1981) A list of ectoparasites of Colombian bats. *Revista de Biología Tropical* 29(1): 11–20.
- Marshall AG (1982) Ecology of Insects Ectoparasitic on Bats. In: Kunz TH (Eds) *Ecology of Bats*. Springer, Boston, MA, 369–401. [https://doi.org/10.1007/978-1-4613-3421-7\\_10](https://doi.org/10.1007/978-1-4613-3421-7_10)
- Mello RM, Muylaert R, Pereira R, Felix G (2016) *Guia para análise de redes ecológicas*, 1 edição. Belo Horizonte, city, 112 pp.
- Mello RM, Laurindo RS, Silva LC, Pyles MV, Bernardi LFO, Mancini MCS, Dáttilo W, Gregorin R (2023) Configuration and composition of human-dominated tropical landscapes affect the prevalence and average intensity of mite and fly infestation in Phyllostomidae bats. *Parasitology Research* 122: 127–37 <https://doi.org/10.1007/s00436-022-07704-3>
- Muñoz Arango, J (2001) Los murciélagos colombianos sistemática, distribución, descripción, historia natural y ecología. *Universidad de Antioquia* 17: 391. <http://catalogo.humboldt.org.co/cgi-bin/koha/opac-detail.pl?biblionumber=2601>
- Nardini A, Yopez S, Zuniga L, Gualtieri C, Bejarano MD (2020) A Computer Aided Approach for River Styles—Inspired Characterization of Large Basins: The Magdalena River (Colombia). *Water* 12(4): 1147. <https://doi.org/10.3390/w12041147>
- Ospina-Pérez EM, Rivera-Páez FA, Ramírez-Chaves HE (2023) Exploring the relationship between bats (Mammalia, Chiroptera) and ectoparasitic flies (Diptera, Hippoboscoidea) of the Orinoquia Region in South America. *ZooKeys* 1179: 1–34. <https://doi.org/10.3897/zookeys.1179.103479>
- Pastrana-Montiel MR, Ballesteros-Correa J, Chacón-Pacheco J (2019) First record of the parasite bat fly *Basilisa mimoni* Theodor & Peterson, 1964 (Diptera: Nycteribiidae)

- in Colombia. *Oecologia Australis* 23(3): 685–689. <https://doi.org/10.4257/oeco.2019.2303.27>
- Patterson BD, Dick CW, Dittmar K (2006) Roosting habits of bats affect their parasitism by bat flies (Diptera: Streblidae). *Journal of Tropical Ecology* 23(2): 177–189. <https://doi.org/10.1017/S0266467406003816>
- Patterson BD, Dick CW, Dittmar K (2008) Parasitism by bat flies (Diptera: Streblidae) on Neotropical bats: effects of host body size, distribution, and abundance. *Parasitology Research* 103: 1091–1100. <https://doi.org/10.1007/s00436-008-1097-y>
- Pilosof S, Dick CW, Korine C, Patterson BD, Krasnov BR (2012) Effects of anthropogenic disturbance and climate on patterns of bat fly parasitism. *PLoS ONE* 7(7): e41487. <https://doi.org/10.1371/journal.pone.0041487>
- Pilosof S, Porter MA, Pascual M, Kéfi S (2017) The multilayer nature of ecological networks. *Nature Ecology and Evolution* 1(4): 0101. <https://doi.org/10.1038/s41559-017-0101>
- Poinar G, Brown A (2012) The first fossil streblid bat fly, *Enischomyia stegosoma* ng, n. sp. (Diptera: Hippoboscoidea: Streblidae). *Systematic parasitology* 81(2): 79–86. <https://doi.org/10.1007/s11230-011-9339-2>
- Presley SJ (2007) Streblid bat fly assemblage structure on Paraguayan *Noctilio leporinus* (Chiroptera: Noctilionidae): nestedness and species co-occurrence. *Journal of Tropical Ecology* 23(4): 409–417. <https://doi.org/10.1017/S0266467407004245>
- R Core Team (2022) R: A Language and Environment for Statistical Computing. R Foundation for Statistical Computing. <https://www.R-project.org> [accessed October 2023]
- Raigosa-Álvarez J, García-Osorio C, Autino AG, Gomes-Dias L (2020) First records of ectoparasitic insects (Diptera: Hippoboscoidea) of bats in the department of Caldas, Colombia. *Papéis Avulsos de Zoologia*, 60 pp. <https://doi.org/10.11606/1807-0205/2020.60.18>
- Ramírez-Chaves HE, Morales-Martínez DM, Rodríguez-Posada ME, Suárez-Castro AF (2021). Checklist of the mammals (Mammalia) of Colombia: Taxonomic changes in a highly diverse country. *Mammalogy Notes* 7(2): 253. <https://doi.org/10.47603/mano.v7n2.253>
- Restrepo JD, Syvitski JP (2006) Assessing the effect of natural controls and land use change on sediment yield in a major Andean River: the Magdalena drainage basin, Colombia. *Ambio: a Journal of the Human Environment* 35(2): 65–74. [https://doi.org/10.1579/0044-7447\(2006\)35\[65:ATEONC\]2.0.CO;2](https://doi.org/10.1579/0044-7447(2006)35[65:ATEONC]2.0.CO;2)
- Saldaña-Vázquez RA, Sandoval-Ruiz CA, Veloz-Maldonado OS, Durán AA, Ramírez-Martínez MM (2019) Host ecology moderates the specialization of Neotropical bat-fly interaction networks. *Parasitology Research* 118: 2919–2924. <https://doi.org/10.1007/s00436-019-06452-1>
- Swann J, Jamshidi N, Lewis NE, Winzeler EA (2015) Systems analysis of host-parasite interactions. *Wiley Interdisciplinary Reviews Systems Biology and Medicine* 7(6): 381–400. <https://doi.org/10.1002/wsbm.1311>
- Tamsitt JR, Fox I (1970) Records of bat ectoparasites from the Caribbean region (Siphonaptera, Acarina, Diptera). *Canadian Journal Zoology* 48: 1093–1097. <https://doi.org/10.1139/z70-193>
- Tarquino-Carbonell A, Gutiérrez-Díaz KA, Galindo-Espinosa EY, Reinoso-Flórez G, Solari S, Guerrero R (2015) Ectoparasites associated with bats in northeastern Tolima, Colombia. *Mastozoología Neotropical* 22(2): 349–358. <https://doi.org/10.11606/1807-0205/2020.60.18>
- Tello SJ, Stevens RD, Dick CW (2008) Patterns of species co-occurrence and density compensation: a test for interspecific competition in bat ectoparasite infracommunities. *Oikos* 117: 693–702. <https://doi.org/10.1111/j.0030-1299.2008.16212.x>

- ter Hofstede HM, Fenton MB (2005) Relationships between roost preferences, ectoparasite density, and grooming behaviour of neotropical bats. *Journal of Zoology* 266(4): 333–340. <https://doi.org/10.1017/S095283690500693X>
- ter Hofstede HM, Fenton MB, Whitaker JO Jr (2004) Host and host-site specificity of bat flies (Diptera: Streblidae and Nycteribiidae) on Neotropical bats (Chiroptera). *Canadian Journal Zoological* 82(2): 616–626. <https://doi.org/10.1139/z04-030>
- Urbieto GL, Gracioli G, Vizentin-Bugoni J (2021) Modularity and specialization in bat-fly interaction networks are remarkably consistent across patches within urbanized landscapes and spatial scales. *Current Zoology* 67(4): 403–410. <https://doi.org/10.1093/cz/zoaa072>
- Wenzel RL (1976) The streblid batflies of Venezuela (Diptera: Streblidae). *Brigham Young University Science Bulletin, Biological Series* 20(4): 1. <https://doi.org/10.5962/bhl.part.5666>
- Wenzel RL, Tipton VJ, Kiewlicz A (1966) The streblid batflies of Panama (Diptera: Callypterae: Streblidae). In: Wenzel RL, Tipton VJ (Eds) *Ectoparasites of Panama*. Chicago, USA: Field Museum 405–675. <https://doi.org/10.5962/bhl.title.2633>
- Wiens JJ, Ackerly DD, Allen AP, Anacker BL, Buckley LB, Cornell HV, Damschen EI, Jonathan Davies TJ, Grytnes JA, Harrison SP, Hawkins BA, Holt RD, McCain CM, Stephens PR (2010) Niche conservatism as an emerging principle in ecology and conservation biology. *Ecology Letters* 13(10): 1310–1324. <https://doi.org/10.1111/j.1461-0248.2010.01515.x>
- Wolff M, Cogollo-Arias JA, Cardona-Duque J, Henao-Sepulveda C, Solari S (2023) New records of *Basilina miranda-ribeiro*, 1903 (Diptera: Hippoboscoidea: Nycteribiidae) from Colombia. *Arquivos de Zoologia* 54(2): 15–19. <https://doi.org/10.11606/2176-7793/2023.54.02>
- Zapata-Mesa N, Montoya-Bustamante S, Hoyos J, Peña D, Galindo-González J, Chacón-Pacheco JJ, Ballesteros-Correa J, Pastrana-Montiel MR, Gracioli G, Nogueira MR, Mello MAR (2024) “BatFly: A Database of Neotropical Bat–Fly Interactions.” *Ecology* 105(3): e4249. <https://doi.org/10.1002/ecy.4249>
- Zarazúa-Carbajal M, Saldaña-Vázquez RA, Sandoval-Ruiz CA, Stoner KE, Benitez-Malvido J (2016) The specificity of host-bat fly interaction networks across vegetation and seasonal variation. *Parasitology Research* 115: 4037–4044. <https://doi.org/10.1007/s00436-016-5176-1>

## Supplementary material 1

### Interaction network between bats and bat-flies in the Magdalena River basin region and null models

Authors: Camila López-Rivera, Laura Natalia Robayo-Sánchez, Alejandro Ramírez-Hernández, Jerson Andrés Cuéllar-Saénz, Juan Diego Villar, Jesús Alfredo Cortés-Vecino, Fredy A. Rivera-Páez, Paula Andrea Ossa-López, Erika M. Ospina-Pérez, Jose J. Henao-Osorio, Alexandra Cardona-Giraldo, Javier Racero-Casarrubia, Miguel E. Rodríguez-Posada, Darwin M. Morales-Martinez, Marylin Hidalgo, Héctor E. Ramírez-Chaves

Data type: docx

Copyright notice: This dataset is made available under the Open Database License (<http://opendatacommons.org/licenses/odbl/1.0/>). The Open Database License (ODbL) is a license agreement intended to allow users to freely share, modify, and use this Dataset while maintaining this same freedom for others, provided that the original source and author(s) are credited.

Link: <https://doi.org/10.3897/zookeys.1221.127890.suppl1>

# Autonomous Reef Monitoring Structures (ARMS) as a tool to uncover neglected marine biodiversity: two new Solenogastres (Mollusca, Aplacophora) from the Gulf of Mexico

M. Carmen Cobo<sup>1</sup>, William J. Farris<sup>2</sup>, Chandler J. Olson<sup>2</sup>, Emily L. McLaughlin<sup>2</sup>, Kevin M. Kocot<sup>2,3</sup>

<sup>1</sup> Department of Invertebrate Zoology, Smithsonian Institution, National Museum of Natural History, Washington, District of Columbia, USA

<sup>2</sup> Department of Biological Sciences, University of Alabama, Tuscaloosa, Alabama, USA

<sup>3</sup> Alabama Museum of Natural History, University of Alabama, Tuscaloosa, Alabama, USA

Corresponding authors: M. Carmen Cobo ([CoboC@si.edu](mailto:CoboC@si.edu)); William J. Farris ([wjfarris1@ua.edu](mailto:wjfarris1@ua.edu))

## Abstract

Solenogastres is a group of mollusks with evolutionary and ecological importance. Nevertheless, their diversity is underestimated and knowledge about the distribution of the approximately 300 formally described species is limited. Factors that contribute to this include their small size and frequent misidentification by non-specialists. Recent deep-sea explorations have resulted in the collection of numerous specimens through effective methods such as epibenthic sledges. However, this is a costly, labor-intensive, and destructive methodology. In contrast, Autonomous Reef Monitoring Structures (ARMS) offer a novel, non-destructive approach, by providing a substrate for benthic organism colonization. This study is the first to describe Solenogastres collected using ARMS, demonstrating that they are an effective tool for biodiversity assessment and characterizing rare marine invertebrates. Following an integrative taxonomic approach, two new solenogaster species are described: *Dondersia tweedtae* Farris, Olson & Kocot, **sp. nov.** (Dondersiidae) and *Eleutheromenia bullescens* Cobo, **sp. nov.** (Pruvotiniidae). The diagnosis of the family Dondersiidae is amended and the necessity of reassessing the validity of the current diagnostic characters for Pruvotiniidae, and its classification is emphasized. The two newly described species exhibit distinct external characteristics; *D. tweedtae* **sp. nov.** has a striking pink color with a bright yellow dorsal keel and *E. bullescens* **sp. nov.** has a unique, discontinuous dorsal keel with nearly spherical protrusions. The presence of cnidocytes in the digestive systems of both species indicate that they feed on cnidarians. It is hypothesized that, like in some nudibranchs, their coloration and body features reflect defensive adaptations related to their diet. This study shows that while habitus alone is typically insufficient for accurate identification in solenogastres, it can sometimes simplify the process. For this, live observations and photographs are essential.

**Key words:** Aculifera, biodiversity, conservation, Dondersiidae, mesophotic, Pruvotiniidae, sampling methods, taxonomy



Academic editor: Andrew Davinack

Received: 4 September 2024

Accepted: 31 October 2024

Published: 31 December 2024

ZooBank: <https://zoobank.org/C48FCB58-0A35-4D73-9EA1-D9943395ED0B>

Citation: Cobo MC, Farris WJ, Olson CJ, McLaughlin EL, Kocot KM (2024) Autonomous Reef Monitoring Structures (ARMS) as a tool to uncover neglected marine biodiversity: two new Solenogastres (Mollusca, Aplacophora) from the Gulf of Mexico. ZooKeys 1221: 401–434. <https://doi.org/10.3897/zookeys.1221.136385>

Copyright: This is an open access article distributed under the terms of the CC0 Public Domain Dedication.

## Introduction

Solenogastres represents an intriguing group within the phylum Mollusca due to their unique characteristics (worm-shaped body, absence of a shell, reduced foot and mantle cavity) that led to their consideration as early-branching mollusks, and thus important to understanding evolutionary relationships within the phylum (e.g., Salvini-Plawen 1967, 1980, 2003a; Scheltema 1978, 1993, 1996; Sigwart and Sutton 2007; Haszprunar et al. 2008; Kocot et al. 2011; Vinther et al. 2012; Scherholz et al. 2013; Salvini-Plawen and Steiner 2014; Vinther 2014; Yap-Chiongco et al. 2024). The most recent phylogenetic studies supported the placement of Solenogastres with Caudofoveata in a clade (Aplacophora) that with Polyplacophora (chitons) is the sister taxon of all other mollusks (Kocot et al. 2019). Solenogastres exhibit a remarkable ecological versatility, with species described from all latitudes and depths and found in diverse marine habitats: interstitial (e.g., Salvini-Plawen 1986; García-Álvarez et al. 2000; Bergmeier et al. 2016), hydrothermal vents (e.g., Salvini-Plawen 2008; Scheltema 2008), abyssal plains (e.g., Scheltema 1999; Gil-Mansilla et al. 2009; Bergmeier et al. 2017, 2019; Cobo and Kocot 2021) and even the hadal zone (Bergmeier et al. 2019). Some species burrow in the first centimeters of the sediment, while many are epibenthic or epizootic on hydrozoans and corals, and one species was even discovered inside a glass sponge in the Southern Ocean (Kocot et al. 2019). Observations of live specimens are limited, although some classic works (e.g., Pruvot 1890; Heath 1911; Salvini-Plawen 1978) include live observations as well as habitat information, and one work (Scheltema and Jebb 1994) reports on observations of specimens kept alive in an aquarium for several weeks. Nevertheless, most of the life history knowledge of Solenogastres has been inferred through indirect observations of prey remains in the digestive system (mostly cnidarians) and more recently due to contaminated sequences (Okusu and Giribet 2003; Meyer et al. 2010). Bergmeier et al. (2021) exploited resistance of the solenogaster 28S gene to routine PCR amplification to sequence gut contents from species broadly spanning the diversity of the group and found evidence for a high level of dietary specialization within most taxa in the deep-sea. Despite these advances, many questions remain about solenogaster feeding, reproductive behavior, and defense strategies, while the few existing reports on these topics suggest intricate ecological interactions and evolutionary adaptations.

Despite interest in Solenogastres for both evolutionary and ecological reasons, our understanding remains inadequate, starting with an underestimation of the group's diversity. Just over 300 species have been described to date, but it has been estimated that the true number is tenfold higher (Todt 2013). Likewise, knowledge of species distributions is limited due to sampling bias and many singletons. This lack of knowledge is driven by several factors (reviewed by Todt 2013). Most notably, solenogasters are typically small animals (most measuring  $\leq 5$  mm) and they are often overlooked or misidentified by non-specialists. In recent years, deep-sea exploration has increased the number of collected solenogasters, mostly due to the efficiency of sampling instruments such as epibenthic sledges (EBS). However, EBS sampling demand significant sorting effort, is a destructive sampling technique, and the

preservation of the samples is not always ideal; particularly when the catch is large and must be preserved before sorting. SCUBA diving and remotely operated vehicles (ROVs) are alternative non-destructive methods that, in the case of solenogasters, work well for locating larger specimens and provide live observations and ecological data that would not be possible otherwise. Nevertheless, both are labor-intensive and are unlikely to fully capture the biodiversity of a given site. SCUBA diving is limited by depth and the collection of samples depends on the diver's eyesight or, in the case of bulk collecting (e.g., sampling reef rubble), how much they can carry. ROV sampling is costly and although it provides valuable images and video, the throughput for specimen collection is low. Autonomous Reef Monitoring Structures (ARMS) represent a novel and standardized approach that offers substrate for benthic organism colonization ([www.oceanarms.org](http://www.oceanarms.org)). Originally developed during the 'Census of Marine Life' to conduct biodiversity assessments and monitoring combining morphological identifications with DNA metabarcoding (Obst et al. 2020), ARMS have proven highly effective for collecting coral reef-associated invertebrates (Zimmerman and Martin 2004). In this study we use an integrative taxonomic approach to describe two new species of Solenogastres collected using ARMS in the Gulf of Mexico as part of the CYCLE project (<https://geome-db.org/record/ark:/21547/EBk2>): *Dondersia tweedtae* sp. nov. (Dondersiidae) and *Eleutheromenia bullescens* sp. nov. (Pruvotiniidae, Eleutheromeniinae). With these two species we increase knowledge of the diversity of Solenogastres in the Gulf of Mexico. To date, only two other species from two different families have been described from the region: *Proneomenia acuminata* Wirén, 1892 (Proneomeniidae) and *Spengelomenia bathybia* Heath, 1912 (Amphimeniidae).

## Materials and methods

### Material examined

Three specimens of Solenogastres were collected during the expedition PS21-04 onboard the R/V Point Sur, part of the CYCLE project (<https://geome-db.org/record/ark:/21547/EBk2>), which aims to assess the connectivity and diversity of mesophotic ecosystems in the Gulf of Mexico. The specimens were collected in two different locations (Fig. 1, Table 1). The specimens were found on Autonomous Reef Monitoring Structures (ARMS) deployed in May 2019 during expedition PS19-25 and recovered in August 2021. All specimens were photographed alive and preserved in 95% ethanol.

**Table 1.** Collection data and final preservation for the examined material (H: Holotype; P: Paratype; Lat: Latitude; Long: Longitude. Depth in meters). Specimens deposited at the Smithsonian National Museum of Natural History.

Museum #	Identification	Type series	Expedition code	Locality	Latitude, Longitude	Depth	Final Preservation
USNM 1718003	<i>Dondersia tweedtae</i> sp. nov.	Holotype	CYCLE_2021	Alderdice	28°5'42.18"N, 92°0'20.38"W	82	Serial sections, SEM stub, DNA extraction
USNM 1718004	<i>Eleutheromenia bullescens</i> sp. nov.	Holotype	CYCLE_2021	Diaphus	28°5'20.26"N, 90°42'5.06"W	82	Serial sections, SEM stub, DNA extraction
USNM 1718005	<i>Eleutheromenia bullescens</i> sp. nov.	Paratype	CYCLE_2021	Diaphus	28°5'20.26"N, 90°42'5.06"W	82	95% ethanol

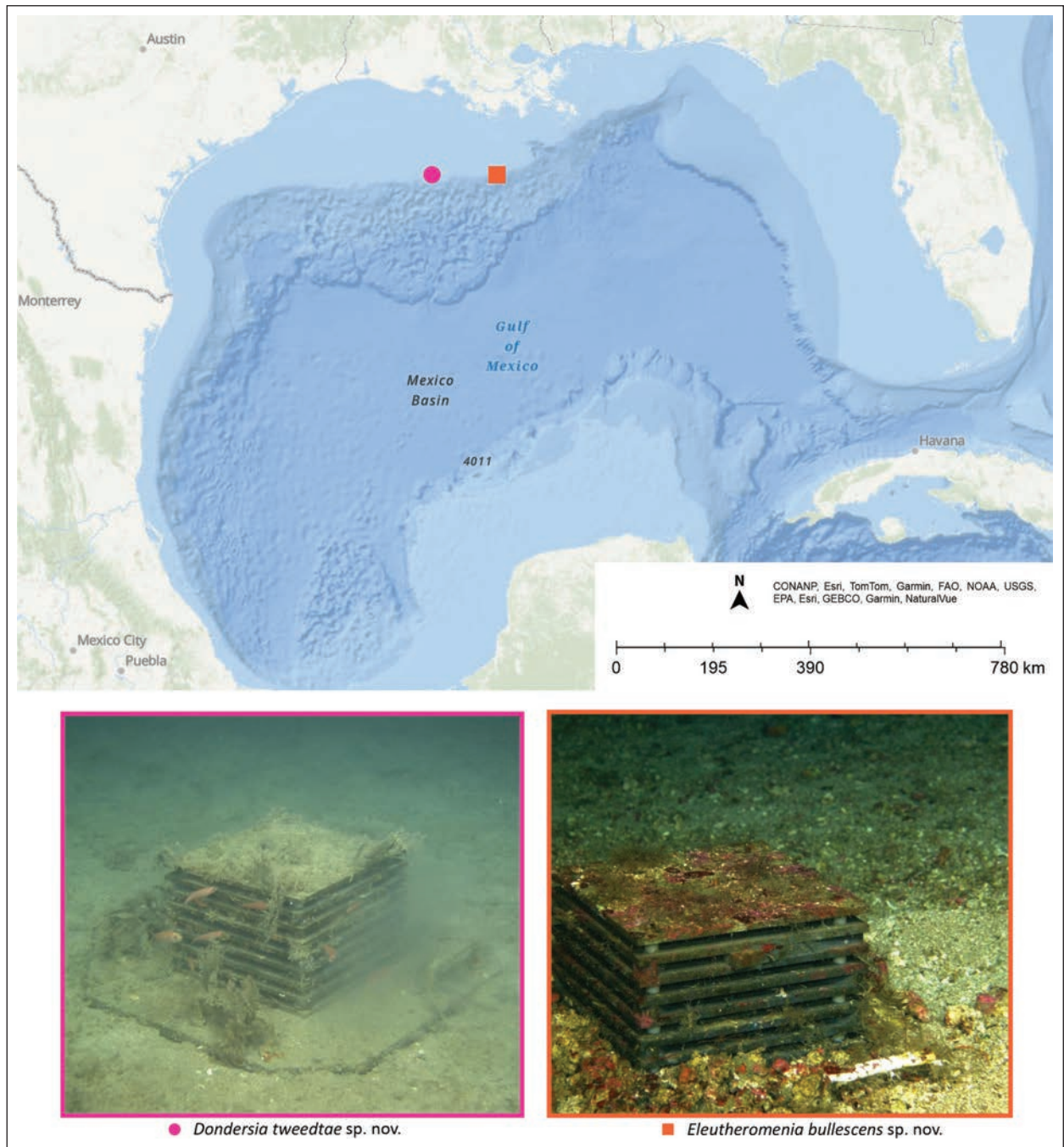


Figure 1. Map with localities where the solenogaster species were found and images of the ARMS.

## Species descriptions

### Habitus and hard parts

Specimens were sorted into two morphospecies based on the study of habitus (coloration, sclerite appearance, body protrusions, body shape). Preserved specimens were observed, photographed using an Olympus SZ40 dissecting microscope with an Olympus DP71 digital camera, and measured. The length of each specimen in lateral view was measured along the axial midline; the dorso-ventral height was also measured in lateral view. In addition, after decalcification (see methodology below) one of the specimens (USNM 1718004)

was photographed using an Olympus DSX100 microscope to observe details of the dorsal body protrusions. Photographs of the fixed material were compared with field photographs for a proper characterization of the external aspect. Two of the specimens (one of each morphospecies) were cut into three parts. The medial body region was air-dried and imaged (uncoated) using a Phenom Pro scanning electron microscope (SEM) under low vacuum with a low accelerating voltage (5–10 kV) to study the sclerites. Subsequently, dried tissue samples were put directly into Omega Bio-tek E.Z.N.A. MicroElute kit tissue lysis (TL) buffer and frozen at -80 °C for later DNA extraction. The anterior and posterior regions were retained in 95% ethanol until they were used for histology.

## Histology

To analyze internal anatomy, the anterior and posterior body regions of two of the specimens (one of each morphospecies; Table 1) were decalcified with EDTA solution (2 ml of distilled water; 1 ml of 10% formalin; and 2 ml of 0.5M EDTA) overnight, dehydrated with a graded ethanol series (20 min for each soak: 70% - 90% - 90% - 95% - 95% - 100% - 100% ethanol) followed by a xylene soak (until the tissue was translucent; ~15 min), embedded in paraffin (Leica Paraplast Regular) following three soaks in fresh paraffin for 1 h each, cut in 5 µm serial transverse sections using a Leica RM2235 rotary microtome and a Reichert-Jung 820 II Histocut Microtome, and stained with Mallory's trichrome stain. The staining protocol followed Gil-Mansilla et al. (2008) except the xylene step was reduced to one soak of < 15 min (just until tissues were translucent), the embedding in paraffin step to two hours instead of three, and the second stain was performed for 20 min. Histological sections of SH20364 were imaged using an Olympus BX53 compound microscope with an SC50 digital camera. Histological sections of SH20192-A and SH20192-B were imaged using an Olympus BX63F compound microscope. A manual reconstruction was made for each species following the structures under the microscope. The manual reconstructions were then digitalized using Corel Draw Standard 2021.

## DNA barcoding and phylogenetic analysis

### DNA barcoding

DNA was extracted from the mid-body tissue used for SEM with the Omega Bio-tek E.Z.N.A. MicroElute kit following the manufacturer's protocol. PCR amplification of a fragment of the mitochondrial 16S rDNA (16S), cytochrome c oxidase subunit I (COI) and cytochrome B (CytB) were performed using Hot Start Taq 2X Master Mix (VWR) following the manufacturer's instructions. For 16S, the solenogaster-specific primers 16Solenor and 16Solenof (Bergmeier et al. 2017) were used with the following cycling parameters: 1 min at 94 °C, (15 s at 94 °C, 30 s at 50 °C, 1 min at 72 °C) × 35 cycles, 7 min 68 °C and finally cooling at 10 °C. For COI, the primers LCO\_Apl (TTTCTACTAAYCATA-ARGATATTGG) and HCO 2198 (Folmer et al. 1994) were used with the following cycling parameters: 1 min at 94 °C, (15 s at 94 °C, 30 s at 52 °C, 1 min at 72 °C) × 30 cycles, 7 min 68 °C and finally cooling at 10 °C. For CytB, the primers 424F and 876R (Boore and Brown 1994) were used with the following cycling

parameters: 1 min at 94 °C, (15 s at 94 °C, 30 s at 47 °C, 1 min at 72 °C) × 40 cycles, 7 min 68 °C and finally cooling at 10 °C. PCR success was determined with gel electrophoresis using 1X SB buffer at 120 volts for 20 min. Products were directly purified either using the Omega Bio-tek E.Z.N.A. Cycle Pure Quick kit or using AMPure SPRI magnetic beads for a one-sided size selection using .95× beads and were eluted in 25 µl of elution buffer. The concentration of the purified PCR products was measured with a Qubit 3.0 Fluorometer using dsDNA HS reagents (Invitrogen). Purified PCR products were sent to GeneWiz for bidirectional Sanger sequencing. Sequencing was performed using the premix option with 10 µl of PCR product and 5 µL of 5 µM primer for each reaction. Successful DNA sequences were assembled into contigs, inspected, and manually edited for quality, if needed, using Geneious Prime 2024. Finally, a BLAST search against the NCBI Nucleotide database was performed to check for any contaminated sequences. All newly generated sequences have been made publicly available via NCBI (Table 2).

**Table 2.** Accession numbers of the sequences used for the phylogenetic analysis (16S and COI) and of the obtained sequences for the new species.

Species	COI	16S	CytB	Reference
<i>Alexandromenia crassa</i> Odhner, 1920	MG855758	MG855855		Mikkelsen et al. 2019
<i>Anamenia gorgonophila</i> (Kowalevsky, 1880)	OQ597876	OQ600030		Cobo et al. 2023
<i>Apodomenia enigmatica</i> Kocot, Todt, Mikkelsen & Halanych, 2019	MK404653	PQ226473		Kocot et al. 2019
<i>Chaetoderma nitidulum</i> Lovén, 1844	AY377726	AY377612		Okusu et al. 2003
<i>Dondersia festiva</i> Hubrecht, 1888	OR458916	OR456222		Cobo et al. 2024
<i>Dondersia tweedtae</i> sp. nov.	PQ246886	PQ249005	PQ241521	Present study
<i>Dorymenia tricarinata</i> (Thiele, 1913)	OQ600547	OQ618431		Todt and Kocot 2014; Cobo et al. 2023
<i>Eleutheromenia bullescens</i> sp. nov.	PQ246885	PQ249006	PQ241520	Present study
<i>Eleutheromenia sierra</i> (Pruvot, 1890)	OR458913	OR456216		Cobo et al. 2024
<i>Epimania babai</i> Salvini-Plawen, 1997	AY377724	AY377616		Okusu et al. 2003
<i>Falcidens sagittiferus</i> Salvini-Plawen, 1968	MG855748	MG855834		Mikkelsen et al., 2019
<i>Gymnomenia pellucida</i> Odhner, 1920	OQ600550	OQ618433		Cobo et al. 2023
<i>Helluherpia aegiri</i> Handl & Büchinger, 1996	PQ222747	PQ226470		Present study
<i>Hypomenia sanjuanensis</i> Kocot & Todt, 2014	OQ600549	OQ618434		Cobo et al. 2023
<i>Kruppomenia genslerae</i> Ostermair et al. 2018	MN531184	MG603271		Bergmeier et al. 2019; Ostermair et al. 2018
<i>Macellomenia schanderi</i> Kocot & Todt, 2014	KJ568516	PQ226471		Kocot et al. 2017
<i>Micromenia fodiens</i> (Schwabl, 1955)	PQ222750	n/a		Kocot et al. 2019
<i>Nematomenia banyulensis</i> (Pruvot, 1890)	OR458911	OR456215		Cobo et al. 2024
<i>Neomenia megatrapezata</i> Salvini-Plawen & Paar-Gausch, 2004	PQ222749	PQ226472		Present study
<i>Proneomenia custodiens</i> Todt & Kocot, 2014	KJ568518	OQ618430		Cobo et al. 2023; Kocot and Todt 2014
<i>Proneomenia sluiteri</i> Hubrecht, 1880	KJ568517	OQ618429		Todt and Kocot 2014; Cobo et al. 2023
<i>Pruvotia</i> cf. <i>sopita</i> (Pruvot, 1891)	OR458908	OR456214		Cobo et al. 2024
<i>Pruvotina impexa</i> (Pruvot, 1890)	OR458907	n/a		Cobo et al. 2024
<i>Scutopus ventrolineatus</i> Salvini-Plawen, 1968	MG855751	MG855840		Mikkelsen et al. 2019
<i>Simrothiella margaritacea</i> (Koren & Danielssen, 1877)	OQ600548	OQ618432		Cobo et al. 2023
<i>Stylomenia sulcodoryata</i> Handl & Salvini-Plawen, 2001	OR452313	PQ226469		Cobo et al. 2024; present study
<i>Tegulaherpia tasmanica</i> Salvini-Plawen, 1988	PQ222746	PQ226468		Yap-Chiongco et al. 2024
<i>Unciherpia hirsuta</i> Urgorri & Salvini-Plawen, 2001	OQ597875	OQ600031		Cobo et al. 2023
<i>Wirenia argentea</i> Odhner, 1920	MG855759	MG855856		Mikkelsen et al. 2019

## Phylogenetic analysis

To confirm our morphology-based identifications, a phylogenetic analysis was performed based on COI and 16S sequences. In addition to data from the new species, sequences broadly spanning the diversity of Solenogastres were obtained from NCBI based on the results of Kocot et al. (2019) as well as available sequences of close relatives of the new described species (Table 2). The caudofoveates *Chaetoderma nitidulum* Lovén, 1844. *Scutopus ventrolineatus* Salvini-Plawen, 1968, and *Falcidens sagittiferus* Salvini-Plawen, 1968 were used as the outgroup. Sequences were aligned with MAFFT v. 7 (Katoh et al. 2002), and the resulting alignments were manually refined to ensure protein-coding sequences (COI) were in the correct open reading frame prior to concatenation with Mesquite 3.81. (Maddison and Maddison 2023). A phylogenetic analysis was conducted on the resulting alignment using maximum likelihood in IQ-TREE 2 (Minh et al. 2020) with the best-fitting model of nucleotide substitution for each partition and 1000 rapid bootstraps. For 16S, the model used was GTR+F+I+G4. COI was additionally partitioned by codon position. Codon position 1 used GTR+F+R3, position 2 used TN+F+R3, and position 3 used TIM2+F+I+G4.

## Results

### Species descriptions

**Order Pholidoskepia Salvini-Plawen, 1978**

**Family Dondersiidae Simroth, 1893**

**Genus *Dondersia* Hubrecht, 1888**

**Type species.** *Dondersia festiva* Hubrecht, 1888, by monotypy. Type locality. Mediterranean Sea (northern Gulf of Naples); 60 m.

***Dondersia tweedtae* Farris, Olson & Kocot, sp. nov.**

<https://zoobank.org/FE62C5A8-71BD-40C4-9E76-288CD3D93AE6>

**Examined material. Holotype:** SH20364 (USNM 1718003). Gulf of Mexico. 28°5'42.18"N, 92°0'20.38"W. 82 m depth. Serial sections (23 slides), light microscopy preparations of the sclerites (two slides, sclerite from mid-body); SEM stub with sclerites; COI, 16S, and CytB sequences (NCBI PQ246886, PQ249005, and PQ241521, respectively).

**Derivatio nominis.** Named after Dr. Sarah Tweedt who provided us with the material and for her outstanding work studying invertebrate biodiversity using ARMS; *tweedtae* is feminine in the genitive.

**Diagnosis.** Elongate animal (~ 14 mm), bright pink with a yellow dorsal keel bearing 17 distinct lobes. Smooth, scaled appearance with three distinct scale-like sclerite types. Large anterior pedal glands. Atrium with about 14 trilobed papillae. Mouth separated from the atrium. Ventrolateral foregut glands of type A. Monoserial radula with two denticles joined at their apex. Midgut with

a short dorsal caecum, without lateral constrictions. With five dorsoterminal sensory organs. Without accessory copulatory structures.

**Description.** Description based on the holotype. Reconstruction of the internal anatomy based on manual reconstruction of the histological sections (Fig. 8A, A').

**Habitus.** Long animal (14 mm, 0.55 mm wide in the midbody), pink color aside from the bright yellow, continuous dorsal keel composed of 17 serially arranged lobes (Fig. 2A). Body with shiny and slightly scaly appearance. Coloration fades to off-white in 95% ethanol (Fig. 2B). Animal extends and contracts the body significantly; it varies in length, ranging from ~ 6–14 mm, and its width spans from 0.8–2 mm. (Fig. 2A). Tapered anterior. Posterior with a slight finger-like projection. Pedal groove, mantle cavity and mouth apertures visible externally (Fig. 2B).

**Mantle.** Thin epidermis (17.54–36.57  $\mu\text{m}$  thick, thickness decreases to ~ 10  $\mu\text{m}$  in areas of the posterior end of the body) without epidermal papillae. Three types of sclerites as scales inserted in one layer (Fig. 3): 1) Oval-shaped scales, relatively small (14–17.61  $\mu\text{m}$  long, 7.69–9.79  $\mu\text{m}$  wide) with a proximal rim and an elongated distal end (Fig. 3B, D), most common type, which forms a base layer across the entire body; 2) Lanceolate scales, long and narrow (38.57–39.75  $\mu\text{m}$  long, 5.28–6.86  $\mu\text{m}$  wide) with an acute distal end (Fig. 3B, C, F), distributed intermittently among the oval-shaped sclerites and are less abundant and shorter on the lobes of the dorsal keel; and 3) Pedunculated paddle-like (i.e., oar-shaped scales (Fig. 3B, E; 38.57–39.75  $\mu\text{m}$  long, 5.28–6.86  $\mu\text{m}$  wide), 'paddle' portion with a proximal rim, distal edge finely serrated ending in an acuminate point. Paddle-like sclerites inserted in the cuticle amongst the oval-shaped scales, found in the dorsal keel. Scales of the pedal groove not observed.

**Pedal groove and mantle cavity.** Pedal pit (100  $\mu\text{m}$  long, 165  $\mu\text{m}$  wide, 100–140  $\mu\text{m}$  high) located posteriorly to the mouth. Pedal glands very large, reaching the dorsal part of the body, surrounding the foregut (Fig. 4B–E). Well-defined pedal groove with a single triangular fold (30–60  $\mu\text{m}$  wide, 40–65  $\mu\text{m}$  tall). Mantle cavity (170  $\mu\text{m}$  long, 320  $\mu\text{m}$  high in the middle region) opens ventrally, with posterior pouch (Fig. 4O). Without respiratory folds, walls of the mantle cavity appear slightly folded and ciliated (Fig. 4N).

**Nervous system and sensory organs.** Cerebral ganglion circular to oval shape in cross section (85  $\mu\text{m}$  long, 50–180  $\mu\text{m}$  wide, 57–110  $\mu\text{m}$  high; Fig. 4C, D). Atrium (182  $\mu\text{m}$  long, 120–200  $\mu\text{m}$  wide 100  $\mu\text{m}$ –260  $\mu\text{m}$  high) opens ventrally with about 24 atrial papillae distally trilobed (27.5–52.5  $\mu\text{m}$  long, 2.5–7.5  $\mu\text{m}$  wide). Five dorsoterminal sensory organs observed both externally and in the serial sections (Fig. 4O).

**Digestive system.** Mouth opens ventrally, separated from the atrium (Figs 4B, C, 8A). Foregut rounded and narrow (50–70  $\mu\text{m}$  diameter), surrounded by a glandular epithelium and a thin muscular layer. Monoserial radula composed of a broad, non-serrated base (~ 20–25  $\mu\text{m}$  wide, 5–10  $\mu\text{m}$  high) and two long and narrow denticles that join at their apex (20–25  $\mu\text{m}$  high, 2.5–5  $\mu\text{m}$  wide; Fig. 4E, E'). Fragments of what seems to be two small lateral teeth observed in the edges of the base (Fig. 4E'). Radular sac extends posteriorly (Fig. 4F; 35  $\mu\text{m}$  long, and up to 45  $\mu\text{m}$  wide, 75  $\mu\text{m}$  high). Ventrolateral foregut



**Figure 2.** Habitus of *Dondersia tweedtae* sp. nov. **A** field photographs of the holotype showing the contractions and extension range (usnm 1718003) **B** photograph of the holotype preserved in ethanol **B'** detail of the lobes of the dorsal keel. Star indicates the anterior end of the animal.

glands of type A (García-Álvarez and Salvini-Plawen 2007) join the foregut via a common opening (Fig. 4E). Esophagus (95 µm long, 35–40 µm in diameter) forms a sphincter as it joins the midgut centrally (Fig. 8A). Midgut with a single dorso-anterior caecum (Fig. 8A) that contains cnidocytes (Fig. 4F, F'), also found in the midgut. Rectum (80–150 µm in diameter) discharges dorsally into the mantle cavity.

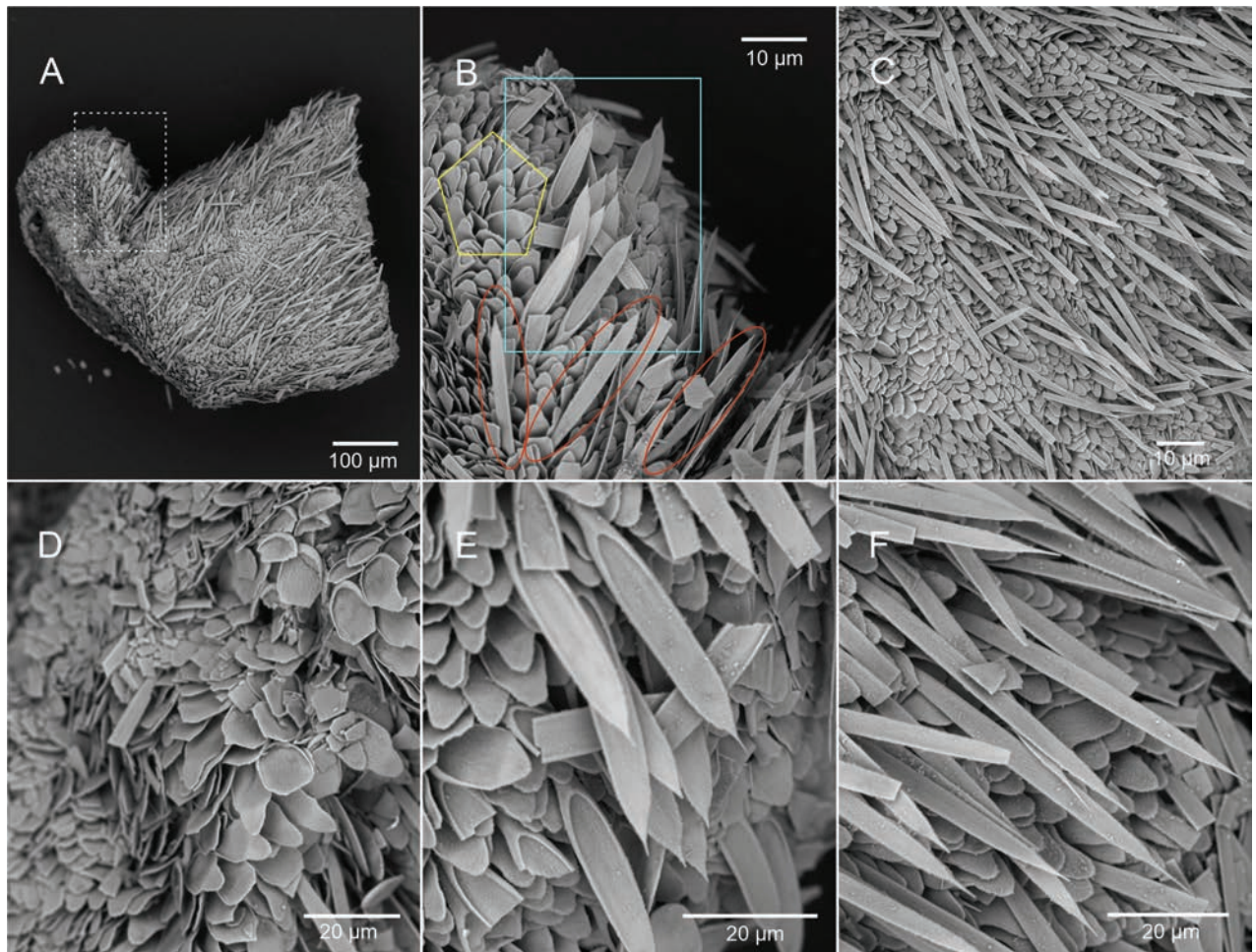


**Figure 3.** SEM images of the sclerites of *Dondersia tweedtae* sp. nov. **A** general SEM image of the dorsal and mid body **B** corresponds with the white square in **A** oval-shaped scales (yellow pentagon), lanceolate scales (red ovals) and pedunculated leaf-shaped scales (blue square) **C** lanceolate scales among oval-shaped scales **D** detail of the layer of oval-shaped scales **E** pedunculated leaf-shaped scales among oval-shaped scales **F** detail of the lanceolate scales. (Images of the holotype: USNM 1718003).

**Gonopericardial system.** Mature animal. Large pericardium (640 µm long, 100 to 530 µm diameter; significantly narrow in its posterior region: 70 µm diameter) (Fig. 8A'), closely associated with gonads, separated only by a thin tissue layer without defined gonoducts (Fig. 4G, H). Heart attached to the dorsal wall of the pericardium (Fig. 4H). Short pericardiodycts (60 µm long, 10–20 µm diameter) that connect to the very posterior end of the pericardium and with the spawning ducts in their origin (Fig. 4I). One seminal vesicle attached to each pericardiodyct (Fig. 4I). Fused region of the spawning ducts (400 µm long, up to 320 µm in diameter) about double the length of the paired region (Fig. 4J). Spawning ducts terminate into the antero-dorsal region of the mantle cavity (Fig. 8A') as a single duct (Fig. 4M), with two glandular lateral pouches in its posterior region (Figs 4K, L, 8A').

**Anatomy of the dorsal keel.** Continuous cuticular dorsal keel made up of 17 lobes covered by cuticle and sclerites. The serially arranged lobes are connected as can be seen externally through the yellow coloration in the

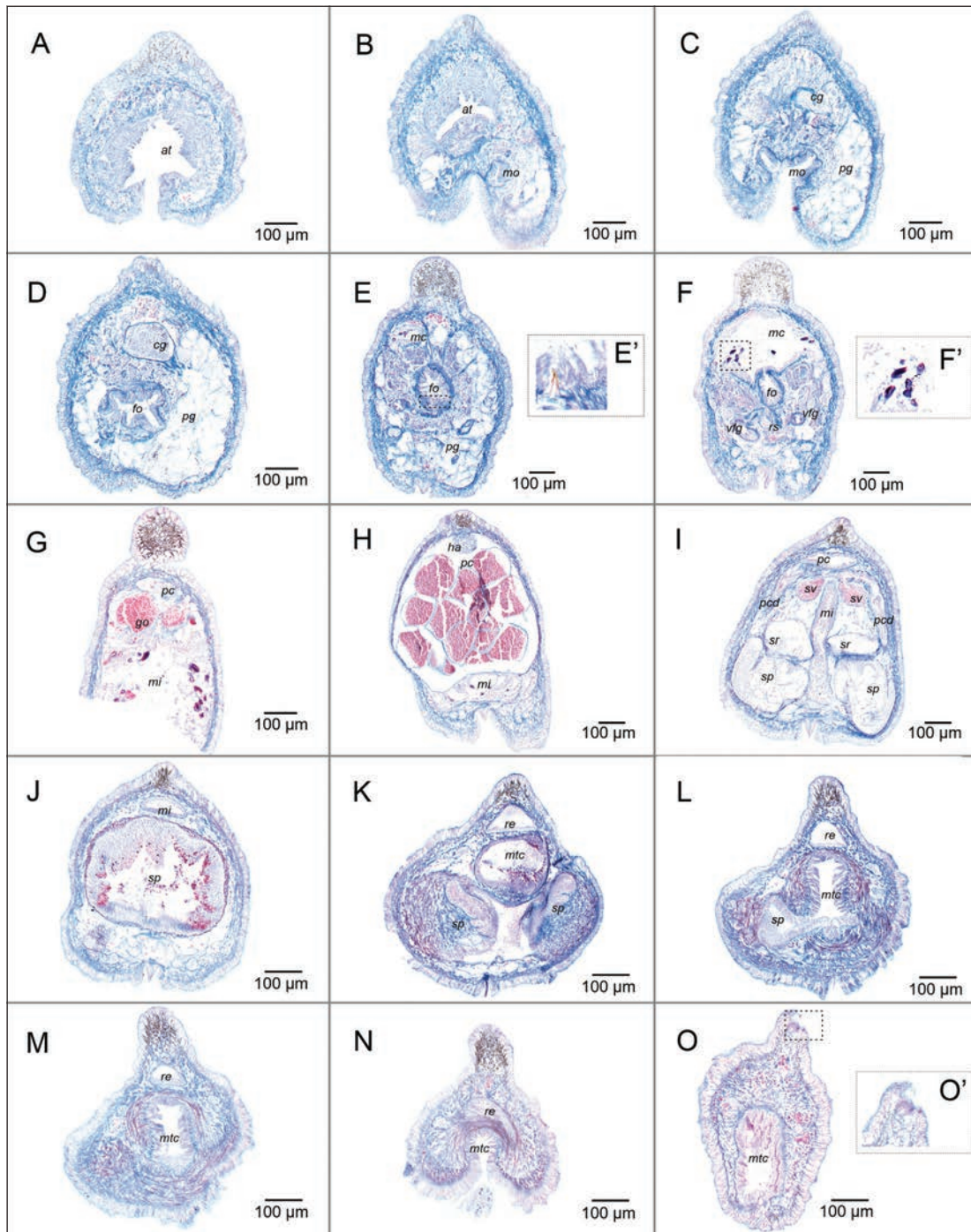


**Figure 4.** Serial section of *Dondersia tweedtae* sp. nov. **A–F** anterior region **A** atrium **B** atrium and mouth **C** opening of the mouth and cerebral ganglion **D** pre-radular region of the foregut and cerebral ganglion **E** radular region of the foregut and midgut caecum **E'** detail of the radula **F** radular region of the foregut: radular sac, ventrolateral foregut glands and midgut caecum **F'** detail of the cnidocytes in the midgut caecum **G** mid-posterior region of the body **H–O** posterior region **H** pericardium bearing the heart and reproductive cells **I** paired origin of the spawning ducts, termination of the pericardium **J** pericardium bearing the heart and reproductive cells **K–M** evolution of the fused region of the spawning ducts **N** opening of the mantle cavity **O** posterior pouch of the mantle cavity and dorsoterminal sensory organ. Abbreviations: at – atrium; cg – cerebral ganglia; fo – foregut; mc – midgut caecum; mi – midgut; mo – mouth; mtc – mantle cavity; pcd – pericardioducts; pg – pedal gland; re – rectum; rs – radular sac; sp – spawning duct; sv – seminal vesicle; sr – seminal receptacles; vfg – ventrolateral foregut glands. (Images of the holotype: USNM 1718003).

living specimen (Fig. 2A). Lateral view of the animal shows how the region between lobes is a bit elevated and thus constitutes a continuous keel. Serial sections show stained dark brown cells (with Mallory's Trichrome) contained in the lobes. This stained content is concentrated in the cavity of the lobules, but also continues into the cuticle. The fact that this can be seen in all the series of sections is an additional proof to the morphological continuity of the keel (Fig. 4).

**Comparisons.** Considering the traditional classification of Solenogastres (*sensu* Salvini-Plawen 1978), the order Pholidoskepia is characterized by a thin cuticle and sclerites as scales. Some authors have identified issues within this order calling for a taxonomic revision (Scheltema 1999; Scheltema and Schander 2000; Scheltema et al. 2012; Bergmeier et al. 2016, 2019; Yap-Chiongco et al. 2024). Nevertheless, the grouping of Pholidoskepia *sensu stricto* (Yap-Chiongco et al. 2024) is well-supported by the mentioned mantle characteristics and molecular data. Thus, we follow the traditional classification here. Within Pholidoskepia, the mantle sclerites, radula, and type of ventrolateral foregut glands, as well as some posterior organs, are important characters used to classify specimens into a family (García-Álvarez and Salvini-Plawen 2007). Particularly important for the identification of Dondersiidae species is the types of sclerites (Scheltema et al. 2012; Cobo and Kocot 2021). The sclerites of the specimen studied here can be compared to those described previously for species of *Dondersia*, especially with those of the type species: *Dondersia festiva* (Hubrecht 1888: fig. 13-2a; Scheltema et al. 2012: figs 1–3). This, with the structure of the radula, justify the classification of the new species within this genus. Moreover, our phylogenetic analysis also supports this classification (see below). The coloration of living specimens is unknown for most solenogasters as most of the species have been described based on preserved material. Within *Dondersia*, two described species are known to have bright colorations: *D. festiva* (bright purple) and *D. annulata* Nierstrasz, 1902 (hot pink with white stripes). Despite similarities, there are clear differences between *Dondersia tweedtae* sp. nov. and these two species and the remaining species of the genus (reviewed in Cobo and Kocot 2021). Particularly, the combination of pink and yellow coloration, along with the dorsal cuticular lobes, is exclusive to *D. tweedtae* sp. nov. Moreover, this constitutes the first Dondersiidae from the Gulf of Mexico (Table 3).

Since this new species bears a cuticular keel, the diagnosis of the family, which states the absence of dorsal keel (Scheltema et al. 2012; Cobo and Kocot 2021), needs to be amended to: "elongate body with or without keel. Anterior end tapered, posterior end with a finger-like projection. Leaf-shaped scales as most abundant type of sclerite, with oar-shaped (= pallet-shaped) or laminar scales scattered between them. With or without common atrio-buccal cavity. Monoserial radula; teeth with four denticles; two central denticles fused and curved distally; two lateral, curved denticles arising from a rounded base. With or without dorsoterminal sensory organs. With or without copulatory stylets. Without respiratory folds. With seminal vesicles and with or without seminal receptacles."

**Table 3.** Species of the families Dondersiidae Simroth, 1893 and Pruvotinidae Heath, 1911 with their know distributions.

Subfamily	Genus	Species	Distribution	Depth (m)
Dondersiidae Simroth, 1893	Dondersia Hubrecht, 1888	<i>Dondersia</i> (?) <i>todtae</i> Klink et al., 2015	Azores (North Atlantic)	26
		<i>Dondersia namibiensis</i> Scheltema, Schander & Kocot, 2012	Namibia (South Atlantic)	619–1007
		<i>Dondersia incali</i> (Scheltema, 1999)	West European Basin (North Atlantic)	2091
		<i>Dondersia cnidevorans</i> Salvini-Plawen, 1978	Ross Sea (Southern Ocean)	659–714
		<i>Dondersia laminata</i> Salvini-Plawen, 1978	Graham Land, Bransfield Strait (Southern Ocean)	311–426
		<i>Dondersia stylastericola</i> Salvini-Plawen, 1978	South Shetland Islands (Southern Ocean)	300
		<i>Dondersia annulata</i> Nierstrasz, 1902	Bima, Sumbawa (Indo-Pacific)	55
		<i>Dondersia festiva</i> Hubrecht, 1888	Gulf of Naples. Corsica (Mediterranean Sea)	60
		<i>Dondersia</i> ? <i>foraminosa</i> Cobo & Kocot, 2021	Brazil Basin (South Atlantic)	4484.7 - 4503
		<b><i>Donderisa tweedtae</i> sp. nov.</b>	<b>Gulf of Mexico</b>	<b>82</b>
	Heathia Thiele, 1913	<i>Heathia porosa</i> (Heath, 1911)	San Diego, California (Northeast Pacific)	920–990
	Helluotherpia Handl & Büchinger, 1996	<i>Helluotherpia vieiralaneroi</i> Cobo & Kocot, 2021	Brazil Basin (South Atlantic)	4484.7-4503
		<i>Helluotherpia aegiri</i> Handl & Büchinger, 1996	Herdlafjord, Bergen. (Norwegian Sea)	185–250
	Ichthyomenia Pilsbry, 1898	<i>Ichthyomenia ichthyodes</i> (Pruvot, 1890)	Rousillon, France (Mediterranean Se)	80
	Inopinatamenia Cobo & Kocot, 2021	<i>Inopinatamenia calamitosa</i> Cobo & Kocot, 2021	Brazil Basin (South Atlantic)	4484.7-4503
	Lyratoherpia Salvini-Plawen, 1978	<i>Lyratoherpia bracteata</i> Salvini-Plawen, 1978	South Sandwich Islands (Southern Ocean)	148–201
		<i>Lyratoherpia carinata</i> Salvini-Plawen, 1978	Ross Sea (Southern Ocean)	344–714
		<i>Lyratoherpia californica</i> (Heath, 1911)	San Diego, California (Northeast Pacific)	38–46
	Micromenia Leloup, 1948	<i>Micromenia amphiatlantica</i> Cobo & Kocot, 2020	Brazil, Angola, Guinea Basins (South Atlantic)	5433–5460
		<i>Micromenia subrubra</i> Salvini-Plawen, 2003	Malta (Mediterranean Sea)	140
		<i>Micromenia simplex</i> Leloup, 1948	Hope Island, Barents Sea (Arctic)	48
		<i>Micromenia fodiens</i> (Schwabl, 1955)	Gullmarfjord, Sweeden (North Atlantic)	40
	Nematomenia Pruvot, 1890	<i>Nematomenia glacialis</i> Thiele, 1913	Gauss Station, Davis Sea (Southern Ocean)	385
		<i>Nematomenia incirrata</i> Salvini-Plawen, 1978	South Orkney Islands (Southern Ocean)	298–302
		<i>Nematomenia protecta</i> Thiele, 1913	Gauss Station, David Sea (Southern Ocean)	385
		<i>Nematomenia ptyalosa</i> Salvini-Plawen, 1978	Sandwich Islands (Antarctica) to Tiera de Fuego	148–210
		<i>Nematomenia squamosa</i> Thiele, 1913	Gauss Station, Davis Sea (Southern Ocean)	385
		<i>Nematomenia tegulata</i> Salvini-Plawen, 1978	South Sandwich Islands (Southern Ocean)	148–201
		<i>Nematomenia</i> ? <i>guineana</i> Cobo & Kocot, 2021	Guinea Basin (South Atlantic)	5142
		<i>Nematomenia brasiliensis</i> Cobo & Kocot, 2021	Brazil Basin (South Atlantic)	4500
		<i>Nematomenia divae</i> Cobo & Kocot, 2021	Guinea Basin (South Atlantic)	5144
		<i>Nematomenia platypoda</i> (Heath, 1911)	Aleutian Islands, Bering Sea (North Pacific)	880
		<i>Nematomenia banyulensis</i> (Pruvot, 1890)	Dalmatia (Mediterranean Sea) to Trondheimsfjord (Norwegian Sea)	45–300

Subfamily	Genus	Species	Distribution	Depth (m)
Dondersiidae Simroth, 1893	<b>Nematomenia</b> Pruvot, 1890	<i>Nematomenia corallophila</i> (Kowalevsky, 1881)	Algeria (Mediterranean Sea)	73–183
		<i>Nematomenia flavens</i> (Pruvot, 1890)	Banyuls, Costa Brava, Corsica (Mediterranean Sea) to Shetland Islands (North Sea)	45–167
		<i>Nematomenia arctica</i> Thiele, 1913	Spitzbergen, Svalbard Archipelago (Arctic)	
	<b>Squamatoherpia</b> Büchinger & Handl, 1996	<i>Squamatoherpia tricuspadata</i> Büchinger & Handl, 1996	Bergen (Norwegian Sea)	250
	<b>Stylomenia</b> Pruvot, 1899	<i>Stylomenia salvatori</i> Pruvot, 1899	Banyuls sur Mer (Mediterranean Sea)	Littoral
		<i>Stylomenia sulcodoryata</i> Handl & Salvini-Plawen, 2001	Bergen (Norwegian Sea)	185
Pruvotinae Heath, 1911	<b>Pruvotina</b> Cockerell, 1903	<i>Pruvotina cryophila</i> (Pelseneer, 1901)	Bellinghausen Sea (Southern Ocean)	342–550
		<i>Pruvotina gauszi</i> Salvini-Plawen, 1978	Gauss Station, David Sea (Southern Ocean)	385
		<i>Pruvotina longispinosa</i> Salvini-Plawen, 1978	Drake Strait, South Sandwich Islands (Southern Ocean)	64–220/3890?
		<i>Pruvotina manifesta</i> Zamarro, García-Álvarez & Ugorri, 2013	Antarctic Peninsula (Southern Ocean)	254
		<i>Pruvotina pallioglandulata</i> Salvini-Plawen, 1978	South Shetland Islands (Southern Ocean)	210–220
		<i>Pruvotina praegnans</i> Salvini-Plawen, 1978	South Sandwich Islands (Southern Ocean)	148–220
		<i>Pruvotina providens</i> Thiele, 1913	Gauss Station, David Sea (Southern Ocean)	385
		<i>Pruvotina uniperata</i> Salvini-Plawen, 1978	Ross Sea (Southern Ocean)	210–2306
		<i>Pruvotina impexa</i> (Pruvot, 1890)	Banyuls sur Mer, Corsica (Mediterranean Sea)	60–80
		<i>Pruvotina artabara</i> Zamarro, García-Álvarez & Ugorri, 2013	NW Iberian Peninsula (North Atlantic)	1132–1191
		<i>Pruvotina megathecata</i> Salvini-Plawen, 1978	Tierra de Fuego (South Pacific)	118–903
		<i>Pruvotina peniculata</i> Salvini-Plawen, 1978	Tierra de Fuego (South Pacific)	119–549
		<i>Pruvotina bathyalis</i> Pedrouzo, García-Álvarez & Ugorri, 2022	NW Iberian Peninsula (North Atlantic)	566–581
		<i>Pruvotina glandulosa</i> Pedrouzo, García-Álvarez & Ugorri, 2022	NW Iberian Peninsula (North Atlantic)	980–2516
		<i>Pruvotina harpagone</i> Pedrouzo, García-Álvarez & Ugorri, 2022	NW Iberian Peninsula (North Atlantic)	709–728
		<i>Pruvotina zamarroae</i> Pedrouzo, García-Álvarez & Ugorri, 2022	NW Iberian Peninsula (North Atlantic)	600
	<b>Pararrhopalia</b> Simroth, 1893	<i>Pararrhopalia fasciata</i> Salvini-Plawen, 1978	South Sandwich Islands (Southern Ocean)	220–240
		<i>Pararrhopalia pruvoti</i> Simroth, 1893	Banyuls sur Mer (Mediterranean Sea)	80–150
		<i>Pararrhopalia oscar</i> Pedrouzo & Ugorri, 2022	NW Iberian Peninsula (North Atlantic)	438–459
	<b>Labidoherpia</b> Thiele, 1903	<i>Labidoherpia spinosa</i> (Thiele, 1913)	Gauss Station, (Southern Ocean)	385
		<i>Labidoherpia lucus</i> Pedrouzo, García-Álvarez & Ugorri, 2022	NW Iberian Peninsula (North Atlantic)	616
		<i>Labidoherpia vitucoi</i> Pedrouzo & García-Álvarez, 2022	NW Iberian Peninsula (North Atlantic)	438–459
	Eleutheromeniinae Salvini-Plawen, 1978	<b>Eleutheromenia</b> Salvini-Plawen, 1967	<i>Eleutheromenia sierra</i> (Pruvot, 1890)	Mediterranean Sea to Norway
<i>Eleutheromenia antarctica</i> Salvini-Plawen, 1978			Ross Sea (Southern Ocean)	342–714
<b><i>Eleutheromenia bullescens</i> sp. nov.</b>			<b>Gulf of Mexico</b>	<b>82</b>
<b>Luitfriedia</b> García-Álvarez & Ugorri, 2001		<i>Luitfriedia minuta</i> García-Álvarez & Ugorri, 2001	NW Iberian Peninsula (North Atlantic)	760–769
Lophomeniinae Salvini-Plawen, 1978	<b>Lophomenia</b> Heath, 1911	<i>Lophomenia spiralis</i> Heath, 1911	Nilhau Islands, Hawaii (East Pacific)	100–1200
		<i>Lophomenia dorsocaeca</i> Gil-Mansilla, García-Álvarez & Ugorri, 2011	Angola Basin (South Atlantic)	5390–5415

Subfamily	Genus	Species	Distribution	Depth (m)
Lophomeniinae Salvini-Plawen, 1978	<b>Hypomenia</b> van Lummel, 1930	<i>Hypomenia sanjuanensis</i> Kocot & Todt, 2014	San Juan Channel (Northeast Pacific)	59
		<i>Hypomenia nierstraszi</i> Van Lummel, 1930	Gulf of Naples (Mediterranean Sea)	150–200
	<b>Metamenia</b> Thiele, 1913	<i>Metamenia intermedia</i> Thiele, 1913	Gauss Station, David Sea (Southern Ocean)	293–385
		<i>Metamenia triglandulata</i> Salvini-Plawen, 1978	Ross Sea (Southern Ocean)	342–1610
Halomeniinae Salvini-Plawen, 1978	<b>Halomenia</b> Heath, 1911	<i>Halomenia gravida</i> Heath, 1911	Kuril Islands (Northwest Pacific)	420
	<b>Forcepimonia</b> Salvini-Plawen, 1969	<i>Forcepimonia protecta</i> Salvini-Plawen, 1969	Red Sea and Gulf of Aden	30
Unciherpiinae Garcia-Alvarez, Urganorri & Salvini-Plawen, 2001	<b>Uncimonia</b> Nierstrasz, 1903	<i>Uncimonia neapolitana</i> Nierstrasz, 1903	Gulf of Naples (Mediterranean Sea)	70
	<b>Sialoherpia</b> Salvini-Plawen, 1978	<i>Sialoherpia aculeitecta</i> Salvini-Plawen, 1978	Drake Strait	2782–2827
Scheltemaiinae Pedrouzo, Garcia-Alvarez & Urganorri, 2022	<b>Scheltemaia</b> Salvini-Plawen, 2003	<i>Scheltemaia mimus</i> (Scheltema & Schander, 2000)	Bass Strait (Tasmania)	140
		<i>Scheltemaia bassensis</i> (Scheltema & Schander, 2000)	Bass Strait (Tasmania)	70

### Order “Cavibelonia” Salvini-Plawen, 1978

#### Family Pruvotinidae Heath, 1911

#### Subfamily Eleutheromeniinae Salvini-Plawen, 1978

#### Genus *Eleutheromenia* Salvini-Plawen, 1967

**Type species.** *Paramenia sierra* Pruvot, 1890, by monotypy. Type locality. Costa Brava (Mediterranean Sea); 80 m. Type material missing (García-Álvarez and Salvini-Plawen 2007).

#### *Eleutheromenia bullescens* Cobo, sp. nov.

<https://zoobank.org/B6796295-A389-4B86-80CE-CA4C61C1A5C1>

**Examined material. Holotype:** SH20192-A (USNM 1718004) Gulf of Mexico. CYCLE 2021 event ID CYCLE\_2021\_ARMS\_01\_DIAback: 28.088295, -90.701405. 82 m depth. Serial sections (16 slides 5 µm), light microscopy preparation of the sclerites (1 slide); SEM stub with sclerites; COI, 16S, and CytB Sequences (NCBI PQ246885, PQ249006, and PQ241520, respectively). **Paratype** SH20192-B (USNM 1718005) Gulf of Mexico. 28.088295, -90.701405. 82 m depth. Animal preserved in 95% ethanol.

**Derivatio nominis.** From Latin *bullesco*, *bullesciscis*, *bullescere*; meaning “to bubble” or “to form bubbles” due to the aspect given by the protrusion of the dorsal keel.

**Diagnosis.** Elongate animal (~ 12 mm), light orange with a discontinuous dorsal keel with protrusions as lobes (number variable, protrusions simple or trilobed). Sclerites as hollow acicular spines, with hook-shaped and harpoon-shaped sclerites. Without epidermal papillae. Mouth and atrium partially separated. Atrium with numerous (≤20) single and branched papillae. Distichous radula. Ventrolateral foregut gland of type A / *Pararrhopalia* type. Foregut with a dorso-pharyngeal papilla gland. With 12 respiratory folds. With abdominal spicules. With one dorso-terminal sensory organ.

**Description.** Description based on the holotype, external aspect of the paratype also considered. Reconstruction of the internal anatomy (Fig. 8B, B') built from the manual reconstruction based on serial sections of the holotype.

**Habitus.** Elongate animal (10–12 × 0.5–1 mm), light orange in life (Fig. 5A, B), but white after preservation in ethanol (Fig. 5C). With a dorsal, discontinuous keel

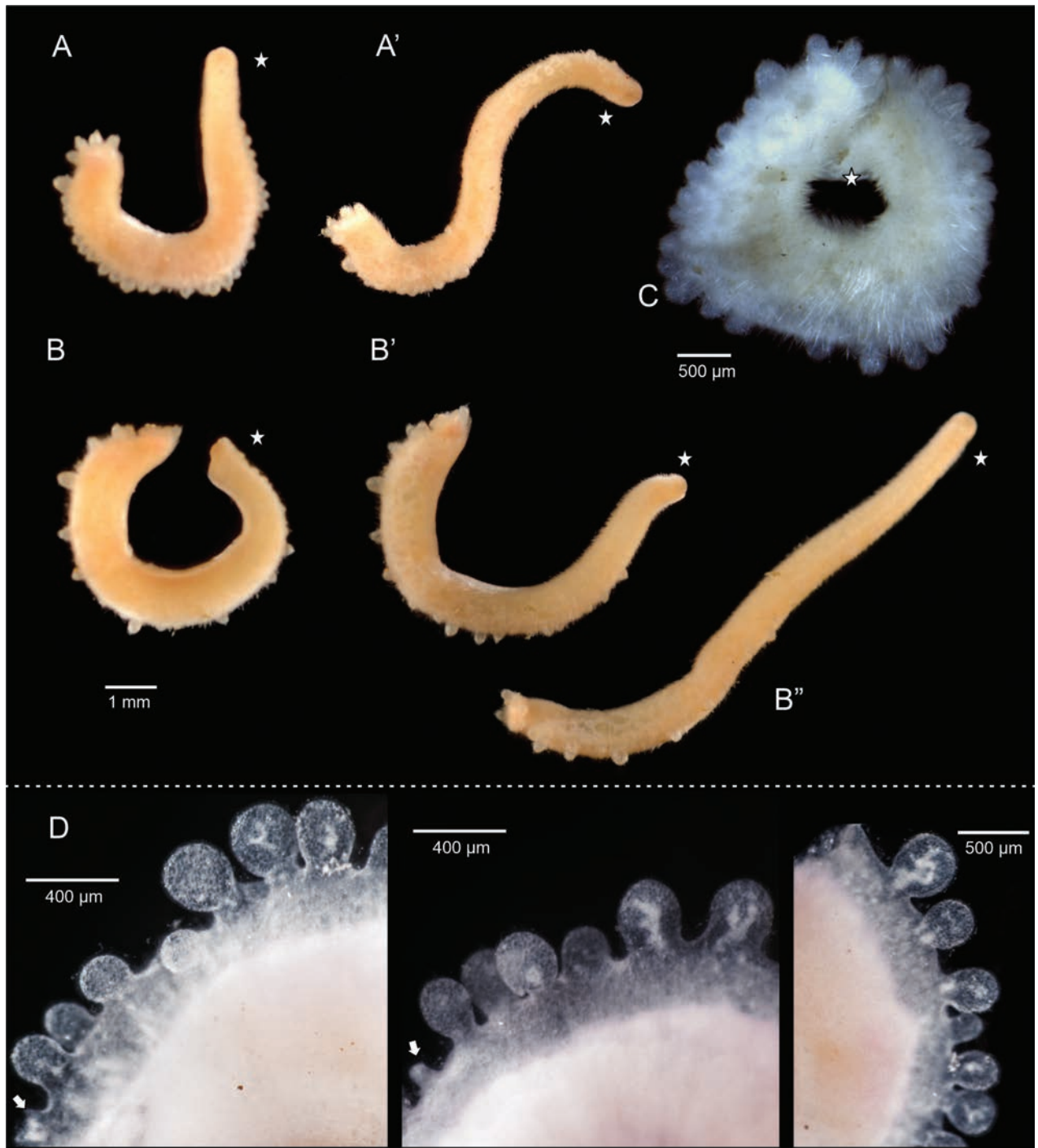


**Figure 5.** Habitus of *Eleutheromenia bullescens* sp. nov. **A, A'** field images of the Holotype (USNM 1718004) **B, B'** field images of the paratype (USNM 1718005) **C** paratype in 95% ethanol **D** detail of the dorsal lobes in the holotype (decalcified mid-body region). Images were captured using Olympus DSX100 optical microscope (Olympus Corporation, Tokyo, Japan) with anti-halation and fast HDR adjustments; brightness 0016 to 0022, texture 50-71, contrast 36-50. Star indicates the anterior end of the animal. Arrow indicates detached lobes and their "pedunculi."

formed by nearly spherical lobes of different sizes. Lobes without organized arrangement, which varies between the holotype and paratype and depending on the degree of extension of the body. Lobes single or grouped as pairs or groups of three.

**Mantle.** Thin cuticle (18.31–27.6  $\mu\text{m}$ ) without distinct papillae and with five main types of hollow acicular sclerites protruding from it (Fig. 6): 1) Hook-shaped sclerites (Fig. 6A–C; 80–90  $\times$  9–6  $\mu\text{m}$ ; the inner part of the hook is 30  $\mu\text{m}$  long) with a small distal protrusion and a short internal region of the hook are particularly abundant in the dorsal region of the body and on the dorsal lobes; 2) Harpoon-shaped sclerites (Fig. 6A, D; 200–210  $\times$  8  $\mu\text{m}$ ), present all over the body and are the dominant sclerite type in the mid-ventral region, also larger than elsewhere on the body (Fig. 6E; 200–300  $\times$  8–10  $\mu\text{m}$ ); 3) Very thin and long acicular sclerites (Fig. 6D, E; 80–150  $\times$  2  $\mu\text{m}$ ), distributed all over the surface of the body, but are less abundant in the dorsal lobes; 4) Acicular sclerites that look almost flat, but are hollow and elliptical in cross-section (Fig. 6A, D–F; 100–160  $\times$  10  $\mu\text{m}$ ), present all over the body; 5) Slightly curved acicular sclerites of varying length (Fig. 6A, F; 80–160  $\times$  6–7  $\mu\text{m}$ ), present all over the body. With knife-shaped scales characteristic of the pedal groove.

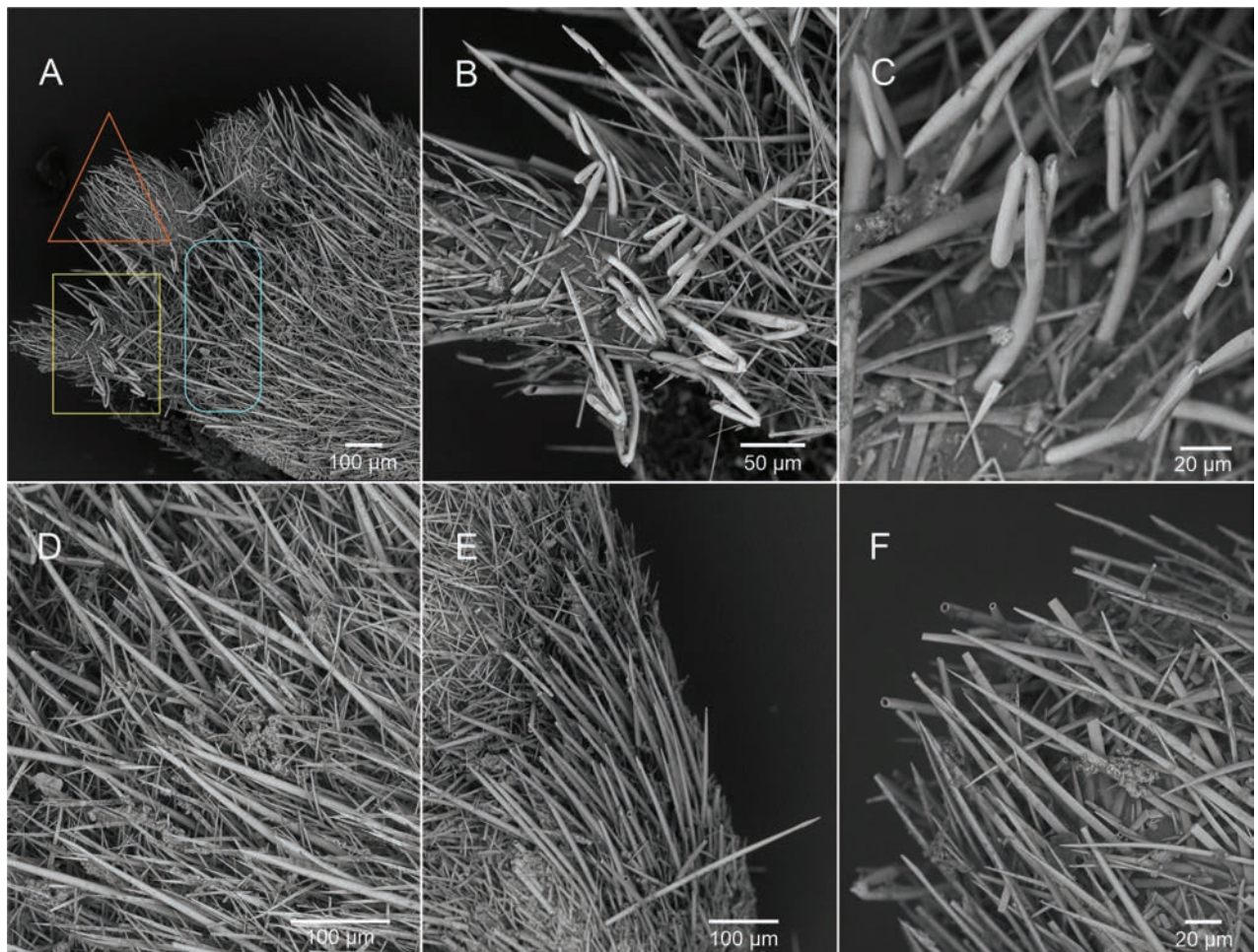


**Figure 6.** SEM images of the sclerites of *Eleutheromenia bullescens* sp. nov. **A** general view of the sclerites in the dorsal region **B** corresponds with the area in the yellow rectangle in **A** detail of sclerites **C** detail of the hook-shaped sclerites **D** corresponds with area in the blue oval rectangle in **A** detail of harpoon-like sclerites and flat acicular sclerites **E** harpoon-like sclerites in the mid-ventral body region **F** corresponds with the area in the red triangle in **A** harpoon-like sclerites, slightly curved acicular sclerites and flat acicular sclerites. (Images of the holotype: USNM 1718004).

**Pedal groove and mantle cavity.** Small pedal pit (90  $\mu\text{m}$  long, 16  $\mu\text{m}$  wide, 4–6  $\mu\text{m}$  high). Pedal groove well marked, extending along the entire length of the body, with a single wide triangular pedal fold (Fig. 7H–L; 5–10  $\mu\text{m}$  wide in the middle region of the fold  $\times$  5–12  $\mu\text{m}$  high). Mantle cavity with 12 unbranched respiratory folds (Fig. 7M, N).

**Nervous system and sensory organs.** Cerebral ganglion of circular shape in cross section (Fig. 7B–D; 35  $\mu\text{m}$  long, 20 to 22  $\mu\text{m}$  wide, 10 to 14  $\mu\text{m}$  high). Atrium (160  $\mu\text{m}$  long, 17 to 34  $\mu\text{m}$  wide, 8 to 10  $\mu\text{m}$  high) with numerous ( $\leq 20$ ) single and branched papillae (Fig. 7A, B). Without dorsoterminal sensory organ.

**Digestive system.** Mouth and atrium partially separated (mouth separated from the atrium by a ridge with musculature but without cuticle; Fig. 7C). Mouth (Fig. 7D) leads to a rounded foregut that enlarges dorsally, where it forms a connection with a dorso-pharyngeal papilla gland (Fig. 7D–F). Short radular sac (Figs 7G, 8B). Ventrolateral foregut glands of type-A (García-Álvarez and Salvini-Plawen 2007) / *Pararrhopalia*-type (Handl and Todt 2005 that are very glandular posteriorly (Fig. 7H). Radula distichous, formed by hook-shaped teeth (radula broken in the sections so the number of middle denticles, if present, cannot be estimated). Midgut with a dorsal caecum that projects anteriorly above the foregut and dorsal pharyngeal gland (Figs 7G, 8B) and marked lateral constrictions (Fig. 7I). Rectum ends dorsally in the mantle cavity (Fig. 7L).

**Gonopericardial system.** Mature animal. Gonoducts connect with a large pericardium (540  $\mu\text{m}$  long, 40 to 200  $\mu\text{m}$  high). Heart not evident in most of the serial sections. Pericardiodycts (340  $\mu\text{m}$  long, 10–20  $\mu\text{m}$  diameter) connect to the posterior end of the pericardium and the mid-posterior spawning duct (Figs 7J, 8B'). Spawning duct paired in most of its longitude (400  $\mu\text{m}$ ), ending as a single tube (160  $\mu\text{m}$  long) in the middle of the mantle cavity (Fig. 7K, L). Seminal receptacles attached dorsally to each of the spawning ducts (Fig. 7J), posterior to the fusion of the pericardiodycts with the spawning ducts (Fig. 8B'). Without seminal vesicles. Without copulatory stylets. With abdominal spicules.

**Anatomy of the dorsal keel.** Dorsal keel consists of a discontinuous series of cuticular lobes. Number of lobes variable among individuals ( $\sim 30$  in the holotype and 24 in paratype 1; Fig. 5A, B). In living specimens, lobes protrude less from the cuticle when the animal expands the body (Fig. 5B'). This and the orientation of the animal makes it difficult to get an exact number of lobes. Concentration of lobes along the body seems uniform in preserved specimens (Fig. 5C), but in living specimens the density of lobes is higher in the posterior region of the body (Fig. 5A, B). This variation of the dorsal keel in the living specimens and after fixation was already described for *Eleutheromenia sierra* Pruvot, 1890 (Cobo et al. 2024). The lobes are mostly single in the mid body, but they can occur as pairs or groups of three, especially toward the anterior and posterior ends. In the decalcified animal it was evident that the lobes have a proximal peduncle in connection with the body (Fig. 5D). Both in the living and fixed specimens, and after decalcification it was observed that the lobes are easily detached from the body, breaking at the peduncular area (Fig. 5D). Histology of the dorsal keel is reminiscent of what has been described for the keel of *E. sierra* (Pruvot 1890; Salvini-Plawen 2003b: fig. 11): connection between lobes not evident externally nor in the histological series. Study of the lobes under the microscope after decalcification (Fig. 5D) revealed that they contain an unidentified material that is in some way connected with the internal

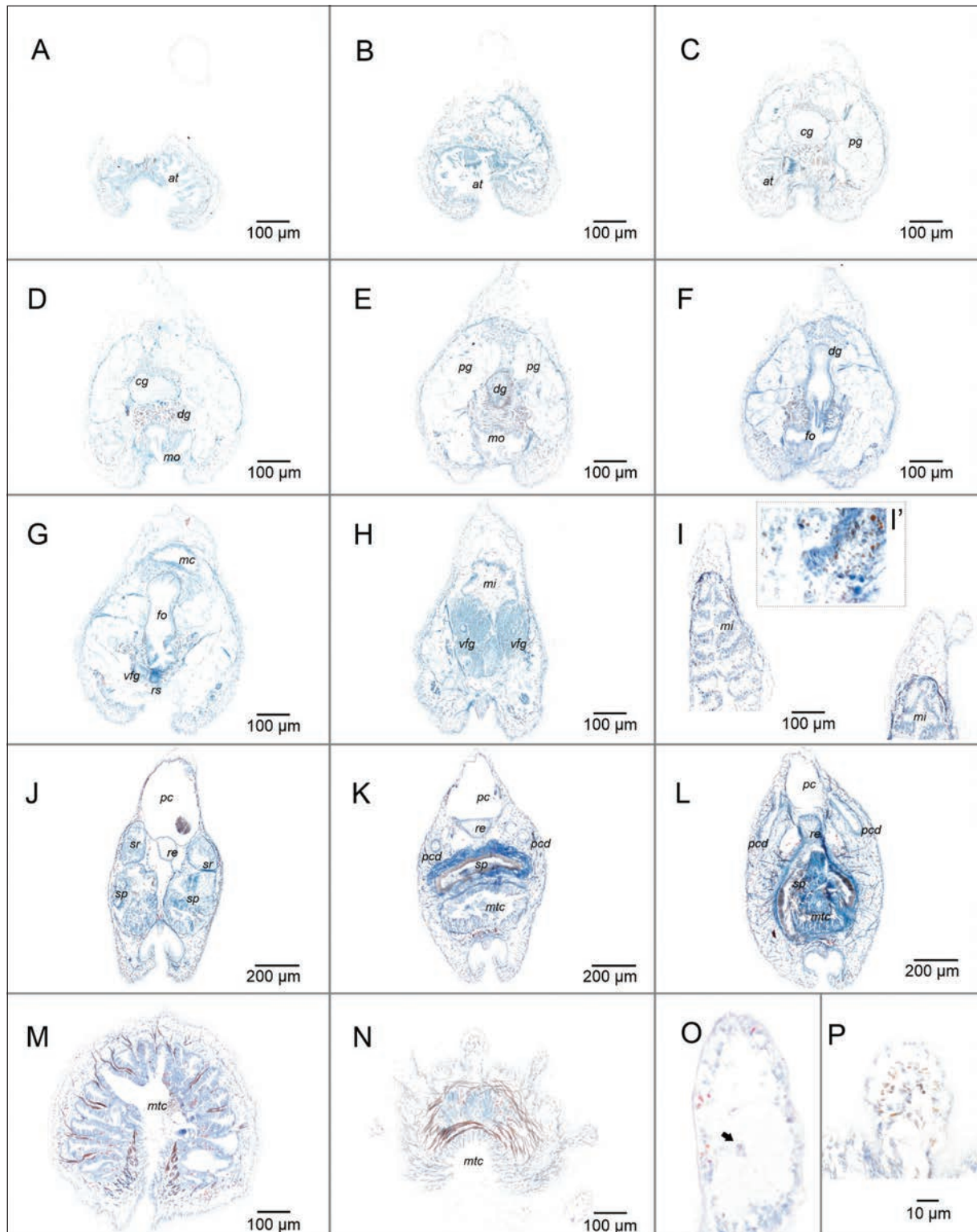


**Figure 7.** Sections of *Eleutheromenia bullescens* sp. nov. **A–G** anterior region **A–C** atrium (detail of the ventral region: muscular groove between mouth and atrium) **D, E** mouth and dorsal gland **F** foregut and dorsal gland **G** ventrolateral foregut glands, radular sac and pedicel **H** posterior region of the ventrolateral foregut glands, midgut, and detail of the cnidocytes (**I'**) **I** midgut with constrictions **J–N** posterior region **J** paired spawning ducts, seminal vesicles and pericardioducts **K, L** fusion of the rectum, spawning ducts, and mantle cavity **M, N** respiratory folds **O, P** details of the dorsal lobes. Abbreviations: at – atrium; cg – cerebral ganglia; dg – dorsal gland; fo – foregut; mc – midgut caecum; mi – midgut; mo – mouth; mtc – mantle cavity; pcd – pericardioducts; pp – pedicel; re – rectum; rs – radular sac; sp – spawning duct; sr – seminal receptacles; vfg – ventrolateral foregut glands. (Images of the holotype: USNM 1718004).

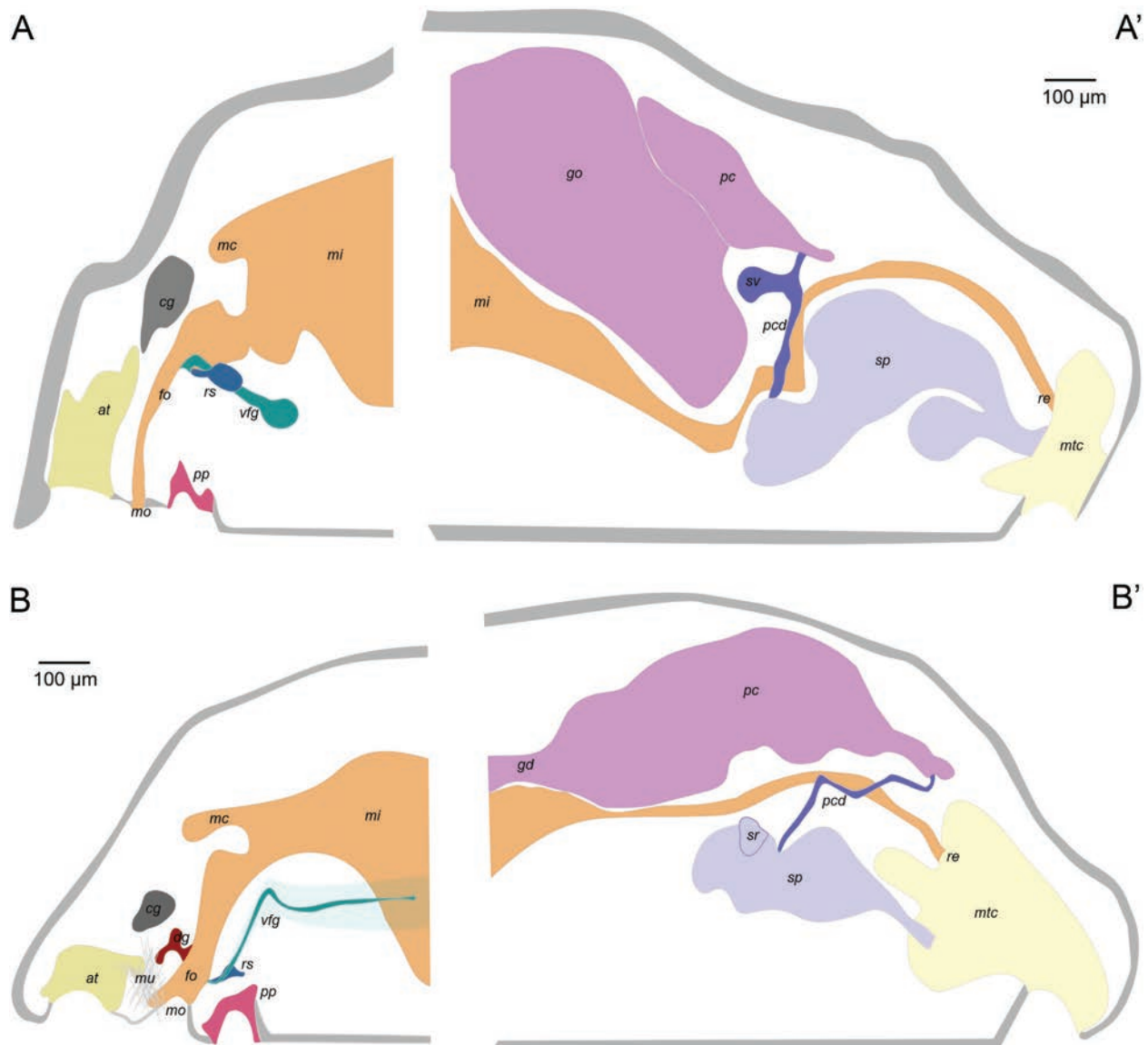


**Figure 8.** Reconstruction of the internal anatomy of **A** *Dondersia tweedtae* sp. nov. **B** *Eleutheromenia bullescens* sp. nov. (A anterior reconstruction, B posterior reconstruction). Abbreviations: at – atrium; cg – cerebral ganglia; dg – dorsal gland; fo – foregut; go – gonad; mu – musculature; mc – midgut caecum; mi – midgut; mo – mouth; mtc – mantle cavity; pcd – pericardioducts; pg – pedal gland; pp – pedal pit; re – rectum; rs – radular sac; sp – spawning duct; sc – seminal vesicle; sr – seminal receptacles; vfg – ventrolateral foregut glands. (Drawings based on the manual reconstruction built on the study of serial sections of the holotypes.).

organs. Content not easily characterized, although diverse types of cells could be observed (Fig. 7P), including one that was tentatively identified as a cnidocyte (Fig. 7O).

**Comparisons.** The presence of hollow sclerites with a hook-shaped distal end is characteristic of two subfamilies within the family Pruvotinidae: Pruvotininae Heath, 1911 and Eleutheromeniinae Salvini-Plawen, 1978 (García-Álvarez and Salvini-Plawen 2007). The main distinguishing feature between these subfamilies is the presence of a dorso-pharyngeal papilla gland in Pruvotininae (García-Álvarez and Salvini-Plawen 2007; Pedrouzo et al. 2022). Although several works have shown that some of the diagnostic characters of the family are somehow ambiguous and the group is in need of systematic revision

(García-Álvarez and Salvini-Plawen 2007; Zamarro et al. 2013; Pedrouzo et al. 2022; Martínez-Sanjuán 2024), the presence/absence of the dorso-pharyngeal papilla gland has been considered as a good diagnostic character to distinguish these subfamilies (Cobo et al. 2024). The new species described here has a dorso-pharyngeal papilla gland, which would place it within Pruvotinae.

The subfamily Pruvotinae includes three genera: *Pruvotina* Cockerell, 1903; *Pararrhopalia* Simroth, 1893 and *Labidoherpia* Salvini-Plawen, 1978. Traditionally, these three genera are distinguished by a combination of internal morphological characters including the presence/absence of atrio-buccal cavity (García-Álvarez and Salvini-Plawen 2007; Zamarro et al. 2013; Pedrouzo et al. 2022). Nevertheless, it was recently concluded (Cobo et al. 2024) that this is not a valid character to differentiate between genera in the subfamily Pruvotinae, and that the only apparently reliable defining morphological characteristics among these genera are the respiratory folds and copulatory stylets: respiratory folds are present both *Pruvotina* and *Labidoherpia*, but absent in *Pararrhopalia* (García-Álvarez and Salvini-Plawen 2007; Pedrouzo et al. 2022) and *Pruvotina* is the only genus in the subfamily that lacks copulatory stylets. The species described here has respiratory folds and lacks copulatory stylets and thus it would be classified as *Pruvotina*. However, the results of our phylogenetic analysis (see below and Fig. 9) place the new species as the sister taxon to a species of *Eleutheromenia* Salvini-Plawen, 1967 (Eleutheromeniinae) with maximal support and thus a classification of the new species based just on internal morphological characters is called into question.

Externally, the new species resembles *Eleutheromenia sierra* (Pruvot, 1890) due to the lobular dorsal keel (Pruvot 1890; Salvini-Plawen and Ozturk 2006; Zamarro et al. 2013; Cobo et al. 2024). Prior to the discovery of the species described here, *E. sierra* was the only species within Pruvotinidae with a distinct dorsal keel. A subtle dorsal keel has been described for *Pruvotina peniculata* Salvini-Plawen, 1978 (Pedrouzo et al. 2022), but while a slight keel can be seen in the drawings included in the original description of the species (Salvini-Plawen 1978: figs 129, 130), this character was not apparent in our study of the sections deposited at the Smithsonian National Museum of Natural History (USNM 1604160, 1604162, 1604163, and 1604174). Further, the study of the syntypes of *P. peniculata* preserved in ethanol revealed a spiny habitus without a dorsal keel (USNM 749729). Considering the sclerites, the new species has harpoon-shaped hollow acicular sclerites, which is also a characteristic of *E. sierra* (Pruvot, 1890). This sclerite type has been reported just for one of the 16 species of *Pruvotina*, *P. harpagone* Pedrouzo, Garcia-Alvarez & Urgorri, 2022 (Pedrouzo et al. 2022). Therefore, considering the external aspect and sclerites along with the results of our molecular phylogenetic analysis, the new species is classified in the subfamily Eleutheromeniinae, despite the presence of a dorso-pharyngeal papilla gland.

Eleutheromeniinae includes two genera. No radula is present in the monospecific *Luitfriedia* García-Álvarez & Urgorri, 2001 while a distichous radula was described for the two accepted species of *Eleutheromenia*, supporting placement of the new species in this genus. *Eleutheromenia bullescens* sp. nov. can be clearly differentiated from the two known species of the genus. The dorsal keel distinguishes it clearly from *E. antarctica* (Salvini-Plawen, 1978), which lacks a keel. Despite the similarities in their external aspect, *E. bullescens* sp.

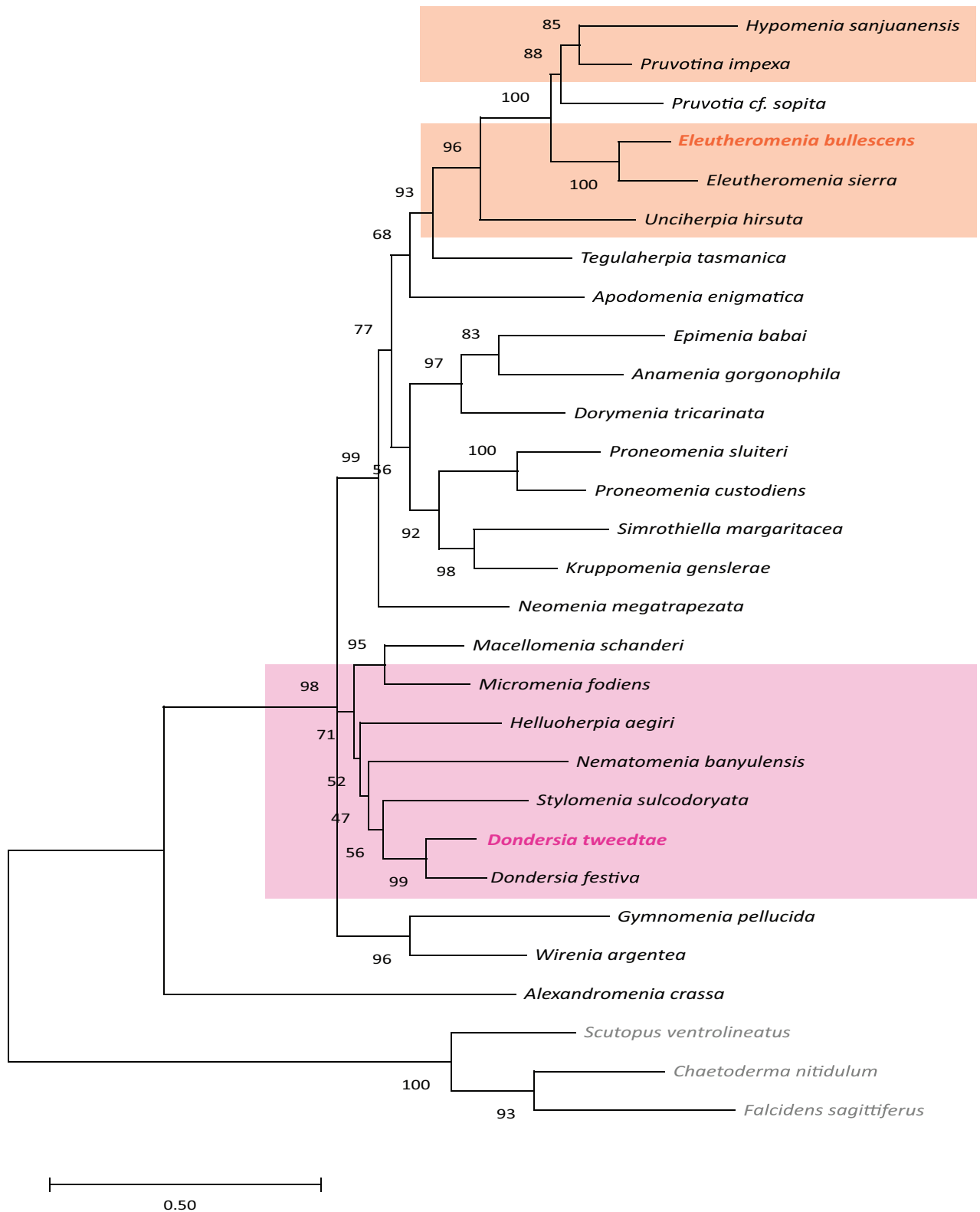


**Figure 9.** Maximum likelihood phylogenetic reconstruction based on 16S and COI genes showing the position of the new species described in this work. Bootstrap support values are shown.

nov. can be easily distinguished from *E. sierra*. The new species is orange while *E. sierra* is white to cream when alive (Pruvot 1890; Cobo et al. 2024). Moreover, the arrangement of the  $\leq 30$  lobes in the new species differs from what was

described for *E. sierra*, which has ~ 17 single lobes, none of which are grouped, and they are spaced more regularly along the body (Cobo et al. 2024). Internally, *E. bullescens* sp. nov. has a dorso-pharyngeal papilla gland and lacks a glandular esophagus, in contrast to *E. sierra* (Salvini-Plawen 1978; Pruvot 1890; Pedrouzo et al. 2022). With the new species included here the distribution of Pruvotinidae is extended to the Gulf of Mexico (Table 3).

Considering all the above, a thorough re-evaluation of the systematics of Pruvotinidae is required. In particular, the generation and analysis of molecular data from already described species seem essential, along with a better characterization of the habitus, sclerites, radula, and digestive glands. The currently accepted classification of the family and diagnoses of the subfamilies and genera, if they prove to represent monophyletic groups, need to be amended, but more research is needed to do this adequately. Given the need for a systematic revision of Pruvotinidae, we refrain from formally amending the diagnosis of Eleutheromeniinae but note that the presence of a dorso-pharyngeal papilla gland in the new species is contrary to the current diagnosis of the group.

### DNA barcoding and phylogenetic analysis

Successful COI, 16S, and CytB sequences were obtained for both newly described species. The phylogenetic analysis performed based on COI and 16S sequences corroborated our morphology-based identification of *D. tweedtae* sp. nov. (Fig. 9), placing it as the sister taxon of *D. festiva* (bootstrap support, bs = 99). *Dondersia* was recovered within a clade of other dondersiids plus the one sampled species of Macellomeniidae, although this clade was only moderately-well supported (bs = 71).

*Eleutheromenia bullescens* sp. nov. was recovered as the sister taxon of *E. sierra* with maximal support (bs = 100). Eleutheromeniinae was recovered as the sister taxon of a clade (bs = 88) in which *Pruvotia sopita* (Pruvot, 1891) (Rhopalomeniidae Salvini-Plawen, 1978) was recovered as the sister (bs = 85) of *Pruvotina impexa* (Pruvot, 1890) (Pruvotinidae, Pruvotininae) and *Hypomenia sanjuanensis* Kocot & Todt, 2014 (Pruvotinidae, Lophomeniinae). Given the presence of a dorsal pharyngeal papilla gland, we had considered taxonomic assignment of *E. bullescens* sp. nov. within the genus *Pruvotina*, but results of this phylogenetic analysis support our decision to classify the new species within *Eleutheromenia*, which is also supported by the presence of a dorsal keel and harpoon-shaped sclerites. Although the goal of our analysis was to confirm our taxonomic assignment of the new species, it is noteworthy that the overall topology of the tree reconstructed based on 16S and COI is fairly consistent with recent transcriptome-based analyses of solenogaster phylogeny (Kocot et al. 2019; Yap-Chiongco et al. 2024), albeit with lower resolution and generally weaker bootstrap support values. Amphimeniidae was recovered as the sister taxon to all other sampled solenogasters with strong support (bs = 100), Neomeniidae was recovered in a clade with the other sampled members of Cavibelonia plus Lepidomeniidae and Apodomeniidae with strong support (bs = 99), and a clade including Epimeniidae, Proneomeniidae (which was recovered non-monophyletic as previously shown: Cobo et al. 2023; Yap-Chiongco et al. 2024), Strophomeniidae, and Simrothiellidae was recovered, albeit with weak bootstrap support (bs = 56).

## Discussion

### Morphological adaptations

The two species included in this study belong to distantly related families but show intriguing similarities in their external morphology, both with a lobulated keel. Nevertheless, a detailed examination of the structure of both species reveals notable differences between them. Externally, the attachment to the body and the consistency appears stronger in *D. tweedtae* sp. nov. where the keel is continuous, while in *E. bullescens* sp. nov., the lobes are not connected, and they have a more delicate appearance (they detach easily). The serial sections reveal darkly stained contents in the lobes of *D. tweedtae* sp. nov. that continues into the cuticle, suggesting a secretion or accumulative function. We did not observe anything like this in the sections of *E. bullescens* sp. nov. where the lobes contain isolated cells, and we identified at least one as a cnidocyte. Both species feed on hydrozoans, as evidenced by cnidocytes in the gut (Figs 4F', 7I').

In the absence of a shell, mollusks adopt other defensive strategies for protection such as mimicry, crypsis, autotomy, production of defensive chemicals, or the retention of exogenous biochemically active compounds and cnidocytes from their prey (e.g., Avila 1995; Ros 1977; Wägele and Klussmann-Kolb 2005; Paul and Ritson-Williams 2008; Greenwood 2009; Neves et al. 2009; Moles et al. 2015; Goodheart et al. 2018, 2022; Winters et al. 2018; Wägele et al. 2022). Solenogastres lack a shell but are protected by a body covered by sclerites. Nevertheless, their defensive value has not been evaluated. The thickness of the cuticle and the layers and density of sclerites vary significantly among different groups. Given the lobulated keel and coloration exhibited by the species described here, in addition to their thin cuticle and sclerite cover, other defensive strategies might be hypothesized.

In *D. tweedtae* sp. nov., the nature of the dark-stained granules in the dorsal lobes is unknown. However, we speculate that the bright, contrasting coloration of this animal may represent aposematic coloration that warns would-be predators of a foul tasting, or toxic compound(s) stored in the lobes. Chemical defense has been described for many "Opisthobranchia" (reviewed in Wägele and Klussmann-Kolb 2005). In Chromodorididae Bergh, 1891 (Gastropoda, Nudibranchia) the storage of secondary metabolites occurs in dermal formations (MDFs) located in exposed parts of the mantle (usually near a distinct coloration, e.g., Carbone et al. 2013: fig. 1). The arrangement of the MDFs is specific to each chromodorid genus (Rudman 1984) and this, together with the coloration patterns, is supposed to play an important defensive role (reviewed in Carbone et al. 2013). Some chromodorid species lack typical MDFs but metabolites are still accumulated in the mantle rim (Harber et al. 2010). Further studies, including semithin sectioning or transmission electron microscopy, would be necessary to determine if the histology of the lobes of *D. tweedtae* sp. nov. can be compared with the MDFs (histology described in e.g., García-Gómez et al. 1991; Wägele and Klussmann-Kolb 2005). Besides, the chemical determination of metabolites in the tissues, and their evaluation, is also mandatory to determine putative toxicity. Aposematic coloration has also been associated with defense mechanisms related with nematocysts-based defense in Nudibranchia (Aguado and Marin 2007). Although we did find cnidocytes in the digestive system of *D. tweedtae* sp. nov., we did not find them in the bulbs of the keel.

Two other species of *Dondersia* (*D. festiva* and *D. annulata*) also exhibit a bright coloration and it is known that all the species of the genus but two (whose placement in the genus is uncertain: *D. ? todtiae* and *D. foraminosa*; Klink et al. 2015; Cobo and Kocot 2021) feed on cnidarians (Salvini-Plawen 1972, 1978; Scheltema et al. 2012).

We speculate that the dorsal lobes in *E. bullescens* sp. nov. may be an adaptation analogous to those observed in nudibranchs. Some taxa within the nudibranch clade Cladobranchia are known to have the ability to sequester nematocysts (kleptocnidae) from their cnidarian prey (Edmunds 1966). The structure that houses the kleptocnidae is called a cnidosac and is located at the tips of the dorsal cerata (review within a phylogenetic context in Goodheart and Bely 2017; Goodheart et al. 2018). Again, further studies would be necessary to advance in the histological characterization of the structure of the bulbs of *E. bullescens* sp. nov. and the closely related species *E. sierra*, also known to feed on cnidarians (Pruvot 1890; Salvini-Plawen 1972).

### Species identification and taxonomic characters

In Solenogastres, the external aspect is uniform in most groups (reviewed by Cobo et al. 2023). Nevertheless, the study of the habitus is essential for the initial sorting of species within morphotypes and can be crucial in the identification and distinction between species of specific families, such as the ones described in this work, especially if images or videos of living animals are available. Live observations of solenogasters can be considered rare, and most known species have been described based on fixed material. Thus, samples like those studied here are important for a better understanding of external morphological variation in these mollusks. Here, we present two examples of solenogasters in which the external features (characterized by distinctive body protuberances and bright colorations) were useful for recognizing them as new species (*D. tweedtae* sp. nov.) or to justify their classification (*E. bullescens* sp. nov.) and will aid in their distinction and identification in the future.

Sclerites are commonly just useful for the classification of solenogasters within the four traditional orders (García-Álvarez and Salvini-Plawen 2007). Nevertheless, there are exceptions. In Dondersiidae sclerites have been shown to be useful for species delimitation (Scheltema et al. 2012; Cobo and Kocot 2021) and this is also demonstrated in this study with the description of *D. tweedtae* sp. nov. Within Pruvotinidae the reliance on sclerites alone is insufficient, but the presence/absence of hook-shaped sclerites along with some internal characteristics allows one to classify specimens to at least the subfamily level (reviewed in Pedrouzo et al. 2022). Our results support several previous works where the pivotal role of sclerites and other hard parts in solenogaster identification has been highlighted (e.g., Scheltema et al. 2012) and we agree that there is a need for detailed characterization of sclerites as they can constitute an important diagnostic character (Scheltema et al. 2012). We consider that they could be a key trait in the revision of Pruvotinidae if used in parallel with molecular data, but sequences of most described species are still unavailable and more detailed description of the sclerites of many of those is also needed.

The combination of DNA barcoding and sclerites is a promising tool for species identification (following Bergmeier et al. 2016) pending of a more com-

plete DNA barcode library and better characterization of sclerites in most of the solenogaster groups. In this study the use of DNA barcoding is shown as a powerful tool in combination with sclerites but also considering the habitus of the species. Previous works have suggested the need for a revision of the family Pruvotinidae (García-Álvarez and Salvini-Plawen 2007; Zamarro et al. 2013; Pedrouzo et al. 2022; Martínez-Sanjuán 2024). In the present work, we include molecular evidence that supports the need for a review of the family. Moreover, with the classification of *E. bullescens* sp. nov. in *Eleutheromenia* despite having a dorso-pharyngeal papilla gland, we show that even the diagnostic characters that seemed more robust need to be reconsidered. We consider that habitus and sclerites, in combination with other traits, can be essential to solve the taxonomy of the family.

Our results recover *P. sopita* (Rhopalomeniidae) within Pruvotinidae. Considering the diagnostic characters currently accepted for Rhopalomeniidae, there is overlap with those of Pruvotinidae (García-Álvarez and Salvini-Plawen 2007): Rhopalomeniidae is supposed to lack hook-shaped sclerites, as do three subfamilies within Pruvotinidae (Lophomeniinae Salvini-Plawen, 1978; Halomeniinae Salvini-Plawen, 1978; and Unciherpiinae Garcia-Alvarez, Ugorri & Salvini-Plawen, 2001), and hook-shaped sclerites have recently been found in *P. sopita* (Cobo et al 2024); the type of radula (if present) is the same (distichous) in both families; the lack of respiratory folds established for Rhopalomeniidae is also known for Pruvotinidae (*Pararrhopalia* Simroth, 1893; *Metamenia* Thiele, 1913; *Hypomenia* van Lummel, 1930, and *Forcepimenia* Salvini-Plawen, 1960) and the variety of ventrolateral foregut glands (A or C; García-Álvarez and Salvini-Plawen 2007) established within Rhopalomeniidae is also established in Pruvotinidae. Therefore, our findings warrant additional research using more conserved molecular markers to enhance our understanding of the relative phylogenetic placement of these families. Furthermore, a thoughtful review of the morphological characters and their significance is needed.

### **New insights from the Gulf of Mexico using ARMS**

Autonomous Reef Monitoring Structures (ARMS) are shown here, as in previous works, as a useful tool for biodiversity assessment and characterizing cryptic biodiversity (e.g., Brainard et al. 2009; Ransome et al. 2017; Hazeri et al. 2019; Vital et al. 2023). Moreover, this study highlights their use for live observations of relatively small and difficult-to-find taxa such as solenogasters, and thus their role in advancing the taxonomy and ecological knowledge. The findings of this study provide new data on the distribution of species within Dondersiidae and Pruvotinidae (Table 3).

To date, only two species of solenogasters from the Gulf had been formally described: *Proneomenia acuminata* Wirén, 1892, originally described from the Antilles and later recorded in the Florida Channel (Wirén 1892; Heath 1911) and *Spengelomenia bathybia* Heath, 1912 described from a specimen found among “a small collection of alcyonarian corals that had been secured from a cable ship operating to the Northwest of the Florida” (Heath 1912: 30). Besides these two species, the aplacophoran fauna of the Gulf of Mexico was documented in 1979 with the additional record of 134 specimens of unnamed Caudofoveata (Treece 1979).

Since then, eight Caudofoveata species have been formally described (*Chaetoderma felderi* Scheltema & Ivanov, 2007; *Chevroderma cuspidatum*, *Claviderma amplum*, *Spathoderma bulbosum*, *Claviderma mexicanum*, *Prochaetoderma gilrowei*, *Niteomica captainkiddae* and *Spathoderma quadratum*; Ivanov and Scheltema 2008) and numerous other specimens, including several unnamed Solenogastres, have been collected and are held in scientific collections, particularly at the Smithsonian National Museum of Natural History. Despite the substantial number of available specimens most solenogaster species from the Gulf of Mexico remain undescribed.

The Gulf of Mexico (GOM) faces significant anthropogenic pressures, notably from coastal human activities, the Mississippi River discharge, and the oil industry (McKinney et al. 2021). Moreover, although the GOM is considered a well-studied region, new species from various taxa, specially neglected small-bodied invertebrates, continue to be discovered (e.g., Hernández-Alcántara and Solís-Weiss 2000; Järnegren et al. 2007; Opresko et al. 2020; Ortiz and Cházaro-Olvera 2022, 2024). To protect this area and to create conservation figures, addressing gaps in biodiversity knowledge is essential. The two species included in this work (*D. tweedtae* sp. nov. and *E. bullescens* sp. nov.) constitute an example of these efforts.

## Conclusions

The findings reported here underscore the importance of ARMS as a sampling method to collect rare taxa and of integrative taxonomic approaches including the study and observation of living specimens. The identification of these remarkable new species offers fresh insights into the diversity, systematics, morphological variety, and ecology of the group. The obtained molecular data contributes to a growing database for solenogasters which is helping to accelerate the process of identification and species discovery, and advance understanding relationships within the group. However, available data for the group remains limited and continued work is necessary to represent much of its diversity. This research also marks a step forward in understanding the real diversity of Solenogastres from the Gulf of Mexico.

## Acknowledgements

We thank Drs. Chris Meyer, Sarah Tweedt, and Santiago Herrera for kindly sharing the specimens on which this study is based and for sharing their photographs of the living specimens. Thank you to Heather Shull, Savannah Bryant, and Mark Lehtonen for their help managing the collection. We also want to thank Scott Whittaker for his assistance with the photographs at the Scientific Imaging Lab of the NMNH.

## Additional information

### Conflict of interest

The authors have declared that no competing interests exist.

### Ethical statement

No ethical statement was reported.

## Funding

This work was supported by the United States National Science Foundation (NSF) grant number DEB-1846174 to KMK. The CYCLE project is funded by the NOAA's National Centers for Coastal Ocean Science, Competitive Research Program and Office of Ocean Exploration and Research under award NA18NOS4780166 to Santiago Herrera at Lehigh University.

## Author contributions

KMK and MCC conceived and designed research. MCC wrote the manuscript and made the figures. KMK and MCC supervised the work. WJF, CJO, and KMK conducted taxonomic work of *Dondersia tweedtae* sp. nov. MCC conducted taxonomic work of *Eleutherozenia bullescens* sp. nov. WJF and ELM conducted molecular laboratory work. ELM and MCC conducted molecular analysis. All authors read and approved the manuscript.

## Author ORCIDs

M. Carmen Cobo  <https://orcid.org/0000-0002-8481-2086>

William J. Farris  <https://orcid.org/0009-0001-8687-6657>

Chandler J. Olson  <https://orcid.org/0000-0002-1524-1339>

Emily L. McLaughlin  <https://orcid.org/0009-0006-0297-2067>

Kevin M. Kocot  <https://orcid.org/0000-0002-8673-2688>

## Data availability

All specimens are deposited in the collections of the National Museum of Natural History (NMNH), Smithsonian Institution, Washington DC. Specimens' occurrences are included in GBIF via the NMNH Extant Specimen Records dataset (<https://www.gbif.org/dataset/821cc27a-e3bb-4bc5-ac34-89ada245069d>). Generated sequences are deposited in the National Center for Biotechnology Information (<https://www.ncbi.nlm.nih.gov/>). This article is registered in ZooBank under <https://zoobank.org/C48FCB58-0A35-4D73-9EA1-D9943395ED0B>.

## References

- Aguado F, Marin A (2007) Warning coloration associated with nematocyst-based defences in aeolidiodean nudibranchs. *Journal of Molluscan Studies* 73(1): 23-28. <https://doi.org/10.1093/mollus/eyl026>
- Avila C (1995) Natural products of opisthobranch molluscs: a biological review. *Oceanography and Marine Biology: An Annual Review* 33: 487-559.
- Bergmeier FS, Haszprunar G, Todt C, Jörger KM (2016) Lost in a taxonomic Bermuda Triangle: comparative 3D-microanatomy of cryptic mesopsammic Solenogastres (Mollusca). *Organisms Diversity & Evolution* 16: 613-639. <https://doi.org/10.1007/s13127-016-0266-6>
- Bergmeier FS, Brandt A, Schwabe E, Jörger KM (2017) Abyssal Solenogastres (Mollusca, Aplacophora) from the Northwest Pacific: scratching the surface of deep-sea diversity using integrative taxonomy. *Frontiers in Marine Science* 4: 410. <https://doi.org/10.3389/fmars.2017.00410>
- Bergmeier, FS, Haszprunar, G, Brandt A, Saito H, Kano Y, Jörger KM (2019) Of basins, plains, and trenches: Systematics and distribution of Solenogastres (Mollusca, Aplacophora) in the Northwest Pacific. *Progress in Oceanography* 178: 102187. <https://doi.org/10.1016/j.pocan.2019.102187>

- Bergmeier FS, Ostermair L, Jörger KM (2021) Specialized predation by deep-sea Solenogastres revealed by sequencing of gut contents. *Current Biology* 31(13): R836-R837. <https://doi.org/10.1016/j.cub.2021.05.031>
- Boore JL, Brown WM (1994) Complete DNA sequence of the mitochondrial genome of the black chiton, *Katharina tunicata*. *Genetics* 138(2): 423-443. <https://doi.org/10.1093/genetics/138.2.423>
- Brainard R, Moffitt R, Timmers M, Paulay G, Plaissance L (2009) Autonomous reef monitoring structures (ARMS): a tool for monitoring indices of biodiversity in the Pacific Islands [Abstr]. 11<sup>th</sup> Pacific Science Inter-Congress. Papeete, Tahiti, 197 pp.
- Carbone M, Gavagnin M, Haber M, Guo Y-W, Fontana A, Manzo E, Genta-Jouve G, Tsoukatou M, Rudman WB, Cimino G, Ghiselin MT, Mollo E (2013) Packaging and delivery of chemical weapons: a Defensive Trojan Horse stratagem in chromodorid nudibranchs. *PLoS ONE* 8: e62075. <https://doi.org/10.1371/journal.pone.0062075>
- Cobo MC, Kocot KM (2021) On the diversity of abyssal Dondersiidae (Mollusca: Aplacophora) with the description of a new genus, six new species, and a review of the family. *Zootaxa* 4933 (1): 063–097. <https://doi.org/10.11646/zootaxa.4933.1.3>
- Cobo MC, McLaughlin EL, Kocot KM (2023) Four new Solenogastres (Mollusca, Aplacophora) from the South China Sea and parphyly of Proneomeniidae Simroth, 1893. *Invertebrate Systematics* 37(6): 301-333. <https://doi.org/10.1071/IS22062>
- Cobo, MC, Farris WJ, Kocot KM (2024) New data on the biodiversity of Solenogastres (Mollusca, Aplacophora) in the Mediterranean Sea: findings from the program “Our Planet Reviewed” Corsica 2019-2022. *Zoosystema* 46(21): 543-576. <https://doi.org/10.5252/zoosystema2024v46a21>
- Edmunds M (1966) Protective mechanisms in the Eolidacea (Mollusca Nudibranchia). *Zoological Journal of the Linnean Society* 46(308): 27-71. <https://doi.org/10.1111/j.1096-3642.1966.tb00082.x>
- Folmer O, Black M, Hoeh W, Lutz R, Vrijenhoek R (1994) DNA primers for amplification of mitochondrial cytochrome c oxidase subunit I from diverse metazoan invertebrates. *Molecular Marine Biology and Biotechnology* 3: 294–299.
- García-Álvarez O, Salvini-Plawen L (2007) Species and diagnosis of the families and genera of Solenogastres (Mollusca). *Iberus* 25 (2): 73–143.
- García-Álvarez O, Urgorri V, Cristobo FJ (2000) Synopsis of the interstitial Solenogastres (Mollusca). *Argonauta* 14(2):27-37.
- García-Gómez JC, Medina A, Coveñas R (1991) Formations (MDFs) of *Chromodoris* and *Hypselodoris* (Opisthobranchia: Chromodorididae). *Malacologia* 32(2): 233-240.
- Gil-Mansilla E, García-Álvarez O, Urgorri V (2008) Metodología para la recolección, conservación y estudio de los moluscos Solenogastros. *Reseñas Malacológicas XIII*: 1–31.
- Gil-Mansilla E, García-Álvarez O, Urgorri V (2009) A new genus and two new species of Simrothiellidae (Solenogastres: Cavibelonia) from the Abyssal Angola Basin. *Journal of the Marine Biological Association of the United Kingdom* 89(7): 1507-1515. <https://doi.org/10.1017/S0025315409000666>
- Goodheart JA, Bely AE (2017) Sequestration of nematocysts by divergent cnidarian predators: mechanism, function, and evolution. *Invertebrate Biology* 136(1): 75-91.
- Goodheart JA, Bleidisel S, Schillo D, Strong EE, Ayres DL, Preisfeld A, Collins AG, Cummings P, Wägele H (2018) Comparative morphology and evolution of the cnidosac in Cladobranchia (Gastropoda: Heterobranchia: Nudibranchia). *Frontiers in Zoology* 15: 43. <https://doi.org/10.1186/s12983-018-0289-2>

- Goodheart JA, Barone V, Lyons DC (2022) Movement and storage of nematocysts across development in the nudibranch *Berghia stephanieae* (Valdés, 2005). *Frontiers in Zoology* 19(1): 16. <https://doi.org/10.1186/s12983-022-00460-1>
- Greenwood P G (2009) Acquisition and use of nematocysts by cnidarian predators. *Toxicon* 54(8): 1065-1070. <https://doi.org/10.1016/j.toxicon.2009.02.029>
- Handl CH, Todt C (2005) Foregut glands of Solenogastres (Mollusca): anatomy and revised terminology. *Journal of Morphology* 265(1): 28-42. <https://doi.org/10.1002/jmor.10336>
- Harber M, Cerfeda S, Carbone M, Calado G, Gaspar H, Neves R, Maharajan V, Cimino G, Gavagnin M, Ghiselin MT, Mollo E (2010) Coloration and defense in the nudibranch gastropod *Hypselodoris fontandraui*. *The Biological Bulletin* 218(2): 181-188. <https://doi.org/10.1086/BBLv218n2p181>
- Haszprunar G, Schander C, Halanych, KM (2008). Relationships of higher molluscan taxa. *Phylogeny and Evolution of the Mollusca 1*: 18-32. <https://doi.org/10.1525/california/9780520250925.003.0002>
- Hazeri G, Rahayu DL, Subhan B, Sembiring A, Anggoro AW, Ghozali AT, Madduppa HH (2019) Latitudinal species diversity and density of cryptic crustacean (Brachyura and Anomura) in micro-habitat Autonomous Reef Monitoring Structures across Kepulauan Seribu, Indonesia. *Biodiversitas Journal of Biological Diversity* 20(5): 1466-1474. <https://doi.org/10.13057/biodiv/d200540>
- Heath H (1911) Reports on the scientific results of the expedition to the Tropical Pacific, in charge of Alexander Agassiz, by the US Fish Commission Steamer Albatross, from August 1899 to June 1900, Commander Jefferson F. Moser. XVI. 'The Solenogastres' *Memoirs of the Museum of Comparative Zoology at Harvard College* 45: 1-182.
- Heath H (1912) *Spengelomenia*, a new genus of Solenogastres. *Zoologische Jahrbücher [Suppl.]* 15: 465-479.
- Hernández-Alcántara P, Solís-Weiss V (2000) Magelonidae from the Mexican Pacific and northern Gulf of Mexico, with the description of a new genus (*Meredithia*) and four new species. *Bulletin of Marine Science* 67(1): 625-644.
- Hubrecht W (1888) *Dondersia festiva* gen. et spec. nov. Feestbundel aan Franciscus Cornelis Donders op den 27sten. Mei 1888, aangeboden door het Nederlandsch Tijdschrift voor Geneeskunde. F. van Rossen, Amsterdam, 324-339.
- Ivanov DL, Scheltema AH (2008) Western Atlantic Prochaetodermatidae from 35 N south to the Argentine Basin including the Gulf of Mexico (Mollusca: Aplacophora). *Zootaxa* 1885(1): 1-60. <https://doi.org/10.11646/zootaxa.1885.1.1>
- Järnegren J, Schander C, Sneli JA, Rønningen V, Young CM (2007) Four genes, morphology and ecology: distinguishing a new species of *Acesta* (Mollusca; Bivalvia) from the Gulf of Mexico. *Marine Biology* 152: 43-55. <https://doi.org/10.1007/s00227-007-0651-y>
- Katoh K, Misawa K, Kuma KI, Miyata T (2002) MAFFT: a novel method for rapid multiple sequence alignment based on fast Fourier transform. *Nucleic Acids Research* 30(14): 3059-3066. <https://doi.org/10.1093/nar/gkf436>
- Klink SP, Bergmeier FS, Neusser TP, Jörger KM. (2015) Stranded on a lonely island: description of *Dondersia* (?) *todtae* sp. nov., the first shelf solenogaster (Mollusca, Aplacophora) from the Azores. *Açoreana* 10: 603-618.
- Kocot KM, Cannon JT, Todt C, Citarella MR, Kohn AB, Meyer A, Santos SR, Schander C, Moroz LL, Lieb B, Halanych KM (2011) Phylogenomics reveals deep molluscan relationships. *Nature* 477(7365): 452-456. <https://doi.org/10.1038/nature10382>
- Kocot KM, Todt C, Mikkelsen NT, Halanych KM (2019) Phylogenomics of Aplacophora (Mollusca, Aculifera) and a solenogaster without a foot. *Proceedings of the Royal Society B* 286(1902): 20190115. <https://doi.org/10.1098/rspb.2019.0115>

- Maddison WP, Maddison DR (2023) Mesquite: a modular system for evolutionary analysis. Version 3.81. <http://www.mesquiteproject.org>
- Martinez-Sanjuán JM (2024) Moluscos solenogastos Pruvotinidae de las campañas IceAge: estudio morfoanatómico en 3D y sistemática molecular (Doctoral dissertation, Universidade de Santiago de Compostela).
- McKinney LD, Shepherd JG, Wilson CA, Hogarth WT, Chanton J, Murawski SA, Sutuon ST, Yoskowitz D, Wowk K, Özgökmen TM, Joye SB, Caffey R (2021) The Gulf of Mexico. *Oceanography* 34(1): 30-43. <https://doi.org/10.5670/oceanog.2021.115>
- Meyer A, Todt C, Mikkelsen NT, Lieb B (2010) Fast evolving 18S rRNA sequences from Solenogastres (Mollusca) resist standard PCR amplification and give new insights into mollusk substitution rate heterogeneity. *BMC evolutionary biology* 10: 1-12. <https://doi.org/10.1186/1471-2148-10-70>
- Minh BQ, Schmidt HA, Chernomor O, Schrempf D, Woodhams MD, Von Haeseler A, Lanfear R. (2020). IQ-TREE 2: new models and efficient methods for phylogenetic inference in the genomic era. *Molecular biology and evolution* 37(5): 1530-1534. <https://doi.org/10.1093/molbev/msaa015>
- Moles J, Núñez-Pons L, Taboada S, Figuerola B, Cristobo J, Avila C (2015) Anti-predatory chemical defences in Antarctic benthic fauna. *Marine Biology* 162: 1813–1821. <https://doi.org/10.1007/s00227-015-2714-9>
- Neves R, Gaspar H, Calado G. (2009) Does a shell matter for defence? Chemical deterrence in two cephalaspidean gastropods with calcified shells. *Journal of Molluscan Studies* 75(2): 127-131. <https://doi.org/10.1093/mollus/eyp004>
- Nierstrasz HF (1902) The Solenogastres of the Siboga-Expedition. In: Weber M (Ed.) *Uitkomsten op Zoologisch, Botanisch, Oceanographisch en Geologisch Gebied verzameld in Nederlandsch Oost-Indië 1899-1900 aan boord H.M. Siboga onder commando van Luitenant ter zee 1e. kl. G.F. Tydeman. Siboga-Expeditie Monographie* 47(Livraison 5): 1-46. <https://doi.org/10.5962/bhl.title.10915>
- Obst M, Exter K, Allcock AL, Arvanitidis C, Axberg A, Bustamante M, Cancio I, Carreira-Flores D, Chatzinikolaou E, Chatzigeorgiou G, Christmas N, Clark MS, Comtet T, Dailianis T, Davies N, Deneudt KI, de Cerio O D, Fortič A, Gerovasileiou V, Hablützel Pascal I, Keklikoglou K, Kotoulas G, Lasota R, Leite BR, Loisel S, Lévêque L, Levy L, Malachowicz M, Mavrič B, Meyer C, Mortelmans J, Norkko J, Pade N, Power AM, Ramšak A, Reiss H, Solbakken J, Staehr PA, Sundberg P, Thyrring J, Troncoso JS, Viard F, Wenne R, Yperifanou EI, Zbawicka MPavlouci C (2020) A marine biodiversity observation network for genetic monitoring of hard-bottom communities (ARMS-MBON). *Frontiers in Marine Science* 7: 572680. <https://doi.org/10.3389/fmars.2020.572680>
- Okusu A, Giribet G (2003) New 18S rRNA sequences from neomenioid aplacophorans and the possible origin of persistent exogenous contamination. *Journal of Molluscan Studies* 69(4): 385-387. <https://doi.org/10.1093/mollus/69.4.385>
- Opresko D M, Goldman SL, Johnson R, Parra K, Nuttall M, Schmahl GP, Brugler MR (2020) Morphological and molecular characterization of a new species of black coral from Elvers Bank, north-western Gulf of Mexico (Cnidaria: Anthozoa: Hexacorallia: Antipatharia: Aphanipathidae: Distichopathes). *Journal of the Marine Biological Association of the United Kingdom* 100(4): 559-566. <https://doi.org/10.1017/S002531542000051X>
- Ortiz M, Cházaro-Olvera S (2022) A new species of the genus *Eudevenopus* (Crustacea: Amphipoda: Platyschnopidae) from the Gulf of Mexico. *Revista Mexicana de biodiversidad* 93: e933852. <https://doi.org/10.22201/ib.20078706e.2022.93.3852>

- Ortiz M, Cházaro-Olvera S (2024) A new species of the genus *Upogebia* Leach, 1802 (Crustacea, Decapoda, Upogebiidae) from the north coast of Cuba. *Novitates Caribaea* (24):11-18. <https://doi.org/10.33800/nc.vi24.354>
- Paul VJ, Ritson-Williams R (2008) Marine chemical ecology. *Natural Product Reports* 25(4): 662-695. <https://doi.org/10.1039/b702742g>
- Pedrouzo L, García-Álvarez Ó, Urgorri V (2022) New species of Pruvotininae (Solenogastres, Cavibelonia) from bathyal bottoms off the NW Iberian Peninsula, with a taxonomical discussion about the family Pruvotinidae. *Iberus* 40(2): 317-354.
- Pruvot G (1890) Sur quelques Néoméniées nouvelles de la Méditerranée. *Archives de Zoologie Expérimentale et Générale* (2)8: notes, [xxi-xxiv].
- Pruvot G (1891) Sur l'organisation de quelques Néoméniens des côtes de France. *Archives de Zoologie Expérimentale et Générale* 2(9): 699-805.
- Ransome E, Geller JB, Timmers M, Leray M, Mahardini A, Sembiring A, Collins AG, Meyer CP (2017) The importance of standardization for biodiversity comparisons: A case study using autonomous reef monitoring structures (ARMS) and metabarcoding to measure cryptic diversity on Moorea coral reefs, French Polynesia. *PLoS ONE* 12(4): e0175066. <https://doi.org/10.1371/journal.pone.0175066>
- Ros J (1977) La defensa en los opisthobranchios. *Investigación y Ciencia* 12: 48-60.
- Rudman WB (1984) The Chromodorididae (Opisthobranchia: Mollusca) of the Indo-West Pacific: a review of the genera. *Zoological Journal of the Linnean Society* 81(2-3):115-273. <https://doi.org/10.1111/j.1096-3642.1984.tb01174.x>
- Salvini-Plawen L (1967) Kritische Bemerkungen zum System der Solenogastres (Mollusca, Aculifera). *Zeitschrift für zoologische Systematik und Evolutionsforschung* 5: 398-444.
- Salvini-Plawen L (1972) Cnidaria as food-sources for marine invertebrates. *Cahiers de Biologie Marine* 13(3): 385-400.
- Salvini-Plawen L (1978) Antarktische Und Subantarktische Solenogastres. Eine Monographie: 1898-1974. *Zoologica (Stuttgart)* 128: 1-155.
- Salvini-Plawen L (1980) A reconsideration of systematics in the Mollusca. *Malacologia* 19: 249-278.
- Salvini-Plawen L (1986) Einige Solenogastres (Mollusca) der europäischen meiofauna. *Annalen Des Naturhistorischen Museums in Wien Serie B Für Botanik Und Zoologie*, 373-385.
- Salvini-Plawen L (2003a) On the phylogenetic significance of the aplacophoran Mollusca. *Iberus* 21: 67-97.
- Salvini-Plawen L (2003b) Contributions to West-Mediterranean Solenogastres (Mollusca) with three new species. *Iberus* 21(2): 37-60.
- Salvini-Plawen L (2008) Three new species of Simrothiellidae (Solenogastres) associated with the hot-vent biotope. *Journal of Molluscan Studies* 74(3): 223-238. <https://doi.org/10.1093/mollus/eyn010>
- Salvini-Plawen L, Ozturk B (2006) New records of Caudofoveata (*Falcidens guttuosus*, *Prochaetoderma raduliferum*) and of Solenogastres (*Eleutheromenia carinata*, spec. nov.) from the eastern Mediterranean Sea (Mollusca). *Spixiana* 29(3): 217-224.
- Salvini-Plawen L, Steiner G (2014) The Testaria concept (Polyplacophora + Conchifera) updated. *Journal of Natural History* 48(45-48): 2751-2772. <https://doi.org/10.1080/00222933.2014.964787>
- Scheltema AH (1978) Position of the Class Aplacophora in the phylum Mollusca. *Malacologia* 17: 99-109.

- Scheltema AH (1993) Aplacophora as progenetic aculiferans and the coelomate origin of mollusks as the sister taxon of Sipuncula. *The Biological Bulletin* 184(1): 57–78. <https://doi.org/10.2307/1542380>
- Scheltema AH (1996) Phylogenetic position of Sipuncula, Mollusca and the progenetic Aplacophora. In *Origin and Evolutionary Radiation of the Mollusca* (Ed. J. D. Taylor), 53–58. Oxford University Press, Oxford. <https://doi.org/10.1093/oso/9780198549802.003.0003>
- Scheltema AH (1999) New eastern Atlantic neomenioid aplacophoran molluscs (Neomeniamorpha, Aplacophora). *Ophelia* 51: 1–28. <https://doi.org/10.1080/00785326.1999.10409397>
- Scheltema AH (2008) Biogeography, diversity, and evolution through vicariance of the hydrothermal vent aplacophoran genus *Helicoradomenia* (Aplacophora, Mollusca). *Journal of Shellfish Research* 27(1): 91–96. [https://doi.org/10.2983/0730-8000\(2008\)27\[91:BDAETV\]2.0.CO;2](https://doi.org/10.2983/0730-8000(2008)27[91:BDAETV]2.0.CO;2)
- Scheltema AH, Jebb M (1994) Natural history of a solenogaster mollusc from Papua New Guinea, *Epimения australis* (Thiele) (Aplacophora: Neomeniomorpha). *Journal of Natural History* 28(6): 1297–1318. <https://doi.org/10.1080/00222939400770661>
- Scheltema AH, Schander C (2000) Discrimination and phylogeny of solenogaster species through the morphology of hard parts (Mollusca, Aplacophora, Neomeniomorpha). *Biological Bulletin* 198: 121–151. <https://doi.org/10.2307/1542810>
- Scheltema AH, Schander C, Kocot KM (2012) Hard and soft anatomy in two genera of Dondersiidae (Mollusca, Aplacophora, Solenogastres). *Biological Bulletin* 222(3): 233–269. <https://doi.org/10.1086/BBLv222n3p233>
- Scherholz M, Redl E, Wollesen T, Todt C, Wanninger A, (2013) Aplacophoran mollusks evolved from ancestors with polyplacophoran-like features. *Current Biology* 21: 2130–2134. <https://doi.org/10.1016/j.cub.2013.08.056>
- Sigwart JD, Sutton MD (2007) Deep molluscan phylogeny: synthesis of palaeontological and neontological data. *Proceedings of the Royal Society B: Biological Sciences* 274(1624): 2413–2419. <https://doi.org/10.1098/rspb.2007.0701>
- Todt C (2013) Aplacophoran mollusks—still obscure and difficult? *American Malacological Bulletin* 31(1): 181–187. <https://doi.org/10.4003/006.031.0110>
- Treece GD (1979) Four new records of aplacophorous mollusks from the Gulf of Mexico. *Bulletin of Marine Science* 29(3): 344–364.
- Vinther, J., 2014. A molecular palaeobiological perspective on aculiferan evolution. *Journal of Natural History* 48(45–48): 2805–2823. <https://doi.org/10.1080/00222933.2014.963185>
- Vinther J, Sperling EA, Briggs DEG, Peterson KJ (2012) A molecular palaeobiological hypothesis for the origin of aplacophoran molluscs and their derivation from chiton-like ancestors. *Proceedings of the Royal Society B: Biological Sciences* 279(1732): 1259–1268. <https://doi.org/https://doi.org/10.1098/rspb.2011.1773>
- Vital XG, Palomino-Alvarez LA, Ortigosa D, Guerra-Castro EJ, Simões N (2023) Sea slugs (Gastropoda: Heterobranchia) associated with Autonomous Reef Monitoring Structures (ARMS) in southern Gulf of Mexico and Mexican Caribbean Sea. *Journal of the Marine Biological Association of the United Kingdom* 103: e50. <https://doi.org/10.1017/S0025315423000334>
- Wägele H, Klussmann-Kolb A (2005) Opisthobranchia (Mollusca, Gastropoda)—more than just slimy slugs. Shell reduction and its implications on defence and foraging. *Frontiers in Zoology* 2: 1–18. <https://doi.org/10.1186/1742-9994-2-3>

- Wägele H, Knezevic K, Moustafa, AY (2022) Defensive acid-secreting glands in Cypraeoidea (Caenogastropoda, Mollusca). *Molluscan Research* 42(4): 320–327. <https://doi.org/10.1080/13235818.2022.2124581>
- Winters AE., White AM, Dewi AS., Mudianta IW, Wilson NG, Forster LC, Garson MJ, Cheney KL (2018) Distribution of defensive metabolites in nudibranch molluscs. *Journal of Chemical Ecology* 44: 384–396. <https://doi.org/10.1007/s10886-018-0941-5>
- Wirén A (1892) Studien über die Solenogastren. II. *Chaetoderma productum*, *Neomenia*, *Proneomenia acuminata*. [Studies on the Solenogastra. II. *Chaetoderma productum*, *Neomenia*, *Proneomenia acuminata*.] *Kungliga Svenska Vetenskaps-Akademiens Handlingar* 25(6): 1–99.
- Yap-Chiongco M K, Bergmeier FS, Roberts NG, Jörger KM, Kocot KM (2024) Phylogenomic reconstruction of Solenogastres (Mollusca, Aplacophora) informs hypotheses on body size evolution. *Molecular Phylogenetics and Evolution* 194: 108029. <https://doi.org/10.1016/j.ympev.2024.108029>
- Zamarro M, García-Álvarez O, Urgorri V (2013) Three new species of Pruvotinidae (Mollusca: Solenogastres) from Antarctica and NW Spain. *Helgoland Marine Research* 67(3): 423–443. <https://doi.org/10.1007/s10152-012-0333-0>
- Zimmerman TL, Martin JW (2004) Artificial reef matrix structures (ARMS): an inexpensive and effective method for collecting coral reef-associated invertebrates. *Gulf and Caribbean Research* 16(1): 59–64. <https://doi.org/10.18785/gcr.1601.08>

# Taxonomic and molecular characterization of *Pseudosteringophorus profundis* sp. nov. (Digenea, Fellodistomidae), a parasite of *Macrourus holotrachys* Günther, 1878 (Gadiformes, Macrouridae) from the deep sea southeastern Pacific Ocean

Marcelo E. Oliva<sup>1,2</sup>, Fabiola A. Sepúlveda<sup>3</sup>, Rubén Escribano<sup>2</sup>, Luis A. Ñacari<sup>2,4</sup>

1 Instituto Ciencias Naturales Alexander von Humboldt, Universidad de Antofagasta, Angamos 601, Antofagasta, Chile

2 Instituto Milenio de Oceanografía, Universidad de Concepción, Concepción, Chile

3 Laboratorio de Eco – Parasitología y Epidemiología Marina, Facultad de Ciencias del Mar y Recursos Biológicos, Universidad de Antofagasta, 601 Angamos, Antofagasta 1240000, Chile

4 Laboratorio de Ecología y Evolución de Parásitos, Facultad de Ciencias del Mar y Recursos Biológicos, Universidad de Antofagasta, 601 Angamos, Antofagasta 1240000, Chile

Corresponding author: Luis A. Ñacari ([luis.nacari.enciso@ua.cl](mailto:luis.nacari.enciso@ua.cl))



Academic editor: David Gibson

Received: 20 August 2024

Accepted: 15 November 2024

Published: 31 December 2024

ZooBank: <https://zoobank.org/26824BD6-7720-4EDD-BE00-60A5F9A2A0C8>

**Citation:** Oliva ME, Sepúlveda FA, Escribano R, Ñacari LA (2024) Taxonomic and molecular characterization of *Pseudosteringophorus profundis* sp. nov. (Digenea, Fellodistomidae), a parasite of *Macrourus holotrachys* Günther, 1878 (Gadiformes, Macrouridae) from the deep sea southeastern Pacific Ocean. ZooKeys 1221: 435–447. <https://doi.org/10.3897/zookeys.1221.135086>

Copyright: © Marcelo E. Oliva et al.  
This is an open access article distributed under terms of the Creative Commons Attribution License (Attribution 4.0 International – CC BY 4.0).

## Abstract

*Pseudosteringophorus profundis* sp. nov. a new species of deep-sea digenean, parasitizing the gallbladder of the “Bigeye grenadier” (*Macrourus holotrachys* Günther, 1878) in the deep waters of the southeastern Pacific Ocean is described on the basis of morphological and molecular (28S rRNA) data. The new species is distinguishable from *Pseudosteringophorus hoplognathi* Yamaguti, 1940, the only other member of the genus, by its subterminal oral sucker, the position of the ovary and testes, the larger anterior seminal vesicle compared to the posterior one, and its larger eggs. In addition, the new species is a parasite of a deep-sea fish, whereas *P. hoplognathi* is a parasite of shallow-water fish. A phylogenetic tree, based on 28S rDNA sequences, indicates that this species is included in a clade of deep-sea fellodistomid species (*Steringophorus* spp.). We provide the first molecular data on the genus *Pseudosteringophorus* Yamaguti, 1940 and expand the molecular database for the family Fellodistomidae. Further studies, including sequences from other fellodistomid taxa, are needed to more precisely infer relationships within this family.

**Key words:** 28S rDNA, Bigeye grenadier, cox1 mDNA, deep-sea fishes, gallbladder parasite, integrative taxonomy, new species, southeastern Pacific Ocean

## Introduction

The deep sea is one of the world’s most vulnerable and unexplored ecosystems and is considered an important reservoir of biodiversity (Danovaro et al. 2010; Ramirez-Llodra et al. 2010). Knowledge of this biodiversity remains scarce (Danovaro et al. 2010) and this is particularly true for the deep waters of the southeastern Pacific Ocean (SEPO) (Danovaro et al. 2002; Sabbatini et al. 2002; Gambi et al. 2003; Fujii et al. 2013; Weston et al. 2021; Ramírez-Flandes et al. 2022). Parasites are a critical component in aquatic ecosystems and

play important roles in the food web and the population dynamics of hosts (McLaughlin et al. 2020). Knowledge of metazoan parasites, especially Digenea in deep-water fishes from SEPO, is limited (Rodríguez and George-Nascimento 1996; Oliva et al. 2008; Salinas et al. 2008; Ñacari and Oliva 2016; Espínola-Novelo et al. 2018; Ñacari et al. 2022).

A few families of digeneans (Fellodistomidae Nicoll, 1909, Gonocercidae Skrjabin & Guschanskaja, 1955, Gorgoderidae Looss, 1899, Hemiuridae Looss, 1899, Lecithasteridae Odhner, 1905, Lepidapedidae Yamaguti, 1958, Opecoelidae Ozaki, 1925, Zoogonidae Odhner, 1902) are reported from the deep sea, especially in bathyal areas (>1000 m) (Bray 2020). So far, 23 species of digeneans are recorded as parasites of fishes of the genus *Macrourus* (Gadiformes) of which nine species parasitize *Macrourus holotrachys* Günther, 1878 (Münster et al. 2016; Ñacari et al. 2022). In this study, we describe a new species of digenean, *Pseudosteringophorus profundis* sp. nov. (Fellodistomidae) from the gallbladder of *M. holotrachys* collected in the deep sea off northern Chile based on morphological and molecular analyses.

## Material and methods

### Collection and morphological analysis

Thirty-six adult specimens of *M. holotrachys* were obtained periodically during 2017 as bycatch from the artisanal longline fishery (9.26 km length) of the Patagonian toothfish, *Dissostichus eleginoides* Smitt, 1898, in northern Chile ( $\approx 22^{\circ}30'S$ ,  $70^{\circ}40'W$ ) at depths between 1000 and 2000 m. The fish were frozen onboard at  $-18^{\circ}C$  immediately after capture and transported to the parasitology laboratory at the Universidad de Antofagasta for further analysis. Digeneans were removed from the gallbladder, fixed in AFA (ethanol: formalin: acetic acid), preserved in 70% ethanol and stained with acetocarmine or Gomori's thrichrome, dehydrated in an alcohol series (70% to 100%), cleared in oil of clove® (Sigma-Aldrich, Madagascar) and mounted in Entellan (Merck-Millipore, Billerica, Massachusetts). Illustrations were prepared with Adobe Illustrator CS9 from draft line drawings made with a camera lucida. Measurements are in micrometres and are given as the range followed by the mean in parentheses. Taxonomic identification of fellodistomids follows Bray (2002). Paratypes of *Pseudosteringophorus hoplognathi* and *Benthotrema hoplognathi* Yamaguti, 1938 (MPM coll. 23037 and coll. 230370, respectively) were examined.

### DNA extraction, amplification and sequencing

DNA was isolated from two Fellodistominae specimens following a modified version of the salting out protocol (Miller et al. 1988). This involved treatment with sodium dodecyl sulphate, digestion with proteinase K, NaCl protein precipitation, and subsequent ethanol precipitation. The DNA was eluted in nuclease-free water and quantified using a BioSpec-nano spectrophotometer (Shimadzu, Japan).

For the molecular analyses, regions within the 28S ribosomal DNA large subunit (LSU rDNA) and the mitochondrial cytochrome c oxidase 1 gene (*cox1* mDNA) were amplified by polymerase chain reaction (PCR). The LSU rDNA region 28S

was amplified by PCR using the forward primer C1 (5'-ACCCGCTGAATTTAAG-CAT-3') and reverse primer D2 (5'-TGGTCCGTGTTTCAAGAC-3') (Chisholm et al. 2001); *cox1* mtDNA was amplified using the forward primer JB3 (5'-TTTTTTGGG-CATCCTGAGGTTTAT-3') and the reverse primer COX1 (5'-AATCATGATGCAAAAG-GTA-3') (Leung et al. 2009). The reaction was carried out in a final volume of 35  $\mu$ L comprising five standard units of GoTaq DNA polymerase (Promega), 7  $\mu$ L of 5 $\times$  PCR buffer, 5.6  $\mu$ L of MgCl<sub>2</sub> (25 mM), 2.1  $\mu$ L of BSA (10 mg/mL), 0.7  $\mu$ L of deoxynucleotide triphosphate (dNTP; 10 mM), 10 pM of each primer, 3  $\mu$ L of template DNA, and sufficient nuclease-free H<sub>2</sub>O to make the total volume up to 35  $\mu$ L. A Boeco Ecogermany M-240R Thermal Cycler (Boeckel, Hamburg, Germany) was used to carry out PCR for LSU rDNA and *cox1* mDNA using the programs reported in Chisholm et al. (2001) and Leung et al. (2009) respectively. The PCR products were sent to Macrogen (Seoul, Korea; <http://www.macrogen.com>) for purification and sequencing of both the DNA forward and reverse strands. The sequences were edited and contigs were assembled using ProSeq 2.9 beta (Filatov 2002). New sequences obtained were compared with the GenBank databases through a nucleotide BLAST (<https://blast.ncbi.nlm.nih.gov/Blast.cgi>). All unique sequences obtained during this study were deposited into GenBank (28S rDNA: PQ109082–PQ109083; *cox1* mDNA: PQ110033–PQ110034).

For phylogenetic analysis, new 28S rDNA sequences obtained in this study were aligned with those of 31 members of Fellodistomidae available in GenBank, 28 sequences belonging to Fellodistominae and three sequences belonging to Tergestiinae (Suppl. material 1). The sequence of *Prosogonarium angelae* Cribb & Bray, 1994 (Tandanicolidae Johnston, 1927) was used as an outgroup, following Bray and Waeschenbach (2020). The alignment was performed using Mafft v.7 (Katoh et al. 2019) with the Q-INS-i algorithm. The aligned sequences were then visualized in ProSeq v. 2.91 (Filatov 2002) and trimmed at the ends. Poorly aligned positions were removed using Gblocks 0.91b (Castresana 2000). Phylogenetic reconstruction was performed using Bayesian inference (BI) and maximum-likelihood (ML) analyses. The jModelTest v. 0.1.1 tool (Posada 2008) was used to identify the best evolutionary model under the Corrected Akaike information criterion (Akaike 1973).

The best model for 28S rDNA aligned sequences was GTR+I+G. The BI analyses were conducted using MrBayes v. 3.2.2 (Ronquist et al. 2012) with the following parameters: nst = 6 and rates invgamma according to the evolutionary model determined by jModelTest. The analysis was performed for 10,000,000 generations, with one run of four chains, sampling every 1000 generations. The initial 25% was discarded as burn-in. Visual inspection of log-likelihood scores against generation time was performed in TRACER v. 1.7 (Rambaut et al. 2018). Support for nodes in the BI tree topology was obtained by posterior probability (PP). The ML analyses were performed using W-IQ-TREE (<http://iqtree.cibiv.univie.ac.at/> accessed on 18 July 2024), with 1000 bootstrap replicates for statistical support. The trees were visualized and edited in FigTree v. 1.4.4 (<http://tree.bio.ed.ac.uk/software/figtree/>). Finally, the pairwise p-distances for 28S rDNA were analyzed using the MEGA v. 6 software (Tamura et al. 2013).

Following Muff et al. (2022) we defined the following five categories for BI nodal support as: PP = 1: fully supported; PP = 0.99–0.90: strongly supported; PP = 0.89–0.80: moderately support; PP = 0.79–0.70: weakly supported; PP = < 0.69: not supported.

## Result

### Taxonomy

#### Family Fellodistomidae Nicoll, 1909

#### Genus *Pseudosteringophorus* Yamaguti, 1940

#### *Pseudosteringophorus profundis* sp. nov.

<https://zoobank.org/BCBF8A63-920C-4795-849D-A1F20E7A99B1>

Fig. 1A, B

**Host.** *Macrourus holotrachys* Günther, 1878 (Gadiformes: Macrouridae).

**Site of infection.** Gallbladder.

**Type locality.** northern Chile ( $\approx 22^{\circ}30'S$ ,  $70^{\circ}40'W$ ), at depth ranging from 1000 to 2000 m.

**Prevalence.** 21 of 36 (39%).

**Intensity.** 1–333 (17).

**Material examined.** • **Holotype:** (MPM coll. no. 25292) and two **paratypes** (MPM coll. no. 25293) in the Meguro Parasitological Museum, Tokyo, Japan (MPM) • Three **paratypes** (MNHCL PLAT-15073-15075) in the Museo Nacional de Historia Natural, Santiago, Chile • Three **paratypes** (MUSM-HEL 5480) in the Museo de Historia Natural, Universidad Nacional Mayor de San Marcos, Lima, Peru (MHN-UNMSM).

**Representative DNA sequences.** GenBank accession number, 28S rDNA (PQ109082–PQ109083) and *cox1* mDNA (PQ110033–PQ110034).

**Differential diagnosis.** The new species belongs to the family Fellodistomidae, a large family of marine fish digeneans characterized by restricted fields of vitelline follicles (Bray 2002). The new species *Pseudosteringophorus profundis* was assigned to the genus *Pseudosteringophorus* based on morphological characteristics typical of the genus, including a fusiform body, intestinal bifurcation in mid-forebody, caeca reaching ventral suckers, internal vesicle seminal bipartite, ovary dextrodorsal and entire, Y-shaped excretory vesicle, and eggs without spines (Bray 2002). Until now, the genus was monotypic, with *Pseudosteringophorus hoplognathi* Yamaguti, 1940, from the intestine of *Oplegnathus punctatus* (Temminck & Schlegel, 1844) from Hamazima, Japan, being the only recorded species. Machida et al. (2007) later examined *P. hoplognathi* from the intestine of *Oplegnathus fasciatus* (Temminck & Schlegel, 1844) at the Tokyo Wholesale Market (NSMT-PI 798), which are larger than Yamaguti's specimens and divided into two groups (large and small specimens) (Table 1). *Pseudosteringophorus profundis* sp. nov. differs from both Yamaguti's and Machida's specimens of *P. hoplognathi* by: (1) ovary overlapping the right testes and close to the anterior margin of ventral sucker, whereas in *P. hoplognathi* the ovary is pretesticular; (2) testes are asymmetrical, behind and partly overlapping the ventral sucker, while in *P. hoplognathi*, they are symmetrical and situated in the anterior hindbody; and (3) egg size is larger ( $35\text{--}50 \times 21\text{--}30 \mu\text{m}$ ) compared to *P. hoplognathi* ( $27\text{--}34 \times 15\text{--}20 \mu\text{m}$  in Yamaguti (1940), and  $21\text{--}26 \times 13\text{--}16 \mu\text{m}$  in Machida et al. (2007) (Table 1). The site of infection also differs: the intestine for *P. hoplognathi* but gall bladder for the new species. In addition, the new species is a parasite of a deep-sea gadiform whereas *P. hoplognathi* parasitizes a shallow-water centrarchiform.

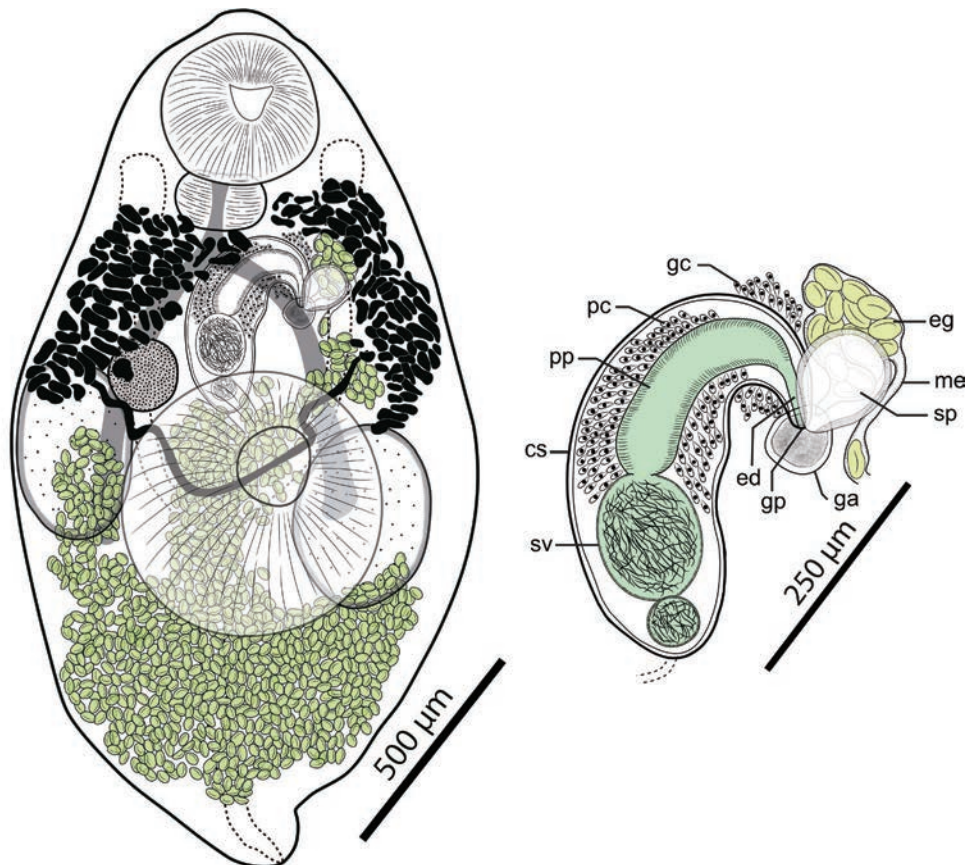


**Figure 1.** *Pseudosteringophorus profundis* sp. nov. **A** holotype, ventral view **B** terminal genitalia, ventral view. Abbreviations: gc: glandular cells; pc: prostate cells; pp: pars prostatica; sv: seminal vesicle; ed: ejaculatory duct; gp: genital pore; ga: atrium genital; sp: spermatophore; me: metaterm; eg: eggs.

**Description.** (Based on 11 stained whole-mounts, Table 1, Fig. 1A, B) Body fusiform, more pointed at posterior than at extremity anterior, 1313–2120 (1747) in length, with maximum breadth of 673–1030 (873) at ventral sucker level. Oral sucker subterminal, rounded, with ventral concavity in lateral view, 269–413 (335) × 299–395 (346). Ventral sucker bowl-shaped, 358–561 (456) × 377–622 (468), near mid-body. Sucker ratio 1.1–1.8 (1.4). Forebody 41.8–53.5 (47.3) % of body length. Prepharynx very short. Pharynx subglobular, 112–211 (147) × 145–192 (167). Esophagus indistinct bifurcates to form intestinal caeca in mid-forebody. Caeca blind, ending at mid-acetabular level.

Testes two, ovoid asymmetrical, one on each body side, posterior to and partly overlapping ventral sucker; right testis 218–389 (320) × 129–307 (237) and left testis 205–432 (319) × 108–338 (236). Cirrus sac elliptical, with anterior end turned sinistral toward genital atrium, with thick wall of inner circular and outer longitudinal muscle fibers, extending to obliquely just inside of right caecum with posterior end passing dorsal to anterior border of ventral sucker, containing seminal vesicle, pars prostatica and short ejaculatory duct opening into genital atrium. Seminal vesicle internal, thin-walled, bipartite, constricted into unequal chambers; anterior chamber 72–136 (109) × 58–122 (90); posterior chamber 39–79 (52) × 30–75 (49). Pars prostatica long, cylindrical surrounded by prostatic cells. Genital pore in left submedian line at anterior part of middle third of body, just ventral and opening to left caecum. Genital atrium wide, muscular. Spermatophore detected attached to genital atrium in several individuals.

**Table 1.** Morphometric data comparisons of *Pseudosteringophorus hoplognathi* and our specimens of *P. profundis* sp. nov. Measurements are shown in  $\mu\text{m}$  with the mean followed by the range (when available).

	<i>Pseudosteringophorus hoplognathi</i>	<i>Pseudosteringophorus hoplognathi</i>	<i>Pseudosteringophorus hoplognathi</i>	<i>Pseudosteringophorus profundis</i> sp. nov.
Definitive host	<i>Oplegnathus punctatus</i>	<i>Oplegnathus fasciatus</i>	<i>Oplegnathus fasciatus</i>	<i>Macrourus holotrachys</i>
Author	Yamaguti 1940	Machida et al. 2007*	Machida et al. 2007*	This study
Specimens examined		10	4	11
Body length	1100–1800	2330–2880	2020–2380	1313–2120 (1747)
Body width	300–480	1150–1430	670–780	673–1030 (873)
Ratio body length:width		2	3.0–3.1	1.7–2.3 (2.0)
Oral sucker length	160–280	340–450	210–240	269–413 (335)
Oral sucker width	100–200	340–420	160–210	299–395 (346)
Pharynx length	39–60			112–211 (147)
Pharynx width	45–54			145–192 (167)
Esophagus length	60–150			32–32 (32)
Ventral sucker length		490–690	260–340	358–561 (456)
Ventral sucker width	175–310	680–900	280–370	377–622 (468)
ratio oral sucker/ ventral sucker	0.65–0.67	1: 1.8–2.4	1:1.6–1.8	1.1–1.8 (1.4)
Forebody length				623–947 (820)
Forebody (%) of body length		48–54	43–52	41.8–53.5 (47.3)
Hindbody length				250–724 (481)
Hindbody (%) of body length				18.0–34.3 (27.0)
Right testes length		280–340	200–290	218–389 (320)
Right testes width		200–280	170–240	129–307 (237)
Left testes length		250–320	210–260	205–432 (319)
Left testes width		180–240	170–210	108–338 (236)
Testes length (average)	110–160	265–330	205–275	220.5–410.5 (319.7)
Testes width (average)	90–140	190–260	170–225	122.5–322.5 (236.5)
Cirrus pouch length	250–360	660–740	520–570	365–617 (522)
Cirrus pouch width	70–135	240–290	180–200	78–169 (135)
Posterior seminal vesicle length	45–60			72–136 (109)
Posterior seminal vesicle width	24–48			58–122 (90)
Anterior seminal vesicle length	50–105			39–79 (52)
Anterior seminal vesicle width	24–60			30–75 (49)
Ovary length	100–150	230–320	180–240	105–197 (155)
Ovary width	70–95	150–200	90–190	82–221 (134)
Eggs length	27–34	21–24	23–26	34.6–49.5 (45.2)
Eggs width	15–20	15–16	13–16	21.4–29.6 (25.8)

\* Measurements of larger and smaller specimens of Machida et al. (2007), respectively.

Ovary ovoid to spherical, 105–197 (155) × 82–221 (134), dextrodorsal to ventral sucker, near or overlapping right testes. Proximal region of uterus forms uterine seminal receptacle. Mehlis' gland and Laurer's canal not observed. Uterus occupies most of post-testicular region, ascends anteriorly between testes, or dorsally to right testis. Metraterm thin-walled, indistinct. Eggs numerous, elongated and oval, operculate, tanned, thick-shelled, 34.6–49.5 (45.2) × 21.4–29.6 (25.8). Vitellarium follicular; follicles numerous, small, closely massed in two fields; fields lie immediately lateral to anterior half of each caecum, between pharynx level and ovarian to anterior border testicular level. Excretory vesicle Y-shaped; branching point obscured by eggs; arms reach just pre-bifurcal.

**Etymology.** The name “profundis” of the new species refers to the depth at which their hosts were captured.

### Phylogenetic data

Two sequences of 839 base pairs (bp) each were obtained from *Pseudosteringophorus profundis* sp. nov. for the 28S rDNA gene. No polymorphic sites were detected between the two sequences. The final alignment dataset consisted of 34 sequences of 818 bp in length. Both inference methods, BI and ML, resulted in the same topology but with different statistical support. *Pseudosteringophorus profundis* sp. nov. was clustered with moderate to weak support (PP = 0.89; ML = 51) within a clade that included ten species of *Steringophorus* (Fig. 2) suggesting that *Steringophorus* is a paraphyletic group. According to genetic distance, the most closely related species to *P. profundis* sp. nov. was *Steringophorus dorsolineatus* (Reimer, 1985) Bray, 1995 with 98.4% similarity (12 nucleotide difference, Suppl. material 2).

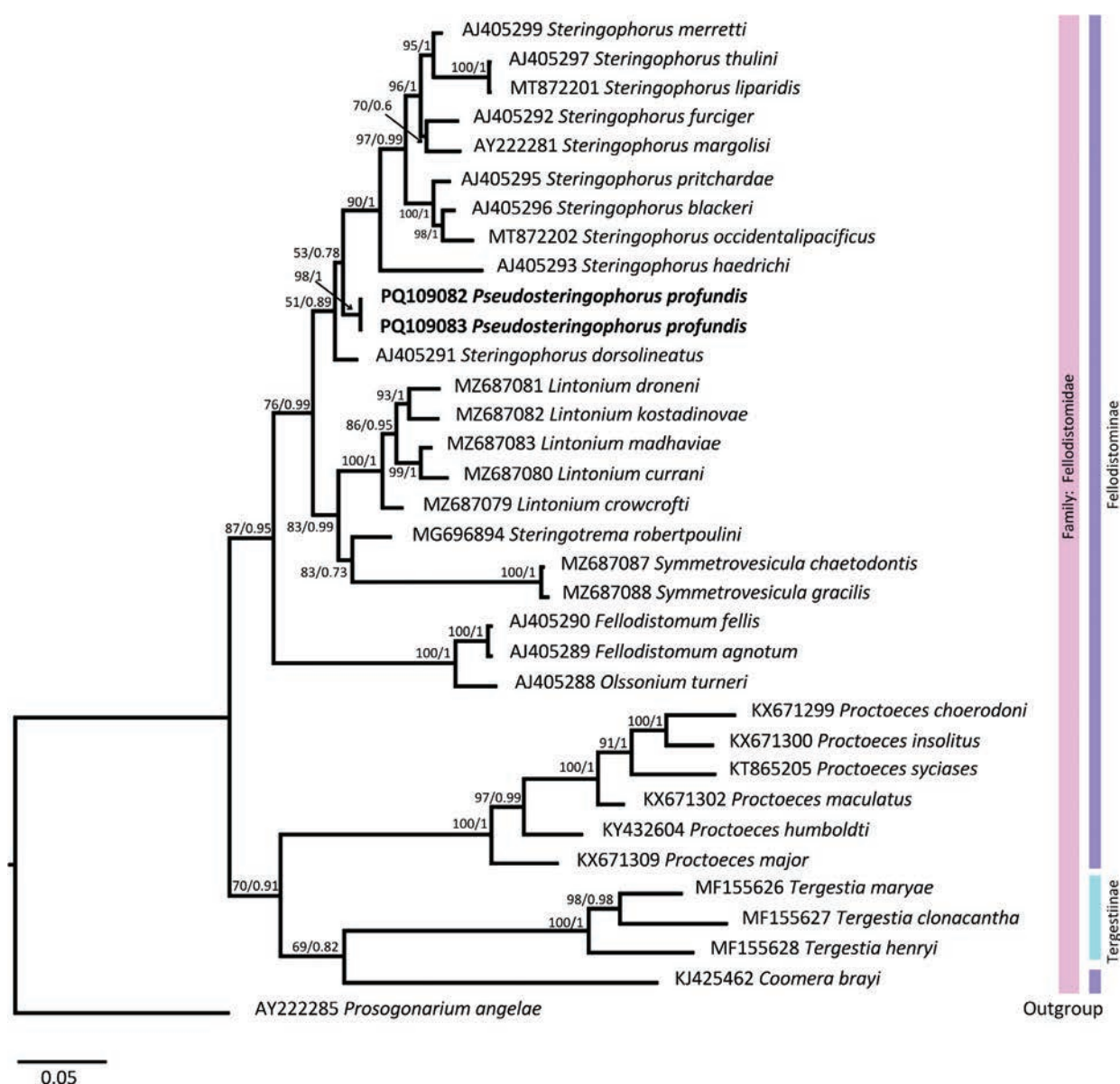


Figure 2. Relationships between fellodistomid taxa based on maximum likelihood (ML) and Bayesian inference (BI) of the partial 28S rDNA dataset. Bootstrap and posterior probability support values are shown at the nodes as ML/BI. The scale bar indicates the expected number of substitutions per site.

In addition, two 727-bp sequences were obtained for *P. profundis* sp. nov. from the *cox1* mRNA gene. One polymorphic site was detected between the two sequences. Sequences for the *cox1* mRNA are available only for two genera of Fellodistomidae (*Proctoeces* Odhner, 1911 and *Lintonium* Stunkard & Nigrelli, 1930), which precludes a phylogenetic analysis.

## Discussion

Members of Fellodistomidae are parasitic in the intestines, pyloric caeca, bile ducts, and gallbladders of marine and occasionally freshwater fishes but also occur as adults in molluscs (bivalves and gastropods) (Bray 2002; Oliva et al. 2018). The family comprises 26 genera with 138 species, of which 39 species are parasites of deep-sea fishes (Klimpel et al. 2009; Glover et al. 2024). *Pseudosteringophorus profundis* sp. nov., parasitizes the gallbladder of the deep-sea *Macrourus holotrachys*, unlike other genera in the family Fellodistomidae, which typically parasitize the intestines of deep-sea fishes. These genera include *Benthotrema* Manter, 1934, *Pseudobenthotrema* Machida, Kamegai & Kuramochi, 2007, *Hypertrema* Manter, 1960, *Lomasoma* Manter, 1935, *Megenteron* Manter, 1934, *Olssonium* Bray & Gibson, 1980, *Prudhoeus* Bray & Gibson, 1980, *Pseudosteringophorus* Yamaguti, 1940, *Steringophorus* Odhner, 1905, *Steringovermes* Bray, 2004 and *Steringotrema* Odhner, 1911 (Bray 2002; Glover et al. 2024).

The genus *Pseudosteringophorus*, is closely related to the genus *Steringophorus*. The main differences include the vitellaria located immediately lateral to the anterior half of each caecum, between the pharynx level and the ovary to the anterior border at testicular level, and an oval ovary in *Pseudosteringophorus*. In contrast, the vitellaria in *Steringophorus* are located between the level of the ventral sucker and the level just posterior to the testes; in addition, the ovary is multilobulate (Table 2). To date, *Pseudosteringophorus* is monotypic, with *P. hoplognathi* being the type species of the genus. *Pseudosteringophorus hoplognathi* was reported parasitizing the intestines of the shallow-water *Oplegnathus punctatus* and *Oplegnathus fasciatus* (Centrarchiformes: Oplegnathidae) in Japan (Yamaguti 1940; Machida et al. 2007), as well as *Plectorhinchus cinctus* (Temminck & Schlegel, 1843) (Eupercaria *incertae sedis*: Haemulidae) in China (Wang 1982). In addition, *Pseudosteringophorus* sp. has been reported from the intestines of *Ephippus orbis* (Bloch, 1787) (Acanthuriformes: Ephippidae) (Mamaev 1970). Unfortunately, accurate descriptions were not provided by Wang (1982) and Mamaev (1970). Kuramochi (2001) reported an undescribed species of *Pseudosteringophorus* from the deep-sea *Congriscus megastoma* (Günther, 1877) (Anguilliformes: Congridae). Kuramochi's specimens differ from *P. profundis* sp. nov. by the size of the ventral sucker as well as the ending of the caecae (see fig. 4 in Kuramochi 2001).

Manter (1954) and Bray (2002) expressed doubts regarding the generic status of *Benthotrema hoplognathi* Yamaguti, 1938, which they found to be closely related to *Pseudosteringophorus hoplognathi*. Both species are parasites of fishes of the genus *Hoplognathus* (= *Oplegnathus*). Machida et al. (2007) reviewed Yamaguti's specimens of *P. hoplognathi* and *B. hoplognathi*, along with their own specimens of *P. hoplognathi*. Their analysis found no significant differences between the two species and suggested that both are

**Table 2.** Taxonomic differences between *Pseudosteringophorus* and *Steringophorus*.

	<i>Pseudosteringophorus</i>	<i>Steringophorus</i>
Body	fusiform, more pointed at the posterior extremity than at the anterior	large, oval to elongate oval, deep-bodied to dorsoventrally flattened
Oral sucker	terminal, oval with ventral concavity in lateral view	rounded or subglobular and subterminal
Ventral sucker	bowl-shaped, located at middle of body or a little further behind	usually larger than oral sucker, located in anterior half of body
Caeca	narrow, simple, terminating at acetabular-ovarian level	wide to narrow, extent variable, extending to testes, to about middle of post-testicular region or occasionally beyond
Testes	oval, entire, symmetrical, anterior hindbody	oval, entire, indented or deeply lobed, symmetrical to tandem, in anterior or mid-hindbody
Cirrus sac	recurved, claviform, just reaching ventral sucker	oval
Internal seminal vesicle	bipartite	bipartite
Genital atrium	with a diverticulum totally lined with hairs and surrounded by glandular cells	often with a diverticulum
Genital pore	sinistrally submedian, post-bifurcal	anterior margin of ventral sucker, sinistrally submedian
Ovary	rounded or oval, near or overlapping with the right testes or pretesticular, dextrodorsal to ventral sucker	multilobate, just pretesticular
Uterus	post-testicular region	coiled posteriorly to testes
Eggs	tanned, embryonated, eggshells no ornamented	eggshells occasionally ornamented
Vitelline follicles	in form of single field of small follicles between pharynx level and ovary to anterior border testicular level	in two lateral fields between level of ventral sucker and level just posterior to testes

synonymous because of the presence of a bipartite internal seminal vesicle, a characteristic in *Pseudosteringophorus*. Meanwhile, Bray (2002) indicated that the genus *Benthotrema* is characterized by a coiled, tubular internal seminal vesicle, and consequently, *B. hoplognathi* should be considered a member of *Pseudosteringophorus*.

Our study provides the first DNA sequences for species of the genus *Pseudosteringophorus* which nest within members of the genus *Steringophorus*, but the position of *S. dorsolineatus* suggests a possible parafly, although with low nodal support among *Steringophorus* as previously noted (Pérez-Ponce de León et al. 2018; Bray and Waeschenbach 2020; Cribb et al. 2021). The classification of *S. dorsolineatus*, originally described as *Occultacetabulum dorsolineatum* by Reimer (1985), has been questioned regarding its inclusion in the genus *Steringophorus* (Bray and Waeschenbach 2020; Sokolov et al. 2021). This has led to a proposal to reinstate the genus *Occultacetabulum*, based on differences in ventral sucker morphology, a narrow ventral slit-like opening in contrast to the unspecialized, rounded ventral sucker of *Steringophorus* (Sokolov et al. 2021). Our phylogenetic analyses support the hypothesis of parafly.

## Conclusion

This study provides the first description of a new species of digenean from the family Fellodistomidae from the deep waters of SEPO, infecting the gallbladder of *Macrourus holotrachys*. Our results suggest the need for increasing sampling efforts for other fellodistomid species that are morphologically close to the genus *Pseudosteringophorus*, such as *Benthotrema* and *Pseudobenthotrema*. This would help to clarify and improve the resolution of the *Steringophorus* spp. + *Pseudosteringophorus* clade.

## Acknowledgements

We appreciate the support of the crew of the fishing boat “Huayca” and its Captain, Mr Dani Manso. We thank Dr Kazuo Ogawa of the Meguro Parasitological Museum, Meguro, Tokyo, Japan for providing us access to the holotype and paratypes of *Benthotrema hoplognathi* and *Pseudosteringophorus hoplognathi*. IDEAWILD Foundation (NACACHIL0324-00) provided equipment support for the identification of specimens.

## Additional information

### Conflict of interest

The authors have declared that no competing interests exist.

### Ethical statement

No ethical statement was reported.

### Funding

This research was funded by MINEDUC-UA project, ANT 1855; Plan de Fortalecimiento a Universidades Estatales—Chile RED21992 and AIM23-0003-INSTITUTO MILENIO DE OCEANOGRAFIA.

### Author contributions

Conceptualization: [Marcelo E. Oliva, Luis A. Ñacari]; Methodology: [Luis A. Ñacari, Fabiola A. Sepúlveda]; Formal analysis and investigation: [Marcelo E. Oliva, Luis A. Ñacari, Fabiola A. Sepúlveda, Rubén Escribano]; Writing - original draft preparation: [Marcelo E. Oliva, Luis A. Ñacari]; Writing - review and editing: [Marcelo E. Oliva, Luis A. Ñacari, Fabiola A. Sepúlveda, Rubén Escribano]; Funding acquisition: [Marcelo E. Oliva, Rubén Escribano]; Resources: [Marcelo E. Oliva].

### Author ORCIDs

Marcelo E. Oliva  <https://orcid.org/0000-0003-1759-2797>

Fabiola A. Sepúlveda  <https://orcid.org/0000-0002-7876-7231>

Rubén Escribano  <https://orcid.org/0000-0002-9843-7723>

Luis A. Ñacari  <https://orcid.org/0000-0001-9692-8476>

### Data availability

All of the data that support the findings of this study are available in the main text or Supplementary Information.

## References

- Akaike H (1973) Maximum likelihood identification of gaussian autoregressive moving average models. *Biometrika* 60: 255–265. <https://doi.org/10.1093/biomet/60.2.255>
- Bray RA (2002) Family Fellodistomidae Nicoll, 1909. In: Jones A, Bray RA, Gibson DI (Eds), *Keys to the Trematoda Vol. 1*. Wallingford: CABI Publishing and the Natural History Museum, 261–293. <https://doi.org/10.1079/9780851995472.0261>

- Bray RA (2020) Digenean parasites of deep-sea teleosts: A progress report. *International Journal for Parasitology: Parasites and Wildlife* 12: 251–264. <https://doi.org/10.1016/j.ijppaw.2020.01.007>
- Bray RA, Waeschenbach A (2020) *Steringophorus merretti* n. sp. (Digenea: Fellodistomidae) from the deep-sea fish *Cataetyx laticeps* Koefoed (Ophidiiformes: Bythitidae) from the Goban Spur, Northeastern Atlantic Ocean. *Systematic Parasitology* 97: 321–334. <https://doi.org/10.1007/s11230-020-09919-3>
- Castresana J (2000) Selection of conserved blocks from multiple alignments for their use in phylogenetic analysis. *Molecular Biology and Evolution* 17: 540–552. <https://doi.org/10.1093/oxfordjournals.molbev.a026334>
- Chisholm LA, Morgan JAT, Adlard RD, Whittington ID (2001) Phylogenetic analysis of the Monocotylidae (Monogenea) inferred from 28S rDNA sequences. *International Journal for Parasitology* 31: 1253–1263. [https://doi.org/10.1016/S0020-7519\(01\)00223-5](https://doi.org/10.1016/S0020-7519(01)00223-5)
- Cribb TH, Martin SB, Diaz PE, Bray RA, Cutmore SC (2021) Eight species of *Lintonium* Stunkard & Nigrelli, 1930 (Digenea: Fellodistomidae) in Australian tetraodontiform fishes. *Systematic Parasitology* 98: 595–624. <https://doi.org/10.1007/s11230-021-10000-w>
- Danovaro R, Gambi C, Della Croce N (2002) Meiofauna hotspot in the Atacama Trench, eastern South Pacific Ocean. *Deep Sea Research Part I: Oceanographic Research Papers* 49: 843–857. [https://doi.org/10.1016/S0967-0637\(01\)00084-X](https://doi.org/10.1016/S0967-0637(01)00084-X)
- Danovaro R, Company JB, Corinaldesi C, D’Onghia G, Galil B, Gambi C, Gooday AJ, Lampadariou N, Luna GM, Morigi C, Olu K, Polymenakou P, Ramirez-Llodra E, Sabbatini A, Sardá F, Sibuet M, Tselepides A (2010) Deep-sea biodiversity in the Mediterranean Sea: The known, the unknown, and the unknowable. *PLoS ONE* 5: e11832. <https://doi.org/10.1371/journal.pone.0011832>
- Espínola-Novelo JF, Escribano R, Oliva ME (2018) Metazoan parasite communities of two deep-sea elasmobranchs: the southern lanternshark, *Etmopterus granulosus*, and the largenose catshark, *Apristurus nasutus*, in the Southeastern Pacific Ocean. *Parasite* 25: 53. <https://doi.org/10.1051/parasite/2018054>
- Filatov DA (2002) PROSEQ: A software for preparation and evolutionary analysis of DNA sequence data sets. *Molecular Ecology Notes* 2: 621–624. <https://doi.org/10.1046/j.1471-8286.2002.00313.x>
- Fujii T, Kilgallen N, Rowden A, Jamieson A (2013) Deep-sea amphipod community structure across abyssal to hadal depths in the Peru-Chile and Kermadec trenches. *Marine Ecology Progress Series* 492: 125–138. <https://doi.org/10.3354/meps10489>
- Gambi C, Vanreusel A, Danovaro R (2003) Biodiversity of nematode assemblages from deep-sea sediments of the Atacama Slope and Trench (South Pacific Ocean). *Deep-Sea Research Part I: Oceanographic Research Papers* 50: 103–117. [https://doi.org/10.1016/S0967-0637\(02\)00143-7](https://doi.org/10.1016/S0967-0637(02)00143-7)
- Glover A, Higgs N, Horton T (2024) World Register of Deep-Sea species (WoRDSS). Fellodistomidae Nicoll, 1909.
- Katoh K, Rozewicki J, Yamada KD (2019) MAFFT online service: Multiple sequence alignment, interactive sequence choice and visualization. *Briefings in Bioinformatics* 20: 1160–1166. <https://doi.org/10.1093/bib/bbx108>
- Klimpel S, Busch MW, Kellermanns E, Kleinertz S, Palm HW (2009) Metazoan Deep Sea Fish Parasites. *Acta Biologica Benrodis*.
- Kuramochi T (2001) Digenean Trematodes of Anguilliform and Gadiform Fishes from Deep-Sea Areas of Tosa Bay, Japan. *National Science Museum monographs* 20: 19–30.

- Leung TLF, Donald KM, Keeney DB, Koehler A V, Peoples RC, Poulin R (2009) Trematode parasites of Otago Harbour (New Zealand) soft-sediment intertidal ecosystems: Life cycles, ecological roles and DNA barcodes. *New Zealand Journal of Marine and Freshwater Research* 43: 857–865. <https://doi.org/10.1080/00288330909510044>
- Machida M, Kamegai S, Kuramochi T (2007) Fellodistomidae (Trematoda, Digenea) from deep-sea fishes of Japan. *Bulletin of the National Science Museum. Series A (Zoology)* 33: 93–103.
- Mamaev YL (1970) [Helminths of some commercial fishes in the Gulf of Tong King]. In: Oshmarin PG, Mamaev YL, Lebedev BI (Eds) *Helminths of Animals of South-East Asia*. Moscow, Izdatel'stvo Nauka, 127–190. [In Russian]
- Manter H (1954) Some digenetic trematodes from fishes of New Zealand. *Transactions of the Royal Society of New Zealand* 82: 475–568.
- McLaughlin JP, Morton DN, Lafferty KD (2020) Parasites in marine food webs. In: *Marine Disease Ecology*. Oxford University Press, 45–60. <https://doi.org/10.1093/oso/9780198821632.003.0002>
- Miller SA, Dykes DD, Polesky HF (1988) A simple salting out procedure for extracting DNA from human nucleated cells. *Nucleic Acids Research* 16: 1215. <https://doi.org/10.1093/nar/16.3.1215>
- Muff S, Nilsen EB, O'Hara RB, Nater CR (2022) Rewriting results sections in the language of evidence. *Trends in Ecology and Evolution* 37: 203–210. <https://doi.org/10.1016/j.tree.2021.10.009>
- Münster J, Kochmann J, Klimpel S, Klapper R, Kuhn T (2016) Parasite fauna of Antarctic *Macrourus whitsoni* (Gadiformes: Macrouridae) in comparison with closely related macrourids. *Parasites & Vectors* 9: 403. <https://doi.org/10.1186/s13071-016-1688-x>
- Ñacari LA, Oliva ME (2016) Metazoan parasites of deep-sea fishes from the South Eastern Pacific: Exploring the role of ecology and host phylogeny. *Deep-Sea Research Part I: Oceanographic Research Papers* 115: 123–130. <https://doi.org/10.1016/j.dsr.2016.06.002>
- Ñacari LA, Escribano R, Oliva ME (2022) Endoparasites and diet of the “bigeye grenadier” *Macrourus holotrachys* Günther, 1878 from the deep sea in the Southeastern Pacific Ocean. *Deep Sea Research Part I: Oceanographic Research Papers* 190: 103903. <https://doi.org/10.1016/j.dsr.2022.103903>
- Oliva ME, Fernández I, Oyarzún C, Murillo C (2008) Metazoan parasites of the stomach of *Dissostichus eleginoides* Smitt 1898 (Pisces: Nototheniidae) from southern Chile: A tool for stock discrimination? *Fisheries Research* 91: 119–122. <https://doi.org/10.1016/j.fishres.2007.11.012>
- Oliva ME, Valdivia IM, Cárdenas L, Muñoz G, Escribano R, George-Nascimento M (2018) A new species of *Proctoeces* and reinstatement of *Proctoeces humboldti* George-Nascimento and Quiroga 1983 (Digenea: Fellodistomidae) based on molecular and morphological evidence. *Parasitology International* 67: 159–169. <https://doi.org/10.1016/j.parint.2017.10.004>
- Pérez-Ponce de León G, Anglade T, Randhawa HS (2018) A new species of *Steringotrema* Odhner, 1911 (Trematoda: Fellodistomidae) from the New Zealand sole *Peltorhamphus novaezeelandiae* Günther off Kaka point in the Catlins, South Island, New Zealand. *Systematic Parasitology* 95: 213–222. <https://doi.org/10.1007/s11230-018-9773-5>
- Posada D (2008) jModelTest: Phylogenetic Model Averaging. *Molecular Biology and Evolution* 25: 1253–1256. <https://doi.org/10.1093/molbev/msn083>
- Rambaut A, Drummond AJ, Xie D, Baele G, Suchard MA (2018) Posterior Summarization in Bayesian Phylogenetics Using Tracer 1.7. *Systematic Biology* 67: 901–904. <https://doi.org/10.1093/sysbio/syy032>

- Ramírez-Flandes S, González CE, Aldunate M, Poulain J, Wincker P, Glud RN, Escribano R, Haond SA, Ulloa O (2022) High genetic diversity in the pelagic deep-sea fauna of the Atacama Trench revealed by environmental DNA. bioRxiv: 2022.04.14.488404. <https://doi.org/10.1101/2022.04.14.488404>
- Ramirez-Llodra E, Brandt A, Danovaro R, De Mol B, Escobar E, German CR, Levin LA, Martinez Arbizu P, Menot L, Buhl-Mortensen P, Narayanaswamy BE, Smith CR, Tittensor DP, Tyler PA, Vanreusel A, Vecchione M (2010) Deep, diverse and definitely different: Unique attributes of the world's largest ecosystem. *Biogeosciences* 7: 2851–2899. <https://doi.org/10.5194/bg-7-2851-2010>
- Reimer L (1985) *Occultacetabulum dorsolineatum* ng, n. sp. (Occultacetabulinae n. subf.), a fellodistomine digenean from a deep-sea fish in the Mozambique Channel (in German). *Angewandte Parasitologie* 26: 107–109.
- Rodriguez L, George-Nascimento M (1996) La fauna de parásitos metazoos del bacalao de profundidad *Dissostichus eleginoides* Smitt, 1898 (Pisces: Nototheniidae) en Chile central: aspectos taxonómicos, ecológicos y zoogeográficos. *Revista Chilena de Historia Natural* 69: 21–33.
- Ronquist F, Teslenko M, Van Der Mark P, Ayres DL, Darling A, Höhna S, Larget B, Liu L, Suchard MA, Huelsenbeck JP (2012) MrBayes 3.2: Efficient Bayesian Phylogenetic Inference and Model Choice Across a Large Model Space. *Systematic Biology* 61: 539–542. <https://doi.org/10.1093/sysbio/sys029>
- Sabbatini A, Morigi C, Negri A, Gooday AJ (2002) Soft-shelled benthic foraminifera from a hadal site (7800 m water depth) in the Atacama Trench (SE Pacific): preliminary observations. *Journal of Micropalaeontology* 21: 131–135. <https://doi.org/10.1144/jm.21.2.131>
- Salinas X, González MT, Acuña E (2008) Metazoan parasites of the thumb grenadier *Nezumia pulchella*, from the south-eastern Pacific, off Chile, and their use for discrimination of host populations. *Journal of Fish Biology* 73: 683–691. <https://doi.org/10.1111/j.1095-8649.2008.01967.x>
- Sokolov SG, Shchenkov S V., Gordeev II (2021) A phylogenetic assessment of *Pronoprymna* spp. (Digenea: Faustulidae) and Pacific and Antarctic representatives of the genus *Steringophorus* Odhner, 1905 (Digenea: Fellodistomidae), with description of a new species. *Journal of Natural History* 55: 867–887. <https://doi.org/10.1080/00222933.2021.1923852>
- Tamura K, Stecher G, Peterson D, Filipski A, Kumar S (2013) MEGA6: Molecular evolutionary genetics analysis version 6.0. *Molecular Biology and Evolution* 30: 2725–2729. <https://doi.org/10.1093/molbev/mst197>
- Wang PQ (1982) Some digenetic trematodes of marine fishes from Fujian Province, China. *Oceanologia et Limnologia Sinica* 13: 179–194. [In Chinese]
- Weston JNJ, Espinosa-Leal L, Wainwright JA, Stewart ECD, González CE, Linley TD, Reid WDK, Hidalgo P, Oliva ME, Ulloa O, Wenzhöfer F, Glud RN, Escribano R, Jamieson AJ (2021) *Eurythenes atacamensis* sp. nov. (Crustacea: Amphipoda) exhibits ontogenetic vertical stratification across abyssal and hadal depths in the Atacama Trench, eastern South Pacific Ocean. *Marine Biodiversity* 51: 51. <https://doi.org/10.1007/s12526-021-01182-z>
- Yamaguti S (1938) Studies on the helminth fauna of Japan. Part 21. Trematodes of fishes, IV. Published by author, Japan, 139 pp.
- Yamaguti S (1940) Studies on the helminth fauna of Japan. Part 31. Trematodes of fishes, VII. *Journal of Zoology* 9: 35–108.

## Supplementary material 1

### Data on the 28S rDNA sequences used in the phylogenetic analysis

Authors: Marcelo E. Oliva, Fabiola A. Sepúlveda, Rubén Escribano, Luis A. Ñacari

Data type: xlsx

Copyright notice: This dataset is made available under the Open Database License (<http://opendatacommons.org/licenses/odbl/1.0/>). The Open Database License (ODbL) is a license agreement intended to allow users to freely share, modify, and use this Dataset while maintaining this same freedom for others, provided that the original source and author(s) are credited.

Link: <https://doi.org/10.3897/zookeys.1221.135086.suppl1>

## Supplementary material 2

### Pairwise sequence divergences for 28S rDNA sequences of family Fellostomidae

Authors: Marcelo E. Oliva, Fabiola A. Sepúlveda, Rubén Escribano, Luis A. Ñacari

Data type: xlsx

Explanation note: The p-distance is shown as a percentage (below the diagonal) and the raw number of bp-pairwise differences above the diagonal.

Copyright notice: This dataset is made available under the Open Database License (<http://opendatacommons.org/licenses/odbl/1.0/>). The Open Database License (ODbL) is a license agreement intended to allow users to freely share, modify, and use this Dataset while maintaining this same freedom for others, provided that the original source and author(s) are credited.

Link: <https://doi.org/10.3897/zookeys.1221.135086.suppl2>

# Three new species of *Atkinsoniella* (Hemiptera, Cicadellidae, Cicadellinae) from southwestern China

Yan Jiang<sup>1,2</sup>, Xiao-Fei Yu<sup>1,3</sup>, Mao-Fa Yang<sup>1,3</sup>

<sup>1</sup> Institute of Entomology, Guizhou Provincial Key Laboratory for Agricultural Pest Management of the Mountainous Region, Guizhou University, Guiyang 550025, China

<sup>2</sup> Department of Pharmacy, Guizhou Provincial Engineering Research Center of Medical Resourceful Healthcare Products, Guiyang Healthcare Vocational University, Guiyang 550000, China

<sup>3</sup> College of Tobacco Sciences, Guizhou University, Guiyang 550025, China

Corresponding author: Mao-Fa Yang ([ggdgly@126.com](mailto:ggdgly@126.com))

## Abstract

Three new species of the genus *Atkinsoniella* (Hemiptera: Cicadellidae: Cicadellinae), *A. chongqingana* Jiang & Yang, *A. likuni* Jiang & Yang and *A. biostiolum* Jiang & Yang, **sp. nov.**, collected from southwestern China, are described and illustrated. The two new species, *A. chongqingana* Jiang & Yang, **sp. nov.** and *A. likuni* Jiang & Yang, **sp. nov.**, are similar to *A. nigrominiatula* (Jacobi, 1944), *A. latior* Young, 1986, *A. limba* Kuoh, 1991, *A. dormana* Li, 1992, *A. divaricata* Yang, Meng & Li, 2017, *A. peaka* Yang, Meng & Li, 2017, and *A. zizhongji* Jiang & Yang, 2022 in appearances, but can be distinguished from these species by the characteristic of aedeagus, paraphysis, and pygofer. *Atkinsoniella biostiolum* Jiang & Yang, **sp. nov.** can be distinguished from all the known *Atkinsoniella* species by its special color and markings, as well as males having one ostiole in the center of the base of each subgenital plate. A key to *Atkinsoniella* species from China is provided.

**Key words:** Auchenorrhyncha, China, leafhopper, morphology, taxonomy



Academic editor:

J. Adilson Pinedo-Escatel

Received: 6 June 2024

Accepted: 3 November 2024

Published: 31 December 2024

ZooBank: <https://zoobank.org/3EC18A44-6767-41D1-B85C-8D14CEC3B560>

**Citation:** Jiang Y, Yu X-F, Yang M-F (2024) Three new species of *Atkinsoniella* (Hemiptera, Cicadellidae, Cicadellinae) from southwestern China. ZooKeys 1221: 449–469. <https://doi.org/10.3897/zookeys.1221.129125>

Copyright: © Yan Jiang et al.

This is an open access article distributed under terms of the Creative Commons Attribution License (Attribution 4.0 International – CC BY 4.0).

## Introduction

Southwestern China includes Sichuan Province, Guizhou Province, Yunnan Province, Tibet Autonomous Region, and Chongqing Municipality. Due to its complex topography characterized by significant variations in altitude and numerous mountainous basins, many insects, including Cicadellidae, are rich in biodiversity in Southwest China. Of the 102 valid known species of the genus *Atkinsoniella*, 92 occur in China and distributed in 20 provincial administrative regions (Feng and Zhang 2015; Yang et al. 2017; Naveed and Zhang 2018; Jiang et al. 2022, 2023). Of the 92 known Chinese *Atkinsoniella* species, 72 species are distributed in Yunnan Province, 26 species in Guizhou Province, 21 species in Tibet Autonomous Region, 20 species in Sichuan Province, and 17 species are distributed in Chongqing Municipality (Yang et al. 2017; Jiang et al. 2023). In this study, the descriptions, male genitalia, and habitus photographs of three new species, *Atkinsoniella chongqingana* Jiang & Yang, **sp. nov.**, *A. likuni* Jiang & Yang, **sp. nov.** and *A. biostiolum* Jiang & Yang, **sp. nov.** from southwestern China are provided with a key to all Chinese species.

## Materials and methods

The specimens were collected by sweeping (27–35 sweeps per collecting event) on shrubs and weeds using 2.5 m insect sweep nets (200 mesh) in daylight, and at sunset using a 500W high-pressure mercury lamps; all materials were preserved in absolute ethanol and stored at -20 °C in the laboratory. The abdomens of specimens were detached and soaked in 10% NaOH solution, boiled for ~ 3 min, rinsed with water to remove traces of NaOH, and transferred to glycerol for further dissection, photography, and eventually preserved in PCR tubes with glycerol. The habitus and male genitalia were photographed using a KEYENCE VHX-6000 digital camera and a Nikon Eclipse Ni-E microscope, respectively. Adobe Photoshop 2020 was used to edit compiled images. The length of the body was measured from the vertex to the rear of the forewings using a KEYENCE VHX-6000 digital camera. The morphological terminology is adapted from Young (1968, 1986) and Yang et al. (2017). The holotype and paratypes were deposited at the Institute of Entomology, Guizhou University, Guiyang, China (**GUGC**).

## Taxonomy

### Genus *Atkinsoniella* Distant, 1908

*Atkinsoniella* Distant, 1908: 235.

*Soibanga* Distant, 1908: 236.

*Curvufacies* Kuoh, 1993: 38.

**Type species.** *Atkinsoniella decisa* Distant, 1908, type locality India.

**Distribution.** Palearctic, Oriental.

**Note.** The comparison of male genitalia morphological characteristics of the nine similar *Atkinsoniella* species is provided in Table 1.

### *Atkinsoniella chongqingana* Jiang & Yang, sp. nov.

<https://zoobank.org/23F7EE43-2C83-44DB-A454-43F1DC100C76>

Figs 1A–D, 2A–F

**Material examined. Holotype:** • ♂, Wulipo National Nature Reserve, Chongqing Municipality, CHINA, 781 m, 21 July 2021, coll. Li-Kun Zhong. **Paratypes:** • 3 ♂♂ (light trapped), Wulipo National Nature Reserve, Chongqing Municipality, CHINA, 790 m, 24 July 2021, coll. Li-Kun Zhong.

**Description.** Length of male 6.9–7.3 mm. Dorsum orange. Crown with one black spot in center of vertex, and one black spot below each ocelli at basal margin; eyes black; ocellus brown; pronotum with one large inverted T-shaped black spot, and one or two black vimineous spots at each lateral margin; scutellum with one large black spot at each basal angle and connected to inverted T-shaped marking on pronotum to form seemingly lung lobe-shaped marking; forewing with black longitudinal stripe in clavus, corium, and clavus suture, respectively; posterior margin, anterior margin, and veins black, apical portion black brown, anterior marginal area black-brown in some specimens; face saffron-yellow, antennal ledge with one black spot; thorax and abdomen black in ventral view; legs brown or yellowish brown.

**Table 1.** Comparison of male genitalia morphological characteristics of the nine similar *Atkinsoniella* species.

Species	Pygofer	Pygofer process	Aedeagus	Paraphysis	Style
<i>A. nigrominiatula</i> (Jacobi, 1944)	Posterior portion slightly widened, dorsal margin straight.	Posterior 1/2 tapered, tip acute and not exceeding posterior margin of pygofer.	Entirely short, dorsal margin nearly straight.	Paraphysis with tip tapered and bent dorsad, articulating with aedeagus apically.	Y-shaped
<i>A. latior</i> Young, 1986	Nearly rectangular with posterior margin broadly rounded.	Pygofer process extending posterodorsally, then posteriorly, attenuated and sharply curved apically.	Aedeagus wide, dorsal margin straight, apical part narrower.	Paraphysis pygofer process extending posterodorsally, then posteriorly, attenuated, and sharply curved apically.	Y-shaped
<i>A. limba</i> Kuoh, 1991	Dorsal margin with 1 angular flat process near base.	Pygofer process arising basiventrally and tapered posteriorly.	Aedeagus slender and posterior portion bent dorsad.	Paraphysis with laterally produced flattened part subapically.	Y-shaped
<i>A. dormana</i> Li, 1992	Dorsal margin with 1 angular flat process near base.	Pygofer process bent posterodorsally from median, tip acute.	Aedeagus wide basally, median with pair of triangular flat processes, tip bent dorsad.	Paraphysis with tip tapered and bent dorsad, articulating with aedeagus apically.	Nearly V-shaped
<i>A. divaricata</i> Yang, Meng & Li, 2017	Posterior margin broadly rounded, basal 1/3 of dorsal margin convex and with several macrosetae.	Posterior 1/2 bending dorsad, tip acute.	Base wide, proximal portion slightly curved dorsad.	Medially with wrinkle in ventral view, tip forked and clamped median of aedeagus.	V-shaped
<i>A. peaka</i> Yang, Meng & Li, 2017	Medially bulging outwards, tip sharply flattened and contracted into rounded protrusion, resembling peak of peaked cap.	Base with several microsetae, posterior portion acute and extending straight, tip not reaching posterior margin of pygofer.	Basal 1/3 bent dorsad, medial 1/3 portion approaching paraphysis, tip rounded.	Tip hooked and articulated with proximal aedeagus apically.	V-shaped
<i>A. zizhongji</i> Jiang & Yang, 2022	Posterior portion broadly rounded and bent dorsally.	Arising basiventrally and extending dorsolateral posteriorly of pygofer, apex with transparent membrane dorsad and exceeding posterior margin of pygofer.	Base and tip concave, ventral margin concave medially, apical 1/3 portion bent dorsad, tip obtuse.	Apex acute and slightly bent dorsad, ventral margin undulating medially, and articulating with aedeagus apically.	Y-shaped
<i>A. chongqingana</i> Jiang & Yang, sp. nov.	Entirety broad, tip convex arcuately and bent dorsally	Base with short microsetae, extending arcuately and dorsolateral posteriorly of pygofer, posterior portion with lamellar membranous structures, tip acute.	Posterior 1/2 warped dorsally, tip rounded, ventral margin articulate with paraphysis at basal 1/4 and 1/2.	Basal 1/2 stipiform, posterior 1/2 widened, tip narrowed into a cusp and curved dorsally, and articulating with aedeagus apically.	Nearly V-shaped
<i>A. likuni</i> Jiang & Yang, sp. nov.	Basal 1/2 broad, posterior 1/2 narrow, tip warped dorsally, posterior margin truncate.	Entirety slender, arising basiventrally and extending along ventral margin of pygofer, slightly curved dorsally, median broadened with lamellar membranous structure, apical 1/3 narrow strip-shaped.	Entirety slender and straight, tip slightly bent dorsally, median and subbase concave at ventral margin.	Entirety slender and straight, posterior portion dilated, apex sharply tooth-shaped and bent dorsally, articulating apically with aedeagus at apical 2/5.	Y-shaped

Crown with anterior margin rounded and convex; crown surface flat except for lateral area of ocellus concave; ocellus located at imaginary line between anterior eye angles and tip of lateral clypeal suture; each ocellus further from other one than to adjacent eye; pronotum equal wide to head, anterior margin cambered, posterior margin slightly concave medially, lateral margins convergent anteriorly; scutellum with transverse depression slightly arcuate; face with frontoclypeus flat medially, muscle impressions distinct, clypeal sulcus slightly fuzzy medially; forewings with apical membranous area distinct and four apical cells, base of second cells more proximal than third cells transversely.

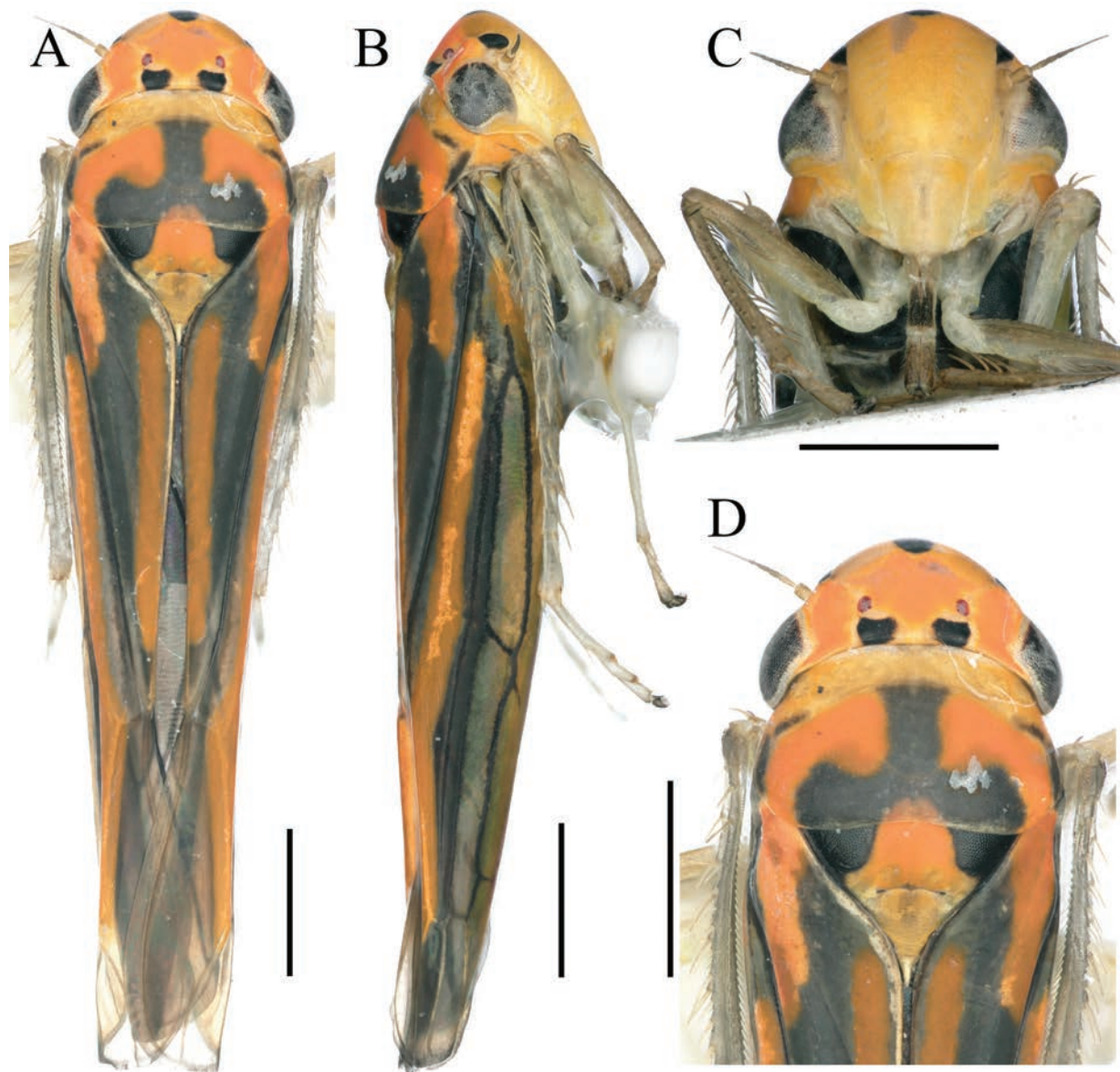


**Figure 1.** External features of *Atkinsoniella chongqingana* Jiang & Yang, sp. nov., male holotype **A** habitus, dorsal view **B** habitus, lateral view **C** face, anterior view **D** head and pronotum, dorsal view. Scale bars: 1000  $\mu\text{m}$ .

Male pygofer broadly short, tip arcuately convex and bent dorsally, posterior 1/2 and median of dorsal margin with macrosetae; pygofer process with short microsetae at base, and arcuately extending dorsolateral posteriorly of pygofer, posterior portion with lamellar membranous structures, tip acute; subgenital plate broad at base, posterior 1/2 narrow and bent dorsally, with one uniseriate row of macrosetae obliquely, lateral margin and apical 1/2 with long and short microsetae; aedeagus stout, with posterior 1/2 relatively narrow and warped dorsally, tip rounded, ventral margin articulate with paraphysis at basal 1/4 and 1/2; paraphysis basal 1/2 stipiform, posterior 1/2 gradually widened, tip narrowed into cusp and dorsally curved, articulating with aedeagus apically; connective V-shaped; style broad and short, with tip acute and bent.

**Distribution.** China (Chongqing).

**Etymology.** The name of the new species is derived from Chongqing where the type specimens were collected.

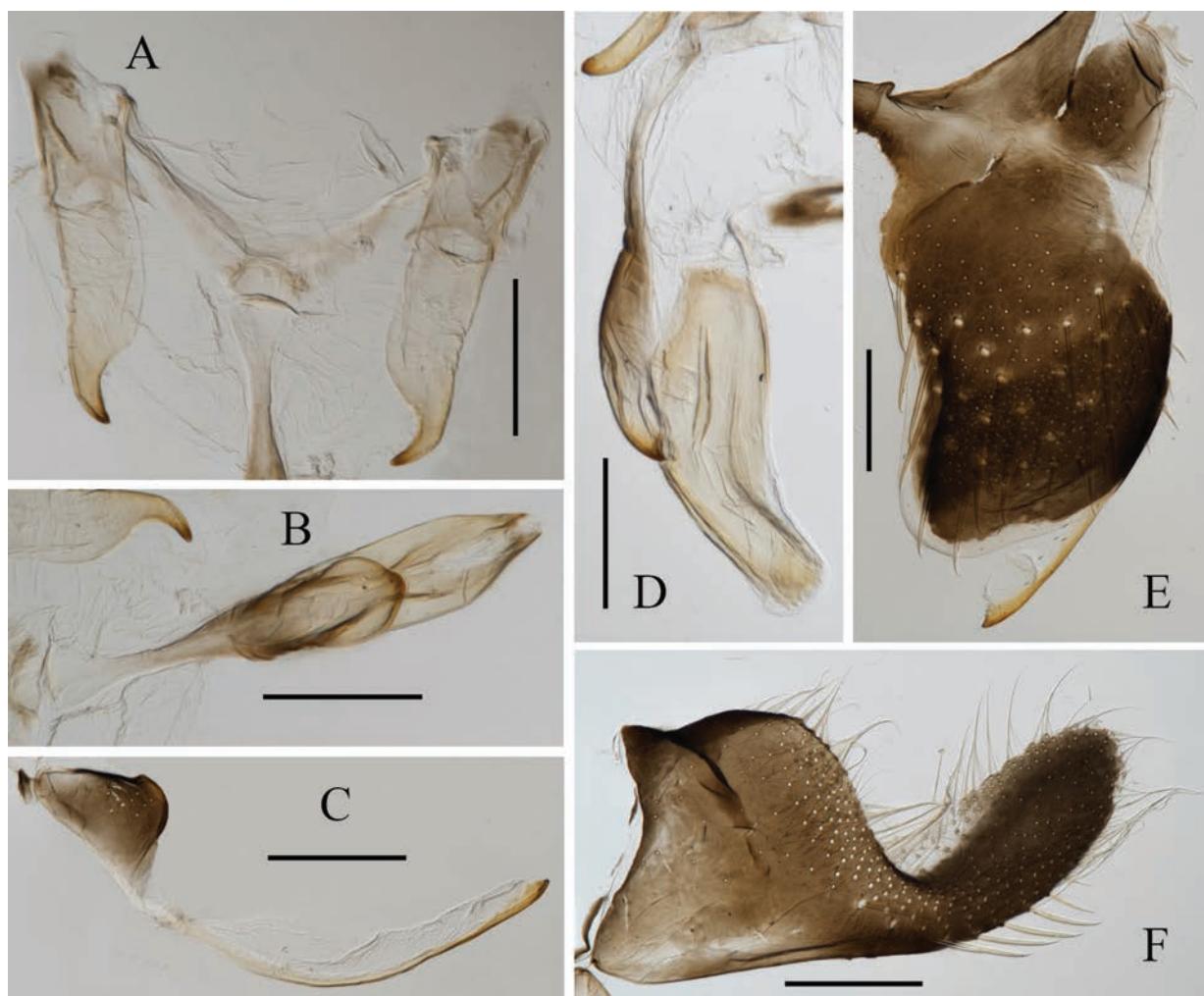


**Figure 2.** Male genitalia of *Atkinsoniella chongqingana* Jiang & Yang, sp. nov. **A** style **B** aedeagus and paraphysis, ventral view **C** pygofer process **D** aedeagus and paraphysis, lateral view **E** pygofer, lateral view **F** subgenital plate, ventral view. Scale bars: 200  $\mu$ m.

**Remarks.** This species is similar to *A. nigrominiatula* (Jacobi, 1944), *A. latior* Young, 1986, *A. limba* Kuoh, 1991, *A. dormana* Li, 1992, *A. divaricata* Yang, Meng & Li, 2017, *A. peaka* Yang, Meng & Li, 2017, and *A. zizhongji* Jiang & Yang, 2022 in appearance, but can be easily differentiated from these species by the following characteristics: pygofer process extending dorsolateral posteriorly of the pygofer, and its posterior portion having lamellar membranous structures; the aedeagus has its posterior 1/2 warped dorsally, and the ventral margin is articulated with the paraphysis at basal 1/4 and 1/2.

***Atkinsoniella likuni* Jiang & Yang, sp. nov.**

<https://zoobank.org/70C0BBCC-7E32-4CBF-B33E-A461F4BACAC0>

Figs 3A–D, 4A–F

**Material examined. Holotype:** • ♂, Wulipo National Nature Reserve, Chongqing Municipality, CHINA, 781 m, 21 July 2021, coll. Li-Kun Zhong. **Paratypes:** • 7 ♂♂ (light trapped) 2 ♂♂, Wulipo National Nature Reserve, Chongqing Municipality, CHINA, 781–1348 m, 18–24 July 2021, coll. Li-Kun Zhong.

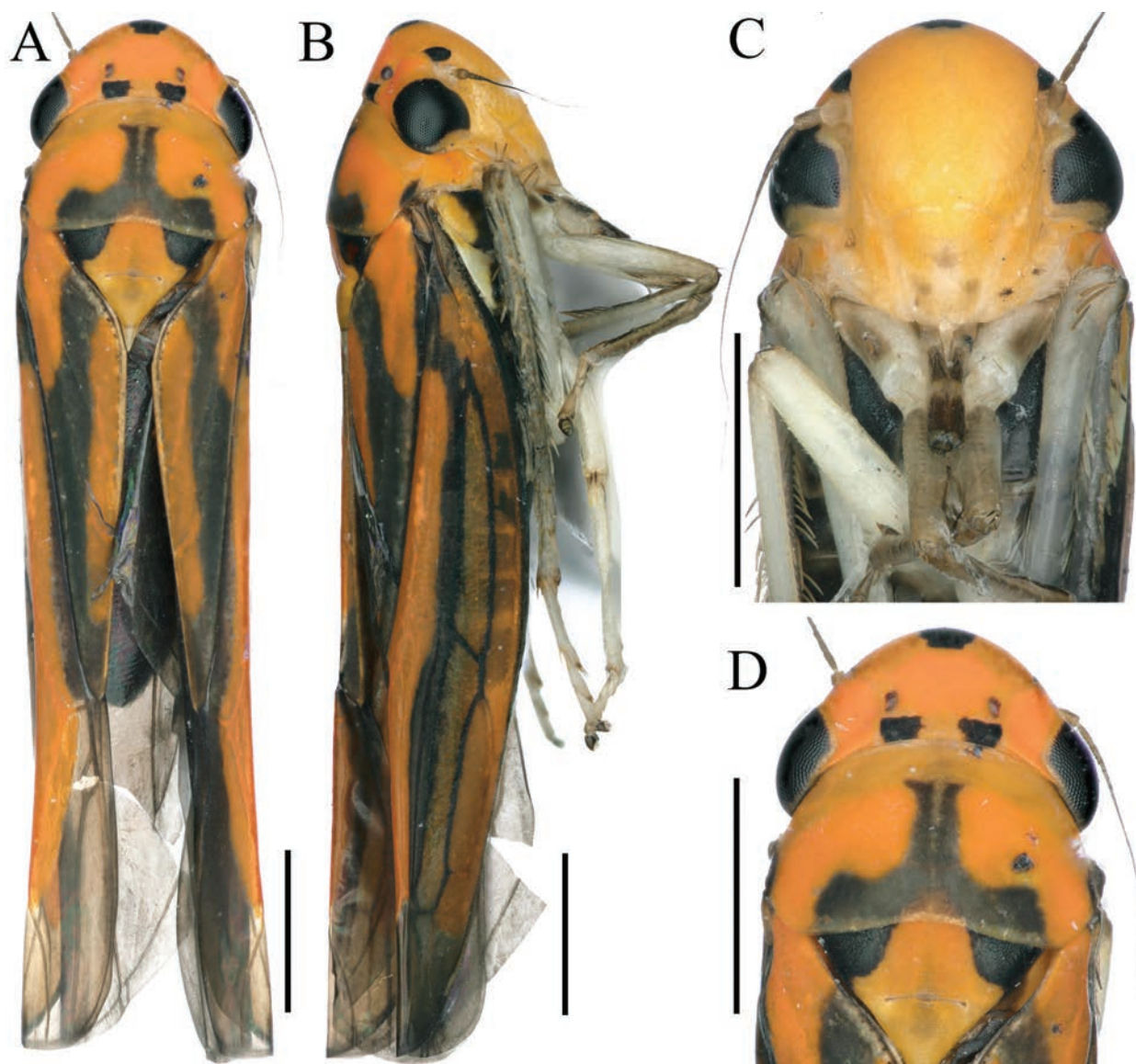


**Figure 3.** External features of *Atkinsoniella likuni* Jiang & Yang, sp. nov., male holotype **A** habitus, dorsal view **B** habitus, lateral view **C** face, anterior view **D** head and pronotum, dorsal view. Scale bars: 1000  $\mu$ m.

**Description.** Length of male 6.6–6.8 mm. The appearance is similar to *Atkinsoniella chongqingana* Jiang & Yang, sp. nov. Male pygofer broadly short, tip rounded and warped dorsally, median of dorsal margin and posterior 1/2 with long macrosetae; pygofer process slender and short, arising basiventrally and extending along ventral margin of pygofer, slightly curved dorsally and not as far posteriorly as pygofer apex, median lamellar broadened with membranous structure, apical 1/3 thin strip-shaped; subgenital plates basal 3/5 area broad, apical 2/5 narrow and bent dorsally, with one row of macrosetae uniseriate obliquely, long and short dense microsetae at outer lateral area of macrosetae; aedeagus slender and straight, with tip slightly bent dorsally, subbase concave at ventral margin, ventral margin articulating with dorsal margin of paraphysis medially and basally; paraphysis slender and straight, tip dilated, apex sharp teeth shaped and bent dorsally, articulating apically with aedeagus



**Figure 4.** Male genitalia of *Atkinsoniella likuni* Jiang & Yang, sp. nov. **A** style **B** aedeagus and paraphysis, lateral view **C** subgenital plate, ventral view **D** pygofer, lateral view **E** aedeagus and paraphysis, ventral view **F** pygofer process. Scale bars: 200  $\mu$ m.

at apical 2/5 and median with aedeagus at base; connective Y-shaped; style broad at basal 2/3 and tapered at apical 1/3, apex acute and incurved.

**Distribution.** China (Chongqing).

**Etymology.** The new species is named after the first name of the collector Li-Kun Zhong.

**Remarks.** This species is similar to *A. nigrominiatula* (Jacobi, 1944), *A. latior* Young, 1986, *A. limba* Kuoh, 1991, *A. dormana* Li, 1992, *A. divaricata* Yang, Meng & Li, 2017, *A. peaka* Yang, Meng & Li, 2017, *A. zizhong* Jiang & Yang, 2022, and *A. chongqingana* Jiang & Yang, sp. nov. in appearance, but it can be distinguished from these species by the following characteristics: (1) pygofer process smaller and not extending beyond the posterior margin of the pygofer, the median lamella is broadened with a membranous structure; (2) the aedeagus is slender and straight, its base articulating with the median of paraphysis; (3) the articulation of the aedeagus and paraphysis is located in the apical 2/5 of the aedeagus.

***Atkinsoniella biostiolum* Jiang & Yang, sp. nov.**

<https://zoobank.org/4CA025A0-8798-4419-BD1D-57543DDB5D10>

Figs 5A–E, 6A–E, 7A–E

**Material examined. Holotype:** • ♂, Nongdao Town, Ruili City, Yunnan Province, CHINA, 755 m, 4 August 2020, coll. Xian-Yi Wang. **Paratypes:** • 1 ♂, the same data as holotype; 1 ♂ 4 ♀♀, Daweishan national forest park, Pingbian County, Honghe Hani and Yi Autonomous Prefecture, Yunnan Province, CHINA, 1158 m, 5 June 2019, coll. Tie-Long Xu.

**Description.** Length, male 5.3–5.4 mm, female 5.6–5.9 mm. Crown orange, posterior 1/2 with trapezoidal and yellow-white area medially, and one small drop-shaped black spot in center between ocellus, basal margin with triangular black spot medially and small triangular black brown spot below each ocellus, and coronal suture black with median discontinuous; eyes orange-black to black brown; ocelli grayish with black border distinctly; pronotum orange, with posterior 1/2 black, triangular orange macular area, concave medially, in center of black area, and one orange spot at each basal area laterally. Scutellum

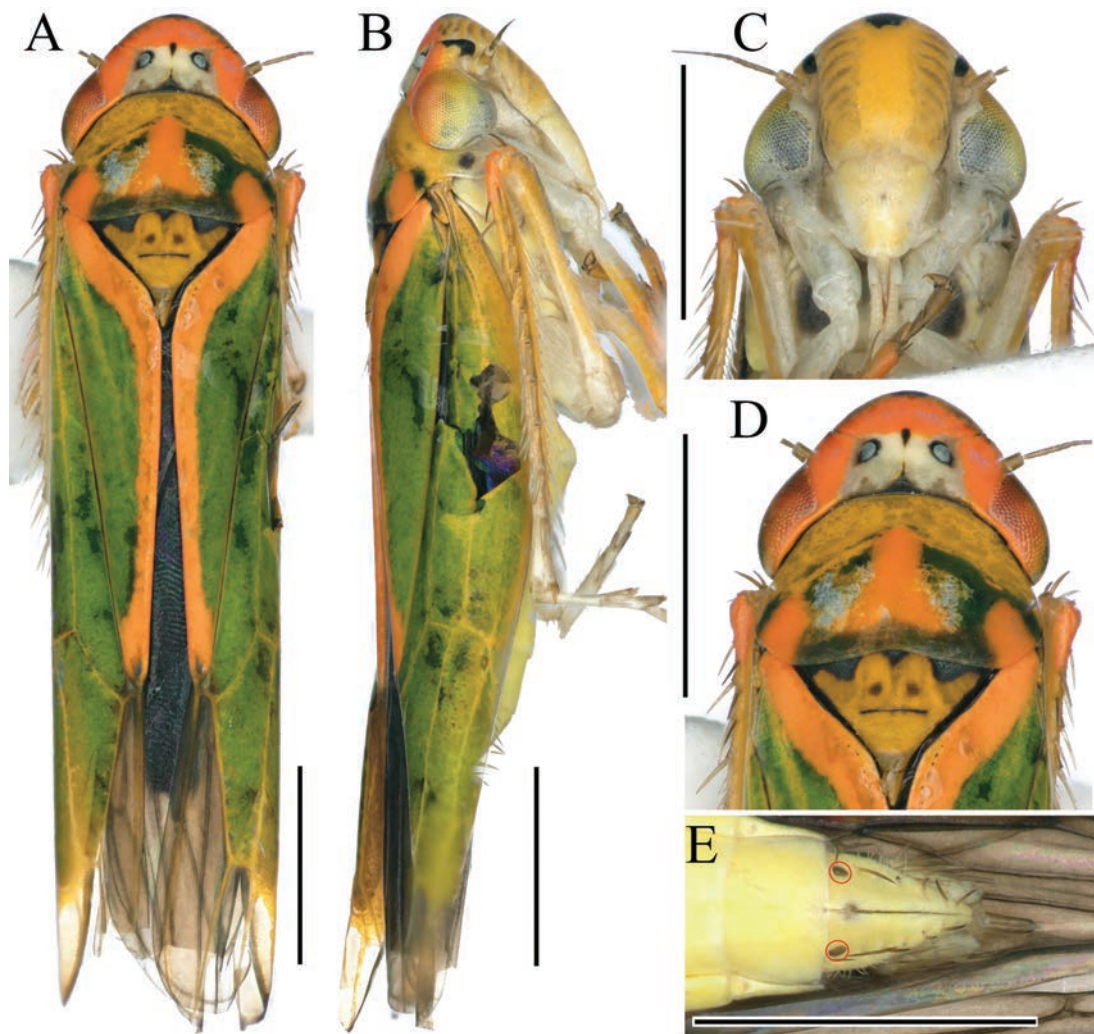


**Figure 5.** External features of *Atkinsoniella biostiolum* Jiang & Yang, sp. nov., male holotype **A** habitus, dorsal view **B** habitus, lateral view **C** face, anterior view **D** head and pronotum, dorsal view **E** apical portion of abdomen, ventral view (red circles indicates ostioles). Scale bars: 1000  $\mu$ m.

with three triangular black spots at basal margin and apical corner dark brown, lateral margin and transverse depression black, two small black spots above transverse depression; forewings green with yellow veins, clavus bordered with orange stripes laterally and connected with orange spots laterally on pronotum, apical membranous area black-brown; face with frontoclypeus and anteclypeus orange-yellow, muscle impressions and remaining areas dark brown, with one black spot above basal margin of antennal ledge; thorax pale yellow in ventral view, with two large black spots, legs yellow-white to gray-white, forelegs with femur and tibia orange-red, tarsus and pretarsus black-brown; abdomen yellow.

Crown with anterior margin rounded and convex; coronal suture distinct and equal to median length of crown; ocelli located slightly in front of imaginary line between anterior eye angles and tip of lateral clypeal suture, distance between ocellus equal to adjacent eye; pronotum wider than head, anterior margin rounded and convex, posterior margin with median concavity angular; scutellum with medial transverse depression slightly arcuate; forewings with distinct apical membranous area, base of second cells more proximal than third cells transversely; face with frontoclypeus flat medially, muscle impressions and clypeal sulcus blurred medially; males with one ostiole in center of base of each subgenital plate (marked by red circles in Fig. 5E).

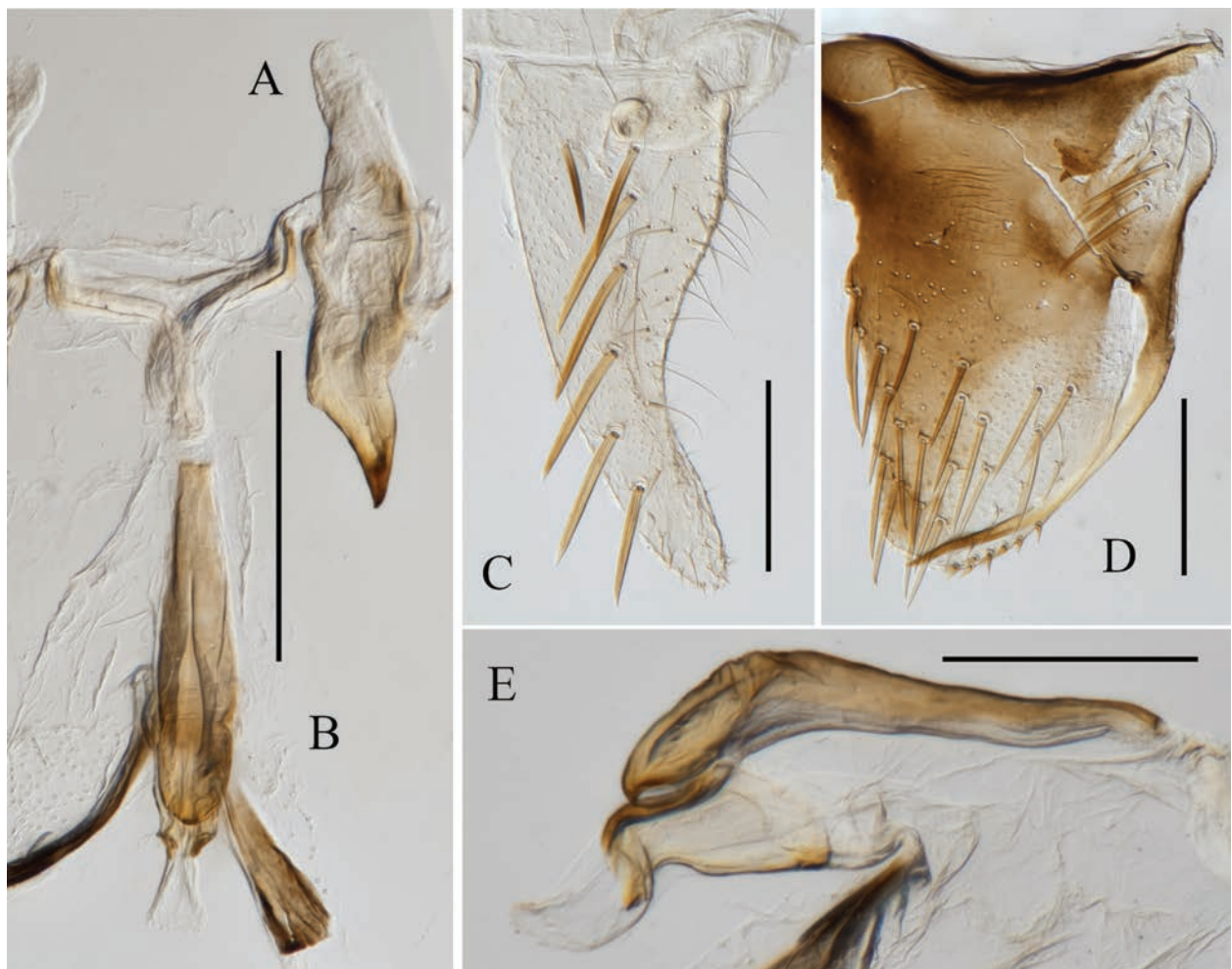


**Figure 6.** Male genitalia of *Atkinsoniella biostiolum* Jiang & Yang, sp. nov. **A** style **B** aedeagus and paraphysis, ventral view **C** subgenital plate, ventral view **D** pygofer, lateral view **E** aedeagus and paraphysis, lateral view. Scale bars: 200  $\mu$ m.

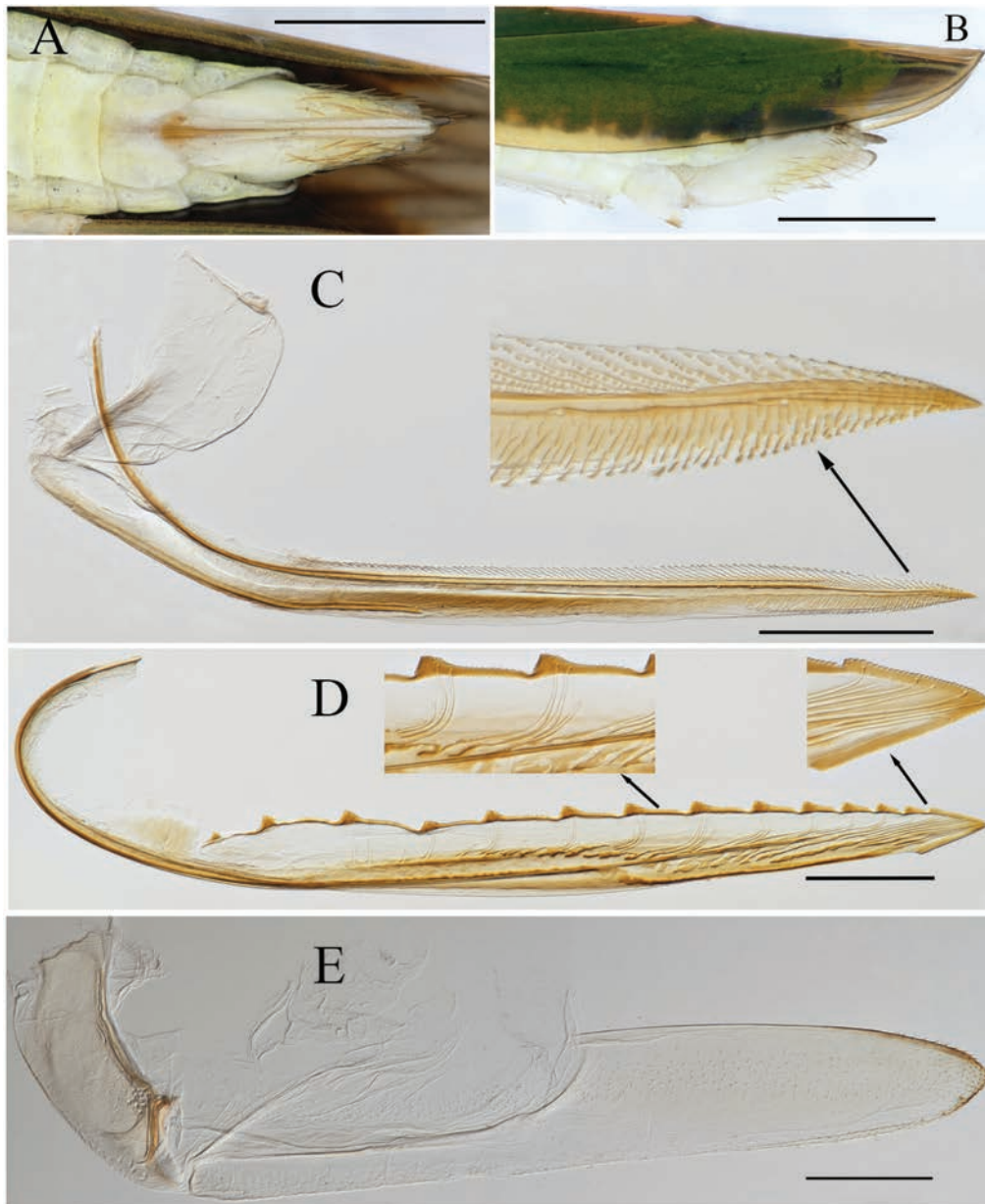


**Figure 7.** Female genitalia of *Atkinsoniella biostiolum* Jiang & Yang, sp. nov. **A** apical portion of abdomen, ventral view **B** apical portion of abdomen, lateral view **C** first valvifer and first valvula, lateral view **D** second valvula, lateral view **E** second valvifer and gonoplac, lateral view. Scale bars: 1000  $\mu$ m (**A**, **B**), 200  $\mu$ m (**C**, **D**, **E**).

Male pygofer broad, short, apex truncated, median of dorsal margin and posterior 1/2 with long macrosetae; pygofer process slender, arising basiventrally and extending along ventral margin of pygofer, slightly curved dorsally and just beyond pygofer apex posteriorly, median lamellar area broadened with membranous structure, apical 1/3 thin strip-shaped; subgenital plates with basal 3/5 broad, apical 2/5 narrow and bent dorsally, with one row of macrosetae uniseriate obliquely, long and short dense microsetae at outer lateral area of macrosetae; aedeagus warped medially and 8-shaped in lateral view, ventral margin articulating with dorsal margin of paraphysis medially; paraphysis slender and straight, tip dilated, apex teeth sharp and bent dorsally, articulating apically with aedeagus at apical 1/2; connective Y-shaped; style broad at basal 2/3 and tapered at apical 1/3, apex acute and incurved.

Female abdominal sternite VII, shorter than wide, posterior margin with median concavity; pygofer, in lateral view, produced posteriorly, posterior margin narrowly rounded with macrosetae at posterior portion and ventral margin; first valvifer longer than wide; first valvula apex acute, dorsal area with sculptured striae extending from basal portion of blade to apex; second valvula ventral preapical margin protruding, posterior portion arrow-shaped, blade with ~ 11 continuous large triangular teeth on expanded subapical portion and smaller teeth apically, all large teeth as well as ventral and dorsal margin of apical blade with denticles, ducts distributed in area of third teeth to apex of blade; third valvula basal 1/2 narrow and posterior 1/2 distinctly expanded, apex obtuse, and tiny setae distributed on apical portion and posterior 1/3 ventral margin of blade.

**Distribution.** China (Yunnan).

**Etymology.** The new species is named after the ostiole in the base of each subgenital plate.

**Remarks.** This species can be easily differentiated from other *Atkinsoniella* species by its color, markings, characteristics of the aedeagus, especially subgenital plates with ostioles, which is the first reported characteristics in subfamily Cicadellinae.

### Key to species of *Atkinsoniella* Distant, 1908 from China (updated from Yang et al. 2017)

- 1 Forewing completely black ..... ***A. nigripennis* Yang & Li, 1999**
- Forewing not black or not completely black ..... **2**
- 2 Pronotum uniform black, without distinct spots or stripes ..... **3**
- Pronotum not black or not completely black ..... **20**
- 3 Apical portion of crown with a median red spot .....  
..... ***A. xinfengi* Yang, Meng & Li, 2017**
- Crown without red spots ..... **4**
- 4 Forewing black with 2 brown-yellow longitudinal stripes .....  
..... ***A. guttata* Li, 1993 (part)**
- Forewing black with red spots or stripes ..... **5**
- 5 Forewing with red longitudinal stripes ..... **6**
- Forewing with red spots or macular area ..... **10**
- 6 Forewing with 2 red longitudinal stripes ..... **7**
- Forewing with 3 red longitudinal stripes ..... **8**
- 7 Forewing with the 2 red longitudinal stripes completely disjunctive .....  
..... ***A. nigra* Kuoh & Cai, 1994**
- Forewing with the 2 red longitudinal stripes connecting in the middle .....  
..... ***A. flavilega* Yang, Meng & Li, 2017 (part)**
- 8 Male head and frontoclypeus completely black .....  
..... ***A. nigrita* Zhang & Kuoh, 1993 (part)**
- Male crown anterior margin and face yellow-white with black spots or stripes ..... **9**
- 9 Male vertex with a small black spot, face yellow-white without stripes .....  
..... ***A. nigridorsum* Kuoh & Zhuo, 1996 (part)**
- Anterior portion of male crown with single median gray spot, frontoclypeus with black longitudinal stripe on each side .....  
..... ***A. fishtaila* Yang, Meng & Li, 2017**

10	Claval suture black, dividing forewing red spots or area into 2 parts.....	11
–	Claval suture black partly, forewing red spots or area complete piece ...	12
11	Forewing red area apex not exceeding the end of claval suture, frontoclypeus black.....	<b>A. lili Yang &amp; Zhang, 2000</b>
–	Forewing red area apex exceeding the end of claval suture, frontoclypeus black with a median yellow-white longitudinal stripe .....	<b>A. tuberosityla Yang, Meng &amp; Li, 2017</b>
12	Forewing red area long, apex exceeding the end of claval suture .....	13
–	Forewing red area short, apex not exceeding or only reaching the end of claval suture.....	14
13	Male pygofer process with a short horn-like branch at apical 1/3; paraphysis bifurcate at middle, clamping aedeagus .....	<b>A. nigricens Yang &amp; Li, 2004</b>
–	Male pygofer process without branches; paraphysis not furcate with acute apex, preapical portion expanded laterally and with large dental process dorsally.....	<b>A. atrata Yang, Meng &amp; Li, 2017</b>
14	Male pygofer process apex fork-like, paraphysis with apex longitudinally concave medially.....	<b>A. longiaurita Yang, Meng &amp; Li, 2017</b>
–	Characters not as above.....	15
15	Apical 1/2 of male pygofer process with broad dorsal membranous lobe .	<b>A. membrana Yang, Meng &amp; Li, 2017</b>
–	Male pygofer process smooth, without membranous lobe.....	16
16	Male pygofer process curved dorsad at base 1/3, becoming straight near apex 1/3 .....	<b>A. recta Yang, Meng &amp; Li, 2017</b>
–	Male pygofer process curved not as above.....	17
17	Male pygofer process particularly long, extending posteriorly farther than apex of pygofer.....	<b>A. longa Yang, Meng &amp; Li, 2017</b>
–	Male pygofer process at most extending to apex of pygofer.....	18
18	Male pygofer posterodorsal angle finger-like, pygofer process right-angled and curved dorsad at middle .....	<b>A. rectangulata Yang, Meng &amp; Li, 2017</b>
–	Characters not as above .....	19
19	Male pygofer with apical portion raised dorsad, apicodorsal margin acute and fishtail-shaped; aedeagus apex not expanded.....	<b>A. biundulata Meng, Yang &amp; Ni, 2010</b>
–	Male pygofer with apical portion produced round-horned; aedeagus apex expanded .....	<b>A. expanda Yang, Meng &amp; Li, 2017</b>
20	Forewing without distinct spots or stripes .....	21
–	Forewing with distinct spots or stripes.....	53
21	Forewing black-brown, the joint area of 2 forewings orange-red, veins of costal margin and corium orange .....	<b>A. xanthovena Yang &amp; Li, 2002</b>
–	Characters of forewing not as above.....	22
22	Forewing of living body cyan, exsiccatae yellow-brown, forewing hyaline next to costal margin .....	<b>A. variata Young, 1986</b>
–	Characters of forewing not as above.....	23
23	Pronotum with distinct spots or stripes .....	24
–	Pronotum without distinct spots or stripes.....	27
24	Scutellum tawny or orange, with basal black side spots.....	25
–	Scutellum black completely.....	26

25	Scutellum tawny, apex with a black spot.....	
	.....	<b>A. sulphurata (Distant, 1908) (part)</b>
–	Scutellum orange, apex without black spots.....	
	.....	<b>A. longiuscula Feng &amp; Zhang, 2015 (part)</b>
26	Crown black, anterior 1/2 with a median yellow-white spot; inside eyes yellowish-white, region broad; male pygofer posterodorsal margin finger-like.....	<b>A. fuscopenna Yang &amp; Li, 2004</b>
–	Crown black, anterior 1/2 without median yellow-white spots, inside eyes yellowish white, region narrow; male pygofer posterodorsal margin angular.....	<b>A. guttata Kuoh, 1992 (part)</b>
27	Basal portion of crown without median black spots.....	<b>28</b>
–	Basal portion of crown with single median black spot.....	<b>31</b>
28	Male pygofer process with apical 1/2 straightened posteriorly, exceeding apical margin of pygofer, without branch.....	<b>A. uniguttata Li, 1993</b>
–	Male pygofer process with small branch at subapex.....	<b>29</b>
29	Apical portion of crown with large, median black squared spot; aedeagus broad and short, apex truncated.....	<b>A. cyclops (Melichar, 1914)</b>
–	Apical portion of crown without black spots or only with a minimal spot; aedeagus not as above.....	<b>30</b>
30	Apical portion of crown without black spots, face yellowish brown, frontoclypeus with a median yellow-white longitudinal stripe; aedeagus with finger-like rounded tip.....	<b>A. duna Yang, Meng &amp; Li, 2017</b>
–	Apical portion of crown without black spots or only with a minimal spot, face uniform yellowish white; aedeagus with acute tip not finger-like.....	
	.....	<b>A. xanthoabdomena Yang, Meng &amp; Li, 2017</b>
31	Crown with 2 black, median, parallel rhomboid spots.....	
	.....	<b>A. rhomboida Yang, Meng &amp; Li, 2017</b>
–	Crown with none or 1 median black spot.....	<b>32</b>
32	Apical portion of crown without black spots, the spot of basal portion V-shaped.....	<b>A. curvata Yang &amp; Li, 1980</b>
–	Apical portion of crown with median black spot, spot of basal portion not V-shaped.....	<b>33</b>
33	Crown with large basal black spot, distinctly larger than anterior median one.....	<b>34</b>
–	Crown with small basal black spot, as large as or smaller than anterior median.....	<b>35</b>
34	Scutellum without black spots, forewing orange, subapical region orange-red or red.....	<b>A. wui Yang, Meng &amp; Li, 2017</b>
–	Scutellum with a black spot in each basal angle, forewing ivory.....	
	.....	<b>A. albipenna Yang, Meng &amp; Li, 2017</b>
35	Forewing ivory, base orange-red or red.....	<b>36</b>
–	Forewing orange, yellow-green, gray-brown, or red-brown except apical membrane.....	<b>37</b>
36	Abdominal venter black completely; male subgenital plate without macrosetae.....	<b>A. punica Yang &amp; Li, 2002</b>
–	Abdomen yellow, or yellow-brown, or only with black apex; male subgenital plate with uniseriate macrosetae.....	<b>A. longiuscula Feng &amp; Zhang, 2015 (part)</b>

37	Mesothethium with 2 large black or black-brown spots.....	38
–	Mesothethium without spots or stripes.....	44
38	Scutellum without black spots .....	39
–	Scutellum with a black spot in each basal angle .....	40
39	Male pygofer process slender; aedeagus narrowed to the end, apex acute .....	<b>A. multiseta Yang, Meng &amp; Li, 2017</b>
–	Male pygofer process broad and long, tapering apically and bending inside; aedeagus with approximately parallel sides, apex round .....	<b>A. changae Yang, Meng &amp; Li, 2017</b>
40	Forewing gray-brown; male pygofer process with a small branch subapically .....	<b>A. zhangmuensis Yang, Meng &amp; Li, 2017</b>
–	Forewing orange; male pygofer process without branches.....	41
41	Male pygofer process with apical 1/3 constricted and contorted .....	42
–	Male pygofer process normal, not constricted or contorted.....	43
42	Apical 1/3 portion of male pygofer process willow-leaf-shaped, straight; aedeagus broad and short.....	<b>A. flavipenna Li &amp; Wang, 1992</b>
–	Apical 1/3 portion of male pygofer process sickle-shaped; aedeagus slender .....	<b>A. liui Yang, Meng &amp; Li, 2017</b>
43	Frontoclypeus with a median thin tumor near apex; whole paraphysis curved dorsad.....	<b>A. rinkihonis (Matsumura, 1912)</b>
–	Frontoclypeus without the tumors; paraphysis arched, apical 1/2 right-angled curved dorsad.....	<b>A. bowa Yang, Meng &amp; Li, 2017</b>
44	Male pygofer process with branch or toothed process subapically .....	45
–	Male pygofer process without branch or process.....	47
45	Male pygofer process with membranous branch; paraphysis curved dorsad from median portion, and with apical 1/3 curved posteroventrally .....	<b>A. yunnanana Yang, Meng &amp; Li, 2017</b>
–	Male pygofer process with toothed process subapically, paraphysis curved not as above .....	46
46	Male pygofer with posterodorsal margin arc-shaped, apex of pygofer process thick; aedeagus slender, apical 1/2 straight.....	<b>A. thaloidea Young, 1986</b>
–	Male pygofer process with posterodorsal margin roundly angular, apex of pygofer process thin; aedeagus stout, apex curved dorsad.....	<b>A. thalia (Distant, 1918)</b>
47	Male pygofer truncated apically; pygofer process contorted and curved medially.....	<b>A. aurantiaca Cai &amp; Kuoh, 1995</b>
–	Male pygofer rounded apically; pygofer process not contorted or curved medially.....	48
48	Scutellum without spots and stripes .....	49
–	Scutellum with black or black-brown spot in each basal angle .....	51
49	Male pygofer process lamellate, posterior 1/3 portion broadly lamellate and twisted backwards, apex acute; connective V-shaped .....	<b>A. wangi Jiang &amp; Yang, 2023</b>
–	Male pygofer process slender, posterior 1/3 not as above; connective Y-shaped .....	50
50	Male aedeagus with posterior portion angular .....	<b>A. warpa Yang, Meng &amp; Li, 2017</b>
–	Male aedeagus with posterior margin truncate .....	<b>A. stenopyga Jiang &amp; Yang, 2023</b>

51	Head, thorax, and base of forewing ivory in dorsal view; male pygofer process broad and flat, apex beak-shaped, abruptly acute and slightly curved; aedeagus slightly curved dorsad medially .....	<b>A. beaka Yang, Meng &amp; Li, 2017</b>
–	Head, thorax, and forewing orange-yellow or gray-brown in dorsal view; male pygofer process slender, apex not beak-shaped; aedeagus straight.....	<b>52</b>
52	Head, thorax, and forewing gray-brown in dorsal view; male pygofer nearly truncated apically, apical margin with minute dents, apical 1/3 portion of pygofer process abruptly narrowed; aedeagus with ventral tumor medially .....	<b>A. heae Yang, Meng &amp; Li, 2017</b>
–	Head, thorax, and forewing orange-yellow in dorsal view; male pygofer with apex roundedly angular dorsad, apical margin smooth, pygofer process tapering to the end; aedeagus without ventral tumor .....	<b>A. tiani Yang, Meng &amp; Li, 2017</b>
53	Forewing dark yellow-brown, with muddy yellow or gray-white transparent or translucent spots .....	<b>A. huangi Yang &amp; Zhang, 2000</b>
–	Forewing not as above.....	<b>54</b>
54	Forewing black, with 3 longitudinal grayish white stripes; pronotum with 2 small black spots abreast in the center, and posterior area with 2 large black spots transversely .....	<b>A. yingjiangensis Jiang &amp; Yang, 2023</b>
–	Forewing and pronotum not as above .....	<b>55</b>
55	Forewing green, clavus bordered with orange stripes laterally, males with 1 ostiole in the center of the base of each subgenital plate .....	<b>A. biostiolum Jiang &amp; Yang, sp. nov.</b>
–	Forewing and subgenital plates not as above.....	<b>56</b>
56	Forewing white or gray-white, with brown or black-brown stripes .....	<b>57</b>
–	Forewing black with red or brown-yellow stripes, or forewing brown-yellow with black or yellow-brown stripes.....	<b>58</b>
57	Basal portion of crown with ⊥-shaped black stripe medially; forewing gray-white, costal margin, inner margin, and veins black-brown, broad longitudinal brown stripe along claval suture.....	<b>A. motuoensis Meng, Yang &amp; Ni, 2010</b>
–	Basal portion of crown with large black spot medially; forewing ivory, costal and inner margins black-brown, with longitudinal black-brown stripe parallel to costal and inner margins.....	<b>A. alcmena (Distant, 1908)</b>
58	Scutellum completely black.....	<b>59</b>
–	Scutellum not completely black .....	<b>85</b>
59	Pronotum with 2 large white spots; forewing clavus with broad longitudinal white strip .....	<b>A. albimacula Yang &amp; Li, 2002</b>
–	Characters not as above .....	<b>60</b>
60	Forewing with red stripes or spots.....	<b>61</b>
–	Forewing without red stripes or spots .....	<b>81</b>
61	Forewing clavus base with red spot or short stripe, costal margin with or without orange-red stripe.....	<b>A. alternata Young, 1986</b>
–	Forewing with red stripes not as above .....	<b>62</b>
62	Forewing with 2 longitudinal red stripes.....	<b>63</b>
–	Forewing with 3 longitudinal red stripes.....	<b>72</b>
63	Red stripes of forewing short, extending only to end of claval suture.....	<b>A. furipygofera Yang &amp; Meng, 2011</b>
–	Red stripes of forewing long, extending farther than end of claval suture ...	<b>64</b>

- 64 Forewing with the 2 longitudinal red stripes connecting in the middle .....  
 ..... **A. flavilega Yang, Meng & Li, 2017(part)**
- Forewing with the 2 longitudinal red stripes completely separated ..... **65**
- 65 Male paraphysis with 3 toothed processes apically .....  
 ..... **A. tridentata Yang & Li, 2011**
- Male paraphysis with single pointed process apically ..... **66**
- 66 Head and thorax with many small scattered red spots; caudodorsal margin of male pygofer not produced in angular or flat finger-shaped process .....  
 ..... **A. rufistigma Yang, Meng & Li, 2017 (part)**
- Head and thorax without small red spots; caudodorsal margin of male pygofer produced in angular or flat finger-shaped process ..... **67**
- 67 Caudodorsal margin of male pygofer extended posteriorly forming angular process ..... **68**
- Caudodorsal margin of male pygofer extended posteriorly forming flat finger-shaped process ..... **70**
- 68 Basal portion of crown with transverse black band; pronotum with 2 transverse red stripes medially; male pygofer process with flat angular process medially ..... **A. zaihuai Yang & Meng, 2011**
- Basal portion of crown without black strip, but middle portion of crown with 2 longitudinal black stripes across ocelli; pronotum with 2 large orange-red spots; male pygofer process without flat angular process ..  
 ..... **69**
- 69 Face orange-red, frontoclypeus with small black spot medially, clypeal suture with triangular black spot; male pygofer process with apical 1/3 flat and broad, aedeagus slender ..... **A. angula Kuoh, 1992**
- Face black, frontoclypeus with a longitudinal orange-red stripe medially, anteclypeus with lateral orange-red spot, gena and maxillary plate yellow-white; male pygofer process strip-shaped, apical 1/2 tapering, aedeagus stout ..... **A. nigrosteaka Li & Wang, 1994**
- 70 Crown black except muddy yellow posterolateral margin; red band of pronotum short and narrow ..... **A. xanthonota Kuoh, 1994**
- Crown muddy yellow or orange-red, basal and apical portion with black stripes; red band of pronotum long, width variable ..... **71**
- 71 Crown with 3 black spots, 1 at vertex, 2 under ocelli; red band of pronotum broad and long ..... **A. grahami Young, 1986 (part)**
- Crown with irregular transverse black bands on apical and basal portion; red band of pronotum slender ..... **A. rubrostriata Kuoh, 1992**
- 72 Pronotum with an uninterrupted median transverse red band, face yellow-white without stripe ..... **A. nigradorsum Kuoh & Zhuo, 1996 (part)**
- Characters not as above ..... **73**
- 73 Frontoclypeus and anteclypeus black completely ..... **74**
- Frontoclypeus and anteclypeus not all black ..... **76**
- 74 Median portion of pronotum with a transverse red band or several continuous red spots; red stripes of forewing broad .....  
 ..... **A. transfasciata Yang, Meng & Li, 2017**
- Median portion of pronotum with 2 red spots or oblique stripes; red stripes of forewing narrow and thin ..... **75**

- 75 Two red longitudinal stripes on corium of forewing disjunctive completely, legs yellow-white ..... **A. *yani* Yang, Meng & Li, 2017**
- Two red longitudinal stripes on corium of forewing joined at base, legs black..... **A. *insignata* (Haupt, 1924)**
- 76 Pronotum with 2 rounded red spots, frontoclypeus completely black ..... **A. *nigrita* Zhang & Kuoh, 1993 (part)**
- Pronotum with red spots not rounded, frontoclypeus not completely black.....77
- 77 Crown with a large fork-shaped black spot on basal-median portion; frontoclypeus with a large lateral black spot; anteclypeus with a long median black stripe ..... **A. *contrariuscula* (Jacobi, 1944)**
- Characters not as above .....78
- 78 Pronotum with a transverse red stripe medially..... **A. *mediofasciola* Yang & Li, 2002**
- Pronotum with 2 transverse red stripes medially.....79
- 79 Crown completely black..... **A. *goosenecka* Yang, Meng & Li, 2017**
- Crown orange-red with black spots.....80
- 80 Face yellow-white, but frontoclypeus with basal margin black, basal 1/2 with lateral longitudinal black stripe, whole inverted U-shaped ..... **A. *hupehna* Young, 1986**
- Face orange-red, with Y-shaped or T-shaped black stripes ..... **A. *dactylia* Yang & Li, 2000**
- 81 Forewing yellow-green, costal and inner margins black, corium with 2 black spots ..... **A. *nigricephala* Li, 1992**
- Forewing black with orange stripes .....82
- 82 Forewing with 4 large orange spots..... **A. *dubia* Young, 1986**
- Forewing with 2 longitudinal orange or yellow-brown stripes .....83
- 83 Crown yellow-brown, with 2 Y-shaped black stripes medially; face with lorum completely black..... **A. *flexa* Kuoh, 1992**
- Crown with stripes not as above; face with lorum orange-yellow or only basal portion black.....84
- 84 Crown black except yellow-white posterolateral margin and inner side of eyes; anteclypeus black, lorum black basally. **A. *guttata* Kuoh, 1992 (part)**
- Crown orange-red or orange-yellow, with 3 distinct black spots, 1 at vertex, 2 under ocelli; anteclypeus with a black spot basally, lorum orange-yellow ..... **A. *grahami* Young, 1986 (part)**
- 85 Scutellum black with red spots .....86
- Scutellum without red spots.....87
- 86 Pronotum bright red, anterior margin with a large median black spot, posterior margin with black boundary, median portion with or without black stripe linked; scutellum with a large red spot medially ..... **A. *brevistyla* Yang & Li, 2004**
- Pronotum black, anterior margin with 2 transverse red stripes or spots, median portion with 2 long transverse red stripes; scutellum with 2 or 4 red spots ..... **A. *rufistigma* Yang, Meng & Li, 2017 (part)**
- 87 Forewing with red stripes.....88
- Forewing without red stripes ..... 101

88	Pronotum dark red, with 3 black spots arranged in regular triangle.....	
	.....	<b>A. trimaculata Li, 1992</b>
–	Characters not as above.....	<b>89</b>
89	Forewing with 3 longitudinal red stripes.....	<b>90</b>
–	Forewing with more than 3 red stripes.....	<b>93</b>
90	Male pygofer constricted medially, apex arrow-shaped.....	
	.....	<b>A. cuspidata Meng, Yang &amp; Ni, 2010 (part)</b>
–	Characters not as above.....	<b>91</b>
91	Male pygofer process with thumb-shaped dorsal projection subapically...	
	.....	<b>A. jini Yang, Meng &amp; Li, 2017</b>
–	Male pygofer process without any projections.....	<b>92</b>
92	Male pygofer process with membranous lobe at apicodorsal margin; paraphysis narrow and straight, apex expanded and curved sickle-shaped, ventral margin deeply concave medially.....	<b>A. nigrisigna Li, 1992 (part)</b>
–	Male pygofer process without membranous lobe, paraphysis with apical portion curved dorsad, apex acute.....	<b>A. heiyuana Li, 1992</b>
93	Male paraphysis forked apically and clamping median of aedeagus.....	
	.....	<b>A. divaricata Yang, Meng &amp; Li, 2017</b>
–	Male paraphysis not forked apically.....	<b>94</b>
94	Male pygofer process extending posterodorsally, then posteriorly attenuated and sharply curved apically.....	<b>A. latior Young, 1986</b>
–	Characters not as above.....	<b>95</b>
95	Aedeagus with paired flat dorsal triangular processes at middle.....	
	.....	<b>A. dormana Li, 1992</b>
–	Aedeagus with dorsal aspect straight.....	<b>96</b>
96	Apical portion of male pygofer peaked; apex of paraphysis extending posteriorly nearly to apex of aedeagus.....	<b>A. peaka Yang, Meng &amp; Li, 2017</b>
–	Apical portion of male pygofer not peaked; apex of paraphysis extending posteriorly only to middle of aedeagus.....	<b>97</b>
97	Dorsal margin of male pygofer with an angular flat process near base, aedeagus long, paraphysis with lateral produced flatly subapically.....	
	.....	<b>A. limba Kuoh, 1991</b>
–	Characteristics not as above.....	<b>98</b>
98	Dorsal margin of male pygofer straight, aedeagus short and dorsal margin near straight, paraphysis with apex tapered.....	
	.....	<b>A. nigrominiatula (Jacobi, 1944)</b>
–	Characteristics not as above.....	<b>99</b>
99	Aedeagus stout with posterior 1/2 relatively narrow and warped dorsally, aedeagus 2× wider than paraphysis in lateral view.....	
	.....	<b>A. chongqingana Jiang &amp; Yang, sp. nov.</b>
–	Aedeagus slender, aedeagus and paraphysis subequal in width in lateral view.....	<b>100</b>
100	Male pygofer process median lamellar broadened with membranous structure, apical 1/3 thin strip-shaped, acute at apex; paraphysis articulating apically with aedeagus at apical 2/5.....	<b>A. likuni Jiang &amp; Yang, sp. nov.</b>
–	Male pygofer process dorsad membranous transparent apically, not acute at the apex; paraphysis articulating apically with aedeagus at apical 1/2..	
	.....	<b>A. zizhongji Jiang &amp; Yang, 2022</b>

- 101 Forewing orange-yellow or brown-yellow, with black spots..... **102**  
 – Forewing black, with longitudinal orange-yellow stripes; or orange-yellow with black stripes ..... **103**
- 102 Apical margin of crown with black spot medially; forewing with 4 large black spots, 1 located at subbasal portion of clavus, other 3 located at subbasal, median, and subapical portions of corium, respectively .....  
 ..... **A. sulphurata (Distant, 1908) (part)**  
 – Apical 1/2 of crown with a shawl-shaped black stripe; forewing with 3 black spots, 1 located at apical portion of clavus, others located at basal 1/3 and 2/3 portions of corium, respectively ..... **A. malaisei Young, 1986 (part)**
- 103 Forewing orange-yellow, with a longitudinal black stripe medially ..... **104**  
 – Characters not as above ..... **105**
- 104 Apical margin of crown with a black spot medially .....  
 ..... **A. sulphurata (Distant, 1908) (part)**  
 – Apical 1/2 of crown with a shawl-shaped black stripe .....  
 ..... **A. malaisei Young, 1986 (part)**
- 105 Forewing with 2 longitudinal muddy-yellow stripes .....  
 ..... **A. xanthovitta Kuoh, 1994**  
 – Forewing with > 2 longitudinal stripes ..... **106**
- 106 Body smaller, length < 5.5 mm; clavus orange-yellow, with a longitudinal black stripe medially ..... **A. opponens (Walker, 1851)**  
 – Body larger, length > 6 mm; clavus orange-yellow, without longitudinal black stripes medially ..... **107**
- 107 Male pygofer constricted medially, apex arrow-shaped .....  
 ..... **A. cuspidata Meng, Yang & Ni, 2010 (part)**  
 – Male pygofer with apex curved dorsally, apical margin roundly produced..  
 ..... **A. nigrisigna Li, 1992 (part)**

## Discussion

Currently, the identification of Cicadellinae species is mainly based on their external morphology and male genitalia characteristics of adults. However, there are some species that exhibit similar external morphologies, but the characteristics of the male genitalia are obviously different, or the characteristics of male genitalia are similar, but external morphologies are different. These situations make the identification of some Cicadellinae species difficult at species level, especially for the female specimens. *Atkinsoniella nigrominiatula* (Jacobi, 1944), *A. latior* Young, 1986, *A. limba* Kuoh, 1991, *A. dormana* Li, 1992, *A. divaricata* Yang, Meng & Li, 2017, *A. peaka* Yang, Meng & Li, 2017, *A. zizhongji* Jiang & Yang, 2022, *A. chongqingana* Jiang & Yang, sp. nov., and *A. likuni* Jiang & Yang, sp. nov. are similar in appearance but differ in their male genitalia. As the characteristics of female genitalia of subfamily Cicadellinae species are not obvious, those of the female specimens of *A. chongqingana* Jiang & Yang, sp. nov. and *A. likuni* Jiang & Yang, sp. nov. cannot be provided as the females have the same appearance, making their identification confusing; therefore, molecular methods are necessary to help solve these difficulties and provide more accurate species delimitations. In addition, the investigations into the biology and ecology may be good directions for better understanding the known and newly described leafhopper species in the future.

## Acknowledgements

We are grateful to Li-Kun Zhong, Xian-Yi Wang, and Tie-Long Xu (Institute of Entomology, Guizhou University) for collecting specimens.

## Additional information

### Conflict of interest

The authors have declared that no competing interests exist.

### Ethical statement

No ethical statement was reported.

## Funding

This study is supported by the National Natural Science Foundation of China (32360125, 32360393), Guizhou Province Science and Technology Innovation Talent Team Project (Qian Ke He Pingtai Rencai - CXTD [2021] 004), and the Scientific Research Foundation of Guiyang Healthcare Vocational University (Guikangda K2024-4).

## Author contributions

Conceptualization: YJ. Formal analysis: YJ. Methodology: XFY, YJ. Software: XFY, YJ. Supervision: MFY. Writing - original draft: YJ. Writing - review and editing: MFY.

## Author ORCIDs

Yan Jiang  <https://orcid.org/0000-0002-8980-5344>

Xiao-Fei Yu  <https://orcid.org/0000-0002-1362-9524>

Mao-Fa Yang  <https://orcid.org/0000-0002-5523-6825>

## Data availability

All of the data that support the findings of this study are available in the main text.

## References

- Distant WL (1908) The Fauna of British India Including Ceylon and Burma: Rhynchota. Vol. IV. Homoptera and Appendix (Pt.). Taylor and Francis, London, 501 pp.
- Feng L, Zhang YL (2015) The leafhopper genus *Atkinsoniella* Distant (Hemiptera: Cicadellidae: Cicadellinae) with descriptions of two new species from China. *Zootaxa* 4028: 274–286. <https://doi.org/10.11646/zootaxa.4028.2.7>
- Jacobi A (1944) Die Zikadenfauna der Provinz Fukien in Südchina und ihre tiergeographischen Beziehungen. *Mitteilungen der Münchener Entomologischen Gesellschaft* 34: 5–66.
- Jiang Y, Li HX, Yu XF, Yang MF (2022) Description and complete mitochondrial genome of *Atkinsoniella zizhongji* sp. nov. (Hemiptera: Cicadellidae: Cicadellinae) from China and its phylogenetic implications. *PeerJ* 10: e14026. <https://doi.org/10.7717/peerj.14026>
- Jiang Y, Yu XF, Yang MF (2023) Three new species of *Atkinsoniella* (Arthropoda, Insecta, Hemiptera, Cicadellidae, Cicadellinae) from China, with an updated checklist to the known species worldwide. *ZooKeys* 2023: 89–115. <https://doi.org/10.3897/zookeys.1161.101062>

- Kuoh CL (1991) Five new species of Cicadellidae from Fujian (Homoptera: Cicadelloidea). *Wuyi Science Journal* 8: 15–22. [In Chinese]
- Kuoh CL (1993) A new genus and a new species of Cicadellidae (Homoptera: Cicadelloidea). *Acta Zoologica Sinica* 39(1): 38–40. [In Chinese]
- Li ZZ (1992) Five new species of the genus *Atkinsoniella* from China (Homoptera: Tettigellidae). *Acta Zootaxonomica Sinica* 17(3): 344–351. [In Chinese]
- Naveed H, Zhang YL (2018) Newly recorded leafhoppers of the subfamily Cicadellinae (Hemiptera: Cicadellidae) with description of a new species from Pakistan. *Zootaxa* 4504: 285–295. <https://doi.org/10.11646/zootaxa.4504.2.9>
- Yang MF, Meng ZH, Li ZZ (2017) Hemiptera: Cicadellidae (II): Cicadellinae. *Fauna Sinica: Insecta*. Vol. 67. Science Press, Beijing, China, 637 pp. [In Chinese]
- Young DA (1968) Taxonomic study of the Cicadellinae (Homoptera: Cicadellidae), Part 1, Proconiini. *Bulletin - United States National Museum* 261: 1–287. <https://doi.org/10.5962/bhl.part.20869>
- Young DA (1986) Taxonomic study of the Cicadellinae (Homoptera: Cicadellidae), Part 3, Old World Cicadellini. *Bulletin of the North Carolina Agricultural Experimental Station* 281: 1–639.

